British Journal of Pharmacology

August 1992

Volume 106 Number 4 pages 757–1042

Dr S J Coker
Department of Pharmacology
University of Liverpool
P.O. Box 147
LIVERPOOL L69 3BX

Br. J. Pharmacol. (1992), **106**, 759–761

SPECIAL REPORT

© Macmillan Press Ltd, 1992

Pharmacological evidence for distinct endothelin receptors in guinea-pig bronchus and aorta

D.W.P. Hay

Department of Pharmacology, SmithKline Beecham Pharmaceuticals, P.O. Box 1539, King of Prussia, PA 19406-0939, U.S.A.

The ET_A receptor antagonist, BQ-123 (1 μM) potently antagonized endothelin-1 (ET-1) concentration-response curves in guinea-pig aorta ($pK_B = 7.1$). However, 10 μM BQ-123 was without effect on ET-1-induced contractions in guinea-pig bronchus. The ET_B-selective agonist, sarafotoxin S6c did not contract the aorta but was a potent and effective contractile agonist in the bronchus. BQ-123 (10 μM) was without effect on sarafotoxin S6c-induced contractions in the bronchus. These data provide evidence for distinct endothelin receptors in guinea-pig aorta and bronchus, which appear to be predominantly of the ET_A and non-ET_A, perhaps ET_B, subtypes, respectively.

Keywords: Endothelin-1; guinea-pig aorta; guinea-pig bronchus; BQ-123; ET_A receptor antagonist; sarafotoxin S6c; ET_B agonist; endothelin receptor subtypes; ET_A receptor; ET_B receptor

Introduction Endothelin-1 (ET-1) belongs to a family of recently discovered 21-amino acid vasoconstrictor peptides which also includes ET-2 and ET-3 (Yanagisawa & Masaki, 1989). Researchers have provided evidence for distinct endothelin receptors in several cells and tissues including rat lung (Masuda *et al.*, 1989). Recently the cloning and expression of cDNA for a selective and also a non-selective endothelin receptor, designated ET_A and ET_B, respectively, was described (Arai *et al.*, 1990; Sakurai *et al.*, 1990; Sakamoto *et al.*, 1991).

A comparison of the contractile effects of the endothelins and fragments provided preliminary evidence for distinct endothelin receptors in airway versus vascular smooth muscle (Maggi *et al.*, 1989; Cardell *et al.*, 1992).

The endothelins bear a close structural homology with a group of snake venoms, the sarafotoxins (Yanagisawa & Masaki, 1989), of which sarafotoxin S6c exhibits selectivity for the ET_B receptor (Williams *et al.*, 1991). In addition, BQ-123, a cyclic pentapeptide (D-Asp-L-Pro-D-Val-L-Leu-D-Trp), has been identified as a potent and selective ET_A receptor antagonist (Ihara *et al.*, 1991). In the present study, sarafotoxin S6c and BQ-123 were used to explore further potential differences in endothelin receptors mediating contraction in guinea-pig airway and vascular smooth muscles.

Methods Primary bronchi and thoracic aortae were removed from male Hartley guinea-pigs (Hazelton Research Animals, Denver, PA, U.S.A.; 450–650 g body weight). The epithelium and endothelium were removed mechanically from the bronchial and aortic rings, respectively. The preparations were placed under approximately 1.5 g tension in 10-ml water-jacketed siliconized organ baths containing modified Krebs-Henseleit solution. The composition of the Krebs-Henseleit solution, which was gassed with 95% O_2:5% CO_2 and maintained at 37°C, was (mM): NaCl 113.0, KCl 4.8, $CaCl_2$ 2.5, KH_2PO_4 1.2, $MgSO_4$ 1.2, $NaHCO_3$ 25.0 and glucose 5.5. Mechanical responses were recorded isometrically with multi-channel polygraphs. Experiments were conducted in the presence of the cyclo-oxygenase inhibitor, meclofenamic acid (1 μM). One hour after equilibration, and also at the end of the experiment, the bronchi and aortae were exposed to 10 μM carbachol and 10 μM phenylephrine, respectively; subsequent responses were expressed as a percentage of the reference contractions obtained following completion of the experiment. Cumulative concentration-response curves to ET-1 and sarafotoxin S6c were constructed by 3 fold increases in agonist concentration; in some experiments BQ-123 was added 30 min before starting the agonist concentration-response curves.

Geometric mean EC_{50} values were calculated from linear regression analysis of data, which are given as mean ± s.e.mean.

BQ-123 was synthesized by Dr Michael Moore and colleagues in the Department of Peptide Chemistry, SmithKline Beecham Pharmaceuticals. ET-1 and sarafotoxin S6c were purchased from Peninsula Laboratories (Belmont, CA, U.S.A.), phenylephrine and carbachol from Sigma Chemical Co. (St. Louis, MO, U.S.A.).

Results The ET_A receptor antagonist BQ-123 (1 μM) produced a marked shift to the right of ET-1 concentration-response curves in guinea-pig aorta (Figure 1a) with a $pK_B = 7.1$. In contrast, BQ-123 (1 or 10 μM) was without effect on contractions elicited by ET-1 in guinea-pig bronchus (illustrated for 10 μM in Figure 1b).

Sarafotoxin S6c (0.1 nM–0.1 μM) did not contract guinea-pig aorta but was a potent and effective contractile agent in guinea-pig bronchus (Figure 2). BQ-123 (10 μM) was without effect on sarafotoxin S6c-induced contractions in guinea-pig bronchus (Figure 2b).

Discussion Studies exploring the activity of various agonists provided preliminary evidence for the existence of different endothelin receptors responsible for contraction in vascular versus airway smooth muscle (Maggi *et al.*, 1989; Cardell *et al.*, 1992). The present study extends these observations and provides strong evidence for distinct endothelin receptors mediating ET-1-induced contraction in guinea-pig aorta and bronchus. Thus, the ET_A receptor antagonist, BQ-123 (Ihara *et al.*, 1991), potently antagonized ET-1 concentration-response curves in the aorta but was without effect on responses in the bronchus. Furthermore, sarafotoxin S6c, the ET_B-selective agonist (Williams *et al.*, 1991), did not contract the aorta but was a potent and effective contractile agonist in the bronchus. Selectivity of action of BQ-123 for ET_A-mediated responses was confirmed by its lack of effect against sarafotoxin S6c-induced contraction in bronchus. The potency of BQ-123 in guinea-pig aorta ($pK_B = 7.1$) is similar to that reported previously for inhibition of ET-1-induced contraction in porcine coronary artery ($pA_2 = 7.4$) (Ihara *et al.*, 1991).

The present data indicate that contraction of guinea-pig aorta induced by ET-1 is produced by activation of ET_A

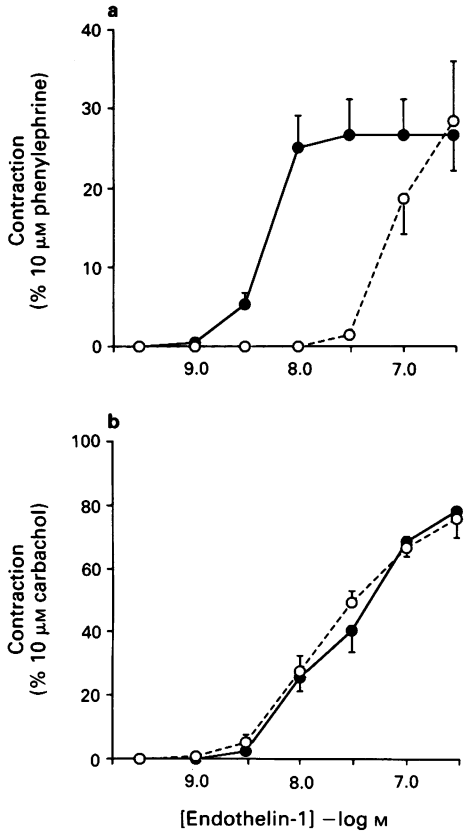

Figure 1 Effect of BQ-123 on endothelin-1 (concentration-response curves in (a) guinea-pig aorta and (b) guinea-pig bronchus. Results are expressed as a percentage of the response to (a) 10 μM phenylephrine or (b) 10 μM carbachol and are the mean with s.e.mean shown by vertical bars. (a) (●) Control; (○) 1 μM BQ-123, $n = 6$; (b) (●) control; (○) 10 μM BQ-123, $n = 4$.

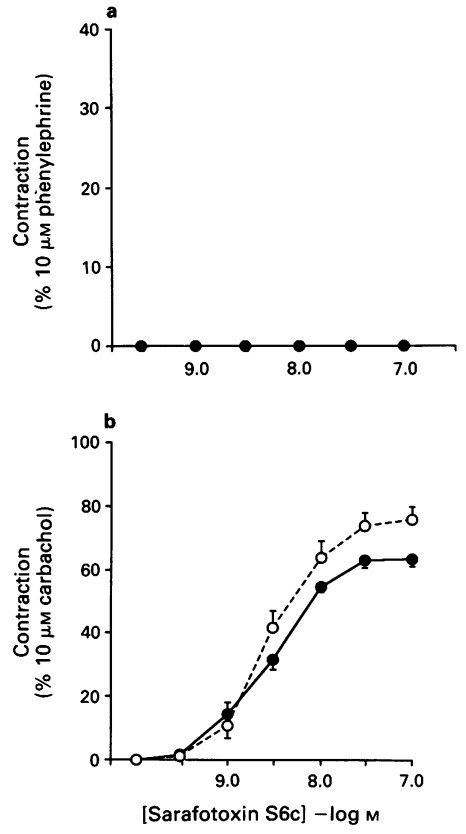

Figure 2 Concentration-response curves to sarafotoxin S6c in (a) guinea-pig aorta and (b) guinea-pig bronchus; also indicated in (b) is the effect of BQ-123 (10 μM) on sarafotoxin S6c-induced contractions. Results are expressed as a percentage of the response to (a) 10 μM phenylephrine or (b) 10 μM carbachol and are given as the means with s.e.mean (vertical bars) of 4 tissues: (b) (●) control; (○) 10 μM BQ-123.

receptors. Without the availability of a selective ET_B receptor antagonist, it is uncertain whether the ET-1-induced contraction of guinea-pig bronchus is due to stimulation of ET_B receptors or perhaps a non-ET_A, non-ET_B receptor subtype similar to that recently proposed following functional studies in porcine coronary artery with various members of the endothelin and sarafotoxin families (Harrison *et al.*, 1992). The functional identification of endothelin receptor subtypes will be important in the development of selective endothelin receptor antagonists for the treatment of diseases in which endothelin has been implicated.

In summary, the results of this study, in addition to previous findings, suggest that ET-1-induced contractions of guinea-pig aorta and bronchus are mediated predominantly via an ET_A-type and a non-ET_A-type, perhaps ET_B-type, receptor, respectively.

The author thanks Mark Luttmann for excellent technical assistance, Dr Eliot Ohlstein for helpful discussion and Dotti Lavan for typing this material.

References

ARAI, H., HORI, S., ARAMORI, I., OHKUBO, H. & NAKANISHI, S. (1990). Cloning and expression of a cDNA encoding an endothelin receptor. *Nature*, **348**, 730–732.

CARDELL, L.O., UDDMAN, R. & EDVINSSON, L. (1992). Evidence for multiple endothelin receptors in the guinea-pig pulmonary artery and trachea. *Br. J. Pharmacol.*, **105**, 376–380.

HARRISON, V.J., RANDRIANTSOA, A. & SCHOEFFTER, P. (1992). Heterogeneity of endothelin-sarafotoxin receptors mediating contraction of pig coronary artery. *Br. J. Pharmacol.*, **105**, 511–513.

IHARA, M., NOGUCHI, K., SAEKI, T., FUKURODA, T., TSUCHIDA, S., KIMURA, S., FUKAMI, T., ISHIKAWA, K., NISHIKIBE, M. & YANO, M. (1991). Biological profiles of highly potent novel endothelin antagonists selective for the ET_A receptor. *Life Sci.*, **50**, 247–255.

MAGGI, C.A., GIULIANI, S., PATACCHINI, R., SANTICIOLI, P., ROVERO, P., GIACHETTI, A. & MELI, A. (1989). The C-terminal hexapeptide, endothelin-(16-21), discriminates between different endothelin receptors. *Eur. J. Pharmacol.*, **166**, 121–122.

MASUDA, Y., MIYAZAKI, H., KONDOH, M., WATANABE, H., YANAGISAWA, M., MASAKI, T. & MURAKAMI, K. (1989). Two different forms of endothelin receptors in rat lung. *F.E.B.S. Lett.*, **257**, 208–210.

SAKURAI, T., YANAGISAWA, M., TAKUWA, Y., MIYAZAKI, H., KIMURA, S., GOTO, K. & MASAKI, T. (1990). Cloning of a cDNA encoding a non-isopeptide-selective subtype of the endothelin receptor. *Nature*, **348**, 732–735.

SAKAMOTO, A., YANAGISAWA, M., SAKURAI, T., TAKUWA, Y., YANAGISAWA, H. & MASAKI, T. (1991). Cloning and functional expression of human cDNA for the ET_B endothelin receptor. *Biochem. Biophys. Res. Commun.*, **178,** 656–663.

WILLIAMS, D.L., Jr., JONES, K.L., PETTIBONE, D.J., LIS, E.V. & CLINESCHMIDT, B.V. (1991). Sarafotoxin S6c: an agonist which distinguishes between endothelin receptor subtypes. *Biochem. Biophys. Res. Commun.*, **175,** 556–561.

YANAGISAWA, M. & MASAKI, T. (1989). Endothelin, a novel endothelium-derived peptide. Pharmacological activities, regulation and possible roles in cardiovascular control. *Biochem. Pharmacol.*, **38,** 1877–1883.

(Received March 19, 1992
Accepted April 16, 1992)

Br. J. Pharmacol. (1992), **106**, 762–763

SPECIAL REPORT

© Macmillan Press Ltd, 1992

ATP mediates excitatory synaptic transmission in mammalian neurones

[1] E.M. Silinsky, *V. Gerzanich & [2] S.M. Vanner

Department of Pharmacology, Northwestern University Medical School, 303 East Chicago Avenue, Chicago, Illinois and *Vollum Institute for Advanced Biomedical Research, 3181 SW Sam Jackson Park Road, Portland, Oregon 97201, U.S.A.

Adenosine 5'-triphosphate (ATP, 0.1–100 μM), produced inward currents in patch-clamped coeliac neurones from guinea-pig when studied in either the whole cell configuration or in excised (outside-out) patches. The P_2-purinoceptor antagonists suramin (80–230 μM) or reactive blue 2 (2–20 μM) depressed the ATP-induced currents but not those produced by acetylcholine. Excitatory post-synaptic currents (e.p.s.cs) were observed in cultured neurones. E.p.s.cs had similar current-voltage relationships to currents evoked by ATP in excised patches and were reduced by suramin or reactive blue 2 to a similar extent as ATP currents. The results suggest that ATP is the excitatory neurotransmitter in cultures of these neurones.

Keywords: ATP; synaptic currents; suramin; reactive blue 2; acetylcholine; purinergic

Introduction Adenosine 5'-triphosphate (ATP) has the potential to serve as a rapid excitatory neurotransmitter in the mammalian nervous system (Burnstock, 1972; Sneddon & Westfall, 1984; Silinsky, 1989; Allen & Burnstock, 1990; Fieber & Adams, 1991). Such a role for ATP is implied in studies on intracardiac ganglia (Allen & Burnstock, 1990; Fieber & Adams, 1991) and sensory transmission from the periphery to the central nervous system (Jahr & Jessell, 1983; Fyffe & Perl, 1984). However, there has been no direct evidence forthcoming to suggest that ATP mediates excitatory synaptic transmission between neurones. In preliminary experiments, we have found that ATP receptors in neurones of the guinea-pig coeliac ganglion, a sympathetic prevertebral ganglion, are ionic channels the activation of which produces excitation in a manner more potent and efficacious than acetylcholine (ACh) (Gerzanich *et al.*, 1991; unpublished observations). It would thus be of interest to determine whether synaptic currents observed in coeliac neurones are purinergic.

Methods Experiments were carried out on neurones acutely dissociated from young adult guinea-pigs (150–250 g) by conventional methods. The coeliac ganglia were dissected (Kreulen & Szurszewski, 1979; McLachlan & Meckler, 1989), washed in modified Liebowitz 1:15 solution (free of divalent cations), and then treated sequentially with papain and collagenase (1 mg ml^{-1}) plus dispase (4 mg ml^{-1}). After trituration, washing and centrifugation, the cells were plated onto collagen-coated cover slips in growth medium (supplemented Eagle's essential medium). Cells were used from 2–24 h after dissociation or kept in culture from 1–8 days (being fed 2 times per week). Experiments in this paper were all carried out using patch clamp methods (Sakmann & Neher, 1983) on isolated neurones (Axopatch 1B or 1C, Axon Instruments) at room temperature but similar effects of ATP were observed with intracellular electrodes in the freshly-dissected ganglion studied at 37°C *in vitro* (Vanner *et al.*, 1991; Silinsky, 1992, see Figures 6 and 12). Recording micropipettes had resistances ranging from 3–5 MΩ for whole cell recording and 10–15 MΩ for single channels in excised (outside-outside) patches. Internal solutions in the patch electrodes contained (mM): Cs gluconate 160, Na^+ 24, EGTA 10, Ca^{2+} 0–1, Mg^{2+} 0–1. External solutions contained (mM): NaCl 160, glucose 11, CsCl 0–1, $CaCl_2$ 1–2.5 and $MgCl_2$ 0–1; intracellular and extracellular solutions were buffered to pH 7.3–7.4 with 5–10 mM HEPES. Mean values of membrane currents are presented ± 1 standard error of the mean (s.e.mean). ATP, and reactive blue 2 were obtained from the Sigma Chemical Company. Suramin sodium was the generous gift of Dr John Daly.

Results and Discussion ATP, at concentrations beginning in the hundred nanomolar range, depolarized unclamped coeliac neurones to threshold for action potential generation (Silinsky, 1992) or produced inward currents in neurones voltage clamped at the resting potential (Figure 1). These excitatory effects of ATP were associated with conductance increases to cations (Silinsky, 1992). Figure 1 illustrates that ATP is more potent than acetylcholine (ACh) in isolated neurones. ATP was also more efficacious than ATP. Indeed, at a holding potential near the normal resting potential (– 50 mV), ACh generally required an order of magnitude higher concentration to produce maximal effects less than 75% of those produced by ATP (73 ± 10%, $n = 11$). Suramin (80–230 μM), a selective antagonist of P_2-purinoceptors (Dunn & Blakely, 1988; Nakazawa *et al.*, 1990), reversibly reduced the ATP-induced current to approximately 50% of control (50.8% ± 2.9%, $n = 10$) but did not affect the current evoked by ACh in the same cell (Figure 1).

A proportion of neurones in culture possess excitatory postsynaptic currents (e.p.s.cs, Figure 2a). The current-voltage relationship for the e.p.s.cs were similar to those

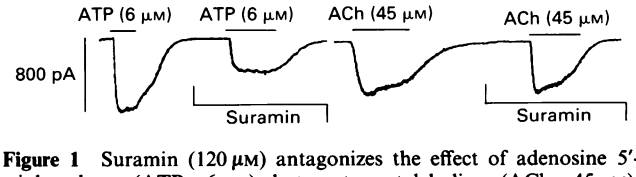

Figure 1 Suramin (120 μM) antagonizes the effect of adenosine 5'-triphosphate (ATP, 6 μM) but not acetylcholine (ACh, 45 μM). Suramin was delivered from fast flow pipes (300 μM inner diameter) between the arrows. First application of ATP lasted 7 s (bar, which was also the duration of the maximal response) and was 800 pA in magnitude. Reactive blue 2 (2–20 μM) produced similar effects to suramin ($n = 6$). The nicotinic antagonists tubocurarine, (50–100 μM, $n = 4$), hexamethonium (25–100 μM, $n = 7$), or trimethaphan (25 μM, $n = 3$) blocked the effects of ACh but did not affect the response to ATP (data not shown). These results were also observed at the level of single ion channels (outside-out patches).

[1] Author for correspondence.
[2] Present address: Gastroenterology Research Unit, Queens University, Kingston, Ontario, Canada

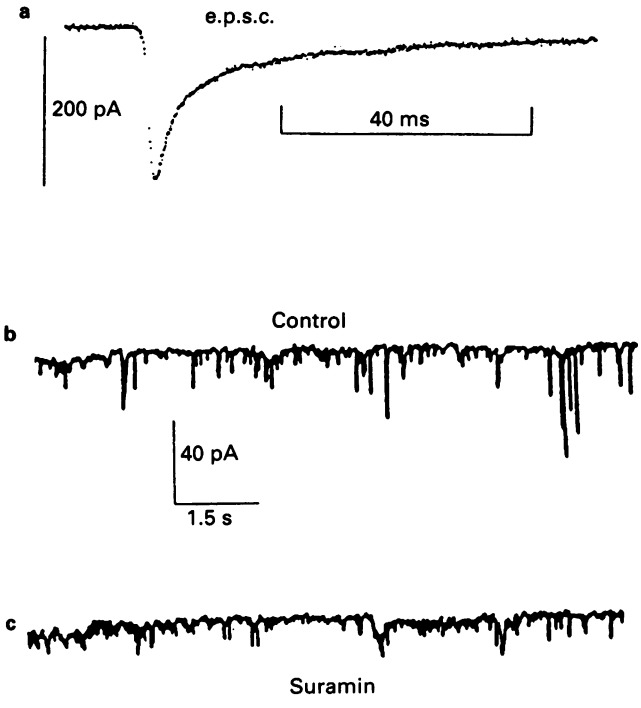

Figure 2 Synaptic currents in cultures of coeliac neurones and their antagonism by suramin: (a) shows typical excitatory synaptic current (e.p.s.c.), holding potential − 86 mV; (b) shows control e.p.s.c. from another neurone in solutions containing 1 μM tetrodotoxin, holding potential − 115 mV. Bottom trace (c) shows the same cell during suramin application—mean e.p.s.c. amplitude was reduced by 53% in this experiment (from 14.8 ± 1 pA, $n = 139$ in control to 7.9 pA ± 0.7 pA, $n = 151$ in suramin). The inhibitory effect of suramin ranged from 48% to 53% of control and was reversible. Reactive blue 2 also reduced e.p.s.c. amplitudes ($n = 2$).

produced by ATP in outside-out patches, reversing near − 10 mV and exhibiting inward rectification. The e.p.s.cs were not blocked by the Na^+ channel blocker, tetrodotoxin (TTX, Figure 2b) or by antagonists at nicotinic synapses (unpublished). Figure 2 presents a representative experiment ($n = 4$) illustrating that the e.p.s.cs were reduced in amplitude by suramin to approximately 50% of control, an effect similar to the depression of ATP-induced currents by suramin. Suramin has not been found to affect transmitters other than ATP (e.g. Dunn & Blakely, 1988; Nakazawa *et al.*, 1991). Reactive blue 2 (2–20 μM), another P_2-purinoceptor antagonist that affects ATP-gated channels (see e.g. Fieber & Adams, 1991), produced results similar to those illustrated for suramin in Figure 1 (antagonism of the effects of ATP but not ACh, $n = 6$) and Figure 2 (reduction in size of e.p.s.cs, $n = 2$).

Further evidence for the role of ATP as a neurotransmitter was found in experiments in which evoked secretion was studied. Depolarization of the presynaptic nerve fibre by the local application of 10 mM K^+, increased the frequency of e.p.s.cs in a Ca^{2+}-dependent manner and also opened ATP-gated channels in outside-out patches; this only occurred when the ATP-detector patches were positioned at the presynaptic nerve fibre near the cell soma. Evoked responses were also antagonized reversibly by suramin.

The results suggest that ATP but not ACh is the neurotransmitter mediating e.p.s.cs in isolated coeliac neurones. These isolated neurones may thus provide a model system in which to study the electrophysiological correlates of quantal purinergic transmission.

This work was supported by a grant from the U.S. Public Health Service to E.M.S. V.G. is grateful for support from Dr R.A. North. We wish to thank Ms Rosa Barajas-Lopez and Dr S. Matsumoto for assistance in the isolation and culturing of coeliac neurones, Dr John Daly for the gift of suramin sodium, and Drs R.A. North/A.M. Suprenant for the loan of select items of electrophysiological equipment and for finding E.M.S. a splendid dwelling whilst he was on sabbatical leave in Oregon.

References

ALLEN, T.G.J. & BURNSTOCK, G. (1990). The actions of adenosine 5'-triphosphate on guinea-pig intracardiac neurones in culture. *Br. J. Pharmacol.*, **100**, 269–276.

BURNSTOCK, G. (1972). Purinergic nerves. *Pharmacol. Rev.*, **24**, 509–581.

DUNN, P.M. & BLAKELY, A.G.H. (1988). Suramin: a reversible P_2-purinoceptor antagonist in the mouse vas deferens. *Br. J. Pharmacol.*, **93**, 243–245.

FIEBER, L.A. & ADAMS, D.J. (1991). Adenosine triphosphate-evoked currents in cultured neurons dissociated from rat parasympathetic cardiac ganglia. *J. Physiol.*, **434**, 239–256.

FYFFE, R.E. & PERL, E.R. (1984). Is ATP a central synaptic transmitter for certain primary afferent fibres from mammalian skin. *Proc. Natl. Acad. Sci. U.S.A.*, **81**, 6890–6893.

GERZANICH, V., MATSUMOTO, S., NORTH, R.A. & SILINSKY, E.M. (1991). Currents evoked by adenosine 5'-triphosphate in guinea-pig celiac ganglion cells. *Soc. Neurosci. Abs.*, **17**, 410(abs).

JAHR, C.E. & JESSELL, T.M. (1983). ATP excites a subpopulation of rat dorsal horn neurones. *Nature*, **304**, 730–733.

KREULEN, D.L. & SZURSZEWSKI, J.H. (1979). Nerve pathways in celiac plexus of the guinea pig. *Am. J. Physiol.*, **237**, E90–E97.

MCLACHLAN, E.M. & MECKLER, R.L. (1989). Characteristics of synaptic input to three classes of sympathetic neurone in the coeliac ganglion of the guinea-pig. *J. Physiol.*, **415**, 109–129.

NAKAZAWA, K., FUJIMORI, K., TAKANAKA, A. & INOUE, K. (1990). Reversible and selective antagonism by suramin of ATP-activated inward current in PC12 phaeochromocytoma cells. *Br. J. Pharmacol.*, **101**, 224–226.

SAKMANN, B. & NEHER, E. (1983). *Single-Channel Recording*. New York: Plenum Press.

SILINSKY, E.M. (1989). Adenosine derivatives and neuronal function. *Sem. Neurosci.*, **1**, 155–165.

SILINSKY, E.M. (1992). Intracellular recording methods for neurons. In *Monitoring Neuronal Activity: a Practical Approach*. ed. Stamford, J.A., pp. 29–57. London: Oxford University Press (IRL).

SNEDDON, P. & WESTFALL, D.P. (1984). Pharmacological evidence that adenosine triphosphate and noradrenaline are co-transmitters in the guinea-pig vas deferens. *J. Physiol.*, **347**, 561–580.

VANNER, S., SILINSKY, E.M. & GERZANIC, V. (1991). Purinoceptors mediate fast excitatory depolarizations in celiac ganglia of the guinea-pig. *Clin. Invest. Med.*, **14** (Suppl), A265.

(Received April 8, 1992
Accepted April 22, 1992)

Br. J. Pharmacol. (1992), **106**, 764–765

SPECIAL REPORT

© Macmillan Press Ltd, 1992

Ca^{2+} release from isolated sarcoplasmic reticulum of guinea-pig psoas muscle induced by K^+-channel blockers

[1]Yukisato Ishida, Hiromi Honda & *Takushi X. Watanabe

Mitsubishi Kasei Institute of Life Sciences, Machida, Tokyo 194, Japan and *Peptide Institute Inc., Protein Research Foundation, Minoh, Osaka, 562, Japan

A Ca^{2+}-sensitive electrode was used to measure the Ca^{2+} concentration of the medium containing the heavy fraction of the fragmented sarcoplasmic reticulum (SR) prepared from guinea-pig psoas muscle. Among K^+-channel blockers tested, 4-aminopyridine (4-AP), tetraethylammonium (TEA) and charybdotoxin elicited Ca^{2+} release from the SR, but apamin and glibenclamide did not. These results suggest that a reduction of SR K^+ conductance leads to Ca^{2+} release from the SR.

Keywords: K^+-channel blocker; 4-aminopyridine; tetraethylammonium; charybdotoxin; apamin; glibenclamide; Ca^{2+}-release; sarcoplasmic reticulum; guinea-pig skeletal muscle

Introduction Striated muscle contraction is initiated by a rapid release of Ca^{2+} through Ca^{2+} channels on the sarcoplasmic reticulum (SR) membrane (Endo, 1985). The SR also possesses K^+ channels which it has been suggested form a counter-ion pathway during Ca^{2+} movement upon contraction, following extensive studies using planar phospholipid bilayer membranes (Miller *et al.*, 1984). In the present experiments, we investigated the effects of various potassium channel blockers on Ca^{2+}-filled fragmented SR prepared from guinea-pig psoas muscle to determine if a relationship exists between K^+ and Ca^{2+} channels on the SR membrane.

Methods The heavy fraction of the fragmented SR was prepared by the modified method of Kim *et al.* (1983). Male guinea-pigs (about 400 g) were stunned and exsanguinated. The psoas muscle (a white muscle) was isolated and homogenized. The homogenate in 5 volumes of 5 mM Tris-maleate (pH 7.0) was fractionated by differential centrifugation. The SR heavy fraction remaining in the supernatant after centrifugation at 5000 *g* for 5 min were pelleted at 12000 *g* for 30 min. The pellet was washed with a buffer containing 0.1 M KCl and 5 mM Tris-maleate by centrifugation at 70000 *g* for 30 min. The heavy fraction of the fragmented SR was stored at 0°C and used within 3 days.

A Ca^{2+}-sensitive electrode was used to measure the Ca^{2+} concentration of the medium containing the fragmented SR as described elsewhere (Kobayashi *et al.*, 1988). The electrode showed Nernstian responsiveness (slope, 27–29 mV/pCa unit) in the calibration solutions between pCa 3 to 6.5 with Ca^{2+} and ethylene glycol-*bis*(β-aminoethylether)-N,N,N,N-tetraacetic acid (EGTA). The time for 90% response was approximately 0.6 s when pCa was lowered from 6 to 4. For the assay, $CaCl_2$ 50 μM, fragmented SR 0.5–1 mg protein ml^{-1}, phosphocreatine 5 mM and ATP 1 mM plus creatine kinase 0.1 mg ml^{-1} were successively added to the basic solution of the following composition (mM): KCl 100, $MgCl_2$ 0.5 and 4-morpholinepropane sulphonic acid (MOPS) 50 (pH 7.0, 30°C). After Ca^{2+} in the medium was taken up by the SR, various drugs were administered (number of experiments, at least 3). The Ca^{2+} concentration in the nominally Ca^{2+}-free solution was estimated to be 1.28 ± 0.21 μM (mean ± s.e. mean, $n = 6$).

To make the Ca^{2+}-sensitive electrode, a small amount of the Ca^{2+} sensor, a mixture of Ca^{2+}-cocktail (Fluka 21048, Switzerland) and polyvinyl chloride in tetrahydrofuran, was attached at the tip of a polyethylene pipette (C20, Gilson, France) ~0.3 mm in diameter. Then, the pipette was filled with an internal solution of the following composition (mM): $CaCl_2$ 5, EGTA 5, $MgCl_2$ 5, KCl 100 and MOPS 50 (pH 7.0). The reference electrode (glass pipette) was filled with 1.5% agar in the internal solution without $CaCl_2$ and EGTA. The electrodes were fed into a pH meter (model GT-01, Mitsubishi Kasei, Tokyo).

Drugs used were: 4-aminopyridine and tetraethylammonium chloride (Tokyo Kasei, Tokyo), caffeine (Wako Pure Chemicals, Tokyo), apamin and glibenclamide (Sigma, St Louis, MO). Charybdotoxin was synthesized as reported elsewhere (Lambert *et al.*, 1990). Cromakalim and nicorandil were generous gifts from Beecham Pharmaceuticals, Surrey, U.K. and Chugai Pharmaceutical Co., Tokyo, Japan, respectively.

Results The effects of various K^+-channel blockers on the SR prepared from the guinea-pig psoas muscle were investigated by directly monitoring the Ca^{2+} concentration in the medium with a Ca^{2+}-sensitive electrode (Figure 1). The prompt reduction and the subsequent gradual decrease in Ca^{2+} concentration after addition of ATP are due to the formation of the Ca-ATP complex and active Ca^{2+} uptake by SR, respectively. The early part of the Ca^{2+} uptake was almost linear in an antilogarithmic plot (data not shown). When the Ca^{2+} concentration was reduced to submicromolar levels, the rate of Ca^{2+} uptake decreased. Addition of caffeine (0.5 mM), which is known to release Ca^{2+} from SR (Endo, 1985), elicited a transient increase in the Ca^{2+} concentration of the medium (Figure 1), indicating Ca^{2+} release from SR followed by reuptake, as reported previously (Kobayashi *et al.*, 1988). Addition of 4-AP (1 mM), TEA (10 mM) or charybdotoxin (1 μM) elicited a similar increase in the Ca^{2+} concentration of the medium. High concentrations of 4-AP (10 mM) and TEA (30 mM) prolonged the duration of the increase in the Ca^{2+}-concentration of the medium. 4-AP (10 mM) caused oscillation of the Ca^{2+}-level to occur. Lower concentrations of 4-AP (less than 0.3 mM) and TEA (3 mM) did not release Ca^{2+} from the fragmented SR. Apamin (1 μM) and glibenclamide (10 μM) did not elicit Ca^{2+} release from the fragmented SR. The presence of cromakalim or nicorandil (both 10 μM), so-called K^+-channel activators (Weston & Abbot, 1987), did not elicit Ca^{2+} release or affect the Ca^{2+} release induced by 4-AP, TEA, charybdotoxin or caffeine (data not shown).

[1] Author for correspondence.

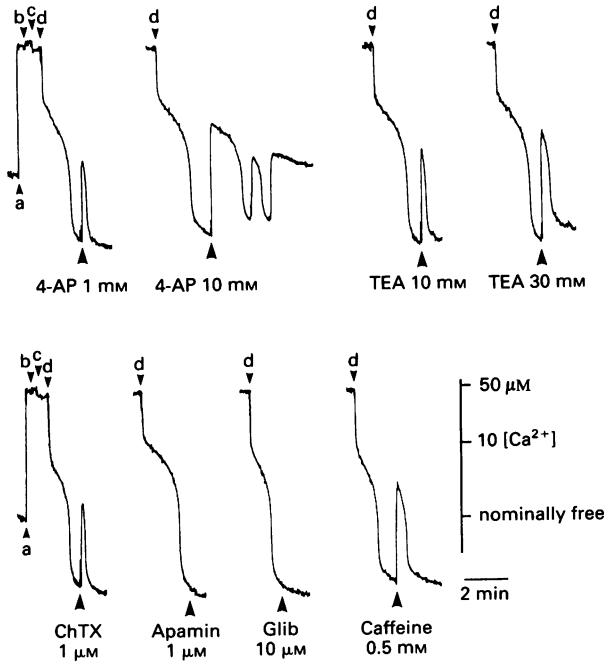

Figure 1 Effects of various K^+-channel blockers and caffeine on the Ca^{2+}-filled sarcoplasmic reticulum (SR) prepared from guinea-pig psoas muscle. Following accumulation of Ca^{2+} from the medium by the SR, 4-aminopyridine (4-AP), tetraethylammonium (TEA), charybdotoxin (ChTX), apamin, glibenclamide (Glib) and caffeine were administered. The following additions were made: (a) $CaCl_2$; (b) fragmented SR; (c) phosphocreatine and (d) ATP and creatine kinase. Calibration of the Ca^{2+} concentration of the medium is shown in the logarithmic scale on the right of the lower panel. The level before addition of Ca^{2+} represents the nominally Ca^{2+}-free level (1.25 μM).

Discussion TEA has been reported to be able to impede the K^+ conductance of channels when applied to the inside of the lipid bilayer, presumably representing the inside membrane of the SR (Miller *et al.*, 1984). Thus, one might speculate that TEA as well as 4-AP, although administered to the cytosolic side in the present experiments, could gain entry to the SR and by an action on the inner membrane elicit Ca^{2+} release. The large molecular size of charybdotoxin is likely to preclude its entry into the SR, but it too elicited Ca^{2+} release. It seems likely, therefore, that all three K^+ channel blockers can trigger the Ca^{2+} release from the SR by an action on the outer, cytosolic membrane of the SR. It is possible that K^+ channel blockade produces a depolarization of the SR membrane which leads to Ca^{2+} release (Endo, 1985), although the role of depolarization in SR is not yet fully understood.

Miller *et al.* (1985) reported that charybdotoxin, an inhibitor of the large-conductance Ca^{2+}-activated K^+ channel, had no effect on K^+ channels from mammalian SR. Presumably, the concentration of charybdotoxin used by these workers was inappropriately low (the highest concentration described was 1.3 $\mu g\ ml^{-1}$ of the partially purified toxin). The concentration of 1 μM used here was higher than that required to block K^+ channels on the plasma membrane, however, the same concentration of another peptide blocker, apamin, did not elicit Ca^{2+} release from SR, suggesting that the inhibitory effect of charybdotoxin is rather specific. Recently, Uehara *et al.* (1991) found a class of Ca^{2+}-activated K^+ channels in cardiac SR with a large conductance of 184 pS. This SR K^+ channel had properties distinct from other reported Ca^{2+}-activated K^+ channels on the plasma membrane with respect to the channel open time and voltage sensitivity. Thus, the need for a high concentration of charybdotoxin in our experiments may be because the K^+ channel in the SR is atypical.

In skeletal muscle, cromakalim was reported to open the ATP-sensitive K^+ channels of the plasma membrane (Spuler *et al.*, 1989). Glibenclamide is known to inhibit ATP-sensitive K^+ channels (Sturgess *et al.*, 1988). Neither cromakalim nor glibenclamide elicited Ca^{2+} release from the SR or affected the Ca^{2+} release induced by caffeine and the K^+ channel blockers described above. These results suggest that K^+ channels distinct from the ATP-sensitive K^+ channel play a substantial role in the regulation of Ca^{2+} movements in the SR.

References

ENDO, M. (1985). Calcium release from sarcoplasmic reticulum. *Curr. Top. Membr. Transp.*, **25**, 181–230.

KIM, D.H., OHNISHI, S.T. & IKEMOTO, N. (1983). Kinetic studies of calcium release from sarcoplasmic reticulum *in vitro*. *J. Biol. Chem.*, **258**, 9662–9668.

KOBAYASHI, M., ISHIDA, Y., SHOJI, N. & OHIZUMI, Y. (1988). Cardiotonic action of [8]-gingerol, an activator of the Ca^{2+}-pumping adenosine triphosphatase of sarcoplasmic reticulum, in guinea pig atrial muscle. *J. Pharmacol. Exp. Ther.*, **246**, 667–673.

LAMBERT, P., KURODA, H., CHINO, N., WATANABE, T.X., KIMURA, T. & SAKAKIBARA, S. (1990). Solution synthesis of charybdotoxin (ChTX), a K^+ channel blocker. *Biochem. Biophys. Res. Commun.*, **170**, 684–690.

MILLER, C., BELL, J.E. & GARCIA, M. (1984). The potassium channel of sarcoplasmic reticulum. *Curr. Top. Membr. Transp.*, **21**, 99–132.

MILLER, C., MOCZYDLOWSKY, E., LATORRE, R. & PHILLIPS, M. (1985). Charybdotoxin, a protein inhibitor of single Ca^{2+}-activated K^+ channels from mammalian skeletal muscle. *Nature*, **313**, 316–318.

SPULER, A., LEHMANN-HORN, F. & GRAFE, P. (1989). Cromakalim (BRL 34915) restores *in vitro* the membrane potential of depolarized human skeletal muscle fibres. *Naunyn-Schmiedebergs Arch Pharmacol.*, **339**, 327–331.

STURGESS, N.C., KOZLOWSKI, R.Z., CARRINGTON, C.A., HALES, C.N. & ASHFORD, M.L.J. (1988). Effects of sulphonylureas and diazoxide on insulin secretion and nucleotide-sensitive channels in an insulin-secreting cell line. *Br. J. Pharmacol.*, **95**, 83–94.

UEHARA, A., YASUKOHCHI, M., OGATA, S. & IMANAGA, I. (1991). Activation by intracellular calcium of a potassium channel in cardiac sarcoplasmic reticulum. *Pflügers Arch. Eur. J. Physiol.*, **417**, 651–653.

WESTON, A.H. & ABBOTT, A. (1987). New class of antihypertensive acts by opening K^+ channels. *Trends Pharmacol. Sci.*, **8**, 283–284.

(Received March 24, 1992
Accepted April 28, 1992)

Br. J. Pharmacol. (1992), **106**, 766–767

SPECIAL REPORT

© Macmillan Press Ltd, 1992

The neuroprotective effect of a nitric oxide inhibitor in a rat model of focal cerebral ischaemia

[1]A. Buisson, M. Plotkine & R.G. Boulu

Laboratoire de Pharmacologie, Faculté des Sciences Pharmaceutiques et Biologiques, Université René Descartes, 75006 Paris, France

Recent data showed that glutamate toxicity in primary cortical cultures is mediated by nitric oxide. In order to investigate the effect of inhibition of NO synthase on focal cerebral ischaemia in rats, we studied the histological consequences of a middle cerebral artery (MCA) occlusion after post-operative treatment with N^G-nitro-L-arginine methyl ester, an inhibitor of nitric oxide synthase. We found a significant reduction of cortical (−43%) and striatal (−25%) necrotic volumes induced by MCA occlusion, indicating that NO synthesis plays an important role in the neurotoxic cascade leading to neuronal damage after focal cerebral ischaemia in rats.

Keywords: Cerebral focal ischaemia in rats; nitric oxide; NO synthase inhibitor

Introduction Nitric oxide (NO) is an ubiquitous messenger molecule which has been shown to be produced enzymatically in the central nervous system in response to activation of N-methyl-D-aspartate (NMDA) receptors. This activation results in a raised influx of Ca^{2+} ions into post-synaptic structures, which in turn activates NO-synthase under physiological conditions (Snyder, 1991).

As the overstimulation of NMDA receptors by excitatory amino acids may initiate several phenomena which lead to neuronal death during cerebral ischaemia (Choi, 1991), and as the blockade of NO synthesis reduces the glutamate-induced neurotoxicity in cultured cortical neurones (Dawson *et al.*, 1991), it might be hypothesized that NO would mediate, at least in part, the ischaemia-induced neuronal damage. In order to investigate the possibility that NO participates in the neuronal damage induced by a focal cerebral ischaemia, we studied the effect of the systemic administration of a competitive inhibitor of NO-synthase, N^G-nitro-L-arginine methyl ester (L-NAME) (Rees *et al.*, 1990), on the histological consequences of permanent occlusion of the MCA in rats.

Methods Male Sprague Dawley rats (280–300 g) were anaesthetized with chloral hydrate (300 mg kg^{-1}, i.p.) and the left MCA was cauterized at its proximal site. Rectal and temporal muscle temperatures were maintained at 36–37°C during the experiment. L-NAME was administered (1 or 3 mg kg^{-1}, i.p.), 5 min, 3 h, 6 h, 24 h and 36 h after ischaemia. The rats were killed 2 days later. Their brains were removed and frozen in isopentane (−40°C). Cryostat coronal brain sections were stained with cresyl violet and analysed with an image analyser (IMSTAR, PARIS). Twelve coronal slices were digitized for each animal. The areas of ischaemic damage were measured by outlining the necrotic cortical and striatal regions on the digitized image and measuring the enclosed area. By using values for the distances between respective coronal sections, a linear integration was used to calculate the cortical and striatal necrotic volumes.

In other groups of rats subjected to the same experimental condition of anaesthesia, mean arterial blood pressure (MABP) was continuously recorded with a chronically implanted femoral catether.

[1] Author for correspondence at: Alain Buisson, Laboratoire de Pharmacologie, 4 avenue de l'Observatoire, 75006 Paris, France.

Results MCA occlusion in rats induced a highly reproducible infarction that affected both the cortex and the striatum. The total volume (mean ± s.e.mean) of the infarction in the vehicle-treated rats was 194 ± 14 mm^3 ($n = 9$). The low dose (1 mg kg^{-1}, i.p.) of L-NAME failed to induce any significant change in the infarcted volume in ischaemic rats. Treatment with 3 mg kg^{-1} of L-NAME significantly reduced the total infarct volume by 35% (125 ± 18 mm^3, $n = 9$, $P<0.05$), the cortical infarct volume by 43% (84 ± 16 mm^3 versus 139 ± 15 mm^3, $P<0.05$) and the striatal infarct volume by 25% (41 ± 5 mm^3 versus 55 ± 4 mm^3, $P<0.05$) (Figure 1).

In chloral anaesthetized rats, treatment with L-NAME at 1 mg kg^{-1} did not induce any significant modification of MABP. Under the same conditions, a hypertension (21 ± 6 mmHg) appeared 30 min after treatment with L-NAME 3 mg kg^{-1} (Figure 2). The repeated treatment at 3 h,

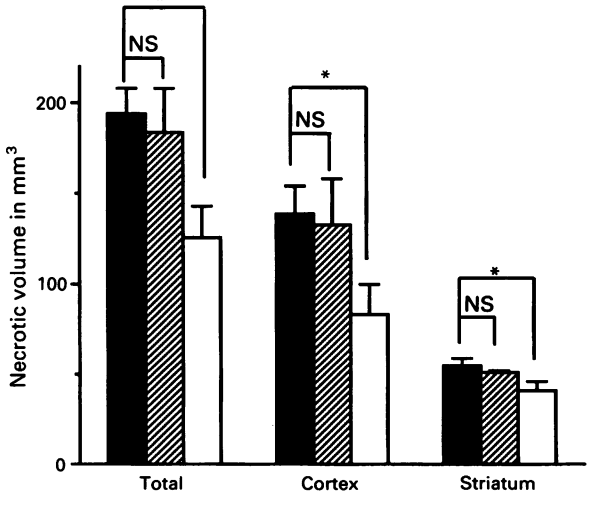

Figure 1 Effect of middle cerebral artery occlusion on striatal, cortical and total cerebral necrotic volumes developed by control rats (solid columns), and by rats treated with N^G-nitro-L-arginine methyl ester (L-NAME) 1 mg kg^{-1}, i.p. (hatched columns) and 3 mg kg^{-1}, i.p. (open columns) administered 5 min, 3 h, 6 h, 24 h and 36 h after induction of cerebral focal ischaemia. Each column is the mean of 8–9 experiments with s.e.mean shown by vertical bars. Statistical significance was assessed by ANOVA followed by a Dunnett test. *$P<0.05$; NS, not significant.

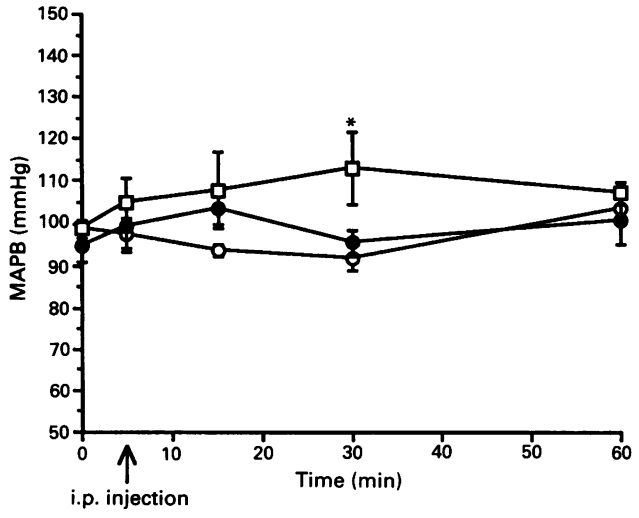

Figure 2 Mean arterial blood pressure of chloral anaesthetized rats, treated with N^G-nitro-L-arginine methyl ester (L-NAME) 1 mg kg^{-1}, i.p. (●), 3 mg kg^{-1}, i.p. (□) or vehicle-treated rats (○). Each point is the mean of 5 experiments with s.e.mean shown by vertical bars. Statistical significance was assessed by ANOVA followed by a Dunnett test. $*P<0.05$.

6 h, 24 h and 36 h on rats that were awake did not induce any modification of MABP.

Discussion The infarcted volume obtained in our control Sprague Dawley rats is consistent with the recent data of Mackay *et al.* (1991) obtained after MCA occlusion in the same strain. The present study represents the first demonstration that blockade of NO synthesis markedly reduces the cerebral infarct volume induced by a cauterisation of the MCA in rats. These results are in accordance with those of Nowicki *et al.* (1991), showing that in mice, a post treatment with N^G-nitro-L-arginine protects the cortex from ischaemic insult induced by irreversible focal ischaemia. The hypertension observed in anaesthetized rats after the first treatment with L-NAME (3 mg kg^{-1}) is a consequence of the inhibition of endothelial NO-synthase (Rees *et al.*, 1990). However, as Jacewicz *et al.* (1990) have shown in this model of focal ischaemia, the infarct size is not influenced by a moderate variation of blood pressure, it is unlikely that the minor hypertension induced by the treatment with L-NAME explains the neuroprotection. It can be hypothesized that the stimulation of the N-methyl-D-aspartate (NMDA) receptor induced by the ischaemic insult, could raise cytosolic calcium, due largely to influx though the receptor-operated ions channels, and that this calcium influx will activate NO-synthase and lead to an overproduction of NO (Garthwaite, 1991). NO is a free radical which reacts with the oxygen superoxide (O_2^-) to form peroxynitrite anions ($ONOO^-$) (Blough & Zafiriou, 1985). Peroxynitrite could diffuse for several μm before decomposing to form the powerful and cytotoxic oxidants: hydroxyl radical and nitrogen dioxide (Beckman, 1991). Therefore, inhibition of NO synthase might have reduced the ischaemic superoxide-mediated neuronal injury induced by MCA occlusion in the striatum and in the cortex of rats. However, as NMDA antagonists exert few if any protective effects on striatal infarcts induced by focal ischaemia (Park *et al.*, 1988), our results indicate that NO synthase inhibitors may constitute a more efficient treatment than NMDA antagonists, and suggest that the ischaemic NO production may be, at least in part, unrelated to NMDA receptor overstimulation. The above data demonstrate that inhibition of NO synthesis might represent a new pharmacological strategy for neuroprotection in cerebral ischaemia.

We are most grateful to Dr E.T. McKenzie for his help. A.B. is a fellow of the Institut Scientifique Roussel.

References

BECKMAN, J.S. (1991). The double edged role of nitric oxide in brain function and superoxide-mediated injury. *J. Dev. Physiol.*, **15**, 53–59.

BLOUGH, N.V. & ZAFIRIOU, O.C. (1985). Reaction of superoxide with nitric oxide to form peroxinitrite in alkaline aqueous solution. *Inorg. Chem.*, **24**, 3504–3505.

CHOI, D.W. (1990). Methods for antagonizing glutamate toxicity. *Cerebrovasc. Brain Metab. Rev.*, **2**, 105–134.

DAWSON, V.L., DAWSON, T.M., LONDON, E.D., BREDT, D.S. & SNYDER, S.H. (1991). Nitric oxide mediates glutamate neurotoxicity in primary cortical cultures. *Proc. Natl. Acad. Sci. U.S.A.*, **88**, 6368.

GARTHWAITE, J. (1991). Glutamate, nitric oxide and cell-cell signalling in the nervous system. *Trends Neurol. Sci.*, **14**, 60–67.

JACEWICZ, M., BRINT, S., TANABE, J. & PULSINELLI, W.A. (1990). Continuous nimodipine treatment attenuates cortical infarction in rats subjected to 24 hours of focal cerebral ischemia. *J. Cereb. Blood Flow Metab.*, **10**, 89–96.

MACKAY, K.B., KUSUMOTO, K. & MCCULLOCH, J. (1991). The neuroprotective effect of the kappa agonist CI-977 in a rat model of focal cerebral ischaemia. *Br. J. Pharmacol.*, **104**, 303P.

NOWICKI, J.P., DUVAL, D., POIGNET, H. & SCATTON, B. (1991). Nitric oxide mediates neuronal death after focal cerebral ischemia in the mouse. *Eur. J. Pharmacol.*, **204**, 339–340.

PARK, C.K., NEHLS, D.G., GRAHAM, D.I., TEASDALE, G.M. & MCCULLOCH, J. (1988). The glutamate antagonist MK-801 reduces focal ischaemic brain damage in rats. *Ann. Neurol.*, **24**, 543–551.

REES, D.D., PALMER, R.M.J., SCHULZ, R., HODSON, H.F. & MONCADA, S. (1990). Characterisation of three inhibitors of endothelial nitric oxide synthase *in vitro* and *in vivo*. *Br. J. Pharmacol.*, **101**, 746–752.

SNYDER, S.H. (1991). Nitric oxide as a neuronal messenger. *Trends Pharmacol. Sci.*, **12**, 125–127.

(Received April 9, 1992
Accepted April 29, 1992)

Br. J. Pharmacol. (1992), **106**, 768–773 © Macmillan Press Ltd, 1992

Characterization and localization of nitric oxide synthase in non-adrenergic non-cholinergic nerves from bovine retractor penis muscles

[1]*Hong Sheng, †Harald H.H.W. Schmidt, *Masaki Nakane, †Jane A. Mitchell, *Jennifer S. Pollock, *†Ulrich Föstermann & *†Ferid Murad

*Abbott Laboratories, Abbott Park, IL 60064, and †Department of Pharmacology, Northwestern University Medical School, Chicago, IL 60611, U.S.A.

1 Partially purified soluble nitric oxide (NO) synthase was isolated from the bovine retractor penis muscle (BRP), a tissue in which the inhibitory response to non-adrenergic non-cholinergic nerve (NANC) stimulation appears to be mediated by NO or NO-like material.

2 NO synthase from BRP used L-arginine as a substrate, required NADPH, tetrahydrobiopterin, and FAD as co-factors and was Ca^{2+}/calmodulin-dependent. The activity of NO synthase was inhibited by N^G-methyl-L-arginine and N^G-nitro-L-arginine, and haemoglobin blocked the effect of NO formed by the enzyme.

3 On reducing SDS polyacrylamide gel electrophoresis the apparent molecular mass of NO synthase from BRP was 160 ± 2 kDa, which is similar to that of the cerebellar NO synthase. Protein immunoblot and immunoprecipitation showed that NO synthase from BRP cross-reacted with the selective antiserum to neuronal NO synthase from rat cerebellum.

4 Immunohistochemistry using the same antiserum demonstrated that NO synthase in BRP was located exclusively within nerve fibres. Thus, autonomic nerves synthesizing the NANC neurotransmitter seem to contain an isoform of NO synthase which is similar to that from rat cerebellum.

Keywords: Calcium/calmodulin-dependent; calmodulin antagonist; cyclic GMP; L-arginine; nitric oxide; nitric oxide synthase; N^G-methly-L-arginine; N^G-nitro-L-arginine; non-adrenergic non-cholinergic nerve; retractor penis

Introduction

Field stimulation of autonomic nerves in many organs produces inhibitory responses which are not regulated by the release of adrenergic or cholinergic neurotransmitters. In many tissues such as anococcygeus and retractor penis muscle, the relaxations caused by non-adrenergic non-cholinergic (NANC) nerve stimulation appear to be mediated by nitric acid or nitric oxide-like material (NO) (Gillespie *et al.*, 1989; Gibson *et al.*, 1990; Gillespie & Sheng, 1990; Sheng, 1991; Liu *et al.*, 1991). NO has also been shown to be released from NANC innervated canine ileocolonic junction upon field stimulation (Bult *et al.*, 1990). However, it is unclear whether the NANC neurotransmitter itself is NO or whether an unidentified neurotransmitter causes NO release from adjacent cells.

Various cell types have been found to synthesize NO. The enzyme responsible for NO synthesis (NO synthase) has been characterized and purified from cerebellum (Bredt & Snyder, 1990; Mayer *et al.*, 1990; Schmidt *et al.*, 1991), endothelial cells (Förstermann *et al.*, 1991; Pollock *et al.*, 1991), neutrophils (Yui *et al.*, 1991b), and cytotoxic macrophages (Yui *et al.*, 1991a). In all cases No synthase requires NADPH as a co-factor and utilizes L-arginine as a substrate. The cerebellum contains a soluble, constitutive isoform of NO synthase (Bredt & Snyder, 1990; Mayer *et al.*, 1990; Schmidt *et al.*, 1991) whereas most of the constitutive NO synthase in endothelial cells is particulate (Förstermann *et al.*, 1991; Pollock *et al.*, 1991). Both isoforms are regulated by Ca^{2+} and calmodulin. In contrast, the NO synthase induced in macrophages by endotoxin and/or cytokines is Ca^{2+}/calmodulin-independent (Yui *et al.*, 1991a).

In bovine retractor penis muscle (BRP) the inhibitory response to nerve stimulation is mediated by the activation of soluble guanylyl cyclase and formation of guanosine 3′:5′-cyclic monophosphate (cyclic GMP) (Bowman & Drummond, 1985). Nitric oxide mimics the response to NANC nerve stimulation and both effects can be inhibited by oxyhaemoglobin (Bowman *et al.*, 1982; Gillespie & Sheng, 1988; 1989). Further experiments showed that the endogenous formation of NO from L-arginine may be involved in NANC neurotransmission (Liu *et al.*, 1991; Sheng, 1991). Recently we showed that a Ca^{2+}-dependent NO synthase was present in rat anococcygeus muscle (Mitchell *et al.*, 1991), a tissue which has an anatomical and pharmacological profile similar to BRP (Gillespie & Sheng, 1989). However, since smooth muscle preparations may contain more than one isoform of NO synthase, it is important to classify the isozyme responsible for the formation of NANC neurotransmitter. Here we show that NO synthase isolated from BRP is neuronal in origin and synthesizes the material which mediates NANC neurotransmission. Some of these observations have been reported in abstract from (Sheng *et al.*, 1991b).

Methods

Crude soluble fraction

BRP muscles from the local slaughter house were frozen in liquid nitrogen immediately after tissue dissection. The following experiments were performed at 4°C except when indicated otherwise. Muscles were homogenized (1:5) in buffer 1 (50 mM Tris/HCl, pH 7.4 containing 0.1 mM EDTA, 0.1 mM EGTA, 12 mM 2-mercaptoethanol, 1 mM phenylmethylsulphonyl fluoride, 3 μM leupeptin, and 1 μM pepstatin A) with a commercial blender. The homogenate was filtered through muslin, centrifuged (100,000 *g* for 1 h) and the supernatant (crude soluble fraction) collected.

[1] Author for correspondence at present address: Dept. of Pharmacology, UCLA School of Medicine, The Center for Health Science, Los Angeles, CA 90024, U.S.A..

DEAE Sephacel chromatography

The crude soluble fraction (500 ml) was loaded into a DEAE Sephacel anion exchange column (1 ml) by recirculating it 3–4 times through the column. The column was then washed with 10 column volumes of buffer 2 (buffer 1 containing 10% glycerol) and partially purified NO synthase was eluted with 3 column volumes of buffer 2 containing 0.3 M NaCl.

2', 5'-ADP-Sepharose chromatography

The crude soluble fraction (500–1000 ml) was loaded onto a 2', 5'-ADP-Sepharose column (0.5 ml) by recirculating it 3–5 times through the column. The column was washed with 10 column volumes of buffer 2, then 3 column volumes of buffer 2 containing 0.5 M NaCl, followed by 10 column volumes of buffer 2. Partially purified soluble NO synthase was eluted with 5 column volumes of buffer 2 containing NADPH (10 mM).

Assay of activation of guanylyl cyclase in RFL-6 cells

The increase of cyclic GMP in rat foetal lung fibroblasts (RFL-6 cells) was used as a measure of NO activity as described by Ishii *et al.* (1991). Briefly, RFL-6 cells cultured in 12-well plates (5×10^5 cells per well) were washed twice with Locke solution (composition mM: NaCl 154, KCl 5.6, $CaCl_2$ 2, $MgCl_2$ 1, $NaHCO_3$ 3.6, glucose 5.6 and HEPES 10; pH 7.4) containing 3-isobutyl-1-methylxanthine (IBMX, 0.3 mM). Cells were then equilibrated at 37°C for 20 min in the same solution. Superoxide dismutase (SOD, 20 units ml^{-1}) was added 3 min before addition of L-arginine (100 μM), NADPH (100 μM), calmodulin (30 units ml^{-1}), tetrahydrobiopterin (3 μM), and FAD (1 μM). The reaction was started by adding partially purified NO synthase from BRP. In some experiments, some of the co-factors were omitted. The incubation was continued for another 3 min. The reaction was stopped by aspirating the medium, adding 0.5 ml of ice-cold sodium acetate (50 mM, pH 4.0) to the RFL-6 cells, and rapidly freezing the samples with liquid nitrogen. The content of cyclic GMP in each sample was determined by radioimmunoassay. Experiments with defined Ca^{2+} concentrations were performed in Ca^{2+}-free Locke solution (pH 7.4) containing IBMX (0.3 mM), SOD (20 units ml^{-1}), and EGTA (1 mM). Various amounts of $CaCl_2$ were added and free Ca^{2+} concentrations were calculated (Segal, 1986). In some experiments the calmodulin antagonists, calmidazolium or trifluoperazine were added to the RFL-6 cells in the absence of exogenous calmodulin. In another series of experiments, the L-arginine analogues N^G-methyl-L-arginine (L-NMA) or N^G-nitro-L-arginine (L-NNA) were added to the cells in the presence of 10 μM L-arginine.

Western blot analysis of NO synthase from BRP

Polyclonal antisera against NO synthase from rat cerebellum were raised in three rabbits (Schmidt *et al.*, 1992). NO synthase from BRP, rat cerebellum and endothelial cells was partially purified by 2', 5'-ADP affinity chromatography and separated on a 7.5% SDS polyacrylamide gel, then transferred to a nitrocellulose membrane. All subsequent procedures were performed at room temperature. The transferring buffer contained 40 mM Tris/HCl pH 7.55, 0.3 M NaCl and 0.3% Tween 20. The membrane was blocked with 7% fat-free dried milk and then incubated with antiserum at a 1:1000 dilution for 1 h. The NO synthase band were identified with a horseradish peroxidase-conjugated secondary antibody against rabbit IgG (1:5000) and chemiluminescence (Amersham).

Immunoprecipitation of NO synthase from BRP

Polyclonal IgG against NO synthase from rat cerebellum was purified by protein A Superose chromatography (Pharmacia). Partially purified soluble NO synthase from BRP (by 2', 5'-ADP chromatography, 18 μg per aliquot) was incubated overnight with different concentrations of purified antibody. The control experiment was performed by using normal rabbit IgG. After adding protein A Sepharose beads (18 μg per aliquot) to each aliquot, samples were centrifuged (20,000 *g*) for 1 h. The supernatant from each aliquot was assayed for NO synthase activity by activation of guanylyl cyclase in RFL-6 cells.

Histochemical determination of NO synthase in BRP

Frozen BRP was mounted onto microtome chucks. Oblique or longitudinal sections (8 μm thick) were cut and thaw-mounted onto microscope slides, fixed by immersion in acetone for 5 min and then air-dried. For NO synthase staining, the sections were incubated with polyclonal antiserum to rat cerebellar NO synthase (1:100) or the pre-immune serum (1:100) diluted in phosphate buffered saline (PBS) containing 1% bovine serum albumin (BSA) at 37°C for 30 min and then, in peroxidase conjugate (1:50, in 1% BSA/PBS) for 30 min. The peroxidase label was developed by using 3', 3'-diaminobenzidine dissolved in imidazole buffer for 6–10 min, washed with Tris buffer (50 mM, pH 7.6), dehydrated and mounted. It has been reported that NO synthase from rat cerebellum has NADPH diaphorase activity (Hope *et al.*, 1991). For labelling NADPH diaphorase, the tissue sections were incubated for 20–30 min at 37°C with nitro blue tetrazolium (0.5 mM) and NADPH (1 mM) in Tris (50 mM, pH 7.6) containing Triton X-100 (2%), counterstained with eosin, and then dehydrated by use of a graded series of ethyl alcohol concentrations.

Protein determination

Protein concentrations were determined as described by Bradford (1976) with bovine serum albumin used as the standard.

Drugs

Compound R24571 (calmidazolium), calmodulin, 3', 3'-diaminobenzidine, ethylenediaminetetraacetic acid (EDTA), ethylene glycol-*bis* (β-aminoethylether)-N,N,N',N'-tetraacetic acid (EGTA), flavin adenine dinucleotide (FAD), haemoglobin, 3-isobutyl-1-methylxanthine (IBMX), leupeptin, L-arginine hydrochloride, 2-mercaptoethanol, nitro blue tetrazolium, N^G-nitro-L-arginine (L-NNA), pepstatin A, phenylmethylsulphonyl fluoride, superoxide dismutase, trifluoperazine dihydrochloride were purchased from Sigma (U.S.A.); NADPH tetrasodium salt was obtained from Boehringer Mannheim (Germany); Tetrahydrobiopterin from Schirks (Switzerland); N^G-methyl-L-arginine (L-NMA) was synthesized as described (Patthy *et al.*, 1977).

Results

Soluble NO synthase isolated from BRP produced NO as deduced by stimulation of cyclic GMP accumulation and conversion of L-arginine to L-citrulline (data not shown). The results mentioned below were obtained by measuring the cyclic GMP content in RFL-6 cells as this is a sensitive bioassay technique for the detection of NO (Ishii *et al.*, 1991). The specific activities of partially purified NO synthase from BRP (detected in 5×10^5 RFL-6 cells) were 28.08 ± 8.69 nmol cyclic GMP mg^{-1} protein by 2',5'-ADP affinity chromatography ($n = 9$) and 11.82 ± 0.32 pmol cyclic GMP mg^{-1} protein by DEAE anion exchange chromatography ($n = 3$). Figure 1a shows that NO synthase from BRP used L-arginine as a substrate. Superoxide dismutase (20 units ml^{-1}) was required for the detection of NO synthase activity, while oxyhaemoglobin (10^{-5} M) completely inhibited

the effect of NO formed by NO synthase from BRP (Figure 1a). The L-arginine analogues, L-NMA and L-NNA showed a concentration-dependent inhibition of the enzyme activity (Figure 1b). The acitivities of NO synthase partially purified by DEAE anion exchange chromatography were reduced in the absence of exogenous NADPH (36.62 ± 6.13% of control activity, $n = 3$) or tetrahydrobiopterin (19.9 ± 3.9% of control activity, $n = 3$). The material eluted from 2',5'-ADP Sepharose showed very little dependence on tetrahydrobiopterin (87.97 ± 12.89% of control activity, $n = 3$). We have found that NO synthase from other tissues partially purified by 2', 5'-ADP chromatography still contained tetrahydrobiopterin (Schmidt *et al.*, unpublished observations). The enzyme activity was partially reduced in the absence of FAD (46.44 ± 3.13% of control activity, $n = 3$) or calmodulin (64.31 ± 1.87% of control activity, $n = 3$). NO synthase from BRP was found to be Ca^{2+}-dependent. There was no detectable enzyme activity at a Ca^{2+} concentration ≤ 1 nM, and enzyme activity reached a maximum at 500 nM Ca^{2+} (Figure 1c). Partially purified NO synthase showed only a partial dependence on exogenous calmodulin, probably because the sample still contained significant amounts of endogenous calmodulin as we reported previously for partially purified preparations from endothelial cells (Förstermann *et al.*, 1991). To test whether NO synthase from BRP is calmodulin-dependent, we also investigated the effects of two calmodulin antagonists on the enzyme activity. Figure 1d shows that both calmidazolium (0.1 or 0.3 μM) and trifluoperazine (1 or 3 μM) markedly inhibited the activity of NO synthase with calmidazolium being approximately 10 fold more potent than trifluoperazine.

Protein immunoblot analysis showed that soluble NO synthase from BRP partially purified by 2', 5'-ADP affinity chromatography cross-reacted with a polyclonal antiserum generated against NO synthase from rat cerebellum (Figure 2a). The denatured molecular mass of NO synthase from BRP was 160 ± 2 kDa. The antiserum was selective in that it did not cross-react with soluble (data not shown) and particulate NO synthase from endothelial cells (Figure 2a). Identical results were obtained by using similar antisera raised in two other rabbits (data not shown). The partially purified NO synthase from BRP (by 2', 5'-ADP chromatography) contained many other proteins, as SDS polyacrylamide gel electrophoresis revealed more than 20 protein bands when stained with Coomassie blue (data not shown). To ensure the single band shown in Figure 2a was NO synthase, we performed immunoprecipitation experiments. NO synthase from BRP bound to purified IgG to rat cerebellar NO synthase and was precipitated by adding protein A Sepharose beads. Figure 2b shows that the activity of NO synthase was reduced by higher concentration of purified IgG to cerebellar NO synthase but not by normal rabbit IgG.

Immunohistochemistry demonstrated that antiserum raised against rat cerebellar NO synthase stained only nerve fibres in BRP from both longitudinal (Figure 3a) and oblique sections (Figure 3b). Similar results were obtained with nitro blue tetrazolium used to demonstrate the NADPH diaphorase activity (Figure 3c). In contrast, Figure 3d shows no staining in a longitudinal section treated with rabbit preimmune serum.

Discussion

It has been known for several years that some smooth muscle preparations contain an inhibitory neurotransmitter, the response of which cannot be blocked by any known receptor antagonists, but can be inhibited by oxyhaemoglobin (Bowman *et al.*, 1982; Gillespie & Sheng, 1989). Recently, as L-arginine analogues such as L-NMA and L-NNA became established as inhibitors to the synthetic pathway of endothelium-derived relaxing factor, these compounds were found to inhibit the relaxation caused by stimulation of NANC

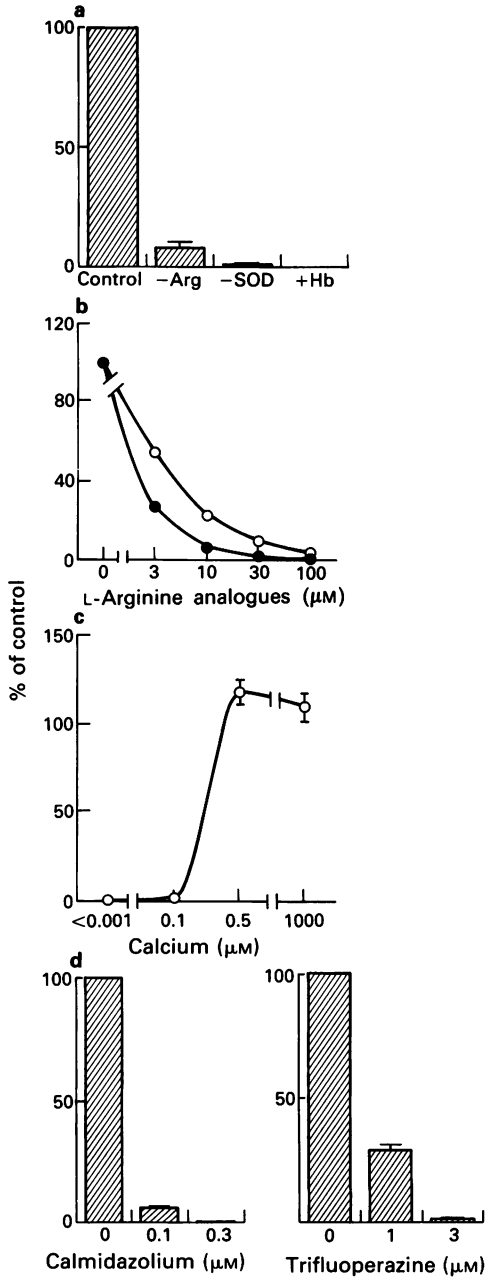

Figure 1 Characterization of NO synthase from bovine retractor penis muscle. Activity of NO synthase partially purified by 2', 5'-ADP affinity chromatography was detected by the cyclic GMP accumulation in 5×10^5 RFL-6 cells in the presence of L-arginine (100 μM), superoxide dismutase (20 units ml^{-1}), NADPH (100 μM), tetrahydrobiopterin (3 μM), and calmodulin (CaM, 30 units ml^{-1}) (control). (a) The activity of NO synthase was reduced in the absence of L-arginine (– Arg) or superoxide dismutase (– SOD) and in the presence of oxyhaemoglobin (+ Hb). Control activity was 18.66 ± 1.20 nmol cyclic GMP mg^{-1} protein. (b) NO synthase activity was inhibited in a concentration-dependent fashion by N^G-methyl-L-arginine (○) or N^G-nitro-L-arginine (●) in the presence of 10 μM L-arginine. Control activity was 45.43 ± 3.65 nmol cyclic GMP mg^{-1} protein. (c) The activity of NO synthase was tested at different concentrations of Ca^{2+} buffered with EGTA (1 mM). Control activity (20.25 ± 1.68 nmol cyclic GMP mg^{-1} protein) was measured in normal Locke buffer containing 2 mM Ca^{2+}. (d) Calmidazolium (0.1 or 0.3 μM) and trifluoperazine (1 or 3 μM) inhibited the activity of NO synthase. Control activity was 12 ± 0.77 nmol cyclic GMP mg^{-1} protein in the absence of exogenous calmodulin. Columns or points represent means with s.e. shown by vertical bars except where the error lies within the symbol, $n = 3$.

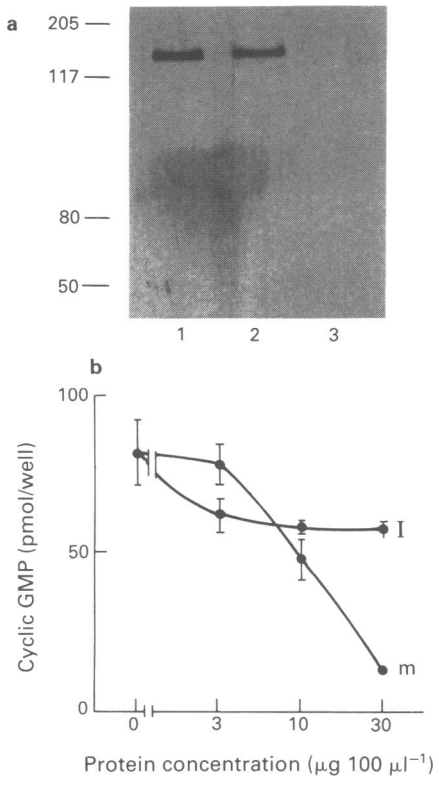

Figure 2 Western blot and immunoprecipitation of NO synthase from bovine retractor penis (BRP) muscle. (a) Soluble NO synthase from rat cerebellum (lane 1, 2 μg) and from BRP (lane 2, 18 μg) but not solubilized particulate NO synthase from bovine aortic endothelial cells (lane 3, 15 μg) cross-reacted with the antiserum against NO synthase from rat cerebellum. All NO synthase preparations were partially purified by 2′, 5′-ADP affinity chromatography. Positions of molecular mass (Mr) markers are shown (Mr × 10^3). (b) NO synthase from BRP bound to purified rabbit IgG raised against NO synthase from rat cerebellum (m) was precipitated by protein A Sepharose beads. The enzyme which did not bind to normal rabbit IgG (I) was not precipitated. The activity of NO synthase in the supernatant fraction was determined by cyclic GMP accumulation in 5×10^5 RFL-6 cells. Points represent means with s.e. shown by vertical bars, $n = 3$.

nerves in these tissues (Gillespie *et al.*, 1989; Gibson *et al.*, 1990; Liu *et al.*, 1991). In a bioassay cascade, stimulation of NANC-innervated canine ileocolonic junction leads to relaxation of the subjacent detector tissues (Bult *et al.*, 1990). It is still unclear, however, whether NO is released directly from nerve endings or from other cells within the donor tissue. The results of the present study clearly demonstrate that NO synthase in the NANC-innervated BRP is located exclusively in nerves. Therefore, NO, which causes relaxation following electrical stimulation of BRP and other NANC-innervated tissues, is likely to be synthesized within nerves and act as a NANC neurotransmitter.

The co-factor requirement of the BRP enzyme and its regulation by Ca^{2+} and calmodulin was very similar to the constitutive NO synthase from rat cerebellum and from endothelial cells (Bredt & Snyder, 1990; Schmidt *et al.*, 1991; Pollock *et al.*, 1991). The antiserum raised against NO synthase from rat cerebellum was selective in that it did not cross-react with NO synthase from endothelial cells either from immunoblot or from immunohistochemical staining (Figure 2a; Schmidt *et al.*, unpublished observations). Therefore, the soluble NO synthase isolated from BRP is clearly not from vascular endothelial cells in this preparation. In addition, staining for NADPH diaphorase activity showed a distribution similar to NO synthase activity in BRP. This co-localization has previously been shown for cerebellar NO synthase and NADPH diaphorase (Hope *et al.*, 1991). According to protein immunoblot analysis, the denatured molecular mass of NO synthase in BRP was 160 ± 2 kDa, which is very similar to that of the enzyme isolated from cerebellum (Bredt & Snyder, 1990; Mayer *et al.*, 1990; Schmidt *et al.*, 1991). Also, on FPLC Superose 6 gel permeation chromatography (Pharmacia) the NO synthase from BRP eluted in the same fraction as NO synthase isolated from rat cerebellum (data not shown; Schmidt *et al.*, 1991). Thus, BRP contains an isoform of NO synthase which is similar to that from rat cerebellum. Since immunohistochemical staining of BRP with the antiserum to rat cerebellar NO synthase was only detected in nerve fibres, the soluble NO synthase in BRP is neuronal in origin and is responsible for NANC neurotransmission.

Some NO synthase activity was also detected in the particulate fraction of BRP showing similar characteristics to the soluble enzyme (data not shown). However, the small amount of particulate material we obtained was not enough for a detailed study of particulate NO synthase from BRP. Whether the particulate NO synthase from BRP is derived from microvascular endothelial cells (which contain predominantly particulate enzyme) or from nerves warrants further investigation.

It has been reported that L-NNA but not L-NMA inhibited the inhibitory response to NANC nerve stimulation in BRP (Liu *et al.*, 1991). In our experiment using RFL-6 cells to detect NO-like activity, both L-NMA and L-NNA inhibited the activity of NO synthase in either the soluble or the particulate fraction. The difference between our results and the previous report (Liu *et al.*, 1991) may be due to differences in uptake and/or metabolism of NMA in intact vesus broken tissue (Hecker *et al.*, 1990).

The amount of NO synthesized within NANC nerves during electrical stimulation was enough to increase cyclic GMP content in BRP (Bowman & Drummond, 1985). We have previously reported that the increase of cyclic GMP in the bovine trachea is due to the generation of NO following addition of carbachol (Sheng *et al.*, 1991a). However, it was not clear whether NO was generated within the smooth muscle or other cells. Possibly in this latter tissue carbachol may stimulate the release of NO from NANC nerves within the trachea, rather than from the smooth muscle cells.

Unlike the induced NO synthase from macrophages or smooth muscle cells (Busse & Mülsch, 1990; Rees *et al.*, 1990; Yui *et al.*, 1991a) the enzyme isolated from BRP is Ca^{2+}/calmodulin-dependent. Therefore, the synthesis of NO in NANC nerves is likely to be regulated by the intracellular Ca^{2+} concentration. Depolarization of NANC nerves can lead to Ca^{2+} influx which, in turn, can activate NO synthase. The synthesized NO will be released from the NANC nerves and directly activates guanylyl cyclase in adjacent smooth muscle cells. Thus, unlike classical neurotransmitters, the NANC neurotransmitter does not act on a membrane receptor, but the haeme-moiety of soluble guanylyl cylcase functions as its 'receptor'. As NANC nerves are present in many tissues in the gastrointestinal, urino-genital, and vascular systems (Toda *et al.*, 1990a,b; Boeckxstaens *et al.*, 1990; 1991; Tøttrup *et al.*, 1991; Dokita *et al.*, 1991; Kim *et al.*, 1991; Liu *et al.*, 1991). NO, acting as a neurotransmitter, may play an important physiological role in the regulation of smooth muscle tone in these organs.

The authors wish to acknowledge Dr M.F. Miller and Mr G.D. Gagne for their invaluable help in the preparation of the histochemical specimens and Ms R. Huang, J. Azzarello and T. Gray for excellent technical assistance.

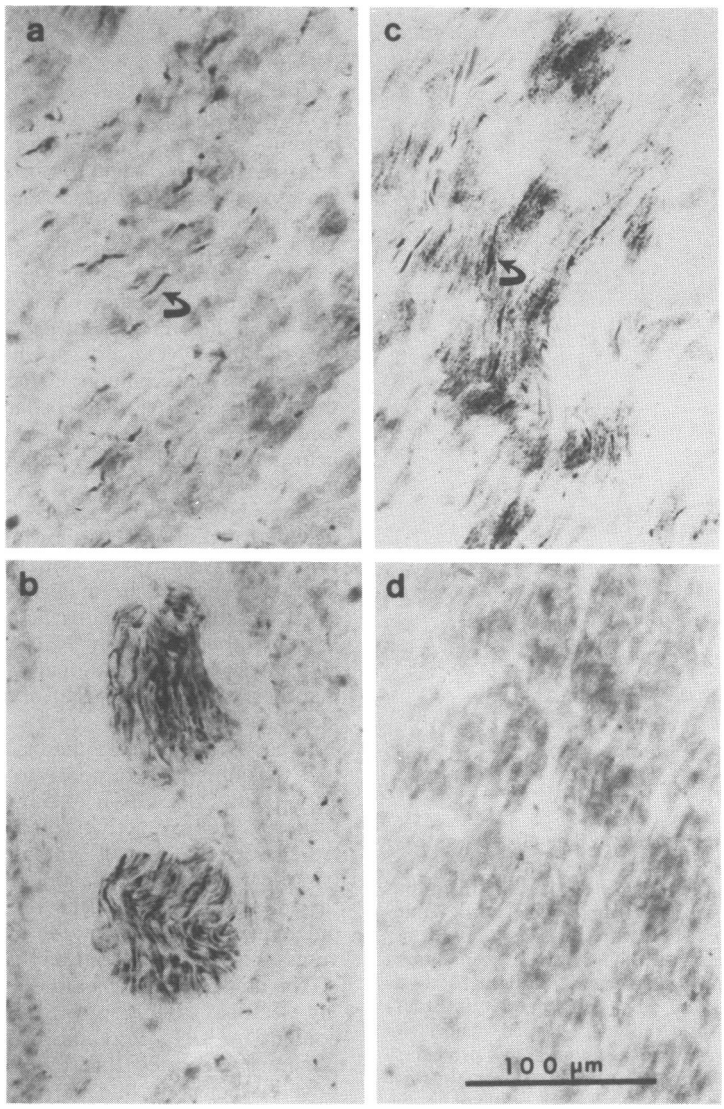

Figure 3 Localization of NO synthase in bovine retractor penis muscle (BRP). NO synthase stained with antiserum against NO synthase from rat cerebellum in (a), an oblique section and (b), longitudinal section was located in BRP in the nerve fibres traversing the smooth muscle. NADPH diaphorase, the localization of which is similar to NO synthase in brain, was also localized to nerves in the longitudinal section (c). The control (d) shows no staining in muscle longitudinal section treated with pre-immune rabbit serum. The arrows indicate the nerve fibres in BRP.

References

BOECKXSTAENS, G.E., PELCKMANS, P.A., BORGERS, J.J., BULT, H., DE MAN, J.G., OOSTERBOSCH, L., HERMAN, A.G. & VAN MAERCKE, Y.M. (1991). Release of nitric oxide upon stimulation of nonadrenergic noncholinergic nerves in the rat gastric fundus. *J. Pharmacol. Exp. Ther.*, **256**, 441–447.

BOECKXSTAENS, G.E., PELCKMANS, P.A., BULT, H., DE MAN, J.G., HERMAN, A.G. & VAN MAERCKE, Y.M. (1990). Non-adrenergic non-cholinergic relaxation mediated by nitric oxide in the canine ileocolonic junction. *Eur. J. Pharmacol.*, **190**, 239–246.

BOWMAN, A. & DRUMMOND, A.H. (1985). Cyclic GMP mediates neurogenic relaxations in the bovine retractor penis muscles. *Br. J. Pharmacol.*, **81**, 665–674.

BOWMAN, A., GILLESPIE, J.S. & POLLOCK, D. (1982). Oxyhaemoglobin blocks non-adrenergic non-cholinergic inhibition in the bovine retractor penis muscle. *Eur. J. Pharmacol.*, **85**, 221–224.

BRADFORD, M.M. (1976). A rapid and sensitive method for the quantitation of microgram quantities of protein utilizating the principle of protein dye binding. *Anal. Biochem.*, **72**, 248–254.

BREDT, D.S. & SNYDER, S.H. (1990). Isolation of nitric oxide synthase, a calmodulin-requiring enzyme. *Proc. Natl. Acad. Sci. U.S.A.*, **87**, 682–685.

BULT, H., BOECKXSTAENS, G.E., PELCKMANS, P.A., JORDEANS, F.H., VAN MAERCKE, Y.M. & HERMAN, A.G. (1990). Nitric oxide as an inhibitory non-adrenergic non-cholinergic neurotransmitter. *Nature*, **345**, 346–347.

BUSSE, R. & MÜLSCH, A. (1990). Induction of nitric oxide synthase by cytokines in vascular smooth muscle cells. *FEBS Lett.*, **275**, 87–90.

DOKITA, S., MORGAN, W.R., WHEELER, M.A., YOSHIDA, M., LATIFPOUR, J. & WEISS, R.M. (1991). N^G-nitro-L-arginine inhibits non-adrenergic, non-cholinergic relaxation in rabbit urethral smooth muscle. *Life Sci.*, **48**, 2429–2436.

FÖSTERMANN, U., POLLOCK, J.S., SCHMIDT, H.H.H.W., HELLER, M. & MURAD, F. (1991). Calmodulin-dependent endothelium-derived relaxing factor/nitric oxide synthase activity is present in the particulate and cytosolic fractions of bovine aortic endothelial cells. *Proc. Natl. Acad. Sci. U.S.A.*, **88**, 1788–1792.

GIBSON, A., MIRZADEH, S., HOBBS, A.J. & MOORE, P.K. (1990). L-N^G-monomethyl arginine and L-N^G-nitro arginine inhibit non-adrenergic, non-cholinergic relaxation of the mouse anococcygeus muscle. *Br. J. Pharmacol.*, **99**, 602–606.

GILLESPIE, J.S., LIU, X. & MARTIN, W. (1989). The effects of L-arginine and N^G-monomethyl L-arginine on the response of the rat anococcygeus muscle to NANC nerve stimulation. *Br. J. Pharmacol.*, **98,** 1080–1082.

GILLESPIE, J.S. & SHENG, H. (1988). Influence of haemoglobin and erythrocytes on the effets of EDRF, a smooth muscle inhibitory factor, and nitric oxide on vascular and non-vascular smooth muscle. *Br. J. Pharmacol.*, **95,** 1151–1156.

GILLESPIE, J.S. & SHENG, H. (1989). A comparison of haemoglobin and erythrocytes as inhibitors of smooth muscle relaxation by the NANC transmitter in the BRP and rat anococcygeus and by EDRF in the rabbit aortic strip. *Br. J. Pharmacol.*, **98,** 445–450.

GILLESPIE, J.S. & SHENG, H. (1990). The effects of pyrogallol and hydroquinone on the response to NANC nerve stimulation in the rat anococcygeus and the bovine retractor penis muscles. *Br. J. Pharmacol.*, **99,** 194–196.

HECKER, M., MITCHELL, J.A., HARRIS, H.J., KATSURA, M., THIEMERMANN, C. & VANE, J. (1990). Endothelial cells metabolize N^G-monomethyl-L-arginine to L-citrulline and subsequently to L-arginine. *Biochem. Biophys. Res. Commun.*, **167,** 1037–1043.

HOPE, B.T., MICHAEL, G.J., KNIGGE, K.M. & VINCENT, S.R. (1991). Neuronal NADPH diaphorase is a nitric oxide synthase. *Proc. Natl. Acad. Sci. U.S.A.*, **88,** 2811–2814.

ISHII, K., SHENG, H., WARNER, T.D., FÖRSTERMANN, U. & MURAD, F. (1991). A simple and sensitive bioassay method for detection of EDRF with RFL-6 rat lung fibroblasts. *Am. J. Physiol.*, **261,** H598–603.

KIM, N., AZADZOI, K.M., GOLDSTEIN, I. & DE TEJADA, I.S. (1991). A nitric oxide-like factor mediates nonadrenergic-noncholinergic neurogenic relaxation of penile corpus carvernosum smooth muscle. *J. Clin. Invest.*, **88,** 112–118.

LIU, X., GILLESPIE, J.S., GIBSON, I.F. & MARTIN, W. (1991). Effects of N^G-substituted analogues of L-arginine on NANC relaxation of the anococcygeus and retractor penis muscles and the bovine penile artery. *Br. J. Pharmacol.*, **104,** 53–58.

MAYER, B., JOHN, M. & BÖHME, E. (1990). Purification of a Ca^{2+}/calmodulin-dependent nitric oxide synthase from porcine cerebellum. *FEBS Lett.*, **277,** 215–219.

MITCHELL, J.A., SHENG, H., FÖRSTERMANN, U. & MURAD, F. (1991). Characterization of nitric oxide synthase in non-adrenergic non-cholinergic nerve containing tissue from the rat anococcygeus muscle. *Br J. Pharmacol.*, **104,** 289–291.

PATTHY, A., BAJUSZ, S. & PATTHY, L. (1977). Preparation and characterization of N^G-mono, di- and trimethylated arginines. *Acta Biochem. Biophys. Sci. Hung.*, **12,** 191–196.

POLLOCK, J.S., FÖRSTERMANN, U., MITCHELL, J.A., WARNER, T.D., SCHMIDT, H.H.H.W. & MURAD, F. (1991). Purification and characterization of particulate nitric oxide synthase from cultured and native bovine aortic endothelial cells. *Proc. Natl. Acad. Sci. U.S.A.*, **88,** 10480–10484.

REES, D.D., CELLEK, S., PALMER, R.M.J. & MONCADA, S. (1990). Dexamethasone prevents the induction by endotoxin of a nitric oxide synthase and associated effects on vascular tone: an insight into endotoxin shock. *Biochem. Biophys. Res. Commun.*, **173,** 541–547.

SCHMIDT, H.H.H.W., POLLOCK, J.S., NAKANE, M., GORSKY, L.D., FÖRSTERMANN, U. & MURAD, F. (1991). Purification of a soluble isoform of guanylyl cylcase-activating factor synthase. *Proc. Natl. Acad. Sci. U.S.A.*, **88,** 365–369.

SCHMIDT, H.H.H.W., WARNER, T.D., ISHII, K., SHENG, H. & MURAD, F. (1992). Insulin secretion in pancreatic b-cells: signal transduction through L-arginine-derived nitrogen oxides. *Science*, (in press).

SEGAL, J. (1986). Cation chelators and their utilization in the preparation of low concentrations of calcium. *Biotechnol. Appl. Biochem.*, **8,** 423–429.

SHENG, H. (1991). Effect of LY 83583 on the NANC nerve stimulation in rat anococcygeus and bovine retractor penis muscles. *Br. J. Pharmacol.*, **104,** 137P.

SHENG, H., ISHII, K. & MURAD, F. (1991a). Generation of an endothelium-derived relaxing factor-like substance in bovine tracheal smooth muscle. *Am. J. Physiol.*, **260,** L489–493.

SHENG, H., MITCHELL, J.A., NAKANE, M., WARNER, T.D., POLLOCK, J.S., FÖRSTERMANN, U. & MURAD, F. (1991b). Characterisation of NO-synthase from NANC nerve-containing tissues: rat anococcygeus and bovine retractor penis muscles. *Br. J. Pharmacol.*, **104,** 7P.

TODA, N., BABA, H. & OKAMURA, T. (1990a). Role of nitric oxide in non-adrenergic, non-cholinergic nerve-mediated relaxation in dog duodenal longitudinal muscle strips. *Jpn. J. Pharmacol.*, **53,** 281–284.

TODA, N., MINAMI, Y. & OKAMURA, T. (1990b). Inhibitory effects of L-N^G-nitro-arginine on the synthesis of EDRF and the cerebroarterial response to vasodilator nerve stimulation. *Life Sci.*, **47,** 345–351.

TØTTRUP, A., SVANE, D. & FORMAN, A. (1991). Nitric oxide mediating NANC inhibition in opossum lower esophageal sphincter. *Am. J. Physiol.*, **260,** G385–389.

YUI, Y., HATTORI, R., KOSUGA, K., EIZAWA, H., HIKI, K. & KAWAI, C. (1991a). Purification of nitric oxide synthase from rat macrophages. *J. Biol. Chem.*, **266,** 12544–12547.

YUI, Y., HATTORI, R., KOSUGA, K., EIZAWA, H., HIKI, K., OHKAWA, S., OHNISH, K., TERAO, S. & KAWAI, C. (1991b). Calmodulin-independent nitric oxide synthase from rat polymorphonuclear neutrophils. *J. Biol. Chem.*, **266,** 3369–3371.

(Received January 22, 1992
Revised February 28, 1992
Accepted March 10, 1992)

Br. J. Pharmacol. (1992), **106**, 774–782 © Macmillan Press Ltd, 1992

Adenosine receptors on human airway epithelia and their relationship to chloride secretion

[1]E.R. Lazarowski, S.J. Mason, L. Clarke, *T.K. Harden & R.C. Boucher

Departments of Medicine and *Pharmacology, University of North Carolina, Chapel Hill, North Carolina 27599, U.S.A.

1 We have characterized an adenosine receptor subtype present in human airway epithelial cells by measuring the changes in the intracellular levels of adenosine 3':5'-cyclic monophosphate (cyclic AMP) and the rate of transepithelial Cl^- secretion.

2 Primary cultures of human nasal epithelium obtained from excised surgical airway epithelial tissues and the cell lines BEAS39 and CF/T43 derived from human airway epithelium were grown on plastic dishes and labelled with [^{3}H]-adenine for measurement of intracellular cyclic AMP accumulation. Primary cultures were loaded with the calcium indicator fura-2 to measure $[Ca^{2+}]_i$ and studied as polarized, ion transporting epithelia on collagen matrix supports for measurement of Cl^- secretion.

3 Adenosine analogues stimulated cyclic AMP accumulation with a rank order of potency characteristic of an A_2-receptor: 5-N-ethyl-carboxamidoadenosine (NECA) > adenosine > **R**-phenylisopropyladenosine (**R**-PIA), 6-N-cyclopentyladenosine (CPA) > S-PIA. NECA increased cyclic AMP accumulation in normal and cystic fibrosis (CF) primary cells as well as in the CF/T43 and BEAS39 cell lines with $K_{0.5}$ values ranging from 0.3 to 3 μM. Preincubation with NECA resulted in the homologous desensitization of airway epithelial cells. The effect of NECA was specifically inhibited by the adenosine receptor antagonist, aminophylline, in a competitive manner.

4 The A_1-adenosine receptor agonists CPA and **R**-PIA did not inhibit isoprenaline-stimulated cyclic AMP accumulation in CF/T43 cells, and potentiating effects of the adenosine analogues were observed on forskolin-stimulated cyclic AMP accumulation. Adenosine analogues did not cause significant changes in intracellular Ca^{2+} ($[Ca^{2+}]_i$) in airway epithelium.

5 Adenosine analogues, applied to either the serosal or mucosal side of the polarized amiloride pretreated primary cultures, induced changes in I_{sc} with a rank order of potency of agonists similar to that observed for stimulation of cyclic AMP accumulation. Intracellular microelectrode studies indicated that the locus of action was the apical membrane Cl^- conductance. Adenosine failed to stimulate Cl^- secretion in CF airway epithelium.

6 These results provide evidence for the existence of an A_2-adenosine receptor that modulates intracellular levels of cyclic AMP in human airway epithelium. Activation of this receptor might lead to stimulation of Cl^- secretion in amiloride pretreated normal but not CF cells.

Keywords: Epithelium; adenosine receptors; cyclic AMP; aminophylline; chloride secretion; cystic fibrosis; purinoceptors

Introduction

Extracellular adenosine and adenine nucleotides modulate a variety of physiological processes by interacting with specific membrane bound receptors, termed P_1-purinoceptors for those activated by adenosine and P_2-purinoceptors for receptors activated by adenosine 5'-triphosphate (ATP) (Burnstock, 1978). The adenosine receptors have been subclassified into two major subtypes, A_1 and A_2, according to their ability to increase (A_2) or decrease (A_1) adenylate cyclase activity and the relative potencies of a series of adenosine analogues (Van Calker *et al.*, 1979; Londos *et al.*, 1980; Daly, 1982; Stone, 1991). The A_2-receptor exhibits a potency order of 5-N-ethyl-carboxamidoadenosine (NECA) > adenosine > **R**-phenylisopropyladenosine (**R**-PIA), N-6-cyclopentyladenosine (CPA) > S-PIA, while the order of potency at the A_1-receptor is **R**-PIA, CPA > adenosine > NECA > S-PIA. Activation of both classes of adenosine receptors is competitively antagonized by methylxanthines (Sattin & Rall, 1970; Fredholm, 1980; Daly *et al.*, 1983; Parsons & Stiles, 1985).

Recent findings suggest that adenosine receptors may regulate second messenger systems in addition to adenylate cyclase. For example, an adenosine-mediated increase of intracellular Ca^{2+} ($[Ca^{2+}]_i$) in rat mast cells has been reported to be secondary to activation of phosphoinositide turnover (Ali *et al.*, 1990). Adenosine receptors may also regulate cardiac K^+ conductance by a mechanism not involving adenosine 3':5'-cyclic monophosphate (cyclic AMP) (Bohm *et al.*, 1986). Ribeiro & Sebastiao (1986) have proposed that a third type of adenosine receptor, termed A_3, is coupled to calcium channels and exhibits an agonist potency order not consistent with that of the A_1- or A_2-receptor subtypes.

In epithelia, adenosine receptor activation is functionally coupled to regulation of ion transport rates. Adenosine regulates the rate of chloride ion secretion in a variety of epithelial tissues including frog cornea (Spinowitz & Zadunaisky, 1979), rabbit ileum (Dobbins *et al.*, 1984), canine trachea (Pratt *et al.*, 1986), rabbit kidney cortical collecting duct (CCD) (Schwiebert *et al.*, 1990) and T84 human colonic epithelial cells (Barrett *et al.*, 1989). In a number of these target tissues the effect of adenosine on Cl^- transport is accompanied by elevation of cyclic AMP suggesting involvement of an A_2-adenosine receptor.

Cl^- transport by airway epithelia is likely to play an important role in modulating the volume and composition of pulmonary secretions. A defective regulation of Cl^- transport by airway epithelia may be involved in lung diseases, e.g. cystic fibrosis (CF) (Frizzell *et al.*, 1986; Welsh & Liedtke, 1986; Boucher *et al.*, 1988; Riordan *et al.*, 1989; Rommens *et al.*, 1989). We previously observed that extracellular nucleotides such as ATP and UTP stimulate Cl^- secretion in both normal and CF airway epithelial cells pretreated with amiloride (Mason *et al.*, 1991). This effect was associated with an

[1] Author for correspondence.

elevation of intracellular Ca^{2+} (Mason *et al.*, 1991) and inositol phosphates (Brown *et al.*, 1991). The objective of the present study was to determine the presence of adenosine receptors on human airway epithelia and to establish whether adenosine receptors modulate Cl^- secretion in amiloride pretreated human airway epithelia.

Methods

Cell culture

Cell lines derived from airway epithelium from a normal subject (BEAS39, Reddel *et al.*, 1988) and from a CF patient (CF/T43, Jetten *et al.*, 1989) by introduction of SV40T, were grown to confluence in hormone supplemented serum-free medium (KGM) on plastic tissue culture 12 well plates (Costar, Cambridge, MA, U.S.A.) Human nasal epithelium from normal or cystic fibrosis subjects was obtained from freshly excised nasal tissue by standard techniques (Wu *et al.*, 1985). Epithelial cells were harvested from these specimens and cultured to confluence on plastic 12 well plates for cyclic AMP studies, on non-fluorescent vitrogen coated glass coverslips for intracellular Ca^{2+} measurements, or on permeable collagen matrix supports for bioelectric measurements. An F12 based, serum-free medium supplemented with hydrocortisone 5 ng ml^{-1}, insulin 10 μg ml^{-1}, transferrin 5 μg ml^{-1}, endothelial cell growth substance 3.7 μg ml^{-1}, and 30 nM T_3 (F12, 4.1X) was the culture medium for primary cells. In previous studies using cholera toxin (CTX)-containing medium, negligible Cl^- secretory response to adenosine was observed (Mason *et al.*, 1991). For this reason, CTX was omitted from the culture medium for these studies.

Measurement of cyclic AMP accumulation

Cyclic AMP accumulation was monitored essentially as described previously (Hughes & Harden, 1986). Briefly, cells were incubated for 3 h with 1 ml of HEPES-buffered (20 mM, pH 7.5) Eagle's modified essential medium (EMEM) containing 2–3 μCi ml^{-1} of [^{3}H]-adenine. The medium was aspirated, the cells were washed twice with 1 ml of HEPES-EMEM and fresh aliquots of 1 ml HEPES-EMEM were added. Except where indicated, papaverine 200 μM, was added 10 min before incubation with agonists. The reactions were carried out at 37°C and they were terminated at the indicated times by aspiration of the medium followed by the immediate addition of 1 ml 5% trichloroacetic acid containing 0.5 mM cyclic AMP. [^{3}H]-cyclic AMP was separated from [^{3}H]-ATP by sequential passage of the trichloroacetic acid extract over Dowex and alumina columns as described previously (Harden *et al.*, 1982). Aliquots of the cyclic AMP fractions were assayed spectrophotometrically at 259 nm to correct for recovery of cyclic AMP. Experiments were carried out with triplicate samples that differed less than 10% from the mean. The results are expressed as the precentage conversion of [^{3}H]-ATP to [^{3}H]-cyclic AMP. Except where indicated, the cell cultures were supplemented with adenosine deaminase 2 u ml^{-1} for 12 h before measurement of cyclic AMP accumulation.

Measurement of intracellular calcium

Primary nasal epithelial cells grown to confluence on vitrogen-coated coverslips were loaded with a final concentration of 3 μM Fura-2 acetomethylester (Fura-2/AM) at 37°C for 30 min. $[Ca^{2+}]_i$ was measured as described by Mason *et al.* (1991) with a modular microspectrofluorimeter (SPEX Industries Inc., Edison, NJ, U.S.A.).

Bioelectric studies

Confluent monolayers of primary human nasal epithelium were mounted in modified Ussing chambers (Knowles *et al.*, 1983; Boucher *et al.*, 1988). The cultures were maintained at 37°C and continuously perfused with a standard Krebs Ringer bicarbonate solution with amiloride (100 μM) added to the apical bath to block transepithelial Na^+ transport. The current required to clamp the spontaneous transepithelial potential difference (V_t), the short circuit current (I_{sc}), was measured under voltage clamp (short circuit) conditions. Changes in I_{sc} (ΔI_{sc}), transepithelial resistance (R_t) and V_t were measured as described previously (Mason *et al.*, 1991). Intracellular microelectrode techniques for electrophysiological measurement have been described in detail elsewhere (Willumsen *et al.*, 1989; Clarke *et al.*, 1991). In brief, the culture cups were inserted in a horizontally-oriented Ussing chamber and perfused as indicated above. V_t was continuously measured and constant current pulses ($\sim$40 μA cm^{-2}, I) were passed across the tissue for measurement of transepithelial resistance ($R_t = \Delta V_t/I$). The equivalent short circuit current (I_{eq}) was calculated from Ohm's law. Cells were impaled vertically across the apical membrane with conventional microelectrodes backfilled with 3 mM KCl (tip resistance $\sim$130 mΩ). The apical membrane potential (V_a) and V_t were referenced to the apical bath and the basolateral membrane potential ($V_b = V_t - V_a$) was referenced to the basolateral bath. The fractional resistance of the apical membrane (fR_a) was calculated from the equation, $fR_a = R_a/(R_a + R_b) = \Delta V_a/\Delta V_t$ where R_a and R_b are the resistance of the apical and basolateral membranes, respectively, and ΔV_a and ΔV_t are the changes in the voltage signals in response to I.

Chemicals and solutions

Forskolin, NECA, **R**-PIA, 2-methylthio-ATP, papaverine and aminophylline were from Research Biochemicals Inc. (Natick, MA, U.S.A.). Isoprenaline, cyclic AMP, CPA, 3-isobutyl-1-methylxanthine (IBMX), adenosine deaminase, ADP, grade I neutral alumina and all nucleosides were purchased from Sigma (St. Louis, MO, U.S.A.). AG 50W-X4 Dowex resin was purchased from Bio-Rad Laboratories (Richmond, CA, U.S.A.). UTP, ATP and other adenine nucleotides were from Boehringer Mannheim Biochemicals (Indianapolis, IN, U.S.A.). Fura-2/AM and Fura-2 pentapotassium salt were purchased from Molecular Probes (Eugene, OR, U.S.A.). [2,8-^{3}H]-adenine was purchased from Amersham Corp (Arlington Heights, IL, U.S.A.). Hormones for culture medium were from Collaborative Research Inc (Waltham, MA, U.S.A.). Keratinocyte growth medium (KGM) was purchased from Clonetics (San Diego, CA, U.S.A.). Eagle's modified essential medium and Ham's F-12 cell culture medium were purchased from Gibco (Grand Island, NY, U.S.A.).

Results

Under resting conditions, there was no detectable accumulation of [^{3}H]-cyclic AMP from [^{3}H]-ATP in [^{3}H]-adenine prelabelled CF/T43 cells without or with cyclic nucleotide phosphodiesterase (PDE) inhibitors (Table 1). Exposure of the cells to isoprenaline or the adenosine analogue, NECA, resulted in stimulation of [^{3}H]-cyclic AMP accumulation (Table 1). The methylxanthine PDE inhibitors such as IBMX are known to antagonize competitively P_1-purinoceptors (Parsons & Stiles, 1985). In contrast, papaverine does not interact with A_1- or A_2-adenosine receptors. As illustrated in Table 1, 200 μM papaverine potentiated cyclic AMP elevation at concentrations of NECA that had no effect on cyclic AMP accumulation in the presence of 200 μM IBMX. The response to isoprenaline was similar, irrespective of whether IBMX or papaverine was used as a PDE inhibitor (Table 1). Based on these and other results, 200 μM papaverine was routinely included as a PDE inhibitor in all assays. The nature of the effect of methylxanthines on the adenosine receptor response is examined further below.

Table 1 Effect of phosphodiesterase (PDE) inhibitors on cyclic AMP accumulation in CF/T43 cells

	% Conversion of [^{3}H]-ATP to [^{3}H]-cyclic AMP
Control	0.00
IBMX	0.00
Papaverine	0.00
Isoprenaline (10 μM)	0.38 ± 0.03
Isoprenaline (10 μM) + IBMX	4.46 ± 0.32
Isoprenaline (10 μM) + papaverine	4.36 ± 0.42
NECA (1 μM)	0.00
NECA (1 μM) + IBMX	0.00
NECA (1 μM) + papaverine	2.78 ± 0.08
NECA (100 μM)	0.86 ± 0.04
NECA (100 μM) + IBMX	2.04 ± 0.06
NECA (100 μM) + papaverine	2.86 ± 0.05

Cells were labelled and washed as described in Methods and preincubated for 10 min with vehicle, 200 μM isobutylmethylxanthine (IBMX), or 200 μM papaverine. The cells were challenged for 5 min with the indicated concentration of isoprenaline or 5-N-ethyl-carboxamidoadenosine (NECA). The data are means ± s.d. from one experiment performed in triplicate and are representative of 3 different experiments.

The pharmacological characteristics of the adenosine receptor involved in the elevation of cyclic AMP in CF/T43 cells was examined. Accumulation of cyclic AMP was stimulated with an order of potency of NECA > adenosine > CPA, R-PIA > S-PIA (Figure 1). Thymidine, cytidine, uridine, guanidine or inosine did not stimulate cyclic AMP accumulation at millimolar concentrations (data not shown). These results suggest that an A_2-adenosine receptor activates adenylyl cyclase in CF/T43 cells.

The time course of accumulation of cyclic AMP in CF/T43 cells was compared in the presence of maximal concentrations of NECA or isoprenaline. The initial rate of cyclic AMP accumulation in the presence of NECA was approximately one half of that observed for isoprenaline (Figure 2). After a 3–4 min exposure of cells to NECA no further increase in cyclic AMP occurred and addition of fresh NECA did not induce further cyclic AMP formation. In contrast, addition of isoprenaline to NECA-treated cells resulted in a further increase in cyclic AMP formation with an initial rate similar to that observed in cells treated with isoprenaline alone (Figure 2). These results suggest that CF/T43 cells underwent a rapid and receptor-specific desensitization to NECA, as previously described for A_2-receptors in other cells (Kenimer & Nirenberg, 1981; Newman & Levitzki, 1983; Ramkumar *et al.*, 1991).

The theophylline analogue, aminophylline, has been shown to block the effect of adenosine on A_2-receptors (Hartzell, 1979). Preincubation of CF/T43 cells with aminophylline resulted in a concentration-dependent reduction in NECA-stimulated cyclic AMP accumulation (Figure 3). In contrast, aminophylline had no effect on the action of isoprenaline (Figure 3). The apparent potency of aminophylline for inhibition of the NECA response varied with the time of preincubation with antagonist and with the length of drug challenge (data not shown). Thus, concentration-effect curves for NECA were generated in the presence of varying concentrations of aminophylline, under conditions in which aminophylline and NECA were added concurrently. Incubations were for 2 min in order to minimize the contribution of agonist-induced desensitization. The concentration-effect curve for NECA was shifted to the right in a parallel fashion by increasing concentrations of aminophylline (Figure 4). These data suggest competitive inhibition of the NECA response by aminophylline. The apparent inhibition constant for aminophylline was estimated by Schild analysis (Arunlakshana & Schild, 1959). The calculated pA_2 value was 4.8 which corresponds to a K_i value of 5.3 μM. The validity of this value is brought into question by the fact that the slope of the line of the transformed data (−1.7) differs significantly from the value (−1) expected for a competitive antagonist. Lack of achievement of equilibrium conditions under the necessary restricted conditions of this experiment seems likely.

Forskolin, which directly activates adenylate cyclase (Seamon & Daly, 1981), is also known to potentiate the actions of receptors activating this enzyme through G_s, e.g. β-adrenoceptors and adenosine receptors (Seamon *et al.*, 1981; Daly *et al.*, 1982). We examined the effect of forskolin

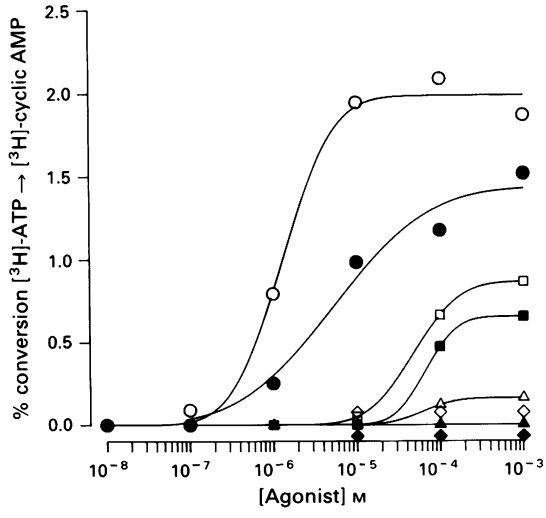

Figure 1 Effect of adenosine analogues on the accumulation of cyclic AMP in CF/T43 cells. Cells were labelled and preincubated as indicated in Methods and challenged for 2 min with the indicated concentrations of NECA (○), adenosine (●), CPA (□), R-PIA (■), S-PIA (△), ADP (◇), ATP (▲) or UTP (◆). Adenosine deaminase was omitted from the incubations. The data are representative of results from four experiments. For abbreviations, see text.

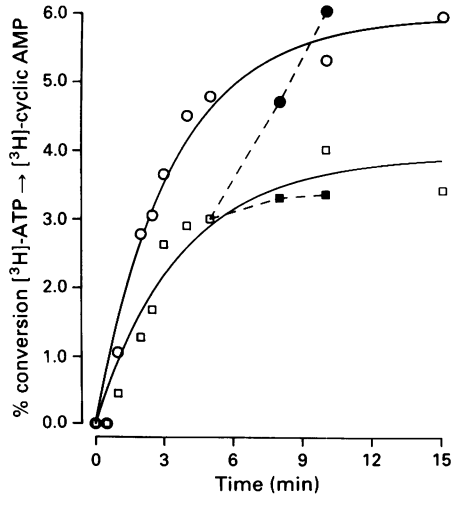

Figure 2 Time-dependent effect of isoprenaline and NECA on the accumulation of cyclic AMP in CF/T43 cells. Cells were labelled and preincubated with 200 μM papaverine as indicated in Methods. The cells were challenged with 10 μM isoprenaline (○) or 100 μM NECA (□) for the indicated times or they were preincubated with 100 μM NECA for 5 min and further incubated for 3 and 5 min with 10 μM isoprenaline (●) or 100 μM NECA (■). Results are the mean of triplicate determinations. The data are representative of results from three experiments. For abbreviations, see text.

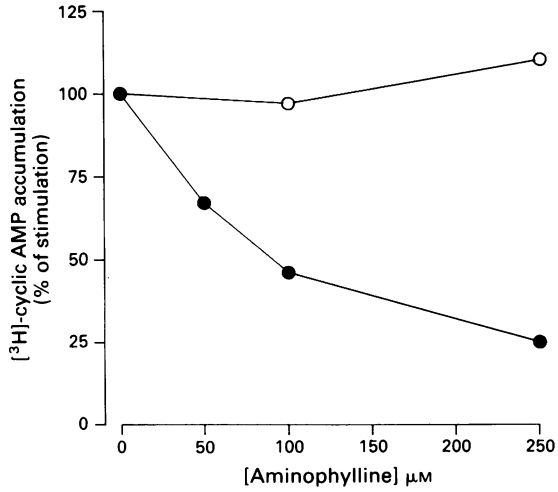

Figure 3 Effect of aminophylline on NECA and isoprenaline stimulated accumulation of cyclic AMP in CF/T43 cells. The cells were preincubated for 10 min with the indicated concentrations of aminophylline and challenged for 5 min with 10 μM isoprenaline (○) or NECA (●). The results are plotted as the percentage of the response in the absence of aminophylline and are the mean of triplicate determinations. For abbreviations, see text.

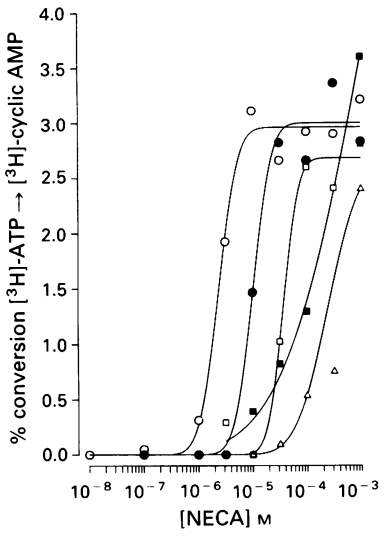

Figure 4 Effect of aminophylline on the stimulation of cyclic AMP accumulation by NECA. CF/T43 cells were labelled and preincubated as indicated in the legend of Figure 2. The cells were incubated for 2 min with the indicated concentrations of NECA alone (○) or with the concurrent addition of 10 μM (●), 20 μM (□), 50 μM (■), or 100 μM (△) aminophylline. The results are plotted as percentage conversion of [3H]-ATP to [3H]-cyclic AMP and are the mean of triplicate determinations. For abbreviations, see text.

on cyclic AMP accumulation in isoprenaline or adenosine-stimulated CF/T43 cells. Addition of isoprenaline with forskolin to CF/T43 cells, resulted in cyclic AMP accumulation at levels 2–3 times larger than that expected for simple additivity between the two stimuli (not shown). Similar results were obtained in CF/T43 cells stimulated with forskolin combined with NECA (Figure 5a) or with adenosine, R-PIA or CPA (not shown). Incubation of cells for 5 min with 1 μM NECA or higher resulted in maximal accumulation of cyclic AMP, and a similar level of cyclic AMP accumulation was produced by 10 μM forskolin. However, the addition of forskolin in combination with NECA resulted in marked potentiation of their respective effects. Forskolin potentiated cyclic AMP elevation at concentrations of NECA (10^{-8} M) that did not cause apparent cyclic AMP accumulation if added alone (Figure 5a). Preincubation of CF/T43 cells with increasing concentrations of aminophylline or IBMX resulted in a concentration-dependent inhibition of the formation of cyclic AMP in response to 30 μM NECA plus 10 μM forskolin. The IC_{50} values for aminophylline and IBMX were 35 μM and 72 μM, respectively (Figure 5b). The inhibitory effect of the methylxanthines was not observed in CF/T43 cells stimulated with forskolin alone (not shown).

To test whether the CF/T43 cells selected for study accurately reflected adenosine receptor activation in human airway epithelium, the ability of NECA to stimulate the formation of cyclic AMP in primary culture of human airway epithelial cells from normal and CF patients, as well as in a cell line (BEAS39) derived from a normal subject, was examined. Incubation of the cells for 2 min with NECA caused concentration-dependent increases in cyclic AMP accumulation in each cell type studied (Figure 6). NECA, at a maximal stimulatory concentration, was similarly efficacious in stimulating cyclic AMP accumulation in normal and CF cells, being 3–4 times more effective in the cell lines than in primary cells (Figure 6). The $K_{0.5}$ values for NECA (in μM) were as follows: normal primary cells, 0.6 ($n = 3$); CF primary cells, 3.0 ($n = 2$); BEAS39 cells, 3.0 ($n = 2$), and CF/T43 cells, 1.1 ($n = 5$).

We also examined whether an A_1-adenosine receptor capable of inhibiting cyclic AMP accumulation was present on CF/T43 cells. Combined addition of NECA and submaximal concentrations of isoprenaline resulted in slightly (24% ± 11) enhanced cyclic AMP accumulation over that observed with isoprenaline alone. No significant inhibitory effect of CPA or R-PIA on isoprenaline-stimulated cyclic AMP levels occurred (not shown). These data suggest that A_1-adenosine receptors are not expressed on airway epithelial cells.

The effect of P_2-purinoceptor agonists on the levels of cyclic AMP in CF/T43 cells was also studied. Incubation of the cells with either ADP, ATP or UTP (Figure 1), or with ADPβS, 2-methylthio-ATP or α,β-methylene ATP (not shown) did not result in increased cyclic AMP accumulation. Neither ATP, adenosine-5′-*O*-3-thiotriphosphate (ATPγS) or UTP (each at 100 μM) caused changes in a 1 to 10 min time course of isoprenaline-stimulated cyclic AMP accumulation

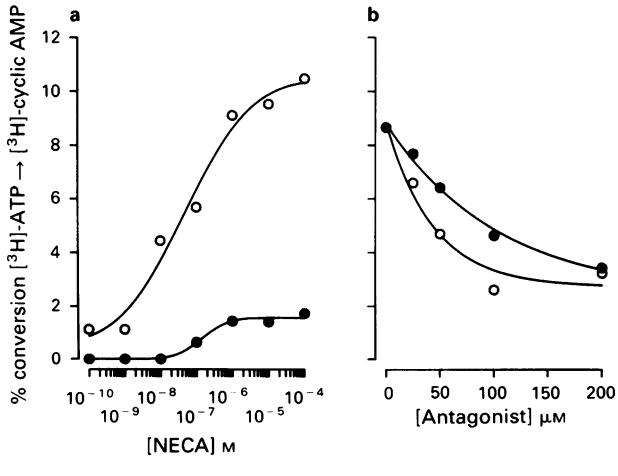

Figure 5 Potentiation of NECA-stimulated cyclic AMP accumulation by forskolin. CF/T43 cells were labelled and preincubated as indicated in the legend of Figure 2. (a) The cells were challenged for 5 min with the indicated concentrations of NECA with (○) or without (●) the concurrent addition of 10 μM of forskolin. (b) The cells were preincubated for 10 min with the indicated concentrations of aminophylline (○) or IBMX (●) and challenged for 5 min with 30 μM NECA plus 10 μM of forskolin. Results are plotted as the percentage conversion of [3H]-ATP to [3H]-cyclic AMP and they are the mean of triplicate determinations. For abbreviations, see text.

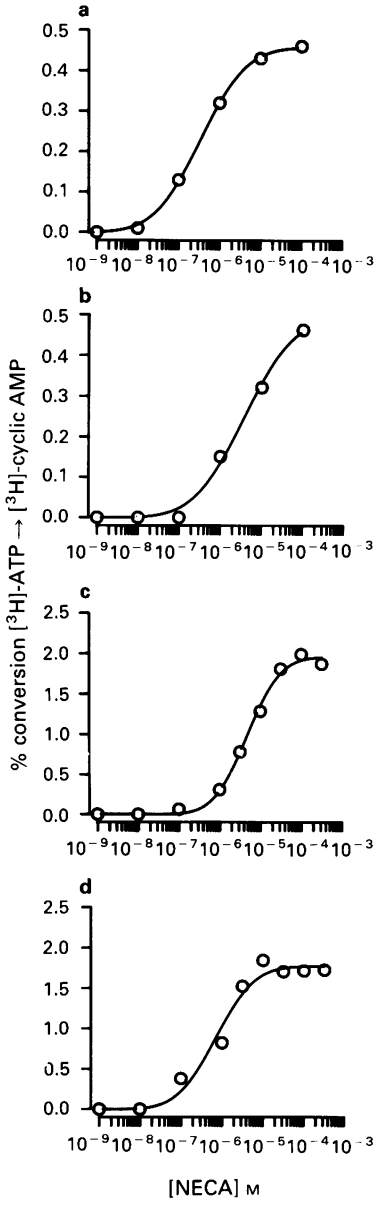

Figure 6 Effect of NECA on [^{3}H]-cyclic AMP accumulation in human airway epithelial cells. Primary tissue from human airway epithelia excised from control subjects (a) or cystic fibrosis (CF) patients (b) and BEAS39 (c) and CF/T43 (d) cells were labelled with [^{3}H]-adenine as indicated in Methods. Cells were preincubated for 10 min with 200 μM papaverine and then challenged with the indicated concentration of NECA for 2 min. The results are plotted as the percent conversion of [^{3}H]-ATP to [^{3}H]-cyclic AMP and are the mean of triplicate determinations. For abbreviations, see text.

(isoprenaline = 10 μM, data not shown). These data suggest that cyclic AMP levels are not regulated by P_2-purinoceptors in CF/T43 cells.

We have previously shown that the P_2-purinoceptor agonist, ATP, induces a rapid increase in $[Ca^{2+}]_i$ (net increase: 739 ± 171 nM) in human nasal epithelium (Mason *et al.*, 1991). To determine whether airway epithelial cells possess a P_1-receptor subtype linked to elevation of $[Ca^{2+}]_i$, we studied the effect of the adenosine analogues on fura-2-loaded human nasal epithelial cells. In contrast to the effect of ATP, addition of 100 μM adenosine or NECA caused delayed (1–2 min after addition) and negligible (10–20 nM) changes in $[Ca^{2+}]_i$. Addition of CPA and **R**-PIA initiated no change in $[Ca^{2+}]_i$ (data not shown).

In bioelectric studies of human nasal epithelium, we have recently demonstrated that extracellular adenine nucleotides stimulate Cl^- secretion, as measured by changes in I_{sc} in amiloride-pretreated cells (Mason *et al.*, 1991). Pretreatment of monolayers with amiloride (100 μM) effectively removes the Na^+ absorptive component of I_{sc}, so that the residual I_{sc} reflects a basal Cl^- secretory activity (Boucher *et al.*, 1986; Willumsen *et al.*, 1989). The effect of adenosine receptor agonists on I_{sc} in amiloride pretreated polarized human nasal epithelium is illustrated in Figure 7. The observed rank order of potency of Cl^- secretory stimulation for the adenosine analogues was NECA > adenosine > **R**-PIA ≥ CPA when applied to either the apical (Figure 7a) or basolateral (Figure 7b) surface.

Representative tracings of I_{sc} in normal and CF primary nasal epithelium are shown in Figure 8. Exposure of amiloride pretreated normal nasal epithelium to a NECA concentration causing maximal cyclic AMP accumulation resulted in the complete lack of response to a second addition of NECA and in a markedly diminished response to isoprenaline (Figure 8a). In contrast, the I_{sc} response to ATP following NECA and isoprenaline was in the range reported for untreated tissues (Mason *et al.*, 1991). Amiloride pretreated CF tissue showed no Cl^- secretory response to NECA or isoprenaline, but a large response was observed to ATP (Figure 8b).

Additivity between P_1-purinoceptor and β-adrenoceptor agonists and between P_1 and P_2-purinoceptor agonists for stimulation of Cl^- secretion was tested in normal tissues (Figure 9). When amiloride pretreated cells were stimulated

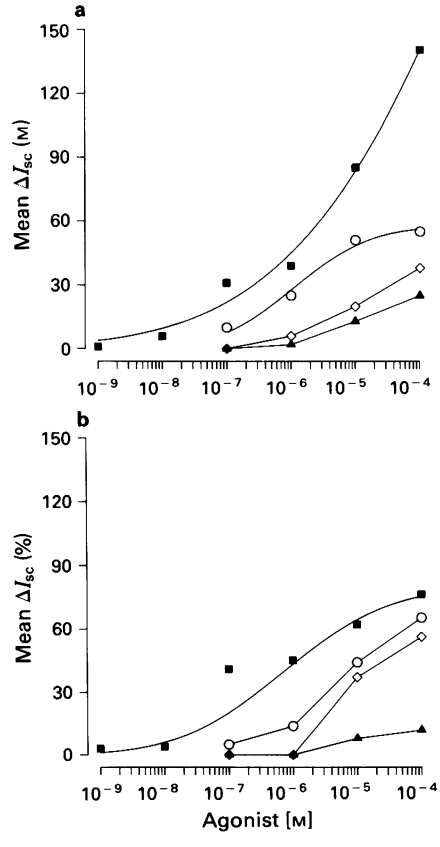

Figure 7 Effect of adenosine analogues on I_{sc} changes in human airway epithelium. Confluent monolayers of primary human nasal epithelium were pretreated with amiloride as indicated in Methods followed by apical (a) or basolateral (b) addition of NECA (■), adenosine (○), **R**-PIA (◇) or CPA (▲). The results are based on the agonist-stimulated peak change in I_{sc} and are plotted as percentage change in I_{sc}. The data represent the mean of 3–12 determinations from tissues obtained from 3–10 different normal donors. I_{sc} values of amiloride pretreated unstimulated cells were 15.5 ± 4.6 μA cm^{-2} in (a) and 15.7 ± 6.1 μA cm^{-2} in (b). For abbreviations, see text.

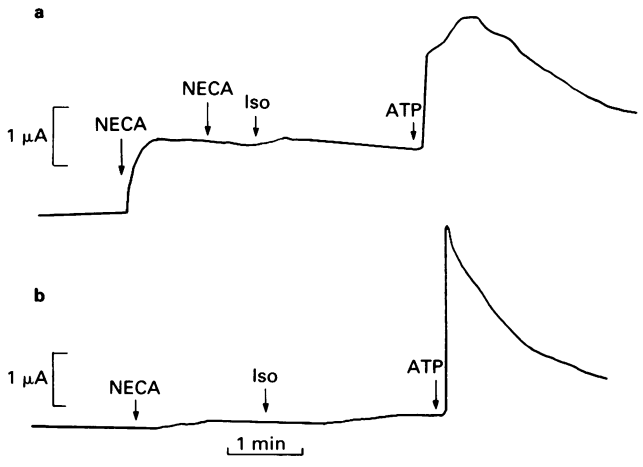

Figure 8 Representative bioelectric tracings of I_{sc} in human airway epithelium. Primary cultures of human nasal epithelium from a normal (a) or a cystic fibrosis (b) donor were pretreated with amiloride as indicated in Methods and stimulated with consecutive (apical) addition of 100 μM NECA, 10 μM isoprenaline (Iso) and 100 μM ATP. Control post-amiloride I_{sc} were 24 μA cm^{-2} in (a) and 38 μA cm^{-2} in (b). The data are representative of experiments performed with tissue from at least four different donors.

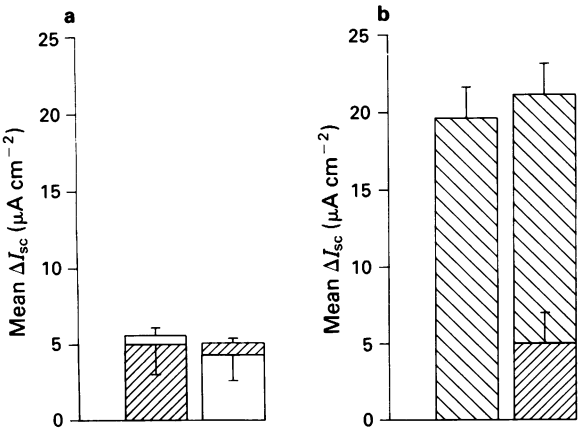

Figure 9 I_{sc} changes in human airway epithelium stimulated by combined addition of NECA, isoprenaline and ATP. Human nasal epithelium from normal donors were treated with amiloride as indicated in Methods. (a) The cells was challenged with 100 μM NECA (hatched columns) either before (left) or after (right) the addition of 10 μM isoprenaline (open columns). (b) The cells were stimulated by 100 μM ATP alone (left) or after the addition of 100 μM NECA (right). In each set of experiments, the addition of the second agonist followed stabilization of the response to the first one. All additions were on the apical surface of the monolayer. For abbreviations, see text.

with sequential additions of NECA and isoprenaline, the I_{sc} response to the second agonist was substantially reduced, irrespective of the order of the additions (Figure 9a). These results suggest that these agonists stimulated Cl^- transport at least in part through a common mechanism. In contrast, the ATP response following NECA was not significantly different from the response to ATP alone suggesting additivity of these agents (Figure 9b).

Cyclic AMP-dependent activation of Cl^- secretion in human airway epithelium, e.g. in response to isoprenaline, results from a primary activation of an apical membrane Cl^- conductance (Widdicombe *et al.*, 1985; Boucher *et al.*, 1988). To test whether activation of A_2-receptors with NECA induces Cl^- secretion by a similar mode, changes in the individual membrane potentials and resistances were studied during cellular impalement with conventional microelectrodes. As shown in Figure 10, upper trace, luminal application of NECA (100 μM) to amiloride pretreated human nasal epithelium cultures induced an increase in transepithelial potential difference (V_t) and a decrease in transepithelial resistance (R_t), indicated by a decrease in the amplitude of the current-induced voltage deflection. These changes indicate an increase in the equivalent short circuit current. As shown in the lower trace, NECA application induced an abrupt depolarization of the apical membrane potential (V_a). Note also that the apical membrane voltage response to the current pulses decreased to a relatively greater degree than in the V_t tracing, indicating a decrease in the fractional resistance of the apical membrane. Like the previous Ussing chamber data (see Figure 8), NECA stimulated a significant increase in Cl^- secretion (I_{eq}) (Table 2). During the response, the cellular changes were (1) depolarization of V_a and (2) a decrease in fR_a, which coupled with a decrease in R_t, indicated a decrease in the resistance (i.e., increased conductance) of the apical membrane. Thus, the Cl^- secretory response resulting from NECA application was associated with the induction of a depolarizing conductance in the apical membrane, which is consistent with activation of an apical membrane Cl^- conductance.

Discussion

In this study we have expanded our previous investigations of the effect of adenosine and adenine nucleotides in human airway epithelial cells. Previously, we have shown that extracellular ATP stimulates the formation of inositol phosphates (Brown *et al.*, 1991), raises $[Ca^{2+}]_i$, and increases the rate of Cl^- transport (Mason *et al.*, 1991) in human nasal epithelium. Here, we demonstrate that extracellular adenosine modulates the intracellular levels of cyclic AMP in human

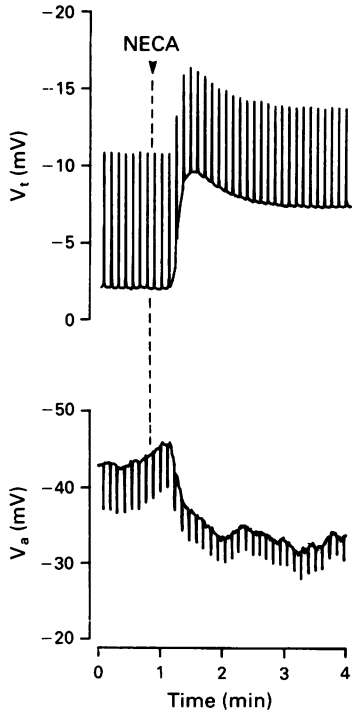

Figure 10 Representative microelectrode tracings of transepithelial and apical membrane responses to NECA. Amiloride pretreated human nasal epithelium was challenged with 100 μM NECA added to the apical bath. Upper trace, transepithelial potential difference (V_t). Lower trace, apical membrane potential (V_a). Voltage deflections are in response to constant current pulses (~40 μA cm^{-2}).

Table 2 Effect of 5-N-ethyl-carboxamidoadenosine (NECA) on Cl^- secretion in amiloride pretreated nasal epithelial cell cultures

	Transepithelial parameters			*Cellular parameters*		
	V_t (mV)	R_t ($\Omega.cm^2$)	I_{eq} ($\mu A\ cm^{-2}$)	V_a (mV)	V_b (mV)	fR_a
A Basal	-2.9 ± 0.9	298 ± 29	-9.5 ± 3.1	-30.2 ± 3.9	-33.1 ± 4.4	0.56 ± 0.06
B NECA	-7.2 ± 1.0	251 ± 21	-28.6 ± 4.0	-23.4 ± 4.3	-30.6 ± 4.4	0.43 ± 0.05
D (B−A)	-4.3 ± 1.4	-47 ± 13 *	-19.1 ± 5.9 *	6.8 ± 1.6 *	2.5 ± 1.7	-0.14 ± 0.01 *

Basal and NECA (100 μM, luminal application) data values were measured during a continuous cellular impalement of each primary culture with microelectrodes as indicated in Methods. The values represent the means ($\pm$ s.e.mean) from four experiments. All NECA values were recorded simultaneously with the maximal change in I_{eq}. Amiloride (100 μM) was added to the luminal bath prior to experiment. *$P<0.05$ (paired t test). Abbreviations: V_t, V_a and V_b, transepithelial, apical and basolateral membrane potential differences, respectively; R_t, transepithelial resistance; I_{eq} equivalent short-circuit current; and fR_a, fractional resistance of the apical membrane.

airway epithelium, and that this effect appears to be mediated by a cell surface receptor that responds to adenosine but not to adenine nucleotides.

The effect of adenosine on cyclic AMP suggests the existence of a stimulatory A_2-adenosine receptor on airway epithelium. Most notably, the A_2-adenosine receptor agonist, NECA, is the most potent and effective agonist at this receptor. The order of potency of the adenosine analogues is consistent with that observed in other tissues for stimulatory A_2-adenosine receptors (Van Calker, 1979; Londos *et al.*, 1980; Daly, 1982; Stone, 1990). The potency of NECA for stimulation of cyclic AMP accumulation in epithelial cells was lower than that reported for other tissues, e.g. rat liver (Londos, 1980), and rat brain (Daly *et al.*, 1983). However, Daly (1982) has pointed out that the apparent potencies of adenosine analogues show considerable range in different tissues and the $K_{0.5}$ values of NECA observed with primary tissue and cell lines from human airway epithelium are within this range.

The phenomenon of homologous desensitization is known to occur following the activation of receptors coupled in a stimulatory fashion to the enzyme adenylyl cyclase, e.g. β-adrenoceptors (Harden, 1983; Sibley & Lefkowitz, 1985). Previous studies in NG108-15 neuroblastoma-glioma hybrid cells (Kenimer & Nirenberg, 1981), rat normal kidney (RNK) fibroblasts (Newman & Levitzki, 1983) and DDT_1 MF-2 smooth muscle cells (Ramkumar *et al.*, 1991) have shown that the A_2-receptor undergoes homologous desensitization during exposure of cells to adenosine analogues. Consistent with these reports, we have shown (Figure 2) that NECA-treated CF/T43 cells became refractory to further stimulation with the adenosine analogue but not with the β-receptor agonist isoprenaline.

It is widely recognized that membrane-bound adenosine receptors are competitively antagonized by methylxanthines (Sattin & Rall, 1970; Fredholm, 1980; Daly *et al.*, 1983; Parsons & Stiles, 1985). As shown in Figures 3–5, the effect of NECA on cyclic AMP accumulation in CF/T43 cells was inhibited by IBMX and aminophylline and this effect was specific for adenosine and its analogues.

Recently, it has been reported that adenosine stimulatory receptors can co-exist in the same cell type with those coupled to inhibition of adenylate cyclase (Ramkumar *et al.*, 1990). However, our results show that A_1-adenosine receptor agonists R-PIA or CPA did not inhibit the effect of isoprenaline on cyclic AMP accumulation and potentiating interactions rather than inhibitory ones were observed by the adenosine analogues on forskolin-stimulated CF/T43 cells (Figure 5). The later observation supports the premise that the action of adenosine is mediated through G_s.

A recent report showed that adenosine stimulates phospholipase C and Ca^{2+} mobilization in RBL-2H3 cells with a rank order of potency of agonists characteristic of an A_2-adenosine receptor (Ali *et al.*, 1990). However, there was only a negligible increase in $[Ca^{2+}]_i$ in NECA or adenosine-stimulated human airway epithelial cells. Furthermore, we have shown recently that adenosine does not stimulate inositol phosphate accumulation in CF/T43 cells (Brown *et al.*, 1991).

While adenylate cyclase is likely to be the earliest effector of A_2-adenosine receptor activation, the spectrum of distal targets of this pathway in human airway epithelium has not been fully identified. There have been previous reports that adenosine-stimulated cyclic AMP accumulation and cyclic AMP-dependent protein kinase in epithelial cells is associated with increased Cl^- secretion (Spinowitz & Sadunaitzki, 1979; Dobbins *et al.*, 1984; Pratt *et al.*, 1986; Barrett *et al.*, 1990). Similarly, cyclic AMP plays an important role in regulating Cl^- transport in human airway epithelium. Evidence for this notion comes from studies showing that isoprenaline and other agents that increase cyclic AMP levels as well as cyclic AMP-dependent protein kinase activate Cl^- transport or channels in normal human airway epithelia but not in CF cells (Frizzel *et al.*, 1986; Welch *et al.*, 1986; Schoumacher *et al.*, 1987; Li *et al.*, 1988; Boucher *et al.*, 1988; 1989). From these studies, we might expect adenosine and its analogues to activate Cl^- transport in normal epithelium but not in cells from CF patients. Importantly, the direction of stimulated Cl^- transport, absorption versus secretion, is only known for amiloride pretreated human nasal epithelia. In this condition adenosine would be expected to induce an increase in secretion.

The data presented here confirm these predictions. Indeed, activation of Cl^- secretion by adenosine (or analogues) primarily reflects its actions on raising cyclic AMP levels as indicated by the following data: (1) adenosine analogues showed the same order of potency for stimulating Cl^- secretion and cyclic AMP accumulation; (2) NECA-stimulated Cl^- secretion and cyclic AMP accumulation occurred with similar concentration-dependence; (3) analysis of the microelectrode data indicate that NECA, like isoprenaline, initiates Cl^- secretion via an action on the apical membrane Cl^- conductance, a conductance previously shown to be regulated by cyclic AMP-dependent mechanisms; and (4) NECA failed to induce Cl^- secretion in cells obatined from patients with a genetic inability to activate a Cl^- conductance in response to cyclic AMP, i.e., CF patients.

Data from studies of other cell systems indicate that regulatory mechanisms in addition to cyclic AMP might activate Cl^- secretion subsequent to adenosine stimulation of airway epithelial cells. Recently, it has been shown that transepithelial Cl^- secretion can be stimulated by Ca^{2+} ionophores and by agonists that increase $[Ca^{2+}]_i$ and the formation of inositol phosphates (Boucher *et al.*, 1989; Mason *et al.*, 1991; Brown *et al.*, 1991). Furthermore, adenosine-stimulated Cl^- secretion in CDD cells was associated with increased inositol phosphate formation (Schwiebert *et al.*, 1990). However, as discussed above with reference to the absence of changes in $[Ca^{2+}]_i$ in response to adenosine, this is not the case in human airway epithelium.

In conclusion, BEAS39, CF/T43 and primary cultures of

both normal and CF human airway epithelial cells express an A_2-type adenosine receptor that stimulates cyclic AMP accumulation. This receptor is located functionally on both the apical and basolateral surface of polarized airway epithelia. The A_2-receptor appears coupled via adenylate cyclase activation to regulating the rate of Cl^- secretion in normal airway epithelium. Like the β-adrenoceptor, the stimulatory adenosine receptor is functionally uncoupled from stimulating Cl^- secretion in CF airway epithelial cells due to a defect in a distal effector element, probably the CF protein itself, and not due to abnormality in A_2-receptor or its coupling to adenylate cyclase.

This work was supported by the National Institute of Health grant HL34322 and the Cystic Fibrosis Foundation grant R025.

References

ALI, H., CUNHA-MELO, J.R., SAUL, W.F. & BEAVEN, M.A. (1990). Activation of phospholipase C via adenosine receptors provides synergistic signals for secretion in antigen-stimulated RBL-2H3 cells. *J. Biol. Chem.*, **265**, 745–753.

ARUNLAKSHANA, O. & SCHILD, H.O. (1959). Some quantitative uses of drug antagonists. *Br. J. Pharmacol. Chemother.*, **14**, 48–58.

BARRETT, K.E., COHN, J.A., HUOTT, P.A., WASSERMAN, S.I. & DHARMSATHAPHORN, K. (1990). Immune-related intestinal chloride secretion II. Effect of adenosine on T84 cell line. *Am. J. Physiol.*, **258** (Cell. Physiol. 27), C902–C912.

BOHM, M., BRUCKNER, R., NEUMMAN, J., SCHMITZ, W., SCHOLZ, H. & STARBATTY, J. (1986). Role of guanine nucleotide binding-protein in the regulation by adenosine of cardiac potassium conductance and force of contraction. Evaluation with pertussis toxin. *Naunyn-Schmiedebergs Arch. Pharmacol.*, **332**, 403–405.

BOUCHER, R.C., STUTTS, M.J., KNOWLES, M.R., CANTLEY, L. & GATZY, J.T. (1986). Na^+ transport in cystic fibrosis respiratory epithelia. Abnormal basal rate and response to adenylate cyclase activation. *J. Clin. Invest.*, **78**, 1245–1252.

BOUCHER, R.C., COTTON, C.U., GATZY, J.T., KNOWLES, M.R. & YANKASKAS, J.R. (1988). Evidence for reduced Cl^- and increased Na^+ permeability in cystic fibrosis human primary cell cultures. *J. Physiol.*, **405**, 77–103.

BOUCHER, R.C., CHENG, H.C., PARADISO, A.M., STUTTS, M.J., KNOWLES, M.R. & EARP, H.S. (1989). Chloride secretory response of cystic fibrosis human airway epithelia. Preservation of calcium but not protein kinase C- and A mechanisms. *J. Clin. Invest.*, **84**, 1424–1431.

BROWN, H.A., LAZAROWSKI, E.R., BOUCHER, R.C. & HARDEN, T.K. (1991). Evidence that UTP and ATP regulate phospholipase C through a common extracellular 5′-nucleotide receptor in human airway epithelial cells. *Mol. Pharmacol.*, **40**, 648–655.

BURNSTOCK, G. (1978). A basis for distinguishing two types of purinergic receptor. In *Cell Membrane Receptors for Drug and Hormones: A Multidisciplinary Approach.* ed. Straub, L.B. pp. 107–118. New York: Raven Press.

CLARKE, L.L., PARADISO, A.M., MASON, S.J. & BOUCHER, R.C. (1992). Effect of bradykinin on Na^+ and Cl^- transport in human nasal epithelium. *Am. J. Physiol.*, (Cell Physiol.), **31** C644–C655.

DALY, J.W. (1982). Adenosine receptors: target for future drugs. *J. Med. Chem.*, **25**, 197–207.

DALY, J.W., PADGETT, W. & SEAMON, K.B. (1982). Activation of cyclic AMP-generating systems in brain membranes and slices by the diterpene forskolin. Augmentation of receptor-mediated responses. *J. Neurochem.*, **38**, 532–544.

DALY, J.W., BUTTS-LAMB, P. & PADGETT, W. (1983). Subclasses of adenosine receptors in the central nervous system: Interaction with caffeine and related methylxanthines. *Cell. Mol. Neurobiol.*, **3**, 69–80.

DOBBINS, J.W., LAURENSON, J.P. & FORREST, J.N. Jr (1984). Adenosine and adenosine analogues stimulate adenosine cyclic 3′,5′-monophosphate-dependent chloride secretion in the mammalian ileum. *J. Clin. Invest.*, **74**, 929–935.

FREDHOLM, B.B. (1980). Are methylxanthine effects due to antagonism of endogenous adenine? *Trends Pharmacol. Sci.*, **1**, 129–132.

FRIZZELL, R.A., RECHKEMMER, G. & SHOEMAKER, R.L. (1986). Altered regulation of airway epithelial cell chloride channels in cystic fibrosis. *Science*, **233**, 558–560.

HARDEN, T.K. (1983). Agonist-induced desensitization of the β-adrenergic receptor-linked adenylate cyclase. *Pharmacol. Rev.*, **35**, 5–32.

HARDEN, T.K., SCHEER, A.G. & SMITH, M.M. (1982). Differential modification of the interaction of cardiac muscarinic and beta-adrenergic receptors with a guanine nucleotide binding component(s). *Mol. Pharmacol.*, **21**, 570–580.

HARTZELL, H.C. (1979). Adenosine receptors in frog sinus venus: slow inhibitory potentials produced by adenine compounds and acetylcholine. *J. Physiol.*, **293**, 23–49.

HUGHES, A. & HARDEN, T.K. (1986). Adenosine and muscarine receptors attenuate cyclic AMP accumulation by different mechanisms in 1321 N1 astrocytome cells. *J. Pharmacol. Exp. Ther.*, **237**, 173–178.

JETTEN, A.M., YANKASKAS, J.R., STUTTS, M.J., WILLUMSEN, N.J. & BOUCHER, R.C. (1989). Persistence of abnormal chloride conductance regulation in transformed Cystic Fibrosis epithelia. *Science*, **244**, 1472–1475.

KENIMER, J.G. & NIREMBERG, M. (1981). Densensitization of adenylate cyclase to prostaglandin E_1 or 2-chloroadenosine. *Mol. Pharmacol.*, **20**, 585–591.

KNOWLES, M.R., STUTTS, M.J., SPOCK, A., FISHER, N., GATZY, J.T. & BOUCHER, R.C. (1983). Abnormal ion permeation through cystic fibrosis respiratory epithelium. *Science*, **221**, 1067–1070.

LI, M., MCCANN, J.D., LIEDTKE, C.M., NAIRN, A.C., GREENGARD, P. & WELSH, M.J. (1988). Cyclic AMP-dependent protein kinase open chloride channels in normal but not cystic fibrosis airway epithelium. *Nature*, **331**, 358–360.

LONDOS, C., COOPER, D.M.F. & WOLFF, J. (1980). Subclasses of external adenosine receptors *Proc. Natl. Acad. Sci. U.S.A.*, **77**, 2551–2554.

MASON, S.J., PARADISO, A.M. & BOUCHER, R.C. (1991). Regulation of ion transport and intracellular calcium by adenosine triphosphate in human normal and cystic fibrosis airway epithelium. *Br. J. Pharmacol.*, **103**, 1649–1656.

NEWMAN, M.E. & LEVITZKI, A. (1983). Desensitization of normal rat kidney cells to adenosine. *Biochem. Pharmacol.*, **32**, 137–140.

PARSONS, W.J. & STILES, G.L. (1985). Methylxanthines as adenosine receptor antagonists. *Ann. Intern. Med.*, **103**, 643.

PRATT, A.D., CLANCY, G. & WELSH, M.J. (1986). Mucosal adenosine stimulates chloride secretion in canine tracheal epithelium. *Am. J. Physiol.*, **251** (Cell Physiol., 20), C167–C174.

RAMKUMAR, V., BARRINGTON, W.W., JACOBSON, K.A. & STILES, G.L. (1990). Demonstration of both A_1 and A_2 adenosine receptors in DTT_1 MF-2 smooth muscle cells. *Mol. Pharmacol.*, **37**, 149–156.

RAMKUMAR, V., OLAH, M.E., JACOBSON, K.A. & STILES, G. (1991). Distinct pathways of desensitization of A_1- and A_2- adenosine receptors in DDT_1 MF-2 cells. *Mol. Pharmacol.*, **40**, 639–647.

REDDEL, R.R. YANG KE, GERWIN, B.I., MCMENAMIN, M.G., LECHNER, J.F., SU, R.T., BRASH, D.E., PARK, J.B., RHIM, J.S. & HARRIS, C.C. (1988). Transformation of human bronchial epithelial cells by infection with SV40 or adenovirus-12 SV40 hybrid virus, or transfection via strontium phosphate coprecipitation with a plasmid containing SV40 early region genes. *Cancer Res.*, **48**, 1904–1909.

RIBEIRO, J.A. & SEBASTIAO, A.M. (1986). Adenosine receptors and calcium: Basis for proposing a third (A3) adenosine receptor. *Prog. Neurobiol.*, **26**, 179–207.

RIORDAN, J.R., ROMMENS, J.M., KEREM, B.-T., ALON, N., ROZMAHEL, R., GRZELCZAK, Z., ZIELENSKI, J., LOK, S., PLAVSIC, N., CHOU, J.-L., DRUM, M.L., IANNUZZI, M.C., COLINS, F.S. & TSUI, L.C. (1989). Identification of the cystic fibrosis gene: Cloning and characterization of complementary DNA. *Science*, **245**, 1066–1073.

ROMMENS, J.M., IANNUZZI, M.C., KEREM, B.-T., DRUM, M.L., MELMER, G., DEAN, M., ROZMAHEL, R., COLE, J.L., KENNEDY, D., HIDAKA, N., ZSIGA, M., BUCHWALD, M., RIORDAN, J.R., TSUI, L.-C. & COLLINS, F.S. (1989). Identification of the cystic fibrosis gene: chromosome walking and jumping. *Science*, **245**, 1059–1065.

SATTIN, A. & RALL, T.W. (1970). The effect of adenosine and adenine nucleotides on cyclic adenosine 3',5'-phosphate content of guinea pig cerebral cortex slices. *Mol. Pharmacol.*, **6,** 13–23.

SCHWIEBERT, E., LIGHT, D., DIETEL, P., FEJES-TOTH, G., NARAY-FEJES-TOTH, A. & STANTON, B. (1990). Protein kinase C and a G protein, α_{-3}, regulate a Cl^- channel in the cortical collecting duct (CCD). *Kidney Int.*, **37,** 216.

SEAMON, K.B. & DALY, J.W. (1981). Activation of adenylate cyclase by the diterpene forskolin does not require the guanine nucleotide regulatory protein. *J. Biol. Chem.*, **256,** 9799–9801.

SEAMON, K.B., PADGETT, W. & DALY, J. (1981). Forskolin: unique diterpene activator of adenylate cyclase in membranes and in intact cells. *Proc. Natl. Acad. Sci. U.S.A.*, **78,** 3363–3367.

SCHOUMACHER, R.A., SHOEMAKER, R.L., HALM, D.R., TALLANT, E.A., WALLACE, R.W. & FRIZZELL, R.A. (1987). Phosphorylation fails to activate chloride channels from cystic fibrosis airway cells. *Nature*, **330,** 752–754.

SIBLEY, D.R. & LEFKOWITZ, R.J. (1985). Molecular mechanisms of receptor desensitization using the β-adrenergic receptor-coupled adenylate cyclase system as a model. *Nature*, **317,** 124–129.

SPINOWITZ, B.S. & ZADUNAISKY, J.A. (1979). Action of adenosine on chloride active transport of isolated frog cornea. *Am. J. Physiol.*, **237,** (Renal Fluid Electrolyte Physiol., 6), F121–F127.

STONE, T.W. (1991). Receptor for adenosine and adenine nucleotides. *Gen. Pharmacol.*, **22,** 25–31.

VAN CALKER, D.M., MULLER, M. & HAMPRECHT, B. (1979). Adenosine regulates via two different types of receptors, the accumulation of cyclic AMP in culture brain cells. *J. Neurochem.*, **33,** 99–1005.

WELSH, M.J. & LIEDTKE, C.M. (1986). Chloride and potassium channels in cystic fibrosis airway epithelia. *Nature*, **322,** 467–470.

WIDDICOMBE, J.H., WELSH, M.J. & FINKBEINER, W.E. (1985). Cystic fibrosis decreases the apical membrane chloride permeability of monolayers cultured from cells of tracheal epithelium. *Proc. Natl. Acad. Sci. U.S.A.*, **82,** 6167–6171.

WILLUMSEN, N.J., DAVIS, C.W. & BOUCHER, R.C. (1989). Intracellular Cl^- activity and cellular pathways in cultured human airway epithelium. *Am. J. Physiol.*, **256,** C1033–C1044.

WU, R., YANKASKAS, J., CHENG, E., KNOWLES, M.R. & BOUCHER, R.C. (1985). Growth and differentiation of human nasal epithelial cells in culture. Serum free, hormone-supplemented medium and proteoglycan synthesis. *Am. Rev. Respir. Dis.*, **132,** 311–320.

(Received January 9, 1992
Accepted February 17, 1992)

Br. J. Pharmacol. (1992), **106**, 783–789 © Macmillan Press Ltd, 1992

GR94839, a κ-opioid agonist with limited access to the central nervous system, has antinociceptive activity

[1]H. Rogers, P.J. Birch, S.M. Harrison, †E. Palmer, †G.R. Manchee, *D.B. Judd, *A. Naylor, *D.I.C. Scopes & A.G. Hayes

Departments of Neuropharmacology, †Biochemical Pharmacology and *Medicinal Chemistry, Glaxo Group Research Ltd, Ware, Herts SG12 0DP

1 The pharmacological profile of GR94839, a κ-opioid agonist with limited access to the central nervous system, has been investigated. Its antinociceptive activity has been compared with that of GR103545, a centrally-penetrating κ-agonist and ICI204448, the previously described peripherally-selective κ-agonist.

2 GR94839 was a potent agonist in the rabbit vas deferens *in vitro* assay for κ-opioid receptors (IC_{50}: 1.4 ± 0.3 nM; $n = 6$), but had limited activity at μ- or δ-opioid receptors.

3 In the mouse abdominal constriction test, GR94839 was 238 fold more potent when given i.c.v. (ED_{50}: 0.008 (0.004–0.029) mg kg^{-1}; $n = 18$) than when s.c. (ED_{50}: 1.9 (0.7–3.1) mg kg^{-1}; $n = 30$). In comparison, GR103545 was equipotent when given i.c.v. or s.c.

4 After intravenous administration, the maximum plasma to brain concentration-ratio attained by GR94839 was 18 compared with 2 for GR85571, a structurally-related κ-agonist that is centrally-penetrating.

5 GR94839 inhibited the 2nd phase of the rat formalin response at doses 7 fold lower than those required to inhibit the 1st phase (ED_{50} vs 1st phase: 10.2 (6.7–17.1) mg kg^{-1}, s.c.; ED_{50} vs 2nd phase: 1.4 (1.0–1.8) mg kg^{-1}, s.c.; $n = 18$). GR103545 was equipotent against the two phases.

6 Intraplantar administration of the opioid antagonists, norbinaltorphimine (100 μg) or naltrexone (1 μg), reversed the antinociceptive effect of systemic GR94839 (3 mg kg^{-1}, s.c.) against the 2nd phase of the formalin response and intraplantar injection of GR94839 (30–100 μg) selectively inhibited the 2nd phase.

7 GR94839 and ICI204448 reversed the hyperalgesia in the zymosan-inflamed rat paw at doses (ED_{50} GR94839: 2.0 (1.1–3.2) mg kg^{-1}, s.c.; ED_{50} ICI204448: 1.2 (0.8–1.7) mg kg^{-1}, s.c.), lower than those required to raise the noxious pressure threshold in the non-inflamed paw (ED_{50} GR94839: 16.4 (8.6–46.7) mg kg^{-1}, s.c.; ED_{50} ICI204448: 68.0 (22.1–32000) mg kg^{-1}, s.c.). GR103545 raised the noxious presure threshold in the inflamed and non-inflamed paws at the same doses.

8 GR94839 was sedative in the rat rotarod test (ED_{50}: 35 (12–245) mg kg^{-1}, s.c.) at doses higher than those required to inhibit the 2nd phase of the formalin response or reverse hyperalgesia in the zymosan-inflamed rat paw. The doses were comparable to those that inhibited the 1st phase of the formalin response and raised the noxious pressure threshold in the non-inflamed paw.

9 The results suggest that GR94839 is a selective κ-agonist which has antinociceptive activity against inflammatory pain at doses that produce limited central effects. These antinociceptive effects are probably mediated at peripheral opioid receptors.

Keywords: κ-Opioid agonist; antinociception; peripheral opioid receptor

Introduction

There is evidence to suggest that κ-opioid receptors are present on the peripheral terminals of primary afferent neurones (Stein *et al.*, 1989) and that activation of these receptors reduces hyperalgesia in a rat model of arthritic pain. A κ-opioid agonist, ICI204448, which has limited access to the central nervous system has been described previously by Shaw and colleagues (1989), however, the analgesic profile of this compound has not been investigated in detail. A κ-opioid agonist with limited access to the central nervous system could be antinociceptive against inflammatory pain but lack the adverse side-effects, e.g. sedation and dysphoria, of a centrally-penetrating κ-agonist. This paper describes the pharmacological profile of a second peripherally-selective κ-agonist, GR94839, including its activity in nociceptive tests with an inflammatory pain component.

GR94839 is a κ-opioid receptor agonist, closely related in structure to the potent κ-agonist, GR103545 (Hayes *et al.*, 1990). GR103545 has the behavioural profile of a centrally-penetrating κ-agonist, having antinociceptive activity in a variety of tests and producing sedation and diuresis (Hayes *et al.*, 1990). In the present study pharmacological and biochemical data suggest that GR94839 is a potent κ-agonist but, unlike GR103545, has limited access to the cental nervous system. The antinociceptive activity of GR94839 is compared with GR103545 and ICI204448. Also, the plasma and brain concentrations of GR94839 are compared with a centrally-penetrating κ-agonist, GR85571. The structures of the κ-agonists are shown in Figure 1. A preliminary communication of these results has been made (Hayes *et al.*, 1991).

Methods

Isolated tissue preparations

Vasa deferentia were removed from Californian rabbits (weight range 2.5–3.5 kg), Random Hooded rats (weight range 150–200 g) and Golden Syrian hamsters (weight range

[1] Author for correspondence.

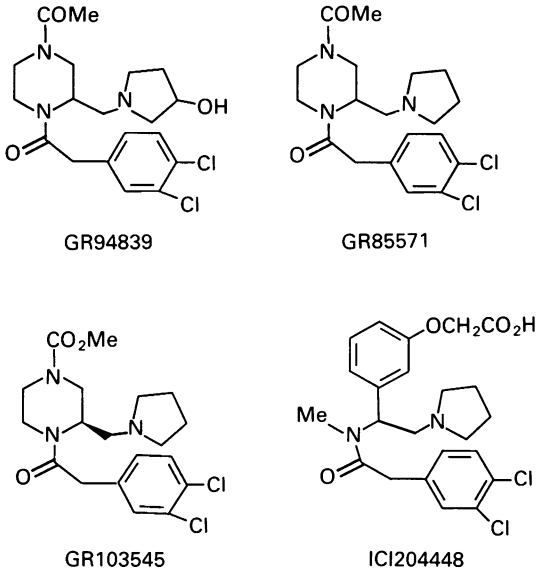

Figure 1 Chemical structures of the κ-opioid agonists: GR94839, GR85571, GR103545, and ICI204448.

250–300 g) and suspended between platinum electrodes in 5 ml organ baths containing Krebs-Henseleit solution of composition (mM): NaCl 118, $NaHCO_3$ 29, glucose 11, KCl 4.7, $CaCl_2$ 2.5 and KH_2PO_4 1.2, pH 7.4, gassed with 95% O_2:5% CO_2 at 37°C. Contractions were evoked by field-stimulation with a single square-wave pulse (width 0.5 ms; frequency 0.1 Hz; 1 V above maximum voltage) in rabbit or rat vasa deferentia, and a train of three similar pulses 200 ms apart in the hamster vas deferens. Cumulative concentration-response curves were constructed and the IC_{50} values (50% inhibition of the twitch height) ± standard error of the mean were determined where appropriate.

In vivo *experiments*

Abdominal constriction test Male CRH mice (weight range 14–22 g) were used. Intraperitoneal injections of acetylcholine 3 mg kg^{-1}, carba-prostacyclin 0.1 mg kg^{-1}, or acetic acid 0.6% (dose volume 10 ml kg^{-1}) were used to induce abdominal constrictions. The number of abdominal constrictions occurring 0–3.5 min post-acetylcholine, 0–10 min post-carba-prostacyclin and 5–20 min post-acetic acid injection were recorded. Kappa agonists were administered subcutaneously (dose volume 10 ml kg^{-1}) or directly into the cerebral ventricles (i.c.v.; dose volume 5 μl) 30 min prior to the observation period.

Determination of plasma and brain concentrations GR94839 or GR85571 were administered to male albino rats ($n = 2$; weight range 150–200 g) at 10 mg kg^{-1} i.v. via the tail vein. At various times post-dosing, animals were anaesthetized and exsanguinated via the dorsal aorta. The brain was then removed and homogenized with acetone, the samples centrifuged, and the supernatant removed. This was evaporated to dryness, resuspended in water and subjected to extraction on diol columns. Drug was extracted from the plasma by solid phase extraction with diol columns. The eluate was analysed by high performance liquid chromatography using a cyano spherisorb column and a mobile phase of sodium acetate (0.01 M, pH 4.2): acetonitrile (35:65 volume:volume).

Formalin-induced paw licking Male Random Hooded rats (weight range 50–80 g) were used. A solution of 5% formalin in phosphate-buffered saline (pH 7.4; dose volume 50 μl) was injected into the pad of one-hind-paw (intraplantar). A biphasic licking of the injected paw was observed, and the duration of licking was recorded 0–5 min (1st phase) and 15–30 min post-formalin injection (2nd phase). The 1st phase of the formalin response is thought to be due to direct activation of sensory nerve terminals by formalin and the 2nd phase is thought to involve local inflammation (Hunskaar & Hole, 1986). GR94839 or GR103545 were administered s.c. 30 min before each phase of licking in separate rats, and ICI204448 was injected 15 min before the 1st phase. The dose volume used was 4 ml kg^{-1}. In some experiments, drugs were administered intraplantar (dose volume 50 μl) immediately before the 1st or 2nd phases of licking.

Zymosan-induced hyperalgesia Male Random Hooded rats (weight range 80–120 g) or male Dunkin-Hartley guinea-pigs (weight range 150–220 g) were used. Intraplantar injection of 100 μl of a 20% suspension of zymosan in saline lowered the noxious pressure threshold of the injected paw at greater than 3 h post-zymosan in both guinea-pigs and rats. The noxious pressure threshold of each hind-paw was determined, before intraplantar injection of zymosan and at 5 h post-injection in rats and at 3 h and 4 h post-injection in guinea-pigs. Kappa-agonists were administered s.c. 4.5 h post-zymosan in rats (dose volume 4 ml kg^{-1}) and 3.5 h post-zymosan in guinea-pigs (dose volume 2 ml kg^{-1}).

Rotarod Male Random Hooded rats (weight range 80–120 g) were used. Rats were placed on a rotating horizontal rod which accelerated in a linear fashion from 0 to 50 rev min^{-1}. The score (proportional to the acceleration of the tread-mill) when the rat fell from the rod was recorded as a measure of the incapacitating effect of the drug. κ-Agonists or saline were administered 30 min before testing.

Experimental design and data analysis

Behavioural tests were performed on 6 or 8 animals/drug treatment. In some cases data have been pooled from more than one experiment. In all experiments animals were colour-coded and drug treatments randomized between groups. Observers were unaware of the drug treatments that animals had received. The methods of Finney (1964) were used to determine regression slopes, linearity and parrallelism for dose-response curves and also the ED_{50} values (50% reduction in response compared to saline pretreated animals) with 95% confidence limits. For the noxious pressure threshold experiments, the ED_{50} value in the inflamed paw (50% reversal of the fall in noxious pressure threshold) and the ED_{30} value in the non-inflamed paw (30% increase in noxious pressure threshold) were determined. The significance of drug effects was tested by a Student's unpaired t test ($P < 0.05$).

Drugs and solutions

Drugs were freshly made up in saline for each experiment, and administered in the dose volumes indicated. A control group of animals injected with an appropriate volume of saline was included in each experiment. Drugs were obtained from the following sources: acetylcholine (Sigma), carba-prostacyclin (Cayman Chemical Co. Inc.), [D-Ala^2, MePhe^4, Gly(ol)^5] enkaphalin (DAMGO, Bachem), [D-Pen^2,D-Pen^5] enkephalin (DPDPE, Bachem), ethylketocyclazocine methane sulphonate (EKC; Sterling-Winthrop), ICI204448 (**R,S**)-3-[1-[[(3,4-dichlorophenyl) acetyl] methylamino]-2-(pyrrolidinyl) ethyl] phenoxyacetic acid hydrochloride, Cambridge Research Biochemicals), morphine hydrochloride (Macfarlan-Smith), naltrexone hydrochloride (Endo). GR85571 (4-acetyl-1-[(3,4-dichlorophenyl) acetyl] -2 - (1-pyrrolidinylmethyl) piperazine), GR94839 (4-acetyl-1-(3,4-dichlorophenyl)acetyl]-2-[(3-hydroxy-1-pyrrolidinyl) methyl] piperazine), GR103545 ((**R**)-methyl 4-[(3,4-dichlorophenyl)acetyl]-3- (1-pyrrolidinylmethyl) -1-piperazinecarboxylate fumarate), M8008 (16-methylcyprenorphine), and norbinaltorphimine (norBNI) were all synthesized in the Department of Medicinal Chemistry, Glaxo Group Research Ltd, Ware.

Results

Field-stimulated vasa deferentia

In the rabbit vas deferens assay for κ-opioid receptors, GR94839 was a potent agonist, inhibiting the electrically-evoked twitch with an IC_{50} value of 1.4 ± 0.3 nM ($n = 6$). For comparison, the κ-agonist, ethylketocyclazocine had an IC_{50} value of 36 ± 8 nM ($n = 6$). Pre-equilibration of the tissue with naloxone (300 nM) for 30 min caused a rightward shift of the dose-response curve to GR94839 ($n = 4$). The pK_B value for naloxone antagonizing GR94839 was 7.5 ± 0.1 ($n = 4$), which is consistent with an action of GR94839 on κ-receptors. In the rat vas deferens assay for μ-opioid receptors, GR94839 at a dose of 100 μM reduced the twitch height by 42% ($n = 2$) whereas the selective μ-agonist [D-Ala^2,MePhe^4,Gly^5-ol]enkephalin (DAMGO) had an IC_{50} value of approximately 7 μM ($n = 2$). In the hamster vas deferens assay for δ-opioid receptors, GR94839 had an IC_{50} value of approximately 13 μM ($n = 2$) compared with approximately 0.12 μM for the selective δ-agonist, D-Pen^2,D-Pen^5]enkephalin (DPDPE; $n = 2$). Thus, *in vitro*, GR94839 was a potent κ-agonist with limited activity at μ- or δ-receptors.

In vitro experiments

Mouse abdominal constriction test In the mouse abdominal constriction test, GR94839 had EC_{50} values of 1.9 (0.7–3.1) mg kg^{-1}, s.c. ($n = 30$) and 0.16 (0.08–0.57) μg ($n = 18$) which is equivalent to approximately 0.008 mg kg^{-1}, i.c.v. Thus, the ratio of ED_{50} values after subcutaneous administration and i.c.v. administration was 238. In contrast, GR103545 had very similar ED_{50} values following subcutaneous (0.015 (0.005–0.025) mg kg^{-1}) and i.c.v. administration (0.010 (0.005–0.020) mg kg^{-1}), giving a subcutaneous to i.c.v. ED_{50} ratio of 1.5 ($n = 6$). ICI204448 was more potent given i.c.v. than subcutaneously with ED_{50} values of 0.14 (0.04–0.41) mg kg^{-1}, i.c.v. and 4.4 (2.5–7.4) mg kg^{-1}, s.c. ($n = 6$) with a subcutaneous to i.c.v. ED_{50} ratio of 31. GR94839 also inhibited carba-prostacyclin-induced and acetic acid-induced abdominal constrictions with ED_{50} values of 0.8 (0.3–1.7) and 4.1 (2.6–6.7) mg kg^{-1}, s.c. respectively ($n = 6$).

The inhibition produced by GR94839 at a dose of 10 mg kg^{-1}, s.c. was reversed by a co-injection of the opioid antagonist, naltrexone (10 mg kg^{-1}, s.c.) i.e. mean number of abdominal constrictions: saline 8.0 ± 0.7; naltrexone 8.7 ± 1.4; GR94839 0 ± 0; GR94839 + naltrexone 7.7 ± 1.1 ($n = 6$).

Plasma and brain concentration-time profiles of GR94839 and GR85571 The plasma and brain concentrations of GR94839 were measured up to 5 h following an i.v. injection at 10 mg kg^{-1} (Figure 2). Peak levels of GR94839 observed in plasma (1282 ng ml^{-1} at 15 min) were significantly higher than those observed in brain tissue (103 ng g^{-1} at 30 min). The maximum plasma:brain concentration ratio attained by GR94839 was 18, 15 min after injection. GR85571 has a similar *in vitro* potency to GR94839 (IC_{50} in rabbit vas deferens: 10 nM; $n = 2$) but has an ED_{50} in the mouse acetylcholine-induced abdominal constriction test of 0.08 (0.04–0.15) mg kg^{-1}, s.c. ($n = 6$), suggesting that it readily penetrates into the central nervous system. The concentrations of GR85571 achieved in brain and plasma following a dose of 10 mg kg^{-1} i.v. were very similar throughout the time-course and similar to the plasma levels attained by GR94839. The maximum plasma:brain concentration ratio attained was 2, 30 min after injection. These findings are consistent with GR94839 having limited access to the central nervous system.

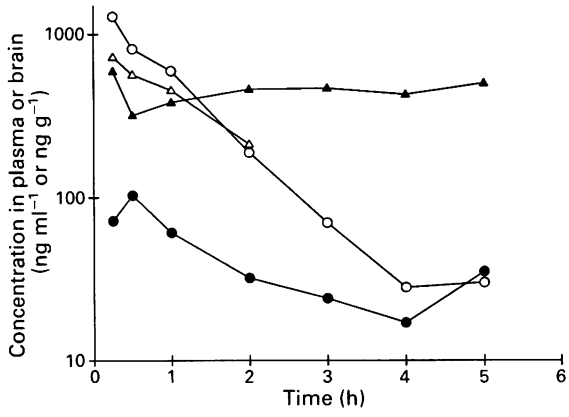

Figure 2 A comparison of the plasma and brain concentration-time profiles for GR94839 and GR85571. Rats were dosed ($n = 2$/drug) with either GR94839 (circles) or GR85571 (triangles) at 10 mg kg^{-1}, i.v. and killed at various times post-dosing, shown on the abscissa scale. The concentrations of drug in the plasma (ng ml^{-1}; open symbols) or the brain (ng g^{-1}; closed symbols) were measured by h.p.l.c. and are shown on the ordinate scale. See Methods for further technical details.

Rat formalin-induced paw licking GR94839 (1–10 mg kg^{-1}, s.c.) caused a significant decrease in the duration of licking recorded in the 2nd phase of the formalin response (Figure 3) with the highest dose virtually abolishing licking. However, the same doses had a lesser effect on licking in the 1st phase (Figure 3), and a dose of GR94839 30 mg kg^{-1}, s.c., was required to cause a marked inhibition of the 1st phase. The ED_{50} values for GR94839 vs the 1st and 2nd phases of the formalin response are given in Table 1. ICI204448 (1–100 mg kg^{-1}, s.c.) caused a decrease of the 2nd phase of the formalin response at slightly lower doses than inhibited the 1st phase (Table 1). In contrast, the centrally-penetrating κ-agonist, GR103545 was equi-effective against both phases (Table 1).

The inhibition of the 2nd phase by GR94839 (3 mg kg^{-1}, s.c.) was reversed by co-administration of naltrexone (0.3 mg kg^{-1}, s.c.; duration of licking in the 2nd phase: saline 153 ± 18 s; GR94839 19 ± 5 s; naltrexone 172 ± 18 s; GR94839 + naltrexone 141 ± 24 s; $n = 6$). However, co-administration of the μ/δ-opioid receptor antagonist, M8008 (Smith, 1987; Birch *et al.*, 1988) at a dose of 1 mg kg^{-1}, s.c., caused no significant reversal of the inhibition of the 2nd phase by the same dose of GR94839 (duration of licking in the 2nd phase: saline 136 ± 13 s; GR94839 37 ± 5 s; M8008

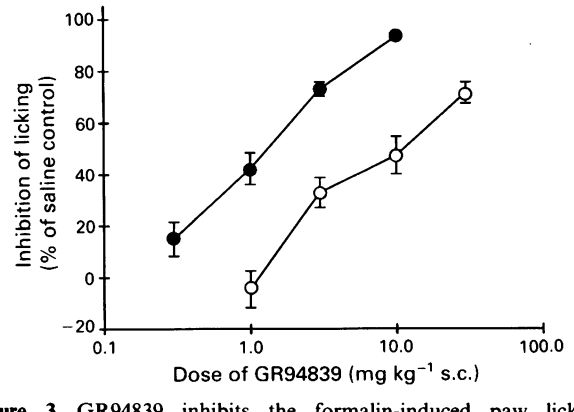

Figure 3 GR94839 inhibits the formalin-induced paw licking observed 0–5 min (○) or 15–30 min post-formalin (●) in a dose-dependent manner. Ordinate scale: inhibition of licking expressed as a percentage of licking in saline dosed rats. Abscissa scale: dose of GR94839 mg kg^{-1}, s.c. Rats were given GR94839 s.c. 30 min before intraplantar injection of formalin ($n = 18$).

Table 1 A comparison of the ED_{50} values for inhibition of the 1st and 2nd phases of the rat formalin response

κ-Agonist	ED_{50} mg kg^{-1} s.c., (95% confidence levels) 1st phase	2nd phase	1st/2nd	(n)
GR94839	10.2 (6.7–17.1)	1.4 (1.0–1.8)	7.3	(18)
GR103545	0.0004 (0.0002–0.0013)	0.0004 (0.0002–0.0005)	1	(6)
ICI204448	49% ↓ at 30 mg kg^{-1}	8.9 (5.4–36.5)	≃3.3	(6)

134 ± 14 s; GR94839 + M8008 68 ± 9 s; $n = 12$). M8008 (1 mg kg^{-1}, s.c.; co-injection) reversed the inhibition of the 2nd phase by the μ-agonist, morphine (duration of licking in 2nd phase: saline 163 ± 11 s; M8008 131 ± 30 s; morphine 0 ± 0 s; morphine + M8008 164 ± 17 s ($n = 6$)).

To see whether GR94839 could inhibit the 2nd phase of the formalin response by a local action in the paw, GR94839 (30–100 μg; $n = 6$–12) was injected into the same paw as formalin immediately before either phase of the formalin response. Following intraplantar injection of saline the duration of licking in the 2nd phase was 147 ± 10 s, which was reduced to 109 ± 15 s by GR94839 at a dose of 30 μg and to 55 ± 10 s ($P < 0.05$ vs saline) at a dose of 100 μg. The same doses of GR94839 had no effect on the duration of paw licking when injected into the contralateral paw (GR94938 30 μg: 155 ± 12 s; GR94839 100 μg: 142 ± 9 s). GR94839 (30–100 μg; $n = 6$) also failed to inhibit licking in the 1st phase of the formalin response when injected into the ipsilateral paw immediately before formalin injection (saline: 75 ± 6 s; GR94839 30 μg: 75 ± 3; GR94839 100 μg: 73 ± 8 s).

To establish that the inhibition of the 2nd phase by intraplantar injection of GR94839 was a receptor-mediated effect and not due to local anaesthesia, the effect of pretreatment with systemic opioid antagonists was examined. Naltrexone (0.3 mg kg^{-1}, s.c.; 30 min pretreatment) reversed the effect of intraplantar GR94839 (duration of licking in 2nd phase: saline 172 ± 12 s; GR94839 100 μg 84 ± 10 s; GR94839 + naltrexone 144 ± 21 s; $n = 6$). M8008 at a dose of 1 mg kg^{-1}, s.c., had no effect on the inhibition of licking by intraplantar GR94839 (duration of licking in 2nd phase: saline 110 ± 19 s; M8008 136 ± 6 s; GR94839 67 ± 19 s; GR94839 + M8008 61 ± 12 s; $n = 6$).

Intraplantar injection of the non-selective opioid antagonist, naltrexone (1 μg; $n = 18$) or the κ-receptor selective antagonist, norbinaltorphimine (100 μg; $n = 6$), immediately before the 2nd phase of licking, reversed partially, but significantly, the inhibition of the 2nd phase of the formalin response by systemic GR94839 (3 mg kg^{-1}, s.c.; 15 min before formalin; Figure 4). Injection of the antagonists alone into the formalin-injected paw had no effect on the duration of licking in the 2nd phase, and injection of antagonist into the contralateral paw did not reverse the antinociceptive effects of systemic GR94839.

Zymosan-induced hyperalgesia In the rat, GR94839 (0.3–10 mg kg^{-1}, s.c.) reversed significantly the hyperalgesia observed in the zymosan-injected paw (Figure 5). Higher doses of GR94839 (10–30 mg kg^{-1}, s.c.) were required to raise significantly the noxious presure threshold in the normal paw. The ED_{50} value for GR94839 in the inflamed paw and the ED_{30} value in the non-inflamed paw are given in Table 2. ICI204448 also reversed the hyperalgesia in the inflamed paw at lower doses than raised the noxious pressure threshold in the non-inflamed paw (Table 2), whereas for GR103545 the ED_{50} values for both paws were similar. Thus, at doses similar to those that inhibit the 2nd phase of the formalin response GR94839 reversed the zymosan-induced hyperalgesia.

In the guinea-pig, GR94839 (0.3–10 mg kg^{-1}, s.c.) raised the noxious pressure threshold in the inflamed and non-inflamed paws equally (ED_{50} inflamed paw: 1.4 (0.2–2.6) mg kg^{-1}, s.c.; ED_{30} non-inflamed paw: 1.0 (0.2–2.6) mg kg^{-1}, s.c. ($n = 16$). GR103545 was also equipotent in raising the noxious pressure threshold in the inflamed and non-inflamed paws (ED_{50} inflamed paw: 0.4 (0.2–1.1) μg kg^{-1}, s.c.; ED_{30} non-inflamed paw: 0.12 (0.01–0.67) μg kg^{-1}, s.c. ($n = 16$)).

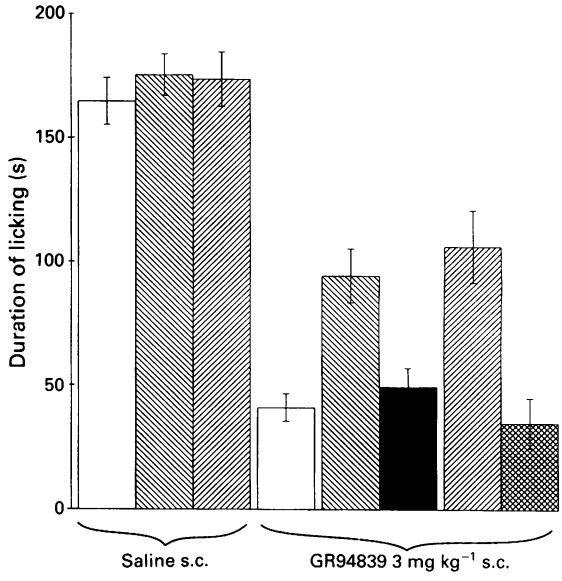

Figure 4 Intraplantar injection of naltrexone or norbinaltorphimine antagonizes the inhibition of the 2nd phase of the formalin response by systemic GR94839. Rats were injected with GR94839 3 mg kg^{-1} or saline s.c. (as indicated beneath the histogram) 15 min before intraplantar injection of formalin. Fifteen min after formalin injection saline or the opioid antagonists were injected intraplantar either ipsilateral or contralateral to the formalin injection ($n = 6$–18). Open columns indicate an ipsilateral saline injection; left-hatched columns, ipsilateral naltrexone 1 μg; and right-hatched columns, ipsilateral norbinaltorphimine 100 μg. The solid column indicates a contralateral injection of naltrexone 1 μg and the cross-hatched column a contralateral injection of norbinaltorphimine 100 μg. Ordinate scale: duration of licking 15–30 min post-formalin. *$P < 0.05$ vs saline s.c. and ipsilateral saline intraplantar. **$P < 0.05$ vs GR94839 3 mg kg^{-1}, s.c. and ipsilateral saline intraplantar.

Rat rotarod GR94839 (10–100 mg kg^{-1}, s.c.) decreased the rotarod score. The rats were considered to be mildly sedated at these doses. ED_{50} values for GR94839 and also ICI204448 and GR103545 are given in Table 3. The doses of GR94839 that had sedative effects were similar to those that decreased the duration of licking in the 1st phase of the rat formalin response and raised the noxious pressure threshold in the non-inflamed paw of the rat.

Discussion

It has been shown previously that opioid agonists selective for the μ,κ-, and δ-opioid receptor subtypes can mediate antinociception in a rat model of arthritis by activation of

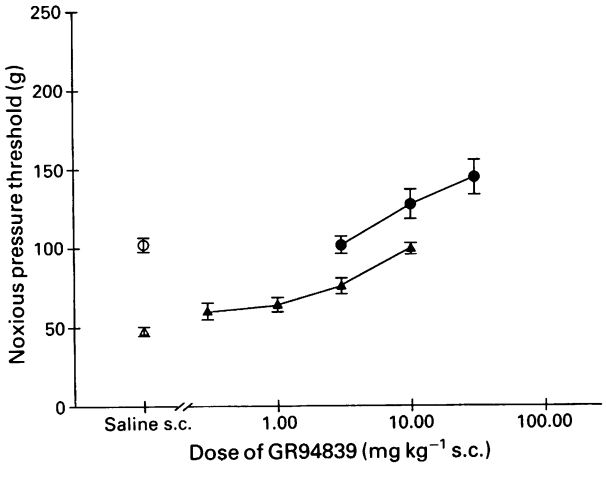

Figure 5 GR94839 raises the noxious pressure threshold in the zymosan-inflamed and the normal paw of the rat. Zymosan was injected into one hind-paw and the noxious pressure threshold of the zymosan-injected paw (triangles) and the non-injected paw (circles), was measured 5 h post-injection. GR94839 (closed symbols) or saline (open symbols) was administered s.c., 4.5 h post-zymosan ($n = 18$). Ordinate scale: paw pressure threshold (g). Abscissa scale: dose of GR94839 mg kg^{-1}, s.c.

opioid receptors in the periphery (Stein *et al.*, 1989). These experiments suggest that an opioid agonist with limited access to the CNS could be analgesic without possessing the undersirable effects of centrally-acting opioids, e.g. for μ-opioids, dependence and respiratory depression and for κ-opioids, sedation and dysphoria. Peripherally-selective μ- or δ-agonists could have effects on gastrointestinal function (Birch *et al.*, 1986; Tavani *et al.*, 1990), thus a peripherally-selective κ-agonist may be the best candidate for a novel analgesic. The pharmacological and biochemical profile described for the κ-agonist, GR94839, in the present study suggests that it has both limited access to the CNS and can mediate antinociception at a peripheral site and may thus have potential as an analgesic.

Two sets of experiments strongly suggest that GR94839 has limited access to the central nervous system. In the mouse acetylcholine-induced abdominal constriction test, GR94839 was weakly active when given subcutaneously, but underwent a marked enhancement of potency when it was given i.c.v. The lack of potency after systemic administration was not dependent on the agent used to induce abdominal constriction, and the effects were opioid receptor-mediated as they were naltrexone reversible. In fact the effect seen after systemic administration was probably due to penetration of GR94839 into the central nervous system, because the potency correlated poorly with the nanomolar potency the compound has for κ-receptors in the rabbit vas deferens, whereas the potency i.c.v. correlated well. In contrast, the potent, centrally penetrating κ-agonist, GR103545 (Hayes *et al.*, 1990), was highly effective and equipotent at inhibiting acetylcholine-induced abdominal constrictions after subcutaneous or i.c.v. administration. Co-administration of GR94839 with acetylcholine failed to inhibit abdominal constrictions, suggesting that the site of action of GR94839 is distant from the site of injection and as the pretreatment time for intraperitoneal injection of GR94839 was increased the ability of GR94839 to inhibit abdominal constrictions increased (data not shown). This could suggest that GR94839 gains slow access to its site of action i.e. the central nervous system. These findings together suggest that the ratio of the subcutaneous and i.c.v. ED_{50} values for GR94839 and ICI204448 in the abdominal constriction test, 238 and 31 respectively, reflects the ability of the compounds to enter the CNS.

Table 3 A comparison of the ED_{50} values in the rat rotarod test for sedation

κ-Agonist	*Rotarod test* (ED_{50} mg kg^{-1}, s.c.)	(n)
GR94839	35 (12–245)	(6)
GR103545	0.0017 (0.0013–0.0023)	(8)
ICI204448	Inactive at 30 mg kg^{-1}	(6)

Measurement of the plasma and CNS levels of GR94839 following i.v. administration in the rat, showed that the levels of GR94839 attained in the CNS were always lower than the levels of GR85571, a structurally similar but centrally-penetrating κ-agonist. This finding is direct evidence for the inability of GR94839 to accumulate within the CNS. The lack of penetration of GR94839 into the CNS may be due to its lower lipophilicity: the log P of GR94839 is 1.25, compared with 3.14 for GR103545 and 2.47 for GR85571.

It has been suggested that opioid analgesics are more effective at peripheral opioid receptors in the presence of inflammation (Ferreira & Nakamura, 1979; Stein *et al.*, 1988; 1989; Bartho *et al.*, 1990). For this reason, the antinociceptive activity of GR94839 was investigated in two nociceptive tests that had an inflammatory pain component: the rat formalin-induced licking test and the zymosan-induced mechanical hyperalgesia model. In the rat formalin test, a biphasic response has been described both behaviourally (Dubuisson & Dennis, 1977; Hunskaar *et al.*, 1985; Wheeler-Aceto *et al.*, 1990) and electrophysiologically (Banna *et al.*, 1986; Heapy *et al.*, 1987; Dickenson & Sullivan, 1987). The first phase is thought to be due to a direct activation of C-fibres because it is only inhibited by high doses of non-steroidal anti-inflammatory drugs but is inhibited by centrally-acting opioids (Dickenson & Sullivan, 1987; Shibata *et al.*, 1989). The 2nd phase is thought to have a peripheral inflammatory component because it is selectively inhibited by indomethacin and steroids (Hunskaar & Hole, 1986; Hunskaar *et al.*, 1987; Shibata *et al.*, 1989), and bradykinin (B_2) antagonists (Haley *et al.*, 1989), although other studies suggest it can in part be attributed to central plasticity (Dickenson & Sullivan, 1987; Coderre *et al.*, 1990).

In the present study, it was found that not only did systemic GR94839 inhibit the 2nd phase of the formalin response at doses 7 fold lower than those required to inhibit the 1st phase, but local injection of GR94839 selectively inhibited the 2nd phase. Together the data suggest that GR94839 is having its antinociceptive action at a peripheral locus during the 2nd phase of the formalin response. The

Table 2 A comparison of the ED_{50} values to raise the noxious pressure threshold in the zymosan-inflamed or non-inflamed paws of the rat

κ-Agonist	*Non-inflamed* (ED_{50}, mg kg^{-1})	*Inflamed* (ED_{30}, mg kg^{-1})	*Non-inf. /Inf.*	(n)
GR94839	16.4 (8.6–46.7)	2.0 (1.1–3.2)	8.2	(18)
GR103545	0.0011 (0.0008–0.0016)	0.0012 (0.0008–0.0017)	1	(24)
ICI204448	68.0 (22.1–32000)	19.5 (13.3–32.7)	3.5	(8)

antinociception was mediated by opioid receptor activation (rather than local anaesthesia) because it was reversed by systemic naltrexone. The peripherally-selective κ-agonist, ICI204448 also showed some selectivity (approximately 3 fold) for the 2nd phase of the formalin response but was less potent than GR94839. GR103545, in contrast, was equipotent versus both phases of the licking response, consistent with the previously demonstrated ability of κ-opioids to inhibit the formalin response at a central site (Calcagnetti *et al.*, 1988; Pelissier *et al.*, 1990). The opioid receptor activated is probably a κ-receptor because the inhibition by intraplantar GR94839 was not blocked by the μ/δ-antagonist, M8008, at selective doses (Birch *et al.*, 1988). Further evidence for a peripheral activation of κ-receptors by GR94839 was obtained when the inhibition of the 2nd phase of the formalin response was reversed by local injection of naltrexone, and the κ-selective opioid antagonist, norbinaltorphimine. The present findings are in agreement with previous studies (Abbott, 1988; Haley *et al.*, 1990) where a peripheral inhibition of the formalin response by κ-opioids was demonstrated, although we were not able to demonstrate an inhibition of the 1st phase on local administration (Haley *et al.*, 1990). This difference between the studies may be due to the intensity of spinal cord nerve activity not being directly proportional to the behavioural response.

In a second model of nociception associated with inflammation, the rat zymosan-induced mechanical hyperalgesia model, GR94839 caused a significant reversal of inflammation-induced mechanical hyperalgesia at doses that had no significant effect on the noxious pressure threshold in the non-inflamed paw. The doses that reversed the hyperalgesia were similar to the doses that inhibited the 2nd phase of the formalin-induced paw licking, whereas the doses that raised the non-inflamed paw noxious pressure threshold corresponded with the doses that inhibited the 1st phase of the formalin response. The latter were presumably central effects, as these doses are mildly sedative and impair performance in the rat rotarod test. ICI204448 showed less selectivity against the noxious pressure threshold of the inflamed paw than GR94839 and was less potent, whereas GR103545 was highly effective and equipotent at raising the noxious pressure threshold in both paws. Thus, in a second pain model with an inflammatory component GR94839 and ICI204448 have peripheral antinociceptive activity.

The mechanism by which GR94839 mediates antinociception in the periphery has not been rigorously investigated in the present study. Kappa opioids are known to have a diuretic action at a peripheral site (Leander, 1983). However, the local action of GR94839 in the formalin test would exclude this systemic action from mediating the antinociceptive effect. κ-Opioids have been shown to inhibit electrically-evoked plasma protein extravasation in the hind-paw of rats (Bartho & Szolcsanyi, 1981; Smith & Buchan, 1984). Also, a recent study showed that the enhanced antinociceptive activity of morphine against inflammatory pain was eliminated by capsaicin-pretreatment (Bartho *et al.*, 1990). Both studies suggest that the opioid receptors are located on sensory nerve terminals, and indeed κ-opioids have been shown to reduce the spontaneous discharge of sensory afferents in the inflamed knee joint of the cat (Russell *et al.*, 1987).

The doses of GR94839 required locally or systemically to inhibit the 2nd phase of formalin-induced licking and the zymosan-induced hyperalgesia were higher than one would predict from the *in vitro* potency of the compounds and the doses required to inhibit acetylcholine-induced abdominal constriction after i.c.v. administration. This may reflect the density of opioid receptors peripherally or the efficiency of coupling of peripheral receptors to second messenger systems. Unfortunately, the relatively high doses of GR94839 that are required to activate peripheral κ-receptors compared with central receptors may have resulted in the inability to demonstrate a selective effect of GR94839 in the inflamed paw of the guinea-pig. The guinea-pig has a higher density of κ-receptors in the CNS than the rat, and is thought to resemble man in this respect (Mansour *et al.*, 1988). A significantly greater κ-receptor reserve in the central nervous system of the guinea-pig than the periphery, could mean that lower concentrations of GR94839 are required to elicit central effects than peripheral effects. As man resembles the guinea-pig in having abundant central κ-receptors (Mansour *et al.*, 1988), a compound possessing a better separation of central and peripheral effects than GR94839 would be required to be an effective analgesic in the absence of central side-effects.

References

ABBOTT, F.V. (1988). Peripheral and central antinociceptive actions of ethylketocyclazocine in the formalin test. *Eur. J. Pharmacol.*, **152**, 93–98.

BANNA, N.R., SAADE, N.E., ATWEH, S.F. & JABBUR, S.J. (1986). Prolonged discharge of wide dynamic range spinal neurons evoked by formaldehyde injected in their cutaneous receptive fields. *Exp. Neurol.*, **93**, 275–278.

BARTHO, L., STEIN, C. & HERZ, A. (1990). Involvement of capsaicin-sensitive neurones in hyperalgesia and enhanced opioid antinociception in inflammation. *Naunyn-Schmiederbergs Arch. Pharmacol.*, **342**, 666–670.

BARTHO, L. & SZOLCSANYI, J (1981). Opiate agonists inhibit neurogenic plasma extravasation in the rat. *Eur. J. Pharmacol.*, **73**, 101–104.

BIRCH, P.J., HAYES, A.G., SHEEHAN, M.J. & TYERS, M.B. (1988). In vivo studies with the opioid antagonist 16-methyl cyprenorphine. *J. Pharm. Pharmacol.*, **40**, 213–214.

BIRCH, P.J., HAYES, A.G. & SPRAGGS, C.F. (1986). Studies on the δ-opioid receptor-mediated inhibition of I_{sc} in the isolated guinea-pig ileal mucosal preparation. *Br. J. Pharmacol.*, **89**, 833P.

CALCAGNETTI, D.J., HELMSTETTER, F.J. & FANSELOW, M.S. (1988). Analgesia produced by centrally administered DAGO, DPDPE and U50488H in the formalin test. *Eur. J. Pharmacol.*, **153**, 117–122.

CODERRE, T.J., VACCARINO, A.L. & MELZACK, R. (1990). Central nervous system plasticity in the tonic pain response to subcutaneous formalin injection. *Brain Res.*, **535**, 155–158.

DICKENSON, A.H. & SULLIVAN, A.F. (1987). Peripheral origins and central modulation of subcutaneous formalin-induced activity of rat dorsal horn neurons. *Neurosci. Letts*, **83**, 207–211.

DUBUISSON, D. & DENNIS, S.G. (1977). The formalin test: quantitative study of the analgesic effects of morphine, meperidine and brain stem stimulation in rats and cats. *Pain*, **4**, 161–174.

FERREIRA, S.H. & NAKAMURA, M. (1979). III Prostaglandin hyperalgesia: relevance of the peripheral effect for the analgesic action of opioid-antagonists. *Prostaglandins*, **18**, 201–208.

FINNEY, D.J. (1964). *Statistical Method in Biological Assay*. 2nd Ed. London: Griffin.

HALEY, J.E., DICKENSON, A.H. & SCHACHTER, M. (1989). Electrophysiological evidence for a role of bradykinin in chemical nociception in the rat. *Neurosci. Letts*, **97**, 198–202.

HALEY, J.E., KETCHUM, S. & DICKENSON, A.H. (1990). Peripheral κ-opioid modulation of the formalin response: an electrophysiological study in the rat. *Eur. J. Pharmacol.*, **191**, 437–446.

HAYES, A.G., BIRCH, P.J., HAYWARD, N.J., SHEEHAN, M.J., ROGERS, H., TYERS, M.B., JUDD, D.B., SCOPES, D.I.C. & NAYLOR, A. (1990). A series of novel, highly potent and selective agonists for the κ-opioid receptor. *Br. J. Pharmacol.*, **101**, 944–948.

HAYES, A.G., ROGERS, H., BIRCH, P.J., HARRISON, S.M., JUDD, D.B., NAYLOR, A. & SCOPES, D.I.C. (1991). Activation of peripheral opioid receptors by GR94839 mediates antinociception in the rat. *Fundamentals Clin. Pharmacol.*, **5**, 414.

HEAPY, C.G., JAMIESON, A. & RUSSELL, N.J.W. (1987). Afferent C-fibre and A-delta activity in models of inflammation. *Br. J. Pharmacol.*, **90,** 164P.

HUNSKAAR, S., BERGE, O.G. & HOLE, K. (1987). Dissociation between antinociceptive and anti-inflammatory effects of acetylsalicylic acid and indomethacin in the formalin test. *Pain*, **25,** 125–132.

HUNSKAAR, S., FASMER, O.B. & HOLE, K. (1985). Acetylsalicylic acid, paracetamol and morphine inhibit behavioural responses to intrathecally administered substance P or capsaicin. *J. Neurosci. Methods*, **14,** 69–76.

HUNSKAAR, S. & HOLE, K. (1986). The formalin test in mice: dissociation between inflammatory and non-inflammatory pain. *Pain*, **30,** 103–114.

LEANDER, J.P. (1983). A kappa opioid effect: increased urination in the rat. *J. Pharmacol. Exp. Ther.*, **224,** 89–94.

MANSOUR, A., KHACHATURIAN, H., LEWIS, M.E., AKIL, H. & WATSON, S.J. (1988). Anatomy of CNS opioid receptors. *Trends Neurosci.*, **11,** 308–314.

PELISSIER, T., PAEILE, C., SOTO-MOYANO, R., SAAVEDRA, H. & HERNANDEZ, A. (1990). Analgesia produced by intrathecal administration of the κ-opioid agonist, U-50,488H on formalin-evoked cutaneous pain in the rat. *Eur. J. Pharmacol.*, **190,** 287–293.

RUSSELL, N.J.W., SCHAIBLE, H.-G. & SCHMIDT, R.F. (1987). Opiates inhibit the discharge of fine afferent units from the inflammed knee joint of the cat. *Neurosci. Letts*, **76,** 107–112.

SHAW, J.S., CARROLL, J.A., ALCOCK, P. & MAIN, B.G. (1989). ICI204448: a κ-opioid agonist with limited access to the CNS. *Br. J. Pharmacol.*, **96,** 986–992.

SHIBATA, M., OHKUBO, T., TAKAHASHI, H. & INOKI, R. (1989). Modified formalin test: characteristic biphasic pain response. *Pain*, **38,** 347–352.

SMITH, C.F.C. (1987). 16-Me cyprenorphine (RX 8008M): a potent opioid antagonist with some δ selectivity. *Life Sci.*, **40,** 267–274.

SMITH, T.W. & BUCHAN, P. (1984). Peripheral opioid receptors located on the rat saphenous nerve. *Neuropeptides*, **5,** 217–220.

STEIN, C., MILLAN, M.J., SHIPPENBERG, T.S., PETER, K. & HERZ, A. (1989). Peripheral opioid receptors mediating antinociception in inflammation. *J. Pharmacol. Exp. Ther.*, **248,** 1269–1275.

STEIN, C., MILLAN, M.J., YASSOURIDIS, A., & HERZ, A. (1988). Antinociceptive effects of μ- and κ-agonists in inflammation are enhanced by a peripheral opioid receptor specific mechanism. *Eur. J. Pharmacol.*, **155,** 255–264.

TAVANI, A., PETRILLO, P., LA REGINA, A. & SBACCHI, M. (1990). Role of peripheral μ-, and κ-opioid receptors in opioid-induced inhibition of gastrointestinal transit in rats. *J. Pharmacol. Exp. Ther.*, **254,** 91–97.

WHEELER-ACETO, H., PORRECA, F. & COWAN, A. (1990). The rat paw formalin test: comparison of noxious agents. *Pain*, **40,** 229–238.

(Received January 30, 1992
Revised March 19, 1992
Accepted March 23, 1992)

Br. J. Pharmacol. (1992), **106**, 790–796 © Macmillan Press Ltd, 1992

Effect of α_2-adrenoceptor agonists on gastric pepsin and acid secretion in the rat

Khaddouj Tazi-Saad, Jacques Chariot, *Mario Del Tacca & [1]Claude Rozé

INSERM U239, Faculté de Médecine X Bichat, 16 Rue H Huchard, 75018 Paris, France, and *Institute of Pharmacology, Medical School of the University, Via Roma 55, 56100 Pisa, Italy

1 The purpose of the present study was to analyze the effects of the α_2-adrenoceptor agonists clonidine, guanabenz, detomidine and medetomidine on pepsin secretion in conscious rats provided with gastric chronic fistula and to compare this with acid secretion.

2 Basal interdigestive gastric secretion, which is mainly neurally driven in the rat, and the secretion directly stimulated by the two main stimulants of chief cells, cholecystokinin octapeptide (CCK8) and methacholine, were studied.

3 Basal secretion of pepsin and acid was inhibited by all four drugs with comparable EC_{50}s.

4 CCK-stimulated pepsin and acid secretion was less sensitive than basal pepsin and acid secretion to α_2-adrenoceptor inhibition.

5 Methacholine-stimulated pepsin and acid secretion was not changed by clonidine and guanabenz; methacholine-stimulated acid was even marginally increased by clonidine.

6 These results do not favour the presence of α_2-receptors on chief cells in the rat stomach. They rather suggest that pepsin inhibition by α_2-adrenoceptor agonists is indirect and due to central or peripheral inhibition of the discharge of nerve fibres activating pepsin secretion.

Keywords: Gastric fistula rats; pepsin secretion; acid secretion; α_2-adrenoceptors; clonidine; guanabenz; detomidine; medetomidine

Introduction

Both direct inhibition and indirect stimulation of gastric acid secretion by α_2-adrenoceptor agonists have been reported. Inhibition had both central and peripheral components (Taylor & Mir, 1982; Pascaud *et al.*, 1983), whereas stimulation might take place through activation of peripheral histamine receptors (Del Tacca *et al.*, 1982; Soldani *et al.*, 1984). By comparison, the influence of α_2-adrenoceptor agonists on pepsin secretion is poorly documented and the presence of α_2-adrenoceptors on chief cells has not been reported.

The purpose of this study was to determine the effects of four α_2-adrenoceptor agonists, clonidine, guanabenz, detomidine and medetomidine, on gastric pepsin secretion *in vivo*, and compare it with acid secretion. The experiments were conducted in gastric fistula rats under basal conditions, a situation in which gastric secretion is mainly neurally driven, and after direct stimulation of chief cells by cholecystokinin octapeptide (CCK8) or methacholine, two potent stimulants of pepsin secretion (Tazi-Saad *et al.*, 1992).

Methods

Animals

Male Wistar rats (Iffa Credo, Les Oncins, F-69210 L'Arbresle, France), weighing 300 ± 20 g, were used in these studies. They were maintained in the laboratory on a commercial autoclaved pelleted chow (UAR 113, Alimentation Rationnelle, Villemoisson, F-91360 Epinay sur Orge, France).

Gastric chronic fistula

After premedication with 10 mg kg^{-1} of acepromazine i.p. (Vetranquil, Clin Midy, F-45142, St Jean de la Ruelle, France), the rats were anaesthetized with 50 mg kg^{-1} ketamine i.p. (Imalgène 500, Rhône Mérieux, F-69002 Lyon, France). A gastric fistula was set up following the method of Emås *et al.* (1981): a seromuscular purse was prepared in the ruminal part of the stomach, and a Thomas cannula was inserted and secured in place with the help of a square pad of synthetic felt 1.5 × 1.5 cm (Dacron felt, USCI, U.S.A.).

Salivary secretion

In experiments with methacholine, salivary secretion was also stimulated and gastric secretion was therefore contaminated by salivary bicarbonate. To correct for this contamination, salivary secretion was measured in separate experiments. Under ether anaesthesia, a polyethylene catheter (Biotrol No 13) was introduced in the lower oesophagus through a ruminal incision, secured in place by two ligatures at the level of the cardia and rumen, and conducted through the abdominal wall. The muscle and skin were sutured, the rat was placed in a Bollman cage, and an infusion catheter was inserted in a tail vein. After 2 h of post anaesthesia recovery, saliva was collected as 40 min fractions in 5 ml graduated tubes. Methacholine was infused in successive increasing doses under the same conditions as in gastric fistula rats. The volume of saliva samples was measured to the nearest 0.1 ml. Bicarbonate was determined by an auto-analyzer method (Chariot & Rozé, 1976).

Secretory tests

Two weeks of post-operative recovery were allowed before the secretory tests began. During this period, the rats were trained to stand quiet in the Bollman cages during three sham-experiments. Secretory tests were then performed no more than once a week. After a 24 h fasting period with drinking water *ad libitum*, the gastric cannula was opened and the stomach was rinsed with water prewarmed at 37°C. A plastic prolongator was screwed onto the gastric cannula

[1] Author for correspondence.

and a small diameter polyethylene catheter with lateral holes was introduced and secured in the cannula. This catheter helped to collect the gastric juice safely, by guiding it drop by drop into the collecting tube. The rats were placed in Bollman cages, and an infusion catheter was inserted in a tail vein and secured with adhesive tape. A venous infusion of NaCl 0.9% w/v was then started. Gastric secretion was collected as 40 min samples in tared tubes. The weight of gastric juice was measured, and accepted as a measure of gastric volume, assuming that 1 ml = 1 g. Two 40 min samples were collected before injecting any substance. The mean of these two samples was taken as representative of basal secretion.

Acid secretion

Acid was titrated to pH = 7.0 with NaOH 4 mM, on 0.1 ml samples, with an automatic titrator (Metrohm AG, 9100 Herisau, Switzerland). When the pH of gastric samples was greater than or equal to 5.0, the samples were immediately acidified with 20 µl HCl (6 M) per ml of gastric juice, in order to protect pepsin activity, which rapidly fades away in solutions of pH > 5.

Pepsin secretion

Pepsin activity was determined by a semi-automated method derived from the method proposed by Anson & Mirsky (1933), which involves two successive steps: (1) Pepsin present in the samples was allowed to digest an aqueous solution of 2.5% haemoglobin (Sigma, St Louis, MO, U.S.A.), pH = 1.7, for 3 min at 37°C. The reaction was then stopped by adding 5% trichloracetic acid (Prolabo, Paris, France), and soluble hydrolysis products were separated by centrifugation. (2) Soluble hydrolysis products were determined with the Folin-Ciocalteu reagent (Merck, West Point, U.S.A.) in a Technicon auto-analyzer, with tyrosine as a standard. Volume of each sample was 50 µl for the dosage and 50 µl for the blank tube without hydrolysis. Pepsin activity of the gastric juice was determined relative to a control scale of standard purified pepsin (Fluka, Buchs, Switzerland, ref 77152, 0.2 to 1 mg ml^{-1}) and was expressed as pepsin units (PU). One unit corresponds to the amount of pepsin releasing 1 µmol tyrosine min^{-1} under the conditions adopted for the study.

Experimental schedules

Effect of α_2-adrenoceptor agonists on basal secretion Clonidine, guanabenz, detomidine and medetomidine were administered as successive i.v. infusions of increasing doses (4.35, 13.7, 43.5 nmol kg^{-1} h^{-1}), each infused for 80 min. The effect of each dose was measured during the second 40 min half of the 80 min infusion period.

The time course of the effect was analyzed on 240 min i.v. infusions of clonidine (13.7, 43.5 or 137 nmol kg^{-1} h^{-1}) or guanabenz (13.7 or 43.5 nmol kg^{-1} h^{-1}). To test the α_2-specificity of the clonidine effect, the α_2-adrenoceptor antagonist, idazoxan, was administered as a s.c. injection, 40 min before the infusion of clonidine had begun.

Effect of clonidine and guanabenz on CCK-stimulated secretion Clonidine (13.7, 43.5 or 137 nmol kg^{-1} h^{-1}) or guanabenz (13.7 or 43.5 nmol kg^{-1} h^{-1}) were first infused alone i.v. for 120 min, and then accompanied by CCK, 1.9 and 6 nmol kg^{-1} h^{-1} as two successive 40 min infusions. In antagonist experiments, idazoxan was injected s.c., 40 min before clonidine infusion.

Effect of clonidine and guanabenz on methacholine-stimulated secretion Clonidine or guanabenz were first infused alone i.v. for 120 min, and then accompanied by methacholine, 3100 and 9710 nmol kg^{-1} h^{-1}, as two successive 40 min infusions. Since salivary secretion (a source of fluid and bicarbonate) was stimulated by methacholine, acid secretion was underestimated and volume was overestimated in these experiments. Thus, volume and acid data were corrected for salivary secretion measured in separate experiments: the volume of saliva was subtracted from the total volume of juice collected from the gastric fistula, whereas salivary bicarbonate output was added to gastric acid output, assuming that gastric acid had been stoichiometrically neutralized by salivary bicarbonate. To ensure pepsin stability, all samples from methacholine experiments were immediately acidified with 6 M HCl 20 µl ml^{-1}.

Substances tested

The following substances were used: CCK: Boc-Nle_{28}-Nle_{31}-CCK_{26-33} (a gift of J. Martinez, Centre CNRS-INSERM de Pharmacologie Endocrinologie, Montpellier, France), a synthetic analogue of CCK8 the activity of which is equal to that of CCK8 in all models tested to date; methacholine: acetyl-β-methylcholine chloride (Pharmacie Centrale des Hopitaux, Paris, France); clonidine: a gift of Boehringer (Ingelheim, Germany); guanabenz acetate: Sigma (St Louis, MO, U.S.A.); detomidine hydrochloride and medetomidine hydrochloride: a gift of Farmos (Turku, Finland); idazoxan: a gift of Reckitt and Colman (Kingston upon Hull, GB). All drugs were dissolved in NaCl 0.9%. CCK solutions were prepared in 0.9% NaCl with 0.3% bovine serum albumin added.

Expression of results and statistics

The results are expressed as means ± standard error of the mean (s.e.mean). The doses causing 50% inhibition (ED_{50}) were calculated from the linear portion of the regression curve of the effect on log dose, as described by Tallarida & Murray (1984). Statistical significance of the differences between means was tested by one or two way ANOVA, followed when necessary by a multigroup comparison test (Dunnet or Newman-Keuls). A P value $\leqslant 0.05$ was considered significant.

Results

Effect of α_2-adrenoceptor agonists on basal gastric secretion

Dose-response curves by infusion of successive increasing doses Clonidine, guanabenz, detomidine and medetomidine inhibited in a dose-related way the basal output of acid and pepsin (Figure 1). The inhibition observed with the dose of 43.5 nmol kg^{-1} h^{-1} reached about 90% of the basal acid and pepsin outputs. The calculated ED_{50} values (doses causing 50% inhibition) are shown in Table 1: all four drugs had similar ED_{50}s on volume, acid and pepsin outputs.

Time course of the inhibition produced by clonidine and guanabenz The time course of the inhibition produced by long lasting (240 min) i.v. infusions of 13.7 nmol kg^{-1} h^{-1} of clonidine or guanabenz was identical with both drugs. The peak inhibition (about 50% for volume, acid and pepsin) was observed after 120 min of infusion, and remained at this level until the end of the infusion (not shown). The time course was similar when the clonidine or guanabenz dose was increased to 43.5 nmol kg^{-1} h^{-1} (Figure 2): the peak inhibition was reached after 120 min of i.v. infusion, and remained approximately constant for the rest of the infusion period. With this latter dose of clonidine, the inhibition at 120 min was 80% for volume, and 90% for acid and pepsin outputs. With this latter dose of guanabenz, the inhibition at 120 min was 60% for volume, 90% for acid, and 80% for pepsin output (Figure 2). After clonidine (137 nmol kg^{-1} h^{-1}), the

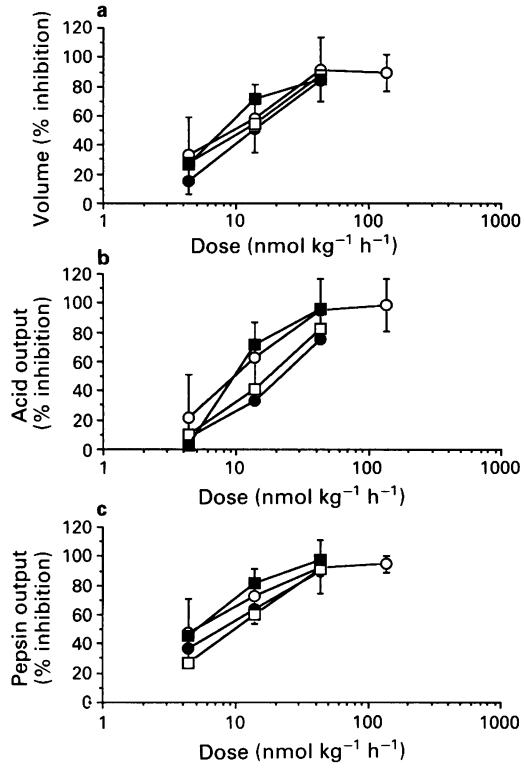

Figure 1 Effects of clonidine (○), guanabenz (●), detomidine (□) and medetomidine (■), on gastric juice volume (a) and on acid (b) and pepsin (c) outputs as a function of doses in conscious rats provided with gastric chronic fistula. The results are expressed as percentage inhibition of basal secretion. The data show the mean of 6 or 7 rats per group. To increase clarity, the vertical lines showing s.e.mean have been drawn only for the group receiving clonidine.

Table 1 The ED_{50} values (dose causing 50% inhibition; nmol kg^{-1} h^{-1}, 95% confidence limits in parentheses) of clonidine, guanabenz, detomidine and medetomidine on basal gastric secretion

Substance	*Volume*	*Acid output*	*Pepsin output*
Clonidine	9.0 (5.4–14.8)	10.2 (5.9–17.6)	4.7 (2.1–10.3)
Guanabenz	13.6 (10.2–18.2)	17.7 (10.7–29.4)	7.7 (5.5–10.8)
Detomidine	10.6 (7.5–14.2)	15.1 (9.6–23.7)	9.8 (7.1–13.6)
Medetomidine	8.9 (6.1–13.2)	12.2 (8.1–18.3)	4.8 (3.6–6.5)

Data are calculated from the experiments shown in Figure 1, $n = 6$ or 7 rats per group.

inhibition at 120 min was 87% for volume, 99% for acid, and 100% for pepsin output (Figure 3).

Pepsin concentration was significantly decreased by 43.5 nmol kg^{-1} h^{-1} of clonidine or guanabenz (Table 2).

Idazoxan alone did not change basal gastric secretion (not shown), but suppressed the clonidine inhibition of volume, acid and pepsin outputs (Figure 3).

Clonidine and guanabenz on CCK-stimulated gastric secretion

Volume, acid and pepsin outputs were stimulated in a dose-related way by CCK (Figure 4), while pepsin concentration was decreased (Table 2).

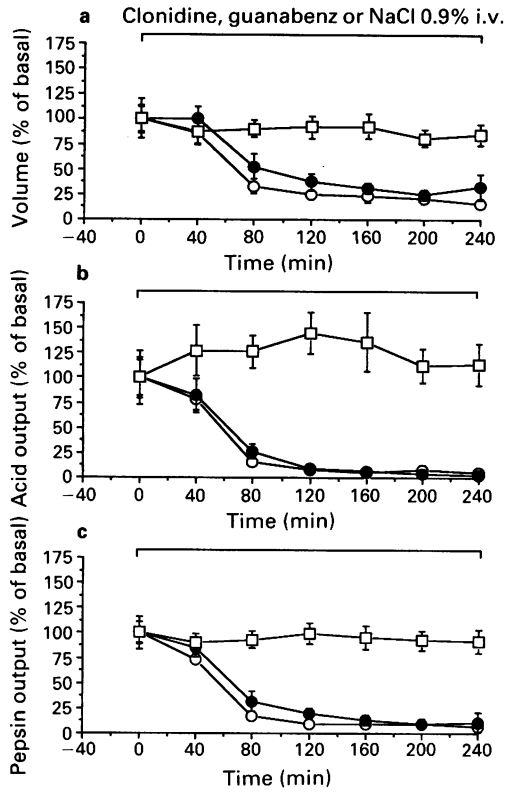

Figure 2 Time course of the inhibitory effect of clonidine (43.5 nmol kg^{-1} h^{-1}, i.v., ○) and guanabenz (43.5 nmol kg^{-1} h^{-1}, i.v., ●) on gastric juice volume (a) and on acid (b) and pepsin (c) outputs in conscious rats provided with gastric chronic fistula. The time course of gastric secretion in a control group receiving only NaCl (□) is shown for comparison. The results are expressed as percentage inhibition of basal secretion, shown as means of 8 rats per group; vertical bars represent s.e.mean. The average basal levels were: volume 980 ± 81.3 µl 40 min^{-1}, acid output 75.0 ± 7.68 µmol 40 min^{-1}, pepsin output 10.3 ± 0.66 PU 40 min^{-1}.

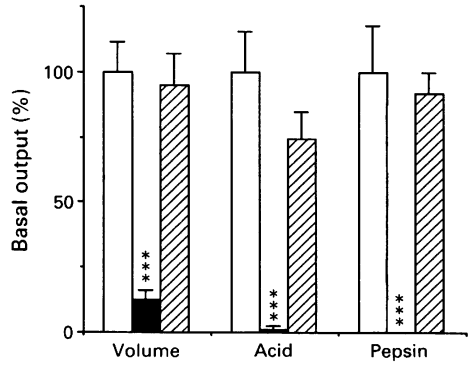

Figure 3 Antagonism by idazoxan (3 mg kg^{-1}, s.c. 40 min before beginning the infusion of clonidine) of the inhibitory effects of clonidine (137 nmol kg^{-1} h^{-1}, i.v.) on basal volume juice, and on acid and pepsin outputs in conscious rats provided with gastric chronic fistula. Basal secretion = open columns; clonidine = solid columns; idazoxan + clonidine = hatched columns. Means of 8 rats per group. Vertical lines show s.e.mean.
***$P < 0.001$ versus basal level (Dunnett's test)

Clonidine decreased CCK-stimulated gastric secretion (Figure 4). In Figure 4, the probability values refer to the significance of the difference between the three dose levels of clonidine (0, 13.7 and 43.5 nmol kg^{-1} h^{-1}), under basal conditions (Control groups) and during the infusion of 1.9 or

Table 2 Effect of clonidine and guanabenz on pepsin concentration in the gastric juice (PU ml^{-1}), in basal conditions (control) and with cholecystokinin (CCK) stimulation

	Control	*CCK 1.9*	*CCK 6*	P *(CCK effect)*
Control	11.1 ± 0.9	7.6 ± 0.2	8.4 ± 0.2	<0.001
Clonidine [13.7*]	11.0 ± 0.6	7.5 ± 0.3	9.1 ± 0.5	<0.001
Clonidine [43.5]	5.6 ± 1.6	7.1 ± 0.9	9.1 ± 0.7	NS
P (Clonidine effect)	<0.01	NS	NS	
Guanabenz [13.7]	9.2 ± 0.2	7.8 ± 0.3	9.9 ± 0.4	<0.001
Guanabenz [43.5]	6.0 ± 1.2	8.5 ± 0.8	11.3 ± 1.3	<0.05
P (Guanabenz effect)	<0.01	NS	NS	

*Doses are in nmol kg^{-1} h^{-1}. The values are shown as mean ± s.e.mean of 6 to 16 rats per group. The *P* levels correspond to the result of the ANOVA between doses of CCK, clonidine or guanabenz. NS: not significant.

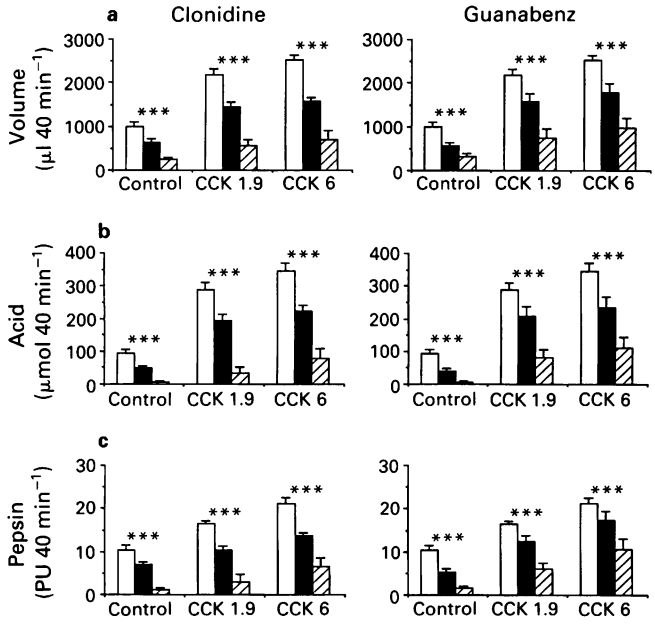

Figure 4 Effects of clonidine (left panel) and guanabenz (right panel) on gastric juice volume (a) and on acid (b) and pepsin (c) outputs in basal conditions (Control) and under cholecystokinin (CCK) stimulation (1.9 and 6 nmol kg^{-1} h^{-1}) in conscious rats provided with gastric chronic fistula. The stimulation consisted of two successive 40 min infusions of CCK 1.9 and 6 nmol kg^{-1} h^{-1} from 120 min after the beginning of clonidine or guanabenz infusion. The doses of clonidine and guanabenz were: zero = open columns: 13.7 nmol kg^{-1} h^{-1} = solid columns and 43.5 nmol kg^{-1} h^{-1} = hatched columns. Means of 6 to 16 rats per group. Vertical lines show s.e.mean.
The probability values, $^{**}P<0.01$ and $^{***}P<0.001$ refer to the significance between the dose levels of clonidine or guanabenz (0, 13.7 and 43.5 nmol kg^{-1} h^{-1}) under basal conditions (control) and under CCK stimulation (1.9 and 6 nmol kg^{-1} h^{-1}) (ANOVA).

6 nmol kg^{-1} h^{-1} of CCK. The clonidine ED_{50} values were twice as great for CCK-stimulated (Table 3) as compared to the basal volume and acid secretion (Table 1, $P<0.05$ to 0.01), and about four times as great for CCK-stimulated as compared to the basal pepsin output. Pepsin concentration was not significantly changed by clonidine in CCK-treated rats (Table 2). When using large doses of clonidine, CCK-stimulated secretion was almost abolished: after 137 nmol kg^{-1} h^{-1} of clonidine, volume was decreased by 70%, acid output by 99%, and pepsin output by 90% (Figure 5).

Guanabenz (13.7 and 43.5 nmol kg^{-1} h^{-1}) was also given with CCK (1.9 and 6 nmol kg^{-1} h^{-1}) (Figure 4). The effects of guanabenz were very similar to those of clonidine on the CCK-stimulated gastric juice volume, acid output and pepsin output. The ED_{50} values of guanabenz were significantly greater on CCK-stimulated volume and pepsin output (Table 3) than on the basal secretion (Table 1). Pepsin concentration was not significantly changed by guanabenz in CCK-stimulated rats (Table 2).

Idazoxan antagonism of the clonidine inhibition of CCK-stimulated pepsin secretion

In these studies, a maximally effective dose of 137 nmol kg^{-1} h^{-1} of clonidine was used to ensure a nearly complete inhibition of pepsin secretion. The prior s.c. injection of idazoxan (3 mg kg^{-1}) totally suppressed the clonidine-induced inhibition of pepsin output and decreased the clonidine-induced inhibition of volume ($P<0.05$) and acid output ($P=0.14$) (Figure 5).

Effect of clonidine and guanabenz on methacholine-stimulated gastric secretion

Methacholine stimulated in a dose-related way the volume and the acid and pepsin outputs, as shown in Figure 6. The volume and acid values were corrected for salivary con-

Table 3 The ED_{50} values (doses causing 50% inhibition; nmol kg^{-1} h^{-1}, 95% confidence limits in parentheses) of clonidine and guanabenz on cholecystokinin (CCK)-stimulated gastric secretion

Substance	*CCK dose* (nmol kg^{-1} h^{-1})	*Volume*	*Acid output*	*Pepsin output*
Clonidine	1.9	21.5[b] (16.4–28.2)	19.3[a] (14.9–25.0)	19.4[c] (15.3–24.5)
	6	20.9[b] (16.1–27.0)	20.4[a] (15.9–26.1)	22.7[c] (17.5–29.4)
Guanabenz	1.9	26.8[a] (16.2–44.0)	24.4 (15.4–38.7)	29.2[c] (16.4–52.1)
	6	28.8[a] (16.0–52.0)	24.1 (13.8–42.1)	43.3[c] (15.6–120)

Data are calculated from the experiments shown in Figure 4, $n=6$ to 14 rats per group, where [a]: $P<0.05$, [b]: $P<0.01$, [c]: $P<0.001$ versus the corresponding ED_{50} values on basal secretion (Table 1).

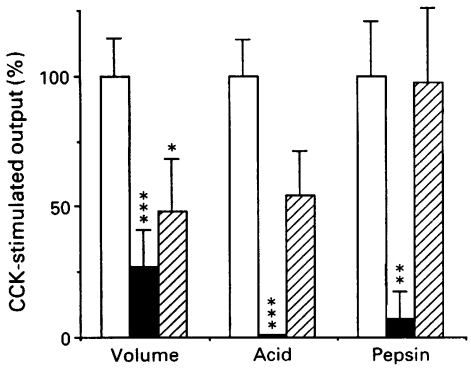

Figure 5 Antagonism by idazoxan (3 mg kg^{-1}, s.c. 40 min before beginning the infusion of clonidine) of the inhibitory effects of clonidine (137 nmol kg^{-1} h^{-1}, i.v.) on gastric juice volume, and on acid and pepsin outputs stimulated by CCK (1.9 nmol kg^{-1} h^{-1}, i.v., accompanying the infusion of clonidine for 40 min from 120 min after the beginning of clonidine infusion) in conscious rats provided with gastric chronic fistula. CCK = open columns; CCK + clonidine = solid columns; CCK + idazoxan + clonidine = hatched columns. The results are expressed as percentage of the CCK-stimulated secretion. Means of 8 to 12 rats per group. Vertical lines show s.e.mean.
*$P<0.05$; **$P<0.01$; ***$P<0.001$ versus group CCK (Dunnett's test).

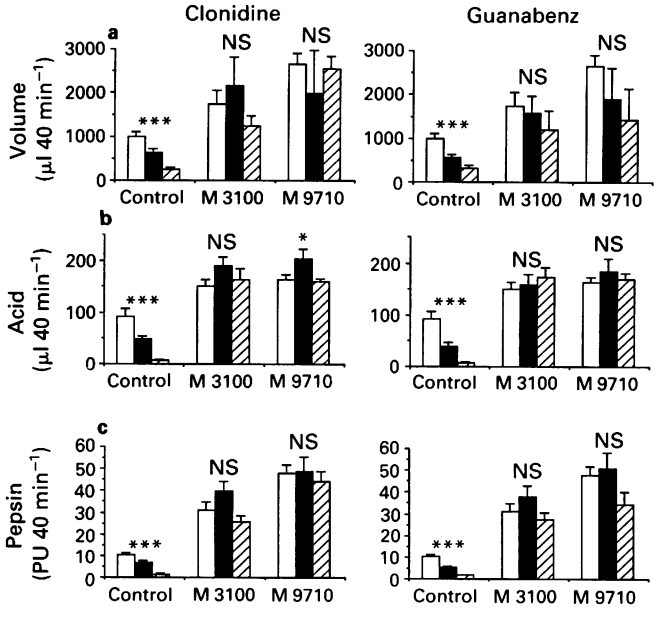

Figure 6 Effects of clonidine (left panel) and guanabenz (right panel) on gastric juice volume (a) and on acid (b) and pepsin (c) outputs in basal conditions (Control) and under methacholine (M) stimulation (3100 and 9710 nmol kg^{-1} h^{-1}) in conscious rats provided with gastric chronic fistula. The stimulation consisted of two successive 40 min infusions of methacholine 3100 and 9710 nmol kg^{-1} h^{-1} from 120 min after the beginning of clonidine or guanabenz infusion. The doses of clonidine and guanabenz were: zero = open columns; 13.7 nmol kg^{-1} h^{-1} = solid columns and 43.5 nmol kg^{-1} h^{-1} = hatched columns. Means of 6 to 12 rats per group. Vertical lines show s.e.mean. NS = no significant difference.
*$P<0.05$ and ***$P<0.001$ = values of the difference between the doses of clonidine and guanabenz (0, 1.37, and 43.5 nmol kg^{-1} h^{-1}) under basal conditions (Control) and under methacholine stimulation (3100 and 9710 nmol kg^{-1} h^{-1}) (ANOVA).

tamination, by use of the average data of methacholine stimulation of salivary secretion, shown in Table 4. This correction was also made in clonidine treated groups, since clonidine (43.5 nmol kg^{-1} h^{-1}) did not change the methacholine-induced stimulation of salivary volume and bicarbonate output (Table 4).

Clonidine and guanabenz (13.7 or 43.5 nmol kg^{-1} h^{-1}) did not decrease significantly gastric secretion (volume, acid and pepsin) stimulated either by a submaximal (3100 nmol kg^{-1} h^{-1}) or maximal (9710 nmol kg^{-1} h^{-1}) dose of methacholine (Figure 6). Clonidine (13.7 nmol kg^{-1} h^{-1}) actually caused a slight increase in methacholine-stimulated acid output.

Discussion

The effect of α_2-adrenoceptor agonists on gastric acid secretion has been studied in a variety of species, mainly by use of clonidine (Hoefke & Kobinger, 1966; Cheng *et al.*, 1981; Del Tacca *et al.*, 1982; Pascaud *et al.*,1983; Soldani *et al.*, 1984) but also with guanfacin, xylazine, guanabenz, detomidine and medetomidine (Kunchandy *et al.*, 1985; Bernardini *et al.*, 1986; Savola *et al.*, 1989; Blandizzi *et al.*, 1990). In those studies, small doses of clonidine usually induced an inhibition of gastric acid secretion when this secretion was stimulated by vagal activity or by pentagastrin. Such inhibition was also observed during basal and pentagastrin-stimulated secretion in conscious fistula rats (Pascaud *et al.*, 1983), conscious pylorus-ligated rats (Cheng *et al.*, 1981; Del Tacca *et al.*, 1982; Bernardini *et al.*, 1986), or 2-deoxyglucose stimulated secretion in rats and dogs (Cheng *et al.*, 1981; Soldani *et al.*, 1984). This inhibition has been interpreted as resulting from the action of clonidine at neural α_2-adrenoceptors, located both peripherally (presynaptic α_2-receptors on vagal acetylcholine-producing neurones, Del Tacca *et al.*, 1982) and centrally (Taylor & Mir, 1982; Pascaud *et al.*, 1983; Dettmar & Lord, 1986; Fornai *et al.*, 1990).

In contrast, basal gastric acid secretion in preparations without endogenous vagal tone, such as basal secretion in lumen-perfused anaesthetized rats (Bernardini *et al.*, 1986) or basal secretion in dogs (Soldani *et al.*, 1984) was moderately increased by clonidine. This effect was suppressed by histamine H_2-receptor antagonists, and has been attributed either to direct activation of histamine receptors, or to histamine release by clonidine. The non-imidazole derivative, guanabenz, did not display such stimulating effect (Bernardini *et al.*, 1986). Recently, however, the selective α_2-adrenoceptor agonist, detomidine, which lacks affinity for H_2-receptors (Virtanen & Nyman, 1985), has been found to stimulate gastric acid secretion in urethane-anaesthetized, lumen-perfused, non-vagotomized or vagotomized rats (Blandizzi *et al.*, 1990). This effect was reversed by idazoxan and the authors suggested that it might correspond to the blockade by detomidine of an α_2-mediated sympathetic inhibitory tone on the gastric secretion. In other studies, acid secretion stimulated by cholinergic agents was either unchanged (Pascaud *et al.*, 1983, conscious rats) or even increased (Soldani *et al.*, 1984, conscious dogs) by clonidine.

In contrast to these detailed reports of α_2-adrenoceptor agonist effects on gastric acid secretion, no data have been published as yet concerning pepsin secretion. The present results show that basal pepsin secretion in conscious rats (an animal model submitted to permanent sustained vagal stimulant tone) was decreased in a dose-related way by the four α_2-adrenoceptor agonists tested, with similar potencies (non significantly different ED_{50} values of 4.7 to 9.8 nmol kg^{-1} h^{-1} on pepsin secretion) and efficacies (approaching 100% inhibition at the dose of 43.5 nmol kg^{-1} h^{-1}). This α_2-mediated effect (suppressed by idazoxan), was comparable for volume, acid and pepsin, and we suggest that it may be due to the occupation of either central α_2-adrenoceptors or presynaptic α_2-adrenoceptors located on peripheral cholinergic neurones. Since this inhibition of basal secretion corresponds to the suppression of an endogenous cholinergic stimulus, it does not implicate the presence of inhibitory

Table 4 Effect of methacholine and methacholine plus clon[illegible] on salivary secretion in conscious rats

Methacholine (nmol kg^{-1} h^{-1})	*Clonidine* (nmol kg^{-1} h^{-1})	*(μ* [illegible] *ume* nin^{-1})	*Bicarbonate* *Concentration* (mmol l^{-1})	*Output* (μmol 40 min^{-1})
0	0	[illegible] ± 26	21.6 ± 4.1	2.1 ± 1.2
3100	0	2[illegible] ± 470	39.5 ± 2.2	80.7 ± 14.4
3100	43.5	2[illegible] ± 470	31.1 ± 1.6	71.6 ± 11.1
9710	0	3[illegible] ± 240	42.0 ± 1.2	141 ± 13.2
9710	43.5	3[illegible] ± 410	38.1 ± 0.2	144 ± 15.3
P levels, 2 way ANOVA:				
Between methacholine doses		[illegible]0.01	<0.01	<0.001
Clonidine/no clonidine		[illegible]NS	<0.01	NS
Interactions clonidine/methach.		[illegible]NS	NS	NS

Data are shown as the mean ± s.e.mean of 4 rats per group

α_2-adrenoceptors on chief cells. Thus, the simple decrease in acetylcholine efflux from nerve terminals to chief cells can explain the results.

The effect of clonidine and guanabenz was also tested on stimulated pepsin secretion, and we chose for these experiments CCK and methacholine, which probably are the two main physiological stimulants of pepsin secretion (Hersey, 1987; Tazi-Saad *et al.*, 1992). The results were different with these two stimulants: whereas clonidine and guanabenz both decreased CCK-stimulated acid and pepsin secretion, they did not change (or even marginally increased) methacholine-stimulated acid and pepsin secretion. Since pepsin concentration did not decrease with increasing doses of α_2-adrenoceptors agonists (Table 2), it may be that only the volume flow was decreased by α_2-adrenoceptor agonists in CCK-stimulated gastric glands, thus preventing pepsin from being washed out of the glands. If the inhibition of CCK-induced secretion is due to the absence of cholinergic tone in gastric glands, the effects observed may be attributed to the central decrease of vagal tone and/or to the presynaptic inhibition of acetylcholine release by α_2-adrenoceptor stimulation. Previous experiments comparing clonidine and ST91 a clonidine-like drug (which crosses the blood-brain barrier poorly) indicated that clonidine inhibition of gastric acid secretion in conscious rats had a large central component (Pascaud *et al.*, 1983). Clonidine thus inhibited the effect of the central stimulant 2-deoxy-D-glucose, which acts through the vagus on muscarinic gastric receptors, whereas the peripheral cholinoceptor stimulant methacholine was not affected (Pascaud *et al.*, 1983). It has also been shown that the volume and acid responses to pentagastrin are much decreased in vagotomized rats, and that most of the response to pentagastrin can be restored by infusing small doses of acetylcholine, able to mimic a pseudo-endogenous vagal tone (Chicau-Chovet *et al.*, 1988). This, however, has not been determined with CCK.

The effect of methacholine was not changed, or tended to increase, after clonidine or guanabenz administration. This suggests that the α_2-adrenoceptor agonists did not interfere with the intracellular mechanisms activated by methacholine, and thus that the parietal and chief cell membranes do not bear α_2-adrenoceptors able to interfere with the cellular processes when the muscarinic receptors of these cells are stimulated. Soldani *et al.* (1984) found in the dog an increase of both bethanechol- and histamine-stimulated acid secretion by clonidine. These authors suggested that this result was due to the histamine receptor stimulating effect of clonidine. The mechanism is probably different in our experiments, since guanabenz, which has no histamine-like effects (Bernardini *et al.*, 1986) produced the same effect as clonidine.

In conclusion, we suggest that the effect of the α_2-adrenoceptor agonists on both pepsin and acid is probably due to the central and peripheral inhibition of the neural cholinergic input to gastric glands. Some cholinergic background is necessary for developing the stimulating effect of various agents, which explains why CCK-stimulation is also inhibited by the α_2-adrenoceptor agonists. When methacholine is used, it compensates for the inhibition of cholinergic background, and does not allow α_2-adrenoceptor agonists to inhibit this secretion.

Financial support was provided in part by the Conseil Scientifique of Faculté X. Bichat and by Association Charles Debray.

References

ANSON, M.L. & MIRSKY, A.E. (1933). The estimation of pepsin with hemoglobin. *J. Gen. Physiol.*, **16**, 59–63.

BERNARDINI, C. DEL TACCA, M., SOLDANI, G. & MARTINOTTI, E. (1986). The effects of α_2-agonists and antagonists on gastric acid secretion. *Arch. Int. Pharmacodyn.*, **281**, 134–144.

BLANDIZZI, C., BERNARDINI, M.C., NATALE, G. & DEL TACCA, M. (1990). α_2-Adrenoceptor-mediated inhibitory and excitatory effects of detomidine on rat gastric acid secretion. *J. Pharm. Pharmacol.*, **42**, 685–688.

CHARIOT, J. & ROZÉ, C. (1976). Détermination automatisée de très faibles concentrations de bicarbonate. Application au suc pancréatique. *Ann. Biol. Clin. (Paris)*, **34**, 269–272.

CHENG, H.C., GLEASON, E.M., NATHAN, B.A., LACHMANN, P.J. & WOODWARD, J.K. (1981). Effects of clonidine on gastric acid secretion in the rat. *J. Pharmacol. Exp. Ther.*, **217**, 121–126.

CHICAU-CHOVET, M., DUBRASQUET, M., CHARIOT, J., LECOMTE, J.M. & ROZÉ, C. (1988). Thiorphan and acetorphan inhibit gastric secretion by a central, non-opioid mechanism in the rat. *Eur. J. Pharmacol.*, **154**, 247–254.

DEL TACCA, M., SOLDANI, G., BERNARDINI, C., MARTINOTTI, E. & IMPICCIATORE, M. (1982). Pharmacological studies on the mechanisms underlying the inhibitory and excitatory effects of clonidine on gastric acid secretion. *Eur. J. Pharmacol.*, **81**, 255–261.

DETTMAR, P.W. & LORD, J.A.H. (1986). The effect of α_2-adrenoceptor agonists on the acid secretory responses of rat isolated gastric mucosa to electrical field stimulation. *Br. J. Pharmacol.*, **89**, 361–366.

EMÅS, S., NYLANDER, G. & WALLIN, B. (1981). Comparison of the dose-response curves for acid output to pentagastrin determined by two techniques on chronic gastric fistula rats. *Digestion*, **22**, 94–100.

FORNAI, F., BLANDIZZI, C. & DEL TACCA, M. (1990). Central α_2-adrenoceptors regulate central and peripheral functions. *Pharmacol. Res.*, **22**, 541–554.

HERSEY, S.J. (1987). Pepsinogen secretion. In *Physiology of the Gastro-Intestinal Tract*, 2nd ed., ed. Johnson, L.R., Christensen, J., Jackson, M.J., Jacobson, E.D. & Walsh, J.H. pp. 947–957. New York: Raven Press.

HOEFKE, W. & KOBINGER, W. (1966). Pharmakologische wirkungen des 2-(2,6-dichlor-phenylamino)-2-imidazolinhydrochlorids, einer neuen, antihypertensiven substanz. *Arzneimittelforsch,*, **16,** 1038–1050.

KUNCHANDY, J., KHANNA, S. & KULKARNI, S.K. (1985). Effect of α_2 agonists clonidine, guanfacine and B-HT 920 on gastric acid secretion and ulcers in rats. *Arch. Int. Pharmacodyn.*, **275,** 123–138.

PASCAUD, X., ROGER, A., GENTON, M. & ROZÉ, C. (1983). Further support for the central origin of the gastric antisecretory properties of clonidine in conscious rats. *Eur. J. Pharmacol.*, **86,** 247–257.

SAVOLA, M., SAVOLA, J.M. & PUURUNEN J. (1989). α_2-Adrenoceptor-mediated inhibition of gastric acid secretion by medetomidine is efficiently antagonized by atipamezole in rats. *Arch. Int. Pharmacodyn.*, **301,** 267–276.

SOLDANI, G., DEL TACCA, M., BERNARDINI, C., MARTINOTTI, E. & IMPICCIATORE, M. (1984). Evidence for two opposite effects of clonidine on gastric acid secretion in the dog. *Naunyn. Schmiedebergs Arch. Pharmacol.*, **327,** 139–142.

TALLARIDA, R.J. & MURRAY, R.B. (1984). Manual of pharmacologic calculations with computer programs. p. 14. New York: Springer-Verlag.

TAYLOR, J.A. & MIR, G.N. (1982). Alpha adrenergic receptors and gastric function. *Drug Develop. Res.*, **2,** 105–122.

TAZI-SAAD, K., CHARIOT, J. & ROZÉ, C. (1992). Control of pepsin secretion by regulatory peptides in the rat stomach. Comparison with acid secretion. *Peptides* (in press).

VIRTANEN, R. & NYMAN, L. (1985). Evaluation of the α_1- and α_2-adrenoceptor effects of detomidine, a novel veterinary sedative analgesic. *Eur. J. Pharmacol.*, **108,** 163–169.

(Received November 28, 1991
Revised March 2, 1992
Accepted March 23, 1992)

Br. J. Pharmacol. (1992), **106**, 797–801 © Macmillan Press Ltd, 1992

Haemodynamic effects of dicentrine, a novel α_1-adrenoceptor antagonist: comparison with prazosin in spontaneously hypertensive and normotensive Wistar-Kyoto rats

Sheu-Meei Yu, *Shih-Yuan Hsu, Feng-Nien Ko, *Chien-Chih Chen, *Yu-Ling Huang, Tur-Fu Huang & [1]Che-Ming Teng

Pharmacological Institute, College of Medicine, National Taiwan University and *National Research Institute of Chinese Medicine, Taipei, Taiwan

1 The haemodynamic effects of dicentrine, an aporphine derivative isolated from the plant *Lindera megaphylla*, were investigated and compared with prazosin in rats.

2 In anaesthetized normotensive Wistar-Kyoto (WKY) rats, i.v. administration of dicentrine (0.1, 0.5, 1.0 mg kg^{-1}) and prazosin (0.01, 0.05, 0.1 mg kg^{-1}) induced a dose-related reduction of mean arterial pressure (MAP) which reached a maximal effect 5–10 min after injection and persisted for 2 h.

3 In anaesthetized WKY rats, a higher dose of dicentrine (1.0 mg kg^{-1}, i.v.) did not cause any significant changes in heart rate (HR), cardiac output (CO) and stroke volume (SV) but markedly increased tail blood flow. In contrast, a higher dose of prazosin (0.1 mg kg^{-1}, i.v.) produced a decrease in HR which paralleled the time course of the hypotensive response.

4 The hypotensive activity of dicentrine was completely abolished by α-adrenoceptor blockade. Both dicentrine and prazosin significantly attenuated pressor responses to noradrenaline but failed, even at maximal hypotensive doses, to impair the pressor effects of angiotensin II or vasopressin. These observations suggest that dicentrine appears to exert its hypotensive action through α_1-adrenoceptor blockade.

5 In conscious normotensive and spontaneously hypertensive (SH) rats, dicentrine (0.5– 2.0 mg kg^{-1}, i.v.) and prazosin (0.05–0.2 mg kg^{-1}, i.v.) also evoked dose-related decreases in MAP which were of greater magnitude in SH rats. Oral administration of dicentrine (5 and 8 mg kg^{-1}) to conscious SH rats caused a hypotensive effect which persisted for over 15 h.

6 These results suggest that dicentrine may have therapeutic potential as an oral antihypertensive drug via α_1-adrenoceptor blockade.

Keywords: Dicentrine; prazosin; α_1-adrenoceptor antagonist; mean arterial pressure; spontaneously hypertensive rats; Wistar-Kyoto rats

Introduction

α-Adrenoceptors are involved in a variety of physiological processes, including regulation of blood pressure (Minneman, 1988). However, the role played by α-adrenoceptors in hypertensive disease remains unclear. Nevertheless, the blockade of α-adrenoceptors by appropriate antagonistic drugs is effective in lowering blood pressure, particularly with the selective α_1-antagonists such as prazosin (Cavero & Roach, 1980; Stanaszek *et al.*, 1983; Titmarsch & Monk, 1987).

The chemical structures of these α-adrenoceptor antagonists may be of pharmaceutical interest and/or useful for pharmacological study. Phenoxybenzamine is a phenylethylamine derivative which is chemically related to endogenous catecholamines. Phentolamine is an imidazoline derivative. Prazosin is 1-(4-amino-6,7-dimethoxy-2-quinazolinyl)-4-(2-furoyl)-piperazine monochloride which shows some resemblance both to papaverine and to the aminopyrimidine moiety of adenosine 3':5'-cyclic monophosphate (cyclic AMP) and guanosine 3':5'-cyclic monophosphate (cyclic GMP). In general, the chemical structure of α-adrenoceptor blocking agents is strikingly unrelated to their pharmacological activity. Recently, we found that dicentrine, an aporphine derivative (Figure 1) isolated from the plant *Lindera megaphylla*, possesses α_1-adrenoceptor antagonistic action in isolated vessels (Teng *et al.*, 1991). In this paper, we have examined the haemodynamic effects of dicentrine and compared it with prazosin in spontaneously hypertensive (SH) and normotensive Wistar-Kyoto (WKY) rats.

Methods

Animal preparation

Male SH rats weighing 320–340 g (Iffa Credo Laboratories, L'Arbresle, France) (mean arterial pressure (MAP) 180 ±

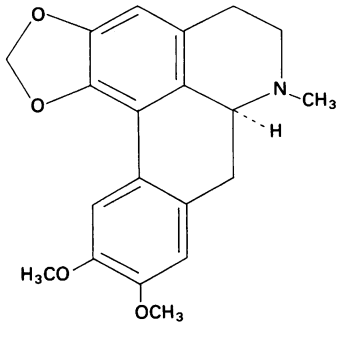

Figure 1 Chemical structure of (+)-dicentrine.

[1] Author for correspondence.

5 mmHg; heart rate (HR): 365 ± 12 beats min^{-1}) and age-matched WKY control animals weighing 320–330 g (Biological Research Laboratories, Fullinsdorf, Switzerland) (MAP: 120 ± 10 mmHg; HR: 357 ± 9 beats min^{-1}) were used in this study. Rats were anaesthetized with sodium pentobarbitone (40 mg kg^{-1}, i.p.). The left carotid artery and the femoral vein were cannulated for blood pressure measurement and i.v. injections, respectively. The arterial cannula was connected via a Statham pressure transducer to a Grass model 7 polygraph (Grass Instruments Co., Quincy, MA) for arterial pressure measurement. HR was monitored on a tachograph (Grass Instruments Co.) triggered by a standard Lead II ECG. Cardiac output (CO) was determined by use of a thermodilution cardiac output computer (Model 85, Columbus Instruments). Pulsed Doppler flowprobes (Haywood *et al.*, 1981) were placed around the tail artery and the lower abdominal aorta just above the iliac bifurcation (equated to hindquarters blood flow) and were connected to a pulsed Doppler flowmeter (Cristal Biotech Inc., Holliston, MA, U.S.A.). After a 30 min-stabilization period, the basal values of all parameters investigated were recorded.

Male conscious WKY and SH rats weighing 300–350 g were also used in this study. The animals were given food and water *ad libitum*. They were housed in the Laboratory Animal Centre of NTUMC at a controlled ambient temperature of 22°C with 50 ± 10% relative humidity and a 12 h light/dark cycle. Polyethylene (PE-50) catheters were inserted into the tail artery and vein for blood pressure measurement and i.v. injections, respectively. After cannulation, the animals were housed separately with food and water freely available. The second day after this surgical procedure, the animals were placed in separate cages for continuous measurement of MAP and HR with an electronic analyzer.

Experimental protocols

The animals were randomly assigned to one of the three following treatment groups: controls, dicentrine and prazosin. After the end of the stabilization period, dimethylsulphoxide (DMSO, control), dicentrine or prazosin was injected (i.v. bolus), and MAP, HR, CO, stroke volume (SV) and blood flow were monitored.

Experiment A: dose-response curves to dicentrine (0.1, 0.5, 1.0 mg kg^{-1}) or prazosin (0.01, 0.05, 0.1 mg kg^{-1}) administered as i.v. bolus injections were obtained in anaesthetized rats. Each dose was studied in separate groups of rats.

Experiment B: the pharmacological mechanism of action of dicentrine or prazosin was investigated in anaesthetized rats. Control pressor responses to angiotensin II (0.1 μg kg^{-1}), noradrenaline (1 μg kg^{-1}) and vasopressin (0.03 iu kg^{-1}) given i.v. were determined. After 30 min, dicentrine (1.0 mg kg^{-1}) or prazosin (0.1 mg kg^{-1}) was administered i.v. Pressor responses to further doses of angiotensin II, noradrenaline and vasopressin were again determined at 30 min after the i.v. bolus of dicentrine or prazosin. In additional groups of rats, α-adrenoceptor blockade was achieved by previous i.v. administration of prazosin (0.1 mg kg^{-1}) or phentolamine (2.0 mg kg^{-1}). After the reduction in MAP to stable levels, the effect of i.v. dicentrine (1.0 mg kg^{-1}) administration was studied.

Experiment C: dicentrine (0.5, 1.0, 2.0 mg kg^{-1}) or prazosin (0.05, 0.1, 0.2 mg kg^{-1}) was administered by i.v. bolus, and each dose was studied in separate groups of conscious SH or WKY rats. MAP was calculated as [(systolic pressure-diastolic pressure)/3 + diastolic pressure]. In additional groups of SH rats, the effect of oral dicentrine (5 or 8 mg kg^{-1}) was followed over time. Dicentrine was suspended in arabic gum and distilled water. Control rats were given 1 ml kg^{-1} of the vehicle.

Data analysis

The experimental results are expressed as the mean ± s.e.mean and accompanied by the number of observations. Statistical significance was assessed by Student's t test and P values less than 0.05 were considered significant.

Drugs

(+)-Dicentrine (Figure 1) was prepared according to the method as described previously (Chen *et al.*, 1991). The following drugs were used: noradrenaline, prazosin, phentolamine, angiotensin II, indomethacin, propranolol and vasopressin, all obtained from Sigma Chemical Co. (St. Louis, MO, U.S.A.). Dicentrine and indomethacin were dissolved in DMSO; prazosin and phentolamine were dissolved in saline.

Results

Haemodynamic effects of dicentrine in anaesthetized WKY rats

Administration of dicentrine (0.1, 0.5, 1.0 mg kg^{-1}, i.v. bolus) caused a dose-related reduction of MAP which reached a maximal effect 5–10 min after injection and persisted for 2 h. Relationships between the dose of dicentrine and MAP or HR responses in anaesthetized rats are depicted in Figure 2. Dicentrine solvent did not exert any significant effects on MAP or HR. A higher dose of dicentrine (1.0 mg kg^{-1}) did not cause any significant changes in HR, CO and SV but markedly and significantly ($P<0.001$) increased tail blood flow (E_{max}, 200 ± 27% change from baseline value) (Table 1).

Haemodynamic effects of prazosin in anaesthetized WKY rats

Intravenous administration of prazosin (0.01, 0.05, 0.1 mg kg^{-1}) produced similar and prolonged (over 2 h) reductions of MAP in anaesthetized rats. Peak responses were observed within 5 min after prazosin injection. Prazosin (0.1 mg kg^{-1}) produced a decrease in HR ($P<0.05$) which paralleled its hypotensive effect (Figure 2). These effects of the higher dose of prazosin (0.1 mg kg^{-1}) were accompanied by increases in SV and tail blood flow (Table 1).

Studies on the mechanism of action of dicentrine

In anaesthetized rats, pressor responses to intravenous injection of noradrenaline (1 μg kg^{-1}), angiotensin II (0.1 μg kg^{-1}) or vasopressin (0.03 iu kg^{-1}) amounted to 50 ± 9, 41 ± 7 and 46 ± 8 mmHg, respectively. The pressor response of noradrenaline was significantly reduced by intravenous pretreatment with dicentrine (0.5, 1.0 mg kg^{-1}) or prazosin (0.05, 0.1 mg kg^{-1}), but was unchanged after saline. Even at maximal hypotensive doses, dicentrine (1.0 mg kg^{-1}) and prazosin (0.1 mg kg^{-1}) failed to impair pressor responses to angiotensin II and vasopressin (Figure 3).

When dicentrine was administered at a maximal hypotensive dose (1.0 mg kg^{-1}, i.v.), it reduced MAP to a plateau value (Δ MAP 55 ± 7 mmHg) which did not differ significantly from that achieved after α-adrenoceptor blockade with phentolamine (2.0 mg kg^{-1}, i.v., Δ MAP 58 ± 9 mmHg) or prazosin (0.1 mg kg^{-1}, i.v., Δ MAP 50 ± 6 mmHg). Pretreatment with phentolamine (2.0 mg kg^{-1}) or prazosin (0.1 mg kg^{-1}) resulted in significant decreases in MAP from 124 ± 6 to 66 ± 9 mmHg and 120 ± 4 to 70 ± 6 mmHg, respectively. Subsequent administration of dicentrine (1.0 mg kg^{-1}) caused no further reduction in MAP (Figure 4). After dicentrine (1.0 mg kg^{-1}) pretreatment, prazosin also did not produce a further fall in MAP. Indomethacin and propranolol pretreatment did not change the base-line blood pressure of anaesthetized rats.

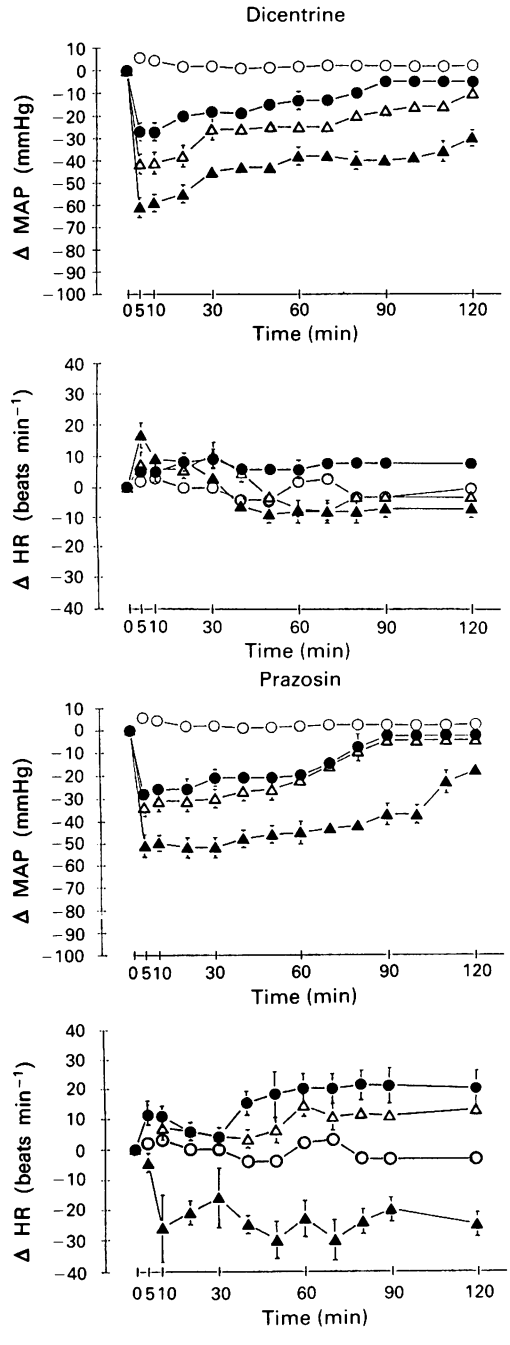

Figure 2 Changes in mean arterial pressure (ΔMAP) and heart rate (ΔHR) produced by i.v. injection of dicentrine (●, 0.1; △, 0.5; ▲, 1.0 mg kg^{-1}), prazosin (●, 0.01; △, 0.05; ▲, 0.1 mg kg^{-1}) or vehicle control (○, dimethylsulphoxide) in anaesthetized WKY rats. Each point represents the mean and vertical bars show s.e.mean ($n = 6$).

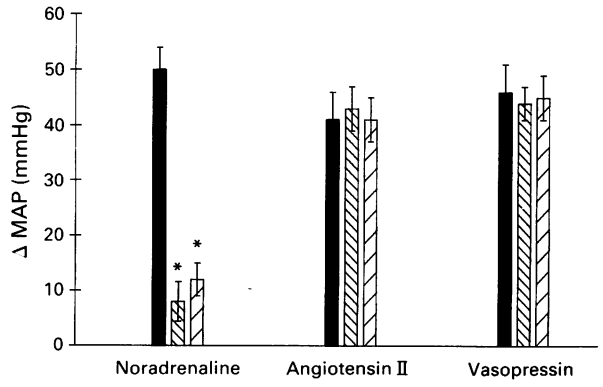

Figure 3 Pressor responses to noradrenaline (1 μg kg^{-1}), angiotensin II (0.1 μg kg^{-1}) and vasopressin (0.03 iu kg^{-1}) before (■) and after dicentrine (▨, 1.0 mg kg^{-1}) and prazosin (▨, 0.1 mg kg^{-1}) in anaesthetized rats. All drugs were i.v. bolus injections. Values are presented as mean with s.e.mean shown by vertical bars. ($n = 6$). *$P < 0.001$ as compared with the respective control.

These compounds failed to modify significantly the hypotensive effects produced by dicentrine (1.0 mg kg^{-1}, i.v.) (data not shown).

Hypotensive effect of dicentrine in conscious WKY and SH rats

Administration of dicentrine (0.5, 1.0, 2.0 mg kg^{-1}, i.v.) to conscious SH rats, induced dose-related decreases in MAP which reached a maximum within 30 min after injection and persisted for at least 4 h. Even at maximal hypotensive doses of dicentrine (2.0 mg kg^{-1}), no change in HR was noted (Figure 5). Intravenous injections of dicentrine and prazosin promptly evoked decreases in MAP which were of greater magnitude in conscious SH than WKY rats. In both conscious WKY and SH rats, prazosin afforded concomitant decreases in HR and blood pressure. However, dicentrine did not significantly affect HR. Oral administration of dicentrine (5 or 8 mg kg^{-1}) to conscious SH rats resulted in decreased MAP ($P < 0.05$) and the duration as well as the magnitude of the effect was dose-dependent (Figure 6). A significant reduction in MAP was observed 1 h after the smaller oral dose of dicentrine (5 mg kg^{-1}) and the hypotensive effect persisted for over 15 h at oral doses of 5 and 8 mg kg^{-1}. Dicentrine at 5 mg kg^{-1} was still effective 15 h but not 24 h after oral administration. No changes in the appearance or behaviour of the rats was evident.

Discussion

These experiments demonstrate that dicentrine is an antihypertensive agent since it effectively lowers the blood pres-

Table 1 Comparison of the effects of approximately equi-effec[illegible] hypotensive doses of dicentrine and prazosin in anaesthetized rats

	Dicentrine ([illegible] mg kg^{-1}) (n = [illegible])		*Prazosin* (0.1 mg kg^{-1}) ($n = 8$)	
Haemodynamic parameters	*Pre-*	*Post-*	*Pre-*	*Post-*
MAP (mmHg)	122 ± 5	62 ± 5**	120 ± 4	68 ± 6**
HR (beats min^{-1})	353 ± 10	348 ± 8	357 ± 9	327 ± 10*
CO (ml min^{-1})	21 ± 2	25 ± 4	27 ± 3	32 ± 3
SV (μl min^{-1}beat^{-1})	50 ± 3	55 ± 9	64 ± 4	79 ± 7*
TBF (% change)	–	200 ± 27**	–	171 ± 14**

Values are means ± s.e.mean for n observations. MAP, mea[illegible]terial pressure (mmHg); HR, heart rate (beats min^{-1}); CO, cardiac output (ml min^{-1}); SV, stroke volume (μl min^{-1}beat^{-1}); [illegible]BF, tail blood flow (mean % change over baseline values). *$P < 0.05$ and ** $P < 0.001$ denote significant differences bet[illegible] pre- and post-drug values.

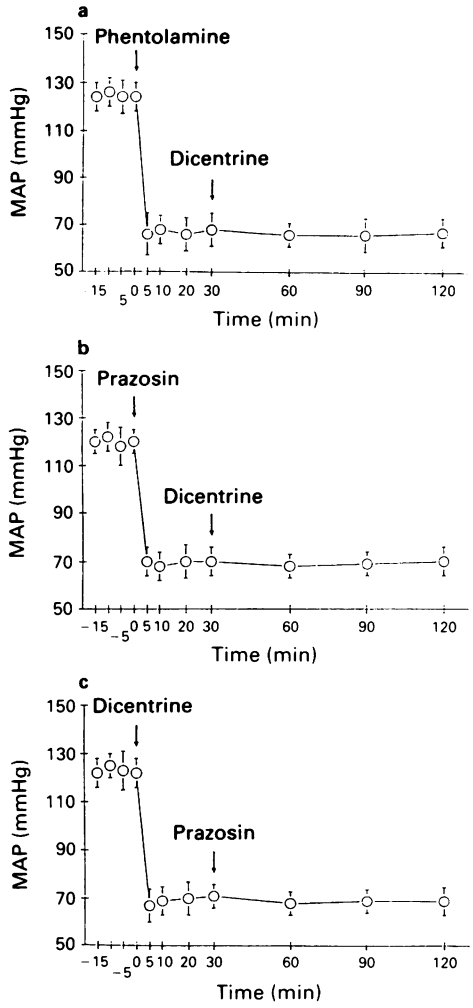

Figure 4 Effects of dicentrine (1.0 mg kg^{-1}, i.v.) on mean arterial pressure (MAP) in anaesthetized WKY rats pretreated with (a) phentolamine (2.0 mg kg^{-1}, i.v.); (b) prazosin (0.1 mg kg^{-1}, i.v.). (c) Effect of prazosin (0.1 mg kg^{-1}, i.v.) on MAP in anaesthetized rats pretreated with dicentrine (1.0 mg kg^{-1}, i.v.). Each point represents the mean and vertical bars show s.e.mean ($n = 6$).

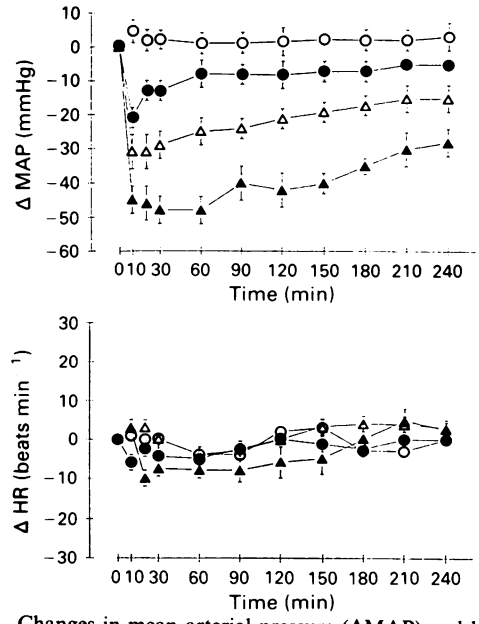

Figure 5 Changes in mean arterial pressure (ΔMAP) and heart rate (ΔHR) produced by dicentrine (●, 0.5; △, 1.0; ▲, 2.0 mg kg^{-1}, i.v.) or vehicle control (○, dimethylsulphoxide) in conscious SH rats. Each point represents the mean and vertical bars show s.e.mean ($n = 8$).

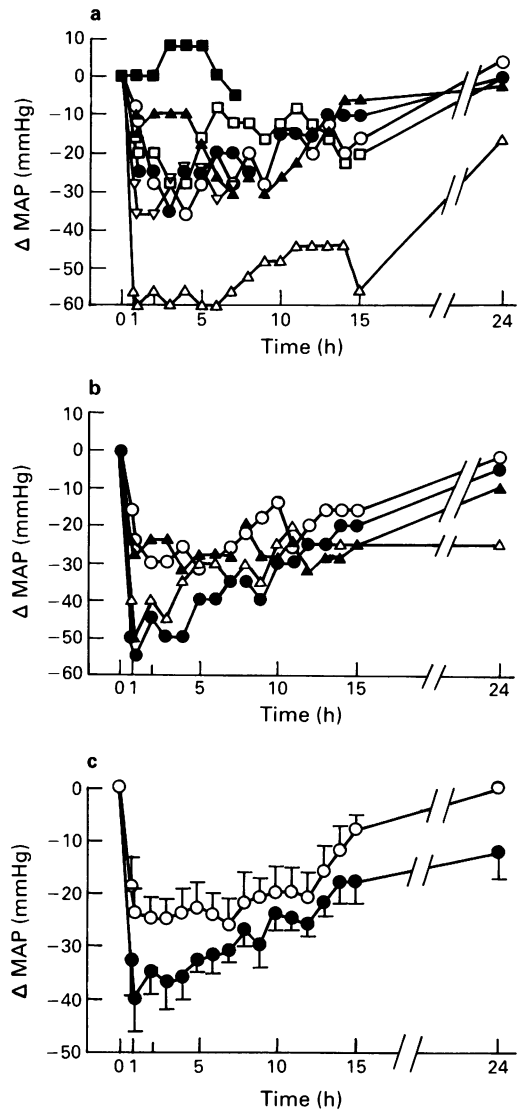

Figure 6 Effects of oral administration of dicentrine on mean arterial pressure (MAP) in conscious SH rats. Dicentrine (a, 5 mg kg^{-1}, $n = 7$; b, 8 mg kg^{-1}, $n = 4$) was orally administered at time 0 and then blood pressure was monitored for 24 h. Time axis is interrupted between 15 and 24 h. The changes in mean arterial pressure (ΔMAP) of each individual rat by dicentrine (5 or 8 mg kg^{-1}) are depicted. The mean data of changes in MAP produced by dicentrine (5 (○), or 8 (●) mg kg^{-1}) is shown in (c). Each point represents the mean and vertical bars show s.e.mean ($n = 4$–7).

sure in anaesthetized WKY as well as in conscious SH and WKY rats. When dicentrine (1.0 mg kg^{-1}) was administered i.v. to anaesthetized and conscious rats, it caused a decrease in blood pressure of similar magnitude to that caused by prazosin (0.1 mg kg^{-1}). Classic α-adrenoceptor antagonists, such as phentolamine, phenoxybenzamine, tolazoline and hydrogenated ergot alkaloids have not proven useful for long-term blood pressure control in hypertensive patients (Craham & Pettinger, 1979; Van Zwieten, 1990). The administration of these drugs is accompanied by marked reflex tachycardia, triggered by the baroreceptor reflex system and autonomic nervous system. However, according to Constantine *et al.* (1978), prazosin does not cause reflex tachycardia in conscious dogs due perhaps to reduced baroreceptor modulation since prazosin depresses the baroreflex function in cats (Cambridge *et al.*, 1977), dogs (Hardey & Lokhandwala, 1979) and rats (Persson *et al.*, 1981). In this study, with dicentrine treatment, there was no significant change in heart rate at the doses employed. Because dicentrine causes little or

no heart rate increase, it differs from, and has therapeutic advantages over peripheral direct vasodilators (such as hydralazine) and classic α-adrenoceptor antagonists (phentolamine) (Massingham & Hayden, 1975).

Prazosin does not decrease cardiac output (Constantine *et al.*, 1973). Its hypotensive effect is mainly due to decreases in total peripheral resistance, reflecting dilatation of arterioles as a result of vascular α_1-adrenoceptor blockade. Because the hypotensive activity of prazosin is abolished by either ganglionic blockade or by α-adrenoceptor blockade, prazosin clearly acts by interference with peripheral sympathetic function and is devoid of direct vasodilator activity (Graham *et al.*, 1977; Van Zwieten, 1990). Administration of dicentrine i.v. to anaesthetized rats pretreated with prazosin or phentolamine did not lead to any futher fall in MAP. This suggests that dicentrine, prazosin and phentolamine may act on a common receptor to mediate a depressor response. Thus, the mechanism of action of dicentrine differs from that of direct-acting vasodilators such as hydralazine and diazoxide.

Pressor responses to noradrenaline are impaired by α-adrenoceptor blockade (Freis *et al.*, 1951; Ablad *et al.*, 1975). In the present studies, both prazosin and dicentrine significantly attenuated pressor responses to noradrenaline. On the other hand, both failed, even at maximal hypotensive doses, to impair the pressor activity of angiotensin II or vasopressin. In addition, Teng *et al.* (1991) demonstrated that dicentrine did not affect the aortic contraction induced by U-46619, angiotensin II, KCl or carbachol and it specifically displaced only [^{3}H]-prazosin binding. These results are indicative of specific α-adrenoceptor blockade.

Results from several studies have demonstrated that noradrenaline levels in a variety of vascular and nonvascular tissues are elevated in SH rats compared to their normotensive genetic control, the WKY rats (Donohue *et al.*, 1988).The tissues examined include mesenteric artery (Head *et al.*, 1985), caudal artery (Cassis *et al.*, 1985), kidney, aorta and vas deferens (Head *et al.*, 1985). There is evidence to suggest that the elevated noradrenaline concentration in these tissues is due to a greater sympathetic innervation in the hypertensive strain. This may explain why intravenous bolus injections of dicentrine and prazosin evoked greater decreases in MAP in conscious SH rats and support the concept that dicentrine acts via inhibition of α-adrenoceptor activity.

Assessment of the effects of dicentrine in conscious SH rats showed that it is a potent and long-acting hypotensive agent when administered orally. Although the onset of action was very rapid, blood pressure diminutions of >25 mmHg were evident 10 h after administration, suggesting good bioavailability.

In conclusion, like prazosin, dicentrine decreases MAP, reduces TPR and enhances blood flow whilst affording minimal changes in CO. However, unlike prazosin, dicentrine does not influence HR. The drug appears to block vascular α-adrenoceptors and is orally active. Dicentrine may thus hold therapeutic potential as an oral antihypertensive agent.

This work was supported by research grants of the National Science Council of the Republic of China (NSC 81-0412-B002-113) and the National Research Institute of Chinese Medicine.

References

ABLAD, B., BORG, K.O., CARLSSON, E., EK, L., JOHNSSON, G., MALMFORS, T. & REGARDH, C.G. (1975). A survey of the pharmacological properties of metoprolol in animals and man. *Acta Pharmacol. Toxicol.*, **36**, 7–23.

CAMBRIDGE, D., DAVEY, M.J. & MASSINGHAM, R. (1977). The pharmacology of antihypertensive drugs with special reference to vasodilators, α_1-adrenergic blocking agents and prazosin. *Med. J. Aust.*, **5** (Suppl. 2), 2–5.

CASSIS, L.A., STITZEL, R.E. & HEAD, R.J. (1985). Hypernoradrenergic innervation of the caudal artery of the spontaneously hypertensive rats: An influence upon neuroeffector mechanism. *J. Pharmacol. Exp. Ther.*, **234**, 792–803.

CAVERO, I. & ROACH, A.G. (1980). The pharmacology of prazosin, a novel antihypertensive agent. *Life Sci.*, **27**, 1525–1540.

CHEN, C.C., HUANG, Y.L., OU, J.C., SU, M.J., YU, S.M. & TENG, C.M. (1991). Bioactive principles from the roots of *Lindera megaphylla*. *Planta Medica*, **57**, 406–408.

CONSTANTINE, J.W., MC SHANE, W.K., SCRIABINE, A. & HESS, H.J. (1973). Analysis of the hypotensive action of prazosin. In *Hypertension: Mechanisms and Management*. ed. Onesti, G., Kim, K.E. & Moyer, J.H. pp. 429–444. New York: Grune and Stratton.

CONSTANTINE, J.W., WEEKS, R.A. & MC SHANE, W.K. (1978). Prazosin and presynaptic α-receptors in the cardioaccelerator nerve of the dog. *Eur. J. Pharmacol.*, **50**, 51–60.

CRAHAM, R.M. & PETTINGER, W.A. (1979). Drug therapy, prazosin. *N. Engl. J. Med.*, **300**, 232–236.

DONOHUE, S.J., STITEEL, R.E. & HEAD, R.J. (1988). Time course of changes in the norepinephrine content of tissues from spontaneously hypertensive and Wistar kyoto rats. *J. Pharmacol. Exp. Ther.*, **245**, 24–31.

FREIS, E.D., MACKAY, J.C. & OLIVER, W.F. (1951). The effect of sympatholytic drugs on the cardiovascular responses to epinephrine and norepinephrine in man. *Circulation*, **3**, 254–259.

GRAHAM, R.M., OATES, H.F., STOKER, L.M. & STOKES, G.S. (1977). Alpha-blocking action of the antihypertensive agent, prazosin. *J. Pharmacol. Exp. Ther.*, **201**, 747–752.

HARDEY, D.W. & LOKHANDWALA, M.F. (1979). Influence of prazosin on cardiac reflex function. *Eur. J. Pharmacol.*, **57**, 251–254.

HAYWOOD, J.R., SHAFFER, R.A., FASTENOW, C., FINK, G.D. & BRODY, M.J. (1981). Regional blood flow measurement with pulsed Doppler flowmeters in conscious rat. *Am. J. Physiol.*, **241**, H273–H278.

HEAD, R.J., CASSIS, L.A., ROBINSON, R.L., WESTFALL, D.P. & STITZEL, R.E. (1985). Altered catecholamine contents in vascular and nonvascular tissues in genetically hypertensive rats. *Blood Vessels*, **22**, 196–204.

MASSINGHAM, R. & HAYDEN, M.L. (1975). A comparison of the effects of prazosin and dihydralazine on blood pressure, heart rate and plasma renin activity in conscious renal hypertensive drugs. *Eur. J. Pharmacol.*, **30**, 121–124.

MINNEMAN, K.P. (1988). α_1-Adrenergic receptor subtypes, inositol phosphates, and sources of cell Ca^{2+}. *Pharmacol. Rev.*, **40**, 87–119.

PERSSON, B., YAO, T. & THOREN, P. (1981). Correlation between decreased heart rate and central inhibition of sympathetic discharges after prazosin administration in the spontaneously hypertensive rat. *Clin. Exp. Hypertens.*, **3**, 245–250.

STANASZEK, W.F., KELLERMAN, D. & BROGDEN, R.N. (1983). Prazosin update. A review of its pharmacological properties and therapeutic use in hypertension and congestive heart failure. *Drugs*, **25**, 339–384.

TENG, C.M., YU, S.M., KO, F.N., CHEN, C.C., HUANG, Y.L. & HUANG, T.F. (1991). Dicentrine, a natural vascular α_1-adrenoceptor antagonist, isolated from *Lindera megaphylla*. *Br. J. Pharmacol.*, **104**, 651–656.

TITMARSCH, S. & MONK, J.P. (1987). Terazosin. A review of its pharmacodynamic and pharmacokinetic properties, and therapeutic efficacy in essential hypertension. *Drugs*, **33**, 461–477.

VAN ZWIETEN, P.A. (1990). α-Adrenoceptor antagonists. In *Handb. Exp. Pharmacol.: Pharmacology of Antihypertensive Therapeutics*. ed. Ganten, D. & Mulrow, P.J. pp. 105–125. New York: Springer Verlag.

(Received February 19, 1992
Revised March 18, 1992
Accepted March 23, 1992)

Br. J. Pharmacol. (1992), **106**, 802–812 © Macmillan Press Ltd, 1992

The mechanism by which procaine inhibits catecholamine secretion from bovine chromaffin cells

P. Charlesworth, [1]I. Jacobson, G. Pocock & [2]C.D. Richards

Department of Physiology, Royal Free Hospital School of Medicine, Rowland Hill Street, London NW3 2PF

1 We have investigated the action of procaine on stimulus-secretion coupling in bovine adrenal chromaffin cells.

2 Procaine inhibited the catecholamine secretion evoked by 500 μM carbachol (CCh) with an IC_{50} of 35 μM and the associated calcium influx (IC_{50} 60 μM). It inhibited the catecholamine secretion evoked by depolarization with high potassium by less than 20% even at the highest concentrations tested (3.2 mM).

3 The secretion evoked by CCh was associated with an increase in sodium influx. This evoked influx was also inhibited by procaine (IC_{50} 80 μM).

4 This selective action of procaine on the CCh-evoked catecholamine secretion was investigated further by patch-clamp techniques.

5 In agreement with the ion flux studies, procaine inhibited the inward current evoked by CCh. Procaine also altered the spectral characteristics of the noise associated with the agonist-induced current by adding an additional high frequency component. The amplitude of this component showed an e-fold increase for a 55 mV membrane hyperpolarization.

6 Data from cell-attached patches showed that increasing concentrations of procaine produced a progressive fall in the mean channel open time and an increase in mean blocked time. This combination led to a decrease in mean burst length. In addition, P_{open} was reduced by 50 μM procaine. These changes in channel conducting time were sufficient to account for the reduction in inward current. A limited study of the action of procaine on nicotinic channels in outside-out patches gave similar results.

7 The data were considered in relation to various schemes of anaesthetic-channel interactions. The data did not fit the sequential blocking model or the extended channel block model but could be fitted to a modified sequential blocking model in which the rate constant for channel reopening after block was itself subject to modulation by the anaesthetic and the blocked channel could close without passing through the open state.

Keywords: Anaesthetic; chromaffin cells; catecholamines; nicotinic receptor; patch-clamp; procaine; secretion

Introduction

Bovine adrenal chromaffin cells secrete catecholamines in response to nicotinic stimulation or to direct depolarization (Baker & Knight, 1984; Douglas & Rubin, 1963). We have previously shown that general anaesthetics such as pentobarbitone and halothane interfere with this secretion by depressing the influx of sodium and calcium ions (Pocock & Richards, 1987; 1988). Although local anaesthetics such as procaine are primarily used as nerve blocking agents they are also known to modify the response of the nicotinic acetylcholine receptors of the neuromuscular junction (Katz & Miledi, 1975; Adams, 1976; Ruff, 1977; Neher, 1983) and those of *Aplysia* neurones (Marty, 1978). In addition, procaine inhibits chemical transmission in the olfactory cortex (Richards, 1982) an action it shares with general anaesthetic agents (see Pocock & Richards, 1991 for a recent review).

To examine in greater detail the mechanism by which procaine modifies chemical transmission, we have investigated its action on stimulus-secretion coupling in bovine isolated adrenal medullary cells. These cells are derived from embryonic neural crest tissue and are homologous with sympathetic postganglionic neurones. Following isolation they retain the secretory characteristics of the intact tissue (Baker & Knight, 1984) and offer a suitable experimental model for detailed study of neurosecretion at the cellular and molecular level. Here we describe experiments in which we have made parallel measurements of ion fluxes and catecholamine secretion in intact cells and employed patch clamp recording techniques to characterize the actions of procaine on the events underlying stimulus-secretion coupling. We show that while procaine has little effect on secretion evoked by direct depolarization, it selectively inhibits the secretion evoked by nicotinic agonists such as carbachol (CCh). This inhibition of catecholamine secretion occurs at concentrations of procaine much less than those required for nerve block and can be fully accounted for by blockade of the channels gated by the nicotinic receptor. A preliminary account has been given to the Physiological Society (Charlesworth *et al.*, 1990).

Methods

Preparation and handling of cells

Bovine chromaffin cells were isolated by enzymic digestion as described previously (Pocock, 1983a). For tissue culture, the cell isolation procedure was carried out under sterile conditions and the resulting suspension was purified by differential plating as described by Waymire *et al.* (1983). For the patch-clamp experiments, cells were plated on glass coverslips at a density of 0.5×10^6 ml^{-1}. The coverslips were coated with poly-L-lysine or collagen prior to plating. A small number of experiments were performed with cells immobilised on cytodex beads. For these studies the cells were plated at a density of $2-5 \times 10^6$ ml^{-1} and maintained in culture in petri dishes. Cultures were maintained in a 1:1 mixture of Dulbecco's minimum essential medium and Ham's F12 medium supple-

[1] Present address: Institute of Neurobiology, University of Göteborg, POB 33031, S-400 33 Göteborg, Sweden.
[2] Author for correspondence.

mented with newborn bovine serum (usually 10% but supplements of 2% or 5% were occasionally used) and kept at 37°C in a humidified atmosphere containing 5% CO_2.

Measurement of catecholamine secretion and ion fluxes in cell suspensions

Basal and evoked secretion of catecholamines and the associated ion fluxes were measured by centrifuging cell suspensions through a layer of oil as described previously (Pocock, 1983b; Pocock & Richards, 1987). To measure the ^{22}Na influx evoked by CCh it was necessary to inhibit the sodium efflux via the sodium pump and sodium influx via voltage-gated sodium channels respectively by including ouabain (20 μM) and tetrodotoxin (TTX; 10 μM) in the bathing medium. The catecholamine content of the cell suspension and supernatant was assayed by the method of von Euler & Floding (1955) using a Perkin-Elmer fluorescence spectrophotometer. Catecholamine secretion could then be expressed as a percentage of the total (see Pocock, 1983a and Pocock & Richards, 1987 for further details).

Continuous measurement of catecholamine secretion from immobilised cells

Cytodex beads carrying cells were mounted in a small perspex column (10 × 3 mm) and perfused continuously at 1 ml min^{-1} with sodium Locke solution. Where appropriate to the experimental design, procaine was included in the perfusate. The cells were stimulated by injecting either 100 μl or 2 ml of a 500 μM solution of CCh in sodium Locke solution into the perfusing stream via an injection loop. The injected solution contained procaine when required. The catecholamine content of the perfusate was monitored continuously by an electrochemical detector (Applied Chromatography Systems model 350/06). Neither procaine nor CCh interfered with the electrochemical assay of the catecholamine.

Electrophysiological methods

Experiments were carried out using three variants of the patch-clamp recording technique of Hamill *et al.* (1981). The configurations used were on-cell (cell attached) recording, whole cell recording under voltage clamp and recording from excised outside-out patches. All experiments were performed on small spherical chromaffin cells (10–15 μm diameter) which had a capacitance of less than 10 pF. Patch pipettes were fabricated from thick-walled borosilicate glass (Clarke Electromedical GC150) and had tip diameters of 1–2 μm. The electrode tips were fire polished on a microforge before use. Their resistance was 5–15 MΩ and the series resistance was always less than 60 MΩ and usually less than 20 MΩ. As the input resistance of chromaffin cells was more than 1 GΩ in all of our recordings and as the currents flowing through the pipette during the experiment were small, the voltage errors due to series resistance were also small and membrane holding potentials were not corrected for these errors. All experiments were performed at room temperature (18–22°C).

Recording and analysis Signals were recorded with either a List electronic L/M EPC-5 or Axopatch 1D patch clamp amplifier and were stored on magnetic tape (flat bandwidth d.c.-2.5 kHz or in later experiments d.c.-20 kHz). For analysis of whole cell current noise the signal from the tape recorder was filtered with a 7-pole Cauer eliptical filter (Frequency Devices model 675, bandpass d.c.-1 kHz) and digitized at 2.5 kHz. These anti-aliasing filters give a flat frequency – response (typically ± 0.02 dB) to their cutoff frequency with a phase shift similar to that of an eight pole Butterworth filter but have a much greater attenuation rate above the cutoff (−94 dB at twice the corner frequency). The residual high frequency ripple lies below the resolution of the least significant bit of our 12 bit analogue to digital converter. Records were divided into 0.4 s blocks prior to calculation of the spectral density. CCh or CCh plus procaine was applied for 60 s in order to acquire sufficient time blocks for averaging and each spectrum was derived from a single continuous application. The mean power spectrum was calculated by averaging at least sixty four of the spectra obtained from the 0.4 s time blocks. To obtain the noise spectrum due to application of agonist alone the spectrum obtained before application of agonist was subtracted from that obtained during its application. The resulting spectra were then fitted by either a single or a double Lorentzian function using a least-squares Levenberg-Marquart algorithm with proportional weighting of the data points. The quality of the fitted curve was judged from the value of χ^2 and the random distribution of residuals. The amplitude of single channel currents was estimated from the parameters derived from the fitted power spectra and the mean inward current (Anderson & Stevens, 1973; Cull-Candy *et al.*, 1988).

For the analysis of the single channel events, signals were low-pass filtered at 1 kHz with a four-pole Bessel Filter and digitised at 10 kHz. To determine the frequency and duration of channel openings an all-points histogram of current amplitude was first constructed and Gaussian distributions fitted to the peaks in the histogram. The detection threshold for channel opening was then set at 50% of the amplitude for a single channel opening. Each transition was inspected and an idealized reconstruction of the open-closed transitions made. From this transition list we constructed frequency distribution histograms of open state and closed state durations. For analysis of the transition list, multiple channel openings were excluded from the formal data analysis together with openings of less than full amplitude (apparent substates), the excluded states were considered closed and their time values amalgamated with the preceding closed times. For the data obtained from some patches we also analysed the distribution of open and closed times taking the substate to be equivalent to a full opening. The time constants of the distributions of open and closed times derived in this way were little different from those obtained solely from full amplitude openings. The minimum resolvable time of single channel events for a low pass filter of 1 kHz was taken as 0.3 ms. Shorter events were considered unresolved. These unresolved openings and closures bias the recorded value in the first bin of frequency histograms leading to a consistent under-estimate of the true value. For this reason, the value of the first bin was always excluded from the curve fitting procedures

Very long openings in the cell attached configuration tended to show a distinct relaxation. As chromaffin cells have a high input resistance (> 1 GΩ) the current flowing through a single nicotinic channel may well be sufficient to depolarize the cell by a few mV, sufficient to account for the observed relaxation (seen Fenwick *et al.*, 1982). Nevertheless, the amplitude of these long openings rarely falls by more than 20% and so the openings do not fall below the 50% detection threshold. The relaxation of current amplitude will not contribute significantly to the all points current distribution as long openings are comparatively rare.

For the anlaysis of 'bursts' of openings we calculated a critical gap length for bursts below which a closure is classified as a gap within a burst (Colquhoun & Sakmann, 1983; Clapham & Neher, 1984). This is calculated so that the proportion of short intervals misclassified as closures between bursts was equal to the proportion of long intervals misclassified as closures within bursts. In practice the value of this time interval (t_{crit}) under control conditions was about 3 ms but the calculation of burst frequency and duration was not unduly sensitive to small changes in the chosen value.

The curve fitting procedure employed an unweighted least-squares Levenberg-Marquart algorithm as this procedure has previously been shown to be relatively insensitive to truncation of data sets (Dionne & Liebowicz, 1982).

To record whole cell calcium currents, cells were subjected to a depolarizing step of 100 ms duration from a holding

potential of −80 mV to zero at 10 s intervals. The mean inward current flowing in response to the voltage step was then plotted as a time sequence to give the final record. The pulse sequence was controlled by a Tandon PCA computer coupled to a Cambridge Electronic Design 1401 interface.

The spectral noise analysis (SPAN), voltage clamp (VCAN) and channel transition (PAT) detection programmes were kindly supplied by Dr John Dempster, University of Strathclyde, U.K.

Solutions

The external bathing medium (Locke solution) contained (mM): NaCl 140, KCl 5, $MgCl_2$ 1.8, $CaCl_2$ 1.0, HEPES 15, glucose 5.5; the pH was adjusted to 7.4 with NaOH. For the experiments designed to study the correlation between catecholamine secretion and ion movements procaine and CCh were dissolved in Locke solution at concentrations appropriate to the experimental design and cell suspensions were added to these solutions. For studies of the effects of procaine on secretion evoked by direct depolarization, cell suspensions were added to an equal volume of Locke solution in which the concentration of sodium and potassium ions had been reversed. The cells are therefore depolarized by a solution containing 75 mM K^+. Further experimental details can be found in the papers by Pocock & Richards (1987, 1988).

For the experiments on the nicotinic receptor we wished to define the equilibrium potentials for sodium and potassium. To achieve this the pipettes used for whole cell recordings contained (mM): KCl 120, NaCl 20, $MgCl_2$ 2, $CaCl_2$ 1, EGTA 11; the pH was adjusted to 7.2 with KOH and free calcium was measured as less than 10^{-7} M with an Orion 93-20 calcium electrode. For recording from outside-out patches, KCl was 140 mM and NaCl was omitted and other ions were as for the whole cell recordings. For cell attached patches the electrode was filled with sodium Locke solution containing either 10 μM CCh or 10 μM CCh plus an appropriate concentration of procaine.

To maximize the amplitude of the calcium channel currents we used barium as the main charge carrier (see Nowycky *et al.*, 1985) and for these experiments the bathing medium contained mM: tetraethyl ammonium chloride 120, $CsCl_2$ 5, $BaCl_2$ 10, HEPES 10, glucose 10 and tetrodotoxin 10 μM pH 7.4. The pipette contained mM: $CsCl_2$ 120, EGTA 10, $MgCl_2$ 5, HEPES 40, ATP 2 and GTP 0.3, pH 7.2

In the whole-cell patch-clamp experiments procaine and CCh were applied by microperfusion by use of a U-tube similar to that described by Krishtal & Pidoplichko (1980) and for the outside-out patches procaine was applied by pressure from a micropipette. For cell-attached patch-clamp experiments both CCh and procaine were present in the patch pipette at appropriate concentrations. Both carbachol and procaine were obtained from Sigma Chemicals Co.

Statistical analysis

Combined values are shown as mean ± s.e.mean unless otherwise indicated. Differences between data sets were assessed using the *t* test and were considered statistically significant when $P < 0.05$.

Results

The action of procaine on catecholamine secretion

In agreement with our previous work (Pocock & Richards, 1987; 1988) the total catecholamine content of the cell suspensions was around 70 nmol/10^6 cells. In the absence of secretagogues, the catecholamine present in the medium after 10–15 min incubation was 3–5% of the total. Concentrations of procaine up to 200 μM produced no significant change in this basal secretion. Higher concentrations of anaesthetic (400–3200 μM) produced statistically significant increases ($P < 0.05$) in basal secretion e.g. from 4.43 ± 0.28% ($n = 14$; control) to 6.27 ± 0.60% (mean ± s.e.mean; for 1600 μM procaine; $n = 4$).

As described previously (Pocock & Richards, 1987) the chromaffin cells were stimulated to secrete by exposure to either 500 μM CCh or a solution nominally containing 75 mM potassium. These stimuli caused an additional 3.82 ± 0.18% of total catecholamine to be secreted following potassium depolarization ($n = 7$) and 3.83 ± 0.33% following stimulation by CCh ($n = 14$). Figure 1 shows the effects of procaine (5–3200 μM) on catecholamine secretion evoked by both CCh and high potassium. CCh-evoked secretion was strongly inhibited by the anaesthetic with an IC_{50} of 35 μM. In contrast, the secretion evoked by high potassium was scarcely inhibited (less than 20%) even at the highest concentrations of anaesthetic tested (3.2 mM). The Hill coefficient for the inhibition of CCh-evoked catecholamine secretion by procaine was 1.1.

Effect of procaine on the time-course of secretion

To determine the effect of procaine on the rate of catecholamine secretion, beads carrying chromaffin cells were mounted in a small column and continously perfused with Locke solution at approximately 1 ml min^{-1}. The effluent from the column was continuously monitored to determine the rate of catecholamine secretion (see Methods). In response to a brief pulse of 200 μM CCh (about 6 s duration) injected into the superfusate the catecholamine secretion from the immobilised cells rose to a peak within 15–20 s as shown in Figure 2a and declined over the ensuing 40–45 s. When cells were exposed to CCh for 80–120 s, secretion reached a plateau before declining slowly in the continuing presence of the agonist, with a half time of about 80 s. Repeated applications of identical pulses of CCh led to decreasing responses similar to the progressive decrease in the secretory response of intact glands (Douglas & Rubin, 1963; Holmes & Schneider, 1973).

In the presence of procaine (50 μM) both the rate of rise and the extent of secretion seen in response to CCh were depressed as shown in Figure 2. The rate of decline of secretion was accelerated during prolonged exposure to the agonist. The half time for decay decreased from 80 ± 1 s in control to 41 ± 2 s in the presence of 50 μM procaine ($n = 3$). Nevertheless, this effect was insufficient to account for the overall decrease in catecholamine secretion. These effects of procaine were partially reversible (see Figure 2).

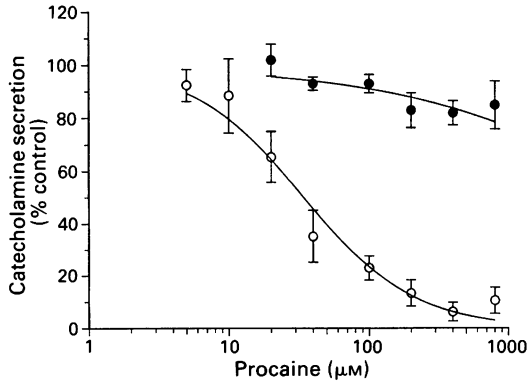

Figure 1 The concentration-dependence of the inhibition of catecholamine secretion by procaine. Freshly isolated bovine chromaffin cells were stimulated by either 75 mM potassium (●) or 500 μM carbachol (CCh, ○) as described in the Methods. The line for CCh-evoked secretion was fitted to the Hill equation with a coefficient of 1.1.

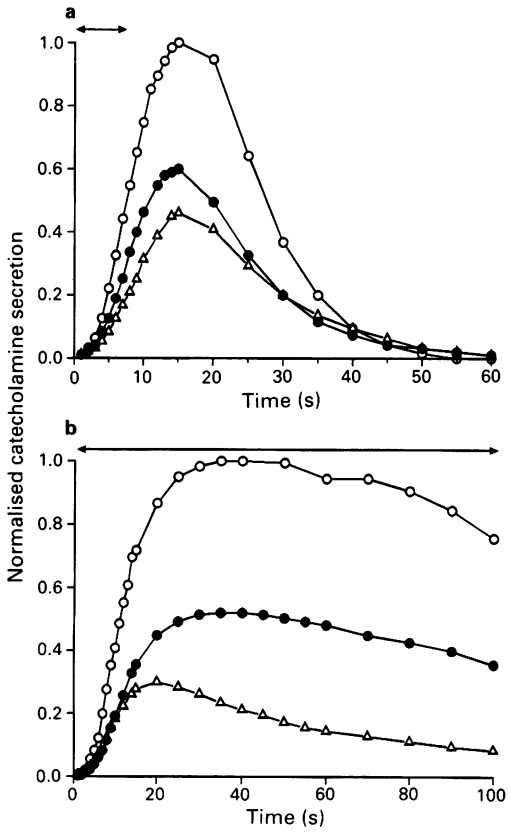

Figure 2 The effect of procaine on the time course of catecholamine secretion from cultured chromaffin cells attached to cytodex beads. The secretory response was normalised to the maximum seen following the initial challenge with carbachol (CCh). (a) The time course of catecholamine secretion seen in response to a 6 s pulse of 200 μM CCh as indicated by the double-headed arrow. (b) The time course of secretion during a 100 s application of CCh as indicated by the double-headed arrow. In (a) and (b): (○) control, (△) 50 μM procaine, (●) recovery.

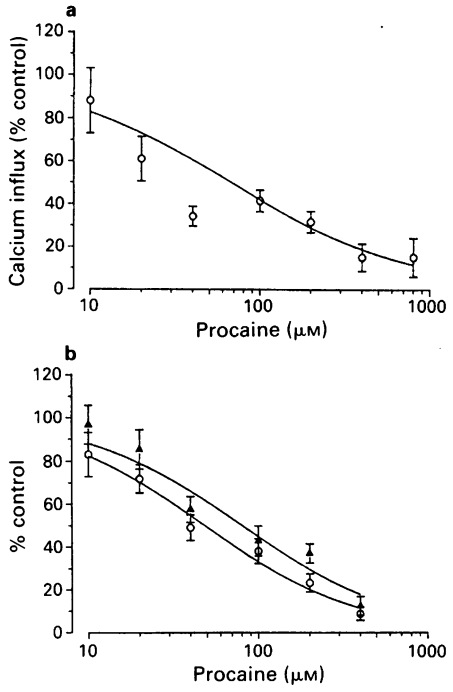

Figure 3 The concentration-dependence of the effect of procaine on carbachol on (CCh)-evoked ^{45}Ca influx (a) and on the CCh-evoked ^{22}Na influx and the associated catecholamine secretion (b) both expressed as a percentage of control. Lines were fitted to the Hill equation with coefficients of 0.82 for Ca^{2+} influx (a) and 0.97 and 0.95 for procaine inhibition of CCh-evoked catecholamine secretion (b, ○) and sodium influx (b, ▲).

The action of procaine on ^{45}Ca influx

Freshly isolated bovine chromaffin cells have a resting influx of ^{45}Ca of 21.1 ± 2.3 μmol (l cells)$^{-1}$ min^{-1}. When they were stimulated by either CCh or high potassium the increase in catecholamine secretion was paralleled by an increase in ^{45}Ca influx of 219 ± 39 and 581 ± 46 μmol (l cells)$^{-1}$ ($n = 6$) most of which occurred within the first minute of stimulation (see also Holz *et al.*, 1982; Pocock & Richards, 1987; 1988). Procaine at concentrations up to 800 μM had no significant effect on basal ^{45}Ca uptake but inhibited that seen in response to CCh with an IC_{50} of approximately 60 μM (see Figure 3a). In agreement with the data for secretion, procaine had little effect on the potassium-evoked ^{45}Ca influx. The inhibition by procaine of the ^{45}Ca influx evoked by CCh could be fitted to a Hill equation with a coefficient of 0.82.

The action of procaine on carbachol-evoked ^{22}Na influx and catecholamine secretion

It is generally agreed that activation of nicotinic receptors is associated with the inward movement of sodium ions (Fenwick *et al.*, 1982; Cull-Candy *et al.*, 1988; Jacobson *et al.*, 1991). In agreement with this we have shown previously a strong dependence of CCh-evoked secretion upon extracellular sodium ions (Pocock & Richards, 1987; 1988). Under the conditions for measuring sodium influx given in the Methods, procaine inhibited the CCh-evoked catecholamine secretion with an IC_{50} of approximately 50 μM (see Figure 3b). Concentrations of procaine up to 400 μM had no significant effect on resting ^{22}Na influx which was 3.02 ± 0.10 mmol (l cells)$^{-1}$ min^{-1} ($n = 6$). In the absence of procaine the CCh-evoked ^{22}Na influx was 13.5 ± 0.8 mmol (l cells)$^{-1}$ almost all of which occurred within the first minute of stimulation. The ^{22}Na influx evoked by CCh was inhibited by the anaesthetic with an IC_{50} of approximately 80 μM (Figure 3b), in parallel with the inhibition of secretion. As for the experiments with ^{45}Ca influx, the inhibition of both catecholamine secretion and ^{22}Na influx by procaine could be fitted by a Hill equation with a coefficient close to unity (0.97 and 0.95 respectively).

Electrophysiological analysis of the effect of procaine

Action of procaine on carbachol-evoked inward current By use of the whole cell variant of the patch clamp technique it is possible to record an inward current in response to application of CCh to adrenal chromaffin cells. This inward current is the electrical parallel of the agonist-evoked ^{22}Na influx. Figure 4 shows typical current records observed in single chromaffin cells in response to a 5 s pulse of 200 μM CCh. There is a fast initial transient followed by a rapid decline, reflecting receptor desensitization. The initial amplitude varied from cell to cell and tended to desensitize with repeated applications. For the control tests the peak inward current had a mean value of 261 pA and ranged from 458 pA to 35 pA (6 tests in three cells). During a 5 s application of 200 μM CCh the total charge carried ranged from 40 to 721 pC and had a mean value of 347 pC. The decay of the inward current could be fitted by a single exponential with a mean time constant of 1.06 ± 0.06 s. In paired tests, co-application of procaine (50 μM) reduced the total charge carried to 46 ± 7% of control (mean ± s.e.mean; 6 paired tests in three cells). This decrease resulted both from a reduction in peak amplitude (59 ± 7% of control) and from a reduction in the time constant of current decay (66.5 ± 9.3%

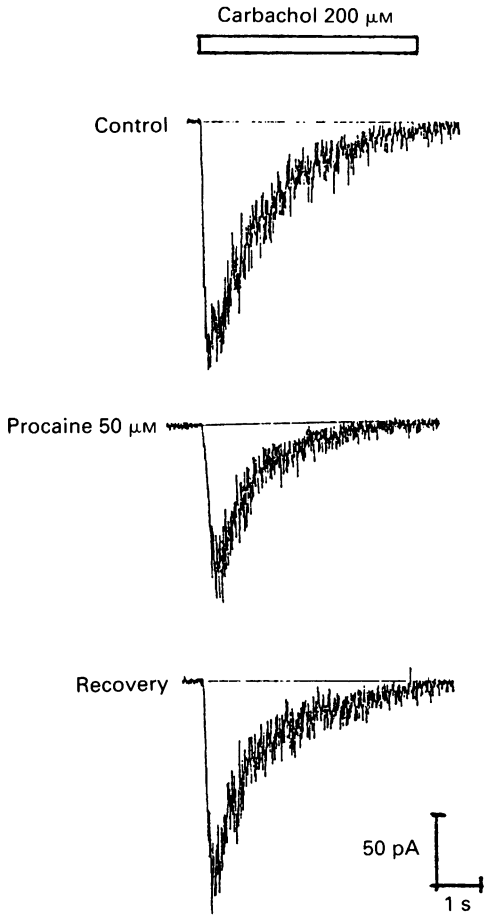

Figure 4 The action of 50 μM procaine on the carbachol (CCh)-evoked inward current. The record was obtained by the whole cell voltage clamp technique and shows the response of a single chromaffin cell to a 5 s pulse of 200 μM CCh before, during and after exposure to 50 μM procaine. Holding potential was −80 mV. The interval between each record was 30 s. Inward currents are shown by downward deflections.

of control). These effects of procaine on the CCh-evoked inward current were largely reversed on washing. After recovery the total charge carried was 87 ± 9%, the peak amplitude was 80 ± 9% and time constant of decay was 90 ± 9% of the paired control values. An example of the action of procaine on the inward current is shown in Figure 4.

Low concentrations of CCh (10 μM) evoke a small inward current that does not show an obvious time-dependent decay. With a holding potential of −80 mV the steady-state inward current evoked by 10 μM CCh had a mean value of 1.58 ± 0.22 pA. Co-application of 20 μM procaine with 10 μM CCh reduced the inward current to 0.66 ± 0.12 pA (seven cells). When expressed as a percentage of the paired control the inward current was inhibited by 56 ± 6% ($n = 7$). In two cells, 50 μM procaine reduced the steady-state inward current by 80%.

Noise analysis An increase in noise is associated with the inward current (see Figure 4) and this noise can be attributed to activation of nicotinic channels (Anderson & Stevens, 1973; Fenwick *et al.*, 1982; Cull-Candy *et al.*, 1988). In the experiments described here the CCh concentration was kept low (10 μM) to avoid significant desensitization of the response and the mean inward current at a holding potential of −80 mV was very low at 1.58 ± 0.22 pA. With this holding potential a spectral analysis of the agonist-induced noise yielded a frequency distribution that was adequately fitted by a single Lorentzian function with a corner frequency of 15.6 ± 1.1 Hz ($n = 7$). This corner frequency corresponds to a time constant for channel closure of 10.2 ms for the simple model of channel behaviour proposed by Anderson & Stevens (1973). Similar values were found at other holding potentials (e.g. Figure 5a,c). A slightly better fit could be obtained by the sum of two Lorentzian functions in some instances (see also Jacobson *et al.*, 1991). The main component had a corner frequency around 15 Hz and the second a corner frequency around 100 Hz but the low-frequency intercept (S(0)) value of the high frequency component was usually less than 1% of the low frequency component. As the high frequency component was very small and the errors in estimating its parameters correspondingly large we have fitted our control data to single Lorentzian functions (Figure 5). The single channel conductance estimated from the noise spectra and the mean inward current was 32 ± 1.5 pS ($n = 7$). The reversal potential of CCh-evoked inward current was found to be −13 mV by extrapolation, a value close to the expected value of −3 mV assuming the nicotinic channel to be equally permeable to both sodium and potassium ions.

In addition to its depressant action on inward current, procaine caused a second, higher frequency, component to

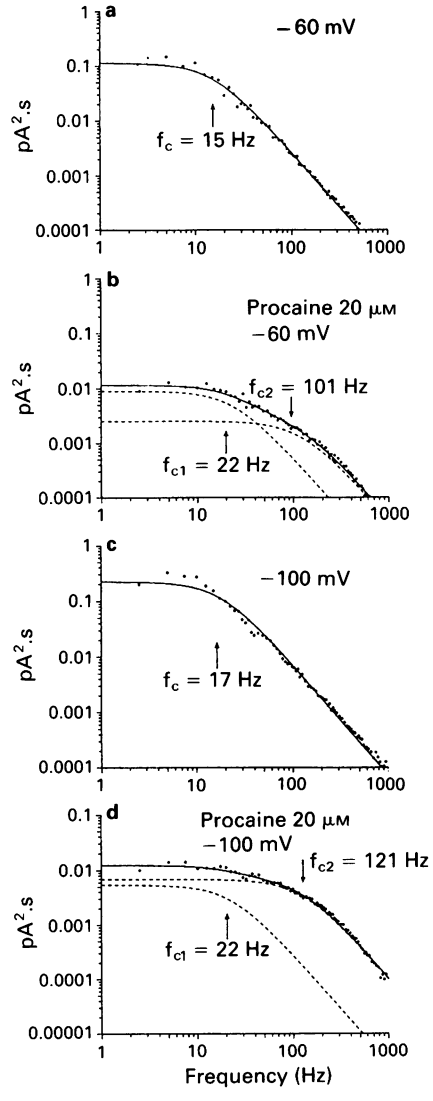

Figure 5 Spectral analysis of carbachol (CCh)-induced current noise in the presence and absence of 20 μM procaine. (a, c) Show the control spectra for holding potentials of −60 mV (a) and −100 mV (c). Panels (b, d) show spectra for the same holding potentials in the presence of anaesthetic. All data are from a single chromaffin cell.

appear prominently in the noise spectrum (see also Katz & Miledi, 1975). With a holding potential of −80 mV, co-application of 10 μM CCh and 20 μM procaine gave noise spectra that were best fitted by the sum of two Lorentzians with corner frequencies of 22.5 ± 1.2 Hz and 122 ± 6 Hz ($n = 7$) corresponding to time constants for channel closure of 7.1 and 1.3 ms respectively. The S(0) intercept of the low frequency component was on average 2.4 times that of the high frequency component when the holding potential was −80 mV. A similar pattern is seen at other holding potentials (see Figure 5b,d). In two cells, co-application of 10 μM CCh with 50 μM procaine the corner frequencies were higher at 36 Hz and 280 Hz (corresponding to time constants of 4.4 and 0.6 ms). At this concentration of procaine the relative amplitude of the S(0) value of the high frequency component was also increased. Procaine had no effect on the apparent single channel conductance calculated from the noise spectra. The conductance was 32.6 ± 1.3 pS ($n = 7$) in 20 μM procaine and 36 and 35 pS for two determinations in 50 μM procaine.

Voltage-dependence of procaine action The voltage-dependence of the noise spectra was examined in seven cells. In the absence of procaine the corner frequency showed no consistent change as the holding potential was varied between −100 mV and −50 mV (see Figure 5a,c). This is somewhat at variance with the weak voltage-dependence of corner frequency reported by Cull-Candy *et al.* (1988). The reason for this discrepancy is not clear. In the presence of 20 μM procaine, neither the corner frequency of the low frequency component nor that of the high frequency component showed any statistically significant trend with membrane potential. In contrast, the S(0) intercept of the high frequency component increased approximately linearly with increasing hyperpolarization showing an e-fold increase for a 55 mV hyperpolarization (Figures 5 and 6). At a holding potential of −100 mV the S(0) values for both components were almost equal.

Single channel studies

The lignocaine derivatives QX222 and QX314 have previously been shown to produce an increase in the high-frequency components of the noise induced by acetylcholine at the neuromuscular junction (Ruff, 1977; Neher & Steinbach, 1978). This behaviour has been explained in terms of a simple sequential blocking model (see Ruff, 1977; Neher & Steinbach, 1978; Colquhoun & Hawkes, 1983) which makes a number of predictions for anaesthetic-channel interactions. The most readily tested predictions are:

(1) That the mean channel open time should decrease as the anaesthetic concentration increases.

(2) That the mean time for which the channel is blocked should be independent of the anaesthetic concentration.

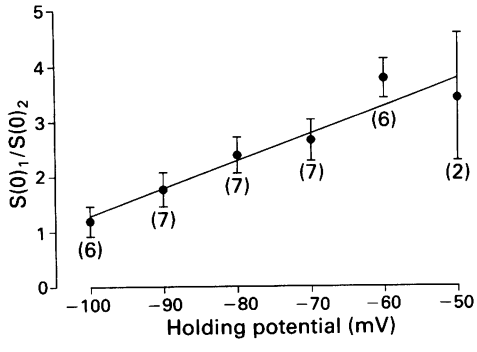

Figure 6 The influence of holding potential on the ratio between the zero-frequency intercepts ($S(0)_1/S(0)_2$) observed during the application of 20 μM procaine. The numbers in parentheses give the number of observations for each data point. The regression line was fitted to the equation $y = 0.05(x) + 6.27$ by the method of least squares.

(3) That the total channel open time within a burst of openings should be independent of the anaesthetic concentration.

(4) That the mean burst length should increase with increasing anaesthetic concentration.

The single channel studies described below were performed both to provide a detailed description of the action of procaine on a neuronal type of nicotinic channel and to test these predictions.

Cell attached patches With the cell attached configuration, CCh (10 μM) was always present in the patch pipette to activate the channels. In this configuration, application of procaine to the region outside the patch was ineffective in modifying the kinetics of channel opening so, where appropriate, procaine was included in the solution within the patch pipette at 2–50 μM.

When activated by CCh alone, the channel openings were seen as inward currents of approximately 2pA (Figure 7). The individual channel openings were usually single events and were not interrupted by brief closures (see below). In 6 out of 7 patches examined, the distribution of current amplitudes showed a second peak corresponding to a channel with 70% of the conductance of a full channel opening. These events appear to represent a substate of the nicotinic channel as direct transitions between the full and low conductance states were occasionally observed. The substate accounted for about a quarter of all transitions and, although we found no difference between the action of procaine on the low conductance state and its action on the full conductance state, we have excluded low conductance states from the formal analysis presented here (see Methods). The amplitude of the channel openings was unchanged by 2 and 10 μM procaine but 50 μM caused a statistically significant reduction in amplitude when assessed by the t test ($P < 0.05$; see Table 1). At this concentration, however, the channel openings are very brief with an open time distribution time constant of approximately 0.8 ms (see below). About two thirds of these fast openings will be shorter than 0.8 ms and will be attenuated by our low-pass filter (−3 dB at 1 kHz). In addition, when channel openings are very brief, it is not easy to distinguish substates from attenuated full openings. This apparent reduction in channel conductance can, therefore, be fully explained by the filter characteristics of the recording system.

In the absence of procaine the duration of channel open times was best fitted by the sum of two exponentials with time constants of 1.07 ms and 6.94 ms. The combined data for seven separate patches are shown in Figure 7a. The probability of the channel being in the open state (P_{open}) was low with a mean value of 0.0068 (Table 1).

Addition of procaine (2–50 μM) to the patch pipettes reduced the number of long duration openings and shifted the distribution of open times progressively to shorter intervals as the concentration of procaine increased (see Figure 7b–d). At the highest concentration tested, the open time distribution could be fitted by a single exponential with a time constant of 0.78 ms. The open time distributions of Figure 7 represent the combined data of between five and seven separate patches. The mean open time of the channels progressively decreased as the concentration of procaine increased (Figure 9) as predicted by the sequential blocking model. The channel blocking rate constant was estimated from these data as $2 \times 10^7\ M^{-1}\ s^{-1}$ (the value determined from the noise spectra was about $6 \times 10^6\ M^{-1}\ s^{-1}$). This decrease in mean channel open time was associated with marked oscillations of the open state which increased in frequency as the procaine concentration was increased from 2 to 10 μM (Figure 7). The open state probability was not significantly different from control for 2 and 10 μM procaine but was reduced in the presence of 50 μM procaine (see Table 1).

The closed times were distributed in a biphasic manner with a high incidence of brief closures (<2 ms) and a broad

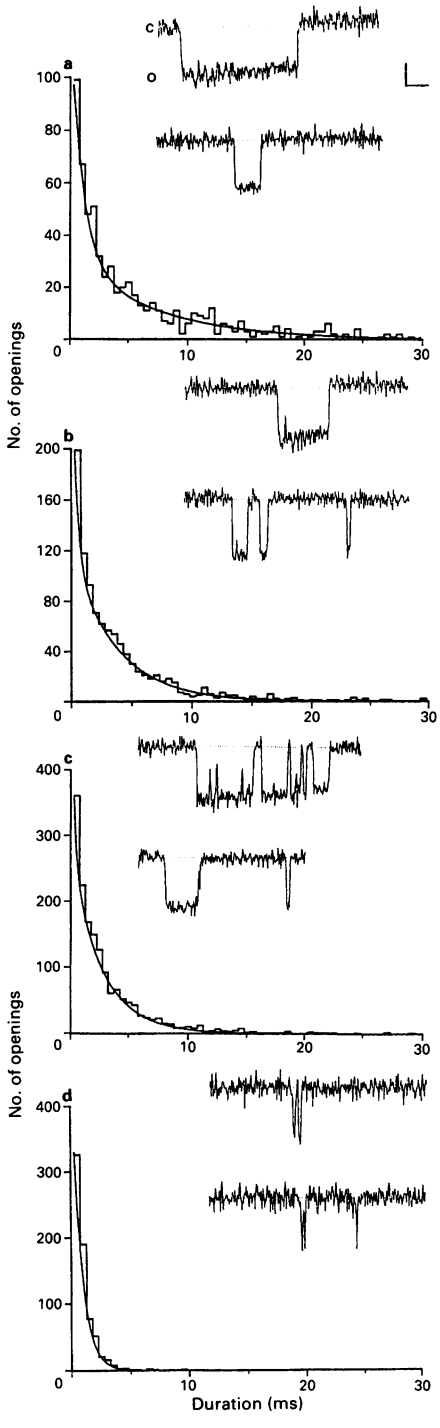

Figure 7 The effect of increasing concentrations of procaine on the distribution of the open times of the channels activated by 10 μM carbachol (CCh). Each panel shows combined data for 5–7 cell attached patches. The pipette potential was set at zero. The smooth curves are the calculated exponential functions fitted to the frequency distribution of open times greater than 0.5 ms (see Methods). The histograms shown are (a) control, (b) 2 μM procaine, (c) 10 μM procaine and (d) 50 μM procaine. The original records are examples of channel openings and bursts recorded under the stated conditions. Calibration bars in (a) apply to all traces and are 1 pA (vertical bar) and 10 ms (horizontal bar). The open state of the channel (reflecting *inward* current) is shown by downward deflections (o) from the closed state (c).

distribution of longer closed times which could be fitted with a time constant of about 500 ms (not shown). We interpret this biphasic distribution as follows: the brief closures represent closures within bursts and the longer closures are intervals between bursts (see also Colquhoun & Sakmann, 1983; Clapham & Neher, 1984). Application of procaine (2–50 μM) caused a progressive increase in the proportion of brief closures and their distribution was then best fitted by two exponentials (Figure 8 and Table 1). As the time constant for the distribution of the long closures reflects the gap between bursts and as the number of channels in a patch is not known, the long time constants are difficult to interpret and have therefore been ignored in our analysis.

Effects of procaine on bursting behaviour In the absence of procaine, the channel open times were exponentially distributed and there were few short channel closures. The distribution of burst length was therefore very similar to the distribution of channel open time. In the presence of procaine, channel openings were more frequently interrupted by brief closures so giving a characteristic pattern which is typical of burst behaviour. A similar effect on burst behaviour has been reported for the action of benzocaine and the lignocaine derivative QX222 at muscle nicotinic receptors (Ogden *et al.*, 1981; Neher, 1983). Nevertheless, even in the presence of 50 μM procaine the majority of channel openings were single events. For the experiments described here the classification of groups of openings as bursts was determined according to the criteria given by Clapham & Neher (1984) (see Methods). In the absence of procaine the distribution of burst length could be described adequately by the sum of two exponentials but as the concentration of procaine increased the time constants of the distributions became shorter and mean burst length decreased e.g. from 7.94 ms in control to 5.21 ms in 2 μM and 2.91 ms in 50 μM procaine.

As the distribution of closed times progressively changed with increasing procaine concentration (see Figure 8 and Table 1) the t_{crit} for calculating burst characteristics also changed. This will bias the calculation of mean blocked time. To compensate for this we have also analysed the data with a fixed value for t_{crit} of 8 ms which is the value appropriate for 50 μM procaine. Although this reanalysis gives different mean values for burst length and blocked time at other concentrations of procaine (e.g. 8.4 ms burst length in control compared to 7.94 ms with a t_{crit} of 5 ms), the tendency for burst length to decrease and blocked time to increase with increasing procaine concentration remains (Table 1). Overall, increasing concentrations of procaine caused an increase in the number of gaps per burst and an increase in the mean blocked time but a reduction in mean burst length (Figure 9).

Excised outside out patches To gain better control of the membrane potential during drug application and to permit acquisition of data from the same channels in the presence and absence of anaesthetic, we have also examined the effect of procaine in three excised outside-out patches. With a holding potential of −70 mV the channel openings are seen as inward current movements of 2.72 ± 0.098 pA amplitude. As with the cell attached patches, the distribution of channel open times was best fitted by the sum of two exponentials with time constants of 0.47 ms and 6.7 ms (combined data from three patches). Application of procaine (50 μM) reduced the amplitude of single channel events to 2.52 ± 0.71 pA, abolished long duration openings and shifted the open time distribution curve to the left. As for the studies with cell attached patches, the distribution of channel open times in the presence of 50 μM procaine was best fitted by a single exponential which, in this case, had a time constant of 1.33 ms.

As for channels activated by 10 μM CCh in cell attached patches, the distribution of channel closed times was skewed with a large number of brief closures (<2 ms) and a broad distribution of longer closed times with a time constant close to 500 ms. The distribution of brief closures could be fitted by the sum of two exponentials with time constants of 0.65 ms and 17 ms. Application of procaine caused a higher incidence of brief closures (from 12.5% of closures of 2 ms or less in control to 26% of closures of 2 ms or less duration

Table 1 Procaine modulation of the kinetic constants of currents induced by 10 μM carbachol (CCh) in cell attached patches

	Control	*Procaine*		
Parameter		2 μM	10 μM	50 μM
Open state				
Unit current (pA)	2.35 ± 0.03	2.29 ± 0.05	2.28 ± 0.04	1.98 ± 0.03*
τ_{fast} (ms)	1.07 ± 0.11	0.36 ± 0.03	0.27 ± 0.04	—
τ_{slow} (ms)	6.94 ± 0.68	3.64 ± 0.09	2.63 ± 0.06	0.79 ± 0.01
$Area_f/Area_s$	0.54	0.35	0.73	—
Mean open time (ms)	7.32 ± 0.59	4.26 ± 0.18*	2.67 ± 0.12*	1.07 ± 0.04*
P_{open} (%)	0.68 ± 0.03	0.70 ± 0.06	1.1 ± 0.02*	0.21 ± 0.04*
F_{open} (s^{-1})	1.05 ± 0.12	1.83 ± 0.19*	4.06 ± 0.54*	2.16 ± 0.28*
Closed state				
τ_{fast} (ms)	0.75 ± 0.03	0.50 ± 0.03	0.96 ± 0.03	0.85 ± 0.27
τ_{slow} (ms)	—	13 ± 4	11 ± 3	8.8 ± 2.6
$Area_f/Area_s$	—	1.89	2.65	1.09
Burst behaviour				
Burst length (ms)	8.4 ± 0.67	5.62 ± 0.20*	5.13 ± 0.56*	2.91 ± 0.24*
Mean blocked time (ms)	0.81 ± 0.05	1.11 ± 0.05*	1.21 ± 0.06*	1.82 ± 0.06*
Gaps/burst	0.18 ± 0.04	0.33 ± 0.04*	0.63 ± 0.19*	0.75 ± 0.17*
τ_{fast} (ms)	0.74 ± 0.08	0.47 ± 0.06	0.36 ± 0.08	0.74 ± 0.06
τ_{slow} (ms)	7.31 ± 0.53	5.01 ± 0.29	4.30 ± 0.28	4.13 ± 0.83
$Area_f/Area_s$	0.43	0.69	0.47	1.17

The time constants for open times and bursts were calculated using a bin width of 0.5 ms. Those for closed times were calculated for closures of less than 50 ms using a bind width of 1 ms. The burst characteristics were calculated assuming a t_{crit} of 8 ms (see text). The mean open time, burst length, blocked time, P_{open} and F_{open} for 5–7 patches are given ± s.e.mean. Statistical comparisons were made where appropriate (* denotes $P<0.05$ for the difference between control patches and those exposed to procaine). The time constants are calculated form amalgamated data and are given together with the standard error of the estimate. F_{open} is frequency of opening.

when 50 μM procaine was applied). The distribution of brief closures during application of procaine was best fitted by exponentials with time constants of 0.71 ms and 4.37 ms. In the absence of procaine, the distribution of burst length was well fitted by the sum of two exponentials which had time constants of 0.88 ms and 14.6 ms. In agreement with the studies in cell-attached patches, procaine decreased mean burst length from 7.34 ms to 4.31 ms, this decrease being evident in each of the patches studied. The data are summarised in Table 2.

Effect of procaine on voltage-activated calcium currents

Under whole cell voltage-clamp and with the pipette and bathing solutions given in the Methods, a voltage step from a holding potential of −80 mV to 0 mV elicits an inward current which has the characteristics of the calcium currents previously described in chromaffin cells by Bossu *et al.* (1991a,b) and Charlesworth *et al.* (1991). We have conducted a brief study of the effect of procaine on these currents in eight cells. In agreement with the calcium influx data, 200 μM procaine had a barely detectable effect on the inward calcium current, 500 μM procaine produced a 23% reduction while a concentration of 2 mM procaine reduced the current by about half (see Figure 10). Procaine did not alter the rate of decay of the inward current.

Discussion

We have examined the effect of the local anaesthetic, procaine, on stimulus-secretion coupling in bovine adrenal chromaffin cells. At micromolar concentrations this agent inhibits both the catecholamine secretion and the ionic fluxes (Na^+ and Ca^{2+}) evoked by CCh. At comparable concentrations, procaine neither inhibits the K^+-evoked catecholamine secretion and the associated ^{45}Ca influx nor does it inhibit the voltage-gated Ca^{2+} currents. Our previous studies have shown that catecholamine secretion in response to nicotinic agonists is directly related to the Na^+ influx (Pocock & Richards, 1987; 1988) and we have shown here that the inhibition of Na^+ influx can quantitatively account for the reduction in catecholamine secretion (Figure 3b). This suggests that procaine exerts its action at the nicotinic receptor-channel complex without significantly inhibiting either the secretory pathway beyond the level of the plasma membrane or the voltage gated Ca^{2+} channels.

Procaine could depress catecholamine secretion by simply increasing the rate of desensitization of the activated nicotinic receptors. This possibility has been investigated in experiments in which catecholamine secretion was monitored continuously and in studies of the action of procaine on the CCh-evoked inward current. These experiments showed that procaine accelerated the rate of receptor desensitization (see Figures 2 and 4). Nevertheless, this effect is modest and, as the experiments with low CCh concentrations show, procaine is able to reduce steady-state inward currents without inducing a time-dependent desensitization.

The electrophysiological studies of Bossu *et al.* (1991a,b) and of Charlesworth *et al.* (1991) have shown that voltage-activated Ca^{2+} channels of chromaffin cells appear to be of the N and L subtypes originally described in dorsal root ganglion cells by Nowycky *et al.* (1985). Procaine had little effect on the voltage-activated Ca^{2+} currents whether measured directly or indirectly by ^{45}Ca flux measurements (see Results). Nevertheless, agonist-evoked Ca^{2+} entry was powerfully inhibited by procaine. What is the mechanism of this inhibition? A reduction of Na^+ influx caused by a reduction in extracellular Na^+ leads to a decrease in both catecholamine secretion and the agonist-induced Ca^{2+} influx (Pocock & Richards, unpublished observations). Morever, Mulle *et al.* (1992) found that Ca^{2+} current of neuronal nicotinic channels recorded in Na^+ -free media with 5 mM Ca^{2+} , was only 2% of the Na^+ current. This suggests that Ca^{2+} entry through the nicotinic channel is likely to be very small under physiological conditions. Instead it is more likely that voltage-activated Ca^{2+} channels open following depolarization by the CCh-evoked Na^+ influx. The depressant action of procaine on the Na^+ movement gated by the nicotinic receptor would therefore inhibit both Ca^{2+} entry and catecholamine secretion.

The decrease in agonist-evoked ion fluxes is paralleled by a

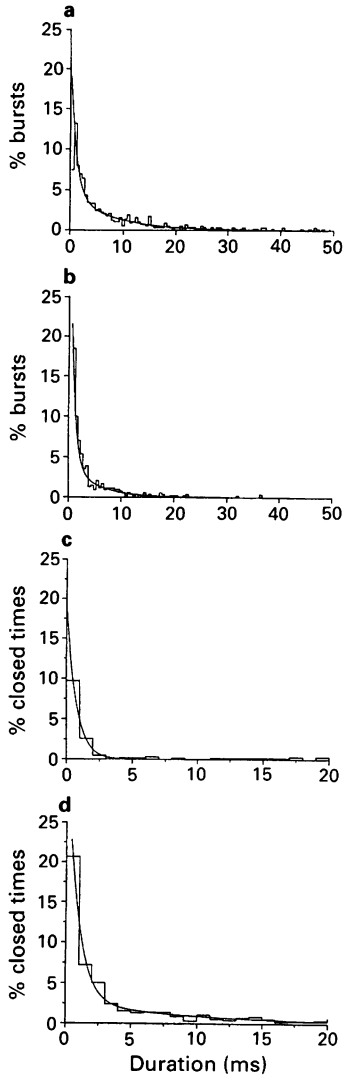

Figure 8 The effect of 50 μM procaine on the frequency distribution of burst length (a, b) and closed times (c, d). In each case the ordinates are expressed as a percentage of the total number of events. Combined data from 5–7 cell attached patches are shown. The smooth curves are the calculated exponential functions fitted to the data points. The time constants of the burst length distributions (τ_f and τ_s) were 1.03 ms and 7.93 ms in control (a), 0.74 ms and 5.0 ms in 50 μM procaine (b). The distribution of brief closed times was fitted by a single exponential with a time constant of 0.75 ms under control conditions (c), and by two exponentials with time constants of 0.85 and 8.8 ms in 50 μM procaine (d). The total number of bursts was 578 for (a) and 524 for (b). The total number of closures was 668 for (c) and 914 for (d). Note that in this figure t_{crit} was determined separately for each condition and was 5 ms for control and 8 ms for 50 μM procaine (see text).

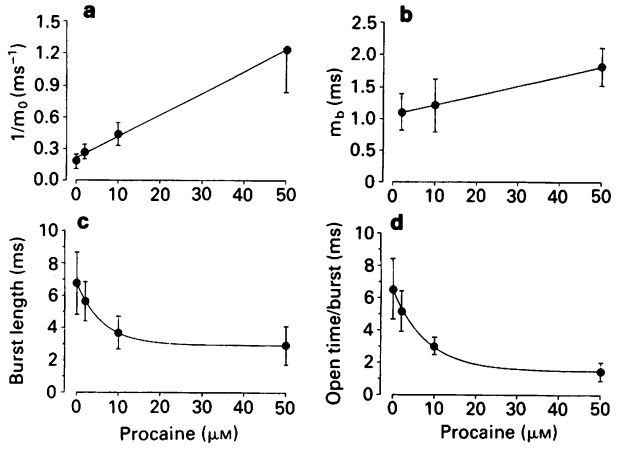

Figure 9 Tests of the principal predictions arising from the sequential blocking model (see text for details). (a) A plot of the reciprocal of mean channel open time (m_o) against procaine concentration. The line is fitted to the equation $y = 0.02(x) + 0.21$ by the method of least squares. (b) A plot of mean blocked time against procaine concentration. (c) A plot of mean burst length against procaine concentration (burst length calculated using a critical time of 8 ms (see text and Table 1)). (d) A plot of open time per burst against procaine concentration.

Table 2 Effect of procaine on the kinetic properties of currents induced by 10 μM carbachol (CCh) recorded from outside-out patches

	Control	*Procaine* 50 μM
Open state		
Unit current (pA)	2.72 ± 0.098	2.52 ± 0.071*
τ_f (ms)	0.47 ± 0.05	—
τ_s (ms)	6.70 ± 0.11	1.33 ± 0.07
$Area_f/Area_s$	1.61	—
Mean open time (ms)	5.8 ± 1.2	1.44 ± 0.15*
Closed state		
τ_f (ms)	0.65 ± 0.04	0.71 ± 0.12
τ_s (ms)	17 ± 12	4.37 ± 0.67
$Area_f/Area_s$	1.58	0.58
Burst behaviour		
Burst length (ms)	7.34 ± 1.79	4.31 ± 1.44
Mean blocked time (ms)	1.07 ± 0.05	1.8 ± 0.14*
Gaps/burst	0.18 ± 0.02	0.73 ± 0.30
τ_f (ms)	0.88 ± 0.04	0.92 ± 0.05
τ_s (ms)	14.6 ± 4.8	11.7 ± 4.6
$Area_f/Area_s$	2.14	2.59

Mean values ± s.e.mean are calculated from data obtained from three outside-out patches and statistical comparisons made where appropriate (* denotes $P<0.05$). The fitted time constants were calculated for amalgamated data from three patches and are given together with the standard error of the estimate.

decrease in the agonist-evoked inward current measured electrophysiologically. Neglecting any changes in receptor desensitization, there are two possible ways in which procaine could inhibit the inward current: it could reduce the probability of the channel being open or it could reduce the conductance of the channel. Direct measurement of the channel openings shows that procaine does not significantly reduce the conductance of the channel when the effects of filtering are taken into account (see Results). Although low concentrations of procaine shift the distribution of channel open times to shorter values, the probability of the channel being in the open state is not significantly affected by 2 μM and 10 μM procaine. At these concentrations procaine had little effect on catecholamine secretion or Na^+ influx. In the presence of 50 μM procaine, however, the probability of the channel being open is reduced by about two thirds. This is sufficient to account for its action in reducing the inward current evoked by low concentrations of CCh. (The P_{open} was reduced by approximately 70% and the mean steady-state inward current was reduced by 80% by 50 μM procaine, the slight difference being readily attributable to sampling error, see Results).

By what mechanism does procaine modulate the nicotinic receptor complex to reduce the inward current? As discussed above, increasing concentrations of procaine shorten mean channel open time and alter the spectral characteristics of the channel noise by inducing an excess of high frequency noise

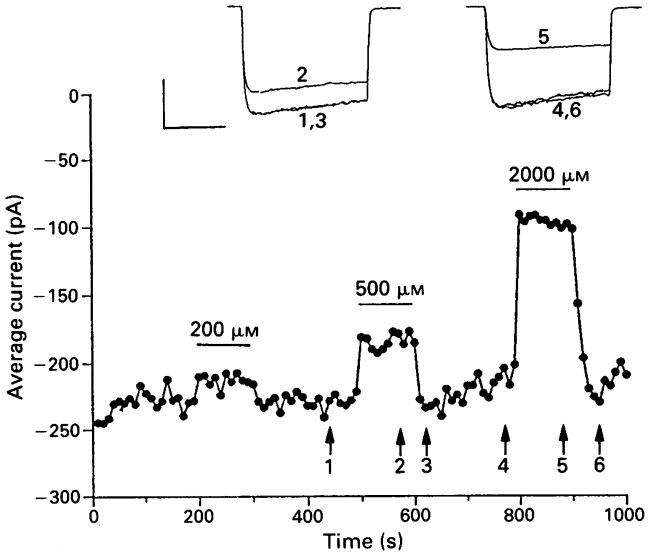

Figure 10 The effect of successive applications of 200, 500 and 2000 μM procaine on the inward calcium current. Each point is the mean current of four successive voltage steps from a holding potential of −80 mV to zero (see Methods for further details). Left inset shows the effect of 500 μM procaine and that on the right shows the effect of 2000 μM procaine on the mean inward Ca^{2+} current. The numbered arrows relate the traces shown in the insets to the overall timecourse. Calibration bars are: vertical 100 pA, horizontal 100 ms.

(Figure 5). Similar effects on channel noise have previously been reported for the action of local anaesthetics at the neuromuscular junction (Ruff, 1977; Neher & Steinbach, 1978; Ogden *et al.*, 1981) and have been interpreted in terms of a simple sequential blocking model in which transitions between closed, open and blocked states must occur in strict sequence. The dose-response curves for the action of procaine on catecholamine secretion and the CCh-evoked influx of Na^+ and Ca^{2+} have Hill coefficients close to unity. This suggests that the action of procaine is not cooperative and that a simple model such as the sequential blocking model outlined above may be sufficient to explain its action at the molecular level. This model has been proposed to account for the action of barbiturates and mepacrine at the neuromuscular junction (Adams, 1976; Adams & Feltz, 1980) and has been discussed by Gurney & Rang (1984) for the action of methonium compounds at ganglionic cholinoceptors.

In the absence of anaesthetic, the time constant for channel closure estimated from the noise is about 9 ms which corresponds to the long time constant for the distribution of burst length. When procaine was applied, a second high frequency component appeared in the noise spectrum and the low frequency time constant decreased. The time constants estimated from the spectra decreased as the procaine concentration increased from 20 to 50 μM and those estimated in the presence of 50 μM procaine corresponded to the time constants for burst length determined from the single channel studies (τ_f 0.6 and 0.74 ms; τ_s 4.4 and 5 ms respectively). The voltage-sensitivity of the high frequency component of the noise suggests that the positively charged procaine ions enter the channel to cause an open channel block. This interpretation is consistent with the sequential blocking model.

More stringent tests of the model have been made by investigating the effect of procaine on single channel currents. The results show that, while increasing concentrations of procaine progressively reduce the mean open time as predicted, they also increased the mean blocked time, decreased the mean open time within a burst and decreased burst length. As a burst may be terminated either by channel closure or by the channel entering a long-lived blocked state, a more detailed analysis of burst behaviour is unhelpful. Nevertheless, it is clear that the basic three state model is inadequate to account for our experimental findings. Gage & Wachtel (1984) and Gage & MacKinnon (1985) have previously reported similar results for the action of both procaine and pentobarbitone at the motor endplate. The three state model also fails to account for the action of the positively charged lignocaine derivative, QX222, at concentrations greater than 40 μM (Neher, 1983).

A model that could provide a reasonable framework for explaining our data is the extended block model discussed by Murrell *et al.* (1991), Murrell & Haydon (1991) and more fully by Dilger & Brett (1991). These authors propose the existence of a long-lived blocked state beyond the blocked open state. This modification of the original scheme correctly predicts the reduction in burst length and the increase in the number of openings per burst observed with procaine, alkanols and the volatile anaesthetics, enflurane and isoflurane, but it does not predict the concentration-dependence of the mean blocked time which increases in a concentration-dependent manner. In the cell-attached patches the closed time distributions in the presence of procaine reveal an increase in the proportion of brief closures (<2 ms) and an additional kinetically distinguishable component with a time constant of 8 ms. This latter component becomes more evident as the concentration of procaine increases. These data suggest that there are at least two blocked states that lead directly from the open state and there may be other blocked states we are unable to resolve. Moreover, the open state probability density function in the absence of procaine suggests the existence of at least two open states. A minimum of five discrete states are therefore required to describe the action of procaine on the nicotinic channel. In view of the complexity of the kinetics and the absence of any ready means of differentiating between the various blocked states, we have elected to describe the action of procaine (Pr) in terms of the simple three state model shown below:

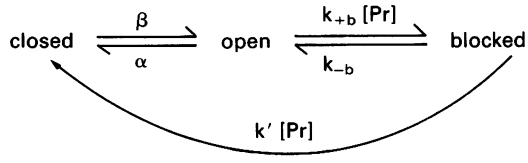

These states are not regarded as unique but encompass blocked, closed and open states which may themselves be modulated by the anaesthetic. In essence our model proposes that procaine both blocks the open channel and binds to an allosteric site to modulate the rate at which the blocked channel can close without passing through the open state. Once the channel has entered the blocked state, the probability that it will close without passing through the open state rises as the concentration of procaine increases.

The simplified model accounts for the following observations: (1) The fall in mean open time with increasing concentration of anaesthetic. (2) The increase in mean blocked time with increasing concentration of anaesthetic. (3) The decrease in mean open time per burst as anaesthetic concentration increases and (4) the non-linear decrease in mean burst length with increasing concentration of anaesthetic. From the mean open times we are able to estimate the rate constant for channel closure in the absence of procaine as $176 \pm 26\ s^{-1}$ and the apparent rate constant for channel block as approximately $2 \times 10^7\ M^{-1}\ s^{-1}$. Comparable values have been obtained by Dilger & Brett (1991) for the higher alcohols in their action on the nicotinic receptors of BC3H-1 cells. Short chain alkanols and volatile agents such as enflurane and isoflurane have somewhat lower values close to $10^6\ M^{-1}\ s^{-1}$ (see also Wachtel & Wergrzynowicz, 1991). The rate con-

stants for unblocking can be estimated from the high resolution closed time distribution as 1000–2000 s^{-1} for the fast component and 77–114 s^{-1} for the slow component.

To conclude, procaine inhibits CCh-evoked catecholamine secretion from bovine chromaffin cells by depressing the agonist-evoked inward current. This depression can be largely explained by a dual action of procaine on the nicotinic receptor-channel complex.

We thank Dr A. Mathie for constructive comments on the manuscript and the Wellcome Trust for financial suppport.

References

ADAMS, P.R. (1976). Drug blockade of open endplate channels. *J. Physiol.*, **260,** 531–552.

ADAMS, P.R. & FELTZ, A. (1980). Quinacrine (mepacrine) action at frog end-plate. *J. Physiol.*, **306,** 261–281.

ANDERSON, C.R. & STEVENS, C.F. (1973). Voltage clamp analysis of acetylcholine produced endplate current fluctuations at frog neuro-muscular junction. *J. Physiol.*, **235,** 655–691.

BAKER, P.F. & KNIGHT, D.E. (1984). Calcium control of exocytosis in bovine adrenal medullary cells. *Trends Neurosci.*, **7,** 120–126.

BOSSU, J.-L., DE WAARD, M. & FELTZ, A. (1991a). Inactivation characteristics reveal two calcium currents in adult bovine chromaffin cells. *J. Physiol.*, **437,** 603–620.

BOSSU, J.-L., DE WAARD, M. & FELTZ, A. (1991b). Two types of calcium channels are expressed in adult bovine chromaffin cells. *J. Physiol.*, **437,** 621–634.

CHARLESWORTH, P., JACOBSON, I., POCOCK, G. & RICHARDS, C.D. (1990). Procaine selectively inhibits channels opened by nicotinic agonists in bovine adrenal chromaffin cells. *J. Physiol.*, **425,** 69P.

CHARLESWORTH, P., POCOCK, G. & RICHARDS, C.D. (1991). Calcium currents in bovine adrenal chromaffin cells. *J. Physiol.*, **438,** 105P.

CLAPHAM, D.E. & NEHER, E. (1984). Substance P reduces acetylcholine-induced currents in isolated bovine chromaffin cells. *J. Physiol.*, **347,** 255–277.

COLQUHOUN, D. & HAWKES, A.G. (1983). The principles of the stochastic interpretation of ion channel mechanisms. Ch. 9, pp. 135–176. In *Single Channel Recording*. Sakmann, B. & Neher, E. New York: Plenum.

COLQUHOUN, D. & SAKMANN, B. (1983). Bursts of openings in transmitter-activated ion channels. Ch 16, pp. 345–364. In *Single Channel Recording*. Sakmann, B. & Neher, E. New York: Plenum.

CULL-CANDY, S.G., MATHIE, A. & POWIS, D.A. (1988). Acetylcholine receptor channels and their block by clonidine in cultured bovine chromaffin cells. *J. Physiol.*, **402,** 255–278.

DILGER, J.P. & BRETT, R.S. (1991). Actions of volatile anesthetics and alcohols on cholinergic receptor channels. *Ann N.Y. Acad. Sci.*, **625,** 616–627.

DIONNE, V.E. & LEIBOWITZ, M.D. (1982). Acetylcholine receptor kinetics: a description from single channel currents at snake neuromuscular junctions. *Biophys. J.*, **39,** 253–261.

DOUGLAS, W.W. & RUBIN, R.P. (1963). The mechanism of catecholamine release from the adrenal medulla and the role of calcium in stimulus-secretion coupling. *J. Physiol.*, **167,** 288–310.

FENWICK, E.M., MARTY, A. & NEHER, E. (1982). A patch clamp study of bovine chromaffin cells and of their sensitivity to acetylcholine. *J. Physiol.*, **331,** 577–597.

GAGE, P.W. & MCKINNON, D. (1985). Effects of pentobarbitone on acetylcholine-activated channels in mammalian muscle. *Br. J. Pharmcol.*, **85,** 229–235.

GAGE, P.W. & WACHTEL, R.E. (1984). Some effects of procaine at the toad end-plate are not consistent with a simple channel blocking model. *J. Physiol.*, **346,** 331–339.

GURNEY, A.M. & RANG, H.P. (1984). The channel blocking action of methonium compounds on rat submandibular ganglion cells. *Br. J. Pharmacol.*, **82,** 623–642.

HAMILL, O.P., MARTY, A., NEHER, E., SAKMANN, B. & SIGWORTH, F.J. (1981). Improved patch clamp techniques for high resolution current recordings from cells and cell-free membrane patches. *Pfügers Arch.*, **391,** 85–100.

HOLMES, J.C. & SCHNEIDER, F.H. (1973). Pentobarbitone inhibition of catecholamine secretion. *Br. J. Pharmacol.*, **49,** 517–528.

HOLZ, R.W., SENTER, R.A. & FRYE, R.A. (1982). Relationship between Ca^{2+} uptake and catecholamine secretion in primary dissociated cultures of adrenal medulla. *J. Neurochem.*, **39,** 635–646.

JACOBSON, I., POCOCK, G. & RICHARDS, C.D. (1991). Effects of pentobarbitone on the properties of nicotinic channels of chromaffin cells. *Eur. J. Pharmacol.*, **202,** 331–339.

KATZ, B. & MILEDI, R. (1975). The effect of procaine on the action of acetylcholine at the neuromuscular junction. *J. Physiol.*, **249,** 269–284.

KRISHTAL, O.A. & PIDOPLICHKO, V.I. (1980). A receptor for protons in the nerve cell membrane. *Neuroscience*, **5,** 2325–2327.

MARTY, A. (1978). Noise and relaxation studies of acetylcholine induced currents in the presence of procaine. *J. Physiol.*, **278,** 237–250.

MULLE, C., CHOQUET, D., KORN, H. & CHANGEUX, J.-P. (1992). Calcium influx through nicotinic receptor in rat central neurons: its relevance to cellular regulation. *Neuron*, **8,** 135–143.

MURRELL, R.D. & HAYDON, D.A. (1991). Actions of n-alcohols on nicotinic acetylcholine receptor ion channels in cultured rat muscle cells. *Ann N.Y. Acad. Sci.*, **625,** 365–374.

MURRELL, R.D., BRAUN, M.S. & HAYDON, D.A. (1991). Actions of n-alcohols on nicotinic acetylcholine receptor channels in cultured rat myotubes. *J. Physiol.*, **437,** 431–448.

NEHER, E. (1983). The charge carried by single-channel currents of rat cultured muscle cells in the presence of local anaesthetics. *J. Physiol.*, **339,** 663–678.

NEHER, E. & STEINBACH, J.H. (1978). Local anaesthetics transiently block currents through single acetylcholine-receptor channels. *J. Physiol.*, **277,** 153–176.

NOWYCKY, M.C., FOX, A.P. & TSIEN, R.W. (1985). Three types of neuronal calcium channel with different calcium agonist sensitivity. *Nature*, **316,** 440–443.

ODGEN, D.C., SIEGELBAUM, S.A. & COLQUHOUN, D. (1981). Block of acetylcholine-activated ion channel by an uncharged local anaesthetic. *Nature*, **289,** 596–598.

POCOCK, G. (1983a). Ionic and metabolic requirements for stimulation of secretion by ouabain in bovine adrenal medullary cells. *Mol. Pharmacol.*, **23,** 671–680.

POCOCK, G. (1983b). Ion movements in isolated bovine adrenal medullary cells treated with ouabain. *Mol. Pharmacol.*, **23,** 681–697.

POCOCK, G. & RICHARDS, C.D. (1987). The action of pentobarbitone on stimulus-secretion coupling in adrenal chromaffin cells. *Br. J. Pharmacol.*, **90,** 71–80.

POCOCK, G. & RICHARDS, C.D. (1988). The action of volatile anaesthetics on stimulus-secretion coupling in bovine adrenal chromaffin cells. *Br. J. Pharmacol.*, **95,** 209–217.

POCOCK, G. & RICHARDS, C.D. (1991). Cellular mechanisms in general anaesthesia. *Br. J. Anaesth.*, **66,** 116–128.

RICHARDS, C.D. (1982). The actions of pentobarbitone, procaine and tetrodotoxin on synaptic transmission in the olfactory cortex of the guinea-pig. *Br. J. Pharmacol.*, **75,** 639–646.

RUFF, R.L. (1977). A quantitative analysis of local anaesthetic alteration of miniature endplate current fluctuations. *J. Physiol.*, **264,** 89–124.

VON EULER, U.S. & FLODING, T. (1955). A fluorimetric micromethod for differential estimation of adrenaline and nor-adrenaline. *Acta Physiol. Scand.*, Suppl 118., **33,** 45–56.

WACHTEL, R.E. & WEGRZYNOWICZ, E.S. (1991). Mechanism of volatile anesthetic action on ion channels. *Ann. N.Y. Acad. Sci.*, **625,** 116–128.

WAYMIRE, J.C., BENNETT, W.F., BOEHME, R., HANKINS, L., GILMER-WAYMIRE, K. & HAYCOCK, J.W. (1983). Bovine adrenal chromaffin cells: high yield purification and viability in suspension culture. *J. Neurosci. Methods*, **7,** 329–351.

(Received October 15, 1991
Revised March 13, 1992
Accepted March 24, 1992)

Br. J. Pharmacol. (1992), **106**, 813–818 © Macmillan Press Ltd, 1992

Tracheal relaxation induced by potassium channel opening drugs: its antagonism by adrenergic neurone blocking agents

J.L. Berry, [1]R.C. Small & R.W. Foster

Smooth Muscle Research Group, Department of Physiological Sciences, University of Manchester, Oxford Road, Manchester M13 9PT

1 We have studied the ability of some adrenergic neurone blocking agents to inhibit the tracheal relaxant actions of isoprenaline, theophylline and the potassium channel openers (KCOs) BRL 38227, pinacidil and RP 52891.

2 BRL 38227, isoprenaline, pinacidil, RP 52891 and theophylline each caused concentration-dependent suppression of the spontaneous tone of guinea-pig isolated trachealis. The maximal relaxant effects of isoprenaline and pinacidil were equal to that of theophylline. In contrast, the maximal effects of BRL 38227 and RP 52891 were approximately 85–95% of that of theophylline.

3 Guanethidine (5–500 μM) did not itself modify the spontaneous tone of the trachealis muscle but antagonized BRL 38227 in a concentration-dependent manner. Guanethidine (50 μM) also antagonized pinacidil and RP 52891. However, guanethidine did not antagonize either isoprenaline or theophylline.

4 Bretylium (50 μM) did not itself modify the spontaneous tone of the trachealis muscle but antagonized BRL 38227, pinacidil and RP 52891. Bretylium did not antagonize either isoprenaline or theophylline.

5 Guanidine (50 and 500 μM) did not itself modify the spontaneous tone of the trachea and failed to modify the tracheal relaxant activity both of BRL 38227 and theophylline.

6 BRL 38227 (1 and 10 μM) stimulated, in a concentration-dependent manner, the efflux of $^{86}Rb^+$ from strips of bovine trachealis muscle that had been pre-loaded with the radiotracer. Guanethidine (50 μM), bretylium (50 μM) and debrisoquine (50 μM) did not themselves modify the efflux of $^{86}Rb^+$ from bovine trachealis but each of these agents markedly inhibited the stimulant effect of BRL 38227 (10 μM) on $^{86}Rb^+$ efflux.

7 It is concluded that the adrenergic neurone blocking agents guanethidine and bretylium can inhibit the tracheal relaxant actions of KCOs such as BRL 38227, pinacidil and RP 52891 without antagonizing isoprenaline or theophylline. The ability of the adrenergic neurone blocking agents to antagonize BRL 38227 in promoting $^{86}Rb^+$ efflux from trachealis muscle may suggest that the adrenergic neurone blocking agents act to prevent the opening of the plasmalemmal K^+-channel that is involved in the tracheal relaxant actions of the KCOs.

Keywords: Trachealis muscle; BRL 38227; RP 52891; theophylline; isoprenaline; guanethidine; bretylium; debrisoquine; guanidine; $^{86}Rb^+$ efflux

Introduction

In order to study the effects of cromakalim (a potassium channel opener) on excitatory, non-adrenergic, non-cholinergic (NANC) neuroeffector transmission in guinea-pig isolated trachealis, Burka *et al.* (1991) set up tracheal segments for the isometric recording of tension changes in Krebs solution containing atropine (1 μM), indomethacin (2.8 μM) and propranolol (1 μM). The tracheal segments were subjected to transmural electrical stimulation and cromakalim was observed to cause a concentration-dependent inhibition of the NANC contractile responses. Whilst performing further, similar experiments, we decided to compare the effects of isoprenaline with those of cromakalim against excitatory NANC neuroeffector transmission in the trachea. The use of isoprenaline in these experiments dictated that an alternative sympatholytic agent be substituted for propranolol as a component of the antagonist cocktail in the Krebs solution. Accordingly, guanethidine (50 μM) was substituted for propranolol. Under these conditions we noticed that the inhibitory potency of cromakalim against excitatory NANC neuro-effector transmission was reduced. This raised the possibility that guanethidine might antagonize cromakalim in suppressing the spontaneous tone of guinea-pig trachealis muscle.

Our preliminary observation that guanethidine, indeed, antagonized cromakalim in suppressing the spontaneous tone of the trachea prompted the experiments of the present study. In these experiments we have attempted to assess the selectivity of guanethidine as an antagonist of BRL 38227 (a benzopyran derivative; the active enantioner of cromakalim), whether guanethidine antagonizes other KCOs (e.g. the cyanoguanidine derivative, pinacidil and the tetrahydrothiopyran derivative, RP 52891) and whether the antagonism of KCOs provided by guanethidine is a property shared by other adrenergic neurone blocking agents (e.g. debrisoquine and bretylium).

Methods

Tissue preparation

Guinea-pigs (300–500 g) of either sex were killed by stunning and bleeding. Tracheae were excised, cleaned of adhering fat and connective tissue and opened by cutting longitudinally through the cartilage rings diametrically opposite the trachealis. The open trachea was cut into small segments each containing 3–4 cartilage rings. Bovine tracheae were collected from the local abbatoir and transported to the laboratory immersed in cold Krebs solution. The bovine tracheae were opened in a fashion similar to that described for guinea-pig

[1] Author for correspondence.

tissue. However, a segment of bovine tracheal wall containing the trachealis muscle was then dissected from the opened organ and pinned out under Krebs solution with the adventitial surface uppermost. Adventitial tissue was carefully dissected from the preparation to expose the dorsal surface of the trachealis muscle. The preparation was then pinned out mucosal surface uppermost and the mucosal and submucosal tissue was carefully removed in order to expose the ventral surface of the trachealis muscle. Strips (approximately 10 mm in length) of the cleaned trachealis muscle were prepared by cutting in the longitudinal axis of the muscle bundles.

Tissue bath studies of mechanical activity of guinea-pig trachealis

Small segments of guinea-pig trachea were set up for the isometric recording of tension changes essentially as described by Foster *et al.* (1983). At the outset of each experiment, tissues were subjected to an imposed tension of 1.5 g. Approximately 20 min later aminophylline (1 mM) was added in order to determine the recorder pen position at zero tone. The aminophylline was washed from the tissues (initial wash followed by two further washes at 10 min intervals) and when tone subsequently became maximal (40 min after initial wash), study of bronchodilator drugs started.

Cumulative log concentration-effect curves were constructed for all relaxant drugs studied. Half-$\log_{10}$ unit concentration increments were used. Each concentration increment of BRL 38227, pinacidil or RP 52891 was allowed 8 min tissue contact. For isoprenaline and theophylline the contact times were 4 and 5 min respectively. In order to minimize desensitization to the KCOs, a concentration-effect curve for theophylline was always interposed between successive concentration-effect curves of each KCO. The effects of the various relaxants were measured in terms of the maximal relaxation induced by aminophylline.

Following the construction of initial log concentration-relaxation curves for the bronchodilator drugs, test tissues were exposed to Krebs solution containing one of the following modifying agents: bretylium (50 μM), debrisoquine (16 or 50 μM), guanethidine (5, 16, 50 or 500 μM), or guanidine (50 or 500 μM). Following 40 min tissue equilibration with the modifying agent, the log concentration-relaxation curves of the bronchodilator drugs were reconstructed in the presence of the modifying agent. Time-matched control tissues were treated identically to the test tissues but were not exposed to the modifying agent.

Studies of $^{86}Rb^+$ efflux from bovine trachealis

The efflux of $^{86}Rb^+$ from bovine trachealis was studied essentially as described by Longmore *et al.* (1991). In brief, strips of bovine trachealis (wet weight approximately 150 mg) were impaled on hypodermic needles and loaded with $^{86}Rb^+$ by incubation for 90 min in Krebs solution maintained at 37°C and gassed with a mixture of 95% O_2 and 5% CO_2. This loading medium contained 185 kBq ml^{-1} $^{86}Rb^+$ and the Rb^+ concentration was less than 50 μM. Following loading with the radiotracer, each tissue strip was transferred to the first of a series of efflux tubes containing 3 ml of Krebs solution gassed with a mixture of 95% O_2 and 5% CO_2 and maintained at 37°C. Each tissue strip was transferred to the next tube in the series at 3 min intervals. At the end of the efflux period the contents of each of the efflux tubes was assayed for radioactivity in a gamma counter. Each tissue strip was blotted and similarly assayed for radioactivity.

In the case of test tissues, BRL 38227 (1 or 10 μM) was present in the efflux medium for the period 30 to 60 min from the start of the efflux. In the case of time-matched control tissues, the efflux medium contained the appropriate vehicle for BRL 38227 over the same time period. In experiments where the effects of guanethidine (50 μM), bretylium (50 μM) or debrisoquine (50 μM) alone, or in combination with BRL 38227 (10 μM) were examined, the adrenergic neurone blocking agent (or appropriate vehicle) was added to the efflux medium for the whole of the efflux period.

Drugs and solutions/statistical analysis of results

Drug concentrations are expressed in terms of the molar concentration of the active species. The following substances were used: aminophylline (BDH), bretylium tosylate (Wellcome Foundation), BRL 38227 ((−)-6-cyano-3,4-dihydro-2,2-dimethyl-*trans*-4-(2-oxo-1-pyrrolidyl)-2H-benzo[b]pyran-3-ol, SmithKline Beecham Pharmaceuticals), debrisoquine sulphate (Roche Products Ltd), guanethidine sulphate (Ciba), guanidine sulphate (Sigma), (−)-isoprenaline hydrochloride (Sigma), (±)-pinacidil (Leo), RP 52891 ((−)-N-methyl-2-(3-pyridinyl)-tetrahydrothiopyran-2-carbothioamide-1-oxide, RhonePoulenc-Rorer), theophylline (Sigma).

A stock solution of isoprenaline was prepared in 0.1 M HCl. Dilutions from this stock were prepared with distilled water containing 0.57 mM ascorbic acid as an antioxidant. Stock solutions of BRL 38227, pinacidil and RP 52891 were prepared in 70% ethanol. Stock solutions of other drugs were prepared using twice-distilled water.

The Krebs solution had the following composition (mM): NaCl 118, KCl 4.8, $CaCl_2$ 2.5, $MgSO_4$ 1.2, KH_2PO_4 1.2, $NaHCO_3$ 25 and glucose 11.1. This solution (pH 7.4) was maintained at 37°C and was gassed with a mixture of 95% O_2 and 5% CO_2.

The significance of differences between means was assessed by use of a two-tailed, unpaired t test. The null hypothesis was rejected when $P<0.05$.

Results

Tissue bath studies of mechanical activity of guinea-pig trachealis

Isoprenaline (1–300 nM), theophylline (3 μM–1 mM), BRL 38227 (0.03–100 μM), pinacidil (0.1–100 μM) and RP 52891 (0.03–100 μM) each evoked concentration-dependent suppression of the spontaneous tone of guinea-pig isolated trachealis. The maximal relaxant effects of BRL 38227 and RP 52891 were only 85–95% of that of theophylline, but the maximal relaxant effects of pinacidil and isoprenaline were identical to that of theophylline (Figures 1–3).

Guanethidine (5, 16, 50 or 500 μM) did not itself modify the spontaneous tone of the tracheal segments (Table 1). However, guanethidine antagonized BRL 38227 in a concentration-dependent manner. The antagonism was characterized by a rightwards shift in the log concentration-relaxation curve for BRL 38227 (Figure 1). The greatest rightward shift (approximately 10 fold) was obtained with guanethidine (50 μM). Increasing the concentration of guanethidine to 500 μM produced no greater antagonism. Guanethidine (50 μM) also antagonized RP 52891 and pinacidil. In the presence of guanethidine, the log concentration-relaxation curve for RP 52891 was shifted to the right and there was some reduction in the slope of the curve and in the maximal response. In contrast, the presence of guanethidine caused a rightward shift of the log concentration-relaxation curve of pinacidil without reducing the maximal response (Figure 2). Guanethidine (50 μM) did not affect the shape or position of the log concentration-relaxation curve for theophylline but caused approximately 4 fold potentiation of isoprenaline (Table 2, Figure 2).

Bretylium (50 μM) did not itself modify the spontaneous tone of the tracheal segments (Table 1). However, bretylium antagonized BRL 38227, pinacidil and RP 52891. In the case of pinacidil the antagonism was characterized by a rightward shift in the log concentration-relaxation curve of the KCO without depression of the maximal response. In the cases of

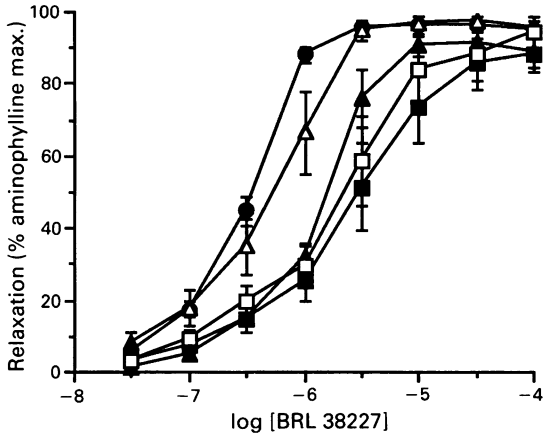

Figure 1 Effect of guanethidine on the action of BRL 38227 in suppressing the spontaneous tone of guinea-pig isolated trachealis. Abscissa scale: molar concentration of BRL 38227 on a $\log_{10}$ scale. Ordinate scale: relaxation as a percentage of the maximum relaxation induced by aminophylline. Symbols: (●) indicates the log concentration-effect curve for BRL 38227 obtained in time-matched control tissues; (△), (▲), (■) and (□) indicate subsequent log concentration-effect curves for BRL 38227 obtained in test tissues equilibrated with guanethidine 5, 16, 50 and 500 μM respectively. Data points indicate means of values from at least 8 tissues. Vertical bars indicate s.e.mean.

Table 1 Effects of some adrenergic neurone blocking agents and guanidine on the spontaneous tone of guinea-pig isolated trachealis

Agents tested	*Vehicle-treated, time-matched control tissues*	*Test tissues*
Bretylium (50 μM)	95.1 ± 1.5	94.3 ± 2.2
Debrisoquine (50 μM)	98.7 ± 2.4	44.8 ± 6.0*
Guanethidine (5 μM)	104.5 ± 3.4	101.4 ± 3.4
Guanethidine (16 μM)	103.5 ± 3.2	105.2 ± 5.9
Guanethidine (50 μM)	99.4 ± 1.8	99.7 ± 2.3
Guanethidine (500 μM)	102.5 ± 2.3	98.4 ± 4.0
Guanidine (50 μM)	94.0 ± 2.2	94.8 ± 4.5

Data indicate the spontaneous tone observed after 40 min tissue equilibration with vehicle (time-matched control tissues) or with the indicated adrenergic neurone blocking agent (test tissues) and expressed as a percentage of the spontaneous tone observed at the beginning of the experiment. Data indicate the mean (± s.e.mean) of values from at least 12 tissues.

* indicates a significant ($P<0.05$) difference from the corresponding time-matched control tissues (two-tailed, unpaired t test).

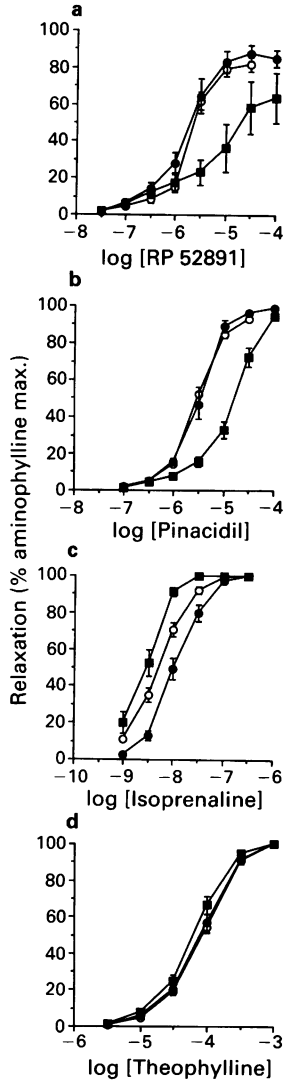

Figure 2 Effects of guanethidine (50 μM) on the actions of RP 52891 (a), pinacidil (b), isoprenaline (c) and theophylline (d) in suppressing the spontaneous tone of guinea-pig isolated trachealis. Abscissa scales: molar concentration of RP 52891, pinacidil, isoprenaline or theophylline on a $\log_{10}$ scale. Ordinate scale: relaxation as a percentage of the maximal relaxation evoked by aminophylline. Symbols: (○) indicates the pooled initial log concentration-relaxation curve for RP 52891, pinacidil, isoprenaline or theophylline; (●) indicates the subsequent log concentration-relaxation curve obtained in time-matched control tissues; (■) indicates the subsequent log concentration-relaxation curve for RP 52891, pinacidil, isoprenaline or theophylline obtained in test tissues equilibrated with guanethidine (50 μM). Data points indicate means of values obtained from at least 6 tissues. Vertical bars indicate s.e.mean.

BRL 38227 and RP 52891 the log concentration-relaxation curves were shifted rightward with some reduction in slope and maximal response (Figure 3). Bretylium (50 μM) failed to affect the shape and position (Table 2) of the log concentration-relaxation curves of theophylline or isoprenaline.

In contrast to guanethidine and bretylium, debrisoquine (16 and 50 μM) tended to suppress the spontaneous tone of the tracheal segments and to induce phasic tension changes (Table 1). These effects made it extremely difficult to test debrisoquine for inhibitory activity against the tracheal relaxant activity of the KCOs. However, in the 4 out of 12 tissues where debrisoquine failed to suppress spontaneous tone, it was clear that debrisoquine antagonized BRL 38227 and that such antagonism was characterized by a reduction in the maximal response to BRL 38277 (data not shown). Since the guanidine moiety forms part of the structure of guanethidine, it seemed worthwhile to examine whether guanidine might be the active species rendering guanethidine able to antagonize the KCOs. Guanidine (50 and 500 μM) did not modify the spontaneous tone of the tracheal segments (Table 1), nor did it antagonize BRL 38227 or theophylline (Table 2).

Studies of $^{86}Rb^+$ efflux from bovine trachealis

Fifteen minutes after the start of the efflux period, the $^{86}Rb^+$ efflux rate coefficient had declined to a relatively low (approximately 0.3% min^{-1}) value, suggesting that the rapidly-exchanging compartment for $^{86}Rb^+$ had cleared. This was true for both test and control tissues. In the case of the control tissues, the $^{86}Rb^+$ efflux rate coefficient thereafter fell very slowly throughout the remainder of the efflux period (Figures 4 and 5). Addition of the ethanolic vehicle for BRL

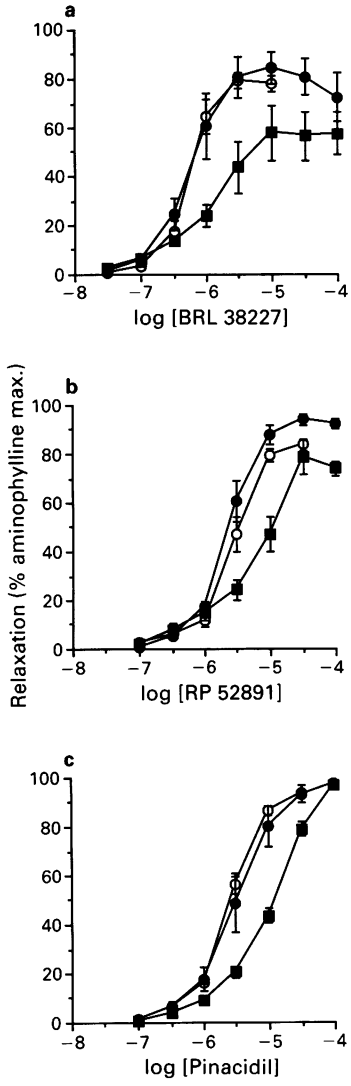

Figure 3 Effect of bretylium (50 μM) on the actions of BRL 38227 (a), RP 52891 (b) and pinacidil (c) in suppressing the spontaneous tone of guinea-pig isolated trachealis. Abscissa scale: molar concentration of BRL 38227, RP 52891 or pinacidil on a $\log_{10}$ scale. Ordinate scales: relaxation as a percentage of the maximal relaxation evoked by aminophylline. Symbols: (○) indicates the pooled initial log concentration-relaxation curve for BRL 38227, RP52891 or pinacidil; (●) indicates the subsequent log concentration-relaxation curve obtained in time-matched control tissues; (■) indicates the subsequent log concentration-relaxation curve for BRL 38227, RP 52891 or pinacidil obtained in test tissues equilibrated with bretylium (50 μM). Data points indicate means of values from at least 6 tissues. Vertical bars indicate s.e.mean.

Table 2 The effects of some adrenergic neurone blocking agents and guanidine on the potencies of some tracheal relaxant drugs

	−log EC_{50} for isoprenaline	
	Control tissues	*Test tissues*
Guanethidine (50 μM)	7.96 ± 0.07	8.55 ± 0.09*
Bretylium (50 μM)	7.92 ± 0.09	7.99 ± 0.07
	−log EC_{50} for theophylline	
	Control tissues	*Test tissues*
Guanethidine (50 μM)	4.42 ± 0.04	4.62 ± 0.10
Bretylium (50 μM)	4.09 ± 0.05	4.14 ± 0.08
Guanidine (50 μM)	4.28 ± 0.04	4.24 ± 0.04
Guanidine (500 μM)	4.24 ± 0.03	4.23 ± 0.04
	−log EC_{50} for BRL 38227	
	Control tissues	*Test tissues*
Guanidine (50 μM)	6.35 ± 0.02	6.32 ± 0.05
Guanidine (500 μM)	6.30 ± 0.05	6.22 ± 0.05

Data indicate the mean (± s.e.mean) of values from at least 6 tissues.
* indicates a significant ($P < 0.05$) difference from the corresponding value for the vehicle-treated, time-matched control tissues.

38227 to the efflux medium (30 min into the efflux period) caused no detectable change in the efflux rate coefficient. In contrast, the addition of BRL 38227 (1 or 10 μM) to the efflux medium at this time caused a concentration-dependent increase in the efflux rate coefficient (Figure 4). The concentration-dependency of the effect was manifest principally by the rate at which the peak effect was attained.

Addition of guanethidine (50 μM) to the efflux medium caused no change in the efflux rate coefficient at any time point as evident from comparisons with vehicle-treated control tissues. However, the presence of guanethidine markedly inhibited the ability of BRL 38227 to increase the efflux rate coefficient (Figure 4). Similar results were obtained with bretylium (50 μM) and debrisoquine (50 μM) (Figure 5).

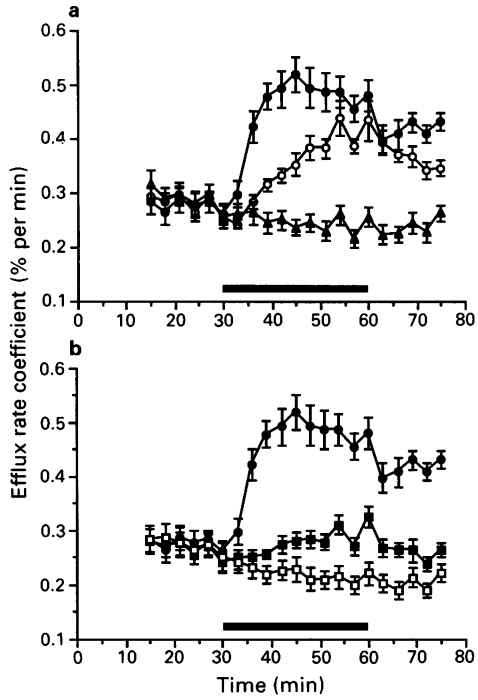

Figure 4 The effect of guanethidine (50 μM) on the action of BRL 38227 in promoting the efflux of $^{86}Rb^{+}$ from strips of bovine trachealis muscle preloaded with the radiotracer. In each panel the abscissa scale indicates the time (min) measured from the start of the efflux period. The ordinate scale indicates the efflux rate coefficient (% per min). In (a) the effects of ethanolic vehicle (▲), 1 μM BRL 38227 (○) and 10 μM BRL 38227 (●) are shown; (b) the effects of 50 μM guanethidine alone (□) of 10 μM BRL 38227 alone (●) [same data as in (a)] and 10 μM BRL 38227 in combination with 50 μM guanethidine (■). Data points indicate the mean of values from tissue strips from at least 6 tracheae. Vertical bars indicate s.e.mean. Where used, the adrenergic neurone blocking agent was present throughout. The horizontal bar indicates the period for which BRL 38227 or its ethanolic vehicle was present.

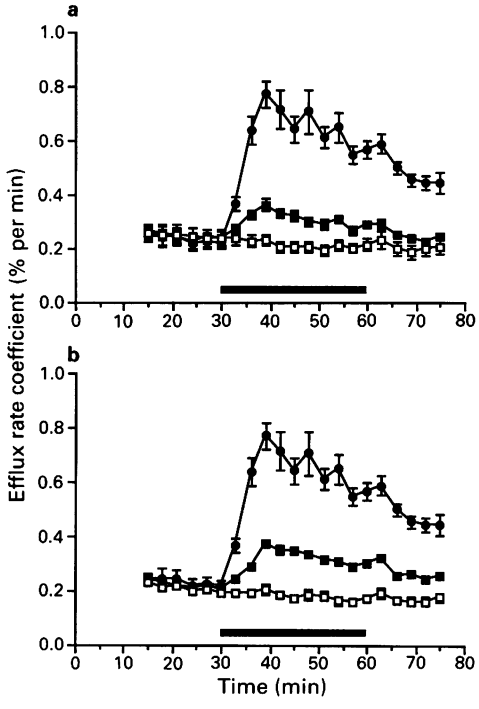

Figure 5 The effect of bretylium and debrisoquine (each 50 μM) on the action of BRL 38227 in promoting the efflux of $^{86}Rb^+$ from strips of bovine trachealis muscle preloaded with the radiotracer. In each panel the abscissa scale indicates the time (min) measured from the start of the efflux period. The ordinate scale indicates the efflux rate coefficient (% per min). In (a) are shown the effects of bretylium (50 μM) alone (□), BRL 38227 (10 μM) alone (●) and bretylium (50 μM) in combination with BRL 38227 (10 μM) (■); (b) shows the effects of debrisoquine (50 μM) alone (□), BRL 38227 (10 μM) alone (●) [same data as in (a)] and debrisoquine (50 μM) in combination with BRL 38227 (10 μM) (■). Data points indicate the mean of values from tissue strips from at least 6 tracheae. Vertical bars indicate s.e.mean. Where used, the adrenergic neurone blocking agent was present throughout. The horizontal bar indicates the period for which BRL 38227 or its ethanolic vehicle was present.

Discussion

Interactions between adrenergic neurone blocking agents and drugs causing tracheal relaxation

The ability of guanethidine to potentiate isoprenaline in suppressing the spontaneous tone of the guinea-pig isolated trachea (Figure 2) confirms results obtained in our earlier studies (Boyle *et al.*, 1987) and may be explained in terms of guanethidine inhibiting the extraneuronal uptake of isoprenaline (Foster, 1969). The present observation that bretylium failed to potentiate isoprenaline (Table 2) may suggest that, in contrast to guanethidine, bretylium does not inhibit the sequestration of isoprenaline into extraneuronal sites.

Among the group of KCOs chosen for study, BRL 38227 is a benzopyran derivative, pinacidil is a cyanoguanidine derivative and RP 52891 is a tetrahydrothiopyran derivative (Small *et al.*, 1992). The experiments of the present study have shown that guanethidine can antagonize each of these agents in suppressing the spontaneous tone of the trachea without antagonizing the effect of isoprenaline or theophylline (Figures 1 and 2). Clearly, the antagonism provided by guanethidine exhibits selectivity for the KCOs as opposed to agonists at β-adrenoceptors or alkylxanthines. Furthermore, the antagonism of KCOs provided by guanethidine is not restricted to one particular chemical class (e.g. benzopyrans) of KCO. The present experiments have also shown that bretylium can antagonize BRL 38227, pinacidil and RP 52891 in suppressing spontaneous tracheal tone (Figure 3) without antagonizing isoprenaline or theophylline (Table 2). In addition, guanethidine, bretylium and debrisoquine were each able to antagonize BRL 38227 in promoting the efflux of $^{86}Rb^+$ from strips of bovine trachealis muscle preloaded with the radiotracer (Figures 4 and 5). These observations suggest that antagonism of the tracheal relaxant actions of KCOs is a property shared by several agents classically described (Louis & Howes, 1990) as adrenergic neurone blocking agents. The ability of the adrenergic neurone blocking agents selectively to inhibit the airways smooth muscle relaxant actions of the KCOs without antagonizing agonists at β-adrenoceptors or alkylxanthines is shared both by sulphonylureas such as glibenclamide (Murray *et al.*, 1989; Black *et al.*, 1990; Nielsen-Kudsk *et al.*, 1990; Berry *et al.*, 1991; Raeburn & Brown, 1991) and by phentoamine (Murray *et al.*, 1989; McPherson & Angus, 1990). That such a structurally-diverse group of agents can provide selective antagonism of the KCOs may have important implications concerning the site or mechanism of action of the KCOs.

Mechanisms by which adrenergic neurone blocking agents antagonize KCOs in suppressing the spontaneous tone of the trachea

The scientific literature currently contains very few reports linking the cellular pharmacology of adrenergic neurone blocking agents to the activity of plasmalemmal K^+-channels. Kirpekar *et al.* (1978) observed that the K^+-channel inhibitors tetraethylammonium (TEA) and 4-aminopyridine (4-AP) could reverse the ability of guanethidine to inhibit the neural release of noradrenaline in the *in situ* perfused spleen of the cat. Stutzin *et al.* (1983) observed that the K^+-channel inhibitor, apamin, could antagonize guanethidine in inhibiting contractile responses to the electrical stimulation of nerves in the guinea-pig isolated vas deferens. Such observations led Stutzin *et al.* (1983) to suggest that, by promoting an increase in the cytosolic concentration of free Ca^{2+}, guanethidine might cause the opening of Ca^{2+}-dependent K^+-channels in the neuronal plasmalemma, hyperpolarize the neuronal terminals and thereby inhibit transmitter release. However, the present finding that adrenergic neurone blocking agents antagonize KCOs acting on airways smooth muscle is difficult to reconcile with the idea that the adrenergic neurone blocking agents promote K^+-channel opening.

Tested on cardiac myocytes from the chick embryo, bretylium (applied either extracellularly or intracellularly) was observed to inhibit the outward K^+-current induced by a depolarizing voltage step (Bkaily *et al.*, 1988) and the antidysrhythmic activity of this agent has been attributed to K^+-channel blockade (Bacaner *et al.*, 1986). The present observation that adrenergic neurone blocking agents, including bretylium, antagonize KCOs in suppressing the spontaneous tone of the trachea is entirely consistent with the idea that the former group of compounds have K^+-channel inhibitory activity.

If guanethidine, indeed, is an inhibitor of the K^+-channels opened by BRL 38227, pinacidil and RP 52891, then the failure of guanethidine to convert the spontaneous electrical slow waves of guinea-pig trachealis into regenerative action potentials (Boyle *et al.*, 1987) suggests that the K^+-channel opened by BRL 38227, pinacidil and RP 52891 does not play an important role in determining the strong outward rectifying behaviour of the trachealis cells. Electrophysiological studies of the effect of glibenclamide and phentolamine (Murray *et al.*, 1989) have led to a similar conclusion.

The present observation that guanethidine, bretylium and debrisoquine each inhibited the ability of BRL 38227 to promote $^{86}Rb^+$ efflux from strips of bovine trachealis (Figures 4 and 5) is consistent with the idea that these adrenergic neurone blocking agents inhibit the K^+-channel that is opened by the KCOs. However, at present, it has not been established whether the KCOs act directly on the K^+-

channel protein or whether they act at a site distant from the channel and, there, initiate a series of biochemical changes that culminate in the opening of the channel. In view of this, the mechanism of action of any agent having antagonist activity against the KCOs must remain somewhat speculative.

J.L.B. was supported by Sandoz Pharma Ltd. R.W.F. and R.C.S. were supported by both Sandoz Pharma Ltd and the National Asthma Campaign. We thank Mr A.J. Miller for expert technical assistance. Bretylium, BRL 38227, RP 52891 and debrisoquine were gifts from the respective manufacturers.

References

BACANER, M.B., CLAY, J.R., SHRIER, A. & BROCHU, R.M. (1986). Potassium channel blockade: a mechanism for suppressing ventricular fibrillation. *Proc. Natl. Acad. Sci. U.S.A.*, **83,** 2223–2227.

BERRY, J.L., ELLIOTT, K.R.F., FOSTER, R.W., GREEN, K.A., MURRAY, M.A. & SMALL, R.C. (1991). Mechanical, biochemical and electrophysiological studies of RP 49356 and cromakalim in guinea-pig and bovine trachealis muscle. *Pulm. Pharmacol.*, **4,** 91–98.

BKAILY, G., PAYET, M.D., BENABDERRAZIK, M., SAUVE, R., RENAUD, J.F., BACANER, M. & SPERELAKIS, N. (1988). Intracellular bretylium blocks Na^+ and K^+ currents in heart cells. *Eur. J. Pharmacol.*, **151,** 389–397.

BLACK, J.L., ARMOUR, C.L., JOHNSON, P.R.A., ALOUAN, L.A. & BARNES, P.J. (1990). The action of a potassium channel activator, BRL 38227 (lemakalim) on human airway smooth muscle. *Am. Rev. Respir. Dis.*, **142,** 1384–1389.

BOYLE, J.P., DAVIES, J.M., FOSTER, R.W., MORGAN, G.P. & SMALL, R.C. (1987). Inhibitory responses to nicotine and transmural stimulation in hyoscine-treated guinea-pig isolated trachealis; an electrical and mechanical study. *Br. J. Pharmacol.*, **90,** 733–744.

BURKA, J.F., BERRY, J.L., FOSTER, R.W., SMALL, R.C. & WATT, A.J. (1991). Effects of cromakalim on neurally-mediated responses of guinea-pig tracheal smooth muscle. *Br. J. Pharmacol.*, **104,** 263–269.

FOSTER, R.W. (1969). An uptake of radioactivity from (±)-[^{3}H]-isoprenaline and its inhibition by drugs which potentiate the responses to (−)-isoprenaline in the guinea-pig isolated trachea. *Br. J. Pharmacol.*, **35,** 418–427.

FOSTER, R.W., SMALL, R.C. & WESTON, A.H. (1983). Evidence that the spasmogenic effect of tetraethylammonium in guinea-pig trachealis is both direct and dependent on the cellular influx of Ca^{2+} ion. *Br. J. Pharmacol.*, **79,** 255–263.

KIRPEKAR, M., KIRPEKAR, S.M. & PRAT, J.C. (1978). Reversal of guanethidine blockade of sympathetic nerve terminals by tetraethylammonium and 4-aminopyridine. *Br. J. Pharmacol.*, **62,** 75–78.

LONGMORE, J., BRAY, K.M. & WESTON, A.H. (1991). The contribution of ^{86}Rb-permeable potassium channels to the relaxant and membrane hyperpolarizing actions of cromakalim, RP 49356 and diazoxide in bovine tracheal smooth muscle. *Br. J. Pharmacol.*, **102,** 979–985.

LOUIS, W.J. & HOWES, L.G. (1990). Guanethidine and related compounds. In *Handbook of Experimental Pharmacology*, vol. 93, Pharmacology of Anti-hypertensive Therapeutics. ed. Ganten, D. & Mulrow, P.J. pp. 287–299. Berlin: Springer Verlag.

MCPHERSON, G.A. & ANGUS, J.A. (1990). Characterization of responses to cromakalim and pinacidil in smooth and cardiac muscle by use of selective antagonists. *Br. J. Pharmacol.*, **100,** 201–206.

MURRAY, M.A., BOYLE, J.P. & SMALL, R.C. (1989). Cromakalim-induced relaxation of guinea-pig isolated trachealis: antagonism by glibenclamide and by phentolamine. *Br. J. Pharmacol.*, **98,** 865–874.

NIELSEN-KUDSK, J.E., BANG, L. & BRONSGAARD, A.M. (1990). Glibenclamide blocks the relaxant action of pinacidil and cromakalim in airway smooth muscle. *Eur. J. Pharmacol.*, **180,** 291–296.

RAEBURN, D.M. & BROWN, T.J. (1991). RP 49356 and cromakalim relax airway smooth muscle in vitro by opening a sulphonylurea-sensitive K^+-channel: a comparison with nifedipine. *J. Pharmacol. Exp. Ther.*, **256,** 492–499.

SMALL, R.C., BERRY, J.L., BURKA, J.F., COOK, S.J., FOSTER, R.W., GREEN, K.A. & MURRAY, M.A. (1992). Potassium channel activators and bronchial asthma. *Clin. Exp. Allergy*, **22,** 11–18.

STUTZIN, A., PARAVIC, F., ORMENO, G. & ORREGO, F. (1983). Guanethidine effects on the guinea-pig vas deferens are antagonized by the blockers of calcium-activated potassium conductance, apamin, methylene blue and quinine. *Mol. Pharmacol.*, **23,** 409–416.

(Received February 10, 1992
Revised March 19, 1992
Accepted March 24, 1992)

Br. J. Pharmacol. (1992), **106**, 819–822 © Macmillan Press Ltd, 1992

The contribution of charge to affinity at functional (M_3) muscarinic receptors in guinea-pig ileum assessed from the effects of the carbon analogue of 4-DAMP methiodide

[1,2]*†R.B. Barlow, †Susan Bond, *D.W. Holdup, [1]**J.A.K. Howard, †D.S. McQueen, †Anne Paterson & *M.A. Veale

*Department of Pharmacology, Bristol University, †Department of Pharmacology, University of Edinburgh and **Department of Inorganic Chemistry, University of Bristol.

1 4-Diphenylacetoxy-1:1-dimethyl *cyclo*hexane (carbo-4-DAMP) is the carbon analogue of 4-diphenylacetoxy-*N*-methylpiperidine (4-DAMP) methiodide. The compounds differ only in that the quarternary nitrogen atom in 4-DAMP methiodide is replaced by a quaternary carbon atom, which is uncharged.

2 Carbo-4-DAMP appears to act competitively at functional (M_3) muscarinic receptors in guinea-pig ileum. Estimates of log affinity constant are 6.0 at 30°C and 5.9 at 37°C, i.e. the compound has 0.1% of the affinity of 4-DAMP methobromide.

3 The absence of charge makes little difference to the conformation as determined by X-ray crystallography. The bond lengths and angles are very similar, though the bonds in the *cyclo*hexane ring of carbo-4-DAMP are consistently slightly longer than those in the piperidinium ring of 4-DAMP methiodide, and the presence of the charge slightly reduces the space between molecules.

4 The difference between the affinities of 4-DAMP methobromide and carbo-4-DAMP indicates that the contribution of coulombic forces to the binding between 4-DAMP methiodide and muscarinic (M_3) receptors is at least 17 kJ mol^{-1} (4.1 kcal mol^{-1}) at 37°C. How much this is an underestimate depends upon how much hydrophobic binding is greater with the uncharged compound.

Keywords: M_3 muscarinic receptors; guinea-pig ileum; 4-DAMP methiodide; carbo-4-DAMP; quaternary nitrogen; coulombic interaction; X-ray crystal structure; affinity

Introduction

Coulombic forces between charged groups are assumed to contribute greatly to drug-receptor interactions but it is not easy to assess the size of this contribution experimentally. Two methods have been used. The first is to compare the properties of compounds containing quaternary nitrogen (charged) and quaternary carbon (uncharged), e.g. acetylcholine and its carbon analogue (Adams & Whittaker, 1949; Banister & Whittaker, 1951). The second method is to study the effects of pH on the activity of compounds which are bases and the ionisation of which is appreciably affected in the pH range which can be tested. From the effects of pH on the activity of arecoline on guinea-pig ileum, Burgen (1965) concluded that the contribution of the charge to binding was greater with agonists than with antagonists. Measurements of the affinities of the carbon analogues of antagonists (Barlow & Tubby, 1974), however, showed that the contribution varied greatly, with the effect on the affinity of acetylcholine lying within the range for the antagonists.

The effects of pH on the affinity of antagonists at muscarinic receptors in guinea-pig ileum also indicate great variation in the contribution of charge to affinity. From dose-ratio experiments with guinea-pig ileum, Barlow & Winter (1981) concluded that the uncharged form of hyoscine (also called scopolamine) has about 10% of the affinity of the protonated form whereas the uncharged form of hyoscine-N-oxide is virtually inactive. The uncharged form of pirenzepine had less than 1% of the affinity of pirenzepine (Barlow & Chan, 1982). In these experiments the response is a muscular contraction involving muscarinic M_3 receptors (Candell *et al.*, 1990).

From binding experiments Ehlert & Delen (1990) estimated the affinity of the uncharged form of hyoscine to be 1.4% of that of the charged form for muscarinic receptors in rat corpus striatum (mainly M_1 receptors) and 1.5% for those in rat heart (M_2 receptors), much less than the value (10%) in dose-ratio experiments. Changes in pH, however, may alter the structure of the receptor and whichever method is used it is possible that the conformations of the charged and uncharged forms are different, so the observed effect on binding may have been affected by a change in conformation.

This paper describes results obtained with 4-diphenylacetoxy, 1,1-dimethyl*cyclo*hexane (carbo-4-DAMP) which is the carbon analogue of 4-diphenylacetoxy-*N*-methylpiperidine (4-DAMP) methiodide. Carbo-4-DAMP was obtained crystalline and an X-ray crystal structure determination was made so that the effects of the charge on molecular dimensions could be assessed by comparing it with 4-DAMP methiodide (Barlow *et al.*, 1987). Quaternary nitrogen and quarternary carbon should be similar in size – in *Interatomic Distances* (Sutton, 1965) the average distance between saturated carbon atoms is 1.54Å and the average distance between carbon and quarternary nitrogen is 1.48Å – but a direct comparison needs to be made because appreciable differences were noted between the apparent molal volumes of some quarternary carbon and quaternary nitrogen compounds (Barlow & Tubby, 1974).

[1] Present addresses: (R.B.B.) Ash Lea Cottage, Ravenstonedale, Kirkby Stephen, Cumbria CA17 4NG.
(J.A.K.H.) Department of Chemistry, University of Durham, South Road, Durham DH1 3LE.
[2] Author for correspondence.

Methods

Preparation of 4-diphenylacetoxy-1,1-dimethyl-cyclohexane (carbo-4-DAMP)

4,4-Dimethyl-2-*cyclo*hexen-1-one (Aldrich) was reduced with lithium aluminium hydride in ether to give 4,4-dimethl-2-*cyclo*hexen-1-ol which was reduced with hydrogen and palladium charcoal to give 4,4-dimethyl-*cyclo*hexan-1-ol. This was heated for 4 h at 80°C with diphenylacetylchloride and the ester was dissolved in ether, washed with sodium hydroxide (2 M), dried and distilled. The fraction boiling at 175–180°C/0.3 mmHg was redistilled and had b.p. 140–142°C/2×10^{-3} mmHg. This subsequently crystallized and was recrystallized from ethanol and water and had m.p. 81–82°C. Found C, 81.5; H, 8.13: $C_{22}H_{26}O_2$ requires C, 81.9; H, 8.22%.

Crystal structure determination

Crystal data for 4-diphenylacetoxy-1,1-dimethyl-*cyclo*hexane (carbo-4-DAMP) $C_{22}H_{26}O_2$, M = 322.45, orthorhombic, Pbca (No: 61), a = 11.448(7), b = 16.999(6), c = 19.073(7)Å, U = 3712(2)Å^3, Z = 8, $D_g = 1.16\ gcm^{-2}$, F(000) = 1392, T = 298K, $R(R_w) = 0.070(0.071)$ for 611 unique reflections with $I > 3\sigma(I)$.

Diffracted intensity data were collected on a Siemens P3m/V four-circle automated diffractometer and the data collection parameters and details of data reduction, structure solution and refinement were as previously described (Barlow & Johnson, 1989).

All crystallographic data have been deposited with the Cambridge Crystallographic Data Centre, Lensfield Road, Cambridge.

Measurement of affinity constants

Ileum from Dunkin-Hartley guinea-pigs was set up as described by Edinburgh Staff (1974). The responses were recorded isotonically with a load of about 0.5 g. The tissue was suspended in modified Krebs-Henseleit solution (Edinburgh Staff, 1974), aerated with a mixture of 95% oxygen and 5% carbon dioxide, and experiments were done at 29.8 ± 0.3°C and 37.0 ± 0.1°C.

The agonist, carbachol, was allowed to act for 30 s and added once every 90 s by relays controlled from a PET microcomputer. Alternate small and large control responses were obtained and when these were regular the tissue was exposed to a solution of the antagonist. In some experiments the concentration of the agonist was increased to try to obtain responses which roughly matched the controls. In others, where only slight antagonism was expected, the concentration of agonist was not altered. When these were regular the approximate dose-ratio is given by the ratio of the concentrations of the agonist used in the presence and in the absence of the antagonist and an exact dose-ratio was calculated from the size of the responses by a calculation similar to a 4-point assay (Edinburgh Staff, 1974; Barlow, 1983). In nearly all experiments, further concentrations of antagonist were tested on the preparation with a fresh set of control responses, though recovery was often very slow, possibly because the compound was retained by lipid in the tissue.

These methods are the same as those used by Barlow & Shepherd (1986) and Barlow *et al.* (1988) but the results have been complicated by the limited solubility of the compound in water. Stock solutions of carbo-4-DAMP were made up in absolute ethanol and a 1 mM solution in ethanol was diluted to 1 litre with Krebs solution to obtain concentrations in the range 0.1–1.0 μM. Solutions which should be stronger than this are cloudy. A check was made that the concentration of ethanol present in the Krebs solution (up to 1 ml litre^{-1}, i.e. approximately 20 mM) had no visible effect on the responses to carbachol.

Results

Although carbo-4-DAMP could only be tested in concentrations that produced small effects, consistent estimates of log affinity constant could be obtained (Table 1). The results at 37°C give a Schild plot with a slope of 1.13 ± 0.24 and the intercept on the X-axis (pA_2) is 6.00.

As a further test for competition, dose-ratios were obtained with carbo-4-DAMP given in combination with 4-DAMP methobromide, which is known to act competitively (Abramson, 1964; Barlow & Shepherd, 1985). For two antagonists tested in concentrations producing dose-ratios DR_1 and DR_2 separately, the dose-ratio in the presence of the two together should be $DR_1 + DR_2 - 1$ if both are competitive: otherwise the dose-rato should be $DR_1 \times DR_2$ (Ariens *et al.*, 1964; Paton & Rang, 1965; Abramson *et al.*, 1969). With 1.0 μM carbo-4-DAMP and 10 nM 4-DAMP methobromide at 37°C the dose-ratios were 1.84 and 10.5, with a combined dose-ratio of 10.2 in one experiment and 1.92 and 9.53, with a combined dose-ratio of 9.91 in another. With 0.6 μM carbo-4-DAMP and 10 nM 4-DAMP methobromide the dose-ratios were 2.02 and 11.0, with a combined dose-ratio of 11.8 in one experiment and 1.65 and 8.47, with a combined dose-ratio of 10.7 in another. The mean difference between the combined dose-ratio observed and the value expected for competition ($DR_1 + DR_2 - 1$) is 0.2 ± 0.6 (mean ± s.e.mean, 4 measurements).

The final fractional atomic coordinates calculated from the X-ray structure determination are shown in Table 2: the numbering is indicated in Figure 1.

Discussion

From published values of log affinity constant for 4-DAMP methobromide (Barlow *et al.*, 1976; Barlow & Shepherd, 1985) and the values for carbo-4-DAMP in Table 1, the difference in affinity can be calculated: at 30°C this is 9.0–6.0 = 3 log units: at 37°C it is 8.8 – 5.9 = 2.9 log units. These correspond to differences in the free-energy of adsorption of 18 kJ mol^{-1} (4.25 kcal mol^{-1}) and 17 kJ mol^{-1} (4.11 kcal mol^{-1}), respectively, which may indicate the contribution of charge to binding to functional (M_3) muscarinic receptors in guinea-pig ileum. They are considerably less than the value of 42 kJ mol^{-1} (10 kcal mol^{-1}) suggested by Albert (1951) for interactions between amino and carboxyl group but are bigger than the biggest difference (1.8 log units) observed with the compounds studied by Barlow & Tubby (1974). They also appear to be bigger than between the ionised and unionised forms of arecoline (Burgen, 1965) and of hyoscine (Barlow & Winter, 1981) acting at M_3 receptors, and of hyoscine in binding experiments to M_1 and M_2 receptors (Ehlert & Delen, 1990). The difference is even bigger than that between the ionised and unionised forms of pirenzepine on ileum (Barlow & Chan, 1982).

In the crystal the structures of carbo-4-DAMP and

Table 1 Log affinity constants (± s.e.mean and number of estimates) obtained with the carbon analogue of 4-diphenylacetoxy-*N*-methylpiperidine (4-DAMP) tested on guinea-pig isolated ileum with carbachol as agonist

	Log affinity constant	
Concentration of carbo-4-DAMP	*30°C*	*37°C*
0.2 μM		5.54 ± 0.35 (4)
0.3 μM	5.97 ± 0.05 (6)	5.87 ± 0.03 (3)
0.4 μM	6.14 ± 0.08 (5)	6.10 ± 0.07 (5)
0.6 μM	6.10 ± 0.13 (3)	6.01 ± 0.06 (6)
1.0 μM	5.82 ± 0.12 (5)	5.86 ± 0.10 (5)
Mean	5.99 ± 0.05 (19)	5.89 ± 0.07 (25)

Table 2 Atomic coordinates ($\times 10^4$) and equivalent isotropic thermal parameters ($A^2 \times 10^3$) for 4-diphenylacetoxy-1:1-dimethyl *cyclo*hexane (carbo-4-DAMP)

	x	*y*	*z*	*U**
C(1)	1141(13)	9446(8)	4159(7)	46(5)
C(2)	2021(14)	8918(9)	3817(8)	68(7)
C(3)	2581(13)	8370(9)	4344(7)	65(6)
C(4)	1681(14)	7880(9)	4764(8)	61(6)
C(5)	804(13)	8446(9)	5074(7)	63(6)
C(6)	200(13)	8980(7)	4528(7)	57(6)
O(7)	543(7)	9899(5)	3613(5)	49(3)
C(8)	1074(15)	10559(9)	3414(8)	52(7)
O(9)	1930(10)	10829(6)	3650(6)	79(5)
C(10)	434(14)	10880(7)	2766(8)	52(6)
C(11)	811(12)	10460(7)	2099(7)	44(4)
C(12)	− 17(12)	10372(7)	1578(7)	63(4)
C(13)	295(14)	10012(8)	947(8)	76(5)
C(14)	1426(13)	9744(9)	865(8)	75(5)
C(15)	2242(13)	9840(8)	1374(7)	76(5)
C(16)	1906(13)	10188(7)	2004(7)	62(4)
C(17)	562(13)	11766(8)	2693(7)	49(4)
C(18)	− 236(14)	12260(8)	2998(7)	70(5)
C(19)	− 153(14)	13074(9)	2924(7)	73(5)
C(20)	708(14)	13386(9)	2554(7)	66(4)
C(21)	1528(14)	12947(10)	2256(8)	80(5)
C(22)	1439(15)	12114(9)	2338(7)	84(6)
C(23)	2314(15)	7443(9)	5367(8)	99(8)
C(24)	1074(14)	7256(9)	4300(8)	99(9)

*Equivalent isotropic U defined as one-third of the trace of the orthogonalized U_{ij} tensor.

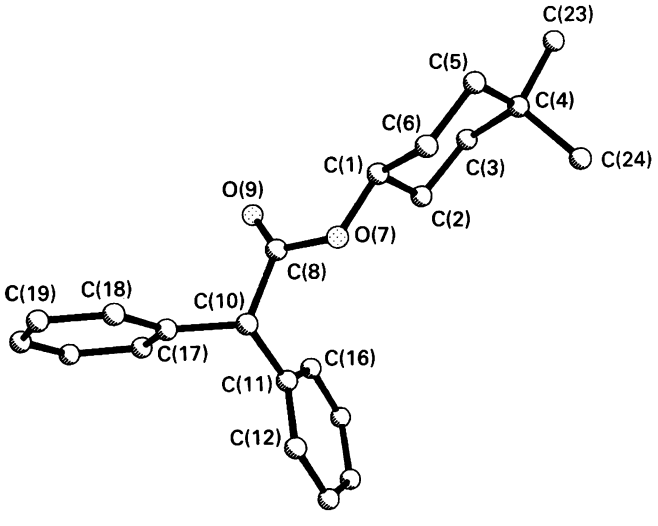

Figure 1 The structure of 4-diphenylacetoxy-1:1-dimethyl *cyclo*hexane (carbo-4-DAMP) showing the numbering scheme.

Table 3 Interatomic distances (Å) at 25°C in the six-membered saturated ring

Atoms	*4-DAMP MeI*	*Carbo-4-DAMP*
1–2	1.503	1.499
2–3	1.496	1.513
3–4	1.508	1.549
4–5	1.517	1.510
5–6	1.497	1.544
6–1	1.532	1.512
4–23	1.511	1.548
4–24	1.474	1.547
Mean*	1.505	1.528
s.e.mean	0.006	0.008

*Significant difference: an analysis of variance gives $P < 0.05$ and with a Mann-Whitney U-test, $P = 0.03$.

4-DAMP methiodide are very similar and it is unlikely that differences in comformation can account for much of the difference in affinity. It is possible to see that the presence of the charge produces a small (but significant) reduction in the size of the six-membered non-aromatic ring (Table 3), but the distance between the acetyl carbon and quarternary carbon in carbo-4-DAMP (6.52Å) is only marginally bigger than that between the acetyl carbon and quaternary nitrogen in 4-DAMP methiodide (6.48Å). The overall similarity is shown in Figure 2, in which the two structures are superimposed.

There are, however, differences between the packing of the molecules in the crystal. The molecular volume of carbo-4-DAMP (464.0Å^3) is slightly less than that for 4-DAMP methiodide (489.9Å^3) and the latter also contains the iodide ion. For an ionic radius of 2.16Å (Pauling, 1967) the volume of iodide should be 42.2Å^3, so the estimate of the volume of the 4-DAMP cation would be 447.7Å^3, i.e. 16Å^3 smaller than carbo-4-DAMP. These observations are similar to what was observed in solution in water by Barlow & Tubby (1974) who compared the apparent molal volumes of choline bromide and its carbon analogue. The choline ion was smaller than carbocholine by 5–17 cm^3 mol^{-1} (depending on how the size of the bromide ion in solution is measured) which is 8–28Å^3 for each molecule. Thus although the presence or absence of the charge in carbo-4-DAMP has little effect on the conformation of individual molecules, it can be seen to affect interactions between molecules in the crystal and probably also affects interactions between molecules in water, including hydrophobic binding.

The simplest explanation for the difference in affinity is that it measures the electrostatic contribution of the charge to the binding of 4-DAMP methiodide and shows that this part of the molecule fits closely to muscarinic M_3 receptors. This is unlikely to be the reason why the compound is selective for these receptors, however, because there is also a large difference between the charged and uncharged forms of pirenzepine tested on ileum and this drug is selective for M_2

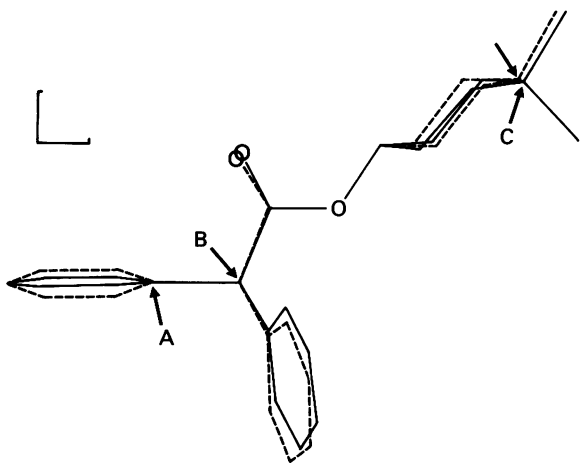

Figure 2 A comparison of the X-ray crystal structures of 4-diphenylacetoxy-*N*-methylpiperidine (4-DAMP) methiodide (broken line) and 4-diphenylacetoxyl:1-dimethyl *cyclo*hexane (carbo-4-DAMP, full line). The two molecules have been superimposed with the near end of one benzene ring (A), the acetyl carbon atom (B) and the quaternary nitrogen or quaternary carbon (C) lying in the same plane, with B as the origin. There are slight differences in the positions of the benzene rings, one of which is viewed almost edge-on, and between the orientation of the piperidine ring, also viewed edge-on, and the *cyclo*hexane ring, which is slightly twisted out of plane. Overall the conformations are very similar with several of the bonds superimposed. The scale marks are 1Å (100 picometres).

receptors. It is also possible, particularly in view of the effects on size discussed above, that the contribution from hydrophobic binding is greater with uncharged molecules, thus reducing what is assumed to be the electrostatic contribution. Even if there is uncertainty about this, a limit can be set; it must be at least as big as the experimental difference.

Although the amino acid sequences of muscarinic receptors are known (review: Hulme *et al.*, 1990) it is not yet possible to produce detailed pictures of the environment of the binding site. Binding experiments (Birdsall *et al.*, 1990; Ehlert & Delen, 1990) suggest that there may be more than one carboxyl group involved but in dose-ratio experiments with functional tissue the binding must be to the M_3 receptor concerned with the response and drugs are likely to compete with protons for the carboxyl group which is most strongly acidic. This could well be in the aspartic acid, which is 105 in the sequence.

We thank the MRC for support for part of this work and Professor F.G.A. Stone for the use of facilities in the Inorganic Chemistry Department in Bristol. We are particularly grateful to Professor J.S. Kelly for the use of facilities in Edinburgh.

References

ABRAMSON, F.B. (1964). The synthesis and pharmacological properties of some alicyclic compounds related to acetylcholine. *Ph.D. Thesis, University of Edinburgh.* pp. 20 & 28.

ABRAMSON, F.B., BARLOW, R.B., MUSTAFA, M.G. & STEPHENSON, R.P. (1969). Relationship between chemical structure and affinity for acetylcholine receptors. *Br. J. Pharmacol.*, **37**, 207–233.

ADAMS, D.H. & WHITTAKER, V.P. (1949). The cholinesterases of human blood. I. The specificity of the plasma enzyme and its relation to the erythrocyte cholinesterase. *Biochim. Biophys. Acta*, **3**, 358–366.

ALBERT, A. (1951). *Selective Toxicity*, p. 26. London: Methuen.

ARIENS, E.J., SIMONIS, A.M. & VAN ROSSUM, J.M. (1964). Drug-receptor interaction: interaction of one or more drugs with different receptor systems. In *Molecular Pharmacology*, vol. 1 p. 336, section IIB. New York: Academic Press.

BANISTER, J. & WHITTAKER, V.P. (1951). Pharmacological activity of the carbon analogue of acetylcholine. *Nature*, **167**, 605.

BARLOW, R.B. (1983). *Biodata Handling with Microcomputers.* pp. 55–61. Cambridge: Elsevier Biosoft.

BARLOW, R.B., BERRY, K.J., GLENTON, P.A.M., NIKOLAOU, N.M. & SOH, K.S. (1976). A comparison of affinity constants for muscarine-sensitive acetylcholine receptors in guinea-pig atrial pacemaker cells at 29°C and in ileum at 29°C and 37°C. *Br. J. Pharmacol.*, **58**, 613–620.

BARLOW, R.B. & CHAN, M. (1982). The effects of pH on the affinity of pirenzepine for muscarinic receptors in the guinea-pig ileum and rat fundus strip. *Br. J. Pharmacol.*, **77**, 559–563.

BARLOW, R.B., HOWARD, J.A.K., JOHNSON, O. & SANDERS, T.M. (1987). Structures of 4-diphenylacetoxy-N-methylpiperidine methiodide and hyoscine methiodide. *Acta Cryst.*, **C43**, 671–674.

BARLOW, R.B. & JOHNSON, O. (1989). The X-ray crystal structure of 4-diphenylcarbamyl-N-methyl-piperidine methobromide (the carbamate analogue of 4-DAMP methiodide). *Br. J. Pharmacol.*, **98**, 425–428.

BARLOW, R.B. & SHEPHERD, M.K. (1985). A search for selective antagonists at M_2 muscarinic receptors. *Br. J. Pharmacol.*, **85**, 427–435.

BARLOW, R.B. & SHEPHERD, M.K. (1986). A further search for selective antagonists at M_2 muscarinic receptors. *Br. J. Pharmacol.*, **89**, 837–843.

BARLOW, R.B., SHEPHERD, M.K., TYDEMAN, H. & VEALE, M.A. (1988). The affinity of some acetylenic analogues of 4-DAMP methobromide for muscarinic receptors in guinea-pig ileum and atria. *Br. J. Pharmacol.*, **94**, 947–951.

BARLOW, R.B. & TUBBY, J.H. (1974). Actions of some esters of 3,3-dimethylbutan-1-ol (the carbon analogue of choline) on the guinea-pig ileum. *Br. J. Pharmacol.*, **51**, 95–100.

BARLOW, R.B. & WINTER, E.A. (1981). Affinities of the protonated and non-protonated forms of hyoscine and hyoscine N-oxide for muscarinic receptors of the guinea-pig ileum and a comparison of their size in solution with that of atropine. *Br. J. Pharmacol.*, **72**, 657–664.

BIRDSALL, N.J.M., CHAN, S.C., EVELEIGH, P., HULME, E.C. & MILLER, K.W. (1990). The modes of binding of ligands to cardiac muscarinic receptors. *Trends Pharmacol. Sci.* (suppl), 31–34.

BURGEN, A.S.V. (1965). The role of ionic interactions at the muscarinic receptor. *Br. J. Pharmacol. Chemother.*, **25**, 4–17.

CANDELL, L.M., YUN, S.H., TRAN, L.L.P. & EHLERT, F.J. (1990). Differential coupling of subtypes of the muscarinic receptor to adenylate cyclase and phosphoinositide hydrolysis in the longitudinal muscle of the rat ileum. *Mol. Pharmacol.*, **38**, 689–697.

EDINBURGH STAFF (1974). *Pharmacological Experiments on Isolated Preparations.* 2nd edition. pp. 2, 25–28, 58–62, 112. Edinburgh: Churchill Livingstone.

EHLERT, F.J. & DELEN, F.M. (1990). Influence of pH on the binding of scopolamine and N-methylscopolamine to muscarinic receptors in the corpus striatum and heart of rats. *Mol. Pharmacol.*, **38**, 143–147.

HULME, E.C., BIRDSALL, N.J.M. & BUCKLEY, N.J. (1990). Muscarinic receptor subtypes. *Annu. Rev. Pharmacol. Toxicol.*, **30**, 633–673.

PATON, W.D.M. & RANG, H.P. (1965). The uptake of atropine and related drugs by intestinal smooth muscle of the guinea-pig in relation to acetylcholine receptors. *Proc. R. Soc.*, **B163**, 1–44.

PAULING, L. (1967). *The Chemical Bond* p. 151. Ithaca, New York: Cornell University Press.

SUTTON, L.E. (1965). *Tables of Interatomic Distances and Configuratiion in Molecules and Ions*, Special Publication No. 18, pp. 14 & 19. London: The Chemical Society.

(Received January 15, 1992
Revised March 23, 1992
Accepted March 24, 1992)

Br. J. Pharmacol. (1992), **106**, 823–827 © Macmillan Press Ltd, 1992

Strychnine-induced potassium current in CA1 pyramidal neurones of the rat hippocampus

Satoru Ebihara & [1] Norio Akaike

Department of Neurophysiology, Tohoku University School of Medicine, Sendai 980, Japan

1 Direct actions of strychnine (Str) and brucine (Bru) on the dissociated hippocampal CA1 neurones of the rat have been investigated with the whole-cell mode of the patch-clamp technique.

2 At a holding potential (V_H) of − 20 mV, both Str and Bru elicited outward current at concentrations over 10^{-5} M. The reversal potential of Str-induced current (E_{Str}) was − 77.8 mV, which was close to the K^+ equilibrium potential (E_K = − 80.3 mV). The change in E_{Str} for a ten fold change in extracellular K^+ concentration was 58 mV, indicating that the membrane behaves like a K^+ electrode in the presence of Str.

3 The concentration-response curves for Str and Bru were bell-shaped, and nearly maximum response occurred at 10^{-4} M for Str and 3×10^{-4} M for Bru. The maximum current amplitude induced by Bru was about 80% of that induced by Str. A transient 'hump' current appeared immediately after the wash-out of external solutions containing Str and Bru at concentrations higher than 10^{-4} and 3×10^{-4} M, respectively.

4 The Str-induced current (I_{Str}) was antagonized by K^+ channel blockers such as Ba^{2+}, tetraethylammonium (TEA)-chloride, and 4-aminopyridine (4-AP) in a concentration-dependent manner. I_{Str} was insensitive to glibenclamide, a blocker of ATP-sensitive K^+ channels.

5 Internal perfusion with 10 mM BAPTA did not affect the Str-induced I_K. Depletion of the intracellular Ca^{2+} store by caffeine had no effect, indicating that intracellular Ca^{2+} does not mediate the Str-induced activation of K^+ conductance.

6 Both guanosine-5'-O-3-thiotriphosphate (GTPγS) and guanosine-5'-O-thiodiphosphate (GDPβS) suppressed the Str-induced I_K, the former action appearing more rapidly than the latter. The results suggest that the GTP binding proteins are involved in this Str response.

7 When neurones were loaded with cholera toxin (CTX) or pertussis toxin (PTX) through a patch pipette, PTX suppressed the Str response whereas CTX did not, suggesting that G_i and/or G_o might be involved in the Str-induced I_K.

Keywords: Hippocampal CA1 neurone in rat; strychnine; brucine; K^+ current; G protein

Introduction

Strychnine (Str) is prepared from dried ripe seeds of *Strychnos nux-vomica* that contains 1.1 to 1.4% Str and a similar amount of closely related alkaloid, brucine (Bru). The Str is known as a selective and competitive antagonist of the glycine receptor Cl^- channel complex, and Str has been used as a valuable tool in physiological and pharmacological studies on glycine receptors. However, many studies also showed that Str inhibits not only the glycine-induced Cl^- current (I_{Cl}) but also the γ-aminobutyric acid (GABA)-induced I_{Cl} in a competitive manner in a concentration range between 0.1 μM and 100 μM (Aibara *et al.*, 1991; Shirasaki *et al.*, 1991). Moreover, at the higher concentration, Str inhibits the responses induced by acetylcholine (Phillis & York, 1967; Faber & Klee, 1974), noradrenaline (Phillis & York, 1967), 5-hydroxytryptamine (Phillis & York, 1967; Faber & Klee, 1974), histamine (Groul & Weinreich, 1979), dopamine (Faber & Klee, 1974) or N-methyl-D-aspartate (NMDA) (Bertolino & Stefano, 1988). In addition, voltage-dependent Na^{2+} (Shapiro, 1977), K^+ (Shapiro, 1977) and Ca^{2+} (Oyama *et al.*, 1988) channels are also blocked by Str. Recently, we also found that Str itself induces the K^+ current in rat dorsal root ganglion (DRG) cells (Aibara *et al.*, 1991). These results suggest that Str has multiple pharmacological actions in the concentrations used. In this study, we investigated whether Str could also induce K^+ outward currents in mammalian CNS neurones as well as in DRG neurones. In addition, we studied the intracellular mechanisms of this response.

[1] Author for correspondence.

Methods

Preparations

The method used to dissociate rat hippocampal CA1 pyramidal neurones has been described in a previous paper (Ito *et al.*, 1991). Briefly, 1- to 2-week-old Wistar rats were decapitated under ether anaesthesia and 350 μm transverse slices of the brains were prepared with a microslicer (D.S.K., DTK-1000). The brain slices were incubated in Krebs solution containing 0.01% pronase [Calbiochem] for 15 to 20 min at 31°C, and subsequently treated with 0.01% thermolysin [Sigma]. The CA1 region of the hippocampus was micropunched out of the slices, then dissociated mechanically with fine glass pipettes. Dissociated hippocampal CA1 pyramidal neurones adhered to the bottom of the culture dish within 30 min. In the present experiment, we used neurones that maintained their original morphological features, such as the dendritic processes.

Solutions

The normal external solution contained (in mM): NaCl 150, KCl 5, $CaCl_2$ 2, $MgCl_2$ 1, glucose 10 and HEPES 10, buffered to pH 7.4 with Tris-base. The Ca^{2+}-free 2 mM EGTA solution contained (in mM): NaCl 150, KCl 5, $MgCl_2$ 1, EGTA 2, glucose 10 and HEPES 10, buffered to pH 7.4 with Tris-base. In the conventional patch-clamp study, the normal internal solution contained (in mM): KCl 50, K-gluconate 70, NaCl 20, $CaCl_2$ 0.25, $MgCl_2$ 6, Na_2ATP 5,

EGTA 5 and HEPES 10, buffered to pH 7.2 with Tris-base. In the perforated patch-clamp study, nystatin was added at a final concentration of 150 $\mu g\ ml^{-1}$ to the normal internal solution, the composition of which was (in mM): KCl 150 and HEPES 10. The pH was adjusted to 7.2 with Tris-base.

Electrical recording

Two types of voltage-clamp recordings were made in the whole-cell mode, either by use of a conventional patch-clamp (Hamill *et al.*, 1981) or by a nystatin perforated patch-clamp technique (Horn & Marty, 1988). In both recordings, the resistance between the glass pipette filled with internal solution and the reference electrode was 4 to 8 MΩ. The current and voltage were measured with a patch-clamp amplifier (List Medical, EPC-7), monitored on a storage oscilloscope (Toshiba, 10M63) and a pen-recorder (Sanei, RECTI-HORIZ-8K), and recorded on video tapes after digitization with a PCM processor (Sony, PCM-501ES). All experiments were carried out at room temperature (20 to 23°C).

Drugs

The following drugs were used: strychnine hydrochloride (Str), kainic acid (KA), 10,11-dimethoxystrychnine, glibenclamide, *bis*(γ-aminophenoxy) ethane-*N*,*N*,*N*′,*N*′,-tetraacetic acid (BAPTA), guanosine-5′-O-3-thiotriphosphate (GTPγS), guanosine-5′-O-thiodiphosphate (GDPβS), cholera toxin (CTX) [Sigma], 4-aminopyridine (4-AP), tetraethylammonium (TEA)-chloride [Tokyo Kasei], caffeine [Ishizu] and pertussis toxin (PTX) [Seikagaku Corporation]. All drugs were dissolved in the external or internal solution just before use. External solutions were exchanged by a rapid application technique termed the 'Y-tube' method, which allows the exchange of solutions surrounding a neurone within 10 to 20 ms (Akaike *et al.*, 1989; Murase *et al.*, 1989).

Results

Strychnine- and brucine-induced currents

Experiments were carried out at a holding potential (V_H) of − 20 mV in the conventional whole-cell mode. Str and Bru were applied every 2 min, at which interval constant responses could be repeatedly evoked for 1 h or more. The threshold concentrations for both the Str- and Bru-induced current (I_{Str} and I_{Bru}, respectively) were approximately 10^{-5} M. The I_{Str} increased with increasing Str concentration in the range 10^{-5} to 10^{-4} M. The I_{Bru} also increased as Bru concentration increased in the range 10^{-5} to 3×10^{-4} M (Figure 1). The amplitude of the maximum I_{Bru} was about 80% of that of the maximum I_{Str}. Further increase in Str or Bru concentration beyond that which induced the maximum response decreased the peak current during a continuous application of these drugs. The 'wash-out' of external solution containing Str or Bru at concentrations higher than 10^{-4} M for the former and 3×10^{-4} M for the latter always induced a transient outward 'hump' current (Figure 1a). Figure 1b summarizes the Str- and Bru-induced peak currents plotted as functions of Str and Bru concentrations. When all responses were normalized to the peak current induced by 10^{-4} M Str, the concentration-response curves for Str and Bru showed a bell-shaped pattern.

Current-voltage (I-V) relationship for Str response

Figure 2a shows the currents induced by 10^{-4} M Str at various V_Hs. In the *I*-V relationship, the responses at various V_Hs were normalized to the peak response induced by Str at a V_H of − 50 mV (*). The reversal potential of I_{Str} (E_{Str}) estimated from the intersection on the voltage axis in the *I*-V curve was − 77.8 ± 1.3 mV (mean ± s.e.mean, $n = 5$). The

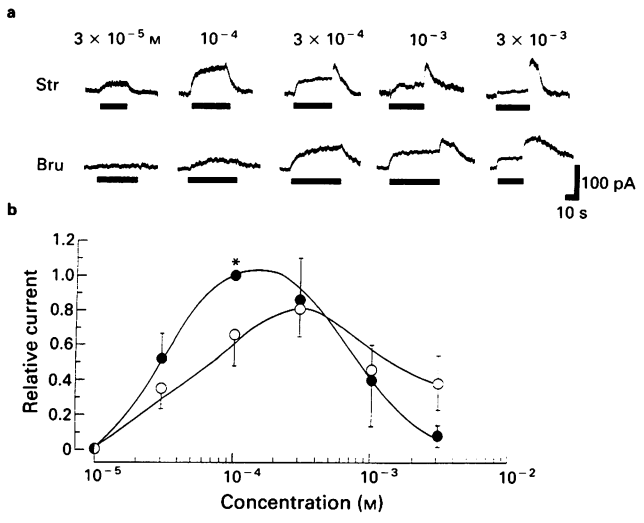

Figure 1 (a) Strychnine (upper panel) - and brucine (lower panel)-induced outward currents in dissociated hippocampal CA1 neurones. V_H was − 20 mV. The neurones were exposed to various concentrations of strychnine (Str) or brucine (Bru) during the periods indicated by the horizontal bar below each response. (b) Concentration-response curves for Str (●) and Bru (○). Each point shows the average of 5–7 experiments and the vertical bars show ± s.e.mean. All responses were normalized to the peak current induced by 10^{-4} M Str (see symbol marked with asterisk). The continuous curves were drawn by eye.

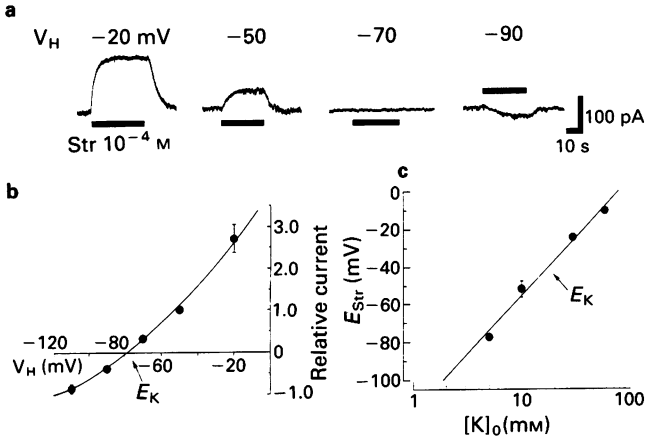

Figure 2 Strychnine (Str)-induced currents: (a) 10^{-4} M Str-induced currents at various V_Hs in the same cell; (b) current-voltage (*I*-V) relationship of 10^{-4} M Str-induced responses. All responses were normalized to the peak response induced by Str at a V_H of − 50 mV (see symbol marked with asterisk). The vertical bars show ± s.e.mean. (c) Effect of $[K^+]_o$ on the E_{Str}. Dissociated hippocampal CA1 neurones were perfused with external solutions containing various concentrations of K^+. The $[K^+]_i$ was 120 mM throughout this experiment. Each point is the average of 4–5 experiments. A straight line shows E_K. The vertical bars represent ± s.e.mean.

value was quite close to the K^+ equilibrium potential (E_K) of − 80.3 mV calculated with the Nernst equation for the given extra- and intracellular K^+ concentrations ($[K^+]_o$ and $[K^+]_i$, respectively) (Figure 2b). Moreover, the 'hump' current induced by the removal of high concentrations of Str also reversed at nearly E_K (data not shown). The results indicate that I_{Str} and the 'hump' current are carried by K^+ ions.

When the dissociated neurones were perfused with the normal internal solution containing 120 mM K^+ and the external solutions containing various K^+ concentrations ($[K^+]_o$ = 5, 10, 30 and 60 mM), the measured E_{Str} values are

-77.4 ± 1.3 mV ($n = 5$), -52.0 ± 4.2 mV ($n = 4$), -24.5 ± 1.8 mV ($n = 5$), -10.6 ± 0.8 mV ($n = 4$) for 5, 10, 30 and 60 mM $[K^+]_o$, respectively (Figure 2c). The change in E_{Str} for a ten fold change in $[K^+]_o$ was 58 mV, indicating that the cell membrane behaves like a K^+ electrode in the presence of Str.

Effects of various K^+ channel blockers on strychnine response

In order to elucidate pharmacological properties of the K^+ channel activated by Str, the effects of K^+ channel blockers on I_{Str} were tested at a V_H of -20 mV. The neurones were perfused with normal internal and external solutions. In these experiments, glibenclamide and $BaCl_2$ were directly dissolved in the standard external solution. The external solution containing 4-AP or TEA was made by replacement of NaCl in the external solution. Ba^{2+}, 4-AP and TEA suppressed I_{Str} in a concentration-dependent manner (Figure 3). The inhibitory potency was in the order $Ba^{2+} > 4\text{-AP} > \text{TEA}$. Glibenclamide, an ATP-sensitive K^+ channel blocker, had no effect on I_{Str} at concentrations of 10 to 100 μM.

Effects of intracellular Ca^{2+} depletion on I_{Str}

To find whether a rise in intracellular free Ca^{2+} is necessary for the Str-induced response, the following two types of study were performed. In the first study, we chelated the intracellular Ca^{2+} by an internal solution containing 10 mM BAPTA. In this experiment, the current recordings were made in the nystatin perforated-patch mode and successively in the conventional whole-cell mode by rupture of the cell membrane. After the I_{Str} was recorded at a V_H of -20 mV using the nystatin perforated patch-clamp technique, the patched membrane was ruptured by applying negative pressure. Successive intracellular perfusions of BAPTA had little effects on the amplitude and kinetics of the I_{Str} in all cells tested ($n = 4$) (Figure 4a). The next study was performed with the nystatin perforated patch-clamp technique. Caffeine (10^{-2} M), which is known to release Ca^{2+} from a caffeine-sensitive Ca^{2+} (CICR) pool in excitable cells (Endo *et al.*, 1970), induced an outward current, and the caffeine response completely recovered within 4 min from a previous exposure to caffeine. In the absence of extracellular Ca^{2+}, the first application of caffeine induced an almost identical response. However, the 2nd application after 4 min induced only a small response. Even in this condition of Ca^{2+} depletion of the CICR pool (Akaike & Sadoshima, 1989), Str could induce I_{Str} having a current amplitude ($n = 4$) similar to that in the normal external solution (Figure 4b). These results suggest that the I_{Str} is induced by a mechanism different from that of the caffeine-induced K^+ current: i.e., the Str response does not result in activation of K^+ conductance by intracellular Ca^{2+}.

Effects of guanosine derivatives on I_{Str}

In order to examine the possible involvement of guanine nucleotide binding proteins (G proteins), the effects of intracellular perfusion with GTPγS or GDPβS on I_{Str} were examined with the conventional whole-cell patch-clamp technique. The Str was applied every 2 min between each application of kainate (KA), which constantly activates the receptor-channel complex (Wang *et al.*, 1991). When neurones were loaded with 100 μM GTPγS through the pipettes at a V_H of -20 mV, I_{Str} was abolished within 12 min whereas the KA-induced inward current was little affected. Intracellular perfusion with 100 μM GDPβS also suppressed I_{Str} within 30 min. In contrast, during perfusion with the normal internal solution (control), almost the same responses were maintained for more than 30 min (Figure 5). The results suggest that I_{Str} is mediated by G proteins.

Effects of cholera toxin and pertussis toxin on I_{Str}

We examined the type of G proteins involved in I_{Str}. When a conventional whole-cell patch was made with a patch-pipette containing pertussis toxin (PTX) 1 μg ml^{-1}, the A protomer of islet-activating protein (IAP), together with 1 mM nicotinamide-adenine dinucleotide (NAD), I_{Str} gradually declined to about 35% of its initial amplitude within 30 min

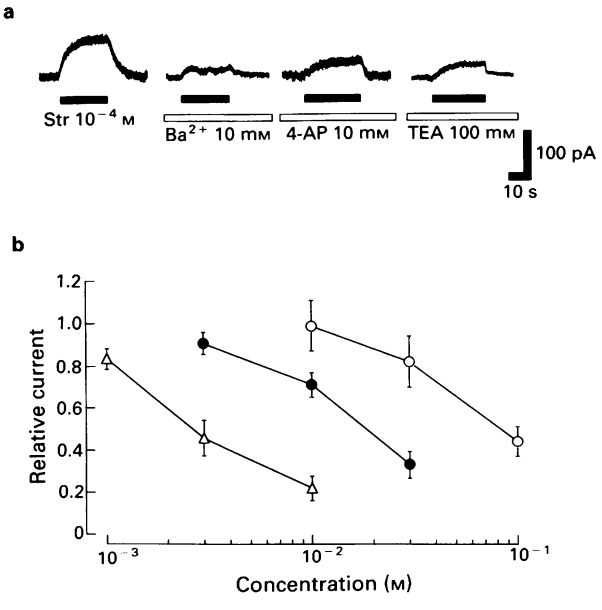

Figure 3 Effects of various K^+ channel blockers on the I_{Str}. The neurones were pretreated for 1 min with normal external solution containing various K^+ channel blockers and 10^{-4} M (Str) together with one of the blockers was applied, in succession. V_H was -20 mV. (a) All recordings were obtained from the same cell. Open and closed horizontal bars indicate the application of the blockers and Str, respectively. (b) All responses induced by a mixture of 10^{-4} M Str and one of the blockers at various concentrations were normalized to the peak current induced by 10^{-4} M Str alone. Abscissa scale shows the concentration of blockers: (Δ) Ba^{2+}; (●) 4-aminopyridine (4-AP); (○) tetraethylammonium (TEA). Each point shows the mean of 4–6 experiments and vertical bars show ± s.e.mean.

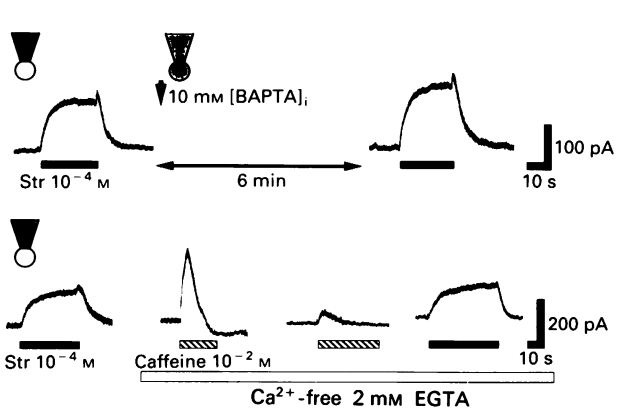

Figure 4 Effects of intracellular Ca^{2+} depletion on I_{Str}. V_H was -20 mV. (a) Effect of intracellular Ca^{2+} chelator, *bis* (γ-aminophenoxy)ethane-*N*,*N*,*N*′,*N*′,-tetraacetic acid (BAPTA), on I_{Str}. Strychnine (Str)-induced (10^{-4} M) currents before (left) and 6 min after (right) rupture of the patch membrane with a pipette containing 10 mM BAPTA. I_{Str} was not affected by intracellular perfusion of 10 mM BAPTA. Arrow indicates rupture of the patch membrane. The results are typical of four reproducible observations. (b) Effects of depletion of Ca^{2+} in an intracellular Ca^{2+} store by 10 mM caffeine. Str was given to the neurone before and during superfusion with Ca^{2+}-free 2 mM EGTA external solution. The results are typical of four reproducible observations.

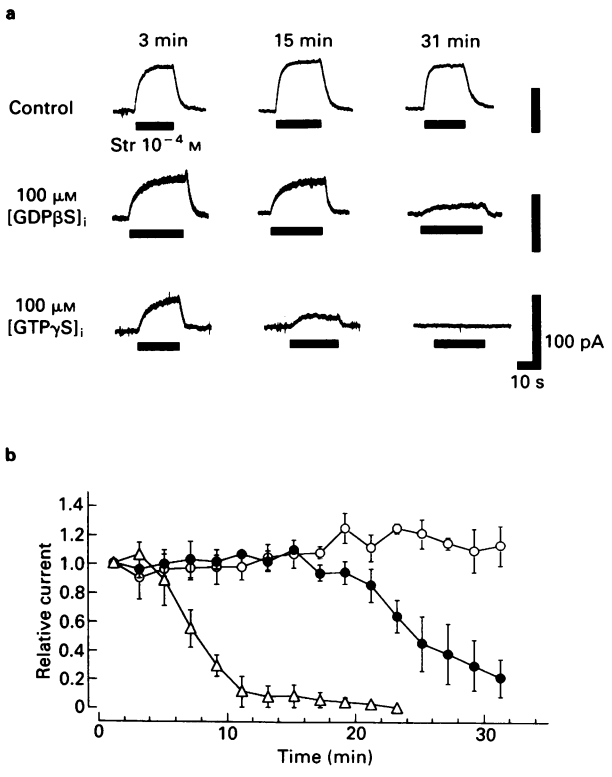

Figure 5 Effects of guanosine-5'-O-thiodiphosphate (GDPβS) and guanosine-5'-O-3-thiotriphosphate (GTPγS) on I_{Str}. (a) Representative recordings of I_{Str}s after 3, 15 and 31 min perfusion with normal (upper), 100 μM GDPβS containing (middle) and 100 μM GTPγS containing (lower) internal solutions. The horizontal bars indicate the period of application of 10^{-4} M Str. (b) Relationships between the time of intracellular perfusion and the relative peak amplitude of I_{Str}s. All responses were normalized to the peak amplitude of I_{Str} 1 min after rupture of the patch membrane. (○), Control; (●) GDPβS; (△), GTPγS. Data are mean ± s.e.mean (vertical bars) obtained from 4 to 6 experiments. $V_H = -20$ mV.

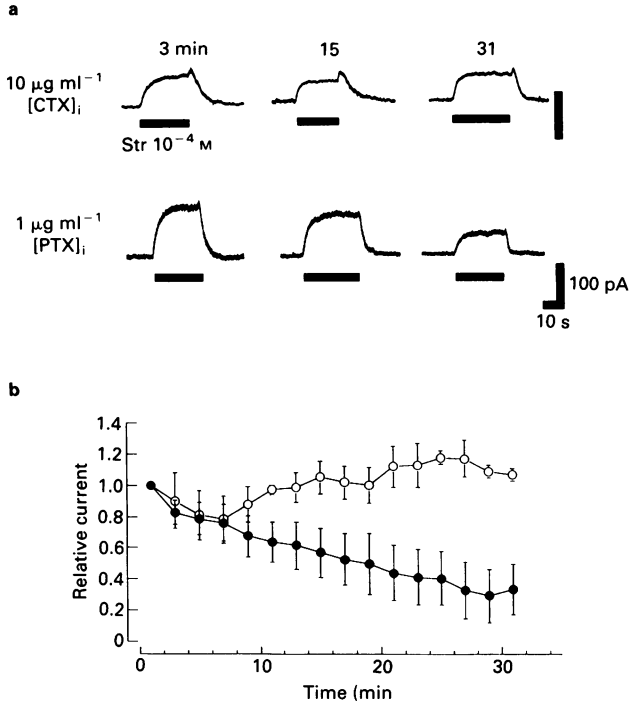

Figure 6 Effects of cholera toxin (CTX) and pertussis toxin (PTX) on I_{Str}. (a) Representative recordings of I_{Str} after 3, 15 and 31 min intracellular perfusion of CTX, 10 μg ml^{-1}, containing (upper) or PTX, 1 μg ml^{-1}, containing (lower) internal solutions. The horizontal bars indicate the period of application of 10^{-4} M strychnine (Str). $V_H = -20$ mV. (b) Relationship between the time of internal perfusion and the relative peak amplitude of I_{Str}. All responses were normalized to the peak amplitude of I_{Str} 1 min after rupture of the patch membrane. (○) CTX; (●) PTX. Data are mean ± s.e.mean (vertical bars) obtained from 5 to 7 experiments.

after the beginning of PTX perfusion. In contrast, intracellular perfusion with cholera toxin (CTX) 1 μg ml^{-1} exerted little effect on I_{Str} (Figure 6). Since PTX is known to inhibit specifically G_i and G_o by ADP-ribosylation (Katada & Ui, 1982; Florio & Sternweis, 1985; Ewald *et al.*, 1988) the present result suggests that G_i and/or G_o may be involved in the I_{Str}.

Discussion

In these experiments we clearly showed that at high concentrations over 10^{-5} M, Str induced K^+ currents in mammalian CNS neurones (hippocampal CA1 pyramidal neurones). The concentration-response relationship, the current-voltage relationship and the pharmacological properties of I_{Str} in hippocampal CA1 pyramidal neurones were almost identical to those in rat dorsal root ganglion (DRG) cells (Aibara *et al.*, 1991). We also showed that I_{Str} does not result from activation of the ATP-sensitive K^+ channel, based on the absence of an inhibitory effect of glibenclamide.

Shapiro (1977) showed that blockade of voltage-dependent K^+ channels by Str resembles that by intracellular application of certain quaternary ammonium (QA) ions, such as tetraethylammonium compounds and demonstrated that the molecular structure of the most potent QA, φC_3 (Armstrong, 1971), is nearly superimposed on that of Str. Using *N*-methylstrychnine, he also reported that Str must cross the membrane and block from the cytoplasmic side in the same fashion as QA ions do. In the present experiments, when the peak I_{Str} was suppressed with concentrations of Str over 10^{-4} M, the wash-out of Str always induced a transient 'hump' current (Figure 1a). Such decreases of the peak currents in the presence of Str may be due to blockade of Str-activated K^+ channels by the Str molecule itself, in the same fashion as Str blocks voltage-dependent K^+ channels. The hump immediately after the wash-out of high concentrations of Str is probably due to activation of undesensitized receptors by Str, released from channels blocked by Str. Similar humps were observed at the wash-out of high concentrations of acetylcholine in the voltage-clamped frog endplate (Adams, 1975) and pentobarbitone in the frog DRG neurone (Akaike *et al.*, 1987).

Bru is less potent than Str as a convulsant. It produces convulsions only with 40 times the effective dose of Str (Webster, 1930) but in this study, the potency of Bru as an agonist for evoking K^+ current seemed to be almost 10 times as weak as that of Str, judging from the concentration-response relationship (Figure 1b).

A vast array of cellular signal transduction processes arise from combinations of many different types of agonists, receptors, effectors and coupling molecules such as heterotrimeric G proteins or protein kinases that connect the receptors to effectors. In this case, we supposed that Str might activate the simplest multiple signalling pathway that is composed of three elements: receptor, G protein and ion channel. There are three reasons for this: (1) The conventional whole-cell patch configuration cannot preserve cytoplasmic constitutions that are necessary to maintain the second messenger system in the dissociated neurones because of 'wash out' (Wakamori *et al.*, 1991). However, I_{Str} was evoked even 30 min after the conventional whole-cell had been initiated. (2) Guanosine derivatives and PTX suppressed the Str res-

ponses. (3) The Str response was not involved in intracellular Ca^{2+}.

In GTPγS-loaded cells, I_{Str} was suppressed within 15 min, suggesting that inhibition occurred at the level of the G protein, due to its continuous activation. As a result, the activity of the G protein would not be transmitted efficiently to the K^+ channel. A similar mechanism has been proposed for the muscarinic activation of the anomalous rectification in heart muscle cells (Kurachi *et al.*, 1987). Under normal conditions, however, an apparent desensitization of the Str-induced outward currents was scarcely observed in hippocampal CA1 neurones, even when almost saturated concentrations of the agonists were applied. This result is not compatible with inactivation of the G protein involved. In heart muscle cells, increased concentrations of ACh markedly facilitated inactivation of the muscarinic receptor-activated anomalous rectifying K^+ current. Our results may suggest that infusion of GTPγS through the patch-pipette spontaneously activates not only a G protein inducing the K^+ current by Str but also another G protein which may be involved in inactivation of the activated K^+ channel. It is well known that adenylate cyclase is controlled in opposing ways by an inhibitory G protein (G_i) and an excitatory G protein (G_s) (reviewed by Gilman, 1987). Therefore, a similar mechanism might function in the Str-activated K^+ channel. In the present case, the inhibitory G protein system may act on the activated K^+ channel since in the GTPγS-loaded cells inactivation of the Str response occurred only after the current was produced. Recently, closing of the S-channel produced by 5-hydroxytryptamine (5-HT) was found to be overridden by Phe-Met-Arg-Phe-NH_2 (FMRFamide; Belardetti *et al.*, 1987), probably by a reversal of the phosphorylation of the channel or its closely related protein induced by 5-HT (Sweatt *et al.*, 1989). Moreover, Inoue & Kuriyama (1991) reported that intracellular GTPγS suppressed muscarinic responses in guinea-pig chromaffin cells and they considered the same mechanism in discussing that phenomenon. Therefore, it is of interest that Str induced K^+ current, probably due to activation of G proteins, particularly G_i and/or G_o, in mammalian CNS.

This study was supported by Grants-in-Aid for Scientific Research (No. 02241101, 02557005 and 03304026) to N.A., from the Ministry of Education, Science and Culture, Japan.

References

ADAMS, P.R. (1975). A study of desensitization using voltage clamp. *Pflügers Arch.*, **60**, 135–144.

AIBARA, K., OONUMA, M. & AKAIKE, N. (1991). Strychnine-induced potassium current in isolated dorsal root ganglion cells of the rat. *Br. J. Pharmacol.*, **102**, 492–496.

AKAIKE, N. & SADOSHIMA, J. (1989). Caffeine affects four different ionic currents in the bull-frog sympathetic neurone. *J. Physiol.*, **412**, 221–244.

AKAIKE, N., SHIRASAKI, T. & YAKUSHIJI, T. (1989). Quinolones and fenbufen interact with $GABA_A$ receptor in rat isolated CA1 pyramidal neurons. *Acta Physiol. Scand.*, **136**, Supplement 582, p 21.

AKAIKE, N., MARUYAMA, T. & TOKUTOMI, N. (1987). Kinetic properties of the pentobarbitone-gated chloride current in frog sensory neurones. *J. Physiol.*, **394**, 85–98.

ARMSTRONG, C.M. (1991). Interaction of tetraethylammonium ion derivatives with potassium channels of giant axons. *J. Gen. Physiol.*, **58**, 413–437.

BELARDETTI, F., KANDEL, E.R. & SIEGELBAUM, S.A. (1987). Neuronal inhibition by the peptide FMRFamide involves opening of S K^+ channels. *Nature*, **325**, 345–346.

BERTOLINO, M. & STEFANO, V. (1988). Voltage-dependent block by strychnine of *N*-methyl-D-aspartic acid-activated cation channels in rat cortical neurons in culture. *Mol. Pharmacol.*, **34**, 98–103.

ENDO, M., TANAKA, M. & OGAWA, Y. (1970). Calcium induced release of calcium from the sarcoplasmic reticulum of skinned muscle fibers. *Nature*, **288**, 34–36.

EWALD, D.A., STERNWEIS, P.C. & MILLER, R.J. (1988). Guanine nucleotide binding protein G_o induced coupling of NPY receptors to calcium channels in sensory neurons. *Proc. Natl. Acad. Sci. U.S.A.*, **88**, 3633–3637.

FABER, D.S. & KLEE, M.R. (1974). Strychnine interactions with acetylcholine, dopamine and serotonin receptors in *Aplysia* neurons. *Brain Res.*, **65**, 109–126.

FLORIO, V.A. & STERNWEIS, P.C. (1985). Reconstitution of resolved muscarinic cholinergic receptors with purified GTP-binding proteins. *J. Biol. Chem.*, **260**, 3477–3483.

GILMAN, A.G. (1987). G proteins: transducers of receptor-generated signals. *Annu. Rev. Biochem.*, **56**, 615–649.

GROUL, D. & WEINREICH, D. (1979). Two pharmacologically distinct histamine receptors mediating membrane hyperpolarizations on identified neurons of *Aplysia californica*. *Brain Res.* **162**, 281–301.

HAMILL, O.P., MARTY, A., NEHER, E., SAKMANN, B. & SIGWORTH, F.J. (1981). Improved patch-clamp technique for high resolution current recording from cells and cell-free membrane patch. *Pflügers Arch.*, **391**, 85–100.

HORN, R. & MARTY, A. (1988). Muscarinic activation of ionic currents measured by a new whole-cell recording method. *J. Gen. Physiol.*, **92**, 145–159.

INOUE, M. & KURIYAMA, H. (1991). Muscarinic receptor is coupled with a cation channel through a GTP-binding protein in guinea-pig chromaffin cells. *J. Physiol.*, **436**, 511–529.

ITO, C., WAKAMORI, M. & AKAIKE, N. (1991). Dual effect of glycine on isolated rat suprachiasmatic neurons. *Am. J. Physiol.*, **260**, C213–218.

KATADA, T. & UI, M. (1982). Direct modification of the membrane adenylate cyclase system by islet-activating protein due to ADP-ribosylation of a membrane protein. *Proc. Natl. Acad. Sci. U.S.A.*, **79**, 3129–3133.

KURACHI, Y., NAKAJIMA, T. & SUGIMOTO, T. (1987). Short-term desensitization of muscarinic K^+ channel current in the isolated atrial myocytes and possible role of GTP-binding proteins. *Pflügers Arch.*, **410**, 227–233.

MURASE, K., RYU, P.D. & RANDIC, M. (1989). Excitatory and inhibitory amino acids and peptide-induced response in acutely-isolated rat spinal dorsal horn neurones. *Neurosci. Lett.*, **103**, 56–63.

OYAMA, Y., AKAIKE, N. & CARPENTER, D.O. (1988). Strychnine decreases the voltage-dependent Ca^{2+} current of both *Aplysia* and frog ganglion neurons. *Cell. Mol. Neurobiol.*, **8**, 307–314.

PHILLIS, J.W. & YORK, D.H. (1967). Strychnine block of neural and drug-induced inhibition in the cerebral cortex. *Nature*, **216**, 922–923.

SHAPIRO, B.I. (1977). Effects of strychnine on the potassium conductance of the frog node of Ranvier. *J. Gen. Physiol.*, **69**, 897–914.

SHIRASAKI, T., KLEE, M.R., NAKAYE, T. & AKAIKE, N. (1991). Differential blockade of bicuculline and strychnine on GABA- and glycine-induced responses in dissociated rat hippocampal pyramidal cells. *Brain Res.*, **561**, 77–83.

SWEATT, J.D., VOLTERRA, A., EDMONDS, B., KARL, K.A., SIEGELBAUM, S.A. & KANDEL, E.R. (1989). FMRFamide reverses protein phosphorylation produced by 5-HT and cAMP in *Aplysia* sensory neurons. *Nature*, **342**, 275–278.

WAKAMORI, M., UNEYAMA, H. & AKAIKE, N. (1991). Muscarinic response in acutely dissociated rat hippocampal CA1 neurons. *Third IBRO world congress of neuroscience abstracts*, P54.44, 352.

WANG, L., SALTER, M.W. & MACDONALD, J.F. (1991). Regulation of kainate receptors by cAMP-dependent protein kinase and phosphatases. *Nature*, **253**, 1132–1135.

WEBSTER, R.W. (1930). *Legal Medicine and Toxicology*, W.B. Saunders Co., Philadelphia.

(Received January 20, 1992
Accepted March 25, 1992)

Br. J. Pharmacol. (1992), **106**, 828–832 © Macmillan Press Ltd, 1992

Involvement of inflammatory mediators in the airway responses to trimellitic anhydride in sensitized guinea-pigs

*†James, P. Hayes, *Jan O. Lotvall, *Peter J. Barnes, †Anthony J. Newman Taylor & [1]*K. Fan Chung

*Department of Thoracic Medicine and †Department of Occupational & Environmental Medicine, National Heart and Lung Institute, Royal Brompton National Heart & Lung Hospital, London

1 We examined the effect of various pharmacological agents on the acute bronchoconstrictor response and airway microvascular leakage in a model of guinea-pig sensitization to trimellitic anhydride (TMA) a cause of low molecular weight occupational asthma in man.

2 Guinea-pigs were given intradermal injections of 0.1 ml of 0.3% TMA in corn oil; 21–28 days later, anaesthetized guinea-pigs were challenged with TMA conjugated to guinea-pig albumin by tracheal instillation. Changes in lung resistance were measured and airway microvascular leakage was quantified by measuring the extravasation of Evans blue dye into the airway tissue.

3 Sensitized guinea-pig ($n = 9$ in each group) were pretreated with chlorpheniramine (2.5 mg kg^{-1}, i.v.), WEB 2086 (10 $\mu g\ kg^{-1}$, i.v.), BW 4AC (50 mg kg^{-1}, i.p.), nedocromil sodium (2% aerosol for 60 s) or vehicle alone.

4 Pretreatment with chlorpheniramine inhibited both the acute bronchoconstrictor response and the increase in airway microvascular leakage. WEB 2086 and nedocromil sodium partially inhibited the bronchoconstrictor response but had no significant effect on airway microvascular leakage. BW 4AC caused a non-significant reduction of the bronchoconstrictor response and airway microvascular leakage.

5 These results indicate that both the bronchoconstrictor response and the airway microvascular response in this model of sensitization is mediated to a large extent by histamine. PAF but not 5-lipoxygenase products also partially mediates the bronchoconstrictor response but not the airway microvascular leakage. Nedocromil sodium partially inhibits the bronchoconstrictor response only.

Keywords: Trimellitic anhydride; occupational asthma; airway microvascular leakage; bronchoconstriction; histamine; platelet activating factor; leukotriene; nedocromil sodium

Introduction

Trimellitic anhydride (TMA), a reactive chemical widely used in industry as a curing agent for epoxy resins, may cause asthma in individuals exposed to it in the workplace (Fawcett *et al.*, 1977). Occupational asthma due to trimellitic anhydride has been associated with the development of a specific IgE antibody response (Venables, 1989). Inhalation challenge with TMA in sensitized individuals may induce an immediate, late or dual asthmatic response and an increase in airway responsiveness. Symptoms of asthma and increased bronchial responsiveness may persist in spite of avoidance of further exposure (Newman Taylor, 1987). The exact mechanisms of these responses remains unclear.

We have developed a model of occupational asthma due to TMA in the guinea-pig. An intradermal injection of TMA in guinea-pigs can induce a specific IgG1 and IgE antibody response to TMA conjugated to guinea-pig serum albumin (TMA-GPSA). We have also shown that exposure to free TMA dust in sensitized guinea-pigs is accompanied by an increase in airway reactivity and airway eosinophilia (Hayes *et al.*, 1990). Most recently we have shown that tracheal instillation of TMA-GPSA in sensitized guinea-pigs induces acute bronchoconstriction and an increase in airway microvascular leakage (Hayes *et al.*, 1991). In order to characterize further this guinea-pig model of sensitization, we have studied the involvement of various putative mediators of the acute response to TMA-GPSA and in particular histamine, platelet activating factor (PAF) and products of the 5-lipoxygenase pathway. In addition we have examined the effect of nedocromil sodium, a non steroidal anti-inflammatory agent used for the prophylaxis of asthma.

[1] Author for correspondence.

Methods

Sensitization

Female Dunkin-Hartley guinea-pigs, weighing 200–250 g, were injected intradermally with 0.1 ml of 0.3% of TMA in corn oil. Controls ($n = 9$) were injected with 0.1 ml of corn oil alone. All guinea-pigs were challenged intratracheally 21–28 days later with 50 µl TMA-GPSA, a protein conjugate of TMA prepared as described below.

Pretreatment protocols

Prior to challenge, sensitized guinea-pigs were divided into 5 groups ($n = 9$) and treated as indicated. Group 1: chlorpheniramine (2.5 mg kg^{-1}, i.v., 5 min before TMA-GPSA), an H_1 histamine receptor antagonist (Evans *et al.*, 1988a). Group 2: BW 4AC (N-(3-phenoxy-cinnamyl)-acetohydroxamic acid; 50 mg kg^{-1} in 10% Tween, i.p.; 1 h before challenge) a 5-lipoxygenase inhibitor (Payne *et al.*, 1988). Group 3: WEB 2086 (3-(4-(2-chlorophenyl)-9-methyl-6H-thieno (3,2-f) (1,2,4)triazolo- (4,3-a) (1,4)diazepin-2-yl)-1- (4-morpholinyl)-1-propanone); 10 $\mu g\ kg^{-1}$, i.v., 5 min before TMA-GPSA), a PAF receptor antagonist (Evans *et al.*, 1988b). Group 4: nedocromil sodium (60 breaths of 2% aerosolized solution via ultrasonic nebulizer, Model 2512; PulmonoSonic, DeVillbiss Co, PA, U.S.A.), an anti-inflammatory agent used for the treatment of asthma. Group 5 were injected with vehicle (10% Tween) 1 h before exposure and were also exposed to normal saline in the same manner as group 4.

Measurement of lung resistance

On days 21–28, guinea-pigs were anesthetized with pentobarbitone 60 mg ml^{-1}, intraperitoneally. A tracheal cannula (10 mm length and 2.7 mm internal diameter) was inserted into the lumen of the trachea through a tracheostomy. A polyethylene catheter was inserted into the left carotid artery to monitor blood pressure with a pressure transducer (PDCR 75 S/N 1572, Druck, U.K.). Transpulmonary pressure was measured with a pressure transducer (Model FCO 40; ± 1000 mmH_2O, Furness Controls Ltd, Bexhill, Sussex) with one side attached to a catheter inserted into the right pleural cavity and the other side attached to a catheter connected to a side port of the intra-tracheal cannula. The ventilatory circuit had a total volume of 20 ml. Airflow was measured with a pneumotachograph (Model F1L; Mercury Electronics Ltd., Glasgow) connected to a transducer (Model FCO 40; ± 20 mmH_2O: Furness Controls Ltd). The signals from the transducers were digitalized with a 12-bit analog-digital board (NB-MIO-16, National Instruments, Austin, TX, U.S.A.) connected to a Macintosh II computer (Apple Computer Inc., Cupertino, CA, U.S.A.) and analysed with a software (Labview National Instruments), which was programmed to calculate lung resistance (R_L) instantaneously by the method of von Neergaard & Wirz (1927). Transpulmonary pressure and mean blood pressure were also monitored throughout the experiment.

Measurement of airway microvascular leakage

Evans blue dye (20 mg ml^{-1}) was injected intravenously over 1 min. After another minute, 50 µl of 1% TMA-GPSA in saline was instilled into the trachea though a polyethylene cannula (internal diameter 0.9 mm) which was inserted into the trachea having passed through the length of the tracheal cannula. Lung resistance was monitored for 5 min after which the guinea-pigs were hyperinflated with twice the tidal volume and 60 s later the guinea-pigs were disconnected from the ventilator. The chest was opened and a cannula was inserted into the aorta through the left ventricle. This cannula was perfused with 0.9% NaCl at a pressure of 100–120 mmHg to eliminate dye from the bronchial circulation. After 90 s of perfusion, a second cannula was inserted into the pulmonary artery through the right ventricle and perfused with 20 ml of saline over 60 s to eliminate dye from the pulmonary circulation. The trachea and lungs were dissected out *en bloc*, the parenchyma carefully scraped off, and extraneous tissue removed. The trachea, major bronchi and intrapulmonary airways were then separated from each other, and the intrapulmonary airways were divided into two equal portions, arbitrarily named proximal (PIP) and distal (DIP). All tissues were weighed after having been freeze-dried for 36 h. Evans blue dye was extracted by placing each sample of tissue in 2 ml of formamide in a 40°C water bath overnight. Absorption at 620 nm was measured in a spectrophotometer (Model 8480, Philips, Cambridge, U.K.). Extravasated Evans blue dye was quantified by interpolation on a standard curve of dye concentrations in the range of 0.5–10 µg ml^{-1} and expressed as ng dye mg^{-1} tissue. Evans blue dye measurements have been shown to correlate highly with the extravasation of radiolabelled albumin into guinea-pig airways (Rogers *et al.*, 1989).

Preparation of trimellitic anhydride conjugate

TMA was conjugated to guinea-pig serum albumin (GPSA) as follows. Four aliquots of 250 mg GPSA (Sigma, Poole, Dorset) were mixed with 50 ml of 9% $NaHCO_3$ on ice and 250 mg of ground TMA (Aldrich, Gillingham, Kent) dust was added and allowed to stand for 10 min. Each aliquot was stirred separately for 1 h. The aliquots were pooled and spun for 10 min at 600 *g* (MSE Centaur 2). The supernatant was separated and dialysed with 0.02 M NH_4HCO_3 for 48 h with 6 changes. This was further dialysed with distilled water for 24 h and lyophilized. The degree of substitution was assessed by u.v. spectrophotometry. Briefly 1.0 mg TMA-GPSA was added to 1 ml of 0.1 M borate buffer at pH 9.3. A 0.03 M solution of 2,4,6,trinitrobenzenesulphonic acid (TNBS: Aldrich, Gillingham, Kent) in borate buffer was prepared. Then 25 µl of TNBS solution was added to 1 ml of the TMA-GPSA solution and incubated for 20 min at room temperature. The sample was read on the spectrophotometer at an optical density of 420 nm. The substitution ratio for TMA-GPSA was 21:1.

ELISA for assessment of IgG1 antibodies

Plates (Maxisorb F96, A/S Nunc, DK-4000 Roskilde, Denmark) were coated with 5 µg ml^{-1} TMA-GPSA in coating buffer and incubated overnight at 4°C. On the next day the plates were washed 4 times in PBS/Tween. Serum was diluted to 1:50 solution and plates were coated with PBS/Tween. Serum was added in doubling dilutions across the plate and incubated for 3 h at 27°C. The plates were again washed 4 times with PBS/Tween and 1:2500 of rabbit anti-guinea pig IgG1 (ICN Biomedicals Ltd, High Wycombe, Bucks) was added and incubated for 2 h at 27°C. Again the plates were washed with PBS/Tween. Anti-rabbit IgG-peroxidase (ICN Biomedicals Ltd, High Wycombe, Bucks) was added at 1:5000 dilution and incubated at 27°C for 2 h. Finally the plates were washed in PBS/Tween and chromogen was added. The reaction was stopped after 6 min with 1 M H_2SO_4 and read at an optical density of 492 nm.

Statistical analysis

Data are expressed as mean ± s.e.mean. To determine the effect of various treatments on the overall response of lung resistance, areas under the curves (AUC) were calculated over the 6 min period of R_L measurements. Kruskal-Wallis non-parametric analysis of variance was used to determine significant variance among the groups. Multiple Mann-Whitney U tests were used to compare significant differences between groups and the Bonferoni correction applied to take account of the multiple comparisons. A P value of less than 0.012 was considered significant.

Results

All guinea-pigs injected with 0.3% TMA developed IgG1 antibodies to TMA-GPSA (Figure 1). Intratracheal instillation of 50 µl of 1% TMA-GPSA induced a significant increase in lung resistance in sensitized untreated guinea-pigs (24.2 ± 6.7 cmH_2O ml^{-1}s^{-1}) compared to the control group (0.9 ± 0.2; $P<0.0005$). The response started within 30 s of instillation and reached a peak within 3 min (Figure 2). There was an overall difference in both the maximal increase in lung resistance and area under the curve over 6 min between the groups as analysed by Kruskal-Wallis test ($P<0.0001$, Figure 3). There was a significant decrease in peak lung resistance following challenge with TMA-GPSA in guinea-pigs treated with chlorpheniramine (2.8 ± 0.9 cmH_2O ml^{-1} s^{-1}; $P<0.005$), WEB 2086 (5.8 ± 1.3; $P<0.012$) and nedocromil sodium (5.5 ± 2.3; $P<0.01$) when compared to the sensitized untreated group. Although pretreatment with BW 4AC appeared to inhibit the maximal increase in lung resistance after TMA-GPSA (13.3 ± 2.2; $P<0.012$) compared to sensitized untreated guinea-pigs, this did not achieve statistical significance. Similar results were obtained for all these pharmacological agents when these were analysed in terms of area under the curve measurements (Figure 3b).

There was an overall difference between the groups in the degree of airway microvascular leakage found in the trachea ($P<0.0002$), main bronchi ($P<0.0003$), PIP ($P<0.005$) and DIP ($P<0.01$, Table 1). There was a significant difference

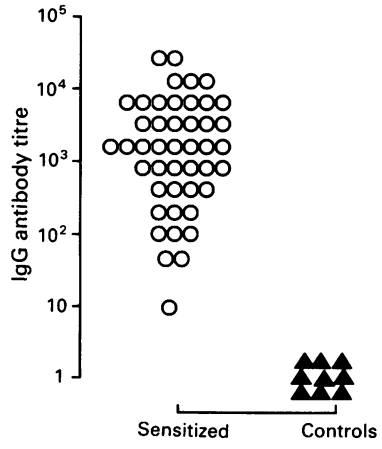

Figure 1 Individual IgG1 antibodies to trimellitic anhydride conjugated to guinea-pig serum albumin (TMA-GPSA) measured by ELISA (see text) in guinea-pigs injected intradermally with 0.3% TMA compared to control guinea-pigs injected with corn oil alone.

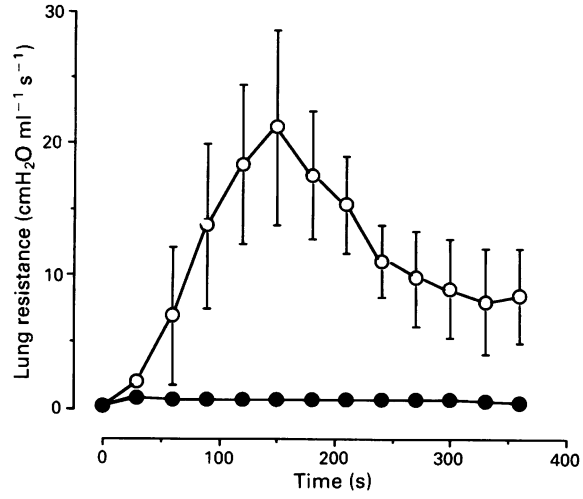

Figure 2 Time course of changes in lung resistance induced by tracheal instillation of 1% trimellitic anhydride conjugated to guinea-pig serum albumin (TMA-GPSA) in sensitized untreated (○) and control (●) guinea-pigs. Data are expressed as mean with s.e.mean shown by vertical bars.

between the degree of airway microvascular leakage found in sensitized untreated guinea-pigs compared to control guinea-pigs at all levels of the airways examined ($P<0.0005$). Similarly, pretreatment with chlorpheniramine in sensitized guinea-pigs significantly inhibited airway microvascular leakage compared with the sensitized untreated group at all levels of the bronchial tree ($P<0.005$). Pretreatment with WEB 2086, BWA4C or nedocromil sodium had no significant effect on airway microvascular leakage found at any level of the tracheo bronchial tree ($P<0.012$).

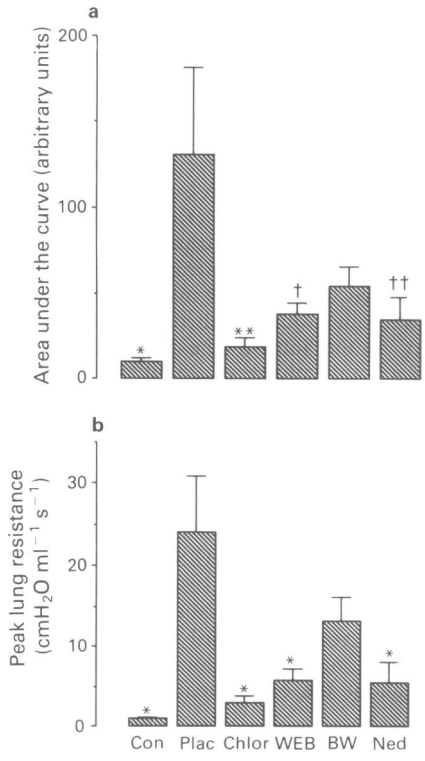

Figure 3 Maximal and total (area under the curve) changes in lung resistance after tracheal instillation of 1% trimellitic anhydride conjugated to guinea-pig serum albumin (TMA-GPSA, 50 µl) in sensitized animals pretreated with chlorpheniramine (Chlor), WEB 2086 (WEB), BW 4AC (BW) and nedocromil sodium (Ned) compared to sensitized untreated guinea-pigs (Plac) and guinea-pigs injected with corn oil alone (Con). Data are expressed as mean with s.e.mean shown by vertical bars.
*$P<0.0005$; **$P<0.005$; †$P<0.012$; ††$P<0.012$.

Table 1 Effect of pharmacological agents on airway microvascular leakage induced by trimellitic anhydride conjugated to guinea-pig serum albumin (TMA-GPSA) in guinea-pigs sensitized with TMA

	Evans blue dye (ng mg^{-1} tissue)			
	Trachea	*Bronchi*	*PIP*	*DIP*
Untreated	134 ± 21	143 ± 23	126 ± 22	107 ± 17
Chlorpheniramine	49 ± 6‡	55 ± 9‡	48 ± 8‡	47 ± 9‡
WEB 2086	89 ± 19	94 ± 18	75 ± 12	74 ± 9
BW A4C	102 ± 20	105 ± 17	89 ± 12	77 ± 11
Nedocromil	80 ± 18	86 ± 23	86 ± 22	85 ± 22
Controls*	34 ± 4†	33 ± 4†	39 ± 5†	42 ± 7†

PIP = proximal intrapulmonary airways; DIP = distal intrapulmonary airways.
†$P<0.0005$; ‡$P<0.005$ compared to corresponding tissue in the sensitized untreated group.
*Controls were unsensitized guinea-pigs given i.p. injections of vehicle and inhaled saline before tracheal instillation of TMA-GPSA.

Discussion

We have found that airway responses induced by instillation of TMA-GPSA in guinea-pigs sensitized with intradermal injections of unconjugated TMA in corn oil can be in part inhibited by pretreatment with chlorpheniramine (a histamine H_1 receptor antagonist), WEB 2086 (a PAF antagonist) and nedocromil sodium which can inhibit inflammatory cell activation. This response was reduced by pretreatment with BWA4C, a lipoxygenase inhibitor but this did not reach statistical significance. We have also found that pretreatment with chlorpheniramine inhibits airway microvascular leakage induced by TMA-GPSA at all levels of the bronchial tree but that pretreatment with WEB 2086, BWA4C and nedocromil sodium has no significant effect. All guinea-pigs given intradermal injections of TMA developed IgG1 antibodies to TMA-GPSA.

Occupational asthma due to low molecular chemicals such as the acid anhydrides accounts for 10% of all adult asthma and is of interest as symptoms of asthma and bronchial hyperresponsiveness may persist in spite of avoidance of further exposure to the causative agent. It differs from allergic asthma in that non-atopic workers have the same risk of developing symptoms of asthma as atopic workers (Chang-Yeung & Lam, 1986). An animal model may be of value in elucidating the underlying mechanisms of these responses to low molecular weight chemicals. Previous studies have demonstrated that sensitization with TMA is associated with specific IgG1 antibodies and IgE antibodies in a number of species (Dearman & Botham, 1990). We have previously described airway responses and airway microvascular leakage to intratracheally administered TMA-GPSA in guinea-pigs sensitized with TMA (Hayes *et al.*, 1991). We have also demonstrated that this occurs in the post-capillary venules. In this study we did not instill TMa dust into the airways because of the difficulty of ensuring distribution throughout the airway. Also we have previously shown that the antibody response to the TMA-GPSA is directed against the protein conjugate as has been previously demonstrated in man (Topping *et al.*, 1986) and therefore it would seem more appropriate to examine the effect of TMA-GPSA on airway responses. The TMA-GPSA was instilled into the trachea as it does not nebulize well with an ultrasonic nebulizer.

As in previous studies of ovalbumin-sensitized guinea-pigs, we found that both the increase in lung resistance and airway microvascular leakage was effectively inhibited by a histamine H_1 receptor antagonist (Woodward *et al.*, 1983). In another study, pretreatment with chlorpheniramine significantly inhibited airway microvascular leakage in the trachea and main bronchi in ovalbumin-sensitized guinea-pigs challenged with intravenous antigen (Evans *et al.*, 1988a). In the present study, pretreatment with chlorpheniramine almost completely inhibited leakage throughout the trancheobronchial tree. Other workers have found a similar effect of histamine on airway microvascular leakage in the trachea in ovalbumin-sensitized guinea-pigs (Saria *et al.*, 1983). WEB 2086, a highly potent PAF antagonist, inhibited in part the increase in lung resistance but had no effect on airway microvascular leakage following challenge with TMA-GPSA. This is in keeping with previous studies where PAF has been demonstrated to have a role in bronchoconstriction induced by antigen challenge in ovalbumin-sensitized guinea-pigs (Casals-Stenzel, 1987) and other studies which demonstrated that PAF antagonists did not affect the increase in airway microvascular leakage after antigen challenge (Evans *et al.*, 1988b). It is unlikely that the bronchoconstrictor effects of PAF are mediated by histamine release in the guinea-pig (Vargaftig *et al.*, 1982).

The 5-lipoxygenase inhibitor, BW 4AC, had no significant effect on the bronchoconstrictor and airway microvascular leakage induced by tracheal instillation of TMA-GPSA. At the doses used, the compound has been shown to be an effective 5-lipoxygenase inhibitor *in vivo* in the guinea-pig. A greater inhibitory effect against ovalbumin-induced bronchoconstriction in sensitized guinea-pigs was observed with a combination of BW 4AC with an antihistamine than with the antihistamine alone (Payne *et al.*, 1988). Similarly, in sensitized guinea-pigs pretreated with antihistamines, allergen-induced bronchoconstriction was found to be partly mediated by sulphidopeptide leukotrienes (Kreutner *et al.*, 1989). Although Woodward *et al.* (1983) did not find any inhibitory effect of FPL 55712, a leukotriene receptor antagonist, against airway microvascular leakage in the guinea-pig, the 5-lipoxygenase inhibitor A-63162 has recently been shown to inhibit both the bronchoconstrictor and airway microvascular leakage induced by ovalbumin aerosol in the guinea-pig (Hui *et al.*, 1991). Thus, our guinea-pigs sensitized to TMA may show a different profile of mediator release when challenged with TMA-GPSA compared to ovalbumin. However, in both models histamine release appears to be the predominant contributor to the airway responses.

Nedocromil sodium, a pyranoquinoline dicarboxylic acid, has been shown to inhibit significantly the release of histamine, leukotriene C_4 and prostaglandin D_2 from bronchoalveolar mast cells obtained from sensitized monkeys challenged with antigen (Eady *et al.*, 1985). We found that nedocromil sodium partially inhibited the bronchoconstrictor response to challenge with TMA-GPSA, with some effect on airway microvascular leakage which did not achieve statistical significance. In a previous study of ovalbumin-sensitized guinea-pigs (Evans *et al.*, 1988a), the extravasation of Evans blue dye induced by intravenously administered ovalbumin was significantly inhibited by nedocromil sodium administered intravenously. It is possible that the intravenous route of administration may have resulted in an effectively higher concentration being achieved in the airway. In our study, nedocromil sodium at the dose used was more effective at inhibiting the increase in lung resistance than in preventing the airway microvascular leakage, as also seen with the airway responses to the PAF antagonist, WEB 2086 and to the 5-lipoxygenase inhibitor, BW 4AC. This effect may result from inhibition of mediator release from inflammatory cells.

In conclusion, in guinea-pigs sensitized to TMA, TMA-GPSA challenge induces bronchoconstrictor and airway microvascular leakage which are predominantly mediated by histamine release. PAF rather than the 5-lipoxyygenase products may be involved in the increase in lung resistance. It appears that the induction of airway microvascular leakage is less inhibitable than the increase in lung resistance. Whether important interactions between the mediators released during TMA-GPSA challenge occur is not known but can be tested in our guinea-pig model.

We are grateful to Boehinger Ingleheim (Germany), Fisons (U.K.) and Wellcome Laboratories (U.K.) for providing WEB 2086, nedocromil sodium and BW 4AC respectively.

References

CASALS-STENZEL, J. (1987). Effects of WEB 2086, a novel antagonist of platelet activating factor, in active and passive anaphylaxis. *Immunopharmacol.*, **13**, 7–24.

CHAN-YEUNG, M. & LAM, S. (1986). Occupational asthma. *Am. Rev. Respir. Dis.*, **133**, 686–703.

DEARMAN, R.J. & BOTHAM, P.A. (1990). Inhalation exposure to respiratory sensitising chemicals down-regulate guinea pig IgE and pulmonary responses. *Int. Arch. Allergy Appl. Immunol.*, **92**, 425–432.

EADY, R.P., GREENWOOD, B., JACKSON, D.M., ORR, T.S.C. & WELLS, E. (1985). The effect of nedocromil sodium and sodium chromoglycate on antigen-induced bronchoconstriction in the Ascaris-sensitive monkey. *Br. J. Pharmacol.*, **85**, 323–325.

EVANS, T.W., ROGERS, D.F., AURSUDKIJ, B., CHUNG, K.F. & BARNES, P.J. (1988a). Inflammatory mediators involved in antigen-induced airway microvascular leakage in guinea pigs. *Am. Rev. Respir. Dis.*, **138**, 395–399.

EVANS, T.W., DENT, G., ROGERS, D.F., AURSUDKIJ, B., CHUNG, K.F. & BARNES, P.J. (1988b). Effect of a PAF antagonist, WEB 2086, on airway microvascular leakage in the guinea-pig and platelet aggregation in man. *Br. J. Pharmacol.*, **94**, 164–168.

FAWCETT, I.W., NEWMAN TAYLOR, A.J. & PEPYS, J. (1977). Asthma due to inhaled chemical agents-epoxy resins systems containing phthalic acid anhydride, trimellitic acid anhydride. *Clin. Allergy*, **7**, 1–14.

HAYES, J.P., DANIEL, R., TEE, R.D., BARNES, P.J., NEWMAN TAYLOR, A.J. & CHUNG, K.F. (1990). The effect of free trimellitic anhydride dust on airway responses in guinea pigs sensitised to the free hapten. *Eur. Resp. J.*, **3** (Suppl 10), 340S.

HAYES, J.P., LOTVALL, J.O., DANIEL, R., BARNES, P.J., NEWMAN TAYLOR, A.J. & CHUNG, K.F. (1991). Airway microvascular leakage to a protein conjugate of trimellitic anhydride in guinea pigs sensitised to the free hapten. *Am. Rev. Respir. Dis.*, **3**, 111s.

HUI, K.P., LOTVALL, J.O., CHUNG, K.F. & BARNES, P.J. (1991). Attenuation of allergen induced airflow obstruction and airway microvascular leakage in actively sensitised guinea pigs by 5-lipoxygenase inhibition (A-63162). *Am. Rev. Respir. Dis.*, **143**, 1015–1019.

KREUTNER, W., SHERWOOD, J. & RIZZO, C. (1989). The effect of leukotriene antagonists, lipoxygenase inhibitors and selected standards on leukotriene-mediated allergic bronchospasm in guinea pigs. *Agents Actions*, **28**, 173–183.

NEWMAN TAYLOR, A.J., VENABLES, K.M., DURHAM, S.R., GRANEEK, B.J. & TOPPING, M.D. (1987). Acid anhydrides and asthma. *Int. Arch. Allergy Clin. Immunol.*, **82**, 435–439.

PAYNE, A.N., GARLAND, L.G., LEES, I.W. & SALMON, J.A. (1988). Selective inhibition of arachnidonate 5-lipoxygenase by novel acetohydroxamic acids: effects of bronchial anaphylaxis in anaesthetised guinea-pigs. *Br. J. Pharmacol.*, **94**, 540–546.

ROGERS, D.F., BOSCHETTO, P. & BARNES, P.J. (1989). Plasma exudation correlation between Evans Blue dye and radiolabelled albumin in guinea pig airways *in vivo*. *J. Pharmacol. Methods*, **21**, 309–313.

SARIA, A., LUNDBERG, J.M., SKOFITISCH, G. & LEMBECK, F. (1983). Vascular protein leakage in various tissues is induced by substance P, capsaicin, bradykinin, serotonin, histamine and by antigen challenge. *Arch. Pharmacol.*, **324**, 212–218.

TOPPING, M.D., VENABLES, K.M., LUCZYNSKA, C.M., HOWE, W. & NEWMAN TAYLOR, A.J. (1986). Specificity of the human IgE response to inhaled acid anhydrides. *J. Allergy Clin. Immunol.*, **77**, 834–842.

VARGAFTIG, B.B., LEFORT, J., WAL, F., CHIGNARD, M. & MEDEIROS, M.C. (1982). Interference of non-steroidal non-inflammatory drugs associated with anti-histamine and anti-serotonin agents on the bronchial and platelet effects of "platelet-activating factor" (PAF-acether). *Eur. J. Pharmacol.*, **82**, 121–130.

VENABLES, K.M. (1989). Low molecular weighy chemicals, hypersensitivity, and direct toxicity: the acid anhydrides. *Br. J. Ind. Med.*, **46**, 222–232.

VON NEERGAARD, K. & WIRZ, K. (1927). Die Messung der Stromungswiderstande in den Atemwegen des Menschen: inbesondere bei Asthma und Emphysem. *Z. Klin. Med.*, **105**, 51–82.

WOODWARD, D.F., WASSERMAN, M.A. & WEICHMANN, B.M. (1983). Investigation of leukotriene involvement in the vasopermeability response associated with guinea pig tracheal anaphylaxis: comparison with cutaneous anaphylaxis. *Eur. J. Pharmacol.*, **93**, 9–19.

(Received December 6, 1991
Revised March 23, 1992
Accepted March 26, 1992)

Br. J. Pharmacol. (1992), **106**, 833–837 © Macmillan Press Ltd, 1992

Ca^{2+}-stores mobilization by diadenosine tetraphosphate, Ap_4A, through a putative P_{2Y} purinoceptor in adrenal chromaffin cells

[1]E. Castro, J. Pintor & M.T. Miras-Portugal

Departamento de Bioquímica, Facultad de Veterinaria, Universidad Complutense de Madrid, 28040 Madrid, España

1 Diadenosine tetraphosphate (Ap_4A) evoked a concentration-dependent increase in cytosolic [Ca^{2+}] in resting chromaffin cells. The EC_{50} value for this action was 28.2 ± 6.6 μM. This effect was also produced by diadenosine pentaphosphate (Ap_5A) with an EC_{50} of 50 ± 7 μM.

2 In contrast with this effect, pretreatment with Ap_4A or Ap_5A induced a 30% reduction in Ca^{2+} entry following 10 μM dimethylphenylpiperazinium.

3 The elevation in cytosolic [Ca^{2+}] induced by Ap_4A was persistent in $\approx$100 nM external [Ca^{2+}] and was sensitive to depletion of internal Ca^{2+} stores by a bradykinin prepulse or whole cell depletion in Ca^{2+}.

4 The effect of Ap_4A was mimicked and desensitized by the agonist adenosine 5'-O-(2-thiodiphosphate), and blocked by the P_{2Y}-receptor antagonist, cibachrome blue. The P_{2X}-receptor agonist α,β-methylene adenosine 5'-triphosphate was inactive both by itself or in combination with Ap_4A. This is compatible with a P_{2Y}-purinoceptor-mediated action.

Keywords: Cytosolic calcium; diadenosine polyphosphates; bradykinin; purinoceptors

Introduction

Diadenosine polyphosphates are a novel class of compounds with emerging extracellular actions being added to their known intracellular role. Diadenosine tetraphosphate (adenosine (5')tetraphospho (5') adenosine, Ap_4A), the major representative of this type of nucleotides, is found in eukaryotic cells at micromolar concentrations (Zamecnik, 1983; Coste *et al.*, 1987), fluctuating with the cellular growth rate (MacLennan & Prescott, 1984). The localization of Ap_4A is mainly nuclear (Weinmann-Dorsch & Grummt, 1986) inside the cells. Ap_4A has been implicated in the initiation of DNA replication (Weinmann-Dorsch *et al.*, 1984) through its binding to DNA polymerase α (Rapaport *et al.*, 1981) and in the processing of ADP-ribosylated histones (Surowy & Berger, 1983). So, this metabolite is now considered as a delayed intracellular messenger molecule involved in the regulation of the eukaryotic cell cycle (Baril *et al.*, 1983; Grummt, 1988) and in the response to cellular stress (Baker & Jacobson, 1986; Coste *et al.*, 1987).

Besides this role as a nuclear signal, diadenosine polyphosphates can also be found at high concentrations in the secretory granules of platelets (Flodgaard & Klenow, 1982; Lüthje & Ogilvie, 1983) and adrenal chromaffin cells (Rodriguez del Castillo *et al.*, 1988), co-stored with ATP and 5-hydroxytryptamine or catecholamines respectively. These compounds are exocytotically released to the extracellular medium during platelet aggregation (Lüthje & Ogilvie, 1983) and chromaffin cells catecholamine secretion stimulation (Pintor *et al.*, 1991a). Acting from the extracellular side, diadenosine polyphosphates have been found to be active in the platelet aggregation process (Lüthje *et al.*, 1985) both inhibiting (Harrison *et al.*, 1975) and promoting it (Lüthje & Ogilvie, 1984); they are also known to have vasomotor properties in peripheral arteries (Busse *et al.*, 1988), and to modulate catecholamine release from chromaffin cells (Castro *et al.*, 1990).

Recently we have described high affinity binding sites for [^{3}H]-Ap_4A in chromaffin cells membranes (Pintor *et al.*, 1991b) showing a putative P_{2Y}-purinoceptor pharmacological profile according to the currently accepted classification of purinoceptors (Burnstock & Kennedy, 1985). Little is known about purinoceptors in chromaffin cells. In other tissues P_{2Y} receptors are linked to phospholipase C (Forsberg *et al.*, 1987; Boyer *et al.*, 1989). In chromaffin cells ATP is known to induce inositol phosphates mobilization and release of intracellular Ca^{2+} stores (Sasakawa *et al.*, 1989). Here we examine the action of Ap_4A on cytosolic Ap_4A in chromaffin cells to discover the mechanism of diadenosine polyposphate modulation of catecholamine release and to characterize further Ap_4A receptors in these cells.

[1] Author for correspondence.

Methods

Preparation of chromaffin cells

The chromaffin cells were obained after digestion of adrenal glands with collagenase in retrograde perfusion as described by Miras-Portugal *et al.* (1985). Briefly, glands supplied by a local slaughterhouse were trimmed of fat, cannulated through the adrenal vein and washed with Ca^{2+}/Mg^{2+}-free saline containing (in mM) NaCl 154, KCl 5.6, $NaHCO_3$ 3.6, glucose 5.6 and HEPES 5.0, buffered at pH 7.4. Digestion was performed with a 0.2% collagenase plus 0.5% bovine serum albumin (BSA) solution in the above medium. After digestion glands were cut, soft medullae were removed, minced and dispersed cells filtered through a nylon mesh. Cells were purified by buoyant sedimentation in a Percoll gradient to greater than 95% chromaffin cells as assayed by neutral red staining. Purified cells were maintained in suspension cultures, dispersed in Dulbecco's Modified Eagle's Medium (DMEM) containing 10% foetal calf serum and standard antibiotics, with continuous stirring. Cells were used on 4th–6th culture day. Anchorage dependent cells do not grow, but gradually die, in these culture conditions.

Measurement of cytosolic [Ca^{2+}]

Cytosolic Ca^{2+} concentration was determined with the fluorescent indicator fura-2. The cells were dispersed in a Locke solution containing (in mM). NaCl 140, KCl 4.4, $CaCl_2$ 2.5, $MgSO_4$ 1.2, KH_2PO_4 1.2, glucose 5.5 and HEPES 10, pH 7.4. Cells were loaded with 2.5 μM fura-2 AM for

45 min and washed by centrifugation. The recordings were performed in 1 ml sample containing 10^6 cells in thermostated and stirred cuvettes, in a Perkin-Elmer LS-50 fluorimeter. The probe was excited at 340 nm and fluorescence read at 510 nm. At the end of each experiment the cells were lysed in 0.4% Triton X-100 and the dye content calibrated from measurements at 2.5 mM Ca^{2+} and 7.5 mM EGTA/45 mM Tris ($[Ca^{2+}] < 0.2$ nM). The cytosolic Ca^{2+} concentration ($[Ca^{2+}]_i$) was derived from fluorescence traces with the equation of Grynkiewicz *et al.* (1985). Additions to the cuvette were made with Hamilton syringes from at least 100 fold concentrated stock solutions, to avoid large volume variations.

Data expression and analysis

All data were interfaced to a computer to allow off-line analysis and record average. Data are presented as averaged traces of usually 3 records. Numerical values are presented as mean ± s.e.mean. Difference between averaged records were within noise range. Experiments with identical results were obtained in different batches of cells.

The EC_{50} ± s.e.mean estimates were derived from a logistic fit to the concentration-response curves. Six concentrations were used in the range from 1 to 300 μM, in triplicate. For 10 and 100 μM points, pooled data from nine different experiments were used. The fit was performed with a computer programme written by one of us (E.C.). This programme uses the Newton-Gauss-Mardquadt algorithm for least-squares fitting. Weighting proportional to experimental variance was introduced.

Materials

Inorganic salts were from Merk (F.R.G.). Ap_4A, Ap_5A (adenosine (5') pentaphospho (5') adenosine) and collagenase (EC 3.4.24.3) were from Boehringer (Mannheim, Germany). Adenosine 5'-O-(2-thiodiphosphate) (ADPβS), α,β-methylene adenosine-5'-triphosphate (α,β-MeATP) and dimethylphenylpiperazinium (DMPP) were from Sigma (Saint Louis, U.S.A.). Percoll is a registered mark of Pharmacia (Upsala, Sweden). Culture products and media were from Flow (Irvine, U.K.). Fura-2 was from Molecular Probes (Eugene, U.S.A.).

Results

Ap_4A and Ap_5A actions on resting and stimulated $[Ca^{2+}]_i$

The resting cytosolic $[Ca^{2+}]_i$ in chromaffin cells was found to be consistently low, usually in the 25–75 nM range (average 34 ± 5 nM). Challenging chromaffin cells with Ap_4A induced a rapid and transient rise in the cytosolic Ca^{2+} level, as shown in Figure 1a. The rise in $[Ca^{2+}]_i$ induced by Ap_4A was small, amounting to 80 ± 9 nM as a maximal effect. The action was dependent on the concentration of the agonist, with an EC_{50} of 28.2 ± 6.6 μM. Ap_5A was also active in increasing $[Ca^{2+}]_i$ levels, although somewhat less potent that Ap_4A, with an EC_{50} of 50 ± 7 μM.

In contrast, Ap_4A slightly reduced the Ca^{2+} peak evoked by the nicotinic agonist DMPP (Figure 2). The effect was small, a 30.5 ± 7.5% inhibition, but statistically significantly when tested in paired form within each experiment. A similar result was obtained with Ap_5A (not shown).

Source of Ca^{2+} during Ap_4A-induced $[Ca^{2+}]_i$ elevation

The $[Ca^{2+}]_i$ increasing effect of Ap_4A was not abolished by the absence of a Ca^{2+} gradient across the membrane. The response was present when extracellular $[Ca^{2+}]$ was buffered at ≈100 nM with a mixture of Ca/EGTA as employed in Figure 3. This fact suggests that $[Ca^{2+}]_i$ rise by Ap_4A was due

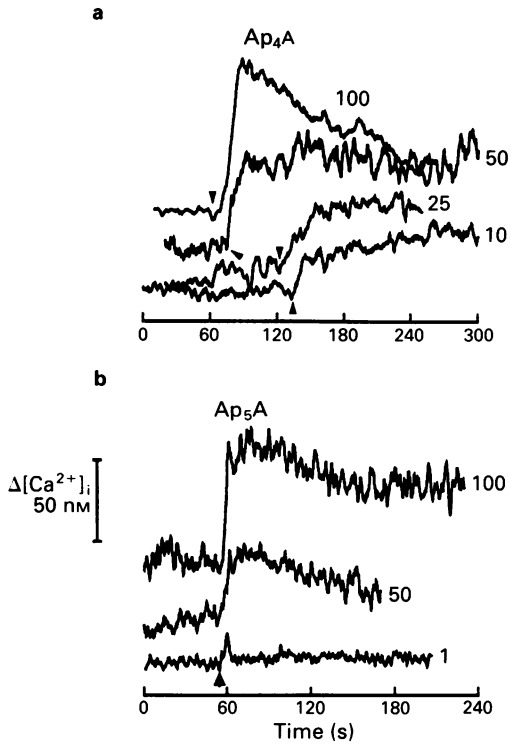

Figure 1 Elevation of cytosolic $[Ca^{2+}]$ by diadenosine tetraphosphate (Ap_4A) (a) and diadenosine pentaphosphate (Ap_5A) (b). At the time marked by the arrows Ap_4A or Ap_5A were added to the final concentration indicated (in μM).

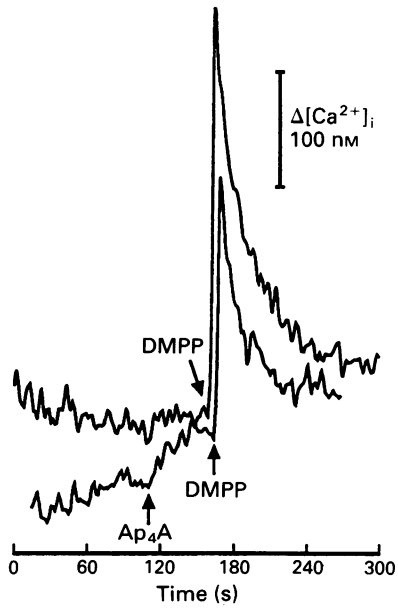

Figure 2 Reduction of 10 μM dimethylphenylpiperazinium (DMPP)-evoked Ca^{2+} entry by diadenosine tetraphosphate (Ap_4A) 100 μM. Peaks correspond to successive cuvettes.

to Ca^{2+} release from internal stores. To test this possibility further we tried to deplete these stores in two different ways. First, previous stimulation of the chromaffin cells with bradykinin severely compromises their ability to respond to Ap_4A (Figure 4). In contrast, Ap_4A stimulation had only a little effect on the response to bradykinin challenge. As a second strategy, the internal stores were emptied by incubating the cells for 45 min in a medium containing only ≈100 nM free $[Ca^{2+}]$ plus 10 mM caffeine to promote depletion by pump-

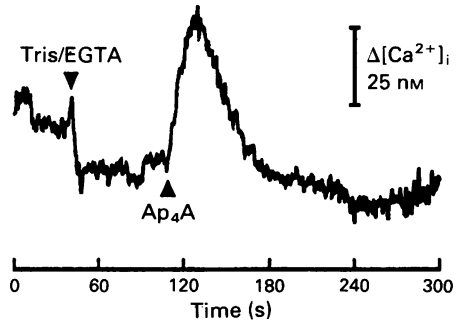

Figure 3 Response to diadenosine tetraphosphate (Ap_4A) in a nominal 100 nM $[Ca^{2+}]$ medium. $[Ca^{2+}]$ was buffered with a mixture of Ca/EGTA/Tris, $[EGTA]_t = 5$ mM. Ap_4A was 100 μM.

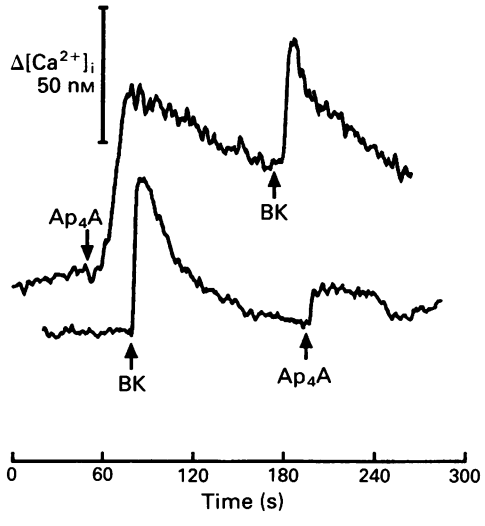

Figure 4 Response to diadenosine tetraphosphate (Ap_4A) after depletion of Ca^{2+}-stores. Inhibition of Ap_4A (100 μM) effect by a previous stimulation with 25 μM bradykinin (BK) and *vice versa*. Cells were incubated in normal medium including 2.5 mM Ca^{2+}.

ing out internal Ca^{2+} (Liu *et al.*, 1989). This treatment completely abolished the response to Ap_4A and profoundly diminished the effect of bradykinin, as shown in Figure 5. The reintroduction of Ca^{2+} to the medium restored the ability of the cells to respond to Ap_4A.

Interaction with P_2 purinoceptor drugs

The pharmacological identification of the Ap_4A receptor was assessed in the experiments summarized in Figure 6. Cibachrome Blue has been used as a selective P_{2Y}-receptor antagonist at moderate concentrations (Houston *et al.*, 1987). This agent completely and specifically blocked the Ca^{2+} rise induced by Ap_4A but not bradykinin. Furthermore, ADPβS is a potent P_{2Y}-receptor agonist which can induce receptor desensitization (Boyer *et al.*, 1989; Nanoff *et al.*, 1990). Figure 6 shows that ADPβS is a good agonist inducing $[Ca^{2+}]_i$ increase and that in the continuous presence of 100 μM ADPβS, the Ap_4A effect was lost, although a bradykinin-sensitive pool of Ca^{2+} was still present. In contrast, the selective P_{2X} agonist α,β-MeATP (Burnstock & Kennedy, 1985) produced only a minimal, possibly marginal, increase in $[Ca^{2+}]_i$, and failed to prevent the subsequent action of Ap_4A.

Discussion

In the present work we show how Ap_4A and Ap_5A stimulation of diadenosine polyphosphate receptors in chromaffin

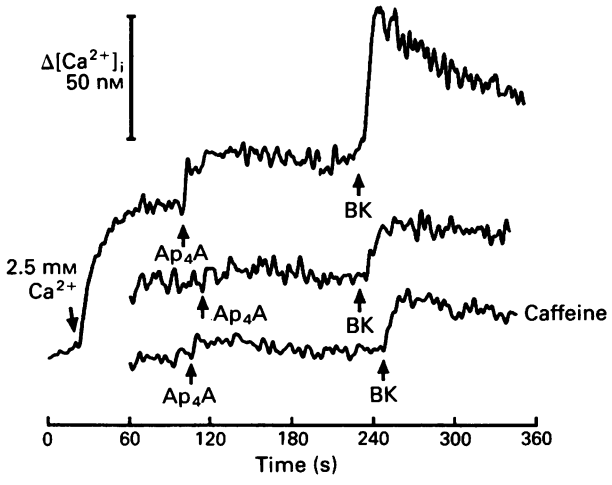

Figure 5 Response to diadenosine tetraphosphate (Ap_4A) after depletion of Ca^{2+}-stores. Depletion of Ca^{2+} from cells after incubation in 100 nM $[Ca^{2+}]_0$ plus 10 mM caffeine medium for 45 min. Lower trace, cells assayed with caffeine in the medium; middle trace, cells washed and resuspended for assay in the same medium without caffeine; upper trace, reintroduction of Ca^{2+} to a 2.5 mM final concentration. Ap_4A 100 μM, BK, bradykinin 25 μM.

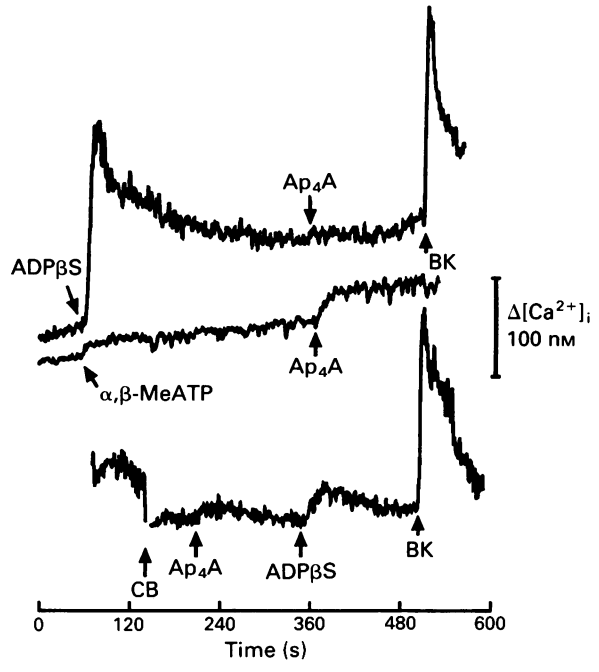

Figure 6 Pharmacology of diadenosine tetraphosphate (Ap_4A) effect. Upper trace, adenosine 5′-O-(2-thiodiphosphate) (ADPβS 100 μM) mimics and prevents the subsequent action of Ap_4A (100 μM) but not bradykinin (BK, 25 μM). Middle trace, α,β-methylene adenosine-5′-triphosphate (α,β-MeATP, 100 μM) shows a marginal action on $[Ca^{2+}]$ and does not prevent the Ap_4A (50 μM) effect. Lower trace, cibachrome blue (CB, 50 μM) effectively antagonizes the effects of Ap_4A (100 μM) and ADPβS (100 μM), without a major effect on the bradykinin (25 μM) peak. Drop produced by cibachrome blue is due to autoabsorption by the coloured dye, this effect was corrected in the calibration of $[Ca^{2+}]$.

cells is coupled to modulation of Ca^{2+}-signalling in these cells in a way parallel to diadenosine polyphosphate modulation of catecholamine release. The EC_{50} value for elevation of $[Ca^{2+}]_i$ is similar to that found for the action of diadenosine polyphosphates on catecholamine secretion and the potency order $Ap_4A > Ap_5A$ is the same (Castro *et al.*, 1990). This EC_{50} value is within an order of magnitude of the EC_{50} for

ATP stimulation of phosphoinositide turnover and Ca^{2+} mobilization (Sasakawa *et al.*, 1989). It is important to appreciate that the lifetime of nucleotides in the extracellular medium of the adrenal medulla may be very much shortened by the ectonucleotidase activity of chromaffin cells (Torres *et al.*, 1990). The ecto-phosphodiesterase (Ap_4Aase) activity present in the plasma membranes of these cells is three orders of magnitude lower than ecto-ATPase activity (Miras-Portugal *et al.*, 1990), so the lifetime of Ap_4A and Ap_5A will probably be much longer than that of ATP. This relative resistance of Ap_4A to ectonucleotidases present in chromaffin cells suggests that, after co-release with ATP (at approximately 1:10 dinucleotides:ATP ratio), Ap_4A-mediated effects become predominant with time and distance from release sites.

The source of Ca for the Ap_4A-induced increase in $[Ca^{2+}]_i$ seems to be the release of intracellularly stored Ca^{2+}, rather than Ca^{2+} entry through plasma membrane. This conclusion is supported by our findings that the Ca^{2+} signal remained in a low Ca^{2+} medium, when there is not a Ca^{2+} gradient across the membrane and so Ca^{2+} flux is negligible, and the sensitivity of this signal to store depletion. In addition to this, there is still a component of the response which is dependent on extracellular Ca^{2+}, as revealed by the smaller size and width of $[Ca^{2+}]_i$ peak of Figure 3 as compared with Figure 1 or 4. This component probably represents the replenishment of internal Ca^{2+} stores by extracellular Ca^{2+} entry. This same phenomenon has been observed in other tissues, although the precise pathway for this Ca^{2+} entry is not clear (Putney, 1987). However, this pathway is different from voltage-dependent Ca^{2+}-channels, since these are tightly coupled to secretion in chromaffin cells, while Ca^{2+} peaks induced by Ap_4A are not accompanied by corresponding secretory responses.

Diadenosine polyphosphates have only very small effects on basal catecholamine release (Castro *et al.*, 1990), which correlates perfectly with the size and origin of the Ap_4A-induced Ca^{2+} peak. A similar failure of intracellularly released Ca^{2+} to evoke catecholamine secretion has been described for bradykinin, angiotensin II, muscarinic agonists and nucleotides (O'Sullivan & Burgoyne, 1989; Cheek *et al.*, 1989b; Kim & Westhead, 1989). This fact is due to the spatial organization of the secretory machinery, which require $[Ca^{2+}]_i$ elevation just beneath the plasma membrane (i.e. Ca^{2+} flux through Ca^{2+} channels is fully active), while the release of intracellular Ca^{2+} takes place deep in the cytoplasm and becomes diluted (i.e. inactive) at secretory sites (Cheek *et al.*, 1989a,b). In contrast, Ap_4A slightly reduced the Ca^{2+} peak evoked by the nicotinic agonist DMPP, largely due to extracellular Ca^{2+} entry, which explains the small inhibitory action of diadenosine polyphosphates on nicotine-evoked catecholamine secretion (Castro *et al.*, 1990). The mechanism underlying this reduction, whether a direct modulation of Ca^{2+} channels, a modulation by cytosolic Ca^{2+}, or the activation of K^+ channels remains to be investigated.

The messenger linking receptor activation and Ca^{2+} release from intracellular stores is accepted as usually inositol (1,4,5)trisphosphate (IP_3) (Berridge, 1987). P_{2Y} receptors have been shown to be coupled to PLC/IP_3 pathway in vascular cells (Boyer *et al.*, 1989; Forsberg *et al.*, 1987). The [^{3}H]-Ap_4A binding site found previously in chromaffin cells showed a P_{2Y} displacing profile (Pintor *et al.*, 1990a). Therefore, our results are consistent with the view that Ap_4A exerts its effects through P_{2Y} purinoceptors, coupled to IP_3 formation, leading to release of intracellular Ca^{2+}, a mechanism which is common to other IP_3 generating agonists such as bradykinin (Challiss *et al.*, 1991). This functional assignment is reinforced by the pharmacological data. Although cibachrome blue is not an ideal antagonist, the reduction of Ap_4A and ADPβS responses selectively with respect to bradykinin, and the almost lack of Ca^{2+} response to α,β-Me-ATP, argue against a P_{2X}-purinoceptor as the site of action of Ap_4A.

However, the amplitude, kinetics, and sensitivity to acute or prolonged Ca^{2+}-depletion of Ap_4A and bradykinin were different. This probably reflects the complexity of the Ca^{2+} signalling pathway in chromaffin cells, which is more than a single messenger acting in a single target Ca^{2+} store. There are multiple intracellular Ca^{2+} pools in chromaffin cells, some sensitive to IP_3 and others responding to other (unknown) messengers. The non-IP_3-sensitive pools can be released experimentally by caffeine. These different Ca^{2+} pools are not completely separate, but are probably intercommunicated. We have had to include caffeine in order to abolish completely the response to Ap_4A, which probably means participation of different pools in the response to Ap_4A (and bradykinin). Since caffeine has P_1-purinoceptor antagonistic properties, an interfering effect could be suspected. However the result was identical whether caffeine was present during the assay or had been washed out beforehand, showing that its effect is not due to a competitive receptor blockade.

Altogether, these findings indicate that extracellular Ap_4A is a good ligand for a population of receptors present in chromaffin cell membranes, putatively identified as P_{2Y} type purinoceptors, and linked to the intracellular Ca^{2+} signalling pathway. To our knowledge this is the first time the mechanism of action of diadenosine polyphosphates has been directly addressed in neurosecretory cells.

This work was supported by grant CICYT PB-89/0095 from Ministerio de Educación y Ciencia. J.P. holds a fellowship from Universidad Complutense de Madrid.

References

BAKER, J.C. & JACOBSON, M.K. (1986). Alteration of adenyl dinucleotide metabolism by environmental stress. *Proc. Natl. Acad. Sci. USA*, **83**, 2350–2352.

BARIL, E., BONIN, P., BURNSTEIN, D., MARA, K. & ZAMECNIK, P. (1983). Resolution of diadenosine 5',5''-P^1,P^4-tetraphosphate binding subunit from a multiprotein form of HeLa cell DNA polymerase α. *Proc. Natl. Acad. Sci. USA*, **80**, 4931–4935.

BERRIDGE, M.J. (1987). Inositol trisphosphate and diacylglycerol: two interacting messengers. *Annu. Rev. Biochem.*, **56**, 159–193.

BOYER, J.L., DOWNES, C.P. & HARDEN, T.K. (1989). Kinetics of activation of phospholipase C by P_{2Y} purinergic receptor agonists and guanine nucleotides. *J. Biol. Chem.*, **264**, 884–890.

BURNSTOCK, G. & KENNEDY, C. (1985). Is there a basis for distinguishing two types of P_2-purinoceptors? *Gen. Pharmacol.*, **16**, 433–440.

BUSSE, R., OGILVIE, A. & POHL, U. (1988). Vasomotor activity of diadenosine triphosphate and diadenosine tetraphosphate in isolated arteries. *Am. J. Physiol.*, **254**, H828–H832.

CASTRO, E., TORRES, M., MIRAS-PORTUGAL, M.T. & GONZALEZ, M.P. (1990). Effect of diadenosine polyphosphates on catecholamine secretion from isolated chromaffin cells. *Br. J. Pharmacol.*, **100**, 360–364.

CHALLIS, R.A.J., JONES, J.A., OWEN, P.J. & BOARDER, M.R. (1991). Changes in inositol, 1,4,5-trisphosphate and inositol 1,3,4,5-tetrakisphosphate mass accumulations in cultured adrenal chromaffin cells in response to bradykinin and histamine. *J. Neurochem.*, **56**, 1083–1086.

CHEEK, T.R., JACKSON, T.R., O'SULLIVAN, A.J., MORETON, R.B., BERRIDGE, M.J. & BURGOYNE, R.D. (1989a). Simultaneous measurements of cytosolic calcium and secretion in single bovine adrenal chromaffin cells by fluorescent imaging of fura-2 in cocultured cells. *J. Cell Biol.*, **109**, 1219–1227.

CHEEK, T.R., O'SULLIVAN, A.J., MORETON, R.B., BERRIDGE, M.J. & BURGOYNE, R.D. (1989b). Spatial localization of the stimulus-induced rise in cytosolic Ca^{2+} in bovine adrenal chromaffin cells. *FEBS Lett.*, **247**, 429–434.

COSTE, H., BREVET, A., PLATEAU, P. & BLANQUET, S. (1987). Non-adenylated bis(5'-nucleosidyl) tetraphosphate occur in Saccharomyces cerevisiae and in Escherichia coli and accumulate upon temperature shift or exposure to cadmium. *J. Biol. Chem.*, **262**, 12096–12103.

FLODGAARD, H. & KLENOW, H. (1982). Abundant amounts of diadenosine 5',5''-P_1,P_4-tetraphosphate are present and releasable, but metabolically inactive in human platelets. *Biochem. J.*, **208**, 737–742.

FORSBERG, E.J., FEUERSTEIN, G., SHOHAMI, E. & POLLARD, H.B. (1987). Adenosine triphosphate stimulates inositol phospholipid metabolism and prostacyclin formation in adrenal medullary endothelial cells by means of P_2-purinergic receptors. *Proc. Natl. Acad. Sci. USA*, **84**, 5630–5634.

GRUMMT, F. (1988). Diadenosine tetraphosphate as a putative intracellular signal of eukaryotic cell cycle control. *Modern Cell Biol.*, **6**, 29–64.

GRYNKIEWICZ, G., POENIE, M. & TSIEN, R.Y. (1985). A new generation of calcium indicators with greatly improved fluorescence properties. *J. Biol. Chem.*, **240**, 3440–3450.

HARRISON, M.J., BROSSMER, R. & GOODY, R.S. (1975). Inhibition of platelet aggregation and platelet release reaction by α,ω-diadenosine polyphosphates. *FEBS Lett.*, **54**, 57–60.

HOUSTON, D.A., BURNSTOCK, G. & VANHOUTTE, P.M. (1987). Different P_2-purinergic receptor subtypes of endothelium and smooth muscle in canine blood vessels. *J. Pharmacol. Exp. Ther.*, **241**, 501–506.

KIM, K.-T. & WESTHEAD, E.W. (1989). Cellular responses to Ca^{2+} from extracellular and intracellular sources are different as shown by simultaneous measurements of cytosolic Ca^{2+} and secretion from bovine chromaffin cells. *Proc. Natl. Acad. Sci. USA*, **86**, 9881–9885.

LIU, P.-S., LIN, Y.-J. & KAO, L.-S. (1991). Caffeine-sensitive calcium stores in bovine adrenal chromaffin cells. *J. Neurochem.*, **56**, 172–177.

LÜTHJE, J. & OGILVIE, A. (1983). The presence of diadenosine 5',5''-P_1,P_3-triphosphate (AP_3A) in human platelets. *Biochem. Biophys. Res. Commun.*, **115**, 253–260.

LÜTHJE, J. & OGILVIE, A. (1984). Diadenosine triphosphate (AP_3A) mediates human platelet aggregation by liberation of ADP. *Biochem. Biophys. Res. Commun.*, **118**, 704–709.

LÜTHJE, J., BARINGER, K. & OGILVIE, A. (1985). Effects of diadenosine triphosphate (AP_3A) and diadenosine tetraphosphate (AP_4A) on platelet aggregation in unfractioned human blood. *Blut*, **51**, 405–413.

MACLENNAN, A.G. & PRESCOTT, M. (1984). Diadenosine 5',5''-P_1,P_4-di(adenosine-5')tetraphosphate in developing embryos of Artemia. *Nucleic Acids Res.*, **12**, 1609–1619.

MIRAS-PORTUGAL, M.T., ROTLLAN, R. & AUNIS, D. (1985). Incorporation of adenosine into nucleotides in chromaffin cells maintained in primary cultures. *Neurochem. Int.*, **7**, 89–93.

MIRAS-PORTUGAL, M.T., PINTOR, J., ROTLLAN, P. & TORRES, M. (1990). Characterization of ectonucleotidases in chromaffin cells. *Ann. N.Y. Acad. Sci.*, **603**, 523–526.

NANOFF, C., FREISSMUTH, M., TUILS, E. & SCHÜTZ, W. (1990). P_2- but not P_1-purinoceptors mediate formation of 1,4,5-inositol trisphosphate and its metabolites via pertussis toxin-insensitive pathway in the rat renal cortex. *Br. J. Pharmacol.*, **100**, 63–68.

O'SULLIVAN, A.J. & BURGOYNE, R.D. (1989). A comparison of bradykinin angiotensin II and muscarinic stimulation of cultured bovine adrenal chromaffin cells. *Biosci. Rep.*, **9**, 243–252.

PINTOR, J., TORRES, M., CASTRO, E. & MIRAS-PORTUGAL, M.T. (1991a). Characterization of diadenosine tetraphosphate (Ap_4A) binding sites in cultured chromaffin cells: evidence for a P_{2Y} site. *Br. J. Pharmacol.*, **103**, 1980–1984.

PINTOR, J., TORRES, M. & MIRAS-PORTUGAL, M.T. (1991b). Carbachol induced release of diadenosine polyphosphates-Ap_4A and Ap_5A- from perfused bovine adrenal medulla and isolated chromaffin cells. *Life Sci.*, **48**, 2317–2324.

PUTNEY, J.W. (1987). Calcium mobilizing receptors. *Trends Pharmacol. Sci.*, **233**, 305–312.

RAPAPORT, E., ZAMECNIK, P.C. & BARIL, E.F. (1981). HeLa cell DNA polymerase α is tightly associated with tryptophanyl-transfer RNA synthetase and diadenosine-5',5''-P_1,P_4-tetraphosphate binding activities. *Proc. Natl. Acad. Sci. U.S.A.*, **78**, 838–892.

RODRIGUEZ DEL CASTILLO, A., TORRES, M., DELICADO, E.G. & MIRAS-PORTUGAL, M.T. (1988). Subcellular distribution studies of diadenosine polyphosphates -AP_4A and Ap_5A- in bovine adrenal medulla: presence in chromaffin granules. *J. Neurochem.*, **51**, 1696–1703.

SASAKAWA, N., NAKAKI, T., YAMAMOTO, S. & KATO, R. (1989). Stimulation of inositol trisphosphate accumulation and calcium mobilization in cultured adrenal chromaffin cells. *J. Neurochem.*, **52**, 441–447.

SUROWY, C.S. & BERGER, N.A. (1983). Diadenosine 5',5''-P_1,P_4-tetraphosphate stimulates processing of ADP-ribosylated poly (ADP-ribose) polymerase. *J. Biol. Chem.*, **258**, 579–583.

TORRES, M., PINTOR, J. & MIRAS-PORTUGAL, M.T. (1990). Presence of ectonucleotidases in cultured chromaffin cells: hydrolysis of extracellular adenine nucleotides. *Arch. Biochem. Biophys.*, **279**, 37–44.

WEINMANN-DORSCH, C. & GRUMMT, F. (1986). Diadenosine tetraphosphate is compartimentalized in nuclei of mammalian cells. *Exp. Cell. Res.*, **165**, 550–554.

WEINMAN-DORSCH, C., HEDL, A., GRUMMT, I., ALBERT, I., FERDINAN, F.J., FRIIS, R.R., PIERRON, G., MOLL, W. & GRUMMT, F. (1984). Drastic rise of intracellular adenosine (5') tetraphosphate (5'') adenosine correlates with onset of DNA-synthesys in eukaryotic cells. *Eur. J. Biochem.*, **138**, 179–185.

ZAMECNIK, P. (1983). Diadenosine 5',5''-P_1,P_4-tetraphosphate (AP_4A): its role in cellular metabolism. *Anal. Biochem.*, **134**, 1–10.

(Received November 7, 1991
Revised February 18, 1992
Accepted March 25, 1992)

Br. J. Pharmacol. (1992), **106**, 838–845 © Macmillan Press Ltd, 1992

Modulation of the pharmacological actions of nitrovasodilators by methylene blue and pyocyanin

*R.J. Gryglewski, *A. Zembowicz, D. Salvemini, †G.W. Taylor & [1]J.R. Vane

The William Harvey Research Institute, St. Bartholomew's Hospital Medical College, Charterhouse Square, London EC1M 6BQ; *Copernicus Academy of Medicine, Department of Pharmacology, 16 Grzegorzecka 31-531 Cracow, Poland and †Royal Postgraduate Medical School, Department of Clinical Pharmacology, Du Cane Road, London W12 0NN

1 In superfused precontracted strips of rabbit aorta, methylene blue (MeB) or pyocyanin (Pyo, 1-hydroxy-5-methyl phenazinum betaine) at concentrations of 1–10 μM inhibited relaxations induced by endothelium-derived relaxing factor (EDRF), glyceryl trinitrate (GTN), S-nitroso-N-acetyl-penicillamine (SNAP) or 3-morpholino-sydnonimine (SIN-1). However, the vasorelaxant actions of sodium nitroprusside (NaNP) or sodium nitrite ($NaNO_2$) were enhanced by MeB or Pyo. Oxyhaemoglobin (HbO_2, 1 μM) inhibited the activities of EDRF and all of the nitrovasodilators studied. Vascular preparations were not relaxed by Pyo unless pretreated with NaNP (0.05–10 μM).

2 In bathed, precontracted rings of rabbit aorta, Pyo (10 μM) produced a shift to the left of the cumulative concentration-response curve for NaNP (0.01–10 μM). The rise in guanosine-3′:5′-cyclic monophosphate (cyclic GMP) content of aortic tissue was also enhanced.

3 The vasorelaxant potency of NaNP (30 μM) at pH 5–8 and at 37°C remained unchanged over 2.5 h while a solution of SNAP (30 μM) progressively lost its biological activity over 60 min. The *in vitro* degradation of the biological activity of SNAP was accelerated by MeB (150 μM) or Pyo (150 μM), whereas the vasorelaxant potency NaNP (30 μM) was doubled when incubated with MeB or Pyo.

4 In human platelet-rich plasma, MeB or Pyo (0.3–3.0 μM) uncovered an anti-aggregatory action of subthreshold concentrations of NaNP (4–8 μM). This was abrogated by HbO_2 (10 μM). In contrast to NaNP the anti-aggregatory effect of SNAP (2–20 μM) was antagonized by MeB (10 μM), Pyo (10 μM) or HbO_2 (10 μM).

5 We conclude that MeB or Pyo differ from HbO_2 in their mode of interaction with nitrovasodilators. HbO_2 scavenges nitric oxide that is released from all types of nitrovasodilators. MeB and Pyo exert a similar action towards organic nitrovasodilators (e.g. SNAP, SIN-1). However, the pharmacological actions of inorganic nitrovasodilators (e.g. NaNP or $NaNO_2$) are potentiated by MeB and Pyo owing to facilitation of the intracellular release of nitric oxide from the inorganic nitrovasodilators.

Keywords: Glyceryl trinitrate; methylene blue; pyocyanin; sodium nitroprusside; sodium nitrite; oxyhaemoglobin; S-nitroso-*N*-acetyl-penicillamine; morpholino-sydnonimine

Introduction

Methylene blue (MeB) is a synthetic phenothiazine dye with redox properties. It is used for the treatment of methaemoglobinaemias (Layne & Smith, 1969), as an uroseptic drug and as an antidote for paraquat poisoning (Kelner *et al.*, 1988). Human erythrocytes accumulate MeB as a consequence of its reduction to poorly permeable leuko-MeB. The intracellular reduction of MeB is catalyzed by flavoproteins such as NADH-dependent cytochrome c reductase or NADPH-dependent cytochrome P_{450} reductase (Kelner *et al.*, 1988).

MeB inhibits vasorelaxations induced by endothelium-derived relaxing factor (EDRF) (Griffith *et al.*, 1985; Martin *et al.*, 1985), nitric oxide, hydrogen peroxide (Burke & Wolin, 1987) or organic peroxides (Thomas & Ramwell, 1986). MeB also suppresses the activation of soluble guanylate cyclase by nitrovasodilators (Gruetter *et al.*, 1981; Martin *et al.*, 1985; Ignarro *et al.*, 1986), but it does not prevent the activation of this enzyme by arachidonic acid, protoporphyrin IX (Ignarro & Wood, 1987) or phenylhydrazine (Ignarro, 1989). Particulate guanylate cyclase is not inhibited by MeB (Martin *et al.*, 1988).

Like oxyhaemoglobin (HbO_2) (Doyle & Hoekstra, 1981), MeB binds nitric oxide and destroys its biological activity (Marshall *et al.*, 1988; Wolin *et al.*, 1990). Apart from its NO-scavenging property, MeB has been claimed to interfere directly with the activity of soluble guanylate cyclase either by oxidation of its active haeme centre (Martin *et al.*, 1985) or by inactivation of its haeme-deficient apoenzyme (Tsai *et al.*, 1983).

MeB also hinders the release of nitric oxide from organic nitrates (Feelisch & Noack, 1987a,b), blocks Ca^{2+}-activated low conductance potassium channels in smooth muscle (Cook, 1988), releases noradrenaline from adrenergic nerve endings (Matsuoka *et al.*, 1987) and inhibits arterial production of prostacyclin (Martin *et al.*, 1989).

Pyocyanin (Pyo), 1-hydroxy-5-methyl-phenazinum betaine (Watson *et al.*, 1986; 1988) is produced by *Pseudomonas aeruginosa*, the anaerobic bacterium that frequently colonizes the lungs of patients with cystic fibrosis and other forms of severe bronchiectases. Pyo and the product of its alkaline hydrolysis 1-hydroxyphenazine are toxic for the respiratory epithelium (Wilson *et al.*, 1988).

Pyo also inhibits the biological activity of EDRF released from cultured endothelial cells and forms a nitrosated derivative during its reaction with nitric oxide at room temperature (Warren *et al.*, 1990).

The similarity between the chemical structures of MeB and Pyo prompted us to compare the pharmacological interactions between MeB or Pyo and the nitrovasodilators which are known to exert their pharmacological actions through the release of nitric oxide (Feelisch & Noack, 1987,a,b; Feelisch, 1991) and activation of soluble guanylate cyclase (Waldman & Murad, 1987).

[1] Author for correspondence.

Unlike that with organic nitrovasodilators the antagonism betwen NaNP and MeB in some vascular preparations is weak or non-existent (Gruetter *et al.*, 1981, bovine coronary artery; Kreye, 1984, rabbit aorta, Marshall *et al.*, 1988, cat cerebral arterioles; Okamura *et al.*, 1990, dog and monkey mesenteric arteries) whereas in other blood vessels this antagonism is in line with that for organic nitrovasodilators (Ignarro *et al.*, 1986, bovine intrapulmonary artery; Okamura *et al.*, 1990, rat and guinea pig aorta). Therefore, we focused our attention on the differences in the interaction between organic nitrovasodilators (glyceryl trinitrate, GTN; N-acetyl-*S*-nitrosopenicillamine, SNAP; 3-morpholino-sydnonimine, SIN-1) and inorganic nitrovasodilators (sodium nitrite, $NaNO_2$; sodium nitroprusside, NaNP) with MeB or Pyo in vascular and blood platelet preparations.

Methods

Bioassay in superfused cascade of arterial strips

Three to four spirally cut strips of rabbit aorta (RbA), mesenteric artery (RbMA), common carotid artery (RbCA) or jugular vein (RbJV) were denuded of endothelium and superfused in a Vane cascade (5 ml min^{-1} at 37°C) with gassed (95% O_2:5% CO_2) Krebs buffer composed of (mM): NaCl 118, KCl 4.7, KH_2PO_4 1.2, $MgSO_4.7H_2O$ 1.17, $CaCl_2.6H_2O$ 2.5, $NaHCO_3$ 25 and glucose 5.6. Strips were allowed to equilibrate for 1–2 h with a preload of 2 g. They were then contracted with an infusion of U 46619 (9,11-dideoxy-9α,11α-methanoepoxyprostaglandin $F_{1\alpha}$, 10–30 nM) or phenylephrine hydrochloride (Phe, 100 nM). The tone of the vascular strips was recorded by auxotonic levers attached to Harvard isotonic transducers connected to Linearcorder mark VII WR3101 (Graphtec). The amplification of the recorder was adjusted so that standard doses of glyceryl trinitrate (GTN, 30–100 pmol) induced similar recordings (approximately 5 cm) for all four tissues.

Generation of EDRF

EDRF was generated and assayed as described previously (Gryglewski *et al.*, 1986). Briefly, bovine aortic endothelial cells were grown onto Cytodex microcarrier beads. Then, 2–3 ml of beads covered with $1-2 \times 10^7$ cells were packed into a heated (37°C) column which was perfused (5 ml min^{-1} at 37°C) with gassed (95% O_2:5% CO_2) Krebs buffer containing superoxide dismutase (SOD, 10 u ml^{-1}). The effluent from the column superfused a bioassay cascade arranged as described above. Effluent from the column reached the consecutive RbA strips after 1, 3, 7 and 10 s. EDRF was released from the endothelial cells by a single bolus injection of bradykinin (BK 5 pmol) given through the column (t.c.). When required MeB (1–30 μM) or Pyo (0.3–10 μM) was infused over the bioassay tissues (o.t.).

Alternatively, EDRF was generated from native endothelium of strips of RbA by including strips of RbA with preserved endothelium in the cascade and stimulating them with acetylcholine (1–5 nmol) given as a bolus injection o.t.

Interaction of nitrovasodilators with methylene blue or pyocyanin

GTN (30–100 pmol), SNAP (100–300 pmol), SIN-1 (3 nmol), $NaNO_2$ (1–2 μmol) or NaNP (100–300 pmol) were given o.t. as a single bolus injection in the absence and in the presence of MeB (1–30 μM), Pyo (0.3–10 μM) or HbO_2 (1 μM) infused o.t.

Alternatively, MeB (150 μM) or Pyo (150 μM) were dissolved in saline and incubated in an Eppendorf Thermomixer 5436 at 37°C with gentle shaking in the presence of either NaNP (30 μM) or SNAP (30 μM). Samples (10 μl) of these mixtures containing 300 pmol of NaNP or SNAP were tested for their vasorelaxant potencies on RbA strips after incubation for 0.1 to 180 min.

The effect of MeB, Pyo or HbO_2 on the vasorelaxant activity of nitrovasodilators was expressed as a ratio of the relaxation in the presence of MeB, Pyo, or HbO_2 to the relaxation without MeB, Pyo or HbO_2.

Organ bath experiments

The thoracic aorta of the rabbit was cut into rings 4 mm in width. The rings were cut open, denuded of endothelium and mounted in 20 ml organ baths filled with warmed (37°C), oxygenated (95% O_2:5% CO_2) Krebs buffer. Changes in isometric tension were measured with Biegestab K30 type 351 transducers (Hugo Sachs Electronic) attached to MK II transducer coupler (Z.T.S., London, UK) and recorded with Linearcorder mark VII WR3101 (Graphtec). The tissues were equilibrated under resting tension of 2 g for 2 h and the Krebs buffer was changed every 15 min. Tissues were then washed and cumulative concentration-response curves to Phe (0.03–10 μM) were produced. After 1.5 h of washing, the strips were contracted with Phe (0.6–1 μM) to produce a 75–80% maximal contraction. Pyo (1 μM) or saline were instilled for 1 h and a cumulative concentration-response curve to NaNP was produced. Then aortic preparations were thoroughly washed for 1.5 h and again contracted with the same concentrations of Phe. In a cross-over manner Pyo (1 μM) or saline was added to baths and after stabilization of the baseline the second concentration-response curves to NaNP were obtained. NaNP- or Pyo-induced responses were expressed as the percentage change in the Phe-induced tone.

Guanosine 3':5'-cyclic monophosphate (cyclic GMP) measurements

The thoracic aorta of a rabbit was cut into rings 2 mm in width and placed in oxygenated (95% O_2:5% CO_2), warmed (37°C) Krebs buffer. Rings were incubated for 4 h and the buffer was changed every 30 min. Then rings were placed on steel hooks with attached thread and incubated for 30 min with Pyo (1–10 μM), MeB (1–10 μM) or with their solvents. The aortic rings were then transferred together with 1 ml of the incubation medium to Eppendorf tubes. After 5 min of incubation in an Eppendorf Thermomixer at 37°C with mild shaking, the aortic rings were treated with NaNP (1 μM) or saline (10 μl) and incubation was continued for another 3 min. The aortic rings were then rapidly removed, frozen in liquid nitrogen and stored at − 20°C. Rings were ground in a glass-glass homogenizer precooled in liquid nitrogen and then homogenized for 1 min in ice-cold 6% trichloroacetic acid (TCA) with an Ultra Turrax set at maximal speed. The resultant suspension was centrifuged at 11,000 *g* for 15 min and TCA from the supernatant was extracted with two volumes of 0.5 M tri-n-octylamine dissolved in 1,1,2 trichlorotrifluoroethane. Levels of cyclic GMP in the aqueous phase were measured by radioimmunoassay (Steiner *et al.*, 1972) with prior acetylation of samples with acetic anhydride (Harper & Brooker, 1975) using antibodies obtained from Dr H. Strobach (Institute of Pharmacology, University of Düsseldorf, Germany) and iodinated tracer purchased from Amersham, U.K. The sensitivity of the assay was 2 fmol and the cross-reactivity with adenosine 3':5'-cyclic monophosphate (cyclic AMP) was less than 0.001%. The residue remaining after centrifugation of the homogenate was incubated with 1 M NaOH for 2 h at 80°C and the protein content was estimated by the method of Bradford (1976) with bovine serum albumin used as a standard. The cyclic GMP content of each ring was expressed as pmol mg^{-1} protein.

Preparation of human platelet-rich plasma

Blood from healthy volunteers who had not taken any drugs for at least 15 days was collected by venopuncture into a

plastic flask containing 3.15% sodium citrate (1:9 v/v). Platelet rich plasma (PRP) was prepared by centrifugation (800 $g \times 8$ min). Platelet poor plasma (PPP) was obtained by further centrifugation of the PRP at 4,000 g for 3 min.

Platelet aggregation

Platelet aggregation was studied in a Payton Dual Channel aggregometer calibrated with PRP (optical density, OD = 0%) and PPP (OD = 100%) with respect to light transmission. PRP was incubated at 37°C for 3 min with stirring at 1,000 r.p.m. (Born & Cross, 1963) and then platelets were aggregated with near maximal concentrations of collagen (0.5–1.5 $\mu l\ ml^{-1}$). MeB (0.01–10 μM), Pyo (0.01–10 μM) or their solvents (10 μl) were added to the PRP 2 min before stimulation with collagen. NaNP (4–8 μM) or SNAP (2–20 μM) i.e. at their minimal anti-aggregatory concentrations were given 1 min after MeB or Pyo and then 1 min later collagen was added. The change in OD was monitored for 5 min after the addition of collagen. Near maximal concentrations of collagen were defined as those which caused 80–90% change in OD.

In some experiments, HbO_2 (10 μM) was added 30 s to 5 min after collagen was instilled to PRP and the response monitored for a sufficient time (5 min) to achieve a plateau phase. The addition of MeB or Pyo increased the OD of the system. Therefore the following equation (Salvemini *et al.*, 1990) was used to express the data: % inhibition of platelet aggregation = $100 - (Y/X \times 100)$ where X = % fall in OD of collagen-treated PRP without MeB or Pyo and Y = % fall in OD of collagen-treated PRP with MeB or Pyo at various concentrations.

Materials

Sodium nitroprusside, sodium nitrite, superoxide dismutase, methylene blue, bradykinin, acetylcholine chloride, bovine serum albumin, phenylephrine hydrochloride and haemoglobin (from bovine blood) were obtained from Sigma (Poole, Dorset, U.K.). S-nitroso-*N*-acetylpenicillamine was synthesized in our laboratory by Dr M. Katsura by the method of Field *et al.* (1978). SIN-1 was a generous gift from Hoechst, Germany and U46619 from Dr J. Pike of Upjohn Co. Pyocyanin was synthesized by photolysis of phenazine methosulphate in air (Warren *et al.*, 1990). Collagen (fibril suspension) was obtained from Hormon-Chemie (München, Germany). Glyceryl trinitrate (Nitronal) was supplied by Lipha Pharmaceuticals Ltd. (West Drayton, U.K.). Oxyhaemoglobin was prepared by reduction of bovine haemoglobin with sodium hydrosulphite as described previously (Salvemini *et al.*, 1989). Stock solutions of nitrovasodilators were freshly made in distilled water at pH 6 and kept on ice.

Statistics

Unless specifically indicated, all the values in the figures and text are expressed as mean ± s.e.mean of n observations. Statistical methods are referred to in legends to tables and figures.

Results

The effect of infusion of MeB, Pyo or HbO_2 over the strips of RbA on their vasorelaxant responses to EDRF and nitrovasodilators

Either Pyo or MeB (1 to 10 μM) suppressed the vasorelaxant action of EDRF that was released either by BK from cultured bovine aortic endothelial cells (Figure 2; results for MeB not shown) or by ACh for native endothelium of strips of RbA (Figure 3; results for MeB not shown).

Pyo or MeB (3–30 μM) inhibited relaxations induced by the organic nitrovasodilators SNAP, SIN-1, or GTN. In contrast, relaxations induced by NaNP or $NaNO_2$ were enhanced in the presence of either MeB or Pyo (Table 1; Figure 1, results with MeB not shown). These effect of Pyo but not MeB were reversed by washing the RbAs with Pyo-free Krebs buffer for 30 min (Figures 2 and 3; results with MeB not shown). In addition MeB and Pyo transformed the slow pattern of relaxation of NaNP to a more rapid one (Figures 1, 2 and 3; results for MeB not shown). Either Pyo or MeB potentiated the relaxations to NaNP or $NaNO_2$ on RbCA, RbMA or RbJV ($n = 7$), while inhibiting those induced by SIN-1, SNAP or GTN (results not shown).

HbO_2 (1 μM) inhibited the responses of superfused RbAs to all nitrovasodilators studied (Table 1).

The effect of incubation of MeB or Pyo with NaNP or SNAP on relaxations of strips of RbA

Incubation of NaNP in saline at 37°C for 2–2.5 h did not change the potency of its vasorelaxant action on RbA.

Table 1 The degree of relaxation of superfused strips of rabbit aorta induced by nitrovasodilators (GTN, SNAP, SIN-1, NaNP and $NaNO_2$) was measured in the presence and in the absence of methylene blue (MeB 1 μM, 3 μM, 10 μM and 30 μM), pyocyanin (Pyo 1 μM, 3 μM and 10 μM) or oxyhaemoglobin (HbO_2, 1 μM)

	GTN	*SNAP*	*SIN-1*	*NaNP*	*$NaNO_2$*
MeB (1 μM) ($n = 8-12$)	0.81 ± 0.1*	0.81 ± 0.3	0.67 ± 0.1*	1.40 ± 0.3*	1.15 ± 0.2
MeB (3 μM) ($n = 4-16$)	0.76 ± 0.1*	0.54 ± 0.1*	0.77 ± 0.2*	1.97 ± 0.6*	1.33 ± 0.2*
MeB (10 μM) ($n = 8-15$)	0.83 ± 0.2*	0.57 ± 0.1*	0.71 ± 0.2*	2.52 ± 1.0*	1.88 ± 0.4*
MeB (30 μM) ($n = 10-15$)	0.71 ± 0.1*	0.31 ± 0.2*	n.t.	4.31 ± 1.4*	2.95 ± 1.1*
Pyo (1 μM) ($n = 8-23$)	0.99 ± 0.1	0.69 ± 0.1*	1.07 ± 0.2	1.82 ± 0.6*	1.30 ± 0.3*
Pyo (3 μM) ($n = 10-18$)	0.48 ± 0.2*	0.49 ± 0.2*	0.69 ± 0.1*	3.62 ± 1.1*	1.35 ± 0.3*
Pyo (10 μM) ($n = 8-12$)	0.50 ± 0.1*	0.35 ± 0.2*	0.44 ± 0.2*	3.17 ± 0.7*	1.80 ± 0.6*
HbO_2 (1 μM) ($n = 4-8$)	0.28 ± 0.09*	0.15 ± 0.03*	0.30 ± 0.09*	0.56 ± 0.09*	0.32 ± 0.06*

Figures represent mean ratio ± s.d. of n experiments, n.t. – not tested. *$P < 0.05$ – different from 1 as estimated by two-way one sample t-test. Figure 1 shows a typical design of experiments which were used for the construction of Table 1. Note that HbO_2 inhibits responses to all nitrovasodilators (the ratio < 1) whereas MeB or Pyo suppress vasorelaxation only by glyceryltrinitrate (GTN), S-nitroso-*N*-acetyl-penicillamine (SNAP) or 3-morpholino-sydnonimine (SIN-1) but augment vasorelaxation by sodium nitroprusside (NaNP) or sodium nitrite ($NaNO_2$) (the ratio > 1).

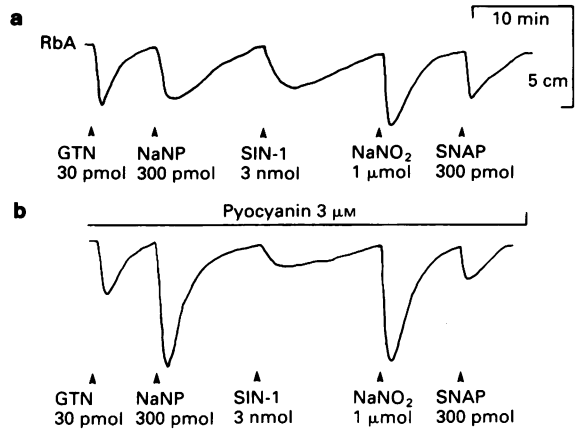

Figure 1 Pyocyanin (3 μM) inhibits relaxations of a superfused precontracted rabbit aortic strip (RbA) by glyceryl trinitrate (GTN), 3-morpholino-sydnonimine (SIN-1) or S-nitroso-*N*-acetyl-penicillamine (SNAP) but it potentiates vasorelaxant effect of sodium nitroprusside (NaNP) or sodium nitrite ($NaNO_2$). (a) Relaxations of RbA in the absence of pyocyanin; (b) relaxations of RbA following 30 min infusion of pyocyanin. Ratios of the latter to the former were used for the construction of Table 1.

Incubation of NaNP with MeB or Pyo resulted in an enhancement of its vasorelaxant properties. This effect appeared as soon as 6 s after incubation and remained unchanged for up to 2.5 h (Figure 4; results for MeB not shown). In contrast to NaNP, SNAP in saline solution at 37°C progressively lost its vasorelaxant action until it disappeared after 1 h of incubation. The presence of MeB or Pyo in the solution accelerated the disappearance of the biological activity of SNAP (Figure 4; results for MeB not shown).

The interaction between Pyo and NaNP in rabbit aortic ring preprations

Addition of Pyo (1 μM) to the organ bath potentiated the action of NaNP resulting in a shift to the left of the concentration-response curve (Figure 5).

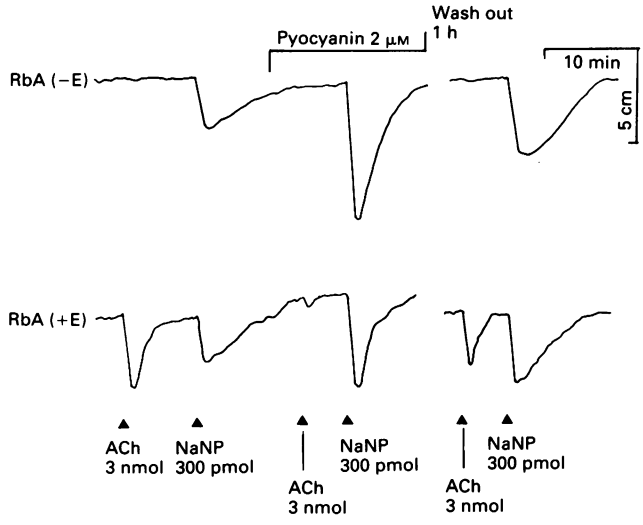

Figure 3 The effect of pyocyanin (2 μM) on relaxations induced by acetylcholine (ACh, 3 nmol) or sodium nitroprusside (NaNP, 300 pmol) in precontracted superfused in cascade rabbit aortic strips, one of which was denuded of endothelium [RbA(− E)] and the other had preserved endothelium [RbA(+ E)]. ACh relaxed only RbA(+ E) whereas NaNP relaxed both strips and thus relaxation of RbA(+ E) by ACh might be ascribed to the release of endothelium-derived relaxing factor (EDRF). Pyocyanin reversibly blocked the effects of EDRF and enhanced the vasorelaxant action of NaNP.

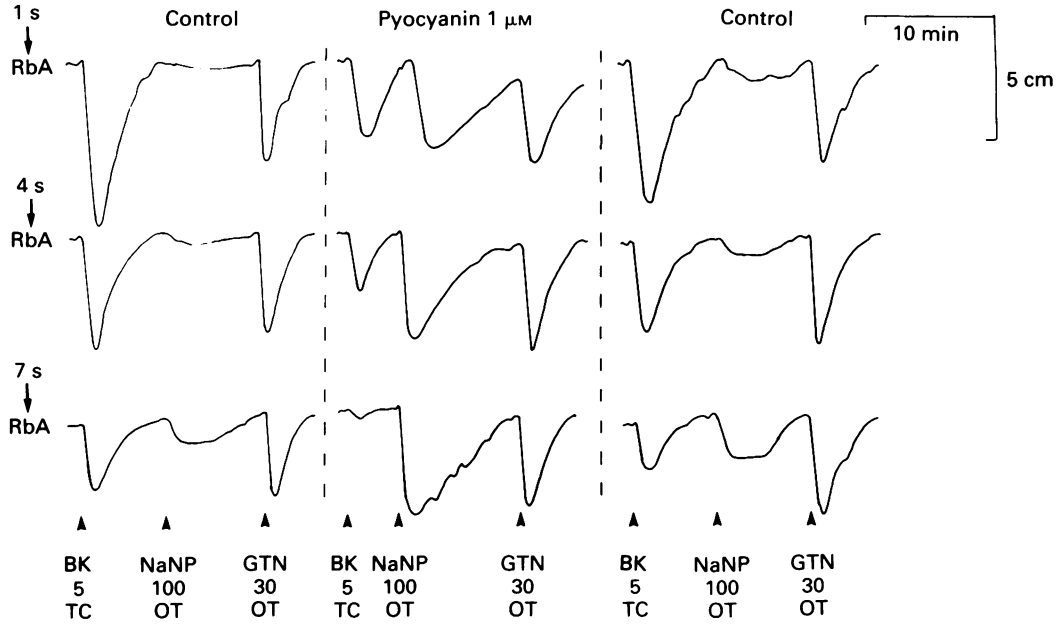

Figure 2 The effect of pyocyanin (1 μM) given over assay tissues (o.t.) on relaxations induced by endothelium-derived relaxing factor (EDRF), sodium nitroprusside (NaNP, 100 pmol, o.t.) or glyceryl trinitrate (GTN, 30 pmol, o.t.) in three precontracted endothelium-denuded rabbit aortic strips (RbA) which were superfused in cascade. EDRF was generated by an injection of bradykinin (BK, 5 pmol) through a column (t.c.) packed with cultured bovine aortic endothelial cells. The EDRF elicited relaxations of RbA strips which disappeared down the cascade. BK (5 pmol, o.t.) had no effect on the tone of RbA strips. The first vertical dashed line represents a 30 min period of treatment with pyocyanin that was continued throughout the middle panel. The second vertical dashed line indicates a 30 min period of washout with Krebs buffer. Infusion by pyocyanin (1 μM) had little effect on relaxations induced by GTN, while it inhibited relaxations induced by EDRF and potentiated relaxations induced by NaNP. This action of pyocyanin (1 μM) was partially reversible.

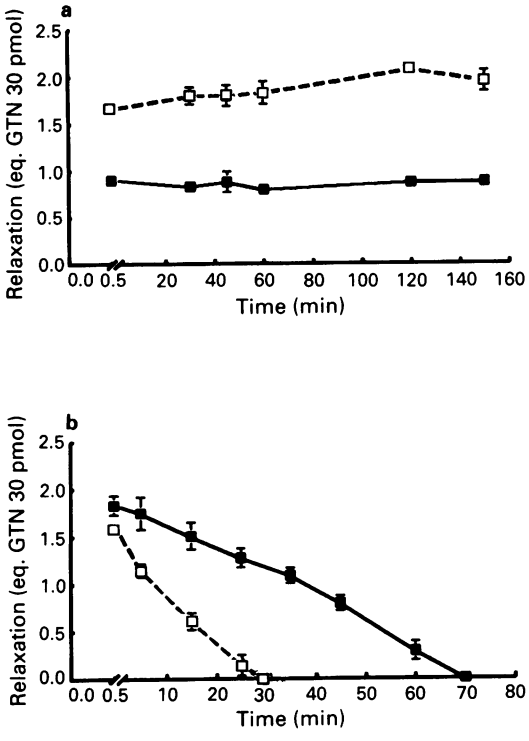

Figure 4 The effect of preincubation of pyocyanin (150 μM) with sodium nitroprusside (NaNP, 30 μM) (a) or S-nitroso-*N*-acetyl-penicillamine (SNAP, 30 μM) (b) on their vasorelaxant action in precontracted superfused rabbit aortic strips. Incubations were performed as described in methods. Abscissa scale: incubation time in min. Ordinate scale: vasorelaxant response expressed as a ratio of vasorelaxation by NaNP or SNAP to vasorelaxation induced by glyceryl trinitrate (GTN) at a standard dose of 30 pmol. Solid lines represent vasorelaxation induced by 10 μl samples of nitrovasodilators incubated in the absence of pyocyanin, and dashed line in the presence of pyocyanin. Each point represents mean of 8–12 experiments and vertical bars represent s.e.mean. Pyocyanin augmented the stable vasorelaxant action of NaNP and accelerated the deterioration of labile vasorelaxant activity of SNAP.

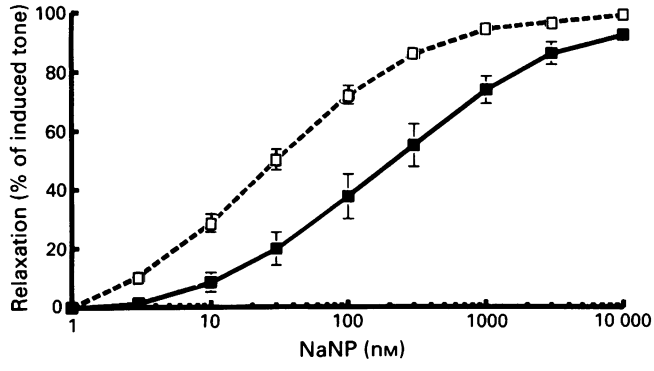

Figure 5 The enhancement by pyocyanin (1 μM; dashed line) of sodium nitroprusside (NaNP, solid line)-induced relaxations in phenylephrine-contracted open ring preparations of rabbit aorta in an organ bath. ($n = 5$ rabbits).
$P < 0.05$ by two way ANOVA.

Residual activity of NaNP after removal from bath

Pyo itself slightly increased the tone of endothelium-denuded RbA rings provided that the rings were not treated with NaNP. However, after treatment of the assay tissues with NaNP (up to 10 μM) and a subsequent extensive washing out of NaNP (up to 1.5 h) the first instillation of Pyo (1 μM) into the bath resulted in a rapid and transient relaxation (45 ± 14% of Phe-induced tone, $n = 5$) (Figure 6). Pyo (10 μM) produced similar relaxations in strips of RbA superfused with NaNP (50 nM) for 15 min and then with Krebs buffer (n = 3; results not shown).

The effect of Pyo or MeB on the cyclic GMP levels in rings of RbA stimulated with NaNP

As shown in Figure 7, NaNP (1 μM) increased the levels of cyclic GMP in rings of RbA and this effect was significantly ($P < 0.05$) potentiated by preincubation of the rings with Pyo (3 or 10 μM) or MeB (3 or 10 μM). Pyo (1 μM) potentiated the NaNP-induced increase in cyclic GMP in 7 out of 8 experiments.

The effect of MeB or Pyo on the anti-aggregatory action of NaNP or SNAP in human platelet-rich plasma

In human PRP, collagen (0.5–1.5 μl ml^{-1}) produced near maximal aggregation within 5 min. This aggregation was not

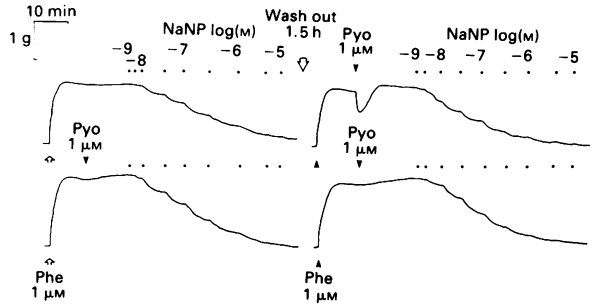

Figure 6 Pyocyanin (Pyo) relaxes bathed rings of rabbit aorta treated with sodium nitroprusside (NaNP). The upper trace shows a rabbit aortic ring precontracted with phenylephrine (Phe 1 μM) relaxing to NaNP. After wash out (1.5 h), Phe (1 μM) was again added followed by Pyo (1 μM) and NaNP. The lower trace shows a second ring precontracted with Phe (1 μM) treated with Pyo (1 μM) followed by NaNP. After wash out (1.5 h) the second ring was contracted with Phe (1 μM) again then treated with Pyo (1 μM) and NaNP. Pyo (1 μM) enhanced the concentration-dependent relaxations to NaNP. Moreover, Pyo (1 μM), when added after extensive wash out (6 times every 15 min) and constriction with Phe (upper trace), caused a sharp, transient relaxation of the ring previously treated with NaNP. The aortic ring previously treated with Pyo (1 μM; lower trace) did not relax to a second addition of Pyo. (Original traces representative of 5 different experiments).

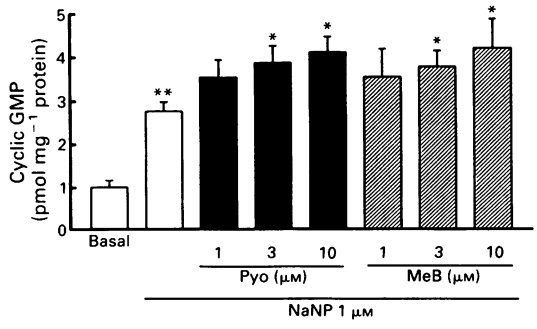

Figure 7 Potentiation by pyocyanin (Pyo) or methylene blue (MeB) of sodium nitroprusside (NaNP)-induced elevation of cyclic GMP in rings of rabbit aorta. NaNP (1 μM) evoked accumulation of cyclic GMP in aortic tissue and that was further potentiated by preincubation of the rings with Pyo (1–10 μM) or MeB (1–10 μM). Columns represent means (with s.e.mean shown by vertical bars) from 7–9 rabbits.
*,** denote significant differences ($P < 0.05$) when compared to basal (**) or to NaNP alone (*).

influenced by 1 min preincubation with MeB (10 μM) or Pyo (10 μM). The subthreshold anti-aggregatory concentration of NaNP was 6.5 ± 1.9 μM, $n = 4$.

The preincubation (1 min) of MeB or Pyo (1 μM) with subthreshold anti-aggregatory concentrations of NaNP (4–8 μM) in PRP revealed the anti-aggregatory actions of the latter (Figure 8). This potentiation of the anti-aggregatory effects of NaNP by MeB or Pyo was reversed by HbO_2 (10 μM). The effect of HbO_2 was inversely proportional to the time (30 s–5 min) that elapsed between the instillation of collagen and the treatment with HbO_2 (Figure 9). When HbO_2 (10 μM) was present in PRP before Pyo (1 μM) and NaNP (4–8 μM) were added then the potentiating effect of Pyo on the anti-aggregatory action of NaNP was ablated ($n = 3$).

SNAP (2–20 μM) inhibited platelet aggregation induced by collagen. Its action was antagonized by either Pyo (10 μM) or MeB (10 μM; data not shown).

Discussion

EDRF has been identified as nitric oxide (Palmer *et al.*, 1987; Moncada *et al.*, 1991). Nitrovasodilators exert their action through the formation of nitric oxide (Feelisch *et al.*, 1988; Feelisch, 1991) which combines with the active haeme centre of soluble guanylate cyclase (Gerzer *et al.*, 1988). Oxyhaemoglobin (Martin *et al.*, 1985), MeB (Griffith *et al.*, 1985; Martin *et al.*, 1985; Pearce *et al.*, 1990; Kaiser *et al.*, 1986; Watanabe *et al.*, 1988; Hyman *et al.*, 1989) and Pyo (Warren *et al.*, 1990) abolish vascular relaxations induced by EDRF.

Thus, MeB and Pyo could be expected to attenuate the vasorelaxant and platelet-suppressant effects of all nitrovasodilators as did HbO_2, but this was not so. MeB and Pyo (1–10 μM) attenuated the relaxations of strips of rabbit aorta induced by SNAP, SIN-1 and GTN. However, these blue dyes enhanced the relaxations induced by NaNP or $NaNO_2$. Furthermore, the anti-aggregatory effect of NaNP in human platelets was potentiated by MeB and Pyo, whereas the anti-aggregatory effect of SNAP was inhibited by both dyes.

It may well be that this paradoxical augmentation of the pharmacological effects of inorganic nitrovasodilators by MeB or Pyo reflects different mechanisms for the release of nitric oxide from the nitrovasodilators. In aqueous solutions SNAP (Ignarro *et al.*, 1981; Gryglewski *et al.*, 1989) and SIN-1 (Gerzer *et al.*, 1988; Feelisch, 1991) spontaneously release nitric oxide which is readily scavenged by MeB, Pyo or HbO_2 as we have seen in our experiments.

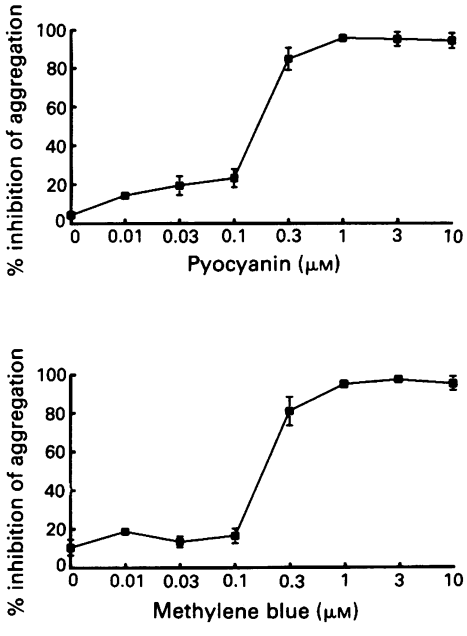

Figure 8 Pyocyanin or methylene blue (0.01–10 μM) reveal anti-aggregatory activity of subthreshold concentrations (6.5 ± 2 μM) of sodium nitroprusside in human platelet rich plasma. Aggregation was induced by collagen (0.5–1.5 μg ml^{-1}). The points represent the mean and vertical bars show s.d. of 4 experiments.

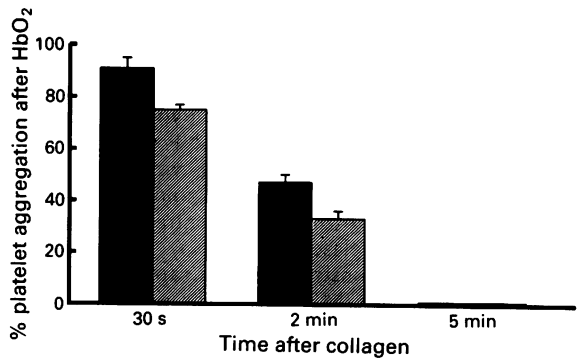

Figure 9 Reversal by oxyhaemoglobin (HbO_2, 10 μM) of the inhibition of platelet aggregation that was induced by a combined administration of sodium nitroprusside (NaNP, 6.1 ± 1 μM) and pyocyanin (Pyo, 3 μM) (solid columns) or methylene blue (MeB, 3 μM) (hatched columns) to human platelet-rich plasma that was aggregated by collagen (0.5–15 μg ml^{-1}). HbO_2 acted in a time-dependent manner when instilled 30 s or 2 min after collagen was added. Columns represent percentage of platelet aggregation in the presence of NaNP, Pyo or MeB and HbO_2 as compared to the control aggregation that was induced by collagen alone. Columns show mean of 4 experiments and vertical bars show s.d.

Relatively small amounts of nitric oxide are released from NaNP in aqueous solution at physiological pH (Feelisch & Noack, 1987b; Gryglewski *et al.*, 1989). It does not fit the correlation between formation of nitric oxide and activation of a soluble guanylate cyclase *in vitro* – the correlation that is seen with organic nitrovasodilators (Feelisch, 1991). Moreover, the generation of nitric oxide from NaNP is not enhanced by cysteine, as occurs with GTN; in fact it appears to be reduced (Feelisch & Noack, 1987b). Thus, there is a discrepancy between the low yield of nitric oxide from NaNP *in vitro* and its potent vasorelaxant and platelet-suppressant actions (Gryglewski *et al.*, 1989; Salvemini *et al.*, 1990). An intracellular site for the biotransformation of NaNP is therefore proposed.

Any substantial release of nitric oxide from $NaNO_2$ requires either light energy (Matsunga & Furchgott, 1989; Wigilius *et al.*, 1990) or an acid pH (Furchgott, 1988). In an organ bath at low pH, $NaNO_2$ generates, along with nitrous acid, an unstable vasorelaxant principle which is likely to be nitric oxide (Furchgott, 1988), and we have at present no explanation for the potentiation of its vasorelaxant action by Pyo or MeB.

The results of *in vitro* incubations of NaNP with Pyo might suggest that a direct chemical interaction leads to the formation of nitric oxide in a test tube. However, if Pyo causes the release of NO from NaNP, a time-dependent decrease in the vasorelaxant activity of the incubation mixture, due to the consumption of substrate, should have been observed. This was not the case, since the vasorelaxant activity of the mixture of NaNP and Pyo remained unchanged during 2.5 h of incubation suggesting that this interaction occurred at the level of the smooth muscle rather than in the test tube. Importantly, in organ bath experiments Pyo relaxed rabbit aortic rings which were previously treated with NaNP even after extensive wash out, further suggesting an intracellular site of interaction between NaNP and Pyo. Most probably, Pyo reacted with intracellular remnants of NaNP which by themselves were unable to activate guanylate

cyclase. The second instillation of Pyo was unable to produce relaxation, hence indicating an exhaustion of intracellular stores of NaNP. Therefore, it is possible that a more complex mechanism than a simple chemical reaction in watery solution explains the interaction between Pyo and NaNP. We suggest that the nitrosyl moiety of NaNP interacts with the cloud of pi electrons of Pyo or MeB, weakening, but not breaking, the Fe-NO bond of NaNP and thus facilitating transfer of nitric oxide to the haeme centre at the active site of soluble guanylate cyclase.

Indeed, we have demonstrated that a rapid NaNP-induced accumulation of cyclic GMP in vascular rings is augmented by MeB or Pyo along with the shift to the left of the vasorelaxant dose-response curve. This finding accords with the concept that MeB and Pyo are intracellular carriers for NaNP to soluble guanylate cyclase, and activate transfer of nitric oxide from NaNP to the active haeme centre.

This phenomenon may be responsible for the enhancement of platelet-suppressant and vasorelaxant activities of NaNP by MeB or Pyo in human platelets and rabbit vasculature. Species and tissue specificity of this interaction are likely to be regulated by various isoforms of guanylate cyclase or by intracellular pH and redox potential. Perhaps, these regulatory mechanisms are responsible for a variety of interactions between NaNP and MeB in blood vessels (Gruetter *et al.*, 1981; Kreye, 1984; Ignarro *et al.*, 1986; Marshall *et al.*, 1988; Okamura *et al.*, 1990) and in tracheal muscle (Zhou & Torphy, 1991).

HbO_2 is a specific inhibitor of nitric oxide-induced suppression of platelet aggregation for it does not affect the anti-aggregatory action of prostacyclin analogues or phosphodiesterase inhibitors (Salvemini *et al.*, 1990). It inhibits the activity of soluble guanylate cyclase by binding to nitric oxide in the extracellular space (Martin *et al.*, 1985) and acting as a 'sink' for intracellular nitric oxide. Moreover, the reversal of nitric oxide-induced inhibition of platelet aggregation by HbO_2 coincides with a time-dependent fall in the intracellular levels of cyclic GMP (Salvemini *et al.*, 1990). This time-dependent decrease of the effect of HbO_2 indicates that some time (min) of continuous stimulation of guanylate cyclase by nitric oxide is required before the inhibition of platelet aggregation becomes irreversible. Therefore, our data on HbO_2 indicate that the increased availability of nitric oxide from NaNP for guanylate cyclase is involved in the potentiation of the action of NaNP by Pyo or MeB.

In conclusion, we consider that Pyo is a suitable replacement for MeB as a scavenger of either endogenous or exogenous nitric oxide in biological systems. Moreover, NaNP, although a potent stimulator of soluble guanylate cyclase, vasorelaxant and platelet-suppressant, cannot be considered as a donor of nitric oxide in the same way as sydnonimines, S-nitrosothiols or organic nitrates.

This work was supported by a grant from Glaxo Group Research Ltd. We would like to thank Miss E. Wood for preparing the cultured bovine endothelial cells used in this study and Dr R. Botting for editorial assistance.

References

BORN, G.V.R. & CROSS, M.J. (1963). The aggregation of blood platelets. *J. Physiol.*, **168**, 178–195.

BRADFORD, M.M. (1976). A rapid and sensitive method for the quantitation of microgram quantities of protein utilizing the principle of protein binding. *Anal. Biochem.*, **72**, 248–254.

BURKE, T.M. & WOLIN, M.S. (1987). Hydrogen peroxide elicits pulmonary arterial relaxation and guanylate cyclase activation. *Am. J. Physiol.*, **252**, H721–731.

COOK, N.S. (1988). The pharmacology of potassium channels and their therapeutic potential. *Trends Pharmacol. Sci.*, **9**, 21–28.

DOYLE, M.P. & HOEKSTRA, J.W. (1981). Oxidation of nitric oxides by bound dioxygen on hemoproteins. *J. Inorg. Biochem.*, **14**, 351–354.

FEELISCH, M. (1991). The biochemical pathways of nitric oxide formation from nitrovasodilators: appropriate choice of exogenous NO donors and aspects of preparation and handling of aqueous NO solutions. *J. Cardiovasc. Pharmacol.*, **17**, S25–S33.

FEELISCH, M. & NOACK, E.A. (1987a). Correlation between nitric oxide formation during degradation of organic nitrates and activation of guanylate cyclase. *Eur. J. Pharmacol.*, **139**, 19–30.

FEELISCH, M. & NOACK, E.A. (1987b). Nitric oxide (NO) formation from nitrovasodilators occurs independently of hemoglobin or non-heme iron. *Eur. J. Pharmacol.*, **142**, 465–469.

FEELISCH, M., NOACK, E. & SCHRÖDER, H. (1988). Explanation of the discrepancy between the degree of organic nitrate decomposition, nitrite formation and guanylate cyclase stimulation. *Eur. Heart J.*, **9**, 57–62.

FIELD, L., DILTS, R.V., RAVICHANDRAN, R., LENHERT, P.G. & CARNAHAN, G.E. (1978). An unusually stable thionitrate from N-acetyl-D,L-penicillamine: X-ray crystal and molecular structure of 2-acetylamino-2-carboxyl-1,1-dimethylethyl thionitrite. *J. Chem. Soc. Perkin. Trans.*, **1**, 249–250.

FURCHGOTT, R.F. (1988). Studies on relaxation of rabbit aorta by sodium nitrite: the basis for the proposal that the acid-activable inhibitory factor from retractor penis is inorganic nitrite and the endothelium-derived relaxing factor is nitric oxide. In *Vasodilation: Vascular Smooth Muscle, Peptides, Autonomic Nerves and Endothelium.* ed. Vanhoutte, P.M. pp. 401–414. New York: Raven Press.

GERZER, R., KARRENBROCK, B., SIESS, W. & HEIM, J.M. (1988). Direct comparison of the effects of nitroprusside, SIN-1, and various nitrates on platelet aggregation and soluble guanylate cyclase. *Throm. Res.*, **52**, 11–21.

GRIFFITH, T.M., EDWARDS, D.H., LEWIS, M.J. & HENDERSON, A.H. (1985). Evidence that cyclic guanosine monophosphate (c-GMP) mediates endothelium-dependent relaxation. *Eur. J. Pharmacol.*, **112**, 195–202.

GRUETTER, C.A., GRUETTER, D.Y., LYON, J.E., KADOWITZ, P.J. & IGNARRO, L.J. (1981). Relationship between cyclic guanosine 3′5′-monophosphate formation and relaxation of coronary arterial smooth muscle by glyceryl trinitrate, nitroprusside, nitrite and nitric oxide: effects of methylene blue and methemoglobin. *J. Pharmacol. Exp. Ther.*, **219**, 181–186.

GRYGLEWSKI, R.J., MONCADA, S. & PALMER, R.M.J. (1986). Bioassay of prostacyclin and endothelium-derived relaxing factor (EDRF) from porcine aortic endothelial cells. *Br. J. Pharmacol.*, **87**, 685–694.

GRYGLEWSKI, R.J., KORBUT, R., KALECINSKA, A. & ZEMBOWICZ, A. (1989). Interaction between stimulators of adenylate and guanylate cyclases in human leukocytes, platelets and arteries. *Tissue React. Int. J.*, **11**, 269–275.

HARPER, J.F. & BROOKER, G. (1975). Fentomole sensitive radioimmunoassay for cyclic AMP and cyclic GMP after 2′O acetylation by acetic anhydride in aqueous solution. *J. Cyclic Nucleotide Res.*, **1**, 207–218.

HYMAN, A.L., KADOWITZ, P.J. & LIPTON, H.L. (1989). Methylene blue selectively inhibits pulmonary vasodilator responses in cats. *J. Appl. Physiol.*, **66**, 1513–1517.

IGNARRO, L.J. (1989). Heme-dependent activation of soluble guanylate cyclase by nitric oxide: regulation of enzyme activity by porphyrins and metalloporphyrins. *Sem. Haematol.*, **26**, 63–76.

IGNARRO, L.J. & WOOD, K.S. (1987). Activation of purified soluble guanylate cyclase by arachidonic acid requires absence of enzyme bound heme. *Biochem. Biophys. Acta*, **928**, 160–170.

IGNARRO, L.J., HARBISON, R.G., WOOD, K.S. & KADOWITZ, P.J. (1986). Dissimilarities between methylene blue and cyanide on relaxation and cyclic GMP formation in endothelium-intact intrapulmonary artery caused by nitrogen oxide-containing vasodilators and acetylcholine. *J. Pharmacol. Exp. Ther.*, **236**, 30–36.

IGNARRO, L.J., LIPPTON, H., EDWARDS, J.C., BARICOS, W.H., HYMAN, L., KADOWITZ, P.J. & GRUETTER, C.A. (1981). Mechanism of vascular smooth muscle relaxation by organic nitrates, nitrites, nitroprusside and nitric oxide: evidence for the involvement of S-nitrosothiols as active intermediates. *J. Pharmacol. Exp. Ther.*, **218**, 739–749.

KAISER, L., HULL, S.S. Jr & SPARKS, H.V. Jr (1986). Methylene blue and ETYA block flow-dependent dilatation in canine femoral artery. *Am. J. Physiol.*, **250**, H974–H981.

KELNER, M.J., BAGNELL, R., HALE, B. & ALEXANDER, N.M. (1988). Methylene blue competes with paraquat for reduction by flavoenzymes resulting in decreased superoxide production in the presence of heme proteins. *Arch. Biochem. Biophys.*, **262**, 422–426.

KREYE, V.A.W. (1984). Direct vasodilators with unknown modes of action: the nitro-compounds and hydralazine. *J. Cardiovasc. Pharmacol.*, **6**, S646–S655.

LAYNE, W.R. & SMITH, R.P. (1969). Methylene blue uptake and the reversal of chemically induced methemoglobinemias in human erythrocytes. *J. Pharmacol. Exp. Ther.*, **169**, 36–44.

MARSHALL, J.J., WEI, E.P. & KONTOS, H.A. (1988). Independent blockade of cerebral vasodilatation from acetylcholine and nitric oxide. *Am. J. Physiol.*, **255**, H847–H854.

MARTIN, W., DRAZAN, K.M. & NEWBY, A.C. (1989). Methylene blue but not changes in cyclic GMP inhibits resting and bradykinin-stimulated production of prostacyclin by pig aortic endothelial cells. *Br. J. Pharmacol.*, **97**, 51–56.

MARTIN, W., VILLANI, G.M., JOTHIANANDAN, D. & FURCHGOTT, R.F. (1985). Selective blockade of endothelium-dependent and glyceryl trinitrate-induced relaxation by hemoglobin and by methylene blue in the rabbit aorta. *J. Pharmacol. Exp. Ther.*, **232**, 708–716.

MARTIN, W., WHITE, D.G. & HENDERSON, A.H. (1988). Endothelium-derived relaxing factor and atriopeptin II elevate cyclic GMP levels in pig aortic endothelial cells. *Br. J. Pharmacol.*, **93**, 229–239.

MATSUNGA, K. & FURCHGOTT, R.F. (1989). Interaction of light and sodium nitrite in producing relaxation of rabbit aorta. *J. Pharmacol. Exp. Ther.*, **248**, 687–695.

MATSUOKA, I., SAKURAI, K., ONO, T. & NAKANISHI, H. (1987). Involvement of endogenous noradrenaline release in methylene blue induced contractions of isolated rabbit aorta. *Jpn. J. Pharmacol.*, **44**, 23–33.

MONCADA, S., PALMER, R.M.J. & HIGGS, E.A. (1991). Nitric oxide: physiology, pathophysiology, and pharmacology. *Pharmacol. Rev.*, **43**, 109–142.

OKAMURA, T., INOUE, M. & TODA, N. (1990). Methylene blue sensitive and insensitive responses to sodium nitroprusside of blood vessels isolated from animals of different species. *Eur. J. Pharmacol.*, **183**, 1267–1268.

PALMER, R.M.J., FERRIGE, A.G. & MONCADA, S. (1987). Nitric oxide accounts for the biological activity of endothelium-derived relaxing factor. *Nature*, **88**, 411–415.

PEARCE, W.J., REINIER-REBUFFEL, A.-M., LEE, J., AUBINEAU, P., IGNARRO, L. & SEYLAZ, J. (1990). Effect of methylene blue on hypoxic cerebral vasodilatation in the rabbit. *J. Pharmacol. Exp. Ther.*, **254**, 616–625.

SALVEMINI, D., DE NUCCI, G., GRYGLEWSKI, R.J. & VANE, J. (1989). Human neutrophils and mononuclear cells inhibit platelet aggregation by releasing a nitric oxide-like factor. *Proc. Natl. Acad. Sci. U.S.A.*, **86**, 6328–6332.

SALVEMINI, D., RADZISZEWSKI, A., KORBUT, R. & VANE, J. (1990). The use of oxyhaemoglobin to explore the events underlying inhibition of platelet aggregation induced by NO-donors. *Br. J. Pharmacol.*, **101**, 991–995.

SALVEMINI, D., MOLLACE, V., PISTELLI, A., ÄNGGÅRD, E. & VANE, J. (1992). Metabolism of glyceryl trinitrate to nitric oxide by endothelial cells and smooth muscle cells and its induction by *Eschericha coli* lipopolysaccharide. *Proc. Natl. Acad. Sci. U.S.A.*, **89**, 982–986.

STEINER, A.L., PARKER, C.W. & KIPNIS, D.M. (1972). Radioimmunoassay for cyclic nucleotides. *J. Biol. Chem.*, **247**, 1106–1113.

THOMAS, G. & RAMWELL, P. (1986). Induction of vascular relaxation by hydroperoxides. *Biochem. Biophys. Res. Commun.*, **139**, 102–108.

TSAI, S.C., ADAMIK, R., MANGANIELLO, V.C. & VAUGHAN, M. (1983). Regulation of activity of purified guanylate cyclase from liver that is unresponsive to nitric oxide. *Biochem. J.*, **215**, 447–455.

WALDMAN, S.A. & MURAD, F. (1987). Cyclic GMP synthesis and function. *Pharmacol. Rev.*, **39**, 163–196.

WARREN, J.B., LOI, R., RENDEL, N.B. & TAYLOR, G.W. (1990). Nitric oxide is inactivated by the bacterial pigment pyocyanin. *Biochem. J.*, **266**, 921–923.

WATANABE, M., ROSENBLUM, W.I. & NELSON, G.H. (1988). *In vivo* effect of methylene blue on endothelium-dependent and endothelium-independent dilatations of brain microvessels in mice. *Circ. Res.*, **62**, 86–90.

WATSON, D., MCDERMOT, J., WILSON, R., COLE, P.J. & TAYLOR, G.W. (1986). Purification and structural analysis of pyocyanin and 1-hydroxyphenazine. *Eur. J. Biochem.*, **159**, 309–313.

WATSON, D., TAYLOR, G.W., WILSON, R., COLE, P.J. & ROWE, C. (1988). Thermospray mass spectrometric analysis of phenazines. *Biomed. Environ. Mass Spectrometr.*, **17**, 251–255.

WIGILIUS, I.M., AXELSSON, K.L., ANDERSSON, R.G.G., KARLSSON, J.O.G. & ODMAN, S. (1990). Effects of sodium nitrite on ultraviolet light-induced relaxation and ultraviolet light-dependent activation of guanylate cyclase in bovine mesenteric arteries. *Biochem. Biophys. Res. Commun.*, **169**, 129–135.

WILSON, R., SYKES, D.A., WATSON, D., RUTMAN, A., TAYLOR, G.W. & COLE, P.J. (1988). Measurement of Pseudomonas aeruginosa phenazine pigments in sputum and assessment of their contribution to sputums of toxicity for respiratory epithelium. *Infect. Immun.*, **56**, 2515–2517.

WOLIN, M.S., CHERRY, P.D., RODENBURY, J.M., MESSINA, E.J. & KALEY, G. (1990). Methylene blue inhibits vasodilatation of skeletal muscle arterioles to acetylcholine and nitric oxide via the extracellular generation of superoxide anion. *J. Pharmacol. Exp. Ther.*, **254**, 872–876.

ZHOU, H.L. & TORPHY, T.J. (1991). Relationship between cyclic guanosine monophosphate accumulation and relaxation of canine tracheaolis induced by nitrovasodilators. *J. Pharmacol. Exp. Ther.*, **250**, 972–978.

(Received December 18, 1991
Revised March 16, 1992
Accepted March 26, 1992)

Br. J. Pharmacol. (1992), **106**, 846–852 © Macmillan Press Ltd, 1992

Modulation by opioids and by afferent sensory neurones of prostanoid protection of the rat gastric mucosa

J.V. Esplugues, [1,*] B.J.R. Whittle & *S. Moncada

Department of Pharmacology, University of Valencia, Valencia, Spain and *Wellcome Research Laboratories, Langley Court, Beckenham, Kent BR3 3BS

1 Pretreatment with capsaicin, to deplete sensory neuropeptides from primary afferent neurones or the administration of morphine (9 mg kg^{-1}, i.v.), which can inhibit neuropeptide release, augmented gastric mucosal injury induced by a 5 min challenge with intragastric ethanol in the rat, as assessed by macroscopic and histological evaluation.

2 Morphine administration substantially attenuated the protective actions of the prostaglandin analogue 16,16 dimethyl prostaglandin E_2 (dm PGE_2; 0.5–20 $\mu g\ kg^{-1}$, p.o.) against ethanol-induced damage. This reduced degree of protection by dmPGE_2 was not however, the consequence of the enhanced level of damage.

3 These actions of morphine in reducing prostaglandin protection against mucosal injury were abolished by pretreatment (5 min) with naloxone (1 mg kg^{-1}, i.v.) or the peripherally acting opioid antagonist, N-methyl nalorphine (6 mg kg^{-1}, i.v.).

4 Capsaicin pretreatment (2 weeks before study), likewise attenuated the protective actions of dmPGE_2, although to a lesser degree than did morphine.

5 These findings, thus implicate the involvement of capsaicin- and opioid-sensitive afferent neurones in the processes by which exogenous prostanoids can protect the gastric mucosa from damage.

Keywords: Opioids; morphine, capsaicin; 16,16-dimethyl PGE_2; prostaglandins; sensory neurones; mucosal protection; gastric damage

Introduction

It has been proposed that the maintenance of gastric mucosal integrity is regulated by the interaction between local mediators such as sensory neuropeptides, nitric oxide (NO) and prostaglandins (Whittle *et al.*, 1990).

A role for sensory neuropeptides has been deduced from the findings that chronic systemic administration of capsaicin, which depletes sensory neuropeptides from primary afferent neurones, can substantially enhance gastric mucosal injury induced by a number of pro-ulcerogenic agents (Szolcsanyi & Bartho, 1981; Holzer & Sametz, 1986; Esplugues *et al.*, 1989). Under such conditions, the inhibitor of NO biosynthesis, N^G-monomethyl-L-arginine (L-NMMA), induces acute mucosal haemorrhage and erosion, indicating the involvement of NO in mucosal integrity and its interaction with sensory neuropeptides (Whittle *et al.*, 1990).

Opioids, that can act peripherally on sensory neurones (Ferreira & Nakamura, 1979; Bartho & Szolcsanyi, 1981; Smith & Buchan, 1984) and can inhibit neuropeptide release (Lembeck & Donnerer, 1985), can likewise augment mucosal damage (Esplugues *et al.*, 1989; Esplugues & Whittle, 1990; Whittle & Lopez-Belmonte, 1991; Holzer *et al.*, 1991). Conversely, acute intragastric capsaicin administration, which stimulates the neuronal release of sensory neuropeptides, protects the mucosa against damage (Holzer & Lippe, 1988; Holzer *et al.*, 1990). Furthermore, intra-arterial administration of calcitonin-gene related peptide (CGRP), the predominant sensory neuropeptide in the rat gastric mucosa (Green & Dockray, 1988), also reduces gastric injury (Lippe *et al.*, 1989; Whittle & Lopez-Belmonte, 1991).

The involvement of endogenous prostaglandins in the modulation of mucosal integrity is suggested by the enhanced susceptibility of the gastric mucosa to challenge following treatment with indomethacin and other cyclo-oxygenase inhibitors (Whittle, 1983; Whittle & Vane, 1987). In addition, it is well-established that naturally-occuring prostaglandins and their synthetic analogues can potently protect against most forms of experimental gastric damage, although their mechanisms of action are complex and not clearly defined (Robert, 1976; Whittle, 1976; Robert *et al.*, 1979; Guth *et al.*, 1984; Henagan *et al.*, 1984; Whittle & Steel, 1985; Whittle & Vane, 1987).

The acute mucosal damage induced by indomethacin is augmented in capsaicin-pretreated rats, suggesting interactions between endogenous prostanoids and sensory neuropeptides (Holzer & Sametz, 1986; Whittle *et al.*, 1990). In the present study, the interactions of these local mediators in the processes by which the gastric mucosa can resist challenge and injury, have been further explored. Thus, the dependence on endogenous sensory neuropeptides of a prostaglandin E_2 analogue (16, 16, dimethyl PGE_2) to exert its protective actions against ethanol challenge, has been investigated by use of opioids and capsaicin treatment to modulate their release in the rat.

Methods

Induction and assessment of mucosal damage

Male Wistar rats (220–260 g body weight) were deprived of food, but not water, for 18–20 h before the experiment. One ml of ethanol (50% or 100% v/v in saline) or saline alone was administered orally by gavage, and the rats killed by cervical dislocation 5 min later. The stomachs were opened, pinned to a wax block immersed in neutral buffered formalin and photographed on colour transparency film.

The extent of macroscopically visible damage was subsequently determined from these slides in a randomized fashion via computerised planimetry. The area of mucosal damage was calculated as the % of the total gastric mucosal area showing macroscopically visible damage. The extent of macroscopic damage in both the corpus and antral regions

[1] Author for correspondence.

was also expressed as a % of the area of these individual regions.

Effects of 16, 16 dimethyl PGE_2

16, 16-dimethyl PGE_2 ($dmPGE_2$; 0.5, 1, 5 or 20 $\mu g\,kg^{-1}$), in doses chosen from previous studies (Whittle & Steel, 1985) or saline (1 $ml\,kg^{-1}$) was administered orally by gavage 10 min before challenge with intragastric ethanol. Macroscopic damage of the gastric mucosa was assessed as described above, 5 min after ethanol challenge.

Effects of morphine and opioid antagonists

Morphine (9 $mg\,kg^{-1}$) or saline (1 $ml\,kg^{-1}$) was injected into the tail vein 15 min before the intragastric challenge with ethanol. This dose of morphine has been shown in previous studies to induce a consistent near-maximal potentiation of ethanol-induced gastric damage in the rat (Esplugues & Whittle, 1990). Macroscopic mucosal damage was assessed 5 min after challenge.

In a further series of experiments, rats were pretreated with the opioid antagonists naloxone (1 $mg\,kg^{-1}$, i.v.) or N-methyl-nalorphine (6 $mg\,kg^{-1}$, i.v.) 5 min before the administration of morphine, in doses derived from previous studies in the rat (Esplugues & Whittle, 1990). Macroscopic damage was assessed 5 min after intragastric ethanol challenge.

Effects of pretreatment with capsaicin

Adult rats (190–220 g) were treated with capsaicin for three consecutive days (20, 30 and 50 $mg\,kg^{-1}$, s.c.). This regimen has been shown to lead to functional ablation of primary afferent neurones (see Holzer, 1988; 1991). All capsaicin injections were administered under halothane anaesthesia and, to counteract the respiratory impairment associated with the administration of capsaicin, the rats were pretreated with terbutaline (0.1 $mg\,kg^{-1}$, i.m.) and aminophylline (10 $mg\,kg^{-1}$, i.m.) prior to capsaicin injection. Control rats received a similar regimen with the capsaicin vehicle.

Two weeks after completion of the capsaicin treatment, $dmPGE_2$ (0.5, 1 or 20 $\mu g\,kg^{-1}$) or saline (1 $ml\,kg^{-1}$), was administered by gavage 10 min before intragastric ethanol challenge (50 or 100%, 1 ml) and the gastric damage was assessed 5 min later.

Histological assessment of mucosal damage

Two 1.5 × 0.5 cm segments of the corpus mucosa were excised from standardized areas of the stomach with tissue from both the dorsal and ventral aspects of the mid-corpus region being obtained 0.5 cm below the forestomach limiting ridge. Following processing by routine techniques and embedding in paraffin, the sections (4 μm) were stained with haematoxylin and eosin and examined under a light microscope.

The 1.5 cm length of each histological section was assessed for vasocongestion or haemorrhagic damage in the upper third of the mucosa (Type 1 damage); glandular disruption, vasocongestion or oedema in the mid mucosa (Type 2 damage); and haemorrhagic damage and necrosis in the lower mucosa (Type 3 damage). In this study, epithelial cell damage induced by ethanol and the various treatments was not separately assessed, since previous studies have shown it is affected by prostaglandin pretreatment only at high doses (Lacy & Ito, 1982; Whittle & Steel, 1985). All determinations were performed in a randomized manner with the histological sections coded to eliminate observer bias. The length of each section exhibiting each type of damage was expressed as a % of the total section length, and the mean value for the two sections of each corpus mucosa was calculated.

Drugs

Morphine hydrochloride (MacFarlane Smith, Edinburgh, U.K.) naloxone hydrochloride (Endo Labs, New York, U.S.A.), 16, 16-dimethyl PGE_2 (stored in absolute ethanol, Cayman Chemicals, MI, U.S.A.), aminophylline (Sigma Chemical Co., Poole, Dorset), terbutaline sulphate (Astra, Kings Langley, U.K.) and N-methyl-nalorphine (synthesized in the Dept. of Medicinal Chemistry, Wellcome Research Labs.) were dissolved in isotonic saline immediately before use. Capsaicin (Fluka Chemic AG Buchi, Switzerland) was prepared in a 50 $mg\,ml^{-1}$ solution containing absolute ethanol, Tween 80 and isotonic saline (10:10:80 v/v/v). Ethanol (analar; B.D.H. Poole, Dorset) was diluted with saline as appropriate.

Statistical analysis

All data are expressed as the mean ± s.e.mean. Comparisons between groups of parametric data were made by Student's *t* test for unpaired data. Comparisons between groups of non-parametric data (histological evaluation) were made by the Mann-Whitney U-test. *P* values of less than 0.05 were taken as significant.

Results

Effects of 16, 16-dimethyl PGE_2 on ethanol-induced mucosal damage

Intragastric challenge with 1 ml of ethanol (50 or 100%) for 5 min induced a concentration-dependent degree of macroscopically assessed mucosal injury. Intragastric administration of ethanol (100%) resulted in macroscopic damage involving 40 ± 6% ($n = 17$) of the total mucosal area (Figure 1). This damage was of a haemorrhagic nature and located both in the corpus and antral regions (Table 1). Likewise, intragastric challenge with 50% ethanol induced mucosal damage (Figure 2) that occurred in both corpus and antral

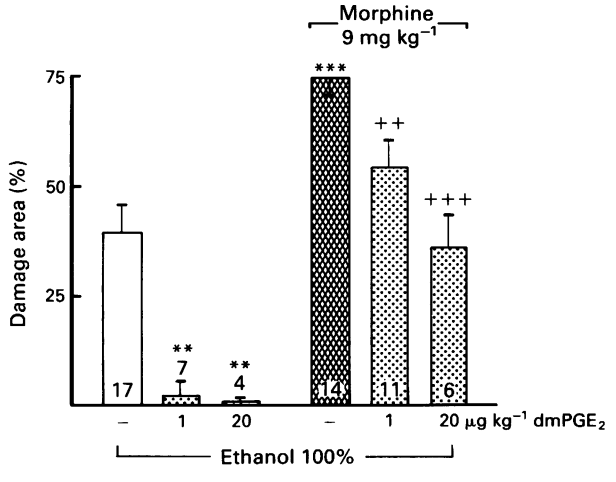

Figure 1 Effects of pretreatment with 16,16-dimethyl prostaglandin E_2 ($dmPGE_2$, 1 and 20 $\mu g\,kg^{-1}$, p.o.) on the gastric mucosal damage induced by the intragastric administration of 100% ethanol (1 ml) alone, or in combination with morphine (9 $mg\,kg^{-1}$, i.v.). Results, shown as the % of the total mucosal area that exhibited macroscopically assessed damage, 5 min after challenge, are the mean with s.e.mean (vertical bars) of (*n*) experiments in each group. Significant difference from the control (ethanol-alone) group is given as $^{**}P<0.01$ and $^{***}P<0.001$, and from the corresponding ethanol and morphine group as $\dagger\dagger P<0.01$ and $\dagger\dagger\dagger P<0.001$. The inhibitory effects of $dmPGE_2$ (1 and 20 $\mu g\,kg^{-1}$) against ethanol-induced mucosal damage were significantly less ($P<0.001$ for both) in rats treated concurrently with morphine.

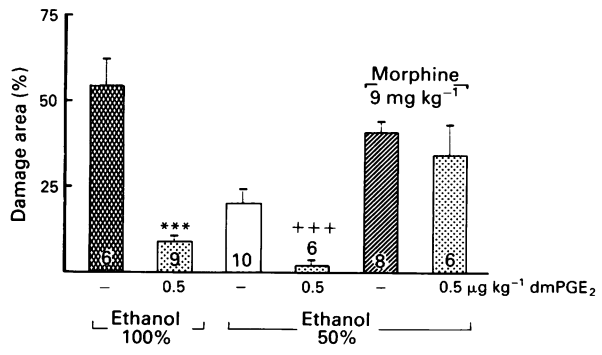

Figure 2 Effects of pretreatment with 16, 16-dimethyl prostaglandin E_2 ($dmPGE_2$, 0.5 μg kg^{-1}, p.o.) on the gastric mucosal damage induced by the intragastric administration of ethanol (50% or 100%, 1 ml) alone, or in combination with morphine (9 mg kg^{-1}, i.v.). Results, shown as the % of the total mucosal area that exhibited macroscopically assessed damage, 5 min after challenge, are the mean with s.e.mean (vertical bars) of (n) experiments in each group. Significant difference from the respective control ethanol group is given as ***$P<0.001$; †††$P<0.001$. The inhibitory effects of $dmPGE_2$ against ethanol (50%)-induced damage were significantly less ($P<0.01$) in rats treated concurrently with morphine.

Table 1 Effect of morphine administration or capsaicin pretreatment on prostaglandin protection of different regions of the rat gastric mucosa

	Damage (% area)		
	Corpus	*Antrum*	*(n)*
Ethanol (100%)	31 ± 7	32 ± 7	(12)
+ $dmPGE_2$	5 ± 1**	11 ± 4*	(14)
Ethanol (50%)	19 ± 4	14 ± 5	(10)
+ $dmPGE_2$	2 ± 1**	1 ± 1**	(9)
Ethanol (50%)			
+ morphine	35 ± 4†	37 ± 6†	(11)
+ morphine + $dmPGE_2$	26 ± 6	32 ± 9	(9)
Ethanol (50%)			
+ capsaicin	30 ± 5†	47 ± 13†	(5)
+ capsaicin + $dmPGE_2$	10 ± 2*	21 ± 8	(5)

The data show mucosal damage in the antral and corpus regions of the rat stomach following a 5 min intragastric challenge with 50% or 100% ethanol (1 ml) and the effects of administration of 16,16-dimethyl prostaglandin E_2 ($dmPGE_2$, 0.5 μg kg^{-1}, p.o.) morphine (9 mg kg^{-1}, i.v.) or capsaicin pretreatment.

Results, shown as the % of the mucosal area of the antrum or of the corpus that exhibited macroscopic damage, are the mean ± s.e.mean of (n) experiments in each group. Significant difference between the ethanol-challenged groups treated with vehicle and those treated with $dmPGE_2$ are shown as *$P<0.05$, **$P<0.01$. The significant increase in ethanol (50%)-induced damage by morphine or capsaicin treatment in both regions is shown as †$P<0.05$.

regions of the mucosa (Table 1). Gastric mucosal damage was not observed in any rat receiving only intragastric administration of 1 ml saline ($n = 5$).

Intragastric pretreatment with $dmPGE_2$ (1 or 20 μg kg^{-1}) near-maximally inhibited ($P<0.01$ for both) the macroscopic damage induced by intragastric instillation of 100% ethanol (Figure 1). Lower doses of $dmPGE_2$ (0.5 μg kg^{-1}) likewise caused significant inhibition (85 ± 5%, $n = 5$; $P<0.01$) of the mucosal damage induced by ethanol (100%), and near-maximally inhibited that induced by ethanol (50%), as shown in Figure 2. Inhibition of ethanol-induced macroscopic damage by $dmPGE_2$ (0.5 μg kg^{-1}), was seen in both the corpus and antral regions of the mucosa (Table 1). Administration of $dmPGE_2$ (20 μg kg^{-1}) alone did not cause any macroscopically detectable damage to the rat gastric mucosa ($n = 5$).

Effects of pretreatment with morphine

The area of damage induced by 100% ethanol was significantly ($P<0.001$) increased to 74 ± 4% ($n = 14$) of the gastric mucosa by pretreatment (15 min) with morphine (9 mg kg^{-1}, i.v.), as shown in Figure 1. Pretreatment with this dose of morphine alone did not cause any macroscopically detectable damage to the rat gastric mucosa ($n = 5$).

Under such conditions of morphine pretreatment, administration of $dmPGE_2$ (1 μg kg^{-1}, p.o.) did not substantially inhibit the degree of damage induced by ethanol challenge (Figure 1). Furthermore, following morphine administration, the reduction of ethanol-induced damage by $dmPGE_2$ (20 μg kg^{-1}) was markedly attenuated (from 99 ± 1%, $n = 7$ to 54 ± 6%, $n = 6$, $P<0.001$), as shown in Figure 1.

Since the reduced ability of $dmPGE_2$ to inhibit the damage induced by 100% ethanol following pretreatment with morphine could have reflected the increased extent of mucosal damage, further studies were conducted with a lower ethanol concentration under similar conditions. Thus, pretreatment with morphine (9 mg kg^{-1}, i.v.) augmented the area of damage induced by intragastric challenge with 50% ethanol to a level not significantly different from that observed with 100% ethanol alone (Figure 2). However, even under these conditions, $dmPGE_2$ (0.5 μg kg^{-1}, p.o.) did not significantly inhibit damage caused by 50% ethanol following morphine pretreatment, although damage induced by intragastric challenge with 50% or 100% ethanol alone was reduced by 85% and 98% respectively ($P<0.001$ for both) as shown in Figure 2. This ablation of the protective actions of $dmPGE_2$ (0.5 μg kg^{-1}) by morphine pretreatment was observed in both the corpus and antral regions of the mucosa (Table 1).

In further studies, 5 min pretreatment (i.v.) with either the opioid antagonist naloxone (1 mg kg^{-1}), which acts on both central and peripheral opioid receptors, or N-methyl nalorphine (6 mg kg^{-1}), a peripherally acting quaternary opioid receptor antagonist, restored the protective effects of $dmPGE_2$ (0.5 μg kg^{-1}) as shown in Figure 3. Neither naloxone nor N-methyl nalorphine significantly affected the area of damage induced by 50% ethanol alone ($n = 4$ for each, data not shown).

Effects of pretreatment with capsaicin

Capsaicin pretreatment, 2 weeks before the study, significantly ($P<0.01$) increased the area of macroscopic damage induced by the intragastric administration of 50 or 100% ethanol (Table 1 and Figure 4 respectively). Gastric damage was not observed in capsaicin-pretreated animals receiving a similar intragastric volume (1 ml) of saline ($n = 4$). The increase in ethanol-induced mucosal damage by capsaicin pretreatment was seen in both the corpus and antral regions (Table 1).

Pretreatment (10 min) with $dmPGE_2$ (1 μg kg^{-1}, p.o.) near-maximally inhibited the macroscopically assessed mucosal damage induced by 100% ethanol in control vehicle-pretreated rats, as shown in Figure 4. However, in capsaicin-pretreated rats, the effects of $dmPGE_2$ (1 μg kg^{-1}) were significantly ($P<0.001$) attenuated (Figure 4). Furthermore, under these conditions, even high doses of $dmPGE_2$ (20 μg kg^{-1}) failed to abolish this macroscopic damage (Figure 4).

Further studies were conducted to ensure that the reduced protection by $dmPGE_2$ in capsaicin-pretreated rats was not simply a reflection of the higher degree of mucosal damage induced by ethanol challenge. Thus, the level of damage induced by intragastric 50% ethanol in capsaicin-pretreated rats was not significantly different from that induced by 100% ethanol in vehicle-pretreated animals (Figure 5).

Administration of $dmPGE_2$ (0.5 $\mu g\ kg^{-1}$) near-maximally inhibited the mucosal damage induced by challenge with 100% ethanol alone, whereas in capsaicin-pretreated rats, there was a significant attenuation of the protective actions of $dmPGE_2$ against challenge with 50% ethanol (Figure 5), which was observed in both corpus and antral mucosal regions (Table 1).

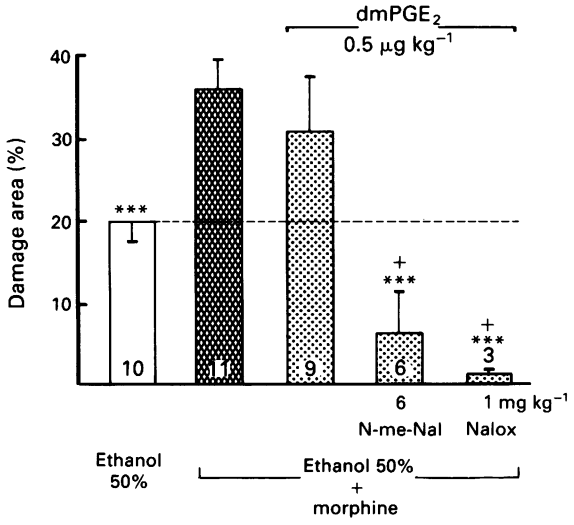

Figure 3 Pretreatment with the opioid antagonist naloxone (1 mg kg^{-1}, i.v.) and the peripherally acting antagonist, N-methyl nalorphine (N-me-Nal 6 mg kg^{-1}, i.v.) restores the protective effect of 16, 16-dimethyl prostaglandin E_2 ($dmPGE_2$, 0.5 $\mu g\ kg^{-1}$, p.o.) against gastric mucosal damage induced by 50% ethanol (1 ml, p.o.) in rats treated with morphine (9 mg kg^{-1}, i.v.). Results, shown as the % of the total mucosal area that exhibited macroscopically assessed damage 5 min after challenge, are the mean with s.e.mean (vertical bars) of (n) experiments in each group. Significant difference from the control ethanol-morphine group is given as $^{***}P<0.001$, and from the ethanol, morphine and $dmPGE_2$ group as $\dagger P<0.001$.

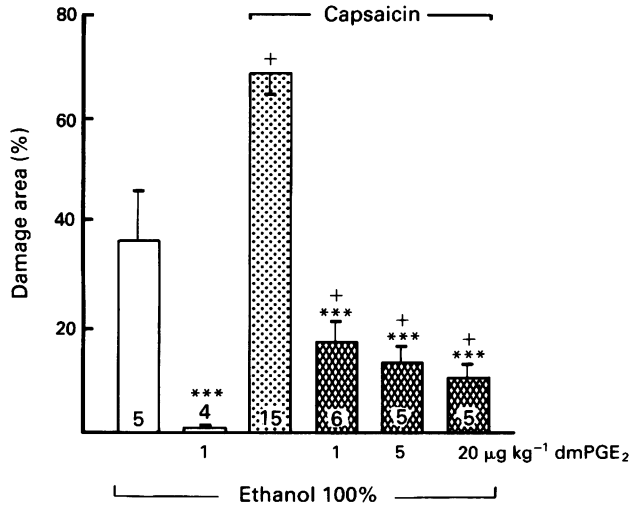

Figure 4 Effects of 16, 16-dimethyl prostaglandin E_2 ($dmPGE_2$ 1, 5 and 20 $\mu g\ kg^{-1}$, p.o.) on the gastric mucosal damage induced by the intragastric administration of 100% ethanol (1 ml), in control or capsaicin-pretreated rats. Results, shown as the % of the total mucosal area that exhibited macroscopically assessed damage, 5 min after challenge, are the mean with s.e.mean (vertical bars) of (n) experiments in each group. Significant difference from the control (ethanol-alone) group is given as $^{***}P<0.001$ and from the corresponding ethanol or ethanol-capsaicin group as $\dagger P<0.01$.

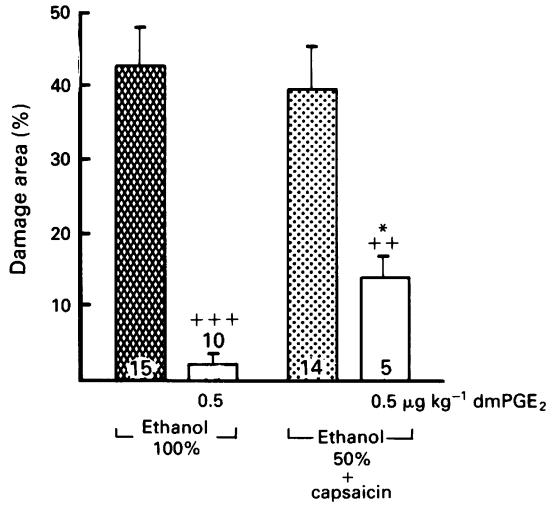

Figure 5 Effects of pretreatment with 16, 16-dimethyl prostaglandin E_2 ($dmPGE_2$, 0.5 $\mu g\ kg^{-1}$, p.o.) on the gastric mucosal damage induced by the intragastric administration of 100% ethanol (1 ml) alone, or 50% ethanol in capsaicin pretreated rats. Results, shown as the % of the total mucosal area that exhibited macroscopically assessed damage, 5 min after challenge, are the mean with s.e.mean (vertical bars) of (n) experiments in each group. Significant difference from the respective control ethanol-challenge group is given $\dagger\dagger P<0.01$ or $\dagger\dagger\dagger P<0.001$, and between prostaglandin treated groups as $^{*}P<0.01$.

Histological assessment of gastric damage

Intragastric administration of 100% ethanol (1 ml) caused damage to the upper (Type 1 damage) and, mid (Type 2 damage) regions of the mucosa, accompanied by Type 3 damage (characterized as deep haemorrhagic damage and necrosis), as shown in Table 2. Administration of $dmPGE_2$ (0.5 $\mu g\ kg^{-1}$) reduced the level of histological damage after challenge with 100% ethanol to values similar to those of the non-challenged control group receiving intragastric saline (Table 2).

Rats treated with morphine (9 mg kg^{-1}) or pretreated with capsaicin prior to challenge with 50% ethanol showed levels of histologically assessed damage similar to that following challenge with 100% ethanol alone (Table 2). Pretreatment with either morphine or capsaicin alone did not significantly modify the extent of Type 1, 2 or 3 damage compared to vehicle control groups in the absence of ethanol challenge (Table 2).

Following pretreatment with morphine (9 mg kg^{-1}), $dmPGE_2$ (0.5 $\mu g\ kg^{-1}$) failed to reduce significantly the degree of Type 1, Type 2 and Type 3 damage induced by 50% ethanol (Table 2). Likewise, in capsaicin-pretreated rats, the protective effects of $dmPGE_2$ (0.5 $\mu g\ kg^{-1}$) against Type 1, 2 and 3 damage induced by 50% ethanol were substantially less than its actions against the mucosal damage induced by 100% ethanol alone (Table 2).

Discussion

The present study demonstrates that morphine administration or capsaicin pretreatment, which alone do not induce detectable damage to the gastric mucosa, potentiated the mucosal injury following a 5 min challenge with intragastric ethanol, confirming previous studies (Esplugues & Whittle, 1990). Since capsaicin administration depletes sensory neuropeptides from afferent sensory neurones (Holzer, 1988; 1991), while morphine can affect capsaicin-sensitive neurones and inhibit neuropeptide release (Bartho & Szolcsanyi, 1981; Lembeck & Donnerer, 1985; Mantelli *et al.*, 1989) these

Table 2 Histological assessment of the effect of morphine administration or capsaicin-pretreatment on prostaglandin protection of the rat gastric mucosa

	Histological damage type (% total length)			
	1	*2*	*3*	*(n)*
Control	3 ± 2	0	0	(4)
Morphine	2 ± 3	0	0	(6)
Capsaicin	5 ± 3	0	0	(4)
Ethanol (100%)	85 ± 7	47 ± 7	18 ± 8	(7)
Ethanol (100%) + $dmPGE_2$	9 ± 3***	3 ± 3**	0***	(8)
Ethanol (50%) + morphine	79 ± 9	55 ± 6	21 ± 3	(15)
Ethanol (50%) + morphine + $dmPGE_2$	66 ± 5	47 ± 4	19 ± 3	(6)
Ethanol (50%) + capsaicin	89 ± 5	60 ± 5	26 ± 8	(14)
Ethanol (50%) + capsaicin + $dmPGE_2$	43 ± 7†	23 ± 4†	6 ± 2††	(5)

The influence of morphine (9 mg kg^{-1}, i.v.) or capsaicin pretreatment on the histologically assessed protective effects of 16, 16-dimethyl prostaglandin E_2 ($dmPGE_2$; 0.5 μg kg^{-1}, p.o.) on gastric mucosal damage induced by a 5 min intragastric challenge with ethanol (50 or 100%) is shown.

The data are expressed as the length of section exhibiting damage of varying degrees, Type 1 (vasocongestion or haemorrhagic damage in the upper mucosa), Type 2 (glandular disruption and haemorrhagic damage in the mid mucosa) and Type 3 (deeper haemorrhage and necrosis), expressed as % of total section length. Results are given as mean ± s.e.mean of (*n*) values, where statistically significant difference from the ethanol 100% group is shown as $^{**}P<0.01$, $^{***}P<0.001$ and difference from the 50% ethanol with capsaicin as $^{\dagger}P<0.05$, $^{\dagger\dagger}P<0.05$.

findings support the concept that such endogenous sensory neuropeptides play an important role in the regulation of mucosal protection against challenge (Szolcsanyi & Bartho, 1981; Holzer & Sametz, 1986; Esplugues *et al.*, 1989). Furthermore, the present findings demonstrate that the protection of the gastric mucosa by the prostaglandin analogue 16,16-dimethyl PGE_2 ($dmPGE_2$) is also modulated by capsaicin or morphine administration, implicating a role for endogenous sensory neuropeptides in its mechanism of action. In other studies, morphine has likewise been shown to attenuate the mucosal protection elicited by PGE_2 (Esplugues & Whittle, 1991).

The enhanced mucosal injury induced by morphine and capsaicin pretreatment, observed macroscopically, in both antral and corpus regions, was characterized histologically as an increase in vasocongestion, haemorrhage and glandular disruption. With such techniques, it was demonstrated by varying the concentration of the intragastric ethanol, that the attenuation by capsaicin and morphine of the protective actions of $dmPGE_2$ was not a result of the enhanced degree of damage. These actions of morphine were abolished by the opioid μ receptor antagonist naloxone and by the peripherally acting N-methyl nalorphine, consistent with an action of morphine on peripheral sensory neurones (Ferreira & Nakamura, 1979; Smith & Buchan, 1984; Esplugues & Whittle, 1990). However, although both morphine and capsaicin treatment augmented mucosal damage to a comparable degree, morphine was more effective than capsaicin pretreatment in attenuating the mucosal protective actions of $dmPGE_2$. This may reflect the ability of morphine to affect additional processes other than those that are capsaicin-sensitive. Thin unmyelinated C-fibres are primarily susceptible to the actions of capsaicin pretreatment in adult rats leading to neuropeptide depletion (Holzer, 1988; 1991), while morphine can not only prevent neuropeptide release from such neurones, but can also modulate the excitability of other sensory neurones such as A-delta afferents (Sastry, 1978). Additional effects of morphine through actions on opioid receptors located on other tissues or cells cannot, however, be excluded.

The processes involved in the interactions between prostanoids and sensory neurones in the gastric mucosa are not clear. However, it is known that PGE_2 potently stimulates afferent vagal C-fibres in the lungs after a single systemic exposure in the cat (Coleridge *et al.*, 1976; 1978). In rat skin, capsaicin-pretreatment reduces the oedema induced by intracutaneous injection of PGE_1, (Arvier *et al.*, 1979), while morphine inhibits the acute hyperalgesic actions of PGE_2 on cutaneous sensory neurones (Ferreira & Nakamura, 1979). Furthermore, a long lasting hyperalgesia action in the rat paw is induced by multiple intraplantar injections of PGE_2 or prostacyclin which reflects actions on sensory nerves (Nakamura-Craig & Smith, 1989). PGE_2 can also activate a capsaicin-sensitive reflex micturition in the rat (Maggi *et al.*, 1988). Since capsaicin-sensitive vagal afferent fibres are known to influence gastric function (Raybould & Tache, 1989; Esplugues *et al.*, 1990; Thiefin *et al.*, 1990), it is pertinent that earlier studies have demonstrated that vagotomy could abolish the protective actions of $dmPGE_2$ against ethanol-induced challenge (Henagan *et al.*, 1984).

The mechanisms underlying the protective actions of prostanoids in the stomach are complex, but local vascular actions are strongly implicated (Robert, 1981; Whittle & Vane, 1987). While direct vasodilator actions on the gastric mucosa by PGE_2, prostacyclin and their analogues may play a role (Whittle & Vane, 1987), prostanoids have also been shown to prevent stasis in the microcirculation following challenge by ethanol (Guth *et al.*, 1984; Pihan *et al.*, 1986), perhaps by altering cellular interactions within the microvasculature and preventing endothelial cell damage. Capsaicin-sensitive sensory neurones are located in close association with the submucosal vessels that regulate mucosal blood flow (Sharkey *et al.*, 1984; Ekblad *et al.*, 1985; Sternini *et al.*, 1987; Su *et al.*, 1987; Green & Dockray, 1988) while functional ablation of such neurones with capsaicin or morphine augments the detrimental microvascular changes following intravascular challenge (Pique *et al.*, 1990). Furthermore, sensory neuropeptide release induced by capsaicin, or close arterial infusion of CGRP, which protect against mucosal injury (Holzer & Lippe, 1988; Lippe & Holzer, 1989; Whittle & Lopez-Belmonte, 1991), also can elevate mucosal blood flow (Holzer *et al.*, 1991; Holzer & Guth, 1991) although it is possible that sensory neuropeptides can exert a direct action on the endothelium, preventing microvascular injury in the mucosa. Although not abolished, the protective actions of even high doses of $dmPGE_2$ were substantially attenuated by morphine or capsaicin treatment, and it is therefore feasible that sensory neuronal activation and neuropeptide release contribute to the vascular actions of prostanoids involved in the mucosal protective processes.

Endogenous prostanoids do not appear to be directly involved in the protective actions of endogenous sensory

neuropeptides since cyclo-oxygenase inhibition by indomethacin or aspirin did not modulate the protection following acute intragastric capsaicin administration (Holzer & Sametz, 1986; Holzer *et al.*, 1990). However, recent studies suggest that an inhibitor of NO biosynthesis can reduce the protective actions of such acute capsaicin application (Peskar *et al.*, 1991), which is consistent with the actions of L-NMMA in attenuating the cardiovascular actions of CGRP (Whittle, 1990). Furthermore, the reduction in resting gastric mucosal blood flow induced by L-NMMA (Pique *et al.*, 1989; 1992) or N^G-nitro-L-arginine methyl ester is substantially enhanced by capsaicin pretreatment, indicating an interactive role of endogenous neuropeptides and NO in the mucosal microcirculation (Whittle & Tepperman, 1991; Tepperman & Whittle, 1992). The present findings that gastric mucosal protection by an E-type prostaglandin can be modulated by sensory neuronal mechanisms thus further re-inforce the concept of interactions between sensory neuropeptides and prostanoids, which together with NO are involved in the regulation of mucosal integrity (Whittle *et al.*, 1990).

References

ARVIER, P.T., CHAL, L.A. & LADD, R.J. (1977). Modification by capsaicin and compound 48/80 of dye leakage induced by irritants in the rat. *Br. J. Pharmacol.*, **59**, 61–68.

BARTHO, L. & SZOLCSANYI, J. (1981). Opiate agonists inhibit neurogenic plasma extravasation in the rat. *Eur. J. Pharmacol.*, **73**, 101–104.

COLERIDGE, H.M., COLERIDGE, J.C.G., BAKER, D.G., GINZEL, K.H. & MORRISON, M.A. (1978). Comparison of the effects of histamine and prostaglandin on afferent C-fiber endings and irritant receptors in the intrapulmonary airways. *Adv. Exp. Med. Biol.*, **99**, 291–305.

COLERIDGE, H.M., COLERIDGE, J.C.G., GINZEL, K.H., BAKER, D.G., BANZETT, R.B. & MORRISON, M.A. (1976). Stimulation of 'irritant' receptors and afferent C-fibres in the lungs by prostaglandins. *Nature*, **264**, 451–453.

EKBLAD, E., EKEBLUND, M., GRAFFNER, H., HAKANSON, R. & SUNDLER, F. (1985). Peptide-containing nerve fibres in the stomach wall of rat and mouse. *Gastroenterology*, **89**, 73–85.

ESPLUGUES, J.V., RAMOS, E.G., GIL, L. & ESPLUGUES, J. (1990). Influence of capsaicin-sensitive afferent neurones on the acid secretory responses of the rat stomach *in vivo*. *Br. J. Pharmacol.*, **100**, 491–496.

ESPLUGUES, J.V. & WHITTLE, B.J.R. (1990). Morphine potentiation of ethanol-induced gastric mucosal damage in the rat. *Gastroenterology*, **98**, 82–89.

ESPLUGUES, J.V. & WHITTLE, B.J.R. (1991). Peripheral opioid-sensitive mechanisms of mucosal injury and protection. In *Mechanisms of Injury, Protection and Repair of the Upper Gastrointestinal Tract*. ed. Garner, A. & O'Brien, P.E. pp. 115–125, Chichester: John Wiley & Sons.

ESPLUGUES, J.V., WHITTLE, B.J.R. & MONCADA, S. (1989). Local opioid-sensitive afferent sensory neurones in the modulation of gastric damage induced by PAF. *Br. J. Pharmacol.*, **97**, 579–585.

FERREIRA, S.H. & NAKAMURA, M. (1979). II-Prostaglandin hyperalgesia: the peripheral analgesic activity of morphine, enkephalines and opioid antagonists. *Prostaglandins*, **18**, 191–200.

GREEN, T. & DOCKRAY, G.J. (1988). Characterization of the peptidergic afferent innervation of the stomach in the rat, mouse and guinea-pig. *Neuroscience*, **25**, 181–193.

GUTH, P.H., PAULSEN, G. & NAGATA, H. (1984). Histologic and microcirculatory changes in alcohol-induced gastric lesions in the rat: effect of prostaglandin cytoprotection. *Gastroenterology*, **87**, 1083–1090.

HENAGAN, M., SMITH, S., SEIDEL, E. & MILLER, A.T. (1984). Influence of vagotomy on mucosal protection against alcohol-induced gastric damage in the rat. *Gastroenterology*, **87**, 903–908.

HOLZER, P. (1988). Local effector functions of capsaicin-sensitive sensory nerve endings: involvement of tachykinins, calcitonin gene-related peptide and other neuropeptides. *Neuroscience*, **24**, 739–768.

HOLZER, P. (1991). Capsaicin: Cellular targets, mechanism of action, and selectivity for thin sensory neurones. *Pharmacol. Rev.*, **43**, 143–201.

HOLZER, P. & GUTH, P.H. (1991) Neuropeptide control of rat gastric mucosal blood flow: increase by calcitonin gene-related peptide and vasoactive intestinal polypeptide, but not substance P and neurokinin A. *Circ. Res.*, **68**, 100–105.

HOLZER, P. & LIPPE, I.Th. (1988). Stimulation of afferent nerve endings by intragastric capsaicin protect against ethanol-induced damage of gastric mucosa. *Neuroscience*, **27**, 981–987.

HOLZER, P., LIVINGSTON, E.H., SARIA, A. & GUTH, P.H. (1991). Sensory neurones mediate protective vasodilatation in rat gastric mucosa. *Am. J. Physiol.*, **260**, G363–G370.

HOLZER, P., PABST, M.A., LIPPE, I.Th., PESKAR, B.M., PESKAR, B.A., LIVINGSTON, E.H. & GUTH, P.H. (1990). Afferent nerve-mediated protection against deep mucosal damage in the rat stomach. *Gastroenterology*, **98**, 838–848.

HOLZER, P. & SAMETZ, W. (1986). Gastric mucosal protection against ulcerogenic factors in the rat mediated by capsaicin-sensitive afferent neurones. *Gastroenterology*, **91**, 975–991.

LACY, E.R. & ITO, S. (1982). Microscopic analysis of ethanol damage to the rat gastric mucosa after treatment with a prostaglandin. *Gastroenterology*, **83**, 619–625.

LEMBECK, F. & DONNERER, J. (1985). Opioid control of the function of primary afferent substance P fibres. *Eur. J. Pharmacol.*, **144**, 241–246.

LIPPE, I.T., LORBACH, M. & HOLZER, P. (1989). Close arterial infusion of calcitonin gene-relate peptide into the rat stomach inhibits aspirin- and ethanol-induced hemorrhagic damage. *Regul. Pept.*, **26**, 35–46.

MAGGI, C.A., GIULIANI, S., CONTE, B., FURIO, M., SANTICIOLI, P., MELI, P., GRAGNANI, L. & MELI, A. (1988). Prostanoids modulate reflex micturition by acting through capsaicin-sensitive afferents. *Eur. J. Pharmacol.*, **145**, 105–112.

MANTELLI, L., AMERINI, S. & LEDDA, F. (1989). Effects of opioid drugs on capsaicin-sensitive neurones in guinea-pig atria. *Eur. J. Pharmacol.*, **170**, 217–223.

NAKAMURA-CRAIG, M. & SMITH, T.W. (1989). Substance P and peripheral inflammatory hyperalgesia. *Pain*, **38**, 91–98.

PESKAR, B.M., RESPONDEK, M., MULLER, K.M. & PESKAR, B.A. (1991). A role of nitric oxide in capsaicin-induced gastroprotection. *Eur. J. Pharmacol.*, **198**, 113–114.

PIHAN, G., MAJZOUBI, D., HOUNDENSCHILD, C., TRIER, J.S. & SZABO, S. (1986). Early microcirculatory stasis in acute gastric mucosal injury in the rat and prevention by 16,16-dimethyl prostaglandin E_2 or sodium thiosulfate. *Gastroenterology*, **91**, 1415–1426.

PIQUE, J.M., ESPLUGUES, J.V. & WHITTLE, B.J.R. (1990). Influence of morphine or capsaicin pretreatment on rat gastric microcirculatory response to PAF. *Am. J. Physiol.*, **258**, G352–G357.

PIQUE, J.M., ESPLUGUES, J.V. & WHITTLE, B.J.R. (1992). Endogenous nitric oxide as a mediator of gastric mucosal vasodilatation during acid secretion. *Gastroenterology*, **102**, 168–174.

PIQUE, J.M., WHITTLE, B.J.R. & ESPLUGUES, J.V. (1989). The vasodilator role of endogenous nitric oxide in the rat gastric microcirculation. *Eur. J. Pharmacol.*, **174**, 293–296.

RAYBOULD, H.E. & TACHE, Y. (1989). Capsaicin-sensitive vagal afferent fibres and stimulation of gastric acid secretion in anaesthetized rats. *Eur. J. Pharmacol.*, **167**, 237–243.

ROBERT, A. (1976). Antisecretory, anti-ulcer, cytoprotective and diarrhoegenic properties of prostaglandins. In *Advances in Prostaglandin and Thromboxane Research*, Vol. 2, ed. Samuelsson, B. & Vane, J.R., pp. 507–520. New York: Raven Press.

ROBERT, A. (1981). Prostaglandins and the gastrointestinal tract. In *Physiology of the Gastrointestinal Tract*. ed. Johnson, L.R., pp. 1407–1434. New York: Raven Press.

ROBERT, A., NEZAMIS, J.E., LANCASTER, C. & HANCHAR, A.J. (1979). Cytoprotection by prostaglandins in rats–Prevention of gastric necrosis produced by alcohol, HCl, NaOH, hypertonic NaCl and thermal injury. *Gastroenterology*, **77**, 433–443.

SASTRY, B.R. (1978). Morphine and met-enkephalin effects on sural A afferent terminal excitability. *Eur. J. Pharmacol.*, **50**, 269–273.

SHARKEY, K.A., WILLIAMS, R.G. & DOCKRAY, G.J. (1984). Sensory substance P innervation of the stomach and pancreas. Demonstration of capsaicin-sensitive sensory neurones in the rat by combined immunohistochemistry and retrograde tracing. *Gastroenterology*, **87**, 914–921.

SMITH, T.W. & BUCHAN, P. (1984). Peripheral opioid receptors on rat saphenous nerve. *Neuropeptides*, **5**, 217–220.

STERNINI, C., REEVE, J.R. & BRECHA, N. (1987). Distribution and characterisation of calcitonin gene-related peptide immunoreactivity in the digestive system of normal and capsaicin-treated rats. *Gastroenterology*, **93**, 852–862.

SU, H.C., BISHOP, A.E., POWER, R.F., HAMADA, Y. & POLAK, J.M. (1987). Dual intrinsic and extrinsic origins of CGRP- and NPY-immunoreative nerves of rat gut and pancreas. *J. Neurosci.*, **7**, 2647–2687.

SZOLCSANYI, J. & BARTHO, L. (1981). Impaired defense mechanism to peptic ulcer in the capsaicin-desensitized rat. In *Gastrointestinal Defense Mechanisms*. ed. Mozsik, Gy., Hanninen, O. & Javor, T. pp. 39–51. Oxford and Budapest: Pergamon Press and Akademiai Kiado.

TEPPERMAN, B.L. & WHITTLE, B.J.R. (1992). Endogenous nitric oxide and sensory neuropeptides interact in the modulation of the rat gastric microcirculation. *Br. J. Pharmacol.*, **105**, 171–175.

THIEFIN, G., RAYBOULD, H.E., LEUNG, F.W., TACHE, Y. & GUTH, P.H. (1990). Capsaicin-sensitive afferent fibres contribute to gastric mucosal blood flow response to electrical vagal stimulation. *Am. J. Physiol.*, **259**, G1037–G1043.

WHITTLE, B.J.R. (1976). Relationship between the prevention of rat gastric erosions and the inhibition of acid secretion by prostaglandins. *Eur. J. Pharmacol.*, **40**, 233–239.

WHITTLE, B.J.R. (1983). The potentiation of taurocholate-induced rat gastric erosions following parenteral administration of cyclooxygenase inhibitors. *Br. J. Pharmacol.*, **80**, 545–551.

WHITTLE, B.J.R. (1990). Role of endogenous nitric oxide in the mechanisms underlying gastric mucosal integrity. In *Nitric oxide from L-Arginine: a Bioregulatory System*. ed. Moncada, S. & Higgs, E.A. pp. 365–371. Amsterdam: Elsevier Science Publishers B.V.

WHITTLE, B.J.R. & LOPEZ-BELMONTE, J. (1991). Interactions between the vascular peptide endothelin-1 and sensory neuropeptides in gastric mucosal injury. *Br. J. Pharmacol.*, **102**, 950–954.

WHITTLE, B.J.R., LOPEZ-BELMONTE, J. & MONCADA, S. (1990). Regulation of gastric mucosal integrity by endogenous nitric oxide: interactions with prostanoids and sensory neuropeptides in the rat. *Br. J. Pharmacol.*, **99**, 607–611.

WHITTLE, B.J.R. & STEEL, G. (1985). Evaluation of the protection of rat gastric mucosa by a prostaglandin analogue using cellular enzyme marker and histologic techniques. *Gastroenterology*, **88**, 315–327.

WHITTLE, B.J.R. & TEPPERMAN, B.L. (1991). Role of endogenous vasoactive mediators, nitric oxide, prostanoids and sensory neuropeptides in the regulation of gastric mucosal blood flow and mucosal integrity. In *Mechanism of Injury, Protection and Repair in the Upper Gastrointestinal Tract*. ed. Garner, A. & O'Brien, P. pp. 127–137. Chichester: John Wiley & Sons.

WHITTLE, B.J.R. & VANE, J.R. (1987). Prostanoids as regulators of gastrointestinal function. In *Physiology of the Gastrointestinal Tract*. ed. Johnston, L.R. (Second Edition)., Vol. 1, pp. 143–180. New York: Raven Press.

(Received January 24, 1992
Revised March 23, 1992
Accepted March 27, 1992)

Br. J. Pharmacol. (1992), **106**, 853–858 © Macmillan Press Ltd, 1992

The nucleotide receptors on mouse C2C12 myotubes

[1]Robert H. Henning, Adriaan Nelemans, Jan van den Akker & Adriaan den Hertog

Department of Pharmacology/Clinical Pharmacology, University of Groningen, Bloemsingel 1, 9713 BZ Groningen, The Netherlands

1 The response of C2C12 mouse myotubes to stimulation with adenosine triphosphate (ATP) and other nucleotides was studied by measuring changes in membrane potential.

2 A transient hyperpolarization followed by a slowly declining depolarization of the cells was observed in the presence of ATP (10 μM– 1 mM).

3 The hyperpolarization was not observed in the absence of external calcium, and was abolished in the presence of tetraethylammonium (20 mM) or the bee toxin, apamin (0.1 μM). The depolarization was reduced under low sodium conditions.

4 A biphasic change in membrane potential was also recorded in the presence of adenosine 5'-O-(3-thiotriphosphate) (ATPγS) and the pyrimidine uridine triphosphate (UTP), while the ATP derivatives and analogues, adenosine diphosphate, adenosine, α,β-methylene ATP and 2-methylthio ATP and the nucleotides, guanosine triphosphate and cytidine triphosphate, did not affect the membrane potential of the myotubes.

5 The hyperpolarization elicited by ATPγS or UTP was also blocked by apamin and abolished under Ca^{2+}-free conditions.

6 In contrast to ATP and ATPγS, the depolarization evoked by UTP was unaffected under low Na^+ and less sensitive to the antagonistic action of suramin.

7 The ATP and UTP responses at maximal concentration were not additive after simultaneous application. ATP elicited a depolarization if applied after UTP, while UTP did not change membrane potential following the application of ATP.

8 The concentration-response curves of the effective nucleotides were shifted to the right in the presence of suramin, suggesting competitive antagonism.

9 These results can be explained by the presence of 'nucleotide receptors' mediating the ATP/UTP-induced hyperpolarization and depolarization in C2C12 myotubes. Furthermore, an increase in Na^+-conductivity can be exclusively activated by ATP.

Keywords: P_2-purinoceptor; ATP; UTP; nucleotide receptor; C2C12 cells; myotubes

Introduction

The action of adenosine triphosphate (ATP) observed in many cell types including myotube, has been ascribed to stimulation of P_2-purinoceptors (Kolb & Wakelam, 1983; Burnstock, 1990). Suramin has been recognized as an antagonist of the P_2-purinoceptor on smooth muscle (Dunn & Blakely, 1988; Den Hertog *et al.*, 1989) and on phaeochromocytoma cells (Nakazawa *et al.*, 1991). Subclassification of the P_2-purinoceptors is based on the relative sensitivity to the various ATP analogues (Burnstock, 1990; Cusack & Hourani, 1990). The ATP-sensitive receptors of *Xenopus* and embryonic chick skeletal muscle, however, appeared to be insensitive to α,β-methylene ATP and 2-methylthio ATP (Igusa, 1988; Hume & Honig, 1986). Recently, a 'nucleotide receptor' was defined showing a similar sensitivity to ATP and to the pyrimidine uridine triphosphate (UTP) (Davidson *et al.*, 1990; O'Connor *et al.*, 1991).

To examine the nature of the receptor involved in stimulation by ATP, the C2C12 mouse skeletal muscle cell line was used (Yaffee & Saxel, 1977). Exponentially proliferating myoblasts can be fused into multinucleated myotubes, which exhibit many of the characteristics of primary skeletal muscle cultures, like the expression of the acetylcholine receptor (Revah *et al.*, 1987), acetylcholinesterase (Inestrosa *et al.*, 1983), creatine kinase (Whitson *et al.*, 1989), phosphofructokinase (Gekakis *et al.*, 1989) and the neural cell adhesion molecule (N-CAM) (Moore *et al.*, 1987). The aim of this study was (1) to establish the response to ATP in these myotubes by measuring changes in membrane potential, (2) to characterize the ATP sensitive receptor site by determining the action of different nucleotides and (3) to examine the action of suramin on the responses induced by the effective nucleotides.

[1] Author for correspondence.

Methods

Cell culture

C2C12 cells, a murine myoblast cell line (Yaffee & Saxel, 1977) were obtained from the American Tissue Type Collection, Rockville, U.S.A. and cultured at 37°C on glass cover slips in Dulbecco's modified essential medium, 7 mM $NaHCO_3$ and 10 mM HEPES (DMEM) supplemented with 10% foetal calf serum. When cells reach 80% confluence, the medium was changed to DMEM supplemented with 5% horse serum. Myotubes were used 7–10 days later.

Electrophysiology

The membrane potential of C2C12 myotubes was measured by the conventional microelectrode technique (Molleman *et al.*, 1989). Experiments were performed at 25°C in a 1 ml bath superfused at a rate of 1.5 ml min^{-1} with a solution containing (mM): NaCl 125, KCl 6, $CaCl_2$ 1.2, $MgCl_2$ 2.5, NaH_2PO_4 1.2, glucose 11, HEPES 10, pH 7.4. In the low Na^+ solution (23 mM), NaCl was replaced with glucamine-

chloride. In the Ca^{2+}-free solution $CaCl_2$ was omitted and EGTA (0.4 mM) and $MgCl_2$ (3.5 mM) were added.

Data analysis

Data are presented as mean ± s.e. and are considered statistically different at $P<0.05$ (unpaired Student's t test). A biphasic response was evoked by the nucleotides, showing a short-lasting hyperpolarization and a slower depolarization. Apamin caused inhibition of the hyperpolarization as described in the Results section. Responses at different agonist concentrations (ATP, UTP, ATPγS) were recorded in the presence of apamin to serve as a series of reference traces showing only the depolarizing phase. To quantify the response in subsequent experiments, the reference depolarizations were used to overlay the biphasic response. The hyperpolarization was quantified as the maximum difference between the actual and the reference response (Figure 1).

Drugs

Adenosine, adenosine 5'-diphosphate (ADP), α,β-methylene adenosine 5'-triphosphate (α,β-meATP), guanosine 5'-triphosphate (GTP), cytidine 5'-triphosphate (CTP) and adenosine 5'-O-(3-thiotriphosphate) (ATPγS) were obtained from Boehringer, Mannheim (Germany). Adenosine 5'-triphosphate (ATP) and uridine 5'-triphosphate (UTP) from Serva, Heidelberg (Germany) and 2-(methylthio) adenosine 5'-triphosphate (2-MeSATP) from Research Biochemicals Inc., Natrick, Mass. (U.S.A.). Suramin was obtained from Bayer, Leverkusen (Germany), tetraethylammonium (TEA) was from Janssen Chimica, Beerse (Belgium) and diltiazem, tetrodotoxin and apamin were from Sigma, St. Louis (U.S.A.).

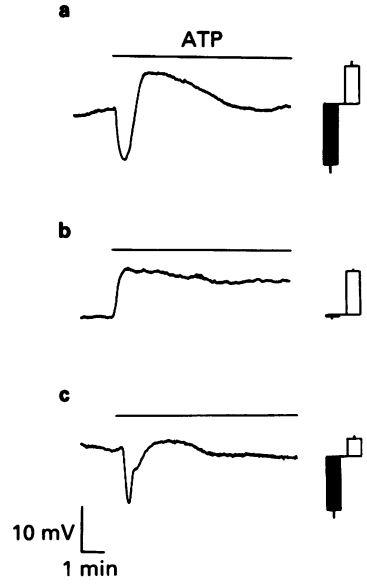

Figure 2 The effect of adenosine 5'-triphosphate (ATP) on the membrane potential of mouse C2C12 myotubes under different experimental conditions. (a) The transient hyperpolarization (downward deflection) and depolarization (upward deflection) evoked by ATP (300 μM). The column represent the maximal amplitude of the hyperpolarization and the depolarization, respectively, determined in 4 different experiments. (b) The response evoked by ATP in the absence of external Ca^{2+} (15 min), only showing depolarization of the cell. (c) The response elicited under low Na^+ (23 mM; 15 min) conditions, causing a marked reduction of the depolarization.

Results

The response to ATP

The membrane potential of C2C12 was about − 55 mV (− 54.8 ± 1.2 mV, $n = 26$). Exposure of the myotubes to ATP (10 μM–1 mM) resulted in a biphasic change in membrane potential, represented by a transient hyperpolarization followed by a depolarization, which declined slowly after reaching a maximum (Figures 2a, 3a). The amplitude of both the hyperpolarization and the depolarization induced by ATP increased at higher agonist concentrations, reaching its maximum value at a concentration of 300 μM (Figure 4). Involvement of the different ions in the development of the biphasic ATP-induced response was investigated by changing the ionic composition of the external solutions or by applying channel blocking agents to the cell. The membrane potential was slightly depolarized after exposure of the cells to Ca^{2+}-free conditions for 15 min (membrane potential: − 50.3 ± 3.4 mV, $n = 8$). Under Ca^{2+}-free conditions, application of ATP induced only the depolarization, the hyperpolarization being abolished (Figure 2b). Further, the decline of the depolarization was extremely slow under these conditions and was not terminated by the withdrawal of ATP, but addition of extracellular Ca^{2+} caused recovery towards the pre-ATP membrane potential. Reduction of the Na^+-gradient across the plasma membrane by lowering the external Na^+ concentration to 23 mM for 15 min depolarized the cells to about − 49 mV (− 48.7 ± 3.4 mV; $n = 6$). Under low Na^+ conditions a 50% reduction of the depolarization evoked by ATP was observed (Figure 2c). The hyperpolarization was still present and remained transient in nature. These Na^+-channels were not sensitive to tetrodotoxin (1 μM; not shown). The ATP-induced response was unaffected by diltiazem (10 μM) added 15 min before agonist addition (not shown), suggesting that the Ca^{2+} entry was not occurring via high threshold, voltage-dependent calcium channels. To reduce the passage via K^+-channels the cells were pretreated (10 min) with TEA^+ (20 mM) before evoking the ATP response. The membrane potential was reduced to − 48.2 ± 1.1 mV ($n = 4$). The hyperpolarization was abolished in the presence of ATP, but the depolarization was still present and was not markedly changed in amplitude compared to the response in the absence of TEA^+ (Figure 3a, b). A similar action on the hyperpolarization to that with TEA^+ was observed in the presence of the bee-toxin apamin (Figure 3c), known to block K^+ channels in certain cells (Den Hertog, 1982; Hugues *et al.*, 1982; Marty, 1983; Traoré *et al.*, 1986). Apamin (0.1 μM) applied for 15 min did not affect the membrane potential, but caused suppression of the ATP-evoked hyperpolarization (Figure 3c).

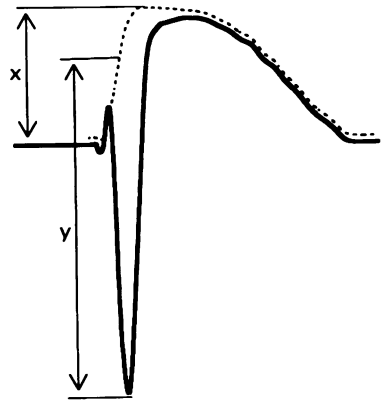

Figure 1 Diagram depicting the analysis of the biphasic response (solid line) evoked by the nucleotides in mouse C2C12 myotubes, using the reference tracing obtained in the presence of apamin (0.1 μM; dashed line). The amplitude of the depolarizing phase is represented by x and of the hyperpolarizing phase by y.

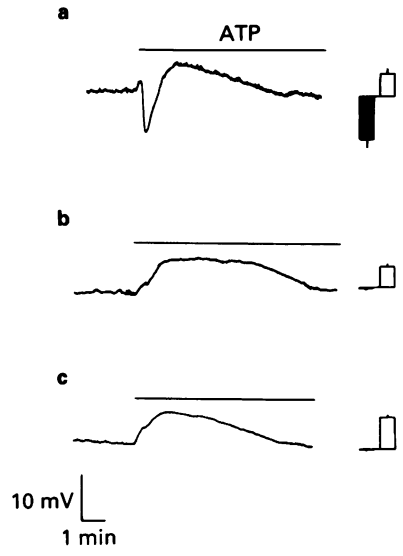

Figure 3 The effect of adenosine 5'-triphosphate (ATP) on the membrane potential under different experimental conditions. (a) The transient hyperpolarization (downward deflection) and depolarization (upward deflection) evoked by ATP (30 μM). The columns represent the maximal amplitude of the hyperpolarization and depolarization, respectively, measured in 4 different experiments. (b) The response evoked by ATP (300 μM) in the presence of tetraethylammonium (15 min; 20 mM), only showing depolarization of the cell. (c) The response elicited in the presence of apamin (15 min, 0.1 μM) showing abolition of the hyperpolarization.

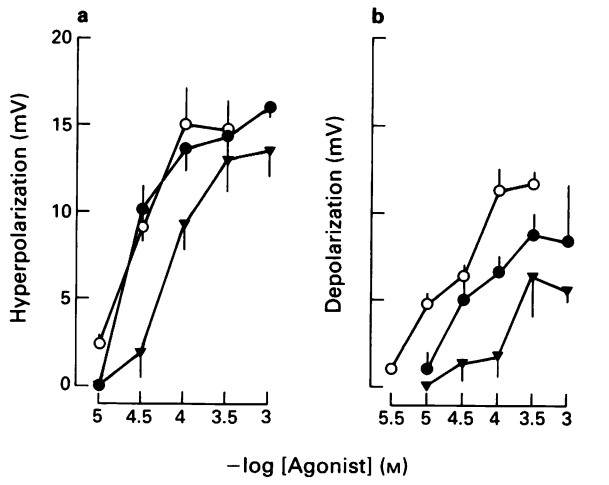

Figure 4 Concentration-dependent changes in membrane potential evoked by the effective nucleotides. The response after stimulation of the cells with adenosine 5'-triphosphate (ATP, ●), adenosine 5'-O-(3-thiotriphosphate) (ATPγS, ○) and uridine triphosphate (UTP, ▼) respectively, is represented by the hyperpolarization (a) and the depolarization (b).

The response to other nucleotides

To characterize the receptor site interacting with ATP, its sensitivity to a variety of ATP derivatives, analogues and other nucleotides was tested. The dephosphorylated metabolites ADP and adenosine, thought to interact with P_2-purinoceptors and P_1-purinoceptors (Cusack & Hourani, 1990), respectively, did not affect the membrane potential of the C2C12 myotubes. The analogues α,β-meATP, considered to act as a potent P_{2x}-purinoceptor agonist and 2-MeSATP, known as a P_{2y}-purinoceptor agonist (Burnstock, 1990; Cusack & Hourani, 1990), did not change the membrane potential either. The stable analogue ATPγS, however, caused a transient hyperpolarization and a pronounced depolarization, components which were also observed with ATP (Figures 5a,b). It was noticed that the decline of the depolarization is slower in the presence of ATPγS. The ATPγS induced hyperpolarization was abolished in the presence of apamin (0.1 μM; Figure 5a) and the depolarization was suppressed under low-Na^+ conditions as was the ATP-induced response (not shown). GTP did not change the membrane potential significantly, while cytidine triphosphate (CTP) produced only a small depolarization (1.0 ± 0.3 mV, $n = 4$). The pyrimidine UTP however, caused effects similar to ATP on C2C12 myotubes (Figure 5b). The transient hyperpolarization observed in the presence of UTP was suppressed completely by apamin (0.1 μM) and under Ca^{2+}-free conditions (not shown). The UTP-evoked depolarization was relatively small but not changed under low-Na^+ conditions, in contrast to the depolarization evoked by ATP (not shown). ATP and ATPγS showed the same potency in evoking a hyperpolarization (EC_{50}: 30 μM), while UTP showed a 4 fold lower potency (EC_{50}: 120 μM; Figure 4). The hyperpolarization evoked by ATPγS was abolished by apamin (0.1 μM). The remaining depolarization obtained in the presence of ATPγS was about twice the amplitude found with UTP (Figure 4).

Thus, the cells were responding with a biphasic change in membrane potential to ATP, ATPγS as well as to UTP. Therefore, the reaction of the cells to subsequent or simultaneous stimulation of the ATP- and UTP-sensitive receptor was investigated. Exposure of the cells to an optimal ATP concentration (300 μM) elicited the expected response, while after reaching the pre-ATP value still in the presence of ATP, subsequent addition of UTP (1 mM) did not affect the membrane potential (Figure 5b). Reversing the experimental procedure showed that cells responded with a small depolarization to ATP if UTP was added in advance (4.1 ± 0.7 mV, $n = 4$). Simultaneous application of both agonists (ATP: 300 μM; UTP: 1 mM) resulted in a response of similar magnitude to that obtained on application of ATP alone (hyperpolarization: 14.8 ± 0.9 mV; depolarization: 7.6 ± 1.7 mV; $n = 5$), showing that the responses were not additive.

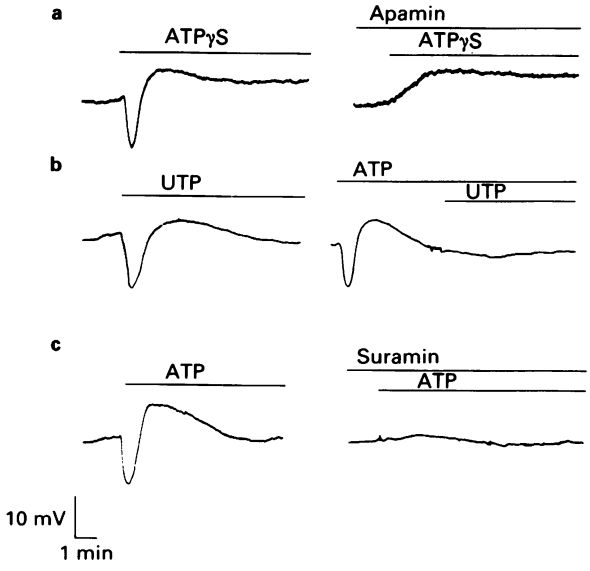

Figure 5 The effect of nucleotides on the membrane potential under different experimental conditions. The response evoked by adenosine 5'-O-(3-thiotriphosphate) (ATPγS), uridine triphosphate (UTP) or adenosine 5'-triphosphate (ATP) represented as a hyperpolarization (downward deflection) and depolarization (upward deflection). (a) ATPγS (100 μM) and in the presence of apamin (0.1 μM, 15 min); (b) UTP (1 mM) and abolition of the UTP response in the presence of ATP (300 μM) added beforehand; (c) ATP (300 μM) and abolition of the response in the presence of suramin (500 μM).

Suramin and the nucleotide responses

The effect of suramin on the responses evoked by the effective nucleotides on C2C12 myotubes was investigated in view of its antagonistic properties on P_2-purinoceptors (Dunn & Blakely, 1988; Den Hertog *et al.*, 1989; Nakazawa *et al.*, 1991). The hyperpolarization evoked by ATP and UTP was inhibited by suramin (Figures 5c, 6a), as demonstrated by a rightward shift of the concentration-response curves in the presence of suramin (100 μM; Figure 6a). The concentration-response curve for the depolarization in presence of ATP also exhibited a rightward shift in the presence of suramin (100 μM), in contrast to the depolarization evoked by UTP, which was not affected at this suramin concentration (Figure 6b). However, the depolarization evoked by UTP (300 μM) was completely abolished by a higher suramin concentration (300 μM, $n = 4$).

Discussion

This study shows that the ATP-sensitive receptors on C2C12 mouse myotubes mediate a biphasic change in membrane potential. The early transient hyperpolarization is most probably carried by K^+-ions in view of the action of TEA^+ and apamin, assumed to block certain Ca^{2+}-regulated K^+-channels (Den Hertog, 1982; Hugues *et al.*, 1982; Marty, 1983; Traoré *et al.*, 1986). A similar ATP-induced K^+-current has also been observed in DDT_1MF-2 smooth muscle cells (Molleman *et al.*, 1989). It is likely that a different K^+-channel is involved in the two cell types, because the K^+-current in DDT_1MF-2 cells is insensitive to apamin (Molleman *et al.*, 1989). High threshold voltage-dependent Ca^{2+}-channels are not involved in the ATP-receptor-mediated hyperpolarization, because blocking Ca^{2+} entry via these channels with diltiazem did not affect the response in the presence of external Ca^{2+}. However, the hyperpolarization was abolished under Ca^{2+}-free conditions, indicating that a Ca^{2+} influx is necessary to activate the K^+-efflux, in contrast to observations in smooth muscle cells (Molleman *et al.*, 1989). In chick myotubes, ATP-induced release of Ca^{2+} from internal stores, due to phospholipase C mediated formation of inositol trisphosphate (Häggblad & Heilbron, 1988). A coupling of the 'nucleotide receptor' to the phospholipase C pathway has also been reported (Davidson *et al.*, 1990; O'Connor *et al.*, 1991). The dependency of the hyperpolarization on external Ca^{2+} in C2C12 myotubes, however questions the contribution of Ca^{2+} released from internal stores to the hyperpolarization, but does not exclude it. The hyperpolarizing phase of the response evoked by the effective agonists ATPγS and UTP displayed the same characteristics as the ATP-induced response. The hyperpolarization was abolished in the presence of TEA^+ or apamin. Under Ca^{2+}-free conditions and in the presence of suramin the hyperpolarization was abolished, which suggests that the hyperpolarization is mediated via one receptor type, sensitive to both ATP and UTP.

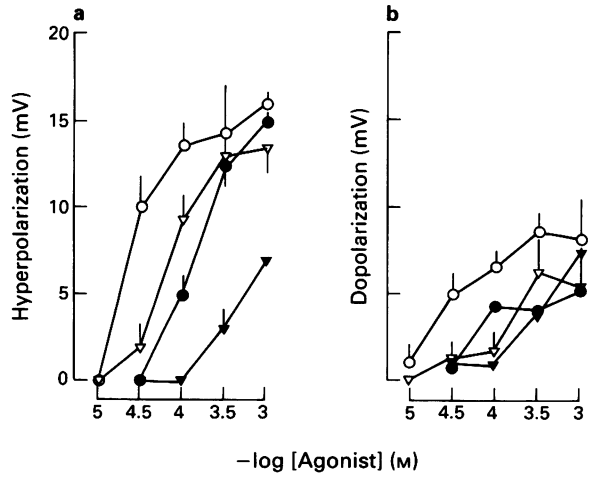

Figure 6 The antagonistic effect of suramin on the nucleotide response. The effect of changes in membrane potential of different concentrations of ATP (○, ●) and UTP (▽, ▼) in the absence (open symbols) and in the presence of suramin (100 μM; 15 min; solid symbols) represented by hyperpolarization (a) and depolarization (b).

The ATP-induced depolarization following the transient hyperpolarization is partly carried by Na^+ entering the cell, as the magnitude of the depolarization is decreased after reducing the Na^+ gradient. These ion channels are not sensitive to tetrodotoxin (TTX), known to block voltage-dependent Na^+-channels. The ATP-receptor-activated channels may allow Na^+ ions as well as Ca^{2+} ions to pass, as described for the ATP-sensitive ion channel of chick myotube (Kolb & Wakelam, 1983), *Xenopus* striated muscle (Igusa, 1988) and smooth muscle cells (Benham & Tsien, 1987; Molleman *et al.*, 1989; 1991). The slow development and the long time course of the depolarization, similar to the earlier observations in myotubes (Hume & Honig, 1986) and DDT_1MF-2 cells (Molleman *et al.*, 1989), probably reflect the properties of the receptor or ion-channel involved. By contrast, the ATP-activated inward currents with much faster characteristics as described by others (e.g. Benham & Tsien, 1987) are mediated by a different receptor type since they were activated by purinoceptor agonists not effective in C2C12 cells.

The depolarizations evoked by the agonists showed different characteristics. The UTP-evoked depolarization was not affected under low Na^+ conditions and showed a lower sensitivity to the antagonistic action of suramin than ATP. The depolarizations evoked by ATP and UTP were not additive. In addition, still in the presence of UTP, ATP elicited a small depolarization when applied after the decline of the UTP-induced depolarization, but UTP did not cause a response following an ATP application. These experiments suggest the involvement of different receptors mediating the depolarization. The receptor exclusively activated by ATP has a greater sensitivity to suramin, is involved in the increased Na^+ conductivity and is possibly related to the ATP-activated Na^+-channel observed in chick myotubes (Kolb & Wakelam, 1987) and *Xenopus* myotomal muscle cells (Igusa, 1988). The other receptor type, activated by both UTP and ATP, is less sensitive to suramin and mediates the transport of ions other than Na^+. The presence of two receptors mediating the depolarization also explains the apparent biphasic concentration-response curves obtained for this component, in contrast to the monophasic curves observed for the hyperpolarization. The similarity between the ATP and the ATPγS response is demonstrated by the observation that a monophasic depolarization was recorded after suppression of the hyperpolarization by blocking the apamin-sensitive K^+-channels and by the observation that the depolarizing phase was lowered by reducing external Na^+. However, the decline in depolarization caused by ATPγS was extremely slow and comparable to the ATP-evoked depolarization under Ca^{2+}-free conditions. These differences in the decline of the depolarization cannot be explained by differences in the rate of degradation by ectonucleotidases, for the myotubes were continuously superfused with agonist containing solution during the experiment. Thus, the decline in depolarization is most probably due to a Ca^{2+}-dependent inactivation of the ion-channel, since repolarization under Ca^{2+}-free conditions occurred only if external Ca^{2+} was applied. The ion-channel is apparently permanently activated in the presence of ATPγS, suggesting opening of the channel in the ATP bound form. Whether the regulatory protein involved is part of the ATP receptor itself or belongs to a class of proteins equivalent to GTP-binding proteins (Fortes *et al.*, 1973), merits further investigation.

Classification of ATP-sensitive receptors recognized in a

variety of cell types other than myotubes has been reviewed recently (Cusack & Hourani, 1990). The involvement of P_1-purinoceptors sensitive to adenosine, P_{2x}-purinoceptors sensitive to α,β-meATP or P_{2y}-purinoceptors sensitive to 2-MeSATP, has to be excluded in the myotubes studied by us. The P_{2t}-subtype recognized in platelets, on which ADP acts as agonist and ATP as antagonist (Cusack & Hourani, 1990) and the P_{2z}-purinoceptors found in mast cells and insensitive to UTP (Cusack & Hourani, 1990) cannot explain the effects caused by these purines. So far, we have discussed that in addition to ATP and ATPγS, the less potent pyrimidine, UTP, generated a biphasic change in membrane potential of the myotubes. The hyperpolarization is likely to be mediated by one receptor type sensitive to UTP and ATP, while the depolarization is thought to be mediated by two receptor types, one exclusively sensitive to ATP and one sensitive to ATP and UTP as discussed above. The responsiveness of C2C12 myotubes to ATP, ATPγs and UTP supports the presence of 'nucleotide receptors' (Davidson *et al.*, 1990) on C2C12 myotubes, mediating the hyperpolarization and the UTP-sensitive depolarization. Additionally, a receptor type sensitive to ATP and ATPγS is present, which mediates a UTP-insensitive depolarization.

The polysulphonated naphtylurea, suramin, known to inhibit the P_{2x}-and P_{2y}-receptor induced responses (Dunn & Blakely, 1988; Den Hertog *et al.*, 1989; Leff *et al.*, 1990; Hoyle, *et al.*, 1990; Hoiting *et al.*, 1990), also appeared to interact with the 'nucleotide receptors' in myotubes as studied by us. It was shown that both components of the biphasic response evoked by ATP or UTP were antagonized. Since suramin has been reported to inhibit ATP-dependent mechanisms other than nucleotide or P_2-receptor, like ion pumps (Moriyama & Nelson, 1988; Fortes *et al.*, 1973), kinase (Mahoney *et al.*, 1990) and the growth factor receptor (Coffey *et al.*, 1987; Hosoi & Edidin, 1989), one may speculate that the sulphonyl moiety of the molecule blocks the access for the γ-phosphate group involved in all these processes.

In conclusion, the biphasic changes in membrane potential evoked by ATP or UTP are mediated by 'nucleotide receptors' and inhibited by suramin. Furthermore, ATP exclusively activates an increase in Na^+ conductivity via a yet unclassified receptor.

References

BENHAM, C.D. & TSIEN, R.W. (1987). ATP receptor-operated channels permeable to calcium in arterial smooth muscle. *Nature*, **328**, 275–278.

BURNSTOCK, G. (1990). Purinergic mechanisms. *Ann. N.Y. Acad. Sci.*, **603**, 1–17.

COFFEY, R.J., LEOF, E.B., SHIPLEY, G.D. & MOSES, H.L. (1987). Suramin inhibition of growth factor receptor binding and mitogenicity in AKR-2B cells. *J. Cell. Physiol.*, **132**, 143–148.

CUSACK, N.J. & HOURANI, S.M.O. (1990). Subtypes of P_2-purinoceptors. *Ann. N.Y. Acad. Sci.*, **603**, 172–81.

DAVIDSON, J., WAKEFIELD, I.K., SOHNINS, U., VAN DER MERWE, P.A. & MILLER, R.P. (1990). A novel extracellular nucleotide receptor coupled to phosphoinositidase-C in pituitary cells. *Endocrinology*, **126**, 80–87.

DEN HERTOG, A. (1982). Calcium and the action of adrenaline, adenosine triphosphate and carbachol on guinea-pig taenia caeci. *J. Physiol.*, **325**, 423–439.

DEN HERTOG, A., NELEMANS, A. & VAN DER AKKER, J. (1989). The inhibitory action of suramin on the P_2-purinoceptor response in smooth muscle cells of guinea-pig taenia caeci. *Eur. J. Pharmacol.*, **166**, 531.

DUNN, P.M. & BLAKELY, A.G. (1988). Suramin: a reversible P_2-purinoceptor antagonist in mouse vas deferens. *Br. J. Pharmacol.*, **93**, 243.

FORTES, P.A.G., ELLORY, J.C. & LEW, V.L. (1973). Suramin: a potent ATPase inhibitor which interacts on the inside surface of the sodium pump. *Biochem. Biophys. Acta*, **318**, 262–272.

GEKAKIS, N., GEHNRICH, S.C. & SUL, H.S. (1989). Phosphofructokinase Isozyme expression during myoblast differentiation. *J. Biol. Chem.*, **264**, 3658–61.

HÄGGBLAD, J. & HEILBRON, E. (1988). P2-purinoceptor-stimulated phosphoinositide turnover in chick myotubes. *FEBS Lett.*, **235**, 133–6.

HOITING, B., MOLLEMAN, A., NELEMANS, A. & DEN HERTOG, A. (1990). P_2-purinoceptor-activated membrane currents and inositol tetrakisphosphate formation are blocked by suramin. *Eur. J. Pharmacol.*, **181**, 127–131.

HOSOI, K. & EDIDIN, M. (1989). Exogenous ATP and other nucleoside phosphates modulate epidermal growth factor receptors of A-431 epidermoid carcinoma cells. *Proc. Natl. Acad. Sci. U.S.A.*, **86**, 4510–4514.

HOYLE, C.H.V., KNIGHT, G.E. & BURNSTOCK, G. (1990). Suramin antagonizes responses to P_2-purinoceptor agonists and purinergic nerve stimulation in the guinea-pig urinary bladder and taenia coli. *Br. J. Pharmacol.*, **99**, 617–621.

HUGUES, M., SCHMID, H., ROMEY, G., DUVAL, D., FRELIN, C. & LAZDUNSKI, M. (1982). Apamin as a selective blocker of the calcium dependant potassium channel in neuroblastoma cell: voltage clamp and biochemical characterization of the toxin receptor. *Proc. Natl. Acad. Sci. U.S.A.*, **79**, 1308–1312.

HUME, R.I. & HONIG, M.G. (1986). Excitatory action of ATP on embryonic chick muscle. *J. Neurosci.*, **6**, 681–90.

IGUSA, Y. (1988). Adenosine 5'-triphosphate activates acetylcholine receptor channels in cultured Xenopus myotomal muscle cells. *J. Physiol.*, **405**, 169–185.

INESTROSA, N.C., MILLER, J.B., SILBERSTEIN, L., ZISKIND-CONHAIM, L. & HALL, Z. (1983). Developmental regulation of 16S acetylcholinesterase and acetylcholine receptors in a mouse muscle cell line. *Exp. Cell. Res.*, **147**, 393–405.

KOLB, H.A. & WAKELAM, M.J.O. (1983). Transmitter-like action of ATP on patched membranes of cultured myoblasts and myotubes. *Nature*, **303**, 621–3.

LEFF, P., WOOD, B.E. & O'CONNOR, S.E. (1990). Suramin is a slowly-equilibrating but competitive antagonist at P_2 receptors in rabbit isolated ear artery. *Br. J. Pharmacol.*, **101**, 645–649.

MAHONEY, C.W., AZZI, A. & HUANG, K.P. (1990). Effect of suramin, an anti-human immunodeficiency virus reverse transcriptase agent, on protein kinase C. *J. Biol. Chem.*, **265**, 5424–5428.

MARTY, A. (1983). Ca^{2+}-dependant K^+-channels with large unitary conductance. *Trends Pharmacol. Sci.*, **6**, 262–265.

MOLLEMAN, A., NELEMANS, A. & DEN HERTOG, A. (1989). P_2-purinoceptor operated conductances in DDT_1-MF-2 smooth muscle cells. *Eur. J. Pharmacol.*, **169**, 167–74.

MOLLEMAN, A., HOITING, B., DUIN, M., VAN DEN AKKER, J., NELEMANS, A. & DEN HERTOG, A. (1991). Potassium channels regulated by inositol 1,3,4,5-tetrakisphosphate and internal calcium in DDT_1-MF-2 smooth muscle cells. *J. Biol. Chem.*, **266**, 5658–63.

MOORE, S.E., THOMPSON, J., KIRKNESS, V., DICKSON, J.G. & WALSH, F.S. (1987). Skeletal muscle neural cell adhesion molecule (N-CAM): changes in protein and mRNA species during myogenesis of muscle cell lines. *J. Cell Biol.*, **105**, 1377–86.

MORIYAMA, Y. & NELSON, N. (1988). Inhibition of vacuolar H^+-ATPases by fusidic acid and suramin. *FEBS Lett.*, **234**, 383–386.

NAKAZAWA, K., FUJIMORI, K., TAKANAKA, A. & INOUE, K. (1990). Reversible and selective antagonism by suramin of ATP-activated inward current in PC12 phaeochromocytoma cells. *Br. J. Pharmacol.*, **101**, 224–226.

O'CONNOR, S.E., DAINTY, I.A. & LEFF, P. (1991). Further subclassification of ATP receptors based on agonist studies. *Trends Pharmacol. Sci.*, **12**, 137–41.

REVAH, F., MULLE, C., PINSET, C., AUDHYA, T., GOLDSTEIN, G. & CHANGEUX, J.P. (1987). Calcium-dependent effect of the thymic polypeptide thymopeoietin on the densensitization of the nicotinic acetylcholine receptor. *Proc. Natl. Acad. Sci. U.S.A.*, **84**, 3477–81.

TRAORÉ, F., COGNARD, C., PROTREAN, D. & RAYMOND, G. (1986). The apamin sensitive potassium current in frog skeletal muscle: its dependency on the extracellular calcium and sensitivity to calcium channel blockers. *Pflügers Archiv. Eur. J. Physiol.*, **407**, 199–203.

WHITSON, P.A., STUART, C.A., HULS, M.H., SAMS, C.F. & CINTRON, N.M. (1989). Dexamethason effects on creatine kinase activity and insulin-like growth factor receptors in cultured muscle cells. *J. Cell. Physiol.*, **140,** 8–17.

YAFFEE, D. & SAXEL, O. (1977). Serial passage and differentiation of myogenic cells isolated from dystrophic mouse muscle. *Nature*, **270,** 725–7.

(Received October 28, 1991
Revised March 25, 1992
Accepted March 30, 1992)

Br. J. Pharmacol. (1992), **106**, 859–864 © Macmillan Press Ltd, 1992

Noradrenaline-stimulated inositol phosphate accumulation in arteries from spontaneously-hypertensive rats

[1]S.B. Guild, [2]S. Jenkinson & T.C. Muir

Department of Pharmacology, University of Glasgow, Glasgow G12 8QQ

1 The effects of noradrenaline upon polyphosphoinositide (PPI) breakdown was investigated by measuring the accumulation of inositol phosphates (IPs) in tail arteries from normo- (WKY) and spontaneously-hypertensive (SHR) rats.

2 Noradrenaline (10^{-7}–10^{-3} M) evoked a concentration-dependent increase in total IP accumulation in both WKY and SHR rats but no significant differences between the populations were detected.

3 In contrast, significant differences in the accumulation of the individual IPs, which contributed to the total IP, occurred. A significantly greater noradrenaline-stimulated accumulation of inositol trisphosphate (IP_3) was observed in tissues from SHR compared with those from WKY rats at each effective concentration of noradrenaline. This was paralleled by an equivalent reduction in inositol monophosphate (IP_1) accumulation, consistent with the lack of a significant difference in noradrenaline-stimulated total IP accumulation between the two populations.

4 In time course studies, an enhanced noradrenaline-induced accumulation of IP_3, in SHR compared to WKY rats, occurred from the earliest time point studied after the addition of the catecholamine both in the presence and absence of LiCL (10 mM). In the presence of LiCl (10 mM) no significant difference in noradrenaline-evoked total IP accumulation between SHR and WKY rats was observed; in the absence of LiCl noradrenaline-evoked a greater total IP accumulation in SHR than in WKY rats at all time points investigated.

5 These studies suggest that the main reason for the enhanced noradrenaline-induced accumulation of IP_3 in arteries from SHR rats is a reduced rate of dephosphorylation of both IP_3 and inositol bisphosphate (IP_2) rather than a greater formation of IP_3 from PPIs.

6 This enhanced accumulation of IP_3 may result in an increased calcium mobilisation accounting for the increased contractility to noradrenaline of tail arteries from SHR as compared with those from WKY rats.

Keywords: Hypertension; smooth muscle; vascular; polyphosphoinositides; noradrenaline

Introduction

The enhanced contractile response of the vasculature to both nerve stimulation (Ekas & Lokhandwala, 1981; Muir & Wardle, 1989) and to exogenous catecholamines, such as noradrenaline (Fouda *et al.*, 1987; Muir & Wardle, 1989), in hypertensive compared to normotensive rat models, implicates a postsynaptic locus for this effect. Alterations in signal-transduction systems, recently implicated in other cardiovascular diseases such as hypertension and congestive heart disease (Brodde *et al.*, 1989; Brodde & Michel, 1989), could underlie the development of hypertension and account for the increased contractility of vascular smooth muscle in this disease.

A signal-transduction mechanism closely associated with contraction in vascular smooth muscle, including the rat tail artery (Bao *et al.*, 1989; Schwarze *et al.*, 1990) involves stimulation of polyphosphoinositide (PPI) metabolism to generate inositol phosphates (IPs) and diacylglycerol (DAG) (Abdel-Latif, 1986). Noradrenaline increases intracellular inositol trisphosphate (IP_3) concentrations in vascular smooth muscle cells which, through a mobilization of IP_3-sensitive intracellular calcium, results in contraction (Abdel-Latif, 1986). It is possible that an enhanced contractile response in vascular smooth muscle could be evoked by an enhanced accumulation of IP_3 resulting in an increased mobilization of intracellular calcium. The PPI transduction system is, therefore, an obvious target for study when mechanisms underlying postsynaptic changes responsible for the increased responsiveness of arteries from spontaneously hypertensive (SHR) rats as compared to arteries from normotensive (WKY) control rats are sought.

We have already reported an enhanced pressor response to nerve stimulation and exogenous noradrenaline in the tail artery from SHR rats compared to that from WKY rats (Muir & Wardle, 1989). Furthermore, we have shown that noradrenaline increased total IP accumulation, taken as a measure of PPI metabolism (Jenkinson *et al.*, 1990) in tail arteries from both WKY and SHR rats. However, no significant differences between results from SHR and WKY rats emerged. In a further attempt to explain the enhanced contractile responsiveness of tissues from hypertensive animals, we have measured the rates of formation, accumulation and metabolism of individual IPs, inositol monophosphate (IP_1), inositol bisphosphate (IP_2) and IP_3.

The study revealed no significant difference in the total accumulation of IPs or in the degree of breakdown of PPIs between SHR and WKY rats. There were significant differences, however, in the relative proportions of the individual IPs which constitute the total. Importantly, an enhanced accumulation of IP_3 in tissues from SHR rats was observed.

Methods

Preparation of arteries

Age-matched albino WKY and SHR rats (200–250 g) were killed by stunning followed by exsanguination. The tail was severed, the cornified epithelium removed and a length (7–8

[1] Author for correspondence at present address: School of Biological and Medical Sciences, Bute Medical Building, University of St Andrews, St Andrews KY16 9TS.

[2]Present address: Pharmacology and Therapeutics, University of Leicester, PO Box 138, Medical Sciences Building, University Road, Leicester LE1 9NH.

cm) of artery dissected out from the proximal end (Holman & Suprenant, 1980). Arteries were then cleaned of connective tissue and cut into segments (1 cm long, 5 mg wet wt). Changes in PPI metabolism in the segments were quantified by measuring IP accumulation (Akhtar & Abdel-Latif, 1984). To do this the segments were transferred to a glass vial containing a bicarbonate buffered salt solution (2 ml), of the following composition (mM): NaCl 118, $NaHCO_3$ 25, KCl 4, $CaCl_2$ 2.6, $MgCl_2$ 1.2, NaH_2PO_4 1, glucose 11, pH 7.4, saturated with O_2/CO_2 (19:1), to which was added *myo*-[2-^{3}H]-inositol (8 μCi ml^{-1}). This vial was incubated for 3 h at 37°C then the segments were transferred to another similar vial containing either an identical medium or one of the buffered salt solution supplemented with LiCl (10 mM) and *myo*-[2-^{3}H]-inositol (8 μCi ml^{-1}). The time course of accumulation of IPs was measured both in the presence of LiCl, to inhibit the inositol monophosphatase and therefore the recycling of the IPs (Berridge, 1983), and in the absence of LiCl. These vials and contents were then incubated for a further 15 min at 37°C. After this preliminary incubation, segments were placed in other identical glass vials (3–4 segments per vial) at 37°C in Li-free or Li-containing medium and used in the following studies.

Effect and time course of noradrenaline on IP accumulation

The effects of noradrenaline (10^{-7}–10^{-3} M) upon IP accumulation were examined 30 min after its addition to the Li-containing medium. The time course of accumulation of IPs was examined by incubating segments of artery for 1, 2, 5, 10, 20 or 30 min with or without 10^{-4} M noradrenaline in either Li-free or Li-containing bicarbonate buffer. The time course of the decay in the levels of IP accumulation, in response to 10^{-4} M noradrenaline, was investigated. The time course of metabolism of IPs was examined by the method of Batty & Nahorski (1989) which required that the incubations be carried out in the absence of LiCl (10 mM) to permit the recycling of the IPs unhindered by the inhibition of inositol monophosphatase by this salt. Segments were incubated in Li-free medium with 10^{-4} M noradrenaline for 30 min at which point the α_1-adrenoceptor antagonist, prazosin (10^{-6} M; a concentration known to be effective in blocking both nerve- and exogenous noradrenaline-stimulated contraction of this tissue; Schwarze *et al.*, 1990), was added to terminate the stimulation of PPI metabolism by noradrenaline. Alternatively, in control vials, stimulation of PPI metabolism by noradrenaline was continued; controls received an equal volume of medium instead of prazosin. Segments were incubated for a further 1, 2, 5, 10, 15 or 20 min in this medium at 37°C. In all cases, incubations were terminated by transferring the segments to ice-cold trichloroacetic acid (TCA) (1 ml, 10% w/v).

Inositol phosphate extraction

TCA was extracted from the samples (1 ml) by repeated (3 times) addition and thorough mixing with water-saturated diethyl-ether. The pH of the samples was then adjusted to 7 with NaOH (0.2 ml, 0.1 M). The IPs were extracted and separated from the samples by anion exchange chromatography (Berridge, 1983) on Dowex 1-X8 anion exchange columns (100–200 mesh, formate form). Inositol trisphosphates (IP_3), bisphosphates (IP_2) and monophosphates (IP_1) were eluted separately. This was done by successive applications of (1) formic acid (0.1 M)/ammonium formate (0.2 M) solution to elute IP_1; (2) formic acid (0.1 M)/ammonium formate (0.4 M) solution to elute IP_2 and (3) formic acid (0.1 M)/ammonium formate (0.8 M) solution to elute IP_3. The amount of individual IPs and, when summated, total IP accumulation was thus measured. The eluted IPs were counted by liquid scintillation counting.

Measurement of systolic blood pressure

Systolic blood pressure was measured in conscious rats, acclimatized to 37°C for 15 min. Readings were made without anaesthesia by inflating a tail cuff; a piezo-electric crystal detector connected to a storage oscilloscope was used to determine when systolic blood pressure had been reached and a sphygmomanometer was used to measured blood pressure. The mean (± s.e.mean) systolic blood pressure measured was: 125 ± 3.0 mmHg in WKY rats and 195 ± 1.9 mmHg in SHR rats ($n = 10$).

Analysis of results

Results are expressed as the mean ± standard error of mean (s.e.mean) of a number (n) of observations. Data were analysed by the Mann Whitney U-test. At t value of $P<0.05$, or less, was taken as significant. * is used to donate $P<0.05$; **$P<0.01$ and ***$P<0.001$.

Drugs and chemicals

Myo-[2-^{3}H]-inositol (18.3 Ci mmol^{-1}) in an aqueous ethanol solution (10% v:v) was purchased from Amersham International. (±)-Noradrenaline bitartrate was purchased from Sigma, (±)-prazosin hydrochloride was a gift from Pfizer Research, UK. Concentrations in text refer to the salts.

Results

Noradrenaline-stimulated inositol phosphate accumulation in arteries from WKY and SHR rats

Noradrenaline concentrations (10^{-6}–10^{-3} M) which evoked contractions of this tissue (Schwarze *et al.*, 1990) evoked similar concentration-dependent, prazosin (10^{-6} M)-sensitive, increases in total IP accumulation in arteries from both SHR and WKY rats (Figure 1a). Analysis of the individual IPs, however, revealed differences between SHR and WKY rats. Noradrenaline (10^{-6}–10^{-3} M) evoked a concentration-dependent increase in IP_1 (Figure 1b), IP_2 (Figure 1c) and IP_3 (Figure 1d) accumulation in both SHR and WKY rats with respect to controls. IP_1 accumulation was significantly greater in WKY rats at concentrations of noradrenaline of 10^{-6}–10^{-4} M (Figure 1b). In the case of IP_2 (Figure 1c), no significant difference was observed between WKY and SHR populations except at the low concentrations of 10^{-7} M and 10^{-6} M at which IP_2 accumulation was significantly greater in WKY rats (Figure 1c). In contrast to the effects on IP_1 and IP_2, IP_3 accumulation was significantly greater in SHR than in WKY rats at all effective concentrations of noradrenaline (10^{-5}–10^{-3} M) (Figure 1d).

Time course of noradrenaline (10^{-4} M)-stimulated inositol phosphate accumulation

The differences in the accumulation of individual IPs in response to noradrenaline (Figure 1) were investigated further by studying the time course of their accumulation. In the presence of LiCl, paralleling the conditions used in studies of the concentration-dependence of IP accumulation, 10^{-4} M noradrenaline stimulated a time-dependent accumulation of total IP in both SHR and WKY rats (Figure 2a). No significant difference emerged, at any time point measured, between tissues from SHR and WKY animals, confirming the results presented in Figure 1a. In contrast to measurements of total IP accumulation, 10^{-4} M noradrenaline-stimulated IP_1 accumulation in arteries from WKY rats was significantly greater after 20 min than in those from SHR rats (Figure 2b) consistent with the data in Figure 1b. Noradrenaline (10^{-4} M)-stimulated IP_2 accumulation was not different at any time point studied (Figure 2c) but accumulation of IP_3 at

every time point was significantly greater, including the zero time point (Figure 2d), in arteries from SHR than from WKY rats. These results are consistent with the data presented in Figure 1d.

Time course studies of the accumulation of the IPs were repeated in the absence of LiCl to confirm that (a) significant IP accumulation in response to noradrenaline could be detected and that (b) differences in the accumulation of individual IPs persisted in the absence of the salt. Noradrenaline (10^{-4} M) stimulated a time-dependent, but significantly smaller, accumulation of total IP (Figure 3a), IP_1 (Figure 3b), IP_2 (Figure 3c) and IP_3 (Figure 3d) in the absence, compared with that in the presence, of LiCl. However, there were significant differences from the data presented in Figure 2.

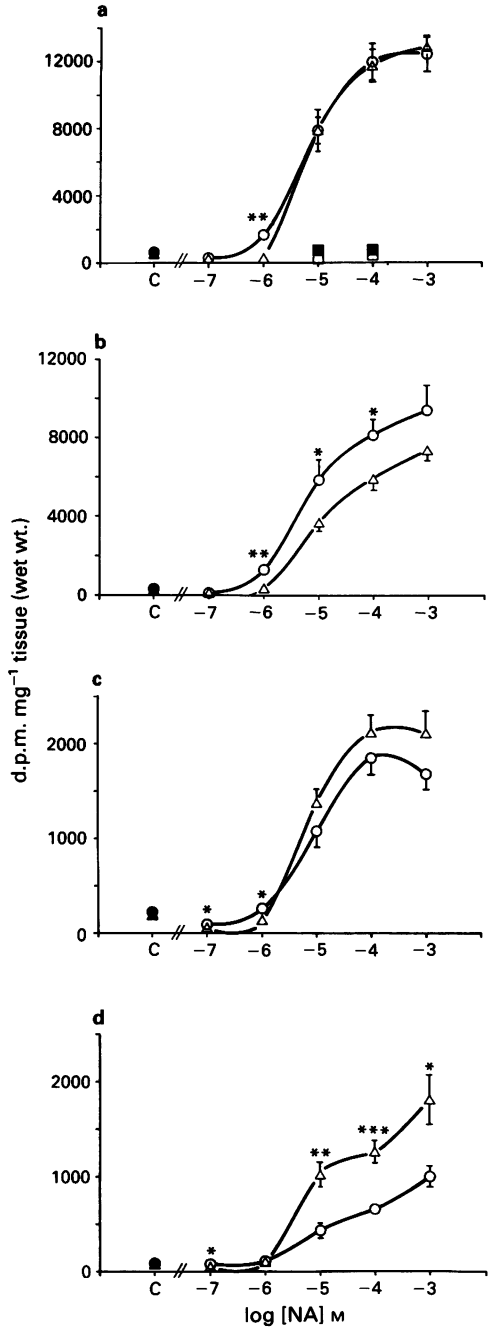

Figure 1 The mean (± s.e.mean, vertical bars, $n \geq 6$) increase in noradrenaline-evoked accumulation of total (a) and individual inositol phosphates (IPs), IP_1 (b), IP_2 (c) and IP_3 (d) expressed as disintegrations per minute (d.p.m.) mg^{-1} tissue wet weight (ordinate scale) in tail arteries from WKY (○) and SHR (△) rats compared with the respective controls (C). Noradrenaline evoked a concentration-dependent, prazosin (10^{-6} M)-sensitive (WKY, □; SHR, ■) increase in the accumulation of both total and individual IPs. This was significantly greater, for IP_3 (d), at concentrations of noradrenaline of 10^{-5} M and above in tissues from SHR compared to those from WKY rats. IP_1 levels (b) at 10^{-6}–10^{-4} M noradrenaline were significantly greater in tissues from WKY than in those from SHR rats. There was no significant difference in total IP (a) or IP_2 (c) accumulation in response to noradrenaline between tissues from WKY and SHR rats.

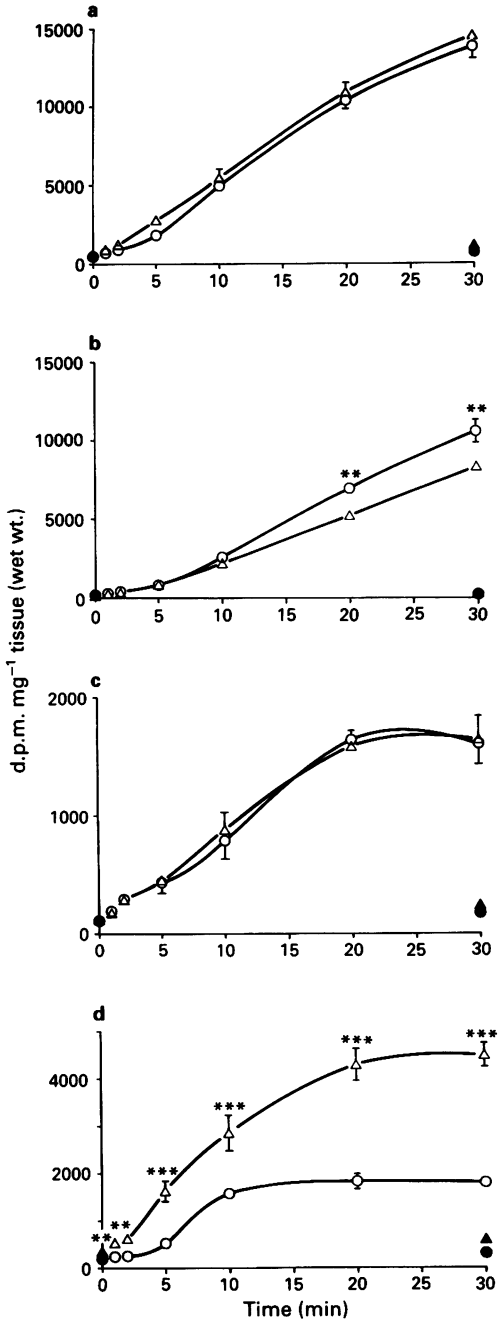

Figure 2 The effect of time (abscissa scale, min) on the noradrenaline (10^{-4} M)-evoked accumulation (mean with s.e.mean, shown by vertical bars, $n \geq 6$) of total (a) and of individual inositol phosphates (IPs) (IP_1 (b), IP_2 (c), IP_3 (d)) expressed as disintegrations per minute (d.p.m.) mg^{-1} tissue wet wt (ordinate scale) in tail arteries from SHR (△) and WKY (○) rats compared with the respective controls (WKY, ●; SHR, ▲). LiCl was present throughout. The accumulation of IP_3 (d) in response to noradrenaline in arteries from SHR was greater than in those from WKY rats at each time point studied; for IP_2 (c), accumulation was not significantly different between the two populations and for IP_1 (b), accumulation was significantly greater in arteries from WKY rats after 20 min. Interestingly, control IP_3 (d) levels in SHR (▲) rats were significantly greater than in WKY (●) rats.

Noradrenaline (10^{-4} M) stimulated a significantly greater total IP accumulation, in incubations longer than 2 min, in SHR compared to WKY rats (Figure 3a); an effect not evident in the presence of LiCl. With the exception of the 30 min time point, no significant difference between IP_1 accumulation evoked by 10^{-4} M noradrenaline in SHR and WKY rats (Figure 3b) was observed. The difference in total IP accumulation between SHR and WKY rats, observed in Figure 3a, is therefore due to differences in the accumulation of the other two IPs measured. IP_2 (Figure 3c) and IP_3 (Figure 3d)-accumulations in response to 10^{-4} M noradrenaline were greater at all time points studied (up to 30 min) in tissues from SHR than in those from WKY rats.

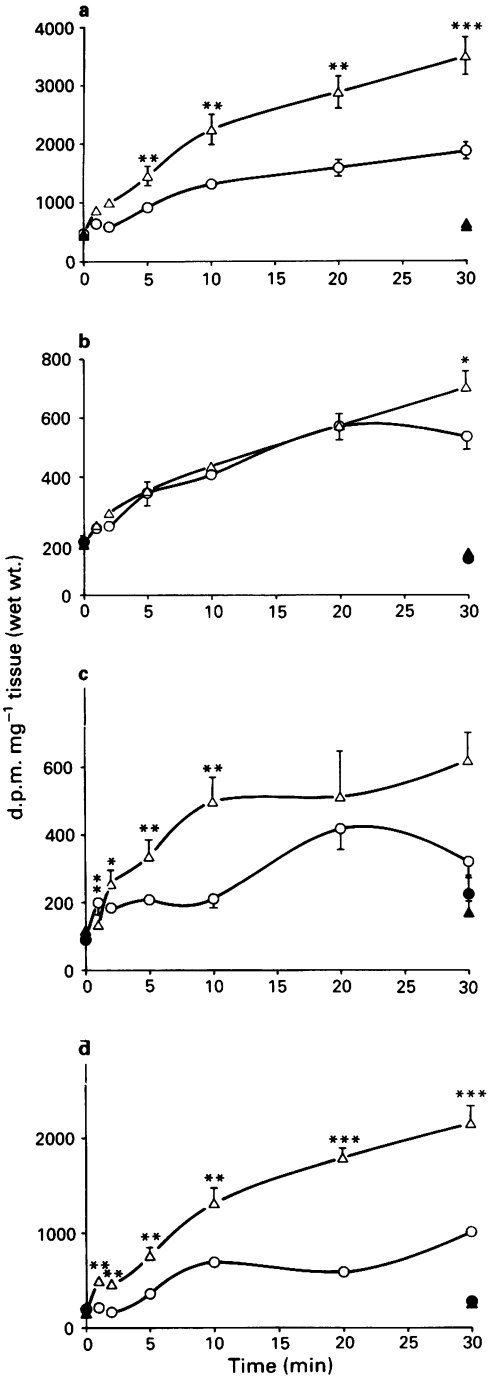

Figure 3 The effect of time on the noradrenaline (10^{-4} M)-evoked accumulation (mean with s.e.mean, shown by vertical bars, $n \geq 6$) of total inositol phosphates (IP) (a) and individual IPs (IP_1 (b), IP_2 (c), IP_3 (d)) expressed as disintegrations per minute (d.p.m.) mg^{-1} tissue wet wt (ordinate scale) in tail arteries from SHR (△) and WKY (○) rats compared with the respective controls (SHR, ▲; WKY, ●). LiCl was absent. The accumulation of IPs was significantly smaller than in the presence of LiCl (c.f. Figure 2). Accumulation of total IP (a), IP_2 (c), and IP_3 (d) was significantly greater in tissues from SHR than in those from WKY rats where indicated. Noradrenaline-evoked accumulation of IP_1 (b) in tissues from SHR and WKY rats did not differ significantly.

The decay of noradrenaline (10^{-4} M)-stimulated inositol phosphate accumulation

The declines in the accumulated total IP and individual constituent IPs were measured after addition of 10^{-6} M of the α_1-adrenoceptor antagonist, prazosin, to terminate further PPI metabolism. In the absence of prazosin, noradrenaline (10^{-4} M)-stimulated IP accumulation remained constant throughout the 20 min period examined (Figure 4) confirming that metabolism of PPIs continued during this time.

Total inositol phosphate accumulation

In WKY rats, total IP accumulation in response to noradrenaline was greater than in non-stimulated controls (Figure 4a) at all time points studied. Within 5 min of the addition of 10^{-6} M prazosin, the levels of total IP were significantly lower than at time 0 but then no further decreases were observed. Similarly, noradrenaline-stimulated total IP accumulation in SHR rats declined with time from the addition of prazosin but remained significantly greater than in non-stimulated controls throughout the 20 min period studied. Total IP accumulation in SHR rats remained significantly greater than those values at equivalent time points in WKY rats until 15 min after addition of prazosin when total IP accumulation in tissues from both SHR and WKY rats were indistiguishable (Figure 4a). Prazosin alone had no effect upon basal total IP accumulation; basal levels were 611 ± 49 (SHR) and 580 ± 48 (WKY) d.p.m. mg^{-1} tissue (wet weight) in the absence and 812 ± 159 (SHR) and 622 ± 59 (WKY) d.p.m. mg^{-1} tissue (wet wt.) in the presence of prazosin.

Inositol monophosphate accumulation

Noradrenaline-induced increases in IP_1 levels were similar in both WKY and SHR rats and declined with time, but remained significantly above those in non-stimulated controls, throughout the 20 min period following the addition of prazosin (Figure 4b) to arrest stimulation. However, the rate at which IP_1 levels declined differed between the two groups, being greater in WKY rats. This resulted in IP_1 levels in SHR rats remaining significantly greater than those at equivalent time points in WKY rats for up to 10 min; after this time values in the two groups were indistinguishable (Figure 4b). Prazosin alone had no effect upon basal IP_1 accumulation; basal levels were: 184 ± 21 (SHR) and 181 ± 11 (WKY) d.p.m. mg^{-1} tissue (wet wt.) in the absence and 189 ± 24 (SHR) and 204 ± 21 (WKY) d.p.m. mg^{-1} tissue (wet wt.) in the presence of prazosin.

Inositol bisphosphate accumulation

Although IP_2 levels decayed with time in the presence of prazosin, in both WKY and SHR rats (Figure 4c), they remained significantly greater than the respective non-stimulated controls at all time points examined. In SHR rats, noradrenaline-stimulated IP_2 accumulation initially increased within 1 min of the addition of prazosin and remained significantly elevated compared to values in WKY tissues for 10 min after the addition of the antagonist (Figure 4c). Prazosin alone had no effect upon basal IP_2 accumulation; basal levels were: 129 ± 6 (SHR) and 114 ± 6 (WKY) d.p.m. mg^{-1} tissue (wet wt.) in the absence and 147 ± 33 (SHR) and 129 ± 15 (WKY) d.p.m. mg^{-1} tissue (wet wt.) in the presence of prazosin.

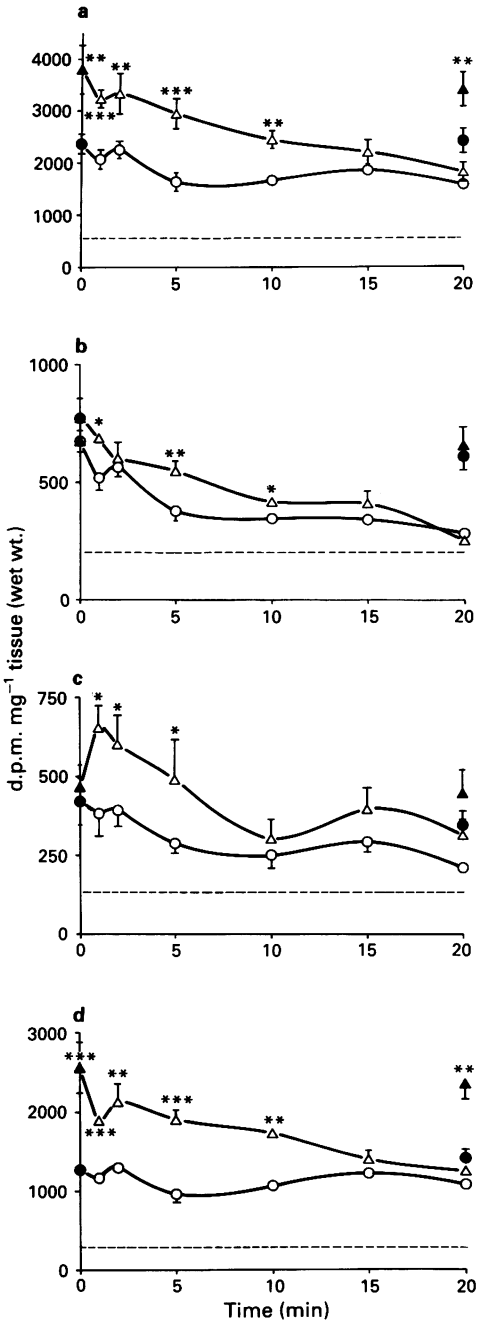

Figure 4 The decay of noradrenaline (10^{-4} M)-stimulated inositol phosphate (IP) accumulation (mean with s.e.mean, shown by vertical bars, $n \geq 6$) of total (a) and individual IPs (IP_1 (b), IP_2 (c) and IP_3 (d)) with time (abscissa scale, min) in tail arteries from SHR (△) and WKY (○) rats in the presence of prazosin (10^{-6} M, time 0) to arrest the effects of noradrenaline. IP accumulations in the absence of prazosin are represented thus (SHR, ▲; WKY, ●). In all cases IP levels remained above basal (----) levels.

Inositol trisphosphate accumulation

IP_3 accumulation in response to noradrenaline was higher in WKY rats than in non-stimulated controls (Figure 4d) but, in contrast to that of the other IPs, did not decline significantly with time after the addition of 10^{-6} M prazosin. In contrast, noradrenaline-stimulated IP_3 levels in SHR rats declined from the time of addition of the antagonist, but remained significantly greater than in the non-stimulated controls throughout the 20 min period investigated. This decline took place from a significantly greater level in SHR rats, compared to that at the equivalent time point in tissues from WKY rats. IP_3 levels remained significantly greater than those values at equivalent time points in WKY rats until 10 min after addition of prazosin at which point IP_3 levels in tissues from both SHR and WKY rats were indistinguishable. Prazosin alone had no effect upon basal IP_3 accumulation; basal levels were 298 ± 22 (SHR) and 285 ± 30 (WKY) d.p.m. mg^{-1} tissue (wet wt.) in the absence and 476 ± 101 (SHR) and 290 ± 24 (WKY) d.p.m. mg^{-1} tissue (wet wt.) in the presence of prazosin.

Discussion

Measurement of total IP accumulation, as an indication of alterations in the PPI signal-transduction pathway, can be misleading. The lack of difference in total IP accumulation measured in the presence of LiCl contrasted with the significant differences in the accumulation of individual IPs between SHR and WKY rats. Significantly greater levels of IP_3 accumulated, at each effective concentration of noradrenaline, in tissues from SHR compared to those from WKY rats. This was paralleled by a reduction in IP_1 accumulation and no significant differences in IP_2 accumulation, consistent with the lack of a significant difference in noradrenaline-stimulated total IP accumulation between the two populations. Since IP_3 is the PPI product responsible for calcium mobilization (Berridge & Irvine, 1989), its enhanced accumulation could account for the increased contractility of tissues from SHR rats. Interestingly, basal IP_3 level were found to be significantly greater in arteries from SHR than in WKY rats and may be a contribution to the increased contractility of such tissues. The measured accumulation of IP_3 reflects the liberation of IP_3 from PIP_2, the net metabolism of IP_3 to IP_2 and the formation of IP_3 from higher phosphorylated IPs such as inositol tetrakisphosphate (IP_4), inositol pentakisphosphate (IP_5) and inositol hexakisphosphate (IP_6). (1,4,5)-IP_3 can be further phosphorylated to (1,3,4,5)IP_4 which is then dephosphorylated to (1,3,4)IP_3 and further rephosphorylated to (1,3,4,5)IP_4 (for review see Berridge & Irvine, 1989). Of the two major IP_3 isomers (1,4,5)IP_3 and (1,3,4)IP_3, only the former is responsible for the liberation of calcium from internal stores (Berridge & Irvine, 1989). (1,3,4)IP_3 is formed by the dephosphorylation of (1,3,4,5)IP_4 and is an intermediary in the recycling of inositol back into the PPIs. Since anion exchange chromatography does not permit the relative proportions of the two isomers in the IP_3 fraction to be resolved, it cannot be determined whether or not the increased accumulation of IP_3 in arteries from SHR rats is of the important calcium mobilizing (1,4,5)IP_3 isomer.

The lack of difference in total IP accumulation between tissues from SHR and WKY rats indicates that the extent of noradrenaline-induced stimulation of phospholipase C (PLC) in tissues from SHR and WKY rats may have been similar. This implies that the enhanced accumulation of IP_3 in tissues from SHR rats is due to differences in the subsequent metabolism of IPs following their liberation from PPIs. From time course studies, the reason for the enhanced noradrenaline-induced accumulation of IP_3 in arteries from SHR rats may be a reduced rate of dephosphorylation of IP_3.

In the presence of LiCl, the rate of noradrenaline-stimulated IP_3 accumulation was greater in SHR rats from the moment of addition of the catecholamine. This was matched by a corresponding decrease in the rate of IP_1 accumulation resulting in no net difference in total IP accumulation between SHR and WKY rats over the time period studied. Studies on the metabolism of IPs are complicated by the presence of LiCl. This salt is used to block recycling of inositol back to PPIs and so facilitates measurement of IPs (Berridge, 1983). However, this results in the successive accumulation of IP_1 and IP_2 which will produce an inhibition of the IP_2 and IP_3 phosphatases as accumulation of these products occurs (Shears *et al.*, 1987). It is therefore difficult to separate changes in the rate of metabolism of IPs by

phosphatases from those which arise from the altered sensitivity of these enzymes to inhibition by accumulation of reaction products (IP_1, IP_2 and IP_3). These problems are absent when LiCl is removed. Interestingly, in the absence of LiCl, significant differences were observed in the time course of noradrenaline-stimulated total IP accumulation, an observation masked in studies performed in the presence of the salt. In the absence of LiCl, the accumulation of IP_1 was reduced to about 5% of that seen in the presence of LiCl and no differences were evident between the levels of this IP in either SHR or WKY rats. However, a substantial accumulation of IP_3 in both SHR and WKY rats remained and this was enhanced by noradrenaline to a greater extent in tissues from SHR rats than in those from WKY rats. An enhanced accumulation of IP_2 in response to noradrenaline in SHR rats was also revealed. The lack of difference in net PPI metabolism (and therefore IP liberation) between SHR and WKY rats, compatible with an enhanced accumulation of IP_2 and IP_3 but not IP_1 in arteries from SHR rats, may arise from a reduced metabolism of IP_3 to IP_2 to IP_1 in these arteries.

We attempted to investigate differences in the rates of metabolism of IPs between arteries from SHR and WKY rats by measuring the rates of decay of the individual IPs after the termination of the hydrolysis of PPIs. This was achieved by the addition of the α_1-adrenoceptor antagonist, prazosin, which itself had no effect upon basal levels of any of the IPs measured. The rates of decay in the levels of the IPs, in particular the rates of decay of IP_3, may reveal differences in the metabolism of IPs between the two groups but unfortunately, measuring the time course of the decays in the levels of IPs did not reveal any differences. IP_3 levels declined after the addition of prazosin in SHR rats from an initially greater value and remained significantly greater than in WKY rats. However, any comparison with the rate of decay of IP_3 levels in WKY rats was impossible as IP_3 levels in tissues from WKY rats did not decline significantly after addition of prazosin. This could have been due to insufficient prazosin being added to terminate noradrenaline-stimulation of PPI hydrolysis, but is unlikely as 10^{-6} M prazosin completely blocked the contraction and IP accumulation stimulated by this concentration of noradrenaline in these arteries (Schwarze *et al.*, 1990). One possible explanation is that changes in the specific activity of the ^{3}H-labelled-product may be responsible for the lack of decay of IP_3 after the addition of prazosin in WKY rats, as changes in specific radioactivity are revealed in that fraction of the response which is not reversible by antagonist (Batty & Nahorski, 1989). However, the apparent steady state of IP_3 levels is most likely to be a reflection of the complicated, and as yet ill-defined, metabolism of IPs which may result in a constant metabolism and formation of IP_3s via various routes. It may require the resolution of the isomers of the IPs and the additional measurement of more highly phosphorylated IPs (e.g. IP_4, IP_5 and IP_6) before more meaningful results are obtained from the measurement of the metabolism of IPs in these tissues.

In conclusion, this study suggests that, in tail arteries of SHR rats, there is an altered signal-transduction mechanism which mediates noradrenaline-evoked contractions and which results in an enhanced accumulation of IP_3. This change may be an altered metabolism of IPs resulting in accumulation of more of the calcium-releasing IP_3. Although the particular isomer of IP_3 was not identified, it is tempting to speculate that the enhanced accumulation of IP_3 may result in an increased calcium mobilization and so account for the increasing contractility to noradrenaline.

The authors gratefully acknowledge the support of the Scottish Home and Health Department, the Nuffield Foundation, The Wellcome Trust, Smith Kline Beecham and the medical research funds of the University of Glasgow.

References

ABDEL-LATIF, A.A. (1986). Calcium mobilising receptors, polyphosphoinositides and the generation of second messengers. *Pharmacol. Rev.*, **38**, 227–272.

AKHTAR, R.A. & ABDEL-LATIF, A.A. (1984). Carbachol causes rapid phosphodiesteric cleavage of phosphatidylinositol 4,5-bisphosphate in rabbit iris smooth muscle; prazosin inhibits noradrenaline- and ionophore A23187-stimulated accumulation of inositol phosphates. *Biochem. J.*, **224**, 291–300.

BAO, J.X., ERIKSSON, I.E. & STJARNE, L. (1989). Neurogenic contraction in the tail artery of normotensive rats is mediated by noradrenaline and ATP via post-junctional α_1- and α_2-adrenoceptors and P_{2X}-purinoceptors. *Acta Physiol. Scand.*, **136**, 139–140.

BATTY, I.H. & NAHORSKI, S.R. (1989). Rapid accumulation and sustained turnover of inositol phosphates in cerebral-cortex slices after muscarinic-receptor stimulation. *Biochem. J.*, **260**, 237–241.

BERRIDGE, M.J. (1983). Rapid accumulation of inositol trisphosphate reveals that agonists hydrolyse polyphosphoinositides instead of phosphatidylinositol. *Biochem. J.*, **212**, 849–858.

BERRIDGE, M.J. & IRVINE, R.F. (1989). Inositol phosphates and cell signalling. *Nature*, **341**, 197–205.

BRODDE, O.E., ZERKOWSKI, H.R., BORST, H.G., MAIER, W. & MICHEL, M.C. (1989). β-adrenoceptor regulation in the human heart: can it be monitored in circulating lymphocytes? *Eur. Heart J.*, **10**, 38–44.

BRODDE, O.E. & MICHEL, M.C. (1989). Disease states can modify both receptor number and signal-transduction pathways. *Trends Pharmacol. Sci.*, **10**, 383–384.

EKAS, R.D. & LOKHANDWALA, M.F. (1981). Sympathetic nerve function and vascular reactivity in spontaneously hypertensive rats. *Am. J. Physiol.*, **240**, R379–R383.

FOUDA, A.K., MARAZZI, A., BOILLAT, N., GUILLAN, H. & ATKINSON, J. (1987). Changes in vascular reactivity of the isolated tail arteries from spontaneously and renovascular hypertensive rats to endogenous and exogenous noradrenaline. *Blood Vessels*, **24**, 63–75.

HOLMAN, M.E. & SURPRENANT, A. (1980). An electrophysiological analysis of the effects of noradrenaline and α-receptor agonists on neuromuscular transmission in mammalian muscular arteries. *Br. J. Pharmacol.*, **71**, 651–661.

JENKINSON, S., GUILD, S. & MUIR, T.C. (1990). Differences in inositol phosphate accumulation in response to noradrenaline in tail arteries from spontaneously hypertensive rats. *Br. J. Pharmacol.*, **101**, 534P.

MUIR, T.C. & WARDLE, K.A. (1989). Vascular smooth muscle responses in normo- and hypertensive rats to sympathetic nerve stimulation and putative transmitters. *J. Autonom. Pharmacol.*, **9**, 23–34.

SCHWARZE, J., GUILD, S.B. & MUIR, T.C. (1990). The mechanical and biochemical interactions of individual co-transmitters in rat tail artery. *Br. J. Pharmacol.*, **101**, 532P.

SHEARS, S.B., STOREY, D.J., MORRIS, A.J., CUBITT, A.B., PARRY, J.B., MICHELL, R.H. & KIRK, C.J. (1987). Dephosphorylation of myo-inositol 1,4,5-trisphosphate and myo-inositol 1,3,4-triphosphate. *Biochem. J.*, **242**, 393–402.

(Received September 13, 1991
Revised February 6, 1992
Accepted March 31, 1992)

Br. J. Pharmacol. (1992), **106**, 865–870 © Macmillan Press Ltd, 1992

The effects of noradrenaline and adenosine 5′-triphosphate on polyphosphoinositide and phosphatidylcholine hydrolysis in arterial smooth muscle

[1]Jane E. Nally, T.C. Muir & [2]S.B. Guild

Department of Pharmacology, University of Glasgow, Glasgow G12 8QQ

1 The effects of noradrenaline and α,β,methylene adenosine 5′-triphosphate (α,β,methylene ATP) on polyphosphoinositide metabolism, phosphatidylcholine hydrolysis and contraction in rabbit saphenous arteries were investigated. The effect of noradrenaline upon polyphosphoinositide metabolism was also investigated in the rat tail artery.

2 Noradrenaline (10^{-7}– 10^{-4} M) evoked a concentration-dependent increase in total inositol phosphate accumulation in the rat tail but not in the rabbit saphenous artery. Propranolol (3×10^{-6} M) did not alter this result in the rabbit saphenous artery. In addition, α,β,methylene ATP (10^{-6} M) significantly increased total inositol phosphate accumulation in the rabbit saphenous artery, while potassium chloride (8×10^{-2} M) was ineffective.

3 Phorbol 1,2-myristate 1,3-acetate (3×10^{-8} M) enhanced noradrenaline (10^{-2}–10^{-4} M)-evoked contractions in rabbit saphenous artery. The contractile responses to potassium chloride (1– 16×10^{-2} M) in tissues treated with 6-hydroxydopamine (5×10^{-4} M), *in vitro*, were unaffected by these concentrations of the phorbol ester.

4 Noradrenaline (10^{-6}– 10^{-4} M) evoked a concentration-dependent increase in the levels of choline and choline phosphate, but not in those of glycerophosphocholine, in the rabbit saphenous artery. Choline levels increased significantly over the first 15–30 s then declined to control levels within 2 min of addition of noradrenaline (10^{-5} M). A smaller initial rise in choline phosphate levels (15–30 s) was followed by a larger secondary rise at 2–4 min.

5 α,β,methylene ATP (10^{-7}–10^{-4} M) also evoked a concentration-dependent increase in the levels of both choline and choline phosphate, but not those of glycerophosphocholine, in the rabbit saphenous artery. α,β,methylene ATP (10^{-4} M) significantly increased levels of both of these products within the first 15–30 s of addition of the drug; these levels reached a stable plateau 1 min after addition.

6 The maximum accumulation of choline or choline phosphate evoked by either noradrenaline or α,β,methylene ATP, acting alone or in combination, was not significantly different. No evidence of synergism between noradrenaline and α,β,methylene ATP was observed.

7 This study demonstrates that each of the co-transmitters in the rabbit saphenous artery, noradrenaline and adenosine 5′-triphosphate (ATP), promote phosphatidylcholine hydrolysis. Noradrenaline seems to rely on phosphatidylcholine hydrolysis to mediate its contractile effects, whilst ATP promotes both polyphosphoinositide and phosphatidylcholine metabolism suggesting that multiple signal-transduction mechanisms are involved in stimulus-contraction coupling in this artery.

Keywords: Noradrenaline; adenosine 5′-triphosphate; vascular smooth muscle; phosphatidylcholine; polyphosphoinositides; rabbit saphenous artery

Introduction

Stimulation of sympathetic nerves to the rabbit saphenous artery releases two excitatory substances, noradrenaline and adenosine 5′-triphosphate (ATP, or a related substance), which may act as co-transmitters (Burnstock & Warland, 1987). Investigation of the electrical and mechanical response to field stimulation of the extrinsic nerves in this tissue (Nally & Muir, 1992) has already shown that the non-adrenergic (purinergic) component comprises both excitatory junction potentials (e.j.ps) and contractions, while noradrenaline produces contractions but no change in membrane potential. There remained the question of how neuronally-released noradrenaline produced contractions in this tissue and of how, if co-transmission existed, the components interacted to fulfil their co-operative function.

In the absence of voltage-dependent mechanisms, several biochemical transduction systems could account for noradrenaline-mediated contractions. In some arteries, e.g. that of the rat tail (Fox *et al.*, 1985) and the rabbit mesenteric artery (Hashimoto *et al.*, 1986), transmitter-receptor interactions lead to hydrolysis of the membrane phospholipid, phosphatidylinositol 4,5, bisphosphate (PIP_2), by phosphatidylinositol-specific phospholipase C. This hydrolysis produces the 'second messengers' inositol (1,4,5) trisphosphate, which releases Ca^{2+} from the endoplasmic reticulum (Burgess *et al.*, 1983), and diacylglycerol, which stimulates protein kinase C (Nishizuka, 1983). There may, however, be several different forms of diacylglycerol liberated from membrane phospholipids to interact with a family of protein kinase C isozymes (see Billah & Anthes, 1990).

In addition to the breakdown of PIP_2, diacylglycerol may be released by the hydrolysis of phosphatidylcholine, a more common membrane phospholipid than PIP_2 (see Loffelholz, 1989). A number of phospholipases may be involved in the hydrolysis of phosphatidylcholine, including phospholipase D which produces choline and phosphatidic acid. Further hydrolysis of phosphatidic acid by phosphohydrolase leads to

[1] Present address: Institute of Physiology, University of Glasgow, Glasgow G12 8QQ.
[2] Author for correspondence at: School of Biological and Medical Sciences, University of St. Andrews, St. Andrews, Fife KY16 9AJ.

the production of diacylglycerol. Diacylglycerol and choline phosphate are the products of phosphatidylcholine hydrolysis by phosphatidylcholine-specific phospholipase C, whilst diacylglycerol itself is also produced by the action of phospholipase A_2.

The formation of diacylglycerol and hence protein kinase C activation, has already been established as an important component of excitation-contraction coupling (Rink *et al.*, 1983; Nishizuka, 1986; Singer *et al.*, 1989) but the contribution of phosphatidylcholine in smooth muscle contraction has not. Accordingly, the present study had two objectives; firstly, to determine if PIP_2 and phosphatidylcholine hydrolysis could provide a mechanistic basis for the contractile responses to noradrenaline and ATP in the rabbit saphenous artery and, secondly, to examine if any interaction between noradrenaline and ATP occurred in terms of these biochemical mechanisms, in a tissue in which co-transmission has been proposed. Preliminary accounts of this study have been communicated to the British Pharmacological Society (Nally *et al.*, 1991a,b).

Methods

Preparation of tissues

Male New Zealand white rabbits (1.5–2.5 kg) and male Wistar rats (200–400 g) were killed either by Halothane overdose or, alternatively, by a blow to the head, followed, in each case, by exsanguination. Lengths (as detailed in the text) of rabbit saphenous artery (from 1 cm below to 3 cm above the knee) and rat tail artery were dissected out by the method of Holman & Surprenant (1979).

Measurement of phosphatidylinositol 4,5,bisphosphate hydrolysis

The effects of noradrenaline and ATP (using the stable analogue of ATP, α,β,methylene ATP) on PIP_2 hydrolysis were measured in both rabbit saphenous and rat tail arteries by analysis of the water soluble products of hydrolysis, the inositol phosphates (expressed as total inositol phosphates), using a modification of the method of Akhtar & Abdel-Latif (1986). Briefly, lengths (2–4 cm) of each artery were pre-incubated for 3 h in a physiological salt solution supplemented with *myo*-[2-^{3}H]-inositol (8 μCi ml^{-1}), followed by a further 15 min in fresh isotope-containing physiological solution containing lithium chloride (10 mM) to inhibit inositol monophosphatase (Hallcher & Sherman, 1980). The physiological salt solution had the following composition (mM): NaCl 118.4, $NaHCO_3$ 25, NaH_2PO_4 1.1, KCl 4.7, $CaCl_2$ 2.7, $MgCl_2$ 1.3, glucose 11. Agonists were added for 25 min and antagonists 15 min before agonists. Incubations were terminated by placing artery segments in 1 ml of ice cold trichloroacetic acid (10% w:v). Tissues were homogenized and centrifuged (2,000 *g*, 15 min, 4°C). Excess trichloroacetic acid was extracted with water-saturated diethyl ether (4 times, 4 ml) and the samples were neutralised with NaOH (0.1 M). Separation of the inositol phosphates from other water soluble components of the extract was carried out by anion exchange chromatography (Downes *et al.*, 1986).

Contractile studies

Rabbit saphenous arteries were used to examine the effects of the phorbol ester, phorbol 1,2-myristate 1,3-acetate, which stimulates protein kinase C (Nishizuka, 1983), on noradrenaline-and potassium chloride-evoked contractions. Contractions of ring segments (1–2 cm) of rabbit saphenous artery in organ baths (10 ml) were recorded isometrically in physiological solution at 37°C. Segments of this artery were mounted, under 1 g tension, on two Pt wires (0.3 mm diameter) placed in the lumen. One wire was fixed and the other attached to a force displacement transducer. Phorbol 1,2,-myristate 1,3-acetate was added 1 h before challenge with agonists. In order to minimize any presynaptic effects of depolarization, contractions to potassium chloride were examined after pretreatment with 6-hydroxydopamine (5×10^{-4} M) *in vitro* to destroy adrenergic nerves (Wadsworth, 1973).

Measurement of phosphatidylcholine hydrolysis

The effects of noradrenaline and α,β,methylene ATP, acting either alone or in combination, on hydrolysis of phosphatidylcholine were estimated in the rabbit saphenous artery, by measurement of changes in the levels of choline, choline phosphate and glycerophosphocholine, the respective products of phospholipase D, phosphatidylcholine – specific phospholipase C and phospholipase A_2 activity, using a modification of the method of Cook & Wakelam (1989). Briefly, lengths of artery (2–4 cm) were pre-incubated with Krebs solution supplemented with [methyl-^{3}H]-choline chloride (2 μCi ml^{-1}). Tissues were then washed twice in fresh physiological solution and agonists added for the appropriate time. Antagonists were added 15 min before the agonists. The incubations were terminated by placing the artery segments in ice-cold methanol (1 ml) and the products of the hydrolysis of phosphatidylcholine extracted by a methanol:chloroform:water mixture (10:10:9). Samples were homogenized, centrifuged (2,000 *g*, 15 min, 4°C) and the liberated [^{3}H]-choline, [^{3}H]-choline phosphate and [^{3}H]-glycerophosphocholine, in the aqueous phase, separated by anion exchange chromatography (Cook & Wakelam, 1989).

The chemicals used were obtained from the following sources; α,β,methylene ATP, 6-hydroxydopamine hydrobromide, (−)-noradrenaline bitartrate, phorbol 1,2-myristate 1,3-acetate and (±)-propranolol hydrochloride from Sigma, St. Louis Mo. U.S.A.; *myo*-[2-^{3}H]-inositol (18.3 Ci mmol^{-1} in an ethanol solution) and [methyl ^{3}H]-choline chloride (75–85 Ci mmol^{-1} in an ethanol solution) from Amersham International, Amersham, Bucks; prazosin hydrochloride was a gift from Pfizer Research, Sandwich, Kent. Halothane was purchased from I.C.I. Alderly Edge, Lancs. Concentrations in the text refer to the salts.

Analysis of results

Results are expressed as means ± s.e.mean; *n*, the number of observations refers to the number of animals used. Student's *t* test was used in all cases to test for significance between means except in Figure 3 where one-way regression analyses were used. A *P* value of <0.05 was taken as significant.

Results

Stimulated total inositol phosphate accumulation in rat tail and rabbit saphenous arteries

Noradrenaline (10^{-7}–10^{-4} M) evoked a concentration-dependent increase in total inositol phosphate accumulation in the rat tail but not in the rabbit saphenous artery (Figure 1). The pD_2 value for noradrenaline in the rat tail artery was 5.47 ± 0.2, $n = 12$. The stimulation of total inositol phosphate accumulation by noradrenaline in the rat tail artery was inhibited by prazosin (10^{-6} M; d.p.m. mg^{-1} tissue, control, 1076 ± 73.8; in the presence of prazosin (10^{-6} M) and noradrenaline (10^{-4} M) 1210 ± 58.7, $n = 8$ in each case). Propranolol (3×10^{-6} M), added to inhibit any β-adrenoceptor-mediated inhibition of PIP_2 hydrolysis, as occurs in bovine trachea (Hall & Hill, 1988), did not alter the absence of total inositol phosphate accumulation to noradrenaline in the rabbit saphenous artery (d.p.m. mg^{-1} tissue, control, 1085 ± 73.8; in the presence of propranol (3×10^{-6} M) and noradrenaline (10^{-4} M) 1210 ± 58.7, $n = 8$ in each case). This suggested that

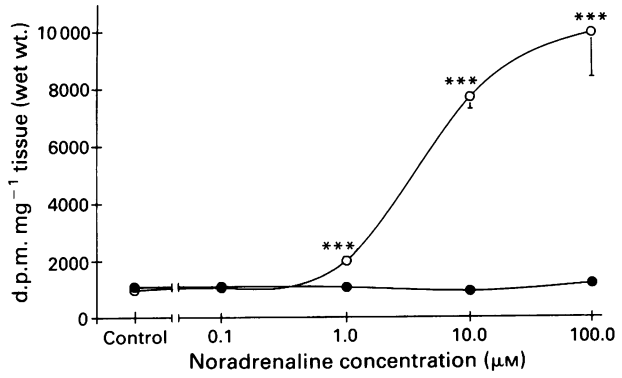

Figure 1 The effect of increasing doses of noradrenaline (10^{-7}–10^{-4} M) on the accumulation of total [^{3}H]-inositol phosphates, measured as disintegrations per minute (d.p.m.) per mg of tissue (wet weight), in rat tail ($n = 12$, O) and rabbit saphenous ($n = 10$, ●) arteries pre-incubated with *myo*-(2-^{3}H]-inositol, compared with the respective unstimulated controls. ***Indicates a significant ($P < 0.001$) response. Vertical bars represent s.e.mean.

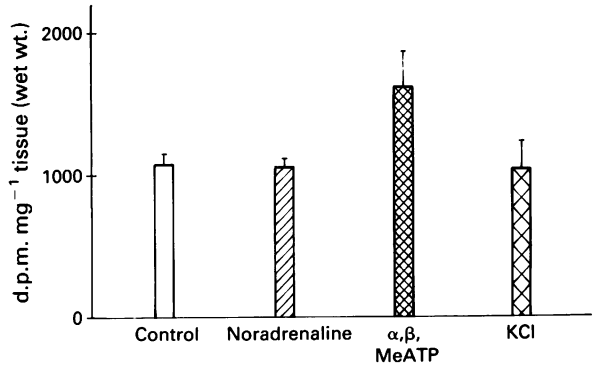

Figure 2 The effect of noradrenaline (10^{-5} M), α,β,methylene adenosine 5'-triphosphate, (α,β,Me ATP, 10^{-6} M) and potassium chloride (KCl 8×10^{-2} M), on the accumulation of total [^{3}H]-inositol phosphates measured as disintegrations per minute (d.p.m.) per mg of tissue (wet weight), compared with controls in rabbit saphenous arteries pre-incubated with *myo*-[2-^{3}H]-inositol. While noradrenaline and potassium chloride (KCl) were each ineffective, α,β,methylene ATP evoked a significant rise in total inositol phosphate levels (**$P < 0.005$) compared with controls. Number of observations (n) = 23 in each case. Vertical bars represent s.e.mean.

PIP_2 hydrolysis was not utilised in the contractions evoked by noradrenaline in the rabbit saphenous artery.

In contrast, α,β,methylene ATP (10^{-6} M, the EC_{50} value for contraction; Muir & Nally, 1989), significantly increased total inositol phosphate accumulation in the rabbit saphenous artery (Figure 2), indicating that the phosphoinositide transduction mechanism is present and operative. Potassium chloride, at a concentration (8×10^{-2} M) which evoked a degree of contraction similar to that of 10^{-6} M α,β,methylene ATP, did not increase accumulation of total inositol phosphates, thus indicating that a rise in the cytosolic calcium, evoked by the membrane depolarizing effects of α,β,methylene ATP, is not the stimulus for polyphosphoinositide metabolism.

The effect of phorbol esters on agonist-induced contractions in the rabbit saphenous artery

Phorbol 1,2-myristate 1,3-acetate (10^{-8}–10^{-7} M) enhanced, in a concentration-dependent manner, the contractions to noradrenaline (10^{-7}–10^{-4} M, Figure 3a). The maximum response to noradrenaline was increased (2 fold by 3×10^{-5} M noradrenaline) in the presence of phorbol ester (3×10^{-8} M). In contrast, in tissues which had been treated *in vitro* with 6-hydroxydopamine (5×10^{-4} M) for 2 h to destroy adrenergic nerves and so remove depolarization-evoked transmitter release (Wadsworth, 1973), the phorbol ester did not affect contractions to potassium chloride ($1-16 \times 10^{-2}$ M) (Figure 3b). Since potassium chloride produces contraction by depolarization-evoked increases in intracellular calcium concentration, the failure of the phorbol ester to augment potassium chloride-evoked contractions suggests that the synergism between the phorbol ester and noradrenaline is not due to a synergism between protein kinase C activation and increased intracellular calcium concentration.

The effect of noradrenaline on phosphatidylcholine hydrolysis in rabbit saphenous artery

Figure 4 shows that noradrenaline (10^{-6}–10^{-4} M) evoked a concentration-dependent, prazosin (10^{-6} M)-sensitive, significant increase in the levels of both [^{3}H]-choline and [^{3}H]-choline phosphate (approximately 3 and 8 fold increases respectively). The pD_2 values for noradrenaline against choline and choline phosphate were, respectively, 5.6 ± 0.5 and 5.72 ± 0.6 ($n = 10$ in each case). No accumulation of [^{3}H]-glycerophosphocholine in response to noradrenaline (10^{-6}–10^{-4} M) was detected (d.p.m. mg^{-1} tissue, control, 233 ± 72;

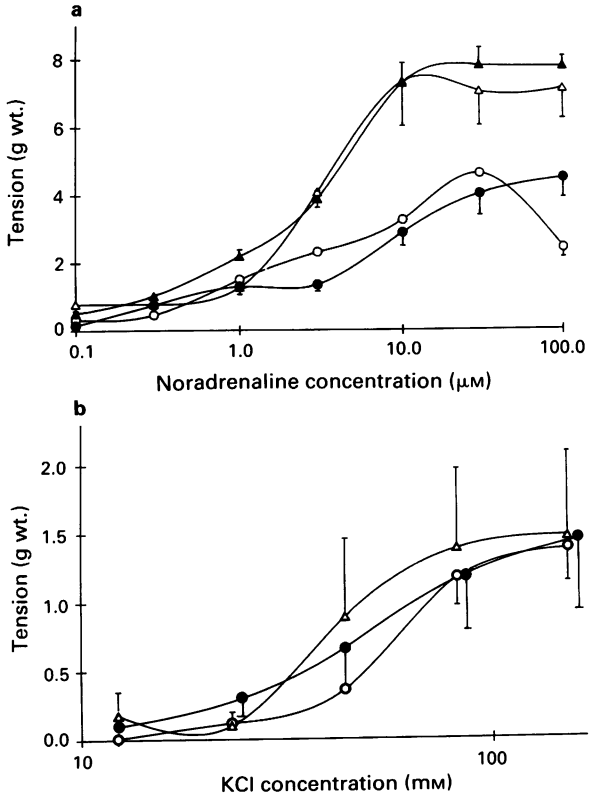

Figure 3 Contractions of the rabbit saphenous artery to noradrenaline (10^{-7}–10^{-4} M) in the absence (O) and presence of phorbol, 1,2-myristate 1,3-acetate (10^{-8} M (●), 3×10^{-8} M (Δ) and 10^{-7} M (▲) a) and to potassium chloride (KCl, $1-16 \times 10^{-2}$ M) in the absence (O) and presence of phorbol 1,2-myristate 1,3-acetate (3×10^{-8} M (●), 10^{-7} M (Δ)) (b). Contractions to KCl were evoked after pretreatment with 6-hydroxydopamine (5×10^{-4} M) *in vitro* to destroy noradrenergic nerves. The responses evoked by noradrenaline ($> 3 \times 10^{-6}$ M) were significantly enhanced by the presence of phorbol, 1,2 myristate-1,3-acetate (3×10^{-8} M, or greater) compared with control, untreated preparations. Number of observations (n) = 8 in each case. Vertical bars represent s.e.mean when it exceeds the size of the symbols.

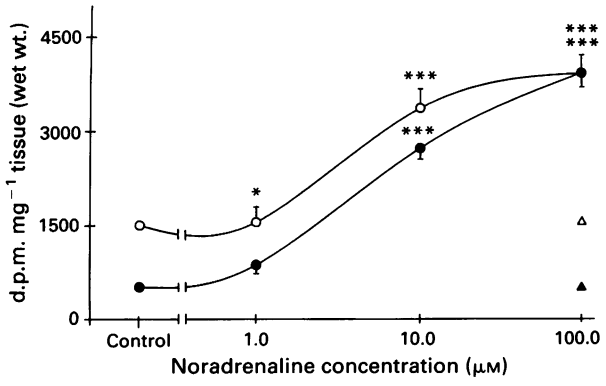

Figure 4 The effect, measured after 30 s, of increasing concentrations of noradrenaline on the accumulation of [^{3}H]-choline (○) and [^{3}H]-choline phosphate (●) in rabbit saphenous arteries, pre-incubated with [methyl ^{3}H]-choline chloride measured as disintegrations per minute (d.p.m.) per mg tissue (wet weight). The effect of prazosin (10^{-6} M) on noradrenaline-evoked responses is indicated by (△) for choline and (▲) for choline phosphate values. Number of observations (n) = 10 in each case. * and ** indicate significant ($P<0.05$ and $P<0.005$ respectively) increases in responses. Vertical bars represent s.e.mean.

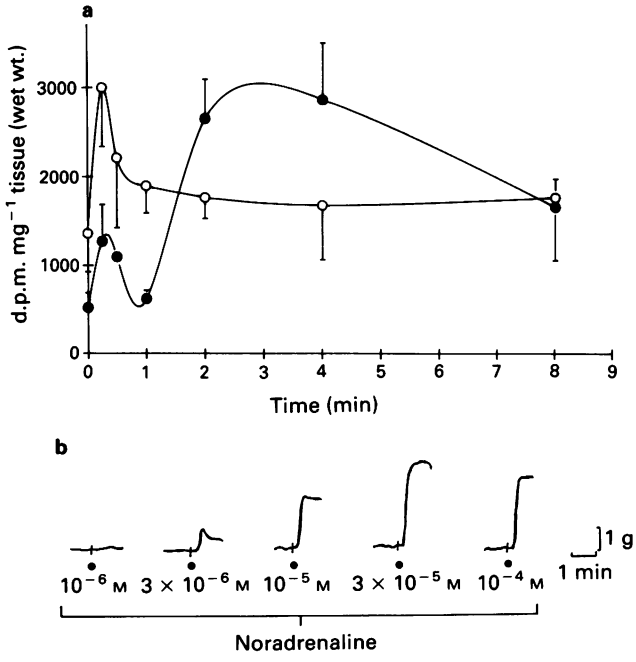

Figure 5 (a) Time-dependent changes in levels of [^{3}H]-choline (○) and of [^{3}H]-choline phosphate (●) in rabbit saphenous arteries, pre-incubated with [methyl-^{3}H]-choline chloride, in response to noradrenaline (10^{-5} M), measured as disintegrations per minute (d.p.m.) per mg tissue (wet weight). There was an initial (15–30 s) significant rise in the levels of choline and of choline phosphate. Number of observations (n) = 10 in each case. (b) The effect of increasing concentrations of noradrenaline (10^{-6}–10^{-4} M) on the tension developed in the rabbit saphenous artery. Vertical bars represent s.e.mean.

in the presence of noradrenaline 10^{-4} M, 211 ± 49, n = 10 in each case).

In time course studies, differences in the accumulation of [^{3}H]-choline and [^{3}H]-choline phosphate to noradrenaline (10^{-5} M) were observed (Figure 5). [^{3}H]-choline levels increased significantly (2.5 fold) over the first 15–30 s, then declined to a steady value not significantly different from controls, within 2 min of addition of noradrenaline. The pattern of [^{3}H]-choline phosphate accumulation (smaller in magnitude than that of [^{3}H]-choline), in the first minute after addition of noradrenaline, parallelled that of [^{3}H]-choline, but a second significant accumulation of [^{3}H]-choline phosphate (approximately 6 fold) was observed some 2 min after addition of the catecholamine. In addition, the time taken to develop the maximum contractile response to noradrenaline (approximately 30 s), corresponded to that at which the initial rises in the levels of choline and choline phosphate occurred (Figure 5b). Together, these results suggest that noradrenaline (10^{-5} M) induced the hydrolysis of phosphatidylcholine by activation of both phospholipase D and phosphatidylcholine-specific phospholipase C but not by phospholipase A_2.

The effect of αβ,methylene adenosine 5'-triphosphate on phosphatidylcholine hydrolysis in the rabbit saphenous artery

α,β,Methylene ATP (10^{-7}–10^{-4} M) evoked a significant concentration-dependent increase in the levels of both [^{3}H]-choline and [^{3}H]-choline phosphate in the rabbit saphenous artery (Figure 6). The pD_2 values for α,β,methylene ATP against choline and choline phosphate were 7.25 ± 0.45 and 6.53 ± 0.5 respectively, n = 10 in each case. From time course studies, it was evident that α,β,methylene ATP (10^{-6} M) increased levels of both of these products significantly within the first 15–30 s of addition of the compound and reached a stable plateau (3 fold increase over control) 1 min after addition (Figure 7a). Accumulation of [^{3}H]-glycerophosphocholine was unaffected by α,β,methylene ATP (d.p.m. mg^{-1} tissue, control, 289 ± 105; in the presence of α,β,methylene ATP 10^{-4} M, 325 ± 60; n = 10 in each case).

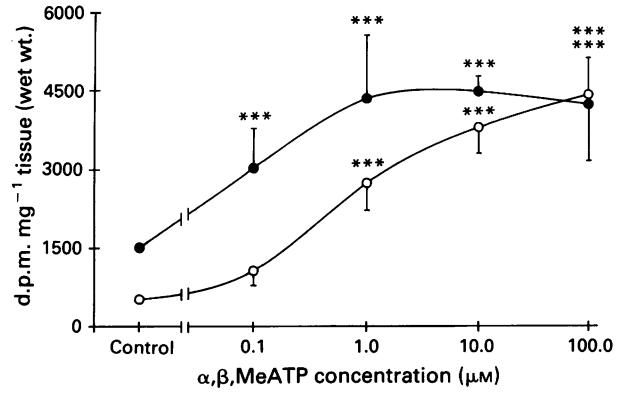

Figure 6 The effect, measured after 30 s, of increasing concentrations of α,β,methylene adenosine 5'-triphosphate (α,β,Me ATP, 10^{-7}–10^{-4} M) on the accumulation of [^{3}H]-choline (○) and of [^{3}H]-choline phosphate (●) in rabbit saphenous arteries, preincubated with [methyl-^{3}H]-choline chloride, measured as disintegrations per minute (d.p.m.) per mg tissue (wet weight). The respective control values (choline, ○ and choline phosphate, ●) are indicated. Number of observation (n) = 10 in each case. ***Indicates a significant ($P<0.001$) increase. Vertical bars represent s.e.mean.

The effect of noradrenaline and α,β,methylene adenosine 5'-triphosphate added together upon phosphatidylcholine hydrolysis in rabbit saphenous artery

Noradrenaline (10^{-6}–10^{-4} M) and α,β,methylene ATP (10^{-6}–10^{-4} M) alone, or combined in equal concentrations, produced concentration-dependent increases in [^{3}H]-choline (Figure 8a) and [^{3}H]-choline phosphate levels (Figure 8b). The maximum response to each agonist alone was not exceeded by that produced by a combination of the two. No evidence of synergism was observed.

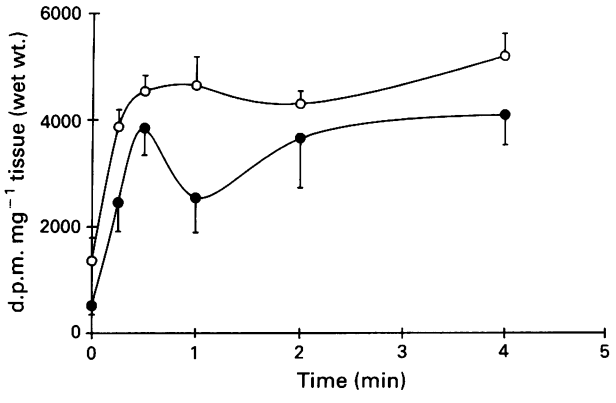

Figure 7 Time-dependent changes in the levels of [^{3}H]-choline (○) and [^{3}H]-choline phosphate(●) in rabbit saphenous arteries, preincubated with [methyl-^{3}H]-choline chloride, in response to α,β,methylene adenosine 5'-triphosphate, (10^{-6} M), measured as disintegrations per minute (d.p.m.) per mg tissue (wet weight). Number of observations (n) = 10 in each case. Vertical bars represent s.e.mean.

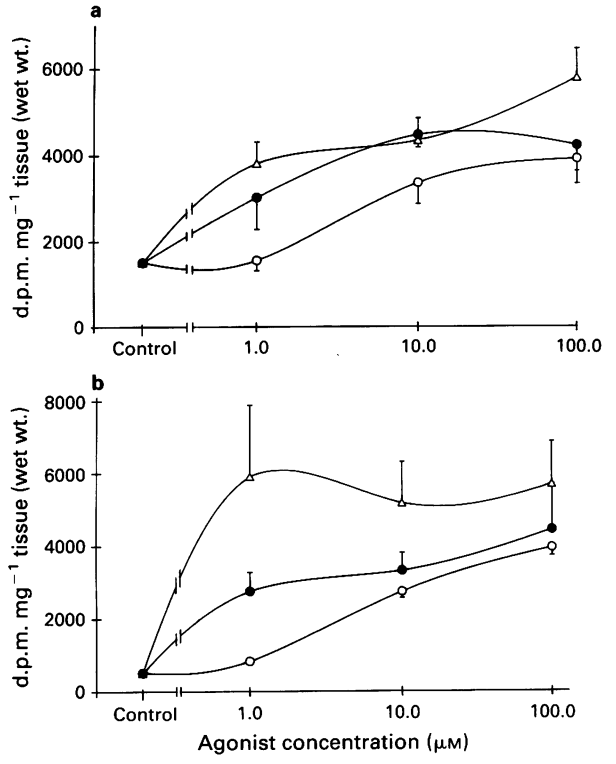

Figure 8 The effect, measured after 30 s, of increasing concentrations of noradrenaline (n = 8, ○) of α,β,methylene adenosine 5'-triphosphate (n = 8, ●), and of the two combined (n = 10, Δ), on accumulation of (a) [^{3}H]-choline and (b) [^{3}H]-choline phosphate, in rabbit saphenous arteries, preincubated with [methyl-^{3}H]-choline chloride. Vertical bars represent s.e.means.

Discussion

PIP_2-hydrolysis, already implicated in noradrenaline-evoked contractions in vascular smooth muscle (Abdel-Latif, 1986), was a logical starting point from which to investigate the biochemical transduction mechanisms involved in arterial smooth muscle contraction. Hence, the absence of noradrenaline-evoked phosphoinositide metabolism in the rabbit saphenous artery was surprising and in contrast to the positive findings in the rat tail artery (Fox *et al.*, 1985; present study), rabbit aorta (Campbell *et al.*, 1985) and rabbit mesenteric artery (Hashimoto *et al.*, 1986). Interestingly, both the rat tail (Sneddon & Burnstock, 1984) and the rabbit mesenteric (Lim *et al.*, 1986) arteries display a similar pattern of electrical responses to their co-transmitters as does the rabbit saphenous artery (Sneddon & Burnstock, 1984; Lim *et al.*, 1986). Thus, in the rabbit saphenous artery the electrical response is mediated by ATP alone, while both noradrenaline and ATP contribute to the contraction (cf. Lim *et al.*, 1986). Failure of noradrenaline to cause accumulation of total inositol phosphates in the rabbit saphenous artery is due neither to the absence of a mechanism for PIP_2 hydrolysis, since α,β,methylene ATP was effective, nor to β-adrenoceptor attenuation of PIP_2 hydrolysis (Hall & Hill, 1988); propranolol did not unmask any accumulation of total inositol phosphates in response to noradrenaline. Nor is the lack of response to noradrenaline in the rabbit saphenous artery due to deficiencies in the methodology used, since the catecholamine was demonstrably effective in stimulating the accumulation of total inositol phosphates in rat tail artery. Interestingly, where phosphoinositide metabolism is evident in the rabbit saphenous artery, it is likely to be mediated via a receptor-operated mechanism. Potassium chloride, which causes contraction via an opening of voltage-dependent calcium channels, did not increase total inositol phosphate levels.

An involvement of, or regulation by, diacylglycerol and hence, by implication, a protein kinase C, at some stage in the α_1-adrenoceptor-mediated contraction to noradrenaline, was implied by the ability of phorbol 1,2-myristate 1,3-acetate to enhance contractions to noradrenaline but not to potassium chloride in the rabbit saphenous artery. Since PIP_2 hydrolysis was not the source of diacylglycerol in this tissue, an alternative, namely phosphatidylcholine hydrolysis, was examined. Phosphatidylcholine can be hydrolysed by a number of phospholipases – phospholipase D, phosphatidylcholine-specific phospholipase C or phospholipase A_2. The respective water soluble intermediates of this hydrolysis are choline, choline phosphate or glycerophosphocholine, along with lipid soluble products which lead to diacylglycerol formation. The particular forms of diacylglycerol produced by these phospholipases acting on phosphatidylcholine differ from those produced by PIP_2 hydrolysis and are very effective activators of protein kinase C *in vitro* (Go *et al.*, 1987). Since a number of forms of protein kinase C exist (Nishizuka, 1988), the molecular species of diacylglycerol produced from phosphatidylcholine may exert differential effects on the various forms of protein kinase C, perhaps leading to different cellular effects from those produced by PIP_2 hydrolysis (Exton, 1990).

Noradrenaline evoked concentration-dependent, increases in levels of choline and choline phosphate demonstrate a role for phosphatidylcholine hydrolysis in the response of smooth muscle to this catecholamine. In addition, noradrenaline-stimulated phosphatidylcholine hydrolysis was demonstrated in the absence of PIP_2 hydrolysis. Although this separation of the two mechanisms has been reported before in some cell lines (for review see Billah & Anthes, 1990), it is much more common for both systems to operate simultaneously. Indeed, it has been suggested that phosphatidylcholine hydrolysis is a consequence of a primary PIP_2 hydrolysis. This is clearly not the case in the rabbit saphenous artery where noradrenaline-stimulated PIP_2 hydrolysis was not detected.

Stimulation of phosphatidylcholine hydrolysis was not unique to noradrenaline; α,β,methylene ATP stimulated both phosphatidylcholine and PIP_2 hydrolysis in the rabbit saphenous artery. This parallel rise in the levels of choline and choline phosphate (but not in those of glycerophosphocholine) implied that phospholipase D and phosphatidylcholine-specific phospholipase C (but not phospholipase A_2) were involved in the response to both noradrenaline and α,β-methylene ATP.

Some further indication of the phospholipases involved was given by the time course studies of the accumulation of the products of phosphatidylcholine hydrolysis. The initial

increase in the levels of choline corresponded with the time course for contraction, suggesting that noradrenaline stimulates the activity of phospholipase D (Figure 5b). Similarly, the (smaller) increase in choline phosphate levels could have arisen from the activity of phosphatidylcholine-specific phospholipase C. The larger, secondary increase in choline phosphate, at about 2–4 min, subsequent to the onset of the maximum contraction, could have resulted from secondary activation of phosphatidylcholine-specific phospholipase C, perhaps as a consequence of protein kinase C stimulation (see Billah & Anthes, 1990). Alternatively, phosphorylation of the choline initially liberated, which has been proposed as being part of the re-synthesis of phosphatidylcholine (see Pelech & Vance, 1989), could have been responsible. The secondary rise in choline phosphate could not be investigated further without a selective inhibitor of choline kinase, the enzyme responsible for the phosphorylation. The time course of α,β,methylene ATP-stimulated phosphatidylcholine hydrolysis also suggests the involvement of both phospholipase D and phosphatidylcholine-specific phospholipase C. Here, the involvement of phosphatidylcholine-specific phospholipase C, as shown by the rise in the levels of choline phosphate, was approximately equivalent to that seen with choline. With α,β, methylene ATP, both phospholipase D and phosphatidylcholine-specific phospholipase C seemed to be involved to a similar extent in the rabbit saphenous artery.

If co-transmission exists in the rabbit saphenous artery, synergism between noradrenaline and α,β,methylene ATP might have been anticipated but none was detected. The rise in choline levels produced by a combination of noradrenaline and α,β,methylene ATP was no greater than that produced by α,β,methylene ATP alone. In terms of choline phosphate levels, the effects of noradrenaline and α,β,methylene ATP were additive; the increase in response to the combined presence of the compounds approximately equalled the sum of the responses to the individual agonists up to a maximum accumulation which could be achieved by either compound alone.

Together, there results suggest that the contraction produced by the co-transmitters in the rabbit saphenous artery involves more than one transduction mechanism. ATP (in the form of the stable analogue α,β,methylene ATP) initiated both PIP_2 and phosphatidylcholine hydrolysis, each of which ultimately produced diacylglycerol to stimulate a protein kinase C. Contractions to field stimulation were accompanied by ATP-mediated e.j.ps (Nally & Muir, 1992). Noradrenaline, on the other hand, seems to rely solely on phosphatidylcholine hydrolysis for its contractile effects in this tissue.

The support of the S.E.R.C., I.C.I., the Wellcome Trust and the medical research funds of the University of Glasgow is acknowledged gratefully.

References

ABDEL-LATIF, A.A. (1986). Calcium-mobilising receptors, polyphosphoinositides and the generation of second messengers. *Pharmacol. Rev.*, **38**, 227–272.

AKHTAR, R.A. & ABDEL-LATIF, A. (1986). Surgical sympathetic denervation increases α_1-adrenoceptor mediated accumulation of *myo*-inositol trisphosphate and muscle contraction in rabbit iris dilator smooth muscle. *J. Neurochem.*, **46**, 96–104.

BILLAH, M.M. & ANTHES, J.C. (1990). The regulation and cellular functions of phosphatidylcholine hydrolysis. *Biochem. J.*, **269**, 281–291.

BURGESS, G.M., MCKINNEY, J.S., FABIATO, A., LESLEY, B.A. & PUTNEY, J.W. (1983). Calcium pools in saponin-permeabilised guinea-pig hepatocytes. *J. Biol. Chem.*, **258**, 15336–15345.

BURNSTOCK, G. & WARLAND, J.I. (1987). A pharmacological study of the rabbit saphenous artery *in vitro*: a vessel with a large purinergic contractile response to sympathetic nerve stimulation. *Br. J. Pharmacol.*, **90**, 111–120.

CAMPBELL, M.D., DETH, R.C., PAYNE, R.A. & HONEYMAN, T.W. (1985). Phosphoinositol hydrolysis is correlated with agonist-induced calcium flux in the rabbit aorta. *Eur. J. Pharmacol.*, **116**, 129–136.

COOK, S.J. & WAKELAM, M.J.O. (1989). Analysis of the water-soluble products of phosphatidylcholine breakdown by anion-exchange chromatography. *Biochem. J.*, **263**, 581–587.

DOWNES, C.P., HAWKINS, P.T. & IRVINE, R.F. (1986). Inositol 1,3,4,5-tetrakisphosphate and not phosphatidylinositol 3,4-bisphosphate is the probable precursor of inositol 1,3,4-trisphosphate in agonist stimulated parotid gland. *Biochem. J.*, **238**, 501–506.

EXTON, J.E. (1990). Signalling through phosphatidylcholine breakdown. *J. Biol. Chem.*, **265**, 1–4.

FOX, A.W., ABEL, P.W. & MINNEMAN, K.P. (1985). Activation of α_1-adrenoreceptors increases [^{3}H]-inositol metabolism in rat vas deferens and caudal artery. *Eur.J. Pharmacol.*, **116**, 145–152.

GO, M., SEKIGUCHI, K., NOMURA, H., KIKKAWA, U. & NISHIZUKA, Y. (1987). Further studies on the specificity of diacylglycerol for protein kinase C activation. *Biochem. Biophys. Res. Commun.*, **144**, 598–605.

HALL, I.P. & HILL, S.J. (1988). β-Adrenoceptor stimulation inhibits histamine stimulated inositol phospholipid hydrolysis in bovine trachea smooth muscle. *Br. J. Pharmacol.*, **95**, 1204–1212.

HALLCHER, L.M. & SHERMAN, W.R. (1980). Effects of lithium ion and other agents on the activity of *myo*-inositol-1-phosphatase from bovine brain. *J. Biol. Chem.*, **155**, 10896–10901.

HASHIMOTO, T., HIRATA, M., ITOH, T., KANMURA, Y. & KURIYAMA, H. (1986). Inositol 1,4,5-trisphosphate activates pharmacomechanical coupling in smooth muscle of the rabbit mesenteric artery. *J. Physiol.*, **370**, 605–618.

HOLMAN, M.E. & SURPRENANT, A. (1979). Some properties of the excitatory junction potentials recorded from saphenous arteries of rabbits. *J. Physiol.*, **287**, 337–351.

LIM, S.P., MUIR, T.C. & WARDLE, K.A. (1986). Are both transmitters involved in the contraction of the isolated superior mesenteric artery of the rabbit? *J. Physiol.*, **378**, 56P.

LOFFELHOLZ, K. (1989). Receptor regulation of choline phospholipid hydrolysis. *Biochem. Pharmacol.*, **38**, 1543–1549.

MUIR, T.C. & NALLY, J.E. (1989). Co-transmission in the rabbit saphenous artery. *Br. J. Pharmacol.*, **96**, 188P.

NALLY, J.E., GUILD, S.B. & MUIR, T.C. (1991a). Phosphatidylcholine metabolism and contraction in arteriolar smooth muscle. *Br. J. Pharmacol.*, **101**, 504P.

NALLY, J.E., GUILD, S.B. & MUIR, T.C. (1991b). The effects of the co-transmitters noradrenaline (NA) and adenosine 5'-triphosphate (ATP) on phosphatidylcholine (PC) hydrolysis in arterial smooth muscle. *Fund. Clin. Pharmacol.*, **5**, 424P.

NALLY, J.E. & MUIR, T.C. (1992). The electrical and mechanical responses of the rabbit saphenous artery to nerve stimulation and drugs. *Br. J. Pharmacol.*, **105**, 367–376.

NISHIZUKA, Y. (1983). Phospholipid degeneration and signal transduction for protein phosphorylation. *Trends Biochem. Sci.*, **8**, 13–16.

NISHIZUKA, Y. (1986). Studies and perspectives of protein kinase C in cell surface signal transduction and tumour promotion. *Nature*, **308**, 693–698.

NISHIZUKA, Y. (1988). The molecular heterogeneity of protein kinase C and its implications for cellular regulation. *Nature*, **334**, 661–665.

PELECH, S.L. & VANCE, D.E. (1989). Signal transduction via phosphatidylcholine cycles. *Trends Biochem. Sci.*, **14**, 28–30.

RINK, T.J., SANCHEZ, A. & HALLAM, T.J. (1983). Diacylglycerol and phorbol esters stimulate secretion without raising cytoplasmic free calcium in human platelets. *Nature*, **305**, 317–319.

SINGER, H.A., OREN, J.W. & BENSCOTER, H.A. (1989). Myosin light chain phosphorylation in ^{32}P-labelled rabbit aorta stimulated by phorbol 12,13-dibutyrate and phenylephrine. *J. Biol. Chem.*, **264**, 21215–21222.

SNEDDON, P. & BURNSTOCK, G. (1984). ATP as a co-transmitter in rat tail artery. *Eur. J. Pharmacol.*, **106**, 149–152.

WADSWORTH, R. (1973). Abolition of neurally evoked responses of the rat vas deferens by 6-hydroxydopamine. *Eur. J. Pharmacol.*, **21**, 383–387.

(Received August 28, 1991
Revised February 18, 1992
Accepted March 31, 1992)

Br. J. Pharmacol. (1992), **106**, 871–876 © Macmillan Press Ltd, 1992

Prejunctional α_2-adrenoceptors in mouse atria function through G-proteins which are sensitive to N-ethylmaleimide, but not pertussis toxin

Timothy V. Murphy, [1]Sylvain Foucart & [2]Henryk Majewski

Department of Pharmacology, University of Melbourne, Parkville 3052, Victoria, Australia

1 The identity of the G-proteins involved in prejunctional α_2-adrenoceptor signal transduction in mouse atria was examined by use of the G-protein inactivators N-ethylmaleimide and pertussis toxin.

2 The α_2-adrenoceptor partial agonist clonidine (0.03 μM) inhibited the electrical stimulation-induced (S-I) outflow of radioactivity from mouse atria which were incubated with [^{3}H]-noradenaline and stimulated at 5 Hz. The partial α_2-adrenoceptor agonist St 363 (10 μM) inhibited the S-I outflow of radioactivity at the lower stimulation frequency of 2.5 Hz. The inhibitory effects of these compounds were not altered in mice pretreated with pertussis toxin (1.5 μg, i.v.).

3 The α_2-adrenoceptor antagonist, idazoxan (0.1 μM), increased the S-I outflow of radioactivity from mouse atria stimulated at 5 Hz, and this effect was not altered in atria from mice pretreated with pertussis toxin.

4 The inhibitory effects of clonidine and St 363 and the facilitatory effect of idazoxan on the S-I outflow of radioactivity from mouse atria were significantly less in atria incubated with N-ethylmaleimide (NEM, 3 μM) for 60 min before the [^{3}H]-noradrenaline incubation.

5 The results suggest that prejunctional α_2-adrenoceptors in mouse atria function through G-proteins which are NEM-sensitive, but pertussis toxin insensitive.

Keywords: G-proteins; prejunctional α_2-adrenoceptors; noradrenaline release; N-ethylmaleimide; pertussis toxin

Introduction

Structurally, α_2-adrenoceptors belong to the guanosine 5'-triphosphate (GTP)-binding protein (or G-protein) coupled family of receptors (Zeng *et al.*, 1990; Harrison *et al.*, 1991). The effects of α_2-adrenoceptor-stimulation are blocked by pertussis toxin, an agent which inactivates some G-proteins (G_i and G_o) by adenosine diphosphate (ADP)-ribosylation (see Ui, 1988). These effects include lipidolysis in fat cells (García-Sáinz, 1981), inhibition of insulin release from rat pancreatic islets (Katada & Ui, 1981) and vasoconstriction in the pithed rat (Boyer *et al.*, 1983; Docherty, 1988; Nichols *et al.*, 1988).

Activation of α_2-adrenoceptors results in inhibition of noradrenaline release from sympathetic nerves (see Starke, 1977; 1987). However, Musgrave *et al.* (1987) demonstrated that prejunctional α_2-adrenoceptors on noradrenergic nerves in mouse atria were not sensitive to pertussis toxin. In addition, pertussis toxin did not alter the inhibitory effect of the α_2-adrenoceptor agonists on cardiac responses to sympathetic nerve stimulation in the pithed rat, even though responses to postjunctional α_2-adrenoceptors in the same studies were attenuated by pertussis toxin (Docherty, 1988; Nichols *et al.*, 1988). Pertussis toxin treatment also did not affect prejunctional α_2-adrenoceptors in rat vas deferens (Docherty, 1988; 1990; however see Lai *et al.*, 1983), mouse vas deferens (Lux & Schultz, 1986), rat atria (Docherty, 1990), rat tail artery (Li, 1990) or rabbit renal artery (Wolk *et al.*, 1991). Furthermore in rat kidney, pertussis toxin abolished the inhibitory effect of the α_1-adrenoceptor agonist, methoxamine but had no effect on the inhibition produced by clonidine (Murphy & Majewski, 1990). These results are in contrast to studies performed on brain tissue, where pertussis toxin attenuated the inhibitory effects of α_2-adrenoceptor agonists on [^{3}H]-noradrenaline release from rabbit hippocampus (Allgaier *et al.*, 1985).

The aim of the present study was to use N-ethylmaleimide (NEM) in mouse atria to determine further whether G-proteins were involved in α_2-adrenoceptor signal transduction in sympathetic nerves. NEM alkylates proteins and is capable of inactivating G-proteins with some degree of selectivity over other cellular structures (Winslow *et al.*, 1987; Ueda *et al.*, 1990). NEM also alkylates G-proteins associated with α_2-adrenoceptors (Kitamura & Nomura, 1987), and has been shown to attenuate α_2-adrenoceptor-mediated inhibition of noradrenaline release from rat tail artery (Weber, 1989; Illes *et al.*, 1990), mouse vas deferens (Kaschube & Brasch, 1990) and rabbit renal artery (Wolk *et al.*, 1991). In contrast to previous studies we decided to use St 363 as our test α_2-adrenoceptor agonist as it is a weak partial agonist on prejunctional α_2-adrenoceptors (Medgett & McCulloch, 1980) and thus must activate a larger proportion of α_2-adrenoceptors to exert its effect which may make it easier to detect changes in functional α_2-adrenoceptors.

Methods

Pertussis toxin treatment

Female random bred Swiss white mice (17–38 g) were treated with pertussis toxin (1.5 μg/mouse in 0.1 ml lysine-glycerol buffer, i.v.) or vehicle solution (0.1 ml lysine-glycerol buffer, i.v.), four days before the experiment.

Atria were taken from vehicle- and pertussis toxin-treated mice. The mice were stunned, decapitated and the whole hearts removed and placed in pre-warmed (37°C) Krebs-Henseleit solution which was continuously gassed with a

[1] Present address: [1]Department of Pharmacological and Physiological Sciences, University of Chicago, 947 East 58th St., Chicago, II. 60637, U.S.A.

[2] Author for correspondence at present address: Prince Henry's Institute of Medical Research, PO Box 152, Clayton 3168, Australia.

mixture of 95% O_2/5% CO_2. The atria were dissected free and suspended in an organ bath containing 2.5 ml Krebs-Henseleit solution maintained at 37°C and continuously gassed with a mixture of 95% O_2/5% CO_2. The basal tension applied to the atria was 0.1 g. The negative chronotropic effects of carbachol (10 μM) on the spontaneously beating whole atria were determined. The atria were equilibrated for 1 h in Krebs-Henseleit solution.

The atria were then incubated with (−)-[7,8-^{3}H]-noradrenaline (0.2 μM, 2.9 μCi ml^{-1}) for 20 min. After this incubation period, the atria were washed every 2 min for 60 min with fresh Krebs-Henseleit solution. After 45 min of this washing procedure an electrical priming stimulation (5 Hz, 60 s, square wave pulses of 15 V cm^{-1}, 1 ms duration) was delivered through two platinum field electrodes. Following the washing period, the bathing solution was collected every 3 min for 54 min. There were two periods of electrical stimulation of the atria, at 9 and 39 min after the start of the sampling period, termed S_1 and S_2 respectively. Drugs were added to the bathing solution from 15 min before the second stimulation period.

At the end of the sampling period the atria were dissolved in 2 ml Soluene (Packard Instruments, U.S.A.). The amount of radioactivity in these samples and the superfusate samples was determined by adding 6 ml Picofluor-40 (Packard Instruments, U.S.A.) to each sample followed by liquid scintillation counting. Corrections were made for counting efficiency with an automatic external standard and results were expressed as disintegrations per minute (d.p.m.).

Calculation of results

The resting (spontaneous) outflow of radioactivity from the atria was taken as the mean radioactive content of the superfusate during the 3 min period immediately before stimulation and the 3 min period starting 6 min after the onset of stimulation. The stimulation-induced (S-I) outflow of radioactivity was calculated by subtracting the total amount of radioactivity in the calculated spontaneous outflow from the total amount of radioactivity in the two 3 min samples collected during and immediately after stimulation.

In all cases the S-I outflow of radioactivity was expressed as a fraction of the total tissue content of radioactivity at the time of stimulation (fractional S-I outflow). The fractional S-I outflow of radioactivity in the second stimulation period (S_2) is expressed as a percentage of that in the first (S_1). The corresponding spontaneous outflows of radioactivity are referred to as R_2 and R_1.

Incubation of mouse atria with N-ethylmaleimide

To allow direct comparison with the pertussis toxin experiments all mice were treated with lysine-glycerol buffer. Some atria from vehicle-treated mice were incubated with N-ethylmaleimide (NEM). After dissection, atria were incubated in drug-free Krebs-Henseleit solution or Krebs-Henseleit solution containing NEM (3 μM) for 60 min. The incubation solution was replaced with fresh solution every 10 min. At the end of this incubation period the atria were washed with drug-free Krebs-Henseleit solution every 1 min for 5 min and the negative chronotropic effects of carbachol (10 μM) on the spontaneously beating whole atria were determined. Experiments on [^{3}H]-noradrenaline outflow from these atria were then carried out.

Statistics

Data are expressed as means ± the standard error of the mean (s.e.mean). Statistical analysis of the data was performed by one- or two-way analyses of variance (ANOVA) followed by unpaired *t* tests between individual groups of data, unless otherwise specified. Where multiple means were compared to a single control value, a Dunnett's test was performed to compare the data. Values of $P < 0.05$ were taken to indicate significant differences between means. The statistical tests were performed with the computer programme CSS (Statsoft, Tulsa, U.S.A.).

Drugs and vehicles

The composition of the Krebs-Henseleit solution was as follows (all concentrations in mM): NaCl 118, KCl 4.7, $CaCl_2$ 2.5, $NaHCO_3$ 25, KH_2PO_3 1.3, $MgSO_4$ 0.45, D-(+)-glucose 11.1, disodium edetate 0.067 and ascorbic acid 0.14.

Pertussis toxin was obtained from Commonwealth Serum Laboratories, Parkville, Victoria. The pertussis toxin was dissolved in 50 mM Tris-HCl buffer/lysine glycerol solution (pH 8.3).

The composition of the lysine-glycerol buffer used to dissolve the pertussis toxin further was (all concentrations in mM): NaCl 250, $NaHCO_3$ 25 and L-lysine 10. All reagents were initially dissolved in deionized water and the pH adjusted to 7.5. Glycerol was then added in a 1:1 ratio to give the above concentrations.

The following drugs were purchased: (−)-[7,8-^{3}H]-noradrenaline (Radiochemical Centre, Amersham, U.K.; specific activity 10.6 Ci mmol^{-1}); carbamyl choline (carbachol), N-ethylmaleimide (Sigma Chemical Co., St. Louis, MO, U.S.A.).

The following drugs were generously donated: idazoxan (Reckitt and Colman, U.K.); clonidine hydrochloride and St 363 (2-(2,4-dichlorophenylimino)-imidazolidine; Boehringer Ingelheim, Australia). All drugs were initially dissolved in deionized water and subsequently diluted in Krebs-Henseleit solution.

Results

Effect of carbachol on spontaneous rate of beating of isolated atria

Carbachol (10 μM) completely inhibited the beating of atria from vehicle-treated mice (0.1 ml lysine-glycerol, i.v.). However, carbachol (10 μM) had no effect on the spontaneous beating of atria isolated from any pertussis toxin-treated mouse (1.5 μg/mouse, i.v.; Table 1).

Carbachol (10 μM) reduced, but did not abolish the spontaneous beating of mouse atria incubated with NEM (3 μM for 60 min) (Table 1). The basal rate of beating of atria incubated with NEM was significantly lower than that of vehicle incubated atria (Table 1).

Influence of pertussis toxin on the effects of clonidine, St 363 and idazoxan in mouse atria

The uptake of radioactivity into, and the resting and the S-I outflow of radioactivity from atria taken from pertussis toxin treated (1.5 μg, i.v.) mice and incubated in [^{3}H]-noradrenaline was not different from that in atria taken from vehicle-treated mice (Table 2).

At a stimulation frequency of 5 Hz, the S-I outflow of radioactivity from the atria of vehicle-treated mice was inhibited by clonidine (0.03 μM) and enhanced by idazoxan (0.1 μM; Figure 1) and the respective effects of clonidine or idazoxan were not significantly different in atria from pertussis toxin-treated mice (Figure 1). The partial α_2-adrenoceptor agonist St 363 (10 μM) had no effect on the S-I outflow of radioactivity from vehicle-treated mouse atria at a stimulation frequency of 5 Hz, but significantly reduced the S-I outflow of radioactivity at 2.5 Hz (Figure 1). The inhibitory effect of St 363 in atria taken from pertussis toxin-treated mice at 2.5 Hz was not significantly different from that observed in atria of vehicle-treated mice (Figure 1). Neither clonidine, St 363 nor idazoxan altered the resting outflow of radioactivity from the mouse atria (not shown).

Table 1 The influence of pertussis toxin or N-ethylmaleimide (NEM) on the effect of carbachol (10 μM) on the spontaneous rate of beating of mouse isolated atria

Treatment	n	*Rate of beating* (beats min^{-1}) *Before carbachol*		*After carbachol*
Mouse atria				
Vehicle	49	350 ± 11	---*---	0 ± 0
Pertussis toxin	23	346 ± 18		333 ± 22
NEM	37	320 ± 18	--*--	132 ± 24

Mice (1.5 μg, i.v.) were treated with pertussis toxin or vehicle solution 4 days before the experiment. NEM incubation (3 μM for 60 min) took place before incubation with [^{3}H]-noradrenaline.
*Indicates a significant effect of carbachol $P < 0.05$ (Student's t test). The inhibitory effect of carbachol was significantly reduced in NEM-incubated atria and atria from pertussis toxin-treated animals compared to that in atria from vehicle-treated animals ($P < 0.05$, two-way ANOVA). Data are represented as means ± s.e.mean. n = number of experiments in each group.

Table 2 Effect of pertussis toxin or N-ethylmaleimide (NEM) on outflow and uptake of [^{3}H]-noradrenaline from mouse atria

Parameter	*Stim. Freq.* (Hz)	*Vehicle*	n	*Treatment pertussis toxin*	n	*NEM*	n
S_1, %	5	1.49 ± 0.13	17	1.31 ± 0.07	15	0.71 ± 0.04▲	21
	2.5	0.63 ± 0.06*	24	0.68 ± 0.13*	8	0.48 ± 0.04*▲	16
	1.75	0.50 ± 0.04*	8				
R_1, %		0.98 ± 0.04	49	0.91 ± 0.04	23	1.49 ± 0.07▲	37
Tissue radioactivity (d.p.m. × 10^{-6})		1.06 ± 0.05	49	1.30 ± 0.13	23	0.71 ± 0.05▲	37

Mice were treated with vehicle solution (0.1 ml lysine-glycerol, i.v.) or pertussis toxin (1.5 μg, i.v.) 4 days before the experiment. NEM incubation (3 μM for 60 min) took place immediately before incubation with [^{3}H]-noradrenaline. There were two periods of electrical stimulation of the atria, S_1 and S_2, 30 min apart, at either 5, 2.5 or 1.75 Hz for 60 s. The fractional S-I outflow of radioactivity in S_1 (S_1, %), the fractional spontaneous outflow of radioactivity corresponding to this stimulation (R_1, %) and the total content of radioactivity at the start of the sampling period (d.p.m.) are shown. Data are represented as means ± s.e.mean. Significant differences from the S-I outflow of radioactivity at 5 Hz are represented by *, which indicates $P < 0.5$ (Student's t test after ANOVA). ▲Indicates a significant effect of NEM compared to the appropriate parameter in atria from vehicle-treated mice ($P < 0.05$, Student's t test after ANOVA).

Influence of NEM on the effects of clonidine and idazoxan in mouse atria

The uptake of radiaoctivity into mouse atria incubated with NEM before incubation with [^{3}H]-noradrenaline was significantly lower than the uptake into atria incubated in vehicle solution (Table 2). Incubation with NEM also reduced the S-I outflow of radioactivity compared with vehicle-incubated atria, at all frequencies tested (Table 2). In mouse atria incubated with NEM, the resting outflow of radioactivity was higher than that from atria incubated in vehicle solution (R_1; Table 2).

At a stimulation frequency of 5 Hz, clonidine (0.03 μM) had no effect on the S-I outflow of radioactivity from the mouse atria pre-incubated with NEM (3 μM for 60 min; Figure 2), in contrast to its inhibitory effect in vehicle-incubated atria. The enhancing effect of idazoxan (0.1 μM) on the S-I outflow of radioactivity at 5 Hz was significantly less in atria incubated with NEM than in atria incubated in vehicle solution (Figure 2). NEM also reduced the inhibitory effect of clonidine at a lower stimulation frequency of 2.5 Hz ($P < 0.05$, ANOVA; Figure 2).

Another comparison of the effects of clonidine was performed under equivalent absolute S-I outflow conditions (2.5 Hz/vehicle vs. 5 Hz/NEM; see Table 2). At 2.5 Hz, clonidine inhibited the S-I outflow of radioactivity from vehicle-treated atria to a significantly greater extent than at 5 Hz (Figure 2). When the effects of clonidine in vehicle and NEM pre-incubated atria were compared under conditions of equivalent S-I outflow of radioactivity (2.5 Hz/vehicle vs. 5 Hz/NEM), the inhibitory effect of clonidine in NEM pre-incubated atria (5 Hz stimulation) was markedly less than that observed in vehicle pre-incubated atria (2.5 Hz stimulation; $P < 0.05$, ANOVA; Figure 2).

The facilitatory effect of idazoxan on the S-I outflow of radioactivity in vehicle-treated atria was significantly less at 2.5 Hz than at 5 Hz (Figure 2). When the effects of idazoxan in vehicle and NEM pre-incubated atria were compared under conditions of equivalent S-I outflow of radioactivity (2.5 Hz/vehicle versus 5 Hz/NEM), the facilitatory effect of idazoxan in NEM pre-incubated atria (5 Hz stimulation) was still significantly less than that at 2.5 Hz in atria from vehicle-treated mice ($P < 0.05$, ANOVA; Figure 2). None of the drugs altered the resting outflow of radioactivity (not shown).

Influence of NEM on the effect of St 363 in mouse atria

St 363 significantly inhibited the S-I outflow of radioactivity from mouse atria incubated with [^{3}H]-noradrenaline and stimulated at 2.5 Hz (Figure 2). In atria pre-incubated with NEM (3 μM for 60 min) and stimulated at 2.5 Hz, St 363 (10 μM) had no effect on the S-I outflow of radioactivity (Figure 2). Another set of experiments was performed in the absence of NEM where the stimulation frequency was lowered to 1.75 Hz so that the fractional S-I outflow of radioactivity was not significantly different from the NEM-incubated atria at 2.5 Hz (Table 2). At 1.75 Hz, St 363 inhibited the S-I outflow of radioactivity from vehicle-treated atria to a significantly greater extent than at 2.5 Hz (Figure 2) and significantly greater extent than from NEM-treated atria at 2.5 Hz ($P < 0.05$, ANOVA; Figure 2). None of the drugs affected the resting outflow of radioactivity (not shown).

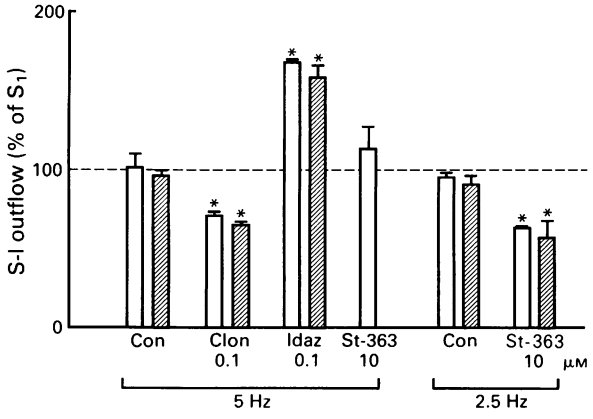

Figure 1 Influence of pertussis toxin treatment on the effects of clonidine (Clon, 0.1 μM), idazoxan (Idaz, 0.1 μM) and St 363 (10 μM) on the S-I outflow of radioactivity from mouse atria incubated in [^{3}H]-noradrenaline. Mice were treated with pertussis toxin or vehicle solution (i.v.) 4 days before the experiment. There were two periods of electrical stimulation of the atria, S_1 and S_2, 30 min apart, both 5 or 2.5 Hz for 60 s. Drugs were present from 15 min before the second stimulation period. The columns represent the fractional S-I outflow of radioactivity in S_2 as a percentage of that in S_1, and show the means with s.e.mean indicated by vertical bars. Significant differences from control experiments (Con) are represented by *, which indicates $P < 0.05$ (Student's t test, after ANOVA). The open columns refer to vehicle experiments and the hatched columns are atria from pertussis toxin-treated mice (1.5 μg). The inhibitory effects of clonidine and St 363 and the facilitatory effect of idazoxan in atria from pertussis toxin-treated mice were not significantly different from those in atria from vehicle-treated mice ($P > 0.05$, ANOVA). The number of experiments in each group (n) is as follows: for vehicle-treated mice, Con (5 Hz) = 7, Clon = 6, Idaz = 4, St 363 = 4, Con (2.5 Hz) = 11, St 363 = 4; for pertussis toxin-treated mice, Con (5 Hz) = 5, Clon = 6, Idaz = 4, Con (2.5 Hz) = 4, St 363 = 4.

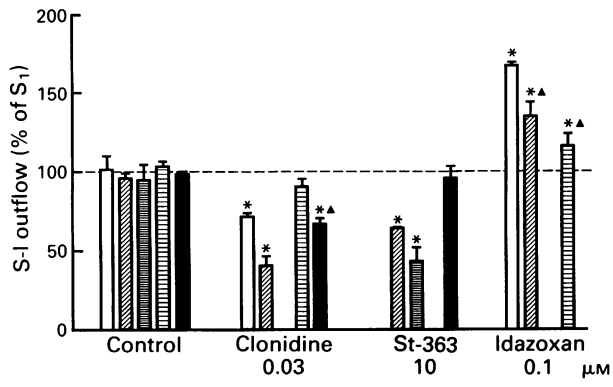

Figure 2 Influence of incubation with N-ethylmaleimide (NEM, 3 μM for 60 min) on the effects of clonidine (Clon, 0.1 μM), idazoxan (Idaz, 0.1 μM) or St 363 (10 μM) on the S-I outflow of radioactivity from mouse atria incubated in [^{3}H]-noradrenaline. There were two periods of electrical stimulation of the atria, S_1 and S_2, 30 min apart, 5, 2.5 or 1.75 Hz for 60 s. Clonidine, idazoxan or St 363 was present from 15 min prior to the second stimulation period. The columns represent the fractional S-I outflow of radioactivity in S_2 as a percentage of that in S_1, and show the means with s.e.mean indicated by vertical bars. The open columns refer to vehicle experiments (5 Hz), the oblique hatched columns are vehicle 2.5 Hz, the narrow spaced horizontal hatched are vehicle 1.75 Hz, the wide space horizontal hatched are NEM-treated 5 Hz and the black columns are NEM-treated 2.5 Hz. Significant differences from corresponding control experiments (Con are represented by *, which indicates $P < 0.05$ (Student's t test, after ANOVA). ▲Indicates that the effects of clonidine and idazoxan were significantly reduced in atria incubated with NEM from those in vehicle-incubated atria ($P < 0.05$, two-way ANOVA). The number of experiments in each group (n) is as follows: for atria from vehicle-treated mice (5 Hz), Con = 7, Clon = 6, Idaz = 4; (2.5 Hz) Con = 11, Clon = 4, St 363 = 4, Idaz = 5; (1.75 Hz) Con = 4, St 363 = 4; for NEM-incubated atria (5 Hz), Con = 9, Clon = 7, Idaz = 6; (2.5 Hz) Con = 5, Clon = 5, St 363 = 5, Idaz = 5.

Discussion

In the present study, clonidine inhibited and idazoxan enhanced stimulation-induced noradrenaline release from mouse atria which suggests that automodulatory, prejunctional α_2-adrenoceptors were functional. In atria from mice treated with the G-protein inactivator, pertussis toxin (Ui, 1988), the effects of clonidine and idazoxan on noradrenaline release were not different from those observed in atria from vehicle-treated mice. In addition, the pertussis toxin treatment had no effect on the absolute levels of noradrenaline release *per se*. All of these results are consistent with a lack of effect of pertussis toxin on the α_2-autoinhibitory mechanism and this is in agreement with an earlier study in mouse atria (Musgrave *et al.*, 1987).

One possible reason for these negative results is that pertussis toxin may have inactivated only a portion of the G-protein pool and if there were an excess of prejunctional α_2-adrenoceptors than that necessary for a full response (spare receptors) then this may not be sufficient to diminish the effects of α_2-adrenoceptor ligands. In rat hepatocytes at least 80% of the G-proteins had to be inactivated to reduce the inhibitory effect of angiotensin II on adenosine 3':5'-cyclic monophosphate (cyclic AMP) production (Pobiner *et al.*, 1985). We therefore used St 363 as an α_2-adrenoceptor agonist since it has a lower efficacy than clonidine (pD_2 of 5.5 compared to 8.8 for clonidine in guinea-pig atria; Medgett & McCulloch, 1980) and therefore has to activate a greater proportion of the α_2-adrenoceptors than clonidine to produce its effect. Indeed, at stimulation frequency of 5 Hz, St 363 had no effect on noradrenaline release (unlike clonidine) and an inhibitory effect was only revealed at a stimulation frequency of 2.5 Hz, presumably because only at the lower frequency was the concentration of neuronally-released noradrenaline low enough to enable St 363 to exert an effect. This frequency-dependence of the effects of partial α_2-adrenoceptor agonists has been shown previously (Medgett *et al.*, 1978; Rand *et al.*, 1980; Rump & Majewski, 1987). Pertussis toxin treatment had no influence on the inhibitory effect of St 363 on noradrenaline release from the mouse atria which again argues against a role for pertussis toxin-sensitive G-proteins in α_2-adrenoceptor inhibition of noradrenaline release. It should be noted that the pertussis toxin treatment was sufficient to inhibit completely muscarinic receptor-mediated bradycardia, an event mediated by pertussis toxin-sensitive G-proteins (e.g. Martin *et al.*, 1985). Similar negative results with pertussis toxin on α_2-adrenoceptor modulation of noradrenaline release have been obtained in other sympathetically innervated tissues (see Introduction). However, Nozaki & Sperelakis (1989) reported that pertussis toxin reduced the inhibitory effect of clonidine on noradrenaline release from the guinea-pig mesenteric artery.

Another tool to investigate G-proteins is N-ethylmaleimide (NEM), which alkylates sulphydryl groups. Despite this relatively non-selective action, with widespread effects at higher concentrations (see for other effects: Smith & Lauf, 1985; Schömig *et al.*, 1988; Sabatini & Kurtzman, 1989; Wölfel *et al.*, 1989; Foucart *et al.*, 1990), it has been suggested that NEM targets G-proteins selectively at lower concentrations (Winslow *et al.*, 1987; Ueda *et al.*, 1990). It has also been reported that pertussis toxin and NEM may inactivate the same G-proteins (Kitamura & Nomura, 1987; Ueda *et al.*, 1990). However, NEM may also affect G-proteins which are not pertussis toxin-sensitive. In mouse atria incubated with NEM, the inhibitory effect of neuropeptide Y and the facilitatory effects of angiotensin II and isoprenaline were reduced by NEM but not by pertussis toxin

(Foucart *et al.*, 1990). Importantly, NEM did not affect the isoprenaline or angiotensin II signal transduction pathways – cyclic AMP and protein kinase C respectively – suggesting that the NEM targeted receptor/G-protein interactions (Foucart *et al.*, 1990). Some caution must nevertheless be used since NEM by itself reduced [^{3}H]-noradrenaline release and the uptake of [^{3}H]-noradrenaline in mouse atria (Foucart *et al.*, 1990) and similar effects were seen in the present study. The reasons for this are unclear but suggest that either alkylation of G-proteins affect these processes or that the effects of NEM are not entirely selective.

In the present study the inhibitory effect of clonidine on S-I noradrenaline release was only slightly attenuated in mouse atria pre-incubated with NEM. One complicating factor in these results is that NEM by itself reduced the S-I outflow of noradrenaline from the mouse atria, as has been previously reported in mouse atria (Foucart *et al.*, 1990). Therefore it may be more appropriate to compare the effects of α_2-adrenoceptor ligands under conditions of equivalent S-I noradrenaline release, since it is well known that in the presence of a lower biophase concentration of noradrenaline, the inhibitory effect of exogenous partial α_2-adrenoceptor agonists like clonidine and St 363 are increased (present study; also Medgett *et al.*, 1978; Rand *et al.*, 1980). When compared under these conditions of equivalent S-I noradrenaline release (2.5 Hz vehicle versus 5 Hz NEM), the inhibitory effect of clonidine was clearly reduced by NEM. Similarly, under these conditions of equivalent noradrenaline release (1.75 Hz vehicle versus 2.5 Hz NEM), the inhibitory effect of St 363 was also clearly reduced in NEM-incubated atria. The facilitatory effect of idazoxan on noradrenaline release from NEM-incubated atria was significantly attenuated, but not abolished, when compared with that in vehicle-treated atria. This effect may have been entirely attributable to the reduction of noradrenaline release caused by NEM, which would result in less 'feedback' inhibition of noradrenaline release. However, when the effects of idazoxan were examined under conditions of equivalent noradrenaline release (2.5 Hz vehicle versus 5 Hz NEM), the facilitatory effect of idazoxan was still significantly attenuated in NEM-incubated atria when compared to that in vehicle-treated atria. This is an indication that the feedback inhibitions exerted by equivalent amounts of neuronally-released noradrenaline is inhibited by NEM. Taken together, these results obtained with clonidine, St 363 and idazoxan suggest that prejunctional α_2-adrenoceptors in mouse atria function through NEM-sensitive G-proteins. Similar effects of NEM on prejunctional α_2-adrenoceptors have been observed in other tissues (see Introduction).

The results suggest that prejunctional α_2-adrenoceptors in mouse atria function through G-proteins which are sensitive to NEM, but not to pertussis toxin, as also observed in rabbit renal artery (Wolk *et al.*, 1991). The question then arises as to which G-protein is involved in prejunctional α_2-adrenoceptor transduction in these tissues. Previous studies have suggested that NEM and pertussis toxin inactivate the G-proteins, G_i and G_o, primarily by acting at the same site, as NEM treatment prevents ADP-ribosylation of these G-proteins by pertussis toxin (Winslow *et al.*, 1987; Hertting & Allgaier, 1988; Ueda *et al.*, 1990). It is possible that NEM affected some other site on the G-protein α-subunit rather than the ADP-ribosylation site, as NEM alkylates several sulphydryl groups in the α-subunit that appear to be functionally important (Asano & Ogasawara, 1986; Winslow *et al.*, 1987); however, this still does not explain the ineffectiveness of pertussis toxin. The most likely explanation seems to be that prejunctional α_2-adrenoceptors in mouse atria function through G-proteins that are sensitive to NEM but not pertussis toxin. Previous results suggest that G-proteins other than G_i and G_o are affected by NEM (Sigafoos & Bramowitz, 1986; Foucart *et al.*, 1990). However, the exact nature of the G-protein involved in prejunctional α_2-adrenoceptors signal transduction on sympathetic nerve varicosities remains an enigma.

T.V.M. is a recipient of a University of Melbourne Postgraduate Writing Award. S.F. is an F.R.S.Q. Research Fellow, H.M. is a Senior Research Fellow of the National Health and Medicial Research Council of Australia. This work was supported by the National Heart Foundation of Australia and the National Health and Medical Research Council of Australia.

References

ALLGAIER, C., FEUERSTEIN, T.J. & HERTTING, G. (1985). Islet-activating protein (pertussis toxin) diminishes α_2-adrenoceptor mediated effects on noradrenaline release. *Naunyn-Schmiedebergs Arch. Pharmacol.*, **331**, 235–239.

ASANO, T. & OGASAWARA, N. (1986). Uncoupling of G-aminobutyric acid B receptors from GTP-binding proteins by N-ethylmaleimide: effects of N-ethylmaleimide on purified GTP-binding proteins. *Mol. Pharmacol.*, **29**, 244–249.

BOYER, J.L., CARDENAS, C., POSADAS, C. & GARCIA-SAINZ, J.A. (1983). Pertussis toxin induced tachycardia and impairs the increase in blood pressure produced by α_2-adrenergic agonists. *Life Sci.*, **33**, 2627–2633.

DOCHERTY, J.R. (1988). Pertussis toxin and pre-junctional α_2-adrenoceptors in rat heart and vas deferens. *J. Autonom. Pharmacol.*, **8**, 197–201.

DOCHERTY, J.R. (1990). No effect of pertussis toxin on peripheral prejunctional α_2-adrenoceptor-mediated responses and on endothelium-dependent relaxation responses in the rat. *Br. J. Pharmacol.*, **100**, 348–252.

FOUCART, S., MURPHY, T.V. & MAJEWSKI, H. (1990). Prejunctional β-adrenoceptors, angiotensin II and neuropeptide Y receptors on sympathetic nerves in mouse atria are linked to N-ethylmaleimide-susceptible G-proteins. *J. Autonom. Nervous Syst.*, **30**, 221–232.

GARCIA-SAINZ, J.A. (1981). Decreased sensitivity to α_2-adrenergic amines, adenosine and prostaglandins in white fat cells from hamsters treated with pertussis vaccine. *FEBS Lett.*, **153**, 183–186.

HARRISON, J.K., PEARSON, W.R. & LYNCH, K.R. (1991). Molecular characterization of α_1- and α_2-adrenoceptors. *Trends Pharmacol. Sci.*, **12**, 62–67.

HERTTING, G. & ALLGAIER, C. (1988). Participation of protein kinase C and regulatory G-proteins in modulation of the evoked noradrenaline release in brain. *Cell. Mol. Neurobiol.*, **8**, 105–114.

ILLES, P., WEBER, H.-D., NEUBURGER, J., BUCHER, B., REGENOLD, J.T. & NÖRENBERG, W. (1990). Receptor interactions at noradrenergic neurones. *Ann. N.Y. Acad. Sci.*, **604**, 197–210.

KASCHUBE, M. & BRASCH, H. (1990). Pre- and postjunctional effects of N-ethylmaleimide in the isolated mouse vas deferens. *Eur. J. Pharmacol.*, **178**, 151–159.

KATADA, T. & UI, M. (1981). In vitro effects of islet-activating protein on cultured rat pancreatic islets. Enhancement of insulin secretion, adenosine 3′:5′-monophosphate accumulation and ^{45}Ca flux. *J. Biochem.*, **89**, 979–990.

KITAMURA, Y. & NOMURA, Y. (1987). Uncoupling of rat cerebral cortical α_2-adrenoceptors from GTP-binding proteins by N-ethylmaleimide. *J. Neurochem.*, **49**, 1894–1901.

LAI, R.-T., WATANABE, Y. & YOSHIDA, H. (1983). Effects of islet-activating protein (IAP) on contractile responses of rat vas deferens: evidence for participation of Ni (inhibitory GTP binding regulating protein) in the α_2-adrenoceptor-mediated response. *Eur. J. Pharmacol.*, **90**, 453–456.

LI, C. (1990). *Studies on modulation of non-adrenergic non-cholinergic transmission.* Ph.D. Thesis, University of Melbourne.

LUX, B. & SHULZ, R. (1986). Effect of cholera toxin and pertussis toxin on opioid tolerance and dependence in the guinea-pig myenteric plexus. *J. Pharmacol. Exp. Ther.*, **237**, 995–1000.

MARTIN, J.M., HUNTER, D.D. & NATHANSON, N.M. (1985). Islet activating protein inhibits physiological responses evoked by cardiac muscarinic acetylcholine receptors. Role of guanosine triphosphate binding proteins in regulation of potassium permeability. *Biochemistry*, **24**, 7521–7525.

MEDGETT, I.C. & MCCULLOCH, M.W. (1980). Receptor sites of action of clonidine: effects of clonidine and three structural isomers on prejunctional and postjunctional α-adrenoceptors and histamine H_2-receptors in guinea-pig isolated cardiovascular tissues. *J. Pharm. Pharmacol.*, **32**, 137–138.

MEDGETT, I.C., MCCULLOCH, M.W. & RAND, M.J. (1978). Partial agonist action of clonidine on prejunctional and postjunctional α-adrenoceptors. *Naunyn-Schmiedebergs Arch. Pharmacol.*, **304**, 215–221.

MURPHY, T.V. & MAJEWSKI, H. (1990). Pertussis toxin differentiates between α_1- and α_2-adrenoceptor inhibition of noradrenaline release in rat kidney cortex. *Eur. J. Pharmacol.*, **179**, 435–439.

MUSGRAVE, I.F., MARLEY, P. & MAJEWSKI, H. (1987). Pertussis toxin does not attenuate α_2-adrenoceptor mediated inhibition of noradrenaline release in mouse atria. *Naunyn-Schmiedebergs Arch. Pharmacol.*, **336**, 280–286.

NICHOLS, A.J., MOTLEY, E.D. & RUFFOLO, R.R. Jr. (1988). Differential effect of pertussis toxin on pre- and postjunctional α_2-adrenoceptors in the cardiovascular system of the pithed rat. *Eur. J. Pharmacol.*, **145**, 345–349.

NOZAKI, M. & SPERELAKIS, N. (1989). Pertussis toxin effects on transmitter release from perivascular nerve terminals. *Am. J. Physiol.*, **256**, H455–H459.

POBINER, B.F., HEWLETT, E.L. & GARRISON, J.C. (1985). Role of Ni in coupling angiotensin receptors to inhibiton of adenylate cyclase in hepatocytes. *J. Biol. Chem.*, **260**, 16200–16209.

RAND, M.J., MAJEWSKI, H., MEDGETT, I.C., MCCULLOCH, M.W. & STORY, D.F. (1980). Prejunctional receptors modulating autonomic neuroeffector transmission. *Circ. Res.*, **46** (Suppl.I), 170–176.

RUMP, L.C. & MAJEWSKI, H. (1987). Modulation of norepinephrine release through α_1- and α_2-adrenoceptors in rat isolated kidney. *J. Cardiovasc. Pharmacol.*, **9**, 500–509.

SABATINI, S. & KURTZMAN, N.A. (1989). Vanadate stimulates the N-ethylmaleimide-sensitive adenosine triphosphatase in rat nephron. *J. Pharmacol. Exp. Ther.*, **250**, 529–533.

SCHÖMIG, E., MICHAEL-HEPP, J. & BÖNISCH, H. (1988). Inhibition of neuronal noradrenaline uptake (uptake 1) and desipramin binding by N-ethylmaleimide (NEM). *Naunyn-Schmiedebergs Arch. Pharmacol.*, **337**, 633–636.

SIGAFOOS, J.F. & ABRAMOWITZ, J. (1986). Effects of N-ethylmaleimide on gonadotropin and β-adrenergic receptor function coupled to rabbit luteal adenylate cyclase. *Endocrinol.*, **119**, 1432–1438.

SMITH, D.K. & LAUF, P.K. (1985). Effects of N-ethylmaleimide on ouabain-insensitive cation fluxes in human red cell ghosts. *Biochim. Biophys. Acta*, **818**, 251–259.

STARKE, K. (1977). Regulation of noradrenaline release by presynaptic receptor systems. *Rev. Physiol. Pharmacol.*, **77**, 1–125.

STARKE, K. (1987). Presynaptic α-autoceptors. *Rev. Physiol. Biochem. Pharmacol.*, **107**, 74–146.

UEDA, H., MISAWA, H., KATADA, T., UI, M., TAKAGI, H. & SATOH, M. (1990). Functional reconstitution of purified G_i and G_o with μ-opioid receptors in guinea-pig striatal membranes pretreated with micromolar concentrations of N-methylmaleimide. *J. Neurochem.*, **54**, 841–848.

UI, M. (1988). The multiple biological activities of pertussis toxin. In *Pathogenesis and Immunity in Pertussis*, ed. Wardlaw, A.C. & Parton, R. pp. 121–145. New York: John Wiley and Sons Ltd.

WEBER, H.-D. (1989). Presynaptic α_2-adrenoceptors at the terminals of perivascular sympathetic nerves are coupled to an N-ethylmaleimide-sensitive G-protein. *Naunyn-Schmiedebergs Arch. Pharmacol.*, **339**, (Suppl.), R35.

WINSLOW, J.W., BRADLEY, J.D., SMITH, J.A. & NEERE, E.J. (1987). Reactive sulfhydryl groups of α_{39}, a guanine nucleotide-binding protein from brain. *J. Biol. Chem.*, **262**, 4501–4507.

WÖLFEL, R., HALBRÜGGE, T. & GRAEFE, K.-H. (1989). Effects of N-ethylmaleimide on 5-hydroxytryptamine transport and sodium content in rabbit platelets. *Br. J. Pharmacol.*, **97**, 1308–1314.

WOLK, V., SCHOLLMEYER, P. & RUMP, L.C. (1991). Pertussis toxin sensitive α_1- and NEM sensitive α_2-adrenoceptor mediated inhibition of noradrenaline release in rabbit renal arteries. *Naunyn-Schmiederbergs Arch. Pharmacol.*, **343** (Suppl.), R35.

ZENG, D., HARRISON, J.K., D'ANGELO, D.D, BARBER, C.M., TUCKER, A.L., LU, Z. & LYNCH, K.R. (1990). Molecular characterization of a rat α_{2B}-adrenergic receptor. *Proc. Natl. Acad. Sci. USA.*, **87**, 3102–3106.

(Received September 10, 1991
Revised March 30, 1992
Accepted March 31, 1992)

Br. J. Pharmacol. (1992), **106**, 877–882 © Macmillan Press Ltd, 1992

Investigation of the 5-hydroxytryptamine receptor mediating the 'maintained' short-circuit current response in guinea-pig ileal mucosa

C.M. Scott, [1]K.T. Bunce & C.F. Spraggs

Department of Gastrointestinal Pharmacology, Glaxo Group Research Ltd., Ware, Herts, SG12 0DP

1 5-Hydroxytryptamine (5-HT) stimulated a biphasic increase in short-circuit current (SCC) in guinea-pig isolated ileal mucosa. The initial 'spike' response to 5-HT was inhibited by tetrodotoxin (0.3 μM). We have investigated the 5-HT receptor mechanism(s) controlling the second 'maintained' component of the response which remained after treatment with tetrodotoxin.

2 5-HT stimulated concentration-related increases in SCC with an EC_{50} value of 5.4 μM. Isobutylmethylxanthine (IBMX, 10 μM) produced a six fold leftward shift of this concentration-response curve, suggesting the involvement of a cyclic nucleotide(s) in these responses.

3 In the presence of IBMX, 5-HT stimulated reproducible increases in SCC with an EC_{50} value of 0.9 μM. The rank order of potency of indole agonists in these tests was 5-HT ≥ 5-methoxytryptamine > 5-carboxamidotryptamine = α-methyl-5-HT >> 2-methyl-5-HT.

4 The substituted benzamides were partial agonists. Metoclopramide and cisapride produced approximately 20% of the 5-HT maximum, and renzapride and **R,S**-zacopride produced approximately 50% of the 5-HT maximum. Metoclopramide and cisapride inhibited the SCC responses to 5-HT with apparent pK_B values of 4.8 and 7.0 respectively.

5 The SCC responses to 5-HT were not inhibited by antagonists selective for 5-HT_1 (methysergide, methiothepin), 5-HT_2 (ketanserin) or 5-HT_3 (ondansetron, ICS205-930) receptors.

6 The SCC responses to 5-methoxytryptamine, 5-carboxamidotryptamine, α-methyl-5-HT and **R,S**-zacopride, but not 5-HT, were selectively inhibited by high concentrations of ICS205-930 with apparent pK_B values of approximately 6.

7 A possible interpretation of these results is that the 'maintained' SCC response to 5-HT is mediated by a heterogeneous population of 5-HT receptors. One of these receptors exhibits the characteristics of the putative 5-HT_4 receptor.

Keywords: Guinea-pig ileum; secretion; 5-hydroxytryptamine receptor; short-circuit current

Introduction

5-Hydroxytryptamine (5-HT) is present in the gastrointestinal tract, located both in enterochromaffin cells (Erspamer, 1954) and neurones within the enteric nervous system (Furness & Costa, 1982; Costa *et al.*, 1982). 5-HT is a potent secretagogue in many species including the rat (Beubler *et al.*, 1990; Zimmerman & Binder, 1984), rabbit (Donowitz *et al.*, 1977) and guinea-pig (Cooke & Carey, 1985).

In guinea-pig isolated ileal mucosa, 5-HT stimulates a biphasic increase in short-circuit current (SCC) which is attributable to an increase in electrogenic chloride secretion (Cooke & Carey, 1985; Hendricks *et al.*, 1989). The first phase of the response to 5-HT is transient and blocked by tetrodotoxin (TTX), thus implicating a neuronal mechanism (Cooke & Carey, 1985; Hendricks *et al.*, 1989). Indeed, this initial response to 5-HT was completely blocked by ICS205-930 (1 μM) which is consistent with the involvement of neuronal 5-HT_3 receptors (Hendricks *et al.*, 1989). In contrast, the second phase of the SCC response to 5-HT was well maintained, and was largely resistant to TTX. It was not affected by ICS205-930 at concentrations up to 10 μM, and was not inhibited by methysergide or cyproheptadine (Cooke & Carey, 1985; Hendricks *et al.*, 1989). Thus the second phase of the SCC response to 5-HT in guinea-pig ileum appears to be mediated by a receptor that cannot clearly be classified as 5-HT_1-like, 5-HT_2 or 5-HT_3 (see Bradley *et al.*, 1986). The purpose of the present study was to characterize the 5-HT receptor mediating this response. A preliminary account of this work was presented to the British Pharmacological Society (Scott *et al.*, 1991).

[1] Author for correspondence.

Methods

Experimental procedure

Female Dunkin-Hartley guinea-pigs (approximately 400 g) were killed by cervical dislocation and the terminal ileum removed. The ileal segment was flushed with oxygenated Krebs-Henseleit solution, and portions of ileum 1–1.5 cm in length were then taken at a distance of approximately 10 cm from the ileo-caecal junction. These were opened along the mesenteric border and pinned as a flat sheet, mucosal side down on a wax block. The longitudinal and circular muscle layers were dissected away, and the mucosa with adherent submucous plexus was then mounted between the two halves of an Ussing chamber (window area 0.8 cm^2). Two paired (adjacent) tissues were used for each experiment.

The Ussing chambers were prepared for the measurement of SCC across the mucosa, as described by Bunce & Spraggs, (1988). The tissues were voltage-clamped at zero potential by passage of current using a voltage clamp amplifier (DVC-1000 World Precision Instruments, CT, USA) and the resulting SCC recorded continuously as a measure of electrogenic chloride transport (see Cooke & Carey, 1985).

The tissues were bathed on both sides with Krebs-Henseleit solution containing (in mM): NaCl 117, KCl 4.7, $CaCl_2$

2.5, $MgSO_4$ 1.2, KH_2PO_4 1.2, $NaHCO_3$ 24.8, at 37°C and gassed with 95% O_2, 5% CO_2. Glucose (11 mM) was added to the serosal solution and mannitol (11 mM) to the mucosal solution. Glucose was omitted from the mucosal side to prevent coupled electrogenic sodium absorption which might have affected subsequent measurements of SCC.

Drugs were added to both sides of the tissue unless otherwise stated. All antagonists were added 30 min before the construction of an agonist concentration-response curve. In some experiments tissues were treated with pargyline (100 μM) for 30 min and then washed several times with fresh Krebs solution. In these pargyline-treated preparations the effect of amine uptake inhibitors was also investigated. All agonist concentration-response curves were constructed in a cumulative manner.

Compounds

5-Hydroxytryptamine creatinine sulphate (5-HT, Sigma), tetrodotoxin (TTX, Sigma), 3-isobutyl-1-methyl-xanthine (IBMX, Sigma), 5-methoxytryptamine hydrochloride (5-MeOT, Sigma), 5-carboxamidotryptamine maleate (5-CT, Glaxo), α-methyl-5-HT maleate (Glaxo), 2-methyl-5-HT hydrochloride (Glaxo), ondansetron hydrochloride (Glaxo), metoclopramide hydrochloride (Sigma), methysergide maleate (Sandoz), methiothepin maleate (Roche), **R,S**-zacopride fumarate (Glaxo), renzapride (Glaxo), ICS205-930 ((3α-tropanyl)-1H-indole-3-carboxylic acid ester; Sandoz), forskolin (Sigma), ketanserin tartrate (Janssen), cocaine hydrochloride (May & Baker Ltd), corticosterone (Sigma), pargyline hydrochloride (Abbott Laboratories Ltd), desmethylimipramine hydrochloride (Geigy). Cisapride base was purchased from Janssen and prepared as the tartrate salt in our own laboratories.

All compounds were soluble in Krebs solution with the following exceptions:- ICS205-930 was dissolved in 0.1 ml of 1 N HCl, forskolin was dissolved at 1 mM in 50% ethanol, IBMX was dissolved in 0.2 ml 0.1 M NaOH. All solutions were then diluted to the required concentration with Krebs solution. When adding test compounds, control tissues received the appropriate solvent. No effects on SCC were observed.

Expression of results

SCC values (μA cm^{-2}) and percentage maximum response are expressed as the arithmetic mean ± s.e.mean. EC_{50} values (determined graphically) and concentration ratios (CR) calculated from them are expressed as the geometric mean with 95% confidence limits. pK_B values were calculated from:-

$$pK_B = \log_{10} (CR\text{-}1) - \log_{10} (\text{antagonist concentration}).$$

A paired t test was used to determine statistical significance between groups of data. A P value of <0.05 was considered to be significant.

Results

5-Hydroxytryptamine-induced SCC response

Guinea-pig ileal mucosa exhibited a high basal SCC of 145.3 ± 10.2 μA cm^{-2} ($n = 8$) (lumen side negative). Addition of a single concentration of 5-HT (3 μM) stimulated a biphasic increase in SCC, as shown in Figure 1a. The initial 'spike' response faded after approximately 2 min, to reveal a second plateau response which was well-maintained. Tetrodotoxin (TTX, 0.3 μM) inhibited the basal SCC to 45.9 ± 8.1 μA cm^{-2} ($n = 10$) and also blocked the initial phase of the response to 5-HT, an example of which is shown in Figure 1b. All further studies were carried out on the component of the SCC response which remained after treatment with TTX (0.3 μM) and, under these conditions, it was possible to construct a cumulative concentration-response curve, an example of which is given in Figure 1c.

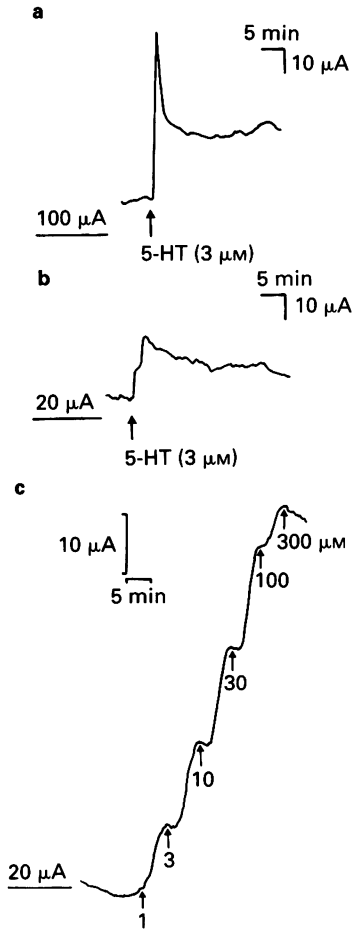

Figure 1 The effect of 5-hydroxytryptamine (5-HT) on short circuit current in guinea-pig ileal mucosa. 5-HT was added to both sides of the tissues. Baseline currents are indicated by the horizontal bars. (a) Response to a single concentration of 5-HT under control conditions; (b) response to a single concentration of 5-HT in the presence of tetrodotoxin (0.3 μM); (c) responses to cumulative additions of 5-HT in the presence of tetrodotoxin (0.3 μM).

In preliminary studies ($n = 7$) two repeated 5-HT concentration-response curves were constructed in each preparation, but with this protocol the responses were not reproducible with the maximum response to 5-HT in the second curve being 49.4 ± 11.5% of that in the first curve. Thus a different experimental protocol was sought, and paired tissues were used from adjacent portions of ileum. The mean results from six such experiments are shown in Figure 2; EC_{50} values of 5.4 (3.3–8.9) μM and 8.0 (4.2–15.3) μM with corresponding maximum responses of 98.0 ± 8.2 and 102.5 ± 7.6 μA cm^{-2} at 100 μM 5-HT were obtained for the paired tissues. On this basis the protocol adopted was that (i) for agonist studies one tissue received 5-HT and the paired tissue received the test agonist, (ii) for antagonist studies one tissue received the agonist alone and the paired partner received agonist plus antagonist.

Effect of 3-isobutyl-l-methyl-xanthine

The effect of the phosphodiesterase inhibitor, IBMX, is shown in Figure 2. IBMX (10 μM) shifted the 5-HT concentration-response curve to the left with no change in the maximum response. The EC_{50} values for 5-HT were 0.9 (0.4–1.9) μM and 1.6 (0.5–4.4) μM for the paired tissues ($P > 0.05$, $n = 6$), with corresponding maximum responses of 99.6 ± 12.2 and 92.4 ± 8.9 μA cm^{-2} ($P > 0.05$). IBMX (10

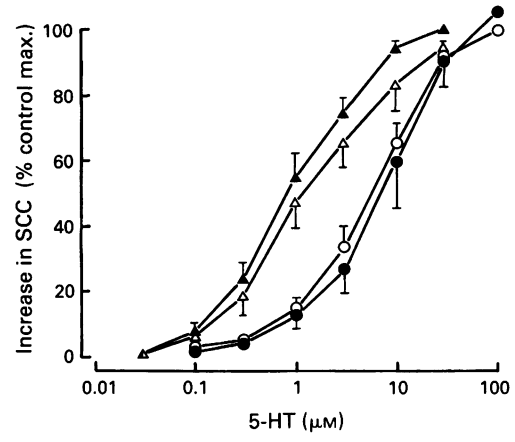

Figure 2 Concentration-response curves to 5-hydroxytryptamine (5-HT) in paired tissues of guinea-pig ileal mucosa. Responses are shown to 5-HT in paired tissues in the absence (○, ●) and presence (△, ▲) of isobutylmethylxanthine (IBMX, 10 μM). In each case the maximum response in one of the tissue pairs is expressed as 100% (control ○; IBMX ▲). Results are expressed as mean with s.e.mean shown by vertical bars; $n = 6$.

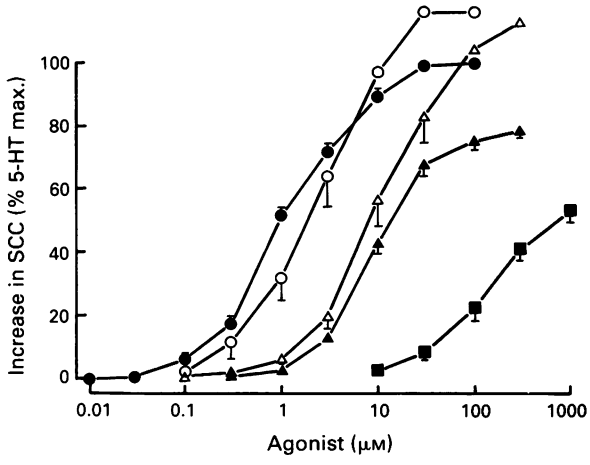

Figure 3 The agonist effect of 5-hydroxytryptamine (5-HT) and other indoleamines in guinea-pig ileal mucosa: 5-HT control (●); 5-methoxytryptamine (○); 5-carboxamidotryptamine (△); α-methyl-5-HT (▲) and 2-methyl-5-HT (■). Results are expressed as mean with s.e.mean shown by vertical bars; $n = 4-7$.

μM) was therefore added to the bathing solutions routinely in subsequent studies; enhancing the potency of 5-HT in this way facilitated studies with antagonists and with agonists which were less potent than 5-HT.

5-Hydroxytryptamine receptor agonists

Previous studies have reported that 5-HT is a substrate for amine uptake mechanisms in rat oesophagus (Baxter *et al.*, 1991), a tissue containing 5-HT_4 receptors. In addition, the possibility existed that 5-HT might be a substrate for metabolism by monoamine oxidase. Such a possibility was examined by investigating the effects of a combination of cocaine (30 μM), corticosterone (30 μM) and pargyline (100 μM). However, under these conditions the maximum response to 5-HT was diminished to 27.5 ± 8.2% of control ($n = 6$). This latter effect was due to the presence of cocaine since replacement of cocaine by desmethylimipramine (0.1 μM) resulted in no change in the control response to 5-HT (EC_{50} values of 1.6 and 1.3 μM and maximum responses of 78.8 and 70.6 μA cm^{-2} in control and test curves respectively). Based on these results, inhibitors of amine uptake or metabolism were not used further.

Four indoleamine agonists were tested. Details of the results are given in Figure 3 with a summary in Table 1. 5-MeOT and 5-CT were full agonists with 5-MeOT being approximately equipotent and 5-CT less potent than 5-HT. α-Methyl-5-HT and 2-methyl-5-HT were partial agonists, the latter compound being particularly weak.

In addition to the indoleamines, four benzamide derivatives were tested. The results are shown in Figure 4 with a summary of the data in Table 1. All of the benzamides exhibited apparent partial agonist activity with renzapride and **R,S**-zacopride producing approximately 50% of the 5-HT maximum. Metoclopramide and cisapride were weak partial agonists and stimulated a maximum response of only 20% of that to 5-HT.

5-Hydroxytryptamine receptor antagonists

5-HT receptor antagonists with some degree of selectivity for the different 5-HT receptor subtypes were tested against the SCC response to 5-HT and the results are shown in Table 2. High concentrations of antagonists with affinity for 5-HT_1-like, 5-HT_2, 5-HT_3 and 5-HT_4 receptors were without effect. The possibility existed that the SCC response to 5-HT, rather than being mediated by a single receptor type, was controlled by a heterogeneous population of 5-HT receptors. For this reason combinations of antagonists were used against 5-HT. ICS205-930 (10 μM) plus methysergide (10 μM) and ICS205-930 (10 μM) plus methiothepin (0.3 μM) were tested against 5-HT and respective concentration-ratios of 1.7 (0.6–4.7) and 1.8 (1.4–2.1) were calculated with no change in the maximum response ($n = 4$ throughout). Thus, these latter experi-

Table 1 Summary of the effects of 5-hydroxytryptamine (5-HT) receptor agonists in guinea-pig ileal mucosa

Compound	*Receptor selectivity of agonists*	**EC_{50} (μM) (95% confidence limits)*	*% 5-HT maximum*
5-HT	Non-selective	0.9 (0.4–1.9)	100
5-MeOT	Non-selective (but inactive at 5-HT_3)	2.6 (2.1–3.1)	116 ± 17
α-methyl-5-HT	5-HT_2	9.1 (7.4–11.1)	79 ± 2
5-CT	5-HT_1	10.6 (7.0–16.2)	110 ± 9
2-methyl-5-HT	5-HT_3	94.7 (43.2–207.9)	53 ± 4
†Renzapride	5-HT_4?	0.5 (0.4–0.8)	57 ± 11
†**R,S**-zacopride	5-HT_4?	1.5 (0.9–2.3)	48 ± 3
†Cisapride	5-HT_4?	1.9 (0.6–6.0)	19 ± 8
†Metoclopramide	5-HT_4?	15.4 (12.7–18.7)	17 ± 3

†Compounds are 5-HT_3 receptor antagonists.
*EC_{50} values calculated using own maximum for each agonist.
5-MeOT = 5-methoxytryptamine; 5-CT = 5-carboxamidotryptamine. $n = 4-7$.

ments did not reveal a significant shift of the response to 5-HT.

The agonist profiles obtained (see Figures 3 and 4), in particular the partial agonist activities of the benzamides, are consistent with the presence of 5-HT_4 receptors (see Clark *et al.*, 1989). We therefore re-examined the effect of the putative 5-HT_4 receptor antagonist, ICS205-930, against a range of agonists and the results are summarized in Table 3. As stated above, ICS205-930 did not inhibit the SCC responses to 5-HT, but this antagonist did inhibit the responses to other indoleamine and benzamide agonists with pK_B values of approximately 6. Notice that with the partial agonists, α-methyl-5-HT and **R,S**-zacopride, ICS205-930 caused a depression of the maximum response achieved by each agonist (Table 3). These findings are not unexpected for a competitive antagonist against responses to partial agonists (see Rang, 1966). At the concentration used (10 μM) ICS205-930 was selective since it did not significantly inhibit the basal SCC or the increase in SCC stimulated by forskolin (0.03–3 μM) [concentration-ratio = 1.56 (0.96–2.53)].

Since metoclopramide and cisapride are weak partial agonists (Figure 4) they were also tested as antagonists. Metoclopramide (100 μM) and cisapride (0.3 μM) both inhibited the SCC response to 5-HT with apparent pK_B values of 4.8 ± 0.2 and 7.0 ± 0.2 (calculated from concentration-ratios determined at the EC_{50} level for 5-HT) and maximum responses to 5-HT of 100 ± 16% and 79 ± 7% respectively (relative to paired control).

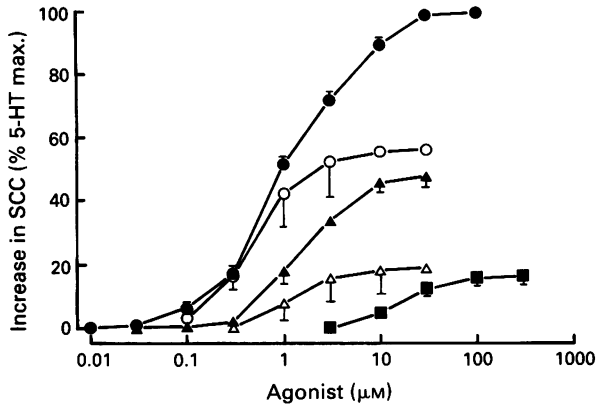

Figure 4 The agonist effect of 5-hydroxytryptamine (5-HT) and certain substituted benzamides in guinea-pig ileal mucosa: 5-HT control (●); renzapride (○); **R,S**-zacopride (▲); cisapride (△) and metoclopramide (■). Results are expressed as mean with s.e.mean shown by vertical bars; $n = 6$.

Discussion

In agreement with the work of Cooke & Carey (1989) and Hendricks *et al.* (1989), we have shown that 5-HT induced a biphasic SCC response in guinea-pig ileal mucosa. The initial 'spike' component of the response was neuronally mediated

Table 2 Antagonist effects against 5-hydroxytryptamine (5-HT)-induced short-circuit current (SCC) in guinea-pig ileal mucosa

Antagonist	*Antagonist selectivity*	**5-HT EC_{50} (μM) (control)*	**5-HT EC_{50} (μM) (+ antagonist)*	*Concentration ratio*	*#% 5-HT_{max} (+ antagonist)*
Ketanserin (1 μM)	5-HT_2	0.99 (0.75–1.28)	1.15 (0.67–1.98)	1.16	99.5 ± 7.4
Methysergide (10 μM)	5-HT_1-like 5-HT_2	1.04 (0.63–1.73)	2.64 (1.38–5.05)	2.54	95.0 ± 4.6
Methiothepin (0.3 μM)	5-HT_1-like 5-HT_2	0.83 (0.37–1.83)	1.05 (0.6–1.8)	1.27	102.0 ± 9.4
Ondansetron (10 μM)	5-HT_3	1.13 (0.75–1.17)	0.8 (0.6–1.1)	0.71	104.0 ± 10.0
ICS205-930 (100 μM)	5-HT_3/5-HT_4	1.07 (0.75–1.52)	1.46 (0.81–2.64)	1.37	99.8 ± 3.1

*Geometric mean, 95% confidence limits. Log_{10} EC_{50} values were compared by a paired t test. None of the antagonists tested produced a significant shift ($P > 0.05$) of the control 5-HT curve.
#Arithmetic mean ± s.e.mean. $n = 4–6$.

Table 3 Mean pK_B values for ICS205-930 against 5-hydroxytryptamine (5-HT) receptor agonists

Agonist	*ICS205-930 concentration (μM)*	n	*#Concentration ratio (95% confidence limits)*	*Apparent pK_B value*	**% agonist max (+ ICS205-930)*
5-Hydroxytryptamine	10	6	1.7 (0.9–3.0)	not calculated	100.2 ± 3.8
5-Methoxytryptamine	10	6	8.1 (3.0–21.7)	5.8 ± 0.2	97.9 ± 9.3
5-Carboxamidotryptamine	10	6	10.3 (5.5–19.2)	6.0 ± 0.1	99.4 ± 6.9
α-Methyl-5-hydroxytryptamine	10	5	8.7 (5.9–13.0)	5.9 ± 0.1	76.2 ± 4.4
R,S-zacopride	10	6	18.5 (8.8–38.7)	6.3 ± 0.1	64 ± 7.6

#Calculated at the EC_{50} level for the control agonist response.
*Expressed as percentage of control maximum response to each agonist.

Table 4 Rank orders of agonist potency of selective compounds at 5-hydroxytryptamine (5-HT) receptors

Receptor subtype	*Agonist potency*	*References*
5-HT_1-like (contraction)	5-CT > 5-HT > α-Me5-HT > 2-Me5-HT = 0	Feniuk *et al.* (1985)
5-HT_1-like (relaxation)	5-CT >> 5-HT >> 2-Me5-HT = α-Me5-HT = 0	Humphrey (1984)
5-HT_2	5-HT = α-Me5-HT > 5-CT > 2-Me5-HT	Humphrey (1984)
5-HT_3	5-HT = 2-Me5-HT > α-Me5-HT >> 5-CT	Humphrey (1984)
Guinea-pig ileal mucosa	5-HT > α-Me5-HT = 5-CT >> 2-Me5-HT	This study

5-CT = 5-carboxamidotryptamine; α-Me5-HT = α-methyl-5-HT; 2-Me5-HT = 2-methyl-5-HT.

(blocked by TTX; Cooke & Carey, 1985) and inhibited by low concentrations of ICS205-930 (< 1 μM), which is consistent with the involvement of 5-HT_3 receptors (Hendricks *et al.*, 1989). Indeed, all of our own studies on receptor classification were carried out in the presence of TTX to allow investigation of the second maintained component of the response to 5-HT.

The effect of inhibitors of amine uptake and metabolism were investigated on the SCC response to 5-HT. This was done since removal of 5-HT from the receptor milieu might affect any assessment of antagonist affinity, or more particularly, rank order of agonist potency (see Kenakin, 1987). However, studies using mixtures of pargyline, corticosterone, cocaine and/or desmethylimipramine indicated that if uptake or metabolism of 5-HT did occur, this did not appear to affect the SCC responses to 5-HT.

The receptor type mediating the SCC maintained response to 5-HT was first examined using agonist rank order of potency to indole compounds. It must be pointed out that not all of the compounds were full agonists compared with 5-HT (see Furchgott, 1972), but with this reservation in mind the rank orders of agonist potency have been compared with published data, and these are shown in Table 4. The rank order of potency of the key indole agonists is not consistent with the presence of 5-HT_1, 5-HT_2 or 5-HT_3 receptors in guinea-pig ileal mucosa. However, these data do indicate the presence of 5-HT_4 receptors as revealed by comparison with other systems exhibiting these receptors. Although some differences in agonist profile do occur between tissues purported to contain 5-HT_4 receptors, in certain preparations, as observed in guinea-pig ileal mucosa in the present study, 5-methoxytryptamine is an agonist almost equipotent with 5-HT (Dumuis *et al.*, 1988), α-methyl-5-HT and 5-CT are somewhat less potent than 5-HT (Reeves *et al.*, 1991) and 2-methyl-5-HT is a very weak agonist (Baxter *et al.*, 1991).

Additional agonist data for receptor classification were obtained by use of substituted benzamides which were partial agonists. Such activity of the benzamides is a key feature of 5-HT_4 receptors where, depending on the preparation used, these compounds are reported to be partial (Eglen *et al.*, 1990; Reeves *et al.*, 1991) or full (Dumuis *et al.*, 1989) agonists. Confirmatory evidence that the benzamides were interacting with a 5-HT receptor in guinea-pig ileal mucosa was derived from the observation that the two compounds with particularly low efficacy, viz. metoclopramide and cisapride, antagonized the SCC response to 5-HT.

Further information on the receptor type controlling the maintained SCC response in guinea-pig ileum was sought by use of antagonists. However, high concentrations of antagonists with affinity for 5-HT_1, 5-HT_2, 5-HT_3 and 5-HT_4 receptors were without effect against 5-HT. It is possible that selective antagonists might fail to inhibit the 5-HT-induced SCC response if a heterogeneous population of 5-HT receptors is present in the mucosa of guinea-pig ileum. For this reason high concentrations of methiothepin plus ICS205-930 or methysergide plus ICS205-930 were used, but no inhibition of the 5-HT-induced SCC response was observed.

Despite this lack of effect of the antagonists, the agonist data appeared to be consistent with the presence of 5-HT_4 receptors. We therefore tested ICS205-930, at a concentration that should antagonize 5-HT_4 receptors (10 μM), against some of the more selective agonists available. In each case ICS205-930 inhibited the agonist-induced SCC response with a pK_B value of approximately 6, a result which is consistent with the presence of 5-HT_4 receptors (Dumuis *et al.*, 1989). These data are difficult to interpret clearly, but one possible explanation is that the maintained SCC response to 5-HT is controlled by a heterogeneous receptor population, one of which is 5-HT_4, and a large proportion of the remaining receptors being of a sub-type(s) which is yet to be defined.

Other workers have also investigated the effect of ICS205-930 against the SCC response to 5-HT in guinea-pig ileal mucosa. Baird & Cuthbert (1987) observed that ICS205-930 (0.1 and 1 μM) inhibited the SCC response and that this was also blocked by tetrodotoxin. Thus it appears that these latter workers were investigating that component of the response to 5-HT which was routinely removed in our studies and mediated by 5-HT_3 receptors. Hendricks *et al.* (1989) state that '. . . there was no reduction in the second component at concentrations of 10^{-6} M or 10^{-5} M ICS205-930 beyond that observed at 10^{-7} M . . .'. Indeed, in the present study we also found that ICS205-930 (10 μM) failed to inhibit the SCC response to 5-HT, as opposed to the positive effect against the other more selective agonists. Cooke & Carey (1985) have reported that cisapride (1.9 μM) inhibited the SCC response to 5-HT in guinea-pig ileum. Cisapride exhibits an affinity constant of approximately 0.1 μM at both 5-HT_3 (Nelson & Thomas, 1989) and 5-HT_4 receptors (present study), so it is likely that cisapride inhibited the SCC response of 5-HT through effects on both the spike and maintained components of the response. Thus, the findings of Cooke & Carey (1985) are consistent with our own work.

Experiments using neuronal tissues (mouse colliculi neurones, Dumuis *et al.*, 1988; guinea-pig hippocampus, Bockaert *et al.*, 1990) have shown that 5-HT_4 receptors are positively coupled to adenylate cyclase. The observation in the present study that IBMX potentiated the response to 5-HT is consistent with this contention.

In summary, the SCC response to 5-HT in guinea-pig ileal mucosa consists of two components, one sensitive and the other insensitive to TTX. We have investigated the receptor types mediating the TTX-insensitive component and found that a heterogeneous population of 5-HT receptors is probably involved. Studies using selective agonists and ICS205-930 have identified a receptor which exhibits the characteristics of the 5-HT_4 receptor. However, the 5-HT_4 receptor apparently mediated only a small component of the response to 5-HT, and the other receptor type(s) involved could not be identified as 5-HT_1, 5-HT_2 or 5-HT_3.

References

BAIRD, A.W. & CUTHBERT, A.W. (1987). Neuronal involvement in type 1 hypersensitivity reactions in gut epithelia. *Br. J. Pharmacol.*, **92**, 647–655.

BAXTER, G.S., CRAIG, D.A. & CLARKE, D.E. (1991). 5-Hydroxytryptamine$_4$ receptors mediate relaxation of the rat oesophageal tunica muscularis mucosae. *Naunyn-Schmiedebergs Arch. Pharmacol.*, **343**, 439–446.

BEUBLER, E., COUPAR, I.M., HARDCASTLE, J. & HARDCASTLE, P.T. (1990). Stimulatory effects of 5-hydroxytryptamine on fluid secretion and transmural potential difference in rat small intestine are mediated by different receptor type. *J. Pharm. Pharmacol.*, **42**, 35–39.

BOCKAERT, J., SEBBEN, M. & DUMUIS, A. (1990). Pharmacological characterisation of 5-HT_4 receptors positively coupled to adenylate cyclase in adult guinea-pig hippocampal membranes: Effect of substituted benzamide derivatives. *Mol. Pharmacol.*, **37**, 408–411.

BRADLEY, P.B., ENGEL, G., FENIUK, W., FOZARD, J.R., HUMPHREY, P.P.A., MIDDLEMISS, D.N., MYLECHARANE, E.J., RICHARDSON, B.P. & SAXENA, P.R. (1986). Proposals for the classification and nomenclature of functional receptors for 5-HT. *Neuropharmacology*, **25**, 563–576.

BUNCE, K.T. & SPRAGGS, C.F. (1988). Stimulation of electrogenic chloride secretion by prostaglandin E_2 in guinea-pig isolated gastric mucosa. *J. Physiol.*, **400,** 381–394.

CLARKE, D.E., CRAIG, D.A. & FOZARD, J.R. (1989). The 5-HT_4 receptor: naughty but nice. *Trends Pharmacol. Sci.*, **10,** 385–386.

COOKE, J.H. & CAREY, H.V. (1985). Pharmacological analysis of 5-hydroxytryptamine actions on guinea-pig ileal mucosa. *Eur. J. Pharmacol.*, **111,** 329–337.

COSTA, M., FURNESS, J.B., CUELLO, A.C., VERHOFSTAD, A.A.J., STEINBUSCH, H.W.J. & ELDE, R.P. (1982). Neurons with 5-hydroxytryptamine-like immunoreactivity in the enteric nervous system: their visualisation and reactions to drug treatment. *Neurosci.*, **7,** 351–363.

DONOWITZ, M., CHARNEY, A.N. & HEFFERNAN, J.M. (1977). Effect of serotonin treatment on intestinal transport in the rabbit. *Am. J. Physiol.*, **232,** E85–E94.

DUMUIS, A., BOUHELAL, R., SEBBEN, M., CORY, R. & BOCKAERT, J. (1988). A non-classical 5-hydroxytryptamine receptor positively coupled with adenylate cyclase in the central nervous system. *Mol. Pharmacol.*, **34,** 880–887.

DUMUIS, A., SEBBEN, M. & BOCKAERT, J. (1989). The gastrointestinal prokinetic benzamide derivatives are agonists at the non-classical 5-HT receptor (5-HT_4) positively coupled to adenylate cyclase in neurons. *Naunyn-Schmiedebergs Arch. Pharmacol.*, **340,** 403–410.

EGLEN, R.M., SWANK, S.R., WALSH, L.K.M. & WHITING, R.L. (1990). Characterisation of 5-HT_3 and 'atypical' 5-HT receptors mediating guinea-pig ileal contractions *in vitro*. *Br. J. Pharmacol.*, **101,** 513–520.

ERSPAMER, V. (1954). Pharmacology of indolealkylamines. *Pharmacol. Rev.*, **6,** 425–487.

FENIUK, W., HUMPHREY, P.P.A., PERREN, M.J. & WATTS, A.D. (1985). A comparison of 5-hydroxytryptamine receptors mediating contraction in rabbit aorta and dog saphenous vein: evidence for different receptor types obtained by use of selective agonists and antagonists. *Br. J. Pharmacol.*, **86,** 697–704.

FURCHGOTT, R.F. (1972). The classification of adrenoceptors. An evaluation from the standpoint of receptor theory. In *Catecholamines, Handbook of Experimental Pharmacology*, Vol. 33, pp. 283–335. ed. Usdin, E. & Snyder, S.H. Oxford: Pergamon.

FURNESS, J.B. & COSTA, M. (1982). Neurons with 5-hydroxytryptamine-like immunoreactivity in the enteric nervous system: their projections in the guinea-pig small intestine. *Neurosci*, **7,** 341–349.

HENDRICKS, R., BORNSTEIN, J.C. & FURNESS, J.B. (1989). Evidence for two types of 5-hydroxytryptamine receptor on secretomotor neurones of the guinea-pig ileum. *Naunyn-Schmiedebergs Arch. Pharmacol.*, **339,** 409–414.

HUMPHREY, P.P.A. (1984). Peripheral 5-hydroxytrypatime receptors and their classification. *Neuropharmacology*, **23,** 1503–1510.

KENAKIN, T.P. (1987). *Pharmacologic Analysis of Drug-Receptor Interaction*. New York: Raven Press.

NELSON, D.R. & THOMAS, D.R. (1989). [^{3}H]-BRL43694 (Granisetron), a specific ligand for 5-HT_3 binding sites in rat brain cortical membranes. *Biochem. Pharmacol.*, **38,** 1693–1695.

RANG, H.P. (1966). The kinetics of action of acetylcholine antagonists in smooth muscle. *Proc. R. Soc.*, **164,** 488–510.

REEVES, J.J., BUNCE, K.T. & HUMPHREY, P.P.A. (1991). Investigation into the 5-hydroxytryptamine receptor mediating smooth muscle relaxation in the rat oesophagus. *Br. J. Pharmacol.*, **103,** 1067–1072.

SCOTT, C.M., BUNCE, K.T. & SPRAGGS, C.F. (1991). Investigation of the 5-HT receptor types controlling the short-circuit current response in guinea-pig ileal mucosa. *Br. J. Pharmacol.*, **104,** 349P.

ZIMMERMAN, T.W. & BINDER, H.J. (1984). Serotonin-induced alteration of colonic electrolyte transport in the rat. *Gastroenterology*, **86,** 310–317.

(Received January 23, 1992
Revised April 1, 1992
Accepted April 3, 1992)

Br. J. Pharmacol. (1992), **106**, 883–887 © Macmillan Press Ltd, 1992

Contractile activity of big endothelin-1 on the human isolated bronchus

[1]C. Advenier, *V. Lagente, Y. Zhang & E. Naline

Département de Pharmacologie, Faculté de Médecine Paris-Ouest, 15 rue de l'Ecole de Médecine, F-75270 Paris Cedex 06, and *Institut Henri Beaufour, 1 avenue des Tropiques, F-91952 Les Ulis, France

1 We have studied the contractile activity of the 39 amino acid precursor of endothelin-1 (ET-1), big endothelin-1 (big ET-1), on human isolated bronchi. The contribution of the metalloproteases, neutral endopeptidase (NEP) and angiotensin converting enzyme (ACE), in the presence or absence of the epithelium lining, by use of specific inhibitors, was also evaluated on the effects of big ET-1.

2 Big ET-1 elicited a potent contraction of human isolated bronchus. The $-\log EC_{50}$ value for big ET-1 was 7.53 ± 0.08 ($n = 11$) and E_{max} $78.5 \pm 3.8\%$ (% of ACh 3 mM).

3 Incubation of human isolated bronchi with the NEP inhibitor phosphoramidon (10^{-5} M) induced a rightward shift of the concentration-response curve induced by big ET-1 (10^{-9} M to 3×10^{-7} M). Similar results were observed when human bronchi were incubated with thiorphan (10^{-5} M), but the shift to the right was significantly less ($P < 0.01$) than that observed in the case of phosphoramidon (-0.35 ± 0.05 vs -0.67 ± 0.07 log unit).

4 The two inhibitors of angiotensin I converting enzyme (ACE), captopril or enalapril diacid, did not affect the concentration-response curve for contraction induced by big ET-1.

5 When the epithelium was removed, a leftward shift of the concentration-response curve of big ET-1 (10^{-9} M to 3×10^{-7} M) was observed. Incubation of human isolated bronchi with phosphoramidon or thiorphan (10^{-5} M) or with enalapril diacid or captopril did not modify the leftward shift of the concentration-response curve for big ET-1 after epithelium removal.

6 These results suggest that big ET-1 elicits potent contractile activity in the human isolated bronchus and that its effect is the consequence of the conversion to ET-1 by a phosphoramidon-sensitive metalloprotease which, although different from NEP and ACE, appears to be similar to the endothelin-converting enzyme (ECE) described in other studies in animals.

Keywords: Big-Endothelin (Big ET-1); human isolated airways; metalloproteases; phosphoramidon; thiorphan

Introduction

The 21-amino acids peptide, endothelin (ET-1), is one of the most potent contractile agents of guinea-pig and human airway smooth muscle *in vitro* (Uchida *et al.*, 1988; Maggi *et al.*, 1989; Hay, 1989; Advenier *et al.*, 1990; Sarriá *et al.*, 1990). Furthermore, ET-1 administered either intravenously or by aerosol in the guinea-pig *in vivo* induces a marked and sustained bronchoconstriction (Payne & Whittle, 1988; Macquin-Mavier *et al.*, 1989; Lagente *et al.*, 1989), suggesting a role for endothelin in airways dysfunction.

By analysis of the nucleotide sequence of the cDNA encoding for ET-1, Yanagisawa *et al.* (1988) proposed that the vasoactive peptide endothelin (ET-1) is produced by a 39-amino-acid precursor named big endothelin (big ET-1). The vasoconstrictor and bronchoconstrictor activities of big ET-1 are much lower than those of ET-1, and conversion of the precursor appears to be essential for the pathophysiological actions of ET-1 (Kimura *et al.*, 1989; Fukuroda *et al.*, 1990; D'Orléans-Juste *et al.*, 1991; Pons *et al.*, 1992). ET-1 is formed from big ET-1 via a single cleavage between amino acids Trp-21 and Val-22. Therefore, the C-terminal fragment (22–39), as well as big ET-1 and ET-1, are present in the culture medium of endothelial cells (Emori *et al.*, 1989; Sawamura *et al.*, 1989). However, the enzyme responsible for this processing has not yet been identified precisely, but it seems to be a metalloprotease and has been called ET-converting enzyme (ECE) (Sawamura *et al.*, 1991; McMahon *et al.*, 1991). Vascular endothelium cells possess such a metalloprotease potentially responsible for the metabolism of big ET-1 into ET-1 via a single cleavage, and this enzyme appears to be sensitive to phosphoramidon (Matsumura *et al.*, 1990a; McMahon *et al.*, 1991). It has recently been demonstrated that phosphoramidon suppresses the hypertensive (Matsumura *et al.*, 1990b; McMahon *et al.*, 1991) effects and modulates the bronchoconstrictor (Fukuroda *et al.*, 1990; Pons *et al.*, 1992) effects of big ET-1 in rats and guinea-pigs respectively.

The ET-converting enzyme appears to be different from other metalloproteases, especially the angiotensin I converting enzyme (ACE) and the neutral endopeptidase 3.4.24.11 (NEP) which are widely distributed and involved in the metabolism of a large variety of hormonal, neuromodulator and neurotransmitter peptides (Erdös, 1984; Turner *et al.*, 1985). In human lung tissues, ACE is localized at the luminal surface of the endothelium, whereas NEP appears to be concentrated within the epithelial cells (Johnson *et al.*, 1985; Naline *et al.*, 1989) and participates in the metabolism of ET-1 in the human and guinea-pig bronchus (Advenier *et al.*, 1990; Candenas *et al.*, 1992).

This led us to study the contractile activity of big ET-1 on the human isolated bronchus. The contribution of the metalloproteases NEP and ACE in the presence or absence of the epithelium lining (by use of specific inhibitors) were also evaluated on the effects of big ET-1.

Methods

Human bronchial tissue preparation

Bronchial tissues were removed from 19 patients with lung cancer at the time of the surgical operation (18 men and 1 women; mean age, 58.4 ± 3.4 years; 12 squamous cell car-

[1] Author for correspondence.

cinomas, 4 oat cell carcinomas and 3 adenocarcinomas). Just after resection, segments of human bronchi with an inner diameter of 3 to 5 mm were taken as far away as possible from the malignancy. They were placed in oxygenated Krebs-Henseleit solution (composition, mM: NaCl 119, KCl 4.7, $CaCl_2$ 2.5, KH_2PO_4 1.2, $MgSO_4$ 1.2, $NaHCO_3$ 25.0 and glucose 11.7) at 4°C and stored overnight at 4°C. After removal of the adhering fat and connective tissue, two to eight adjacent rings from the same bronchus were prepared and suspended in organ baths (10 ml) under an initial tension of 2.5 g in Krebs-Henseleit solution, bubbled with 95% O_2:5% CO_2 and maintained at 37°C. The epithelium of some rings was removed by gently rubbing the luminal surface (over both smooth muscle and cartilage areas) with a cotton tipped applicator (Naline *et al.*, 1989). Changes of force of contraction were measured isometrically with strain gauge amplifiers and I.O.S.-Moise 3 recorder system (Dei Lierre, Mitry Mory, France).

Protocol

Each experiment began with contraction of the bronchial strips to maximal contractile force with acetylcholine (ACh, 3 mM), then maximal relaxation was induced with theophylline (3 mM). During the next 120 min, the tissues were washed every 15 min, and the resting tension was adjusted from 2 to 2.5 g, which has been found to be optimal for recording contractions in such tissues (Advenier *et al.*, 1986; Naline *et al.*, 1989). Thereafter, cumulative concentration-response curves to either ET-1 or big ET-1 were constructed by applying increasing concentrations at 15 to 20 min intervals in logarithmic increments. Acetylcholine (3 mM) was added at the end of the concentration-response curve to determine the maximal response of the preparation. In some experiments, phosphoramidon, thiophan, captopril or enalapril diacid (MK 422) at a final concentration of 10^{-5} M, were added to the bath 30 min before the contractile agents. In all experiments, only one concentration-response curve to ET-1 or big ET-1 was recorded in each strip. Concentrations of big ET-1 up to 3×10^{-7} M were not tested because of the limited availability and the cost of the peptide.

The data are expressed in terms of $-\log EC_{50}$ for potency and E_{max} for efficacy. $-\log EC_{50}$ values were derived graphically from the log concentration-effect curves and defined as the negative log of the drug concentration that caused 50% of maximal effect of ACh 3 mM. The maximal effect (E_{max}) was calculated as the maximal increase in tone induced by ET-1 or big ET-1 and expressed as a percentage of the maximum tension induced by ACh 3 mM.

The maximal contractile force obtained with acetylcholine (3 mM) was not affected by thiorphan, phosphoramidon, captopril and enalapril diacid.

Statistical evaluation of data

Statistical analysis of the results was performed by analysis of variance and with Student's *t* test for paired or unpaired data. All values in the text and tables are expressed as mean ± s.e.mean.

Drugs

Drugs used were: endothelin-1 (ET-1) (human, porcine) and big endothelin-1 (big ET-1) (human) (Peptide Institute Inc, Osaka, Japan), acetylcholine dihydrochloride (PCH, Paris, France), thiorphan (Sigma, St Louis, U.S.A.), phosphoramidon [N-(alpha-L-rhamnopyranosyloxy-hydroxy-phosphinyl)-L-leucyl-L-trytophan] (Sigma), captopril (Squibb, Paris, France), enalapril diacid (MK 422, Merck, Paris, France). All agents were dissolved in distilled water. As with the other drugs, these solutions were diluted with Krebs solution.

Results

Contratile activity of big endothelin-1

Big ET-1 elicited a potent concentration-dependent contraction of the human isolated bronchus. The $-\log EC_{50}$ value for big ET-1 was 7.53 ± 0.08 ($n = 11$) and E_{max} 78.5 ± 3.8% (% of E_{max} for ACh). The big ET-1-induced contraction appeared similar to that of ET-1 ($-\log EC_{50} = 7.64 \pm 0.13$, $E_{max} = 81.7 \pm 4.8$, $n = 11$) (Figure 1).

Effect of enzymatic inhibitors on the contractile activity of big endothelin-1

Incubation of human isolated bronchi with phosphoramidon (10^{-5} M) induced a rightward shift of the concentration-response curve induced by big ET-1 (10^{-9} M to 3×10^{-7} M) (Figure 2a). The displacement of the concentration-response curve was significant as demonstrated by the difference between the $-\log EC_{50}$ values before and after incubation with phosphoramidon (-0.67 ± 0.07 log unit, $P < 0.001$) (Table 1). Similar results were observed when human bronchi were incubated with thiorphan (10^{-5} M) (Figure 2b).

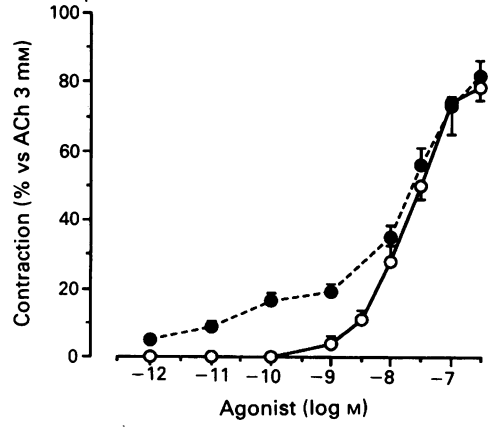

Figure 1 Response of the human isolated bronchus to endothelin-1 (ET-1, ●) or big endothelin-1 (big ET-1, ○). Points represent means; vertical bars represent s.e.mean. $n = 11$.

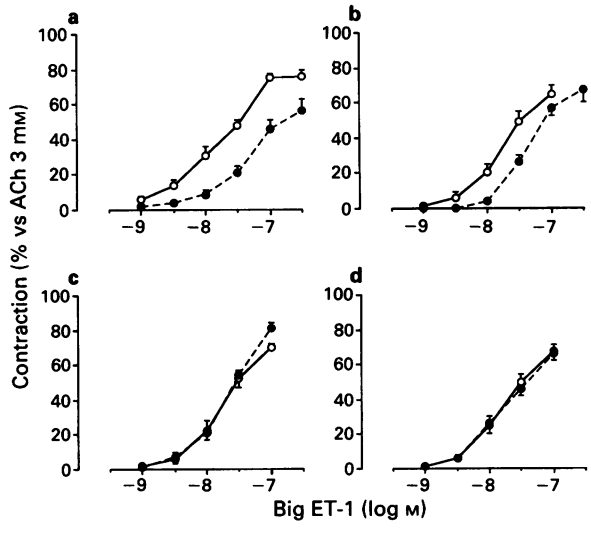

Figure 2 Response of the human isolated bronchus to big endothelin-1 (big ET-1) in the absence (○) or presence (●) of (a) phosphoramidon (10^{-5} M), (b) thiorphan (10^{-5} M), (c) captopril (10^{-5} M) and (d) enalapril diacid (MK 422) (10^{-5} M). Points represent means; vertical bars represent s.e.mean. $n = 5$ to 9.

Table 1 Effect of various enzyme inhibitors of neutral endopeptidase (phosphoramidon, thiorphan) or angiotensin converting enzyme (captopril, enalapril diacid) on big endothelin-1 (big ET-1) induced contraction of human isolated bronchi

Inhibitors	n	*Big ET-1 (−log EC_{50})* Pre-drug	Post-drug	*Shift of the C/R curves* (log unit)
Phosphoramidon 10^{-5} M	9	7.51 ± 0.09	6.84 ± 0.12	−0.67 ± 0.07*
Thiorphan 10^{-5} M	5	7.40 ± 0.12	7.05 ± 0.11	−0.35 ± 0.05*
Captopril 10^{-5} M	5	7.53 ± 0.07	7.54 ± 0.05	0.01 ± 0.06 NS
Enalapril diacid 10^{-5} M	8	7.45 ± 0.10	7.38 ± 0.08	−0.07 ± 0.11 NS

n = number of experiments.
Statistical significance of the shift of the C/R curves are shown as: *$P<0.001$ and NS: not significant.

Table 2 Effect of various enzyme inhibitors on big endothelin-1 (big ET-1)-induced contraction of human isolated bronchi in the presence (+E) or absence (−E) of epithelium (−log EC_{50} values)

Inhibitors	n	*Big ET-1 (−log EC_{50})* +E	−E	*Shift of the C/R curves* (log unit)
Control	6	7.54 ± 0.14	7.94 ± 0.13	0.40 ± 0.05*
Phosphoramidon 10^{-5} M	5	6.81 ± 0.20	7.34 ± 0.17	0.53 ± 0.08§
Enalapril diacid 10^{-5} M	5	7.31 ± 0.05	7.79 ± 0.13	0.48 ± 0.15†
Thiorphan 10^{-5} M	4	7.14 ± 0.09	7.55 ± 0.05	0.41 ± 0.12†

n = number of experiments.
Statistical significance of the shift of the C/R curves are shown as: *$P<0.001$; §$P<0.01$ and †$P<0.05$.

Although significant ($P<0.001$), the shift to the right of the concentration-response curve was significantly less ($P<0.01$) than that observed with phosphoramidon (−0.35 ± 0.05 vs −0.67 ± 0.07 log unit) (Table 1).

In contrast, the two inhibitors of angiotensin I converting enzyme (ACE), captopril or enalapril diacid, did not affect the concentration-response curve induced by big ET-1 (Figure 2c and d) and consequently no significant difference was noted between the −log EC_{50} values before and after incubation with captopril or enalapril diacid (Table 1).

Effect of epithelium removal on the contractile activity of big endothelin-1

When epithelium was removed, a leftward shift of the concentration-response curve of big ET-1 (10^{-9} M to 3×10^{-7} M) was observed (Figure 3a). Indeed, the difference in −log EC_{50} values in the presence (7.54 ± 0.14) or absence (7.94 ± 0.13) of the epithelium was 0.40 ± 0.05 ($P<0.001$, $n=6$) (Table 2).

After incubation of human isolated bronchi with phosphoramidon (10^{-5} M), the same leftward shift (0.53 ± 0.08, $P<0.01$, $n=5$) of the concentration-response curve of big ET-1 was also observed after epithelium removal, suggesting an epithelium-independent effect for the activity of phosphoramidon (Figure 3a, Table 2).

Similar results were observed when the metalloprotease inhibitors thiorphan (10^{-5} M) or enalapril diacid (10^{-5} M) were used under the same conditions (0.41 ± 0.12, $P<0.05$, $n=4$ and 0.48 ± 0.15, $P<0.05$, $n=5$) (Figure 3b, Table 2).

Discussion

The vasoactive peptide endothelin (ET-1) has been shown to elicit potent contractile effect on airway smooth muscle *in vitro* in guinea-pig and rat trachea (Uchida *et al.*, 1988; Maggi *et al.*, 1989; Turner *et al.*, 1989; Sarria *et al.*, 1990). On human airways, Uchida *et al.* (1988) and Advenier *et al.* (1990) also described a potent contractile activity of ET-1.

The present data demonstrate that the 39-amino acid precursor of ET-1, big endothelin-1 (big ET-1), also elicits potent contractile activity in human isolated bronchi. In our preparations, the big ET-1-induced contraction was similar to that of ET-1. Nevertheless, ET-1 was more potent at lower concentrations (10^{-12} to 10^{-9} M) than big ET-1. These data also confirm that, in comparison to big ET-1, ET-1 produced a potent contraction of the human isolated bronchus that proceeded in two steps of different intrinsic activity (Advenier *et al.*, 1990).

These results contrast with those found in rat isolated aorta, where the vasoconstrictor activity of big ET-1 is much lower (about 1/55) than that of ET-1 (Kashiwabara *et al.*, 1989; Kimura *et al.*, 1989). When injected intravenously into ganglion-blocked anaesthetized rats, big ET-1 produces a large pressor response (Kashiwabara *et al.*, 1989). This would suggest that (1) big ET-1 itself has a direct but weak vasoconstrictor activity accounting for the low *in vitro* effect and (2) the conversion of big ET-1 to ET-1 by an endothelin converting enzyme may occur *in vivo* to induce the pressor response, although the response to big ET-1 differs somewhat from the response to ET-1 itself (McMahon *et al.*, 1991).

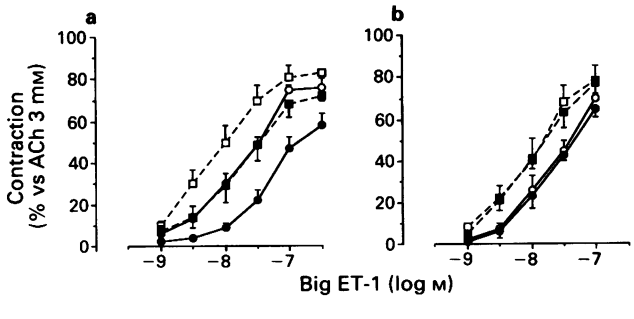

Figure 3 Effect of epithelium removal on the contractile response of the human isolated bronchus to big endothelin-1 (big ET-1) in the absence or presence of (a) phosphoramidon (10^{-5} M) and (b) enalapril diacid (MK 422) (10^{-5} M). Experiments with epithelium: control (○), phosphoramidon or enalapril diacid (●). Experiments after epithelium removal: control (□), phosphoramidon or enalapril diacid (■). Points represent means; vertical bars represent s.e.mean. $n=4$ to 6.

This also indicates that big ET-1 was rapidly and almost totally converted into ET-1 in our preparation since the concentration-response curves observed with both peptides were not significantly different over the mid to upper concentration ranges. Similarly, a rapid generation and degradation of ET-1-like activity was also noted in human polymorphonuclear leukocytes (Sessa *et al.*, 1991).

Previous results showed that a metalloprotease called ET-converting enzyme (ECE) is involved in the conversion of big ET-1 to ET-1. Moreover, the protease inhibitor phosphoramidon is able to inhibit the intracellular conversion of big ET-1 to ET-1 in endothelial cells (Ikegawa *et al.*, 1990; Matsumura *et al.*, 1990a; Sawamura *et al.*, 1991; McMahon *et al.*, 1991) and to reduce the hypertensive and bronchoconstrictor effects of big ET-1 in rat and guinea-pig (Matsumura *et al.*, 1990b; Fukuroda *et al.*, 1990; D'Orléans-Juste *et al.*, 1991; McMahon *et al.*, 1991; Pons *et al.*, 1992). McMahon *et al.* (1991) also reported that in a rabbit lung membrane preparation, ECE activity was blocked by phosphoramidon and 1,10-phenantroline in a concentration-dependent manner. Nevertheless, ECE seems to be different from neutral endopeptidase, although sensitive to phosphoramidon. In ganglion-blocked anaesthetized rats, thiorphan dose-dependently inhibited the pressor response to big ET-1, but was substantially less potent than phosphoramidon (McMahon *et al.*, 1991), even though both compounds inhibited totally NEP activity at the same concentration of 10^{-5} M (Turner *et al.*, 1985). Our results in human bronchus showed that a similar phenomenon can be observed, since it is suggested that the conversion of big ET-1 to ET-1 is under the influence of a phosphoramidon-sensitive metalloprotease and that this enzyme is also different from neutral endopeptidase (NEP), since thiorphan is less efficient than phosphoramidon in reducing the activity of big ET-1 on human isolated bronchi. This possibility has recently been strengthened by the observation that cultured vascular smooth muscle cells contain two types of metalloproteases, which convert big ET-1 to ET-1 and one of them is insensitive to phosphoramidon (Matsumura *et al.*, 1991).

However, it is not possible at this time to specify where ECE is functional in bronchial smooth muscle or near the endothelial cells of bronchial vessels where ECE was originally localized. The present data also confirm that the angiotensin-converting enzyme (ACE) is not involved in the conversion of big ET-1 to ET-1 in human pulmonary tissue, since selective inhibitors of ACE such as captopril and enalapril diacid, have no effects on the contractile activity of big ET-1.

The data obtained in the preparation of human airways after epithelium removal, also suggest the existence of a specific enzyme different from NEP and responsible for the degradation of big ET-1. It has been shown that bronchial epithelium largely modulates the contractile or relaxant activities of various agents. Several hypotheses have been put forward to explain the modulatory role of epithelium. The first hypothesis is to consider epithelium as a diffusion barrier, the removal of which facilitates access of substances to submucosal structures, including smooth muscle, resulting in an increased responsiveness to drug (Small *et al.*, 1990; Iriarte *et al.*, 1990). The second hypothesis is to consider that the epithelium may act as a site of loss (i.e. site of metabolism), limiting the interaction of the agent with its receptor on smooth muscle by reducing its concentration in proportion to the epithelium-dependent rate of degradation. The arguments for this kind of explanation are mainly based on the comparison of the concentration-response curves in the absence or presence of enzyme inhibitors, such as thiorphan or phosphoramidon, which hydrolyse substance P and vasoactive intestinal peptide (VIP) (Devillier *et al.*, 1988; Farmer & Togo, 1990) transport inhibitors (dipyridamole for adenosine) (Advenier *et al.*, 1988). The third hypothesis is that the airway epithelium may release one or more inhibitory factors called epithelium-derived inhibitory factor(s) (or EpDIF) which are able to down-regulate airway responsiveness. The nature of the EpDIF released seems to vary with species and spasmogen agents. It might be a prostanoid, as shown by the effect of cyclo-oxygenase inhibitors on the concentration-response curve to cholinomimetics, leukotrienes and peptides in the guinea-pig isolated trachea or rabbit isolated bronchus (Flavahan *et al.*, 1985; Tschirhart & Landry, 1986), but the release of a non-prostanoid inhibitory factor has been suggested by Fernandes & Goldie (1990).

In the human bronchus, Candenas *et al.* (1992) have found that removal of the epithelium potentiated ET-1-induced contraction. This was shown by a leftward shift of the dose-response curve similar to that observed after incubation of the bronchus with phosphoramidon. This suggests that the neutral endopeptidase plays a role in the degradation and inactivation of ET-1 in the bronchopulmonary system *in vitro* and *in vivo* (Hay, 1989; Boichot *et al.*, 1991; Candenas *et al.*, 1992). Therefore, inhibition of the neutral endopeptidase by phosphoramidon leads to potentiation of the contractile activity of ET-1. On the other hand, in the presence of phosphoramidon, removal of the epithelium does not induce an additional leftward shift of the concentration-response curve to ET-1, suggesting that only epithelium plays a role in the metabolism of this peptide (Candenas *et al.*, 1992).

The situation was markedly different when big ET-1 was used. Removal of the epithelium elicited, as in the case of ET-1, a leftward shift of the dose-response curve to big ET-1, resulting in potentiation of the contractile activity of big ET-1; but in the absence of epithelium, pretreatment with phosphoramidon induced a rightward shift of the concentration-response curve to big ET-1. Metabolic activity of the epithelium cannot be retained and confirms that the enzyme involved in the conversion of big ET-1 to ET-1 is different from that responsible for the degradation of ET-1 (NEP). In contrast, as bronchial epithelium removal potentiates the contractile activity of big ET-1, it is possible to regard the epithelium as a diffusion barrier. The release of a cyclo-oxygenase-derived epithelial mediator under the influence of big ET-1 is not suggested, since indomethacin (3×10^{-6} M) did not modify the concentration-response curve to big ET-1 in the human isolated bronchus (shift of the concentration-response curve: $+0.09 \pm 0.07$ log unit, $n = 4$, unpublished data).

In conclusion, this study shows that in the human isolated bronchus, big ET-1 elicits potent contractile activity, and that this effect is the consequence of the conversion to ET-1 by a phosphoramidon-sensitive metalloprotease which is different from NEP and ACE, but appears to be similar to the ECE described in other studies in animals.

References

ADVENIER, C., DEVILLIER, P., MATRAN, R. & NALINE, E. (1988). Influence of epithelium on the responsiveness of guinea-pig isolated trachea to adenosine. *Br. J. Pharmacol.*, **93**, 295–302.

ADVENIER, C., NALINE, E. & RENIER, A. (1986). Effects of Bay K 8644 on contraction of the human isolated bronchus and guinea-pig isolated trachea. *Br. J. Pharmacol.*, **88**, 33–39.

ADVENIER, C., SARRIA, B., NALINE, E., PUYBASSET, L. & LAGENTE, V. (1990). Contractile activity of three endothelins on the human isolated bronchus. *Br. J. Pharmacol.*, **100**, 168–172.

BOICHOT, E., PONS, F., LAGENTE, V., TOUVAY, C., MENCIA-HUERTA, J.M. & BRAQUET, P. (1991). Phosphoramidon potentiates the ET-1-induced bronchopulmonary response in guinea-pigs. *Neurochem. Int.*, **18**, 477–479.

CANDENAS, M.-L., NALINE, E., SARRIÁ, B. & ADVENIER, C. (1992). Effect of epithelium removal and of enkephalin inhibition of the bronchoconstrictor response to three endothelins of the human isolated bronchus. *Eur. J. Pharmacol.*, **210**, 291–297.

DEVILLIER, P., ADVENIER, C., MARSAC, J., DRAPEAU, G. & REGOLI, D. (1988). Comparison of the influence of epithelium removal and/or of an inhibitor of enkephalinase on the sensitivity of guinea-pig isolated trachealis to neurokinins and agonists analogues. *Br. J. Pharmacol.*, **94,** 675–684.

D'ORLÉANS-JUSTE, P., TÉLÉMAQUE, S. & CLAING, A. (1991). Different pharmacological profiles of big-endothelin-3 and big-endothelin-1 *in vivo* and *in vitro*. *Br. J. Pharmacol.*, **104,** 440–444.

EMORI, T., HIRATA, Y., OTHA, K., SHICHIRI, M. & MARUMO, F. (1989). Secretory mechanism of immunoreactive endothelium in cultured bovine endothelial cells. *Biochem. Biophys. Res. Commun.*, **162,** 93–100.

ERDÖS, E.G. (1984). Multiple functions of human 'converting enzyme' and 'enkephalinase' in peptide metabolism. *Jpn. J. Hypertension*, **6,** 71–80.

FARMER, S.G. & TOGO, J. (1990). Effects of epithelium removal on relaxation of airway smooth muscle induced by vasoactive intestinal peptide and electrical field stimulation. *Br. J. Pharmacol.*, **100,** 73–78.

FERNANDES, L.B. & GOLDIE, R.G. (1990). Pharmacological evaluation of a guinea-pig tracheal epithelium-derived inhibitory factor (EpDIF). *Br. J. Pharmacol.*, **100,** 614–618.

FLAVAHAN, N.A., AARHUS, L.L., RIMELE, T.J. & VANHOUTTE, P.M. (1985). Respiratory epithelium inhibits bronchial smooth muscle tone. *J. Appl. Physiol.*, **58,** 834–838.

FUKURODA, T., NOGUCHI, K., TSUCHIDA, S., NISHIKIBE, M., IKEMOTO, F., OKADA, K. & YANO, M. (1990). Inhibition of biological actions of Big endothelin-1 by phosphoramidon. *Biochem. Biophys. Res. Commun.*, **172,** 390–395.

HAY, D.W.P. (1989). Guinea-pig tracheal epithelium and endothelin. *Eur. J. Pharmacol.*, **171,** 241–245.

IKEGAWA, R., MATSUMURA, Y., TSUKAHARA, Y., TAKAOKA, M. & MORIMOTO, S. (1990). Phosphoramidon, a metalloproteinase inhibitor, suppresses the secretion of endothelin-1 from cultured endothelial cells by inhibiting a big endothelin-1 converting enzyme. *Biochem. Biophys. Res. Commun.*, **171,** 669–675.

IRIARTE, C.F., PASCUAL, R., VILLANEUVA, M.M., ROMÁN, M., CORTIJO, J. & MORCILLO, E.J. (1990). Role of epithelium in agonist-induced contractile responses of guinea-pig trachealis: influence of the surface through which drug enters the tissue. *Br. J. Pharmacol.*, **101,** 257–262.

JOHNSON, A.R., ASTHON, J., SCHULZ, W.W. & ERDÖS, E.G. (1985). Neutral metalloendopeptidase in human lung tissue and cultured cells. *Am. Rev. Respir. Dis.*, **132,** 564–568.

KASHIWABARA, T., INAGAKI, Y., OHTA, H., IWAMATSU, A., NOMIZU, M., MORITA, A. & NISHIKORI, K. (1989). Putative precursors of endothelin have less vasoconstrictor activity in vitro but a potent pressor effect in vivo. *FEBS Lett.*, **247,** 73–76.

KIMURA, S., KASUYA, Y., SAWAMURA, T., SHINMI, O., SUGITA, Y., YANAGISAWA, M., GOTO, K. & MASAKI, T. (1989). Conversion of big endothelin-1 to 21-residue endothelin-1 is essential for expression of full vasoconstrictor activity: structure-activity relationships of big endothelin-1. *J. Cardiovasc. Pharmacol.*, **13** (Suppl. 5), S5–S7.

LAGENTE, V., CHABRIER, P.E., MENCIA-HUERTA, J.M. & BRAQUET, P. (1989). Pharmacological modulation of the bronchopulmonary action of the vasoactive peptide, endothelin, administered by aerosol in the guinea-pig. *Biochem. Biophys. Res. Commun.*, **158,** 625–632.

MCMAHON, E.G., PALOMO, M.A., MOORE, W.M., MCDONALD, J.F. & STERN, M.K. (1991). Phosphoramidon blocks the pressor activity of porcine big endothelin-1 (1-39) in vivo and conversion of big endothelin-1-(1-39) to endothelin-1-(1-21) in vitro. *Proc. Natl. Acad. Sci. U.S.A.*, **88,** 703–707.

MACQUIN-MAVIER, I., LEVAME, M., ISTIN, N. & HARF, A. (1989). Mechanisms of endothelin-mediated bronchoconstriction in the guinea-pig. *J. Pharmacol. Exp. Ther.*, **250,** 740–745.

MAGGI, C.A., PATACCHINI, R., GIULANI, S. & MELI, A. (1989). Potent contractile effect of endothelin in isolated guinea-pig airways. *Eur. J. Pharmacol.*, **160,** 179–182.

MATSUMURA, Y., IKEGAWA, R., TSUKAHARA, Y., TAKAOKA, M. & MORIMOTO, S. (1990a). Conversion of big endothelin-1 to endothelin-1 by two types of metalloproteinases derived from porcine aortic endothelial cells. *FEBS Lett.*, **272,** 166–170.

MATSUMURA, Y., HISAKI, K., TAKAOKA, M. & MORIMOTO, S. (1990b). Phosphoramidon, a metalloproteinase inhibitor, suppresses the hypertensive effect of big-endothelin-1. *Eur. J. Pharmacol.*, **185,** 103–106.

MATSUMURA, Y., IKEGAWA, R., TSUKAHARA, Y., TAKAOKA, M. & MORIMOTO, S. (1991). Conversion of big endothelin-1 to endothelin-1 by two types of metalloproteinases of cultured porcine vascular smooth muscle cells. *Biochem. Biophys. Res. Commun.*, **178,** 899–905.

NALINE, E., DEVILLIER, P., DRAPEAU, G., TOTY, L., BAKDACH, H., REGOLI, D. & ADVENIER, C. (1989). Characterization of neurokinin effects and receptors in human isolated bronchi. *Am. Rev. Resp. Dis.*, **140,** 679–686.

PAYNE, A.N. & WHITTLE, B.J.R. (1988). Potent cyclo-oxygenase-mediated bronchoconstrictor effects of endothelin in the guinea-pig in vivo. *Eur. J. Pharmacol.*, **158,** 303–304.

PONS, F., BOICHOT, E., LAGENTE, V., TOUVAY, C., MENCIA-HUERTA, J.M. & BRAQUET, P. (1992). Role of endothelin in pulmonary functions. *Pulm. Pharmacol.*, (in press).

SARRIÁ, B., NALINE, E., MORCILLO, E., CORTIJO, J., ESPLUGUES, J. & ADVENIER, C. (1990). Calcium dependence of the contraction produced by endothelin (ET-1) in isolated guinea-pig trachea. *Eur. J. Pharmacol.*, **187,** 445–453.

SAWAMURA, T., KIMURA, S., SHINMI, O., SUGITA, Y., YANAGISAWA, M. & MASAKI, T. (1989). Analysis of endothelin related peptide in culture supernatant of porcine aortic endothelial cells: evidence for biosynthetic pathway of endothelin-1. *Biochem. Biophys. Res. Commun.*, **162,** 1287–1294.

SAWAMURA, T., KASUYA, Y., MATSUSHITA, Y., SUZUKI, N., SHINMI, O., KISHI, N., SUGITA, Y., YANAGISAWA, M., GOTO, K., MASAKI, T. & KIMURA, S. (1991). Phosphoramidon inhibits the intracellular conversion of big endothelin-1 to endothelin-1 in cultured endothelial cells. *Biochem. Biophys. Res. Commun.*, **174,** 779–784.

SESSA, W.C., KAW, S., HECKER, M. & VANE, J.R. (1991). The biosynthesis of endothelin-1 by human polymorphonuclear leukocytes. *Biochem. Biophys. Res. Commun.*, **174,** 613–618.

SMALL, R.C., GOOD, D.M., DIXON, J.S. & KENNEDY, I. (1990). The effects of epithelium removal on the actions of cholinomimetic drugs in opened segments and perfused tubular preparations of guinea-pig trachea. *Br. J. Pharmacol.*, **100,** 516–522.

TSCHIRHART, E. & LANDRY, Y. (1986). Airway epithelium does release a relaxant factor: a demonstration with substance P. *Eur. J. Pharmacol.*, **132,** 103–104.

TURNER, A.J., MATSAS, R. & KENNY, A.J. (1985). Are there neuropeptide-specific peptidases? *Biochem. Pharmacol.*, **34,** 1347–1356.

TURNER, N.C., POWER, R.F., POLAK, J.M., BLOOM, S.R. & DOLLERY, C.T. (1989). Endothelin-induced contractions of tracheal smooth muscle and identification of specific endothelin binding sites in the trachea of the rat. *Br. J. Pharmacol.*, **98,** 361–366.

UCHIDA, Y., NINOMIYA, H., SAOTOME, M., NOMURA, A., OHTSUKA, M., YANAGISAWA, M., GOTO, K., MASAKI, T. & HASEGAWA, S. (1988). Endothelin, a novel vasoconstrictor peptide, as potent bronchoconstrictor. *Eur. J. Pharmacol.*, **154,** 227–228.

YANAGISAWA, M., KURIHARA, H., KIMURA, S., TOMOBE, Y., MITSUI, L., GOTO, K. & MASAKI, T. (1988). A novel potent vasoconstrictor peptide produced by vascular endothelial cells. *Nature*, **332,** 411–414.

(Received October 22, 1991
Revised March 16, 1992
Accepted April 3, 1992)

Br. J. Pharmacol. (1992), **106**, 888–892 © Macmillan Press Ltd, 1992

Tachykinin NK_1 receptor in the guinea-pig isolated proximal urethra: characterization by receptor selective agonists and antagonists

Carlo Alberto Maggi & Riccardo Patacchini

Pharmacology Department, A. Menarini Pharmaceuticals, Via Sette Santi 3, 50131 Florence, Italy

1 The tachykinin receptor mediating contraction of the guinea-pig isolated proximal urethra has been characterized by use of receptor selective agonists and antagonists. All experiments were performed in the presence of peptidase inhibitors (bestatin, captopril and thiorphan, 1 μM each) in order to reduce peptide degradation.

2 The natural tachykinins, substance P and neurokinin A produced a concentration-dependent contraction of rings of the proximal urethra which approached the same maximum (about 50% of the response to 80 mM KCl). Substance P (EC_{50} 155 nM) was slightly (3.6 times) more potent than neurokinin A (EC_{50} 560 nM).

3 The tachykinin NK_1 receptor selective agonist, [Sar^9]substance P sulphone (EC_{50} 62 nM), was slightly more potent than substance P and produced the same maximal response of natural tachykinins. The NK_2 receptor selective agonist, [βAla^8] neurokinin A(4–10), was active only at μM concentrations and its maximal effect did not exceed 20% of that to substance P or neurokinin A. The NK_3 receptor selective agonist, senktide, was ineffective up to 30 μM.

4 The response to [Sar^9]substance P sulphone was antagonized in a competitive manner by either (±)-CP 96,345 (pA_2 7.75, slope − 1.10) or GR 82,334 (pA_2 7.31, slope − 1.26), which are selective NK_1 receptor antagonists, while it was unaffected (up to 10 μM) by MEN 10,376, a selective NK_2 receptor antagonist.

5 The response to 10 μM [βAla^8]neurokinin A (4–10) was abolished by either 0.2 μM (±)-CP 96,345 or 1 μM GR 82,334, suggesting the involvement of NK_1 receptors.

6 Electrical field stimulation (5 and 10 Hz, 0.25 ms, 100 V, trains of 5 s duration) produced tetrodotoxin-sensitive phasic contractions of the urethra which were abolished by atropine plus phentolamine (3 μM each). Capsaicin (1 μM) produced a small transient contraction of the urethra which was abolished by (±)-CP 96,345 (0.1 μM). (±)-CP 96,345 did not modify the response to electrical field stimulation.

7 We conclude that tachykinin NK_1 receptors are the main if not the only mediators of the contractile response of guinea-pig proximal urethra to peptides of this family and that this preparation is useful for assessing the affinities of various ligands for the NK_1 receptor. Endogenous tachykinins released from peripheral endings of capsaicin-sensitive primary afferents produce urethral contraction by activating NK_1 receptors.

Keywords: Guinea-pig proximal urethra; tachykinins; tachykinin receptor; receptor antagonists; capsaicin; 'efferent' function of sensory nerves

Introduction

Peptides of the tachykinin family are widely distributed in the urinary tract of various mammalian species, including man. In this region, substance P and neurokinin A are stored in peripheral terminals of primary afferent neurones (capsaicin-sensitive) and, following their release by depolarizing stimuli, exert biological effects (e.g. smooth muscle contraction and plasma protein extravasation) by activating specific receptors located on the membrane of target cells (see Maggi, 1991, for review).

Three distinct types of tachykinin receptors (termed NK_1, NK_2 and NK_3) have been described thus far by pharmacological criteria and subsequently isolated and cloned (see Guard & Watson, 1991; Nakanishi, 1991, for reviews). These receptors are present in the urinary tract (ureter, urinary bladder and urethra) of various species (Maggi, 1991): remarkable species-related variations exist in the types of tachykinin receptor which mediate the same biological function. For instance both NK_1 and NK_2 receptors mediate contraction to tachykinin in the rat and guinea-pig bladder, while only NK_2 receptors do so in the human or hamster urinary bladder (Maggi, 1991, for review). Tachykinins also produce contraction of the mammalian urethral smooth muscle: in rats both NK_1 and NK_2 receptors are present in the proximal urethra (Maggi *et al.*, 1988) while only NK_2 receptors are present in the human urethra (Parlani *et al.*, 1991). Thus NK_2 receptors are consistently expressed, as mediators of the contractile effect of tachykinins in the lower urinary tract, while the expression of NK_1 receptors on smooth muscle seems more susceptible to species-related variations and/or regional differences. In this study we have characterized the tachykinin receptor mediating contraction of the guinea-pig isolated proximal urethra. Evidence has been obtained, by means of receptor selective agonists and antagonists that only NK_1 receptors are present in this preparation. An attempt was also made to establish whether tachykinins may act as excitatory transmitters in the guinea-pig proximal urethra.

Methods

Male albino guinea-pigs weighing 250–350 g were stunned and bled. The whole urinary bladder and urethra were quickly removed and placed in oxygenated (96% O_2 and 4% CO_2) Krebs solution. A ring of proximal urethra was excised and placed in a 5 ml bath for isolated organs. The ring was suspended between two stainless steel hooks and connected to an isotonic transducer (load 3 mN) for recording of mechanical activity.

Experiments were started after a 90 min equilibration period. KCl (80 mM) was added to the bath and the resulting contraction was used as a reference to express contractile response to tachykinin peptides. Concentration-response curves to natural tachykinins and receptor-selective tachykinin agonists were constructed in a cumulative manner, the next concentration being added when the effect of the preceding one had reached its maximum (within 2–3 min of addition to the bath). Preliminary experiments had shown that the maximal response to substance P (3 μM) addition as a single concentration to the bath (55 ± 7% of KCl maximum) was not significantly different from that recorded at the end of the cumulative concentration-response curve (49 ± 6%), indicating absence of a significant tachyphylaxis with this protocol of cumulative application of tachykinins. All experiments were performed in the presence of peptidase inhibitors (bestatin, captopril and thiorphan, 1 μM each, 15 min beforehand).

For studying the effect of tachykinin receptor antagonists, a control curve to the agonist was established first. Then the preparation was thoroughly washed and, 45 min later, the chosen concentration of the antagonist was added to the bath. A new curve to the agonist was performed after a 15 min contact time with the antagonist.

Antagonist potency was evaluated by the Schild plot method (Arunlakshana & Schild, 1959). Since all the antagonists tested provided linear regressions with slopes not significantly different from unity, the antagonists affinity was measured by the constrained plot method (slope constrained to − 1) as proposed by Tallarida *et al.* (1979).

Statistical analysis

All data in the text are means ± s.e. of the mean. Regression analysis was performed by means the least squares method. EC_{50} and 95% confidence limits (CL) were calculated accordingly.

Drugs

Drugs used were: GR 82,334 [D-Pro^9[spiro-γ-lactam]Leu^{10}, Trp^{11}] physalaemin (1–11); Neosystem), bestatin and [Sar^9]substance P sulphone (Peninsula), atropine HCl (Serva), phentolamine mesylate (Ciba-Geigy), tetrodotoxin (Sankyo), captopril (Squibb) and thiorphan (Sigma). Substance P, neurokinin A, [β-Ala^8] neurokinin A (4–10), senktide and MEN 10,376 ([Tyr^5, D-Trp^{6,8,9}, Lys^{10}] NKA(4–10)) were synthesized at Dept. of Chemistry by conventional solid phase methods. (±)-CP 96,345 ([(25,35)-cis-2-(diphenylmethyl)-N-[2-methoxyphenyl)-methyl] - 1-azabicyclo[2.2.2]octan-3-amine]) was synthesized and characterized as described previously (Lecci *et al.*, 1991).

Results

Effect of tachykinin receptor agonists

The guinea-pig isolated proximal urethra was mechanically quiescent. A slowly developing tonic contraction was produced by addition of KCl (80 mM) which was used as a reference response to express the effect of tachykinins and tachykinin-related peptides. The contractile effect of added tachykinins in the guinea-pig isolated proximal urethra developed rapidly (Figure 1) and was rapidly reversed upon washout. Reproducible concentration-response curves were obtained at 30 min intervals with washings intervening between them.

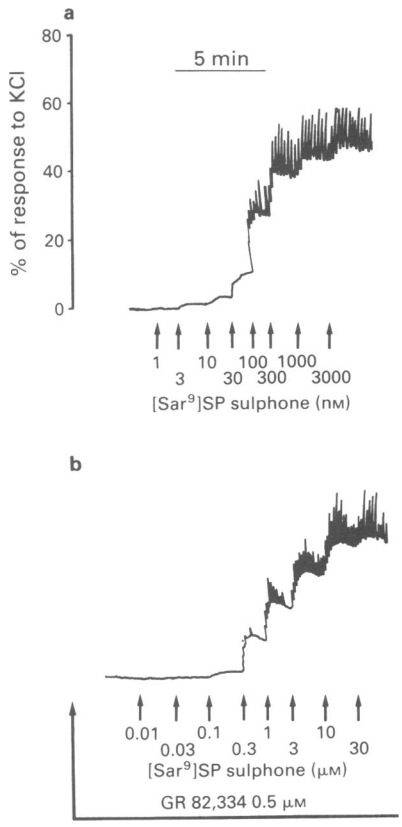

Figure 1 Typical tracings showing the contractile response of the guinea-pig isolated proximal urethra to added [Sar^9]substance P sulphone in the absence (a) and presence (b) of the tachykinin NK_1 receptor antagonist, GR 82,334.

Substance P and neurokinin A both produced a concentration-dependent contraction (Figure 2). The contractile response to each concentration of added peptides was fully developed within 2–3 min of their addition to the bath. The maximum response to substance P and neurokinin A averaged 47 ± 5 and 49 ± 6% of response to KCl ($n = 6$ for each peptide, range 28–89%). Threshold concentrations were 3 nM for substance P and 10 nM for neurokinin A. EC_{50} values and 95% confidence limits are shown in Table 1 and indicate that substance P is slightly (3.6 times) more potent than neurokinin A in contracting the guinea-pig isolated proximal urethra.

The tachykinin NK_1 receptor selective agonist, [Sar^9]-substance P sulphone, behaved as a full agonist (Figures 1 and 2), producing concentration-dependent contractions (threshold concentration 3 nM) which averaged the same maximum (50 ± 3% of the response to KCl) of that produced by natural tachykinins. [Sar^9]substance P sulphone was slightly (2.5 times) more potent than substance P itself and about 9 times more potent than neurokinin A (Table 1).

The NK_2 receptor selective agonist, [βAla^8]neurokinin A(4–10) showed a weak agonist activity at high (μM) concentrations. At the highest concentration tested (30 μM) the response to [βAla^8]neurokinin A(4–10) did not exceed 15% of that to KCl and averaged 23 ± 3% of that produced, in the same urethral rings by a maximally effective concentration of substance P (Figure 2, Table 1).

The NK_3 receptor selective agonist, senktide was ineffective up to 30 μM ($n = 4$, Figure 2, Table 1).

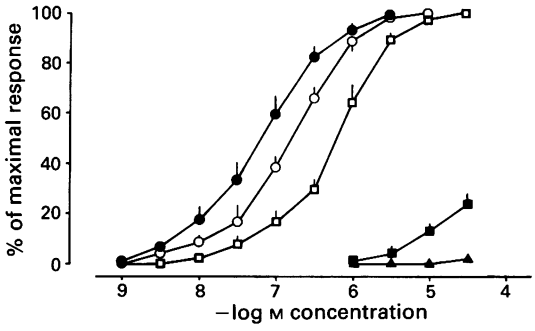

Figure 2 Concentration-dependent contractile response of the guinea-pig isolated proximal urethra to cumulative addition of substance P (○), neurokinin A (□), [Sar^9]substance P sulphone (●), [βAla^8]neurokinin A(4–10) (■) or senktide (▲). Each value is mean of 4–8 experiments; s.e.mean shown by vertical lines.

Table 1 EC_{50} 95% CL values and maximal effect (E_{max}) of natural tachykinins and receptor-selective synthetic agonists in producing contraction of the guinea-pig isolated proximal urethra

Agonist	*EC_{50}* (nM)	*95% CL* (nM)	*E_{max}* (% of KCl)
Substance P	155	92–303	47 ± 5
Neurokinin A	560	142–6273	45 ± 6
[Sar^9]Substance P sulphone	62	34–144	50 ± 3
[βAla^8]Neurokinin A(4–10)	NE	NE	11 ± 4
Senktide	inactive up to 30 μM		—

NE = not evaluatable. Each value originates from 4–8 experiments.

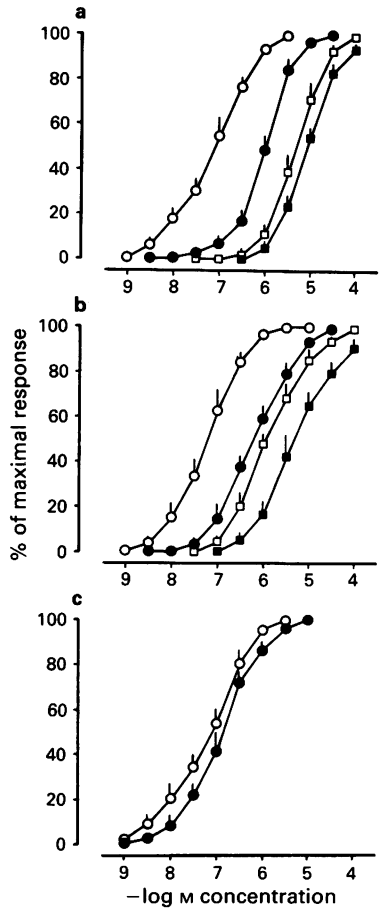

Figure 3 Effect of (±)-CP 96,345 (a) GR 82,334 (b) or MEN 10,376 (c) on the contractile response of the guinea-pig isolated proximal urethra to the tachykinin NK_1 receptor selective agonist, [Sar^9]substance P sulphone. In each panel, control curves to the agonist are shown by (○). Concentrations of the antagonists were as follows: (±)-CP 96,345 0.2 μM (●); 0.5 μM (□) and 1 μM (■); GR 82,334: 0.5 μM (●), 1 μM (□) and 3 μM (■); MEN 10,376 10 μM (●). Each value is mean of at least 4 experiments; s.e.mean shown by vertical lines.

Table 2 Affinity of (±)-CP 96,345, GR 82,334 and MEN 10,376 toward contractions produced by the selective NK_1 treceptor agonist [Sar^9] substance P sulphone in the guinea-pig isolated proximal urethra

Antagonist	*pA_2*	*Slopes of Schild's plot* (95% CL)
(±)-CP 96,345	7.75 ± 0.06	− 1.10 (0.38–1.81)
GR 82,334	7.31 ± 0.08	− 1.26 (0.67–1.86)
MEN 10,376	inactive up to 10 μM	

pA_2 values, calculated by the constrained plot method are mean ± s.e.mean of 9–12 experiments.

Effect of receptor selective antagonists

(±)-CP 96,345, GR 82,334 and MEN 10,376 displayed no agonist activity. Both (±)-CP 96,345 (0.2–1 μM, Figure 3) and GR 82,334 (0.5–3 μM, Figure 1 and 3) produced a concentration-dependent rightward shift of the curve to the NK_1 receptor selective agonist [Sar^9]substance P sulphone without depression of maximal response attainable. Schild's plot analysis revealed the competitive nature of the antagonism (Table 2) and pA_2 values were calculated by the constrained plot method (Tallarida *et al.*, 1979) (Table 2). (±)-CP 96,345 was slightly more potent (0.44 log unit difference in pA_2 values) than GR 82,334. MEN 10,376 (10 μM) failed to affect significantly the concentration-response curve to the NK_1 receptor selective agonist (Figure 3, Table 2).

The question was raised as to whether the small effect produced by [βAla^8]neurokinin A(4–10) may reflect the existence of a minor population of NK_2 receptors in the preparation. The contraction produced by 10 μM [βAla^8]-neurokinin A(4–10) (11 ± 4% of maximal response to neurokinin A, $n = 4$) however, was abolished by 0.2 μM (±)-CP 96,345 ($n = 4$), indicating its dependence upon activation of NK_1 receptor. Similar results were obtained with 1 μM GR 82,334 as antagonist: the response to 10 μM [βAla^8]neurokinin A(4–10) (12.5 ± 2% of maximal response to neurokinin A, $n = 4$) was totally abolished in the presence of GR 82,334.

Effect of (±)-CP 96,345 on contractile responses to capsaicin and electrical field stimulation

These experiments aimed to assess whether tachykinins may act as excitatory transmitters in the guinea-pig proximal urethra following activation of intramural nerves by electrical field stimulation. Electrical stimulation (trains of pulses of 5 s duration, 0.2 ms pulse width, 100 V at a frequency of 5–10 Hz) produced phasic contractions of the urethral rings which were reproducible at 15–20 min intervals. The amplitude of evoked contractions averaged 8 ± 2 and 27 ± 6% of the response to KCl, at 5 and 10 Hz, respectively ($n = 6$). These responses were almostly abolished (>95% inhibition) by 1 μM tetrodotoxin, indicating their neural origin. At both frequencies of stimulation the evoked contractions were also abolished by atropine (3 μM) and phentolamine (3 μM) ($n = 4$). Capsaicin (1 μM) produced a small (7.2 ± 1.5% of the res-

ponse to KCl, $n = 5$), tonic-type contraction of the urethra. A second application of capsaicin, 30 min after the first challenge, had no effect, indicating complete desensitization.

(±)-CP 96,345 (0.1 μM) almost abolished the contractile response to capsaicin, while leaving the response to electrical stimulation (5 Hz) unaffected (Figure 4).

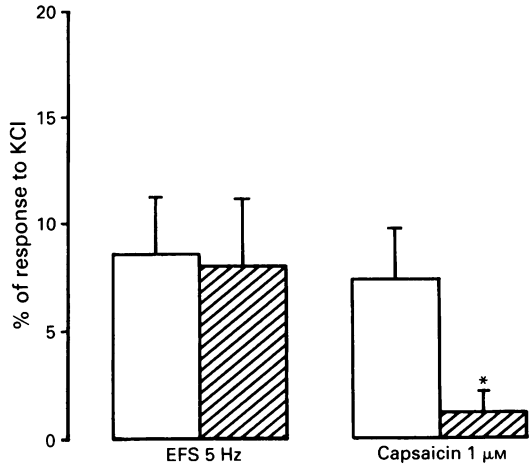

Figure 4 Effect of (±)-CP 96,345 0.1 μM (hatched columns) on contraction of the guinea-pig isolated proximal urethra produced by electrical field stimulation (EFS) or capsaicin; control, open columns. Each column is mean of 4 experiments; vertical bars show s.e.mean. Significantly different from control, $*P < 0.05$.

Discussion

By use of receptor selective agonists and antagonists it appears evident that the contractile response of the guinea-pig isolated proximal urethra to tachykinins is exclusively mediated by tachykinin NK_1 receptors. The evidence supporting this statement is as follows: (a) the response to receptor-selective synthetic agonists, among which only [Sar^9] substance P sulphone, a highly selective NK_1 receptor agonist, produced a response comparable to that of natural tachykinins; (b) antagonism by (±)-CP-96,345 and GR 82,334 which have been previously characterized as selective NK_1 receptor atagonists (Hagan *et al.*, 1991; Snider *et al.*, 1991); (c) failure of MEN 10,376, a selective NK_2 receptor antagonist (Maggi *et al.*, 1991), to affect the response to [Sar^9]substance P sulphone and (d) antagonism of the small reponse to [βAla^8]neurokinin A(4–10) by (±)-CP 96,345 and GR 82,334.

We therefore consider the guinea-pig isolated proximal urethra as a useful 'monoreceptorial' bioassay for the NK_1 tachykinin receptor. In this respect, other preparations with this characteristic have been described, such as the dog carotid artery (D'Orleans-Juste *et al.*, 1986), the guinea-pig vas deferens (Hall & Morton, 1991) the rabbit vena cava and jugular vein (Nantel *et al.*, 1990; 1991). Owing to the recent proposals of the existence of species-related variants of the tachykinin NK_1 receptor vs. NK_1 receptor subtypes (Gitter *et al.*, 1991; Beresford *et al.*, 1991), it is important to compare the activity of various NK_1 receptor antagonists in different preparations from various species. The affinities of (±)-CP 96,345 and GR 82,334 for the NK_1 receptor in the guinea-pig urethra are very similar to those observed in other preparations from this same species (e.g. guinea-pig ileum and vas deferens). Thus pA_2 values of 8.11 and 7.79 have been determined for (±)-CP 96,345 in the guinea-pig ileum and vas deferens, respectively (Lecci *et al.*, 1991; Patacchini & Maggi, unpublished data) vs. a pA_2 value of 7.75 measured here in the guinea-pig urethra. Likewise the pA_2 value of GR 82,334 in the guinea-pig ileum (7.64, Hagan *et al.*, 1991) is very close to that reported here (7.31) for the guinea-pig proximal urethra. Overall, the results of these experiments do not support the idea of heterogeneity of NK_1 receptors in peripheral preparations from guinea-pigs.

Local motor responses ascribable to release of sensory neuropeptides (neurogenic inflammation) have been described as occurring throughout the urinary tract in rats and guinea-pigs (Maggi, 1991 for review). The present findings support the idea that endogenous tachykinins released from peripheral endings of capsaicin-sensitive primary afferents play a role as neurotransmitters by activating NK_1 receptors. The magnitude of the contractile response observed following capsaicin application is small as compared to that produced by exogenous tachykinins or other stimuli (KCl or electrical field stimulation). It may be that other effects produced by tachykinins in the guinea-pig urethra (e.g. plasma protein extravasation) (Abelli *et al.*, 1989) are more important in the general economy of urethral function regulation by sensory nerves in this species. On the other hand, the presence of tachykinin receptors on urethral smooth muscle in this and other species, including man, may indicate a role for locally released tachykinins in the genesis of abnormal urethral contractions (urethral instability) which could take place during chemical or mechanical irritation of primary afferent nerves at this level.

References

ABELLI, L., SOMMA, V., MAGGI, C.A., REGOLI, D., ASTOLFI, M., PARLANI, M., ROVERO, P., CONTE, B. & MELI, A. (1989). Effects of tachykinins and selective tachykinin receptor agonists on vascular permeability in the rat lower urinary tract: evidence for the involvement of NK-1 receptors. *J. Autonom. Pharmacol.*, **9**, 253–263.

ARUNLAKSHANA, O. & SCHILD, H.O. (1959). Some quantitative uses of drug antagonists. *Br. J. Pharmacol Chemother.*, **14**, 48–58.

BERESFORD, I.J.M., BIRCH, B.J., HAGAN, R.M. & IRELAND, S.J. (1991). Investigation into species variants in tachykinin NK-1 receptors by use of the non-peptide antagonist, CP 96,345. *Br. J. Pharmacol.*, **104**, 292–293.

D'ORLEANS-JUSTE, P., DION, S., DRAPEAU, G. & REGOLI, D. (1986). Different receptors are involved in the endothelium-mediated relaxation and the smooth muscle contraction of the rabbit pulmonary artery in response to substance P and related neurokinins. *Eur. J. Pharmacol.*, **125**, 37–44.

GITTER, B.D., WATERS, D.C., BRUNS, R.F., MASON, N.R., NIXON, J.A. & HOWBERT, J.J. (1991). Species differences in affinities of non-peptide antagonists for substance P receptors. *Eur. J. Pharmacol.*, **197**, 237–238.

GUARD, S. & WATSON, S.P. (1991). Tachykinin receptor types: classification and membrane signalling mechanisms. *Neurochem. Internat.*, **18**, 149–165.

HAGAN, R.M., IRELAND, S.J., BAILEY, F., MCBRIDE, C., JORDAN, C.C. & WARD, P. (1991). A spirolactam conformationally-constrained analogue of physalaemin which is a peptidase-resistant, selective neurokinin NK-1 receptor antagonist. *Br. J. Pharmacol.*, **102**, 168P.

HALL, J. & MORTON, I.K.M. (1991). Novel selective agonists and antagonists confirm neurokinin NK-1 receptors in guinea-pig vas deferens. *Br J. Pharmacol.*, **102**, 511–517.

LECCI, A., GIULIANI, S., PATACCHINI, R., VITI, G. & MAGGI, C.A. (1991). Role of NK-1 tachykinin receptors in thermonociception: effect of (±) CP 96,345 a non-peptide substance P antagonist on the hot plate test in mice. *Neurosci. Lett.*, **129**, 299–302.

MAGGI, C.A. (1991). The role of peptides in the regulation of micturition reflex: an update. *Gen. Pharmacol.*, **22**, 1–43.

MAGGI, C.A., GIULIANI, S., BALLATI, L., LECCI, A., MANZINI, S., PATACCHINI, R., RENZETTI, A.R., ROVERO, P., QUARTARA, L. & GIACHETTI, A. (1991). In vivo evidence for tachykininergic transmission using a new NK-2 receptor selective antagonist, MEN 10,376. *J. Pharmacol. Exp. Ther.*, **257,** 1172–1178.

MAGGI, C.A., PARLANI, M., ASTOLFI, M., SANTICIOLI, P., ROVERO, P., ABELLI, L., SOMMA, V., GIULIANI, S., REGOLI, D., PATACCHINI, R. & MELI, A. (1988). Neurokinin receptors in the rat lower urinary tract. *J. Pharmacol. Exp. Ther.*, **246,** 308–315.

NAKANISHI, S. (1991). Mammalian tachykinin receptors. *Annu. Rev. Neurosci.*, **14,** 123–136.

NANTEL, F., ROUISSI, N., RHALEB, N.E., DION, S., DRAPEAU, G. & REGOLI, D. (1990). The rabbit jugular vein is a contractile NK-1 receptor system. *Eur. J. Pharmacol.*, **159,** 457–462.

NANTEL, F., ROUISSI, N., RHALEB, N.E., JUKIC, D. & REGOLI, D. (1991). Pharmacological evaluation of the angiotensin, kinin and neurokinin receptors in the rabbit vena cava. *J. Cardiovasc. Pharmacol.*, **18,** 398–405.

PARLANI, M., CONTE, B., MAJMONE, S., MAGGI, C.A., ROVERO, P. & GIACHETTI, A. (1991). The contractile effect of tachykinins on human prostatic urethra: involvement of NK-2 receptors. *J. Urol.*, **144,** 1543–1545.

SNIDER, R.M., CONSTANTINE, J.W., LOWE III, J.A., LONMGO, K.P., LEBEL, W.S., WOODY, H.A., DROZDA, S.E., DESAI, M.C., VINICK, F.J., SPENCER, R.W. & HESS, H.J. (1991). A potent nonpeptide antagonist of the substance P (NK-1) receptor. *Science*, **251,** 435–437.

TALLARIDA, R.J., COWAN, A. & ADLER, M.W. (1979). pA_2 and receptor differentiation: a statistical analysis of competitive antagonism. *Life Sci.*, **25,** 637–654.

(Received January 27, 1992
Revised March 23, 1992
Accepted April 3, 1992)

Br. J. Pharmacol. (1992), **106**, 893–899 © Macmillan Press Ltd, 1992

Actions of 5-hydroxytryptamine and 5-HT_{1A} receptor ligands on rat dorso-lateral septal neurones *in vitro*

[1] Peter Van den Hooff & [2] Martin Galvan

Marion Merrell Dow Research Institute, 16 rue d'Ankara, B.P. 447 R/9 67009 Strasbourg Cedex, France

1 The actions of 5-hydroxytryptamine (5-HT) and some 5-HT_{1A} receptor ligands on neurones in the rat dorso-lateral septal nucleus were recorded *in vitro* by intracellular recording techniques.

2 In the presence of tetrodotoxin (1 μM) to block any indirect effects, bath application of 5-HT (0.3–30 μM) hyperpolarized the neurones in a concentration-dependent manner and reduced membrane resistance. The hyperpolarization did not exhibit desensitization and was sometimes followed by a small depolarization.

3 The 5-HT_{1A} receptor ligands, 8-hydroxy-2-(di-n-propylamino) tetralin (8-OH-DPAT), N,N-dipropyl-5-carboxamidotryptamine (DP-5-CT) and buspirone but not the non-selective 5-HT_1 receptor agonist, 1-*m*-trifluoromethylphenylpiperazine (TFMPP), also hyperpolarized the neurones.

4 5-HT, 8-OH-DPAT and DP-5-CT appeared to act as full agonists whereas buspirone behaved as a partial agonist. The estimated EC_{50}s were: DP-5-CT 15 nM, 8-OH-DPAT 110 nM, 5-HT 3 μM and buspirone 110 nM.

5 At a concentration of 3 μM, the putative 5-HT_{1A} receptor antagonists, spiperone, methiothepin, NAN-190 (1-(2-methoxyphenyl)-4-[4-(2-pthalimido)butyl]piperazine) and MDL 73005EF (8-[2-(2,3-dihydro-1,4- benzodioxin-2-yl-methylamino)ethyl]-8-azaspiro[4,5]decane-7,9-dione methyl sulphonate), produced a parallel rightward shift in the concentration-response curve to 5-HT with no significant reduction in the maximum response. The estimated pA_2 values were: NAN-190 6.79, MDL 73005EF 6.59, spiperone 6.54 and methiothepin 6.17.

6 The 5-HT_2/5-HT_{1C} receptor antagonist, ketanserin (3 μM) and the $5HT_3$ receptor antagonist, tropisetron (3 μM) did not antagonize the 5-HT-induced hyperpolarizations; however, ketanserin blocked the depolarization which sometimes followed the hyperpolarization.

7 It is concluded that the 5-HT-induced membrane hyperpolarization of rat dorso-lateral septal neurones is mediated by 5-HT_{1A} receptors.

Keywords: 5-Hydroxytryptamine (5-HT); 8-hydroxy-2-(di-n-propylamino) tetralin (8-OH-DPAT); MDL 73005EF; NAN-190; buspirone; $5HT_{1A}$-receptor; lateral septum.

Introduction

There is increasing interest in the neuronal actions of novel, synthetic ligands for 5-HT_{1A} receptors since it appears that these can be of use in the treatment of anxiety conditions in man (Chopin & Briley, 1987; Traber & Glaser, 1987; Taylor, 1988; Palfreyman *et al.*, 1991). Thus it has been demonstrated that buspirone and MDL 73005EF can reduce the firing rate of 5-hydroxytryptaminergic neurones in the dorsal raphe nucleus via activation of 5-HT_{1A} receptors (VanderMaelen *et al.*, 1986; Sprouse & Aghajanian, 1987; 1988; Sprouse, 1991) and it is generally thought that the consequent reduction in 5-hydroxytryptaminergic tone in the postsynaptic target areas can explain the observed behavioural effects of these two compounds (Moser *et al.*, 1990; Palfreyman *et al.*, 1991).

In limbic areas innervated by raphe 5-hydroxytryptaminergic neurones (Andén *et al.*, 1966; Ungerstedt, 1971; Azmitia & Segal, 1978) there is a high density of 5-HT_{1A} receptors (Gozlan *et al.*, 1983; Köhler, 1984; Pazos & Palacios, 1985), the activation of which inhibits neuronal firing (VanderMaelen & Aghajanian, 1983; Sprouse & Aghajanian, 1988). However, the actions of proposed agonists and antagonists at 5-HT_{1A} receptors in these areas is non-uniform and the underlying mechanisms are, at present, far from clear. For example, 8-hydroxy-2-(di-n-propylamino) tetralin (8-OH-DPAT), a compound generally regarded as being an agonist at 5-HT_{1A} receptors, has been reported to have potent antagonist (Colino & Halliwell, 1986; 1987) as well as weak partial agonist actions on hippocampal neurones (Andrade & Nicoll, 1987a). In addition, behavioural, neurochemical and electrophysiological experiments suggest that the novel anxiolytics buspirone and MDL 73005EF act as agonists at the raphe neurone presynaptic 5-HT_{1A} receptors but have partial agonist or even pure antagonist actions at the postsynaptic 5-HT_{1A} receptors (Cornfield *et al.*, 1989; Gartside & Cowan, 1990; Gartside *et al.*, 1990; Moser *et al.*, 1990; Sprouse, 1991; Van den Hooff & Galvan, 1991).

The dorso-lateral septal nucleus receives a dense innervation of 5-hydroxytryptaminergic fibres from the raphe nuclei (Azmitia & Segal, 1978; Köhler *et al.*, 1982) and the presence of 5-HT_{1A} receptors on these neurones has been demonstrated by both quantitative autoradiographical (Pazos & Palacios, 1985) as well as electrophysiological techniques (Joëls *et al.*, 1987). The present experiments were performed to study the actions of a number of high affinity 5-HT_{1A}-receptor ligands currently proposed as being selective agonists or antagonists at this 5-hydroxytryptamine receptor subtype (see Hoyer, 1991 for an overview). A preliminary account of some of these results was presented at the joint meeting of the British Pharmacological Society and the Association Française des Pharmacologistes (Van den Hooff *et al.*, 1991).

[1] Present address: Persijn 39-III, 1082 ET Amsterdam, The Netherlands.
[2] Author for correspondence.

Methods

Slice preparation

Unanaesthetized male Sprague-Dawley rats (100–200 g; Charles River, France) were decapitated and the brains removed and cooled for 1 min in Krebs solution at 2–4°C. The septi were exposed and slices (approximately 500 μm) were cut with an assembly of two razor blades. Slices were either stored until required in a small holding chamber filled with oxygenated Krebs solution (22–26°C) or transferred to the perspex recording chamber where they were sandwiched between two nylon nets and continuously superfused (8 ml min^{-1}) with a modified Krebs solution at 32°C. The composition of the modified Krebs solution was as follows (mM): NaCl 119, KCl 3.0, NaH_2PO_4 1.2, $MgCl_2.6H_2O$ 1.2, $CaCl_2.2H_2O$ 2.0, $NaHCO_3$ 25 and D-glucose 10; all solutions were continuously gassed with 95% O_2/5% CO_2. Compounds were added in fixed concentrations to the bath solution; however, due to the design of the perfusion system, there was a delay of about 30–40 s between changing the perfusion solution and the arrival of the modified solution in the recording chamber.

Intracellular recordings

Intracellular recordings were made with glass microelectrodes filled with 3 M KCl (60–90 MΩ) or 4 M K-acetate (90–150 MΩ). Electrical signals were amplified with an Axoclamp IIA amplifier (Axon Instruments, Foster City, CA, U.S.A.), monitored on a digital oscilloscope and recorded on a chart recorder (TA-2000; Gould Instruments, France) and a personal computer running pClamp software (Axon Instruments). The neurones included in this study exhibited resting membrane potentials more negative than − 60 mV and membrane resistances greater than 70 MΩ. In almost all of the experiments described, tetrodotoxin (TTX; 1 μM) was added to the perfusion medium to block action potential-dependent neurotransmitter release and thus preclude indirect effects of the compounds under study.

Concentration-response curves

Two methods were used to construct concentration-response curves to agonists before and after addition of antagonists. (1) Agonists were applied to single neurones in ascending concentrations with wash periods between each application. Where this was not possible due to the long duration of the agonist response, cells were exposed to only single concentrations of agonist and the results from several cells were pooled. (2) Agonists were applied in ascending concentrations in a cumulative manner without intervening wash periods. In all cases the agonist-induced change in membrane potential (mV) was measured from the chart recordings.

Antagonists were applied for at least 20 min before retesting 5-HT. The pA_2 values were estimated from the shift in the concentration-response curve at the level of the EC_{50} value of 5-HT in control solution by use of the following equation:

$$pA_2 = \log_{10}(\text{dose ratio} - 1) - \log_{10}([\text{antagonist}])$$

Analysis of the results

Unless otherwise stated, all numerical data are given as the means ± s.e.mean. Two-tailed, paired and unpaired *t* tests were calculated as necessary using the programme Instat (Graphpad Software, San Diego, CA, U.S.A.).

Materials

The following substances were used: 5-hydroxytryptamine creatinine sulphate complex, baclofen and tetrodotoxin (Sigma, France); buspirone HCl (Bristol Myers); methiothepin-maleate (Hoffmann La-Roche); ketanserin (Janssen). Spiperone HCl, 8-OH-DPAT HBr (8-hydroxy-2-(di-n-propylamino)-tetralin hydrobromide), TFMPP HCl (1-*m*-trifluoromethylphenylpiperazine hydrochloride) and DP-5-CT (N, N-dipropyl-5-carboxamidotryptamine) were purchased from Research Biochemicals Incorporated, Massachusetts, U.S.A. MDL 73005EF (8-[2-(2,3-dihydro-1,4-benzodioxin-2-yl-methylamino)ethyl]-8-azaspiro[4,5]decane-7,9-dione methyl sulphonate), NAN-190 (1-(2-methoxyphenyl)-4-[4-(2-pthalimido) butyl]piperazine) and tropisetron (3α-tropanyl-1H-indole-3-carboxylic acid ester) were synthesized at the Marion Merrell Dow Research Institute, Strasbourg, France.

Results

The results described are based on stable intracellular recordings from 136 neurones located in the dorso-lateral part of the septum. The resting membrane potential and membrane resistance of these cells was − 70 ± 5.9 mV and 126 ± 42.1 MΩ respectively (means ± s.d.). There were no significant differences in the passive membrane properties of the groups of cells used to test the actions of the various agonists and antagonists.

Actions of putative agonists

Bath application of 5-HT (0.3–30 μM) hyperpolarized the membrane potential and reduced the membrane resistance in a concentration-dependent manner (Figure 1a). The hyperpolarization was maximal after about 1 min and the membrane potential repolarized within 1 to 4 min towards control levels following return to drug-free Krebs solution. During application periods of up to 10 min, no desensitization of the hyperpolarizing response was observed (Figure 1b; $n = 5$ cells). Current-voltage curves constructed before and during application of 5-HT (Figure 2a) indicated that the reversal potential for the underlying ionic conductance change was − 100 ± 1 mV (Figure 2b; $n = 5$).

In most experiments 5-HT was applied in a non-cumulative fashion (e.g. Figure 1a) and the calculated EC_{50} was found to be 3.0 ± 0.4 μM ($n = 8$). Since no obvious desensitization was observed, cumulative concentration-response curves were also constructed. This procedure significantly increased the amount of data that could be obtained from a single neurone and the resulting EC_{50} value (2.5 ± 0.6 μM; $n = 5$) was not significantly different from that obtained with non-cumulative applications.

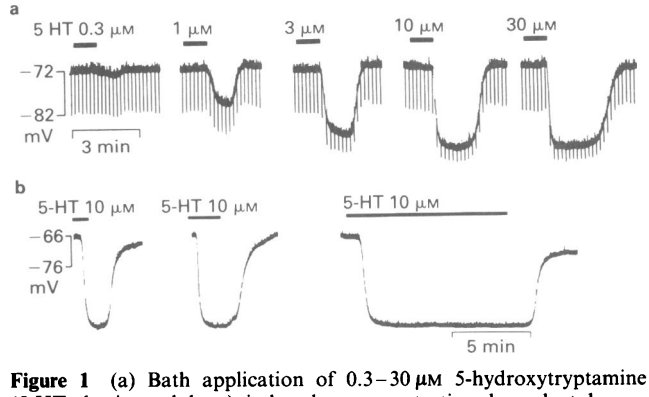

Figure 1 (a) Bath application of 0.3–30 μM 5-hydroxytryptamine (5-HT, horizontal bars) induced a concentration-dependent hyperpolarization and reduced membrane resistance. The transient downward deflections are membrane responses to intracellular injection of constant current pulses (0.1 nA, 350 ms, 0.1 Hz). (b) The 5-HT-induced hyperpolarization did not desensitize during (from left to right) 1, 2 or 10 min applications of 10 μM 5-HT (horizontal bars). The 30–40 s delay in the perfusion line (see methods) has not been corrected for in this and all subsequent figures.

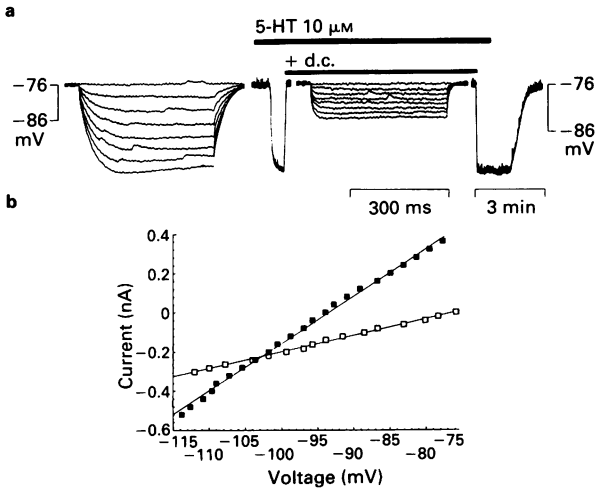

Figure 2 (a) Electrotonic potentials (on a fast time-base) recorded before and during application of 10 μM 5-hydroxytryptamine (5-HT). The 8 superimposed electrotonic potentials resulted from 8 hyperpolarizing current pulses (in − 0.04 nA steps). During the period marked '+ d.c.' steady depolarizing current was injected to restore the membrane potential to the control level. (b) Complete current-voltage relationship recorded from the same cell as (a) in control solution (□) and in the presence of 10 μM 5-HT (■). The reversal potential was about − 102 mV.

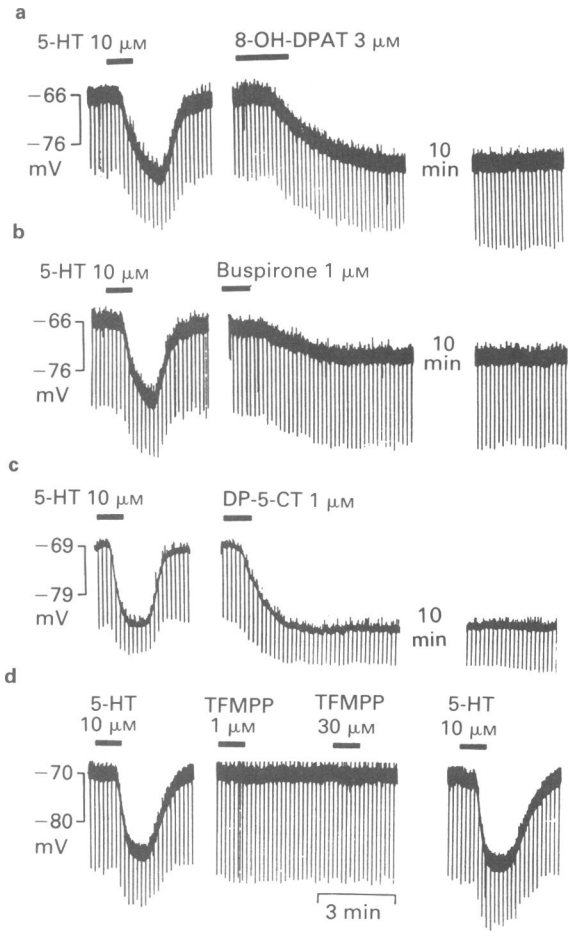

Figure 3 Comparison of the onset and duration of action of (a) 3 μM 8-hydroxy-2-(di-n-propylamino) tetralin (8-OH-DPAT), (b) 1 μM buspirone and (c) 1 μM N,N-dipropyl-5-carboxamidotryptamine (DP-5-CT) in 3 different neurones. Note that the hyperpolarizations persisted following removal of the compounds. 5-Hydroxytryptamine (5-HT) (10 μM) was initially applied to demonstrate sensitivity and reversibility. (d) 1-*m*-Trifluoromethylphenylpiperazine (TFMPP, 1 and 30 μM) was without effect on the membrane potential of a 5-HT responsive cell.

Figure 3 illustrates recordings from 4 different neurones in which the action of 10 μM 5-HT was compared to that of 8-OH-DPAT, buspirone, DP-5-CT and TFMPP. The 5-HT$_{1A}$ receptor agonist 8-OH-DPAT (Figure 3a; 0.03–3 μM), induced hyperpolarizations which were slow in onset (1–5 min) and very poorly reversible. In 5 neurones, 4–5 concentrations of 8-OH-DPAT were applied in a cumulative fashion and the calculated EC_{50} was 112 ± 8 nM.

The anxiolytic drug, buspirone (Figure 3b; 0.1–30 μM), which also has high affinity for 5-HT$_{1A}$ receptors, had actions similar to those of 8-OH-DPAT in that the buspirone-induced hyperpolarizations were slow in onset (several minutes) and very slow to recover. The EC_{50} calculated from pooled data was approximately 110 nM. It was also noted that the maximum response to buspirone (7.0 ± 1.1 mV, $n = 4$) was significantly smaller than that to 8-OH-DPAT (13.8 ± 0.6 mV, $n = 8$; $P < 0.05$) or 5-HT (15.9 ± 0.9 mV, $n = 19$; $P < 0.001$).

DP-5-CT (0.001–1 μM), a potent and selective 5-HT$_{1A}$ receptor agonist, induced a hyperpolarization which was, like 8-OH-DPAT, slow in onset and poorly reversible (Figure 3c; Markstein *et al.*, 1986). In 4 cells, 4–5 concentrations of DP-5-CT were applied in a cumulative manner and the calculated EC_{50} was 17.3 ± 3.0 nM. Figure 3d illustrates that TFMPP, a non-specific ligand for 5-HT receptors with a relatively low affinity for 5-HT$_{1A}$ receptors (Hoyer, 1991), had no significant effect on the membrane potential of a neurone which hyperpolarized in a characteristic manner to 10 μM 5-HT.

MDL 73005EF (1–30 μM), which is equipotent to buspirone as an agonist at 5-HT$_{1A}$ receptors on dorsal raphe neurones (Sprouse, 1991) had no consistent, concentration-dependent effect on the membrane potential or the membrane resistance of dorso-lateral septal neurones. Nevertheless, 6 out of 20 neurones exposed to 3 μM MDL 73005EF were hyperpolarized by 5.7 ± 0.7 mV; the membrane potential change measured in the other 14 cells was ⩽ 1 mV (Figure 4). The onset and offset rates of the hyperpolarizations were similar to those of buspirone and 8-OH-DPAT. The complete concentration-response curves for DP-5-CT, 8-OH-DPAT, 5-HT, buspirone, TFMPP and MDL 73005EF are presented in Figure 5. In contrast to 5-HT, the hyperpolarizations induced by 8-OH-DPAT, DP-5-CT, buspirone and MDL 73005EF showed little or no recovery during a washout period of 10–30 min.

The effects of 5-HT, 8-OH-DPAT, DP-5-CT and buspirone on membrane resistance were calculated from the amplitude of hyperpolarizing electrotonic potentials. The former three compounds reduced membrane resistance in a concentration-dependent manner although there was considerable variation between cells. Thus, membrane resistance was reduced to 49 ± 11% of control by 30 μM 5-HT, 61 ± 15% of control by 3 μM 8-OH-DPAT and 42 ± 12% of control by 1 μM DP-5-CT (means ± s.d., $n = 9$, 9 and 10 respectively). The changes in resistance induced by 3 μM 8-OH-DPAT and 1 μM DP-5-CT were not significantly different from that produced by 30 μM 5-HT ($P > 0.05$, unpaired, 2-tailed t test). Buspirone (3 μM) reduced membrane resistance to 92 ± 5% of control (mean ± s.d., $n = 4$). This small and rather insignificant effect was similar to the reduction induced by a concentration of 5-HT (1 μM) which produced a similar degree of hyperpolarization (95 ± 9%, mean ± s.d., $n = 4$).

Actions of putative antagonists

Previous electrophysiological studies have shown that the 5-HT-induced hyperpolarization of hippocampal CA1 pyramidal neurones can be antagonized by the non-selective

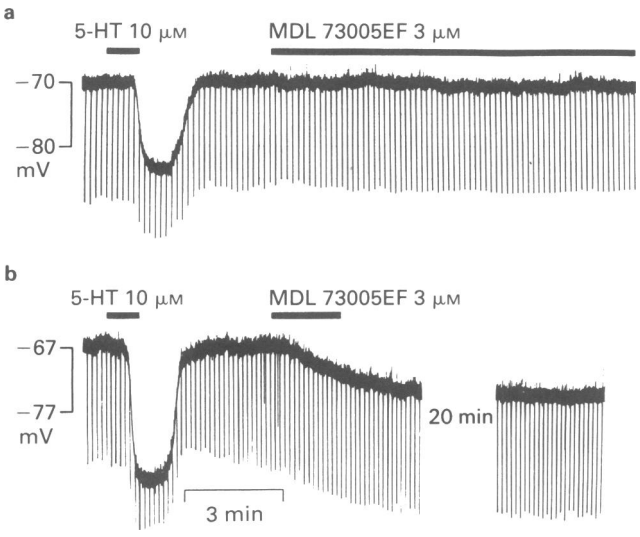

Figure 4 (a) Lack of effect of an 11 min application of 3 μM MDL 73005EF on a 5-hydroxytryptamine (5-HT)-sensitive neurone. (b) An example of the 6 neurones which were hyperpolarized by MDL 73005EF. Note that in each case the action of 5-HT (1 min) was rapidly reversible; however, in (b) the effect of MDL 73005EF outlasted by more than 20 min the 2 min application period.

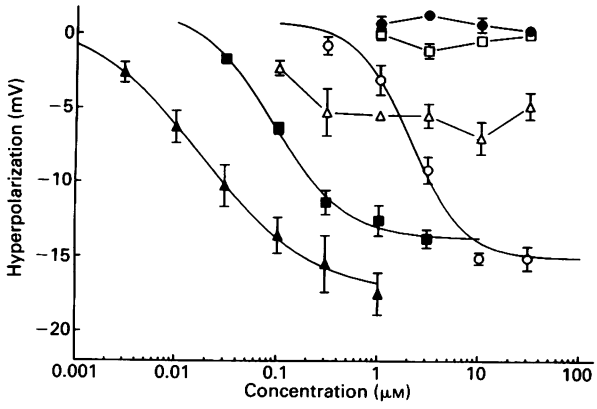

Figure 5 Concentration-response curves for 5-HT_{1A} receptor ligands. The applied concentrations (μM) are on the abscissa scale and the ordinate scale shows the hyperpolarization in mV (mean with s.e.mean shown by vertical bars). The symbols and number of determinations in different cells are as follows: N,N-dipropyl-5-carboxamidotryptamine (DP-5-CT, ▲; $n = 4-10$), 8-hydroxy-2-(di-n-propylamino) tetralin (8-OH-DPAT, ■; $n = 5-8$), 5-hydroxytryptamine (5-HT, ○; $n = 13-99$), buspirone (△; $n = 2-5$), MDL 73005EF (□, $n = 4-20$) and 1-*m*-trifluoromethylphenylpiperazine (TFMPP, ●; $n = 3$).

5-HT_{1A} ligand, spiperone (Andrade & Nicoll, 1987a) and the selective 5-HT_{1A} ligand, MDL 73005EF (Van den Hooff & Galvan, 1991). To characterize further the subtype of 5-HT receptor mediating the 5-HT-induced hyperpolarization of dorso-lateral septal neurones, a series of experiments were performed with MDL 73005EF and spiperone and two additional 5-HT_{1A} receptor antagonists, NAN-190 (Glennon *et al.*, 1988; Hodgkiss *et al.*, 1991) and methiothepin (Hoyer, 1991).

In most (22 out of 29) experiments, several concentrations of 5-HT were applied to a single cell before and during antagonist superfusion. In the remaining experiments ($n = 7$), slices were preincubated in antagonist solution and concentration-response curves to 5-HT were constructed and compared to control data. The small variations in response amplitude both in control and antagonist-containing solution ($\leqslant 20\%$) justified the use of such a procedure. Figure 6a–d illustrates the concentration-response curves obtained in the presence of the 4 putative antagonists. The approximate pA_2 values, calculated from the shift at the level of the EC_{50} value of 5-HT were: NAN-190, 6.79; MDL 73005EF, 6.59; spiperone, 6.54 and methiothepin, 6.17. Figure 6e illustrates, in an exemplary manner, responses to 5-HT measured in a neurone exposed for >20 min to 3 μM NAN-190. Compared to the typical concentration-response relationship illustrated in Figure 1a, it can be seen that NAN-190 reduced the sensitivity of the neurone to 5-HT in a surmountable fashion.

Receptor selectivity

The results of the experiments so far described strongly suggested that the 5-HT-induced hyperpolarization of dorso-lateral septal neurones was mediated via the activation of 5-HT_{1A} receptors. To support this hypothesis further, a series of experiments were performed to assess the selectivity of the 5-HT response and to exclude the involvement of some non 5-HT_{1A} receptors.

It has previously been reported that the $GABA_B$ receptor agonist, baclofen, hyperpolarizes central limbic neurones by activating the same pertussis toxin-sensitive, G-protein linked, potassium channels as does 5-HT (Andrade *et al.*, 1986; Innis & Aghajanian, 1987). In the present experiments MDL 73005EF at a concentration which blocked the hyperpolarization elicited by 6 μM 5-HT, did not reduce the hyperpolarization induced by the $GABA_B$ receptor agonist baclofen (Figure 7a,b and Table 1).

The 5-HT_2/5-HT_{1C}- and α_1-adrenoceptor antagonist, ketanserin (Leysen *et al.*, 1982) did not significantly affect the size of the 5-HT-induced hyperpolarization. The estimated EC_{50} values were 2.3 ± 0.3 μM in control solution and 2.4 ± 0.5 μM after >30 min in 3 μM ketanserin ($n = 3$; Figure 8a). Similar

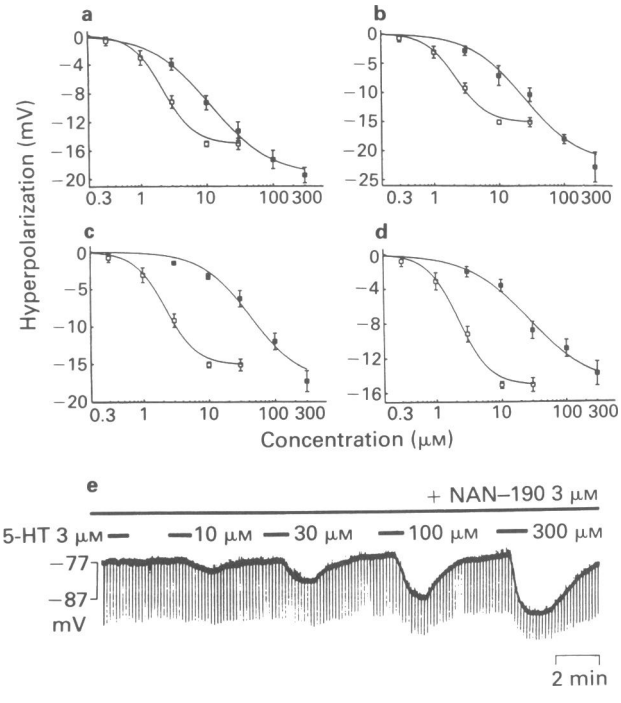

Figure 6 Concentration-response curves for 5-hydroxytryptamine (5-HT) in the absence (open symbols) and presence (solid symbols) of (a) 3 μM methiothepin ($n = 3-8$ cells), (b) 3 μM spiperone ($n = 4-7$), (c) 3 μM NAN-190 ($n = 4$) and (d) 3 μM MDL 73005EF ($n = 4-9$). Ordinates and abscissae are as in Figure 5. In (e) are shown 5-HT-evoked hyperpolarizations recorded from a neurone that had been exposed to 3 μM NAN-190 for 20 min.

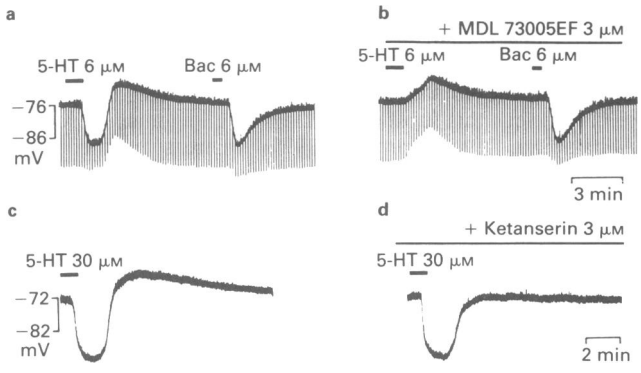

Figure 7 (a) A hyperpolarization/depolarization sequence evoked by 6 μM 5-hydroxytryptamine (5-HT) and a pure hyperpolarization evoked by 6 μM baclofen (Bac) in a single dorso-lateral septal neurone. (b) Responses recorded from the same cell after 20 min superfusion with 3 μM MDL 73005EF. Note the selective blockade of the 5-HT-induced hyperpolarization. The electrotonic potentials were elicited by constant current pulses (− 0.2 nA, 350 ms, 0.1 Hz). (c) A hyperpolarization/depolarization sequence evoked by 30 μM 5-HT in a different neurone. (d) After 55 min in 3 μM ketanserin the 5-HT-induced depolarization was selectively blocked.

Table 1 Actions of MDL 73005EF on hyperpolarizations evoked by 5-hydroxytryptamine (5-HT) or baclofen in rat dorso-lateral septal neurones *in vitro*

Compound	*Hyperpolarization (mV)*
5-HT	11.3 ± 1.9
5-HT + 3 μM MDL 73005EF	2.3 ± 1.2*
Baclofen	14.7 ± 1.8
Baclofen + 3 μM MDL 73005EF	15.0 ± 1.6

Mean changes in membrane potential (± s.e.mean; $n = 3$) evoked by 6 μM 5-HT or 6 μM baclofen, before and after addition of 3 μM MDL 73005EF. Note that MDL 73005EF blocked the action of 5-HT but not that of the $GABA_B$ receptor agonist, baclofen.
*$P < 0.05$ compared to 5-HT alone.

experiments demonstrated that the 5-HT$_3$-receptor antagonist tropisetron (ICS 205–930; Richardson *et al.*, 1985) in a concentration of 3 μM also had no effect on the EC_{50} value for the 5-HT-induced hyperpolarization (2.1 ± 0.9 and 2.1 ± 0.6 μM in the absence and presence of tropisetron, respectively, $n = 5$; Figure 8b).

5-HT-induced depolarizations

In 34 out of 102 cells (33%), the hyperpolarization induced by 6–10 μM 5-HT was followed by a small depolarization of on average 4.5 ± 2.2 mV (mean ± s.d.). This depolarization faded slowly over a period of about 5–15 min and was selectively antagonized by 3 μM ketanserin (Figure 7c,d; Table 2).

Discussion

The aim of this study was to characterize the receptors mediating the actions of 5-HT on single neurones in the rat dorso-lateral septal nucleus. This was achieved by measuring the effects of a number of novel synthetic 5-HT$_{1A}$ receptor agonists and antagonists on the neuronal membrane potential.

5-HT and the high affinity selective 5-HT$_{1A}$ receptor ligands, DP-5-CT (Markstein *et al.*, 1986; Hoyer, 1991) and

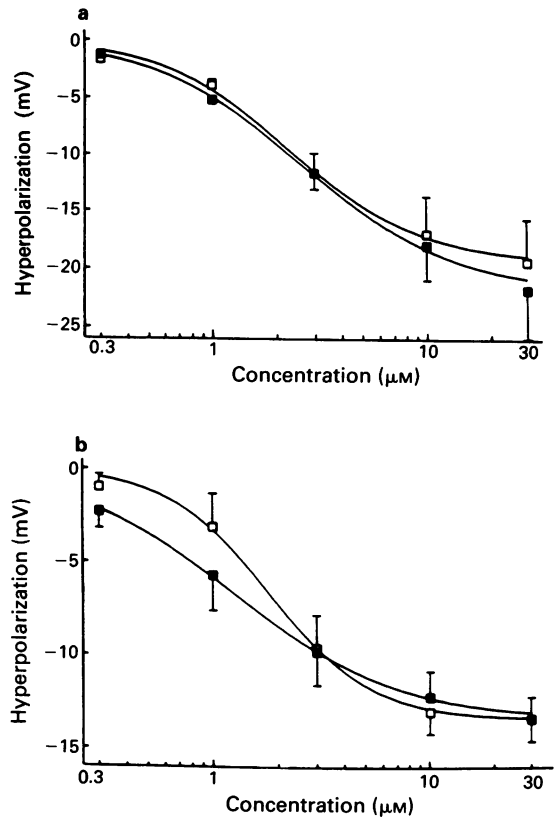

Figure 8 Concentration-response curves for 5-hydroxytryptamine (5-HT)-induced hyperpolarizations measured in control Krebs solution (□) and during superfusion with (a) 3 μM ketanserin (■) and (b) 3 μM tropisetron (■).

Table 2 Actions of ketanserin on membrane potential changes induced by 5-hydroxytryptamine (5-HT) in rat dorso-lateral septal neurones *in vitro*

Compound	*Hyperpolarization (mV)*	*Depolarization (mV)*
5-HT	16.8 ± 1.7	5.0 ± 0.5
5-HT + 3 μM ketanserin	17.6 ± 1.5	0.4 ± 0.2*

Mean changes in membrane potential (± s.e.mean; $n = 5$) during superfusion with 10 μM 5-HT, before and after more than 25 min in 3 μM ketanserin. Note that ketanserin selectively blocked the depolarizing action of 5-HT.
*$P < 0.01$ compared to 5-HT alone.

8-OH-DPAT (Gozlan *et al.*, 1983; Hoyer, 1991) hyperpolarized the membrane potential in a concentration-dependent manner. The concentration-response curves were parallel in nature and the maximum responses to the three agonists were similar. The rank order of potency of these three compounds (DP-5-CT > 8-OH-DPAT > 5-HT) is the same as that determined in radioligand binding experiments ($pK_D = 9.54$, 8.74 and 8.51; Hoyer, 1991) and in second messenger tests ($pEC_{50} = 7.40$, 7.03 and 6.89, respectively; Markstein *et al.*, 1986). Taken together, these findings support the conclusion that all three compounds were acting on the same population of receptors, namely 5-HT$_{1A}$ receptors. Further evidence for the involvement of the 5-HT$_{1A}$ receptor subtype stems from the antagonist experiments in which it was shown that 4 compounds with known high affinity for these receptors antagonized the action of 5-HT. The concentration-response curves measured in the presence of the antagonists were approximately parallel to the control

curves and the maximum response to 5-HT was not significantly reduced in antagonist-containing solution. The lack of effect of TFMPP as an agonist can be explained by the known low affinity for 5-HT_{1A} receptors of this compound ($pK_D = 6.5$; Hoyer, 1991). Furthermore, the lack of antagonist actions of ketanserin and tropisetron exludes an involvement of 5-HT_2-, 5-HT_{1C}- and 5-HT_3-receptors in the membrane hyperpolarization. These results are in agreement with those of Joëls *et al.* (1987) who reported that 5-HT and 8-OH-DPAT, but not TFMPP, hyperpolarized rat dorso-lateral septum neurones *in vitro*. In addition, these authors clearly demonstrated that ritanserin (a non-specific 5-HT_{1C}/5-HT_2 antagonist) did not block the 5-HT-induced hyperpolarization.

In approximately 30% of the neurones tested, 5-HT elicited a small depolarization, which followed the initial hyperpolarization. Similar depolarizations have been reported in hippocampal pyramidal cells (Andrade & Nicoll, 1987a; Colino & Halliwell, 1987), neurones in the nucleus accumbens (North & Uchimura, 1989), the medial prefrontal cortex (Araneda & Andrade, 1991), the cerebral cortex (Davies *et al.*, 1987) and also in the lateral septal nucleus (Joëls *et al.*, 1987). As in the nucleus accumbens (North & Uchimura, 1989) and the prefrontal cortex (Araneda & Andrade, 1991), this 5-HT-induced depolarization of septal neurones was blocked by the 5-HT_2/5-HT_{1C}-receptor antagonist, ketanserin. This is in contrast to reports indicating that the depolarization observed in rat hippocampal neurones is not blocked by ketanserin but rather by putative 5-HT_4-receptor antagonists (Andrade & Chaput, 1991). Similarly, ketanserin failed to block the depolarizing response to 5-HT in rat facial nucleus neurones *in vitro* (Kelly *et al.*, 1988).

The maximum hyperpolarization observed during application of the anxiolytic drug, buspirone, was significantly smaller than that seen during exposure to 5-HT, DP-5-CT, or 8-OH-DPAT and thus it is concluded that buspirone acts as a partial agonist on these cells. This is similar to the conclusion reached by Andrade & Nicoll (1987b), who demonstrated a partial agonist-like profile for buspirone in hippocampal neurones, albeit at far higher concentrations than those employed here. In a previous study of dorso-lateral septal neurones *in vitro*, it was shown that buspirone-induced membrane hyperpolarizations were easily reversible on removal of the drug from the Krebs solution (Joëls *et al.*, 1987). This is in contrast to the present findings in which a rapid recovery from the effects of buspirone was observed in only 1 out of 22 neurones. The underlying cause of this discrepancy is, as yet, unclear.

MDL 73005EF displayed a complex action on dorso-lateral septal neurones. A small proportion of cells (30%) were hyperpolarized by the compound, whereas in the majority of cases no agonist actions were observed. Nevertheless, the hyperpolarization observed in 6 cells was similar in amplitude to that evoked by the same concentration (3 μM) of 5-HT or buspirone. However, the slow rate of onset and poor reversibility suggest that in this subpopulation of neurones MDL 73005EF acts in a manner resembling the other synthetic 5-HT_{1A} agonists and buspirone. Finally, as previously demonstrated in hippocampal CA1 pyramidal cells (Van den Hooff & Galvan, 1991), MDL 73005EF was an effective antagonist of the hyperpolarizing action of 5-HT (see below).

It is interesting to note that in dorsal raphe neurones buspirone and MDL 73005EF are equipotent as inhibitors of cell action potential discharge (Sprouse, 1991), whereas in dorso-lateral septal neurones, MDL 73005EF has predominantly low intrinsic activity and buspirone behaves as a partial agonist. One possible explanation for these data is that there is no receptor reserve for the 5-HT_{1A} receptors in the dorso-lateral septum (Meller *et al.*, 1990). If this is the case, the differences between buspirone and MDL 73005EF could result from differences in efficacy (buspirone having a higher efficacy than MDL 73005EF).

Similar regional differences have been reported for 8-OH-DPAT. In the dorsal raphe nucleus and in the dorso-lateral septal nucleus this substance acts as a full agonist (Sprouse & Aghajanian, 1988; Sprouse, 1991) whereas in the hippocampus it is, at best, a weak partial agonist (Andrade & Nicoll, 1987a) and antagonist properties have been demonstrated at submicromolar concentrations (Colino & Halliwell, 1986). More detailed experiments with partial agonists or agonists of varying efficacy are clearly required to clarify the exact cellular mechanism of action of these compounds.

At present there are no data available to explain the slow onset and particularly the slow recovery (> 30 min), of the hyperpolarizations induced by DP-5-CT, 8-OH-DPAT and buspirone. Radioligand binding experiments with [^{3}H]-8-OH-DPAT (Hall *et al.*, 1985) showed that binding to hippocampal and striatal membranes reached equilibrium within 5–7 min, which might explain the slow onset of hyperpolarization. In contrast, dissociation of the ligand was rapid and 85% of specifically bound [^{3}H]-8-OH-DPAT dissociated within 10 min. Since the ionic conditions employed in the binding assays (50 mM Tris-HCl; Hall *et al.*, 1985) were considerably different from those used in electrophysiology experiments, it cannot yet be excluded that the dissociation rate constant for 8-OH-DPAT (and the other synthetic ligands) is indeed very slow under conventional *in vitro* conditions.

The hyperpolarizing action of 5-HT was antagonized in an apparently competitive manner by NAN-190, MDL 73005-EF, spiperone and methiothepin with estimated pA_2 values of 6.79, 6.59, 6.54 and 6.17, respectively. The so-determined affinities of these compounds for 5-HT_{1A} receptors are significantly lower than the pK_Ds estimated from [^{3}H]-8-OH-DPAT binding (8.9, 8.4, 7.2 and 7.1; Hoyer, 1991). Exactly how such discrepancies could arise is, at present, unknown. One possibility is that equilibrium binding of the antagonists is a very slow process as has been shown for spiperone (Andrade & Nicoll, 1987a) and MDL 73005EF (Van den Hooff & Galvan, 1991) during electrophysiological experiments on hippocampal neurones.

Despite the apparent low potency of the antagonists, it is reasonable to assume that they were acting at 5-HT_{1A} receptors. In particular, the results show that MDL 73005EF acted in a selective manner since the action of baclofen (a $GABA_B$ receptor agonist) was completely unaffected by MDL 73005EF at concentrations that significantly reduced 5-HT-induced hyperpolarizations. Furthermore, the 5-HT-induced depolarizations, which were blocked by the 5-HT_2/5-HT_{1C}-receptor antagonist ketanserin, were also unaffected by 3 μM MDL 73005EF. This selectivity in a functional assay is supported by the results of radioligand binding studies, which revealed that the affinity of MDL 73005EF for 5-HT_{1A} receptors is at least 100 fold higher than for 5-HT_{1B}, 5-HT_{1C}, 5-HT_{1D}, 5-HT_2-receptor, α- and β-adrenoceptor, dopamine D_1 and D_2 and benzodiazepine receptors (Hibert *et al.*, 1988; 1990). Spiperone, a compound with appreciable affinity for 5-HT_{1A}, 5-HT_2 and dopamine receptors was also effective as an antagonist as was the non-specific 5-HT_1 receptor ligand methiothepin (Hoyer, 1991). NAN-190, which is highly specific for 5-HT_{1A} subtype of 5-HT receptors but also has high affinity for α_1-adrenoceptor sites ($K_i = 0.8$ nM; Glennon *et al.*, 1988), was the most potent antagonist tested.

In conclusion, the experiments described here have demonstrated that 5-HT has a dual action on rat dorso-lateral septal neurones *in vitro*. The results of pharmacological experiments with a number of synthetic 5-HT_{1A} receptor ligands lead to the conclusion that the initial hyperpolarization is mediated via activation of 5-HT_{1A} receptors whereas the following depolarization is most probably mediated via activation of 5-HT_2 receptors.

References

ANDÉN, N.E., DAHLSTRÖM, A., FUXE, K., LARSSON, K., OLSON, L. & UNGERSTEDT, U. (1966). Ascending monoamine neurons to the telencephalon and diencephalon. *Acta Physiol. Scand.*, **67**, 313–326.

ANDRADE, R. & CHAPUT, Y. (1991). 5-Hydroxytryptamine$_4$-like receptors mediate the slow excitatory response to serotonin in the rat hippocampus. *J. Pharmacol. Exp. Ther.*, **257**, 930–937.

ANDRADE, R., MALENKA, R.C. & NICOLL, R.A. (1986). A G protein couples serotonin and $GABA_B$ receptors to the same channels in hippocampus. *Science*, **234**, 1261–1264.

ANDRADE, R. & NICOLL, R.A. (1987a). Pharmacologically distinct actions of serotonin on single pyramidal neurones of the rat hippocampus recorded *in vitro*. *J. Physiol.*, **394**, 99–124.

ANDRADE, R. & NICOLL, R.A. (1987b). Novel anxiolytics discriminate between post-synaptic serotonin receptors mediating different physiological responses on single neurones of the rat hippocampus. *Naunyn-Schmiedebergs Arch. Pharmacol.*, **336**, 5–10.

ARANEDA, R. & ANDRADE, R. (1991). 5-Hydroxytryptamine$_2$ and 5-hydroxytryptamine$_{1A}$ receptors mediate opposing responses on membrane excitability in rat association cortex. *Neuroscience*, **40**, 399–412.

AZMITIA, E.C. & SEGAL, M. (1978). Autoradiographic analysis of the differential ascending projections of the dorsal and median raphe nuclei in the rat. *J. Comp. Neurol.*, **179**, 641–668.

CHOPIN, P. & BRILEY, M. (1987). Animal models of anxiety: the effects of compounds that modify 5-HT neurotransmission. *Trends Pharmacol. Sci.*, **8**, 383–388.

COLINO, A. & HALLIWELL, J.V. (1986). 8-OH-DPAT is a strong antagonist of 5-HT action in rat hippocampus. *Eur. J. Pharmacol.*, **130**, 151–152.

COLINO, A. & HALLIWELL, J.V. (1987). Differential modulation of three separate K-conductances in hippocampal CA1 neurones by serotonin. *Nature*, **328**, 73–77.

CORNFIELD, L.J., NELSON, D.L. & MARTIN, A.R. (1989). MDL 73005EF: partial agonist at the 5-HT_{1A} receptor negatively linked to adenylate cyclase. *Eur. J. Pharmacol.*, **173**, 189–192.

DAVIES, M.F., DEISZ, R.A., PRINCE, D.A. & PEROUTKA, S.J. (1987). Two distinct effects of 5-hydroxytryptamine on single cortical neurons. *Brain Res.*, **423**, 347–352.

GARTSIDE, S.E. & COWEN, P.J. (1990). Antagonist effect of MDL 73005EF on postsynaptic 5-HT1A receptors in the rat. *Eur. J. Pharmacol*, **183**, 1961.

GARTSIDE, S.E., COWEN, P.J. & HJORTH, S. (1990). Effects of MDL 73005EF on central pre- and postsynaptic 5-HT1A receptor function in the rat in vivo. *Eur. J. Pharmacol.*, **191**, 391–400.

GLENNON, R.A., NAIMAN, N.A., PIERSON, M.E., TITELER, M., LYON, R.A. & WEISBERG, E. (1988). NAN-190: an arylpiperazine analog that antagonizes the stimulus effects of the 5-HT_{1A} agonist 8-hydroxy-2-(di-n-propylamino)tetralin (8-OH-DPAT). *Eur. J. Pharmacol.*, **154**, 339–341.

GOZLAN, H., EL MESTIKAWY, S., PICHAT, L., GLOWINSKI, J. & HAMON, M. (1983). Identification of presynaptic serotonin autoreceptors using a new ligand: 3H-PAT. *Nature*, **305**, 140–142.

HALL, M.D., EL MESTIKAWY, S., EMERIT, M.B., PICHAT, L., HAMON, M. & GOZLAN, H. (1985). [^{3}H]8-hydroxy-2-(di-n-propylamino) tetralin binding to pre- and postsynaptic 5- hydrotryptamine sites in various regions of the rat brain. *J. Neurochem.*, **44**, 1685–1696.

HIBERT, M.F., MIR, A.K. & FOZARD, J.R. (1990). Serotonin (5-HT) receptors. In *Comprehensive Medicinal Chemistry, The Rational Design, Mechanistic Study and Therapeutic Application of Chemical Compounds*. Vol. 3, *Membranes and Receptors*. ed. Emmett, J.C. pp. 567–600. Oxford: Pergamon Press.

HIBERT, M., MIR, A.K., MAGHIOROS, G., MOSER, P., MIDDLEMISS, D.N., TRICKLEBANK, M.D. & FOZARD, J.R. (1988). The pharmacological properties of MDL 73005EF: a potent and selective ligand at 5-HT_{1A} receptors. *Br. J. Pharmacol.*, **93**, 2P.

HODGKISS, J.P., DAWSON, I.M. & KELLY, J.S. (1991). NAN-190 antagonises the hyperpolarisation mediated by 5-HT_{1A} receptors on rat dorsal raphé neurones. *Br. J. Pharmacol.*, **192**, 135P.

HOYER, D. (1991). The 5-HT receptor family: ligands, distribution and receptor effector coupling. In *5-HT1A Agonists, 5-HT3 Antagonists and Benzodiazepines: their Comparative Behavioural Pharmacology*. ed. Rogers, R.J. & Cooper, S.J. pp. 31–57. Chichester: John Wiley & Sons.

INNIS, R.B. & AGHAJANIAN, G.K. (1987). Pertussis toxin blocks 5-HT_{1A} and $GABA_B$ receptor-mediated inhibition of serotonergic neurons. *Eur. J. Pharmacol.*, **143**, 195–204.

JOËLS, M., SHINNICK-GALLAGHER, P. & GALLAGHER, J.P. (1987). Effect of serotonin and serotonin analogues on passive membrane properties of lateral septum neurons in vitro. *Brain Res.*, **417**, 99–107.

KELLY, J.S., LARKMAN, P.M. & RAINNIE, D.G. (1988). Hyperpolarising and depolarising responses to 5-hydroxytryptamine in the rat brain stem *in vitro*. *Br. J. Pharmacol.*, **95**, 500P.

KÖHLER, C. (1984). The distribution of serotonin binding sites in the hippocampal region of the rat brain, an autoradiographic study. *Neuroscience*, **13**, 667–680.

KÖHLER, C., CHAN-PALAY, V. & STEINBUSCH, H. (1982). The distribution and origin of serotonin-containing fibers in the septal area: a combined immunohistochemical and fluorescent retrograde tracing study in the rat. *J. Comp. Neurol.*, **209**, 91–111.

LEYSEN, J.E., NIEMEGEERS, C.J.E., VAN NUETEN, J.M. & LADURON, P.M. (1982). [^{3}H]Ketanserin (R41 468), a selective ^{3}H ligand for serotonin 2 receptor binding sites. *Mol. Pharmacol.*, **21**, 301–314.

MARKSTEIN, R., HOYER, D. & ENGEL, G. (1986). 5-HT_{1A}-receptors mediate stimulation of adenylate cyclase in rat hippocampus. *Naunyn-Schmiedebergs Arch Pharmacol.*, **333**, 335–341.

MELLER, E., GOLDSTEIN, M. & BOHMAKER, K. (1990). Receptor reserve for 5-hydroxytryptamine$_{1A}$-mediated inhibition of serotonin synthesis: possible relationship to anxiolytic properties of 5-hydroytryptamine$_{1A}$ agonists. *Mol. Pharmacol.*, **37**, 231–237.

MOSER, P.C., TRICKLEBANK, M.D., MIDDLEMISS, D.N., MIR, A.K., HIBERT, M.F. & FOZARD, J.R. (1990). Characterisation of MDL 73005EF as a 5-HT_{1A} selective ligand and its effects in animal models of anxiety: comparison with buspirone, 8-OH-DPAT and diazepam. *Br. J. Pharmacol.*, **99**, 343–349.

NORTH, R.A. & UCHIMURA, U. (1989). 5-Hydroxytryptamine acts at 5-HT_2 receptors to decrease potassium conductance in rat nucleus accumbens neurones. *J. Physiol.*, **417**, 1–12.

PALFREYMAN, M.G., SPROUSE, J.S. & KEHNE, J.H. (1991). Mechanism of action of anxiolytics. In *Current Practices and Future Developments in the Pharmacotherapy of Mental Disorders*. ed. Meltzer, H.Y. & Nerozzi, D. pp. 167–174. Amsterdam: Elsevier.

PAZOS, A. & PALACIOS, J.M. (1985). Quantitative autoradiographic mapping of serotonin receptors in the rat brain. I. Serotonin-1 receptors. *Brain Res.*, **346**, 205–230.

RICHARDSON, B.P., ENGEL, G., DONATSCH, P. & STADLER, P.A. (1985). Identification of serotonin M-receptor subtypes and their specific blockade by a new class of drugs. *Nature*, **316**, 126–131.

SPROUSE, J.S. (1991). Inhibition of dorsal raphe cell firing by MDL 73005EF, a novel 5-HT_{1A} receptor ligand. *Eur. J. Pharmacol.*, **201**, 163–169.

SPROUSE, J.S. & AGHAJANIAN, G.K. (1987). Electrophysiological responses of serotonergic dorsal raphe neurons to 5-HT_{1A} and 5-HT_{1B} agonists. *Synapse*, **1**, 3–9.

SPROUSE, J.S. & AGHAJANIAN, G.K. (1988). Responses of hippocampal pyramidal cells to putative serotonin 5-HT_{1A} and 5-HT_{1B} agonists: a comparative study with dorsal raphe neurons. *Neuropharmacol.*, **27**, 707–715.

TAYLOR, D.P. (1988). Buspirone, a new approach to the treatment of anxiety. *FASEB J.*, **2**, 2445–2452.

TRABER, J. & GLASER, T. (1987). 5-HT_{1A} receptor-related anxiolytics. *Trends Pharmacol. Sci.*, **8**, 432–437.

UNGERSTEDT, U. (1971). Stereotaxic mapping of the monoamine pathways in the rat brain. *Acta Physiol. Scand.*, **82**, (Suppl. 367) 1–48.

VAN DEN HOOFF, P. & GALVAN, M. (1991). Electrophysiology of the 5-HT_{1A} ligand MDL 73005EF in the rat hippocampal slice. *Eur. J. Pharmacol.*, **196**, 291–298.

VAN DEN HOOFF, P., SPROUSE, J. & GALVAN, M. (1991). A comparison of the actions of the 5-HT_{1A} ligand MDL 73005EF on rat dorsal raphe and dorsal lateral septal neurones *in vitro*. *Fundam. Clin. Pharmacol.*, **5**, 432.

VANDERMAELEN, C.P. & AGHAJANIAN, G.K. (1983). Electrophysiological and pharmacological characterization of serotonergic dorsal raphe neurons recorded extracellularly and intracellularly in rat brain slices. *Brain Res.*, **289**, 109–119.

VANDERMAELEN, C.P., MATHESON, G.K., WILDERMAN, R.C. & PATTERSON, L.A. (1986). Inhibition of serotonergic dorsal raphé neurons by systemic and iontophoretic administration of buspirone, a non-benzodiazepine anxiolytic drug. *Eur. J. Pharmacol.*, **129**, 123–130.

(Received February 4, 1992
Revised March 26, 1992
Accepted April 3, 1992)

Br. J. Pharmacol. (1992), **106**, 900–905 © Macmillan Press Ltd, 1992

Blockade of Na^+ current by promethazine in guinea-pig ventricular myocytes

Hideo Tanaka, Yoshizumi Habuchi, †Masao Nishimura, *Nobuyuki Sato & *[1]Yoshio Watanabe

Department of Laboratory Medicine, Kyoto Prefectural University of Medicine, Kyoto, 602, Japan, †The 1st Department of Medicine, Teikyo University, Itabashi, Tokyo, 173, Japan and *Cardiovascular Institute, Fujita Health University, Toyoake, Aichi, 470-11, Japan

1 To elucidate the antiarrhythmic mechanism of promethazine, its effects on the fast Na^+ current (I_{Na}) were examined in single guinea-pig ventricular myocytes by whole-cell voltage clamp methods.

2 Promethazine blocked I_{Na} with a K_D of 42.6 μM and Hill's coefficient of 1.1 at a holding potential of −140 mV.

3 The I_{Na} blockade was enhanced at a less negative holding potential of −80 mV with a change of K_D to 4.4 μM. Although 10 μM promethazine did not change the inactivation time constants of I_{Na}, it shifted the steady-state inactivation curve (h_∞ curve) toward more negative potentials by 19.5 mV with the slope factor unaffected.

4 Double pulse experiments revealed that the development of blockade followed two-exponential functions having time constants of 7 and 220 ms at −20 mV.

5 Promethazine slowed the repriming of I_{Na}. This was associated with the development of slow phase having a time constant of 1160 ± 59 ms.

6 Promethazine produced a profound use-dependent block when the cell was repeatedly stimulated with interpulse intervals shorter than 1 s. However, short pulses of 2 ms duration hardly produced such a use-dependent block. Hence, open channel blockade is considered to play a minor role in the promethazine action on I_{Na}.

7 These results suggest that promethazine blocks cardiac I_{Na} in a manner similar to class I antiarrhythmic drugs and that this effect may account for its antiarrhythmic action.

Keywords: Promethazine; voltage-clamp; Na^+ current; single ventricular myocyte

Introduction

Promethazine, an antihistaminic phenothiazine being widely used for the treatment of allergy, is considered as a competitive antagonist of H_1 histamine receptors (Reinhardt & Borchard, 1982). In addition, this agent has been shown to modify the electrical activity in cardiac tissues. For example, it causes bradycardia and prolongation of the atrioventricular conduction time (Aronson & Hanno, 1979) in perfused rabbit hearts, and exerts a negative chronotropic action on guinea-pig atria (Davis & McNeill, 1973; Hughes & Coret, 1974). Furthermore, promethazine is reported to have anti-tachyarrhythmic effects under certain experimental conditions in atrial (Gupta *et al.*, 1974) and ventricular tissues (Johnson, 1954; Malinow *et al.*, 1955; Rigel & Katona, 1986; Rochette *et al.*, 1988). Some researchers have deduced that these actions are ascribed to a possible 'quinidine-like' local anaesthetic action (Naranjo & de Naranjo, 1958; Giotti & Zilletti, 1981), and not to an H_1 receptor-mediated action (Giotti & Zilletti, 1981; Rigel & Katona, 1986). Indeed, promethazine was reported to suppress the action potential upstroke in skeletal muscle fibres without changing the resting membrane potential, a finding suggesting an inhibitory action on the fast Na^+ current (I_{Na}) (Buttar & Frank, 1976). In cardiac tissues, however, little is known about its effects on I_{Na}. Hence, in a series of experiments on single guinea-pig ventricular myocytes, we measured I_{Na} directly by the use of whole-cell voltage clamp techniques to clarify promethazine-induced changes in the Na^+ channel properties.

[1] Author for correspondence.

Methods

The methods for cell isolation and voltage clamp experiments were identical to those previously described by Habuchi *et al.* (1991). Briefly, the excised guinea-pig hearts were perfused on a Langendorff apparatus for 5 min with a nominally Ca^{2+}-free Tyrode solution having the following composition (in mM): NaCl 142, $MgCl_2$ 5, KCl 5.4, NaH_2PO_4 1, HEPES 5, glucose 20 and 0.2% bovine serum albumin (Sigma, fraction V). The pH was adjusted to 7.4 with NaOH. The perfusate was then changed to an enzyme solution containing 0.3 mg ml^{-1} collagenase, 5 mM $MgCl_2$ and 1% bovine albumin in the Ca-free Tyrode solution. These perfusates were continuously bubbled with 100% O_2 and the temperature was kept at 36 ± 1°C. Enzymatic treatment for 30–40 min was followed by perfusion with a recovery solution with the following composition (in mM): glutamate 110, oxalate 10, KCl 25, KH_2PO_4 10, $MgSO_4$ 2, taurine 20, creatine 5, glucose 20, EGTA 0.5 and HEPES 5 (pH = 7.2 with KOH). The ventricles were subsequently cut into small pieces. The myocytes isolated by gentle agitation were filtered through nylon mesh (200 μm in diameter) and collected by centrifugation. After incubation for 30–40 min in the recovery solution at 32°C, Ca^{2+}-tolerant, rod shape myocytes were obtained, and stocked in a Tyrode solution containing 1.8 mM $CaCl_2$ and 1% albumin.

Voltage-clamp experiments were carried out by the single-pipette whole-cell clamp technique (Hamill *et al.*, 1981). Suction pipettes were made with a two-stage vertical puller (Narishige, Tokyo, Japan), and electrodes having a tip resistance of 0.8–1.5 MΩ were used for the experiment. The internal solution had the following composition (in mM):

NaCl 15, CsF 110, CsCl 20, $MgCl_2$ 2, EGTA-Cs_2 5 and HEPES 5 (pH = 7.2). I_{Na} was measured during superfusion with low-Na^+ test solution with the following composition (in mM): NaCl 18, CsCl 30, $CoCl_2$ 3, $MgCl_2$ 1, tetramethylammonium chloride 20, 4-aminopyridine 5, sucrose 80, glucose 5 and HEPES 5 (pH = 7.4 with CsOH). The liquid junction potential between internal and external solutions (3 mV) was corrected. The series resistance was compensated to a point just before oscillation. A small bath size of 0.15 ml was used and changing of the perfusate was accomplished within 1 min. All the experiments were carried out at room temperature (20–22°C). Promethazine hydrochloride (Sigma, St. Louis, MO, U.S.A.) was stored at a 10^{-2} M concentration.

A voltage-clamp amplifier (ACT ME, 1100T, Japan) designed by M. Yoshii (Narahashi *et al.*, 1987) was used. Current signals were filtered at 10 kHz and stored in a digital cassette recorder (TEAC RD101-T, Japan) or floppy disks attached to a digital oscilloscope (Nicolet 310C). These data were analyzed by a computer (NEC PC 9800, Japan). The linear leakage and capacitive currents were subtracted digitally by P-P/n method (n = 2–5: Bezanilla & Armstrong, 1977), and I_{Na} amplitude was measured from 0 current level to the peak inward current. When I_{Na} exceeded 4 nA under these experimental conditions, voltage errors through the clamp circuit was considered to be within acceptable limits (Habuchi *et al.*, 1991). Fit of the experimental data to exponential equations was performed with a non-linear simplex regression algorithm (Nelder & Mead, 1965; Shavers *et al.*, 1979; Turbo Pascal programme, Borland International Inc.). Statistical analyses were made by Student's paired *t* test and the data are expressed as mean ± s.d.

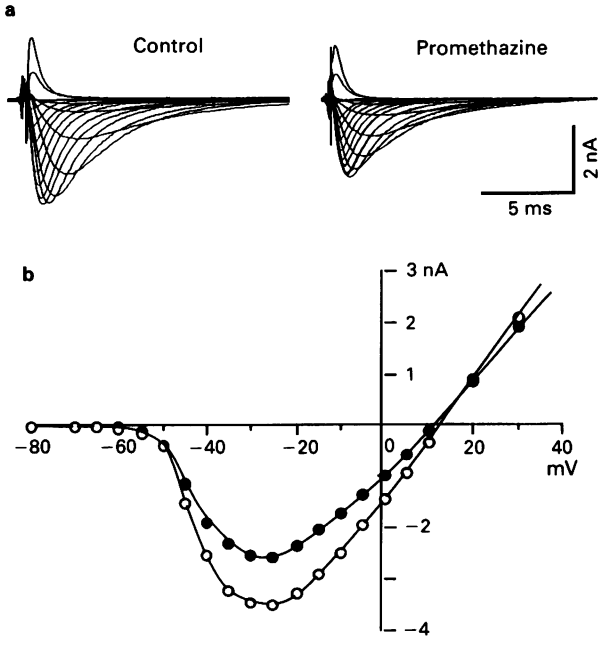

Figure 1 Effect of promethazine on the current-voltage relationship for I_{Na}: 20 ms depolarizing pulses were applied from a holding potential (HP) of −140 mV to various potentials ranging from −80 mV to +30 mV. Test pulses were delivered at a rate of 0.1 Hz. Panel (a) shows families of I_{Na} records before (left) and during (right) superfusion with promethazine 30 μM. In (b), the peak amplitudes of I_{Na} are plotted against the test potentials. Note that promethazine depressed the current amplitudes without affecting the overall configuration of the current-voltage relationship: (○) control; (●) in the presence of promethazine.

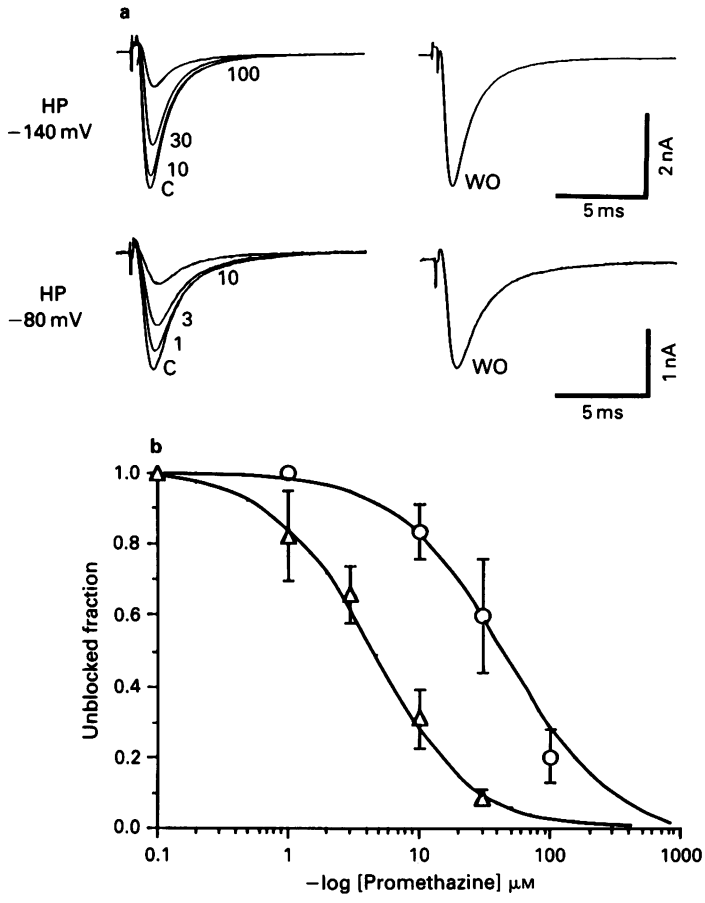

Figure 2 Concentration-dependent effects of promethazine on I_{Na}: (a) shows I_{Na} records obtained by applying 20 ms depolarizing pulses to −20 mV from a HP of −140 mV (upper traces) and −80 mV (lower traces). The numbers along the current traces indicate the drug concentrations in μM, and C denotes the control record. WO denotes the current after washout of the drug. In (b) are shown the concentration-response curves obtained at −140 mV (○) and −80 mV (△). Relative values of I_{Na} normalized by taking the control values as unity are plotted against the drug concentrations. The symbols with vertical bars represent the mean ± s.d. based on 6 (HP = −140 mV) and 4 (HP = −80 mV) experiments.

Results

Steady-state block of Na^+ channel by promethazine

Figure 1 shows typical promethazine effects on the current-voltage relationship for I_{Na} obtained with a holding potential (HP) of −140 mV. The cell was depolarized for 20 ms to various potentials ranging from −80 mV to +30 mV. Under control conditions, I_{Na} developed at potentials positive to −70 mV, attained the maximum value at −25 mV, and reversed its polarity at +13 mV. When promethazine was applied at a concentration of 30 μM, the I_{Na} was reduced by approximately 30% without significant changes in the shape of current-voltage curve.

The concentration-dependent effects of promethazine on I_{Na} are shown in Figure 2. The left upper panel in Figure 2a shows a family of I_{Na} curves obtained with a HP of −140 mV where Na^+ channels are free from inactivation. Promethazine (10–100 μM) decreased the I_{Na} amplitude in a dose-dependent manner. When the HP was decreased to −80 mV, where a fraction of the channels would be in the inactivated state, the block was enhanced (the left lower panel in Figure 2a). Washing out of the drug restored the I_{Na} almost to the control level at either HP (right panels in Figure 2a). In Figure 2b, I_{Na} values relative to the control are

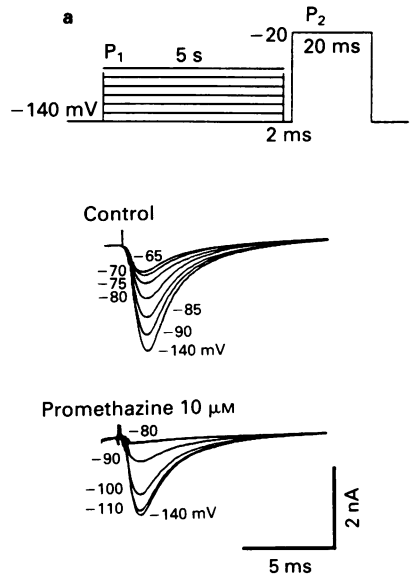

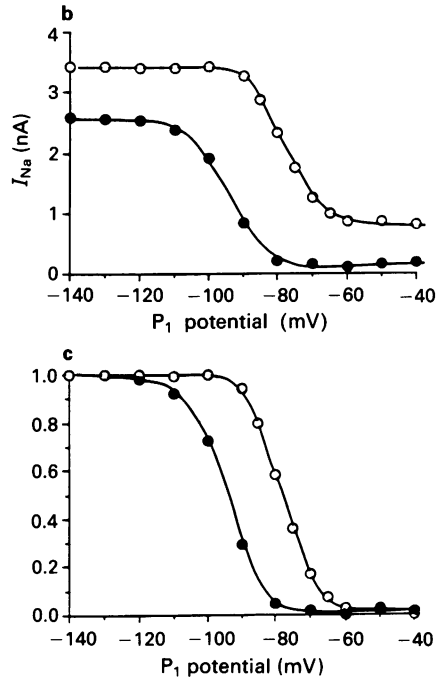

Figure 3 Steady-state inactivation curves for I_{Na} before (○) and during superfusion with 10 μM promethazine (●). As illustrated in the top panel of (a), the application of 5 s conditioning pulses (P_1) to various potentials was followed by a 2 ms interpulse interval and a 20 ms test pulse (P_2) to −20 mV. Families of I_{Na} (I_2) elicited on P_2 are shown in the middle (control) and the lower (promethazine) panels of (a), with the numbers representing the conditioning pulse voltage (P_1). In panel (b), the I_2 amplitudes are plotted against the P_1 potentials. Promethazine at 10 μM depressed I_2 at all the potentials tested. In (c), the steady-state inactivation (h_∞) curves for I_{Na} were obtained by normalizing the I_2 amplitudes to the maximal value in each condition.

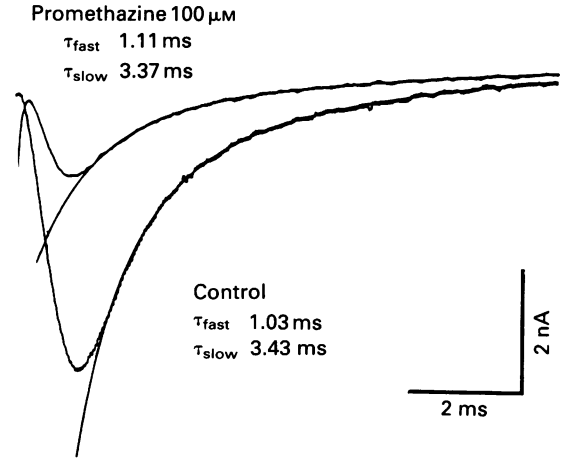

Figure 4 Effect of promethazine on the time course of I_{Na} inactivation in a typical experiment. I_{Na} was elicited by depolarization from the HP of −140 mV to −20 mV.

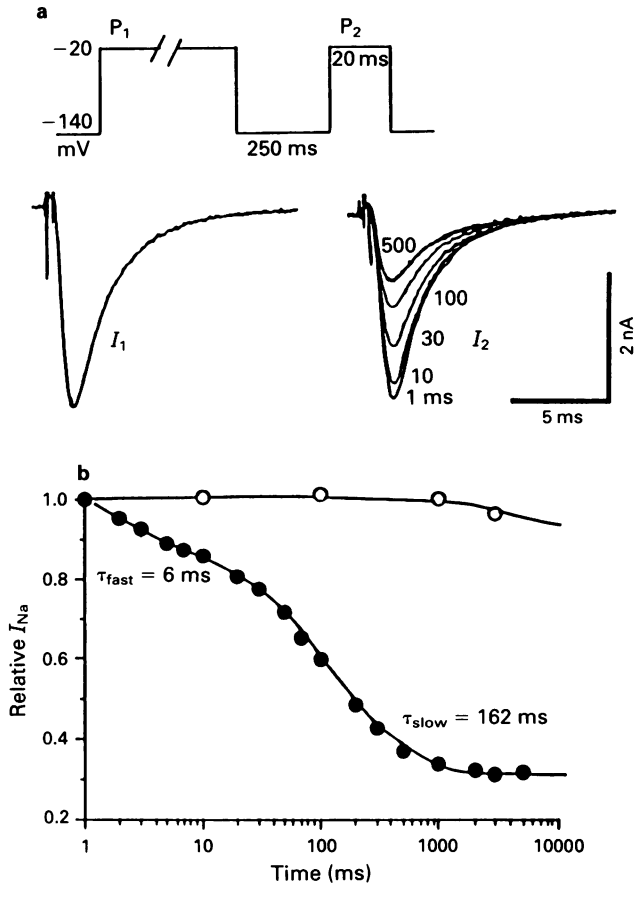

Figure 5 A typical example of the time course of promethazine binding to Na^+ channels. In (a), P_1 pulses of various durations were applied to −20 mV from the HP of −140 mV. After a 250 ms interval at −140 mV during which drug-unbound channels were allowed to reprime fully, a 20 ms test pulse (P_2) was applied again to −20 mV. The lower panels show the current (I_1) elicited on P_1 (left) and that (I_2) elicited on P_2 (right) during superfusion with 10 μM promethazine. In (b), the relative values of I_{Na} (I_2/I_1) are plotted against the duration of P_1 (in ms): (○) and (●) denote the values before and during the application of promethazine, respectively.

plotted against the drug concentration. These relationships obtained from 4 (HP = − 80 mV) and 6 (HP = − 140 mV) experiments were well fitted by the Hill's equation described below:

$$\text{Relative } I_{Na} = 1/[1 + (D/K_D)^n],$$

where D denotes the concentration of promethazine (μM), K_D, the concentration producing the half maximal response, and n, the Hill's coefficient. K_D for the resting state of Na^+ channels was 42.6 μM and n, 1.09. At HP of −80 mV, the curve was shifted toward lower concentrations (K_D = 4.4 μM, n = 1.14).

Effect of promethazine on the kinetics of Na^+ channel inactivation

The effect of promethazine on the steady-state inactivation (h_∞) curve for I_{Na} was studied by use of the double-pulse protocol. Results from a typical experiment are shown in Figure 3. The h_∞ curves were obtained by normalizing the test current amplitudes (I_2) by taking the maximum value under each condition as unity. Curves were fitted by the equation:

$$h_\infty = 1/[1 + \exp((E-V_h)/s)],$$

where E denotes the P_1 potential, V_h, the potential showing $h_\infty = 0.5$, and s the slope factor. Promethazine 10 μM shifted the curve to more negative potentials by 18.1 mV without affecting the slope factor. On average, $V_h = -80.5 \pm 3.6$ mV and $s = -6.2 \pm 0.37$ mV under control conditions, and $V_h = -100.0 \pm 5.7$ mV and $s = -5.8 \pm 0.48$ mV in the presence of 10 μM of promethazine, respectively ($n = 5$, $P < 0.01$ for V_h and $P > 0.1$ for s).

Promethazine did not significantly modify inactivation kinetics (Figure 4). The I_{Na} elicited on depolarization to −20 mV was fitted by double exponential functions by means of a non-linear simplex regression algorithm (Nelder & Mead, 1965; Shavers *et al.*, 1979) according to the following equation:

$$I_{Na} = A \times \exp(-t/\tau_{fast}) + B \times \exp(-t/\tau_{slow}) + C,$$

The I_{Na} decay under the control condition ($n = 5$) showed two time constants of $\tau_{fast} = 1.00 \pm 0.12$ ms and $\tau_{slow} = 3.33 \pm 0.33$ ms. Comparative values in the presence of 100 μM promethazine were 0.98 ± 0.06 ms and 3.13 ± 0.27 ms, respectively.

Time course of the development of I_{Na} block by promethazine

The time course of the development of I_{Na} block by promethazine was studied by double-pulse methods (Figure 5a). P_1 pulses of various durations were applied to −20 mV. After a 250 ms interval at the HP of −140 mV, which allowed the drug-free channels to reprime fully, a 20 ms test pulse (P_2) was applied to −20 mV. The amplitude of I_{Na} produced by the P_2 pulse (I_2) was normalized to that elicited on P_1 (I_1). In Figure 5b, the relative I_{Na} at P_2 is plotted against the P_1 duration. Under control conditions, I_2 was hardly decreased even when the P_1 duration was prolonged to 1 s. Conversely, in the presence of 10 μM promethazine, lengthening of the P_1 duration progressively decreased I_{Na} in two phases. The line connecting the closed circles represents the least squares fit to the following equation:

$$\text{Relative } I_{Na} = 1 - A_{fast} \times \exp(-t/\tau_{fast}) - A_{slow} \times \exp(-t/\tau_{slow}),$$

where A_{fast} and A_{slow} represent the fraction of the fast and slow components, respectively. From 5 experiments, A_{fast}, A_{slow}, τ_{fast}, and τ_{slow} were calculated to be 0.09 ± 0.05, 0.61 ± 0.83, 7.0 ± 5.0 ms, and 220 ± 70 ms, respectively.

Recovery of I_{Na} from inactivation

The speed of the dissociation of promethazine from inactivated Na^+ channels was then assessed. The pulse protocol used is shown in Figure 6a. The Na^+ channels were adequately inactivated by a 5 s pulse to −20 mV (P_1). Following various recovery intervals ranging from 2 to 8000 ms at −140 mV, a test pulse (P_2) was again applied to −20 mV. The unrecovered fraction of I_{Na} at P_2 ($1-I_2/I_1$) was semilogarithmically plotted against the recovery time (Figure 6b). Under control conditions, I_{Na} rapidly recovered from inactivation within 200 ms. In the presence of 3 μM promethazine, on the other hand, I_{Na} recovery was markedly retarded. The semilogarithmic plots obtained from 5 experiments revealed that the retardation could be ascribed to the development of a much slower phase having a mean time constant of 1160 ± 159 ms.

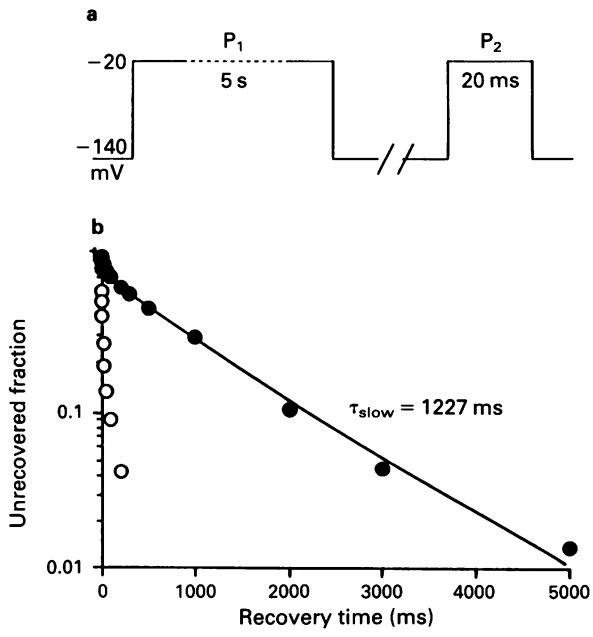

Figure 6 Effect of promethazine on the recovery of I_{Na} from inactivation in a typical experiment. The pulse protocol is shown in (a). The P_1 pulse to −20 mV for 5 s was followed by a 20 ms pulses (P_2) to −20 mV, with an intervening recovery period of various durations. The current (I_2) elicited by P_2 was compared to the current I_1. (b) The unrecovered fraction of I_{Na} ($1-I_2/I_1$) was semilogarithmically plotted as a function of the recovery intervals (in ms): (○) under control conditions; (●) in the presence of 3 μM promethazine. Note that a slow recovery phase (time constant = 1230 ms) developed on superfusion with 3 μM promethazine.

Use-dependent block of I_{Na} by promethazine

The apparent use-dependent effects of promethazine were tested by applying 15 consecutive depolarizing pulses. As shown in Figure 7a, 200 ms pulses to −20 mV were applied in the presence of a HP of either −140 mV or −90 mV. Two interpulse intervals of 500 and 1000 ms were used. Values of I_{Na}, normalized to that on the first pulse in each train, are plotted against the pulse number in Figure 7c and d. It is evident that 3 μM promethazine blocks I_{Na} in a frequency-dependent manner. Such a blocking action was exaggerated when the HP was set at −90 mV. In a subsequent experiment illustrated in Figure 8, the pulse duration was shortened to 2 ms as it is considered that, during such a brief depolarization, I_{Na} inactivation would not develop sufficiently to allow promethazine binding to the inactivated channels. Use-dependent I_{Na} block was hardly observed under these conditions.

Discussion

The present experimental study demonstrated that promethazine would cause a reversible blockade of I_{Na} in guinea-pig ventricular myocytes with a 1 to 1 stoichiometry and a K_D of 42.6 μM in the resting state. Since the therapeutic plasma concentration of this drug ranges from 3 to 23 ng ml^{-1} (less than 0.3 μM: DiGregorio & Ruch, 1980), the drug would be expected barely to bind to the resting Na^+ channels in the clinical situation. However, marked voltage-dependent block of I_{Na} by promethazine, indicated by a shift of the dose-response curve toward lower promethazine concentrations at the HP of −80 mV and a shift of the I_{Na} availability (h_∞)

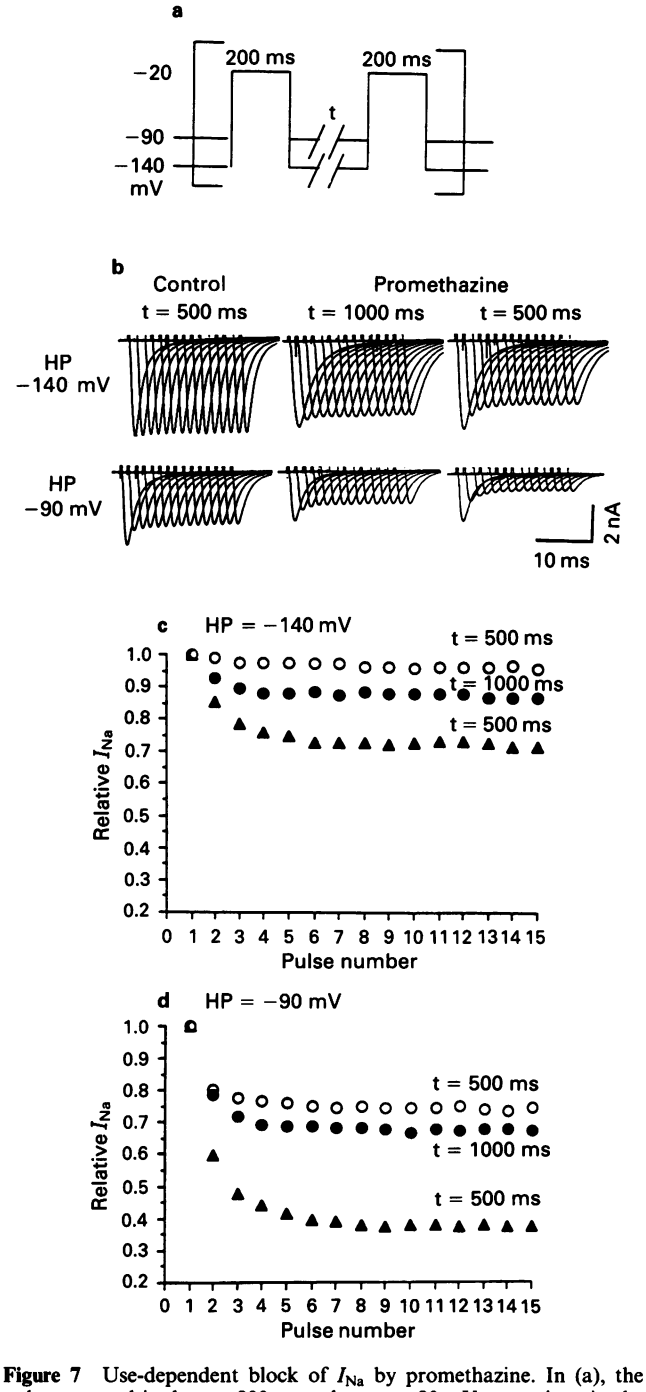

Figure 7 Use-dependent block of I_{Na} by promethazine. In (a), the pulse protocol is shown: 200 ms pulses to −20 mV were given in the presence of the HP of either −140 mV or −90 mV. The interpulse intervals (t) were set at 500 ms or 1000 ms. Panel (b) illustrates the actual current traces obtained at the HP of −140 mV (upper section) and −90 mV (lower section). In (c) and (d), sequential I_{Na} values were normalized to the I_{Na} elicited on the first of the 15 consecutive pulses: (○), under control condition; (●), and (▲), in the presence of 3 μM promethazine. It is evident that promethazine exerts use-dependent block, which is enhanced at a less negative HP.

curve to more negative potentials indicate that promethazine molecules have a higher affinity for inactivated Na^+ channels than for resting channels. We then estimated the K_D of the drug for the inactivated Na^+ channels according to the following equation (Bean *et al.*, 1983):

$$\Delta V_h = s \times \ln((1 + D/K_r)/(1 + D/K_i)),$$

in which ΔV_h is the midpoint shift of the I_{Na} availability curve, s, the slope factor, D, the concentration of promethazine, and K_r and K_i, the dissociation constants for resting and inactivated Na^+ channels, respectively. Using the values of ΔV_h, D, s, and K_r obtained in the present study, the K_i was calculated as 0.36 μM, a value close to the plasma concentration of the drug encountered clinically. In view of such a high affinity of promethazine for inactivated Na^+ channels, the drug may well depress excitability of and conduction in Purkinje fibres and ventricular muscle, especially under pathological conditions associated with rapid heart actions and partially depolarized membranes.

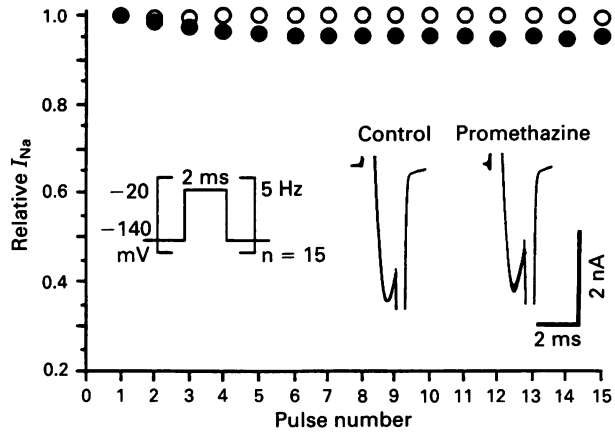

Figure 8 Use-dependent block of I_{Na} caused by shorter depolarizing pulses. As shown in inset at the left, 15 consecutive pulses of 2 ms duration were applied at the rate of 5 Hz. The current traces are shown in the insets at the right. Relative values of I_{Na} are plotted against the pulse number: (○), during control condition; (●), in the presence of 3 μM promethazine. Promethazine produced little use-dependent block with this protocol.

According to the modulated receptor hypothesis, an antiarrhythmic drug binds either to the activated or inactivated state during membrane depolarization (Hille, 1977; Hondeghem & Katzung, 1977). The binding characteristics of promethazine were described by a double exponential function with time constants of 7 ± 5 ms and 220 ± 70 ms at −20 mV. Under these experimental conditions, most of the Na^+ channels were inactivated during the initial 10 ms-depolarization to −20 mV. If a considerable fraction of Na^+ channels is blocked in the open state during the brief activation, the binding process should be faster than development of Na^+ channel inactivation as was demonstrated by Clarkson *et al.* (1988) with lignocaine. Although the rapid phase of promethazine binding may be contaminated with the drug binding to the open channels, this possibility appears remote because (1) promethazine did not affect the I_{Na} decay time course, and (2) repetitive activation of Na^+ channels for 2 ms in the presence of promethazine caused no significant use-dependent block. Therefore, both binding phases would predominantly reflect the binding of the drug to the inactivated channels. Compared to the slow kinetics of lignocaine binding to the inactivated Na^+ channels with a time constant of 350 ms (Clarkson *et al.*, 1988), the time course of promethazine binding to the Na^+ channels is relatively fast.

Another striking finding, which may contribute to the electrophysiological effects of promethazine, is the slow recovery of the Na^+ channel from inactivation. Class I antiarrhythmic drugs are generally characterized by recovery kinetics, which probably represent the process of drug dissociation from inactivated Na^+ channels (Hille, 1977; Hondeghem & Katzung, 1977). In this regard, the time constant of 1230 ms for promethazine to dissociate from Na^+ channels classifies it as an intermediate type Na^+ channel blocker. This relatively slow repriming of I_{Na} leads to an incomplete recovery of Na^+ channels from inactivation during short

diastolic intervals and would contribute to use-dependent block by this agent. Since use-dependent block of I_{Na} was voltage-dependent, being enhanced at a less negative HP of -90 mV than at -140 mV, the drug molecules may dissociate from Na^+ channel receptors after the drug-bound inactivated state is converted to the drug-bound resting state. Hence, promethazine would exert a potent use-dependent blocking action in depolarized and possibly injured myocardium.

Based on the results of the present study, it is concluded that promethazine blocks Na^+ channels in a channel state-dependent manner, much like other class I antiarrhythmic drugs. These features of the Na^+ channel blockade would probably explain previously reported experimental findings such as electrophysiological alterations in the myocardium induced by promethazine (Hughes & Coret, 1972; Davis & McNeill, 1973; Aronson & Hanno, 1979) and the antiarrhythmic properties of this agent (Winbury & Alworth, 1959; Rigel & Katona, 1986; Rochette *et al.*, 1988). Since there is no clinical evidence available to support these experimental findings, clinical study is necessary to elucidate fully the electrophysiological actions of promethazine in man.

References

ARONSON, C.E. & HANNO, E.R.S. (1979). Effects of promethazine on the isolated perfused rat heart. *Gen. Pharmacol.*, **10**, 389–395.

BEAN, B.P., COHEN, C.J. & TSIEN, R.W. (1983). Lidocaine block of cardiac sodium channels. *J. Gen. Physiol.*, **81**, 613–642.

BEZANILLA, F. & ARMSTRONG, C.M. (1977). Inactivation of sodium channel. I. Sodium current experiments. *J. Gen. Physiol.*, **70**, 549–566.

BUTTAR, H.S. & FRANK, G.B. (1976). Effects of antipsychotic drugs on action potential production in skeletal muscle. I. Chlorpromazine and promethazine. *Can. J. Physiol. Pharmacol.*, **55**, 452–461.

CLARKSON, C.W., FOLLMER, C.H., TENEICK, R.E., HONDEGHEM, L.M. & YEH, J.Z. (1988). Evidence for two components of sodium channel block by lidocaine in isolated cardiac myocytes. *Circ. Res.*, **63**, 869–878.

DAVIS, R.S. & MCNEILL, J.H. (1973). The cardiac effects of cocaine and certain antihistamines and antidepressants. *Arch. Int. Pharmacodyn.*, **201**, 262–279.

DiGREGORIO, G.J. & RUCH, E. (1980). Human whole blood and parotid saliva concentrations of oral and intramuscular promethazine. *J. Pharmac. Sci.*, **69**, 1457–1459.

GIOTTI, A. & ZILLETTI, L. (1981). Antiarrhythmic actions of antihistamines. In *Pharmacology of Antiarrhythmic Agents*. ed. Szekeres, L. pp. 195–239. Oxford: Pergamon Press.

GUPTA, S.C., SHARMA, V.N. & SHARMA, H.L. (1974). Antiarrhythmic and antiparkinsonian activity of two new promethazine salts. *Indian J. Exp. Biol.*, **12**, 504–508.

HABUCHI, Y., FURUKAWA, T., TANAKA, H., TSUJIMURA, Y. & YOSHIMURA, M. (1991). Block of Na^+ channels by imipramine in guinea-pig cardiac ventricular cells. *J. Pharmacol. Exp. Ther.*, **256**, 1072–1081.

HAMILL, O.P., MARTY, A., NEHR, E., SAKMANN, B. & SIGWORTH, F.J. (1981). Improved patch clamp techniques for high-resolution current recording from cells and cell-free membrane patches. *Pflügers Arch.*, **391**, 85–100.

HILLE, B. (1977). Local anesthetics: hydrophylic and hydrophobic pathways for the drug-receptor reaction. *J. Gen. Physiol.*, **69**, 497–515.

HONDEGHEM, L.M. & KATZUNG, B.G. (1977). Time- and voltage-dependent interactions of antiarrhythmic drugs with cardiac sodium channels. *Biochim. Biophys. Acta*, **472**, 373–398.

HUGHES, M.J. & CORET, J.A. (1972). On specificity of histamine receptors in the heart. *Am. J. Physiol.*, **223**, 1257–1262.

JOHNSON, E.A. (1954). The effect of antifibrillatory drugs on the cat's heart *in vivo*. *Br. J. Pharmacol. Chemother.*, **9**, 341–345.

MALINOW, M.R., BATLLE, F.F. & MALAMUD, B. (1955). The pharmacology of experimental ventricular arrhythmias in the rat. I. Antihistamic drugs. *Arch. Int. Pharmacodyn. Ther.*, **102**, 55–64.

NARAHASHI, T., TSUNOO, A. & YOSHII, M. (1987). Characterization of two types of Ca^{++} channels in neuroblastoma cells. *J. Physiol.*, **383**, 231–249.

NARANJO, P. & DE NARANJO, E.B. (1958). Local anesthetic activity of some antihistamines and its relationship with the antihistaminic and anticholinergic activities. *Arch. Int. Pharmacodyn.*, **113**, 313–335.

NELDER, J.A. & MEAD, R. (1965). A simplex method for function minimization. *Comput. J.*, **7**, 308–313.

REINHARDT, D. & BORCHARD, U. (1982). H_1-receptor antagonists: comparative pharmacology and clinical use. *Klin. Wochenschr.*, **60**, 983–990.

RIGEL, D.F. & KATONA, P.G. (1986). Effects of antihistamines and local anesthetics on excess tachycardia in conscious dogs. *J. Pharmacol. Exp. Ther.*, **238**, 367–371.

ROCHETTE, L., YAO-KOUAME, J., BRALET, J. & OPIE, L.H. (1988). Effects of promethazine on ischemic and reperfusion arrhythmias in rat heart. *Fundam. Clin. Pharmacol.*, **2**, 385–397.

SHAVERS, C.L., PARSONS, M.L. & DEMING, S.N. (1979). Simplex optimization of chemical systems. *J. Chem. Educ.*, **56**, 307–309.

WINBURY, M.M. & ALWORTH, B.L. (1959). Suppression of experimental atrial arrhythmias by several antihistamines. *Arch. Int. Pharmacodyn.*, **122**, 318–322.

(Received December 24, 1991
Revised March 10, 1992
Accepted April 6, 1992)

Br. J. Pharmacol. (1992), **106**, 906–909 © Macmillan Press Ltd, 1992

Contribution of cyclic GMP formation to KRN2391-induced relaxation in coronary artery of the pig

[1]Yasuhiro Jinno, Hideo Kasai, Hideo Ohta, Koji Nishikori, Hideaki Fukushima & Nobuyuki Ogawa

Pharmaceutical Research Laboratory of Kirin Brewery Co., Ltd., Miyahara-cho 3, Takasaki, Gunma 370-12, Japan

1 In the present study, we investigated the relationship between relaxation and guanosine 3':5'-cyclic monophosphate (cyclic GMP) formation induced by KRN2391, compared with those induced by nicorandil and nitroglycerin, in the coronary artery of the pig.

2 KRN2391 (10^{-8}–3×10^{-5} M), nicorandil (10^{-8}–3×10^{-4} M) and nitroglycerin (10^{-9}–10^{-5} M) antagonized the contraction caused by 25 mM KCl in a concentration-dependent manner.

3 The concentration-relaxation curves for KRN2391, nicorandil and nitroglycerin shifted rightward in the presence of methylene blue (10^{-5} M).

4 KRN2391 (10^{-6} M), nicorandil (10^{-4} M) and nitroglycerin (10^{-6} M) induced an increase in cyclic GMP.

5 The magnitude of the shift of the concentration-relaxation curve caused by methylene blue and the increase in cyclic GMP with KRN2391 were lower than those with nicorandil and nitroglycerin.

6 The adenosine 3':5'-cyclic monophosphate (cyclic AMP) level was not increased by KRN2391 even at a concentration that produced full relaxation.

7 The present results suggest that KRN2391-induced relaxation in the coronary artery of the pig is partly due to the increase in cyclic GMP formation through the stimulation of guanylate cyclase.

Keywords: KRN2391; nicorandil; nitroglycerin; cyclic GMP; porcine coronary artery

Introduction

KRN2391, N-cyano-N'-(2-nitroxyethyl)-3-pyridine-carboximidamide monomethanesulphonate (Figure 1), is a novel vasodilator found in the course of a screening programme. KRN2391 is suggested to have a dual vasodilator mechanism, as a nitrate and a K channel opener, since KRN2391-induced relaxation is antagonized by both a guanylate cyclase inhibitor and a K channel blocker in rat isolated aorta (Kashiwabara *et al.*, 1990). Recently, we obtained results showing that KRN2391-induced relaxation in canine large coronary artery was antagonized by methylene blue but not by glibenclamide.

The K channel opening action of KRN2391 is supported by an increase in efflux of ^{86}Rb, a marker for K^+, in rat aorta (Kashiwabara *et al.*, 1990). However, whether KRN2391 actually increases intracellular guanosine 3':5'-cyclic monophosphate (cyclic GMP) has yet to be elucidated. Therefore, we investigated the relationship between relaxation and cyclic GMP formation caused by KRN2391 in the large coronary artery of the pig. In addition, the effects of KRN2391 were compared with those of nitroglycerin and nicorandil which are reported to increase cyclic GMP formation (Kukovetz & Holzmann, 1987; Meisheri *et al.*, 1991).

Methods

Mechanical experiments

Porcine hearts were obtained from a local abattoir. The left circumflex or the left anterior descending arteries (outer diameter: 2.5–3.0 mm) were dissected and immediately suspended in Krebs-Henseleit solution of the following composition (mM): NaCl 118, KCl 4.7, $MgSO_4$ 1.2, $CaCl_2$ 2.5, KH_2PO_4 1.2, $NaHCO_3$ 25.0 and glucose 10.0. The arteries were cleared of adhering connective tissues and two types of preparation, i.e. 2 mm rings and 4–5 cm long helical strips, were prepared. The endothelium of each preparation was removed by gently abrading the surface with a wooden stick and a moist cotton ball. The endothelium removal was verified by absence of a relaxant response to substance P in preliminary experiments. The 2 mm ring preparation was used for mechanical responses and the helical strip preparation was used for the determination of cyclic nucleotides.

The rings were mounted in an organ bath containing 10 ml Krebs-Henseleit solution gassed with 95% O_2 and 5% CO_2 at 37°C. The preparation was stretched by the initial resting tension of 2 g. After an initial equilibration period of 60 min, contraction was induced by 40 mM K^+, and then the tissues were washed with normal Krebs-Henseleit solution. Subsequently, contraction was induced by 25 mM K^+. The potassium-depolarizing solution was prepared by replacing NaCl with KCl in the control solution (total potassium concentration = 40 or 25 mM). Vasodilators were added cumulatively when the preparations reached stable tension. Isometric tension was measured with a transducer (TB-611T, Nihon Kohden). Methylene blue (10^{-5} M) was added to the organ bath 20 min before the addition of 25 mM K^+ when the effect of methylene blue on KRN2391, nitroglycerin, and nicorandil-induced relaxation was evaluated. Relaxation caused by the test drugs was expressed as a percentage of the maximum relaxation obtained by the addition of 10^{-4} M papaverine at the end of each experiment.

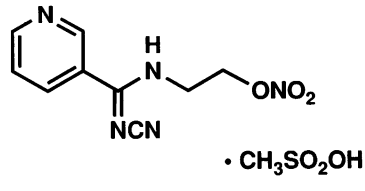

Figure 1 Chemical structure of KRN2391.

[1] Author for correspondence.

EC_{50} values were calculated from each concentration-relaxation curve for vasodilators in the absence and presence of methylene blue.

Determination of cyclic nucleotides

Adenosine 3':5'-cyclic monophosphate (cyclic AMP) and cyclic GMP were measured in the helical strip of the coronary artery incubated under the same conditions as in the relaxation studies. Tissues were removed from the bath at various times after administration of each vasodilator and immediately frozen in liquid nitrogen. Frozen tissue was quickly weighed and stored at −80°C until the measurement of cyclic AMP and cyclic GMP. Frozen tissue, which was homogenized in 6% trichloracetic acid, was centrifuged at 1500 *g* for 10 min. Supernatant fractions were washed 3 times with water-saturated diethyl ether. The upper ether layer was discarded after each wash. Aliquots of the water layer were processed for the content of cyclic AMP and cyclic GMP by radioimmunoassay with commercially available kits (Honma *et al.*, 1977).

Drugs

KRN2391 and nicorandil were synthesized in our laboratory. Methylene blue was purchased from Wako Pure Chemicals and nitroglycerin from Nihon Kayaku Co., Ltd., Japan. The nucleotide assay kit was purchased from Yamasa Shoyu Co., Ltd., Japan.

Statistics

Difference was considered significant when $P<0.05$ by Student's t test and analysis of variance for multiple comparisons. When multiple comparisons were made with a single control, Dunnett's test was used to determine significance. All data are presented as mean ± s.e.mean.

Results

KRN2391 (10^{-8}–3×10^{-5} M), nicorandil (10^{-8}–3×10^{-4} M) and nitroglycerin (10^{-9}–10^{-5} M) produced concentration-dependent relaxation of porcine coronary arteries contracted with 25 mM KCl (Figure 2). The −log EC_{50} values for KRN2391, nicorandil and nitroglycerin were 6.69 M, 5.39 M and 6.94 M, respectively. Thus, KRN2391 was 20 fold more potent than nicorandil and 1.8-fold less potent than nitroglycerin.

The concentration-relaxation curves for KRN2391, nicorandil and nitroglycerin shifted rightward in the presence of 10^{-5} M methylene blue (Figure 2). This concentration of methylene blue had no effect on the relaxation induced by cromakalim, a K channel opener (unpublished observation from our laboratory). The −log EC_{50} values for KRN2391, nicorandil and nitroglycerin in the presence of methylene blue were significantly lower than those in the control (Table 1). The concentration-ratios of KRN2391, nicorandil and nitroglycerin were calculated based on their EC_{50} values and were 2.51, 3.02 and 3.31 at a methylene blue level of 10^{-5} M, respectively.

Figure 3 shows the time course relationships between KRN2391 (10^{-6} M)-induced relaxation, and cyclic GMP and cyclic AMP levels. Relaxation reached a maximum 20 min after administration of KRN2391. Cyclic GMP accumulation reached a maximum level which was maintained thereafter. KRN2391 did not induce an elevation in cyclic AMP.

The time course of relaxation and cyclic GMP accumulation induced by 10^{-4} M nicorandil are shown in Figure 4. Cyclic GMP reached a maximum 5 min after administration, and maintained a fixed level thereafter. The maximum increase in cyclic GMP induced by nicorandil was higher than that induced by KRN2391. The relaxation induced by nicor-

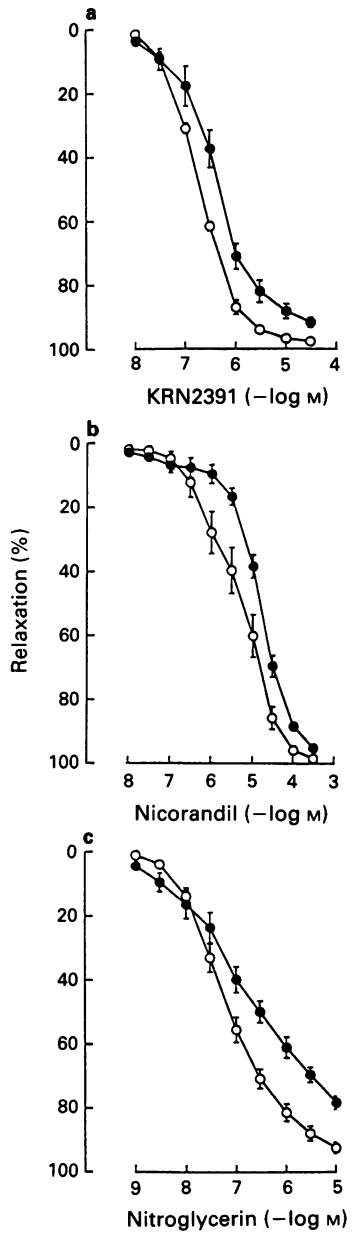

Figure 2 Concentration-relaxation curves for KRN2391 (a), nicorandil (b) and nitroglycerin (c) in porcine coronary arteries contracted by 25 mM KCl in the absence (○) and presence (●) of methylene blue (10^{-5} M). Each point represents mean (s.e.mean shown by vertical bars) of 5–6 experiments.

Table 1 −log EC_{50} values for KRN2391, nicorandil and nitroglycerin in coronary artery of the pig in the absence and presence of methylene blue

Drugs	*Methylene blue* (10^{-5} M)	−*log* EC_{50} (M)	n
KRN2391	−	6.69 ± 0.02	5
	+	6.29 ± 0.14*	6
Nicorandil	−	5.39 ± 0.16	6
	+	4.91 ± 0.06*	6
Nitroglycerin	−	6.94 ± 0.14	5
	+	6.42 ± 0.14*	5

−log EC_{50}; the negative logarithm of the concentration causing half-maximal relaxation.
−log EC_{50} values are means ± s.e.mean.
*$P<0.05$; compared with value in the absence of methylene blue.

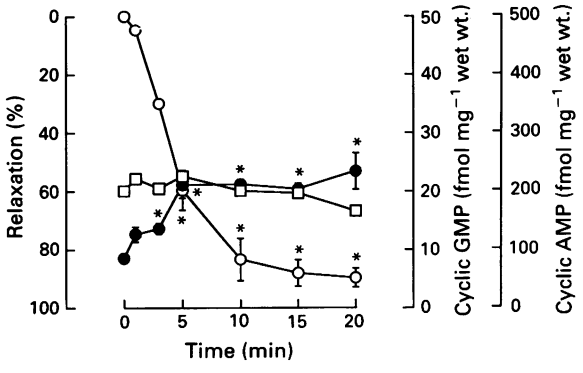

Figure 3 The time course of changes of cyclic nucleotides (cyclic GMP ● and cyclic AMP □) levels and relaxation (○) caused by 10^{-6} M KRN2391 in porcine coronary arteries. Each point represents mean (s.e.mean shown by vertical bars) of 5–7 experiments. *$P<0.05$ significantly different from the value at time 0.

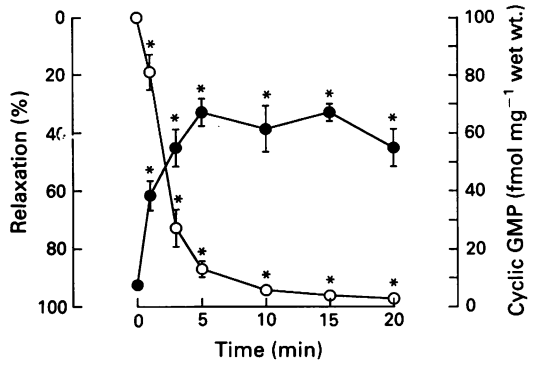

Figure 4 The time course of changes of cyclic GMP concentrations (●) and relaxation (○) caused by 10^{-4} M nicorandil in porcine coronary arteries. Each point represents mean (s.e.mean shown by vertical bars) of 4–6 experiments. *$P<0.05$ significantly different from the value at time 0.

andil also occurred more rapidly than that in response to KRN2391.

Nitroglycerin (10^{-6} M) induced a maximum increase in cyclic GMP 3 min after administration (Figure 5). After 3 min, cyclic GMP gradually returned towards the control values. The relaxations induced by nitroglycerin and by nicorandil occurred more rapidly than those induced by KRN2391 (Figure 5).

The relationship between relaxation and cyclic GMP concentrations in the range of 10^{-8}–10^{-5} M KRN2391 was determined 15 min after administration (Table 2). KRN2391 produced relaxation at more than 10^{-8} M and a significant increase in cyclic GMP at more than 10^{-6} M. The cyclic AMP level did not change at any concentration of KRN2391.

Discussion

The present results showed that an increase in cyclic GMP accompanied relaxation induced by KRN2391 in the coronary artery of the pig. This increase in cyclic GMP appears to be due to the stimulation of guanylate cyclase, because KRN2391-induced relaxation was inhibited by methylene blue, an inhibitor of soluble guanylate cyclase (Gruetter *et al.*, 1981). However, the correlation between relaxation and cyclic GMP with KRN2391 was different from those with nicorandil and nitroglycerin. Despite producing submaximal relaxation at 10^{-6} M KRN2391, the increase in cyclic GMP

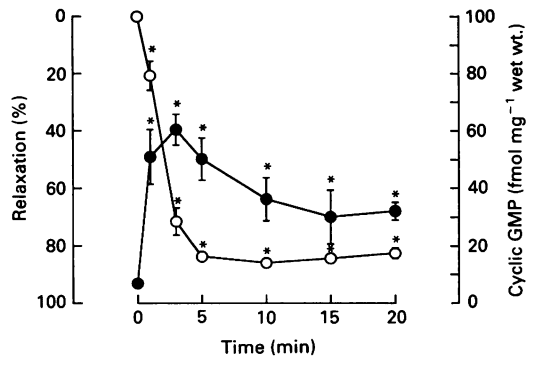

Figure 5 The time course of changes of cyclic GMP level (●) and relaxation (○) caused by 10^{-6} M nitroglycerin in porcine coronary arteries. Each point represents mean (s.e.mean shown by vertical bars) of 5–8 experiments. *$P<0.05$ significantly different from the value at time 0.

Table 2 Relaxation and nucleotide levels after administration of KRN2391 in porcine isolated coronary artery

KRN2391 (M)	*Coronary relaxation* (%)	*Cyclic GMP* (fmol mg^{-1} wet wt.)	*Cyclic AMP*
Control	0	5.38 ± 0.58	187.4 ± 7.8
10^{-8}	1.7 ± 0.8	6.85 ± 1.4	176.4 ± 9.0
10^{-7}	31.2 ± 1.7	8.55 ± 0.88	228.8 ± 14.9
10^{-6}	87.0 ± 2.2	14.88 ± 1.86*	189.4 ± 13.4
10^{-5}	96.7 ± 0.3	30.28 ± 2.69*	188.9 ± 22.4

Results are expressed as mean ± s.e.mean of 5–6 experiments.
*$P<0.01$; compared with control value.

was lower than the increases induced by 10^{-4} M nicorandil and 10^{-6} M nitroglycerin which also produced submaximal relaxation. This is also supported by the observation that the concentration-ratio of KRN2391 to methylene blue was lower than those of nicorandil and nitroglycerin and that 10^{-7} M KRN2391 produced 31.2% relaxation but no change in cyclic GMP (Table 2). These results suggest that KRN2391 possesses an additional relaxant mechanism which does not depend on cyclic GMP formation. However, cyclic AMP formation does not contribute to this additional effect of KRN2391, since it did not affect cyclic AMP levels at any of the concentrations examined.

Kashiwabara *et al.* (1991) reported that KRN2391 showed a dual mechanism of action, as a nitrate and a K channel opener, because KRN2391-induced relaxation was inhibited by methylene blue and some K channel blockers in rat isolated aorta. However, in canine isolated large coronary arteries, the relaxation induced by KRN2391 was inhibited by methylene blue but not by glibenclamide, an ATP-sensitive K channel blocker (Fukata *et al.*, 1991), suggesting that KRN2391 behaves predominantly as a nitrate in canine large coronary arteries. Recently, we observed that KRN2391-induced relaxation was inhibited by both methylene blue and glibenclamide in pig isolated coronary arteries (unpublished data). Therefore, KRN2391 seems to show different characteristics on coronary arteries of the pig and dog. The additional mechanism of KRN2391 implicated in the present experiment may be a K channel opening action.

It is also known that nicorandil possesses a dual mechanism of action as a nitrate and a K channel opener. However, the increase in cyclic GMP induced by nicorandil was higher than that induced by KRN2391 in the present study. This effect of nicorandil was in agreement with the results obtained previously in various vascular smooth muscles (Endoh & Taira, 1983; Holzmann, 1983). Meisheri *et al.* (1991) also

found that nicorandil-induced relaxation was associated with the action of opening K channels at lower concentrations and increase in cyclic GMP at higher concentrations in rabbit isolated superior mesenteric artery. Furthermore, in the coronary vascular bed of a dog, nicorandil behaved predominantly as a nitrate in large coronary artery and as a K channel opener in resistance coronary arterioles (Satoh *et al.*, 1991). Thus, whether nicorandil acts as a nitrate and/or as a K channel opener seems to depend on the type of vascular smooth muscle and the segment of the vascular bed. Though it was not observed whether nicorandil shows a K channel opening action in porcine coronary artery, the effect of nicorandil in increasing cyclic GMP in porcine coronary artery appears to be more potent than that of KRN2391.

It is well known that nitroglycerin-induced relaxation of vascular smooth muscle is based on an increase in cyclic GMP through the stimulation of guanylate cyclase (Itoh *et al.*, 1985; Kukovetz & Holtmann, 1987; Meisheri *et al.*, 1991). The present results also support this, because relaxation induced by nitroglycerin increased cyclic GMP and was inhibited by methylene blue. However, the time course of relaxation and increase in cyclic GMP observed with nitroglycerin was different from that with KRN2391 and nicorandil. Relaxation induced by nitroglycerin was maintained over the observation period, while the level of cyclic GMP decreased. The same results were also obtained by Gruetter *et al.* (1981) and Kukovetz *et al.* (1979). Concerning this phenomenon, Rapoport & Murad (1983) put forward the following explanations: (1) extrusion of cyclic GMP into the surrounding media may have occurred; (2) phosphodiesterase activity may have increased; (3) a step(s) following the formation of cyclic GMP, which is involved in the relaxation mechanism, may have a slower turnover rate than cyclic GMP.

In conclusion, the present results provided evidence that KRN2391 increased cyclic GMP through activation of guanylate cyclase in porcine coronary artery. Another mechanism of action in addition to cyclic GMP formation may partly contribute to KRN2391-induced relaxation because the magnitude of the shift of the concentration-relaxation curve caused by methylene blue and the increase in cyclic GMP with KRN2391 were lower than those with nicorandil and nitroglycerin. Recently, we observed that KRN2391-induced relaxation was inhibited by methylene blue and glibenclamide (unpublished data). Therefore, the additional mechanism of KRN2391 may be a K channel opening action.

References

ENDOH, M. & TAIRA, N. (1983). Relationship between relaxation and cyclic GMP formation caused by nicorandil in canine mesenteric artery. *Naunyn-Schmiedebergs Arch. Pharmacol.*, **322**, 319–321.

FUKATA, Y., HARADA, K., KASHIWABARA, T., OGAWA, N., FUKUSHIMA, H. & NISHIKORI, K. (1991). Different vasodilating mechanism of KRN2391 on isolated canine large coronary and cranial mesenteric arteries. *Jpn. J. Pharmacol.*, **55** (Suppl. 1), 253P.

GRUETTER, C.A., KADOWITZ, P.J. & IGNARRO, L.J. (1981). Methylene blue inhibits coronary arterial relaxation and guanylate cyclase activation by nitroglycerin, sodium nitrite, and amyl nitrite. *Can. J. Physiol. Pharmacol.*, **59**, 150–156.

HOLZMANN, S. (1983). Cyclic GMP as possible mediator of coronary arterial relaxation by nicorandil (SG-75). *J. Cardiovasc. Pharmacol.*, **5**, 364–370.

HONMA, M., SATOH, T., TAKEZAWA, J. & UI, M. (1977). An ultrasensitive method for the simultaneous determination of cyclic AMP and cyclic GMP in small-volume samples from blood and tissue. *Biochem. Med.*, **18**, 257–273.

ITOH, T., KANMURA, Y., KURIYAMA, H. & SASAGURI, T. (1985). Nitroglycerin- and isoprenaline-induced vasodilatation: assessment from the actions of cyclic nucleotides. *Br. J. Pharmacol.*, **84**, 393–406.

KASHIWABARA, T., NAKAJIMA, S., IZAWA, T., FUKUSHIMA, H. & NISHIKORI, K. (1991). Characteristics of KRN2391, a novel vasodilator, compared with those of cromakalim, pinacidil and nifedipine in rat aorta. *Eur. J. Pharmacol.*, **196**, 1–7.

KASHIWABARA, T., ODAI, H., KANETA, S., TANAKA, Y., FUKUSHIMA, H. & NISHIKORI, K. (1990). Vasodilating and hypotensive properties of KRN2391. *Eur. J. Pharmacol.*, **183**, 1266.

KUKOVETZ, W.R. & HOLZMANN, S. (1987). Cyclic GMP in nicorandil-induced vasodilation and tolerance development. *J. Cardiovasc. Pharmacol.*, **10** (Suppl. 8), S25–S30.

KUKOVETZ, W.R., HOLZMANN, S., WURM, A. & PÖCH, G. (1979). Evidence for cyclic GMP-mediated relaxant effects of nitro-compounds in coronary smooth muscle. *Naunyn-Schmiedebergs Arch. Pharmacol.*, **310**, 129–138.

MEISHERI, K.D., CIPKUS-DUBRAY, L.A., HOSNER, J.M. & KHAN, S.A. (1991). Nicorandil-induced vasorelaxation: functional evidence for K^+ channel-dependent and cyclic GMP-dependent components in a single vascular preparation. *J. Cardiovasc. Pharmacol.*, **17**, 903–912.

RAPOPORT, R.M. & MURAD, F. (1983). Agonist-induced endothelium-dependent relaxation in rat thoracic aorta may be mediated through cGMP. *Circ. Res.*, **52**, 352–357.

SATOH, K., YAMADA, H. & TAIRA, N. (1991). Differential antagonism by glibenclamide of the relaxant effect of cromakalim, pinacidil and nicorandil on canine large coronary arteries. *Naunyn-Schmiedebergs Arch. Pharmacol.*, **343**, 76–82.

(Received February 20, 1992
Revised April 3, 1992
Accepted April 7, 1992)

Br. J. Pharmacol. (1992), **106**, 910–916 © Macmillan Press Ltd, 1992

MDL 27,531 selectively reverses strychnine-induced seizures in mice

[1]John H. Kehne, John M. Kane, Francis P. Miller, Herbert J. Ketteler, Donald L. Braun, Yaw Senyah, Stephen F. Chaney, Abdulmuniem Abdallah, Mark W. Dudley, Ann Marie Ogden & Michael G. Palfreyman

Marion Merrell Dow Research Institute, 2110 East Galbraith Road, Cincinnati, Ohio 45215, U.S.A.

1 Strychnine-sensitive glycine receptors are primarily localized in the brainstem and spinal cord where they are the major mediators of postsynaptic inhibition. A compound which acts functionally like a glycine receptor agonist would be potentially useful as a pharmacological tool and as a therapeutic agent for treating disorders of glycinergic transmission.

2 MDL 27,531 (4-methyl-3-methylsulphonyl-5-phenyl-4H-1,2,4-triazole) blocked strychnine-induced tonic extensor seizures in mice following either intraperitoneal (ED_{50} = 12.8 mg kg^{-1}; 30 min) or oral (ED_{50} = 7.3 mg kg^{-1}; 30 min) administration. Time course studies revealed a maximal effect at 30–60 min, though significant activity was still seen after 24 h.

3 MDL 27,531 was selective in antagonizing strychnine seizures and little or no activity was seen against seizures produced by other chemical convulsants (bicuculline; quinolinic acid; mercaptopropionic acid); by electrical stimuli (maximal electroshock); or by sensory stimuli (audiogenic seizure susceptible mice). MDL 27,531 blocked pentylenetetrazol-induced seizures with an ED_{50} = 55 mg kg^{-1}. This profile differed from those of the anticonvulsants diazepam, valproic acid, and diphenylhydantoin.

4 The antagonism of strychnine seizures by MDL 27,531 occurred at doses that did not produce signs of sedation (suppression of spontaneous motor activity), motor ataxia (disruption of rotarod performance), muscle relaxation (inhibition of morphine-induced Straub tail), or CNS depression (potentiation of hexobarbitone sleep time). MDL 27,531 had less side effect potential (as derived from ratios obtained from the above measures) relative to those of the known muscle relaxants diazepam and baclofen.

5 Although MDL 27,531 behaved functionally like a selective agonist at the strychnine-sensitive glycine receptor, the compound did not alter the *in vitro* binding of [^{3}H]-strychnine to mice brainstem/spinal cord membranes at concentrations of up to 100 μM. In further *in vitro* binding assays, MDL 27,531 at concentrations of up to 100 μM, did not displace the binding of [^{3}H]-muscimol, [^{3}H]-flunitrazepam, or [^{35}S]-*t*-butylbicyclophosphorthionate to rat cortical membranes. These ligands bind to the γ-aminobutyric acid (GABA), benzodiazepine, and picrotoxin-convulsant binding sites, respectively.

6 MDL 27,531 (10–100 mg kg^{-1}, i.p.) enhanced binding of the benzodiazepine antagonist [^{3}H]-Ro 15-1788 to mouse cerebral cortex *in vivo* without directly affecting GABA levels.

7 Ro 15-1788 (16, 32 mg kg^{-1}) significantly blocked the MDL 27,531 antagonism of strychnine-induced seizures, though this antagonism was not competitive. The same doses of Ro 15-1788 produced parallel rightward shifts in the dose-response curves for diazepam inhibition of pentylenetetrazol-induced seizures, consistent with a competitive antagonism.

8 Thus, MDL 27,531 acts functionally like an agonist at the strychnine-sensitive glycine receptor in its capacity to reverse selectively strychnine-induced seizures. Though the precise mechanism of action of MDL 27,531 is unknown, MDL 27,531 may act at an allosteric site on the strychnine-sensitive receptor which produces agonist-like activity.

Keywords: Strychnine; convulsions; MDL 27,531; glycine; benzodiazepines; baclofen; epilepsy; spasticity; Ro 15-1788

Introduction

Glycine serves as the major mediator of postsynaptic inhibition in the caudal areas of the central nervous system (CNS) (see Eccles, 1965; Aprison, 1990). Inotophoretically-applied glycine produces well-characterized hyperpolarizing effects on spinal cord and brainstem motor neurones and interneurones, and these effects are selectively reversed by the alkaloid strychnine. Immunohistochemical studies in rat tissues (Triller *et al.*, 1990) and autoradiographic studies in human and non-human tissues (see Cortes & Palacios, 1990, for review) have demonstrated that the strychnine-sensitive glycine receptor is localized primarily in caudal regions of the CNS, particularly in the brainstem and spinal cord.

Recent work has suggested that glycine can also act at a modulatory site of the N-methyl-D-aspartate (NMDA) glutamate ion channel complex, where it facilitates glutamaterigic excitatory amino acid transmission (see Palfreyman & Baron, 1991, for review). This receptor is antagonized by agents such as 5,7-dichlorokynurenic acid but is insensitive to strychnine.

Glycine and its inhibitory effects on central neurones have been studied for three decades, and yet there are surprisingly few pharmacological agents (other than strychnine) which selectively alter glycine activity. Most striking is the lack of agents which are glycine agonists or which act functionally like glycine agonists. Such agents could be useful both as pharmacological tools and as potential therapeutic agents for treating disorders in which a dysfunction of glycine inhibition might exist (e.g. Stern & Bokonjic, 1974; Davidoff, 1978; Hall *et al.*, 1979; Wuis, 1987).

In the process of characterizing a series of 5-aryl-1,2,4-triazole compounds for potential CNS activity, we discovered that MDL 27,531 (4-methyl-3-methylsulphonyl-5-phenyl-4H-

[1] Author for correspondence.

1,2,4-triazole; Figure 1) possessed an unusual pharmacological profile in that it blocked the tonic extensor seizures produced by strychnine at doses that had little or no effect on seizures produced by other convulsants that are mechanistically-different from strychnine. Thus, MDL 27,531 appeared to act functionally like a glycine receptor agonist. This antistrychnine effect was particularly striking in that it occurred without any indications of concomitant sedation or motor impairment.

The studies described herein characterize the antagonism of strychnine seizures by MDL 27,531, with particular consideration to duration of action, oral activity, side effect liability, development of tolerance, and potential mechanism of action. MDL 27,531 was specifically compared to the anticonvulsant/muscle relaxant agents baclofen and diazepam with regard to side effect potential.

Some of the data contained herein were previously presented at the 15th Annual Meeting, Society for Neuroscience (Miller *et al.*, 1989) and at the XIth IUPHAR meeting (Dudley *et al.*, 1990). All experiments described here used procedures which were approved by the Institutional Animal Care and Use Committee and which used the United States Department of Agriculture and National Institutes of Health guidelines on animal care and use.

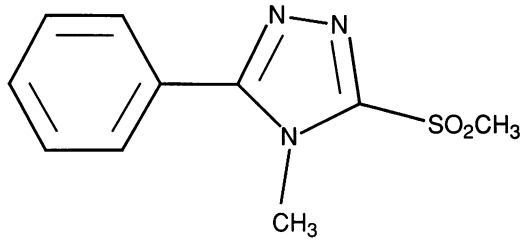

Figure 1 Chemical structure of MDL 27,531 (4-methyl-3-methylsulphonyl-5-phenyl-4H-1,2,4-triazole).

Methods

Adult male Charles River CD-1 mice weighing 20–34 g were used, unless noted otherwise.

Drugs and injection parameters

Compounds were administered intraperitoneally (i.p.), unless otherwise noted. MDL 27,531 (1.6–800 mg kg^{-1}), diazepam (0.25–64 mg kg^{-1}), hexobarbitone sodium (100 mg kg^{-1}) and γ-vinyl-GABA (1.9 g kg^{-1}) were prepared as suspensions in distilled water by use of 1% Tween 80. Strychnine sulphate (2.7 mg kg^{-1}), Ro 15-1788 ([ethyl]-8-fluoro-5,6-dihydro-5-methyl-6-oxo-4H-imidazo (1,5a) (1,4) benzodiazepine -3- carboxylate; 8–32 mg kg^{-1}), pentylenetetrazol (60 mg kg^{-1}), 3-mercaptopropionic acid (3-MPA; 100 mg kg^{-1}), tizanidine (0.4–50.0 mg kg^{-1}), and morphine sulphate (60 mg kg^{-1}) were prepared as solutions in distilled water. Quinolinic acid was prepared as a solution in 0.9% saline. Mice being observed for gross effects were housed in a group in a 30 cm × 30 cm Plexiglas chamber. For all other tests, mice were placed individually in wire mesh cages. Injection volumes were 10 ml kg^{-1} and all doses refer to their respective salts.

Antiseizure activities

Strychnine-induced seizures The method used was modified from Turner (1965). Groups of 10 mice were given a range of doses of the test compounds (MDL 27,531, baclofen, or diazepam) at various times before strychnine (2.7 mg kg^{-1}), in order to determine their ED_{50}s against strychnine-induced seizures. Absence of tonic extension for more than 15 min after strychnine administration was considered significant protection, since >95% of control animals exhibit tonic extension within 15 min after strychnine. MDL 27,531 was tested after both i.p. and oral (p.o.) administration. For Ro 15-1788 experiments, Ro 15-1788 (8–32 mg kg^{-1}) was administered 15 min before strychnine.

Maximal electroshock-induced seizures The method used was modified from Toman *et al.* (1946). Groups of five mice were given MDL 27,531, 200 mg kg^{-1} or diazepam and 30 min later, maximal electroshock (50 mA, 0.2 s, corneal electrodes) was administered. The absence of hindlimb tonic extension was considered to be significant protection, since >95% of the control animals exhibit tonic extension after this electroshock treatment.

Pentylenetetrazol-induced seizures The method used was modified from Goodman *et al.* (1953). Groups of five mice were given MDL 27,531 and 30 min later, pentylenetetrazol was administered by rapid intravenous (i.v.) injection (tail vein) at a dose of 60 mg kg^{-1}. Absence of clonic seizures for 2 min after pentylenetetrazol administration was considered significant protection, since >95% of control animals exhibit clonic seizures within 2 min after pentylenetetrazol.

3-Mercaptopropionic acid (3-MPA)-induced seizures The method used was a modification of those previously described (Lamar, 1970; Loscher, 1979). Groups of five mice were given MDL 27,531 or diazepam and 30 min later, 3-MPA was administered at a dose of 100 mg kg^{-1}, i.v. Absence of seizures for 5 min after 3-MPA was considered significant protection, since >95% of control animals exhibit seizures within 5 min after 3-MPA treatment.

Quinolinic acid-induced seizures Groups of 10 mice were given MDL 27,531 30 min before intracerebroventricularly (i.c.v.) administered quinolinic acid (Haley & McCormick, 1957) at a dose of 7.7 μg in a volume of 5 μl. This dose of quinolinic acid has been found to cause clonic-tonic seizures in 90–100% of the control mice. Immediately following quinolinic acid administration, animals were observed for 15 min for the occurrence of clonic-tonic seizures (Turksi *et al.*, 1985). Those mice not convulsing during the observation period were considered protected.

Audiogenic-induced seizures in DBA/2J male mice DBA/2J male mice (Jackson Laboratories, Bar Harbor, Maine, U.S.A.) were used. The mice (17–18 days old, weighing approximately 6–8 g) were acclimatized for 3 days before testing. On the test day, mice were randomly divided into groups of 5–10 mice. Thirty min post injection of the test compound, each mouse was placed individually in a round glass jar (diameter, 14.5 cm; height 30 cm) inside a sound chamber. The sound chamber was a 30 × 30 × 30 cm insulated box with a lid that had a 20 × 20 cm Plexiglas observation window. The chamber was illuminated by a 40 W light bulb and contained a 4 inch electric bell (Edwards No. 340). Once inside the chamber, the mouse was exposed to the ringing bell (120 dB) for 30 s. During this time, they were observed and scored for the following activities: non-response = 0; wild running for <10 s = 1; wild running for >10 s = 2; clonic seizure = 3; forelimb flexion/hindlimb extension = 4; tonic seizure = 5.

Bicuculline-induced convulsions Male mice (Harlan) were randomly divided into groups of 10 and were placed in individual plastic observation cages. Thirty min after administration of the test compound, bicuculline was administered at dose of 2.7 mg kg^{-1} (subcutaneously, s.c.). Mice were observed for clonic-tonic seizures for a period of 30 min after bicuculline injection. Antagonism of bicuculline seizures was defined as the absence of clonic-tonic seizures for 30 min.

Sedative/depressant activities

Effect on spontaneous motor activity Groups of four mice were given the test compound or vehicle in random order, 30 min before being placed in an Opto-Varimex (Columbus Instruments, Inc.) photocell activity monitor. Motor activity was then recorded for 15 min. A depressant ED_{50}, defined as a 50% reduction of spontaneous motor activity, was determined by linear regression.

Motor ability (rotarod) The method of Kinnard & Carr (1957) was used. Groups of 10 mice were pre-selected for their ability to remain on a horizontal rotating rod (15 r.p.m.) for 120 s. After dosing with the test compound, the mice were treated again at various times. Mice were considered unaffected if they were able to remain on the rotarod for 120 s. Mice unable to remain on the rotarod for 120 s were considered to be motor impaired.

Muscle relaxant activity

Antagonism of morphine-induced Straub tail The method used was modified from Ellis & Carpenter (1974). Mice were administered the test compound (MDL 27,531, diazepam, or baclofen) and 15 min later were injected with morphine (60 mg kg^{-1}, s.c.) and placed singly in vertical, open-ended Plexiglas cylinders. Morphine at this dose produces in control mice an elevation of the tail 90° from the horizontal (Straub tail). Mice observed 15 min after morphine administration were considered significantly affected if the Straub tail was relaxed at a dose that did not also produce loss of righting reflex.

Statistics

ED_{50} values were calculated for analysis of quantal data (Finney, 1978) or by linear regression.

Biochemical tests

In vitro *receptor binding* Brain tissue from young adult male Sprague-Dawley rats (200–250 g) was used for the receptor binding studies. The methods have been described previously: [^{3}H]-flunitrazepam (Braestrup & Squires, 1978), [^{3}H]-muscimol (DeFeudis *et al.*, 1980), [^{35}S]-*t*-butylbicyclophosphorothionate (Trullas *et al.*, 1987), [^{3}H]-baclofen (Bowery *et al.*, 1985) and [^{3}H]-strychnine (Young & Snyder, 1973). MDL 27,531 was dissolved in buffer by sonication.

In vivo *receptor binding* Binding of the benzodiazepine antagonist [^{3}H]-Ro15-1788 to the $GABA_A$ receptor of the mouse cerebral cortex was performed as described by Miller *et al.* (1988). MDL 27,531 were given by i.p. injection 1 h before the ligand; 20 min before the mice were killed 3 μCi of [^{3}H]-Ro 15-1788 was given by i.v. administration. The mice were killed by decapitation, the cortex was removed and the tissue was solubilized in Protosol at 37°C overnight. Beckman Ready Protein scintiallation fluid (10 ml) was added to the vials and radioactivity determined by liquid scintillation spectrophotometry. Non-specific binding of [^{3}H]-Ro 15-1788 was determined by the administration of clonazepam (5 mg kg^{-1}, i.p.) 30 min before [^{3}H]-Ro 15-1788. Specific binding was routinely 85–95% of total bound counts.

GABA levels The method of Lippert *et al.* (1980) was used to determine the effect of MDL 27,531 on mouse cortical GABA levels. Mice were treated with MDL 27,531 (50 mg kg^{-1}, i.p.) and killed 1 h after administration. γ-Vinyl-GABA (2 g kg^{-1}, i.p.) was given 6 h before the mice were killed.

Results

General behavioural observation revealed that MDL 27,531 produced no obvious effects on the overall behaviour of mice in doses of up to 200 mg kg^{-1}, i.p. MDL 27,531 was not lethal (measured at 7 days) in doses as high as 800 mg kg^{-1}, i.p. or p.o.

Antagonism of seizures

MDL 27,531 blocked strychnine-induced seizures in a dose-related manner, after either i.p. or p.o. administration, as summarized in Table 1. The maximal effect was seen following a 30 to 60 min pretreatment time; however, measurable activity was seen 24 h after administration. MDL 27,531 was at least as potent after p.o. administration as after i.p. administration.

Subchronic administration of MDL 27,531 did not produce tolerance. A dose of 64 mg kg^{-1}, i.p. (i.e. 5 × 30′ ED_{50} for antagonism of strychnine-induced seizures) was given once a day for 7 days, followed by an ED_{50} determination on day 8 (18–24 h after the last dose). The ED_{50} was found to be 7.5 mg kg^{-1}.

In marked contrast to its effect on strychnine seizures, MDL 27,531 showed little or no activity in reversing a range of other types of seizures (see Table 2). Chemically-induced seizure tests included: pentylenetrazol (a convulsant that interacts with the $GABA_A$ receptor complex); i.c.v. quinolinic acid (as N-methyl-D-asparatate glutamate agonist); bicuculline (a $GABA_A$ antagonist), and 3-MPA (an inhibitor of glutamate decarboxylase). MDL 27,531 weakly antagonized pentylenetetrazol-induced seizures (ED_{50} = 55.0 mg kg^{-1}) and quinolinic acid-induced seizures (ED_{50} = 269 mg kg^{-1}). In audiogenic seizure-susceptible DBA/2J mice, the administration of 12.5, 25, 50 and 100 mg kg^{-1} of MDL 27,531 (i.p.) protected 10, 60, 40, and 60% of the mice, respectively, against audiogenic seizures. The lack of a consistent dose-response relationship resulted in unacceptable limits and hence the estimated ED_{50}.

In contrast to MDL 27,531, the anticonvulsant diazepam had measurable activity in all anticonvulsant tests run (Table 2). The profile of MDL 27,531 was also distinct from the anticonvulsants sodium valproate and diphenylhydantoin (Table 2). The primary activity of sodium valproate was to antagonize 3-MPA-induced seizures. Diphenylhydantoin antagonized maximal electroshock seizures and, to a lesser extent, 3-MPA seizures. Neither compound affected strychnine seizures in doses of up to 200 mg kg^{-1}.

Side effect profile

Table 3 shows that the separation between the *in vivo* activity of MDL 27,531 as an antistrychnine agent and its possible depressant activity is large, as indicated by measures such as

Table 1 Time course of the antagonism of strychnine-induced seizures by MDL 27,531 following intraperitoneal (i.p.) or oral (p.o.) administration

Route	Pretreat time (h)	ED_{50}[1] (95% confidence interval) (mg kg^{-1})
i.p.	0.5	12.8 (9.3–17.3)
i.p.	1.0	16.5 (12.4–21.9)
i.p.	2.0	23.0 (18.4–28.8)
i.p.	4.0	85.5 (60.1–125.2)
p.o.	0.5	7.3 (5.0–10.8)
p.o.	1.0	8.7 (6.2–12.4)
p.o.	2.0	10.3 (7.3–14.4)
p.o.	4.0	21.6 (16.0–29.2)
p.o.	24.0	182.5 (124.1–272.2)

[1] For each route/pretreatment time group, n = 10–15 per dose for a total n = 40–60.

Table 2 Effects of MDL 27,531, diazepam, sodium valproate, or diphenlyhydantoin (0.5 h pretreatment, i.p.) on seizures induced by chemical or electrical stimuli in normal mice, or on seizures produced by loud sound in DBA/2J audiogenic-seizure susceptible mice

Seizure test	ED_{50}[1] (mg kg^{-1}) (95% conf. interval) *MDL 27,531*	*Diazepam*	*Sodium valproate*	*Diphenylhydantoin*
Strychnine	12.8 (9.3–17.3)	40 (NL)	>200	>200
Maximal electroshock	>200	14.8 (10.7–20.4)	>200	25.9 (19.3–34.8)
Pentylenetetrazol	55.0 (37.2–80.0)	1.5 (1.1–2.0)	100–200	>32
Bicuculline	>100	2.4 (2.0–2.8)	>200	>200
3-Mercaptopropionic acid	>200	0.9 (0.6–1.4)	183 (139–247)	89 (34.4–189.2)
Quinolinic acid i.c.v.	269[2] (NL)	15.7 (9.2–29.9)	NT	NT
Audiogenic seizures	53.2[3] (NL)	0.2 (0.1–0.3)	NT	NT

[1] For each seizure test/drug group, $n = 5–10$ per dose for a total $n = 5–60$.
[2] Estimated, maximum effect 50%
[3] Estimated, maximum effect 60%
NL = no limits
NT = not tested.

disruption of rotarod performance and depression of spontaneous motor activity. To evaluate the side effect potential of MDL 27,531, the ED_{50} against strychnine seizures was used as an estimate of the dose that might be therapeutically useful. Table 3 shows that two anticonvulsant/muscle relaxant compounds, the benzodiazepine agonist, diazepam, and the $GABA_B$ agonist, baclofen, were weakly active against strychnine seizures. Another agent that is currently being tested in the clinic as a muscle relaxant/antispastic agent, the α_2-adrenoceptor agonist, tizanidine (Sayers *et al.*, 1980), antagonized strychnine seizures in a dose-related manner in a dose range of 0.4 to 3.2 mg kg^{-1}. Higher doses (6.3–50 mg kg^{-1}), however, were less effective or inactive in blocking strychnine-induced seizures, and no ED_{50} could be calculated.

Using the ED_{50} for antagonism of strychnine seizures, Table 3 shows that the side effect indices of MDL 27,531 were consistently lower than those calculated for diazepam and baclofen (Table 3). MDL 27,531 (25 and 50 mg kg^{-1}) had little CNS depressant activity as indicated by its lack of effect on hexobarbitone sleep time (Table 4). In contrast, diazepam and baclofen caused significant increases in hexobarbitone sleep time in both groups.

MDL 27,531 had measurable activity in a classic muscle relaxant test, the morphine Straub tail test (ED_{50} = 54 mg kg^{-1}; compared to ED_{50} = 1.2 mg kg^{-1} for diazepam), indicating some separation between the antistrychnine effect and general muscle relaxation *per se*.

Table 4 Effect of i.p. administration of MDL 27,531 or diazepam on sleep time induced by hexobarbitone sodium (100 mg kg^{-1}, i.p.) in mice

Compound	*Dose*[1] (mg kg^{-1}, i.p.)	*Mean sleeptime* (min ± s.e.mean)
Control	—	29.2 ± 2.8
MDL 27,531	25	35.9 ± 4.9
	50	38.5 ± 4.2
Diazepam	4	90.5 ± 5.6*
Baclofen	16	64.7 ± 5.7*

[1] For each group, $n = 10$ mice for a total $n = 50$.
* Significantly different from control group, Student-Newman-Keuls test, $P < 0.001$.

Ro 15-1788 reversal of antistrychnine effects of MDL 27,531

The benzodiazepine antagonist, Ro 15-1788, at doses of 24 or 32 mg kg^{-1}, completely blocked the antagonism of strychnine-induced seizures by i.p. MDL 27,531 (Figure 2). These blockades were not surmountable by even very high doses (e.g. up to 512 mg kg^{-1}) of MDL 27,531, suggesting that MDL 27,531 did not behave like a competitive antagonist. A dose of 16 mg kg^{-1} Ro 15,1788 did not produce a statis-

Table 3 Calculation of side-effect index (SI) ratios for MDL 27,531, diazepam, and baclofen in mice

	ED_{50}[1] (mg kg^{-1}, i.p., 30 min pretreatment)						
Compound	*Anti-strychnine*[2]	*Muscle relaxation*[3]	*SI*[4]	*Sedation*[5]	*SI*	*Ataxia*[6]	*SI*
MDL 27,531	12.8 (9.3–17.3)[7]	53.7 (35.5–80.7)	0.23	299.8 (207–375)	0.04	99.0 (60–154)	0.13
Diazepam	40 (NL)[8]	1.2 (0.8–1.9)	33.3	1.9 (0.5–3.2)[9]	21.05	0.98 (0.6–1.6)	40.8
Baclofen	17.0[10]	5.2 (3.7–7.5)	3.3	2.6 (2.1–3.3)	6.5	7.7 (5.0–11.2)	2.2

[1] For each compound/test group ED_{50} determination, $n = 5–10$ per dose for a total $n = 40–120$.
[2] Reversal of strychnine seizures.
[3] Reversal of morphine-induced Straub tail.
[4] SI = side effect index: $\frac{ED_{50} \text{ antistrychine}}{ED_{50} \text{ measure}}$
[5] Decrease by 50% of spontaneous locomotor activity.
[6] Loss of muscle coordination determined by disruption of rotarod performance.
[7] 95% confidence interval.
[8] NL = no limits.
[9] Estimated ED_{50}.
[10] Lower limit beyond acceptable norm.

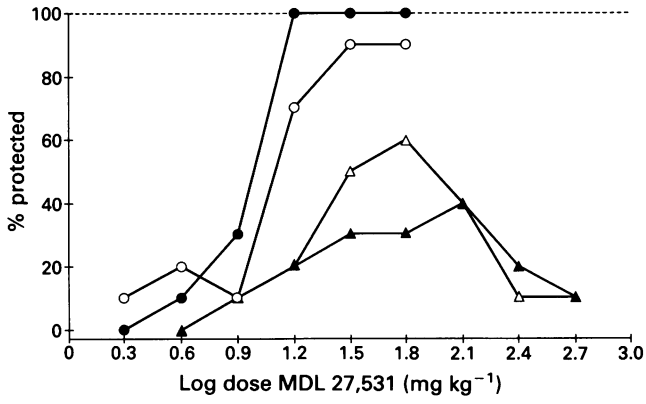

Figure 2 The effects of Ro 15-1788 on the reversal of strychnine-induced seizures by MDL 27,531 in mice. Doses of Ro 15-1788 are: vehicle (●); 16 mg kg^{-1} (○); 24 mg kg^{-1} (△); 32 mg kg^{-1} (▲). For each dose, $n = 10$ mice; total $n = 250$.

tically-significant change relative to vehicle controls (Figure 2). The ED_{50}s for MDL 27,531 reversal of strychnine seizures were: vehicle pretreated: 8.4 (6.2–11.5) mg kg^{-1}; 16 mg kg^{-1} Ro 15-1788 pretreated: 11.4 (7.4–19.8 mg kg^{-1}); 24 mg kg^{-1} Ro 15-1788 pretreated: 40 mg kg^{-1} (estimated, given unacceptable limits), and 32 mg kg Ro 15-1788 pretreated: > 512 mg kg^{-1}.

In contrast to the results obtained against strychnine seizures, Ro 15-1788 (8–32 mg kg^{-1}) produced parallel rightward shifts in the dose-response curves for diazepam-induced antagonism of pentylenetetrazol-induced seizures. The ED_{50}s (and 95% confidence intervals) were: vehicle pretreatment: 0.8 (0.5–1.1) mg kg^{-1}; 8 mg kg^{-1} Ro 15-1788 pretreatment: 3.5 (2.3–5.1) mg kg^{-1}; 16 mg kg^{-1} Ro 15-1788 pretreatment: 16.5 (11.4–24.7); and 32 mg kg^{-1} Ro 15-1788 pretreatment: 11.0 (7.6–15.0). The shifts in the dose-response curves were statistically-significant for all three doses of Ro 15-1788. These data are consistent with the conclusion that at the doses used, Ro 15-1788 acts like a competitive antagonist to reverse the anticonvulsant effects of diazepam.

Receptor binding

MDL 27,531 is a selective antagonist of strychnine seizures in mice, yet, *in vitro*, the compound did not alter [^{3}H]-strychnine binding in mouse brainstem and upper spinal cord membranes at concentrations of up to 100 μM (Table 5). Furthermore, MDL 27,531 *in vitro* did not alter [^{3}H]-flunitrazepam, [^{3}H]-muscimol, [^{35}S]-*t*-butylbicyclophosphorothionate (TBPS) and [^{3}H]-baclofen binding in rat cerebral cortex in concentrations of up to 100 μM (Table 5).

In contrast to the lack of effect *in vitro* on binding to the $GABA_A$ receptor complex, MDL 27,531 (30 and 100 mg kg^{-1}, i.p.) significantly enhanced the binding of [^{3}H]-Ro 15-1788 to the cerebral cortex of mice when measured *in vivo* (Table 6).

Table 6 Effects of MDL 27,531 on *in vivo* binding of [^{3}H]-Ro 15-1788 in mouse cerebral cortex

Dose of MDL 27,531[1] (mg kg^{-1}, i.p.)	*% of control*[2] (mean ± s.e.mean)
1.0	102 ± 7.4
3.0	126 ± 7.0
10.0	152 ± 9.2
30.0	270 ± 16.0*
100.0	501 ± 37.6*

[1] For each dose, $n = 6$, for a total $n = 30$.
[2] Average total bound [^{3}H]-Ro 15-1788 in the control (saline-treated) animals was 37.3 ± 4.5 c.p.m. mg^{-1} of tissue.
* Significantly different from saline controls, $P < 0.05$.

The GABA-transaminase inhibitor, γ-vinyl-GABA, which increases GABA levels, similarly increases [^{3}H]-Ro 15-1788 binding *in vivo* (Dudley *et al.*, 1990). However, MDL 27,531 (50 mg kg^{-1}) did not affect cortical GABA levels (μmol g^{-1}): saline vehicle = 2.91; MDL 27,531 = 2.57; γ-vinyl-GABA = 12.17* (*$P < 0.05$ relative to saline controls).

Discussion

The two major findings of the present study are that MDL 27,531 selectively blocked the seizures produced by the glycine antagonist strychnine and that this antistrychnine effect of MDL 27,531 could be blocked by the benzodiazepine antagonist, Ro 15-1788.

Antistrychnine activity of MDL 27,531

The data confirmed our initial observations that MDL 27,531 was a selective antagonist of strychnine-induced seizures in mice. This antistrychnine activity occurred at doses that lacked other anticonvulsant activities and, importantly, at doses that did not produce any signs of general depression or sedation. In fact, the ED_{50} of MDL 27,531 for depressing spontaneous motor activity was approximately 23 fold higher than the ED_{50} for blocking strychnine seizures (see Table 3).

The anticonvulsant profile of MDL 27,531 as a selective antagonist of strychnine seizures struck us as being unique relative to any other compound that we have tested. For example, representative anticonvulsants such as diazepam, sodium valproate, and diphenylhydantoin had very different anticonvulsant profiles (Table 2), with none of them showing very potent activity against strychnine-induced seizures.

As mentioned in the Introduction, apart from strychnine (which is an antagonist), there are few, if any, pharmacological tools for selectively manipulating activity of inhibitory glycinergic neurones. The selective reversal of strychnine seizures can be interpreted as functional evidence for glycine receptor agonist activity. However, this interpretation

Table 5 Effect of MDL 27,531 on *in vitro* receptor binding activity[1] to glycine[2] or GABA[3] receptors

	IC_{50} (μM)			
Compound	*[^{3}H]-muscimol*	*[^{3}H]-flunitrazepam*	*[^{35}S]-TBPS*	*[^{3}H]-baclofen*
MDL 27,531	> 100	> 100	> 100	> 10
GABA	0.021			
Diazepam		0.003		
Picrotoxin			0.279	
Baclofen				0.100

[1] MDL 27,531 was tested in triplicate at each concentration of up to 100 μM.
[2] MDL 27,531 did not alter [^{3}H]-strychnine binding in mouse brainstem and upper spinal cord membranes at doses of up to 100 μM.
[3] Assays carried out in rat cerebral cortex; [^{3}H]-muscimol, [^{3}H]-flunitrazepam or [^{35}S]-*t*-butylbicyclophosphorothionate (TBPS) ligands bind to the GABA, benzodiazepine and picrotoxin-convulsant binding sites, respectively.

requires the critical assumption that strychnine, at the dose used in the present study (2.7 mg kg^{-1}, the CD_{97}), selectively blocked glycine receptors. A judgement on the glycine selectivity of this dose can only be inferred from published studies. Classic electrophysiological studies (e.g. Curtis *et al.*, 1969) demonstrated that strychnine administered in intravenous doses of 0.1–0.2 mg kg^{-1} selectively reduced the inhibitory effects of iontophoretically applied glycine (but not GABA). However, a direct comparison with the present study is complicated given the differences in factors such as route of administration (s.c. vs intravenous) and species (mouse vs cat). More comparable data comes from studies which have attempted to reverse strychnine seizures with glycine. Although some investigators have reported difficulty in demonstrating glycine reversal (e.g. Freed, 1985), Halsey *et al.* (1989) found that the threshold dose for producing strychnine seizures (2.0–2.5 mg kg^{-1}, as approximated from their graph) was significantly increased by a dose of glycine which did not affect bicuculline- or pentylenetetrazol-induced seizures. These data suggest (but do not prove) a likely glycine selectivity of the 2.7 mg kg^{-1} dose used in the present study.

Ro 15-1788 reversal of antistrychnine activity of MDL 27,531

Although the functional studies suggested that MDL 27,531 behaved like a glycine receptor agonist in selectively reversing strychnine seizures, further studies were needed to begin to evaluate the mechanism of action of this compound.

In vitro receptor binding studies indicated that MDL 27,531 did not readily displace [^{3}H]-strychnine from brainstem/spinal cord membranes, suggesting that there is not simply a competitive interaction of MDL 27,531 with glycine receptors.

The high degree of structural homology between the strychnine-sensitive glycine receptor and the $GABA_A$ receptor (see Langosch *et al.*, 1990; Vandenberg *et al.*, 1992) and the suggested commonalities in mechanism of action of glycine and benzodiazepines (Young *et al.*, 1974) suggested the possibility that the compound might act through a mechanism which might have GABAergic characteristics. Although MDL 27,531 did not affect the binding *in vitro* of various tritiated ligands for $GABA_A$/$GABA_B$ receptors to brainstem/spinal cord membrane preparations, the compound did increase the *in vivo* binding of [^{3}H]-Ro 15-1788 to mouse cerebral cortex in a dose-related manner. γ-Vinyl-GABA, a GABA transaminase inhibitor which increases GABA levels and antagonizes strychnine seizures (Palfreyman *et al.*, 1981), produces a similar effect on [^{3}H]-Ro 15-1788 binding *in vivo* (Dudley *et al.*, 1990). In the present case, MDL 27,531 did not elevate GABA levels, ruling out this as a possible mechanism of action for the observed effects on [^{3}H]-Ro 15-1788 binding.

It is important to emphasize that the observed enhancement of [^{3}H]-Ro 15-1788 binding was measured in cortical tissues (spinal cord/brainstem tissues were not assayed). [^{3}H]-strychnine binding sites are virtually absent from cortex (e.g. Cortes & Palacios, 1990) and therefore it is unlikely that the anti-strychnine seizure activity of MDL 27,531 is mediated in the cortex. Nevertheless, the binding data in cortical tissues did suggest that MDL 27,531 could affect the Ro 15-1788-sensitive binding site and subsequent functional studies found that blockade by MDL 27,531 of strychnine-induced seizures was prevented by Ro 15-1788 (Figure 2). MDL 27,531 is not simply acting like a benzodiazepine agonist (e.g. diazepam) for several reasons: (1) the Ro 15-1788 blockade did not appear to be competitive in nature, in that it was only partially overcome by increasing the dose of MDL 27,531 used (Figure 2). In contrast, as expected, similar doses of Ro 15-1788 reversed in a competitive fashion the blockade of pentylenetetrazol-induced seizures produced by diazepam. (2) Diazepam was only weakly active in blocking strychnine seizures, being approximately 17 fold less potent than in blocking bicuculline seizures (Table 2). In contrast MDL 27,531 was inactive against bicuculline seizures. (3) MDL 27,531 clearly lacked the marked sedative/ataxic effects demonstrated by diazepam (Table 3).

These data, combined with the demonstrated functional profile of MDL 27,531 as a selective antagonist of strychnine seizures and the known structural homology between the strychnine-sensitive glycine receptor and the $GABA_A$ receptor complex, suggests the possibility that MDL 27,531 may affect an allosteric site on the glycine receptor to produce agonist-like activity that is similar to the site it must bind to on the $GABA_A$ receptor to increase Ro 15-1788 binding. Ongoing work to evaluate the further mechanism of action includes measurement of agonist-stimulated chloride fluxes and patch-clamp electrophysiology (J.A. Miller and C. Rogers, personal communication).

It is important to note that MDL 27,531 was orally active, with an ED_{50} similar to that seen following i.p. administration and this oral activity was long-lasting, with detectable activity at 24 h after administration. The fact that MDL 27,531 had oral activity at least as good as after i.p. administration suggests the possibility of an active metabolite. This possibility is consistent with the reported activity in *in vivo* (but not *in vitro*) binding studies reported above. Such a metabolite might (unlike MDL 27,531) have activity in [^{3}H]-strychnine or other binding assays. Clearly, further work is needed to evaluate these and other possibilities.

Finally, though this question was not addressed by the present experiments, it is useful to ask what potential relevance an agent such as MDL 27,531 might have as a therapeutic agent for treating CNS disorders. It has been suggested that certain spastic disorders might result, at least in part, from a decrease in glycinergic inhibition (Davidoff *et al.*, 1967; Stern & Bokonjic, 1974; Davidoff, 1978; Hall *et al.*, 1979; Young & Delwaide, 1981a,b; Wuis, 1987; Mazzochio & Rossi, 1989). If MDL 27,531 can indeed enhance glycinergic tone (as inferred from its selective activity in reversing strychnine seizures), then it might be useful as a potential antispastic agent. Consistent with this possibility, MDL 27,531 has been shown to diminish hindlimb hyperreflexia in a rodent model of spasticity (Kehne *et al.*, unpublished data).

In summary, MDL 27,531 has the profile of a functional agonist at the strychnine-sensitive glycine receptor in its capacity to antagonize selectively strychnine seizures. Though the precise mechanism(s) of action of MDL 27,531 is unknown, it may act at an allosteric site on the strychnine-sensitive glycine receptor which produces agonist-like activity. It is speculated that MDL 27,531 may prove useful for treating disorders of diminished glycinergic inhibition.

We would like to thank Timothy McCloskey, Jerry Miller and Carl Rogers for helpful comments and their reading of the manuscript, and Research Graphics for help in figure preparation.

References

APRISON, M.H. (1990). The discovery of the neurotransmitter role of glycine. In *Glycine Neurotransmission*. ed. Ottersen, O.P. & Storm-Mathisen, J. pp. 1–24. Chichester: John Wiley & Sons.

BOWERY, N.G., HILL, D.R. & HUDSON, A.L. (1985). [^{3}H](−)Baclofen: an improved ligand for $GABA_B$ sites. *Neuropharmacol.*, **24**, 207–210.

BRAESTRUP, C. & SQUIRES, R. (1978). Pharmacological characterization of benzodiazepine receptors in the brain. *Eur. J. Pharmacol.*, **48**, 263–270.

CORTES, R. & PALACIOS, J.M. (1990). Autoradiographic mapping of glycine receptors by [^{3}H]strychnine binding. In *Glycine Neurotransmission*. ed. Ottersen, O.P. & Storm-Mathisen, J. pp. 239–263. Chichester: John Wiley & Sons.

CURTIS, D.R., DUGGAN, A.W. & JOHNSON, G.A.R. (1969). Glycine, strychnine, picrotoxin and spinal inhibition. *Brain Res.*, **14**, 759–762.

DAVIDOFF, R.A. (1978). Pharmacology of spasticity. *Neurology*, **28**, 46–51.

DAVIDOFF, R.A., GRAHAM, L.T., SHANK, R.P., WERMAN, R. & APRISON, M.H. (1967). Changes in amino acid concentrations associated with loss of spinal interneurones. *J. Neurochem.*, **14**, 1025–1031.

DEFEUDIS, F.V., OSSOLA, L., SCHMITT, G., WOLF, P. & MANDEL, P. (1980). Na^+-independent binding of [^{3}H]GABA and [^{3}H]muscimol to subcellular particles of neural primary cultures and whole brain. *J. Neurochem.*, **34**, 216–218.

DUDLEY, M.W., OGDEN, A.M., KANE, J.M., MILLER, F.P. & LIPPERT, B. (1990). The enhancement and inhibition of *in vivo* binding of [^{3}H]Ro 15-1788 in mouse cerebral cortex by a series of 5-aryltriazoles. *Eur. J. Pharmacol.*, **183**, 588–589.

ECCLES, J.C. (1965). Pharmacology of central inhibitory snyapses. *Br. Med. Bull.*, **21**, 19–25.

ELLIS, K.O. & CARPENTER, J.F. (1974). A comparative study of Dantrolene sodium and other skeletal muscle relaxants with the straub tail mouse. *Neuropharmacol.*, **13**, 211–214.

FINNEY, D.J. (1978). *Statistical Method in Biological Assay*, 3rd edition. New York: MacMillan.

FREED, W.J. (1985). Prevention of strychnine-induced seizures and death by the N-methylated glycine derivatives betaine, dimethylglycine and sarcosine. *Pharmacol. Biochem. Behav.*, **22**, 641–643.

GOODMAN, L.S., GREWAL, M.S., BROWN, W.C. & SWINYARD, E.A. (1953). Comparison of maximal seizures evoked by pentylenetetrazol (Metrazol) and electroshock in mice, and their modification by anticonvulsants. *J. Pharmacol. Exp. Ther.*, **108**, 168–176.

HALL, P.V., SMITH, J.E., LANE, J., MOTE, T. & CAMPBELL, R. (1979). Glycine and experimental spinal spasticity. *Neurology*, **29**, 262–267.

HALEY, T.J. & MCCORMICK, W.G. (1957). Pharmacological effects produced by intracerebral injection of drugs in the conscious mouse. *Br. J. Pharmacol. Chemother.*, **12**, 12–15.

HALSEY, M.J., LITTLE, H.J. & WARDLEY-SMITH, B. (1989). Systemically administered glycine protects against strychnine convulsions, but not the behavioral effects of high pressure, in mice. *J. Physiol.*, **408**, 431–441.

KINNARD, W.J. & CARR, C.J. (1957). A preliminary procedure for the evaluation of central nervous system depressants. *J. Pharmacol. Exp. Ther.*, **121**, 354–361.

LAMAR, C. (1970). Mercaptopropionic acid: a convulsant that inhibits glutamate decarboxylase. *J. Neurochem.*, **17**, 165–170.

LANGOSCH, D., BETZ, H. & BECKER, C.-M. (1990). Molecular structure and developmental regulation of the inhibitory glycine receptor. In *Glycine Neurotransmission*. ed. Ottersen, O.P. & Storm-Mathisen, J. pp. 67–82. Chichester: John Wiley & Sons.

LIPPERT, B., METCALF, B.W. & RESVICK, R.J. (1980). Enzyme-activated irreversible inhibition of rat and mouse brain 4-aminobutyric acid-alpha-ketoglutarate transaminase by 5-fluoro-4-oxopentanoic acid. *Biochem. Biophys. Res. Commun.*, **108**, 146–152.

LOSCHER, W. (1979). 3-Mercaptopropionic acid: convulsant properties, effects on enzymes of the gamma-amino-butyrate system in mouse brain and antagonism by certain anti-convulsant drugs. *Biochem. Pharmacol.*, **28**, 1397–1407.

MAZZOCCHIO, R. & ROSSI, A. (1989). Recurrent inhibition in human spinal spasticity. *Ital. J. Neurol. Sci.*, **10**, 337–347.

MILLER, F.P., KANE, J.M., BRAUN, H.J., KETTELER, H.J., MCCLOSKEY, T.C & KEHNE, J.H. (1989). MDL 27,531 is a selective strychnine antagonist. *Soc. Neurosci. Abstr.*, **15**, 1176.

MILLER, L.G., GREENBLATT, D.J., BARNHILL, J.G., SUMMER, W.R. & SHADER, R.I. (1988). 'GABA shift' in vivo: enhancement of benzodiazepine binding in vivo by modulation of endogenous GABA. *Eur. J. Pharmacol.*, **148**, 123–130.

PALFREYMAN, M.G. & BARON, B.B. (1991). Non-competitive NMDA antagonists acting on the glycine site. In *Excitatory Amino Acid Antagonists*. ed. Meldrum, B.S. pp. 101–129. Oxford: Blackwell Scientific Publications.

PALFREYMAN, M.G., SCHECTER, P.J., BUCKETT, W.R., TELL, G.P. & KOCH-WESER, J. (1981). The pharmacology of GABA-transaminase inhibitors. *Biochem. Pharmacol.*, **30**, 817–824.

SAYERS, A.C., BURKI, H.R. & EICHENBERGER, E. (1980). The pharmacology of 5-chloro-4-(2-imidazolin-2-yl-amino)-2,1,3-benzothiadiazole (DS 103-282), a novel myotonolytic agent. *Arzneim. Forsch/Drug Res.*, **30**, 793–803.

STERN, P. & BOKONJIC, R. (1974). Glycine therapy in seven cases of spasticity. *Pharmacol.*, **12**, 117–119.

TOMAN, J.E.P., SWINYARD, E.A. & GOODMAN, L.S. (1946). Properties of maximal seizures and their alteration by anticonvulsant drugs and other agents. *J. Neurophysiol.*, **9**, 231–238.

TRILLER, A., CLUZEAUD, F. & SEITANIDOUS, T. (1990). Immunocytochemical localization of the glycine receptor. In *Glycine Neurotransmission*. ed. Ottersen, O.P. & Storm-Mathisen, J. pp. 83–109. Chichester: John Wiley & Sons.

TRULLAS, R., HAVOUNDJIAN, H. & SKOLNICK, P. (1987). Stress-induced changes in [^{35}S]-t-butylbicyclophorothionate binding to gamma-aminobutyric acid-gated chloride changes are mimicked by in vitro occupation of benzodiazepine receptors. *J. Neurochem.*, **49**, 968–974.

TURNER, R.A. (1965). Anticonvulsants. In *Screening Methods in Pharmacology*. pp. 164–172. New York: Academic Press.

TURKSI, L., MELDRUM, B.S. & COLLINS, J.F. (1985). Anticonvulsant action of β-kainic acid in mice. Is β-kainic acid an N-methyl-D-asparatate antagonist? *Brain Res.*, **336**, 162–166.

VANDENBERG, R.J., FRENCH, C.R., BARRY, P.H., SHINE, J. & SCHOFIELD, P.R. (1992). Antagonism of ligand-gated ion channel receptors: Two domains of the glycine receptor α subunit form the strychnine-binding site. *Proc. Natl. Acad. Sci. U.S.A.*, **89**, 1765–1769.

WUIS, E.W. (1987). Spasticity and drug therapy. *Pharmaceutisch Weekblad Scientific Edition*, **9**, 249–260.

YOUNG, R.R. & DELWAIDE, P.J. (1981a). Drug therapy: Spasticity, Part I. *N. Engl. J. Med.*, **304**, 28–33.

YOUNG, R.R. & DELWAIDE, P.J. (1981b). Drug therapy: Spasticity, Part II. *N. Engl. J. Med.*, **304**, 96–99.

YOUNG, A.B. & SNYDER, S.H. (1973). Strychnine binding associated with glycine receptors of the central nervous system. *Proc. Natl. Acad. Sci. U.S.A.*, **70**, 2832–2836.

YOUNG, A.B., ZUKIN, S.R. & SNYDER, S.H. (1974). Interaction of benzodiazepines with central nervous glycine receptors: possible mechanism of action. *Proc. Natl. Acad. Sci. U.S.A.*, **71**, 2246–2250.

(Received November 26, 1991
Revised April 2, 1992
Accepted April 8, 1992)

Br. J. Pharmacol. (1992), **106**, 917–923 © Macmillan Press Ltd, 1992

Potentiation of ADP-induced aggregation in human platelet-rich plasma by 5-hydroxytryptamine and adrenaline

D.M. Vanags, *S.E. Rodgers, *E.M. Duncan, [1],*J.V. Lloyd & F. Bochner

Department of Clinical and Experimental Pharmacology, University of Adelaide, Adelaide, South Australia, 5000 and *Division of Haematology, Institute of Medical and Veterinary Science, Adelaide, South Australia, 5000

1 We have used dose-response curves to quantitate the potentiation of adenosine 5'-diphosphate (ADP)-induced aggregation and thromboxane (TXA_2) generation by 5-hydroxytryptamine (5-HT) and adrenaline in human citrated platelet-rich plasma. We have also quantitated the inhibition of these responses by aspirin, ketanserin and yohimbine, singly and in pairs.

2 Ketanserin (5 μM) inhibited TXA_2 production and the second wave of platelet aggregation induced by a range of concentrations of ADP alone. This indicates that endogenous 5-HT, released from the platelet dense granules, contributes significantly to responses induced by ADP.

3 When 5-HT (10 μM) was added before ADP, a lower concentration of ADP was required to cause 50% aggregation and TXA_2 generation. The ratio of ADP concentrations (CR) to cause 50% aggregation in the presence and absence of 5-HT was 2.1 when only added 5-HT was considered, and 5.0 when endogenous 5-HT was also taken into account.

4 Potentiation of ADP-induced aggregation by 5-HT also occurred in the presence of aspirin, resulting in a CR of 2.3. As expected, ketanserin inhibited potentiation by 5-HT in the presence and absence of aspirin. Although aspirin caused substantial inhibition of aggregation induced by ADP and 5-HT (CR 3.4), further inhibition occurred when ketanserin was also present (CR 6.5).

5 A subthreshold concentration of adrenaline (0.25 μM) caused substantial potentiation of ADP-induced aggregation in the absence (CR 4.0) and presence (CR 2.0) of aspirin. As expected, yohimbine (9 μM) inhibited this potentiation. Maximum TXA_2 generation induced by ADP increased from 32.5 to 59.4 pg per 10^6 platelets when adrenaline was present. Aggregation induced by ADP and adrenaline was markedly inhibited by aspirin (CR 5.1) but was further inhibited when yohimbine (9 μM) was also present (CR 10.0).

6 Results from this *in vitro* study show ketanserin and yohimbine have the potential to be used in combination with aspirin as antithrombotic agents *in vivo*.

Keywords: Platelet aggregation; thromboxane; 5-hydroxytryptamine; adrenaline; synergism; aspirin; ketanserin; yohimbine; *in vitro*

Introduction

Platelet activation, at a site of vascular injury, by agonists such a collagen, is a receptor-mediated process. A number of biochemical events, including the hydrolysis of phosphatidylinositolbisphosphate, a rise in cytosolic calcium, synthesis of thromboxane (TXA_2) and secretion of adenosine 5'-diphosphate (ADP), 5-hydroxytryptamine (5-HT) and catecholamines from platelet dense granules, are involved, culminating in irreversible platelet aggregation. TXA_2 and 5-HT provide an important mechanism for the enhancement of platelet aggregation, and also contribute to platelet derived vasoconstriction (Mehta, 1990). Single platelet agonists have been classified according to potency with respect to which of the biochemical events are elicited. Adrenaline, 5-HT and ADP when used singly, induce platelet activation with a weak potency and irreversible aggregation will ensue only if TXA_2 synthesis occurs. Relatively few platelets actually adhere to exposed collagen at the site of vessel injury, and therefore the major fraction of platelets are probably activated by ADP, 5-HT, and TXA_2 released from platelets that interact directly wtih the collagen (Holmsen, 1982). It has been demonstrated *in vitro* that 5-HT and catecholamines released from the platelet, potentiate not only the aggregation response initiated by thrombin (Thomas, 1967), but can also potentiate the effects of released ADP (Mills *et al.*, 1968). It is thought that the function of the released agonists *in vivo*, is to potentiate platelet responses induced by other agonists in the milieu of a forming thrombus (De Clerck & De Chaffoy de Courcelles, 1990). It is conceivable that receptor antagonists such as ketanserin or yohimbine, which compete with 5-HT and catecholamines for respective receptor sites, may have a role in the prophylaxis of thrombosis, and associated vascular responses, in addition to, or instead of aspirin.

Synergistic platelet aggregation responses have been described by many investigators for a variety of combinations of agonists (Kinlough-Rathbone & Mustard, 1986). However, the role of TXA_2 in the synergistic aggregation response between weak agonists, in particular, has not been clearly defined. Thromboxane formation has been reported to play a major role in synergism between collagen and other agonists in rabbit platelets (Kinlough-Rathbone & Mustard, 1977). It has been reported that amplification by 5-HT of collagen-induced aggregation, but not ADP-induced aggregation was affected by inhibition of cyclo-oxygenase (De Clerck *et al.*, 1982), indicating that TXA_2 was not essential in the interaction between the weak agonists 5-HT and ADP. Cameron & Ardlie (1982) showed, however, that the interaction between adrenaline and ADP operates via two distinct mechanisms, one TXA_2-dependent and the other TXA_2-independent, although in these experiments TXA_2 production in response to a combination of critical concentrations of agonists only was investigated.

[1] Author for correspondence.

Investigating more thoroughly the mechanism by which 5-HT and adrenaline potentiate ADP-induced aggregation will determine whether additional activation pathways, apart from TXA_2 generation, should be blocked to achieve greater antithrombotic potential. If marked enhancement of aggregation by 5-HT and adrenaline does occur in the presence of aspirin, when there is no TXA_2 production, then it may be reasonable to supplement aspirin therapy with agents that block platelet 5-HT receptors and adrenoceptors.

The aim of this study was to examine platelet aggregation and TXA_2 production induced by the interaction of ADP with either 5-HT or adrenaline, by use of complete dose-response curves. We then wished to quantitate the inhibition of these responses by a combination of aspirin and the appropriate antagonist, ketanserin or yohimbine, and compare it with the effect achieved by each inhibitor alone.

Methods

Platelet preparation

Platelet donors were four healthy volunteers (2 males, 2 females, aged 24–35 years), who had denied taking any medication which may alter platelet function for at least two weeks before the start of the study. Each was studied on two independent occasions because of marked day to day variation in platelet responsiveness. Venous blood was taken into one tenth volume trisodium citrate (0.1 M, pH 7.35), platelet-rich plasma (PRP) prepared by centrifugation at 200 *g* for 11 min at room temperature and adjusted to a platelet count of 300,000 μl^{-1} with autologous platelet-poor plasma, prepared by centrifugation at 900 *g* for 20 min. The standardized PRP was stored at 37°C in an air-free syringe to maintain a constant pH, as previously described (Watts *et al.*, 1985). Aspirin (100 μM) or Tyrode buffer was incubated with PRP in the syringe.

Platelet function tests

Platelet aggregation was measured by turbidometry in two dual channel platelet aggregometers (Payton, Ontario, Canada). PRP (255 μl) was incubated in the aggregation cuvette for 3 min with either ketanserin (0.5–5 μM), yohimbine (0.09–9 μM) or Tyrode buffer (15 μl). Stock solutions of 5-HT and adrenaline were dissolved in HEPES-Tyrode buffer (pH 7.4), (Kinlough-Rathbone *et al.*, 1983) containing 1 mM ascorbic acid to prevent oxidation of the agonists (pH 7.2) (Britt *et al.*, 1988). The dilution of ascorbate containing solutions into PRP did not affect the pH of the solution and the presence of ascorbate did not affect aggregation. 5-HT (10 μM), adrenaline (subthreshold) or HEPES-Tyrode buffer containing ascorbate (15 μl) were then added 20 s before the addition of ADP (0.01–100 μM) (15 μl). (The final volume of PRP + agonists/antagonists was 300 μl). The concentration of 5-HT (10 μM) was chosen because it caused maximal potentiation and when used alone it caused less than 10% aggregation. The subthreshold concentration of adrenaline was determined as the maximum which caused less than 10% aggregation, and varied between subjects and experimental days. The extent of aggregation, 5 min after the addition of agonists, was measured as the percentage of the difference of light transmission between PRP and platelet-free plasma (prepared by centrifugation at 8,000 *g* for 2 min).

The production of TXA_2, 5 min after the addition of agonist, was measured by radioimmunoassay of the stable end-product, TXB_2, as previously described (Herd *et al.*, 1987). The detection limit of the assay was 0.2 ng ml^{-1} PRP or 0.6 pg/10^6 platelets.

Expression of results

Dose-response curves were plotted for concentration of ADP vs % aggregation (semilogarithmic plot) or TXA_2 generation (log-logarithmic plot) and EC_{50} values (concentration of ADP required to produce 50% maximal aggregation or TXA_2 generation) determined. Mean EC_{50} values were calculated from the EC_{50} for each individual experiment. Mean EC_{50} values in tables are shown as geometric mean ($\pm$ geometric s.e.mean) (to 2 significant figures), since it has been demonstrated (Fleming *et al.*, 1972) that EC_{50} and parameters derived therefrom are log-normally distributed. Maximal aggregation and TXA_2 generation responses are expressed as a geometric mean and geometric s.e.mean (g.s.e.).

Potentiation of ADP-induced responses by 5-HT and adrenaline was quantitated as a concentration ratio (CR) by dividing the EC_{50} for ADP alone by the EC_{50} for ADP in the presence of a second agonist. Concentration ratios in Tables 1 and 2 (2 significant figures) are calculated from mean EC_{50}

Table 1 The effect of aspirin $\pm$ ketanserin on aggregation induced by adenosine 5'-diphosphate (ADP) $\pm$ 5-hydroxytryptamine (5-HT, 10 μM)

	ADP EC_{50} (μM)			*ADP + 5-HT EC_{50} (μM)*		
	g.m.	− g.s.e.m.	+ g.s.e.m.	g.m.	− g.s.e.m.	+ g.s.e.m.
Buffer	1.0	0.8	1.2	0.5	0.4	0.6
Ketanserin (5 μM)	2.3	2.0	2.6	1.8	1.6	2.0
Aspirin (100 μM)	3.7	3.4	4.0	1.6	1.4	1.8
Aspirin + ketanserin	4.1	3.4	4.8	3.0	2.7	3.3

EC_{50}^1	*EC_{50}^2*	*Concentration ratio*	
ADP + buffer	ADP + 5-HT + buffer	2.1	$P<0.001$
ADP + ketanserin	ADP + buffer	2.3	$P<<0.001$
ADP + ketanserin	ADP + 5-HT + buffer	5.0	$P<<0.001$
ADP + 5-HT + ketanserin	ADP + 5-HT + buffer	3.8	$P<<0.001$
ADP + 5-HT + aspirin	ADP + 5-HT + buffer	3.4	$P<<0.001$
ADP + 5-HT + aspirin + ketanserin	ADP + 5-HT + buffer	6.5	$P<<0.001$
ADP + 5-HT + aspirin + ketanserin	ADP + 5-HT + aspirin	1.9	$P<0.005$
ADP + aspirin	ADP + 5-HT + aspirin	2.3	$P<<0.001$
ADP + aspirin + ketanserin	ADP + ketanserin	1.7	$P<0.05$
ADP + aspirin + ketanserin	ADP + aspirin	1.1	NS
ADP + aspirin	ADP + buffer	3.7	$P<<0.001$

Values shown are geometric mean (g.m.) $\pm$ geometric s.e.mean (g.s.e.m.) EC_{50} from eight experiments.
Concentration ratios (CR) are calculated from mean EC_{50}^1/EC_{50}^2. NS = not significant. A CR $>$ 1.6 is statistically significant at the 0.05 level.

Table 2 The effect of aspirin ± yohimbine (Yoh) on aggregation induced by adenosine 5'-diphosphate (ADP) ± adrenaline (Ad,0.25 μM)

	ADP EC_{50} (μM)			*ADP + Ad EC_{50} (μM)*		
	g.m.	− g.s.e.m.	+ g.s.e.m.	g.m.	− g.s.e.m.	+ g.s.e.m.
Buffer	0.8	0.7	0.9	0.2	0.1	0.3
Aspirin	2.2	2.0	2.4	1.0	0.9	1.1
Aspirin + yohimbine (0.09 μM)	–	–	–	1.5	1.4	1.6
Aspirin + yohimbine (0.9 μM)	–	–	–	1.8	1.6	2.0
Aspirin + yohimbine (9 μM)	–	–	–	2.2	2.0	2.4

EC_{50}^1	*EC_{50}^2*	*Concentration ratio*	
ADP + buffer	ADP + Ad + buffer	4.0	$P<<0.001$
ADP + Ad + aspirin	ADP + Ad + buffer	5.1	$P<<0.001$
ADP + aspirin	ADP + Ad + aspirin	2.0	$P<0.005$
ADP + Ad + aspirin + Yoh (0.09 μM)	ADP + Ad + aspirin	1.4	NS
ADP + Ad + aspirin + Yoh (0.9 μM)	ADP + Ad + aspirin	1.7	$P<0.05$
ADP + Ad + aspirin + Yoh (9.0 μM)	ADP + Ad + aspirin	2.0	$P<0.005$
ADP + Ad + aspirin + Yoh (9.0 μM)	ADP + Ad	10.0	$P<<0.001$

Values shown are geometric mean (g.m.) ± geometric s.e.mean (g.s.e.m.) EC_{50} from eight experiments.
Concentration ratios (CR) are calculated from mean EC_{50}^1/EC_{50}^2. NS = not significant. A CR > 1.6 is statistically significant at the 0.05 level.

values (3 significant figures). Increasing potentiation was quantitated as an increased CR.

Inhibition of responses was similarly quantitated as a CR, calculated from individual EC_{50} ratios for each experiment, by dividing the EC_{50} in the presence of the inhibitor by that obtained in its absence. Increased inhibition is indicated by an increased CR.

To calculate IC_{50} (the concentration to inhibit the potentiated aggregation response by 50%) for yohimbine and ketanserin (a) the maximal CR was determined, (b) the concentration of receptor antagonists to inhibit this ratio by 50% was determined from a graph of increasing CR vs concentration of receptor antagonist. The geometric mean and geometric s.e.mean (g.s.e.) for IC_{50} values were calculated from the IC_{50} for each individual experiment.

Statistical analyses

EC_{50} data in Tables 1 and 2 were analysed by analysis of variance after logarithmic transformation, and differences between mean values determined by q tests (Dixon & Massey, 1969). The *P* values obtained appear in respective tables.

Chemicals used and their respective sources were:

Aspirin (acetylsalicylic acid), yohimbine, 5-HT (5-hydroxytryptamine-creatinine-sulphate-complex), ADP (adenosine 5'-diphosphate), L-ascorbic acid (Sigma, St. Louis, MO., U.S.A.), ketanserin tartrate (Research Biochemicals Natick, MA., U.S.A.), adrenaline tartrate (David Bull Laboratories, Melbourne, Australia). All concentrations are expressed as final concentrations in PRP.

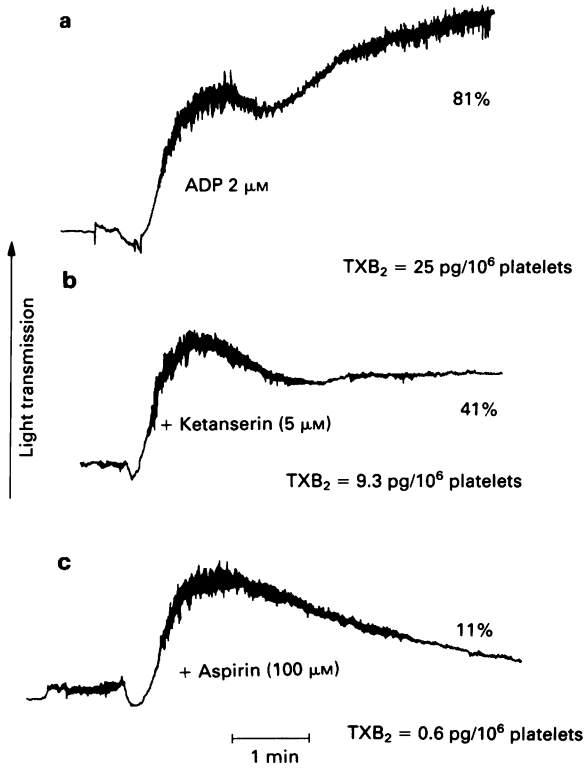

Figure 1 Platelet aggregation and thromboxane (TXB_2) production induced by adenosine 5'-diphosphate (ADP, 2 μM), after preincubation for 3 min with buffer (a), ketanserin (5 μM, b), or aspirin (100 μM, c).

Results

Responses induced by ADP

Ketanserin (5 μM) partially inhibited the second phase of aggregation induced by ADP (Figure 1), but did not affect primary aggregation. The inhibitory effect of ketanserin was observed for a range of ADP concentrations, resulting in a 2.3 fold increase in EC_{50} and a decrease in maximal aggregation response from 93 (g.s.e. 1.02) to 79 (g.s.e. 1.02)% (Figure 2a). Ketanserin also inhibited ADP-induced TXA_2 generation, resulting in a 1.8 fold increase in EC_{50} (Figure 2b). The results indicate that 5-HT released from the platelets contributes significantly to both aggregation and TXA_2 generation.

Aspirin completely inhibited the second phase of aggregation and TXA_2 generation induced by ADP (Figure 1). The inhibitory effect of aspirin on EC_{50} values for ADP-induced aggregation is shown in Tables 1 and 2. Yohimbine (9 μM) had no effect on ADP-induced aggregation or TXA_2 generation (data not shown).

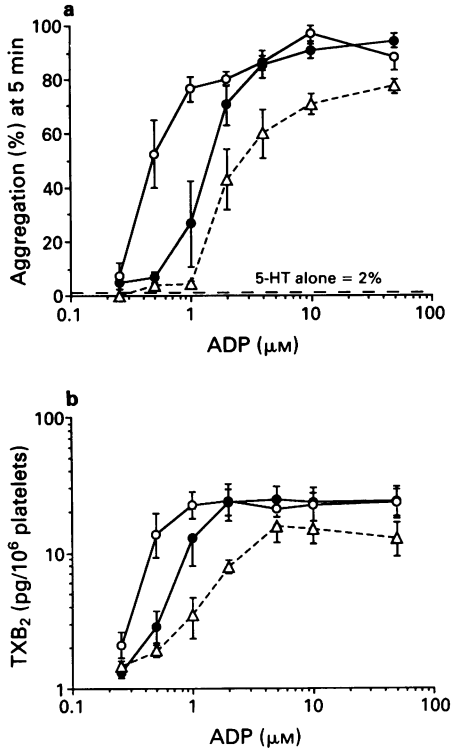

Figure 2 The effect of 5-hydroxytryptamine (5-HT) or ketanserin on platelet aggregation (a) and thromboxane generation (b) induced by adenosine 5'-diphosphate (ADP). Results are shown for 5-HT (10 μM) + ADP (○), ADP alone (●) and ADP + ketanserin (△). All points show geometric mean with s.e.mean shown by vertical bars ($n = 8$). Aggregation EC_{50} values were 0.5 μM, 1.0 μM and 2.3 μM respectively. Thromboxane EC_{50} values were 0.41 μM, 0.75 μM and 1.41 μM respectively. 5-HT (10 μM) alone induced 2 ± 1.13% aggregation (indicated by broken horizontal line) and 0.84 ± 1.63 pg thromboxane.

Responses induced by ADP and 5-HT

When examining the effect of 5-HT concentrations of 1–50 μM, potentiation of ADP-induced aggregation was found to be dose-dependent and maximal at 10 μM 5-HT. This concentration of 5-HT alone caused only 2 (g.s.e. 1.1)% platelet aggregation and TXA_2 production was negligible (0.84 (g.s.e. 1.6) pg/10^6 platelets). Prior addition of 5-HT (10 μM) caused potentiation of aggregation shown by a leftward shift of the dose-response curve to ADP (Figure 2a,b) resulting in a concentration ratio (CR) of 2.1 for ADP-induced platelet aggregation (Table 1) and 1.8 (g.s.e. 1.2) for TXA_2 generation. No increase in maximum for either response was observed.

However, as demonstrated above, endogenous (or released) 5-HT contributes to aggregation induced by ADP alone. Therefore the true aggregation induced by ADP alone is that observed in the presence of ketanserin. Hence enhancement of ADP responses by 5-HT in our study was quantitated as the combined effect of added and endogenous 5-HT, resulting in a CR of 5.0 for platelet aggregation (Figure 2a, Table 1) and 3.4 (g.s.e. 1.2) for TXA_2 generation (Figure 2b).

The effect of inhibitors on responses to ADP potentiated by 5-HT

Ketanserin The effect of added 5-HT (10 μM) on ADP-induced aggregation and TXA_2 generation was inhibited by ketanserin in a dose-dependent manner, (IC_{50} 0.53 (g.s.e. 1.2) μM). The effect of 5 μM ketanserin on the platelet aggregation responses is shown in Table 1.

Aspirin Aspirin caused inhibition of the aggregation response induced by a combination of ADP and 5-HT (CR 3.4, Table 1). However, in the presence of aspirin, ADP-induced aggregation was still potentiated by 5-HT (10 μM), with a CR of 2.3 (Table 1).

Ketanserin + aspirin In the presence of aspirin, ketanserin inhibited the potentiation by 5-HT of ADP-induced aggregation in a dose-dependent manner (IC_{50} 0.52 (g.s.e. 1.4) μM). Ketanserin (5 μM), in combination with aspirin, inhibited aggregation induced by ADP and 5-HT (CR 6.5) further than did aspirin alone (CR 3.4, Table 1).

Responses induced by ADP and adrenaline

The subthreshold concentration of adrenaline (0.25 ± 0.05 μM) caused 2 (g.s.e. 1.9)% platelet aggregation and TXA_2 production was negligible, 1.5 (g.s.e. 1.33) pg/10^6 platelets. Prior addition of this concentration of adrenaline (0.25 μM), resulted in a marked enhancement of ADP-induced aggregation. This resulted in a leftward shift of the ADP dose-response curve (Figure 3a) and a CR of 4.0 for aggregation (Table 2) and 3.5 (g.s.e. 1.2) for TXA_2 generation. No significant increase in maximal aggregation was observed. Maximal TXA_2 generation increased from 32.5 (g.s.e. 1.17) to 59.4 (g.s.e. 1.2) pg/10^6 platelets.

The effect of inhibitors on responses to ADP potentiated by adrenaline

Yohimbine Yohimbine (9 μM) inhibited the potentiation by adrenaline of ADP-induced aggregation and TXA_2 generation (results not shown).

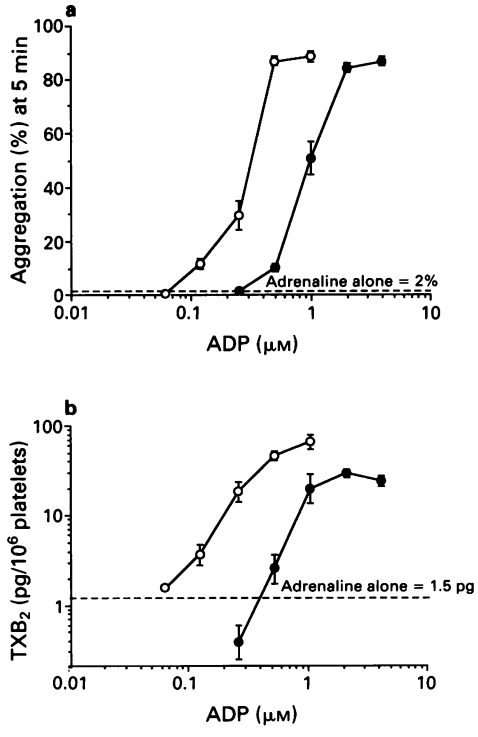

Figure 3 The effect of adrenaline on platelet aggregation (a) and thromboxane generation (b) induced by adenosine 5'-diphosphate (ADP). Results are shown for adrenaline (0.25 μM) + ADP (○) and ADP alone (●). All points show geometric mean with s.e.mean shown by vertical bars ($n = 8$). Aggregation EC_{50} values were 0.2 μM and 0.8 μM respectively. Thromboxane EC_{50} values were 0.24 μM and 0.82 μM respectively. Adrenaline (0.25 μM) alone induced 2 ± 1.9% aggregation and 1.51 ± 1.3 pg thromboxane (indicated by broken horizontal line).

Aspirin Aggregation induced by adrenaline and ADP in combination, was reduced by aspirin (CR 5.1, Table 2). However, in the presence of aspirin, ADP-induced aggregation was still potentiated by adrenaline (0.25 μM) with a CR of 2.0 (Table 2). Increasing potentiation occurred with escalating concentrations of adrenaline, with maximal potentiation achieved with 10 μM, which resulted in a CR of 7.5 (g.s.e. 1.16), ($n = 4$) (results not shown).

Yohimbine and aspirin Yohimbine, in combination with aspirin, caused further inhibition of the aggregation induced by ADP and adrenaline (CR 10.0), than did aspirin alone (CR 5.1, Table 2). In the presence of aspirin, yohimbine inhibited potentiation by adrenaline of ADP-induced aggregation in a dose-dependent manner (Table 2) (IC_{50} 0.22 (g.s.e. 1.36) μM). Yohimbine (9 μM) completely inhibited the effect of added adrenaline, and the EC_{50} for aggregation was then 2.2 μM, the same as for ADP alone in the presence of aspirin (Table 2).

Discussion

We have used complete dose-response curves to show that there was a synergistic interaction for aggregation and thromboxane generation achieved by 5-HT and adrenaline in combination with ADP. To identify true synergism it was necessary to demonstrate a parallel shift to the left of the dose-response curve to one agonist in the presence of a threshold concentration of the other. If an interaction between two agonists is additive rather than synergistic, the dose-response curve for the combined agonists will not be parallel to the dose-response curve for one agonist alone (Draskóczy & Trendelenburg, 1968; Asano & Hidaka, 1980). A superadditive response to a combination of threshold doses of two agonists, as reported in the great majoritiy of previous studies (Kinlough-Rathbone & Mustard, 1986), is therefore not sufficient if true synergism is to be demonstrated.

We have shown that the aggregation response induced by either 5-HT or adrenaline in combination with ADP was synergistic, both in the presence and absence of aspirin. Several studies have demonstrated synergism between platelet agonists in the absence of a cyclo-oxygenase inhibitor (Mills & Roberts, 1967; Michal & Motamed, 1976; Osmani *et al.*, 1983; Steen & Holmsen, 1985). In the presence of a cyclo-oxygenase inhibitor, synergism between ADP and adrenaline or 5-HT was observed only when aggregation was measured by light transmission, but not by decrease in numbers of single platelets in suspension (Thompson *et al.*, 1986). Ours is the first study in which synergism has been investigated both in the presence and absence of aspirin. This has allowed us to assess the contribution of TXA_2 to the synergistic aggregation response.

To quantitate the effects of 5-HT and adrenaline on the ADP response it was necessary first to assess the effects of released (endogenous) 5-HT and adrenaline on the response to ADP alone. When specific inhibitors of these substances were added to platelets prior to ADP, yohimbine was without effect, but ketanserin had an inhibitory effect on the second phase of ADP-induced platelet aggregation. We can conclude therefore, in agreement with previous investigators, that endogenous 5-HT contributes significantly to the second phase of the ADP-induced aggregation response (Bevan & Heptinstall, 1983; De Clerck & Xhonneux, 1985; Heptinstall *et al.*, 1988). In this study we have extended this observation, which in the earlier studies examined aggregation induced by critical agonist concentrations only, to show that ketanserin (5 μM) inhibits both aggregation and TXA_2 generation induced by a range of concentrations of ADP. This finding shows that released 5-HT stimulates the production of TXA_2. Although ketanserin is a selective 5-HT_2 receptor antagonist, it has a moderate α_1-adrenoceptor antagonist effect (Leysen *et al.*, 1981). Kerry & Scrutton (1985) have demonstrated that platelet α_1-adrenoceptor density on platelets is negligible. There has been no reported evidence of ketanserin binding to purinoceptors, which is consistent with the fact that no decrease in ADP-induced primary aggregation was seen. The effect of ketanserin on secondary aggregation induced by ADP is therefore due to blockade of 5-HT_2 receptors and inhibition of positive feedback aggregation and thromboxane generating responses caused by released endogenous 5-HT.

When 5-HT was added prior to ADP, there was a parallel shift to the left for both aggregation and thromboxane formation, confirming previous aggregation results in rabbit platelets (Michal & Motamed, 1976). The degree of shift was more marked when endogenous 5-HT was taken into account. If ADP-induced aggregation and thromboxane formation in the presence of ketanserin are considered the true baseline ADP responses, then an increase in maximum as well as a leftward shift by the addition of 5-HT was observed. In the presence of aspirin, 5-HT retained its ability to enhance ADP-induced aggregation. This effect was less (CR 2.3) than in the absence of aspirin (CR 5.0). Therefore the effect of 5-HT on ADP-induced aggregation is enhanced by, but does not depend on, TXA_2 production. De Clerck *et al.* (1982) found that the effect of 5-HT on ADP-induced aggregation was of the same magnitude whether or not TXA_2 was inhibited, but it is not clear whether the effects of endogenous 5-HT were taken into account.

Experiments with adrenaline also showed a parallel shift to the left of the ADP dose-response curves for both aggregation and TXA_2 generation, confirming previous aggregation data (Mills & Roberts, 1967). The CR of 4.0 achieved for aggregation was reduced to 2.0 in the presence of aspirin, indicating that some of the potentiation previously observed was TXA_2-dependent. However in the presence of aspirin, a sub-threshold dose of adrenaline was still able to potentiate the aggregation response induced by ADP (CR 2.0). Furthermore, in the presence of aspirin, higher doses of adrenaline caused marked potentiation (CR 7.5) of ADP-induced aggregation by a TXA_2-independent mechanism. This extends preliminary observations by Cameron & Ardlie (1982) that critical concentrations of adrenaline and ADP interact to cause a greater than additive response in the presence or absence of aspirin, and Rao *et al.* (1980) who showed that in aspirin-treated platelets, adrenaline (2.5 μM) caused the previously monophasic response induced by ADP (2 μM) to become irreversible. We have quantitated both TXA_2-dependent and independent potentiation by adrenaline of ADP-induced aggregation, and demonstrated that adrenaline and ADP interact in a truly synergistic manner. The intracellular pathways involved remain to be identified.

After examining the nature of the potentiation mechanisms of adrenaline and 5-HT, we considered the ability of the specific 5-HT and adrenaline antagonists, ketanserin and yohimbine, alone and in combination with aspirin, to inhibit the synergistic responses between dual agonists. While previous studies have shown yohimbine and ketanserin effectively inhibit potentiation of platelet responses by adrenaline and 5-HT, to our knowledge the combination of these agents with aspirin has not been reported.

The combination of ketanserin (0.5–5 μM) and aspirin inhibited the platelet aggregation response induced by 5-HT and ADP further than either agent alone. The IC_{50} of ketanserin obtained in our study (0.52 μM) was similar to that obtained in several other *in vitro* studies (Arnout *et al.*, 1985; Schächter *et al.*, 1985), and is consistent with levels shown to be effective *in vivo* (The PACK trial group, 1989). Much lower IC_{50} levels were obtained in some other studies in PRP (16.6 nM, De Clerck *et al.*, 1982; 23 nM, De Clerck *et al.*, 1984; 33 nM, Glusa & Markwardt, 1984). The difference in IC_{50} between these last studies and our study cannot be explained by the 95% protein binding of ketanserin in plasma (Persson *et al.*, 1991), or by uncontrolled platelet storage pH previously stated as the reason for a lower

potency of ketanserin (De Clerck et al., 1985). Our storage conditions, of platelet-rich plasma in an air-free syringe at 37°C, ensure that pH is maintained at 7.3–7.4 throughout the experiment (Watts et al., 1985).

Yohimbine inhibited the enhancement by adrenaline of ADP-induced platelet aggregation, indicating that this enhancement is mediated by α_2-adrenoceptors, as shown previously by others (Grant & Scrutton, 1979; Lanza & Cazenave, 1985). Enhancement by adrenaline of the aggregation response was inhibited to a certain degree in the presence of aspirin alone, but when yohimbine was also present the remaining potentiation was maximally inhibited. In previous studies, not however in the presence of aspirin, yohimbine has been shown to inhibit effectively potentiation by adrenaline of ADP-induced aggregation in PRP (Grant & Scrutton, 1979), with IC_{50} (0.5–1.2 μM) values similar to those obtained in our study (0.22 μM). This is similar to the plasma yohimbine concentration (0.19 μM) achieved *in vivo* after a 10 mg oral dose (Owen et al., 1987), or an 8 mg oral dose (Berlin et al., 1991) which was shown to inhibit effectively platelet aggregation induced by adrenaline (5 μM). Our results are in agreement with those of Rao et al. (1981) who showed that yohimbine (5–10 μM) blocked potentiation by adrenaline of sodium arachidonate-induced aggregation in PRP from donors who had taken aspirin (80 mg, single dose). In washed platelets the IC_{50} (19.5 nM, Lanza & Cazenave, 1985) for the inhibition of potentiation of ADP (1 μM)-induced aggregation by adrenaline (0.5 μM), was lower than in our study in PRP, suggesting that plasma protein binding of the drug may be occurring in PRP.

The maximal potentiating concentration of adrenaline (10 μM) and 5-HT (10 μM) produced a CR of 7.5 and 2.3 respectively, in the presence of aspirin. Therefore adrenaline is more potent for potentiating ADP-induced aggregation in this experimental system. Conversely, the platelet adrenaline content (23 pmol/2.86 × 10^8 platelets) is approximately three orders of magnitude lower than 5-HT (1 μmol/2.86 × 10^8 platelets) (Da Prada & Picotti, 1979). The concentrations of 5-HT and ADP used in this study are within the plasma concentration range that can be achieved after maximal platelet secretion (Meyers et al., 1982). The concentration of adrenaline is approximately 100 times greater than circulating *in vivo* catecholamine concentrations (Ardlie et al., 1984) although this does not take into account conditions of stress or the higher local agonist concentrations which occur in the platelet microenvironment at the site of a thrombus.

Yohimbine or ketanserin have the potential to be used in combination with aspirin as antiplatelet agents *in vivo*. Apart from their action as mediators of platelet aggregation, 5-HT and TXA_2 are also potent vasoconstrictors and inducers of vasospasm, which in conjunction with intracoronary platelet aggregation, may play a crucial role in the genesis of unstable angina and myocardial infarction (Fitzgerald et al., 1986; Mehta, 1990). Ketanserin, in combination with thromboxane receptor antagonists, but not singly, has been reported to inhibit coronary artery reocclusion following thrombolytic therapy with tissue plasminogen activator in canines (Golino et al., 1988), and similarly aspirin has been successful in this regard after streptokinase therapy in man (ISIS-2 collaborative group, 1988). The combination of aspirin and ketanserin to inhibit potentiation by 5-HT of platelet and blood vessel responses may therefore prove to be more successful in the primary and secondary prevention of myocardial ischaemia than aspirin alone.

References

ARDLIE, N.G., CAMERON, H.A. & GARRETT, J. (1984). Platelet activation by circulating hormones: a possible link in coronary heart disease. *Thromb. Res.*, **36**, 315–322.

ARNOUT, J., VAN RUSSELT, M., DECKMYN, H., VERMYLEN, J., FIOCCHI, R., LIJNEN, P. & AMMERY, A. (1985). Platelet hypersensitivity to 5HT after prolonged ketanserin intake? *J. Cardiovasc. Pharmacol.*, **7**, S20–22.

ASANO, M. & HIDAKA, H. (1980). Potentiation of the contractile response to acetylcholine in aortic strips by low concentrations of vascular contractile agents. *Br. J. Pharmacol.*, **69**, 639–646.

BERLIN, I., CRESPO-LAUMONNIER, B., COURNOT, A., LANDAULT, C., ENG, C., AUBIN, F., LEGRAND, J.C. & PUECH, A.J. (1991). The α_2-adrenergic receptor antagonist yohimbine inhibits epinephrine-induced platelet aggregation in healthy subjects. *Clin. Pharmacol. Ther.*, **49**, 362–369.

BEVAN, J. & HEPTINSTALL, S. (1983). Effects of ketanserin and mepyramine on platelet aggregation and on the uptake of 5-hydroxytryptamine into platelets. *Thromb. Res.*, **30**, 415–423.

BRITT, S.G., GONIAS, S.L., SANDERS, J.M. & VAN DENBERG, S.R. (1988). Agonists and antagonist activities of arylpiperazines at human platelet serotonin$_2$ receptors. *J. Pharmacol. Exp. Ther.*, **247**, 965–970.

CAMERON, H.A. & ARDLIE, N.G. (1982). The facilitating effects of adrenaline on platelet aggregation. *Prostaglandin Leukot. Med.*, **9**, 117–128.

DA PRADA, M. & PICOTTI, D. (1979). Content and subcellular localization of catecholamines and 5-hydroxytryptamine in human and animal blood platelets: monoamine distribution between platelets and plasma. *Br. J. Pharmacol.*, **65**, 653–662.

DE CLERCK, F., DAVID, J.L. & JANSSEN, P.A.J. (1982). Inhibition of 5-hydroxytryptamine-induced and -amplified human platelet aggregation by ketanserin (R41 468), a selective $5HT_2$ receptor antagonist. *Agents Actions*, **12**, 388–397.

DE CLERCK, F. & DE CHAFFOY DE COURCELLES, D. (1990). Serotonergic amplification in platelet function: mechanisms and in vivo relevance. *Prog. Pharmacol. Clin. Pharmacol.*, **7**, 51–59.

DE CLERCK, F. & XHONNEUX, B. (1985). Effects of ketanserin, a selective $5HT_2$ serotonergic antagonist, on the secondary recruitment of human platelets in vitro. *Agents Actions*, **17**, 515–526.

DE CLERCK, F., XHONNEUX, B., LEYSEN, J. & JANSSEN, P.A.J. (1984). Evidence for functional $5\text{-}HT_2$ receptor sites on human blood platelets. *Biochem. Pharmacol.*, **33**, 2807–2811.

DE CLERCK, F., XHONNEUX, B., TOLLENAERE, J.P. & JANSSEN, P.A.J. (1985). Dependence of the antagonism at human platelet $5HT_2$-receptors by ketanserin on reaction pH. *Thromb. Res.*, **40**, 581–596.

DIXON, W.J. & MASSEY, F.J. Jr. (1969). *Introduction to Statistical Analysis*, p 163. Third edition. New York: McGraw-Hill.

DRASKOCZY, P.R. & TRENDELENBURG, U. (1968). The uptake of l- and d-norepinephrine by the isolated perfused rabbit heart in relation to the stereospecificity of the sensitizing action of cocaine. *J. Pharmacol. Exp. Ther.*, **159**, 66–73.

FITZGERALD, D.J., ROY, L., CATELLA, F. & FITZGERALD, G.A. (1986). Platelet activation in unstable coronary artery disease. *New Engl. J. Med.*, **315**, 983–989.

FLEMING, W.W., WESTFALL, D.P., DE LA LANDE, I.S. & JELLET, L.B. (1972). Log-normal distribution of equieffective doses of norepinephrine and acetylcholine in several tissues. *J. Pharm. Exp. Ther.*, **181**, 339–345.

GOLINO, P., ASHTON, J.H., GLAS-GREENWAKT, B., MCNATT, J., BUJA, L.M. & WILLERSON, J.T. (1988). Mediation of reocclusion by thromboxane A2 and serotonin after thrombolysis with tissue plasminogen activator in a canine preparation of coronary thrombolysis. *Circulation*, **77**, 678–684.

GLUSA, E. & MARKWARDT, P. (1984). Inhibition of 5-hydroxytryptamine-potentiated aggregation of human blood platelets by 5-hydroxytryptamine receptor blocking agents. *Biomed. Biochim. Acta.*, **43**, 215–220.

GRANT, J.A. & SCRUTTON, M.C. (1979). Novel α_2-adrenoreceptors primarily responsible for inducing human platelet aggregation. *Nature*, **277**, 659–661.

HEPTINSTALL, S., BEVAN, J., HAWKINS, M. & SANDLER, D.A. (1989). Measurements of platelet aggregation in a clinical study of ketanserin in peripheral vascular disease. *Br. J. Clin. Pharmacol.*, **27**, 122P.

HERD, C.M., RODGERS, S.E., TUNBRIDGE, L.J., DUNCAN, E.M., LLOYD, J.V. & BOCHNER, F. (1987). A dose ranging study of the antiplatelet effect of enteric coated aspirin in man. *Austral. N.Z.J. Med.*, **17**, 195–200.

HOLMSEN, H. (1982). Platelet secretion. In *Haemostasis and Thrombosis* ed. Colman, R.W., Hirsh, J., Marder, V.J. & Salzman, E.W. pp. 390–403. Philadelphia: J.B. Lippincott.

ISIS-2 (1988). (Second International Study of Infarct Survival) Collaborative group: randomised trial of intravenous streptokinase, oral aspirin, both or neither in 17,187 cases of acute myocardial infarction. *Lancet*, **ii**, 349–360.

KERRY, R. & SCRUTTON, M.C. (1985). Platelet adrenoceptors. In *The Platelets: Physiology and Pharmacology*. ed. Longenecker, G.L. pp. 113–157. Orlando, Fla: Academic Press Inc.

KINLOUGH-RATHBONE, R.L. & MUSTARD, J.F. (1977). Synergism between platelet aggregating agents: the role of the arachidonate pathway. *Thromb. Res.*, **11**, 567–580.

KINLOUGH-RATHBONE, R.L. & MUSTARD, J.F. (1986). Synergism of agonists. In *Platelet Responses and Metabolism*, Vol. 1. ed. Holmsen, H. pp. 193–207. Florida: CRC press.

KINLOUGH-RATHBONE, R.L., PACKHAM, M. & MUSTARD, J.F. (1983). Platelet aggregation. In *Methods in Haematology. Measurements of Platelet Function* ed. Harker, L.A. & Zimmerman, L.A. pp. 64–91. New York: Churchill Livingstone.

LANZA, F. & CAZENAVE, F. (1985). Studies of α_2-adrenergic receptors of intact and functioning washed human platelets by binding of ^{3}H-dihydroergocryptine and ^{3}H-yohimbine–correlation of ^{3}H-yohimbine binding with potentiation by adrenaline of ADP-induced aggregation. *Thromb. Haemostas.*, **54**, 402–408.

LEYSEN, J.E., AWOUTERS, F., KENNIS, L., LADURON, P.M., VANDENBERK, J. & JANSSEN, P.A.J. (1981). Receptor binding profile of R 41368, a novel antagonist at 5-HT2 receptors. *Life Sci.*, **28**, 1015–1022.

MEHTA, J.L. (1990). Platelet activation in unstable angina: role of thromboxane A2 and other mediators of vasoconstriction. *J.A.C.C.*, **15**, 727–729.

MEYERS, K.M., HOLMSEN, H. & SEACHORD, C.L. (1982). Comparative studies of platelet dense granule constituents. *Am. J. Physiol.*, **243**, R454–461.

MICHAL, F. & MOTAMED, M. (1976). Shape change and aggregation of blood platelets: interaction between the effects of adenosine diphosphate, 5-hydroxytryptamine and adrenaline. *Br. J. Pharmacol.*, **56**, 209–218.

MILLS, D.C.B., ROBB, I.A. & ROBERTS, G.C.K. (1968). The release of nucleotides, 5-hydroxytryptamine and enzymes from human blood platelets during aggregation. *Am. J. Physiol.*, **195**, 715–729.

MILLS, D.C.B. & ROBERTS, G.C.K. (1967). Effects of adrenaline on human blood platelets. *Am. J. Physiol.*, **193**, 443–453.

OSMANI, A.H., CLARE, K.A. & SCRUTTON, M.C. (1983). Synergistic interaction and platelet inhibitory agents. *Thromb. Res.*, **31**, 665–674.

OWEN, J.A., NAKATSU, S.L., FENEMORE, J., CONDRA, M., SURRIDGE, D.H.C. & MORALES, A. (1987). The Pharmacokinetics of yohimbine in man. *Eur. J. Clin. Pharmacol.*, **32**, 577–582.

PERSSON, B., HEYKANTS, J. & HEDNER, T. (1991). Clinical pharmacokinetics of ketanserin. *Clin. Pharmacol.*, **20**, 263–279.

RAO, G.H.R., REDDY, R.K. & WHITE, J.G. (1980). Influence of epinephrine on the aggregation response of aspirin treated platelets. *Prostaglandin Medicine*, **5**, 45–58.

RAO, G.H.R., REDDY, R.K. & WHITE, J.G. (1981). Low dose aspirin, platelet function and prostaglandin synthesis: influence of epinephrine and alpha adrenergic blockade. *Prostaglandin Med.*, **6**, 488–494.

SCHÄCHTER, M., GODFREY, P.P., MINCHIN, M.C.W., MCCLUE, S.J. & YOUNG, M.M. (1985). Serotonergic agonists stimulate inositol lipid metabolism in rabbit platelets. *Life Sci.*, **37**, 1641–1647.

STEEN, V.M. & HOLMSEN, H. (1985). Synergism between thrombin and adrenaline in human platelets: different dose-response relationships for aggregation and dense granule secretion. *Thromb. Haemostas.*, **54**, 680–683.

THE PACK TRIAL GROUP (1989). Platelet function during long-term treatment with ketanserin of claudicating patients with peripheral atherosclerosis. A multi-centre, double-blind, placebo-controlled trial. *Thromb. Res.*, **55**, 13–23.

THOMAS, D.P. (1967). Effects of catecholamines on platelet aggregation caused by thrombin. *Nature*, **215**, 298–299.

THOMPSON, N.T., SCRUTTON, M.C. & WALLIS, R.B. (1986). Synergistic responses in human platelets: comparison between aggregation, secretion and cytosolic calcium concentration. *Eur. J. Biochem.*, **161**, 399–408.

WATTS, S.E., TUNBRIDGE, L.J., DUNCAN, E.M. & LLOYD, J.V. (1985). Storage of platelets for tests of platelet function: comparison of two methods of pH control. *Thromb. Res.*, **37**, 73–83.

(Received November 21, 1991
Revised March 4, 1992
Accepted April 9, 1992)

Br. J. Pharmacol. (1992), **106**, 924–930 © Macmillan Press Ltd, 1992

Effects of K^+ channel blockers on the action potential of hypoxic rabbit myocardium

[1]Elena Ruiz Petrich, [2]Normand Leblanc, [3]Fabien deLorenzi, [2]Yvon Allard & Otto F. Schanne

Department of Physiology and Biophysics, Faculty of Medicine, University of Sherbrooke, Sherbrooke, Québec, Canada J1H 5N4

1 In order to assess the role of different ionic currents in hypoxia-induced action potential shortening, we investigated the effects of blockers of voltage-dependent and ATP-sensitive K^+-channels on the membrane potential of hypoxic rabbit hearts and papillary muscles. The response to blocking of the inward rectifier was studied at three external K^+ concentrations: 2.5, 5, and 7.5 mM.

2 Hypoxia produced a progressive decline in action potential duration (APD) that levelled off after 15 to 20 min. Steady state APD values at 25% and 95% repolarization (APD_{25} and APD_{95}) were 26.0 ± 1.9% and 42.2 ± 2.4% of controls respectively.

3 Tetraethylammonium (TEA, 10 mM) delayed but did not reduce APD shortening at the steady state.

4 Blocking of I_{K1} with a mixture of 0.2 mM Ba^{2+} and 4 mM Cs^+ lengthened APD in normoxia and prevented APD_{95} shortening in hypoxia. The APD_{25} shortening was significantly attenuated at all $[K]_o$.

5 Glibenclamide (Glib, 30 μM) did not prevent APD shortening, but produced a progressive action potential (AP) lengthening after 15 min of hypoxia. Steady levels of 48 ± 3.5% and 62 ± 5.0% of controls for APD_{25} and APD_{95} respectively were reached after 45 min.

6 The relation between APD_{25} and pacing rate was determined in normoxic and hypoxic papillary muscles and the effects of 2 mM 4-aminopyridine (4-AP) were examined. Hypoxia attenuated the APD_{25} shortening currently observed when the stimulation rate was lowered from 1 to 0.1 Hz without altering the plateau reduction occurring at frequencies above 2 Hz. These effects were potentiated by 4-AP.

7 Our data suggest that the accelerated AP repolarization in hypoxic rabbit myocardium represents a delicate balance of several outward currents: I_{K1}, $I_{K\text{-}ATP}$, and at least one yet unidentified current component rather insensitive to changes in $[K]_o$ and to K^+ channel blockers.

Keywords: Hypoxic cardiac muscle; K^+ channel blockers; action potential shortening; I_{K1}; $I_{K\text{-}ATP}$; I_{to}

Introduction

Hypoxia is not only an element of ischaemia but a common sequela of cardiovascular and respiratory disease as well as of anaemia. It has long been recognized that the earliest effect of hypoxia on the cardiac action potential is a marked shortening (Carmeliet, 1978) resulting from a great increase in outward current (Isenberg *et al.*, 1983). The discovery of adenosine 5'-triphosphate (ATP)-sensitive K^+ channels in myocardium by Noma (1983), and subsequent work led to the proposition that activation of these channels underlies the increased outward current observed during metabolic inhibition (Noma & Shibasaki, 1985) as well as the cellular K^+ loss produced by ischaemia (Gasser & Vaughan-Jones, 1990; Wilde *et al.*, 1990). However, discrepancies exist between threshold levels of ATP required for channel opening and the decline in cytosolic ATP measured in whole hearts (Elliot *et al.*, 1989). Cytosolic ATP compartmentation (Weiss & Lamp, 1987), inhomogeneities in ATP distribution (Nichols & Lederer, 1990), and variability of channel sensitivity to ATP (Findlay & Faivre, 1991) have been invoked to explain them. Since the direct and simultaneous measurement of the ATP level in close proximity to the channels and of the current resulting from their opening is not yet possible in intact cells or tissues, blocking of these channels with sulphonylureas has been used to assess the role of $I_{K\text{-}ATP}$ in the action potential (AP) shortening. Some inconsistencies were also found with this approach. Glibenclamide only partially reversed the AP shortening induced by DNP in cardiocytes (Fosset *et al.*, 1988), by hypoxia in papillary muscles (Wilde *et al.*, 1990), and by ischaemia in canine myocardium (Nakaya *et al.*, 1991) whereas AP shortening was completely blocked when induced by ATP depletion (Fosset *et al.*, 1988) or by pinacidil application (deLorenzi *et al.*, 1991). In addition, in hypoxic rabbit hearts blockade of the inward rectifying current I_{K1} antagonized AP shortening near full repolarization but much less so at plateau level (Ruiz-Petrich *et al.*, 1991). It is therefore possible that more than one K conductance is involved in the electrical response of myocardium to metabolic stress compatible with cell survival.

To test that hypothesis, we examined the effects of different K^+ channel blockers on the action potential of rabbit perfused hearts and papillary muscles subjected to mild hypoxia in the presence of glucose. Although tetraethylammonium (TEA) is a rather unspecific blocker of K channels (Stanfield, 1983), we used it as a first approach to assess the role of hypoxia-induced K^+ currents in plateau depression because: (a) 10 mM TEA reduces the K loss in hypoxic rabbit hearts (Leblanc *et al.*, 1987), (b) the plateau shortening is rather insensitive to blockade of I_{K1} with 40 μM Ba^{2+} (Ruiz Petrich *et al.*, 1991), and (c) at low concentrations, TEA should selectively block the delayed rectifier but not the early outward current or I_{K1} (Stanfield, 1983).

Because of the known voltage- and time-dependence of I_{K1} blockade by Ba^{2+} (Hirano & Hiraoka, 1988), we used a combination of 200 μM $BaCl_2$ and 4 mM CsCl to achieve a time- and voltage-independent block of I_{K1}. The effect of varying the external K^+ concentration $[K]_o$ was also tested

[1] Author for correspondence.
[2] Present address: Division of Cardiovascular Sciences, St Boniface General Hospital Research Centre, University of Manitoba, Faculty of Medicine, 351 Tache Ave, Winnipeg, Manitoba, Canada R2H 2A6.
[3] Present address: Wyeth Ayerst, Research, Cardiovascular and Metabolic Disorders Division, Princeton, N.J. 08543-8000, U.S.A.

because of the marked influence of $[K]_o$ on electrogenesis through modifications of the resting membrane potential (RMP) and direct modulation of I_{K1}.

Because of its widely accepted specificity (Arena & Kass, 1989), we used glibenclamide as a blocker of $I_{K\text{-}ATP}$. Since in our hands, none of these blockers completely reversed the reduction of the plateau duration induced by hypoxia, we assessed the possible contribution of the transient outward current I_{to} to the plateau shortening by studying the frequency-dependence of the action potential duration in papillary muscles in normoxia and hypoxia with and without 4-AP. Because of its slow reactivation kinetics (Hiraoka & Kawano, 1987) the 4-AP-sensitive fraction of I_{to} plays a greater role in determining plateau duration at frequencies below 1 Hz to 2 Hz (Hiraoka & Kawano, 1989; Ruiz Petrich & Leblanc, 1989). Papillary muscles were chosen for these experiments because they allowed us to perform continuous recordings from the same cell during long-lasting impalements.

Preliminary accounts of part of this work have appeared in abstract form (Leblanc & Ruiz-Ceretti, 1986; deLorenzi *et al.*, 1990; 1991).

Methods

Experimental models

New Zealand rabbits of either sex weighing 1.5 to 2 kg were killed by cervical dislocation or anaesthetized with a mixture of ketamine (35 mg kg^{-1}) and xylazine (5 mg kg^{-1}) by intramuscular injection. The heart was rapidly removed and rinsed in cold (10°C), oxygenated (95% O_2 : 5% CO_2) Krebs solution.

Perfused hearts

After removal of the pericardium, great veins and connective tissue, the heart was quickly placed in the perfusion apparatus where retrograde aortic perfusion was started at a rate of 20 ml min^{-1} and constant temperature of 33 ± 1.0°C (monitored by an intraventricular thermistor).

The region of the sino-atrial node and adjacent right atrial tissue were removed and the ventricles were driven at a frequency of 2.5 Hz (2 ms long pulses of 1.5 times threshold strength) by means of bipolar platinum electrodes placed at the base of the right ventricle. The preparations were equilibrated for 20 min

Papillary muscle and trabeculae

Papillary muscles and ventricular trabeculae (2–3 mm long and less than 1 mm thick) were excised from the right ventricle. The dissection was carried out in a low calcium (0.2 mM) Krebs solution at room temperature. The preparation was then transferred into a 0.5 ml superfusion chamber lined with Sylgard (Dow Corning, Midland, U.S.A.). One end of the muscle was pinned to the bottom of the chamber and the other was attached to a platinum wire pinned down in the Sylgard. Superfusion was then started at the rate of 5–8 ml min^{-1}. The temperature (33 ± 1°C) was monitored by a thermistor placed near the preparation. The muscle was first superfused without stimulation with the low calcium solution for 10 min followed by 15 min with normal Krebs solution. Stimulation (square pulses of 1 ms duration and 1.5 times the threshold strength) was then applied across the preparation through two platinum electrodes at 1 Hz. The frequency was chosen because higher rates of stimulation resulted in rapid depression of action potential parameters (decreased amplitude, rate of rise, and duration) in these preparations. An equilibration period of at least 45 min preceded experimentation. Dissection and initial superfusion with low calcium medium increased the yield of viable preparations to more than 80%.

Solutions and drugs

The standard perfusate (Krebs solution) had the following composition (mM): NaCl 120, $NaHCO_3$ 25, KH_2PO_4 1.2, KCl 3.8, $MgSO_4$ 1.2, $CaCl_2$ 1.25 and dextrose 5.5. In the experiments in which the potassium concentration was modified, the potassium phosphate buffer was replaced by sodium biphosphate, and KCl was added to the desired final concentration (2.5, 5, or 7.5 mM) without compensation for osmolarity changes. When equilibrated with a gas mixture of 5% CO_2 in O_2 or N_2, the pH was 7.3–7.4. The P_{O_2} of the solution entering the heart (samples obtained anaerobically with a three way stopcock inserted immediately before the aortic cannula, Allied Instrumentation gas analyser model 1312) was between 570 and 640 mmHg (1 mmHg = 133.32 Pa) in normoxia corresponding to an O_2 content between 1.83 and 2.05 ml O_2 100 ml^{-1}. The P_{O_2} declined to 43 to 75 mmHg (0.14 to 0.24 ml O_2 100 ml^{-1}) when the solution was equilibrated with 5% CO_2 in N_2. The P_{CO_2} was between 45.5 and 46.8 mmHg throughout. The P_{CO_2} values indicate that the samples were not significantly contaminated with ambient air. In the experiments with papillary muscles, a constant flow of humidified gas mixture (5% CO_2 in O_2 or N_2) was maintained over the superfusing chamber.

TEA-chloride was purchased from Aldrich Chemical Company (Milwaukee, U.S.A.). Glibenclamide and 4-AP were from Sigma Chemical Company (St Louis, U.S.A.). TEA and 4-AP were directly dissolved in the saline solution. Glibenclamide was dissolved in dimethylsulphoxide (DMSO) and appropriate amounts of the stock solutions were added to saline (0.05 to 0.5 ml l^{-1}) to reach the final concentrations. In 2 control experiments, addition of 0.5 ml l^{-1} DMSO did not modify cell electrical activity.

Recording techniques

In perfused hearts, the transmembrane potential of left ventricular subepicardial cells was recorded with floating glass microelectrodes and a silver-silver chloride reference electrode. Micropipettes were made of Pyrex glass (Corning 7740, 1 mm external diameter) with a vertical puller (David Kopf model 700 D; Tujunga, U.S.A.). When filled with 3 M KCl, the microelectrode resistance was 10 to 20 MΩ in Krebs solution. With papillary muscles and trabeculae, standard (non-floating) microelectrodes were used. The recording equipment consisted of a high impedance amplifier with capacity neutralization (WPI, model KS-700, Sarasota, U.S.A.) and a dual-beam storage oscilloscope (Tektronix 5113, Beaverton, U.S.A.). The traces were photographed with a C4 Grass camera and measured from enlargements under a microfilm reader. A Grass S88 stimulator with a stimulus isolation unit was used to drive the preparation.

Experimental protocols

Control experiments: after the equilbration period, recordings were obtained in normoxic conditions for 15 min followed by hypoxia for 1 h. Recovery in normoxia was tested for an additional 30 min. *Tetraethylammonium*: the perfusate contained 10 mM TEA during 20 min in normoxia followed by 30 min of hypoxia. *Experiments with Ba^{2+} – Cs^+*: three $[K]_o$ were tested: 2.5, 5 and 7.5 mM. Only one concentration was investigated per heart. An initial 20 min exposure to Ba^{2+} and Cs^+ in normoxia at a given $[K]_o$ was followed by 30 to 60 min of hypoxia at the same $[K]_o$. The rate of stimulation had to be lowered to 2 Hz because the blockers lengthened the late repolarization at all $[K]_o$ tested so that full repolarization could not be attained at higher rates. The same protocol was used in controls without blockers but with varied $[K]_o$. *Glibenclamide*: after a control period in normal

Krebs, glibenclamide (3, 10, or 30 μM) was added in normoxia and the action potential was monitored for 15 to 30 min. The effects of 60 min hypoxia in the presence of glibenclamide were then tested. *Papillary muscles*: control experiments were performed with the same protocol described for the perfused heart. In these preparations, continuous recordings of potential from the same cell could be maintained for up to 45 min. The frequency-dependence of the action potential duration was determined in single cells by step changes in frequency within the range 0.1 Hz to 4 Hz in normoxia and hypoxia with and without 2 mM 4-AP. Given the stability of the preparations and the reversibility of 4-AP effects, more than one cell could sometimes be studied in normoxic muscles. Only those relations where the APD value at 1 Hz was the same before and after changes in frequency were retained.

Statistical analysis

The data are presented as means ± s.e.mean from *n* experiments. In experiments with multiple impalements, individual values were measured and taken as data for that heart or muscle. For comparisons of two groups, the non-paired Student's *t* test was used. The s.e.mean of differences was calculated according to Meyer (1975). For comparisons involving more than two groups, an analysis of variance was used (Peritz F test) based on the advantages of Ryan's and Newman-Keuhl's tests for contentious comparisons. For both tests, a probability of error less than 0.05 was accepted as the level of significance. Some sets of data points were fitted with a least-square fitting method to a monoexponetial function.

Results

Perfused hearts

Action potential shortening in hypoxia: seven experiments were performed in normal Krebs (5 mM $[K^+]_o$) to determine the effects of reduced oxygen tension on action potential parameters. Stability of the preparations was assessed in pilot experiments where the membrane potential was monitored for 2 h in normoxia. No significant changes occurred during this observation period. The control record in Figure 1a shows the typical action potential of rabbit ventricle characterized by a fast upstroke and a well developed plateau. Hypoxia produced the well known AP shortening with early plateau depression (Figure 1a(ii)). By the end of 60 min of observation, the action potential had a triangular shape and the overshoot had markedly decreased (Figure 1a(iv)). No significant changes in RMP were observed. The maximum rate of rise of the upstroke ($\dot{V}_{max}$) was not significantly altered: 131 ± 4 Vs^{-1} in normoxia vs 122 ± 6 Vs^{-1} between 45 and 60 min of hypoxia. The change in APD with time in hypoxia was characterized by an early fast decline reaching new steady values after 10 to 20 min of hypoxia (Figure 1b, dashed curves). As a percentage, the decrease in APD was greater at the plateau level than at near full repolarization: after 60 min, APD_{25} was 26.6 ± 1.9% whereas APD_{95} was 42.2 ± 2.4% of the control. These effects were partly reversed (about 80%) by reperfusion with oxygenated solution (not shown).

Delay caused by tetraethylammonium of AP shortening in hypoxia: the effects of 10 mM TEA on the hypoxia-induced AP shortening were tested in 4 hearts. TEA did not affect RMP or APD_{25} in normoxia but slightly lengthened APD_{95} from 219 ± 2.3 ms to 225 ± 1.6 ms ($P<0.05$). In hypoxia, TEA slowed down the rate of APD shortening at both levels of repolarization (Figure 1b, continuous lines). Moreover, the onset of the APD_{95} decline was delayed (no significant change during the first 5 min). However, after 30 min of hypoxia, the APD values approached those observed without TEA. The initial delay of APD_{95} shortening and its absence in APD_{25} reduction suggested that more than one outward current was involved in early AP shortening.

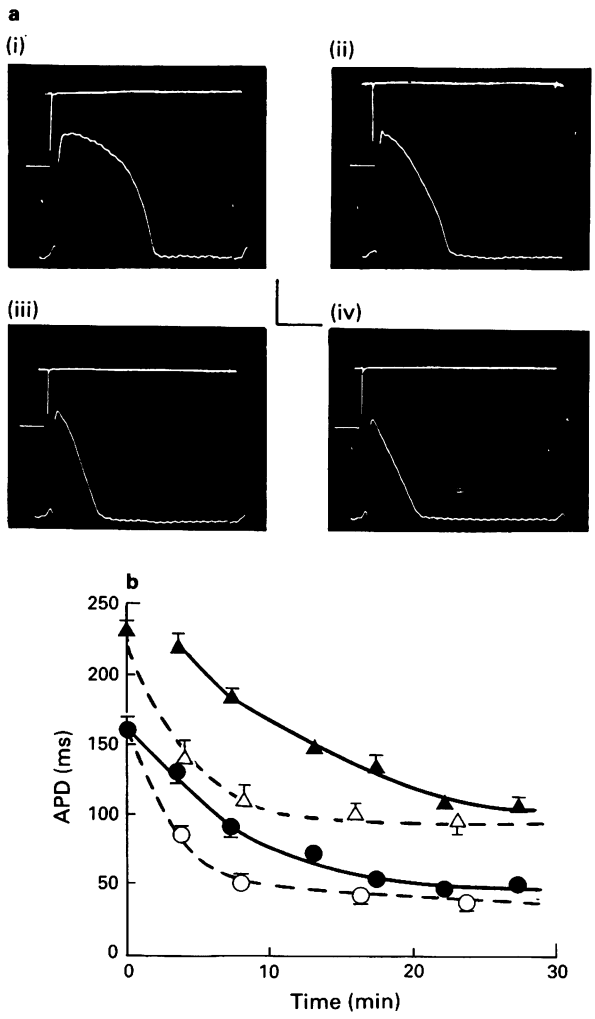

Figure 1 Time course of action potential changes during hypoxia in perfused hearts and the influence of tetraethylammonium (TEA, 10 mM). (a) Action potentials (lower traces) in normoxia (i) and after 4, 11 and 56 min of hypoxia ((ii), (iii) and (iv)). Upper traces are inverted first time derivates of the action potential. Horizontal bars: zero reference lines. Calibrations: vertical, 40 mV and 110 Vs^{-1}; horizontal, 100 ms. (b) Time course of action potential shortening at 25% and 95% repolarization (circles and triangles respectively) in control medium (dashed lines) and in the presence of TEA (solid lines). Control values indicated on the ordinate scale. Data points are means from 7 control hearts and 4 for TEA. Error bars indicated (unless within symbol size). The curves are least square fits of single exponentials with time constants of 4.0 and 4.4 min for APD_{25} and APD_{95} in control hypoxia and of 18.7 min for TEA.

K^+-dependence of APD and I_{K1} blockade: Figure 2 illustrates the steady state values of electrical parameters in normoxia and during the last 15 min of hypoxia at three different $[K]_o$ (7 hearts per concentration) as well as the effects of I_{K1} blockade with a mixture of 0.2 mM Ba^{2+} and 4 mM Cs^+ (4 hearts per $[K]_o$). In normoxia, the resting potential decreased significantly in the presence of Ba^{2+} and Cs^+ at 2.5 and 5 mM $[K]_o$ ($P<0.001$). The depolarization induced by raising $[K]_o$ from 2.5 to 7.5 mM was reduced from 23 ± 0.9 mV in controls to 17 ± 1.4 mV ($P<0.005$). Hypoxia did not affect RMP in the controls but in the presence of Ba^{2+} and Cs^+ a significant depolarization occurred. This effect was greater at low $[K]_o$ and the sensitivity of RMP to changes in $[K]_o$ was

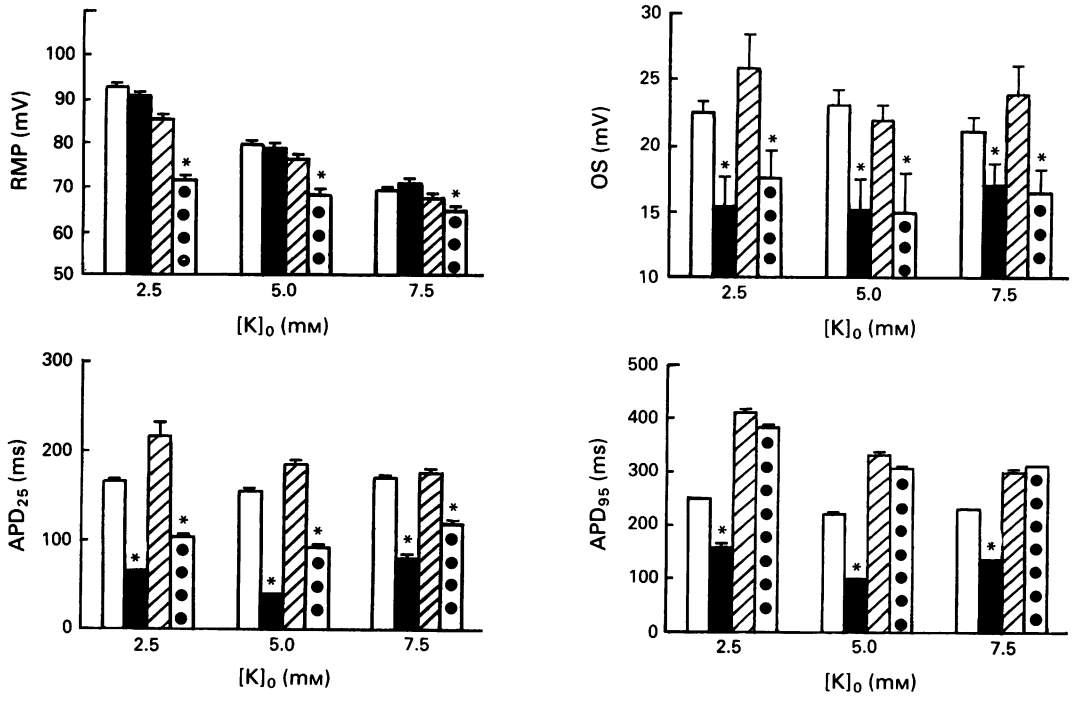

Figure 2 Effects of Ba^{2+} (0.2 mM) and Cs^+ (4 mM) on action potential parameters in normoxia and hypoxia at the steady state: RMP, absolute values of resting membrane potential, OS, overshoot; APD_{25} and APD_{95}, action potential duration at 25% and 95% repolarization at $[K]_o$ of 2.5, 5, and 7.5 mM, as indicated. Values are means from 7 hearts for the control experiments without blockers and 4 for each of the other $[K]_o$ in the presence of Ba^{2+}-Cs^+ . Error bars indicate s.e. unless within trace thickness. Open and solid columns, control normoxia and hypoxia respectively; cross-hatched and dotted columns, Ba^{2+}-Cs^+ in normoxia and hypoxia respectively. $*P<0.05$ or lower, paired t tests between hypoxia and normoxia for each experimental condition.

markedly attenuated (7.8 ± 1.6 mV between 2.5 and 7.5 mV) when compared with hypoxia without the blockers (19.2 ± 1.2 mV, $P<0.001$). Hypoxia significantly reduced the overshoot at all $[K]_o$ regardless of the presence of the blockers but the degree of the reduction was not related to $[K]_o$.

Blocking of I_{K1} with Ba^{2+}-Cs^+ in normoxia significantly increased APD_{25} at 2.5 and 5 mM $[K]_o$ and APD_{95} at all $[K]_o$ but the latter effect became smaller as $[K]_o$ was raised. Moreover, the blockers affected APD shortening and its $[K]_o$ dependence with a different pattern according to the repolarization level. The APD_{25} shortening was attenuated in the presence of the blockers: 55 ± 2.1% vs 61.6 ± 1.9%, 52 ± 2.9% vs 74 ± 1.8%, and 34 ± 4.9% vs 52.7 ± 3.9% at 2.5, 5 and 7.5 mM $[K]_o$ respectively. These differences were highly significant. Most interestingly, the Ba^{2+}-Cs^+ mixture prevented the APD_{95} shortening regardless of $[K]_o$.

Partial restoration of APD by glibenclamide: In 15 hearts, glibenclamide in normoxia did not alter AP configuration at any of the concentrations used (not shown) and at 3 μM the response to hypoxia was not affected. Pre-incubation with 10 or 30 μM glibenclamide for 30 min did not prevent AP shortening upon exposure to hypoxia (Figure 3a). On the contrary, APD values after 15 min were lower than in hypoxic controls. Thereafter, the action potential progressively lengthened and new steady state values were reached at about 45 min of hypoxia. Reoxygenation produced a fast but incomplete recovery of action potential parameters: 90 ± 4% for action potential amplitude, 73 ± 5% for APD_{25} and 85 ± 3.5% for APD_{95} after 30 min (traces not shown). Figure 3b shows that the partial recovery of APD_{25} induced by glibenclamide was dose-dependent and accompanied by a significant increase in APA at 30 μM. In contrast, there was no significant difference between the APD_{95} lengthening observed at 10 and 30 μM (138.6 ± 3.0 ms, vs 132.4 ± 2.9 ms respectively). Higher concentrations of glibenclamide (50 and 100 μM) did not produce further APD lengthening (data not shown). The resting potential slightly but significantly depolarized in hypoxia (3.4 ± 1.1 mV) in the presence of glibenclamide.

Papillary muscles

Figure 4 illustrates the effects of hypoxia on the membrane potential of a single cell in a typical experiment. As in whole hearts, RMP was not significantly altered and the slow decline of APA and the overshoot (Figure 4a) contrasts with the faster decrease in APD (Figure 4b). Similar results were obtained in 4 other preparations. Whereas the decrease in OS was comparable to that seen in rapidly paced hearts, the APD decline was smaller and the new steady state values were reached only after 20 to 30 min of hypoxia.

Figure 5 illustrates the effect of hypoxia and 4-AP on the frequency-dependence of APD_{25}. The control curve (composed from steady state values measured in the same cell at frequencies between 0.1 and 4 Hz) showed a maximum at 1 Hz (Figure 5a). A downward, parallel shift between 1 and 4 Hz was observed after 5 min of hypoxia. Because of the rapid decline of APD, steady state values could not be obtained for low frequency range (8 to 10 stimuli were required to attain the final APD at any given frequency, Ruiz Petrich & Leblanc, 1989). The parallel shift of the APD-frequency curve is compatible with the development of a time-independent outward current. An early depression of $I_{Ca\text{-}L}$ would have selectively depressed the response to higher frequencies. As APD further shortened with time in hypoxia, the influence of the pacing rate diminished, as shown by the curves obtained after 35 and 45 min, once more stable values of APD had been reached. The APD shortening produced by lowering the frequency from 1 to 0.1 Hz was then reduced from 41 ± 2.4% in controls to 25 ± 2.5% in hypoxia (Figure 5b). In addition, the maximum APD shifted from 1 to 2 Hz but the reduction with higher frequencies was maintained. Exposure to 4-AP in normoxia reduced AP shortening at low rates of stimulation and enhanced it as high frequencies. These effects are compatible with the blocking of the 4-AP

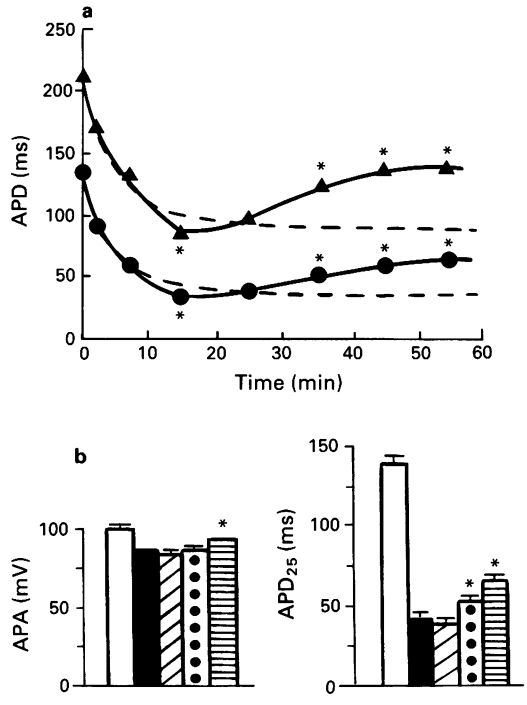

Figure 3 (a) Effects of 30 μM glibenclamide on the time course of action potential shortening during hypoxia (solid lines). Dashed lines: time course of APD decline in the absence of the blocker, same data as in Figure 1b. Control APD values in normoxia in the presence of the drug indicated on the ordinate scale. Data points represent means from 5 hearts with s.e. included in the size of the symbol: (▲) APD_{95}; (●) APD_{25}. Asterisks indicate statistical significance, with respect to hypoxia without glibenclamide, paired *t*-test. (b) Steady state values of action potential amplitude (APA) and APD_{25} in normoxia and hypoxia without drug (open and solid columns respectively) and hypoxia in the presence of 3 (cross hatched), 10 (dotted), and 30 μM (horizontal stripes) glibenclamide. Values are means from 3 hearts for the control and 5 for each glibenclamide concentration with s.e. shown by error bars, except when included within column. Asterisks indicate statistical significance with respect to hypoxia without drug (tested by analysis of variance).

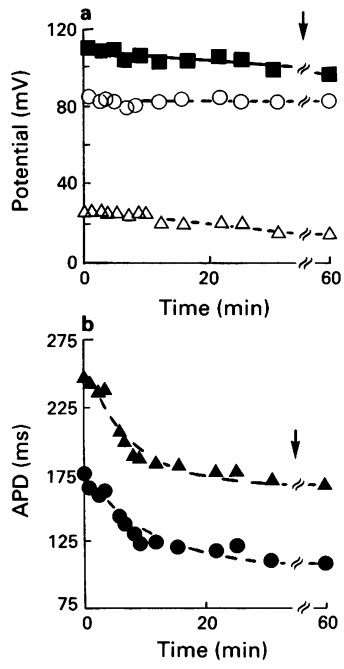

Figure 4 Changes in action potential parameters as a function of time of hypoxic superfusion in a papillary muscle paced at 1 Hz. Control values indicated on the oridinate scale. Data points are individual measurements from the same cell up to 31 min. The arrow indicates spontaneous dislodgement of the electrode. Data at 60 min are from another cell. (a) Action potential amplitude (■); absolute value of membrane resting potential (○), and overshoot (△). (b) Action potential duration at 25% (●) and 95% repolarization (▲). The dashed lines are fitted to single exponential functions with time constants of 9.3 and 7.9 min respectively.

sensitive component of I_{to} (Tseng *et al.*, 1987; Hiraoka & Kawano, 1989). In hypoxia with 4-AP, the AP shortening at 0.1 Hz was only 8 ± 2.7% but the response to higher frequencies was similar in normoxic controls and in hypoxia without 4-AP. These data suggest that the contribution of the 4-AP-sensitive fraction of I_{to} to plateau duration is diminished during metabolic inhibition.

Discussion

Our control experiments showed once more that high flow hypoxia produces a rapid and marked abbreviation of the cardiac action potential (Figure 1). Although the action potential duration is a complex parameter that reflects a delicate balance between outward and inward currents, it is accepted that its shortening during metabolic inhibition results from an early and pronounced increase in outward current (Isenberg *et al.*, 1983; Trube & Hescheler, 1984; Carmeliet *et al.*, 1990; Nichols & Lederer, 1990; Nichols *et al.*, 1991). Our study suggests that more than one ionic conductance needs to be invoked to account fully for the different responses to APD_{25} and APD_{95} to changes in $[K]_o$ and to K^+ channel blockers.

Contribution of I_{K1} to AP shortening

Effective blockade of I_{K1} by the Ba^{2+}-Cs^+ mixture was indicated by the decreased sensitivity of RMP to changes in $[K]_o$

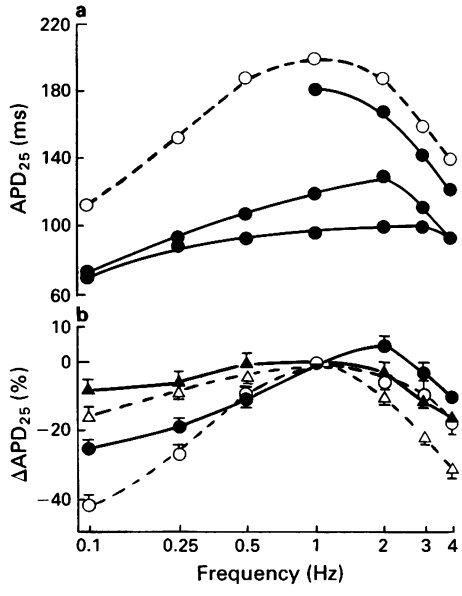

Figure 5 Effects of hypoxia and 4-aminopyridine (4-AP, 2 mM) on the relation between APD_{25} and frequency of stimulation. (a) Typical example of the rate dependence of APD_{25} in normoxia (○) and at different times in hypoxia (●): 5, 35 and 45 min, from top to bottom. Data points represent single measurements from the same cell for each curve. (b) Percentage changes of APD_{25} with frequency (with respect to 1 Hz) at the steady state for different experimental conditions: normoxia (○); hypoxia (●); 4-AP in normoxia (△), and 4-AP in hypoxia (▲). Data points are means from 7 preparations in normoxia and 8 in hypoxia. Error bars indicate s.e. unless included in the size of the symbol.

and the APD lengthening that was greater at 95% than at 25% repolarization, as expected from selective blockade of I_{K1} (Giles & Imaizumi, 1988). The suppression of APD_{95} shortening and the depolarization observed in hypoxia with Ba^{2+}-Cs^+ supports our previous findings that an increase in g_{K1} determines the maintenance of RMP and the AP shortening near full repolarization (Ruiz Petrich *et al.*, 1991). An increased g_{K1} can also explain the inhibitory effects of Ba^{2+} on the hypoxia-induced increase in K^+ efflux (Jiang *et al.*, 1991) and myocardial K^+ loss (Ruiz Petrich *et al.*, 1991). The attenuation of APD_{25} shortening by Ba^{2+}-Cs^+ indicates that either the I_{K1} current was also enhanced at plateau levels or that, at the concentration used, Ba^{2+} was no longer specific for I_{K1} but was also blocking K-ATP channels (Nelson *et al.*, 1990). In either case, these data strengthen the view that more than one outward current is involved in abbreviating APD.

Role of $I_{K\text{-}ATP}$

The involvement of K-ATP channels in AP shortening, increased K^+ efflux, and interstitial K^+ accumulation of hypoxic and ischaemic myocardium has been extensively documented in recent years (Venkatesh *et al.*, 1989; Carmeliet *et al.*, 1990; Wilde *et al.*, 1990; Gasser & Vaughan Jones, 1990; Hicks & Cobbe, 1991; Nakaya *et al.*, 1991; Jiang *et al.*, 1991) and most of these authors agree that blocking of these channels with sulphonylureas does not fully reverse the effects of metabolic inhibition. In our experiments, the enhanced AP shortening observed at about 15 min of hypoxia with glibenclamide (Figure 3) can be explained by a concomitant reduction of coronary flow (Wilde *et al.*, 1990) or to lack of the vasodilatation produced by low O_2 tensions (Daut *et al.*, 1990). The subsequent partial recovery of APD supports the view, also held by others (Hicks & Cobbe, 1991; Nakaya *et al.*, 1991) that K-ATP channels are not the only pathway involved in the response to metabolic stress.

The variability of the glibenclamide effects has been attributed to the drug binding only to open channels (Carmeliet *et al.*, 1990) and to decreased sensitivity of the channels to glibenclamide because of ADP accumulation (Venkatesh & Weiss, 1990). However, glibenclamide blocks $I_{K\text{-}ATP}$ to the same degree whether the channels are open or closed at the time of application (Venkatesh & Weiss, 1990). Moreover, ADP accumulation would result in effects vanishing with time in hypoxia instead of building up, as we and others observed (Carmeliet *et al.*, 1990; Hicks & Cobbe, 1991). The data from our experiments therefore suggest that although $I_{K\text{-}ATP}$ contributes to AP shortening in high flow hypoxia, it may not be a major component of the increased outward current responsible for the early changes, as proposed by Trube & Hescheler (1984).

We have so far identified two current systems (I_{K1} and $I_{K\text{-}ATP}$) the relative contributions of which to APD_{25} and APD_{95} shortening can be estimated by adding up the difference in APDs resulting from their blockade in hypoxia (Figure 6). If these two currents were the only ones involved in APD shortening, their addition should add up to the APD shortening without blockers, which is not the case for APD_{25} where a fraction remains to be accounted for. In contrast, the addition of the Ba^{2+}-Cs^+ and glibenclamide-sensitive fractions exceeds APD_{95} shortening which suggests a certain overlapping of their blocking effects.

Outward currents other than I_{K1} *and* $I_{K\text{-}ATP}$ *involved in plateau shortening*

A delayed rectifier like I_K is very seldom found in rabbit ventricle (Giles & Imaizumi, 1988) and activates too slowly to contribute significantly to AP repolarization (Hiraoka & Kawano, 1989). It seems that this current would also be absent during hypoxia because of the transitory effects of TEA that at 10 mM are believed to be quite specific for I_K (Stanfield, 1983). The remaining K^+ current activated at

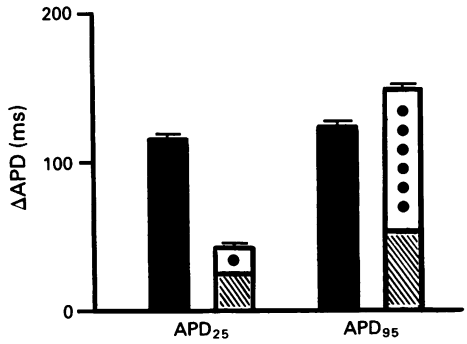

Figure 6 Relative contributions of the Ba^{2+}-Cs^+ and glibenclamide-sensitive currents to AP shortening at 25% and 95% repolarization. Solid columns, APD shortening without blockers; cross hatched columns, glibenclamide-sensitive fraction (difference between filled and dashed curves in Figure 3); spotted columns, Ba^{2+}-Cs^+ sensitive fraction (difference between hypoxia with and without blcokers, corrected for the increase in APD produced by the blockers in normoxia), see Figure 2. The greater size of the 2nd column for APD_{95} could imply a certain degree of overlapping between the blocks induced by glibenclamide and by Ba^{2+}-Cs^+. Means with s.e. (vertical bars); differences between columns were significant.

plateau potentials, I_{to}, determines the fast, early repolarization and the rate-dependent changes of APD. The downward, parallel shift of the relation between APD_{25} and pacing rate at the onset of hypoxia (Figure 5) suggests the rapid development of a time-independent current but the progressive flattening of this curve, particularly in the low frequency range speaks against an increase in I_{to} and rather in favour of another time-independent component of slower development. Inhibition of the 4-AP-sensitive component of I_{to} further enhanced the flattening of the APD_{25} vs frequency curve indicating the persistence of this component in hypoxia. On the other hand, if this current were a major contributor to plateau shortening, the response of APD_{25} to low stimulation rates would be expected to be enhanced, instead of depressed. Our data do not allow us to speculate on the role of the Ca^{2+}-dependent component of I_{to} in APD_{25} shortening at high rates but its contribution could be diminished because AP shortening produces a substantial decrease of the $[Ca^{2+}]_i$ transient (Stern *et al.*, 1988). The Na^+ activated K^+ current is not likely to play a major role in early plateau changes because cytosolic Na^+ accumulation is unlikely to occur within a few minutes of hypoxia.

Other current systems that could be involved in plateau shortening are the catecholamine-induced instantaneous I_{Cl} (Harvey *et al.*, 1990) and (but less probable for the reasons invoked above) a Ca^{2+}-activated transient I_{Cl} (Zygmunt & Gibbons, 1991) that is also enhanced by β-adrenoceptor stimulation. Further experimentation is needed to elucidate the role that these currents could play in AP shortening in hypoxia. Their involvement appears plausible because endogenous catecholamine release occurs early during metabolic inhibition. Moreover, a catecholamine-mediated mechanism could partly explain why APD shortening was less and developed more slowly in papillary muscles (where catecholamine pools should be much smaller) than in whole hearts. Given the multiple regulatory effects of sympathetic innervation on current systems acting at plateau potentials, and on $[Ca^{2+}]_i$, early adrenergic stimulation can markedly affect the delicate balance of inward and outward currents determining plateau duration. Such a mechanism could also explain the controversial evidence reported for perfused hearts vs myocytes where $I_{K\text{-}ATP}$ plays a predominant role in AP shortening.

This work was supported by grants from the Medical Research Council of Canada (MT-2859) and the Quebec Heart Foundation. N.L. was a predoctoral Fellow of the Canadian Heart Foundation. O.F.S. holds the Edwards chair of Cardiology.

The authors acknowledge the skilful collaboration of Denis Chartier and Patrice Yergeau and the expert assistance of Denise Girardin in the preparation of the manuscript.

References

ARENA, J.P. & KASS, R.S. (1989). Activation of ATP-sensitive K channels in heart cells by pinacidil: dependence on ATP. *Am. J. Physiol.*, **257**, H2092–H2096.

CARMELIET, E. (1978). Cardiac transmembrane potentials and metabolism. *Circ. Res.*, **42**, 577–587.

CARMELIET, E., STORMS, L. & VEREECKE, J. (1990). The ATP-dependent K-channel and metabolic inhibition. In *Cardiac Electrophysiology. From Cell to Bedside*. ed. Zipes, D.P. & Jalife, J. pp. 103–108. Philadelphia: W.B. Saunders Corp.

DAUT, J., MAIER-RUDOLPH, W., VON BECKERATH, N., MEHRKE, G., GÜNTHER, K. & GOEDEL-MEINEN, L. (1990). Hypoxic dilation of coronary arteries is mediated by ATP-sensitive potassium channels. *Science*, **247**, 1341–1344.

DELORENZI, F., ALLARD, Y.E., CHARTIER, D. & RUIZ PETRICH, E. (1990). Blockers of ATP-sensitive K channels and the action potential of hypoxic rabbit myocardium. *FASEB J.*, **4**-A559, Abs. 1698.

DELORENZI, F., CHARTIER, D. & RUIZ PETRICH, E. (1991). The ATP-sensitive K channels are not the whole story. *Biophys. J.*, **59**, 291a, Pos. 197.

ELLIOTT, A.C., SMITH, G.L. & ALLEN, D.G. (1989). Simultaneous measurements of action potential duration and intracellular ATP in isolated ferret hearts exposed to cyanide. *Circ. Res.*, **64**, 583–591.

FINDLAY, I. & FAIVRE, J.-F. (1991). ATP-sensitive K channels in heart muscle Spare channels. *FEBS*, **279**, 95–97.

FOSSET, M., DE WEILLE, J.R., GREEN, R.D, SCHMID-ANTOMARCHI, H. & LAZDUNSKI, M. (1988). Antidiabetic sulfonylureas control action potential properties in heart cells via high affinity receptors that are linked to ATP-dependent K^+ channels. *J. Biol. Chem.*, **263**, 7933–7936.

GASSER, R.N.A. & VAUGHAN-JONES, R.D. (1990). Mechanism of potassium efflux and action potential shortening during ischaemia in isolated mammalian cardiac muscle. *J. Physiol.*, **431**, 713–741.

GILES, W.R. & IMAIZUMI, Y. (1988). Comparison of potassium currents in rabbit atrial and ventricular cells. *J. Physiol.*, **405**, 123–145.

HARVEY, R.D., CLARK, C.D. & HUME, J.R. (1990). Chloride current in mammalian cardiac myocytes. *J. Gen. Physiol.*, **95**, 1077–1102.

HICKS, M.N. & COBBE, S.M. (1991). Effect of glibenclamide on extracellular potassium accumulation and the electrophysiological changes during myocardial ischaemia in the arterially perfused interventricular septum of rabbit. *Cardiovasc. Res.*, **25**, 407–413.

HIRANO, Y. & HIRAOKA, M. (1988). Barium-induced automatic activity in isolated ventricular myocytes from guinea-pig hearts. *J. Physiol.*, **394**, 455–472.

HIRAOKA, M. & KAWANO, S. (1987). Mechanism of increased amplitude and duration of the plateau with sudden shortening of diastolic intervals in rabbit ventricular cells. *Circ. Res.*, **60**, 14–26.

HIRAOKA, M. & KAWANO, S. (1989). Calcium-sensitive and insensitive transient outward current in rabbit ventricular myocytes. *J. Physiol.*, **410**, 187–212.

ISENBERG, G., VEREECKE, J., VAN DER HEYDEN, G. & CARMELIET, E. (1983). The shortening of the action potential by DNP in guinea-pig ventricular myocytes is mediated by an increase of a time-independent K conductance. *Pflügers Arch.*, **397**, 251–259.

JIANG, C., CRAKE, T. & POOLE-WILSON, P.A. (1991). Inhibition by barium and glibenclamide of the net loss of $^{86}Rb^+$ from rabbit myocardium during hypoxia. *Cardiovasc. Res.*, **25**, 414–420.

LEBLANC, N. & RUIZ-CERETTI, E. (1986). Hypoxia and the repolarizing phase of the ventricular action potential in altered external K. *Proc. XXX Congress IUPS*, Abst. 364.

LEBLANC, N. & RUIZ-CERETTI, E. (1987). The diffusion and electrogenic components of the membrane potential of hypoxic myocardium. *Can. J. Physiol. Pharmacol.*, **65**, 246–251.

LEBLANC, N., RUIZ-CERETTI, E. & CHARTIER, D. (1987). Potassium loss from hypoxic myocardium: influence of external K concentration. *Can. J. Physiol. Pharmacol.*, **65**, 861–866.

MEYER, S.L. (1975). *Data Analysis for Scientists and Engineers*. p. 237. New York: John Wiley & Sons, Inc.

NAKAYA, H., TAKEDA, Y., TOHSE, N. & KANNO, M. (1991). Effects of ATP-sensitive K^+ channel blockers on the action potential shortening in hypoxic and ischaemic myocardium. *Br. J. Pharmacol.*, **103**, 1019–1026.

NELSON, M.T., PATLAK, J.B., WORLEY, J.F. & STANDEN, N.B. (1990). Calcium channels, potassium channels, and voltage dependence of arterial smooth muscle tone. *Am. J. Physiol.*, **259**, C3–C18.

NICHOLS, C.G. & LEDERER, W.J. (1990). The regulation of ATP-sensitive K^+ channel activity in intact and permeabilized rat ventricular myocytes. *J. Physiol.*, **423**, 91–110.

NICHOLS, C.G., RIPOLL, C. & LEDERER, W.J. (1991). ATP-sensitive potassium channel modulation of the guinea pig ventricular action potential and contraction. *Circ. Res.*, **68**, 280–287.

NOMA, A. (1983). ATP-regulated K^+ channels in cardiac muscle. *Nature*, **305**, 147–148.

NOMA, A. & SHIBASAKI, T. (1985). Membrane current through adenosine-triphosphate-regulated potassium channels in guinea-pig ventricular cells. *J. Physiol.*, **363**, 463–480.

RUIZ PETRICH, E. & LEBLANC, N. (1989). The mechanism of the rate-dependent changes of the conducted action potential in rabbit ventricle. *Can. J. Physiol. Pharmacol.*, **67**, 780–787.

RUIZ PETRICH, E., DELORENZI, F. & CHARTIER, D. (1991). Role of the inward rectifier I_{K1} in the myocardial response to hypoxia. *Cardiovasc. Res.*, **25**, 17–26.

STANFIELD, P.R. (1983). Tetraethylammonium ions and the potassium permeability of excitable cells. *Rev. Physiol. Biochem. Pharmacol.*, **97**, 1–67.

STERN, M.D., SILVERMAN, H.S., HOUSER, S.R., JOSEPHSON, R.A., CAPOGROSSI, M.C., NICHOLS, C.G., LEDERER, W.J. & LAKATTA, E.D. (1988). Anoxic contractile failure in rat heart myocytes is caused by failure of intracellular calcium release due to alteration of the action potential. *Proc. Natl. Acad. Sci. U.S.A.*, **85**, 6954–6958.

TRUBE, G. & HESCHELER, J. (1984). Inward-rectifying channels in isolated patches of the heart cell membrane: ATP-dependence and comparison with cell-attached patches. *Pflügers Arch.*, **401**, 178–184.

TSENG, G.-N., ROBINSON, R.B. & HOFFMAN, B.F. (1987). Passive properties and membrane currents of canine ventricular myocytes. *J. Gen. Physiol.*, **90**, 671–701.

VENKATESH, N., LAMP, S.T. & WEISS, J.N. (1989). Effects of sulfonylureas on K^+ loss during myocardial ischemia and metabolic inhibition. *Circulation*, **80**, (Suppl. II), 607, Abst.

VENKATESH, N. & WEISS, J.N. (1990). ADP interferes with blockade of cardiac ATP-sensitive K^+ channels by glyburide. *Circulation*, **82**, (Suppl. III), 520, Abst.

WEISS, J.N. & LAMP, S.T. (1987). Glycolysis preferentially inhibits ATP-sensitive K^+ channels in isolated guinea-pig cardiac myocytes. *Science*, **238**, 67–69.

WILDE, A.A.M., ESCANDE, D., SCHUMACHER, C.A., THURINGER, D., MESTRE, M., FIOLET, J.W.T. & JANSE, M.J. (1990). Potassium accumulation in the globally ischemic mammalian heart. A role for the ATP-sensitive potassium channel. *Circ. Res.*, **67**, 835–843.

ZYGMUNT, A.C. & GIBBONS, W.R. (1991). Calcium-activated chloride current in rabbit ventricular myocytes. *Circ. Res.*, **68**, 424–437.

(Received October 30, 1991
Revised March 30, 1992
Accepted April 9, 1992)

Br. J. Pharmacol. (1992), **106**, 931–936 © Macmillan Press Ltd, 1992

Cultured astrocytoma cells generate a nitric oxide-like factor from endogenous L-arginine and glyceryl trinitrate: effect of *E. coli* lipopolysaccharide

[1]Daniela Salvemini, *Vincenzo Mollace, [2]Alessandra Pistelli, Erik Änggård & [3]John Vane

The William Harvey Research Institute, St Bartholomew's Hospital Medical College, Charterhouse Square, London EC1M 6BQ and *Department of Biology, University of Rome, Tor Vergata, Via Orazio Raimondo, 00173 Rome, Italy

1 The inhibitory activity of astrocytoma cells ($0.25-3 \times 10^5$) treated with indomethacin (10 μM) on platelet aggregation was enhanced by incubating the cells with *E. coli* lipopolysaccharide (LPS, 0.5 μg ml^{-1}) for 18 h. This effect was attenuated when cycloheximide (10 μg ml^{-1}) was incubated together with LPS. The inhibition of platelet aggregation by cells treated with LPS was potentiated by superoxide dismutase (60 u ml^{-1}) and ablated by oxyhaemoglobin (oxyHb, 10 μM) or N^G-monomethyl-L-arginine (L-NMMA, 30–300 μM). The effects of L-NMMA were reversed by co-incubation with L-arginine (L-Arg, 100 μM) but not D-arginine (D-Arg, 100 μM). LPS also increased the levels of nitrite in the culture media and this increase was ablated by co-incubation with L-NMMA (300 μM) or cycloheximide (10 μg ml^{-1}).

2 Astrocytoma cells (0.5×10^5) treated with indomethacin (10 μM) enhanced the platelet inhibitory activity of glyceryl trinitrate (GTN, 11–352 μM) but not that of sodium nitroprusside (4 μM). Furthermore, when incubated with GTN (200 μM) a 4 fold increase in the levels of guanosine 3':5'-cyclic monophosphate (cyclic GMP) was observed. These effects were abrogated by co-incubation with oxyHb (10 μM) but not with L-NMMA (300 μM). Treatment of the cells with LPS (0.5 μg ml^{-1}) for 18 h did not enhance their capacity to form NO from GTN.

3 Thus, in cultured astrocytoma cells, LPS enhances the formation of nitric oxide from endogenous L-arginine. In addition, these cells can metabolize GTN to nitric oxide but this process is not enhanced by LPS stimulation.

Keywords: Glyceryl trinitrate; nitric oxide; *E. coli* lipopolysaccharide; astrocytoma cells

Introduction

Nitric oxide (NO) is formed from L-arginine (L-Arg) in various areas of the brain where it is linked to stimulation by excitatory amino acids of specific receptors (Garthwaite *et al.*, 1988; Gorsky *et al.*, 1990; Mollace *et al.*, 1991a). This pathway is widely but not uniformly distributed. For example, the highest concentration of the NO synthase in cytosolic preparations from different brain regions was in the cerebellum whereas the lowest concentration was in the medulla oblongata (Förstermann *et al.*, 1990). Its release following activation of the NO-synthase (by excitatory amino acid receptor agonists) is associated with an increase in the levels of guanosine 3':5'-cyclic monophosphate (cyclic GMP), an important messenger in neuronal signal transduction in the brain (Bartfai, 1982).

Endogenous NO from L-Arg in the brain acts as a neuromodulator in both physiological and pathological events. For instance, inhibitors of the NO synthase (1) block the increase in cyclic GMP that occurs following *in vitro* or *in vivo* administration of glutamate, N-methyl-D-aspartate (NMDA) or kainate (Garthwaite *et al.*, 1989a,b; Bredt & Snyder, 1989; Wood *et al.*, 1990a), (2) prevent glutamate or NMDA-induced toxicity in rat primary cortical cultures (Dawson *et al.*, 1991) and (3) decrease electrocortical and locomotor activity or epileptic seizures following intracerebroventricular administration of NMDA (Mollace *et al.*, 1991a) or tachrine (Bagetta *et al.*, 1992).

Glyceryl trinitrate (GTN) relaxes blood vessels (Ignarro *et al.*, 1981; Murad, 1986) and inhibits platelet aggregation (Benjamin *et al.*, 1991; Salvemini *et al.*, 1992) after being converted to NO. In rats the peripheral administration of GTN increases markedly the levels of cyclic GMP in the brain (Torfgard *et al.*, 1989). NO stimulates soluble guanylate cyclase (GC) by interacting with the ferrohaeme centre of the enzyme resulting in the generation of cyclic GMP (Ignarro *et al.*, 1981). The biological activity of NO is destroyed by oxyHb which oxidizes NO to nitrate (Haussman & Werringloer, 1985).

NO is also produced from L-Arg by other cells including endothelial cells (EC) (Palmer *et al.*, 1987), macrophages (Salvemini *et al.*, 1990a), smooth muscle cells (SMC) (Wood *et al.*, 1990b; Mollace *et al.*, 1991b), astrocytes (Murphy *et al.*, 1990) or astrocytoma cells (Mollace *et al.*, 1990). The release of NO from EC, macrophages, and SMC is enhanced by *E. coli* lipopolysaccharide (LPS; Marletta *et al.*, 1988; Radomski *et al.*, 1990; Salvemini *et al.*, 1990a; McCall *et al.*, 1991; Mollace *et al.*, 1991b). In addition, LPS increases the metabolism of GTN to NO in SMC, EC (Salvemini *et al.*, 1992) or macrophages (Salvemini *et al.*, unpublished observations). Whether the induceable L-Arg to NO pathway is expressed in cells of the brain following immunostimulation is at present not known.

The aims of the present study were to investigate whether LPS enhanced the release of NO from L-Arg in cultured astrocytoma cells and whether these cells could metabolize GTN to NO.

[1] Present address: Monsanto Company, 800 North Lindberg Boulevard, St Louis, Missouri 63167, U.S.A. and [2] Department of Preclinical and Clinical Pharmacology 'M. Aiazzi Mancini', Viale G.B. Morgagni 65, 50134 Florence, Italy.

[3] Author for correspondence.

Methods

Preparation of washed platelets

Human washed platelets were prepared as described by Radomski & Moncada (1983). Indomethacin (10 μM) was added to the final platelet suspension to prevent the formation of cyclo-oxygenase products. The platelet count was adjusted to approximately $1.5-2 \times 10^8$ ml^{-1}.

Preparation of astrocytoma cells

Human astrocytoma cells (cell line GO-G-UVW) were obtained from the European Collection of Animal Cell Culture (Salisbury, U.K.) and prepared as described earlier (Mollace *et al.*, 1990). Indomethacin (10 μM) was added to all final cell suspensions. In some experiments LPS (0.5 μg ml^{-1}) and/or cycloheximide (10 μg ml^{-1}) were added to the cells in culture for a period of 4 to 24 h before use. Maximal formation of NO_2^- from endogenous NO derived from L-Arg occurred after 18 h of stimulation. Thus this time of incubation was selected for the experiments performed with the platelet and guanylate cyclase bioassay systems. Cell viability in the absence or presence of LPS was more than 95% as assessed by the uptake of trypan blue. Incubation of the cells with L-NMMA for 60 min did not alter viability.

Platelet aggregation

A suspension of washed platelets was incubated at 37°C for 4 min in a Payton dual channel aggregometer (Born & Cross, 1963) with continuous stirring at 1,000 r.p.m. and then stimulated with thrombin (40 mu ml^{-1}) to give a submaximal aggregation (80–90%). The decrease in optical density was recorded for 5 min. After a 3 min incubation period with platelets, the inhibitory effects of GTN or sodium nitroprusside (NaNP) on platelet aggregation were measured either alone or in the presence of astrocytoma cells non-treated or treated with LPS (0.5 μg ml^{-1} for 18 h). When required oxyHb (10 μM) was added to the platelet mixture for the 3 min incubation period. When using cells or oxyHb, the calibrations were performed in the presence of these agents to compensate for possible changes in light transmission (Salvemini *et al.*, 1989). Inhibition of platelet aggregation was calculated as described previously (Salvemini *et al.*, 1989).

Measurement of cyclic nucleotides

Cyclic GMP levels were measured by radioimmunoassay (Steiner *et al.*, 1972) following prior acetylation of the samples with acetic anhydride (Harper & Brooker, 1975). A suspension of astrocytoma cells (10^5 cells) non-treated or treated with LPS (0.5 μg ml^{-1} for 18 h) was diluted in Krebs buffer and preincubated in an aggregometer for 3 min (37°C, 1,000 r.p.m.). IBMX (0.1 mM) was present in the incubation mixture to inhibit phosphodiesterase activity. GTN (200 μM) was added to the cells for 3 min. When required, oxyHb (10 μM) was added to cells alone or to cells in the presence of GTN for a period of 3 min. Ice cold trichloroacetic acid (TCA, final concentration 5% w/v) was then added, the samples stored at −20°C, and the cyclic nucleotides extracted from TCA with 0.5 M tri-n-octylamine dissolved in 1, 1, 2-trichloro-trifluoroethane. All determinations were performed in duplicate.

Nitrite analysis

Nitrite (NO_2^-) in cell culture medium from astrocytoma cells in the absence or presence of stimulation with LPS (0.5 μg ml^{-1}) for 4 to 24 h was measured by the Griess reaction (Green *et al.*, 1982). In some experiments L-NMMA (300 μM) was added directly in the culture media of non-treated or LPS-treated cells. Aliquots of cell supernatants were mixed with an equal volume of Griess reagent (1% sulphanilamide/0.1% naphthylethylenediamine dihydrochloride/2.5% H_3PO_4). The absorbance was measured at 546 nm, and nitrite concentration was determined with sodium nitrite used as a standard. Results were expressed as nmol NO_2^- ml^{-1}.

Determination of endotoxin levels

Endotoxin levels in the distilled water, Krebs buffer and culture medium were determined by use of Limulus Amoebocyte Lysate (E-Toxate, Sigma). These levels were below the detection limit of the assay (0.03 Eu ml^{-1}).

Materials

The composition of the modified (Sneddon & Vane, 1988) Krebs bicarbonate buffer was (mM): NaCl 137, KCl 2.7, $NaHCO_3$ 11.9, NaH_2PO_4 0.3, $MgSO_4$ 0.8, glucose 5.6 and $CaCl_2$ 1. Human thrombin, *E. coli* lipopolysaccharide (serotype 0127:B8), cycloheximide, bovine serum albumin, haemoglobin (from bovine blood), superoxide dismutase (from bovine erythrocytes), indomethacin, E-Toxate (Limulus Amoebocyte Lysate, No. 210), sodium nitroprusside, L-arginine (free base), D-arginine (free base) sulphanilic acid, N-1-naphthyl ethylene diamine hydrochloride and methylene blue were obtained from Sigma (Poole, U.K.). Tri-n-octylamine and 3′-isobutyl-1-methylxanthine (IBMX) were obtained from Aldrich (Dorset, U.K.) and phosphoric acid from BDR Analar (Essex, U.K.). Stock solutions of IBMX were prepared in 0.1 N NaOH and then diluted in Krebs buffer as required. Kits for radioimmunoassay of adenosine 3′:5′-cyclic monophosphate (cyclic AMP) were purchased from Amersham as was [^{125}I]-cyclic GMP (Bucks, U.K.). N^G-monomethyl-L-arginine (L-NMMA) was obtained from Ultrafine Chemicals Ltd (Manchester, U.K.). Oxyhaemoglobin was prepared by reduction of bovine haemoglobin with sodium hydrosulphite as described previously (Salvemini *et al.*, 1989). Glyceryl trinitrate (Nitronal) was obtained from Lipha Pharmaceuticals Ltd (West Drayton, Middlesex, U.K.). Prostacyclin was a gift from the Wellcome Research Laboratories (Beckenham, U.K.). The cyclic GMP-specific antibodies were kindly provided by Dr K. Schrör (Institute of Pharmacology, University of Düsseldorf, Germany).

Statistics

Results are expressed as mean ± s.e.mean for (n) experiments and each experiment was performed with blood obtained from a different donor. Student's unpaired t test was used to determine the significant difference between means, and a P value of <0.05 was taken as significant.

Results

Release of a NO-like factor from LPS-treated astrocytoma cells

Cultured human astrocytoma cells inhibit platelet aggregation by releasing a NO-like factor (Mollace *et al.*, 1990). Here we show that the anti-platelet activity of astrocytoma cells is enhanced at least 2 fold by treating the cells with LPS (0.5 μg ml^{-1}) for 18 h. Thus, the IC_{50} was $2.2 \pm 0.3 \times 10^5$ without LPS and $0.86 \pm 0.04 \times 10^5$ with LPS (Figure 1). The inhibitory activity of cells treated with LPS was enhanced by SOD (60 u ml^{-1}) and reversed by oxyHb (10 μM) (Figure 1) or L-NMMA (Table 1). L-Arg (100 μM) but not D-Arg (100 μM) when co-incubated together with L-NMMA (30–300 μM) for 60 min counteracted the effects of L-NMMA (Table 1). A preincubation period of 60 min with L-NMMA was necessary in order fully to reverse the inhibitory action of the astrocytoma cells. Thus, when astrocytoma cells (2×10^5) were incubated with L-NMMA for only 30 min a

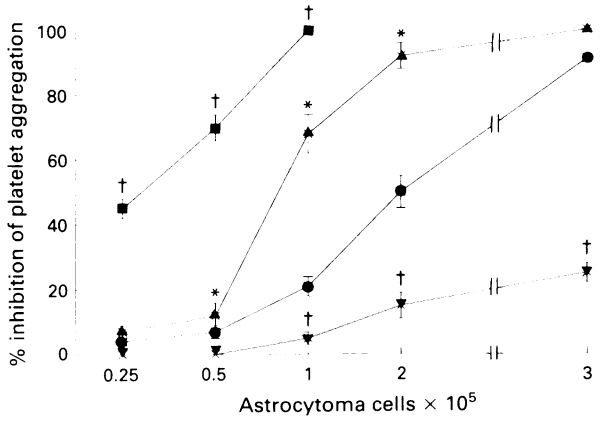

Figure 1 Effects of superoxide dismutase (SOD) or oxyhaemoglobin (oxyHb) on the inhibition of thrombin-induced platelet aggregation by astrocytoma cells treated with *E. coli* lipopolysaccharide (LPS). The inhibitory activity of astrocytoma cells (●) was enhanced by treating the cells with LPS (0.5 μg ml^{-1}) for 18 h (▲). The inhibitory activity of cells treated with LPS was potentiated by SOD (60 u ml^{-1}, ■) and reversed by oxyHb (10 μM, ▼). Results are expressed as % inhibition of platelet aggregation. Each point is the mean of 4 experiments; s.e.mean shown by vertical bars. *$P<0.001$ when compared to control values and †$P<0.001$ when compared to values obtained in the presence of LPS.

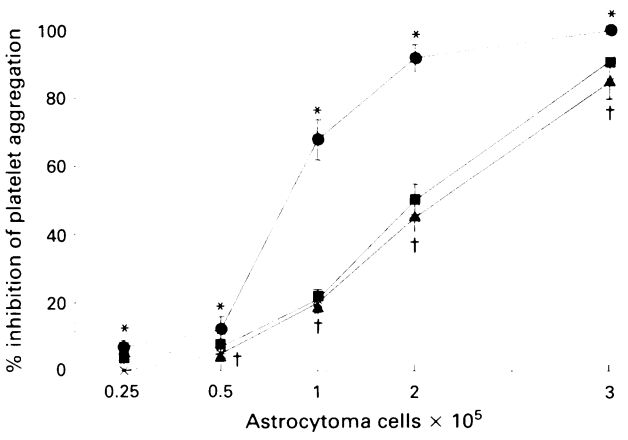

Figure 2 Effects of cycloheximide on the inhibition of thrombin-induced platelet aggregation by astrocytoma cells treated with *E. coli* lipopolysaccharide (LPS). Potentiation of the inhibitory activity of astrocytoma cells (0.25–3 × 10^5, ■) by LPS (0.5 μg ml^{-1} for 18 h, ●) was prevented when cycloheximide (10 μg ml^{-1}) was incubated together with LPS for 18 h (▲). Results are expressed as % inhibition of platelet aggregation. Each point is the mean of 4 experiments; s.e.mean shown by vertical bars. *$P<0.001$ when compared to control value obtained in the absence of LPS and †$P<0.001$ when compared to values obtained in the presence of LPS.

Table 1 Effects of N^G-monomethyl-L-arginine (L-NMMA) on the inhibition of thrombin-induced platelet aggregation by astrocytoma cells treated with *E. coli* lipopolysaccharide (LPS)

L-NMMA (μM)	*Controls*	*+L-Arg*	*+D-Arg*
0	92 ± 4	92 ± 4	92 ± 4
30	47 ± 2*	95 ± 4†	45 ± 4
100	34 ± 3*	90 ± 2†	37 ± 2
300	15 ± 4*	85 ± 4†	22 ± 3

The inhibitory activity of 2 × 10^5 cells was reversed by L-NMMA (30–300 μM) and this effect was attenuated when L-arginine (L-Arg, 100 μM) but not D-arginine (D-Arg, 100 μM) was co-incubated together with L-NMMA. Results are expressed as % inhibition of platelet aggregation. Each value is the mean ± s.e.mean of 4 experiments. *$P<0.001$ when compared to values obtained in the absence of L-NMMA and †$P<0.001$ when compared to values obtained in the presence of L-NMMA.

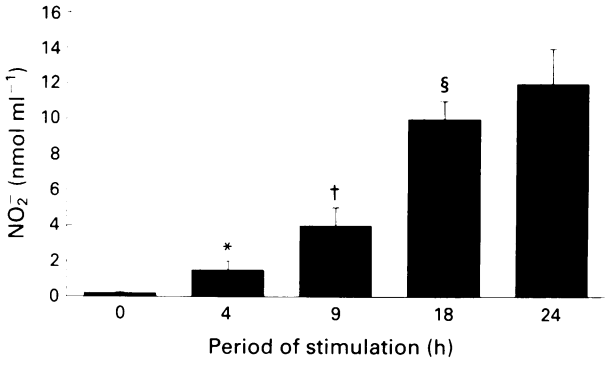

Figure 3 Effects of *E. coli* lipopolysaccharide (LPS)-stimulation on the generation of NO_2^- by cultured astrocytoma cells. Incubation of astrocytoma cells with LPS for 4 to 24 h increased the levels of NO_2^- in a concentration-dependent manner. Maximal production of NO_2^- was obtained after 18 h. Each point is the mean of 10 experiments, vertical bars show s.e.mean. *$P<0.01$ when compared to the value obtained after 0 h; †$P<0.01$ when compared to the value obtained after 4 h and §$P<0.01$ when compared to the value obtained after 9 h of LPS stimulation.

partial reversal of their inhibitory effects was observed (from 92 ± 4% inhibition to 57 ± 4% inhibition, $n = 4$, $P<0.001$). The potentiation of the platelet inhibitory activity by LPS was ablated when cycloheximide (10 μg ml^{-1}) was incubated together with LPS (Figure 2). The anti-platelet effects of non-treated cells were not affected by cycloheximide ($n = 4$, not shown). NO_2^- in the cell culture media was also measured as an index of NO formation. Incubation of astrocytoma cells in culture for 4 to 24 h with LPS (0.5 μg ml^{-1}) increased the levels of NO_2^- in the media; maximal formation was observed after 18 h of stimulation (Figure 3). This time point was used to characterize the origin of the LPS-induced formation of NO_2^- . The increased levels of NO_2^- by LPS (from 0.2 ± 0.05 nmol NO_2^- ml^{-1} in the absence of stimulation with LPS to 10 ± 1 nmol NO_2^- ml^{-1} following stimulation with LPS for 18 h, $n = 10$, $P<0.001$) were due to stimulation of the L-Arg-NO pathway, for L-NMMA (300 μM) when co-incubated with LPS for 18 h abolished this increase (from 10 ± 1 nmol NO_2^- ml^{-1} in the absence of L-NMMA to 0.1 ± 0.04 nmol NO_2^- ml^{-1} in its presence, $n = 10$, $P<0.001$). The effects of LPS were also abrogated when cycloheximide (10 μg ml^{-1}) was added together with LPS for 18 h (from 10 ± 1 nmol NO_2^- ml^{-1} in the absence of cycloheximide to 0.2 ± 0.01 nmol NO_2^- ml^{-1} in its presence, $n = 10$, $P<0.001$).

Potentiation of the anti-platelet activity of glyceryltrinitrate by astrocytoma cells

Salvemini *et al.* (1992) found that the concentration of GTN required to inhibit thrombin-induced platelet aggregation by 50% (IC_{50}) is 110 ± 2 μM and that for NaNP 15 ± 1 μM. This weak anti-platelet action of GTN is enhanced ($IC_{50} = 42 \pm 1$ μM) in the presence of small numbers of astrocytoma cells (Figure 4). Potentiation of the anti-platelet activity of GTN (44 μM) by astrocytoma cells (0.5 × 10^5) was abrogated by co-incubation with oxyHb (10 μM) (80 ± 8% inhibition to 9 ± 4% inhibition, $n = 4$, $P<0.001$). The anti-platelet effects

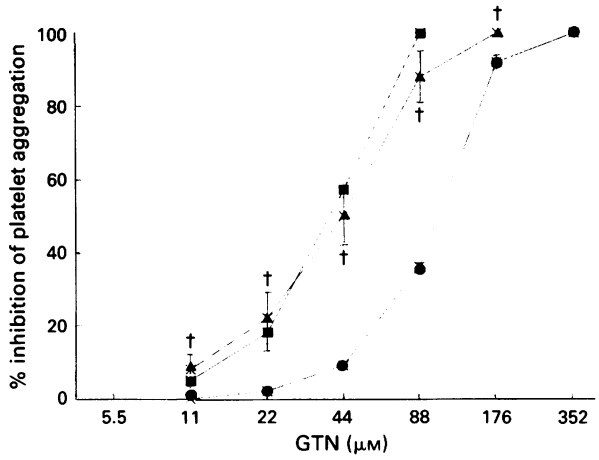

Figure 4 Effects of non-treated or *E. coli* lipopolysaccharide (LPS)-treated astrocytoma cells (0.5×10^5 cells) on the inhibition of thrombin-induced platelet aggregation by glyceryl trinitrate (GTN). The inhibition of platelet aggregation by GTN (●) is magnified by non-treated astrocytoma cells (0.5×10^5, ▲) but this effect is not enhanced further by LPS treatment (■). Results are expressed as % inhibition of platelet aggregation. Each point represents the mean of 4 experiments, vertical bars show s.e.mean; †$P<0.001$ when compared to the values obtained in the absence of cells.

of NaNP were, in contrast, not potentiated by the presence of cells. For instance, NaNP (4 μM) caused approximately a similar degree of inhibition (11 ± 6%, $n = 4$) to that obtained with GTN (44 μM, 9 ± 1%, $n = 16$) but the addition of astrocytoma cells (0.5×10^5 cells, 7 ± 2% inhibition, $n = 4$) did not enhance its inhibitory activity (15 ± 2% inhibition for NaNP together with cells, $n = 4$).

Effects of LPS on the metabolism of glyceryl trinitrate to NO

Figure 4 shows that astrocytoma cells (0.5×10^5) treated with LPS for 18 h are not more effective when compared to the non-treated cells in enhancing the anti-platelet effect of GTN ($IC_{50} = 40 \pm 2$ μM for GTN in the presence of astrocytoma cells treated with LPS). Increasing the period of stimulation with LPS to 24 h did not change the IC_{50} ($n = 3$, not shown). Furthermore, after LPS treatment, these cells did not potentiate the anti-platelet effects of NaNP. Thus the combined effects of NaNP (4 μM, 11 ± 6% inhibition, $n = 4$) and cells treated with LPS (0.5×10^5 cells, 12 ± 4% inhibition, $n = 4$) were only 25 ± 3% inhibition of platelet aggregation ($n = 4$) which is simply an additive effect of the two treatments.

Effects of L-NMMA

When astrocytoma cells (3×10^5) were pretreated with L-NMMA (300 μM, 60 min), their endogenous platelet inhibitory activity was attenuated (from 91 ± 3% inhibition to 15 ± 4% inhibition, $n = 4$, $P<0.0005$). Astrocytoma cells treated with L-NMMA did not, however, lose their ability to potentiate the anti-platelet action of GTN (from 15 ± 4% inhibition to 75 ± 3% inhibition in the absence or presence of GTN, $n = 4$, $P<0.001$). Similarly, when the platelet inhibitory activity of astrocytoma cells (3×10^5) treated with LPS was inhibited by L-NMMA (from 99 ± 2% inhibition to 15 ± 4% inhibition, $n = 4$, $P<0.001$) their ability to metabolize GTN to NO was not changed (from 15 ± 4% inhibition to 80 ± 3% inhibition, $n = 4$, $P<0.001$).

Effect of LPS on cyclic GMP levels

When astrocytoma cells (10^5 cells) were stirred for a period of 3 min, there was an increase in cyclic GMP which was prevented by co-incubation with oxyHb (Figure 5). Exposure of these cells to GTN (200 μM) led to a much greater increase (4 fold) in the levels of cyclic GMP (Figure 5). This increase in cyclic GMP was attenuated by oxyHb (10 μM) (Figure 5). The basal levels of cyclic GMP in astrocytoma cells treated with LPS were 2 fold higher than those in the non-treated cells (Figure 5). OxyHb reduced the increased levels of cyclic GMP in cells treated with LPS (Figure 5). The increase in the levels of cyclic GMP by GTN in astrocytoma cells were not increased by the LPS-pretreatment (Figure 5). GTN did not modify the levels of cyclic AMP in cells with or without LPS ($n = 4$, not shown).

Discussion

LPS enhanced the release in astrocytoma cells of endogenous NO from L-Arg presumably by inducing the expression of the NO-synthase as evidenced by the SOD, oxyHb or L-NMMA-sensitive potentiation of their anti-platelet effects and the increased production of NO_2^- in the culture media of the astrocytoma cells. This effect of LPS requires protein synthesis since its actions were ablated by the protein synthesis inhibitor, cycloheximide. The possible involvement of mediators formed from the cyclo-oxygenases pathway such as prostacyclin (PGI_2) was excluded, for the astrocytoma cells were treated with indomethacin.

Endothelial cells (Salvemini *et al.*, 1990b), J774 cells (Salvemini *et al.*, 1990a) and SMC (Mollace *et al.*, 1991b) when co-incubated with platelets release an inhibitory factor with pharmacological properties identical to NO. Inhibition of platelet aggregation by NO released from these cells can be enhanced 4.4 fold for EC and J774 cells and 2.6 fold for SMC (Mollace *et al.*, 1991b). In this study, LPS potentiated the anti-platelet effects of astrocytoma cells by 2.5 fold which is therefore compared to the effect of LPS on the SMC. This supports the view that after LPS stimulation, expression of the enzyme responsible for the synthesis of NO-like activity and the degree to which it can be induced differs from cell type to cell type (see Moncada *et al.*, 1991a for review).

Two distinct enzymes are responsible for the biosynthesis of NO. One is constitutive, calcium-calmodulin and NADPH-

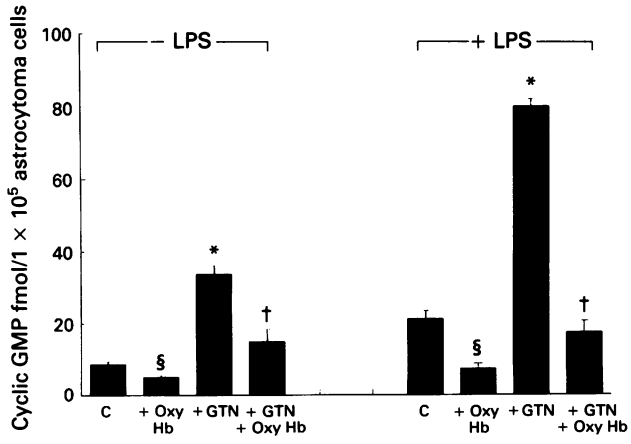

Figure 5 Effects of glyceryl trinitrate (GTN, 200 μM) on cyclic GMP levels in astrocytoma cells (10^5 cells) non-treated or treated with *E. coli* lipopolysaccharide (LPS, 0.5 μg ml^{-1}) for 18 h. Stimulation of astrocytoma cells with GTN (200 μM) increased the levels of cyclic GMP and this increase was blocked by co-incubation with oxyhaemoglobin (oxyHb 10 μM). Treatment of astrocytoma cells with LPS did not increase further the levels of cyclic GMP in response to GTN. Vertical bars represent s.e.mean of 4 experiments performed in duplicate. Results are expressed as cyclic GMP fmol/10^5 cells. *$P<0.001$ when compared to control levels; §$P<0.001$ when compared to values obtained in the absence of GTN; †$P<0.01$ when compared to values obtained in the presence of GTN.

dependent and the other is induced by LPS and various cytokines, is calcium-independent, requires NADPH and tetrahydrobiopterin as cofactors and its induction is inhibited by glucocorticoids (Knowles *et al.*, 1989; Busse & Mülsch, 1990; Radomski *et al.*, 1990). The brain NO synthase in the absence of immunostimulation is calcium-dependent and of the constitutive type (Bredt & Snyder, 1989; 1990; Bredt *et al.*, 1990). In our experiments, the nature of the NO synthase expressed in the presence of LPS stimulation is at present not known since studies on the enzyme activity have not yet been performed.

GTN is converted to NO by several cell types including SMC (Benjamin *et al.*, 1991; Feelisch & Kelm, 1991; Salvemini *et al.*, 1992), EC (Feelisch & Kelm, 1991; Salvemini *et al.*, 1992) and macrophages (Salvemini *et al.*, unpublished observations) and its biological activity is destroyed by oxyHb which oxidizes NO to nitrates (Haussman & Werringloer, 1985). Here we have shown that cultured astrocytoma cells can also metabolize GTN to NO as shown by potentiation of the anti-platelet effects of GTN and increase in cyclic GMP levels, both prevented by oxyHb. However, this metabolism is not increased by LPS treatment. The action of LPS on the astrocytoma cells, therefore, differs from that on the SMC, EC (Salvemini *et al.*, 1992) or macrophages (Salvemini *et al.*, unpublished observations) where induction of the GTN to NO metabolizing system is seen.

Unlike GTN, NaNP releases NO spontaneously (Feelisch, 1991). Thus, its vasodilator and anti-platelet effectiveness do not depend on metabolism by cells (Salvemini *et al.*, 1992) a conclusion supported by our findings that astrocytoma cells failed to alter the anti-platelet activity of NaNP.

Endogenous NO can, through stimulation of cyclic GMP formation, exercise both autocrine and paracrine effects (see Moncada *et al.*, 1991a for review). Inhibition of basal NO formation from EC leads to the development of a supersensitivity to GTN and other vasodilators (Moncada *et al.*, 1991b). This effect may occur at the level of the soluble GC system in the smooth muscle (Moncada *et al.*, 1991b) rather than on a modulatory action of NO on the NO-synthase since endogenous or exogenous NO does not affect the activity of this enzyme, at least in EC (Kuhn *et al.*, 1991; Salvemini *et al.*, 1992) or SMC (Salvemini *et al.*, 1992). Here L-NMMA, an inhibitor or the L-Arg-NO pathways (Hibbs *et al.*, 1987) inhibited the release of NO from non-treated or LPS-treated astrocytoma cells but did not inhibit the metabolism of GTN to NO. Thus endogenous NO does not modulate the metabolism of GTN to NO and NO synthase is not involved in GTN metabolism in these cells, as seen with all other cell types studied (Salvemini *et al.*, 1992).

N^G-nitro-L-arginine, an inhibitor of the L-Arg to NO pathway inhibits the recovery of electrocorticographic activity which occurs after transient global ischaemia in the mongolian gerbil (Sancesario *et al.*, 1992). This indicates that NO may play a physiological role in post-ischaemic recovery in the brain. In the present study we have demonstrated that there is another source of NO generation in the brain, through the conversion of GTN to NO. The presence of this pathway in the brain offers the potential of therapeutic exploration.

Activation of the constitutive NO synthase is a transduction mechanism which underlies several physiological responses, whereas activation of the inducible NO synthase acts as a cytotoxic transduction mechanism or as a mechanism underlying some pathological disorders. In this respect, the findings that astrocytoma cells (and possibly other cell types in the brain) are induced by LPS to form NO synthase indicates that stimulation of the L-Arg to NO pathway may also be involved in some of the pathological changes observed in the brain, for example in sepsis (Trump *et al.*, 1975; Mela *et al.*, 1979).

We thank Dr R. Botting for editorial help and Ms E. Wood for culturing the astrocytoma cells. This work was supported by a grant from Glaxo Group Research Ltd.

References

BAGETTA, G., MOLLACE, V., IANNONE, M. & NISTICO, G. (1992). Possible involvement of nitric oxide in the pathophysiology of seizures and brain damage in rats. In *Biology of Nitric Oxide* ed. Moncada, S., Marletta, M., Hibbs, N & Higgs, E.A. London: Portland Press (in press).

BARTFAI, T. (1982). Cyclic nucleotides and the nervous system. *Trends Pharmacol. Sci.*, **3**, 338–340.

BENJAMIN, N., DUTTON, J.A.E. & RITTER, J.M. (1991). Human vascular smooth muscle cells inhibit platelet aggregation when incubated with glyceryl trinitrate: evidence for generation of nitric oxide. *Br. J. Pharmacol.*, **102**, 847–851.

BORN, G.V.R. & CROSS, M.J. (1963). The aggregation of blood platelets. *J. Physiol.*, **168**, 178–195.

BREDT, D.S. & SNYDER, S.H. (1989). Nitric oxide mediates glutamate-linked enhancement of cGMP levels in the cerebellum. *Proc. Natl. Acad. Sci. U.S.A.*, **86**, 9030–9033.

BREDT, D.S. & SNYDER, S.H. (1990). Isolation of nitric oxide synthase, a calmodulin-requiring enzyme. *Proc. Natl. Acad. Sci. U.S.A.*, **87**, 682–685.

BREDT, D.S., HWANG, P.M. & SNYDER, S.H. (1990). Localization of nitric oxide synthase indicating a neural role for nitric oxide. *Nature*, **347**, 768–770.

BUSSE, R. & MÜLSCH, A. (1990). Calcium-dependent nitric oxide synthesis in endothelial cytosol is mediated by calmodulin. *FEBS Lett.*, **265**, 133–136.

DAWSON, V.L., DAWSON, T.M., LONDON, E.D., BREDT, D.S. & SNYDER, S.H. (1991). Nitric oxide mediates glutamate neurotoxicity in primary cortical cultures. *Proc. Natl. Acad. Sci. U.S.A.*, **88**, 6368–6371.

FEELISCH, M. (1991). The biochemical pathways of nitric oxide formation from nitrovasodilators: Appropriate choice of exogenous NO donors and aspect of preparation and handling of aqueous NO solutions. *J. Cardiovasc. Pharmacol.*, **17**, S25–S33.

FEELISCH, M. & KELM, M. (1991). Biotransformation of organic nitrates to nitric oxide by vascular smooth muscle and endothelial cells. *Biochem. Biophys. Res. Commun.*, **180**, 286–293.

FÖRSTERMANN, U., GORSKY, L.D., POLLOCK, J.S., SCHMIDT, H.H.H.W., HELLER, M. & MURAD, F. (1990). Regional distribution of EDRF/NO synthesizing enzyme(s) in rat brain. *Biochem. Biophys. Res. Commun.*, **168**, 727–732.

GARTHWAITE, J., CHARLES, S.L. & CHESS-WILLIAMS, R. (1988). Endothelium-derived relaxing factor release on activation of NMDA receptors suggests role as intercellular messenger in the brain. *Nature*, **336**, 385–388.

GARTHWAITE, J., CHARLES, S.L. & CHESS-WILLIAMS, R. (1989a). NMDA receptor activation induces nitric oxide synthesis from arginine in rat brain slices. *Eur. J. Pharmacol.*, **172**, 413–416.

GARTHWAITE, J., SOUTHAM, E. & ANDERTON, M. (1989b). A kainate receptor linked to nitric oxide synthesis from arginine. *J. Neurochem.*, **53**, 1952–1954.

GORSKY, L.D., FÖRSTERMANN, U., ISHII, K. & MURAD, F. (1990). Production of an EDRF-like activity in the cytosol of N1E-115 neuroblastoma cells. *FASEB J.*, **4**, 1494–1500.

GREEN, L.C., WAGNER, D., GLOGOWSKI, A., SKIPPER, J., WISHNOK, J.S. & TANNENBAUM, S.R. (1982). Analysis of nitrate, nitrite and [^{15}N] nitrate in biological fluids. *Anal. Biochem.*, **126**, 131–138.

HARPER, J.F. & BROOKER, G. (1975). Fentomole sensitive radioimmunoassay for cyclic AMP and cyclic GMP after 2'0 acetylation by acetic anhydride in aqueous solution. *J. Cyclic Nucleotide Res.*, **1**, 207–218.

HAUSSMANN, H.J. & WERRINGLOER, J. (1985). Nitric oxide and nitrite formation during the degradation of N-nitrosoamines. *Naunyn-Schmiedebergs Arch. Pharmacol.*, **329**, R21.

HIBBS, J.B. Jr, TAINTOR, R.R. & VAVRIN, Z. (1987). Macrophage cytotoxicity; role for L-arginine deiminase and imino nitrogen oxidation to nitrite. *Science*, **235**, 474–476.

IGNARRO, L.J., LIPPTON, H., EDWARDS, J.C., BARICOS, W.H., HYMAN, A.L., KADOWITZ, P.Z. & GRUETTER, C.A. (1981). Mechanism of vascular smooth muscle relaxation by organic nitrates, nitrites, nitroprusside and nitric oxide: evidence for the involvement of S-nitrosothiols as active intermediates. *J. Pharmacol. Exp. Ther.*, **218**, 739–749.

KNOWLES, R.G., PALACIOS, M., PALMER, R.M.J. & MONCADA, S. (1989). Formation of nitric oxide from L-arginine in the central nervous system: a transduction mechanism for stimulation of the soluble guanylate cyclase. *Proc. Natl. Acad. Sci. U.S.A.*, **86**, 5159–5162.

KUHN, M., OTTEN, A., FRÖLISCH, J.C. & FÖSTERMANN, U. (1991). Endothelial cyclic GMP and cyclic AMP do not regulate the release of endothelium-derived relaxing factor/nitric oxide from bovine aortic endothelial cells. *J. Pharmacol. Exp. Ther.*, **256**, 677–682.

MARLETTA, M.A., YOON, P.S., IYENGAR, R., LEAF, C.D. & WISHNOK, J.S. (1980). Macrophage oxidation of L-arginine to nitrite and nitrate: nitric oxide is an intermediate. *Biochemistry*, **27**, 8706–8711.

MCCALL, T.B., FEELISCH, M., PALMER, R.M.J. & MONCADA, S. (1991). Identification of N-iminoethyl-L-ornithine as an irreversible inhibitor of nitric oxide synthase in phagocyte cells. *Br. J. Pharmacol.*, **102**, 234–238.

MELA, L. (1979). Reversibility of mitochondrial metabolic response to circulatory shock and tissue ischemia. *Circ. Shock* (Suppl. 1), 61–67.

MOLLACE, V., SALVEMINI, D., ÄNGGÅRD, E. & VANE, J. (1990). Cultured astrocytoma cells inhibit platelet aggregation by releasing a nitric oxide-like factor. *Biochem. Biophys. Res. Commun.*, **172**, 2, 564–569.

MOLLACE, V., BAGETTA, G. & NISTICO, G. (1991a). Evidence that L-arginine possesses proconvulsant effects mediated through nitric oxide. *Neuro. Rep.*, **2**, 269–272.

MOLLACE, V., SALVEMINI, D., ÄNGGÅRD, E. & VANE, J. (1991b). Nitric oxide from vascular smooth muscle cells: regulation of platelet reactivity and smooth muscle cell guanylate cyclase. *Br. J. Pharmacol.*, **104**, 633–638.

MONCADA, S., PALMER, R.M.J. & HIGGS, E.A. (1991a). Nitric oxide: physiology, pathophysiology and pharmacology. *Pharmacol. Rev.*, **43**, 109–142.

MONCADA, S., REES, D.D., SCHULZ, R. & PALMER, R.M.J. (1991b). Development and mechanism of a specific supersensitivity to nitrovasodilators after inhibition of vascular nitric oxide synthesis in vivo. *Proc. Natl. Acad. Sci. U.S.A.*, **88**, 2166–2170.

MURAD, F. (1986). Cyclic guanosine monophosphate as a mediator of vasodilatation. *J. Clin. Invest.*, **78**, 1–5.

MURPHY, S., MINOR, R.L. Jr, WELK, G. & HARRISON, D.G. (1990). Evidence for an astrocyte-derived vasorelaxing factor with properties similar to nitric oxide. *J. Neurochem.*, **55**, 349–351.

PALMER, R.M.J., FERRIGE, A.G. & MONCADA, S. (1987). Nitric oxide release accounts for the biological activity of endothelium-derived relaxing factor. *Nature*, **327**, 524–527.

RADOMSKI, M.W. & MONCADA, S. (1983). An improved method for washing of human platelets with prostacylin. *Thromb. Res.*, **30**, 383–389.

RADOMSKI, M.W., PALMER, R.M.J. & MONCADA, S. (1990). Glucocorticoids inhibit the expression of an inducible, but not the constitutive nitric oxide synthase in vascular endothelial cells. *Proc. Natl. Acad. Sci. U.S.A.*, **87**, 10043–10047.

SALVEMINI, D., DE NUCCI, G., GRYGLEWSKI, R.J. & VANE, J.R. (1989). Human neutrophils and mononuclear cells inhibit platelet aggregation by releasing a nitric oxide-like factor. *Proc. Natl. Acad. Sci. U.S.A.*, **86**, 6328–6332.

SALVEMINI, D., KORBUT, R. & VANE, J.R. (1990a). N^G-monomethyl-L-arginine inhibits the release of a nitric oxide-like substance induced by E. coli lipopolysaccharide in the mouse macrophage cell line, J774. In *Nitric Oxide from L-Arginine: a Bioregulatory System*. ed. Moncada, S. & Higgs, E.A. pp. 267–274. Amsterdam, New York, Oxford: Excerpta Medica.

SALVEMINI, D., KORBUT, R., ÄNGGÅRD, E.E. & VANE, J.R. (1990b). Immediate release of a nitric oxide-like factor from bovine aortic endothelial cells by Escherichia coli lipopolysaccharide. *Proc. Natl. Acad. Sci. U.S.A.*, **171**, 135–136.

SALVEMINI, D., MOLLACE, V., PISTELLI, A., ÄNGGÅRD, E. & VANE, J. (1992). Metabolism of glyceryl trinitrate to nitric oxide by endothelial cells and smooth muscle cells and its induction by Escherchia coli lipopolysaccharide. *Proc. Natl. Acad. Sci. U.S.A.*, **89**, 982–986.

SANCESARIO, G., IANNONE, M., D'ANGELO, V., BERNARDI, G.L., NISTICO, G. (1992). N^{ω}-nitro-L-arginine ester inhibits electrocortical changes subsequent to transient global brain ischaemia in mongolian gerbil. *Funct. Neurol.* (in press).

SNEDDON, J.M. & VANE, J.R. (1988). Endothelium-derived relaxing factor reduces platelet adhesion to bovine endothelial cells. *Proc. Natl. Acad. Sci. U.S.A.*, **185**, 2800–2804.

STEINER, A.L., PARKER, C.W. & KIPNIS, D.M. (1972). Radioimmunoassay for cyclic nucleotides. *J. Biol. Chem.*, **247**, 1106–1113.

TORFGARD, K., AHLNER, J., AXELSSON, K.L., NORLANDER, B. & BERTLER, A. (1989). Tissue distribution of glyceryl trinitrate and the effect on cGMP levels in rat. *Pharmacol. Toxicol.*, **64**, 369–372.

TRUMP, B.F., VALIGORKY, J.M., JONES, R.T., MERGNER, W.J., GARCIA, J.H. & COWLEY, R.A. (1975). The application of electron microscopy and cellular biochemistry to the autopsy. Observations on cellular changes in human shock. *Hum. Pathol.*, **6**, 499–516.

WOOD, P.L., EMMETT, M.R., RAO, T.S., CLER, J., MICK, S. & IYENGAR, S. (1990a). Inhibition of nitric oxide synthase blocks N-methyl-D-aspartate, quisqualate, kainate, harmaline and pentylenetetrazole-dependent increases in cerebellar cyclic GMP in vivo. *J. Neurochem.*, **55**, 346–348.

WOOD, K.S., BUGA, C.M., BYRNS, R.E. & IGNARRO, L.J. (1990b). Vascular smooth muscle-derived relaxing factor (MDRF) and its close similarity to nitric oxide. *Biochem. Biophys. Res. Commun.*, **170**, 80–87.

(Received February 27, 1992
Revised March 27, 1992
Accepted April 9, 1992)

Br. J. Pharmacol. (1992), **106**, 937–941 © Macmillan Press Ltd, 1992

The influence of endothelin-1 on human foeto-placental blood vessels: a comparison with 5-hydroxytryptamine

[1]Margaret R. MacLean, Alison G.B. Templeton & J.C. McGrath

Autonomic Physiology Unit, Institute of Physiology, Glasgow University, Glasgow G12 8QQ

1 The vasoconstrictor effect of endothelin-1 (3×10^{-11} M–10^{-7} M) was studied in successive generations of blood vessels of the foeto-placental vascular tree. These were the human umbilical arteries and veins, primary surface chorionic plate arteries, secondary chorionic plate arteries, tertiary surface chorionic plate arteries and veins and the secondary stem villus arterioles. The responses to endothelin-1 were compared with those to 5-hydroxytryptamine (10^{-9} M–10^{-5} M). Arterial preparations were gassed with 2.5% O_2, 8% CO_2 balance N_2 and venous preparations were gassed with 5% O_2, 6% CO_2 balance N_2 to simulate the conditions prevalent *in utero*. The influence of increasing the oxygen tension to 16% (that prevalent at birth) on the response to endothelin-1 on the umbilical arteries was also investigated.

2 All the arterial vessels tested were some ten times more sensitive to endothelin-1 than to 5-hydroxytryptamine and the venous preparations were ten times more sensitive to endothelin-1 than were their equivalent arteries. Increasing oxygen tension did not affect the responses to endothelin-1 in the umbilical artery.

3 Whilst the amplitude of the endothelin-1-induced response was uniform throughout the foeto-placental vascular tree, including the stem villus arterioles, the maximum response to 5-hydroxytryptamine decreased with successive generations and it had no significant effect on the stem villus arterioles. The ratios of the responses to 10^{-7} M endothelin-1: 10^{-7} M 5-hydroxytryptamine in human umbilical arteries, primary surface chorionic plate arteries, secondary chorionic plate arteries, tertiary surface chorionic plate arteries and the secondary stem villus arterioles in the vessels (listed in order of decreasing vessel size) were 1:1.2, 1:0.36, 1:0.33, 1:0.35 and 1:0.04 respectively.

4 In conclusion, endothelin-1 is a powerful vasoconstrictor at all levels of the foeto-placental vascular system including the stem villus resistance vessels. It may play an important role in maintaining foeto-plancental vascular resistance at the low oxygen tension which exists in this vascular system *in utero*.

Keywords: Endothelin-1; human foeto-placental blood vessels; vasoconstriction

Introduction

Human umbilical and placental vessels are not innervated (Spivack, 1946). Regulation of vascular tone in the foeto-placental circulation must therefore depend on myogenic factors or on vasoactive factors which are produced locally or carried to their site of action by the blood. Endothelin-1 (ET-1) is a potent endothelium-derived vasoconstrictor (Yanagisawa, 1988) and is present in human umbilical vessels (Haegerstrand *et al.*, 1989). The preproendothelin-1 gene has been identified in human umbilical veins (Inoue *et al.*, 1989) and a cDNA encoding ET-1 has been isolated from a placental cDNA library (Itoh *et al.*, 1988). Umbilical vein endothelial cells can release ET-1 over time (Clozel & Fischli, 1989) or in response to thrombin (Kohno *et al.*, 1990). There is also evidence of increased maternal plasma levels of ET-1 during labour or on delivery and large amounts of ET-1 are present in the amniotic fluid (Usaki *et al.*, 1990). Binding sites for endothelin-1 exist in membranes from whole human placenta (Fischli *et al.*, 1989) and in purified membranes of placental sub-chorionic stem villus vessels (Mondon *et al.*, 1990).

Thus, evidence suggests that ET-1 is capable of being present and so, if it is active, it could be a locally produced modulator of foeto-placental vascular resistance. Whilst Haegerstrand *et al.* (1989) have shown that ET-1 is a potent vasoconstrictor of human umbilical vessels, no study has as yet been conducted to examine the effects of ET-1 on the placental surface chorionic plate arteries and the placental sub-chorionic stem villus arterioles. The sub-chorionic stem villus arterioles are the major site of vascular resistance in the human placenta (Leiser *et al.*, 1991) and if ET-1 is capable of inducing substantial vasoconstriction of these vessels, this would suggest it is an important mediator of placental vascular resistance.

The foetus exists in an environment which is hypoxic by post-natal standards, reflected by the low oxygen tension of blood in the foeto-placental circulation. In the umbilical arteries, blood (returning from the foetus) has a P_{O_2} of approximately 16 mmHg and in the umbilical venous blood (going to the foetus) it is approximately 30 mmHg (Wulf, 1964). There is evidence which suggests that, in the pithed rat, ET-1 and its analogue [$Ala^{1,3,11,15}$]endothelin are more powerful pressor agents in hypoxic conditions *in vivo* (MacLean & Hiley, 1989; MacLean *et al.*, 1989) and that ET-1 is also a more powerful vasoconstrictor of the rat mesenteric bed in hypoxic conditions *in situ* (MacLean *et al.*, 1989) and *in vitro* (Douglas *et al.*, 1991). Hence, there is reason to suppose that ET-1 would be capable of playing a role in the maintenance of foeto-placental vascular resistance in the conditions of low P_{O_2} which prevail *in utero*.

The aim of this study is to assess ET-1-induced vasoconstriction in this unique circulatory system i.e. to assess ET-1-induced vasoconstriction in umbilical vessels and several placental surface chorionic plate arteries and to compare this with its effect in a placental subchorionic plate arteriole. Noradrenaline has no significant vasoconstrictor effect in human foeto-placental vessels and it has been established that 5-hydroxytryptamine (5-HT) is a potent vasoconstrictor of the umbilical artery (MacLennan & McGrath, 1986). Hence, the effects of ET-1 were compared with those of 5-HT. Increasing O_2 tension has been shown to stimulate

[1] Author for correspondence.

thromboxane A_2 production which results in an increase in the sensitivity of umbilical arteries to 5-HT (Templeton *et al.*, 1991b). This can explain the role of 5-HT and thomboxane A_2 in closing down the umbilical circulation at birth (Tuvemo, 1976). The possibility of a similar role for ET-1 was investigated by looking at the effect of a higher oxygen tension, equivalent to that expected at birth, on the activity of ET-1 on umbilical arteries.

A preliminary account of some of this work has been presented to the British Pharmacological Society (MacLean *et al.*, 1991).

Methods

Umbilical cords and placentae were obtained from recent full term normal pregnancies. They were collected from The Queen Mother's Maternity Hospital, Glasgow and used within 1 h of delivery. Tissue was obtained regardless of whether or not the delivery had been drug-free as it has been shown that variability in the responses to agonists in placentae and cords from different women is not related to the method of delivery (MacLennan, 1986). The following vessels were studied and compared: umbilical arteries and veins, primary surface chorionic plate arteries, secondary surface chorionic plate arteries, tertiary surface chorionic plate arteries and veins and the secondary stem villus arterioles (100–180 μm i.d.). All vessels were dissected free, cleaned and cut into rings (2–3 mm wide). All except the stem villus arterioles were suspended in 40 ml organ baths containing Krebs saline at 37°C. The *in vivo* distending pressures of the umbilical artery and chorionic plate arteries are unknown. The rings were stretched to the optimum point of their length active tension relationship as determined by their response to 75 mM KCl at progressive degress of stretch. Thus, 1.5 g of tension was applied to all arteries, regardless of their situation in the vascular tree. Observation of these vessels show that the smooth muscle/lumen ratio appears to increase with each successive generation which probably accounts for this phenomenon. One gram tension was that which optimised the responses to the veins. Arteries were therefore set up under 1.5 g tension whilst veins were set up under 1 g tension. The composition of the Krebs-bicarbonate saline was as follows (in mM): NaCl 118.4, $NaHCO_3$ 25, KCl 4.7, KH_2PO_4 1.2, $MgSO_4$ 1.2. $CaCl_2$ 2.5, glucose 11, Na_2EDTA 0.023. The arteries and arterioles were gassed with 2.5% O_2, 8% CO_2 balance N_2 and the veins were gassed with 5% O_2, 6% CO_2 balance N_2 to mimic the levels present *in utero*. In a further series of experiments, the responses to ET-1 in umbilical arteries gassed with 16% O_2, 8% CO_2 balance N_2 was studied (to mimic the levels present at birth). The gas tensions and pH were determined regularly by use of both an oxygen electrode inserted into one of the organ baths and a blood gas analyser (Instrumentation Laboratory system 1302).

The stem villus arterioles were too small to be set up in standard organ baths. Under a microscope, they were dissected out and mounted as ring preparations (approximately 2 mm long) in a microvascular myograph (Mulvany & Halpern, 1976) by threading the vessels onto two 40 μm stainless steel wires and subsequently securing the wires to supports. They were equilibrated for 1 h at 37°C and set, using a computer programme, to a circumference L_1, estimated to be 0.9 times the circumference they would maintain if relaxed and exposed to a transmural pressure of 100 mmHg, the normalised circumference (Mulvany & Halpern, 1977). This resulted in a force of 305 ± 16 mg wt being applied to the vessels ($n = 7$). The actual *in vivo* distending pressures of human stem villus arterioles is unknown. As this normalisation procedure resulted in optimal response of these vessels to both ET-1 and 5-HT, we considered it acceptable to study differences in sensitivity of these vessels to these two agonists under these conditions.

Cumulative concentration-response curves were constructed to 5-HT (Sigma, Poole) and compared with those elicited by ET-1 (Bio Mac, Glasgow) in the same ring preparations (in random sequence). Results are shown as the absolute response to the vasocostrictor agent as measured in mg wt force. Stock solutions of ET-1 were 10^{-4} M and due to the financial cost of taking the concentration further, the maximum bath concentration used was 10^{-7} M. Hence, a true maximum response was only consistently attained in the umbilical arteries and tertiary surface chorionic plate arteries, preventing calculation of accurate EC_{50} value for ET-1 in all the vessels. To enable a comparison of the responses to ET-1 with those to 5-HT, concentration-response curves to 5-HT and ET-1 were constructed for every ring preparation. The concentration of 5-HT and ET-1 required to induce a response of 200 mg wt ($EC_{200mg\ wt}$) was calculated for every ring preparation and mean values calculated. The ratio of ET-1: 5-HT sensitivity was obtained by calculating the antilog $[(EC_{200(ET\text{-}1)})\text{-}EC_{200(5\text{-}HT)}]$. To compare the magnitude of responses, the responses to 10^{-7} M ET-1 and 5-HT were determined.

A paired Student's t test was used to assess the significance of differences between the responses to ET-1 and 5-HT and an unpaired Student's t test used to assess the significance of differences between the veins and their corresponding arteries.

Results

Blood gas and pH analysis showed that the *in vitro* conditions for the arterial and arteriolar preparations were as follows: P_{O_2}, 14.1 ± 3.1 mmHg; P_{CO_2}, 45 ± 1.5 mmHg; pH 7.27 ± 0.04 and for the venous preparations: P_{O_2}, 30.5 ± 0.6 mmHg; P_{CO_2}, 37.3 ± 1.4 mmHg; pH 7.39 ± 0.01 (all $n = 6$). In those arterial preparations gassed with 16% oxygen, the values were as follows ($n = 6$); P_{O_2}, 122.6 ± 2.8 mmHg; P_{CO_2}, 43.3 ± 1 mmHg; pH 7.3 ± 0.02.

Figure 1 illustrates concentration-response curves for ET-1 and 5-HT in the arterial vessels studied and Table 1 gives a comparison of their $EC_{200\ mg\ wt}$ values and their responses at a concentration of 10^{-7} M. Only two of the seven stem villus arterioles tested responded to 5-HT. Hence no $EC_{200\ mg\ wt}$ value was determined for these vessels. It can be seen that the potency of ET-1 was uniform throughout the arterial tree as was the amplitude of its response at 10^{-7} M. ET-1 was some ten times more potent than 5-HT in the vessels tested. The potency of 5-HT did not vary between the arterial preparations but, as mentioned above, it induced a significant contraction in only two out of the seven stem villus arterioles tested. Table 1 shows that the ratio of ET-1: 5-HT sensitivity tended to increase with successive generations of the foetoplacental vasculature and that the increased potency of ET-1 compared with that to 5-HT was most marked in the umbilical vein. Table 1 shows that, unlike with ET-1, the amplitude of response to 5-HT declined with successive chorionic plate arterial generations and was negligible in the subchorionic stem villus arterioles. It also shows that, in all but the umbilical artery, the amplitude of the response to 10^{-7} M 5-HT was significantly smaller than that elicited by 10^{-7} M ET-1. It can also be seen from Figure 1 that the responses to 5-HT in the primary surface chorionic plate arteries, secondary surface chorionic plate arteries and tertiary surface chorionic plate arteries fall off at concentrations exceeding 3×10^{-7}–10^{-6} M.

Figure 2 illustrates concentration-response curves for ET-1 and 5-HT in the umbilical vein and the tertiary surface chorionic plate vein. It compares these responses with the concentration-response curves for the relevant corresponding arteries. Table 1 also gives a comparison of their $EC_{200\ mg\ wt}$ values and their responses to 10^{-7} M ET-1 and 5-HT. Whilst the potency of 5-HT was the same in the veins and arteries, it can be seen that ET-1 is some ten times more potent in the venous preparations. From Figure 2 and Table 1 it can be

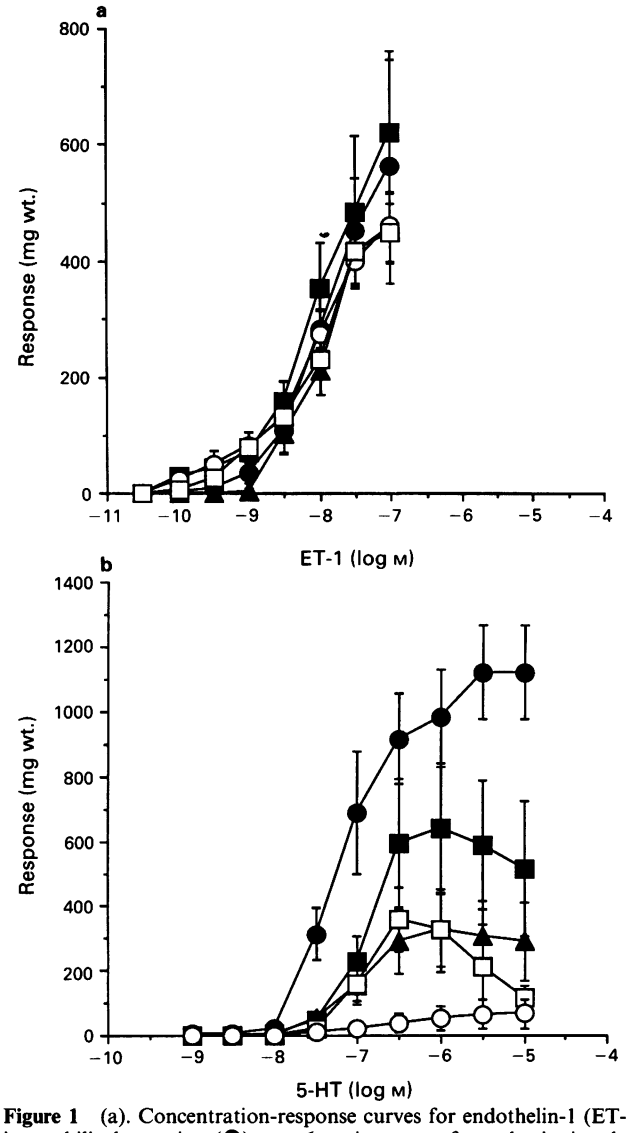

Figure 1 (a). Concentration-response curves for endothelin-1 (ET-1) in umbilical arteries (●) $n = 6$, primary surface chorionic plate arteries (■) $n = 6$, secondary chorionic plate arteries (▲) $n = 6$, tertiary surface chorionic plate arteries (□) $n = 6$ and secondary stem villus arterioles (○) $n = 7$. (b) Concentration-response curves for 5-hydroxytryptamine (5-HT) in umbilical arteries (●) $n = 6$, primary surface chorionic plate arteries (■) $n = 6$, secondary chorionic plate arteries (▲) $n = 6$, tertiary surface chorionic plate arteries (□) $n = 6$ and secondary stem villus arterioles (○) $n = 7$. Responses are expressed as absolute changes in tension (mg wt.). Preparations were gassed with 2.5% O_2, 8% CO_2 balance N_2. All values are given as means with the vertical lines representing s.e.mean.

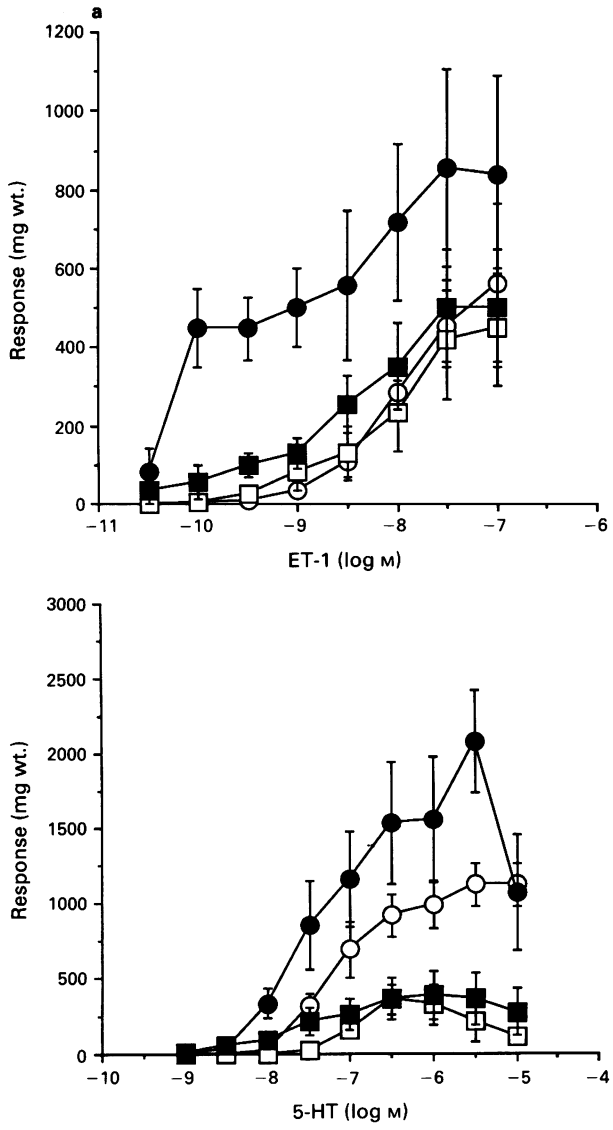

Figure 2 (a). Concentration-response curves for endothelin-1 (ET-1) in umbilical veins (●) $n = 6$, tertiary surface chorionic plate veins (■) $n = 5$, umbilical arteries (○) $n = 6$ and tertiary surface chorionic plate arteries (□) $n = 6$. (b) Concentration-response curves for 5-hydroxytryptamine (5-HT) in umbilical veins (●) $n = 6$, tertiary surface chorionic plate veins (■) $n = 5$, umbilical arteries (○) $n = 6$ and tertiary surface chorionic plate arteries (□) $n = 6$. Responses are expressed as absolute changes in tension (mg wt.). The arteries and arterioles were gassed with 2.5% O_2, 8% CO_2 balance N_2 and the veins were gassed with 5% O_2, 6% CO_2 balance N_2. The values are given as means with the vertical lines representing s.e.mean.

Table 1 $EC_{200\,mg\,wt}$ values and maximum responses to 10^{-7} M endothelin-1 (ET-1) and 10^{-7} M 5-hydroxytryptamine (5-HT) in placental and umbilical blood vessels

	– log concentration of the $EC_{200\,mg\,wt}$			*Response to 10^{-7} M (tension [mg wt.])*		
	ET-1	*5-HT*	*Ratio ET-1:5-HT*	*ET-1*	*5-HT*	n
Umbilical artery	8.3 ± 0.2	7.6 ± 0.1*	5.0	562 ± 200	690 ± 150	6
1° Surface chorionic plate artery	8.1 ± 0.2	6.7 ± 0.1**	31.6	623 ± 100	224 ± 79*	6
2° Surface chorionic plate artery	7.8 ± 0.2	6.6 ± 0.2**	15.8	458 ± 63	153 ± 60*	6
3° Surface chorionic plate artery	8.0 ± 0.4	6.4 ± 0.3*	39.8	450 ± 110	156 ± 50*	6
2° Stem villus arteriole	7.9 ± 0.2	–		460 ± 65	20 ± 16***	7
Umbilical vein	10.0 ± 0.8†	7.5 ± 0.4*	316.2	856 ± 265	757 ± 250	6
3° Surface chorionic plate vein	8.6 ± 0.2††	7.0 ± 0.5**	39.8	580 ± 150	70 ± 5*	5

All arterial preparations were gassed with 2.5% oxygen, 8% carbon dioxide, balance nitrogen whilst the venous preparations were gassed with 5% oxygen, 6% carbon dioxide, balance nitrogen. Statistical differences as assessed by the unpaired Student's t test for veins vs. their relevant arteries

†$P < 0.05$; ††$P < 0.01$; statistical differences as assessed by the paired Student's t test for 5-HT vs. ET-1

*$P < 0.05$; **$P < 0.01$; ***$P < 0.001$.

seen that ET-1 has a particularly profound effect on the umbilical vein with 10^{-10} M ET-1 being the threshold effective concentration. Figure 2 also demonstrates that concentration-response curves to 5-HT in foeto-placental vessels are often bell-shaped, concentrations over $3\ 10^{-6}$ M tending to fall off. This phenomenon is currently under investigation.

Figure 3 shows the responses to ET-1 in the umbilical artery gassed with either 14 mmHg oxygen or 123 mmHg oxygen. Increasing the oxygen tension had no significant effect on the sensitivity to ET-1 in the umbilical artery. In fact the trend, though not significant, was for the increased oxygen tension to decrease absolute responses to ET-1. The $-\log$ concentrations of the $EC_{200\,mg\,wt}$ for ET-1 in the umbilical artery in 16% O_2 and 0% O_2 were 7.9 ± 0.2 and 8.3 ± 0.2 respectively. Alternative statistical tests such as analysis of variance also failed to pick up any significant difference in this data.

Discussion

The aim of this study was to investigate the potential of ET-1 to be a locally produced modulator of foeto-placental vascular resistance by studying the ability of ET-1 to induce vasoconstriction in successive generations of the human foeto-placental vasculature. This is a unique system existing in a low oxygen environment *in utero*, conditions that are known to enhance the effects of ET-1 in other circulatory systems. The results show that ET-1 is a potent agonist at all levels of the foeto-placental circulation. The responses elicited by ET-1 were uniform throughout the foeto-placental vascular tree unlike those to 5-HT which declined with successive generations. Increasing O_2 tension has been shown to stimulate thromboxane A_2 production which results in an increase in the sensitivity of umbilical arteries to 5-HT (Templeton *et al.*, 1991b). It has previously been shown that the maximum responses to thromboxane A_2 diminish with foeto-placental vessel size and that the maximum response achieved in the stem villus arterioles was only 20% of the response seen in the primary surface chorionic plate arteries (Templeton *et al.*, 1991a). The stem villus arterioles are the main site of resistance in the foeto-placental vasculature (Leiser *et al.*, 1991), they are not innervated and as other vasoactive agents have little effect on these vessels, locally produced endogenous ET-1 is the best candidate that we have found, so far, to play a significant role in the maintenance of foeto-placental vascular resistance. Placental vascular ET-1 synthesis may therefore be of great physiological importance.

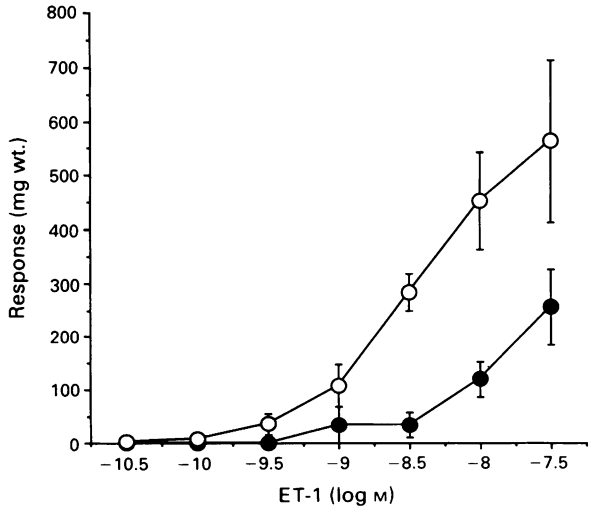

Figure 3 The effect of increasing oxygen tension from 2.5% (+ 8% CO_2 balance N_2) to 16% (+ 8% CO_2 balance N_2) on the responses to endothelin-1 (ET-1) in the umbilical artery. (●) ET-1 at 16% oxygen, (○) ET-1 at 2.5% oxygen. $n = 6$ for both groups. Responses are expressed as absolute changes in tension (mg wt.). The values are given as means with the vertical lines representing s.e.mean.

The results of this study show that ET-1 is an extremely effective vasoconstrictor in the umbilical vein compared with 5-HT with 10^{-10} M being the threshold concentration for a marked vasoconstriction. It may, therefore, play an important role in maintaining umbilical venous pressure and foetal blood supply. Systemic plasma levels of ET-1 have been measured and are in the pM range (Tomita *et al.*, 1989; Saito *et al.*, 1990; Usaki *et al.*, 1990). However, it has been shown by Ånggård *et al.* (1989) that following left ventricular injection of ^{125}I-labelled ET-1, 60% of the ET-1 was removed from the circulation in the first minute after injection. The highest uptake being in the lung, followed by the kidney and liver. Hence, it will be local concentrations of ET-1 which determine the response to this peptide and these are likely to be higher than those detected in plasma. During labour, maternal ET-1 plasma levels can increase though the concentration in the foeto-placental circulation could well be higher still. Indeed, the level of ET-1 detected in the amniotic fluid on delivery exceeds 10 pM (Usaki *et al.*, 1990). The threshold of sensitivity to ET-1 in the vessels studied here were therefore just at physiological levels as measured from the systemic circulation though local levels in the foeto-placental circulation are probably higher than these.

The increase in O_2 tension that occurs at birth is believed to assist in closing down the umbilical circulation by inducing a profound vasoconstriction of the umbilical arteries. This is due to stimulation of thromboxane A_2 production which increases the sensitivity of the umbilical arteries to 5-HT (Templeton *et al.*, 1991b). This study shows that the potency of ET-1 was not increased by increasing oxygen tension in the umbilical artery. These results suggest that the intracellular mechanisms behind the ET-1-induced vasoconstriction are different from those involved in the thromboxane A_2-sensitive 5-HT response. However, as there is an increase in maternal plasma levels of ET-1 on delivery (Usaki *et al.*, 1990), ET-1 may still play a role in closing down the umbilical circulation at birth i.e. because its concentration changes in contrast to the sensitivity of the vessel to it. In particular, increased levels of ET-1 may play an essential role in closing down the umbilical venous circulation at birth.

In the systemic system ET-1 is a relatively better agonist on veins than on arteries. This has previously been demonstrated in various isolated vessel preparations from the rabbit and dog *in vitro* (D'Orléans-Juste *et al.*, 1988). The results of the present study show that it is also the case in human umbilical blood vessels that ET-1 is more potent on the umbilical vein and the tertiary surface chorionic plate vein than in the corresponding arteries, i.e. the umbilical artery and the tertiary surface chorionic plate artery. However an analogy with the systemic system is inappropriate with respect to the metabolic environment since the umbilical 'vein' contains the oxygenated blood. A closer analogy is with the pulmonary circulation where the veins also carry the oxygenated blood although the absolute Po_2 levels are much higher. There is, however, evidence that the primary site of action of ET-1 in the lung is in the pulmonary veins (e.g. in the guinea pig: Horgan *et al.*, 1991) suggesting that there is a greater 'sensitivity' of venous smooth muscle cells to ET-1 (e.g. greater receptor number or affinity).

In conclusion, ET-1 is a potent agonist at all levels of the foeto-placental circulation and hence ET-1 has a unique capacity to maintain foeto-placental vascular resistance in the hypoxic conditions that prevail *in utero*. The increase in ET-1 levels observed during labour and at birth may assist in closing down the umbilical circulation at birth.

M.R.M. is a Wellcome Trust Post-Doctoral Fellow and this work was also funded in part by The British Heart Foundation (grant no. 89/23). The authors wish to thank Mrs J.B. MacMillan for her excellent technical assistance.

References

ANGGÅRD, E., GALTON, S., RAE, G., THOMAS, R., MCLOUGHLIN, DE NUCCI, G. & VANE, J.R. (1989). The fate of radioiodinated endothelin-1 and endothelin-3 in the rat. *J. Cardiovasc. Pharmacol.*, **13** (suppl. 5), S46–S49.

CLOZEL, M. & FISCHLI, W. (1989). Human cultured endothelial cells do secrete endothelin-1. *J. Cardiovasc. Pharmacol.*, **13** (suppl. 5), S229–S231.

D'ORLEANS-JUSTE, P., ANTUNES, E., DE NUCCI, G. & VANE, J.R. (1988). A profile of endothelin on isolated vascular and other smooth muscle preparations. *Br. J. Pharmacol.*, **95,** 809P.

DOUGLAS, S.A., JAMES, S. & HILEY, C.R. (1991). Endothelial modulation and changes in endothelin pressor activity during hypoxia in the rat isolated perfused superior mesenteric arterial blood bed. *Br. J. Pharmacol.*, **103,** 1441–1448.

FISCHLI, W., CLOZEL, M. & GUILLY, C. (1989). Specific receptors for endothelin on membranes from human placenta. Characterization and use in binding assay. *Life Sci.*, **44,** 1429–1436.

HAEGERSTRAND, A., HEMSÉN, A., GILLIS, C., LARSSON, O. & LUNDBERG, J.M. (1989). Endothelin: presence in human umbilical vessels, high levels in fetal blood and potent constrictor effect. *Acta Physiol. Scand.*, **137,** 541–542.

HORGAN, M.J., PINHEIRO, J.M.B. & MALIK, A.B. (1991). Mechanism of Endothelin-1-induced pulmonary vasoconstriction. *Circ. Res.*, **69,** 157–164.

INOUE, A., YANAGISAWA, M., TAKUWA, Y., MITSUI, Y., KOBAYASHI, M. & MASAKI, T. (1989). The human preproendothelin-1 gene. Complete nucleotide sequence and regulation of expression. *J. Biol. Chem.*, **264,** 14954–14959.

ITOH, Y., YANAGISAWA, M., OHKUBO, S., KOSAKA, T., INOUE, A., ISHIDA, N., MITSUI, Y., ONDA, H., FUJINO, M. *et al.* (1988). Cloning and sequence analysis of cDNA encoding the precursor of a human endothelium-derived vasoconstrictor peptide, endothelin: identity of human and porcine endothelin. *FEBS Lett.*, **231,** 440–444.

KOHNO, M., YASUNARI, K., YOKOKAWA, K., MURAKAWA, K., HORIO, T., KANAYAMA, Y., FUZISAWA, M., INOUE, T. & TAKEDA, T. (1990). Thrombin stimulates the production of immunoreactive endothelin-1 in cultured human umbilical vein endothelial cells. *Metabolism*, **39,** 1003–1005.

LEISER, R., KOSANKE, G. & KAUFMANN, P. (1991). In *Placenta: Basic Research for Clinical Application.* ed. Soma, H. Basle: Karger.

MACLEAN, M.R. & HILEY, C.R. (1989). Blood pressure changes induced by [Ala^{1,3,11,15}]endothelin in pithed rats: effects of lowering ventilation volume. *Br. J. Pharmacol.*, **97,** 529P.

MACLEAN, M.R., RANDALL, M.D. & HILEY, C.R. (1989). Effects of moderate hypoxia, hypercapnia and acidosis on haemodynamic changes induced by endothelin-1 in the pithed rat. *Br. J. Pharmacol.*, **98,** 1055–1065.

MACLEAN, M.R, TEMPLETON, A.G.B. & MCGRATH, J.C. (1991). Effect of endothelin-1 on human umbilical and placental blood vessels: a comparison with 5HT. *Br. J. Pharmacol.*, **104,** 102P.

MACLENNAN, S.J. (1986). The influence of oxygen on the isolated human umbilical artery. *PhD. Thesis. Glasgow University.*

MACLENNAN, S.J. & MCGRATH, J.C. (1986). Evidence for 5-HT$_1$-like receptors in human umbilical artery (HUA). *Br. J. Pharmacol.*, **89,** 587P.

MONDON, R.C., FERRE, F. & CAVERO, I. (1990). Identification and characterization of [^{125}I] endothelin binding sites on stem villi vessels from human placenta. *Eur. J. Pharmacol.*, **183,** 1850.

MULVANY, M.J. & HALPERN, W. (1976). Mechanical properties of vascular smooth muscle cells. *in situ. Nature*, **260,** 617–619.

MULVANY, M.J. & HALPERN, W. (1977). Contractile properties of small arterial resistance vessels in spontaneously hypertensive and normotensive rats. *Circ. Res.*, **41,** 19–26.

SAITO, Y., NAKAO, K., MUKOYAMA, M. & IUMURA, H. (1990). Increased plasma endothelin level in patients with essential hypertension. *New Engl. J. Med.*, **322,** 205.

SPIVACK, M. (1946). The anatomical peculiarities of the human umbilical cord and their clinical significance. *Am. J. Obstet. Gynecol.*, **52,** 387–401.

TEMPLETON, A.G.B., MACMILLAN, J.B., MCGRATH, J.C. & WHITTLE, M.J. (1991a). Effect of thromboxane A$_2$ and oxygen in the surface chorionic and stem villus vessels of the human placenta. *Br. J. Pharmacol.*, **104,** 417P.

TEMPLETON, A.G.B., MCGRATH, J.C. & WHITTLE, M.J. (1991b). The role of endogenous thromboxane in contractions to U46619, oxygen, 5-HT and 5-CT in the human isolated umbilical artery. *Br. J. Pharmacol.*, **103,** 1079–1084.

TOMITA, K., UJIIE, K., NAKANISHI, T., TOMURA, S., MATSUDA, O., ANDO, K., SHICHIRA, M., HIRATA, Y. & MARUMO, F. (1989). Plasma endothelin levels in patients with acute renal failure. *New Engl. J. Med.*, **321,** 1127.

TUVEMO, T. (1976). Role of prostaglandins, prostacyclin, and thromboxanes in the control of the umbilical-placental circulation. *Semin. Perinatol.*, **4,** 91–95.

USAKI, S., SAITOH, T., SAWAMURA, T., SUZUKI, N., SHIGEMITSU, S., YANAGISAWA, M., GOTO, K., ONDA, H., FUJINO, M. & MASAKI, T. (1990). Increased maternal plasma concentration of endothelin-1 during labor pain or on delivery and the existence of a large amount of endothelin-1 amniotic fluid. *Gynecol. Endocrinol.*, **4,** 85–97.

WULF, H. (1964). The oxygen and carbon dioxide tension gradients in the human placenta at term. *Am. J. Obstet. Gynecol.*, **88,** 38–44.

YANAGISAWA, M., KURIHARA, H., KIMURA, S., TOMOBE, Y., KOBAYASHI, M., MITSUI, Y., YAZAKI, Y., GOTO, K. & MASAKI, T. (1988). A novel potent vasoconstrictor peptide produced by vascular endothelial cells. *Nature*, **332,** 411–415.

(Received November 28, 1991
Revised April 9, 1992
Accepted April 10, 1992)

Br. J. Pharmacol. (1992), **106**, 942–947 © Macmillan Press Ltd, 1992

The cardiodepressant and vasodepressant effects of tumour necrosis factor in rat isolated atrial and aortic tissues

[1]R. Foulkes & S. Shaw

Immunomodulation Biology, Celltech Research, 216 Bath Road, Slough, SL1 4EN

1 The ability of recombinant human tumour necrosis factor-α (rec huTNF) to elicit cardiodepressor and vasodepressor effects in rat isolated tissues was investigated.

2 rec huTNF (3×10^{-11}–3×10^{-8} M) administered directly to the organ bath, caused a concentration-dependent relaxation of the isoprenaline-induced inotropic response in electrically stimulated rat left atria. This occurred within 20 min of administration. In contrast, rec huTNF was without effect on the chronotropic response to isoprenaline in isolated spontaneously beating atria.

3 rec huTNF (1 μg kg^{-1}) was also given systemically to rats and the atria studied *in vitro*. Only 60 min of rec huTNF pretreatment was sufficient to cause a marked attenuation of the isoprenaline-induced inotropic response. This effect was not further augmented when rats were pretreated with rec huTNF for 24 h.

4 In isolated aortic rings taken from rats 60 min after rec huTNF (1 μg kg^{-1}, i.v.) administration, there was no effect seen on the constriction induced by phenylephrine in either endothelium-intact or denuded tissues. In addition, any responses to L-arginine or N^G-nitro-L-arginine methyl ester (L-NAME) administration were unaffected by rec huTNF pretreatment.

5 In aortic rings taken from rats 24 h after rec huTNF administration, the phenylephrine-induced constriction was significantly attenuated in tissues with an intact endothelium. Furthermore, the relaxation to subsequent L-arginine administration was greater in these tissues than in those from saline-treated rats. In addition, in both endothelium-intact and denuded tissues, the vasoconstrictor response to L-NAME (10^{-3} M) was significantly augmented.

6 These data suggest that rec huTNF possesses both cardiodepressant properties with a rapid onset of action and vasodepressant properties with a slow onset of action. The latter could be mediated through the induction of a non-constitutive form of the NO-synthase enzyme present within the vascular wall.

Keywords: Tumour necrosis factor; nitric oxide; myocardial depression; vasodepression

Introduction

In animals given endotoxin or gram negative bacteria, one of the primary mediators of the ensuing cardiovascular shock state is tumour necrosis factor-α (TNF), a cytokine released from activated monocytes and macrophages as well as other cell types (Beutler & Cerami, 1987). Indeed monoclonal antibodies raised against TNF can improve survival and ameliorate some of the cardiovascular manifestations associated with septic shock in a number of animal species (Beutler *et al.*, 1985; Mathison *et al.*, 1988; Hinshaw *et al.*, 1990). Furthermore, TNF, like lipopolysaccharide (LPS), can induce the expression and synthesis of a form of NO-synthase in macrophages and other cells (Jorens *et al.*, 1991), including smooth muscle (Busse & Mulsch, 1990) and endothelial cells (Kilbourn & Belloni, 1990).

Cardiovascular shock states such as haemorrhagic or endotoxic shock resulting from septicaemia are characterized by marked hypotension, myocardial depression and acidosis often leading to the failure of one or more organs. In man and animal models of these disease states, depression of cardiac performance has been associated with the appearance of a circulating factor which can itself suppress cardiac function in *in vitro* and *in vivo* bioassays (Goodyear, 1967; Lefer, 1970; Lefer & Rovetto, 1970). Although thought to be of peptide origin, the precise nature of this substance(s) remains unknown. In addition, there is growing evidence that the hypotension associated with endotoxin-induced shock states in animals is at least partly dependent on the L-arginine-NO pathway. Indeed, this hypotensive state can be readily reversed by the administration of inhibitors of nitric oxide synthase (Wright *et al.*, 1992). Furthermore, in *in vitro* studies in aortic tissues taken from rats previously given LPS, a reduced vascular responsiveness to phenylephrine has been shown to be associated with the induction of a non-constitutive form of NO-synthase in the tissues (Fleming *et al.*, 1991). However, given the multifarious nature of cytokines and hormones released in response to endotoxin administration, it is unclear which, if any, of these have inherent cardiac and vascular depressive properties.

Hence, the present study investigated whether some of the cardiac and vascular depressant effects known to be associated with LPS administration could also be seen with TNF treatment. This was addressed by studying the effects of recombinant human TNF (rec huTNF) on isolated cardiac and vascular preparations from rats.

Methods

1 Effects of rec huTNF on rat isolated left and right atria

Male Sprague Dawley rats (300–350 g) were killed by a blow to the head and cervical dislocation, the atria rapidly removed and each mounted on electrodes in a 100 ml organ bath. The upper portion of each atrium was connnected to a Grass FT03 force-displacement transducer and isometric tension was recorded on a Gould TA550 recorder. The organ baths were filled with Krebs solution of the following com-

[1] Author for correspondence.

position (in mM): NaCl 118, $NaHCO_3$ 25, D-glucose 11, KCl 4.7, $CaCl_2$ 2.5, KH_2PO_4 1.2 and $MgSO_4.7H_2O$ 1.2, maintained at 37°C and gassed continuously with a mixture of 95% O_2 and 5% CO_2. Left atria were electrically stimulated by a Grass stimulator using a supra-maximal voltage at 90 Hz with a pulse duration of 5 ms whereas the right atria beat spontaneously.

Tissues were allowed to equilibrate for 60 min under a resting tension of 1 g following which a single bolus of isoprenaline (10^{-6} M) was added to the bath to sensitize the tissues (previous pilot studies have shown that after this initial sensitization period up to 4 concentration-response curves (CRCs) to isoprenaline can be carried out without the development of tachyphylaxis). Following repeated washing a CRC to isoprenaline (10^{-10}–10^{-6} M) was performed with a 3 min dosing cycle. The tissues were then washed and a second CRC was performed according to one of the following treatments: (1) CRC to isoprenaline only, ($n = 6$); (2) CRC to isoprenaline in the presence of rec huTNF (3×10^{-12}–3×10^{-8} M) given 15 min earlier ($n = 6$); (3) CRC to isoprenaline in the presence of rec huTNF (3×10^{-10} M) and the additional presence of a specific anti-rec huTNF monoclonal antibody (CB0010, 3×10^{-7} M or 3×10^{-9} M) given 15 min before rec huTNF ($n = 6$). In some tissues ($n = 6$), an isotype-matched control antibody, MOPC21 (3×10^{-7} M) was given instead of CB0010. Neither of these antibodies alone had any effect on the second isoprenaline CRC.

In addition, the effect of prior rec huTNF administration on the inotropic response to 1-isobutyl, 3-methylxanthine (10^{-8}–10^{-4} M) was also studied ($n = 6$).

2 Effect of systemic (i.v.) administration of rec huTNF on rat isolated atria

Male Sprague Dawley rats (300–400 g) were briefly anaesthetized with halothane (2% in O_2) and given either rec huTNF (1 μg kg^{-1} in 1 ml kg^{-1} 0.9% saline bolus, $n = 6$) or 1 ml kg^{-1} 0.9% saline ($n = 6$) via the tail vein. Rats were killed at either 1 h or 24 h post administration, the atria removed and prepared as before. Following the equilibration and isoprenaline sensitization, a single CRC to isoprenaline (10^{-10}–10^{-6} M) was obtained. Previous studies in this laboratory have shown this dose of rec huTNF to be non-hypotensive and non-lethal in this species.

3 Effects of systemic rec huTNF pretreatment on rat isolated aortic rings: interaction with the L-arginine-NO pathway

rec huTNF (1 μg kg^{-1}) or 0.9% saline was administered as a single bolus (1 ml kg^{-1}) via the tail vein to male Sprague Dawley rats (300–400 g). Animals were killed either 1 h or 24 h later and the aortae rapidly removed. Aortic rings (2–3 mm diameter and 1–2 mm in length, $n = 12$) were mounted in 10 ml organ baths, connected to a Grass FT03 transducer and isometric tension recorded on a Grass polygraph. Tissues were bathed in Krebs solution and equilibrated under the optimal resting tension for the tissues (around 1.5 g). In half of the preparations ($n = 6$) the endothelium was removed by gently rubbing the lumen with the barrel of a syringe needle. All experiments were performed in the presence of 10^{-3} M indomethacin to remove any possible influence of cyclo-oxygenase-mediated events.

Rings were preconstricted with 10^{-4} M phenylephrine and the presence of functional endothelium was assessed by observing the vasodilator response to 10^{-6} M acetylcholine (ACh); rings showing no relaxation or a small constriction were considered endothelium-denuded and those showing more than 40% relaxation were considered as endothelium-intact tissues. This was confirmed at the end of the experiment by histological examination. Following repeating washing and a 90 min stabilization period a cumulative CRC to phenylephrine (10^{-9}–10^{-4} M) was performed with a 5 min dosing cycle; tissues were then repeatedly washed and re-equilibrated. All tissues were then constricted to 70% of maximal constriction with phenylephrine and a cumulative CRC to either D- or L-arginine (10^{-6}–10^{-3} M) was carried out with a 15 min dosing cycle. After a further washing and stabilization period, tissues were again constricted to 70% of maximum with phenylephrine but this time in the presence and absence of N^G-nitro-L-arginine methyl ester (L-NAME, 10^{-3} M) given 15 min previously and the change in tension measured.

Data analysis

All data are presented as means ± s.e.mean. In experiment (1), CRCs were compared by calculating the EC_{50} values for the pairs of curves and performing a paired *t*-test. To compare relative shifts at each concentration of rec huTNF, dose ratios were calculated and these were compared by one-way ANOVA. In experiemnt (2), mean EC_{50} values were compared by an unpaired *t* test. In experiment (3), mean EC_{50} values for the phenylephrine constriction curves and the mean changes in tension following L-NAME administration were compared by one-way ANOVA.

Materials

The monoclonal antibodies CB0010 and MOPC21 were manufactured by Celltech. CB0010 specifically neutralizes rec huTNF whereas MOPC21 is a nonspecific isotype matched control antibody. rec huTNF was purchased from Bissendorf Biochem (Hanover, Germany) and all other drugs from Sigma (Poole, UK). Both antibodies and rec huTNF were dissolved in saline before use.

Results

1 Effect of rec huTNF on rat isolated left and right atria

Isoprenaline, administered alone, caused a concentration-dependent increase in force (up to + 0.742 ± 0.13 g) and rate of contraction (up to 440 ± 20 beats per min) in isolated left and right atria, respectively, with a mean EC_{50} of 6 ± 10^{-9} M. Pilot studies indicated that up to 4 CRCs to isoprenaline could be performed on the same tissue without the development of tachyphylaxis.

In left atria, following the first CRC to isoprenaline, 20 min incubation with rec huTNF did not significantly alter the basal contractility. In the presence of rec huTNF, there was concentration-dependent rightward shift in the isoprenaline CRC, the threshold being 3×10^{-11} M rec huTNF (Figure 1a) and the maximum seen at 3×10^{-9} M (Figure 1b). Although the CRC shifts were not large (maximum dose-ratio = 2.7 ± 0.5; $P < 0.01$), they were parallel and not accompanied by a decrease in the maximum isoprenaline response. It should be noted that incubation with rec huTNF for periods up to 60 min did not result in a greater shift in the isoprenaline CRC.

This effect was specific for rec huTNF, since in the presence of a neutralising monoclonal antibody raised against rec huTNF (CB0010, 3×10^{-7} M), the rec huTNF-mediated cardiodepressive response was prevented (dose-ratio = 1.08 ± 0.05). Furthermore, neither a lower concentration (3×10^{-9} M of CB0010 (dose-ratio = 2.62 ± 0.6, $P < 0.05$) nor a non-specific murine monoclonal antibody (MOPC21, 3×10^{-7}M, dose ratio = 2.0 ± 0.17, $P < 0.05$) were able to modify the rec huTNF response.

The effect of rec huTNF on the inotropic response in left atria was not restricted to β-receptor-mediated events since similar shifts in CRCs were seen when the phosphodiesterase inhibitor, IBMX, was used instead of isoprenaline (dose-

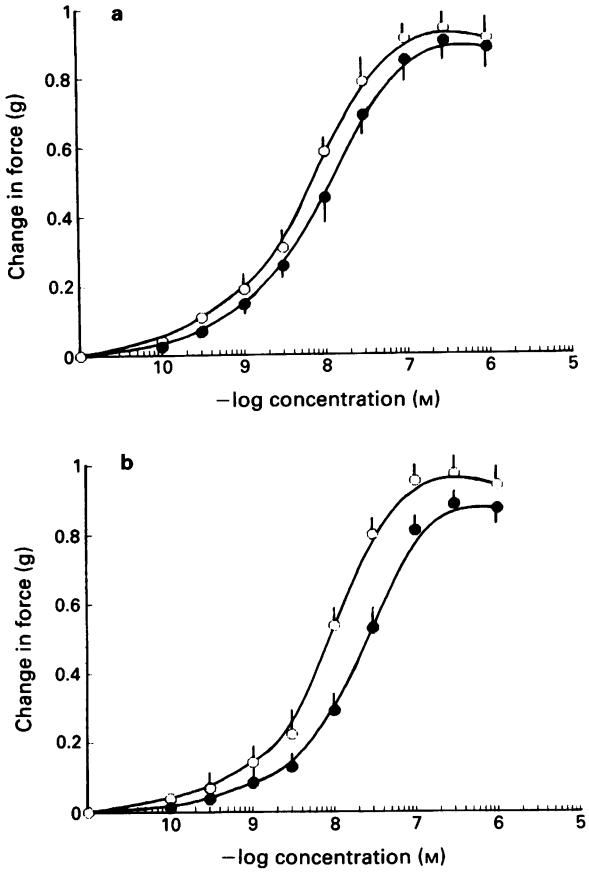

Figure 1 The effect of recombinant human tumour necrosis factor-α (rec huTNF) administration on the isoprenaline-induced inotropic response in rat isolated left atria. A concentration-response curve to isoprenaline was first obtained (○) and, following washing, rec huTNF was administered directly to the bath at either 3×10^{-11} M (a) or 3×10^{-9} M (b) and a second isoprenaline curve obtained (●). Values are mean with s.e.mean shown by vertical lines. $n = 6$ for each group.

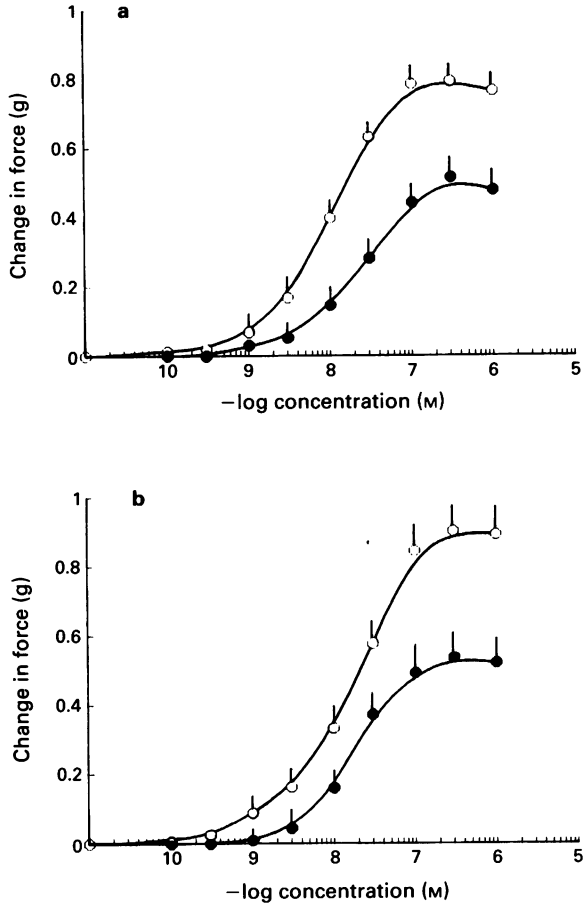

Figure 2 Effect of systemic recombinant human tumour necrosis factor-α (rec huTNF) pretreatment on isoprenaline-induced inotropic responses in rat isolated left atria. Rats received either saline (1 ml kg, i.v., ○) or rec huTNF (1 μg kg^{-1}, i.v., ●) 60 min (a) or 24 h (b) before they were killed and the atria removed. A single isoprenaline curve only was obtained on each tissue. Values are means with s.e.mean shown by vertical lines; $n = 6$ for each group.

ratio = 2.9 ± 0.41, $P < 0.05$).

In spontaneously beating right atria, rec huTNF pretreatment did not affect either the baseline rate of beating or the isoprenaline-induced tachycardia at any concentration.

2 Effect of systemic (i.v.) administration of rec huTNF on rat isolated atria

When rec huTNF was given to rats 1 h before they were killed, the inotropic response of left atria to isoprenaline administration was markedly attenuated; the isoprenaline CRC was shifted to the right accompanied by a decrease in the maximum response (0.475 ± 0.1 g vs 0.765 ± 0.15 g in rec huTNF compared to saline-treated rats, $P < 0.05$; Figure 2a). When the atria were removed 24 h after rec huTNF administration, the suppression of the isoprenaline CRC was no greater than that seen in those removed at 1 h (Figure 2b). Again at neither time point did rec huTNF modify the chronotropic effects of isoprenaline in spontaneously beating right atria.

3 Effects of rec huTNF pretreatment on rat isolated aortic rings-interaction with the L-arginine-NO pathway

Phenylephrine caused a concentration-dependent increase in developed tension in all aortic preparations used.

Tissues removed at 1 h In tissues that had been denuded, the phenylephrine CRC was always to the left of those that had intact endothelium ($P < 0.05$; compare Figures 3a and 3b). This was true for tissues from both saline and rec huTNF-treated rats. However, there was no difference in the response to phenylephrine in either denuded or endothelium intact preparations from saline or rec huTNF-treated rats.

When tissues were constricted to 70% of maximum with phenylephrine, a vasodilator response to L-arginine could be demonstrated only in rings with an intact endothelium. This vasodilatation was similar in rings from both saline and rec huTNF-treated rats (Figure 4a). D-Arginine was without effect in any of the tissues studied.

When phenylephrine was given at a concentration that would normally elicit a 70% constriction, in the additional presence of L-NAME, the constrictor response was enhanced. This occurred only in rings with an intact endothelium. Furthermore, this potentiation was similar in tissues from saline (+ 78 ± 11%) and rec huTNF-treated (+ 81 ± 11%) rats (Figure 4b). No augmentation of the constrictor response to phenylephrine was seen in denuded tissues from either group of rats.

Tissues removed at 24 h In saline-treated rats, the relative potency of phenylephrine was again less in endothelium-intact tissues than in denuded tissues. However, in rings from rec huTNF-treated rats this difference was much more marked; the constrictor response to phenylephrine being attenuated both in terms of the EC_{50} of the CRC and the maximum response in intact compared to denuded tissues (compare Figures 5a and b). Hence, although there were no significant

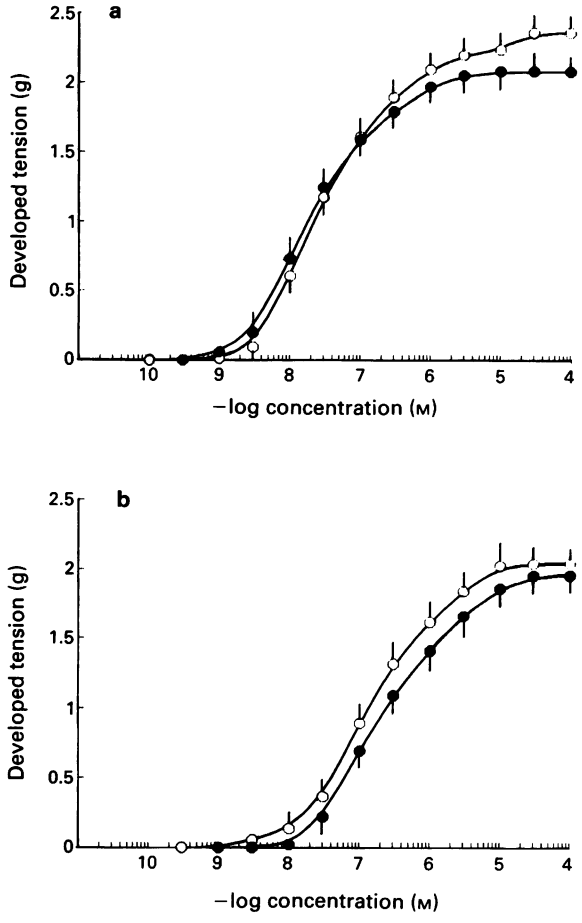

Figure 3 Effect of 1 h saline (1 ml kg^{-1}, i.v., ○) or recombinant human tumour necrosis factor (rec huTNF) (1 μg kg^{-1}, i.v., ●) pretreatment on the phenylephrine-induced constrictor response in rat isolated aortic rings. Tissues were either denuded of endothelium (a) or had the endothelium intact (b). Values are means with s.e.mean shown by vertical lines; $n = 6$ for each group.

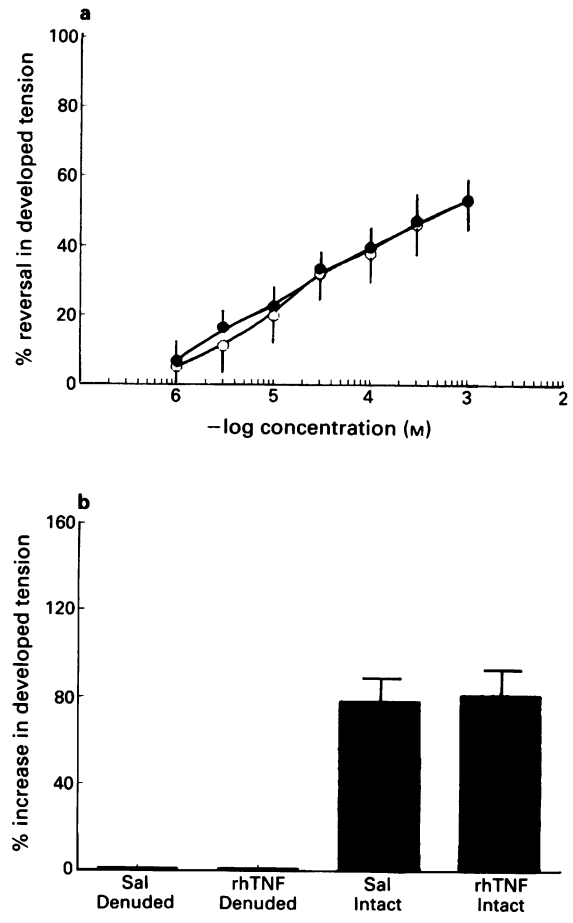

Figure 4 (a) Effect of L-arginine administration on phenylephrine preconstricted aortic rings (endothelium intact) from rats given either saline (1 ml kg^{-1}, i.v., ○) or recombinant human tumour necrosis factor-α (rec huTNF), (1 μg kg^{-1}, i.v., ●) 60 min beforehand. (b) Percentage increase in developed tension following N^G-nitro-L-arginine methyl ester (L-NAME) treatment in rat aortic rings preconstricted to 70% maximum with phenylephrine. Tissues were removed 60 min after saline (Sal, 1 ml kg^{-1}, i.v.) or rec huTNF (1 μg kg^{-1}, i.v.) administration. Values are means with s.e.mean shown by vertical bars; $n = 6$ for each group.

differences in the phenylephrine responses between endothelium-denuded tissues from saline and rec huTNF-treated rats, the response in endothelium intact tissues from rec huTNF-treated rats was significantly ($P < 0.05$) attenuated. In the presence of phenylephrine (giving a 70% maximal constriction), L-arginine caused a concentration-dependent decrease in developed tension in endothelium intact tissues only. This vasodilatation was significantly greater in rings from rec huTNF-treated (81 ± 3%) than from saline-treated rats (41 ± 2%, $P < 0.05$; Figure 6a); D-Arg was without effect.

Furthermore, with the same concentration of phenylephrine, prior administration of L-NAME resulted in an enhanced constrictor response that was significantly greater in tissues from rec huTNF-treated (+ 137 ± 29%) than from saline-treated (+ 66 ± 14%, $P < 0.05$; Figure 6b). Moreover, under these conditions, an enhanced constrictor response to phenylephrine could also be demonstrated in denuded tissues from rec huTNF-treated rats but not from saline-treated rats.

Discussion

Many types of cardiovascular shock, such as haemorrhagic or septic shock, in man and in animals (Lefer, 1970; 1974) are associated with a depression of cardiac contractility. Given that many proteins and peptides, particularly cytokines such as TNF, interleukin-1 (IL-1), IL-6 and IL8, are released into the plasma during shock (Martich *et al.*, 1991) then any of these agents could potentially affect cardiac contractility. Since TNF is a primary cytokine released during shock (Tracey *et al.*, 1986), can cause cardiac injury in rats (Lefer *et al.*, 1990) and is elevated in the plasma of patients with heart failure (Levine *et al.*, 1990) its cardiodepressive potential was investigated in rats.

In isolated, electrically stimulated left atria, rec huTNF antagonized the isoprenaline-induced inotropic response when administered directly to the organ bath; however, it was unable to reduce the basal contractility of the tissues. Although the rightward shift of the isoprenaline CRC was not large, these data clearly indicate that even with an incubation time as short as 20 min, TNF can modulate cardiac contractility to exogenous agents. Such a rapid onset of action has been recently reported by Kumar *et al.* (1991) who showed that rec huTNF administered directly to isolated myocytes can concentration-dependently reduce cell shortening following only 15 min incubation. In addition, in isolated whole heart preparations, myocardial dysfunction is seen only 30 min after administration of LPS (Bardakhchian & Palchikova, 1987). To investigate the temporal effect of rec huTNF on atrial contractility, rec huTNF was administered systemically to rats which were killed either 1 h or 24 h later and the atria removed. Again at neither time point was there a depression of the resting systolic preload but there were similar marked inhibitions of the isoprenaline CRCs at both

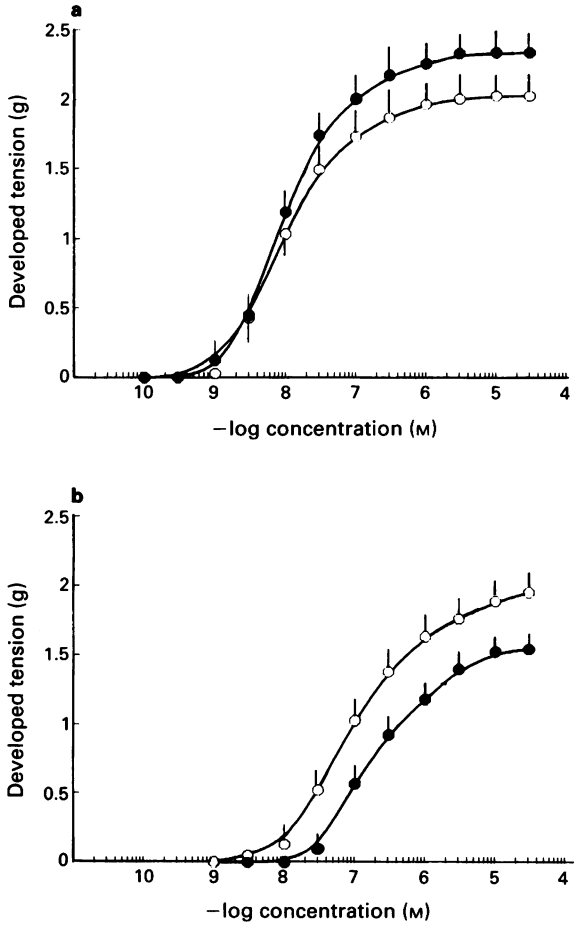

Figure 5 Effect of 24 h saline (1 ml kg^{-1}, i.v., O) or recombinant human tumour necrosis factor-α (rec huTNF, 1 μg kg^{-1}, i.v., ●) pretreatment on the phenylephrine-induced constrictor response in rat isolated aortic rings. Tissues were either denuded of endothelium (a) or had the endothelium intact (b). Values are means with s.e.mean shown by vertical lines; $n = 6$ for each group.

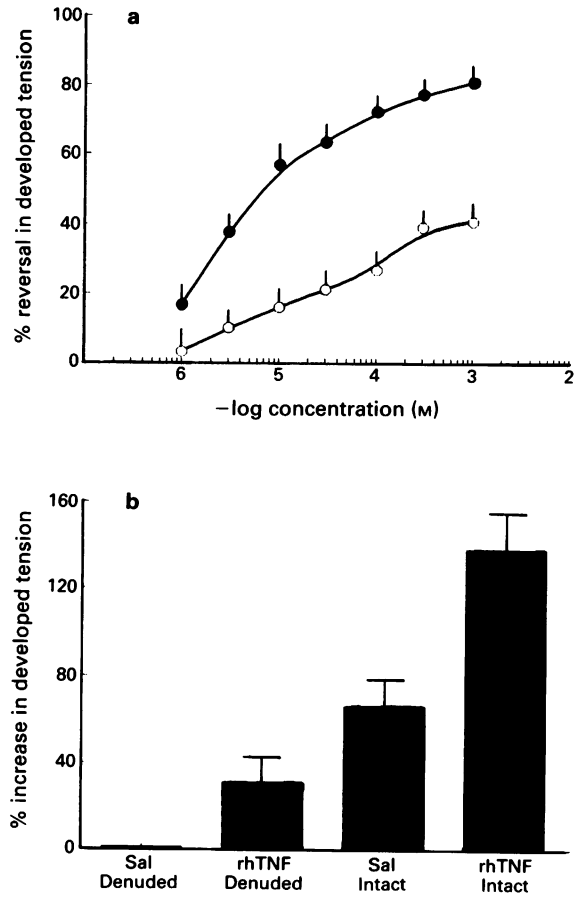

Figure 6 (a) Effect of L-arginine administration on phenylephrine preconstricted aortic rings (endothelium intact) from rats given either saline (1 ml kg^{-1}, i.v., O) or recombinant human tumour necrosis factor-α (rec huTNF, 1 μg kg^{-1}, i.v., ●) 24 h beforehand. (b) Percentage increase in developed tension following L-NAME treatment in rat aortic rings preconstricted to 70% maximum with phenylephrine. Tissues were removed 24 h after saline (1 ml kg^{-1}, i.v.) or rec huTNF (1 μg kg^{-1}, i.v.) administration. Values are means with s.e.mean shown by vertical lines; $n = 6$ for each group.

times. The inhibition seen at 1 h confirms the observation on atrial contractility seen following direct rec huTNF administration to the organ bath. Since many of the physiological and metabolic effects of TNF involve either enzyme induction or the modulation of gene expression (Aoki *et al.*, 1989; Evans *et al.*, 1989), then a greater effect of rec huTNF at 24 h may have been predicted. However, no such greater effect was apparent in this study.

Although the present study reveals little about the possible mechanism of action of rec huTNF in the depression of the β-adrenoceptor-mediated inotropic response, this cytokine was unable to modify the isoprenaline-mediated chronotropic response. However, it is clear that the effects of rec huTNF on atrial function seen here are mediated at a level of the transduction pathway distal to adenylate cyclase since similar results to those seen with rec huTNF were obtained when IBMX was used as the inotropic/chronotropic agent. Taken together, these data shown that rec huTNF is capable of depressing an agonist-induced inotropic response in rat isolated atrial tissue. Hence, this cytokine may be added to the list of other putative myocardial depressive factors that may cause cardiodepression during cardiovascular shock.

In addition to eliciting cardiodepressive effects, endotoxin-induced shock or TNF administration also results in marked hypotension (Schiller *et al.*, 1991; Wright *et al.*, 1992) and reduced sensitivity to vasopressor agents (Fink *et al.*, 1985). Many recent studies have provided evidence that this decreased vascular sensitivity seen in LPS-treated animals (Gray *et al.*, 1991; Wright *et al.*, 1992) may be related, at least in part, to a hyperstimulation of the L-arginine-NO pathway. TNF is known to be released from isolated aortic preparations (McKenna, 1990), macrophages (Jorens *et al.*, 1991) and other cell types, including smooth muscle cells (Busse & Mulsch, 1990) following LPS stimulation and can induce the expression of the non-constitutive form of NO-synthase from these cell types (Drapier *et al.*, 1988; Marsden & Ballerman, 1990) and hence, may itself function as a vasodepressor effector molecule.

In aortae taken from rats treated with rec huTNF 1 h before, neither the vasoconstrictor effect of phenylephrine, nor the responses to L-arginine or L-NAME were modified by rec huTNF pretreatment. This was independent of the presence or absence of endothelium. Hence, unlike the isolated atria experiments described above, rec huTNF seems to have no short term depressive effect on rat vascular tissue. However, these data are somewhat at odds with observations made with LPS or TNF *in vivo* where these agents caused an attenuation of noradrenaline-induced pressor responses associated with NO-synthase activation within 30 min of administration (Kilbourn *et al.*, 1990; Gray *et al.*, 1991). It is important to note that in all of the preparations that had an intact endothelium, this vascular layer remained functional, as reflected by the higher EC_{50} values following phenylephrine administration and the marked responses to L-arginine and L-NAME compared to the denuded preparations.

In contrast, in the tissues removed at 24 h, there was a

clear modulation of the vascular response in rats pretreated with rec huTNF. There was a lower vasoconstrictor response to phenylephrine in tissues with the endothelium intact from rats given rec huTNF. However, this suppression was not apparent in tissues that were devoid of endothelium. Although these data on their own do not indicate the involvement of the L-arginine-NO pathway in these responses, there was also clearly a greater vasodilator effect of L-arginine administration in the endothelium-intact rings from the rec huTNF-treated than in the saline-treated rats. Since no effect of L-arginine was seen in denuded tissues from either group of rats, these data could be interpreted to show a vasodepressor effect of rec huTNF mediated through the induction of a form of NO-synthase present in the endothelial layer only of rat aorta. However, this was not the case, since in the additional presence of L-NAME, an enhanced vasoconstrictor response to subsequent phenylephrine administration was seen in rings from rec huTNF-treated rats, not only when the endothelium was present, but also when it was absent. This observation indicates that rec huTNF can induce a form of NO-synthase in both the endothelial layer and within the smooth muscle layers of the aortic tissue; the latter only being revealed following NO-synthase inhibition. The lack of a vasodilator effect as a result of L-arginine administration to denuded tissues from rec huTNF-treated rats may reflect different mechanisms of L-arginine transport and utilisation in the two layers of the tissue.

Hence, a vasodepressor effect of rec huTNF on phenylephrine-induced vasoconstriction, possibly effected through L-arginine-NO-mediated events, as well as a cardiodepressive action can be demonstrated in isolated tissues from rats. Indeed these effects seen with rec huTNF may be indicative of some of the cardiovascular manifestations (e.g. hypotension, cardiodepression) associated with shock-like states such as septic shock where TNF is thought to be a primary mediator (Tracey *et al.*, 1986). Furthermore, inhibition of TNF action by, for example, anti-TNF monoclonal antibodies, may provide an additional approach to the therapy of patients with profound cardiovascular shock.

References

AOKI, N., SEIGFRIED, M. & LEFER, A.M. (1989). Anti-EDRF effect of tumor necrosis factor in isolated, perfused cat carotid arteries. *Am. J. Physiol.*, **256,** H1509–H1512.

BARDAKHCHIAN, E.A. & PALCHIKOVA, E.I. (1987). Ultrastructural evidences of direct endotoxin action on the heart. *Cor Vasa.*, **29,** 64–69.

BEUTLER, B.D. & CERAMI, A. (1987). Cachectin: more than a tumor necrosis factor. *N. Engl. J. Med.*, **316,** 379–385.

BEUTLER, B.D., GREENWALD, J.D., HULMES, M., CHANG, Y., PAN, C.E., MATHISON, J., ULEVITCH, R. & CERAMI, A. (1985). Identity of tumor necrosis factor and the macrophage secreted factor cachectin. *Nature*, **316,** 552–554.

BUSSE, R. & MULSCH, A. (1990). Induction of nitric oxide synthase by cytokines in vascular smooth muscle cells. *FEBS*, **275,** 87–90.

DRAPIER, J., WIETXERBIN, J. & HIBBS, J.B. (1988). Interferon gamma and tumor necrosis factor induce the L-arginine-dependent cytotoxic effector mechanism in murine macrophages. *Eur. J. Immunol.*, **18,** 1587–1591.

EVANS, R.D., ARGILES, J.M. & WILLIAMSON, D.M. (1989). Metabolic effects of tumour necrosis factor (cachectin) and interleukin-1. *Clin. Sci.*, **77,** 357–364.

FINK, M.P., HOMER, L.D. & FLETCHER, J.R. (1985). Diminished pressor response to exogenous norepinephrine and angiotensin II in septic, non anesthetised rats: evidence for a prostaglandin-mediated effect. *J. Surg. Res.*, **38,** 335–342.

FLEMING, I., JOLOU-SCHAEFFER, G., GRAY, G.A., PARRATT, J.R. & STOCLET, J.-C. (1991). Evidence that an L-arginine/nitric oxide dependent elevation of tissue cyclic GMP content is involved in depression of vascular reactivity by endotoxin. *Br. J. Pharmacol.*, **103,** 1047–1052.

GOODYEAR, A.V.N. (1967). Left ventricular function and tissue hypoxia in irreversible hemorrhagic and endotoxin shock. *Am. J. Physiol.*, **212,** 44.

GRAY, G.A., SCOTT, C., JOLOU-SCHAEFFER, G., FLEMING, I., PARRATT, J.R. & STOCLET, J.-C. (1991). The effect of inhibitors of L-arginine/nitric oxide pathway on endotoxin-induced loss of vascular responsiveness in anaesthetized rats. *Br. J. Pharmacol.*, **103,** 1218–1224.

HINSHAW, L.B., TEKAMP-OLSEN, P., CHANG, A.C.K., LEE, A.P., TAYLOR, F.B., MURRAY, C.K., PEER, G.T., EMERSON, T.E., PASSEY, R.B. & KUO, G.C. (1990). Survival of primates in LD_{100} septic shock following therapy with antibody to tumor necrosis factor (TNF). *Circ. Shock*, **30,** 279–292.

JORENS, P.G., VAN OVERVELD, F.J., BULT, H., VERMIERE, P.A. & HERMAN, A.G. (1991). L-arginine-dependent production of nitrogen oxides by rat pulmonary macrophages. *Eur. J. Pharmacol.*, **200,** 205–209.

KILBOURN, R.G. & BELLONI, P. (1990). Endothelial cell production of nitrogen oxides in response to interferon in combination with tumor necrosis factor, interleukin-1 or endotoxin. *J. Natl. Cancer. Inst.*, **82,** 772–776.

KILBOURN, R.G., JUBRAN, A., GROSS, S.S., GRIFFITH, O.W., LEVI, R., ADAMS, J. & LODATO, R.F. (1990). Reversal of endotoxin-mediated shock by N^G-methyl-L-arginine, an inhibitor of nitric oxide synthesis. *Biochem. Biophys. Res. Commun.*, **172,** 1132–1138.

KUMAR, A., DIMOU, C., HOLLENBERG, S.M., CUNNION, R.E., LAWRENCE, M., URETZ, E., SNELL, R.J. & PARRILLO, J.E. (1991). Tumor necrosis factor produces a concentration-dependent depression of myocardial cell contraction *in vitro*. *Clinical Res.*, **39,** 321A.

LEFER, A.M. (1970). Role of myocardial depressant factor in the pathogenesis of circulatory shock. *Fed. Proc.*, **29,** 1836–1847.

LEFER, A.M. (1974). Myocardial depressant factor and circulatory shock. *Klin. Wochen.*, **52,** 358–370.

LEFER, A.M. & ROVETTO, M.J. (1970). Influence of myocardial depressant factor on physiologic properties of cardiac muscle. *Proc. Soc. Exp. Biol. Med.*, **134,** 269–273.

LEFER, A.M., TSAO, P., AOKI, N. & PALLADINO, M.A. (1990). Mediation of cardioprotection by transforming growth factor-β. *Science*, **249,** 61–64.

LEVINE, B., KALMAN, J., MAYER, L., FILLIT, H. & PACKER, M. (1990). Elevated circulating levels of tumor necrosis factor in severe chronic heart failure. *N. Engl. J. Med.*, **323,** 236–241.

MCKENNA, T.M. (1990). Prolonged exposure of rat aorta to low levels of endotoxin in vitro results in impaired contractility. *J. Clin. Invest.*, **86,** 160–168.

MARSDEN, P.A. & BALLERMAN, B.J. (1990. Tumor necrosis factor activates soluble guanylate cyclase in bovine glomerular mesangial cells via an L-arginine-dependent mechanism. *J. Exp. Med.*, **172,** 1843–1852.

MARTICH, G.D., DANNER, R.L., CESKA, M. & SUFFREDINI, A.F. (1991). Detection of interleukin 8 and tumor necrosis factor in normal humans after intravenous endotoxin: the effect of antiinflammatory agents. *J. Exp. Med.*, **173,** 1021–1024.

MATHISON, J.C., WOLFSON, E. & ULEVITCH, R.J. (1988). Participation of tumor necrosis factor in the mediation of gram negative bacterial lipopolysaccharide-induced injury in rabbits. *J. Clin. Invest.*, **81,** 1925–1937.

SCHILLER, J.H., STORER, B.E., WITT, P.L., ALBERTI, D., TOMBES, M.B., ARZOOMANIAN, R., PROCTOR, R.A., MCCARTHY, D., BROWN, R.R., VOSS, S.D., REMICK, S.C., GREM, J.L., BORDEN, E.C. & TRUMP, D.L. (1991). Biological and clinical effects of tumor necrosis factor-α administered three times weekly. *Cancer. Res.*, **51,** 1651–1658.

TRACEY, K.J., FONG, Y., HESSE, D.J., MANOGUE, K.R., LEE, A.T., KUO, G.C., LOWRY, S.F. & CERAMI, A. (1987). Anti-cachectin/TNF antibodies protect septic shock during lethal bacteremia. *Nature*, **330,** 662–664.

WRIGHT, C.E., REES, D.D. & MONCADA, S. (1992). Protective and pathological roles of nitric oxide in endotoxin shock. *Cardiovasc. Res.*, **26,** 48–57.

(Received March 6, 1992
Revised April 3, 1992
Accepted April 10, 1992)

Br. J. Pharmacol. (1992), **106**, 948–952 © Macmillan Press Ltd, 1992

Regional differences in endothelin converting enzyme activity in rat brain: inhibition by phosphoramidon and EDTA

[1,2]Timothy D. Warner, *Gerald P. Budzik, *Takahiro Matsumoto, [2]Jane A. Mitchell, *Ulrich Förstermann & *Ferid Murad

Department of Pharmacology, Northwestern University Medical School, Chicago, IL 60611 and *Abbott Laboratories, Abbott Park, IL 60064, U.S.A.

1 It has been demonstrated previously that conversion of big endothelin-1 (bET-1) to endothelin-1 (ET-1) is inhibited *in vitro* and *in vivo* by phosphoramidon. In addition, ET-1 binding sites and mRNA have been shown within the brain. Here we expand upon our previous observation that rat brain contains phosphoramidon-inhibitable endothelin converting enzyme (ECE) and show that this activity is not uniformly distributed throughout the brain.

2 ECE activity was detected by a bioassay which depended upon the 10,000 fold difference in potency between bET-1 and ET-1 as stimulants of guanosine 3':5'-cyclic monophosphate (cyclic GMP) accumulation in kidney epithelial (PK_1) cells of the pig. Data were confirmed by specific enzyme-linked immunosorbent assay (ELISA) employing antibody directed against ET-$1/3_{(17-21)}$.

3 Following homogenization of the whole brain and ultracentrifugation the 100,000 *g* pellet contained greater than 4 times more ECE activity than the cytosol. Washing of the pellet with KCl (1 M) and extraction with the detergent CHAPS (20 mM) revealed a phosphoramidon-inhibitable ECE within the residual particulate fraction (nominally classified as the cytoskeletal fraction). Phosphoramidon (IC_{50}, approx. 5 μM) or EDTA inhibited the conversion of bET-1 to ET-1 by the cytoskeletal fraction of rat brain by more than 60%.

4 Following dissection of rat brain into olfactory bulb, cerebral cortex, striatum, hippocampus, cerebellum, midbrain (including thalamus), hypothalamus and medulla oblongata (including pons) the greatest ECE was detected in the hypothalamus and medulla oblongata. After fractionation, the ECE-activities in the cytoskeletal fractions prepared from the hypothalamus or medulla oblongata were inhibited concentration-dependently by phosphoramidon or EDTA, with maximum inhibitions of $>80\%$ and $>70\%$, respectively.

5 These data show that rat brain contains a phosphoramidon- and EDTA-inhibitable ECE which may be similar to that present in endothelial cells. The localization of this enzyme correlates with published reports of immunoreactive-ET-1, ET-1-binding sites, and messenger RNA for ET-1 in the rat brain, and suggests the presence of the entire synthetic pathway for ET-1.

Keywords: Endothelin-1, big endothelin-1; endothelin-converting enzyme; phosphoramidon; EDTA; metalloprotease; endothelin-3; big endothelin-3

Introduction

The biosynthesis of endothelin-1 (ET-1, Yanagisawa *et al.*, 1988) involves the cleavage of its immediate precursor, big ET-1 (bET-1) by a specific endothelin converting enzyme (ECE). Although various candidates have been proposed for this ECE the most likely is a phosphoramidon-inhibitable activity that has been detected in endothelial cells (Ohnaka *et al.*, 1990; Okada *et al.*, 1990; Warner *et al.*, 1992) and vascular smooth muscle cells (Matsumura *et al.*, 1991a). This conclusion is strengthened by the observations that phosphoramidon both decreases the release of ET-1 from cultured endothelial cells (Ikegawa *et al.*, 1990) and diminishes the physiological responses to bET-1 *in vivo* (Matsumura *et al.*, 1991b; Shinyama *et al.*, 1991), and *in vitro* (Hisaki *et al.*, 1991; Télémaque & D'Orleans-Juste, 1991).

Various groups have provided evidence that endothelin has a role within the brain. For instance, there is a selective distribution of endothelin-binding sites (Koseki *et al.*, 1989) and the presence of ET mRNA (MacCumber *et al.*, 1990), particularly in the hypothalamus (Lee *et al.*, 1990), and further it has been suggested that endothelin has an important role in the posterior pituitary system (Yoshizawa *et al.*, 1990). Centrally administered endothelin has also been shown to affect motor activity (Lecci *et al.*, 1990) and arterial blood pressure and blood flows (Hashim & Tadepalli, 1991). In addition, phosphoramidon has been shown to block the vasoconstrictor effects of bET-1 on the basilar artery, *in vivo*, and to inhibit the effects of centrally administered bET-1 (Hashim & Tadepalli, 1991). We have previously reported that rat brain contains a phosphoramidon-inhibitable ECE (Warner *et al.*, 1992). Here we show the further characterization of this enzyme and describe the regional differences in the distribution of ECE activity within the rat brain. The enzyme activity was detected both by enzyme-linked immunosorbent assay (ELISA) and bioassay, using the elevation in guanosine 3' : 5'-cyclic monophosphate (cyclic GMP) induced by ET-1 in kidney epithelial (PK_1) cells of the pig (Warner *et al.*, 1992). The use of the bioassay gives an assurance that the ELISA is detecting biologically active ET-1.

Methods

Preparation of rat brains

Rats (male, Sprague-Dawley, 250–400 g) were rendered unconscious with CO_2 and decapitated. The brains were

[1] Author for correspondence.
[2] Present address: The William Harvey Research Institute, St. Bartholomew's Hospital Medical College, Charterhouse Square, London EC1M 6BQ.

rapidly removed and frozen in liquid N_2. In further experiments brains were allowed to thaw at 4°C to a half-frozen state and dissected into eight different regions (Förstermann *et al.*, 1990) according to the method of Glowinski & Iversen (1966). The regions were olfactory bulb, cerebral cortex, striatum, hippocampus, cerebellum, midbrain (including thalamus), hypothalamus and medulla oblongata (including pons). Following dissection the regions were once again frozen in liquid N_2.

Preparation of subcellular fractions

Rat brains and brain regions were thawed in 5 volumes of buffer A (N-2-hydroxyethyl-piperazine-N'-2-ethanesulphonic acid (HEPES) 50 mM, NaCl 100 mM, pH 7.4) and homogenized on ice by use of a glass tissue grinder with a Teflon pestle. The homogenates were then centrifuged at 100,000 *g* for 1 h. Subsequent fractions were prepared as described previously (Warner *et al.*, 1992). Briefly, the pellet fraction was washed once with buffer A, and resuspended in buffer A by homogenization. In some experiments the particulate fraction was washed with 1 M KCl (in buffer A) for 5 min at 4°C. After centrifugation (100,000 *g*, for 30 min), the pellet was resuspended in buffer A. The particulate fraction was then treated with the detergent 3-[(3-cholamidopropyl)dimethylammonio]-1-propanesulphonate (CHAPS, 20 mM) for 20 min at 4°C. After centrifugation (100,000 *g*, 30 min), the supernatant was collected (CHAPS-solubilized pellet fraction) and the pellet resuspended in buffer A (nominally classified as the cytoskeletal fraction). All fractions were assayed for ECE activity. Protein was determined with the Bradford reagent (Bio-Rad) with bovine serum albumin used as the standard. Aliquots of the subcellular fractions were stored at −70°C.

Assay of endothelin converting enzyme (ECE) activity

The activity of ECE within rat brain fractions was quantified by bioassay and selective ELISA (Warner *et al.*, 1992). Briefly, rat brain protein (22.5 μg protein) was incubated (37°C, 20–180 min), at pH 7.4 in the presence of bET-1 (135 pmol) and any test inhibitors. All samples were incubated in duplicate in the absence and presence of phosphoramidon (100 μM) to permit the calculation of the metalloprotease-ECE activity in each. At the end of this time a mixture of protease/peptidase inhibitors (phenylmethylsulphonyl fluoride 1 mM, leupeptin 2 μM, pepstatin A 1 μM) and EDTA (1 mM) was added to each sample, to a total volume of 62.5 μl. The incubates were than rapidly frozen in liquid N_2 and stored (max. 2 h) at −20°C. To quantitate the amounts of ET-1 in each fraction the samples were rapidly thawed and 12.5 μl of each was bioassayed on PK_1 cells (as described below), the remaining 50 μl was assayed by ELISA. Each ECE/bET-1 combination was assayed in triplicate in each experiment. In some experiments big endothelin-3 (bET-3) was used as a substrate instead of bET-1 and the production of endothelin-3 (ET-3) measured.

Bioassay with LLC-PK_1 cells

PK_1 cells (ATCC CL 101) were grown to confluency in 12-well plates (well diameter, 35 mm) containing Medium 199 with 10% foetal bovine serum, 2 mM L-glutamine, 100 u ml^{-1} penicillin and 0.1 mg ml^{-1} streptomycin at 37°C under an atmosphere of 95% air: 5% CO_2. Prior to experimentation, the culture medium was removed and the cells were washed twice with 1 ml of Locke solution (pH 7.4) of the following composition (mM): NaCl 154.0, KCl 5.6, $CaCl_2$ 2.0, $MgCl_2$ 1.0, $NaHCO_3$ 3.6, glucose 5.6, HEPES 10.0 and 3-isobutyl-1-methylxanthine (IBMX) 0.3. Cells were equilibrated for 20 min in 0.5 ml of the same buffer. Experiments were conducted at 37°C with gentle shaking. After exposing the cells to either ET-1/3 standards or ECE/bET-1/3 mixtures for 4 min, the incubation buffer was removed and reactions were stopped by adding 1 ml of ice-cold sodium acetate buffer (50 mM, pH 4.0). Then, samples were quickly frozen with liquid N_2 (Ishii *et al.*, 1991). After thawing the frozen samples at room temperature, the content of cyclic GMP in the cells was determined by radioimmunoassay (Steiner *et al.*, 1972). The concentration of ET-1/3 present in the sample was then calculated from the levels of cyclic GMP produced in the PK_1 cells compared to the levels produced by known concentrations of ET-1/3 (Warner *et al.*, 1992).

Endothelin ELISA

The amounts of ET-1/3 formed in incubates of bET-1/3 and the test protein fractions were also measured by specific ELISA with antibody directed against the C-terminal fragment of ET-1/3 (ET-$1/3_{(17-21)}$) with approximately 0.01% cross reactivity with bET-1/3. Binding was detected by peroxidase-labelled goat anti-rabbit IgG antibody using *o*-phenylenediamine-2HCl as a substrate. The optical density of each well was measured at 490 nm with a microplate reader (Bio-Tek model EL311).

Chemicals

3-Isobutyl-1-methyl-xanthine (IBMX) and N-(α-rhamno-pyranosyl-oxy-hydroxy-phosphinyl)-Leu-Trp (phosphoramidon) were purchased from Sigma Chemical Company (St. Louis, MO, U.S.A.). Big ET-1 (big endothelin, human) big endothelin-3 (human), ET-1 and ET-3 were obtained from Peninsula Laboratories, Inc. (Belmont, CA, U.S.A.). All other chemicals and reagents used were of the highest quality available.

Statistics

Results are shown as mean ± s.e.mean for *n* experiments. Student's unpaired *t* test was used to determine the significance of differences and a *P* value of less than 0.05 was taken as significant.

Results

Localization of phosphoramidon-inhibitable ECE

Fractionation of the rat brain homogenate revealed four times more ECE activity within the 100,000 *g* pellet than the 100,000 *g* cytosol (Figure 1a), as measured by either bioassay or ELISA. Treatment of the pellet by washing with KCl (1 M, 5 min) and extraction with the detergent CHAPS (20 mM, 20 min) resulted in the greater part of the phosphoramidon-inhibitable activity remaining within the particulate fraction (cytoskeletal fraction, Figure 1b). In the presence of phosphoramidon (100 μM) this activity was decreased by 70.7 ± 10.1% ($n = 7$), as assayed by PK_1 cells, or 52.2 ± 9.8% ($n = 4$), as assayed by ELISA. Similarly, EDTA (1 mM) inhibited the ECE activity by 74.8 ± 14.2 ($n = 5$, PK_1 cells) or 47.2 ± 10.2% ($n = 3$, ELISA). In either assay phosphoramidon inhibited the ECE activity with an IC_{50} of approx. 5 μM (Figure 2). In one experiment employing bET-1 and bET-3 as substrates for the brain fractions, conversion of only bET-1 and not of bET-3 was detected.

Regional distribution of phosphoramidon-inhibitable ECE

At 1 h but not 3 h, inhibition of the formation of immunoreactive (ir)-ET-$1/3_{(17-21)}$ by a mixture of phosphoramidon (100 μM) and EDTA (1 mM) was seen in homogenates prepared from the hypothalamus (29 ± 4%, $n = 3$) or the medulla oblongata (28 ± 75, $n = 3$). By ELISA there was a reduction by 84–99% ($n = 3$ for each) in the formation of ir-ET-$1/3_{(17-21}$, in the presence of the protease and peptidase inhibitors (phenylmethylsulphonyl fluoride

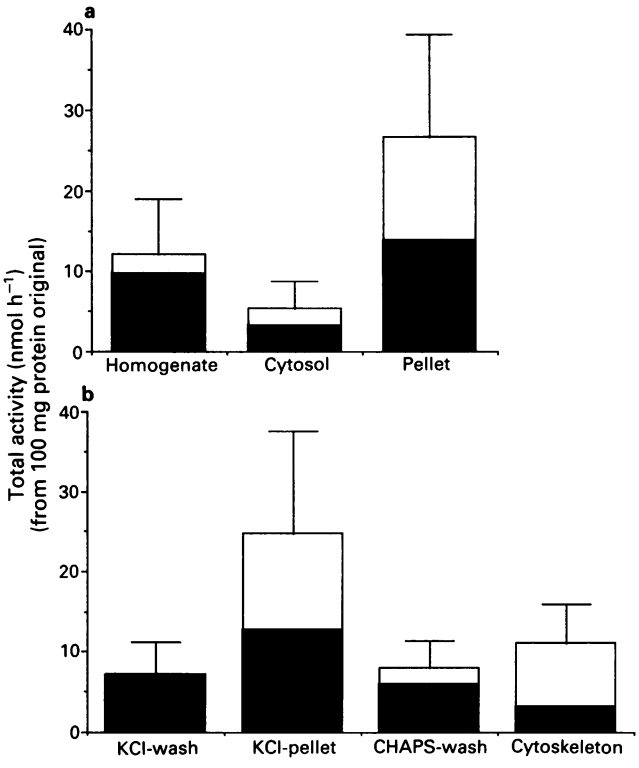

Figure 1 Localization of endothelin converting enzyme (ECE) activity in fractions prepared from the rat brain. The figure represents pooled data from 5 experiments employing both PK_1-cell bioassay and ELISA, each done in triplicate, on 3 different preparations. Results are expressed as the total activities in fractions prepared from homogenates containing 100 mg total protein. Sections within each column indicate the proportion of activity inhibited (open columns) and not inhibited (filled columns) by phosphoramidon (100 μM). (a) ECE activity in homogenate, and 100,000 *g* cytosol and pellet. (b) ECE activity in extracts of the 100,000 *g* pellet.

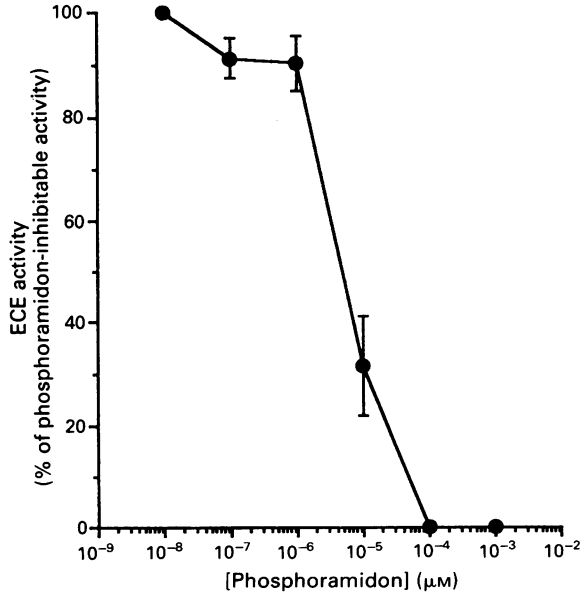

Figure 2 Inhibition of endothelin converting enzyme (ECE) activity by phosphoramidon. Rat brain cytoskeletal fraction (22.5 μg protein) was incubated with bET-1 (135 pmol) for 20 min in the presence of phosphoramidon (0.01–100 μM). Each point with a vertical bar represents the mean ± s.e. of the mean. Data are pooled from three PK_1-cell bioassay and ELISA experiments, each done in triplicate.

1 mM, leupeptin 2 μM, pepsatin A 1 μM) and EDTA (1 mM). Addition of N-ethylmaleimide (1 mM) inhibited all enzymatic activity as assessed by ELISA or bioassay ($n = 3$, for each brain region).

The cytoskeletal fraction of each region was tested by PK_1-cell bioassay and ELISA. The extent of phosphoramidon-inhibitable ECE in each region was, hypothalamus (83 ± 2% by ELISA; 80 ± 7% by PK_1), medulla oblongata (72 ± 2%; 82 ± 6%), midbrain (65 ± 7%; 61 ± 5%), olfactory bulb (0 ± 0%; 38 ± 10%), cerebral cortex (27 ± 5%; 46 ± 12%), striatum (25 ± 13%; 32 ± 17%), cerebellum (28 ± 9%; 51 ± 1%) and hippocampus (33 ± 12%; 61 ± 24%) (Figure 3). EDTA (1 mM) caused similar inhibitions. The activity of both the hypothalamus (Figure 4a) and the medulla oblongata (Figure 4b) was inhibited in a concentration-dependent manner by phosphoramidon and EDTA. In the presence of the peptidase and protease inhibitors and EDTA no production of ir-ET-$1/3_{(17-21)}$ was detected in any of the brain regions or brain fractions (20–60 min, $n = 3$ for each).

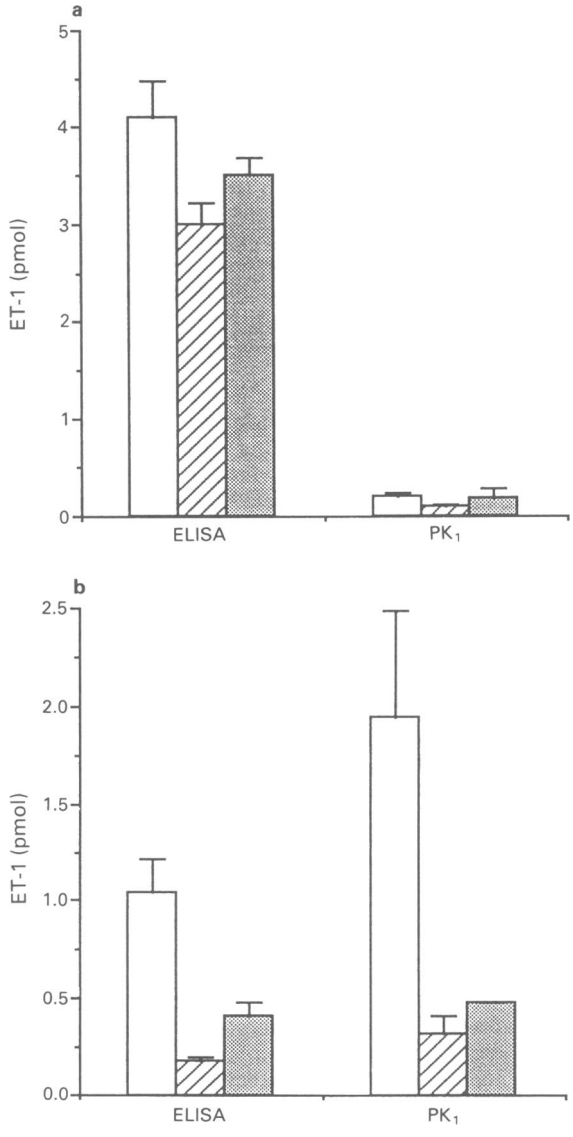

Figure 3 Detection of endothelin converting enzyme (ECE) activity in rat brain regions by ELISA or bioassay. The cytoskeletal fraction (22.5 μg protein) from different rat brain regions was incubated with bET-1 (135 pmol) for 60 min alone ($n = 3$, open columns) or in the presence of phosphoramidon (100 μM, $n = 3$, hatched columns) or EDTA (1 nM, $n = 3$, stippled columns). For comparison, data are shown from three PK_1-cell bioassay and ELISA experiments carried out in parallel: (a) cerebral cortex; (b) hypothalamus. S.e.mean shown by error bars.

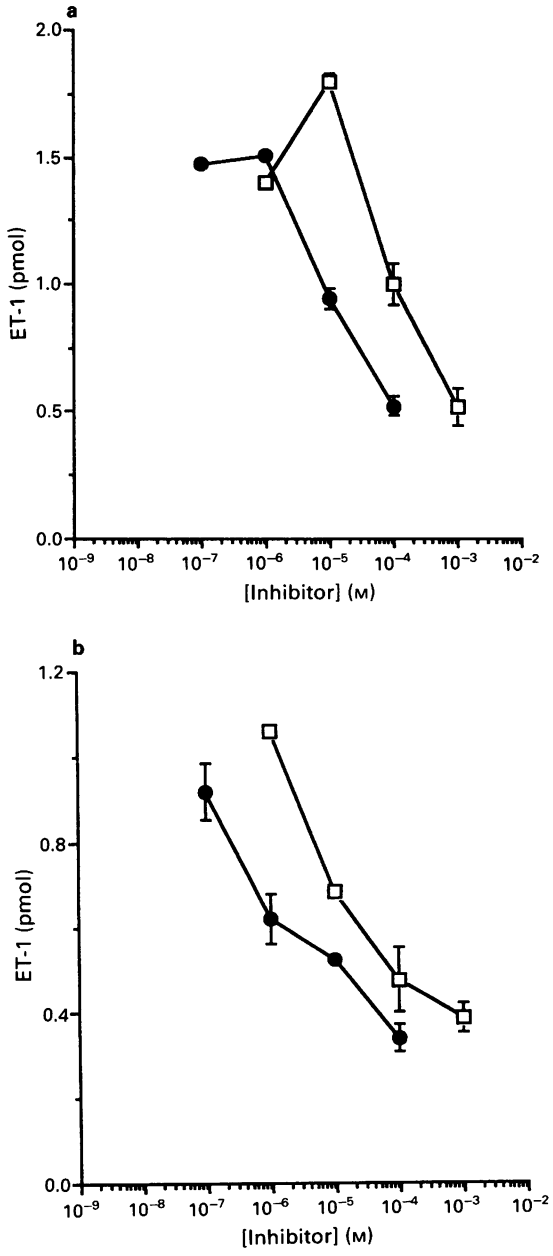

Figure 4 Inhibition of endothelin converting enzyme (ECE) in hypothalamus and medulla oblongata by phosphoramidon or EDTA. The cytoskeletal fraction (22.5 μg protein) from the hypothalalmus or the medulla oblongata was incubated with bET-1 (135 pmol) and either phosphoramidon (0.1–100 μM, $n = 3$, ●) or EDTA (1 μM–1 mM, $n = 3$, □). Data was obtained from ELISA experiments. (a) Hypothalamus; (b) medulla oblongata. s.e.mean shown by error bars.

No phosphoramidon-inhibitable conversion of bET-3 to ET-3 was detected in any of the brain regions ($n = 3$ for each).

Discussion

Our data show that rat brain contains a metalloprotease-ECE activity which is inhibitable by phosphoramidon or EDTA. This suggests that this enzyme is closely related to that present in endothelial cells (Ohnaka *et al.*, 1990; Okada *et al.*, 1990), and to the enzyme responsible for the conversion of exogenous bET-1 to ET-1 in the circulation (Matsumura *et al.*, 1991b). However, unlike the activity in endothelial cells the ECE in brain was largely particulate and was only poorly extractable by detergent. In endothelial cells there is considerably more ECE activity within the cytosol (Takada *et al.*, 1991; Warner *et al.*, 1992), and the activity present in the particulate fraction can be solubilised with detergent (Okada *et al.*, 1990; Warner *et al.*, 1992). Thus, the brain ECE may be located in sites other than the brain endothelium, consistent with the previous findings of endothelin receptors, ET-1-stimulated inositol phosphate turnover, ET-1-promoted mitogenesis, ET-1 messenger RNA, and ET-1 immunoreactivity with brain cells (Koseki *et al.*, 1989; Crawford *et al.*, 1990; MacCumber *et al.*, 1990; Yoshizawa *et al.*, 1990).

In our further experiments to localize the ECE-activity within the rat brain we found that, as in homogenates of whole brain, only very poor phosphoramidon-inhibitable activities were detectable in homogenates of the brain regions. This is probably explained by the presence of other activities masking the phosphoramidon-inhibitable one. This was not revealed, however, by N-ethylmaleimide, which has been reported to discriminate ECE in the particulate fraction of endothelial cells (Matsumura *et al.*, 1991c). Indeed, in these experiments we could not detect any formation of ET-1 by bioassay, or of ir-ET-$1_{(17-21)}$ by ELISA. Thus, the particulate enzyme present in the brain may be different from that in the endothelial cell.

Significant ECE-activities were detected in the cytoskeletal fractions prepared from the hypothalamus and medulla oblongata. Of the remaining regions the highest activity was detected in the midbrain, while the other regions all expressed lower and insignificant activities forming less than 0.2 pmol ET-1 per incubate, as detected by bioassay (data not shown). There was a good correlation in the amount of activity detected in the hypothalamus (Figure 3) and medulla oblongata by ELISA and bioassay, whereas in incubates using protein prepared from other regions the correlation was not so good (Figure 3). For instance, in incubates containing protein prepared from the cerebral cortex, a high level of ir-ET-$1_{(17-21)}$ was detected by ELISA, but no significant activity was detected by bioassay. This was most probably due to the ELISA detecting fragments of bET-1 that were not biologically active. It may also be possible that these regions very rapidly metabolize ET-1 once it is formed, leaving fragments detectable by ELISA but not by bioassay. These suggestions may also explain why in all experiments we found that the ELISA showed either phosphoramidon or EDTA to inhibit the ECE-activity less than did parallel bioassay.

Interestingly, we were not successful in detecting the conversion of bET-3 to ET-3 in any of the rat brain fractions or regions, although it has been reported that rat brain contains more ET-3 than ET-1 (Takahashi *et al.*, 1991). This was not due to the inability of our assays to detect ET-3 since ET-$1_{(17-21)}$ and ET-$3_{(17-21)}$ have the same amino acid sequence, and the PK_1-cell bioassay is equally sensitive to ET-1 and ET-3 (Ishii *et al.*, 1991). The explanation may lie in the fact that the assay employed here was optimised to detect the conversion of bET-1 to ET-1 by the neutral metalloprotease characterized in endothelial cells. It may not be so good for detecting the conversion of bET-3 to ET-3. These results do suggest, however, that the phosphoramidon-inhibitable ECE is selective for bET-1. Due to the close similarity in structure between ET-1 and ET-3 (Inoue *et al.*, 1989) this suggests the possibility of a very strict requirement for binding to the active site of the enzyme.

In our experiments we assayed all samples in duplicate in the absence and presence of phosphoramidon. The difference in ET-1 amounts between the two samples gave a true measure of the ET-1 formation. This protocol provided a control within the bioassay and ELISA for non-specific effects of protein and bET-1 in the assays. The ET-1 thus measured could therefore be taken as an indication of the selective ET-1 formation by the ECE-metalloprotease. The finding that no ir-ET-$1_{(17-21)}$ or ET-1 was detected by ELISA or bioassay after the incubation of brain fractions with bET-

1 and a cocktail of protease/peptidase inhibitors shows that bET-1, at the concentrations used here, did not cross react with the antibody and that the fractions *per se* did not contain detectable amounts of endogenous ET-1.

The localization of phosphoramidon-inhibitable ECE which we describe here correlates well with the reported sites of irET-1 and mRNA for ET-1 in the paraventricular and supraoptic nuclei in the hypothalamus (Yoshizawa *et al.*, 1990), in the thalamus, midbrain, pons, medulla and cerebellum (Yoshimi *et al.*, 1991) and of autoradiographed determinations of the binding sites for ET-1 which are located mainly in the hypothalamic and thalamic areas (Koseki *et al.*, 1989). It also correlates with studies in man which have shown the highest density of cells containing ET-1 mRNA to be in the hypothalamus (Lee *et al.*, 1990). This correlation strongly suggests that the formation of ET-1 in nervous tissue is dependent upon the activity of an ECE which is the same as, or closely related to, the metalloprotease responsible for the processing of bET-1 in endothelial cells. Taken together these data demonstrate the presence of the entire pathway required for the production and effects of ET-1 within the brain.

The authors are indebted to Ms Zei-Jing Huang and Ms Jane Kuk for their excellent technical services and to Drs Pedro D'Orleans-Juste, Masaki Nakane, David M. Pollock and Terry J. Opgenorth for helpful discussions. These studies were supported by grants DK 30787 and HL 28474 from the National Institutes of Health.

References

CRAWFORD, M.L.A., HILEY, C.R. & YOUNG, J.M. (1990). Characteristics of endothelin-1 and endothelin-3 stimulation of phosphoinositide breakdown differ between regions of guinea-pig and rat brain. *Naunyn-Schmiedebergs Arch. Pharmacol.*, **341**, 268–271.

FÖRSTERMANN, U., GORSKY, L.D., POLLOCK, J.S., SCHMIDT, H.H. H.W., HELLER, M. & MURAD, F. (1990). Regional distribution of EDRF/NO-synthesizing enzyme(s) in rat brain. *Biochem. Biophys. Res. Commun.*, **168**, 727–732.

GLOWINSKI, J. & IVERSEN, L.L. (1966). Regional studies of catecholamines in the rat brain – I. The disposition of [^{3}H]-norepinephrine, [^{3}H]dopamine and [^{3}H]DOPA in various regions of the brain. *J. Neurochem.*, **13**, 655–669.

HASHIM, M.A. & TADEPALLI, A.S. (1991). Functional evidence for the presence of a phosphoramidon-sensitive enzyme in rat brain that converts big endothelin-1 to endothelin-1. *Life Sci.*, **49**, PL207–PL211.

HISAKI, K., MATSUMURA, Y., IKEGAWA, R., NISHIGUCHI, S., HAYASHI, K., TAKAOKA, M. & MORIMOTO, S. (1991). Evidence for phosphoramidon-sensitive conversion of big endothelin-1 to endothelin-1 in isolated rat mesenteric artery. *Biochem. Biophys. Res. Commun.*, **177**, 1127–1132.

IKEGAWA, R., MATSUMURA, Y., TSUKAHARA, Y., TAKOAKA, M. & MORIMOTO, S. (1990). Phosphoramidon, a metalloproteinase inhibitor, suppresses the secretion of endothelin-1 from cultured endothelial cells by inhibiting a big endothelin-1 converting enzyme. *Biochem. Biophys. Res. Commun.*, **171**, 669–675.

INOUE, A., YANAGISAWA, M., KIMURA, S., KASUYA, Y., MIYAUCHI, T., GOTO, K. & MASAKI, T. (1989). The human endothelin family: three structurally and pharmacologically distinct isopeptides predicted by three separate genes. *Proc. Natl. Acad. Sci. U.S.A.*, **86**, 2863–2867.

ISHII, K., WARNER, T.D., SHENG, H. & MURAD, F. (1991). Endothelin-1 stimulates cyclic GMP formation in porcine kidney epithelial cells via activation of the L-arginine-dependent soluble guanylate cyclase pathway. *J. Cardiovasc. Pharmacol.*, **17** (Suppl. 7), S246–S250.

KOSEKI, C., IMAI, M., HIRATA, Y., YANAGISAWA, M. & MASAKI, T. (1989). Autoradiographic distribution in rat tissues of binding sites for endothelin: a neuropeptide? *Am. J. Physiol.*, **256**, R858–R866.

LECCI, A., MAGGI, C.-A., ROVERO, P. & MELI, A. (1990). Effect of endothelin-1, endothelin-3 and C-terminal hexapeptide, endothelin (16-21) on motor activity in rats. *Neuropeptides*, **16**, 21–24.

LEE, M.-E., DE LA MONTE, S., NG, S.-C., BLOCH, K.D. & QUERTERMOUS, K. (1990). Expression of the potent vasoconstrictor endothelin in the human central nervous system. *J. Clin. Invest.*, **86**, 141–147.

MACCUMBER, M.W., ROSS, C.A. & SNYDER, S.H. (1990). Endothelin in brain: receptors, mitogenesis, and biosynthesis in glial cells. *Proc. Natl. Acad. Sci. U.S.A.*, **87**, 2359–2363.

MATSUMURA, Y., IKEGAWA, R., TSUKAHARA, Y., TAKAOKA, M. & MORIMOTO, S. (1991a). Conversion of big endothelin-1 to endothelin-1 by two-types of metalloproteinases of cultured porcine vascular smooth muscle cells. *Biochem. Biophys. Res. Commun.*, **178**, 899–905.

MATSUMURA, Y., HISAKA, K., TAKOAKA, M. & MORIMOTO, S. (1991b). Phosphoramidon, a metalloproteinase inhibitor, suppresses the hypertensive effect of big endothelin-1. *Eur. J. Pharmacol.*, **185**, 103–106.

MATSUMURA, Y., IKEGAWA, R., TSUKAHARA, Y., TAKOAKA, M. & MORIMOTO, S. (1991c). N-Ethylmaleimide differentiates endothelin converting activity by two types of metalloproteinases derived from vascular endothelial cells. *Biochem. Biophys. Res. Commun.*, **178**, 531–538.

OHNAKA, K., TAKAYANAGI, R., YAMAUCHI, T., OKAZAKI, H., OHASHI, M., UMEDA, F. & NAWATA, H. (1990). Identification and characterization of endothelin converting activity in cultured bovine endothelial cells. *Biochem. Biophys. Res. Commun.*, **168**, 1128–1136.

OKADA, K., MIYAZAKI, Y., TAKADA, J., MATSUYAMA, K., YAMAKI, T. & YANO, M. (1990). Conversion of big endothelin-1 by membrane-bound metalloendopeptidase in cultured bovine endothelial cells. *Biochem. Biophys. Res. Commun.*, **171**, 1192–1198.

SHINYAMA, H., UCHIDA, T., KIDO, H., HAYASHI, K., WATANABE, M., MATSUMURA, Y., IKEGAWA, R., TAKOAKA, M. & MORIMOTO, S. (1991). Phosphoramidon inhibits the conversion of intracisternally administered big endothelin-1 to endothelin-1. *Biochem. Biophys. Res. Commun.*, **178**, 24–30.

STEINER, A.L., PARKER, C.W. & KIPNIS, D.D. (1972). Radioimmunoassay for cyclic nucleotides. I. Preparation of antibodies and iodinated cyclic nucleotides. *J. Biol. Chem.*, **247**, 1106–1113.

TAKADA, J., OKADA, K., IKENAGA, T., MATSUYAMA, K. & YANO, M. (1991). Phosphoramidon-sensitive endothelin-converting enzyme in the cytosol of cultured bovine endothelial cells. *Biochem. Biophys. Res. Commun.*, **176**, 860–865.

TAKAHASHI, K., GHATEI, M.A., JONES, P.M., MURPHY, J.K., LAM, H.-C., O'HALLORAN, D.J. & BLOOM, S.R (1991). Endothelin in human brain and pituitary gland: comparison with rat. *J. Cardiovasc. Pharmacol.*, **17** (Suppl. 7), S101–S103.

TÉLÉMAQUE, S. & D'ORLEANS-JUSTE, P. (1991). Presence of a phosphoramidon-sensitive endothelin-converting enzyme which converts big-endothelin-1, but not big-endothelin-3, in the rat vas deferens. *Naunyn-Schmiedebergs Arch. Pharmacol.*, **344**, 505–507.

WARNER, T.D., MITCHELL, J.A., D'ORLEANS-JUSTE, P., ISHII, K., FÖRSTERMANN, U. & MURAD, F. (1992). Characterization of endothelin-converting enzyme from endothelial cells and rat brain: detection of the formation of biologically active endothelin-1 by rapid bioassay. *Mol. Pharmacol.*, **41**, 399–403.

YANAGISAWA, M., KURIHARA, H., KIMURA, S., TOMOBE, Y., KOBAYISHI, Y., MITSUI, Y., YAZAKI, Y., GOTO, K. & MASAKI, T. (1988). A novel potent vasoconstrictor peptide produced by vascular endothelial cells. *Nature*, **332**, 411–415.

YOSHIMI, H., KAWANO, Y., AKABANE, S., ASHIDA, T., YOSHIDA, K., KINOSHITA, O., KURAMOCHI, M. & OMAE, T. (1991). Immunoreactive endothelin-1 contents in brain regions from spontaneously hypertensive rats. *J. Cardiovasc. Pharmacol.*, **17** (Suppl. 7), S417–S419.

YOSHIZAWA, T., SHINMI, O., GIAID, A., YANAGISAWA, M., GIBSON, S., KIMURA, S., UCHIYAMA, Y., POLAK, J.M., MASAKI, T. & KANAZAWA, I. (1990). Endothelin: a novel peptide in the posterior pituitary system. *Science*, **247**, 462–464.

(Received February 5, 1992
Revised April 7, 1992
Accepted April 10, 1992)

Br. J. Pharmacol. (1992), **106**, 953–957 © Macmillan Press Ltd, 1992

Endotoxin-induced vasodilatation in anaesthetized rat skin involves nitric oxide and prostaglandin synthesis

[1]J.B. Warren, M.L. Coughlan & T.J. Williams

Department of Applied Pharmacology, National Heart & Lung Institute, London SW3 6LY

1 The effect of intradermally injected endotoxin on skin blood flow was investigated in anaesthetized male Wistar rats *in vivo*.

2 Local skin blood flow changes were measured hourly for 6 h in the shaved dorsal skin with a laser-Doppler flow probe and compared to changes in control sites which had been injected with 100 μl of phosphate-buffered saline. By 3 h, skin blood flow increased above basal by 129 ± 27% and 186 ± 29% with 1 and 10 μg of endotoxin respectively. Blood flow remained significantly elevated at 6 h, the corresponding figures being 129 ± 24% and 154 ± 31% ($P<0.05$, $n=6$ rats, mean ± s.e.mean).

3 In further experiments, the response to 3 μg of endotoxin was measured at 4 h and treatment with a cyclo-oxygenase inhibitor, nitric oxide synthase inhibitors or a topical steroid all significantly inhibited this response ($P<0.05$ in each case, $n=6$ rats in each group with duplicate sites in each animal).

4 Indomethacin 3×10^{-9} mol per site injected 3.5 h after injection of endotoxin suppressed the mean 4 h response to endotoxin by 78%; N^G-nitro-L-arginine methyl ester (L-NAME) 10^{-7} mol per site suppressed the response by 95%; N^G-monomethyl-L-arginine (L-NMMA) 10^{-7} mol per site suppressed the response by 50%; whereas the D-isomer of N^G-monomethyl-arginine 10^{-7} mol per site had no significant effect.

5 Topical application of the corticosteroid, betamethasone 17-valerate (1% solution) 18 h before injection of endotoxin inhibited the mean 4 h response to endotoxin by 66% and the 6 h response by 48%.

6 In the same model, the vasodilator response to arachidonic acid was inhibited by both indomethacin and nitric oxide synthase inhibitors ($P<0.05$ in each case).

7 These data suggest that the microcirculatory vasodilator response to endotoxin and arachidonic acid injected locally involves both nitric oxide synthase and cyclo-oxygenase in this *in vivo* model.

Keywords: Nitric oxide; nitric oxide synthase; endotoxin; vascular smooth muscle; endothelium; vasodilatation; septic shock; prostaglandins; arachidonic acid

Introduction

Bacterial endotoxins are lipopolysaccharides (LPS) found in the outer membrane of Gram negative bacteria. The LPS molecule consists of an oligosaccharide core with a chain of repeating sugar units at one end and lipid A at the other. The structure of lipid A is conserved among Gram negative bacteria and when released from bacteria can bind to the plasma membrane of most cell types. Endotoxin is a powerful stimulus to the immune response and can promote adhesion between leucocytes and the endothelium. Endotoxin can also interact with immune complexes, affect endothelial function to increase permeability and when given systemically can cause endotoxic shock with associated multiple organ failure (Ginsberg & Henson, 1978; Dinarello, 1983; Meyrick *et al.*, 1986).

Endotoxin stimulates the production of many mediators from leucocytes and endothelial cells such as tumour necrosis factor, platelet activating factor, prostacyclin and fragments of complement. Some of these mediators have been implicated in the pathogenesis of endotoxin-induced vasodilatation and pharmacological antagonists to some have protected against septic shock (Beutler *et al.*, 1985; Wise *et al.*, 1985; Casals-Stenzel, 1987).

One likely mediator of the vasodilator response to endotoxin is nitric oxide, synthesized from the amino acid L-arginine by many cell types (Moncada *et al.*, 1991). Two nitric oxide synthase enzymes have been described. The first is a Ca^{2+}-dependent constitutive enzyme which is present in endothelial cells and is involved in the control of vascular tone (Moncada *et al.*, 1991). The second is an inducible Ca^{2+}-independent enzyme which predominates in vascular smooth muscle cells, although it is present to a lesser extent in endothelial cells as well (Wood *et al.*, 1990; Moncada *et al.*, 1991). When precontracted vascular tissue is incubated with endotoxin *in vitro*, relaxation is induced progressively over several hours. This effect is mediated mainly by the inducible enzyme in vascular smooth muscle, requires new protein synthesis and is inhibited by pretreatment with corticosteroids (Julou-Schaeffer *et al.*, 1990; Di-Rosa *et al.*, 1990; Radomski *et al.*, 1990; Kilbourn *et al.*, 1990; Fleming *et al.*, 1991).

Endotoxaemia is characterized by vasodilatation (Wakabayashi *et al.*, 1987) and the subsequent hypotension is often refractory to vasoconstrictors. In both animal models and in man the hypotension can be reversed by inhibitors of nitric oxide synthase (Thiemermann & Vane, 1990; Petros *et al.*, 1991). Pretreatment of animal models with corticosteroids can prevent the hypotension (Rees *et al.*, 1990) suggesting that the vasodilatation is mediated by the inducible form of nitric oxide synthase.

The aim of the present study was to measure the vasodilator effect of endotoxin in the microcirculation and to determine the mechanisms involved. The microcirculatory effects of endotoxin are likely to mediate in part the tissue response to Gram negative bacterial infection.

[1] Author for correspondence.

Methods

Animals

Male Wistar rats weighing 230–350 g were sedated by intramuscular injection of Hypnorm (fentanyl citrate/fluanisone) 0.3 ml kg^{-1}. The dorsal skin was shaved with electric clippers and depilated with a commercial depilating cream (Immac) followed by gentle close shaving with a glass microscope slide. The dorsal skin was then rinsed thoroughly with warm water and the rats left for 1 h before measurements were made.

Blood flow measurements (laser Doppler)

Before injection of test compounds, baseline blood flow was measured in the dorsal skin with a laser-Doppler flow probe (Perimed II, Sweden). This was repeated at either 6 or 8 marked sites, the number depending upon the protocol. During the experiment, the rats were sedated with Hypnorm in an air-conditioned room at 23–25°C. Each reading took 15 s with a 10 s interval between readings and the mean of three readings per site was taken. Results were recorded as red blood cell flux (the number of moving red cells detected by the laser beam × mean cell velocity) and expressed as a percentage of a standardized signal. The laser Doppler was set at 4 Hz, gain 10 and a time constant of 3 s. The output was recorded on a Maclab and Macintosh Apple Computer (Apple Computer Inc, Cupertino, Ca, U.S.A.) set at an input of 10 V and chart speed of 2 mm s^{-1}. Test compounds were injected in a randomized, balanced site pattern.

Experimental protocols

In the first experiment the vasodilator responses to two doses of endotoxin (*E. coli* serotype 055:B5) were determined in six rats. Basal blood flow was measured in six marked sites as described above and then phosphate-buffered saline, endotoxin 1 μg and endotoxin 10 μg were injected in duplicate sites in 100 μl volumes. Red cell flux was measured hourly for 6 h.

To assess the effects of inhibitors on the response to endotoxin, a single dose of 3 μg of endotoxin, assessed at 4 h, was chosen. N^G-nitro-L-arginine methyl ester (L-NAME) and N^G-monomethyl-L-arginine (L-NMMA) were used as nitric oxide synthase inhibitors and N^G-monomethyl-D-arginine (D-NMMA) was used as a control. Endotoxin or control phosphate-buffered saline were injected after taking basal readings. The inhibitors or vehicle control were injected in 100 μl volumes 3.5 h later and the blood flow response measured at 4 h. Batches of six rats were used to test for the effect of L-NAME 10^{-7} mol per site, L-NMMA 10^{-7} mol per site and indomethacin 3×10^{-9} mol per site.

In a further experiment, six rats were pretreated with a corticosteroid 18 h before the injection of endotoxin. Betamethasone 17-valerate was dissolved in 20% diethylacetamide, 40% acetone, 40% ethanol (DAE 2:4:4) and this vehicle was used as the control. The skin was prepared as above and then 0.5 ml of steroid at a 1% w/v concentration was painted evenly on the sites of the right flank and the left flank was treated with vehicle control. Eighteen hours later basal blood flow was measured and then two sites on each flank were injected with phosphate-buffered saline and two with endotoxin as before and the response measured 4 h and 6 h later.

To confirm that the dose of indomethacin used caused effective inhibition of cyclo-oxygenase, six rats were injected in duplicate sites with phosphate-buffered saline, arachidonic acid 3×10^{-9} mol per site, arachidonic acid + indomethacin 3×10^{-9} mol per site and arachidonic acid + L-NAME 10^{-7} mol per site. The change in blood flow from the basal reading was assessed at 30 min. Two other batches of six rats were used to assess the effect of the active L-isomer and inactive D-isomer of NMMA on the response to arachidonic acid and the effect of L-NAME on the response to the stable prostacyclin analogue, iloprost.

Drugs and chemicals

Indomethacin was made as a stock solution of 10^{-2} M in ethanol and then diluted in phosphate-buffered saline. Endotoxin and all other drugs were dissolved and diluted in phosphate-buffered saline. Iloprost was the generous gift of Schering AG Pharmaceutical Research, Berlin, Germany. Pentobarbitone sodium was from May & Baker. All other drugs and chemicals were from the Sigma Chemical Co., Poole, Dorset.

Statistical analysis

Data are presented as mean ± s.e.mean. The suppression of the mean response by inhibitors was calculated as:

$$\frac{(\text{endotoxin and inhibitor} - \text{control})}{(\text{endotoxin} - \text{control})} \times 100$$

Statistical analysis was performed by analysis of variance (ANOVA) and results termed significant if $P < 0.05$.

Results

Figure 1 shows that endotoxin caused slow onset vasodilatation when injected intradermally in rat skin *in vivo*. The response was dose-related and increased progressively over 3 h. A comparison of the mean of the data from 1–6 h showed that both doses of endotoxin were significantly different from control and that the 10 μg dose had a significantly greater effect than the 1 μg dose ($P < 0.05$ in each case, ANOVA). Subsequent experiments were carried out with a 3 μg dose and the response measured at 4 h.

Figure 2 shows that the co-injection of indomethacin at 3.5 h inhibited the vasodilator response to endotoxin when measured at 4 h ($P < 0.05$). The suppression of the mean response by indomethacin was 78% of the response caused by endotoxin alone. Both nitric oxide synthase inhibitors, L-NAME and L-NMMA, inhibited the response to endotoxin by 94% and 50% respectively ($P < 0.05$ in each case, Figure 3). Injection of the inactive isomer D-NMMA had no significant effect on endotoxin-induced vasodilatation (in a further experiment the mean L-NMMA response was 46% of the

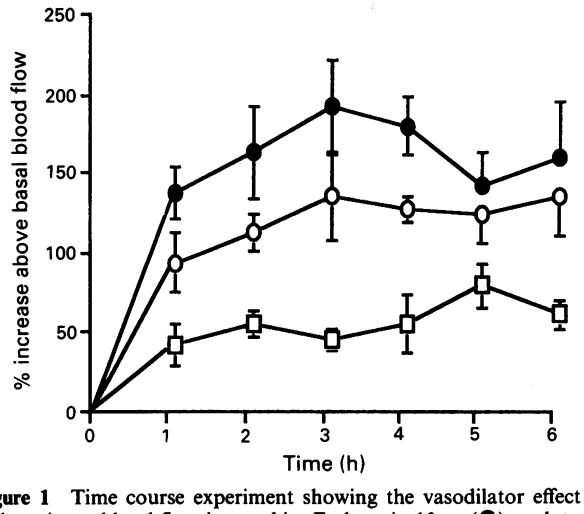

Figure 1 Time course experiment showing the vasodilator effect of endotoxin on blood flow in rat skin. Endotoxin 10 μg (●), endotoxin 1 μg (○) and phosphate-buffered saline (□) were injected in duplicate sites in each animal following the measurement of basal blood flow. Results, expressed as the percentage increase in basal blood flow, are the mean (± s.e.mean, vertical bars) for 6 rats.

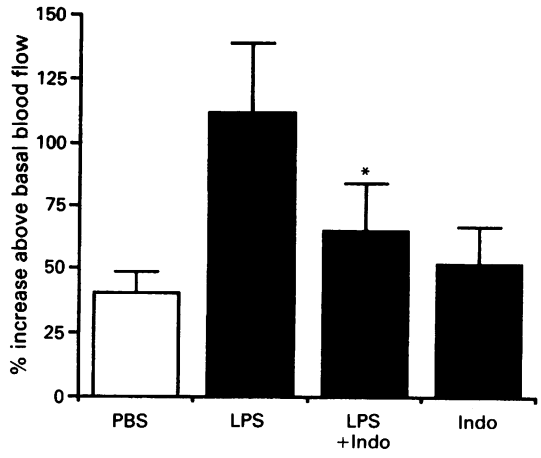

Figure 2 Inhibition of the vasodilator response to endotoxin 3 μg/ site (LPS) by indomethacin in rat skin. Indomethacin 3×10^{-9} mol per site (Indo) or control were injected 3.5 h after the injection of endotoxin or control and the vasodilator response measured at 4 h. The vasodilatation induced by endotoxin was inhibited significantly by indomethacin ($*P<0.05$). Experiments were performed in duplicate in each rat and the results are the mean (± s.e.mean, vertical bars) of 6 rats.

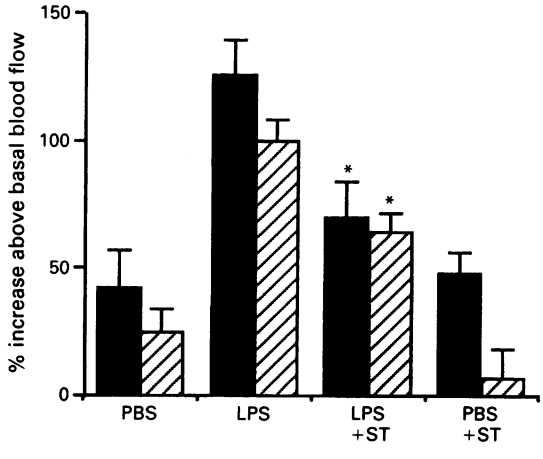

Figure 4 The inhibition of the vasodilator response to endotoxin 3 μg/ site by topical betamethasone-17-valerate in rat skin. The steroid was applied as a 1% solution to one flank and control solution to the other flank 18 h before the injection of endotoxin. The vasodilator response, measured at 4 h (solid columns) and 6 h (hatched columns) after the injection of endotoxin, was inhibited significantly by pretreatment with topical steroid ($*P<0.05$). Experiments were performed in duplicate in each rat and the results are the mean (± s.e.mean, vertical bars) of 6 rats.

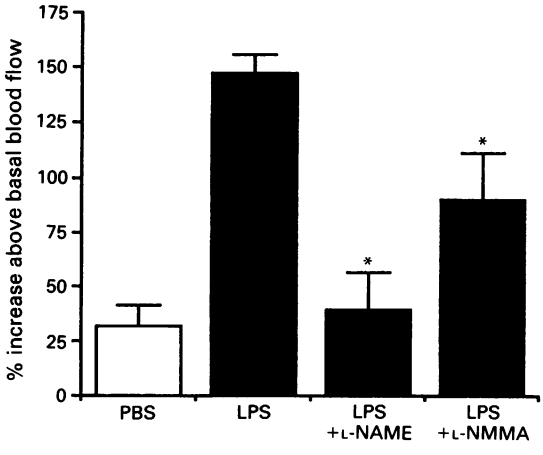

Figure 3 The inhibition of the vasodilator response to endotoxin 3 μg/ site (LPS) by the nitric oxide synthase inhibitors N^G-nitro-L-arginine methyl ester (L-NAME) and N^G-monomethyl-L-arginine (L-NMMA) in rat skin. L-NAME (100 nmol per site), L-NMMA (100 nmol per site) or control were injected 3.5 h after the injection of endotoxin or control and the vasodilator response measured at 4 h. The vasodilatation induced by endotoxin was inhibited significantly by both nitric oxide synthases inhibitors ($*P<0.05$ in each case). Experiments were performed in duplicate in each rat and the results are the mean (± s.e.mean, vertical bars) of 6 rats.

mean LPS response, $P<0.05$, and the D-NMMA response 128%, NS, $n = 6$ rats each in duplicate). It can be seen from Figures 2–5 that the injection of phosphate-buffered saline alone caused a slight increase in blood flow 30 min later, presumably a non-specific response to the 100 μl volume of the injection. In a separate experiment the injection of L-NAME in control sites had no significant effect compared to the injection of buffer when assessed at 30 min: blood flow increased by 24 ± 26% with buffer and 11 ± 7% with L-NAME 10^{-7} mol per site ($n = 4$ rats, experiment performed in triplicate in each rat).

Figure 4 shows the effect of pretreatment with the topical steroid, betamethasone-17-valerate, 18 h before injection of endotoxin or control. The responses were recorded at both 4 h and 6 h after the injection of endotoxin. The steroid significantly inhibited the response to endotoxin at both time points ($P<0.05$ in each case, $n = 6$ rats). Pretreatment with the steroid had no significant effect on blood flow in control sites at 18 h (data not shown in figure), the mean ± s.e.mean change in blood flow at 18 h being −4 ± 11% in sites painted with vehicle solution and 18 ± 13% in sites painted with steroid solution (NS, $n = 6$ rats, each in duplicate).

The vasodilator response to arachidonic acid, assessed at 30 min, was used to test if the chosen dose of indomethacin was sufficient to inhibit cyclo-oxygenase. Figure 5a shows that indomethacin significantly inhibited the response to arachidonic acid with the additional unexpected result that this response was blocked by L-NAME ($P<0.05$ in each case, $n = 6$ rats). Figure 5b shows that L-NAME did not suppress increased blood flow caused by the vasodilator prostaglandin analogue, iloprost ($n = 6$ rats). Figure 5c shows further, that the response to arachidonic acid was blocked by the nitric oxide synthase inhibitor L-NMMA ($P<0.05$, $n = 6$ rats), but not significantly by its inactive D-isomer.

Discussion

The present study shows that endotoxin injected intradermally causes a dose-dependent increase in blood flow in the microcirculation of rat skin *in vivo*. The effect is delayed in onset and can be inhibited by nitric oxide synthase inhibitors. These data suggest that endotoxin-induced arteriolar dilatation is mediated by nitric oxide synthesized by the inducible form of nitric oxide synthase. It is likely that the enzyme is present in vascular smooth muscle as the response to endotoxin in large arteries *in vivo* is endothelium-independent (Fleming *et al.*, 1991), although the endothelium may play a part also, as this tissue can release nitric oxide rapidly in response to endotoxin (Salvemini *et al.*, 1990). The inducible form of nitric oxide synthase has been shown to be steroid-sensitive (Radomski *et al.*, 1990; Knowles *et al.*, 1990) and indeed the response to endotoxin was inhibited in the present experiment by local pretreatment with the steroid betamethasone.

Other cell types may have been involved in the endotoxin-mediated vasodilatation observed in the present experiment. Endotoxin can release intermediates such as tumour necrosis factor or interleukin-1, both of which have been shown to

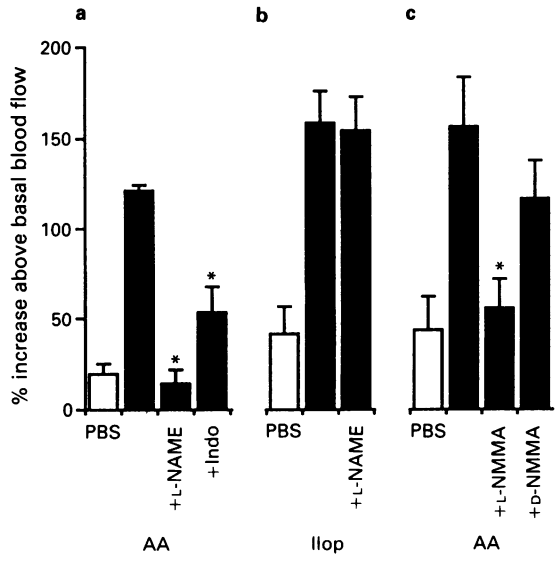

Figure 5 The effect of nitric oxide synthase inhibitors and indomethacin on the vasodilator response to arachidonic acid and iloprost. Responses were measured 30 min after the injection of test compounds. Three groups of 6 rats were studied and experiments carried out in duplicate in each rat. The response to arachidonic acid 3×10^{-9} mol per site (AA) was inhibited significantly by the co-injection of indomethacin 3×10^{-9} mol per site (Indo) and abolished by the co-injection of N^G-nitro-L-arginine methyl ester (L-NAME) 10^{-7} mol per site (a), ($^*P<0.05$ in each case). The response to arachidonic acid was inhibited by the active isomer of methyl arginine, N^G-monomethyl-L-arginine (L-NMMA) ($^*P<0.05$), but not significantly by the inactive isomer, D-NMMA (b). The response to iloprost 10^{-9} mol per site (Ilop) was unaffected by the co-injection of L-NAME 10^{-7} mol per site (c).

induce nitric oxide synthase (Busse & Mulsch, 1990; Robert *et al.*, 1992). When tested at the same dose, the nitric oxide synthase inhibitor L-NAME had a greater effect than L-NMMA in the present experiment, possibly because L-NMMA can be metabolized to L-arginine (Hecker *et al.*, 1990). Interestingly, L-NMMA is a more potent inhibitor than L-NAME in macrophages, where the inducible form of nitric oxide synthase predominates (Gross *et al.*, 1990).

Our results suggest that the endotoxin-induced vasodilatation was mediated, at least in part, by the release of nitric oxide and that this is an important vasodilator in the microcirculation *in vivo*. The nitric oxide-mediated vasodilatation may contribute to the second component of inflammation, oedema formation. Several vasodilators have been shown to potentiate oedema formation (Williams & Peck, 1977; Williams, 1982; Warren *et al.*, 1992) and the oedema response to substance P in rat skin is attenuated by nitric oxide synthase inhibition (Hughes *et al.*, 1990). The injection of *E. coli* intradermally had been used by others to study the response of the rabbit microcirculation where bacteria, probably by the release of endotoxin, can elicit vasodilatation, oedema formation and cell accumulation (Kopaniak *et al.*, 1980).

The inhibition of endotoxin-induced vasodilatation by indomethacin suggests that prostaglandins contribute to the hyperaemia, although we did not measure prostaglandin production directly. The response to endotoxin is slow in onset, suggesting possible induction of an enzyme involved in prostaglandin synthesis. The inhibitory effect of corticosteroids could involve the inhibition of phospholipase A_2 and the suppression of endogenous free arachidonate, and hence prostaglandin and leukotriene synthesis. Vasodilatation induced by arachidonic acid was inhibited by nitric oxide synthase inhibition in the present experiment suggesting that a prostanoid or leukotriene might mediate the release of nitric oxide. One candidate could be prostaglandin D_2 (PGD_2) a vasodilator in rat skin (Flower *et al.*, 1976), which is capable of stimulating nitric oxide synthesis (Braun *et al.*, 1991). Another pathway could be the metabolism of arachidonate to intermediates via the lipoxygenase enzyme, possibly involving leucocytes (Borgeat & Samuelsson, 1979).

There are other possibilities for an interaction between prostaglandins and nitric oxide. One could be that their vasodilator effect on the microcirculation is synergistic, analogous to the synergistic inhibition of platelet aggregation by nitric oxide and prostacyclin (Moncada *et al.*, 1991) or their synergistic action in the gastric mucosa (Whittle *et al.*, 1990). Prostaglandins are vasodilators in the microcirculation, in contrast to their lack of relaxant effect in some large vessels (Gryglewski *et al.*, 1989).

In conclusion, endotoxin induced a delayed vasodilatation in the microcirculation of rat skin *in vivo*. The response was inhibited by pretreatment with a corticosteroid suggesting the inducible form of nitric oxide synthase is involved. That the vasodilator response was inhibited by both indomethacin and nitric oxide synthase inhibition suggests either a synergy between prostaglandins and nitric oxide or that their release is linked in the microcirculation.

This work was supported by the British Heart Foundation.

References

BEUTLER, B., MILSARK, I.W. & CERAMI, A.C. (1985). Passive immunization against cachexin/tumor necrosis factor protects mice from lethal effects of endotoxin. *Science*, **229**, 869–871.

BORGEAT, P. & SAMUELSSON, B. (1979). Arachidonic acid metabolism in polymorphonuclear leukocytes: effects of ionophore A23187. *Proc. Natl. Acad. Sci. U.S.A.*, **76**, 2148–2152.

BRAUN, M., STROBACH, H. & SCHROR, K. (1991). PGD2 relaxes bovine coronary arteries by an endothelium-dependent cyclic GMP-mediated mechanism. *Circulation*, **84**, II-272.

BUSSE, R. & MULSCH, A. (1990). Induction of nitric oxide synthase by cytokines in vascular smooth muscle cells. *FEBS Lett.*, **275**, 87–90.

CASALS-STENZEL, J. (1987). Protective effect of WEB 2086, a novel antagonist of platelet activating factor, in endotoxin shock. *Eur. J. Pharmacol.*, **135**, 117–122.

DINARELLO, C.A. (1983). Molecular mechanisms in endotoxin fever. *Agents Actions*, **13**, 470–486.

DI-ROSA, M., RADOMSKI, M., CARNUCCIO, R. & MONCADA, S. (1990). Glucocorticoids inhibit the induction of nitric oxide synthase in macrophages. *Biochem. Biophys. Res. Commun.*, **172**, 1246–1252.

FLEMING, I., JULOU-SCHAEFFER, G., GRAY, G.A., PARRAT, J.R. & STOCLET, J.-C. (1991). Evidence that an L-arginine/nitric oxide dependent elevation of tissue cyclic GMP content is involved in depression of vascular reactivity by endotoxin. *Br. J. Pharmacol.*, **103**, 1047–1052.

FLOWER, R.J., HARRY, E.A. & KINGSTON, W.P. (1976). Inflammatory effects of prostaglandin D_2 in rat and human skin. *Br. J. Pharmacol.*, **56**, 229–233.

GINSBERG, M.H. & HENSON, P.M. (1978). Enhancement of platelet responses to immune complexes and IgG aggregates by lipid A-rich bacterial lipopolysaccharides. *J. Exp. Med.*, **147**, 207–218.

GROSS, S.S., STUEHR, D.J., AISAKA, K., JAFFE, E.A., LEVI, R. & GRIFFITH, O.W. (1990). Macrophage and endothelial cell nitric oxide synthesis: cell-type selective inhibition by NG-aminoarginine, NG-nitroarginine and NG-methylarginine. *Biochem. Biophys. Res. Commun.*, **170**, 96–103.

GRYGLEWSKI, R.J., KORBUT, R., TRABKA-JANIK, E., ZEMBOWICZ, A. & TRYBULEC, M. (1989). Interaction between NO donors and iloprost in human vascular smooth muscle, platelets and leukocytes. *J. Cardiovasc. Pharmacol.*, **14**, S124–128.

HECKER, M., MITCHELL, J.A., HARRIS, H.J., KATSURA, M., THIEMERMANN, C. & VANE, J.R. (1990). Endothelial cells metabolize NG-monomethyl-L-arginine to L-citrulline and subsequently to L-arginine. *Biochem. Biophys. Res. Commun.*, **167,** 1037–1043.

HUGHES, S.R., WILLIAMS, T.J. & BRAIN, S.D. (1990). Evidence that endogenous nitric oxide modulates oedema formation induced by substance P. *Eur. J. Pharmacol.*, **191,** 481–484.

JULOU-SCHAEFFER, G., GRAY, G.A., FLEMING, I., SCHOTT, C., PARRATT, J.R. & STOCLET, J.C. (1990). Loss of vascular responsiveness induced by endotoxin involves L-arginine pathway. *Am. J. Physiol.*, **259,** H1038–H1043.

KILBOURN, R.G., JUBRAN, A., GROSS, S.S. *et al.* (1990). Reversal of endotoxin-mediated shock by NG-methyl-L-arginine, an inhibitor of nitric oxide synthesis. *Biochem. Biophys. Res. Commun.*, **172,** 1132–1138.

KNOWLES, R.G., SALTER, M., BROOKS, S.L. & MONCADA, S. (1990). Anti-inflammatory glucocorticoids inhibit the induction by endotoxin of nitric oxide synthase in the lung, liver and aorta of the rat. *Biochem. Biophys. Res. Commun.*, **172,** 1042–1048.

KOPANIAK, M.M., ISSEKUTZ, A.C. & MOVAT, H.Z. (1980). Kinetics of acute inflammation induced by E coli in rabbits. *Am. J. Pathol.*, **98,** 485–498.

MEYRICK, B.O., RYAN, U.S. & BRIGHAM, K.L. (1986). Direct effects of E. coli endotoxin on structure and permeability of pulmonary endothelial monolayers and the endothelial layer of intimal explants. *Am. J. Pathol.*, **122,** 140–151.

MONCADA, S., PALMER, R.M.J. & HIGGS, E.A. (1991). Nitric oxide: physiology, pathophysiology and pharmacology. *Pharmacol. Rev.*, **43,** 109–141.

PETROS, A., BENNETT, D. & VALLANCE, P. (1991). Effect of nitric oxide synthase inhibitors on hypotension in patients with septic shock. *Lancet*, **338,** 1557–1558.

RADOMSKI, M.W., PALMER, R.M. & MONCADA, S. (1990). Glucocorticoids inhibit the expression of an inducible, but not the constitutive, nitric oxide synthase in vascular endothelial cells. *Proc. Natl. Acad. Sci. U.S.A.*, **87,** 10043–10047.

REES, D.D., CELLEK, S., PALMER, R.M. & MONCADA, S. (1990). Dexamethasone prevents the induction by endotoxin of a nitric oxide synthase and the associated effects on vascular tone: an insight into endotoxin shock. *Biochem. Biophys. Res. Commun.*, **173,** 541–547.

ROBERT, R., CHAPELAIN, B., JEAN, T. & NELIAT, G. (1992). Interleukin-1 impairs both vascular contraction and relaxation in rabbit isolated aorta. *Biochem. Biophys. Res. Commun.*, **182,** 733–739.

SALVEMINI, D., KORBUT, R., ANGGARD, E. & VANE, J. (1990). Immediate release of a nitric oxide-like factor from bovine aortic endothelial cells by Escherichia coli lipopolysaccharide. *Proc. Natl. Acad. Sci. U.S.A.*, **87,** 2593–2597.

THIEMERMANN, C. & VANE, J. (1990). Inhibition of nitric oxide synthesis reduces the hypotension induced by bacterial lipopolysaccharides in the rat in vivo. *Eur. J. Pharmacol.*, **182,** 591–595.

WAKABAYASHI, I., HATAKE, K., KAKISHITA, E. & NAGAI, K. (1987). Diminution of contractile response of the aorta from endotoxin injected rats. *Eur. J. Pharmacol.*, **141,** 117–122.

WARREN, J.B., LARKIN, S.W., KAJEKAR, R., COUGHLAN, M.L. & WILLIAMS, T.J. (1992). Pituitary adenylate cyclase activating polypeptide (PACAP) is potent vasodilator and oedema potentiator in rabbit skin *in vivo*. *Br. J. Pharmacol.*, **106,** 331–334.

WHITTLE, B.J.R., LOPEZ-BELMONTE, J. & MONCADA, S. (1990). Regulation of gastric mucosal integrity by endogenous nitric oxide: interactions with prostaglandins and sensory neuropeptides in the rat. *Br. J. Pharmacol.*, **99,** 607–611.

WILLIAMS, T.J. (1982). Vasoactive intestinal polypeptide is more potent than prostaglandin E_2 as a vasodilator and oedema potentiator in rabbit skin. *Br. J. Pharmacol.*, **77,** 505–509.

WILLIAMS, T.J. & PECK, M.J. (1977). Role of prostaglandin-mediated vasodilation in inflammation. *Nature*, **270,** 530–532.

WISE, W.C., HALUSHKA, P.V., KNAPP, R.G. & COOK, J.A. (1985). Ibuprofen, methylprednisolone, and gentamicin as cojoint therapy in septic shock. *Circ. Shock*, **17,** 59–71.

WOOD, K.S., BUGA, G.M., BYRNS, R.E. & IGNARRO, L.J. (1990). Vascular smooth muscle-derived relaxing factor (MDRF) and its close similarity to nitric oxide. *Biochem. Biophys. Res. Commun.*, **170,** 80–88.

(Received February 21, 1992
Revised April 9, 1992
Accepted April 10, 1992)

Br. J. Pharmacol. (1992), **106**, 958–965 © Macmillan Press Ltd, 1992

Actions and mechanisms of action of novel analogues of sotalol on guinea-pig and rabbit ventricular cells

S.P. Connors, E.W. Gill & [1]D.A. Terrar

University Department of Pharmacology, Mansfield Road, Oxford, OX1 3QT

1 The actions and mechanisms of action of novel analogues of sotalol which prolong cardiac action potentials were investigated in guinea-pig and rabbit isolated ventricular cells.

2 In guinea-pig and rabbit cells the compounds significantly prolonged action potential duration at 20% and 90% repolarization levels without affecting resting membrane potential. In guinea-pig but not rabbit cells there was an increase in action potential amplitude and in rabbit cells there was no change in the shape or position of the 'notch' in the action potential.

3 Possible mechanisms of action were studied in more detail in the case of compound II (1-(4-methanesulphonamidophenoxy)-3-(N-methyl 3,4 dichlorophenylethylamino)-2-propanol). Prolongation of action potential duration continued to occur in the presence of nisoldipine, and calcium currents recorded under voltage-clamp conditions were not reduced by compound II (1 μM). Action potential prolongation by compound II was also unaffected in the presence of 10 μM tetrodotoxin.

4 Compound II (1 μM) did not influence I_{K1} assessed from the current during ramp changes in membrane potential (20 mV s^{-1}) over the range − 90 to − 10 mV.

5 Compound II (1 μM) blocked time-dependent delayed rectifier potassium current (I_K) activated by step depolarizations and recorded as an outward tail following repolarization. When a submaximal concentration (50 nM) was applied there was no change in the apparent reversal potential of I_K.

6 Submaximal concentrations of compound II were without effect on activation of I_K with time at a membrane potential of + 40 mV, and no changes were detected in the time constants of the two components of I_K decay over the range of potentials − 60 to 0 mV. Compound II (50 nM) appeared to cause a small shift in the activation of I_K with membrane potential (an apparent shift of approximately 10 mV in the depolarizing direction at the mid-point of the curve).

7 Log dose-response curves for action potential prolongation and for blockade of I_K by compound II were similar. The IC_{50} for compound II was approximately 30 nM.

8 It is concluded that this novel series of compounds prolongs action potential duration, and that in the case of compound II the evidence supports a potent selective effect on the time-dependent potassium current I_K, an effect which can account for this prolongation.

Keywords: Sotalol; Class III antiarrhythmic; potassium channel; cardiac, ventricular cell

Introduction

Class III antiarrhythmic agents have been defined by Vaughan Williams (1970) as any compound which increases the duration of the cardiac action potential. Previously the drugs, amiodarone and sotalol, have been the best examples of this type of antiarrhythmic. However, both compounds are not selective in their actions; sotalol is a nonspecific β-adrenoceptor blocker (Singh *et al.*, 1987) while amiodarone has been shown to block both sodium (Sheldon *et al.*, 1989) and calcium channels (Nokin *et al.*, 1986). In a multicentre trial study (Kehoe *et al.*, 1990) with 236 patients, sotalol proved effective in suppression of sustained ventricular tachyarrhythmias of patients that had been refractory to at least 3 other antiarrhythmics. β-Adrenoceptor blockade may be a disadvantage (Soyka *et al.*, 1990) and it is of interest that (+)-sotalol has little or no β-blocking action but retains the ability to prolong cardiac action potentials (Lynch *et al.*, 1984; Carmeliet, 1985). With recent clinical evidence supporting the effectiveness of class III agents there has been great interest in the search for more selective compounds.

The first success in this search was the synthesis of the compounds sematilide (Lumma *et al.*, 1987) and CK-1649c (Randall *et al.*, 1987) from Berlex laboratories. These compounds were shown not to possess any β-blocking ability and to be approximately 10 times more potent than sotalol in prolonging the action potential duration (APD) in canine Purkinje fibres. Subsequently, E-4031 (Oinuma *et al.*, 1990) was developed by Eisai Tsukuba Research Laboratories and even more recently UK-68,798 by Pfizer (Cross *et al.*, 1990; Gwilt *et al.*, 1991). This latter compound has been reported to prolong APD in the concentration range 5 nM-1 μM and is the most potent compound that has been described to date.

The mechanism by which sotalol prolongs the cardiac action potential has been studied in rabbit Purkinje fibres and been shown to be inhibition of the time-dependent potassium current (I_K) and a small decrease in the inward rectifier current (I_{K1}) (Carmeliet, 1985). The aim of the work presented here was to investigate the mechanism of action of a novel series of potent class III agents which have been synthesized in these laboratories. A report on the synthesis of these compounds has been published elsewhere along with preliminary observations on their effects (Connors *et al.*, 1991). The compounds are devoid of β_1-blocking activity as assessed from the suppression of an increase in heart rate induced by intravenous injection of isoprenaline in pithed rats (Connors *et al.*, 1991).

Methods

Experiments were performed on single cardiac ventricular myocytes isolated from guinea-pig and rabbit. The animals

[1] Author for correspondence.

were stunned then killed by cervical dislocation. Hearts were excised and single cells isolated as previously described by Powell *et al.* (1980) and Mitchell *et al.* (1984). After isolation, cells were superfused with an oxygenated solution at 36°C containing (mM): NaCl 118.5, $NaHCO_3$ 14.5, KCl 4.2, KH_2PO_4 1.2, $MgSO_4$ 1.2, glucose 11.1 and $CaCl_2$ 2.5.

All compounds tested were water-soluble either as their free bases or as the corresponding hydrochloride salt (except Pfizer UK 68,798 which was dissolved in 50% v/v aqueous ethanol). Stock solutions were made up to a concentration of 5 mM in twice glass-distilled water. Further dilutions were carried out as needed. Switch to a drug-containing solution was made by a tap placed close to the inflow of the bath. All effects were reversible on washout of the drugs.

Electrical recordings were made via electrodes containing 0.5 M K_2SO_4 and 300 μM KCl; in some voltage-clamp experiments 75 mM BAPTA (1,2-*bis*(2-aminophenoxy) ethane-N,N, N′,N′-tetraacetic acid) was added to this solution. Action potentials were stimulated by 2 ms current pulse injections at 1 Hz (Axoclamp 2 single-microelectrode system; bridge mode). Each measurement of APD was made after continuous recording in the same cell when the effect had reached a steady state approximately 4 min after exposure to the drug.

A switch clamp method of voltage clamping the cells was used. The rate of switching between current passing and voltage recording modes was adjusted to allow settling between transitions, and was normally in the range 2–8 kHz.

In experiments where calcium currents were investigated, both peak current and current at the end of step depolarizations (applied at a frequency of 0.3 Hz) were measured with respect to zero current.

I_K was activated by depolarizing pulses (0.3 or 0.1 Hz) from a holding potential of − 50 mV (except where otherwise indicated). Analysis of the activation of I_K is difficult because of additional currents which may be simultaneously activated by depolarizing pulses. Several additional currents flow during the depolarization including second inward current I_{si}, sodium-calcium exchange current (Beukelmann & Weir, 1989) and calcium activated nonspecific channels (Ehara *et al.*, 1988; Beukelmann & Weir, 1989). Upon repolarization from an activating voltage step an outward tail current is observed which is thought to represent the slow deactivation of I_K and serves as a more reliable index of I_K current. Any residual calcium current would be expected to de-activate much more rapidly than I_K, and currents associated with sodium-calcium exchange or calcium-activated channels are expected to be inward and of much shorter duration (see e.g. Mitchell *et al.*, 1987). Such calcium activated inward tail currents might lead to underestimation of peak I_K. To minimize this possibility, inward tails were suppressed by minimizing the calcium transient in the cell with either nisoldipine applied extracellularly (3 μM) or intracellular BAPTA (Tsien, 1972) from appropriately filled electrodes. The amplitude of the I_K tails measured under these conditions was used as an index for revealing the degree of inhibition by the compounds. Such outward I_K tail currents were similar to those previously described by Matsuura *et al.* (1987). Under the conditions of our experiments, stable records of I_K were obtained for periods of at least 20 min and all experiments were completed within this period.

Voltage and current were recorded on a Racal Store 4 FM tape recorder at 3.75 in/s. Records were displayed on a digital storage oscilloscope (Gould 4020). The data were then either digitized (Data Translation DT 2801A) and analysed with the VCAN software package kindly provided by Dr J. Dempster or sent as an output via an IEEE interface to an Epson H180 plotter.

Results

When the compounds listed in Table 1 were applied to individual guinea-pig ventricular cells the action potential was seen to prolong in a concentration-dependent fashion (see Figure 1). The prolongation reached a steady state in less than two minutes and was reversible. Recovery was slower than onset (see Figure 1b). Observations were compared to those for sotalol since this was used as a lead compound in the development of the series. Sotalol at a concentration of 100 μM gave a prolongation of the action potential duration at 90% repolarization (APD_{90}) of 25 ± 2% under the conditions of our experiments. This compares well with a published value for prolongation of APD_{90} in guinea-pig papillary muscle of 30% at the same concentration (Carmeliet, 1985). UK 68,798 was also tested and found to produce a prolongation of 30 ± 2% at 250 nM. At 50 nM an 8 ± 3% increase in APD_{90} was observed compared with a published value of 28% seen in guinea-pig right papillary muscle (Cross *et al.*, 1990).

The most potent sotalol analogues were 10,000 times more effective than the parent compound (see Table 1). For example, compound I caused a 31% prolongation at a concentration of 10 nM. A detailed study has been made of another potent analogue (compound II). In addition to APD_{90} measurements were made of action potential duration at 20% repolarization (APD_{20}), resting membrane potential and amplitude of the action potential. No change was observed in the resting membrane potential with any of the compounds that were tested, while significant changes were seen in APD_{20} and APD_{90} (see Table 2). An interesting feature of the action potential prolongation was that the maximum achievable

Table 1 Compounds used in this study

	Dose	n	% Δ APD_{90}
Sotalol 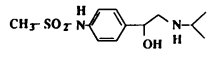	50 μM	4	10 ± 2
	100 μM	7	25 ± 2
Pfizer UK 68,798 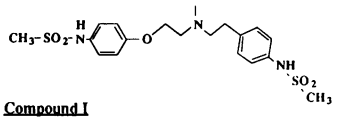	5 nM	4	2 ± 1
	50 nM	6	8 ± 3
	100 nM	4	21 ± 3
	250 nM	4	30 ± 2
Compound I 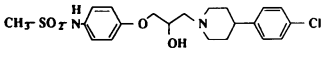	1 nM	4	16 ± 4
	10 nM	4	31 ± 2
	100 nM	4	32 ± 2
Compound II 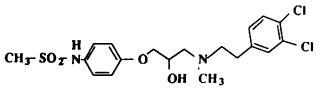	1 nM	6	7 ± 3
	10 nM	6	14 ± 1
	50 nM	6	25 ± 3
	100 nM	6	28 ± 3
	1 μM	6	30 ± 2

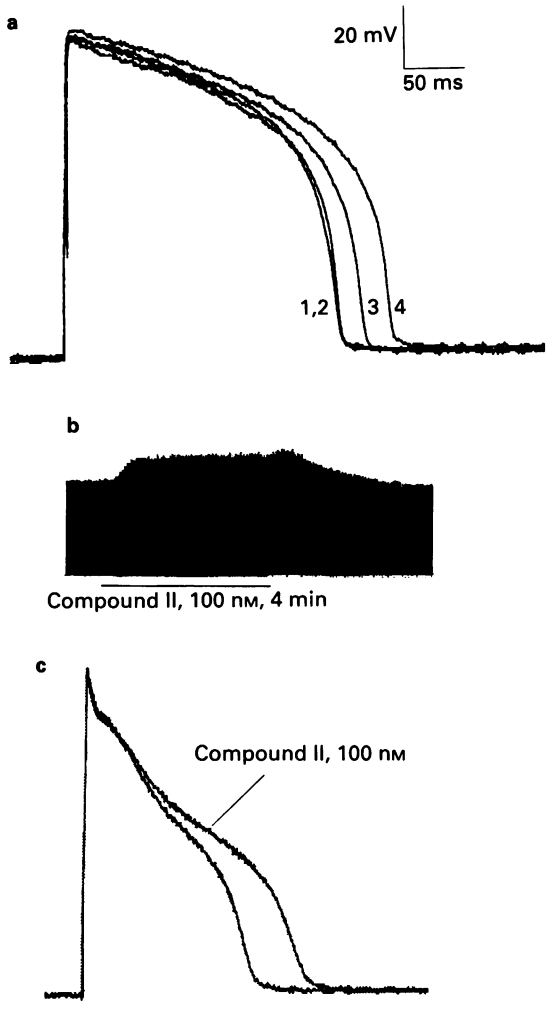

Figure 1 (a) Effect of varying doses of compound II on guinea-pig isolated ventricular cell action potentials at 1 Hz: (1) control; (2) wash (12 min after final exposure to compound II); (3) 10 nM II; (4) 50 nM II. Each dose was allowed to equilibrate for 4 min. (b) The time course of action of 100 nM compound II applied to a guinea-pig isolated ventricular cell. The trace represents a measure of APD_{90} determined from action potentials recorded at 1 Hz. (Each vertical spike represents a ramp voltage the height of which is proportional to the duration of the signal above the threshold. In this case the threshold was set at the 90% repolarization level of the action potential (APD_{90}). The trace above is at a time scale such that all the vertical spikes merge). (c) Influence of compound II (100 nM) on an action potential recorded from rabbit isolated ventricular myocyte. Note prolongation without effect on 'notch'.

effect was 30–35%, an effect also seen with a related compound E-4031 (Sanguinetti & Jurkiewicz, 1990). All the active compounds that were tested were never observed to prolong the action potential more than this amount under our experimental conditions.

It is recognized that in guinea-pig ventricular cells there is no significant transient outward current under physiological conditions (e.g. Fedida *et al.*, 1989). However, in rabbit ventricular cells transient outward current is present and gives rise to a 'notched' appearance in the early repolarization phase (Giles & Imaizumi, 1988). Addition of 100 nM compound II to rabbit isolated ventricular cells did not change the appearance of this notch (see Figure 1c). Similar observations were made in six cells. In these cells, compound II did not cause any significant effect on action potential amplitude (115 ± 3 mV before and 116 ± 3 mV during compound II), while APD_{20} and APD_{90} were significantly increased ($P<0.001$, from 54 ± 6 to 67 ± 7 ms, and from 179 ± 14 to 247 ± 18 ms).

In the presence of nisoldipine (to block 'L-type' calcium channels) action potentials were shortened as a consequence of abolition of inward calcium current during the plateau. Under these conditions, exposure to compound II again caused a dose-dependent increase in the duration. A dose-response curve in the presence of nisoldipine along with an example record in shown in Figure 2a and b (compare also Figure 9 and see later). Compound II (100 nM) in the presence of nisoldipine increased action potential amplitude

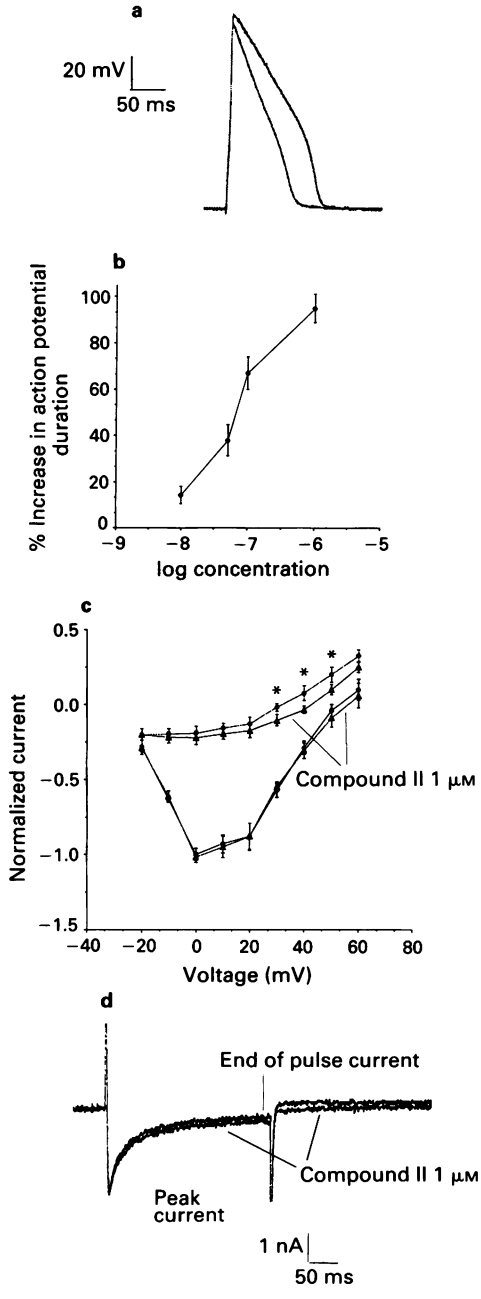

Figure 2 The effects of compound II on nisoldipine-treated guinea-pig ventricular cells: (a) shows a typical record of an action potential at 1 Hz recorded in the presence of 2 μM nisoldipine before and after the effects of 100 nM compound II, (b) shows a dose-response curve for the effects of compound II on nisoldipine-treated action potentials. Data at each dose from 3–5 cells. Vertical bars represent s.e.mean. In the absence of nisoldipine (c) shows both the peak inward current and the current at the end of the depolarizing pulse plotted as a function of membrane voltage before and after the addition of compound II 1 μM. $n = 6$ cells; s.e. shown (*$P<0.05$). Panel (d) A typical current record before and after the addition of II. Holding potential − 40 mV with a 300 ms depolarization to 0 mV.

from 110 ± 2 mV to 120 ± 2 mV, increased APD_{20} from 17 ± 3 to 39 ± 3 ms, and increased APD_{90} from 93 ± 2 to 143 ± 5 ms ($P<0.001$ for all three measurements, $n = 5$).

The possibility that compound II might influence calcium currents was further tested under voltage-clamp conditions by applying step depolarizations from a holding potential of − 40 mV. No change in the magnitude of the peak inward current over the range − 30 mV to + 20 mV could be detected which was consistent with the hypothesis that there was no significant effect on L-type calcium channels (see Figure 2c and d). At more positive membrane potentials a small reduction in outward current at the end of the pulse (significant at + 30 to + 50 mV, see Figure 2c) is consistent with a reduction in I_K which would be expected to contribute more at these depolarized potentials, a possibility which will be considered again later.

The ability to prolong the APD was preserved in the presence of tetrodotoxin (TTX). In Figure 3 it can be seen that 10 μM TTX significantly shortened APD_{90} as has been previously observed (Mitchell *et al.*, 1984; Kiyosue & Atria, 1989). When compound II was added in the continued presence of TTX, significant changes were seen in action potential amplitude, APD_{20}, and APD_{90} (see legend to Figure 3). There was no significant difference in prolongation of the action potential by compound II in the presence of TTX: compound II at a concentration of 1 μM increased APD by 30 ± 4.8% in the absence and by 28 ± 2.9% in the presence of 10 μM TTX.

To test for a potential interaction of these compounds with I_{K1} the voltage across the cell membrane was ramped over the range − 90 to + 20 mV at a rate of 20 mV per second (a rate at which most time-dependent currents including those carried by sodium and calcium are at a steady state). It was seen that concentrations of compound II (1 μM) which caused maximal prolongation of action potentials produced little change in the *I*-V relation of the cell over the range − 90 mV to − 10 mV. At more depolarized membrane potentials where I_{K1} shows marked inward rectification and therefore contributes little to the *I*-V relation of the cell, the current in the presence of compound II was seen to be less outward (or more inward, see Figure 4). These observations are consistent with those of the experiments described above (Figure 2c) where the current at the end of depolarizations used to evoke I_{si} was less outward for membrane potentials between + 30 and + 50 mV while any effects over the range

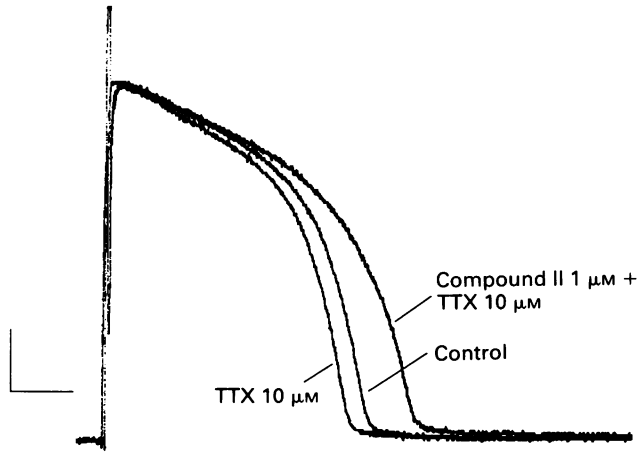

Figure 3 Preservation of the action of compound II in the presence of 10 μM tetrodotoxin (TTX). A typical record is shown on exposure of an action potential stimulated at 1 Hz to first TTX then TTX and compound II together. Changes seen in APD_{20} were as follows: 85 ± 17 ms in control to 80 ± 13 ms on exposure to 10 μM TTX alone and 99 ± 16 ms ($P<0.05$) with 10 μM TTX plus compound II. Values for APD_{90} were 187 ± 14 ms, 169 ± 13 ms ($P<0.001$) and 217 ± 13 ms ($P<0.001$) respectively. Data from 7 cells.

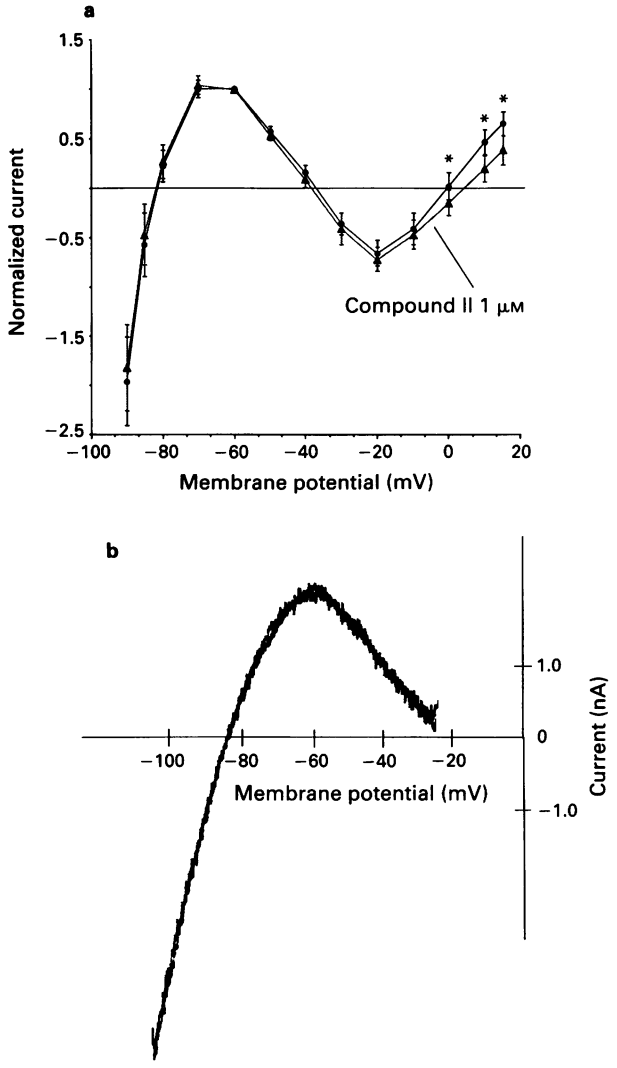

Figure 4 The effects of 1 μM compound II on the *I*-V relationship in guinea-pig isolated ventricular cells: (a) shows the current-voltage relationship plotted over a range of voltages before and after the addition of compound II. Data are taken from ± 40 mV excursions around holding potentials of − 20 mV and − 60 mV. Results are from 7 cells. Data are normalized to current at − 60 mV (*$P<0.05$). (b) shows a typical current record in which voltage was varied at 20 mV per s with an excursion of ± 40 mV about a holding potential of − 60 mV. The effects before and after compound II are shown.

− 30 to + 20 mV were small.

When the possibility of an effect on I_K was tested more directly (measuring I_K as the outward tail on repolarization following a step depolarization to positive potentials from a holding potential of − 50 mV, see Methods) compound II (1 μM) was consistently found to suppress I_K in all cells studied. Examples recorded from three different cells are shown in Figure 5. It can be seen that the influence of compound II on current developing during the step depolarization was variable in contrast to the consistent marked reduction of the I_K tail currents. Contribution of currents other than I_K to the current developing during the step depolarization (and thus its variable sensitivity to compound II) is considered in more detail in the Discussion.

The reversal potential of this outward tail current was found to be approximately − 75 mV, close to the expected value of E_K (Figure 6). A submaximal concentration of compound II (50 nM), which reduced the amplitude by approximately 60% at − 40 mV, caused little or no change in the apparent reversal potential.

In the experiment shown in Figure 7, a range of depolarizations of 350 ms duration from − 30 mV to + 40 mV in 10 mV steps were applied to investigate activation of I_K with membrane potential. The activation of I_K has been described as showing a sigmoid relationship to voltage (Shibasaki, 1987) and the results obtained here followed this pattern. A submaximal dose of compound II reduced the amplitude of the outward I_K tails, showing little dependence on the membrane potential during the activating step. Activation for 350 ms was investigated because although this was not expected to allow full activation of I_K (Matsuura *et al.*, 1987) the duration of depolarization approximates that of the ventricular action potential. Activation of I_K with membrane potential was also investigated using 1 s depolarizations (see Figure 7b) to allow the current to approximate more closely steady state conditions. The effect of compound II on I_K was seen to be similar when the length of depolarization was increased. Depolarizations greater than 1 s were not used in order to avoid possible harmful effects of such long depolarizations (Terrar & White, 1989). When the voltage activation curves for 1 s depolarizations in the presence and absence of 50 nM compound II were compared (following normalization of the current amplitudes to the maximum current elicited) there appeared to be a slight shift in activation of about 10 mV in the depolarizing direction (see Figure 7c). The observations thus appear to indicate that any voltage-dependence of the action of compound II on I_K is small.

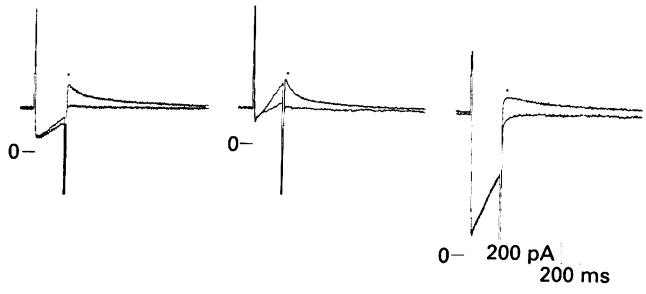

Figure 5 The effects of compound II on the current trace in three different cells (from the guinea-pig) in the presence of 2 μM nisoldipine. Control traces (*) are superimposed on traces in the presence of the compound. Depolarizations are to + 50 mV for 250 ms from a holding potential of − 40 mV. In each case there is a suppression of the decaying outward tail current; however, the effect of compound II on the current during the depolarization is variable. Zero current levels are shown for each cell.

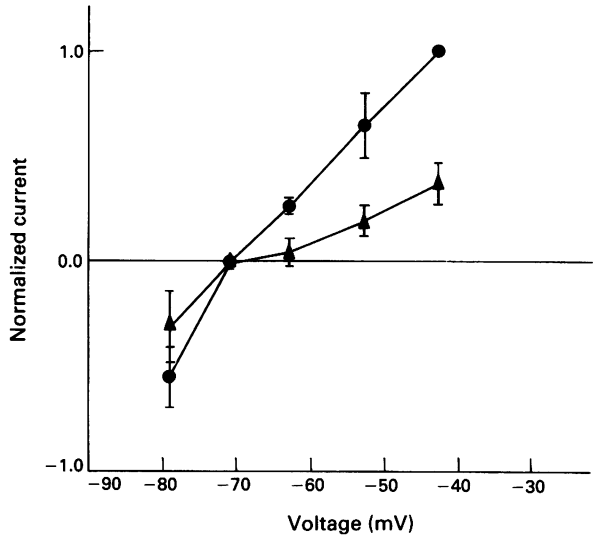

Figure 6 Plot of I_K tail current against membrane potential on repolarization following an activating step depolarization to + 40 mV for 1 s (currents normalized to that at − 40 mV in the absence of compound II). I_K tail currents in the presence of 50 nM compound II (▲); currents in the absence of drug (●). Apparent reversal potential was approximately − 75 mV. Data from 5 guinea-pig cells, BAPTA present throughout. Vertical bars show s.e.

Since activation of I_K depends on time in addition to membrane potential, the effects of compound II upon the time-dependent activation of I_K were also investigated (see Figure 8). Cells were depolarized to + 40 mV for various durations, and the outward I_K tails on repolarization to the holding potential of − 50 mV were recorded. The envelope of deactivating outward tails measured in this way revealed the time-dependence of activation of I_K. Compound II at 50 nM reduced I_K with little or no effect on the kinetics of activation while at 1 μM I_K was virtually abolished at short times up to 200 ms, with approximately 15% of the current remaining at 1000 ms (records not shown). It appears, therefore, that compound II affects the magnitude and not the kinetics of time-dependent activation of I_K.

The possible effect of compound II on the deactivation of I_K was investigated by fitting exponential components to the current deactivation. This decay conformed to biexponential kinetics and could not be fitted well to monoexponential decay as has been previously described in experiments on single cells (e.g. Bennett *et al.*, 1985). In the voltage range − 60 mV to 0 mV, time constants for both the fast and slow components were seen to increase. For voltages positive to this there was a significant steady state activation of I_K such that the deactivating tail current was quite small making analysis difficult. In the absence of I_K inhibitors the time constants were of the order that have been previously reported (Matsuura *et al.*, 1987) and upon addition of compound II no significant change was seen in either the fast or slow component (see Figure 8b and c).

For compound II a dose-response relationship for action potential prolongation and current inhibition is seen in Figure 9. The IC_{50} derived from the relationship of current inhibition and dose was aproximately 30 nM and compares with a value of 10 μM for sotalol (Carmeliet, 1985) representing a substantial increase in potency. It can also be seen in Figure 9 that the log dose-response curve for inhibition of I_K

Table 2 Characteristics of the effects of sotalol 100 μM and compound II 100 nM on the action potentials recorded from guinea-pig isolated ventricular myocytes

	Control (n = 7)	*Sotalol (n = 7)*	*Control (n = 6)*	*Compound II (n = 6)*
RMP	− 75 ± 0.8 mV	− 75 ± 0.9 mV	− 75 ± 0.60 mV	− 75 ± 0.50 mV
AMP	118 ± 1.0 mV	121 ± 0.4 mV*	122 ± 1.6 mV	126 ± 0.60 mV*
APD_{20}	101 ± 13 ms	137 ± 17 ms**	109 ± 10 ms	145 ± 9.8 ms**
APD_{90}	223 ± 16 ms	282 ± 18 ms**	201 ± 12 ms	260 ± 18 ms**

RMP, resting membrane potential.
AMP, amplitude.
APD_{20}, action potential duration at 20% repolarization.
APD_{90}, action potential duration at 90% repolarization.
*$P<0.01$, **$P<0.001$.

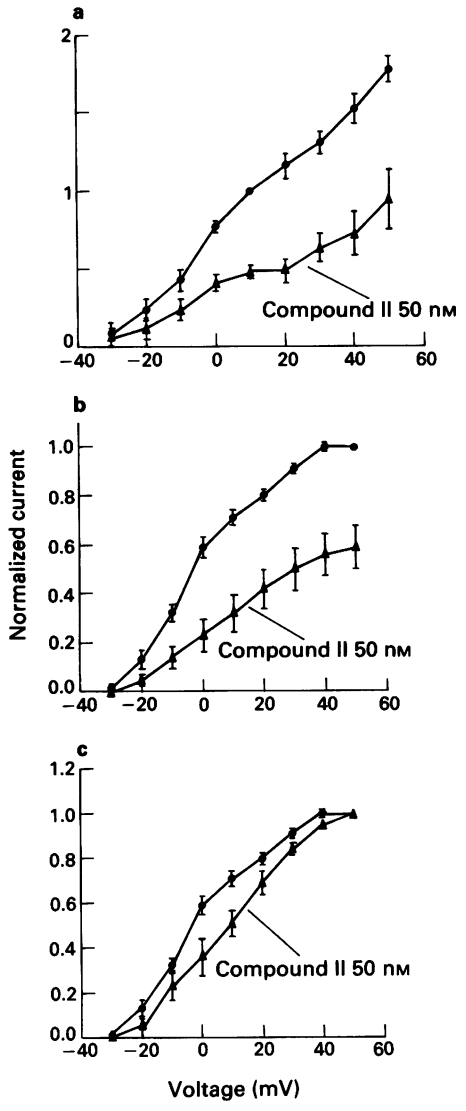

Figure 7 This figure demonstrates the current-voltage relationship of I_K in the presence and absence of compound II: (a) shows the current-voltage relationship in the presence and absence of 50 nM II. Currents were elicited within a 350 ms depolarization. $n = 5$ cells, nisoldipine 2 μM present. (b) shows again the effects of 50 nM compound II on the current-voltage relationship of I_K but currents in this panel were elicited after depolarization for 1 s. $n = 7$ cells, intracellular BAPTA present. (c) shows the results in (b) normalized to I_{Kmax}before and after compound II respectively. Data from 7 cells. s.e. shown. The cells were obtained from guinea-pig.

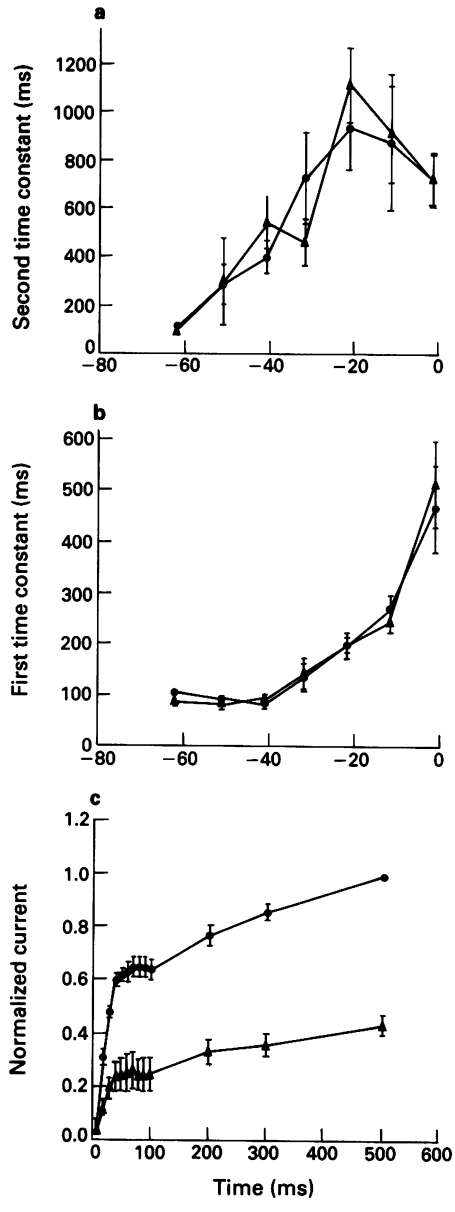

Figure 8 This figure shows the effect of compound II 50 nM on the kinetics of deactivation and activation of I_K. Current was elicited upon returning to a family of voltages from a depolarization to + 40 mV for 1 s: (a) shows the lack of effect on the first time constant (●, control) and (b) shows the lack of effect on the second time constant (●, control). Deactivating tails were fitted to the biexponential equation: $I(t) = A1\exp(-t/t_1) + A2\exp(-t/t_2)$ where $I(t)$ is the value of I_K at time t; A1 and A2 the maximum current value of the two components and t_1 and t_2 the values of the first and second time constants. (c) The time activation of I_K at a constant voltage. Currents were elicited with a depolarization to + 40 mV from a holding potential of − 50 mV in the presence of intracellular BAPTA. The effect of compound II 50 nM (▲) is shown. Currents were normalized to that at 500 ms in control. Data from 6 guinea-pig cells; s.e. shown.

closely follows that of action potential prolongation providing further evidence that the mechanism of action of the compounds is via selective inhibition of I_K.

Discussion

It appears from the observations reported here that under the conditions of our experiments the novel sotalol analogues we have synthesized are among the most potent, perhaps the most potent, agents in prolonging the cardiac action potential described to date. The evidence presented here supports the suggestion that the major mechanism for action potential prolongation is blockade of time-dependent potassium current. This evidence will be briefly discussed below followed by consideration of possible uses of such compounds in electrically dissecting important aspects of cardiac function and as agents of potential therapeutic significance.

Prolongation of action potential duration might have arisen from elevation of depolarizing plateau currents but it appears that enhancement by the compounds either of fast sodium or of calcium currents is unimportant since prolongation of action potentials persisted in the presence of tetrodotoxin or nisoldipine. More direct evidence that compound II did not influence calcium current was provided by the voltage-clamp experiments.

The observation that compound II did not alter resting membrane potential is not by itself convincing in excluding an action on I_{K1}, since changes in the conductance for this

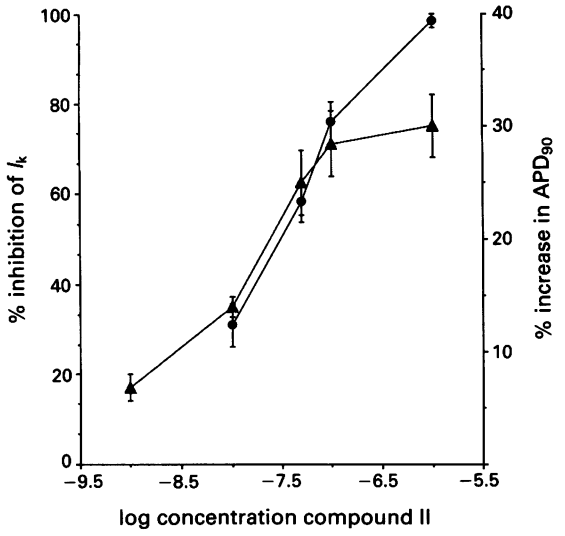

Figure 9 The dose-response relationship for both action potential duration and inhibition of I_K. The prolongation of action potential duration is that at APD_{90} (▲) and is compared with the inhibition of I_K elicited after a 350 ms depolarization to + 40 mV from a holding potential of − 50 mV (●). Each point represents data from 4–6 cells. s.e. shown. Nisoldipine 2 μM present for measurement of the current.

pathway close to the potassium equilibrium potential would be expected to have much less effect than during the repolarization phase of the action potential. However, the ramp voltage-clamp experiments provided additional support for a lack of effect on this pathway.

Compound II caused a consistent suppression of I_K (measured as maximum amplitude of decaying outward tails following an activating depolarization) in all cells studied. No change was detected in the apparent reversal potential of the time-dependent component (I_K) by submaximal concentrations of the drug. It was also shown that compound II did not cause any obvious change either in the activation of I_K with time, or in the two time constants of the decaying I_K tails. Elucidation of precise molecular mechanism requires further experiments but these observations are consistent with an effect to reduce opening of I_K channels without obvious influence on the opening and closing properties of unblocked channels. However, there appeared to be a small change in voltage activation, though the possibility should be considered that this observation might result from differential effects on subtypes of I_K channels (see later) at different membrane potentials. The suggestion that most or all of the action potential prolongation by compound II results from blockade of I_K is supported by the close similarity of log (dose)-response curves for the two effects.

No attempt was made to measure I_K during an activating depolarization since it is known that several components of current are superimposed under these conditions. Even when calcium current is suppressed with nisoldipine, current may flow through Na:Ca exchange and through non-selective cation channels activated by a rise in cytosolic calcium (see e.g. Beukelmann & Wier, 1989; Terrar & White, 1989). When cytosolic calcium is buffered with BAPTA, Na:Ca exchange could support outward current (Ca entry and Na extrusion) at positive potentials and it remains possible that calcium-activated channels could still contribute if buffering of calcium in the 'fuzzy space' beneath the sarcolemma were incomplete (Lederer *et al.*, 1990). Outward current continued to develop during step depolarizations under conditions where the outward tail of I_K was completely suppressed. This observation can be accounted for by the lack of effect of compound II on the above additional currents which contribute to the current during depolarization (see Figure 3). Such compound II-insensitive currents are presumably responsible for continued increase in outward current at the end of these step depolarizations. Indeed, it seems possible that compound II may be useful in future experiments to investigate further these additional current components where I_K is selectively abolished by low concentrations of compound II.

Compound II may also be useful in detecting possible contamination by I_K of other current components. For example it is apparent from Figure 2d that for depolarizations to 0 mV, any contribution of compound II-sensitive I_K is negligible compared to peak calcium current under the conditions of our experiments (consistent with previous work, e.g. Matsuda & Noma, 1984; Mitchell *et al.*, 1987).

It has recently been suggested that there may be two components of the delayed rectifier potassium current (Sanguinetti & Jurkiewicz, 1990) and that sotalol tended to block only one of these components. The complex nature of I_K is supported by other work which demonstrates that I_K does not have a simple activation process (Connors *et al.*, 1990) and that those currents induced by longer depolarizations tend to be selectively increased by forskolin (Connors & Terrar, 1990). In the work of Sanguinetti & Jurkiewicz (1990) evidence for subtypes of I_K was based on currents flowing during activation of I_K compared to those on deactivation of I_K. This approach may not be appropriate if there were contaminating currents during activation (such as Na:Ca exchange) as discussed above. However, this work has raised an important issue from which two possible conclusions may be drawn: either there exist subtypes of I_K channels or a single I_K channel exhibits complex kinetics. The resolution of this question would be important in future investigations and may require single channel evidence which is not yet available.

The observation that the amplitude of the action potential was significantly increased by compound II was interesting. It was argued above that the effects of these compounds were not mediated through an action on sodium or 'L-type' calcium channels or by any large change in the background potassium current. Steady state activation of I_K may occur (Boyett & Jewell, 1980; Delmar *et al.*, 1989) under the conditions of our experiments since the interval between action potentials at 1 Hz may not present sufficient time for deactivation. If there were a steady state level of outward current through I_K, inhibition of this pathway would be expected to increase the amplitude of the action potentials. In the case of the rabbit action potentials, little change in the amplitude was seen presumably because rabbit ventricular cells possess a substantial I_{to} (Giles & Imaizumi, 1988) giving them the 'notched' appearance in the early plateau. Since the current through this pathway is much greater than that of I_K (Giles & Imaizumi, 1988) one would not expect to see the effect of inhibiting I_K on the amplitude of the rabbit ventricular action potential. Following this line of argument, in guinea-pig cells where I_{to} is not prominent (Fedida *et al.*, 1989), nisoldipine decreased the amplitude of the action potential presumably because the contribution of the calcium current to peak amplitude was removed.

The observation that the prolongation of action potential duration was greater in the presence than in the absence of nisoldipine may be accounted for in terms of the relative importance of I_K under these two conditions. In the absence of the calcium channel blocker removal of I_K would tend to approach a natural limit in prolonging action potential duration as there will remain repolarizing influences such as decay of the calcium current and activation of I_{K1}. Thus, a prolongation limit of 30–35% may be reached when repolarization is governed entirely by these I_K-independent mechanisms. In the presence of nisoldipine action potentials in the absence of other drugs are much shorter as a consequence of the absence of the calcium current. Under these different initial conditions this natural limit upon removing I_K need no

longer be the same allowing greater increases in action potential duration by these compounds.

In conclusion compound II, the prototype of a novel series of compounds, has been shown to increase action potential duration through a selective inhibition of the time-dependent potassium current. Future experiments will be required to assess whether compound II and related compounds may have potential therapeutic significance as Class III antiarrhythmic drugs.

References

BENNETT, P.B., MCKINNEY, L.C., KASS, R.S. & BEGENISICH, T. (1985). Delayed rectification in the calf cardiac Purkinje fiber. Evidence for multiple state kinetics. *Biophys. J.*, **48**, 553–567.

BEUCKELMANN, D.J. & WIER, W.G. (1989). Sodium-calcium exchange in guinea-pig cardiac cells: exchange current and changes in intracellular. *Can. J. Physiol.*, **414**, 499–520.

BOYETT, M.R. & JEWELL, B.R. (1980). Analysis of the effects of changes in rate and rhythm upon electrical activity in the heart. *Prog. Biophys. Mol. Biol.*, **36**, 1–52.

CARMELIET, E. (1985). Electrophysiologic and voltage clamp analysis of sotalol effects in cardiac muscle and Purkinje fibers. *J. Pharmacol. Exp. Ther.*, **232**, 817–825.

CONNORS, S.P., DENNIS, D., GILL, E.W. & TERRAR, D.A. (1991). The synthesis and potassium channel blocking activity of some (4-methanesulfonamidophenoxy) propanolamines as potential Class III antiarrhythmic agents. *J. Med. Chem.*, **34**, 1570–1577.

CONNORS, S.P. & TERRAR, D.A. (1990). The effect of forskolin on activation and deactivation of time dependent potassium current in ventricular cells isolated from guinea pig heart. *J. Physiol.*, **429**, 109P.

CONNORS, S.P., GILL, E.W. & TERRAR, D.A. (1990). Activation of the time dependent potassium current in ventricular cells isolated from guinea-pig. *J. Physiol.*, **426**, 13P.

CROSS, P.E., ARROWSMITH, J.E., THOMAS, G.N., GWILT, M., BURGES, R.A. & HIGGINS, A.J. (1990). Selective class III antiarrhythmic agents 1. Bis (arylalkyl)amines. *J. Med. Chem.*, **33**(4), 1151–1155.

DELMAR, M., GLASS, L., MICHEALS, D.C. & JALIFE, J. (1989). Ionic basis and analytical solution of the Wenckebach phenomenon in guinea pig ventricular myocytes. *Circ. Res.*, **65**, 775–788.

EHARA, T., NOMA, A. & ONO, K. (1988). Calcium activated non-selective cation channel in ventricular cells isolated from adult guinea-pig hearts. *J. Physiol.*, **403**, 117–133.

FEDIDA, D., SHIMONI, Y. & GILES, W.R. (1989). A novel effect of norepinephrine on cardiac cells is mediated by a1-receptors. *Am. J. Physiol.*, **256**, H1500–1504.

GILES, W.R. & IMAIZUMI, Y. (1988). Comparison of potassium currents in rabbit atrial and ventricular cells. *J. Physiol.*, **405**, 123–145.

GWILT, M., ARROWSMITH, J.E., BLACKBURN, K.J., BURGES, R.A., CROSS, P.E., DALRYMPLE, H.W. & HIGGINS, A.J. (1991). UK-68,798: a novel, potent and highly selective Class III antiarrhythmic agent which blocks potassium channels in cardiac cells. *J. Pharmacol. Exp. Ther.*, **256**, 318–324.

KEHOE, R.F., ZHEUTLIN, T.A., DUNNINGTON, C.S., MATTIONI, T.A., YU, G. & SPANGENBERG, R.B. (1990). Safety and efficacy of sotalol in patients with drug-refractory sustained ventricular tachyarrhythmias. *Am. J. Cardiol.*, **65**, 58A–64A.

KIYOSUE, T. & ATRIA, M. (1989). Late sodium current and its contribution to action potential configuration in guinea pig ventricular myocytes. *Circ. Res.*, **64**, 389–397.

LEDERER, W.J., NIGGLI, E. & HADLEY, R.W. (1990). Sodium-calcium exchange in excitable cells: Fuzzy space. *Science*, **248**, 283.

LUMMA, W.C., WOHL, R.A., DAVEY, D.D., DIAMOND, J., WONG, S.S. & SULLIVAN, M.E. (1987). Rational design of 4-[(methylsulfonylamino] benzamides as class III antiarrhythmic agents. *J. Med. Chem.*, **30**, 755–758.

LYNCH, J.J., WILBER, D.J., MONTGOMERY, D.G., HSIEH, T.M., PATTERSON, E. & LUCCHESI, B.R. (1984). Antiarrhythmic and fibrillatory actions of levo- and dextro-rotatory isomers of sotalol. *J. Cardiovasc. Pharmacol.*, **6**, 1132–1141.

MATSUDA, H. & NOMA, A. (1984). Isolation of calcium current and its sensitivity to monovalent cations in dialysed ventricular cells of guinea pig. *J. Physiol.*, **357**, 553–573.

MATSUURA, H., EHARA, T. & IMOTO, Y. (1987). An analysis of the delayed outward current in single ventricular cells of the guinea pig. *Pflügers Arch.*, **410**, 596–603.

MITCHELL, M.R., POWELL, T., TERRAR, D.A. & TWIST, V.W. (1984). The effects of ryanodine, EGTA and low sodium on action potentials in rat and guinea-pig ventricular muscle. *Br. J. Pharmacol.*, **81**, 543–550.

MITCHELL, M.R., POWELL, T., TERRAR, D.A. & TWIST, V.W. (1987). Calcium activated inward current and contraction in rat and guinea pig ventricular myocytes. *J. Physiol.*, **391**, 545–560.

NOKIN, P., CLINET, M., SWILLENS, S., DELIZEE, C., MEYSMANS, L. & CHATELAIN, P. (1986). Allosteric modulation of [3H] nitrendipine binding to cardiac and cerebral cortex membranes by amiodarone. *J. Cardiovasc. Pharmacol.*, **8**, 1051–1057.

OINUMA, H., MIYAKE, K., YAMANAKA, M., NOMOTO, K., KATOH, H., SAWADA, K., SHINO, M. & HAMANO, S. (1990). 4'-[(4-Piperidyl) carbonyl] methanesulfonanilides as potent, selective, bioavailable class III antiarrhythmic agents. *J. Med. Chem.*, **33**, 903–905.

POWELL, T., TERRAR, D.A. & TWIST, V.W. (1980). Electrical properties of individual cells isolated from adult rat ventricular myocardium. *J. Physiol.*, **302**, 131–153.

RANDALL, L., MORGAN, T.K., DE VITA, R.J., DAVEY, D.D., LUMMA, W.C., WOHL, R.A., DIAMOND, J., WONG, S.S. & SULLIVAN, M.E. (1987). Synthesis and antiarrhythmic activity of novel 3-alkyl-1-[w-[4-[(alkylsulfonyl) amino] phenyl]-w-hydroxyalkyl]-1H-imidazolium salts and their related compounds. *J. Med. Chem.*, **30**, 696–704.

SANGUINETTI, M.C. & JURKIEWICZ, N.K. (1990). Two components of cardiac delayed rectifier K^+ current. Differential sensitivity to block by class III antiarrhythmic agents. *J. Gen. Physiol.*, **96**, 195–215.

SHELDON, R.S., HILL, R.J., CANNON, N.J. & DUFF, H.J. (1989). Amiodarone: biochemical evidence for binding to a receptor for class I drugs associated with the rat cardiac sodium channels. *Circ. Res.*, **65**, 477–482.

SHIBASAKI, T. (1987). Conductance and kineteics of delayed rectifier potassium channels in nodal cells of rabbit heart. *J. Physiol.*, **387**, 227–250.

SOYKA, L.F., WIRTZ, C. & SPANGENBERG, R.B. (1990). Clinical safety profile of sotalol in patients with arrhythmias. *Am. J. Cardiol.*, **65**, 74A–81A.

TERRAR, D.A. & WHITE, E. (1989). Mechanisms and significance of calcium entry at positive membrane potentials in guinea pig ventricular muscle cells. *Q. J. Exp. Physiol.*, **74**, 121–139.

THOMAS, G., CHUNG, M. & COHEN, C.J. (1985). A dihydropyridine (Bay K 8644) that enhances calcium currents in guinea pig and calf myocardial cells. A new type of positive inotropic agent. *Circ. Res.*, **56**, 87–96.

TSIEN, R.W., GILES, W.R. & GREENGARD, P. (1972). Cyclic AMP mediates the effect of adrenaline on cardiac Purkinje fibers. *Nature, New Biol.*, **240**, 181–183.

VAUGHAN WILLAMS, E.M. (1970). Classification of antiarrhythmic drugs. In *Symposium on Cardiac Arrhythmias*. ed. Sandoe, E., Flensted-Jenson, E. & Olson, K.H. Sodertaljie, Sweden: AB Astra.

(Received April 6, 1992
Accepted April 10, 1992)

Br. J. Pharmacol. (1992), **106**, 966–971 © Macmillan Press Ltd, 1992

In vitro inhibition by endothelins of thrombin-induced aggregation and Ca^{2+} mobilization in human platelets

[1]Catherine Astarie-Dequeker, Lahcen Iouzalen, Monique David-Dufilho & Marie-Aude Devynck

Pharmacology, URACNRS D1482, Necker Medical School, 156, rue de Vaugirard, 75015 Paris, France

1 The *in vitro* effects of endothelins (ET-1 and ET-3) on human platelets were investigated by measurement of the aggregatory responses of washed platelets to thrombin and by the determination of cytosolic pH (pHi) and free Ca^{2+} concentration ($[Ca^{2+}]_i$) determined with the fluorescent indicators, BCECF and Fura-2.

2 ET-1 and ET-3 at concentrations ranging from 10^{-10} to 5×10^{-7} M, did not promote platelet aggregation but inhibited in a dose-dependent manner the aggregation induced by 0.05 u ml^{-1} thrombin ($P < 0.002$ and < 0.001, respectively) with maximal effects reached at 10^{-8} M (17 ± 3 and $15 \pm 2\%$, $n = 11$, $P = 0.002$ for each).

3 Even at 5×10^{-7} M, ET-1 and ET-3 did not cause a measurable change in basal $[Ca^{2+}]_i$ and pHi. When tested in combination with thrombin, 5×10^{-7} M ET-1 and ET-3 decreased the transient peak of $[Ca^{2+}]_i$ by 17 ± 7 and $28 \pm 7\%$ ($n = 7$ and 11, $P = 0.03$ and $P = 0.002$). No effect on pHi variations was detected. In the virtual absence of external Ca^{2+}, 5×10^{-7} M ET-3 inhibited the peak of $[Ca^{2+}]_i$ by $18 \pm 6\%$ ($n = 6$, $P = 0.02$).

4 The anti-aggregating agents, prostacyclin (PGI_2, 10^{-8}–10^{-7} M) and nitroprusside (NP, 10 ng–50 $\mu g\, l^{-1}$) also induced a dose-dependent inhibition of the thrombin-induced $[Ca^{2+}]_i$ peak ($P = 0.001$ for each). A combination of 10^{-9} M PGI_2 and 10 ng l^{-1} NP augmented the inhibitory effect of each drug (PGI_2 alone 52 ± 11, plus NP 90 ± 2; NP alone 26 ± 4, plus PGI_2 $69 \pm 5\%$ inhibition of $[Ca^{2+}]_i$ peak, $n = 6$ for each, $P < 0.01$ and $P < 0.001$, respectively). Platelet preincubation with 5×10^{-7} M ET-3 increased by $34 \pm 11\%$ ($n = 6$, $P = 0.014$) the inhibitory effect of NP 10 ng l^{-1} without a significant influence on the PGI_2 effect.

5 In conclusion, endothelins ET-1 and ET-3 can reduce *in vitro* the aggregating response of human platelets to thrombin by a mechanism that is probably due to decrease Ca^{2+} mobilization.

Keywords: Human platelets; pHi; Ca^{2+}; platelet aggregation; endothelins; prostacyclin; nitroprusside

Introduction

Vascular endothelium generates factors that modulate in the local environment the homeostatic interaction between platelets and vessel wall. Among these agents, both prostacyclin (PGI_2) and the endothelium-derived relaxing factor (EDRF) or nitric oxide (NO) have a significant role in preventing platelet aggregation (Moncada *et al.*, 1976; Azuma *et al.*, 1986). Their potent anti-aggregatory capacity is exerted through an elevation of adenosine 3′:5′-cyclic monophosphate (cyclic AMP) for PGI_2 (Gorman *et al.*, 1977; Tateson *et al.*, 1977) and guanosine 3′:5′-cyclic monophosphate (cyclic GMP) for EDRF/NO (Mellion *et al.*, 1981; Pohl & Busse, 1989) which both in turn lead to a decrease of calcium availability in the cells. Endothelial cells also produce endothelins which belong to a vasoactive peptide family consisting of three isopeptides, endothelin-1, 2 and 3 (ET-1, ET-2 and ET-3) that are structurally and pharmacologically distinct. It has been reported that endothelins exert vasodilator effects which contrast with their vasoconstrictor ability (Fukuda *et al.*, 1991; Takayanagi *et al.*, 1991). For example, Fukuda *et al.* (1991) have recently proposed that ET-3, a more potent depressor agent than ET-1 and ET-2, acts as a vasodilator under physiological conditions whereas it may act as a vasoconstrictor on the endothelium-damaged arteries. However, the precise mechanism of this ET-dependent vasodilatation still remains ambiguous.

Various studies present evidence that endothelins inhibit platelet aggregation when measured both *ex vivo* and *in vivo* (Lidbury *et al.*, 1989; Thiemermann *et al.*, 1989; 1990). This effect is associated with an enhanced platelet cyclic AMP level and seems to be mediated by the endothelial release of PGI_2 into the circulation (Thiemermann *et al.*, 1989). However, the mechanism involved is still unclear because this endothelin effect is only partially blocked by the cyclooxygenase inhibitor, indomethacin (Thiemermann *et al.*, 1989).

The present study was undertaken to evaluate the *in vitro* influence of ET-1 and ET-3 on thrombin-induced aggregating response of human platelets. Changes in cytoplasmic ionized calcium $[Ca^{2+}]_i$ play a major role in many aspects of platelet activation (Siess, 1989). In addition, variations of cytosolic pH (pHi) could modulate platelet responses to various agents (Nachmias *et al.*, 1987; Ishikawa *et al.*, 1989). Endothelin effects were thus investigated on both $[Ca^{2+}]_i$ and pHi and compared with those of PGI_2 and sodium nitroprusside (NP) as a stable analogue of nitric oxide.

Methods

Venous blood from healthy subjects (15–20 ml) was collected into a tube containing 0.1 vol. anticoagulant (2.73% citric acid, 4.48% trisodium citrate, and 2% glucose). Platelet-rich plasma (PRP) was obtained by centrifugation at 530 g_{max} for 5 min at 20°C. All experiments were performed within 3 h after blood sampling on platelets kept at room temperature.

[1] Author for correspondence.

Platelet aggregation study

PRP was centrifuged at 270 *g* for 15 min at 20°C and platelet pellet was resuspended in a buffer containing mM: NaCl 145, KCl 5, $MgCl_2$ 0.5, glucose 5 and HEPES 10, pH 7.4 at 37°C (buffer A). Platelets were counted on a thrombocounter (Coultronics, Margency, France) and their number was adjusted to a final concentration of $8-9 \times 10^7$ cells ml^{-1}. Before each experiment, platelets were incubated with 1 mM $Ca(NO_3)_2$ for 3 min. The aggregatory responses of washed platelets were evaluated at 37°C using continuous stirring by a turbidometric technique (Born, 1962) in a double-channel aggregometer (Coultronics). The concentration of thrombin employed was the lowest that elicited sustained aggregation (0.05 u ml^{-1}). Platelet response was assessed by measurement of the initial rate and the extent of aggregation. Since the effects of endothelin on $[Ca^{2+}]_i$ were rapid and transient, we have also calculated the area under each aggregatory curve recorded for 1 min after the agonist addition. ET-1 or ET-3, PGI_2 or NP (all from Sigma, St Louis, U.S.A.) were added to the platelet suspension 10 and 1 min, respectively, before the addition of thrombin (Roche Diagnostica, Basel, Switzerland). The response to thrombin was repeatedly checked as a control value during the experiment. The inhibition of platelet aggregation was expressed as a percentage of the control value.

Measurement of intracellular ionized calcium concentration

$[Ca^{2+}]_i$ was determined with the fluorescent indicator Fura-2, as described previously (Astarie *et al.*, 1989). Briefly, PRP was incubated at 37°C with 2 μM Fura-2AM for 40 min. After centrifugation at 270 *g* for 15 min at 20°C, platelets were resuspended in buffer A to achieve a final concentration of $8-9 \times 10^7$ cells ml^{-1}. Prior to experimental procedures, the external Ca^{2+} concentration ($[Ca^{2+}]_o$) was adjusted either to 1 mM with a solution of 0.1 M ($Ca(NO_3)_2$ or to 23 nM with the required EGTA-Ca buffer. Cells were then equilibrated at 37°C for about 5 min. Experiments were performed at 37°C in a quartz suprasil micro-cuvette (1 × 5 mm optical pathways) on a Spex Fluorolog CM111 (Instruments S.A., Paris, France) equipped with a 450 W xenon lamp, two excitation monochromators and a dual-mirror chopping mechanism that allows a rapid alternating of excitation wavelength with a fixed emission wavelength. The fluorescence intensities of Fura-2 were recorded at 335 and 385 nm excitation wavelengths that are indicative of the free and Ca-saturated dye, respectively, with an emission wavelength of 510 nm (excitation and emission slits of 1.8 and 4.5 nm, respectively). the fluorescence signals of dye-loaded platelets were corrected for the autofluoresence of the cell suspension. None of the drugs tested modified the intrinsic signal of platelets. Free Ca^{2+} concentration was calculated from the experimental ratio of excitation fluorescence intensities ($R = I_{335}/I_{385}$) (Grinkiewicz *et al.*, 1985; Poenie *et al.*, 1985; Astarie *et al.*, 1989). Under these conditions $[Ca^{2+}]_i$ was measured with inter- and intra-assay reproducibilities of 94.0 ± 4.6% ($n = 5$) and 95.7 ± 4.4% ($n = 10$), respectively. The extent of thrombin-evoked spike of $[Ca^{2+}]_i$ was evaluated as the rise in $[Ca^{2+}]_i$ measured 15 s after the addition of the agonist. The inhibition effect of the drugs was calculated as the percentage of the platelet response induced by thrombin in each experiment.

Measurement of cytosolic pH

Platelet pHi was evaluated with the fluorescent indicator BCECF. As previously described (Astarie *et al.*, 1989), PRP was incubated at 37°C for 20 min with 2 μM BCECF-AM and platelets were then sedimented by centrifugation at 270 *g* for 15 min at 20°C. The pellet was resuspended at a concentration of $8-9 \times 10^7$ cells ml^{-1} in the buffer A adjusted to 1 mM or 23 nM Ca^{2+}. Fluorescence signals of BCECF were recorded at 440 and 503 nm excitation wavelengths with an emission wavelength of 531 nm (1.8 and 4.5 nm slits, respectively). The background fluorescence of platelets was systematically subtracted from each recording. pHi was directly calculated from the ratio of excitation fluorescence intensities (I_{503}/I_{440}). Calibration of pHi versus fluorescence intensities was performed with the K^+-ionophore, nigericin (Thomas *et al.*, 1979; Astarie *et al.*, 1989). The intra- and inter-assays reproductibilities were 98.2 ± 3.7% ($n = 10$) and 97.0 ± 1.5% ($n = 6$), respectively.

Statistical comparison

All results are presented as means ± s.e.mean. Experiments involving multiple groups were first evaluated by one-way analysis of variance. Significance of the differences between groups was assessed by non-parametric Mann-Whitney or Wilcoxon tests. Probability values lower than 5% were considered as significant.

Results

Effect of endothelins on platelet aggregation

Endothelins (ET-1 and ET-3) added to washed platelets at concentrations ranging from 10^{-10} to 5×10^{-7} M did not modify the light transmission of the platelet suspension. However, when preincubated with platelets at 37°C for 10 min, endothelins reduced the thrombin-induced platelet aggregation (Figure 1). Though endothelin effects were small compared to those of PGI_2 and NP (Figure 1), they were dose-dependent (Table 1 and Figure 2). Whatever parameter was used to evaluate the aggregation, the maximal effect was observed with 10^{-8} M ET-1 and ET-3 (Table 1). Nonetheless, the initial rate and the area under the aggregatory curve indicated the inhibitory influence of endothelins better than the extent of aggregation (Table 1).

Effects of endothelins on basal and thrombin-induced $[Ca^{2+}]_i$ and pHi changes

Effects of endothelins on the intracellular modulators of platelet activation, $[Ca^{2+}]_i$ and pHi, were investigated in parallel. Under basal conditions, $[Ca^{2+}]_i$ and pHi averaged 56 ± 2 nM and 7.18 ± 0.01 pH units, respectively ($n = 52$ and 50). The addition of ET-1 or ET-3 at a concentration of 5×10^{-7} M affected neither resting $[Ca^{2+}]_i$ (71 ± 14 vs 70 ± 13 and 61 ± 11 vs 58 ± 9 nM in the presence and absence of ET-1 and ET-3, respectively, $n = 5$ for each) nor pHi value

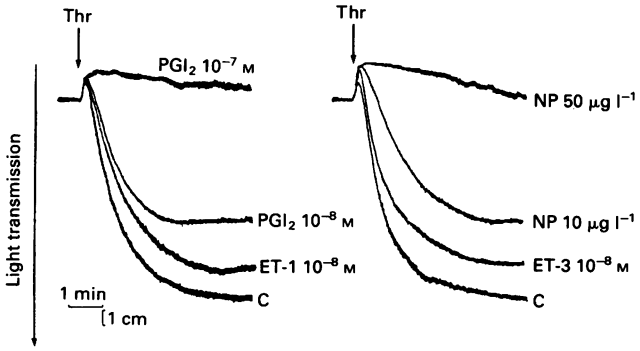

Figure 1 Effect of endothelins (ET-1, ET-3) sodium nitroprusside (NP) and prostacyclin (PGI_2) on aggregation induced by thrombin. Washed platelets were incubated with either ET-1 or ET-3 for 10 min, PGI_2 or NP for 1 min before addition of 0.05 u ml^{-1} thrombin (Thr). These traces are representative of 7–10 independent experiments.

Table 1 Effect of endothelins, prostacyclin (PGI_2) and sodium-nitroprusside (NP) on platelet aggregation induced by thrombin

	Aggregation parameter		
	Initial rate	*Extent*	*Area under curve*
Dose-dependent effects (significance of the analysis of variance)			
ET-1 d.f. (4, 45)	$F = 3.66$	$F = 4.01$	$F = 5.04$
(10^{-10}–5×10^{-7} M)	$P = 0.01$	$P = 0.007$	$P < 0.001$
ET-3 d.f. (4, 45)	$F = 6.37$	$F = 3.11$	$F = 6.80$
(10^{-10}–5×10^{-7} M)	$P < 0.001$	$P = 0.007$	$P < 0.001$
PGI_2 d.f. (2, 19)	$F = 175$	$F = 408$	$F = 408$
(10^{-8}–10^{-7} M)	$P < 0.001$	$P < 0.001$	$P < 0.001$
NP d.f. (3, 21)	$F = 36$	$F = 51$	$F = 204$
(10 ng–50 $\mu g\ l^{-1}$)	$P < 0.001$	$P < 0.001$	$P < 0.001$
Maximal inhibitory effect (% of control)			
10^{-8} M ET-1 ($n = 12$)	14 ± 2	10 ± 2	24 ± 6
	$P = 0.001$	$P = 0.005$	$P = 0.002$
10^{-8} M ET-3 ($n = 12$)	14 ± 3	7 ± 2	16 ± 5
	$P = 0.001$	$P = 0.01$	$P = 0.002$

Dose-dependent effects of endothelins, PGI_2 and NP were evaluated by one-way analysis of variance and the significance of maximal inhibitory effect of endothelins by the Wilcoxon test.

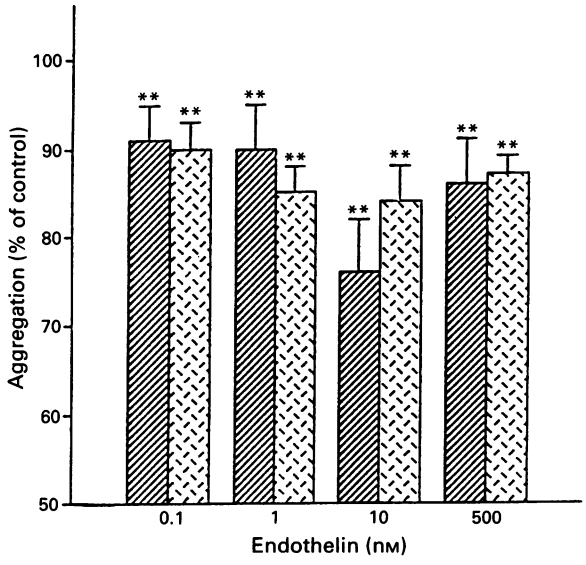

Figure 2 Dose-dependent effects of endothelins on aggregation induced by thrombin. Washed platelets were preincubated with various concentrations of ET-1 (hatched columns) or ET-3 (stippled columns) for 10 min before the addition of 0.05 u ml^{-1} thrombin. Aggregation was measured as the area under the aggregation curve recorded for 1 min. Data are expressed as means (with s.e.mean shown as vertical bars) of 7–12 experiments. *$P < 0.05$ and **$P < 0.01$ when compared to the respective control by Wilcoxon test.

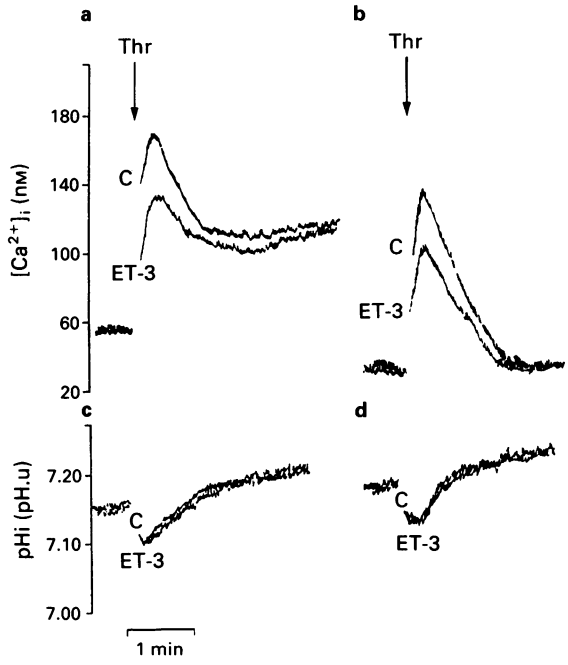

Figure 3 Representation of endothelin-3 (ET-3) effects on cytosolic Ca^{2+} and pH variations induced by thrombin (Thr). Washed platelets loaded with Fura-2 or BCECF were pretreated with 5×10^{-7} M ET-3 for 15 min before 0.05 u ml^{-1} agonist was added. Time course of changes in $[Ca^{2+}]_i$ (a and b) or pHi (c and d) were recorded in the presence of 1 mM (a and c) or 23 nM external Ca^{2+} (b and d). Each trace is representative of 7–10 independent experiments.

(7.13 ± 0.03 vs 7.15 ± 0.04 and 7.10 ± 0.04 vs 7.18 ± 0.04, respectively, $n = 6$ for each). No change in $[Ca^{2+}]_i$ and pHi was detected even when platelets were incubated with endothelins up to 15 min (the longest time studied).

Effects of endothelins were then tested on thrombin-evoked $[Ca^{2+}]_i$ and pHi variations. Figure 3 shows recordings of $[Ca^{2+}]_i$ and pHi transient induced by 0.05 u ml^{-1} thrombin. In the presence of 1 mM $[Ca^{2+}]_o$ thrombin elicited a transient spike of $[Ca^{2+}]_i$ (131 ± 12 nM, $n = 18$) followed by a second phase where $[Ca^{2+}]_i$ was maintained to a value above basal conditions for at least 3 min (80 ± 10 nM, $n = 6$) (Figure 3a). The addition of ET-3 had no immediate effect on $[Ca^{2+}]_i$ variations. However, ET-3 preincubation for 15 min decreased the $[Ca^{2+}]_i$ peak in a dose-dependent manner ($P = 0.02$) (Figure 4), but did not affect $[Ca^{2+}]_i$ value determined 3 min after the addition of the agonist. A significant inhibition was reached with 5×10^{-7} M ET-3 (28 ± 7%, $n = 11$, $P < 0.01$) (Figures 3a and 4) and ET-1 (17 ± 7%, $n = 7$, $P = 0.03$). Platelet preincubation in a Ca-EGTA-buffer which set external Ca^{2+} to 23 nM, decreased the $[Ca^{2+}]_i$ peak to 92 ± 11 nM ($n = 6$, $P < 0.05$) and abolished the second phase (Figure 3b). At this low external Ca^{2+} concentration, 5×10^{-7} M ET-3 still significantly inhibited the $[Ca^{2+}]_i$ peak ($n = 6$, $P = 0.02$) (Figures 3b and 4).

Simultaneously, thrombin provoked a biphasic shift of pHi (Figure 3c). A brief fall of pHi was followed by a rapid alkaline shift raising pHi by 0.03–0.07 pH units above the resting pHi. As previously demonstrated, this alkalinization

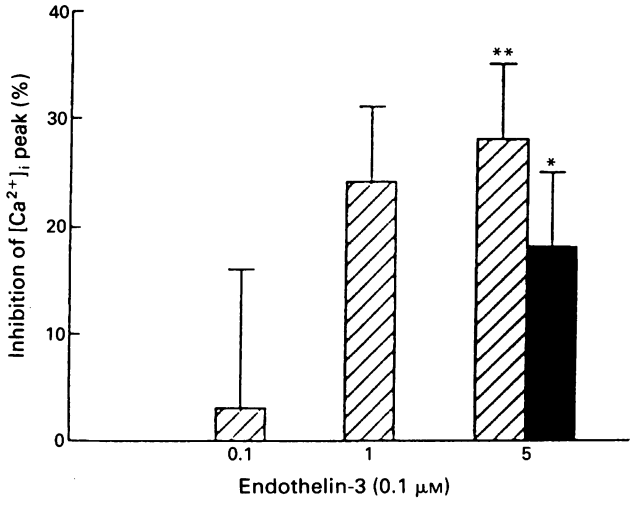

Figure 4 Inhibitory effect of endothelin-3 (ET-3) on the transient peak of $[Ca^{2+}]_i$ induced by thrombin. Fura-2-loaded platelets were pretreated by ET-3 for 15 min and stimulated by 0.05 u ml^{-1} thrombin in the presence of 1 mM (hatched columns) or 23 nM $[Ca^{2+}]_o$ (solid column). Data are expressed as means (s.e.mean shown by vertical bars) of 4–11 experiments. Analysis of variance indicated statistically significant effect of ET-3 [$F = 3.61$, d.f. (3, 29), $P = 0.02$] $*P<0.05$ and $**P<0.01$ when compared to their respective control by Wilcoxon test.

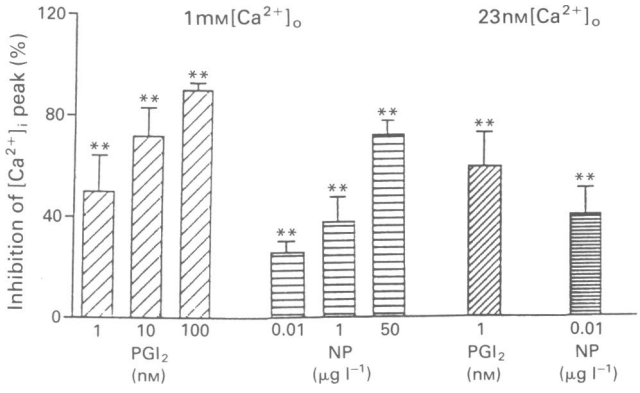

Figure 5 Influence of external Ca^{2+} on the inhibitory effect of prostacyclin (PGI_2) and sodium nitroprusside (NP). Fura-2-loaded platelets were incubated with PGI_2 or NP for 1 min and stimulated by 0.05 u ml^{-1} thrombin in the presence of 1 mM or 23 nM $[Ca^{2+}]_o$. Analysis of variance indicated significant effect of PGI_2 [$F = 24.23$, d.f. (3, 20), $P<0.001$] and NP [$F = 8.10$, d.f. (3,30), $P<0.001$]. Data are expressed as means (s.e.mean shown by vertical bars) of 6–11 experiments. $**P<0.01$ and $***P<0.005$ when compared to their respective control by Wilcoxon test.

was dependent on external Na^+ and sensitive to EIPA, an inhibitor of Na^+/H^+ exchange (Zavoico *et al.*, 1986). Endothelins did not modify pHi changes induced by thrombin, whatever $[Ca^{2+}]_o$ (Figure 3c,d). The similarity of ET-1 and ET-3 effects led us to restrict a further analysis to ET-3 only.

Effect of prostacyclin or sodium nitroprusside combination with endothelin-3 on $[Ca^{2+}]_i$ transients induced by thrombin

The ET-3 effects on $[Ca^{2+}]_i$ were compared to those of PGI_2 and NP. As shown in Figure 5, both PGI_2 and NP progressively decreased the $[Ca^{2+}]_i$ spike ($P<0.001$ for each). Similar effects were observed in the presence of low $[Ca^{2+}]_o$ (Figure 5). A cumulative decrease of the $[Ca^{2+}]_i$ peak was observed either when platelets pretreated with 10 ng l^{-1} NP were incubated with 10^{-9} M PGI_2 or after a successive addition of 10^{-9} M PGI_2 and 10 ng l^{-1} NP (Table 2). Platelet pretreatment with 5×10^{-7} M ET-3 for 15 min increased by 34 ± 11% the NP-inhibitory activity ($P = 0.01$, $n = 6$) while it did not affect the PGI_2 effect (Table 2).

Table 2 Effects of prostacyclin and sodium nitroprusside alone or in combination with other drugs on the $[Ca^{2+}]_i$ spike induced by thrombin

Drugs	*(%) inhibition*
PGI_2	52 ± 11
(NP + PGI_2)	69 ± 5**
(ET-3 + PGI_2)	48 ± 12
NP	26 ± 4
(PGI_2 + NP)	90 ± 2***
(ET-3 + NP)	45 ± 6**

Fura-2-loaded platelets were preincubated at 37°C for 1 min with either 10^{-9} M PGI_2 or 10 ng l^{-1} NP or after pretreatment for 1 min with NP or PGI_2 or for 15 min with 5×10^{-7} M ET-3. Data are expressed as mean ± s.e.mean of 6 experiments. $**P<0.01$ and $***P<0.001$ when compared by Wilcoxon test to the inhibition caused by PGI_2 or NP alone.

Discussion

Endothelial cells have strong anti-thrombogenic properties (Gerlach *et al.*, 1985). One of them concerns the control of platelet responsiveness to agonists and is mediated in particular by the production of physiological inhibitors of platelet aggregation, PGI_2 and EDRF (Moncada *et al.*, 1976; Azuma *et al.*, 1986; Furlong *et al.*, 1987). Our results suggest that endothelins may also contribute to the anti-aggregating properties of endothelium by a direct effect on platelet function.

Under our experimental conditions, ET-1 and ET-3 did not promote platelet aggregation but had a small inhibitory effect on platelet aggregation induced by thrombin. The previous inhibitory effects of endothelins on aggregation observed *ex vivo* with rabbit platelets (Thiemermann *et al.*, 1989) and *in vivo* with platelets of rabbits and dogs (Lidbury *et al.*, 1989; Thiermermann *et al.*, 1990) have been mainly attributed to the release of prostacyclin from the endothelium (Thiemermann *et al.*, 1989). However, even when the platelets were pretreated with indomethacin, an inhibitory effect of ET-1 on ADP-induced aggregation was still observed 15–60 min after peptide injection. This delayed effect *in vivo* agrees with the endothelin effects that we observed *in vitro* after 10–15 min incubation. Our data thus suggest that a direct influence of endothelins could participate in this cyclooxygenase independent mechanism. Previous studies performed *in vitro* have been equivocal. Some have failed to reveal a direct influence of endothelins on stimulated platelets (Patel *et al.*, 1989; Battistini *et al.*, 1990; Joseph *et al.*, 1991) while others have shown inhibition of ADP-induced aggregation by an unknown mechanism (Ohlstein *et al.*, 1990). The probable reason why others have not observed the endothelin-dependent anti-aggregatory effect is because it is small and overcome by high concentrations of thrombogenic stimulus. Platelets were indeed incubated either for a short time or with high thrombin concentrations (Ohlstein *et al.*, 1990; Joseph *et al.*, 1991). In addition to agonist concentration and/or duration of endothelin-incubation, the low number of platelets in our experiments may also be of some importance. Altorjay *et al.* (1989) have indeed observed that an increase in platelet counts was associated with a decreased inhibitory effect of endothelial cells.

In unstimulated platelets, endothelins affect neither intracellular ionized calcium nor cytosolic pH. This is in contrast with what has been described in various types of cells (for review see Simonson & Dunn, 1990) but agrees with other studies on platelets (Ohlstein *et al.*, 1990; Joseph *et al.*, 1991). However, ET-1 and ET-3 clearly decreased the transient $[Ca^{2+}]_i$ peak caused by thrombin without having any effect on the associated pHi variations. We propose that the anti-aggregatory properties of endothelins are mediated by a decrease in Ca^{2+} mobilization from cellular stores. This interpretation agrees with the persistent ET-3-dependent inhibition of $[Ca^{2+}]_i$ peak observed even in the virtual absence of external Ca^{2+}. Pollok & Rink (1986) have indeed demonstrated that the initial $[Ca^{2+}]_i$ spike reflects the thrombin-induced Ca^{2+} release from internal stores. However, we must underline the fact that higher concentrations of ET-3 were required to inhibit Ca^{2+} mobilization than to reduce the aggregation. This can be explained by the effect of Fura-2 as an intracellular Ca^{2+} buffer or by a possible participation of other regulatory mechanisms such as cyclic AMP, in the response to endothelins. Nitroprusside and PGI_2 have been described as exerting a synergistic inhibition of platelet functions (Levin *et al.*, 1982; Bowen & Haslam, 1991) and we could indeed demonstrate their additive effect on $[Ca^{2+}]_i$. A high concentration of NP alone (e.g. 1 $\mu g\,l^{-1}$) decreased the $[Ca^{2+}]_i$ peak by 40% whereas a much lower concentration (0.01 $\mu g\,l^{-1}$) was required to induce a similar effect when ET-3 was present. This indicates an additive effect of NP and ET-3 on Ca^{2+} mobilization.

In various cell types, an increase in $[Ca^{2+}]_i$ constitutes a common pathway of signal transduction for members of the endothelin peptide family (Van Renterghem *et al.*, 1988; Gardner *et al.*, 1989; Simonson *et al.*, 1990). To our knowledge, the present study is the first study concerning an inhibitory effect of endothelins on $[Ca^{2+}]_i$ transients. In addition, endothelins elicit pHi changes in skin fibroblasts and brain capillary endothelial cells (Gardner *et al.*, 1989; Vigne *et al.*, 1991) while we demonstrate here that they affect neither platelet pHi nor the activity of the Na^+/H^+ exchange. This constitutes an example of the different endothelin effects on various cell types. These peptides are also known to exert various effects on different vascular regions which has been explained in part by a different distribution of two distinct endothelin receptors, the stimulation of which may induce either constrictor or relaxant effects, the latter by release of PGI_2 and/or EDRF (De Nucci *et al.*, 1988; Fukuda *et al.*, 1991; Takayanagi *et al.*, 1991).

Endothelins may act in association and/or combination with PGI_2 and EDRF to regulate the interaction of platelets and vessel wall as well as to limit thrombus formation. Their *in vivo* anti-aggregatory activity is mediated for a major part by the release of cyclo-oxygenase products into the circulation. Our study provides evidence that endothelins also exert modest direct anti-aggregatory effects by inhibition of thrombin-induced Ca^{2+} mobilization. The relatively high effective endothelin concentration suggests that they may either bind slowly to platelet receptors or serve as modulators of platelet functions only in the local environment of the endothelium.

The authors thank Dr M. Mazeaud for her assistance with the aggregation experiments. C.A.D. is a recipient of a grant from the Fondation pour la Recherche Médicale.

References

ALTORJAY, I., KIRCHMAIER, C.M. & BREDDIN, H.K. (1989). Changes of spontaneous and induced platelet aggregation in the presence of human endothelial cell monolayer. *Thromb. Res.*, **55**, 69–77.

ASTARIE, C., LEVENSON, J., SIMON, A., MEYER, P. & DEVYNCK, M.A. (1989). Platelet cytosolic proton and free calcium concentrations in essential hypertension. *J. Hypertens.*, **7**, 485–491.

AZUMA, H., ISHIKAWA, M. & SEKIZAKI, S. (1986). Endothelium dependent inhibition of platelet aggregation. *Br. J. Pharmacol.*, **88**, 411–415.

BATTISTINI, B., FILEP, J.G., HERMAN, F. & SIROIS, P. (1990). Endothelin-1 does not affect human platelet aggregation in whole blood and platelet rich plasma. *Thromb. Res.*, **60**, 105–108.

BORN, G.V.R. (1962). Aggregation of blood platelets by adenosine and its reversal. *Nature*, **195**, 927–935.

BOWEN, R. & HASLAM, R.J. (1991). Effects of nitrovasodilatators on platelet cyclic nucleotide levels in rabbit blood. Role for cyclic AMP in synergistic inhibition of platelet function by Sin-1 and prostaglandin E1. *J. Cardiovasc. Pharmacol.*, **17**, 424–433.

DE NUCCI, G., THOMAS, R., D'ORLEANS JUSTE, P., ANTUNES, E., WALDER, C., WARNER, T.D. & VANE, J.R. (1988). Pressor effects of circulating endothelin are limited by its removal in the pulmonary and by the release of prostacyclin and endothelium-derived relaxing factor. *Proc. Natl. Acad. Sci. U.S.A.*, **85**, 9797–9800.

FUKUDA, N., SOMA, M., IZUMI, Y., MINATO, M., WATANABE, Y., WATANABE, M. & HATANO, M. (1991). Low doses of endothelin-3 elicit endothelium dependent vasodilation which accompanies with elevation of cyclic GMP. *Jpn. Circ. J.*, **55**, 617–622.

FURLONG, B., HENDERSON, A.H., LEWIS, M.J. & SMITH, J.A. (1987). Endothelium-derived relaxing factor inhibits *in vitro* platelet aggregation. *Br. J. Pharmacol.*, **90**, 687–692.

GARDNER, J.P., MAHER, E. & AVIV, A. (1989). Calcium mobilization and Na^+/H^+ antiport activation by endothelin in human skin fibroblasts. *FEBS Lett.*, **256**, 38–42.

GERLACH, E., NEES, S. & BECKER, B.F. (1985). The vascular endothelium: a survey of some newly evolving biochemical and physiological features. *Basic Res. Cardiol.*, **80**, 459–474.

GORMAN, R.R., BUNTING, S. & MILLER, O.V. (1977). Modulation of human platelet adenylate cyclase by prostaglandin (PGX). *Prostaglandins*, **13**, 377–388.

GRINKIEWICZ, G., POENIE, M. & TSIEN, R.Y. (1985). A new generation of calcium indicators with greatly improved fluorescence properties. *J. Biol. Chem.*, **260**, 3440–3450.

ISHIKAWA, Y., OGAWA, A. & SASAKAWA, S. (1989). Effect of cytoplasmic pH on platelet activation by arachidonic acid. *Thromb. Res.*, **54**, 17–26.

JOSEPH, R., SCICLI, A.G., HAN, E., GRUNFELD, S., CARRETERO, O.A. & WELCH, K.M.A. (1991). Endothelin-1 and human platelet activity. *Thromb. Res.*, **61**, 529–536.

LEVIN, R.I., WEKSLER, B.B. & JAFFE, E.A. (1982). The interaction of sodium nitroprusside with human endothelial cells and platelets: nitroprusside and prostacyclins synergistically inhibit platelet function. *Circulation*, **66**, 1299–1307.

LIDBURY, P.S., THIEMERMANN, C., THOMAS, G.R. & VANE, J.R. (1989). Endothelin-3: selectivity as an anti-aggregatory peptide in vivo. *Eur. J. Pharmacol.*, **166**, 335–338.

MELLION, B.T., IGNARRO, J.L., OHLSTEIN, E.H., PONTECORVO, E.G. & KADOWITZ, P.J. (1981). Evidence for the inhibitory role of guanosine 3'-5'-monophosphate in ADP-induced human platelet aggregation in the presence of nitric oxide and related vasodilatators. *Blood*, **57**, 946–955.

MONCADA, S., GRYGLEWSKY, R.T. & VANE, J.R. (1976). An enzyme isolated from arteries transforms prostaglandin endoperoxydes to an unstable substance that inhibits platelets aggregation. *Nature*, **263**, 663–665.

NACHIMIAS, V.T., YOSHIDA, K.N. & GLENNON, M.C. (1987). Lowering pH in blood platelets dissociates myosin phosphorylation from shape change and myosin association with cytoskeleton. *J. Cell. Biol.*, **105**, 1761–1769.

OHLSTEIN, E.H., STORER, B., NAMBI, P., GIVEN, M. & LIPPTON, H. (1990). Endothelin and platelet function. *Thromb. Res.*, **57**, 967–974.

PATEL, A., FAIRBANKS, L., GORDGE, M.P. & NEILD, G.H. (1989). Failure of endothelin to influence in vitro platelet responses. *Thromb. Res.*, **56**, 769–770.

POENIE, M., ALDERTON, J., TSIEN, R.Y. & STEINHARDT, R.A. (1985). Changes of free calcium levels with stages of the cell division cycle. *Nature*, **315**, 147–149.

POHL, U. & BUSSE, R. (1989). EDRF increases cyclic GMP in platelets during passage through the coronary vascular bed. *Circ. Res.*, **65**, 1798–1803.

POLLOCK, W.K. & RINK, T.J. (1986). Thrombin and ionomycin can raise platelet cytosolic Ca^{2+} to micromolar levels by discharge of internal Ca^{2+} stores: studies using Fura-2. *Biochem. Biophys. Res. Commun.*, **139**, 308–314.

SIESS, W. (1989). Molecular mechanisms of platelet activation. *Physiol. Rev.*, **69**, 58–141.

SIMONSON, M.S. & DUNN, M.J. (1990). Cellular signaling peptides of the endothelin gene family. *FASEB J.*, **4**, 2989–3000.

SIMONSON, M.S., OSANAI, T. & DUNN, M.J. (1990). Endothelin isopeptides evoked Ca^{2+} signaling and oscillations of cytosolic free $[Ca^{2+}]$in human mesangial cells. *Biochim. Biophys. Acta*, **1055**, 63–68.

TAKAYANAGI, R., KITAZUMI, K., TAKAZAKI, C., OHNAKA, K., AIMOTO, S., TASAKA, K., OHASHI, M. & NAWATA, H. (1991). Presence of non-selective type of endothelin receptor on vascular endothelium and its linkage to vasodilatation. *FEBS Lett.*, **282**, 103–106.

TATESON, J.E., MONCADA, S. & VANE, J.R. (1977). Effects of prostacyclin (PGX) on cyclic AMP concentrations in human platelets. *Prostaglandins*, **13**, 389–397.

THIEMERMANN, C., LIDBURY, P.S., THOMAS, G.R. & VANE, J.R. (1989). Endothelin-1 releases prostacyclin and inhibits ex vivo platelet aggregation in the anesthetized rabbit. *J. Cardiovasc. Pharmacol.*, **13** (Suppl. 5), S138–S141.

THIEMERMANN, C., MAY, G.R., PAGE, C.P. & VANE, J.R. (1990). Endothelin-1 inhibits platelet aggregation *in vivo*: a study with ^{111}indium-labelled platelets. *Br. J. Pharmacol.*, **99**, 303–308.

THOMAS, J.A., BUCHSBAUM, R.N., ZIMNIAK, A. & RACKER, E. (1979). Intracellular pH measurements in Ehrlich ascites tumor cells utilizing spectroscopic probes generated in situ. *Biochemistry*, **18**, 2210–2218.

VAN RENTERGHEM, C., VIGNE, P., BARHANIN, J., SCHMID-ALLIANA, A., FRELIN, C. & LAZDUNSKI, M. (1988). Molecular mechanism of action of the vasoconstrictor peptide endothelin. *Biochem. Biophys. Res. Commun.*, **157**, 977–985.

VIGNE, P., LADOUX, A. & FRELIN, C. (1991). Endothelins activate Na^+/H^+ exchange in brain capillary endothelial cells via a high affinity endothelin-3 receptor that is not coupled to phospholipase C. *J. Biol. Chem.*, **266**, 5925–5928.

ZAVOICO, G.B., CRAGOE, E.J. & FEINSTEIN, M.B. (1986). Regulation of intracellular pH in human platelets. Effect of thrombin, A23187, and ionomycin and evidence for activation of Na^+/H^+ exchange and its inhibition by amiloride analogs. *J. Biol. Chem.*, **261**, 13160–13167.

(Received February 5, 1992
Revised April 8, 1992
Accepted April 14, 1992)

Br. J. Pharmacol. (1992), **106**, 972–977 © Macmillan Press Ltd, 1992

Mode of action and comparative efficacy of pharmacological agents that inhibit calcium-dependent dehydration of sickle cells

[1]*J.C. Ellory, G.B. Nash, P.C.W. Stone, *S.J. Culliford, *E. Horwitz & J. Stuart

Department of Haematology, The Medical School, University of Birmingham, Birmingham and *University Laboratory of Physiology, Parks Road, Oxford

1 Selected Ca-channel antagonists were tested at 20 μM as inhibitors of Ca^{2+}-uptake in human sickle red cells. Nitrendipine, fendiline, and bepridil (and its stereoisomers), were found to be as effective as methoxyverapamil (D-600) in inhibiting a fraction (25%) of Ca^{2+}-uptake. In contrast cetiedil and Org 30701 were ineffective.

2 The drugs were subsequently tested as inhibitors of Ca^{2+}-induced K^+ efflux (Gardos) from sickle cells. They all showed inhibitory activity, with the order of efficacy nitrendipine > fendiline > bepridil > cetiedil > Org 30701.

3 With a 15 h programme of deoxygenation/reoxygenation cycles in a gas exchanger, it was shown that the inhibitors protected against cellular dehydration and loss of filterability in the order nitrendipine > fendiline > bepridil > cetiedil > Org 30701. However, significant stomatocytosis occurred at high concentrations of cetiedil, and bepridil (including its stereoisomers and analogues) impairing cell deformability.

4 It is concluded that Ca-antagonists may partially block both Ca^{2+}-uptake and Ca^{2+}-induced K^+ efflux. The latter pathway is significant in contributing to sickle cell dehydration and nitrendipine is the most effective inhibitor of this route.

Keywords: Dihydropyridines; Ca-channels; calcium-dependent K^+efflux; sickle cells

Introduction

Sickle cells are characterized by abnormal cation homeostasis with net loss of monovalent cation (K^+) and consequential dehydration. Sub-populations of abnormally dense and poorly deformable sickle cells are produced which play an important role in vaso-occlusion (Fabry *et al.*, 1984). The two main cation transport pathways thought to be responsible for loss of cell K^+ (Stuart & Ellory, 1988) are the Ca^{2+}-activated K^+ efflux (Gardos) channel (Gardos, 1958) and the K:Cl co-transporter activated by low pH or hypotonic stress (Ellory *et al.*, 1987). Drugs that prevent loss of cell cation and water are of potential clinical value (Stuart & Johnson, 1987) as polymerisation of sickle haemoglobin is critically dependent on its intracellular concentration (Hofrichter *et al.*, 1974).

Sickle cells have a raised total intracellular [Ca] (Eaton *et al.*, 1973), but near-normal ionised [Ca^{2+}] (Murphy *et al.*, 1987), with the excess Ca being sequestered within membrane vesicles (Lew *et al.*, 1985). Transient increases in cytoplasmic [Ca^{2+}] may be sufficient to activate the Gardos channel with consequential efflux of K^+ (Bookchin *et al.*, 1986). Clinical studies in sickle cell disease have been carried out using nifedipine (Rodgers *et al.*, 1988) and cetiedil citrate (Benjamin *et al.*, 1986), Ca-channel blockers the action of which includes Gardos channel inhibition.

The mode of action of classical Ca^{2+}-entry blockers on the red cell membrane has been questioned by the demonstration that bepridil, a vascular smooth muscle relaxant that inhibits Ca^{2+} entry into excitable cells (Labrid *et al.*, 1979; Vogel *et al.*, 1979), causes inhibition of K^+ efflux via the Gardos channel from normal erythrocytes (Stuart *et al.*, 1989) and prevents dehydration of sickle cells (Johnston *et al.*, 1989). Subsequently, the 1,4-dihydropyridine Ca^{2+}-entry blockers nifedipine and nitrendipine have also been shown to inhibit the Gardos channel (Kaji, 1990; Ellory *et al.*, 1991).

It is clearly important to clarify the mode of action of such inhibitors and to test their potential for preventing dehydration and loss of deformability of sickle cells. We have therefore developed methods for *in vitro* testing of putative anti-sickling compounds that inhibit Ca^{2+}-dependent dehydration of sickle cells. These methods include measurement of Ca^{2+} influx into and Ca^{2+}-activated K^+ efflux from sickle cells and cyclical deoxygenation-reoxygenation of sickle cells over 15 h in the presence of Ca^{2+}. Repeated cycles of deoxygenation-reoxygenation cause repetitive sickling and unsickling with influx of Ca^{2+}, efflux of K^+, cellular dehydration and loss of cell deformability (Johnston *et al.*, 1989).

Methods

Measurement of ^{45}Ca influx

Blood from out-patients with homozygous (SS) sickle-cell disease was washed three times by centrifugation (3,000 *g* for 5 min) in a medium containing (mM): NaCl 144, KCl 5, MOPS (3-[N-morpholino] propane sulphonic acid) 10 (pH 7.4) and 0.1 EGTA (ethylene glycol-*bis*(β-amino ethyl ether) N, N, N^1, N^1-tetracetic acid) 0.1. Washed red cells were finally resuspended to a haematocrit of ~0.10 (10%) and BAPTA-AM (1, 2 *bis*(2-aminophenoxy)ethane N, N, N^1, N^1-tetracetic acid acetomethoxyester) added from a 100 mM stock solution in dimethylsulphoxide (DMSO) to a final concentration of 0.3 mM (0.3% v/v DMSO final concentration). Following incubation at 37°C for 90 min, the cells were washed twice by centrifugation in an identical medium without EGTA. Aliquots of cell suspension were pipetted into Eppendorf 1.5 ml microcentrifuge tubes, and inhibitors to be tested added to the required final concentration. Methoxy verapamil (D-600; 20 μM final concentration) was added as a reference inhibitor of channel-mediated Ca^{2+} influx. The

[1] Author for correspondence.

tubes were cooled in an ice bath and $CaCl_2$ solution (100 mM) added to a final concentration of 0.5 mM together with 1 μCi ml^{-1} ^{45}Ca. The tubes were then incubated at 37°C for 30 min. After this time, the tubes were cooled (2 min at 0°C) and the cells washed 4 times in ice-cold medium (containing EGTA) in a microcentrifuge (10,000 *g* for 10 s). Finally, the cells were lysed in 0.1% v/v Triton X-100, the protein precipitated with 5% w/v TCA and the supernatant assayed for ^{45}Ca in Picofluor 30 by β-scintillation spectroscopy. All experiments were run in triplicate.

Measurement of K (^{86}Rb) efflux

Whole blood taken into heparin was loaded with ^{86}RbCl (as a bioisostere for K^+; Simons, 1976) by incubating 5 ml aliquots with ^{86}RbCl (10 μCi ml^{-1}) for 4 h at 37°C, or overnight (16 h) at 4°C. The cells were washed four times by centrifugation in a medium containing 107 mM $MgCl_2$ and 10 mM MOPS pH 7.4, and then resuspended at 0.02 (2%) haematocrit in a medium containing (mM): KCl 75, NaCl 75, MOPS 10, glucose 5, EGTA 0.1 and A23187 1 μM, at pH 7.4 and 37°C. To start the efflux, $CaCl_2$ solution (110 mM) was added to give a final concentration of 1.5 mM. Aliquots of the suspension were taken at time zero (C_o) and at 5 min intervals (C_t), layered over silicone fluid (density 1.04), and centrifuged (10,000 *g* for 10 s). Samples of the cell-free supernatant were processed for Cerenkov counting in a β-scintillation spectrometer. Further samples of cell suspensions were lysed (0.1% v/v Triton X-100), deproteinized (5% w/v TCA), and counted to give total internal initial ^{86}Rb counts ($C\infty$). The rate constant for K efflux (k) was calculated as $k = \ln(C\infty - C_t)/(C\infty - C_o)/t$ min^{-1}. Parallel incubations were run with the appropriate test compounds.

Cyclical deoxygenation-reoxygenation

Venous blood was taken into lithium heparin (15 i.u. ml^{-1} blood), pre-filtered through IG 500 cotton wool (Terumo Corporation, Tokyo, Japan), washed twice and resuspended in HEPES buffered saline (HBS; 40 mM HEPES, osmolality 290 mM kg^{-1} H_2O, pH 7.4 at 25°C) (Stuart *et al.*, 1985; Keidan *et al.*, 1987). The resulting leucocyte-depleted suspension of SS cells was separated on a Percoll-Isopaque continuous density gradient (modified from Stone *et al.*, 1986) and the more dense 50% of cells were discarded. The remaining light cells were washed three times and resuspended at 0.3×10^{12} cells l^{-1} in HBS (pH 7.4 at 37°C) containing 10 mM glucose, 5 mM KCl, 2 mM $CaCl_2$ and 16 μg ml^{-1} gentamicin sulphate (to inhibit bacterial growth) for incubation in a Cyclical Gas Exchanger.

The Cyclical Gas Exchanger (Mark II) was modified from Johnston *et al.* (1989). Aliquots of SS cell suspensions (0.3×10^{12} cells l^{-1}) in HBS (5 ml) were incubated in 25 ml sterile, plastic Universal tubes (Sterilin Ltd., Feltham, Middlesex) that were inclined at 30°C and mixed by gentle oscillation for 15 h at 37°C. Alternate deoxygenation to a P_{O_2} of 5.3 kPa and reoxygenation to 16.0 kPa was achieved by gassing alternatively with N_2 (10 min at 50 ml min^{-1}) and compressed air (2.5 min at 50 ml min^{-1}) via a humidifier containing water at 45°C. After 15 h incubation and before testing, the cells were reoxygenated by washing three times, resuspended in 5 ml HBS, and mixed in air for 30 min at room temperature.

Stock solutions (50 mM) of the test compounds were made up daily in ethanol (v/v); when the appropriate concentration of compound was added to the incubation mixtures the final concentration of ethanol was 0.02% v/v and this concentration was also added to control tubes.

Rheological measurements

Erythrocyte filterability through pores of 5 μm diameter (Hemafil polycarbonate membranes, batch 5436A10; Nuclepore Corporation, Pleasanton, California, U.S.A.) was measured before and after the 15 h incubation using a St. George's Filtrometer (Carri Med Ltd., Vincent Lane, Dorking, Surrey) at 37°C with a driving pressure of 400 Pa. The membranes were cleaned by ultrasonication (Bilto & Stuart, 1985) and reused. Red cell transit time (RCTT) and clogging rate (CR) were measured as previously described (Dormandy *et al.*, 1985).

Erythrocyte mean cell volume (MCV) and mean cell haemoglobin concentration (MCHC) were calculated from erythrocyte count and haemoglobin concentration as measured by Coulter S Plus IV (Coulter Electronics Ltd., Luton) and packed cell volume (PCV) as measured by microhaematocrit centrifugation (13000 *g* for 5 min) of oxygenated erythrocytes suspended in buffer. Morphology was studied by interference microscopy on oxygenated cells fixed with 1.25% w/v glutaraldehyde in HBS. Erythrocyte K^+ concentration was measured with a Corning Clinical Flame Photometer 410C (Corning Medical and Scientific, Halstead) and expressed as Eq/cell $\times 10^{-16}$.

Statistical significance (two-tailed) was determined by Wilcoxon's signed rank test for paired data.

Materials

Fendiline, bepridil (and its resolved stereoisomers) and Org 30701 (1-[2-(2-methylpropoxy)-1- [[1-(1-propynyl)cyclohexyl]-oxymethyl]-ethyl]-pyrrolidinehydrochloride) were a gift from Organon International BV; nitrendipine was a gift from Bayer UK, Ltd., cetiedil citrate was a gift from Innothéra Laboratories, Arcueil, France; BAPTA-AM and D-600 (methoxy verapamil) were purchased from SIGMA chemicals. All other chemicals were Analar reagent grade.

Results

The results were obtained on blood samples from outpatients in the asymptomatic steady-state of sickle-cell disease. Unless otherwise stated, the sickle cells were studied in the oxygenated state.

Inhibition of ^{45}Ca influx

All test compounds were compared for their inhibitory potency on Ca^{2+}-influx at a concentration of 20 μM. The percentage inhibition of ^{45}Ca influx into oxygenated sickle cells at 37°C is shown in Table 1. All the compounds tested, including the reference Ca^{2+} channel blockers nitrendipine and fendiline but with the exception of Org 30701 and cetiedil citrate, showed significant inhibitory activity on red cell Ca^{2+} uptake at 20 μM. Both stereoisomers of bepridil

Table 1 Percentage inhibition of ^{45}Ca influx by reference Ca^{2+} channel blockers nitrendipine and fendiline, bepridil stereoisomers and analogues, and the Gardos channel inhibitor cetiedil citrate

Drug (20 μM)	*Inhibition (%)*
Nitrendipine	19.1 ± 6.1
Fendiline	23.0 ± 9.2
(±)-Bepridil	17.8 ± 8.9
(+)-Bepridil	25.0 ± 4.0
(−)-Bepridil	26.0 ± 4.6
Org 30701	5.3 ± 10.3
Cetiedil citrate	2.0 ± 10.9

All compounds tested at a final concentration of 20 μM. Results are mean and s.d. for blood from 7 homozygous sickle cell (SS) donors (4 SS donors for nitrendipine (−)-bepridil and Org 30701).

were equally potent as inhibitors. Dose-response curves for inhibition of Ca^{2+} influx were measured for D-600 (a reference Ca^{2+}-channel blocker) which showed a maximal effect (23.1 ± 2.1% inhibition of total Ca^{2+} uptake) at 20 μM.

Inhibition of K^+(^{86}Rb) efflux

Percentage inhibition of $^{86}Rb^+$ efflux from oxygenated sickle cells at 37°C is shown in Table 2. Quinidine HCl and cetiedil citrate were studied as reference Gardos channel inhibitors, causing 42–51% inhibition at 100 μM. As found previously (Johnston *et al.*, 1989; Stuart *et al.*, 1989), (±)-bepridil was a potent inhibitor of Ca^{2+}-activated K^+(^{86}Rb) efflux, and its stereoisomers (+ and −) were nearly equipotent. This agrees with findings on coronary vascular muscle where bepridil has a low stereoselectivity factor (van Amsterdam & Zaagsma, 1988). The bepridil analogue, Org 30701, was a less effective inhibitor. The reference Ca^{2+} entry blockers nitrendipine and fendiline were also tested and nitrendipine was found to inhibit dramatically K^+ (^{86}Rb) efflux i.e. to be a powerful inhibitor of the Gardos channel causing 97% inhibition at 1 μM and 67% inhibition at 0.1 μM (arterial blood concentrations in man are in the region of 0.01–0.1 μM (Goa & Sorkin, 1987)).

Cyclical deoxygenation-reoxygenation

Sickle cells from 20 SS patients were incubated in the Cyclical Gas Exchanger for 15 h in air without cyclical deoxygenation and in the absence of Ca^{2+}. Compared with pre-incubation values (Table 3), there was no significant change in any of the measured parameters after 15 h. When the incubation was performed in the presence of $CaCl_2$ (2 mM) and with cyclical deoxygenation-reoxygenation there was a significant ($P<0.001$) loss of filterability (increase in RCTT and CR) associated with cell dehydration (decrease in cell K^+ and MCV, increase in MCHC). In the absence of $CaCl_2$ these effects are much reduced (Johnston *et al.*, 1989).

The above experiment was also performed in the presence of a range of concentrations of each test compound (Tables 4 and 5), the results being presented as percentage protection against the rheological stress of 15 h cyclical deoxygenation-reoxygenation in the presence of $CaCl_2$ but in the absence of the test compound. Thus a positive value represents percentage correction of the change in RCTT, CR, K, MCV and MCHC compared with 15 h incubation in the absence of the test compound. A negative value represents percentage exacerbation of the abnormality at 15 h.

The Ca^{2+}-entry blocker nitrendipine (Table 4) at all three concentrations gave substantial protection against loss of K^+ and cell dehydration. Fendiline, which also inhibits Ca^{2+} entry, showed a protective effect but caused concentration-dependent stomatocytosis (cup shaped red cells with a mouth-like depression) which, at 100 μM, impaired filterability through the 5 μm diameter pores.

Quinidine HCl and cetiedil citrate were studied as reference Gardos channel inhibitors (Table 4). Quinidine showed slight protection against rheological impairment (RCTT) and loss of cell volume (MCV and MCHC). Cetiedil caused a concentration-dependent improvement in MCV and MCHC but also caused stomatocytosis with consequential loss of filterability.

Bepridil and analogues were studied in the same way for their protective action against cyclical deoxygenation in the presence of $CaCl_2$ (Table V). (±)-Bepridil at 100 μM showed a protective effect against loss of K^+, decrease in MCV and increase in MCHC but this high concentration resulted in stomatocytosis and impairment of filterability. (+)-Bepridil and (−)-bepridil protected against loss of filterability and decrease in MCV at lower concentration than did (±)-bepridil but both caused stomatocytosis at high concentration with consequential impairment of filterability (RCTT and CR). This difference between the racemate and individual stereoisomers is curious, and there is no obvious explanation for this effect. Bepridil has a low stereoselectivity factor (van Amsterdam & Zaagma, 1988).

The analogue Org 30701, in contrast, was minimally stomatocytogenic and showed a rheologically protective effect up to 100 μM.

Table 2 Mean (s.d.) percentage inhibition of Ca^{2+}-activated K^+ (^{86}Rb) efflux from sickle cells of 3 donors

	Drug concentration (μM)				
	0.1	*1*	*10*	*25*	*100*
Quinidine HCl	—	5.6	13.6	11.8	41.9
	—	± 5.1	± 19.2	± 14.2	± 12.5
Cetiedil citrate	—	32.0	17.9	29.7	50.8
	—	± 2.3	± 8.3	± 13.0	± 11.6
(±)-Bepridil	—	24.1	26.6	62.6	98.6
	—	± 10.1	± 4.4	± 11.0	± 1.7
(+)-Bepridil	—	0	24.9	48.1	100.0
	—	± 0	± 6.2	± 6.5	± 0
(−)-Bepridil	—	15.2	20.3	41.8	90.2
	—	± 13.2	± 13.4	± 3.9	± 16.9
Org 30701	—	3.6	10.6	34.8	58.2
	—	± 5.2	± 9.2	± 8.8	± 3.2
Nitrendipine	66.6	97.3	—	—	—
	± 10.2	± 2.4			
Fendiline	—	8.0	38.3	57.3	95.4
	—	± 7.3	± 19.6	± 10.2	± 2.2

Discussion

On deoxygenation of sickle cells, the delay time to polymerization of HbS is inversely proportional to the 30th power of the deoxy HbS concentration (Hofrichter *et al.*, 1974). Any loss of cell water, which crosses the erythrocyte membrane in milliseconds (Sachs *et al.*, 1975), therefore has a disproportionate effect on polymerization and thus on cell deformability. Compounds that prevent loss of, or increase, cell cation content will increase cytoplasmic water, lower MCHC, and reduce the propensity to sickling.

Pilot studies in small numbers of sickle-cell patients have suggested a potential therapeutic effect of Ca^{2+}-entry blockade by nifedipine (Rodgers *et al.*, 1988) and of Gardos channel inhibition by cetiedil citrate (Benjamin *et al.*, 1986). Full clinical trials require a large number of patients because of the biological and clinical variability of this disease and are difficult to execute. Prior *in vitro* screening of test compounds is therefore necessary. Previous *in vitro* studies have demonstrated the potential rheological benefit of Ca^{2+}-entry blockade by nitrendipine (Nash *et al.*, 1989) and of Gardos channel inhibition by bepridil (Johnston *et al.*, 1989). We have now refined these methods by measuring the effect of putative anti-sickling compounds on cation flux and on the rheological changes induced by cyclical deoxygenation-reoxygenation for 15 h in the presence of Ca^{2+}.

Cyclical deoxygenation-reoxygenation over 15 h in the presence of Ca^{2+} resulted in significant loss of cell K^+ and cell volume with an increase in MCHC and loss of filterability through pores of 5 μm diameter. These results confirm the findings of previous workers (Ohnishi *et al.*, 1986; Johnston *et al.*, 1989; Nash *et al.*, 1989) and reflect Ca^{2+} entry into the sickle cell with consequential activation of the Gardos channel.

The 1,4-dihydropyridine nitrendipine, which acts classically as a Ca-channel blocker but in this study has also been shown to act as a Gardos channel inhibitor, produced a substantial protective effect against K^+ loss and dehydration at concentrations down to 0.1 μM, in agreement with Nash *et al.* (1989). Its inhibitory effect on the Gardos channel is 200 fold greater than that of nifedipine (Kaji, 1990; Ellory *et al.*, 1991). Inhibition of the Gardos channel by quinidine or cetiedil citrate gave a weaker protective effect on filterability;

Table 3 Effect of 15 h deoxygenation-reoxygenation in the Cyclical Gas Exchanger

	RCTT	*CR* (ml^{-1})	*K* (Eq/cell $\times 10^{-16}$)	*MCV* (fl)	*MCHC* ($g\ dl^{-1}$)
Pre-incubation	23.3	1.28	76.0	99.2	32.4
	(3.85)	(0.41)	(11.5)	(8.96)	(1.18)
15 h oxy,	25.4	1.33	75.7	98.8	32.5
no $CaCl_2$	(4.48)	(0.37)	(14.8)	(8.14)	(1.12)
*P**	NS	NS	NS	NS	NS
15 h deoxy-	62.9	8.21	15.2	82.1	38.1
reoxy with $CaCl_2$	(31.5)	(3.66)	(10.8)	(7.46)	(1.76)
*P**	<0.001	<0.001	<0.001	<0.001	<0.001

Mean and s.d. for 20 experiments.
*Compared with pre-incubation. NS, not significant.
RCTT: red cell transit time; CR: clogging rate; MCV: erythrocyte mean cell volume; MCHC: mean cell haemoglobin concentration.

Table 4 Effect of reference Ca^{2+}-entry blockers (nitrendipine and fendiline) and Gardos channel inhibitors (quinidine and cetiedil) on the rheological changes induced by 15 h deoxygenation-reoxygenation with added Ca^{2+} in the Cyclical Gas Exchanger

		% change					
		RCTT	*CR* (ml^{-1})	*K* (Eq/cell $\times 10^{-16}$)	*MCV* (fl)	*MCHC* ($g\ dl^{-1}$)	*Stomatocytes*
Nitrendipine	0.1	31.4	11.4	15.8	28.1	28.6	0
(μM)	1	80.3	31.3	11.8	26.1	30.1	0
	10	84.6	44.4	30.3	41.2	42.9	0
Fendiline	1	7.6	− 20.2	− 1.8	2.3	6.2	0
(μM)	10	64.5	14.1	− 7.0	− 0.9	15.0	+
	25	78.9	32.9	− 6.3	19.6	25.0	+
	100	− 112.7	− 46.0	5.0	35.0	55.0	+ + +
Quinidine	1	− 21.2	− 8.0	− 1.3	2.4	− 9.6	0
(μM)	10	33.2	24.7	− 3.1	− 7.1	− 21.2	0
	25	12.4	3.8	− 2.3	13.7	7.7	+
	100	33.6	− 4.9	− 1.6	23.8	11.5	+ +
Cetiedil	1	− 43.0	2.2	− 12.1	8.3	4.4	0
(μM)	10	− 88.1	− 28.0	− 6.3	4.8	0	0
	25	− 160.4	− 20.1	− 1.4	17.2	20.0	+
	100	− 388.1	− 9.8	27.2	79.2	68.9	+ +

Mean percentage protection compared with no drug for 3 experiments; negative values represent adverse effect compared with no drug.
For abbreviations, see Table 3.

Table 5 Effect of bepridil and analogues on the rheological changes induced by 15 h deoxygenation-reoxygenation with added Ca^{2+} in the Cyclical Gas Exchanger

		% change					
		RCTT	*CR* (ml^{-1})	*K* (Eq/cell $\times 10^{-16}$)	*MCV* (fl)	*MCHC* ($g\ dl^{-1}$)	*Stomatocytes*
(±)-Bepridil	1	23.0	1.7	− 9.5	− 14.3	− 16.7	0
(μM)	10	33.5	− 11.4	− 12.3	0.8	− 2.4	0
	25	− 5.0	− 113	− 8.2	6.0	0	+
	100	− 1961*	− 143	− 34.5	70.7	76.2	+ + +
(+)-Bepridil	1	7.1	5.4	3.2	7.3	1.9	0
(μM)	10	37.0	13.1	− 4.6	18.2	11.4	0
	25	8.5	− 9.4	− 0.2	24.2	17.0	+
	100	− 200*	− 200*	15.7	65.5	56.6	+ +
(−)-Bepridil	1	2.0	11.1	4.8	0.8	0	0
(μM)	10	39.5	19.8	2.7	10.2	4.6	0
	25	39.5	− 50.3	2.5	21.1	16.0	0
	100	− 2000*	− 174	55.3	82.8	88.6	+ + +
Org 30701	1	15.7	− 7.2	4.4	− 2.6	− 7.9	0
(μM)	10	25.2	14.3	− 2.6	2.1	− 4.8	0
	25	78.0	33.3	4.8	3.1	− 1.6	0
	100	71.0	29.6	17.4	14.9	14.3	+

Mean percentage protection compared with no drug for 3 experiments; negative values represent adverse effect compared with no drug.
For abbreviations, see Table 3.
*Unfilterable.

this was in part due to their stomatogenic effect at high concentration.

The Ca channel of human red cells has been shown to have similar pharmacological properties to the Ca channel of smooth muscle and cardiac cells (Stimpel *et al.*, 1984), although recently a fraction of Ca^{2+} entry into human red cells has been shown to behave as a reversible carrier-mediated mechanism (Desai *et al.*, 1991). Bepridil inhibits Ca^{2+} entry into excitable cells (Labrid *et al.*, 1979; Vogel *et al.*, 1979) and we have shown in the present study that it also inhibits a component of ^{45}Ca entry into sickle erythrocytes. Further, this paper confirms our previous observation, for bepridil alone (Johnston *et al.*, 1989; Stuart *et al.*, 1989), that bepridil and its stereoisomers and analogues can inhibit Ca^{2+}-dependent K^+ (^{86}Rb) efflux from human erythrocytes. These compounds were less potent than nitrendipine and, at high concentration, most of them had an adverse rheological effect owing to the formation of stomatocytes. Passage of erythrocytes through small pores has been shown previously to be adversely affected by spherostomatocytic shape change (Reinhart & Chien, 1986). Lipophilic compounds that intercalate into the lipid bilayer of erythrocytes can cause echinocytosis (expansion of the outer layer) or stomatocytosis (expansion of the inner layer) according to the bilayer couple hypothesis (Sheetz & Singer, 1974) and this is the probable explanation for the morphological changes observed at high concentrations of these compounds. Membrane expansion by partitioning of lipophilic molecules will eventually increase membrane permeability and cause lysis as was seen for bepridil and its stereoisomers at 100 μM.

Development of the Cyclical Gas Exchanger has allowed *in vitro* comparison of the relative efficacy of test compounds that act as Ca^{2+}-entry blockers or inhibitors of the Gardos channel in SS cells. Bepridil has been shown previously to have an anti-sickling effect *in vitro* (Johnston *et al.*, 1989) but neither bepridil nor its stereoisomers or analogues were as effective as nitrendipine in the present experiments. Despite a rheologically protective effect *in vitro* at 0.1 μM, nitrendipine given orally to patients with sickle cell disease has been found not to improve the rheology of sickle cells in *ex vivo* blood samples (Nash *et al.*, 1991), presumably because lower concentrations are achieved *in vivo*.

This study has demonstrated the potential value of combining cation flux measurements and rheological investigations for examining the mode of action and relative potency of compounds that may prevent dehydration of sickle cells. Compounds originally designed as Ca-channel inhibitors were tested for inhibition of both Ca^{2+}-uptake and Ca^{2+}-dependent K^+ loss in red cells. This identified inhibition of the Ca^{2+}-dependent K^+ loss (Gardos pathway) as the major pharmacologically-effective site of action of certain of these molecules. Subsequent rheological experiments confirmed inhibition of the Ca^{2+}-induced K^+ efflux pathway as a significant parameter in preventing dehydration of sickle cells. The *in vitro* rheological studies indicate the potential therapeutic value of compounds which inhibit this pathway, and suggest that more extensive clinical trials with either nitrendipine or its analogues may be of benefit in preventing sickle cell crisis.

We are indebted to Action Research, The Wellcome Trust and Organon International BV for research grant support; to Dr I.M. Franklin for allowing access to patients in his care; and to the patient volunteers who provided blood samples for this study. E.H. is an M.R.C. Research Student. The Cyclical Gas Exchanger (Mark II) was constructed by Wolfson Research Laboratories, Queen Elizabeth Medical Centre, Birmingham.

References

VAN AMSTERDAM, F.T.M. & ZAAGSMA, J. (1988). Stereoisomers of calcium antagonists discriminate between coronary vascular and myocardial sites. *Naunyn-Schmiedebergs Arch. Pharmacol.*, **337**, 213–219.

BENJAMIN, L.J., BERKOWITZ, L.R., ORRINGER, E., MANKAD, V.N., PRASAD, A.S., LEWKOW, L.M., CHILLAR, R.K. & PETERSON, C.M. (1986). A collaborative, double-blind randomized study of cetiedil citrate in sickle cell crisis. *Blood*, **67**, 1442–1447.

BILTO, Y.Y. & STUART, J. (1985). Ultrasonic cleaning of polycarbonate membranes for measurement of erythrocyte filterability. *Clin. Hemorheol.*, **5**, 437–448.

BOOKCHIN, R.M., ORTIZ, O.E. & LEW, V.L. (1986), Red cell calcium transport and mechanism of dehydration in sickle cell anemia. In *Approaches to the Therapy of Sickle Cell Anaemia*. ed. Beuzard, Y., Charache, S. & Galacteros, F. pp. 291–299. Paris: Les Editions INSERM.

DESAI, S.A., SCHLESINGER, P.H. & KROGSTAD, D.J. (1991). Physiologic rate of carrier-mediated Ca^{2+} entry matches activate extrusion in human erythrocytes. *J. Gen. Physiol.*, **98**, 349–364.

DORMANDY, J., FLUTE, P., MATRAI, A., BOGAR, L., MIKITA, J., LOWE, G.D.O., ANDERSON, J., CHIEN, S., SCHMALZER, E. & HERSCHENFELD, A. (1985). The new St. George's blood filtrometer. *Clin. Hemorheol.*, **5**, 975–983.

EATON, J.W., SKELTON, T.D., SWOFFORD, H.S., KOLPIN, C.E. & JACOB, H.S. (1973). Elevated erythrocyte calcium in sickle cell disease. *Nature*, **246**, 105–106.

ELLORY, J.C., HALL, A.C. & AMESS, J.A.L. (1987). Passive potassium transport in human red cells. *Biomed. Biochim. Acta.*, **46**, 2/3, S31–S35.

ELLORY, J.C., KIRK, K., CULLIFORD, S.J., NASH, G.B. & STUART, J. (1992). Nitrendipine is a potent inhibitor of the Ca^{2+}-activated K^+ channel of human erythrocytes. *FEBS Lett.*, **296**, 291–221.

FABRY, M.E., BENJAMIN, L., LAWRENCE, C. & NAGEL, R.L. (1984). An objective sign in painful crisis in sickle cell anemia: the concomitant reduction of high density cells. *Blood*, **64**, 559–563.

GARDOS, G. (1958). The function of calcium in the potassium permeability of human erythrocytes. *Biochim. Biophys. Acta.*, **30**, 653–654.

GOA, K.L. & SORKIN, E.M. (1987). Nitrendipine: a review of its pharmacodynamic properties, and therapeutic efficacy in the treatment of hypertension. *Drugs*, **33**, 123–155.

HOFRICHTER, J., ROSS, P.D. & EATON, W.A. (1974). Kinetics and mechanism of deoxyhemoglobin S gelation: a new approach to understanding sickle cell disease. *Proc. Natl. Acad. Sci. U.S.A.*, **71**, 4864–4868.

JOHNSTON, M.N., ELLORY, J.C. & STUART, J. (1989). Bepridil protects sickle cells against the adverse rheological effects of cyclical deoxygenation. *Br. J. Haematol.*, **73**, 522–526.

KAJI, D.M. (1990). Nifedipine inhibits calcium-activated K transport in human erythrocytes. *Am. J. Physiol.*, **259**, C332–C339.

KEIDAN, A.J., SOWTER, M.C., MARWAH, S.S., JOHNSON, C.S. & STUART, J. (1987). Evaluation of HEPES and phosphate buffers for rheological studies of sickle cells. *Clin. Hemorheol.*, **7**, 599–610.

LABRID, C., GROSSET, A., DURENG, G., MIRONNEAU, J. & DUCHENE-MARULLAZ, P. (1979). Some membrane interactions with bepridil, a new antianginal agent. *J. Pharmacol. Exp. Ther.*, **211**, 546–554.

LEW, V.L., HOCKADAY, A., SEPULVEDA, M.I., SOMLYO, A.P., SOMLYO, A.V., ORTIZ, O.E. & BOOKCHIN, R.M. (1985). Compartmentalization of sickle cell calcium in endocytic inside-out vesicles. *Nature*, **315**, 586–589.

MURPHY, E., BERKOWITZ, L.R., ORRINGER, E., LEVY, L., GABEL, S.A. & LONDON, R.E. (1987). Cytosolic free calcium levels in sickle red blood cells. *Blood*, **69**, 1469–1474.

NASH, G.B., BOGHOSSIAN, S., PARMAR, J., DORMANDY, J.A. & BEVAN, D. (1989). Alteration of the mechanical properties of sickle cells by repetitive deoxygenation: role of calcium and the effects of calcium blockers. *Br. J. Haematol.*, **72**, 260–264.

NASH, G.B., MILLAR, B., AL SAADY, N., BENNETT, E.D., EVANS, J. & BEVAN, D.H. (1991). Nitrendipine treatment and blood rheology in patients with sickle cell disease. *Br. J. Haematol.*, **78**, 588–589.

OHNISHI, S.T., HORIUCHI, K.Y., HORIUCHI, K., JURMAN, M.E. & SADANAGA, K.K. (1986). Nitrendipine, nifedipine and verapamil inhibit the in vitro formation of irreversibly sickled cells. *Pharmacology*, **32**, 248–256.

REINHART, W.H. & CHIEN, S. (1986). Red cell rheology in stomatocyte-echinocyte transformation: roles of cell geometry and cell shape. *Blood*, **67**, 1110–1118.

RODGERS, G.P., ROY, M.S., NOGUCHI, C.T. & SCHECHTER, A.N. (1988). Is there a role for selective vasodilatation in the management of sickle cell disease? *Blood*, **71**, 597–602.

SACHS, J.R., KNAUF, P.A. & DUNHAM, P.B. (1975). Transport through red cell membranes. In *The Red Blood Cell*, 2nd edition volume 2. ed. Mac N. Surgenor, D. pp. 613–703. New York: Academic Press.

SHEETZ, M.P. & SINGER, S.J. (1974). Biological membranes as bilayer couples. A molecular mechanism of drug-erythrocyte interactions. *Proc. Natl. Acad. Sci. U.S.A.*, **71**, 4457–4461.

SIMONS, T.J.B. (1976). Calcium-dependent potassium exchange in human red cell ghosts. *J. Physiol.*, **256**, 227–244.

STIMPEL, M., NEYSES, L., LOCHER, R., GROTH, H. & VETTER, W. (1984). Human red blood cells – an ideal model system for the action of calcium agonists and antagonists. *J. Hypertension*, **2** (Suppl. 3), 577–580.

STONE, P.C.W., BAREFORD, D., KEIDAN, A.J., JENNINGS, P.E. & STUART, J. (1986). Rheological study of density gradient fractionated erythrocytes in diabetes and atherosclerotic vascular disease. *Clin. Hemorheol.*, **6**, 337–348.

STUART, J. & ELLORY, J.C. (1988). Rheological consequences of erythrocyte dehydration. *Br. J. Haematol.*, **69**, 1–4.

STUART, J., ELLORY, J.C. & STONE, P.C.W. (1989). Rheological action of bepridil on normal and sickle erythrocytes. *Clin. Hemorheol.*, **9**, 247–255.

STUART, J. & JOHNSON, C.S. (1987). Rheology of the sickle cell disorders. *Baillière's Clin. Haematol.*, **1**, 747–775.

STUART, J., STONE, P.C.W., BAREFORD, D., CALDWELL, N.M., DAVIES, J.E. & BAAR, S. (1985). Evaluation of leucocyte removal methods for studies of erythrocyte deformability. *Clin. Hemorheol.*, **5**, 137–147.

VOGEL, S., CRAMPTON, R. & SPERELAKIS, N. (1979). Blockade of myocardial slow channels by bepridil (CERM-1978). *J. Pharmacol. Exp. Ther.*, **210**, 378–385.

(Received December 23, 1991
Revised April 9, 1992
Accepted April 14, 1992)

Br. J. Pharmacol. (1992), **106**, 978–985 © Macmillan Press Ltd, 1992

Adenosine-induced bronchoconstriction of isolated lung and trachea from sensitized guinea-pigs

Julian R. Thorne & [1]Kenneth J. Broadley

Department of Pharmacology, Welsh School of Pharmacy, University of Wales College of Cardiff, P.O. Box 13, Cardiff CF1 3XF

1 The bronchoconstriction of airway-perfused lungs and contraction of superfused tracheal spirals from guinea-pigs in response to adenosine were examined.

2 In lungs from untreated animals, adenosine had little effect unless the perfusion pressure was raised with carbachol (1.1 μM), when it caused a fall in perfusion pressure. However, if removed from guinea-pigs sensitized with ovalbumen (5 mg and 10 mg i.p. 14 and 12 days before use), adenosine was bronchoconstrictor, exerting bronchodilator effects only at high (1 mg) doses. The constrictor response to adenosine (300 μg) was significantly greater than that in lungs from untreated or sham-injected animals.

3 In superfused trachea from untreated animals, adenosine exerted only relaxant responses. In tissues from ovalbumen-sensitized guinea-pigs adenosine produced contracile responses, with relaxation appearing only at high (1 mg) doses.

4 Thus sensitization by antigen challenge revealed a bronchoconstrictor response of isolated airway preparations to adenosine. This is related to the clinical situation where only asthmatic subjects respond to adenosine by bronchoconstriction and suggests that the sensitization may destabilize inflammatory cells for mediator release by adenosine.

5 The response to a second exposure to adenosine was consistently reduced (lungs) or converted to a relaxation (trachea) indicating tachyphylaxis and consistent with a mediator release mechanism.

6 The P_1-purinoceptor antagonist, 8-phenyltheophylline (3.9 μM), antagonized the relaxant responses to higher doses of adenosine. However, it did not affect the contractile responses to lower doses of adenosine. Whether this is due to P_1-purinoceptors not being involved in the contractile response, or whether preferential blockade of the relaxant response leaves the contraction unopposed and apparently unblocked, remains to be established.

Keywords: Adenosine; airway perfused lungs of guinea-pig; superfused trachea; bronchoconstriction; ovalbumen sensitization

Introduction

The predominant response of airway smooth muscle to adenosine is relaxation (Farmer & Farrar, 1976; Karlsson *et al.*, 1982; Darmani & Broadley, 1986) which is mediated via P_1-purinoceptors of the A_2-subtype (Brown & Collis, 1982). In human non-asthmatic subjects, however, adenosine has no effect upon pulmonary function (Cushley *et al.*, 1983) while in asthmatics it produces a bronchoconstriction (Cushley *et al.*, 1983; 1984; Cushley & Holgate, 1985; Mann *et al.*, 1985; Crimi *et al.*, 1988; 1989). To evaluate the relevance of this bronchoconstrictor response to adenosine in asthma and in its treatment with the P_1-receptor antagonist theophylline, it was considered desirable to demonstrate a bronchoconstriction by adenosine in animal tissues.

A bronchoconstrictor response to adenosine or its analogues has been demonstrated *in vivo* in anaesthetized rats (Pauwels & Van Der Straeten, 1987) and guinea-pigs (Manzini & Ballati, 1990), the latter being attributed to vagally-mediated bronchospasm. We have also demonstrated bronchoconstriction to inhaled adenosine in conscious guinea-pigs sensitized to ovalbumen, but not in unsensitized animals (Thorne & Broadley, 1990a).

Small contractile responses of isolated tracheal preparations have also been demonstrated which have been attributed to the presence of longitudinal bands of smooth muscle and favoured by spiral cutting of the tissue (Satchell & Smith, 1984). The small contractile component precedes the predominant relaxation (Coleman, 1976; Karlsson *et al.*, 1982) and appears to depend upon the degree of resting tone (Fredholm *et al.*, 1979; Advenier *et al.*, 1982). There is some disagreement regarding whether the contractile response to the adenosine analogue L-N^6-phenylisopropyladenosine (L-PIA) is antagonized by P_1-receptor antagonists (Caparrotta *et al.*, 1984; Ghai *et al.*, 1987; Farmer *et al.*, 1988). However, the possibility exists for it being mediated via the release of arachidonic acid derivatives (Advenier *et al.*, 1982; Caparrotta *et al.*, 1984).

Because the contractile response to adenosine in these studies was dominated by the relaxation response, the present study was undertaken to establish measurable and reproducible bronchoconstrictor responses to adenosine in guinea-pig isolated lung tissue. Preliminary accounts of some of these results have been given to the British Pharmacological Society (Thorne & Broadley, 1988a,b; 1990b).

Methods

Male Dunkin-Harley guinea-pigs (Halls, Stafford, UK) weighing 300–400 g at purchase, 400–500 g at termination, were used throughout. Groups of 6 animals were housed in grid-bottom cages and kept at an ambient temperature of 22 ± 1°C under 12 h normal phase light-dark cycle.

The guinea-pigs were fed on Special Rabbit Pellet (plain) 680 supplied by Grain Harvesters, Canterbury, Kent or Diet TR2 with vitamin C, supplied by Pilsbury's Ltd., Birmingham. Drinking water was supplemented with ascorbic acid and allowed *ad libitum*.

Sensitization procedures

Guinea-pigs were actively sensitized with ovalbumen administered by intraperitoneal (i.p.) injections (5 mg) on day 0 and

[1] Author for correspondence.

10 mg on day 2. They were used 14–15 days after the start of immunization.

Sham pretreatment was performed, in which the injections were made identically but with vehicle containing no ovalbumen.

Airway-perfused lung preparation

Guinea-pigs were killed by cervical dislocation and trachea and lungs excised. The trachea was removed 5–10 mm above the bifurcation. The entire lung was perfused via the airways by cannulating the trachea. Half-lung preparations were perfused via the bronchi. Perfusion was with warmed (37°C) and gassed (5% CO_2 in oxygen) Krebs-bicarbonate solution of composition in twice-distilled water (mM): NaCl 118, $NaHCO_3$ 24.9, KCl 4.6, $CaCl_2$ 2.5, $MgSO_4$ 1.15, KH_2PO_4 1.15 and glucose 5.5. A constant flow rate of 5 ml min^{-1} was maintained by a Watson-Marlow peristaltic pump (tube internal diameter 0.5 mm) and changes in back-pressure were measured with a Bell and Howell physiological pressure transducer (type 4-327-L221) located at the side-arm on the perfusion cannula. A Condon mercury manometer was included in the system in series with the pressure transducer to accommodate some degree of volume change during drug responses. Perfusion pressure (resting level approximately 15 mmHg) was recorded on a Devices M19 polygraph (Ormed, Welwyn Garden, UK). The surface of the lungs was not scarified to aid outflow of perfusate.

Superfused tracheal spirals

After removal of the trachea from the lungs, it was cut spirally (Constantine, 1965). Lengths of 3–4 cm were suspended in a heated jacket (37°C) and superfused with prewarmed and gassed (5% CO_2 in oxygen) Krebs-bicarbonate solution at a constant flow rate of 5 ml min^{-1}. Changes in isometric tension were measured by attaching the upper end of the spiral to a Devices UF1 transducer (2 oz sensitivity range) and recorded on a Devices M19 polygraph. Intrinsic tone was induced by allowing the spirals to equilibrate under an applied tension of 1 g for 45–60 min.

Experimental protocol

After a 45–60 min equilibration period, agonists were added to lung or tracheal preparations as 0.1 ml bolus injections made into the connecting rubber tubing immediately prior to the warming coil. Antagonists were examined usually in paired tissues from the same animal, one half serving as the control the other being exposed to antagonist from 30 min before and thereafter throughout agonist exposure. For lung halves, left and right lungs were alternated for antagonist exposure. When resting perfusion pressure of the lung was raised, carbachol (1.1 μM) was perfused throughout.

Dose-response curves were constructed by half-logarithmic increments in dose, each dose being added when the perfusion pressure had returned to the resting level following changes from the previous dose. For evaluating different agonists in the same preparation, single bolus doses were usually given in the order: carbachol (10 μg lung, 30 ng trachea), adenosine (300 μg lung, 100 μg trachea), adenosine repeated, ovalbumen (200 μg lung, 500 ng trachea), ovalbumen repeated. The estimated concentration of adenosine after a dose of 300 μg to the lung is 2–3 mM.

Analysis of results

Responses were measured as the peak change in perfusion pressure (lungs) or isometric tension (trachea) induced by each bolus dose of agonist. Mean responses ± s.e.mean were calculated. Statistical comparisons were made between responses for each dose of agonist by Student's paired or unpaired *t* test, a significant difference being assumed at the 5% probability level.

Drugs

The following drugs were used: adenosine, carbachol (carbamylcholine chloride) and 8-phenyltheophylline were obtained from Sigma UK, and ovalbumen and aluminium hydroxide from BDH, Poole, Dorset, UK.

All stock solutions were prepared in 0.9% saline. 8-Phenyltheophylline was initially dissolved in 1 ml 1 M NaOH.

Results

Effect of adenosine in perfused lungs from untreated and ovalbumen-sensitized guinea-pigs

In airway-perfused lungs from untreated guinea-pigs constricted by a constant infusion of carbachol (1.1 μM), bolus doses of adenosine (300 μg and 1 mg) caused dose-related bronchodilatation (Figure 1). However, in the absence of background constriction, adenosine (300 μg) had no effect or produced a small constriction. In lungs from guinea-pigs previously sensitized to ovalbumen, adenosine (300 μg) produced a more marked constriction (Figure 1). Dose-response curves obtained in carbachol-constricted lungs showed a more marked constrictor-effect of adenosine in sensitized tissues at doses up to 300 μg but thereafter a bronchodilator action equivalent to that of untreated tissues (Figure 2).

Single doses of carbachol (10 μg), adenosine (300 μg), adenosine (300 μg), ovalbumen (200 μg) and ovalbumen (200 μg) were next administered, in that order, to lungs from untreated and ovalbumen-sensitized guinea-pigs (Figure 3). The carbachol responses did not differ but there was a significantly greater constriction to adenosine after ovalbumen sensitization (Figure 4). The response to adenosine after ovalbumen sensitization was also significantly greater

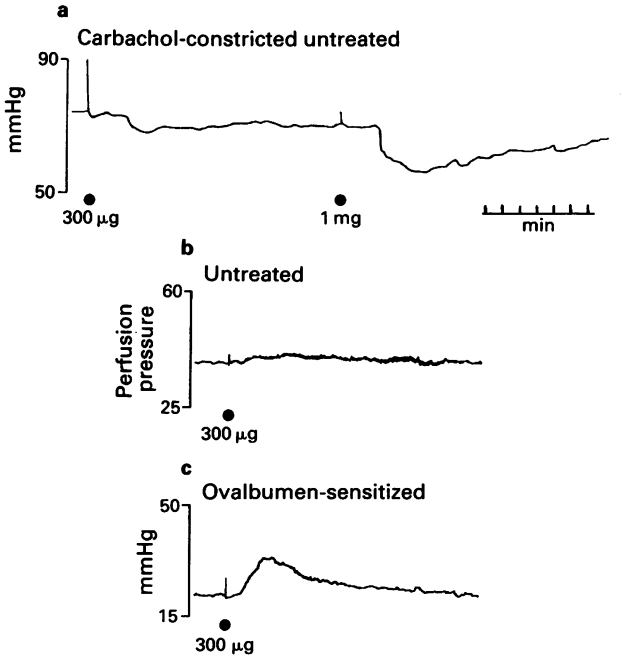

Figure 1 Typical responses to adenosine (●) of isolated airway-perfused lungs from guinea-pigs. Animals were either untreated (a and b) or sensitized with ovalbumen at 14 (5 mg i.p.) and 12 days (10 mg i.p.) before use. In (a) the resting perfusion pressure was raised by perfusion with carbachol (1.1 μM) throughout.

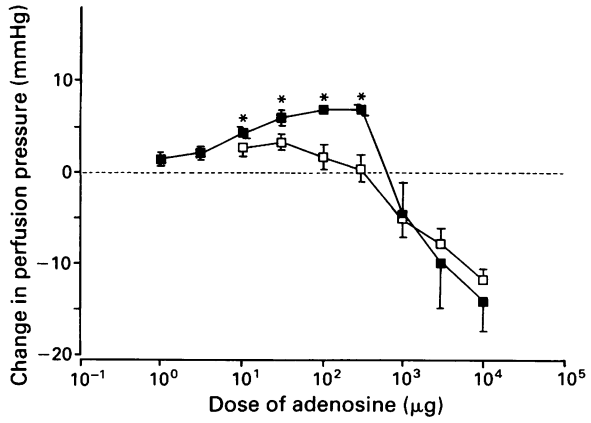

Figure 2 Mean (± s.e.mean, vertical bars) dose-response curves for the effects of bolus doses of adenosine on the perfusion pressure (mmHg) of airway-perfused lungs from untreated (□, $n = 8$) or ovalbumen-sensitized guinea-pigs (■, $n = 6$, 5 mg i.p., 14 days and 10 mg i.p., 12 days before use). Perfusion pressure was raised by perfusion with carbachol (1.1 μM) throughout. A significant difference, by Student's unpaired t test, between responses in untreated and sensitized tissues is indicated by *.

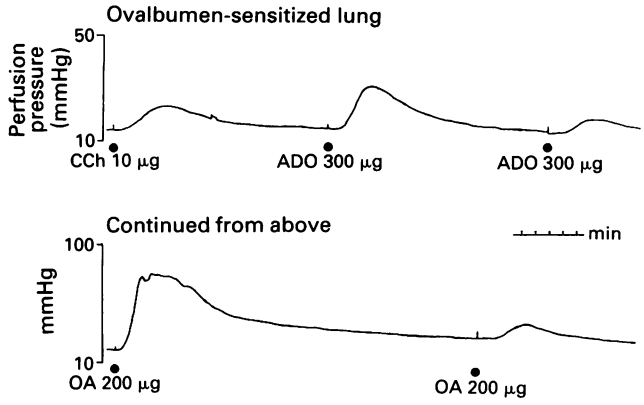

Figure 3 Typical responses of isolated airway-perfused lungs from ovalbumen-sensitized guinea-pigs (5 mg i.p., 14 days and 10 mg i.p., 12 days before use). Bolus doses of carbachol (CCh, 10 μg), adenosine (ADO, 300 μg) and ovalbumen (OA, 200 μg) were added at (●). The lower trace is a continuation from above, but with a change in scale for the vertical axis.

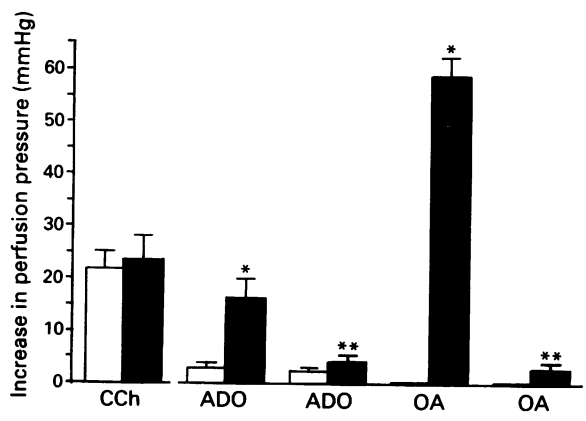

Figure 4 Mean (± s.e.mean, vertical bars) increases in perfusion pressure (mmHg) of isolated airway-perfused lungs in response to bolus doses of carbachol (CCh, 10 μg), adenosine (ADO, 300 μg), repeated adenosine, ovalbumen (OA, 200 μg) and repeated ovalbumen. Doses were added in the above order, as illustrated in Figure 3, to lungs from untreated (open columns, $n = 8$) and ovalbumen-sensitized guinea-pigs (solid columns, $n = 11$) (5 mg i.p., 14 days and 10 mg i.p., 12 days before use). A significant difference, by Student's unpaired t test, between untreated and sensitized tissues is indicated by * and between the first and second doses of adenosine or ovalbumen by **.

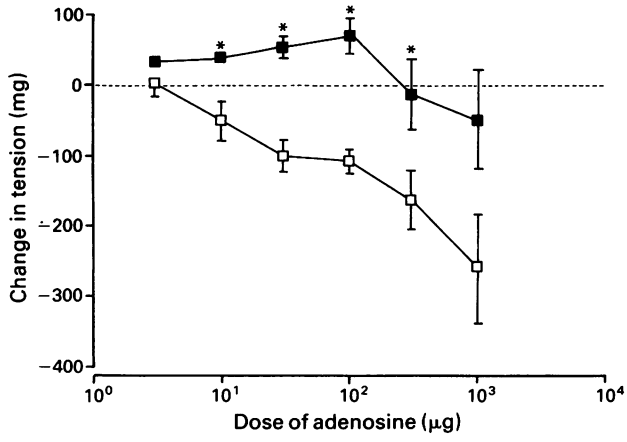

Figure 5 Mean (± s.e.mean, vertical bars) dose-response curves for the effects of bolus doses of adenosine on the tension (mg) of superfused tracheal spirals from untreated (□, $n = 4$) or ovalbumen-sensitized guinea-pigs (■, $n = 4$, 5 mg i.p., 14 days and 10 mg i.p., 12 days before use). A significant difference, by Student's unpaired t test, between responses in untreated and sensitized tissues is indicated by *.

than after sham injection. Ovalbumen induced constriction only after sensitization. The constrictor responses of sensitized lungs to the second administrations of adenosine and ovalbumen were significantly less than to the first exposure (Figures 3 and 4).

Effects of adenosine in superfused tracheae from untreated and ovalbumen-sensitized guinea-pigs

Dose-response curves for bolus injections of adenosine to superfused tracheae revealed only relaxant responses of preparations from untreated animals whereas contractile responses were evident at doses up to 100 μg in preparations from ovalbumen-sensitized guinea-pigs. These were followed by a small relaxation at 1 mg (Figure 5). A single dose of adenosine (100 μg) was also relaxant in untreated tissues but after ovalbumen sensitization, it was contractile in common with ovalbumen (Figure 6).

Effect of 8-phenyltheophylline on constrictor responses to adenosine

Single doses of carbachol, adenosine, adenosine, ovalbumen and ovalbumen, in that order, were examined in paired lung-halves from sensitized guinea-pigs. One half acted as the control and the other was perfused throughout with 8-phenyltheophylline (8-PT, 3.9 μM). 8-PT had no effect upon any of the responses (Figure 7). The responses to the second exposures to adenosine (in the presence of 8-PT only) and to ovalbumen were significantly less than the first exposures.

In superfused tracheae from sensitized guinea-pigs, 8-PT (3.9 μM) was also without effect upon the contractions induced by the first exposures to adenosine and ovalbumen (Figure 8). The second exposures to adenosine and ovalbumen in the absence of 8-PT produced relaxation response of the trachea, but in the present of 8-PT, these relaxations were restored to contractile responses which, in the case of adenosine, were no different from those obtained on the first exposure.

Dose-response curves for adenosine were obtained in superfused tracheae from ovalbumen-sensitized guinea-pigs.

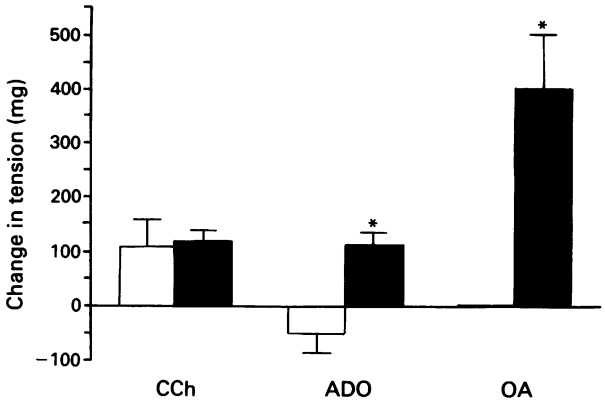

Figure 6 Mean (± s.e.mean, vertical bars) changes in tension (mg) of superfused tracheal spirals in response to bolus doses of carbachol (CCh, 30 ng), adenosine (ADO, 100 μg), and ovalbumen (OA, 500 ng) added in that order. Tissues were removed from untreated (open columns, $n = 7$) and ovalbumen-sensitized guinea-pigs (solid columns, $n = 6$) (5 mg i.p., 14 days and 10 mg i.p., 12 days before use). A significant difference, by Student's unpaired t test, between untreated and sensitized tissues is indicated by * .

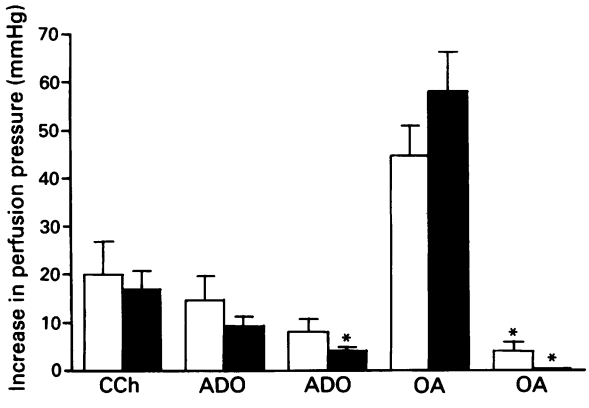

Figure 7 Effects of 8-phenyltheophylline (8-PT) on the mean (± s.e.mean, vertical bars, $n = 7$) increases in perfusion pressure (mmHg) of isolated airway-perfused lung halves from ovalbumen-sensitized guinea-pigs (5 mg i.p., 14 days and 10 mg i.p. 12 days before use). Responses to bolus doses of carbachol (CCh, 10 μg), adenosine (ADO, 300 μg), repeated adenosine, ovalbumen (OA, 200 μg) and repeated ovalbumen, added in that order, were obtained in the absence (open columns) and, in the contralateral lung half, presence of 8-PT (solid columns, 3.9 μM). A significant difference, by Student's paired t test, between first and second exposures to ADO and OA is indicated by *. Values in the absence and presence of 8-PT were not significantly different.

In the absence of 8-PT a biphasic curve was obtained with prominent contractile responses followed, at the higher dose used (1 mg), by a relaxation. In the presence of 8-PT (3.9 μM), the contractions were not blocked but no relaxation occurred at the highest dose used (Figure 9a).

A similar result was obtained in lung halves from ovalbumen-sensitized guinea-pigs that were perfused throughout with carbachol (1.1 μM). The constrictions induced by lower doses of adenosine were unaffected by 8-PT (3.9 μM) whereas the dilator responses to higher doses were significantly antagonized (Figure 9b).

Discussion

Adenosine produced predominantly bronchodilator responses in airway-perfused lungs preconstricted with carbachol and in

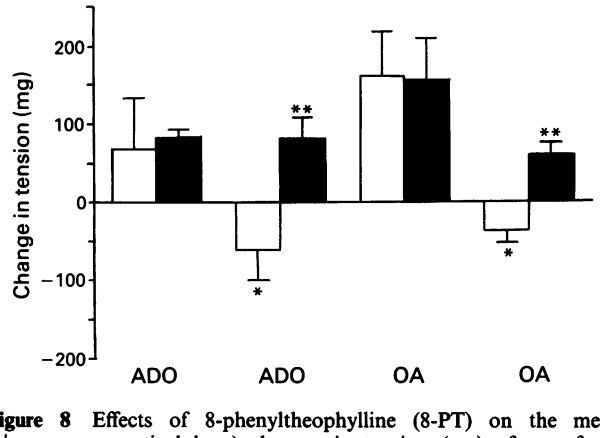

Figure 8 Effects of 8-phenyltheophylline (8-PT) on the mean (± s.e.mean, vertical bars) changes in tension (mg) of superfused tracheal spirals from ovalbumen-sensitized guinea-pigs (5 mg i.p., 14 days and 10 mg i.p. 12 days before use). Responses to bolus doses of adenosine (ADO, 100 μg), repeated adenosine, ovalbumin (OA, 500 ng) and repeated ovalbumen, added in that order, were obtained in the absence (open columns, $n = 5$) and present of 8-PT (solid columns, $n = 8$, 3.9 μM). A significant difference between first and second exposures to ADO and OA is indicated by * and between values in the absence and presence of 8-PT by **, as determined by Student's paired and unpaired t tests respectively.

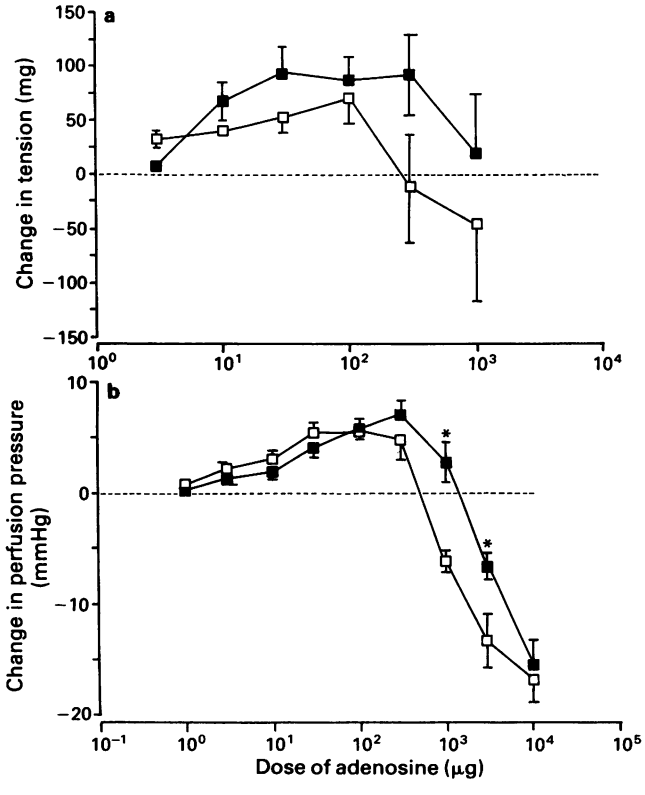

Figure 9 Effects of 8-phenyltheophylline (8-PT) on the mean (± s.e.mean, vertical bars) dose-response curves for (a) changes in tension (mg) of superfused tracheal spirals and (b) changes in perfusion pressure (mmHg) of airway-perfused lung halves, in response to adenosine. Both tissues were obtained from ovalbumen-sensitized guinea-pigs (5 mg i.p., 14 days and 10 mg i.p., 12 days before use). Perfusion pressure of lungs was raised by perfusing with carbachol (1.1 μM) throughout. Increasing bolus doses of adenosine were added to tracheal spirals either in the absence (□, $n = 4$) or presence (■, $n = 11$) of 8-PT (3.9 μM) and to lung halves from the same animals ($n = 9$), one half in the absence (□) and the other in the presence of 8-PT (■). A significant difference, by Student's t test (trachea unpaired; lung paired) between values in the absence and presence of 8-PT is indicated by *.

superfused trachea from untreated guinea-pigs. This confirms numerous reports in the literature of relaxant responses of guinea-pig immersed tracheal preparations (Farmer & Farrar, 1976; Jones *et al.*, 1980; Brown & Collis, 1982; Karlsson *et al.*, 1982; Darmani & Broadley, 1986; Advenier *et al.*, 1988). A small constriction by lower doses of adenosine could be distinguished in the lung but not the trachea. Contractile responses of the immersed trachea have been observed previously to precede the dominant relaxation (Coleman, 1976; Fredholm *et al.*, 1979; Advenier *et al.*, 1982; Karlsson *et al.*, 1982; Farmer *et al.*, 1988), and have been attributed to arachidonic acid breakdown products (Advenier *et al.*, 1982; Caparrotta *et al.*, 1984).

When tissues were removed from ovalbumen-sensitized guinea-pigs, a bronchoconstrictor response to adenosine was revealed in both tissues. In the lungs, the response to a single bolus dose was significantly greater than that of lungs from untreated animals, while the contraction of the trachea compared with relaxation of trachea from untreated animals. Similarly, dose-response curves revealed contractile responses at low doses followed by bronchorelaxation at higher doses. Thus we had achieved our objective of producing reproducible bronchoconstrictor responses of isolated respiratory tissues to adenosine.

Why should sensitization to an antigen such as ovalbumen promote a bronchconstrictor response to adenosine? Sensitized guinea-pigs have long been used as an animal model of asthma, in which aerosol challenge with antigen provokes airway inflammation and bronchoconstriction similar to that of the human early asthmatic response (Kallos & Kallos, 1984) but whether sensitization *per se* induces another feature of asthma, namely airway hyperreactivity, is doubtful. There are reports that tissues removed from sensitized guinea-pigs display raised sensitivity to spasmogens (see Cortijo *et al.*, 1989). However, in the present study there was no apparent increase in the response size to carbachol in tissues from sensitized animals. This agrees with most studies which fail to demonstrate a non-specific increase in sensitivity to histamine (Brink *et al.*, 1981; Saad & Burka, 1983; Hay *et al.*, 1986; Mansour & Daniel, 1987). To observe non-specific hyperreactivity to the bronchoconstrictor effect of spasmogens *in vivo* or *in vitro*, it is necessary to expose the ovalbumen-sensitized animal to antigen several hours before provocation by the bronchoconstrictor. Increased sensitivity to 5-hydroxytryptamine (5-HT), histamine or prostaglandin $F_{2\alpha}$ ($PGF_{2\alpha}$) has been demonstrated *in vivo* (Coyle *et al.*, 1988; Daffonchio *et al.*, 1988; 1989; Sanjar *et al.*, 1990) and increased sensitivity to vagal stimulation of isolated trachea (McCaig, 1987).

The raised sensitivity to adenosine was not therefore a non-specific hyperresponsiveness analogous to that occurring soon after antigen challenge, but probably relatively selective for adenosine. To explain this, it will be necessary to determine the mechanism whereby adenosine induces bronchoconstriction which was not the purpose of the present paper but is for future research. Adenosine has been shown to enhance the IgE-dependent release of histamine and 5-HT from rat serosal mast cells (Marquardt *et al.*, 1978; Church *et al.*, 1986). It also potentiates the release of histamine from human lung mast cells when added before (Peachell *et al.*, 1989) or after (Hughes *et al.*, 1984) immunological challenge with anti-human IgE. The latter report had shown that when added before challenge, adenosine was inhibitory (Hughes *et al.*, 1984). Similarly, when added prior to antigen challenge of human lung parenchymal strips passively sensitized with serum from an atopic patient, the contractile response was attenuated by adenosine (Napier & Temple, 1987a). The potentiating action of adenosine is attributed to its interaction with cell surface A_2-purinoceptors to activate adenylate cyclase, since it is antagonized by the P_1-purinoceptor antagonist 8-phenyltheophylline (Hughes *et al.*, 1984). Furthermore, the potency order of adenosine analogues is consistent with an A_2-receptor involvement (Hughes *et al.*, 1984; Peachell *et al.*, 1989).

Thus a primary candidate for the mechanism of the bronchoconstrictor response to adenosine is through the release of mediators from pulmonary mast cells (Holgate *et al.*, 1990). Indeed, adenosine has been shown to potentiate histamine release by ovalbumen from chopped lung tissue (Welton & Simko, 1980) or perfused lungs (Post *et al.*, 1990) from ovalbumen-sensitized guinea-pigs or rats respectively. Adenosine also enhances non-immunological release of histamine and 5-HT from mast cells (Marquardt *et al.*, 1978; Lohse *et al.*, 1989; Peachell *et al.*, 1989) and chopped lung tissue (Welton & Simko, 1980) by 48/80 and calcium ionophore A23187. Furthermore, the contraction of lung parenchymal strips (Napier & Temple, 1987b) and bronchoconstriction of perfused lungs (Post *et al.*, 1990) from ovalbumen-sensitized guinea-pigs and rats, to antigen challenge was potentiated by adenosine. In spite of this abundant evidence for a potentiating effect of adenosine on histamine release, there is no evidence for its causing release *per se* or enhancing basal release from chopped lung (Welton & Simko, 1980) or mast cells (Marquardt *et al.*, 1978).

The contractile responses observed in the present study were obtained in tissues from sensitized animals but did not require prior challenge of the potential target cells (e.g. mast cells) either immunologically with ovalbumen or non-immunologically. The response to adenosine and its possible release of mediators is, however, a non-immunological process. Immunological and non-immunological release of histmaine from mast cells have different characteristics and requirements, for example, the latter is dependent upon intracellular Ca^{2+} while immunological release relies upon primarily extracellular Ca^{2+} (Rosengard *et al.*, 1986). Thus, although separate mechanisms appear to be involved in histamine release by adenosine and antigen challenge, sensitization with ovalbumen does appear to 'prime' the target cells for mediator release by adenosine. The binding of the antibody (probably IgG in this case) to its target cell receptor may destabilize it for easier non-immunological stimulation by adenosine. We are not aware, however, of any evidence that responses to other non-immunological stimulants such as 48/80 or ionophore A23187 are enhanced by sensitization with ovalbumen. It has recently been suggested that adenosine may promote the release of mediators from primed mast cells in atopic subjects (Holgate *et al.*, 1990).

The constrictor responses to bolus doses of adenosine in the lung and superfused trachea displayed a marked tachyphylaxis. A second administration to the lung produced a significantly smaller constrictor response, while in the trachea, the second administration produced relaxation. Thus the tachyphylaxis was sufficient for the direct smooth muscle relaxant effects of adenosine to be unmasked. Tachyphylaxis of the potentiation of 5-HT release by adenosine from rat mass cells has been reported previously (Church *et al.*, 1986). Marquardt & Walker (1987) also reported that adenosine-induced potentiation of IgE-stimulated granule-derived β-hexosaminidase release is markedly attenuated by prior exposure to the A_2-receptor agonist, N'ethylcarboxamide-adenosine. The bronchoconstrictor response of atopic mildly asthmatic subjects to the related nucleotide AMP, which is used as a precursor for adenosine, was also attenuated on repeated exposure (Phillips *et al.*, 1989). However, there was no cross-tachyphylaxis with the bronchoconstriction induced by allergen challenge. The same conclusion can be drawn from the present results, since although the response to the second exposure to adenosine was consistently reduced, the ovalbumen challenge was still able to induce a substantial response. On repeating the ovalbumen administration, the response was virtually abolished in the lung or converted to a relaxation in the superfused trachea. The appearance of a relaxation response to ovalbumen is worthy of further study. The tachyphylaxis to AMP in man is not associated with refractoriness to histamine. thus the tachyphylaxis to the bronchoconstrictor effect of adenosine is not due to mast cell histamine depletion nor to desensitization of smooth muscle to

released histamine. A down regulation or uncoupling of the adenosine receptor has been suggested (Phillips *et al.*, 1989). However, since the direct smooth muscle relaxation via A_2-receptors has been shown here and elsewhere (Church & Holgate, 1988) not to display tachyphylaxis, this mechanism is unlikely.

The lack of cross-tachyphylaxis between ovalbumen and adenosine may arise through differences in the nature of mediators released. Mast cell-derived histamine is a major mediator of the immediate asthmatic bronchoconstrictor-response (Barnes *et al.*, 1988) and of the constrictor response to ovalbumen of lung tissue from sensitized animals (Mitchell & Denborough, 1979; Napier & Temple, 1987b; Turner & Dollery, 1988). However, whether it is important for the adenosine-induced bronchoconstriction is less clear. The anti-histamine, terfenadine, has been shown to inhibit the response to AMP in man (Rafferty *et al.*, 1987). However, the plasma histamine levels were raised substantially less than with allergen challenge, but both produced equivalent falls in FEV (Phillips *et al.*, 1990). Combined with an earlier report showing no increase in plasma histamine after adenosine challenge of asthmatic patients (Cushley & Holgate, 1985), this suggests that histamine has a minor role in the adenosine response. Furthermore, the contractile response seen here (Thorne & Broadley, 1991) and elsewhere (Advenier *et al.*, 1982; Ghai *et al.*, 1987), is not affected by antihistamines but is blocked by the cyclo-oxygenase inhibitors, indicating that it is more likely to be due to products of arachidonic acid (Caparrotta *et al.*, 1984).

In view of these observations, the earlier studies on augmentation of mast cell histamine release by adenosine may not therefore be directly relevant to the response observed here. If the constrictor response to adenosine is due to the release of cyclo-oxygenase products of arachidonic acid, then it is clearly enhanced or uncovered by ovalbumen sensitization. The tachyphylaxis to adenosine may therefore be due to impaired release of, or sensitivity to, these products. Arachidonic acid-derived mediators originate from mast cells or from alternative cells such as macrophages which also possess IgE and IgG receptors and release arachidonic acid products (Rankin, 1989). Unlike the preformed histamine released from mast cell granules, cyclo-oxygenase products of arachidonic acid are derived from membrane phospholipids of mast cells and macrophages (Barnes *et al.*, 1988). Thus the lack of cross-tachyphylaxis between adenosine and ovalbumen may be explained by the involvement of different cells and/or mediators in their responses.

Tachyphylaxis of the constrictor response to adenosine presumably had an effect when dose-response curves were obtained. Although not examined in this study, it can be assumed that the contractions to subsequent higher doses of adenosine were suppressed by the development of tachyphylaxis.

To determine whether the bronchoconstrictor response to adenosine was mediated via stimulation of extracellular P_1-purinoceptors, its susceptibility to the antagonist 8-phenyltheophylline (8-PT) was examined. The constriction of both the lung and trachea was surprisinngly not blocked by 8-PT. This is in contrast to findings *in vivo* where the bronchoconstriction of asthmatic subjects (Cushley *et al.*, 1984; Mann & Holgate, 1985; Crimi *et al.*, 1989) and of anaesthetized guinea-pigs (Manzini & Ballati, 1990) and rats (Pauwels & Van Der Straeten, 1983) to adenosine were antagonized by theophylline or aminophylline. *In vitro*, however, there is a divergence of opinion, with small contractile responses of the guinea-pig immersed trachea to L-phenylisoprophyladenosine having been shown to be antagonized by theophylline or 8-PT by one group (Farmer *et al.*, 1988), but not by others (Caparrotta *et al.*, 1984; Ghai *et al.*, 1987). The latter authors, however, found antagonism by the selective A_1-receptor antagonist 1,3-dipropyl-8-(2-amino-4-chlorophenyl) xanthine (PACPX) and concluded that the contraction was probably A_1-receptor-mediated. Examination of the dose-response curves revealed blockade of the relaxant component, indicating that the concentration of 8-PT was adequate for P_1-purinoceptor blockade. There was, however, no shift of the contractile response portion of the curve. As evidence for a lack of involvement of cell surface P_1-purinoceptors in the contractile response, however, these results should be treated with caution. The possibility that preferential blockade of the relaxation component of the response leaves the contractile response unopposed and thus apparently unblocked cannot be discounted. Further work is underway to block these two components, selectively.

In conclusion, this study has demonstrated bronchoconstrictor responses in the superfused trachea and airway perfused lungs from guinea-pigs sensitized to ovalbumen. The fact that sensitization to allergen promotes this response indicates that it is related to the allergic state of the animals rather than to any non-specific airway hyperreactivity. It is thus analogous to the situation in human subjects where only asthmatics respond to inhalation of adenosine or AMP with bronchoconstriction (Cushley *et al.*, 1983). Furthermore, in comparison with the human response, it displayed tachyphylaxis (Phillips *et al.*, 1989). Although the resistance to blockade by methylxanthines is in contrast to the situation in asthmatic subjects and awaits a satisfactory explanation, the bronchoconstriction observed in perfused lungs and trachea of sensitized guinea-pigs is a useful simple model for further evaluation of the airway response to adenosine.

This study was initiated by a grant from the Asthma Research Council (now the National Asthma Campaign).

References

ADVENIER, C., BIDET, D., FLOCH-SAINT-AUBIN, A. & RENIER, A. (1982). Contribution of prostaglandins and thromboxanes to the adenosine and ATP-induced contraction of guinea-pig isolated trachea. *Br. J. Pharmacol.*, **77**, 39–44.

ADVENIER, C., DEVILLIER, P., MATRAN, R. & NALINE, E. (1988). Influence of epithelium on the responsiveness of guinea-pig isolated trachea to adenosine. *Br. J. Pharmacol.*, **93**, 295–302.

BARNES, P.J., CHUNG, K.F. & PAGE, C.P. (1988). Inflammatory mediators and asthma. *Pharmacol. Rev.*, **40**, 49–84.

BRINK, C., DUNCAN, P.G. & DOUGLAS, J.S. (1981). The response and sensitivity to histamine of respiratory tissues from normal and ovalbumin-sensitized guinea-pigs: effects of cyclooxygenase and lipoxygenase inhibition. *J. Pharmacol. Exp. Ther.*, **217**, 592–601.

BROWN, C.M. & COLLIS, M.G. (1982). Evidence for an A_2/R_a adenosine receptor in the guinea-pig trachea. *Br. J. Pharmacol.*, **76**, 381–387.

CAPARROTTA, L., CILLO, F., FASSINA, G. & GAION, R.M. (1984). Dual effect of (−)-N^6-phenylisopropyladenosine on guinea-pig trachea. *Br. J. Pharmacol.*, **83**, 23–29.

CHURCH, M.K., HUGHES, P.J. & VARDEY, C.J. (1986). Studies on the receptor mediating cyclic AMP-dependent enhancement by adenosine of IgE-dependent mediator release from rat mast cells. *Br. J. Pharmacol.*, **87**, 233–242.

CHURCH, M.K. & HOLGATE, S.T. (1988). Adenosine in asthmatic lung. In *Mechanisms in Asthma: Pharmacology, Physiology and Management. Prog. Clin. Biol. Res.*, **263**, 159–166.

COLEMAN, R.A. (1976). Effects of some purine derivatives on the guinea-pig trachea and their interaction with drugs that block adenosine uptake. *Br. J. Pharmacol.*, **57**, 51–57.

CONSTANTINE, J.W. (1965). The spirally cut tracheal strip preparation. *J. Pharm. Pharmacol.*, **17**, 384–385.

CORTIJO, J., ORTIZ, J.L., SANZ, C., SARRIA, B., PASCUAL, R., PERPINA, M., ESPLUGUES, J. & MORCILLO, E.J. (1989). Modification by indomethacin of airway contractile responses in normal and sensitized guinea-pigs. *Eur. J. Pharmacol.*, **162**, 467–473.

COYLE, A.J., URWIN, S.C., PAGE, C.P., TOUVAY, C., VILLAIN, B. & BRAQUET, P. (1988). The effect of the selective PAF antagonist BN 52021 on PAF- and antigen-induced bronchial hyperreactivity and eosinophil accumulation. *Eur. J. Pharmacol.*, **148**, 51–58.

CRIMI, N., PALERMO, F., POLOSA, R., OLIVERI, R., MACCARRONE, C., PALERMO, B. & MISTRETTA, A. (1988). Effect of indomethacine on adenocine-induced bronchoconstriction. *J. Allergy Clin. Immunol.*, **83**, 921–925.

CRIMI, N., PALMERMO, F., CICCARELLO, C., OLIVERI, R., VANCHERI, C., PALERMO, B. & MISTRETTA, A. (1989). Effect of theophylline on adenosine-induced bronchoconstriction. *Ann. Allergy*, **62**, 123–127.

CUSHLEY, M.J. & HOLGATE, S.T. (1985). Adenosine-induced bronchoconstriction in asthma: Role of mast cell-mediator release. *J. Allergy Clin. Immunol.*, **75**, 272–278.

CUSHLEY, M.J., TATTERSFIELD, A.E. & HOLGATE, S.T. (1983). Inhaled adenosine and guanosine on airway resistance in normal and asthmatic subjects. *Br. J. Clin. Pharmacol.*, **15**, 161–165.

CUSHLEY, M.J., TATTERSFIELD, A.E. & HOLGATE, S.T. (1984). Adenosine-induced bronchoconstriction in asthma. Antagonism by inhaled theophylline. *Annu. Rev. Resp. Dis.*, **129**, 380–384.

DAFFONCHIO, L., PAYNE, A.N., LEES, I.W. & WHITTLE, B.J.R. (1988). Immediate anaphylactic bronchoconstriction induces airway hyperreactivity in anaesthetized guinea-pigs. *Br. J. Pharmacol.*, **94**, 663–668.

DAFFONCHIO, L., PAYNE, A.N., LEES, I.W. & WHITTLE, B.J.R. (1989). Airway hyperreactivity follows anaphylactic microshock in anaesthetized guinea-pigs. *Eur. J. Pharmacol.*, **161**, 135–142.

DARMANI, N.A. & BROADLEY, K.J. (1986). Actions and interactions of adenosine, theophylline and enprofylline on the guinea-pig spirally cut trachea. *Eur. J. Pharmacol.*, **125**, 353–362.

FARMER, J.B. & FARRAR, D.G. (1976). Pharmacological studies with adenine, adenosine and some phosphorylated derivatives on guinea-pig tracheal muscle. *J. Pharm. Pharmacol.*, **28**, 748–752.

FARMER, S.G., CANNING, B.J. & WILKINS, D.E. (1988). Adenosine receptor-mediated contraction and relaxation of guinea-pig isolated tracheal smooth muscle: effects of adenosine antagonists. *Br. J. Pharmacol.*, **95**, 371–378.

FREDHOLM, B.B., BRODIN, K. & STRANDBERG, K. (1979). On the mechanism of relaxation of tracheal muscle by theophylline and other cyclic nucleotide phosphodiesterase inhibitors. *Acta Pharmacol. Toxicol.*, **45**, 336–344.

GHAI, G., ZIMMERMAN, M.B. & HOPKINS, M.F. (1987). Evidence for A_1 and A_2 adenosine receptors in guinea-pig trachea. *Life Sci.*, **41**, 1215–1224.

HAY, D.W.P., RAEBURN, D., FARMER, S.G., FLEMING, W.W. & FEDAN, J.S. (1986). Epithelium modulates the reactivity of ovalbumin-sensitized guinea-pig airway smooth muscle. *Life Sci.*, **38**, 2461–2468.

HOLGATE, S.T., FINNERTY, J.P. & POLOSA, R. (1990). Mechanisms of purine-induced bronchoconstriction in asthma. *Arch. Int. Pharmacodyn.*, **303**, 122–131.

HUGHES, P.J., HOLGATE, S.T. & CHURCH, M.K. (1984). Adenosine inhibits and potentiates IgE-dependent histamine release from human lung mast cells by an A_2-purinoceptor mediated mechanism. *Biochem. Pharmacol.*, **33**, 3847–3852.

JONES, T.R., LEFCOE, N.M. & HAMILTON, J.T. (1980). Pharmacological study of adenosine and related compounds on isolated guinea pig trachea: evidence for more than one type of purine receptor. *Can. J. Physiol. Pharmacol.*, **58**, 1356–1365.

KALLOS, P. & KALLOS, L. (1984). Experimental asthma in guinea-pigs revisited. *Int. Arch. Allergy Appl. Immunol.*, **73**, 77–85.

KARLSSON, J.A-., KJELLIN, G. & PERSSON, C.G.A. (1982). Effects on tracheal smooth muscle of adenosine and methylxanthines, and their interaction. *J. Pharm. Pharmacol.*, **34**, 788–793.

LOHSE, M.J., MAURER, K., KLOTZ, K.-N. & SCHWABE, U. (1989). Synergistic effects of calcium-mobilizing agents and adenosine on histamine release from rat peritoneal mast cells. *Br. J. Pharmacol.*, **98**, 1392–1398.

MCCAIG, D.J. (1987). Comparison of autonomic response in the trachea isolated from normal and albumin-sensitive guinea-pigs. *Br. J. Pharmacol.*, **92**, 809–816.

MANN, J.S., CUSHLEY, M.J. & HOLGATE, S.T. (1985). Adenosine-induced bronchoconstriction in asthma. Role of parasympathetic stimulation and adrenergic inhibition. *Am. Rev. Resp. Dis.*, **132**, 1–6.

MANN, J.S. & HOLGATE, S.T. (1985). Specific antagonism of adenosine-induced bronchoconstriction in asthma by oral theophylline. *Br. J. Clin. Pharmacol.*, **19**, 685–692.

MANSOUR, S. & DANIEL, E.E. (1987). Responsiveness of isolated tracheal smooth muscle from normal and sensitized guinea pigs. *Can. J. Physiol. Pharmacol.*, **65**, 1942–1950.

MANZINI, S. & BALLATI, L. (1990). 2-Chloroadenosine induction of vagally-mediated and atropine-resistant bronchomotor responses in anaesthetized guinea-pigs. *Br. J. Pharmacol.*, **100**, 251–256.

MARQUARDT, D.L., PARKER, C.W. & SULLIVAN, T.J. (1978). Potentiation of mast cell mediator release by adenosine. *J. Immunol.*, **120**, 871–878.

MARQUARDT, D.L. & WALKER, L. (1987). Inhibition of mast cell adenosine responsiveness by chronic exposure to adenosine receptor agonists. *Biochem. Pharmacol.*, **36**, 4297–4302.

MITCHELL, H.W. & DENBOROUGH, M.A. (1979). Anaphylaxis in guinea-pig peripheral airways in vitro. *Eur. J. Pharmacol.*, **54**, 69–78.

NAPIER, F.E. & TEMPLE, D.M. (1987a). Theophylline's inhibition of antigen-induced contraction of human parenchymal strips is independent of adenosine antagonism. *Eur. J. Pharmacol.*, **142**, 253–260.

NAPIER, F.E. & TEMPLE, D.M. (1987b). The relation between effects of adenosine, theophylline and enprofylline on the contractility of sensitized guinea-pig lung strips. *J. Pharm. Pharmacol.*, **39**, 432–438.

PAUWELS, R. & VAN DER STRAETEN, M. (1983). The in vivo bronchoconstrictory effect of adenosine. *J. Allergy Clin. Immunol.*, **71**, 103P.

PAUWELS, R. & VAN DER STRAETEN, M. (1987). An animal model for adenosine-induced bronchoconstriction. *Am. Rev. Resp. Dis.*, **136**, 374–378.

PEACHELL, P.T., COLUMBO, M., KAGEY-SOBOTKA, A., LICHTENSTEIN, L.M. & MARONE, G. (1989). Adenosine potentiates mediator release from human lung mast cells. *Am. Rev. Resp. Dis.*, **138**, 1143–1151.

PHILLIPS, G.D., BAGGA, P.K., DJUKANOVIC, R. & HOLGATE, S.T. (1989). The influence of refractoriness to adenosine 5'-monophosphate on allergen-provoked bronchoconstriction in asthma. *Am. Rev. Resp. Dis.*, **140**, 321–326.

PHLLIPS, G.D., NG, W.H., CHURCH, M.K. & HOLGATE, S.T. (1990). The response of plasma histamine to bronchoprovocation with methacholine, adenosine 5'-monophosphate and allergen in atopic non-asthmatic subjects. *Am. Rev. Resp. Dis.*, **141**, 9–13.

POST, M.J., TE BIESEBEEK, J.D., WEMER, J., VAN ROOIJ, H.H. & PORSIUS, A.J. (1990). Adenosine enhances antigen-induced bronchoconstriction and histamine release in rat isolated lungs. *Agents Actions*, **30**, 30–33.

RAFFERTY, P., BEASLEY, C.R. & HOLGATE, S.T. (1987). The contribution of histamine to bronchoconstriction produced by inhaled allergen and adenosine 5'-monophosphate in asthma. *Am. Rev. Resp. Dis.*, **136**, 369–373.

RANKIN, J.A. (1989). The contribution of alveolar macrophages to hyperreactive airway disease. *J. Allergy Clin. Immunol.*, **83**, 722–729.

ROSENGARD, B.R., MAHALIK, C. & COCHRANE, D.E. (1986). Mast cell secretion: difference between immunologic and non-immunologic stimulation. *Agents Actions*, **19**, 133–140.

SAAD, M.H. & BURKA, J.F. (1983). Effects of immunological sensitization on the responses and sensitivity of guinea-pig airways to bronchoconstrictors. Modulation by selective inhibition of arachidonic acid metabolism. *Can. J. Physiol. Pharmacol.*, **61**, 876–893.

SANJAR, S., AOKI, S., KRISTERSSON, A., SMITH, D. & MORLEY, J. (1990). Antigen challenge induces pulmonary airway eosinophil accumulation and airway hyperreactivity in sensitized guinea-pigs: the effect of anti-asthmatic drugs. *Br. J. Pharmacol.*, **99**, 679–686.

SATCHELL, D. & SMITH, R. (1984). Adenosine causes contractions in spiral strips and relaxations in transverse strips of guinea-pig trachea: studies on mechanisms of action. *Eur. J. Pharmacol.*, **101**, 243–247.

THORNE, J. & BROADLEY, K.J. (1988a). A bronchoconstrictor response to adenosine in guinea-pig airway perfused lung. *Br. J. Pharmacol.*, **93**, 278P.

THORNE, J. & BROADLEY, K.J. (1988b). Effects of 8-PT and dipyridamole on bronchoconstriction and relaxant responses to adenosine. *Br. J. Pharmacol.*, **95,** 796P.

THORNE, J.R. & BROADLEY, K.J. (1990a). Adenosine-induced bronchoconstriction in the conscious guinea-pig. *Br. J. Pharmacol.*, **101,** 595P.

THORNE, J.R. & BROADLEY, K.J. (1990b). Examination of adenosine on superfused trachea from normal and sensitized guinea-pigs. *Br. J. Pharmacol.*, **99,** 185P.

THORNE, J.R. & BROADLEY, K.J. (1991). Examination of possible mediators of the adenosine-induced bronchoconstriction *in vitro*. *Fund. Clin. Pharmacol.*, **5,** 428P.

TURNER, N.C. & DOLLERY, C.T. (1988). Release of arachidonic acid metabolites and histamine from sensitized guinea-pig lung following antigen challenge. *Br. J. Pharmacol.*, **93,** 751–758.

WELTON, A.F. & SIMKO, B.A. (1980). Regulatory role of adenosine in antigen-induced histamine release from the lung tissue of actively sensitized guinea-pigs. *Biochem. Pharmacol.*, **29,** 1085–1092.

(Received September 3, 1991
Revised January 15, 1992
Accepted April 14, 1992)

Br. J. Pharmacol. (1992), **106**, 986-995 © Macmillan Press Ltd, 1992

[^{3}H]-MK 912 binding delineates two α_2-adrenoceptor subtypes in rat CNS one of which is identical with the cloned pA2d α_2-adrenoceptor

Staffan Uhlén, Yun Xia, Vijay Chhajlani, *Christian C. Felder & Jarl E.S. Wikberg

Department of Pharmacology, Umeå University, S-901 87 Umeå, Sweden and *Department of Health & Human Services, National Institute of Mental Health, Bethesda, MD 20892, U.S.A.

1 Simultaneous computer modelling of control and guanfacine-masked [^{3}H]-MK 912 saturation curves as well as guanfacine competition curves revealed that the drugs bound to two α_2-adrenoceptor subtypes in the rat cerebral cortex with very different selectivities. These α_2-adrenoceptor subtypes were designated α_{2A} and α_{2C}. The K_d value of [^{3}H]-MK 912 for the α_{2A}-subtype was 1.77 nM and for the α_{2C}-subtype 0.075 nM; the receptor sites showing capacities 296 and 33 fmol mg^{-1} protein, respectively. The K_ds of guanfacine were 19.9 and 344 nM, respectively.

2 Binding constants of 26 compounds for the two rat cerebral cortex α_2-adrenoceptor subtypes were determined by simultaneous computer modelling of control and guanfacine-masked drug competition curves as well as plain guanfacine competition curves using [^{3}H]-MK912 as labelled ligand (i.e. a '3-curve assay'). Of the tested drugs WB4101, corynanthine, rauwolscine, yohimbine, ARC 239 and prazosin were found to be clearly α_{2C}-selective with selectivities ranging from 16 to 30 fold whereas guanfacine, oxymetazoline, BRL 44408 and BRL 41992 were found to be α_{2A}-selective with selectivities ranging from 9 to 22 fold.

3 The K_ds of compounds obtained for the cerebral cortex α_{2C}-adrenoceptors showed an almost 1:1 correlation with the corresponding K_ds for α_2-adrenoceptors expressed by the pA2d-gene (the rat 'α_2-C4' adrenoceptor) in CHO-cells. The cerebral cortex α_{2A}-adrenoceptors did not correlate well with the pA2d α_2-adrenoceptor K_ds.

4 In the rat spinal cord [^{3}H]-MK 912 bound to α_{2A}- and α_{2C}-adrenoceptor sites with similar affinities as in the cerebral cortex and with densities 172 and 7.4 fmol mg^{-1} protein, respectively. Drug affinities for some compounds showing major selectivity for α_{2A}- and α_{2C}-adrenoceptors were fully compatible with the notion that the spinal cord sites were α_{2A}- and α_{2C}-adrenoceptors.

Keywords: α-adrenoceptor subtypes; cerebral cortex; spinal cord; α_2-adrenoceptor gene expression; receptor classification; [^{3}H]-MK 912 ligand binding; computer modelling

Introduction

The G-protein coupled receptors represent a large family of receptors with a rapidly growing number of members. Among the G-protein coupled receptors the adrenoceptors have probably been the most intensely studied. Using pharmacological criteria these receptors were originally divided into two classes called α and β by Ahlquist (1948). Subsequent pharmacological studies then showed that they consisted of at least four types: α_1 and α_2 (see Berthelsen & Pettinger, 1977; Wikberg, 1978) and β_1 and β_2 (Lands *et al.*, 1967). More recently both molecular cloning of the genes for several adrenoceptors and pharmacological studies indicate the presence of many more subtypes of the adrenoceptors (reviewed by Harrison *et al.*, 1991a). In particular, for α_2-adrenoceptors molecular cloning data have indicated the presence of at least three different genes in mammals coding for three distinct α_2-adrenoceptor subtypes (Harrison *et al.*, 1991a). However, using functional pharmacological studies it has not been clear how to align the molecularly defined α_2-adrenoceptors with the functional ones. We have previously shown that radioligand binding with [^{3}H]-RX821002 can clearly delineate between α_{2A}- and α_{2B}-adrenoceptors in the rat kidney (Uhlén & Wikberg, 1991b). In another study we have shown that [^{3}H]-RX821002 can label an α_{2A}-type of adrenoceptor in the cerebral cortex and spinal cord of the rat (Uhlén & Wikberg, 1991a). We now present data that a recently introduced radioligand, [^{3}H]-MK 912 (L-657,743) (Pettibone *et al.*, 1989), besides labelling the α_{2A}-adrenoceptor can delineate one additional receptor subtype belonging to the α_2-adrenoceptor family in the cerebral cortex and spinal cord of the rat. The new central system α_2-adrenoceptor has been designated α_{2C} and it shows identical binding properties as the previously cloned pA2d α_2-adrenoceptor ('rat α_2-C4') (Voigt *et al.*, 1991).

Methods

Cell culture

Chinese hamster ovary cells (CHO) transfected and stably expressing the rat pA2d α_2-adrenoceptor clone (Voigt *et al.*, 1991) were grown in MEM alpha medium with 12% (v/v) foetal calf serum. Exponentially growing cultures were trypsinized and subcultured in 225 cm^2 tissue culture flasks in fresh medium.

Membrane preparations

Membranes from cerebral cortex and spinal cord were prepared from Sprague-Dawley rats, as described previously (Uhlén & Wikberg, 1991a). The final pellets were diluted to protein concentrations of ~1.2 mg protein ml^{-1}, using 1.5 mM EDTA, 50 mM Tris-HCl pH 7.5. CHO cell membranes were prepared by washing confluent cultures once with ice-cold phosphate buffered saline (PBS). Cells were scraped into PBS containing 0.54 mM EDTA, pH 7.2, with a rubber policeman. After centrifugation at 800 *g* for 10 min, cells were resuspended in ice-cold 50 mM Tris-HCl, 5 mM EDTA, 0.1 mM phenylmethyl sulphonyl fluoride, 10 μg ml^{-1} soybean trypsin inhibitor and 200 μg ml^{-1} bacitracin, pH 7.5, and

homogenized 15 s × 3 with an Ultra-Turrax T25 at 24,000 r.p.m. The homogenates were then spun at 500 *g* for 10 min and the supernatants collected and spun at 38,000 *g* for 15 min. The final pellets were resuspended in 1.5 mM EDTA, 50 mM Tris-HCl, pH 7.5, and frozen and stored at − 80°C until used for radioligand binding. Protein was measured according to Lowry *et al.* (1951).

Binding studies

Radioligand binding was performed essentially as described (Uhlén & Wikberg, 1991a) by, unless otherwise stated in the text, incubating 60–130 μg of the membranes in 150 μl of 1 mM EDTA, 100 μM Gpp(NH)p (guanyl-5'-yl-imido-diphosphate), 140 mM NaCl, 33 mM Tris-Cl, pH 7.5 with [^{3}H]-MK 912 and drugs for 1 h at 25°C and then filtering and washing on Whatman GF/C filters. Kinetic studies showed that equilibrium of [^{3}H]-MK 912 binding was essentially completely attained after 30 min both in cerebral cortex and in CHO-cells expressing the pA2d gene. All assays were performed in duplicate. Non-specific binding was determined in the presence of 1 μM BDF 8933 (Armah, 1988; Uhlén & Wikberg, 1991b,c). Computer modelling of the data was performed as described (Uhlén & Wikberg, 1991b). In some experiments competition curves were also analyzed by fitting it to the four parameter logistic function by non-linear regression, as described previously (Bergström & Wikberg, 1986), with the purpose of obtaining IC_{50} values and Hill coefficients.

Isotopes, drugs and chemicals

[^{3}H]-MK 912, (2S, 12bS)1',3'dimethylspiro (1,3,4,5',6,6',7,12b-octahydro - 2H - benzo[b]furo[2,3-a]quinazoline) - 2,4'- pyrimidin- 2'-one, (79 Ci mmol^{-1}) was a kind gift from NEN. [^{3}H]-RX821002 (1,4-(6,7(n)-^{3}H)benzodioxan-2-methoxy-2-yl)-2-imidazole; 49 Ci mmol^{-1}) was from Amersham. (−)-Adrenaline, (−)-noradrenaline, chlorpromazine, corynanthine, prazosin and yohimbine were from Sigma Chemical Co.; (+)-adrenaline was from Sterling-Winthrop Res. Inst., Rensselaer, N.Y., U.S.A.; ARC 239 from Thomae, Biberach, Germany; BDF 8933 (4-fluoro-2-(imidazoline-2-ylamino)-isoindoline maleate) from Beiersdorf AG, Hamburg, Germany; benoxathian and WB 4101 (N-[2-(2,6-dimethoxyphenoxy)ethyl]-2,3-dihydro-1,4-benzodioxin-2-methamine HCl) from RBI, Natick, MA, U.S.A.; BRL 44408 (2-[2H-(1-methyl-1,3-dihydroisoindole) methyl]-4,5-dihydroimidazole) and BRL 41992 (1,2-dimethyl-2,3,9,13b - tetrahydro - 1H - dibenzo[c,f]imidazo[1,5-a]azepine) from Beecham, Essex, U.K.; clonidine from Boehringer Ingelheim/Rhein, Germany; guanoxabenz and RU 24969 (5-methoxy-3-(1,2,3,6,tetrahydropridin-4-yl)-1H-indole) from Roussel, Romainville, France; methysergide from Sandoz, Basel, Switzerland; oxymetazoline from Draco, Lund, Sweden; (−)- and (+)-mianserin was from Organon, Oss, Holland; rauwolscine from Roth, Karlsruhe, Germany; RX 821002 (1,4-6,7(n)-benzodioxan-2-methoxy-2-yl)-2-imidazole) was from Reckitt and Coleman, Kingston upon Hull, U.K.; rilmenidine was from Servier, Neuilly-sur-Seine, France; SKF 104078 (6-chloro - 9 - [(3 - methyl-2-butenyl) oxy] - 3 - methyl - 2,3,4,5-tetrahydro-1H- 3-benzapine) was from Smith Kline & French, Swedeland, PA, U.S.A. Guanfacine and guanabenz were gifts from Dr Claes Post, Astra, Södertälje, Sweden. MEM alpha medium and foetal calf serum were from GIBCO BRL. All other chemicals were purchased from Merck or Sigma and were of analytical quality.

Results

Evaluation of [^{3}H]-MK 912 binding in rat cerebral cortex

Preliminary studies indicated that [^{3}H]-Mk 912 bound to two sites with differing affinities in cerebral cortex membranes. Preliminary studies also indicated that guanfacine could compete with [^{3}H]-MK 912 at these sites with distinctly different affinities. As will be discussed in more detail below, one of these sites appears to be very similar to the α_{2A}-adrenoceptor among the α_{2A}- and α_{2B}-adrenoceptor subtypes that we have defined previously (Uhlén & Wikberg, 1991b), whereas the other seems to correspond to a novel α_2-adrenoceptor subtype designated α_{2C}. In order to evaluate the binding of [^{3}H]-MK 912 and guanfacine to these adrenoceptor sites combined saturation and competition experiments were performed as shown in Figure 1a–c. In these experiments, saturation curves of [^{3}H]-MK 912 were obtained by adding various concentrations of the tritiated ligand in the absence as well as in the presence of 0.1, 0.32 or 1 μM guanfacine. In addition, various concentrations of [^{3}H]-MK 912 were added in the presence of 1 μM BDF 8933 in order to define the non-specific binding. Moreover, in the same experiment a competition curve of guanfacine was obtained by adding various concentrations of guanfacine in the presence of a fixed concentration (~0.5 nM) of [^{3}H]-MK 912. The data for both the saturation curves and the competition curve were then simul-

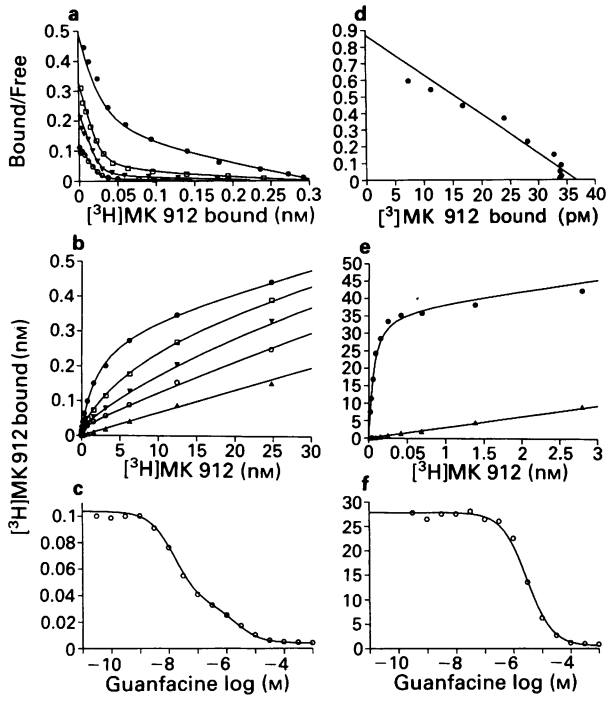

Figure 1 Saturation and competition experiments obtained on rat cerebral cortex membranes (a–c) or membranes prepared from CHO-cells expressing the pA2d α_2-adrenoceptor (d–f) with [^{3}H]-MK 912 as labelled ligand. Shown in (b) are saturation curves for total [^{3}H]-MK 912 binding (●), binding of [^{3}H]-MK 912 in the presence of 0.1 μM guanfacine (□), 0.32 μM guanfacine (▼), 1 μM guanfacine (○) and in the presence of 1 μM BDF 8933 (▲) in the cerebral cortex. Shown in (c) are competition curves of guanfacine obtained in the presence of 0.5 nM [^{3}H]-MK 912, using the same batch of cerebral cortex membranes and performed at the same time as the experiment shown in (b). The lines represent the computer drawn fits from the simultaneous fitting of the data in (b) and (c), assuming that ligands bound reversibly to two independent sites according to the law of mass action. In (a) is shown the Scatchard transform of the data shown in (b): (●) represent the total specific binding and (□), (▼), and (○) the specific binding obtained in the presence of 0.1, 0.32 and 1 μM guanfacine, respectively. Panels (a–c) represents one experiment out of 6 showing essentially the same results. In (e) is shown a saturation curve of [^{3}H]-MK 912 on pA2d α_2-adrenoceptor expressed in CHO-cells: (●) being the total binding and (▲) the non-specific binding, the latter obtained in the presence of 1 μM BDF 8933. In (d) is shown the Scatchard transform of the data shown in (e). In (f) is shown a competition curve of guanfacine obtained on the pA2d α_2-adrenoceptor in CHO-cell membranes using a concentration of ~0.5 nM [^{3}H]-MK 912.

taneously subjected to computer modelling, using the approach described previously (Uhlén & Wikberg, 1991b). The analysis indicated that a 2-site model approximated the data best since fitting the data to a 2-site model resulted in a drastic reduction in the sums of squares as compared to fitting the data to a 1-site model ($P<0.001$). Moreover, fitting the data to a 3-site model did not cause any significant further reductions in the sums of squares compared to the 2-site model. From 6 separate experiments the K_ds of [^{3}H]-MK 912 for the two sites were estimated to be 1.77 ± 0.10 and 0.075 ± 0.005 nM with capacities 296 ± 15 and 33.2 ± 2.6 fmol mg^{-1} protein (mean ± s.e.mean; $n = 6$), for the α_{2A}- and α_{2C}-sites, respectively. These values corresponded to the proportion of sites being $90.2 \pm 0.6\%$ α_{2A} and $9.8 \pm 0.6\%$ α_{2C} and the affinity of the radioligand being 24 fold higher for the α_{2C}-site. The K_ds of guanfacine were in these tests determined to be 19.9 ± 4.9 nM and 344 ± 56 nM for the α_{2A}- and the α_{2C}-sites, respectively. These differences in drug affinities are clearly reflected in the curves shown in Figure 1. Firstly, the competition curve shown in Figure 1c is clearly biphasic reflecting the ~24-fold higher affinity of guanfacine for the α_{2A}-adrenoceptor. Moreover, as can be seen from the Scatchard transform of the saturation studies (Figure 1a), the curve representing total specific binding is non-linear reflecting the binding of [^{3}H]-MK 912 to two sites. However, when increasing concentrations of guanfacine are added the lower affinity component of [^{3}H]-MK 912 binding diminishes progressively so that in the presence of 1 μM of guanfacine almost only the high affinity binding component, which also shows low capacity for [^{3}H]-MK 912, is remaining.

Determination of drug dissociation constants for α_{2A}- and α_{2C}-adrenoceptors in rat cerebral cortex by 3-curve assay

In order to determine the binding constants of drugs for the α_{2A}- and the α_{2C}-sites we used a 3-curve approach that we have documented previously to yield accurate determination of drug binding constants for systems with 2 receptors present (Uhlén & Wikberg, 1991b). In these tests 3 competition curves were obtained for each drug test using ~0.4 nM [^{3}H]-MK 912. One curve was for the tested compound alone and one was for the tested compound obtained in the presence of a fixed concentration of guanfacine (1 μM). The third curve was a full competition curve for guanfacine (see Figure 2a,b for examples of the approach). All three curves were then subjected to simultaneous computer modelling. In Figure 2 representative experiments are shown from these tests. As can be seen, the competition curves of guanfacine are strongly biphasic. Several of the drug competition curves obtained in the absence of guanfacine were also clearly biphasic or shallow. In contrast, all drug competition curves were uniphasic when 1 μM guanfacine was present. Simultaneous computer modelling of the three curves of each experiment showed that a two site model fitted the data best. Thus, fitting the data to a two site model resulted in highly significant decreases in the sums of squares ($P<0.0001$), compared to a one site model. On the other hand use of models involving three sites gave only insignificant reductions in the sums of squares, compared to the two site model.

As can be seen from Figure 2 different patterns are obtained depending on which drug is tested in the assay. Figure 2a shows results for oxymetazoline, a drug which was found to be selective for the α_{2A}-site, similar to guanfacine. In the presence of guanfacine the biphasicity of the oxymetazoline competition curve is eliminated so that the curve covers only the low affinity range of the original oxymetazoline competition curve. This pattern indicates the α_{2A}-selectivity of oxymetazoline.

In contrast, rauwolscine gives a completely different pattern (Figure 2b). The competition curve of rauwolscine obtained in the presence of guanfacine covers only the high affinity range of the plain rauwolscine competition curve.

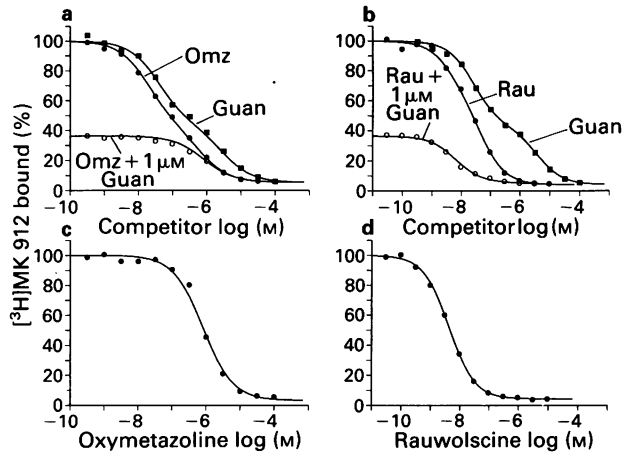

Figure 2 Competition curves of drugs obtained with [^{3}H]-MK 912 and rat cerebral cortex membranes (a,b) or membranes prepared from CHO-cells expressing the pA2d α_2-adrenoceptor (c,d). In (a,b) are shown competition curves obtained by incubating cerebral cortex membranes with ~0.4 nM [^{3}H]-MK 912 and various concentrations of guanfacine (■; Guan), various concentrations of a test compound (●) or various concentrations of the test compound in the presence of a fixed concentration (1 μM) of guanfacine (○). The test compound in (a) was oxymetazoline (Omz) and in (b) rauwolscine (Rau). The curved lines represent the computer drawn fits obtained from the simultaneous fitting of all data in each experiment to a model that assumed that ligands bound to two independent sites according to the law of mass action. In (c,d) are shown competition curves of oxymetazoline and rauwolscine using ~0.4 nM [^{3}H]-MK 912 on the expressed pA2d α_2-adrenoceptor. The curved lines represent the computer drawn fits obtained under the assumption that ligands bound to one site according to the law of mass action. The specific binding of [^{3}H]-MK 912 ranged between 92 and 94%.

Thus, this pattern demonstrates the α_{2C}-selectivity of rauwolscine.

Table 1 gives the binding constants obtained for 26 compounds by the 3-curve approach. Of these compounds WB4101, corynanthine, rauwolscine, yohimbine, ARC 239 and prazosin were found to be clearly α_{2C}-selective; their selectivites ranging from 16 to 30 fold. Guanfacine, oxymetazoline, BRL 44408 and BRL 41992 were found to be α_{2A}-selective with selectivites ranging from 9 to 22 fold. Other compounds were non-selective or showed only minor selectivity for any one of the receptor subtypes. It is also interesting to note that (-)-noradrenaline appeared to be slightly α_{2C}-selective whereas (-)-adrenaline was non-selective for α_{2A}- and α_{2C}-adrenoceptors.

The proportion of sites from all these tests were determined to be 88.2 ± 2.0 and $11.8 \pm 2.0\%$ for the α_{2A}- and α_{2C}-sites, respectively. Thus, these values were almost identical to those obtained above for the proportion of sites determined in the combined saturation and competition studies.

Evaluation of [^{3}H]-MK 912 binding to expressed α_2-pA2d adrenoceptors

In order to obtain data for comparison we also assessed binding of [^{3}H]-MK912 to the expressed pA2d α_2-adrenoceptor. Figures 1d–f and 2c,d show saturation and competition curves from some of these tests. For all tests both the saturation and the competition curves modelled best into one-site fits, as expected. The K_d of [^{3}H]-MK 912 obtained from the saturation studies were 0.046 ± 0.003 nM with a capacity of 99.9 ± 2.2 fmol mg^{-1} protein ($n = 4$). The K_ds of 26 drugs tested in competition with ~0.4 nM [^{3}H]-MK 912 are shown in Table 1.

Table 1 K_d values of drugs for cerebral cortex α_{2A}-, α_{2C}- and expressed pA2d-adrenoceptors obtained by computer analysis of competition curves obtained by use of [^{3}H]-MK 912 radioligand binding

Drugs	*Cerebral cortex* α_{2A}	α_{2C}		*CHO-cells* α_2-pA2d	
BDF 8933	0.412 ± 0.041	0.448 ± 0.033	(3)	0.468 ± 0.046	(4)
RX 821002	0.445 ± 0.034	0.552 ± 0.037	(3)	0.600 ± 0.014	(5)
Oxymetazoline	13.0 ± 0.5	119 ± 24	(3)	98.8 ± 18.5	(3)
BRL 44408	14.1 ± 1.1	128 ± 16	(4)	74.3 ± 2.0	(3)
Guanfacine	19.5 ± 1.2	421 ± 29	(22)	375 ± 30	(3)
BRL 41992	28.0 ± 3.0	276 ± 31	(4)	137 ± 2.0	(3)
Rauwolscine	34.5 ± 2.9	1.64 ± 0.54	(5)	0.851 ± 0.154	(4)
(+)-Mianserin	36.6 ± 1.0	29.4 ± 0.6	(3)	15.6 ± 0.3	(3)
Yohimbine	49.8 ± 1.5	2.79 ± 0.02	(3)	2.38 ± 0.13	(3)
Clonidine	73.0 ± 4.2	81.0 ± 0.9	(3)	88.1 ± 10.0	(3)
WB 4101	138 ± 7	4.53 ± 0.24	(3)	3.03 ± 0.64	(3)
UK 14,304	277 ± 72	221 ± 37	(3)	173 ± 36	(3)
(-)-Mianserin	283 ± 3	1190 ± 90	(3)	670 ± 22	(3)
SKF 104078	296 ± 28	55.7 ± 3.9	(3)	46.3 ± 5.1	(3)
Benoxathian	405 ± 24	41.7 ± 1.9	(3)	15.4 ± 1.6	(3)
Prazosin	492 ± 46	29.9 ± 4.1	(3)	32.3 ± 2.0	(4)
ARC 239	759 ± 14	45.8 ± 4.5	(3)	47.0 ± 4.7	(3)
RU 24969	978 ± 93	2730 ± 130	(3)	2320 ± 400	(3)
Rilmenidine	1320 ± 180	1080 ± 40	(3)	867 ± 174	(3)
Guanoxabenz	2500 ± 550	18,100 ± 3200	(3)	18,000 ± 2600	(4)
Methysergide	2870 ± 150	2500 ± 490	(3)	1820 ± 110	(3)
Chlorpromazine	2950 ± 250	2360 ± 110	(6)	686 ± 46	(4)
(-)-Adrenaline	3040 ± 270	2430 ± 220	(5)	1640 ± 110	(3)
Corynanthine	5900 ± 610	232 ± 34	(3)	143 ± 40	(3)
(-)-Noradrenaline	12,000 ± 1300	3280 ± 460	(3)	3830 ± 290	(3)
(+)-Adrenaline	30,300 ± 2800	15,200 ± 1100	(3)	11,000 ± 700	(3)

For cerebral cortex a 3-curve assay, which included competition curves of guanfacine as well as guanfacine masked and unmasked competition curves of the tested compound, was used (see text for details). For the pA2d α_2-adrenoceptor a single competition curve for the tested compound was used. The table shows the mean ± s.e.mean from 3–22 experiments as is indicated in parentheses, each experiment being based on 24–72 separate duplicate radioligand binding measurements.

Correlation of drug K_ds obtained for cerebral cortex and pA2d α_2-adrenoceptors

In Figure 3 are shown correlations of the $\log_{10}(K_d)$ values of the 26 drugs listed in Table 1 as well as the $\log_{10}(K_d)$ values obtained for [^{3}H]-MK 912 in the combined saturation and competition studies described above. As can be seen from Figure 3a the $\log_{10}(K_d)$ values for the cerebral cortex α_{2C}-adrenoceptor correlate very well ($r = 0.99$; $P < 0.001$) with those obtained for the expressed pA2d α_2-adrenoceptor, indicating that both sites are on the same α_2-adrenoceptor protein. Moreover, since the slope of the regression line was almost unity (0.99) and its intercept was almost exactly through the origin, the methods used seem to give unbiased estimates of drug K_ds. The correlations of cerebral cortex α_{2A}-adrenoceptors with cerebral cortex α_{2C}-adrenoceptors or pA2d α_2-adrenoceptors were clearly inferior (Figure 3b,c), indicating that the α_{2A}-adrenoceptor is distinct from the pA2d/α_{2C}-adrenoceptor.

Evaluation of [^{3}H]-MK 912 binding to rat spinal cord

We also evaluated the binding of [^{3}H]-MK 912 in the rat spinal cord by a similar approach to that used for the cerebral cortex. In Figure 4 are shown the combined saturation and competition studies from these efforts. Figure 4b shows saturation curves of [^{3}H]-MK 912 in the absence as well as in the presence of 0.6 μM guanfacine or 1 μM BDF 8933. In the same experiment competition curves of guanfacine were also obtained with ~0.5 nM [^{3}H]-MK 912 (Figure 4c). In these experiments a slightly lower concentration of guanfacine was used (0.6 μM) than in the cerebral cortex studies (1 μM) because the higher concentration of guanfacine in addition to blocking the α_{2A}-sites also blocked some of the α_{2C}-sites. Thus use of 0.6 μM guanfacine will leave more of the α_{2C}-sites available for [^{3}H]-MK 912 to bind to, while most of the α_{2A}-sites still remain blocked, something which was essential because of the low amount of α_{2C}-sites present in the spinal cord. As seen from the Scatchard transform (Figure 4a) of the saturation experiment of Figure 4b, the pattern obtained is almost identical to that obtained previously in the cerebral cortex, indicating the presence of both α_{2A}- and α_{2C}-sites. Moreover, the guanfacine competition curve is also clearly as biphasic as in the cerebral cortex, supporting this notion. The computer modelling also indicated that a two site model described the data the best. The K_ds of [^{3}H]-MK 912 obtained from the calculations were 1.80 ± 0.09 and 0.0637 ± 0.0078 nM with capacities 172 ± 12 and 7.38 ± 0.39 fmol mg^{-1} ($n = 4$), for the α_{2A}- and α_{2C}-sites, respectively. (The receptor densities corresponded to 95.8 ± 0.5 and 4.2 ± 0.5% of the total number of sites, repectively). K_d values for guanfacine were 23.9 ± 4.9 and 342 ± 46 nM for the α_{2A}- and α_{2C}-sites, respectively. Thus, since the K_d-values obtained in the spinal cord were almost identical to those found for the cerebral cortex α_{2A}- and α_{2C}-sites it is conceivable that [^{3}H]-MK 912 labelled the same adrenoceptor sites in both tissues.

A few drugs that we had found to be major delineators between α_{2A}- and α_{2C}-adrenoceptors in the cerebral cortex were also evaluated in the spinal cord with a similar 3-curve assay to that used in the cortex. In these experiments the masking guanfacine concentration was reduced to 0.6 μM for the same reason as stated above. The data from these tests are given in Table 2. As can be seen from Table 2, the K_d values of the 6 tested compounds for the spinal cord α_{2A}- and α_{2C}-sites compared favourably to those obtained previously for cerebral cortex α_{2A}- and α_{2C}-sites, as well as those obtained for the expressed pA2d α_2-adrenoceptors (Table 1).

Evaluation of assay buffer

It is known from many previous studies that α_2-adrenoceptors may exist in high and low affinity conformations for agonists; the receptor being brought from the low to

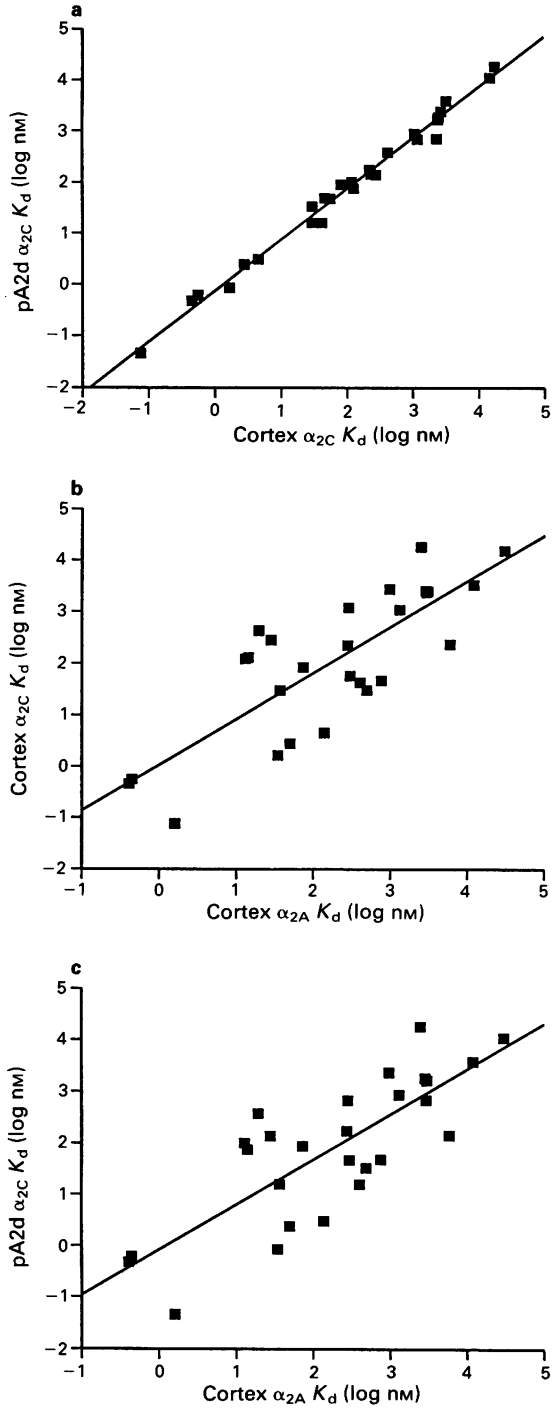

Figure 3 Correlation of $\log_{10}(K_d)$-values of the 26 compounds shown in Table 1. In the correlation was also included the $\log_{10}(K_d)$ values of [^{3}H]-MK 912 obtained by combined saturation and competition studies (data given in the text). (a) Correlation of data obtained for cerebral cortex α_{2C}- and expressed pA2d α_{2C}-adrenoceptor $\log_{10}(K_d$s). (The regression line was $y = 0.99x - 0.13$, with $r = 0.99$ and $P < 0.0001$). (b) Correlation for cerebral cortex α_{2A}-and α_{2C}-adrenoceptor $\log_{10}(K_d$s). ($r = 0.80$; $P < 0.001$). (c) Correlation for cerebral cortex α_{2A}- and pA2d α_{2C}-adrenoceptor $\log_{10}(K_d$s). ($r = 0.79$; $P < 0.001$).

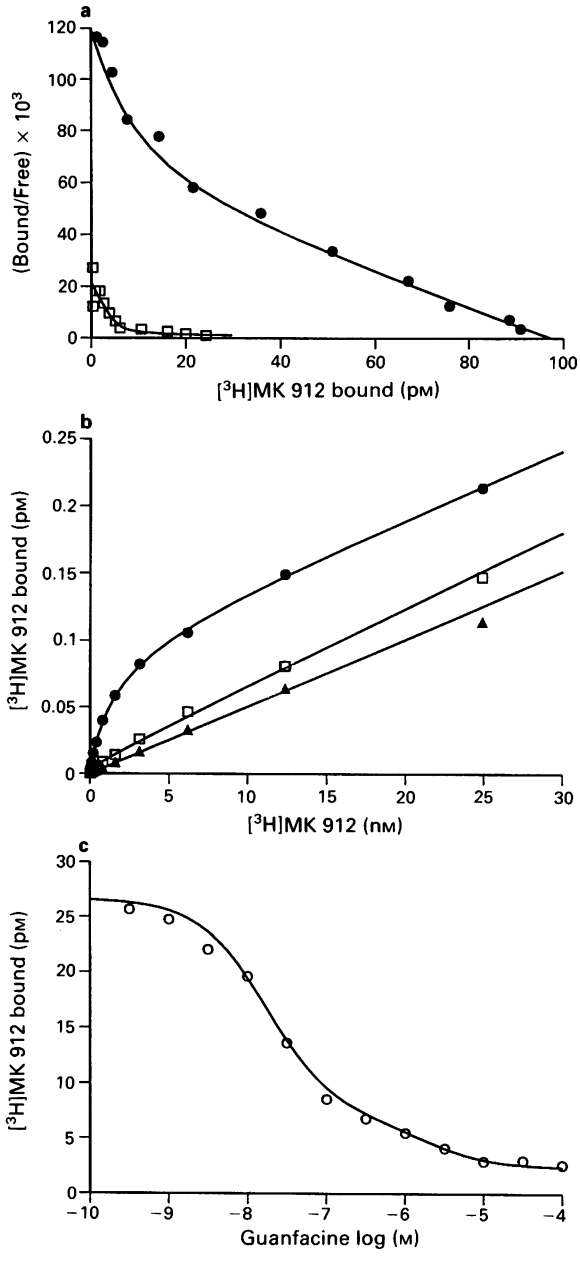

Figure 4 Saturation and competition experiments obtained on rat spinal cord membranes using [^{3}H]-MK 912 as labelled ligand. Shown in (b) are saturation curves for total [^{3}H]-MK 912 binding (●), binding of [^{3}H]-MK 912 in the presence of 0.6 μM guanfacine (□) as well as in the presence of 1 μM BDF 8933 (▲). Shown in (c) are competition curves of guanfacine obtained with ~0.5 nM of [^{3}H]-MK 912 and the same batch of spinal cord membranes and performed at the same time as the experiment shown in (b). The lines represent the computer drawn fits from the simultaneous fitting of the data in (b) and (c) assuming that ligands bound reversibly to two independent sites according to the law of mass action. In (a) is shown the Scatchard transformation of the data shown in (b); (●) represent the total specific binding and (□) the specific binding obtained in the presence of 0.6 μM guanfacine. Panels (a–c) represent one experiment out of 4 showing essentially the same results.

the high affinity conformation by the agonist induced association of the receptor with a G-protein (Hoffman *et al.*, 1980; 1982). Since agonists may have higher affinity for receptor G-protein complexes than for free receptors we sought to eliminate the association of the receptors with G-proteins by including into the assay buffer Gpp(NH)p, NaCl and EDTA. This was because all these agents may counteract the agonist promoted association of receptors with the G-proteins (Schloos *et al.*, 1987; Horstman *et al.*, 1990). In order to verify the effectiveness of this approach we obtained competition curves of (-)-adrenaline with assay buffers including various combinations of 1 mM EDTA, 2 mM $MgCl_2$, 0.1 mM Gpp(NH)p and 140 mM NaCl (Table 3). The α_{2A}-adrenoceptors were studied separately with the radioligand [^{3}H]-RX8210002 in the spinal cord (Uhlén & Wikberg, 1991a). In

Table 2 K_d-values of drugs obtained in competition with [^{3}H]-MK 912 in the rat spinal cord using the 3-curve assay (see text for details)

Drug	α_{2A} K_d (nM)	α_{2C} K_d (nM)	
Rauwolscine	31.8 ± 3.2	2.56 ± 0.74	(4)
ARC 239	744 ± 74	53.0 ± 5.2	(3)
Prazosin	581 ± 40	83.9 ± 5.2	(3)
Oxymetazoline	15.9 ± 1.2	102 ± 16	(3)
Guanfacine	22.8 ± 3.2	355 ± 31	(7)
WB4101	141 ± 4	3.16 ± 0.09	(3)

Number of determinations of K_ds are given in parentheses.

these studies [^{3}H]-RX8210002 was used rather than [^{3}H]-MK 912 because it is nonselective for α_{2A} and α_{2C}-adrenoceptors. Thus, [^{3}H]-RX8210002 will not reveal the minor population of α_{2C}-adrenoceptors in the spinal cord. Instead essentially the whole signal of specific [^{3}H]-RX8210002 binding will be from the α_{2A}-adrenoceptors; see also Table 4 and Uhlén & Wikberg, 1991a. The α_{2C}-adrenoceptors were studied by use of [^{3}H]-MK 912 and expressed pA2d α_{2C}-adrenoceptors. Table 3 gives the slope factors (Hill coefficients; n_H) and the IC_{50} values of the (-)-adrenaline competition curves obtained by fitting the data to the four parameter logistic function. As can be seen from the table, in the presence of Mg^{2+} the (-)-adrenaline competition curves were shallow for both α_{2A}- and α_{2C}-adrenoceptors indicating the presence of high and low affinity sites for the agonist for both the receptor subtypes. The additions of Gpp(NH)p or NaCl as well as the exchange of $MgCl_2$ with EDTA rendered the curves more steep. These effects appeared to be additive so that the combination of EDTA, Gpp(NH)p and NaCl gave the steepest curves for which the Hill coefficients approached unity. Thus, this finding indicates that the EDTA, Gpp(NH)p and NaCl assay buffer used for all the experiments in this study will essentially eliminate completely the agonist high affinity sites for both the α_{2A}- and the α_{2C}-adrenoceptors.

Discussion

In the present study we have shown that [^{3}H]-MK 912 binds to two different sites in rat cerebral cortex. Both sites appear to represent α_2-adrenoceptors. This is because they both show the expected adrenoceptor stereoselectivity for (+)- and (-)-adrenaline and the expected α_2-order of affinities for classical α_1- or α_2-adrenoceptor selective blockers such as prazosin, yohimbine and rauwolscine. Nevertheless the two sites show grossly different binding affinities for certain drugs. The compounds that differed most in their affinities for the two sites were WB4101, corynanthine and rauwolscine as well as [^{3}H]-MK 912 itself (all being 21 to 30 fold α_{2C}-selective), yohimbine, ARC 239 and prazosin (all being about 16 to 18 fold α_{2C}-selective) and guanfacine (22 fold α_{2A}-selective). Moreover, the data obtained in the spinal cord are also fully compatible with the notion that two identical α_2-adrenoceptor sites as in cerebral cortex are labelled by [^{3}H]-MK 912 in this tissue.

In order to simplify the following discussion the K_d-values of some drugs determined for α_{2A}- and α_{2B}-adrenoceptors in some of our recent studies (Uhlén & Wikberg, 1991b; Xia, Uhlén, Lien & Wikberg, unpublished) are given in Table 4, along with the corresponding K_d-values for cerebral cortex and expressed pA2d α_2-adrenoceptors obtained in the present paper. As seen from the table and discussed above, the drug K_ds for the cerebral cortex α_{2C}-adrenoceptor are virtually identical to the K_ds obtained on the expressed pA2d-adrenoceptor, clearly indicating that these sites are on the same α_2-adrenoceptor protein. As can be seen from the table the α_{2C}-adrenoceptor is clearly distinct from the cerebral cortex and kidney α_{2A}-adrenoceptors. The most α_{2C}-selective compounds are WB 4101, corynanthine, rauwolscine, yohimbine and ARC 239, whereas the most α_{2A}-selective is guanfacine. Table 4 also shows that the α_{2C}-adrenoceptor is distinct from the α_{2B}-adrenoceptor. The best compound delineating between α_{2B} and α_{2C}-adrenoceptors is MK-912 itself, the compound being between 10 to 28 fold α_{2C}-selective. Otherwise the best drugs delineating between α_{2C}- and α_{2B}-adrenoceptors are oxymetazoline (between 7 to 17 fold α_{2C}-selective), WB 4101 (between 6 to 18 fold α_{2C}-

Table 3 Hill coefficients (n_H) and IC_{50} values of (-)-adrenaline competition curves obtained by using radioligand binding with 1.4 nM [^{3}H]-RX821002 in spinal cord membranes (**A**) or 0.4 nM [^{3}H]-MK 912 on expressed pA2d α_{2C}-adrenoceptor in CHO-cell membranes (**B**)

A *(-)-Adrenaline/α_{2A}-adrenoceptors*

Assay buffer	n_H	IC_{50}	
2 mM $MgCl_2$	0.48 ± 0.02	84.5 ± 21.8	(4)
+ 0.1 mM Gpp(NH)p	0.69 ± 0.03	1590 ± 450	(4)
+ 0.140 mM NaCl	0.52 ± 0.02	412 ± 51	(4)
+ 0.1 mM Gpp(NH)p, 140 mM NaCl	0.80 ± 0.03	8580 ± 1770	(4)
1 mM EDTA	0.64 ± 0.02	439 ± 131	(4)
+ 0.1 mM Gpp(NH)p	0.74 ± 0.01	1050 ± 210	(4)
+ 0.140 mM NaCl	0.79 ± 0.02	5040 ± 1030	(4)
+ 0.1 mM Gpp(NH)p, 140 mM NaCl	0.89 ± 0.02	9580 ± 204	(8)

B *(-)-Adrenaline/α_{2C}-adrenoceptors*

Assay buffer	n_H	IC_{50}	
2 mM $MgCl_2$	0.69 ± 0.05	358 ± 116	(2)
+ 0.1 mM Gpp(NH)p	0.84 ± 0.07	2300 ± 740	(2)
+ 0.140 mM NaCl	0.70 ± 0.02	2520 ± 110	(2)
+ 0.1 mM Gpp(NH)p, 140 mM NaCl	0.92 ± 0.06	24300 ± 4200	(4)
1 mM EDTA	0.74 ± 0.07	732 ± 198	(2)
+ 0.1 mM Gpp(NH)p	0.80 ± 0.01	1420 ± 720	(2)
+ 0.140 mM NaCl	0.70 ± 0.06	5530 ± 160	(2)
+ 0.1 mM Gpp(NH)p, 140 mM NaCl	0.97 ± 0.05	15200 ± 1800	(6)

The n_Hs and IC_{50} values were determined by fitting the data to the four parameter logistic function. The assay buffer contained 33 mM Tris-HCl, pH 7.5, and the additions shown in the table. Values in parentheses denote number of experiments.

Table 4 K_d-values of drugs for α_2-adrenoceptor subtypes in the rat

	[^{3}H]-RX821002 binding			*[^{3}H]-MK-912 binding*			
	Kidney		Kidney	Lung	Cerebral cortex		pA2d
	α_{2A}	α_{2B}	α_{2B}	α_{2B}	α_{2A}	α_{2C}	α_{2C}
RX-821002	0.68†	2.6†	–	–	0.46	0.55	0.6
MK-912	2.5	1.3	1.1*	0.77*	1.8*	0.075*	0.046*
Guanfacine	31	1900	2000	1600	20	420	380
Oxymetazoline	35	1700	1300	860	13	120	99
Yohimbine	58	16	14	10	50	2.8	2.4
Rauwolscine	68	13	9.3	9.3	34	1.6	0.85
BRL 41992	78	34	43	22	28	276	137
WB 4101	180	53	35	26	140	4.5	3
Prazosin	1400	52	37	19	490	30	32
ARC 239	1500	14	14	8.8	760	46	47
(-)-Adrenaline	3100	4700	5400	3700	3000	2400	1600
Corynanthine	8600	510	–	–	5900	230	140
(-)-Noradrenaline	13000	3600	4800	3000	12000	3300	3800
(+)-Adrenaline	39000	34000	55000	35000	30000	15000	11000

Drug K_d-values for rat kidney α_2-adrenoceptor subtypes obtained with [^{3}H]-RX821002 as radioligand were taken from Uhlén & Wikberg (1991b), except the K_d-values for (-)-noradrenaline and (+)-adrenaline. The latter values were obtained by recalculation of the data reported in Uhlén & Wikberg (1991c) by using exactly the same calculation as described in Uhlén & Wikberg (1991b). The values for rat kidney and neonatal rat lung α_{2B}-adrenoceptors were taken from unpublished results of Y. Xia, S. Uhlén, E.J. Lien & J.E.S. Wikberg. In this study, drug K_ds were determined by using [^{3}H]-MK 912 binding and the NaCl, Gpp(NH)p and EDTA containing assay buffer of the present paper. Values of cerebral cortex and pA2d α_2-adrenoceptors are repeated from Table 1 of the present study. †Denotes that K_d values for RX-8210002 represent those determined for [^{3}H]-RX821002. *Denotes that K_d values for MK-912 represent those determined for [^{3}H]-MK 912.

selective), rauwolscine (between 6 to 15 fold α_{2C}-selective) and BRL 41992 (between 3 to 13 fold α_{2B}-selective). Most other drugs tested show some selectivities for these adrenoceptor subtypes but the selectivities are less marked. Moreover, as shown in Table 4, the correlation between α_{2B}-adrenoceptor K_ds in the kidney and the neonatal lungs are excellent indicating their similar natures. It is also notable that the α_{2B}-adrenoceptor drug K_ds are the same irrespective of whether [^{3}H]-RX821002 or [^{3}H]-MK 912 is used as radioligand (Table 4).

Previous studies have shown that at least three different genes coding for α_2-adrenoceptors are present in mammals. Lefkowitz and coworkers have cloned three different human α_2-adrenoceptor genes, called α_2-C2, α_2-C4 and α_2-C10, which code for distinct α_2-adrenoceptor proteins (Kobilka *et al.*, 1987; Regan *et al.*, 1988; Lomasney *et al.*, 1990). Genes homologous to these human genes have also been cloned in the rat, namely the RNG gene (Zeng *et al.*, 1990), the pA2d gene (Voigt *et al.*, 1991) and the cA20-47 gene (Chalberg *et al.*, 1990). Moreover, Lanier *et al.* (1991) also recently isolated two rat clones, RG10 and RG20, which show only minor differences from the pA2d- and cA2-47 genes, respectively.

Previous studies on the pharmacological properties of expressed α_2-adrenoceptors have clearly indicated that the RG20-gene codes for an α_2-adrenoceptor with an α_{2A}-profile (Harrison *et al.*, 1991b), as it was defined originally by Bylund (1985) (i.e. an α_2-adrenoceptor showing high affinity for oxymetazoline and low affinity for prazosin). The pharmacological properties for the cerebral cortex α_{2A}-adrenoceptor (Table 2) are similar to those found by Harrison *et al.* (1991b) for the expressed RG20-receptor in that it shows relatively low affinity for prazosin and yohimbine but high affinity for oxymetazoline. Northern blot analysis have indicated that both RG10 and RG20, but not RNG, are abundantly expressed in the central nervous system of the rat (Zeng & Lynch, 1991). Since the pharmacological properties of both RG10 and RNG (see below) are very different from those of an α_{2A}-type of adrenoceptor, RG20 may seem to be a strong candidate for the α_{2A}-adrenoceptor observed in the present paper.

As discussed above, the present paper gives unequivocal evidence that the pA2d (RG10) gene codes for a pharmacologically distinct α_2-adrenoceptor which is located in both rat cerebral cortex and spinal cord. The pharmacological properties of this receptor are clearly distinct from those of the α_{2A}- and α_{2B}-adrenoceptor subtypes that we have investigated previously in the rat (Uhlén & Wikberg, 1991b; Xia *et al.*, unpublished) using exactly the same assay buffer as in the present study (see Table 4). Harrison *et al.* (1991b) have suggested that the receptor coded for by RG10, as well as the human α_2-C4, are species analogues of the α_{2C}-adrenoceptor originally found in an oppossum kidney (OK) cell line by Murphy & Bylund (1988). This was because the pharmacology of RG10 and α_2-C4 showed some resemblance to that of the opposum α_{2C}-receptor. (One of the characteristics of the α_{2C}-receptor was that oxymetazoline showed an affinity in between that for α_{2A}- and α_{2B}-adrenoceptors. Moreover, the affinity of rauwolscine and yohimbine was higher for the α_{2C}- than for α_{2A}- and α_{2B}-adrenoceptors, whereas the affinity of prazosin and ARC239 was much higher for the α_{2C}- than for an α_{2A}-adrenoceptor; see Bylund *et al.*, 1991). For these reasons we have chosen to use the nomenclature α_{2C} for the one of the two α_2-adrenoceptors in cerebral cortex and spinal cord which is labelled with the highest affinity by [^{3}H]-MK 912, and which appears to be identical to the adrenoceptor coded for by pA2d/RG10. Moreover, Lorenz *et al.* (1990) reported that the α_2-C4 gene gave a strong hybridization signal from mRNA isolated from OK cells when using northern blot analysis, supporting the view that the OK α_{2C}-adrenoceptor is a species variant of the C4 and pA2d/RG10 adrenoceptors. However, one must still bear in mind that clear differences are present in drug affinities between OK cell, C4, and pA2d/RG10 adrenoceptors (see Bylund *et al.*, 1991; Blaxall *et al.*, 1991). These differences may be due to species differences, the presence of heterogeneous receptor subtypes or to differences in assay conditions between different studies (cf. our K_d values with those reported by Harrison *et al.*, 1991b; see also below). Nevertheless, the contention that the cerebral cortex and spinal cord α_{2C}-adrenoceptor, as defined in the present paper, is identical with pA2d/RG10 is also strongly supported by the finding that RG10 hybridizable mRNA is present in the central nervous system of the rat (Zeng & Lynch, 1991). It is also clear that the expressed RNG α_2-adrenoceptor is not any of the adrenoceptors investigated in the present paper. This is because the RNG receptor shows very low affinity for oxymetazoline and is not expressed in the central nervous

system (Zeng & Lynch, 1991). Instead RNG is expressed in the rat kidney and neonatal rat lung (Zeng *et al.*, 1990); the latter being a tissue which is regarded as the 'prototypic source' for α_{2B}-adrenoceptors (Bylund *et al.*, 1988). It thus seems quite likely that the RNG codes the α_{2B}-adrenoceptor that we have previously detected in the rat (Uhlén & Wikberg, 1991b; Xia *et al.*, unpublished).

In another recent study we have noted that guanoxabenz can delineate the rat kidney α_{2B}-adrenoceptors into two different binding sites which show grossly different affinities ($\sim$70 fold) for guanoxabenz. These sites were designated α_{2B1} and α_{2B2} (Uhlén & Wikberg, 1991c). The rat kidney α_{2B1}- and α_{2B2}-sites clearly represent α_{2B}-types of adrenoceptors because none of the other α_{2A}, α_{2B} and α_{2C}-delineating drugs described in the present study are able to delineate between α_{2B1} and α_{2B2}-sites (Uhlén & Wikberg, 1991b,c). Thus, guanoxabenz appears to be a unique compound capable of the α_{2B1} and α_{2B2}-delineation. Interestingly, comparison of the data of the present study and our previous study in the rat kidney shows that guanoxabenz is $\sim$34-fold more potent for the kidney α_{2A}-adrenoceptor (K_d = 73 nM; Uhlén & Wikberg, 1991c) than for the cerebral cortex α_{2A}-adrenoceptor (K_d = 2500 nM; Table 1). Again this large difference in drug affinity for cerebral cortex and rat kidney α_{2A}-adrenoceptors is not observed for any other of the 20 drugs tested in the present as well as in some of our previous studies (cf. the data of Table 1 of the present study with the data in Uhlén & Wikberg, 1991b,c). The molecular basis for the ability of gunaoxabenz to seemingly delineate both α_{2A}- and α_{2B}-adrenoceptors into further subtypes might be due to the presence of distinct molecular species of α_2-adrenoceptors (e.g. 'α_{2A1}' and 'α_{2A2}' as well as 'α_{2B1}' and 'α_{2B2}'-adrenoceptors). However, this interpretation must be validated by the discovery of additional drugs capable of the guanoxabenz type of delineation, the validation of the guanoxabenz affinities on expressed α_2-adrenoceptor proteins as well as the eventual isolation of novel α_2-adrenoceptors genes capable of expressing receptors showing the matching guanoxabenz affinities. Interestingly, the results of our present study indicate that guanoxabenz cannot delineate between further α_{2C}-subtypes (Table 1).

The data of the present study indicate that the drug K_ds for α_2-adrenoceptor subtypes determined do not represent agonist binding to high affinity forms of α_2-adrenoceptors. This is because the inclusion of NaCl, Gpp(NH)p and EDTA in the assays rendered the slopes of the competition curves of (-)-adrenaline steep, with Hill coefficients approaching unity for both α_{2A}- and α_{2C}-adrenoceptors. These results thus indicate that agonist binding followed simple bimolecular kinetics and that therefore essentially all high affinity conformations of the receptors for agonists had been abolished. Our present results are in complete accord with the results of a previous study in which we have shown that NaCl, Gpp(NH)p and EDTA totally eliminate the agonist high affinity binding sites of α_2-adrenoceptors for agonists for α_{2A}-adrenoceptors in the rat spinal cord (Uhlén & Wikberg, 1991a). Moreover, the present results also show the importance of using all of the three reagents. This was because our data show that any combination which included less than all of the 140 mM NaCl, 0.1 mM Gpp(NH)p and 1 mM EDTA in the assay buffer gave clearly shallow (-)-adrenaline competition curves.

It is also important to note that others who have studied α_2-adrenoceptors with radioligand binding have in general used assay buffers differing from the present NaCl, Gpp(NH)p, EDTA containing buffer. The effects of Gpp(NH)p and EDTA are mediated on the G-proteins while Na^+ is interacting with a highly conserved aspartate residue located to transmembrane segment 2 in the G-protein coupled receptors, including all α_2-adrenoceptors that have been cloned to date (Horstman *et al.*, 1990). Gpp(NH)p and EDTA will affect the apparent K_ds of drugs by counteracting the association of the G-protein with the receptor leading to the elimination of the agonist high affinity state. The sodium ion is believed to induce a conformational change of the receptor which counteracts the association of the G-protein with the receptor. It also appears that this conformational change of the receptor will lower the affinity of agonists but leave the affinity of antagonists essentially unaltered or even increased (see Horstman *et al.*, 1990). Thus, it is of utmost importance to consider the assay conditions when comparison of drug K_ds is made between different studies. For example, in the study of Harrison *et al.* (1991b), chlorpromazine was reported to be a delineator among the three cloned and expressed rat α_2-adrenoceptor subtypes. In our hands chlorpromazine did not delineate between α_{2A}- and α_{2C}-adrenoceptors (Table 1). However, when we exchanged the NaCl, EDTA Gpp(NH)p buffer used in the present study with a 2.5 mM $MgCl_2$-containing buffer the affinity of chlorpromazine increased 13 fold for α_{2C}-sites but only 2-fold for α_{2A}-sites (Uhlén & Wikberg, unpublished observations). Our interpretation of these data is that chlorpromazine is a very weak agonist at the α_{2A}-adrenoceptor but a stronger agonist at the α_{2C}-adrenoceptor. Besides this, it is noteworthy that the correlation between drug K_ds obtained for expressed pA2d receptor and the cerebral cortex and spinal cord α_{2C}-adrenoceptor in the present study is excellent. The good correlations of K_ds of identical α_2-adrenoceptor subtypes verifies the power of the 3 curve approach to recover correct drug K_ds in cerebral cortex and spinal cord where two receptor sites are present (see Uhlén & Wikberg, 1991b, for a theoretical evalueation of the 3 curve assay used here). Moreover, the good correlation seems to indicate that confounding factors such as the formation of agonist high affinity states do not interfere in our assays.

In some previous studies, [^{3}H]-rauwolscine or [^{3}H]-yohimbine were reported to label two different sites in the rat cerebral cortex, presumed to be α_2-adrenoceptor subtypes (Bylund, 1985; Brown *et al.*, 1990). It is possible that these two sites were the α_{2A}- and α_{2C}-adrenoceptors since rauwolscine and yohimbine have higher affinities for the α_{2C}- than for the α_{2A}-adrenoceptors (Table 1) similar to [^{3}H]-MK 912. We have attempted to use [^{3}H]-rauwolscine in the rat cerebral cortex. In our hands, [^{3}H]-rauwolscine appeared to label 3 sites, namely the α_{2A}- and α_{2C}-adrenoceptors as well as a 5-hydroxytryptamine (5-HT) receptor (Uhlén & Wikberg, unpublished results; see also Broadhurst *et al.*, 1988). However, both [^{3}H]-raulwolscine and [^{3}H]-yohimbine are difficult to use because of their low affinities for α_2-adrenoceptors and their high non-specific binding. It is thus conceivable that previous studies using these radioligands in the brain might have been confounded by interference from 5-HT receptors and non-specific sites (cf. our K_ds for RU 24969 and methysergide and BRL 419912 when using [^{3}H]-MK 912 (Table 1) with the K_ds reported by Brown *et al.*, 1990 using [^{3}H]-yohimbine as well as those reported by Young *et al.*, 1989 using [^{3}H]-rauwolscine in the rat cerebral cortex). Compared to [^{3}H]-rauwolscine and [^{3}H]-yohimbine, [^{3}H]-MK 912 is simpler to use since the latter shows both high affinity for α_2-adrenoceptors and low non-specific binding. Moreover, [^{3}H]-MK 912 is not an imidazoline thus precluding imidazoline binding sites from interfering in the assays (see Wikberg & Uhlén, 1990 and references therein for accounts on imidazoline binding sites).

The finding that guanfacine was quite selective for one of the two α_2-adrenoceptors in the central nervous system is interesting. In a recent study we observed that whereas the antinociceptive effect of intrathecal UK-14,304 was highly susceptible to up-regulation after chronic depletion of spinal cord noradrenaline, the antinociceptive effect of intrathecal guanfacine was not (Uhlén *et al.*, 1990). Since our data (Table 1) indicate that UK-14,304 is non-slective for α_{2A}- and α_{2C}-adrenoceptors while guanfacine is about 22 fold α_{2A}-selective, it is tempting to speculate that the difference in susceptibility for the regulation of guanfacine and UK-14,304 effects is caused by the difference in their selectivity for

α_2-adrenoceptor subtypes. It is also interesting to note that while (+)-mianserin is equipotent at α_{2A}- and α_{2C}-adrenoceptors, (-)-mianserin is slightly selective for the α_{2A}-adrenoceptor (Table 1). A few years ago it was reported that while (-)-mianserin was a more potent blocker at presynaptric α_2-adrenoceptors located on 5-HT neurones than it was on presynaptic α_{2A}-adrenoceptors located on noradrenergic neurones of the rat brain, (+)-mianserin was equipotent on these α_2-adrenoceptors (Raiteri *et al.*, 1983; Maura *et al.*, 1985). The possibility that the central nervous system α_{2A}- and α_{2C}-adrenoceptors are located to different types of neurones and that they might show differential susceptibility for regulation is thus a subject that should deserve further studies.

In summary we have shown here that the novel radioligand [^{3}H]-MK 912 is useful for labelling two subtypes of α_2-adrenoceptors in the central nervous system of the rat. These two subtypes of α_2-adrenoceptors have been designated α_{2A} and α_{2C}. The rat CNS α_{2A}- and α_{2C}-adrenoceptors are distinct from the α_{2B}-adrenoceptors that we have previously delineated in the rat kidney and neonatal rat lung. Moreover, the rat CNS α_{2C}-adrenoceptor shows identical binding properties to the cloned and expressed pA2d ('rat α_2-C4') adrenoceptor, strongly linking the rat CNS α_{2C}-adrenoceptor with a molecularly defined structure.

We are indebted to Dr Douglas J. Pettibone, MSD, West Point, PA, U.S.A. for providing [^{3}H]-MK-912 which was used in the preliminary phase of the studies. We are also indebted to Mrs Britt Jacobsson for invaluable technical assistance. Supported by the Swedish MRC (04X-05975), CFN (91-02), the Swedish National Board for Technical Development (89-02211P), the Magnus Bergvall foundation, the Groshinsky foundation and funds from the Medical Faculty of Umeå University.

References

AHLQUIST, R.P. (1948). A study of the adrenotropic receptors. *Am. J. Physiol.*, **153**, 586–600.

ARMAH, B.I. (1988). BDF 8933: A novel alpha-2-receptor antagonist lacking the potential to induce noradrenaline overflow. *Naunyn-Schmiedebergs Arch. Pharmacol.*, (Suppl.) **338**, R55.

BERGSTRÖM, A. & WIKBERG, J.E.S. (1986). Structural and pharmacological differences between cod fish and rat brain α_1 receptors revealed by photoaffinity labeling with ^{125}I-APDQ. *Acta Pharmacol. Toxicol.*, **58**, 148–155.

BERTHELSEN, S. & PETTINGER, W.A. (1977). A functional basis for classification of alpha-adrenergic receptors. *Life Sci.*, **21**, 595–606.

BLAXALL, H., MURPHY, T.J., BAKER, J.C., RAY, C. & BYLUND, D.B. (1991). Characterization of the alpha-2C adrenergic receptor subtype in the opossum kidney and in the OK cell line. *J. Pharmacol. Exp. Ther.*, **259**, 323–329.

BROADHURST, A.M., ALEXANDER, B.S. & WOOD, M.D. (1988). Heterogenous ^{3}H-rauwolscine binding sites in rat cortex: Two alpha$_2$-adrenoceptor subtypes or an additional non-adrenergic interaction? *Life Sci.*, **43**, 83–92.

BROWN, C.M., MACKINNON, A.C., MCGRATH, J.C., SPEDDING, M. & KILPATRICK, A.T. (1990). Heterogeniety of α_2-adrenoceptors in rat cortex but not human platelets can be defined by 8-OH-DPAT, RU 24969 and methysergide. *Br. J. Pharmacol.*, **99**, 481–486.

BYLUND, D.B. (1985). Heterogeneity of alpha-2 adrenergic receptors. *Pharmacol. Biochem. Behav.*, **22**, 835–843.

BYLUND, D.B., RAY-PRENGER, C. & MURPHY, T.J. (1988). Alpha-2A and alpha-2B adrenergic receptor subtypes: antagonist binding in tissues and cell lines containing only one subtype. *J. Pharmacol. Exp. Ther.*, **245**, 600–607.

BYLUND, D.B., BLAXALL, H.S., MURPHY, T.J. & SIMMONEAUX, V. (1991). Pharmacological evidence for alpha-2C and alpha-2D adrenergic receptor subtypes. In *Adrenoceptors: Structure, Mechanisms, Function* ed. Szabadi, E. & Bradshaw, C.M. pp. 27–36. Basel: Birkhäuser.

CHALBERG, S.C., DUDA, T., RHINE, J.A. & SHARMA, R.K. (1990). Molecular cloning, sequencing and expression of an α_2-adrenergic receptor complementary DNA from rat brain. *Mol. Cell Biochem.*, **97**, 161–172.

HARRISON, J.K., PEARSON, W.R. & LYNCH, R.L. (1991a). Molecular characterization of α_1- and α_2-adrenoceptors. *Trends Pharmacol. Sci.*, **12**, 62–67.

HARRISON, J.K., D'ANGELO, D.D., ZENG, D. & LYNCH, K.R. (1991b). Pharmacological characterization of rat α_2-adrenergic receptors. *Mol. Pharmacol.*, **40**, 407–412.

HOFFMAN, B.B., MICHEL, J., MULLIKIN-KILPATRICK, D., LEFKOWITZ, R.J., TOLBERT, M.E.M., GILMAN, H. & FAIN, J.N. (1980). Agonist versus antagonist binding to alpha-adrenergic receptors. *Proc. Natl. Acad. Sci. U.S.A.*, **77**, 4569–4573.

HOFFMAN, B.B., MICHEL, T., BRENNEMAN, T.B. & LEFKOWITZ, R.J. (1982). Interactions of agonists with platelet α_2-adrenergic receptors. *Endocrinol.*, **110**, 926–932.

HORSTMAN, D.A., BRANDON, S., WILSON, A.L., GUYER, C.A., CRAGOE Jr, E.J. & LIMBIRD, L.E. (1990). An aspartate conserved among G-protein receptors confers allosteric regulation of α_2-adrenergic receptors by sodium. *J. Biol. Chem.*, **265**, 21590–21595.

KOBILKA, B.K., MATSUI, H., KOBILKA, T.S., YANG-FENG, T.L., FRANCKE, U., CARON, M.G., LEFKOWITZ, R.J. & REGAN, J.W. (1987). Cloning, sequencing, and expression of the gene coding for the human platelet α_2-adrenergic receptor. *Science*, **238**, 650–656.

LANDS, A.M., LUDUENA, F.P. & BUZZO, H.J. (1967). Differentiation of receptors responsive to isoproterenol. *Life Sci.*, **6**, 2241–2249.

LANIER, S.M., DOWNING, S., DUZIC, E. & HOMCY, C.J. (1991). Isolation of rat genomic clones encoding subtypes of the α_2-adrenergic receptor. *J. Biol. Chem.*, **266**, 10470–10478.

LOMASNEY, J.W., LORENZ, W., ALLEN, L.F., KING, K., REGAN, J.W., YANG-FENG, T.L., CARON, M.G. & LEFKOWITZ, R.J. (1990). Expansion of the α_2-adrenergic receptor family: Cloning and characterization of a human α_2-adrenergic receptor subtype, the gene for which is located on chromosome 2. *Proc. Natl. Acad. Sci. U.S.A.*, **87**, 5094–5098.

LORENZ, W., LOMASNEY, J.W., COLLINS, S., REGAN, J.W., CARON, M.G. & LEFKOWITZ, R.J. (1990). Expression of three α_2-adrenergic receptor subtypes in rat tissues: Implication for α_2 receptor classification. *Mol. Pharmacol.*, **38**, 599–603.

LOWRY, O.H., ROSEBROUGH, N.J., FARR, A.L. & RANDALL, R.J. (1951). Protein measurement with the folin phenol reagent. *J. Biol. Chem.*, **193**, 265–275.

MAURA, G., GEMIGNANI, A. & RAITERI, M. (1985). α_2-adrenoceptors in rat hypothalamus and cerebral cortex: Functional evidence for pharmacologically distinct subpopulations. *Eur. J. Pharmacol.*, **116**, 335–339.

MURPHY, T.J. & BYLUND, D.B. (1988). Characterization of α_2-adrenergic receptors in the OK cell, an apossum kidney cell line. *J. Pharmacol. Exp. Ther.*, **244**, 571–578.

PETTIBONE, D.J., FLAGG, S.D., TOTARO, J.A., CLINESCHMIDT, B.V., HUFF, J.R., YOUNG, S.D. & CHEN, R. (1989). [^{3}H]-L-657,743 (MK-912): A new, high affinity, selective radioligand for brain α_2-adrenoceptors. *Life Sci.*, **44**, 459–467.

RAITERI, M., MAURA, G., GEMIGNANI, A. & PITTALUGA, A. (1983). Differential blockade by (-)mianserin of the α_2-adrenoceptors mediating inhibition of noradrenaline and serotonin release from rat brain synaptosomes. *Naunyn Schmiedebergs Arch Pharmacol.*, **322**, 180–182.

REGAN, J.W., KOBILKA, T.S., YANG-FENG, T.L., CARON, M.G., LEFKOWITZ, R.J. & KOBILKA, B.K. (1988). Cloning and expression of a human kidney cDNA for an α_2-adrenergic receptor subtype. *Proc. Natl. Acad. Sci. U.S.A.*, **85**, 6301–6305.

SCHLOSS, J., WELLSTEIN, A. & PALM, D. (1987). Agonist binding at α_2-adrenoceptors of human platelets using ^{3}H-UK-14,304: regulation by Gp(NH)p and cations. *Naunyn-Schmiedebergs Arch. Pharmacol.*, **336**, 48–59.

UHLÉN, S., PERSSON, M.-L., ALARI, L., POST, C., AXELSSON, K.L. & WIKBERG, J.E.S. (1990). Antinociceptive actions of α_2-adrenoceptor agonists in the rat spinal cord: Evidence for antinociceptive α_2-adrenoceptor subtypes and dissociation of antinociceptive α_2-adrenoceptors from cyclic AMP. *J. Neurochem.*, **55**, 1905–1914.

UHLÉN, S. & WIKBERG, J.E.S. (1991a). Rat spinal cord α_2-adrenoceptors are of the α_{2A}-subtype: Comparison with α_{2A}- and α_{2B}-adrenoceptors in rat spleen, cerebral cortex and kidney using ^{3}H-RX821002 ligand binding. *Pharmacol. Toxicol.*, **69**, 341–350.

UHLÉN, S. & WIKBERG, J.E.S. (1991b). Delineation of α_{2A}- and α_{2B} adrenoceptors in the rat kidney using [^{3}H]RX821002 radioligand binding computer modelling reveals that guanfacine is α_{2A}-adrenoceptor selective. *Eur. J. Pharmacol.*, **202**, 235–243.

UHLÉN, S. & WIKBERG, J.E.S. (1991c). Delineation of three pharmacological subtypes of α_2-adrenoceptors in the kidney. *Br. J. Pharmacol.*, **104**, 657–664.

VOIGT, M.M., MCCUNE, S.K., KANTERMAN, R.Y.& FELDER, C.C. (1991). The rat α_2-C4 adrenergic receptor gene encodes a novel pharmacological subtype. *FEBS Lett.*, **278**, 45–50.

WIKBERG, J.E.S. (1978). Pharmacological classification of adrenergic α-receptors in the guinea pig. *Nature*, **273**, 164–166.

WIKBERG, J.E.S. & UHLÈN, S. (1990). Further characterization of the guinea pig cerebral cortex idazoxan-receptor: Solubilization, distinction from the imidazole-site and demonstration of cirazoline as an idazoxan-receptor selective drug. *J. Neurochem.*, **55**, 192–203.

YOUNG, P., BERGE, J., CHAPMAN, H. & CAWTHORNE, M.A. (1989). Novel α_2-adrenoceptor antagonists show selectivity for α_{2A}- and α_{2B}-adrenoceptor subtypes. *Eur. J. Pharmacol.*, **168**, 381–386.

ZENG, D., HARRISON, J.K., D'ANGELO, D.D., BARBER, C.M., TUCKER, A.L., LU, Z. & LYNCH, K.R. (1990). Molecular characterization of a rat α_{2B}-adrenergic receptor. *Proc. Natl. Acad. Sci. U.S.A.*, **87**, 3102–3106.

ZENG, D. & LYNCH, K.R. (1991). Distribution of α_2-adrenergic mRNAs in the rat CNS. *Mol. Brain Res.*, **10**, 219–225.

(Received December 12, 1991
Revised March 4, 1992
Accepted April 14, 1992)

Br. J. Pharmacol. (1992), **106**, 996–1003 © Macmillan Press Ltd, 1992

Classification of platelet and vascular prostaglandin D_2 (DP) receptors: estimation of affinities and relative efficacies for a series of novel bicylic ligands With an Appendix on Goodness-of-fit analyses

[1]P. Leff & [2]H. Giles

Analytical Pharmacological Group, Biochemical Sciences, Wellcome Research Laboratories, Langley Court, Beckenham, Kent BR3 3BS

1 The DP receptors located on platelets and vasculature were examined in a human washed platelet preparation and in isolated rings of rabbit external jugular vein.

2 A series of eight novel bicyclic compounds were studied for their effects in the two assays. Seven produced agonism, inhibition of aggregation or vascular relaxation, and one compound was 'silent' in both assays.

3 The operational model of agonism (Black & Leff, 1983) was fitted simultaneously to concentration-effect curve data for the seven agonist compounds. The affinity and efficacy estimates so obtained were tested for similarity between the two tissues by analysis of variance, showing that the model could be fitted to both sets of data by assuming the same relative affinity and efficacy values. However, absolute affinity estimates were consistently lower in the vascular preparation.

4 Analysis of two of the seven agonists as antagonists was also possible. This provided pK_B estimates which supported the agonist affinity estimates. The eighth compound was also analysed as an antagonist. It, like the other seven, demonstrated a difference in affinity between the two tissues.

5 The results of this study support the view that platelet and vascular DP receptors are similar, assuming that the systematic difference in affinity estimates for the series of compounds between the two tissues is the consequence of receptor micro-environment and/or accessory binding site differences.

Keywords: Prostaglandin D_2; DP-receptors; classification; dissociation constant; efficacy; 572C85; 192C86; BW A868C

Introduction

In a previous paper (Giles *et al.*, 1989) we described a study of platelet and vascular prostaglandin-D_2 (DP) receptors using a newly available antagonist, BW A868C. The results of that study indicated that the DP-receptors in those two locations belonged to the same class. However, this conclusion had to remain provisional because demonstration of simple competitive antagonism by BW A868C was precluded in the vascular assay due to multiple actions on the part of the available agonists. Thus, while a reliable estimate of the dissociation constant for BW A868C could be obtained for the platelet receptor, this was not possible for the vascular smooth muscle receptor. Furthermore, as shown in the present study, when DP-receptor agonists of appropriate specificity were identified, which should have allowed a quantitative analysis of antagonism by BW A868C to be performed in the vascular assay, further problems of a kinetic nature were revealed.

In an attempt to solve some of these problems we have now identified and analysed the actions of a series of novel bicyclic agonist and antagonist analogues. The objective of this study has been to obtain quantitative information, affinity and efficacy estimates, for these compounds in platelet and vascular assays and thereby provide a more secure basis for the classification of DP-receptors in these tissues.

[1] Present address: Department of Pharmacology, Fisons Research and Development Labs, Bakewell Road, Loughborough, Leicestershire LE11 0RH.

[2] Author for correspondence.

Methods

Tissue preparations

Human washed platelets Blood was drawn from healthy male and female volunteers who had not taken any drugs known to affect platelet function for at least two weeks and collected into sodium citrate (3.15% w/v) in proportion 9:1 w/v. Prostacyclin-washed platelets suspended in Tyrode buffer were prepared as previously described (Giles *et al.*, 1989). Indomethacin (5 $\mu g\,ml^{-1}$) and fibrinogen (400 $\mu g\,ml^{-1}$) were added to the platelet suspension at the start of each experiment. Aggregation responses were measured in 0.5 ml aliquots of the suspension maintained at 37°C and stirred with a metal bar at 900 r.p.m. in 300 BD-S Payton dual channel aggregometers and recorded on Gould BS 272 pen recorders.

Rabbit jugular vein External jugular veins were removed from male New Zealand White rabbits (2.4–3.0 kg) killed by injection of pentobarbitone sodium (Sagatal, 60 $mg\,kg^{-1}$) into a marginal ear vein. The vessels were cannulated, which caused the removal of the endothelium (Leff *et al.*, 1987), and then cleared of adhering tissue. Three 5 mm wide ring segments were obtained from each vein and each was suspended between two wire hooks, one attached to a Grass FT03C force displacement transducer and the other to a stationary support in a 20 ml organ bath containing Krebs solution (pH 7.4) of the following composition (mM): NaCl 118.4, $NaHCO_3$ 25.0, KCl 4.8, KH_2PO_4 1.2, $MgSO_4$ 1.2, glucose 11.1, $CaCl_2$ 2.5, maintained at 37°C and continuously gassed with 95% O_2:5% CO_2. Responses were measured as

changes in isometric force and recorded on Gould BW 272 pen recorders.

Experimental protocols

Human washed platelets Prostaglandin receptor agonists were incubated in the platelet suspension for 6 min before addition of ADP (50 μM). Previous experiments showed that, for all agonists used in this study, this was sufficient time to reach equilibrium. The reproducibility of the ADP-induced aggregation response was checked at intervals throughout the experiment. When an antagonist was used it was added 2 min before the agonist. Responses to the agonist were expressed as percentage inhibition of the control ADP-induced aggregation. The total volume of solutions added to the suspension was always less than 5% of the platelet suspension volume.

Rabbit jugular vein Indomethacin (1 μg ml^{-1}) and the TP receptor antagonist, BM 13.177 (30 μM) were used routinely in all experiments, as described previously (Giles *et al.*, 1989). Initially, jugular vein ring segments were subjected to a force of 0.75 g then allowed to stabilize for a period of 60 min during which time preparations were washed three times. BM 13.177 was incubated for 60 min then histamine (1 μM) was added in order to produce tone. After establishing a stable contraction, relaxation concentration-effect curves were obtained with prostaglandin receptor agonists. A separate experiment demonstrated that the histamine contraction was generally stable (< 5% loss of tone) for the period of time required to construct a concentration-effect curve. Tissues in which there was an initial rapid loss of tone were discarded. Responses were expressed as percentage relaxations of the histamine-induced force. Antagonist studies followed a paired curve design. This was necessary because of substantial inter-tissue variation in the position of prostaglandin receptor agonist concentration-effect curves. Preparations were washed thoroughly following the first concentration-effect curve and allowed to re-stabilize. After re-introduction of BM 13.177, antagonists were incubated for 60 min before constriction with histamine (1 μM) followed by a second prostaglandin agonist concentration-effect curve. A separate experiment established that first and second histamine concentration effect curves, and first and second control prostaglandin agonist concentration-effect curves were superimposable (data not shown).

Analysis of data

Curve fitting A logistic function of the form:

$$E = \frac{\alpha[A]^m}{[A_{50}]^m + [A]^m} \quad \text{(i)}$$

in which α, $[A_{50}]$ and m are the asymptote, location and slope parameters respectively, was fitted to each concentration-effect curve in order to generate average parameter estimates for each group of curves.

Estimation of antagonist affinity: (i) Single curve design A one-way analysis of variance tested for treatment effects on the computed estimates of α and m. In the platelet study, inhibition of aggregation greater than 100% of the ADP aggregation cannot be obtained, therefore analysis of variance on the asymptote (α) was inappropriate. Tests for parallelism relied on slope analysis in this case. If the antagonist did not significantly modify these parameters then computed $\log_{10}[A_{50}]$ values were fitted to the following form of the Schild equation (Black *et al.*, 1985):

$$\log_{10}[A_{50}] = \log_{10}[A_{50}^c] + \log_{10}(1 + [B]^n/K_B) \quad \text{(ii)}$$

where $[A_{50}^c]$ is a control A_{50} value, [B] is the concentration of antagonist, K_B is its equilibrium dissociation constant and n is its order of reaction with the receptor. If n was not significantly different from unity, indicating simple competition, it was constrained to this value in order to obtain an estimate of K_B. The dissociation constant was actually estimated as pK_B ($-\log_{10} K_B$). In this experimental design a complete study of antagonism was conducted on each suspension or tissue and so equation (ii) was used to provide an estimate of pK_B on each occasion. The average of these values is quoted in the text together with the standard error.

(ii) Paired curve design Paired *t* tests were performed on the differences between computed α and m estimates for each pair of concentraton-effect curves. If the antagonist did not significantly modify α or m then the Schild equation was fitted to the computed r − 1 values for each pair of curves:

$$\log(r - 1) = n \log [B] - \log K_B \quad \text{(iii)}$$

where r is the dose-ratio (A_{50}^c/A_{50})

Ideally, a complete study of antagonism should have been conducted on each day (Giles *et al.*, 1989), thus allowing a set of independent estimates of pK_B and n to be obtained. However in the present case, on some occasions data from the jugular vein had to be rejected due to a fading histamine contraction, or because the efficacy of the agonist in that tissue was too small to be defined (presumably due to low receptor reserve). As a result, a complete set of concentration-ratio data was often unobtainable, meaning that a daily analysis was precluded. Therefore, concentration-ratio data obtained over successive days were pooled and fitted simultaneously using the Schild equation. If n was not significantly different from unity, indicating simple competition, it was constrained to this value to obtain an estimate of pK_B together with the standard error. The error estimates on n and pK_B so obtained include fitting error as well as experimental error and are larger than would have been the case had daily estimates been possible. However, the resulting lack of stringency does not compromise interpretation in the present study, as will be seen.

Estimation of agonist affinity and efficacy

The operational model of agonism (Black & Leff, 1983) was fitted to concentration-effect curve data sets where:

$$E = \frac{E_m \tau^n [A]^n}{(K_A + [A])^n + \tau^n [A]^n} \quad \text{(iv)}$$

in which E_m is the maximum effect of a full agonist, τ is the efficacy, K_A is the dissociation constant for the agonist, and n is the slope or sensitivity index for the occupancy-effect relation. Eq. (iv) was fitted to each data set assuming a common K_A but a separate τ value for each curve. The rationale for this, and the associated estimation of error has been described elsewhere (Leff *et al.*, 1990).

As all of the agonists in question behaved as partial agonists a full agonist was required for comparison. In terms of the operational model a standard full agonist is used to provide estimates of E_m and n. This is because for an agonist with high efficacy the shape of the concentration-effect relation is identical to the shape of the occupancy-effect relation (Leff, 1987) which in turn is characterized by the parameters E_m and n. Algebraically, the operational model equation describing a full agonist is a simplified version of equation (iv):

$$E = \frac{E_m [A]^m}{(K_A/\tau)^n + [A]^n} \quad \text{(v)}$$

which is of a logistic form (Leff, 1987). Therefore, E_m and n can be estimated by fitting the full agonist data directly to a logistic function.

Practically, the high efficacy of the standard agonist, that is, its 'fullness' should be checked with an irreversible antagonist. The lack of such an agent for the present receptors meant that evidence for high efficacy had to be sought

elsewhere. Such evidence is available when an agonist naturally varies in its potency ([A_{50}]) in a particular tissue without its maximal effect varying. Assuming that such variation is due to receptor reserve differences between tissues (e.g. to a difference in receptor density or the efficiency of transduction), the implication is that, despite low reserve in some tissues, the agonist can still produce a maximum effect and, therefore, on average it has high intrinsic efficacy. As described later, the standard full agonist used here (BW245C) demonstrated these characteristics.

In order to assess goodness-of-fit and the similarity or otherwise of affinity (pK_A) and efficacy (τ) estimates between tissues, initially a curve was fitted to each individual concentration-effect curve; this allowed estimation of the sum-of-squares associated with fitting. Thereafter, for each tissue, a single curve was fitted to all the data for each agonist under the impositon of various constraints on the parameter estimates (see Appendix).

Drugs

PGE_2 (Cayman Chemical, Denver, Colorado, U.S.A.), 9,11-dideoxy, 9α-11-methanoepoxy-$PGE_{2\alpha}$ (U46619) (Cayman), Epoprostenol sodium Grade 1 (PGI_2) (Wellcome Research Laboratories, Beckenham, Kent), fluprostenol sodium (gift from Coopers Animal Health Ltd., Berkhamstead, Herts), BW 245C (5-(6-carboxyhexyl)-1-(3-cyclohexyl-3-hydroxypropylhydantoin), BW A868C((±)-3-benzyl-5-(6-carboxyhexyl)-1-(2-cyclohexyl-2-hydroxyethylamino)-hydantoin), BM13.177 (4-[2-(benzenesulphonamido) -ethyl] -phenoxyacetic acid) and Compound 1-VIII (Figure 1) (Wellcome), indomethacin (Sigma Chemical Co. St. Louis, MO, U.S.A.), adenosine 5'-diphosphate (ADP) (Sigma), histamine HCl (Sigma), fibrinogen (KabiVitrum Stockholm, Sweden), phenoxybenzamine hydrochloride (Smith, Kline and French, Welwyn Garden City, Herts), atropine sulphate (Sigma).

PGI_2 solutions were made daily in 1 M Tris buffer pH 8.4. All other prostaglandins and their analogues were dissolved initially in ethanol and stored as 20 mM solution at −22°C. Further dilutions were made daily in distilled water, except for BW A868C which required 0.5 M Tris buffer pH 8.4 for the 2 mM dilution. All dilutions were stored on ice. Indomethacin 10 mg ml^{-1} was dissolved in 0.25 mM Tris buffer pH 8.4; histamine HCl 1 mM was prepared in aqueous solution neutralised to pH 7 with 10 mM NaOH; phenoxybenzamine was dissolved in absolute ethanol; ADP, fibrinogen and atropine were aqueous solutions.

At final concentrations to which the tissues were exposed, none of the vehicles influenced tissue responsiveness.

Results

DP receptor effects of compounds I-VIII

Figure 2 illustrates the inhibition of aggregation (a) and vasorelaxation (b) elicited by compounds I-VIII (see Figure 1). The compounds appeared to display a range of intrinsic efficacies and the receptor reserve was apparently higher in the platelets than in the jugular vein (assuming that the receptors are similar in both tissues). Each of the compounds which displayed agonism (I-VII) were antagonized by BW A868C, the previously classified DP receptor antagonist (Giles *et al.*, 1989) in a concentration (100 nM) 100 × its receptor dissociation constant. In the platelet assay, BW A868C elicited an approximately 100 fold parallel rightward displacement of each agonist concentration-effect curve. In the jugular vein assay, this concentration of BW A868C also elicited a rightward displacement of the agonist curves but produced slowing of agonist-induced responses to the extent that steady-state effects could not be measured.

A complete study of antagonism by BW A868C was conducted in the platelet assay using compound I – 572C85

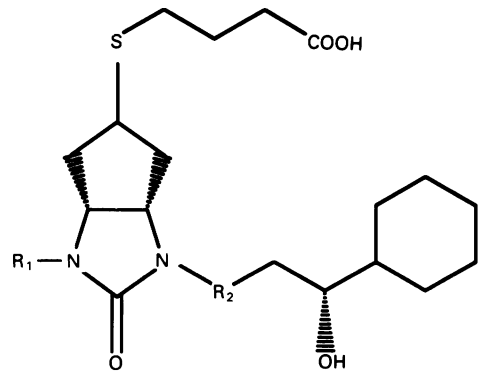

Compound		R_1
I 572C86	○	H
II	●	H
III	□	methyl
IV	■	methyl
V	△	ethyl
VI 192C86	▲	ethyl
VII	▽	propyl
VIII	▼	propyl

Open symbol R_2: NH
Closed symbol R_2: =N

Figure 1 The structures of the eight novel bicyclic prostaglandin analogues used in this study, together with the symbols used in Figures 2 and 5.

(such a study was not possible in the jugular vein assay). In the platelet, the antagonist (3–300 nM) produced parallel rightward displacements of compound I concentration-effect curves (Figure 3a, as assessed by one-way analyses of variance, see Methods). Figure 3b shows the associated Schild plot of all the concentration-ratios obtained. As explained in the Methods section a separate analysis of antagonism was conducted on each day, providing an estimate of the Schild plot slope and a pA_2/pK_B on each occasion. The average slope value over five days was 1.39 ± 0.17 which is significantly higher than unity ($0.025 < P < 0.05$). The average pA_2 value was 8.73 ± 0.13 (a pK_B value is not appropriately quoted under these conditions, see Jenkinson, 1991).

Receptor selectivity of compounds I-VIII

Compounds I-VIII were also studied (on at least one occasion) for possible effects at other prostanoid receptors. All experiments were performed in the presence of 10 μM BW A868C to prevent binding to the DP receptor. None of the compounds, at concentrations up to 10 μM, exerted any effect on baseline tone in the rabbit jugular vein preparation nor on histamine (1 μM)-induced tone in that assay. It has previously been shown that this jugular vein preparation contains TP-receptors which mediate vasoconstriction, IP-receptors and EP_2-receptors which mediate vasorelaxation (Giles *et al.*, 1989; Lawrence *et al.*, 1989). Also, in guinea-pig ileum and rat fundus preparations, which contain respectively EP_1-receptors (Coleman *et al.*, 1984) and FP-receptors (Dong *et al.*, 1986) mediating smooth muscle contraction, compounds I-VIII were without effect at concentrations up to 10 μM.

Antagonist actions were also examined, again at least on one occasion for each compound, in each of these three assays under the same conditions. U46619, prostacyclin and BW 245C concentration-effect curves in the jugular vein assay were unaffected by the compounds, as were concentration-effect curves to prostaglandin E_2 in guinea-pig ileum and to the selective FP-receptor agonist, fluprostenol (Dukes *et al.*, 1974; Coleman *et al.*, 1984) in rat fundus. For one of

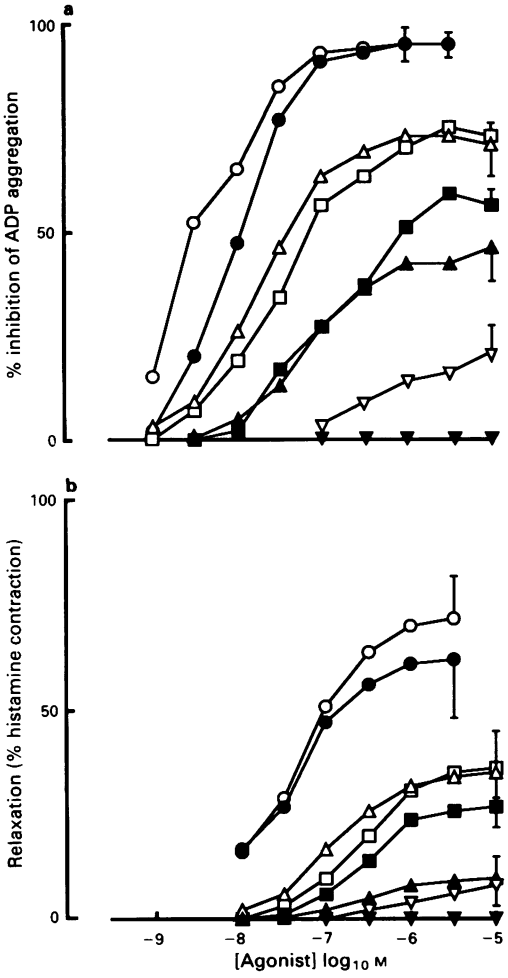

Figure 2 The inhibitory effects of compounds I-VIII on (a) human washed platelet aggregation and (b) histamine-contracted rabbit jugular vein. Responses are the mean of 3–6 replicate curves. See Figure 1 for key to symbols. Vertical bars show s.e.mean. For clarity, error bars have been included only at the highest agonist concentrations.

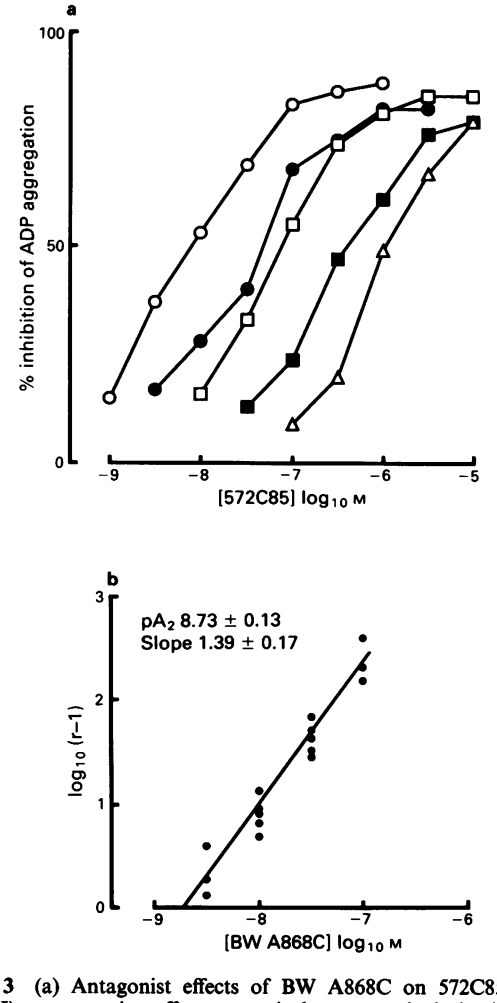

Figure 3 (a) Antagonist effects of BW A868C on 572C85 (compound I) concentration-effect curves in human washed platelets. BW A868C was used at the following concentrations: zero (○), 3 nM (●), 10 nM (□), 30 nM (■), 100 nM (△). Responses are the mean of 3–5 replicate curves. (b) Schild plot antagonism of 572C85 by BW A868C in human platelets. The line through the data was calculated as described in the methods section.

the compounds, compound VI(192C86), actions at other, non-prostanoid receptors (α_1, α_2, β_1, β_2 adrenoceptors, H_1, H_2 histamine receptors, D_1 and D_2 dopamine receptors, muscarinic and purine receptors) were also excluded in appropriate assays.

Quantitative analysis of agonism and antagonism

Agonism Assuming that the data illustrated in Figure 2 are associated with actions on a single homogeneous population of DP-receptors, the following analyses of agonism and antagonism were performed.

As explained in Methods, it was necessary first to analyse a 'full' agonist in order to obtain estimates of E_m and n. BW 245C, a DP receptor agonist (Town *et al.*, 1983; Whittle *et al.*, 1983), was selected because it demonstrated complete inhibition of platelet aggregation and complete relaxation in the jugular vein assay with variations of up to 1 logarithmic unit in the location ($[A_{50}]$) of its concentration-effect curve in different preparations of the same tissue. This indicated that BW 245C possesses a high intrinsic efficacy at DP-receptors. The logistic function (equation i) was fitted to 13 replicated BW 245C concentration-effect curves obtained in the platelet assay, and to 16 replicate curves in the jugular vein assay. In the jugular vein all the BW 245C concentration-effect curves were shifted rightwards by BW A868C, demonstrating that agonism was being mediated through the DP receptor, and not through actions at the EP_2 receptor, since BW 245C has efficacy at both DP and EP_2 receptors (Giles *et al.*, 1989). Average parameter estimates were as follows: platelet: $E_m = 99.85 \pm 0.84$, $n = 1.17 \pm 0.07$; jugular vein: $E_m = 100.70 \pm 1.13$; $n = 1.06 \pm 0.03$. In subsequent model-fits E_m and n were constrained to these values. Average data, along with the average logistic curve fits, are shown in Figure 4.

Concentration-effect curve data for agonists I-VII from both assays were then fitted simultaneously using the operational model of agonism (equation iv). This provided estimates of affinity (pK_A) and efficacy (τ) for each agonist in each tissue (Table 1). These estimates were then tested for their similarity between tissues by imposing a number of selected constraints on the model parameters and analysing the effect of these constraints on the residual sums-of-squares associated with model-fitting.

The results of these analyses are described in full in the Appendix. In brief, it was found that: (i) a significant worsening of fit was obtained when the affinity (pK_A) of each agonist was assumed to be the same in the two tissues, although no worsening occurred when the pK_A values for each agonist were assumed to differ by a constant increment between the two tissues; (ii) a significant worsening of fit occurred when the efficacy (τ) value for each agonist was assumed to be the same in each tissue, but no worsening occurred when a constant ratio was assumed between the values for each agonist acting in the two tissues. Therefore,

the series of agonists were concluded to express the same relative affinities and efficacies in the two tissues. Figure 5 illustrates the average experimental data and model-fitted lines obtained assuming that the relative pK_A and τ values were the same for each agonist (i.e. Fit 9 on Table A1, Appendix).

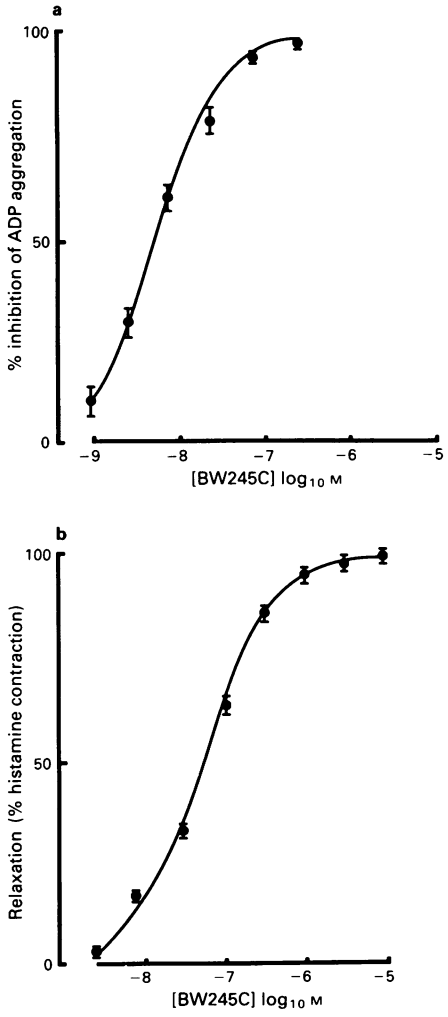

Figure 4 Concentration-effect curves to BW 245C showing (a) inhibition of ADP-induced human platelet aggregation (13 replicates) and (b) inhibition of histamine contraction in rabbit jugular vein (16 replicates). The lines through the data are the average logistic fit (see Methods, curve fitting), which resulted in the following parameter estimates: platelet: log[A_{50}] – 8.17, α 100, m 1.17; jugular: log[A_{50}] – 7.24, α 100, m 1.06. Vertical bars show s.e.mean.

Antagonism On certain occasions when, presumably, receptor reserve was low in the jugular vein, compounds VI and VII produced no agonist effects and, under these circumstances, they could be analysed as competitive antagonists. On these occasions the maximum effect of a saturating concentration of 572C86 (a partial agonist in this tissue) was

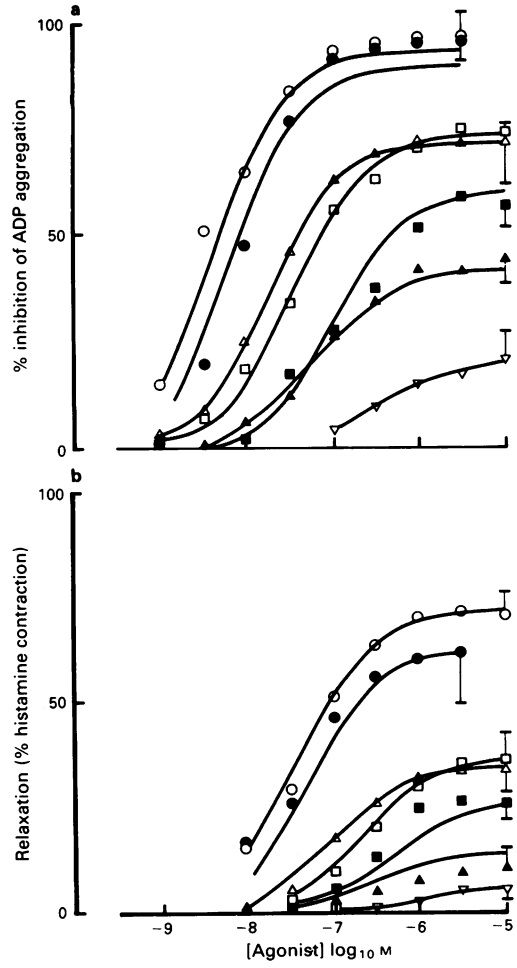

Figure 5 Model-fitted lines using data from Figure 2 which shows the inhibitory effects of compounds I-VII on (a) human platelet aggregation and (b) contraction of rabbit jugular vein. The lines are the result of fitting the operational model of agonism (Eq. iv) to the data (Fit 9 on Table A1, Appendix). A between-tissues fixed increment in both affinity (K_A 0.47 $\log_{10}$ units) and efficacy (τ, 4.04 fold) was allowed, since initial estimates of both parameters were systematically lower in the jugular vein; this constraint caused no significant worsening of fit. Full details of the fitting procedure are described in the Appendix.

Table 1 Operational model parameter estimates

	pK_A		τ	
Compound	*Platelet*	*Jugular*	*Platelet*	*Jugular*
I	7.21 ± 0.29	6.63 ± 0.13	21.34 ± 9.65	4.13 ± 1.66
II	6.69 ± 0.40	6.75 ± 0.15	23.05 ± 10.42	3.31 ± 1.49
III	7.02 ± 0.12	6.31 ± 0.13	2.42 ± 0.31	0.78 ± 0.28
IV	6.69 ± 0.20	6.41 ± 0.26	1.32 ± 0.21	0.44 ± 0.11
V	7.12 ± 0.12	6.80 ± 0.16	3.75 ± 1.42	0.64 ± 0.12
VI	6.94 ± 0.17	6.66 ± 0.45	0.95 ± 0.27	0.27 ± 0.05*
		(6.70 ± 0.05)		
VII	6.51 ± 0.25	5.71 ± 0.49	0.39 ± 0.13	0.31 ± 0.08*
		(5.72 ± 0.03)		
VIII	(7.05 ± 0.03)	(6.21 ± 0.06)		

Parameter estimates ± s.e.mean were estimated as described in the Methods section.
Values in parentheses represent pK_B values obtained as described in the text.
Values are the average of 3–6 estimates.
*On many occasions these compounds did not display agonism in this assay.

always less than on occasions when these compounds showed agonism, supporting the assumption of a decreased receptor reserve in these tissues. Compound VIII was 'silent' on all occasions in both the platelet and jugular vein assays and its antagonist effects were also analysed. In these analyses, Compound I was used as the standard agonist. In all four cases, the antagonist compound produced parallel rightward displacement of agonist concentration-effect curves (as assessed by analyses of variance on slopes and asymptotes) and Schild plot slopes were not significantly different from unity. Figure 6 illustrates the Schild plots for each analysis. The pK_B estimates for compounds VI and VII were similar to the pK_A estimates obtained when these compounds behaved as agonists in the jugular vein (Table 1). For compound VIII, pK_B estimates of 7.05 and 6.21 were obtained in the platelet and jugular vein assays respectively. Statistical analysis of the discrepancy is not strictly appropriate since the error estimates were obtained in different ways (see Methods section). However, the estimates are clearly different, the value obtained in the platelet being 0.84 $\log_{10}$ units higher than that in the vascular assay. This result is qualitatively consistent with the systematic difference (0.47 $\log_{10}$ units) in the agonist pK_A estimates between the two tissues.

Discussion

The recent availability of a highly potent and selective DP receptor antagonist, BW A868C, has allowed significant advances to be made in the identification and classification of prostaglandin receptors (Giles *et al.*, 1989). Using this antagonist, the DP receptors mediating inhibition of aggregation in human platelets and relaxation of rabbit vasculature were provisionally concluded to be of the same DP class. However, those studies were limited by the lack of selectivity of the available agonists which meant that a quantitative analysis of BW A868C was not possible in the vascular assay. The natural agonist, PGD_2, amongst its many actions, elicits vasorelaxation through (presumed) EP_2 receptors; the same is true of BW 245C, the PGD_2 analogue (Giles *et al.*, 1989). Whereas additional actions such as TP receptor activation could be blocked with a suitable antagonist, BM 13.177, the lack of an EP_2 receptor antagonist meant that displacements of agonist-concentration effect curves elicited by BW A868C were confounded by actions through EP_2 receptors.

The series of compounds described in the present paper has allowed this analytical problem to be approached and has enlarged upon the base of information available for the characterization of DP-receptors. In fact, in attempting to perform a quantitative analysis of BW A868C antagonism in the rabbit jugular vein assay using Compound I (572C85) as the agonist a further problem associated with the antagonist was revealed. Despite the specificity of Compound I for DP receptors (evident from the absence of a phase of agonism resistant to BW A868C) it was not possible to analyse concentration-effect curve displacements due to slowing of agonist responses in the presence of BW A868C. This result was suggestive of a 'hemi-equilibrium' state being produced in the jugular vein assay. Hemi-equilibrium is most likely to occur when the antagonist dissociates slowly from the receptor (consistent with the high affinity of BW A868C, pK_B = 9.26 (Giles *et al.*, 1989)) and when the agonist requires a high receptor occupancy in order to elicit a response (Rang, 1966). In the platelet assay, which has a higher receptor reserve than

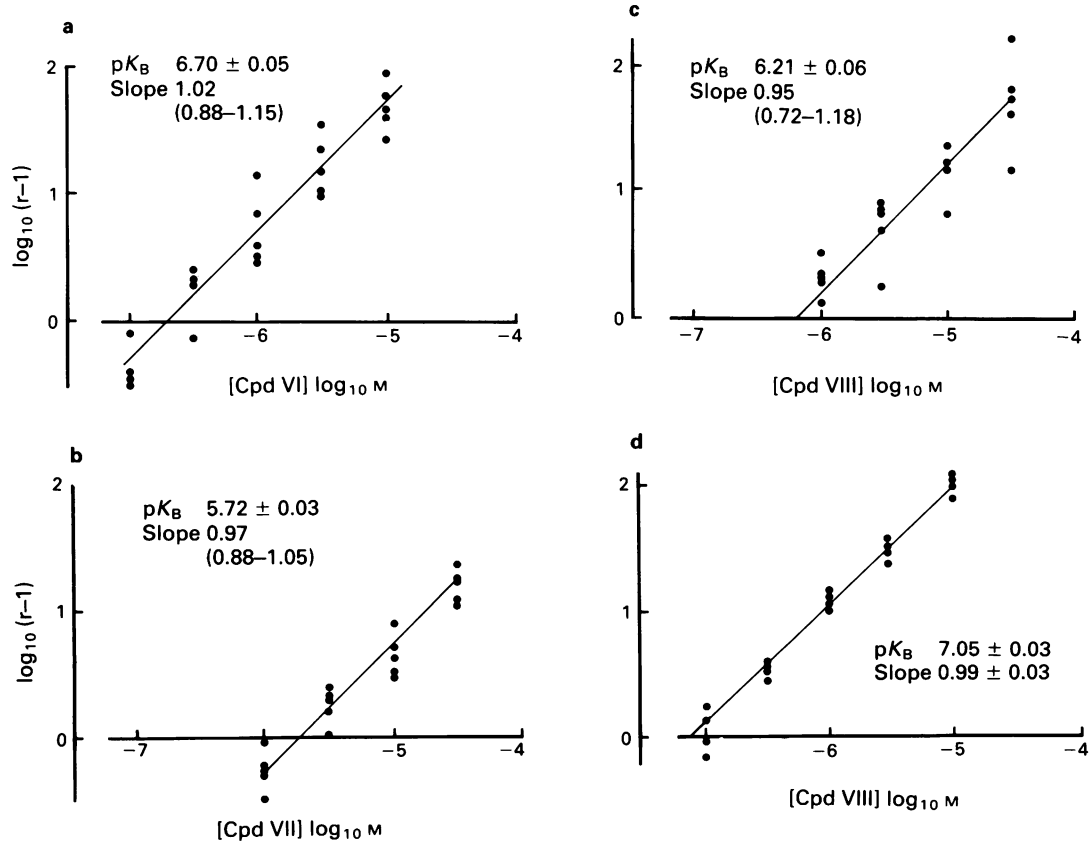

Figure 6 Schild plots showing antagonism of 572C85 (compound I) concentration-effect curves in rabbit jugular vein by (a) compound VI; (b) compound VII; (c) compound VIII and in human platelets by (d) compound VIII. In all cases the slope parameter, n, was not significantly different from unity and the line through each data set was obtained by fitting the data to the appropriate equation (see methods) with n constrained to unity. on this occasion in the platelet assay it was not possible to obtain daily estimates of pK_B therefore all the data were fitted simultaneously to eq. (ii). The pK_B and slope estimates are shown in each panel.

the jugular vein (see Figure 2 and Table 1), such a problem did not occur and the antagonism of Compound I by high concentrations of BW A868C produced no measurable slowing in response. Indeed, the present analysis gave parallel curve displacements and, although the Schild plot slope was slightly greater than unity this, and the pK_B estimate, was indistinguishable from that obtained previously in the platelet assay with BW 245C as the agonist (Giles *et al.*, 1989).

The apparent 'hemi-equilibrium' state in the jugular vein assay was not only produced when Compound I was the agonist employed; the same response slowing was obtained with each of the other agonists. However, when compounds VI-VIII were used as competitive antagonists of compound I, no kinetic problems were revealed and they behaved as simple competitive antagonists in both tissues, presumably because they dissociated from the receptor more quickly than BW A868C. Consistent with this are the estimates of their affinity for the DP receptor, which were 100–1000 fold lower than that of BW A868C (Figure 6 and Table 1).

Therefore, Compound VIII may be preferred to BW A868C for quantitative identification of DP receptors, particularly in assays with a low receptor reserve. It may be wise to recommend BW A868C only for qualitative classification purposes, that is, for discrimination between DP and other types of prostaglandin receptor (its marked selectivity permits this), but not for positive, quantitative definition.

However, despite the problems associated with BW A868C, the tentative conclusion based on its use that the DP receptors in human platelets and rabbit vasculature are the same (Giles *et al.*, 1989) is supported by the combined weight of the affinity and efficacy information obtained here. Figure 5 and analysis (see Appendix) showed that Compounds I-VII demonstrated the same relative affinities and efficacies in the two assays, consistent with similar recognition and transduction of the chemical information in this series by the two receptor populations involved. Similar, that is, but not the same. Evidently, there was a difference between the pK_A estimates for the series between the two tissues (supported in the case of Compounds VI and VII by antagonist affinity (pK_B) estimates) suggesting that the two receptor populations are not identical. However, the difference was systematic and might be explained by minor differences in micro-environment or amino-acid sequence or difference in, say, the type of orientation of binding sites in two otherwise very similar receptors.

Inevitably, such suggestions raise issues of the definition of a receptor, of what 'receptor similarity' really means and what constitutes hard evidence for classifying receptors as the same in different tissues; these issues have been discussed extensively elsewhere (e.g. Stephenson, 1975; Black *et al.*, 1986). In the 5-HT receptor area it has been useful to consider the chemical similarity or otherwise to the natural agonist of the ligands used for classification of the receptor in question (Leff & Martin, 1986; Leff *et al.*, 1986). The argument is that there may be accessory binding sites within the receptor structure which are not utilised by the natural agonist and which may not be conserved between different tissues. As a result, agonists and antagonists which utilise these sites may express different binding affinities between the tissues, whereas the affinity of the natural agonist does not vary. In the present case we cannot claim that Compounds I-VIII are chemical analogues of PGD_2 and it may be that the systematic differences in affinities of these compounds between the platelet and vascular receptor are a consequence of an accessory binding site(s) difference, in which case the ability of these compounds to detect the sameness of the two receptor populations is limited. On the other hand, it seems reasonable to suggest that the 'fingerprint' of affinity and efficacy information generated for Compounds I-VIII can, as it stands, be used to characterize positively and quantitatively DP receptors in new locations. Whether the systematic differences detected here continue to be manifested between different tissues and whether the use of new compounds can lead to a decrease in such analytical noise and, therefore, more quantitively precise receptor classification will no doubt become apparent from future studies.

We would like to thank the medicinal chemists at Wellcome for the synthesis of the novel compounds described here. Particular thanks are due to Dr Alan Robertson, to Mary Bolofo for her technical assistance and to John Wood for statistical advice.

References

BLACK, J.W. & LEFF, P. (1983). Operational models of pharmacological agonism. *Proc. R. Soc. B.*, **220**, 141–162.

BLACK, J.W., LEFF, P. & SHANKLEY, N.P. (1985). Further analysis of anomalous pK_B values for histamine H_2 receptor antagonists on the mouse isolated stomach assay. *Br. J. Pharmacol.*, **86**, 581–587.

BLACK, J.W., JENKINSON, D.H. & GERSKOWITCH, V.P. (ed.) (1986). *Receptor Biochemistry and Methodology*, Vol 6, Perspectives in receptor classification. York: A.R. Liss.

COLEMAN, R.A., HUMPHREY, P.P.A., KENNEDY, I. & LUMLEY, P. (1984). Prostanoid receptors – the development of a working classification. *Trends Pharmacol. Sci.*, **5**, 303–306.

DONG, Y.J., JONES, R.L. & WILSON, N.H. (1986). Prostaglandin E receptor sub-types in smooth muscle: agonist activities of stable prostacyclin analogues. *Br. J. Pharmacol.*, **87**, 97–107.

DUKES, M., RUSSELL, W. & WALPOLE, A.L. (1974). Potent luteolytic agents related to prostaglandin $F_{2\alpha}$. *Nature*, **250**, 330–331.

GILES, H., LEFF, P., BOLOFO, M., KELLY, M.G. & ROBERTON, A.D. (1989). The classification of PGD_2-receptors in platelets and vasculature using BW A868C, a novel, selective and potent competitive antagonist. *Br. J. Pharmacol.*, **96**, 291–300.

JENKINSON, D.H. (1991). How we describe competitive antagonists: three questions of usage. *Trends Pharmacol. Sci.*, **22**, 53–54.

LAWRENCE, R.A., JONES, R.L. & WILSON, N.H. (1989). Relaxant potencies of prostaglandin E analogues on rabbit jugular vein. *Br. J. Pharmacol.*, **98**, 796P.

LEFF, P. (1987). Can operational models of agonism provide a framework for classifying hormone receptors? In *Perspectives on Receptor Classification*. ed. Black, J.W., Jenkinson, D.H. & Gerskowitch, V.P. pp. 157–167. New York: Alan L. Liss Inc.

LEFF, P. & MARTIN, G.R. (1986). Peripheral 5-HT_2 like receptors. Can they be classified with the available antagonists? *Br. J. Pharmacol.*, **88**, 585–593.

LEFF, P., MARTIN, G.R. & MORSE, J.M. (1986). The classification of peripheral 5-HT_2-like receptors using tryptamine agonist and antagonist analogues. *Br. J. Pharmacol.*, **89**, 493–499.

LEFF, P., MARTIN, G.R. & MORSE, J.M. (1987). Differential classification of vascular smooth muscle and endothelial cell 5-HT receptors by use of tryptamine antagonists. *Br. J. Pharmacol.*, **91**, 321–331.

LEFF, P., PRENTICE, D.J., GILES, H., MARTIN, G.R. & WOOD, J. (1990). Estimation of agonist affinity and efficacy by direct, operational model-fitting. *J. Pharmacol. Meth.*, **23**, 225–237.

RANG, H.P. (1966). The kinetics of action of acetylcholine antagonists in smooth muscle. *Proc. R. Soc. B.*, **164**, 488–510.

STEPHENSON, R.P. (1975). Interaction of agonists and antagonists with their receptors. In *Smooth Muscle Pharmacology and Physiology*, (Les Colloques de l Institute National de la Sante et de la Recherche Medicale), Vol 50, ed. Worcel, M. & Vassort, G. pp. 15–28.

TOWN, M.-H., CASALS-STENZEL, J. & SCHILLINGER, E. (1983). Pharmacological and cardiovascular properties of a hydantoin derivative, BW 245C, with high affinity and selectivity for PGD_2 receptors. *Prostaglandins*, **25**, 13–18.

WHITTLE, B.J.R., MONCADA, S., MULLANE, K. & VANE, J.R. (1963). Platelet and cardiovascular activity of the hydantoin BW 245C, a potent prostaglandin analogue. *Prostaglandins*, **25**, 205–223.

(Received January 22, 1992
Revised April 1, 1992
Accepted April 16, 1992)

Appendix: Goodness-of-fit analyses

Analyses of variance

Fit 1 in Table A1 provided an estimate of the error associated with model-fitting. The estimated residual sum of squares (RSS) in Fit 2, which we assume is dominated by inter-preparation variation in receptor reserve, that is, a tissue-dependent contribution to τ, also contains fitting error. Therefore the purely tissue-dependent RSS is 7.98444– 0.35182 which is 7.63262 (132 d.f.). Therefore, the mean RSS associated with tissue variation is 0.05782. This will be considered within the tissues error with which the results of subsequent constraints will be compared.

Analysis of τ

Comparing Fits 2 and 3 shows that the assumption that the τ values for each agonist are the same in each tissue results in an increase in RSS of 2.52906 (7 d.f.) which is equivalent to a mean RSS of 0.36129. Comparing this error with the within tissues error:

$$F_{7,132} = 0.36129/0.05782 = 6.2486$$

which is highly significant ($P<0.001$) and indicating, as expected by inspection of the data (see Figure 2), that the efficacy of each agonist differs between the two assays.

Comparing Fit 4 with Fit 2 shows that the assumption that the relative τ values for the series of agonists are the same in each tissue results in an increase in RSS of 0.14231 (6 d.f.) giving a mean RSS of 0.02372. In this case, comparison with the within tissues error gives:

$$F_{6,132} = 0.02372/0.05782 = 0.4102$$

which is clearly not significant.

Therefore it is reasonable to conclude that the relative efficacies of the compounds are the same in both tissues.

Analysis of pK_A

Comparing Fit 5 with Fit 2 shows that the assumption that the pK_A values for the series of agonists are the same in each tissue results in an increase in RSS of 0.25473 (7 d.f.) giving a mean increase of 0.03639. Therefore,

$$F_{7,132} = 0.03639/0.05782 = 0.6294$$

which is not significant, implying that the assumption is valid. However, comparing Fit 6 with Fit 5, which tests whether the assumption of constant increment in the pK_A values for the agonists between tissues results in an improvement in fit over common pK_A values, yields the following: the decrease in RSS is 0.16595 (1 d.f.), therefore,

$$F_{1,132} = 0.16595/0.05782 = 2.8701$$

which approaches significance ($0.05<P<0.10$).

Furthermore, it was noticed when comparing Fits 5 and 2 that, in order to accommodate the constraint that pK_A values should be the same, the estimates of τ changed dramatically. This indicated that variation of τ values during model-fitting could absorb some of the error associated with pK_A estimation. This is reasonable since τ, as a parameter in the model, contributes to the location [(A_{50})] of concentration-effect curves as well as K_A. Therefore, Fits 7, 8 and 9 were performed which allowed the same tests as those carried out above to be performed without the possibility that error associated with pK_A estimation could be accommodated by τ error. Now, comparing Fits 7 and 8, constraining pK_As to be the same in the two tissues resulted in a significant increase in mean RSS.

The difference in RSS was 0.90388 (7 d.f.) giving a mean of 0.12913. Therefore $F_{7,132} = 0.12913/0.05782 = 2.233$ ($0.025<P<0.05$). Furthermore, constraining the difference in pK_A estimates between the two tissues to be constant (comparing Fit 9 with Fit 7) did not result in a significant worsening of fit. The increase in RSS was 0.17809 (6 d.f.) giving a mean of 0.02968.

$$F_{6,132} = 0.02968/0.05782 = 0.5133$$

which is clearly not significant.

Therefore, from these analyses of variance it appeared sensible to conclude that the τ estimates and the pK_A estimates for the series of agonists were relatively the same in both tissues but differed by constant factors between the two tissues.

Table A1 Goodness-of-fit analyses

Fit	*Constraint*	*Parameters Fitted*	*Comment*	†*RSS*	*d.f.*
1	None: a curve fitted to each replicate data set within each treatment (excluding zeros*)	59 pK_As 59τs	Provides estimate of error associated with fitting	0.35182	319
2	A single curve fitted to all replicate data within a treatment	14 pK_As 14τs	Provides estimates of error associated with tissue-dependent receptor-reserve differences	7.98444	451
3	One curve per treatment assuming same τs between tissues	14 pK_As 7τs		10.51350	458
4	One curve per treatment assuming same relative τs between tissues	14 pK_As 7τs Q	Q denotes the average factor by which τ values differ between the two tissues	8.12675	457
5	One curve per treatment assuming same pK_As between tissues	7 pK_As 14τs		8.23917	458
6	One curve per treatment assuming same relative pK_As between tissues	7 pK_As 14τs C	C denotes the average increment by which pK_A values differ between the two tissues	8.07322	457
7	One curve per treatment assuming τ values fixed to their estimates from Fit 4	14 pK_As		8.12711	465
8	One curve per treatment assuming τ values fixed to their estimates from Fig 4, and assuming same pK_As between tissues	7 pK_As	Fixing the τ values prevents pK_A dependent error being absorbed	9.03099	472
9	As Fit 8 except assuming same relative pK_As between tissues	7 pK_As C		8.30520	464

†RSS = residual sum of squares.
*zeros refers to data sets comprised of zero effect values; such results were occasionally obtained for Compounds VI and VII.

Br. J. Pharmacol. (1992), **106**, 1004–1010 © Macmillan Press Ltd, 1992

Modulation of peristalsis in the guinea-pig isolated small intestine by exogenous and endogenous opioids

Sally A. Waterman, [1]Marcello Costa & *Marcello Tonini

Department of Human Physiology and Centre for Neuroscience, School of Medicine. The Flinders University of South Australia, GPO Box 2100, Adelaide 5001, South Australia and *Department of Internal Medicine and Therapeutics Division of Pharmacology and Toxicology, University of Pavia, 27100, Pavia, Italy

1 A recording method was developed to measure physiological parameters of the preparatory and emptying phases of peristalsis *in vitro*. This method enabled measurement of: the compliance of the intestinal wall during the preparatory phase (a reflection of the resistance of the wall to distension); longitudinal muscle contraction during the preparatory phase; the threshold volume required to trigger the emptying phase; the maximal ejection pressure and the average power generated during the emptying phase, which reflects the rate at which the intestine performs work. Modulation of these parameters by exogenous and endogenous opioids acting at μ, κ and δ opioid receptors was investigated.

2 The compliance of the intestinal wall during the preparatory phase was reduced by the μ opioid receptor agonist, [D-Ala^2, N-methyl-Phe^4, Gly^5-ol] enkephalin (DAMGO) but not by the κ agonist, dynorphin, or the δ agonist, [D-penicillamine^2, D-penicillamine^5] enkephalin (DPDPE). Reflex contraction of the longitudinal muscle during the preparatory phase was inhibited by DAMGO, dynorphin and DPDPE. The threshold volume required to trigger the emptying phase of peristalsis was increased by DAMGO, dynorphin and DPDPE.

3 The maximal ejection pressure generated during the emptying phase was reduced by dynorphin and DPDPE, but not by DAMGO. The average power generated by the intestine when emptying was not altered by any of the agonists.

4 Electrically stimulated contractions of longitudinal muscle in strips of longitudinal muscle-myenteric plexus were not inhibited by DPDPE. Similarly, DPDPE did not significantly inhibit electrically induced contraction of circular muscle in strips of circular muscle-myenteric plexus.

5 Each of the agonist effects on peristaltic parameters was antagonized by the appropriate antagonist: D-Phe-Cys-Tyr-D-Trp-Orn-Thr-Pen-Thr-NH_2 (CTOP) (μ), norbinaltorphimine (nor-BNI) (κ), naltrindole (δ).

6 It is concluded that μ and κ agonists act primarily on excitatory circular and longitudinal muscle motor neurones. The δ agonist probably acts on enteric neurones presynaptic to excitatory circular and longitudinal muscle motor neurones.

7 Antagonists for μ, δ and κ receptors did not affect any parameters of peristalsis when the intestine emptied against a low resistance. However, when emptying against a high outflow resistance, the average power generated by the intestine was increased by the κ antagonist, nor-BNI, but not by CTOP or naltrindole.

8 It is concluded that endogenous opioids appear to have little role in peristalsis when the intestine is working against a low outflow resistance. However endogenous opioids, acting primarily at κ receptors, provide a braking mechanism by inhibiting the emptying phase of peristalsis in conditions in which the intestine empties against a higher resistance.

Keywords: Intestinal motility; endogenous opiates; opioid peptides

Introduction

Peristalsis is an important pattern of motility occurring in the intestine (Cannon, 1912; Kosterlitz & Lees, 1964), involving the coordinated contraction of smooth muscle in both the circular and longitudinal muscle layers to propel intestinal contents in an aboral direction. This activity occurs in isolated segments of intestine and is controlled by the enteric nervous system (Tonini *et al.*, 1981; Costa & Furness, 1982). When fluid is infused continuously into the lumen, the intestine gradually distends (the preparatory phase of peristalsis) until, at a threshold distension, the circular muscle at the oral end of the intestine contracts and a wave of contraction propagates aborally along the intestine (the emptying phase; Kosterlitz & Lees, 1964). Once the intestine has emptied, the cycle starts again if the infusion of fluid continues.

Exogenous opioids alter intestinal motility both *in vivo* and *in vitro* (Kromer, 1988; Miller & Hirning, 1989). Furthermore, endogenous opioids exist in the enteric nervous system of many mammalian species (Hughes *et al.*, 1977; Linnoila *et al.*, 1978; Furness *et al.*, 1983; Costa *et al.*, 1985; Corbett *et al.*, 1988). Opioid receptors have been shown to be present by ligand binding studies (Leslie *et al.*, 1980; Goldstein & Naidu, 1989), electrophysiology (North & Tonini, 1977; Galligan & North, 1991; Pillai & Johnson, 1991) and pharmacology (e.g. Greenberg *et al.*, 1970; Kosterlitz & Waterfield, 1972; Dingledine & Goldstein, 1976). In the guinea-pig ileum, activation of the μ and κ subtypes of opioid receptor on neurones inhibits nerve-mediated contraction of both circular muscle and longitudinal muscle (Kosterlitz & Waterfield, 1972; Johnson *et al.*, 1987) and inhibits peristalsis *in vitro* (Trendelenburg, 1917; Holzer & Lembeck, 1979; Kromer *et al.*, 1980). Specific effects of agonists at the δ receptor subtype on motility in the guinea-pig ileum have been reported in few studies (Kromer, 1988; 1990).

[1] Author for correspondence.

Endogenous opioids are released from enteric neurones during peristalsis (Donnerer *et al.*, 1984) and in response to electrical stimulation (Puig *et al.*, 1977; Glass *et al.*, 1986). The role of endogenous opioids in peristalsis has previously been studied by use of the Trendelenburg preparation or modifications thereof (Van Nueten *et al.*, 1976; Kromer, 1990). However, these methods do not match normal physiological activity, i.e. only the aboral end is open, and fluid inflow and outflow occur through this opening. Hence in this arrangement, the intestine is effectively a blind sac and intestinal contractions force fluid against the inflow head of pressure. At low distending pressures, peristaltic activity rapidly ceases; at higher distending pressures, intermittent, tetrodotoxin-resistant contractile activity is observed (Davison & Najafi-Farashah, 1982). This inhibition of peristalsis has been described as 'fatigue' and has been attributed to the release of endogenous opioids (Van Nueten *et al.*, 1973). However, these experiments were not able to address the role of endogenous opioid peptides in more physiological conditions. Tonini *et al.* (1981) modified the method of Bülbring *et al.* (1958) to study peristalsis. In this modification, the intestine is open-ended; fluid is pumped into the oral end of the intestine and expelled through the aboral end by peristaltic contractions. A one-way valve at the aboral end ensures that expelled fluid does not flow back into the intestine. The method allows a more physiological peristalsis to be studied continuously for several hours without the rapid cessation of contraction seen in previous studies. Based on this technique, we have developed a recording method for measuring physiological parameters of peristalsis *in vitro* (Waterman *et al.*, 1990) and have used this to study the site and mode of action of opioid agonists at μ, κ and δ receptor subtypes and to investigate the possibility that endogenous opioids may have a role in peristalsis.

Methods

Guinea-pigs (strain: IMVS coloured) of either sex and weighing between 250 and 350 g were stunned and bled via the carotid arteries. Segments of ileum just distal to the ligament of Treitz were removed, flushed of luminal contents and placed in Krebs solution at room temperature, gassed with 95% O_2/5% CO_2, until required. The composition of the Krebs solution was (mM): NaCl 118, KCl 4.7, NaH_2PO_4 1.0, $NaHCO_3$ 25, $MgSO_4$ 1.2, D-glucose 5.5 and $CaCl_2$ 2.5, pH 7.4.

Peristalsis

Peristalsis was studied by the method of Tonini *et al.* (1981). Segments of ileum, approximately 7–8 cm in length, were mounted horizontally in a 100 ml organ bath. The organ bath contained Krebs solution maintained at 36–37°C and gassed with 95% O_2/5% CO_2. The Krebs solution was replaced at least every 30 min. Peristalsis was elicited by pumping Krebs solution into the oral end of the intestinal lumen.

Longitudinal muscle contraction was recorded with a Harvard Bioscience isotonic transducer with tension set at 7.5 mN. Intraluminal pressures at the oral and aboral ends of the length of intestine were measured with three Statham pressure transducers. Two transducers measured aboral pressure; one recorded at high sensitivity and the other at low sensitivity. Traces were displayed on a Grass polygraph (Figure 1). The volume expelled at the end of each wave of contraction was measured with a measuring cylinder. The residual volume remaining in the intestine after a peristaltic wave could be estimated by siphoning fluid from the intestine with a fixed length of tubing at the end of each experiment. The intraluminal pressure following removal of the residual volume was defined as the baseline pressure and the length of intestine under these conditions was considered to be the resting length.

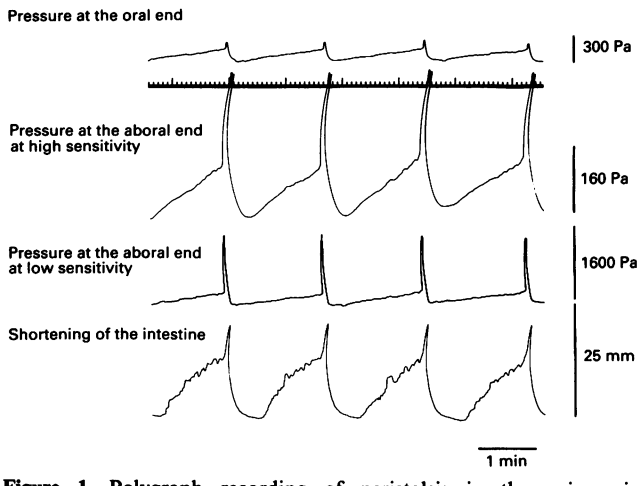

Figure 1 Polygraph recording of peristalsis in the guinea-pig isolated small intestine.

The flow rates used were either 0.63 ml min^{-1} (low rate) or 3.43 ml min^{-1} (high rate). The high flow rate was equivalent to approximately half the average flow rate generated by the intestine itself when emptying. Each peristaltic wave caused the expulsion of fluid from the aboral end of the intestine via a one-way valve. Distal to the valve a length of rigid tubing acted as a resistance to fluid outflow; changing the length of the tubing altered the total outflow resistance. The increase in resistance resulting from lengthening the outflow tubing was estimated in the following manner. A piece of rigid tubing was mounted in the organ bath instead of intestine and the intraluminal pressure measured when different lengths of outflow tubing were in place. Since pressure and resistance are directly proportional if flow rate is constant, an increase in pressure of 21% in response to increasing the length of the tubing indicates that there is a 21% increase in resistance. Fluid leaving the end of the tubing activated a balanced switch that switched off the infusion pump for 10 s to allow the intestine time to finish emptying before more fluid entered.

Physiological parameters of peristalsis

Two phases of peristalsis can be identified: the preparatory phase, when the intestine is being filled with fluid, causing the longitudinal muscle to contract, and the emptying phase, when the circular muscle contracts and forces fluid from the aboral end (see Kosterlitz & Lees, 1964). A number of parameters relating to both phases were calculated from the records (Figure 2).

The compliance of the intestinal wall during the preparatory phase is defined as the change in intraluminal pressure in response to a given change in intraluminal volume (Guyton, 1986). Compliance is a reflection of the resistance of the intestinal wall to infused fluid and can be calculated from the inverse of the slope of the preparatory phase of the intraluminal pressure trace.

$$\text{average compliance} = \frac{\text{volume infused in preparatory phase}}{\text{change in pressure in preparatory phase}}$$

$$= \frac{\text{duration of preparatory phase} \times \text{inflow rate}}{\Delta P}$$

The emptying phase of peristalsis is elicited when the intestine is radially distended to a threshold level. There does not appear to be a pressure threshold (Kosterlitz & Robinson, 1959; Ginzel, 1959). The threshold was therefore measured as the volume of fluid in the intestine when the emptying phase was initiated. The threshold volume consists of the volume infused into the intestine during the preparatory phase

(= duration of preparatory phase × inflow rate) plus the residual volume. In control tissue, the residual volume represents fluid trapped between folds of mucosa and was calculated by siphoning out the contents of the intestine after a peristaltic wave. Changes in residual volume were estimated to be the difference between the volume infused and the volume expelled from the intestine during a peristaltic wave. No significant changes in residual volume were observed in the absence of drugs.

Two parameters of the emptying phase were measured: the maximal ejection pressure (Figure 2) and the average power generated by the intestine when emptying. A positive linear correlation was found between the maximal ejection pressure and the length of segment of intestine. This may reflect the larger volume expelled from the longer segments. To account for slight differences in length of each segment, maximal ejection pressure is therefore expressed per length of intestine. Average power can be defined as pressure × flow rate (Nave & Nave, 1980) and is calculated as:

$$\text{power} = \frac{\text{average pressure in emptying phase} \times \text{volume expelled}}{\text{duration of emptying phase}}$$

The average power generated by the intestine was linearly correlated with the length of intestine. This probably occurs because longer segments of intestine expel a greater volume and because the duration of the emptying phase is longer when a peristaltic wave has further to travel. Consequently, average power is also expressed per length of intestine.

Longitudinal muscle contraction was calculated as the percentage shortening of the intestine at threshold, relative to the resting length.

Circular muscle and longitudinal muscle contraction

The circular muscle-myenteric plexus (CM-MP) preparation of Johnson *et al.* (1987) and a modified version of the longitudinal muscle-myenteric plexus (LM-MP) preparation of Rang (1964) were used to investigate further the actions of the opioid receptor agonists on circular and longitudinal muscle contraction. In the CM-MP preparation, strips of distal ileum, 10 mm in length, from which the mucosa and submucosa had been removed, were mounted in a 5 ml organ bath containing Krebs solution bubbled with 95% O_2/5% CO_2. Circular muscle contractions were recorded with a Harvard isotonic transducer with tension set at 7.5 mN. Following a 90 min equilibration period, the preparations were stimulated electrically via a pair of platinum ring electrodes by a Grass S44 stimulator. The stimulus frequency was 1 pulse every 2 min, pulse duration 0.3 ms and supramaximal pulse amplitude (60 V).

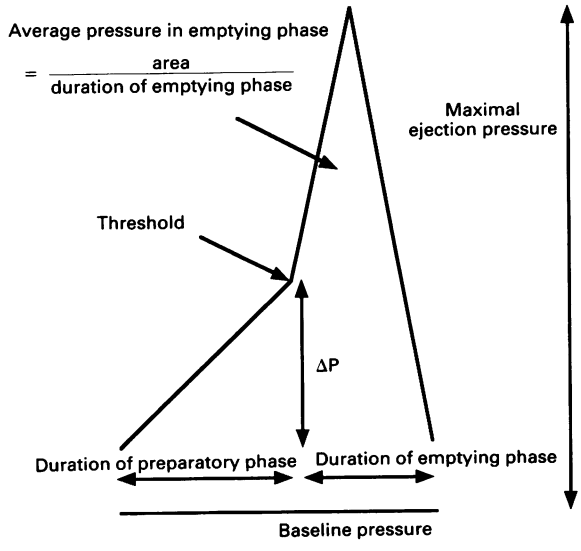

Figure 2 Schematic peristaltic wave showing variables measured in order to calculate values of physiological parameters of peristalsis as described in text.

In the LM-MP preparation, a 2 cm strip of longitudinal muscle-myenteric plexus was folded in half and mounted in a 5 ml organ bath containing Krebs solution. Isotonic contractions of the longitudinal muscle were recorded with a Harvard isotonic transducer with 750 mg counterweight. After a 45 min equilibration period, the strips were stimulated via a pair of platinum ring electrodes with a Grass S44 stimulator. Square wave pulses of supramaximal amplitude (60 V) and 0.5 ms duration were delivered at a frequency of 0.1 Hz. Some opioid receptor agonists probably inhibit neuromuscular transmission by hyperpolarizing neuronal membranes (North & Egan, 1983). Therefore the use of a supramaximal stimulus amplitude may overcome the hyperpolarization and bring the membrane to threshold for initiation of an action potential. In some experiments, the amplitude of the pulses was therefore reduced to produce 50% of the maximal contraction (i.e. EV_{50}).

Experimental design and analysis of results

Data are presented as the means ± s.e.means of experiments using *n* guinea-pigs. Each measurement was made with a separate segment of intestine. Control activity was recorded for at least 5 min before the addition of an agonist. After a further 5 min, an antagonist was added. In some experiments, the antagonist was added 3 min (D-Phe-Cys-Tyr-D-Trp-Orn-Thr-Pen-Thr-NH_2 (CTOP)) or 12 min (nor-binaltorphimine (nor-BNI) and naltrindole) before the agonist. The maximal effect of CTOP occurs within 5 min (Shook *et al.*, 1987). In experiments comparing the effect of an opioid agonist with control recordings, data were analysed with a paired *t* test (two-tailed). Multivariate analysis of variance for repeated measures was used to analyse results from experiments involving control, antagonist and agonist measurements. The General Linear Model procedure of the SAS/STAT System for personal computers (SAS Institute Inc, Cary, NC, 1988) was used. A probability of less than 0.05 was regarded as significant.

Drugs

The following drugs were used: hexamethonium bromide, [D-Ala^2, N-methyl-Phe^4,Gly^5-ol]enkephalin (DAMGO) and tetrodotoxin (Sigma, St Louis, U.S.A.); dynorphin A-(1-13) (Auspep, Melbourne, Australia); [D-Penicillamine^2, D-Penicillamine^5]enkephalin (DPDPE) and D-Phe-Cys-Tyr-D-Trp-Orn-Thr-Pen-Thr-NH_2 (CTOP) (Peninsula, Belmont, Cal, U.S.A.); nor-binaltorphimine (nor-BNI) and naltrindole (RBI, Mass., U.S.A.); and naloxone (Endo Laboratories, New York, U.S.A.).

The peptides were dissolved in 12% trifluoroacetic acid and 0.1% dithiothreitol. At the final concentrations in the bath, these solvents had no effect on the intestinal responses under investigation. The remaining drugs were dissolved in distilled water. The solutions were stored at −4°C and used within 2 weeks (nor-BNI) or 6 weeks (all other drugs). All drugs were administered in volumes less than 1% of the organ bath volume.

Results

Effects of the μ-opioid receptor agonist, DAMGO

The emptying phase of peristalsis was abolished by 200 nM DAMGO in 9 out of 15 preparations. Following addition of the drug, the intestine gradually filled with fluid until the intraluminal pressure increased sufficiently to overcome the outflow resistance. The fluid then moved straight through the

extremely distended intestine as if it were a passive tube. Longitudinal muscle contraction was completely inhibited. In 4 experiments, abolition of peristalsis revealed phasic activity of the circular muscle that was unaffected by tetrodotoxin and therefore probably myogenic. Peristaltic activity could be restored by the addition of 1 μM naloxone, but not by the κ-opioid receptor antagonist, nor-BNI (10 nM) or the δ-opioid receptor antagonist, naltrindole (200 nM). Values of the physiological parameters after peristalsis had been restored by naloxone were not significantly different to control values, with one exception. Contraction of the longitudinal muscle increased significantly from 12.1 ± 1.5% to 14.6 ± 1.5% ($n = 4$; $P < 0.05$). This represents acute dependence to exogenous opioids, as has previously been described by Chahl (1986).

In 6 out of 15 preparations, 200 nM DAMGO did not abolish the emptying phase of peristalsis. In these experiments, values for the physiological parameters of peristalsis were calculated before and after the addition of DAMGO. The compliance of the intestine during the preparatory phase was reduced from 6.9 ± 1.0 μl Pa^{-1} to 4.2 ± 0.7 μl Pa^{-1} ($n = 6$, $P < 0.05$). The threshold volume was increased by 6.9 ± 0.6 ml m^{-1} ($n = 4$; $P < 0.001$). Immediately after the addition of DAMGO, the ensuing preparatory phase was prolonged until the new raised threshold volume was reached. The intestine then emptied to a new, increased, residual volume. The volume of fluid infused during subsequent preparatory phases was not significantly altered. In the experiments in which DAMGO did not abolish the emptying phase, the maximal ejection pressure and the average power generated by the intestine were not altered. Longitudinal muscle contraction was reduced from 14.1 ± 2.5% to 8.1 ± 2.0% ($n = 6$; $P < 0.05$).

Effects of the κ-opioid receptor agonist, dynorphin

Dynorphin (10 nM) abolished the emptying phase of peristalsis in 5 out of 12 experiments. Phasic contractions of the circular muscle were observed in one of these experiments. Peristalsis was restored by 10 nM nor-BNI or 1 μM naloxone, but not by 200 nM naltrindole. Each physiological parameter returned to control levels with the exception of longitudinal muscle contraction. The latter increased significantly from 9.8 ± 1.3% to 13.4 ± 1.1% ($n = 5$; $P < 0.02$) after exposure to dynorphin for approximately 5 min and indicates acute dependence to exogenous opioids, as described previously by Chahl (1986).

Physiological parameters of peristalsis before and after the addition of dynorphin were compared in the experiments in which the emptying phase of peristalsis was not abolished. Dynorphin did not significantly alter the compliance of the intestinal wall in the preparatory phase or the average power generated during the emptying phase. However, there was a large increase in the residual volume. Thus the threshold volume necessary to elicit the emptying phase increased by 5.6 ± 1.4 ml m^{-1} ($n = 6$; $P < 0.02$). There was an increase in the volume of fluid infused into the intestine during the first preparatory phase after the addition of dynorphin, but not in subsequent preparatory phases. Dynorphin reduced the maximal ejection pressure from 30.0 ± 1.7 kPa m^{-1} to 21.7 ± 3.8 kPa m^{-1} ($n = 6$; $P < 0.01$). Longitudinal muscle contraction amplitude at the point of threshold was reduced from 12.0 ± 2.5% to 4.1 ± 1.8% ($n = 6$; $P < 0.01$).

The inhibitory effect of dynorphin on maximal ejection pressure could be due to an action of the drug on excitatory circular muscle motor neurones. In order to investigate this possibility, the effects of dynorphin were tested in the CM-MP preparation. Dynorphin (1 nM, which is the approximate IC_{50}; Johnson, 1991) was added to the preparation following the addition of 30 μM hexamethonium to reduce ganglionic transmission. This concentration of hexamethonium is effective in blocking peristalsis (unpublished observations). Dynorphin significantly reduced the hexamethonium-resistant contractions from 4.86 ± 0.49 mm to 3.18 ± 0.75 mm ($n = 6$; $P < 0.01$).

Effects of the δ-opioid receptor agonist, DPDPE

Unlike the μ- and κ-agonists, DPDPE did not abolish the emptying phase of peristalsis at concentrations up to 1 μM. It did however significantly alter 3 of the 5 physiological parameters (Figure 3). Longitudinal muscle contraction was reduced from 9.4 ± 0.9% to 5.0 ± 0.7% ($n = 23$; $P < 0.0001$) by concentrations above 30 nM. Concentrations of DPDPE up to 77 nM did not affect threshold distension or maximal ejection pressure. Concentrations greater than 115 nM increased the threshold distension through an increase in the residual volume of 2.7 ± 0.6 ml m^{-1} ($n = 15$; $P < 0.0001$). Maximal ejection pressure was reduced from 29.2 ± 1.1 kPa m^{-1} to 25.8 ± 1.1 kPa m^{-1} ($n = 12$; $P < 0.01$) by concentrations of DPDPE above 115 nM. Each of these effects was completely antagonized by the specific δ-opioid receptor antagonist, naltrindole, but not by the μ-(CTOP) or κ-(nor-BNI) receptor antagonists (Table 1). These effects are likely to reflect a very steep concentration-response curve. There was no significant effect of DPDPE on either the compliance of the intestinal wall or on the average power generated during the empyting phase.

Some of the effects of DPDPE could be due to an action of the drug on excitatory circular muscle motor neurones. To test this hypothesis, the effect of DPDPE on electrically stimulated contractions of circular muscle in strips of CM-MP was investigated. Circular muscle contraction was not significantly inhibited by concentrations of DPDPE up to 1 μM.

Longitudinal muscle contraction was reduced by almost 50% by DPDPE during peristalsis. To investigate whether this was due to an action on excitatory longitudinal muscle motor neurones, the effect of DPDPE on electrically stimulated strips of LM-MP was investigated. There was no significant effect of DPDPE at any of the concentrations tested (up to 1 μM). When the LM-MP strip was stimulated by a submaximal voltage (the EV_{50}), there was still no significant effect of DPDPE.

Effects of opioid receptor antagonists

The opioid receptor antagonists CTOP (μ), nor-BNI (κ) and naltrindole (δ), were used to reveal effects of endogenous opioids under different conditions of peristalsis. When fluid was infused into the intestine at a slow rate (0.63 ml min^{-1})

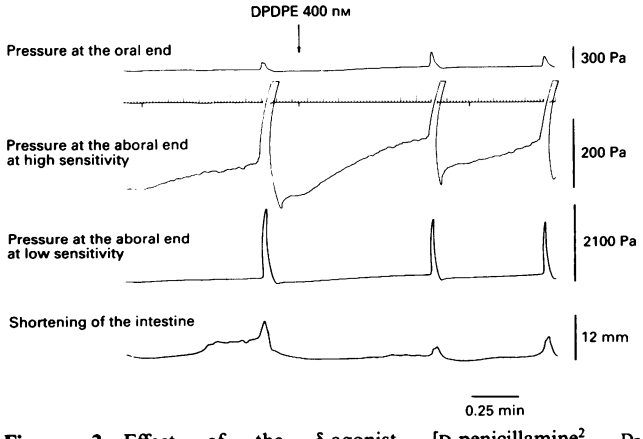

Figure 3 Effect of the δ-agonist, [D-penicillamine^2, D-penicillamine^5]enkephalin (DPDPE) on peristalsis. The duration of the preparatory phase is increased in the first cycle after addition of DPDPE, indicating that a larger volume was infused to trigger the emptying phase. Maximal ejection pressure and shortening of the intestine were both reduced in all cycles following addition of DPDPE.

Table 1 Specificity of effect of [D-penicillamine^2, D-penicillamine^5]enkephalin (DPDPE) on physiological parameters of peristalsis

Condition/Parameter	*Change in residual volume* (ml)	*Maximal ejection pressure* (kPa m^{-1})	*Longitudinal muscle contraction* (%)
Control	−0.013 ± 0.01 (15)	29.22 ± 1.13 (12)	9.39 ± 0.94 (23)
DPDPE	0.194 ± 0.03 (15)****	25.83 ± 1.11 (12)***	5.05 ± 0.68 (23)****
Control	0.012 ± 0.019 (18)	28.18 ± 0.85 (18)	9.49 ± 0.82 (18)
Naltrindole + DPDPE	0.062 ± 0.014 (18)*	27.96 ± 0.82 (18)*	9.18 ± 0.73 (18)*
Control	−0.025 ± 0.023 (4)	22.4 ± 3.29 (5)	9.49 ± 1.71 (5)
CTOP + DPDPE	0.085 ± 0.04 (4)**	18.09 ± 2.94 (5)**	4.38 ± 1.41 (5)****
Control	0.005 ± 0.06 (14)	29.62 ± 0.99 (14)	8.36 ± 5.91 (14)
Nor-BNI + DPDPE	0.21 ± 0.05 (14)**	27.16 ± 1.3 (14)**	5.91 ± 1.03 (14)****

The mean and the s.e.mean are given for experiments on (n) different animals. *$P>0.05$; **$P<0.05$; ***$P<0.01$; ****$P<0.0001$. Probabilities refer to comparisons between DPDPE ± antagonist and the corresponding control. CTOP = D-Phe-Cys-Tyr-D-Trp-Orn-Thr-Pen-Thr-NH_2; nor-BNI = nor-binaltorphimine.

and the intestine emptied against a low resistance, there was no significant effect of any of the antagonists on any of the five parameters measured.

When the intestine was infused with fluid at the higher rate (3.43 ml min^{-1}), it emptied approximately three times more often than at the lower rate, but expelled the same volume of fluid and generated the same average power with each peristaltic wave. Under these conditions, there was also no significant effect of any of the antagonists on any of the parameters measured.

At the low inflow rate, the intestine generated significantly more average power when the resistance of the outflow tubing was increased by 21% by increasing the length of outflow tubing. In these conditions, nor-BNI increased the average power generated from 1.1 ± 0.1 mW m^{-1} to 1.3 ± 0.1 mW m^{-1} ($n = 14$; $P<0.002$). There was no significant effect of nor-BNI on the other four parameters measured, nor were there significant effects of either of the other antagonists on other parameters of peristalsis. The effects of increasing both inflow rate and outflow resistance were not tested.

Discussion

Previous work has shown that in the guinea-pig ileum, opioids inhibit motility by acting on enteric neurones (North & Egan, 1983; Kromer, 1988). Peristalsis involves the coordinated activity of many functional classes of neurones on which opioids might act. The physiological parameters of peristalsis measured in this study reflect the activity of these classes of neurones. We have revealed multiple actions of exogenous and endogenous opioids in peristalsis. In order to interpret the actions of opioids, a brief discussion on the significance of the physiological parameters follows.

Physiological parameters of peristalsis

Radial distension of the intestine as it fills with fluid is detected by mechanoreceptors in the muscularis externa (Yokoyama & North, 1983; Smith *et al.*, 1990) and this must provide the underlying drive for peristalsis. During the preparatory phase, activity of circular muscle motor neurones determines the tone of the circular muscle and the resistance of the muscle to further distension. This was measured as the compliance of the intestinal wall. Activity of longitudinal muscle motor neurones during the preparatory phase causes longitudinal muscle contraction which was measured as shortening of the intestine. Once the threshold distension is reached, contraction of the circular muscle occurs and the threshold distension required to activate this reflex was measured in the present study. The extent of circular muscle contraction and its coordinated propagation determines the peak pressure and average power generated by the intestine.

The effect of selective opioid agonists will be considered on each of the measured parameters in turn, followed by effects of selective antagonists used to reveal the role of released endogenous opioids.

Compliance

The resistance of the intestinal wall to distension (subthreshold for initiation of the emptying phase of peristalsis) is determined by the passive resistance of the wall and the level of contractility of the muscle layer. Neither κ- nor δ-opioid agonists caused any measurable change in the compliance of the intestinal wall during the preparatory phase; however the μ-selective agonist DAMGO significantly reduced compliance. That is, following administration of DAMGO, any infused volume generated a greater luminal pressure change. Mu agonists do not appear to act directly on the muscle in guinea-pig small intestine (Johnson *et al.*, 1987) and have been demonstrated to inhibit enteric neurones (North & Egan, 1983). Therefore these results suggest that the enteric inhibitory neurones are active during the preparatory phase and that the μ-agonist caused a decrease in the output of these neurones to the circular muscle. However, the site of action of DAMGO on compliance remains uncertain; it could inhibitory motor neurones directly or reduce the excitability of sensory neurones or interneurones in the reflex pathway.

Longitudinal muscle contraction

Contraction of the longitudinal muscle layer during the preparatory phase of peristalsis was inhibited by μ-, κ- and δ-opioid agonists. This inhibitory effect of μ- and κ-agonists is likely to be due to inhibition of excitatory motor neurones to the longitudinal muscle layer (Greenberg *et al.*, 1970; Kosterlitz & Waterfield, 1972; Dingledine & Goldstein, 1976). However δ-agonists do not inhibit excitatory transmission to the longitudinal muscle in a comparable manner (Mosberg *et al.*, 1983; Galligan *et al.*, 1984; Shook *et al.*, 1987; Ersparmer *et al.*, 1989; present study). This suggests that δ-agonists inhibit the reflex contraction of longitudinal muscle by acting on either sensory neurones or interneurones rather than directly on motor neurones.

Threshold for triggering the emptying phase

Mu-, κ- and δ-opioid agonists all increased the threshold volume for triggering the emptying phase of peristalsis, in some cases abolishing the emptying phase altogether. In preparations where emptying was not abolished, the threshold volume for eliciting the emptying phase was significantly increased. Both μ- and κ-opioid agonists inhibit excitatory transmission to the circular muscle layer from circular muscle

motor neurones (Johnson *et al.*, 1987; 1988). Greater distension stimuli are known to result in a larger reflex contraction, probably due to a greater activation of the sensory, inter- and motor neurones in the ascending excitatory reflex of the guinea-pig small intestine (Tonini & Costa, 1990). This increase in activation of the reflex pathway may counteract the inhibitory effects of opioids. Similarly, in the preparation used in these experiments to study peristalsis, a greater distension stimulus would counteract the inhibitory effects of opioids on the excitatory motor neurones and trigger the emptying phase. As with the longitudinal muscle layer, δ-agonists do not inhibit excitatory motor neurone transmission to the circular muscle when the motor neurones are electrically stimulated (Johnson *et al.*, 1987; present study). Therefore it is likely that δ-agonists act on sensory neurones or interneurones involved in triggering the emptying phase rather than the final motor neurones.

Maximal ejection pressure and power generated during the emptying phase

During the emptying phase, the peak pressure generated was reduced by κ- and δ-agonists but not by the μ-agonist. These effects can be explained by an action of the κ-agonist on excitatory motor neurones to the circular muscle and of the δ-agonist on sensory neurones or interneurones, as for threshold volume. The lack of effect of the μ-agonist on maximal ejection pressure in contrast to the inhibition evoked by the κ-agonist suggests that there must be differences in the distribution of, or effects mediated by, μ- and κ-receptors on elements of the enteric neurones active during the emptying phase. However, the average power generated by the intestine was unaffected by all the three types of agonist, indicating that the intestine is able to empty equally effectively even after the maximal ejection pressure has been reduced. Nevertheless, there was a reduction in the proportion of the intraluminal volume that was emptied.

Specific effects of δ-opioid receptor agonists

The present study demonstrated several specific effects of DPDPE on motility, as was suggested for the less selective δ-agonist, [D-Ser^2,Leu^5]enkephalin-Thr (DSLET) (Kromer, 1990). The lowest effective concentration of DPDPE differed for each parameter, suggesting that DPDPE acts at more than one site in the reflex pathways underlying peristalsis, and/or that it acts on a single neuronal type which is common to several different pathways. The action of DPDPE could be deduced to be on sensory neurones or interneurones in the pathways innervating both the circular and longitudinal muscle layers, suggesting that these pathways may contain some neurones in common. Thus, using preparations to study peristalsis, δ-agonists have been demonstrated to have effects that were not apparent from studies in simpler preparations (Kromer, 1990; present study) and this reflects the variety of classes of neurones involved in peristalsis. This method of studying peristalsis is highly suitable for revealing multiple sites of action of drugs on enteric neurones.

Modulation of peristalsis by endogenous opioids

Endogenous opioids are released from enteric neurones during peristalsis (Donnerer *et al.*, 1984). Using the methods in which the intestine is forced to empty against the inflow head of pressure (see Introduction), a depression in the amplitude of peristaltic contractions develops which is reversed by naloxone and hence was proposed to be mediated in part by endogenous opioids (Van Nueten *et al.*, 1976). These actions are likely to be mediated predominantly by κ-receptors (Kromer, 1990). Cessation of peristalsis under these conditions represents an extreme situation and has been described as fatigue. In the present study, a role for endogenous opioids was investigated in less extreme conditions. When the intestine was distended by a slow inflow of fluid at the oral end and the emptying at the aboral end was against a low resistance, there was no evidence for the release of endogenous opioids. Similarly, endogenous opioids did not have an effect when the intestine emptied three times as frequently, as a result of an increased rate of distension with fluid. However, when the intestine was forced to empty against a higher outflow resistance, thus being made to work harder, evidence was obtained for endogenous opioids reducing the average power generated by the intestine. This action was predominantly mediated by κ-receptors, and is consistent with the results obtained by Kromer (1990). We propose that endogenous opioids may function as a braking mechanism to prevent the intestine from generating excessive power in response to high resistances. The identification of the class of enteric neurones that is the source of these endogenous opioids remains to be established. However, both pro-enkephalin- and pro-dynorphin-derived peptides are found in different enteric neurones in this tissue (Hughes *et al.*, 1977; Linnoila *et al.*, 1978; Furness *et al.*, 1983; Costa *et al.*, 1985; Corbett *et al.*, 1988).

In conclusion, this study has demonstrated that endogenous opioids are released during peristalsis and reduce the average power generated by the intestine through an action at κ-receptors. This modulatory effect occurs only when the intestine is forced to empty against a high resistance. The study demonstrated specific effects of μ- and κ-opioid receptor agonists on physiological parameters of peristalsis which could be attributed to an action of these agonists on excitatory circular and longitudinal muscle motor neurones and specific effect of a δ-agonist on sensory neurones or interneurones which activate circular or longitudinal muscle motor neurones.

This study was supported by a NH and MRC Medical Undergraduate Scholarship and an AMSA-AMA J.G. Hunter Research Fellowship to S.A.W. and a NH and MRC unit grant to M.C. We are grateful to Mr Charles Humphreys for technical assistance and Dr Simon Brookes for critical comments on the manuscript.

References

BULBRING, E., CREMA, A. & SAXBY, O.B. (1958). A method for recording peristalsis in isolated intestine. *Br. J. Pharmacol.*, **13**, 440–443.

CANNON, W.B. (1912). Peristalsis, segmentation and the myenteric reflex. *Am. J. Physiol.*, **300**, 114–128.

CHAHL, L. (1986). Withdrawal responses of guinea-pig isolated ileum following brief exposure to opiates and opioid peptides. *Naunyn-Schmiedebergs Arch. Pharmacol.*, **333**, 387–392.

CORBETT, A.D., MCKNIGHT, A.T. & KOSTERLITZ, H.W. (1988). Tissue content of opioid peptides in the myenteric plexus-longitudinal muscle of guinea-pig small intestine. *J. Neurochem.*, **51**, 32–37.

COSTA, M. & FURNESS, J.B. (1982). Nervous control of intestinal motility. In *Handbook of Experimental Pharmacology*, ed Bertacchini, A. pp. 279–382. Berlin: Springer-Verlag.

COSTA, M., FURNESS, J.B. & CUELLO, A.C. (1985). Separate populations of opioid containing neurons in the guinea-pig intestine. *Neuropeptides*, **5**, 445–448.

DAVISON, J.S. & NAJAFI-FARASHAH, A. (1982). Role of endogenous opiates in the peristaltic reflex. *J. Physiol.*, **330**, 87P–88P.

DINGLEDINE, R. & GOLDSTEIN, A. (1976). Effect of synaptic transmission blockade on morphine action in the guinea-pig myenteric plexus. *J. Pharmacol. Exp. Ther.*, **196**, 97–106.

DONNERER, J., HOLZER, P. & LEMBECK, F. (1984). Release of dynorphin, somatostatin and substance P from the vascularly perfused small intestine of the guinea-pig during peristalsis. *Br. J. Pharmacol.*, **83**, 919–925.

ERSPARMER, V., MELCHIORRI, P., FALCONIERI-ERSPARMER, G., BARRA, D., SIMMACO, M. & KREIL, G. (1989). Deltorphins: a family of naturally occurring peptides with high affinity and selectivity for δ opioid binding sites. *Proc. Natl. Acad. Sci. U.S.A.*, **86**, 5188–5192.

FURNESS, J.B., COSTA, M. & MILLER, R.J. (1983). Distribution and projections of nerves with enkephalin-like immunoreactivity in the guinea-pig small intestine. *Neuroscience*, **8**, 653–664.

GALLIGAN, J.J., MOSBERG, H.I., HURST, R., HRUBY, V.J. & BURKS, T.F. (1984). Cerebral *delta* opioid receptors mediated analgesia but not the intestinal motility effects of intracerebroventricularly administered opioids. *J. Pharmacol. Exp. Ther.*, **229**, 641–648.

GALLIGAN, J.J. & NORTH, R.A. (1991). Opioid, 5-HT_{1A} and α_2 receptors localized to subsets of guinea-pig myenteric neurons. *J. Auton. Nerv. Syst.*, **32**, 1–12.

GINZEL, K.H. (1959). Investigations concerning the initiation of the peristaltic reflex in the guinea-pig ileum. *J. Physiol.*, **148**, 75P–76P.

GLASS, J., CHAN, W.C. & GINTZLER, A.R. (1986). Direct analysis of the release of methionine-enkephalin from the guinea-pig myenteric plexus: modulation by endogenous opioids and exogenous morphine. *J. Pharmacol. Exp. Ther.*, **239**, 742–747.

GOLDSTEIN, A. & NAIDU, A. (1989). Multiple opioid receptors: ligand selectivity profiles and binding site signatures. *Mol. Pharmacol.*, **36**, 265–272.

GREENBERG, R., KOSTERLITZ, H.W. & WATERFIELD, A.A. (1970). The effects of hexamethonium, morphine and adrenaline on the output of acetylcholine from the myenteric plexus-longitudinal muscle preparation of the ileum. *Br. J. Pharmacol.*, **40**, 553–554P.

GUYTON, A.C. (1986). *Textbook of Medical Physiology* 7th ed. p. 214. Philadelphia: Saunders.

HOLZER, P. & LEMBECK, F. (1979). Effect of neuropeptides on the efficiency of the peristaltic reflex. *Naunyn-Schmiedebergs Arch. Pharmacol.*, **307**, 257–264.

HUGHES, J., KOSTERLITZ, H.W. & SMITH, T.W. (1977). The distribution of methionine-enkephalin and leucine-enkephalin in the brain and peripheral tissue. *Br. J. Pharmacol.*, **61**, 639–647.

JOHNSON, S.M. (1991). Nonspecific tolerance in ileal circular muscle-myenteric plexus preparations from morphine-pretreated guinea-pigs. *J. Pharmacol. Exp. Ther.*, **257**, 239–246.

JOHNSON, S.M., COSTA, M. & HUMPHREYS, C.M.S. (1988). Opioid mu and kappa receptors on axons of cholinergic excitatory motor neurons supplying the circular muscle of guinea-pig ileum. *Naunyn-Schmiedebergs Arch. Pharmacol.*, **338**, 397–400.

JOHNSON, S.M., COSTA, M., HUMPHREYS, C.M.S. & SHEARMAN, R. (1987). Inhibitory effects of opioids in a circular muscle-myenteric plexus preparation of guinea-pig ileum. *Naunyn-Schmiedebergs Arch. Pharmacol.*, **336**, 419–424.

KOSTERLITZ, H.W. & LEES, G.M. (1964). Pharmacological analysis of intrinsic intestinal reflexes. *Pharmacol. Rev.*, **16**, 301–339.

KOSTERLITZ, H.W. & ROBINSON, J.A. (1959). Reflex contractions of the longitudinal muscle coat of the isolated guinea-pig ileum. *J. Physiol.*, **146**, 369–379.

KOSTERLITZ, H.W. & WATERFIELD, A.A. (1972). Differential effects of drugs on the acetylcholine output from the myenteric plexus and the responses of the longitudinal muscle of the guinea-pig ileum. *Br. J. Pharmacol.*, **46**, 569–570P.

KROMER, W. (1988). Endogenous and exogenous opioids in the control of gastrointestinal motility and secretion. *Pharmacol. Rev.*, **40**, 121–162.

KROMER, W. (1990). Reflex peristalsis in the guinea pig isolated ileum is endogenously controlled by kappa opioid receptors. *Naunyn-Schmiedebergs Arch. Pharmacol.*, **341**, 450–454.

KROMER, W., PRETZLAFF, W. & WOINOFF, R. (1980). Opioids modulate periodicity rather than efficacy of peristaltic waves in the guinea pig ileum *in vitro*. *Life Sci.*, **26**, 1857–1865.

LESLIE, F.M., CHAVKIN, C. & COX, B.M. (1980). Opioid binding properties of brain and peripheral tissues: evidence for heterogeneity in opioid ligand binding sites. *J. Pharmacol. Exp. Ther.*, **214**, 395–402.

LINNOILA, R.I., DIAUGUSTINE, R.P., MILLER, R.J., CHANG, K.J. & CUATRESCASAS, P. (1978). An immunohistochemical study of the distribution of (met5) and (leu5)-enkephalin in the gastrointestinal tract. *Neuroscience*, **3**, 1187–1196.

MILLER, R.J. & HIRNING, L.D. (1989). Opioid peptides of the gut. In *Handbook of Physiology: The Gastrointestinal System. Vol. 2.* ed. Schultz, S.G., Wood, J.D. & Rauner, B.B. pp. 631–660. Bethesda: Am. Physiol. Soc.

MOSBERG, H.I., HURST, R., HRUBY, V.J., GEE, K., YAMAMURA, H.I., GALLIGAN, J.J. & BURKS, T.F. (1983). Bis-penicillamine enkephalins possess highly improved specificity toward δ opioid receptors. *Proc. Natl. Acad. Sci. U.S.A.*, **80**, 5871–5874.

NAVE, C.R. & NAVE, B.C. (1980). *Physics for the Health Sciences* 2nd ed. p. 113. Philadelphia: Saunders.

NORTH, R.A. & EGAN, T.M. (1983). Actions and distributions of opioid peptides in peripheral tissues. *Br. Med. Bull.*, **39**, 71–75.

NORTH, R.A. & TONINI, M. (1977). The mechanism of action of narcotic analgesics in the guinea-pig ileum. *Br. J. Pharmacol.*, **61**, 541–549.

PILLAI, N.P. & JOHNSON, S.M. (1991). The electrophysiological effects of [D-Ala^2, N-Me-Phe^4, Gly^5-ol]-enkephalin on guinea-pig myenteric neurons. *Eur. J. Pharmacol.*, **192**, 227–233.

PUIG, M.M., GASCON, P., CRAVISO, G.L. & MUSACCHIO, J.M. (1977). Endogenous opiate receptor ligand: electrically induces release in the guinea-pig ileum. *Science*, **195**, 419–420.

RANG, H.P. (1964). Stimulant actions of volatile anaesthetics on smooth muscle. *Br. J. Pharmacol. Chemother.*, **22**, 356–365.

SAS INSTITUTE INC (1988). *SAS/STAT User's Guide*, release 6.03 edition. Cary, NC.

SHOOK, J.E., PELTON, J.T., WIRE, W.S., HIRNING, L.D., HRUBY, V.J. & BURKS, T.F. (1987). Pharmacological evaluation of a cyclic somatostatin analog with antagonist activity at mu opioid receptors *in vitro*. *J. Pharmacol. Exp. Ther.*, **240**, 772–777.

SMITH, T.K., BORNSTEIN, J.C. & FURNESS, J.B. (1990). Distension-evoked ascending and descending reflexes in the circular muscle of the guinea-pig ileum: an intracellular study. *J. Auton. Nerv. Syst.*, **29**, 203–218.

TONINI, M. & COSTA, M. (1990). A pharmacological analysis of the neuronal circuitry involved in distension-evoked enteric excitatory reflex. *Neuroscience*, **38**, 787–795.

TONINI, M., FRIGO, G., LECCHINI, S., D'ANGELO, L. & CREMA, A. (1981). Hyoscine-resistant peristalsis in guinea-pig ileum. *Eur. J. Pharmacol.*, **71**, 375–381.

TRENDELENBURG, P. (1917). Physiologische und pharmakologische Versuche über die Dünndarmperistaltik. *Arch. Exp. Path. Pharmakol.*, **81**, 55–129.

VAN NUETEN, J.M., JANSSEN, P.A.J. & FONTAINE, J. (1976). Unexpected reversal effects of naloxone on the guinea-pig ileum. *Life Sci.*, **18**, 803–809.

WATERMAN, S.A., COSTA, M. & TONINI, M. (1990). Measurement of physiological parameters of peristalsis in vitro. *Proceedings of the International Symposium on the Pharmacotherapy of Gastrointestinal Motor Disorders Conference*, Adelaide, September 1990.

YOKOYAMA, S. & NORTH, R.A. (1983). Electrical activity of longitudinal and circular muscle during peristalsis. *Am. J. Physiol.*, **244** (*Gastrointest. Liver Physiol.*, **7**), G83–G88.

(Received July 1, 1991
Revised March 13, 1992
Accepted April 16, 1992)

Br. J. Pharmacol. (1992), **106**, 1011–1018 © Macmillan Press Ltd, 1992

[^{3}H]-RS-15385-197, a selective and high affinity radioligand for α_2-adrenoceptors: implications for receptor classification

A.C. MacKinnon, A.T. Kilpatrick, B.A. Kenny, M. Spedding & [1]C.M. Brown

Department of Pharmacology, Syntex Research Centre, Heriot-Watt University Research Park, Riccarton, Edinburgh EH14 4AP

1 RS-15385-197 is the most potent and selective α_2-adrenoceptor antagonist available. We have used [^{3}H]-RS-15385-197 to define α_2-adrenoceptor subtypes. The binding of [^{3}H]-RS-15385-197 to membranes of rat cerebral cortex, rat neonatal lung and human platelets was reversible, saturable and of high affinity. Saturation experiments indicated that [^{3}H]-RS-15385-197 bound to a single population of sites in all 3 tissues with high affinity (0.08–0.14 nM). The density of sites labelled by [^{3}H]-RS-15385-197 was greater in the cortex (275 fmol mg^{-1} protein) than in the neonate lung (174 fmol mg^{-1} protein) and human platelet (170 fmol mg^{-1} protein). The density of sites labelled with [^{3}H]-RS-15385-197 in the cortex was significantly greater than that labelled with [^{3}H]-yohimbine (121 fmol mg^{-1} protein).

2 The selective α_2-adrenoceptor antagonists, idazoxan, yohimbine, rauwolscine and WY 26703 displaced [^{3}H]-RS-15385-197 binding to rat cerebral cortex in a simple manner with Hill slopes close to unity. The affinities derived for these antagonists against [^{3}H]-RS-15385-197 were similar to the values obtained for the displacement of [^{3}H]-yohimbine indicating the α_2-adrenoceptor nature of the binding site.

3 α_{2A}-Adrenoceptor selective compounds, oxymetazoline and BRL 44409, showed high affinity for [^{3}H]-RS-15385-197 binding in the human platelet and lower affinity in the neonate lung, while the α_{2B}-selective compounds, prazosin and imiloxan, showed high affinity for [^{3}H]-RS-15385-197 binding in the neonate lung. This suggests that [^{3}H]-RS-15385-197 labels both α_{2A}- and α_{2B}-adrenoceptor subtypes.

4 Prazosin and methysergide inhibited the binding of [^{3}H]-RS-15385-197 in the rat cerebral cortex in a simple manner consistent with an interaction at a single site. Although oxymetazoline inhibited [^{3}H]-RS-15385-197 with a Hill slope significantly different from unity, the slope was increased to unity in the presence of Gpp(NH)p, suggesting an agonist-like interaction.

5 The site labelled by [^{3}H]-RS-15385-197 in the rat cortex shows high affinity for oxymetazoline and low affinity for prazosin which could be taken as evidence for classifying the site as an α_{2A}-subtype. However, the affinities of yohimbine, rauwolscine and oxymetazoline at this site do not correspond to the population of sites in the human platelet. Yohimbine and rauwolscine were 20 fold selective for the platelet α_{2A}-subtype, whereas phentolamine was 2 fold and imiloxan was 10 fold selective for the cortex subtype. Indeed although the site showed some similarities with the α_{2A}-subtype, the highest degree of homology was observed between this site and the rat submaxillary gland and the RG20 clone, tentatively called the α_{2D}-adrenoceptor subtype. We propose that the α_2-adrenoceptor in the rat cortex may therefore correspond to the putative α_{2D}-subtype of the adrenoceptor.

Keywords: [^{3}H]-RS-15385-197; [^{3}H]-yohimbine; α_2-adrenoceptors, α_2-adrenoceptor subtypes

Introduction

The subdivision of α_2-adrenoceptors into α_1- and α_2 adrenoceptors is based upon a different rank order of potencies for both agonists and antagonists at these receptor subtypes (Starke, 1977; 1987). α_2-Adrenoceptors are historically defined as having high affinity for yohimbine and its stereoisomer rauwolscine but low affinity for prazosin, whereas α_1-adrenoceptors display a high affinity for prazosin but low affinity for yohimbine and rauwolscine.

α_2-Adrenoceptor subtypes have been differentiated on the basis of affinity for prazosin and oxymetazoline; the α_{2A} subtype has low affinity for prazosin and high affinity for oxymetazoline whereas the α_{2B} has higher affinity for prazosin and lower affinity for oxymetazoline (Cheung *et al.*, 1982; Bylund, 1985; Nahorski *et al.*, 1985; Petrash & Bylund, 1986). Although originally proposed as a non-rodent (α_{2A})/rodent (α_{2B}) classification, both subtypes exist in rat cerebrum (Bylund, 1985) and human caudate nucleus (Petrash & Bylund, 1986). The α_2-adrenoceptor on human platelets is considered as a pure population of the α_{2A}-adrenoceptor subtype (Cheung *et al.*, 1982) whereas rat neonate lung contains a homogeneous population of the α_{2B}-adrenoceptor subtype (Latifpour *et al.*, 1982). Cell lines containing the α_{2A}-adrenoceptor subtype (HT29) and α_{2B}-adrenoceptor subtypes (NG108–15) have also been described (Bylund *et al.*, 1988). We have recently confirmed the finding of Bylund (1985), that prazosin and oxymetazoline displace [^{3}H]-yohimbine binding to rat cerebral cortex with high and low affinity (Brown *et al.*, 1990a). Furthermore we have demonstrated that displacement of [^{3}H]-idazoxan by prazosin and oxymetazoline was consistent with binding to a single site; the affinity of prazosin and oxymetazoline suggesting an interaction with the α_{2A}-adrenoceptor subtype (Brown *et al.*, 1990b). Thus labelling of the α_2-adrenoceptor subtypes potentially shows a structural dependence related to the radioligand employed. Recently, RS-15385-197 (Figure 1), has been described as the most potent and selective α_2-adrenoceptor antagonist thus far, having $>$ 1000 fold selectivity over α_1-adrenoceptors and other receptor subtypes (Clark *et al.*, 1989; 1990). In the present studies, we have characterized the binding of [^{3}H]-RS-15385-197 to rat cortex, rat neonatal lung and human platelet and examined its displacement by

[1] Author for correspondence.

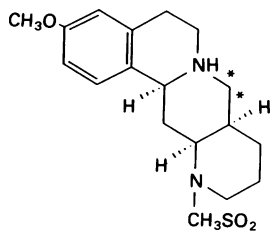

Figure 1 The structure of RS-15385-197; *marks the position of the ^3H.

prazosin and oxymetazoline in order to establish if this radioligand labels α_{2A}-and/or α_{2B}-adrenoceptor subtypes.

Methods

Membrane preparation

Male Sprague-Dawley rats (180–200 g) were stunned, decapitated and the cerebral cortex dissected from the other brain regions over ice. Membranes were prepared as previously described (Brown *et al.*, 1990a). Briefly tissues were homogenized in 25 volumes of ice cold 50 mM Tris HCl, 5 mM EDTA, (pH 7.4 at 25°C) with a polytron PT 10 tissue disruptor. The homogenate was centrifuged at 48000 *g* for 15 min at 4°C. The pellet was resuspended in the same buffer and washed once more under the conditions described. Then the pellet was washed twice in assay buffer (50 mM Tris HCl, 0.5 mM EDTA, pH 7.4 at 25°C) by repeated centrifugation at 48000 *g* for 15 min at 4°C. The final pellet was resuspended in assay buffer at an approximate protein level of 1 mg ml^{-1}. Lungs were dissected from one day old rat pups and membranes were prepared as described for cerebral cortex. Blood was collected from human volunteers and platelet membranes prepared as previously described (Cheung *et al.*, 1982). Platelet rich plasma (PRP) was obtained by centrifugation at 200 *g* for 10 min. The PRP was centrifuged at 25000 *g* for 10 min at 4°C and the resulting pellet resuspended in cold lysing buffer (5 mM Tris HCl, 5 mM EDTA, pH 7.4). The pellet was washed once more in lysing buffer by resuspension and centrifugation followed by a wash in assay buffer 50 mM Tris HCl, 0.5 mM EDTA pH 7.4 at 25°C. The final pellet was resuspended in assay buffer at a protein concentration of 0.3 mg ml^{-1}. Membranes were stored under liquid nitrogen until used in the binding assay.

Saturation experiments

Membranes (50–200 μg protein) and increasing concentrations of [^{3}H]-RS-15385-197 (0.01–5 nM) or [^{3}H]-yohimbine (0.1–15 nM) were incubated to equilibrium in 50 mM Tris HCl buffer, pH 7.4 at 25°C containing 0.5 mM EDTA. Incubations were carried out in a final volume of 1 ml for 90 min for [^{3}H]-RS-15385-197 in the rat cortex and for 60 min in the human platelet and rat neonate lung. [^{3}H]-yohimbine was incubated for 30 min at 25°C in a final volume of 0.5 ml. Bound ligand was separated from free by vacuum filtration over GF/B filters on a Brandell cell harvester. The filters were washed twice for 5 s with incubation buffer and the bound radioactivity determined by liquid scintillation counting. Non-specific binding at each free ligand concentration was determined in the presence of 1 μM phentolamine for [^{3}H]-RS-15385-197 and 10 μM phentolamine for [^{3}H]-yohimbine.

Kinetics

The determination of association kinetics was carried out under conditions described for saturation studies. Binding was initiated with the addition of 0.1–0.2 nM [^{3}H]-RS-15385-197 and terminated, at timed intervals, with rapid filtration. Following the attainment of equilibrium, 1 μM phentolamine was added to dissociate bound [^{3}H]-RS-15385-197 from the receptor. The extent of radioligand dissociation was determined from a second series of timed filtrations of the samples.

Competition experiments

Competition experiments were carried out in the presence of 0.1 nM [^{3}H]-RS-15385-197 or 1.5 nM [^{3}H]-yohimbine and various drugs over the concentration range 1pM–0.1 mM. Conditions for the competition assays were identical to those described for the saturation experiments. Non-specific binding represented $<5\%$ for [^{3}H]-RS-15385-197 in all tissues and between 25–30% of [^{3}H]-yohimbine binding in the rat cortex. Each determination was carried out in duplicate.

Data analysis

Equilibrium binding parameters (K_d and B_{max}) were obtained with the iterative non-linear least square curve fitting programme 'Ligand' (Munson & Rodbard, 1980).

Binding isotherms from displacement studies were analysed with a non-linear least square parametric curve fitting programme capable of estimating the IC_{50} (concentration of drug displacing 50% of specific binding) and iterative curve fitting to a single or two site model. The single site and two site models for each isotherm were compared using the differential F value defined by the following equation

$$F = \frac{(SS_1\text{-}SS_2)/)(d.f._1\text{-}d.f._2)}{SS_2/d.f._2}$$

where SS_1 is the sum of squares error for the single site, SS_2 is the sum of squares error for the two site model, $d.f._1$ is the degrees of freedom for the single site model and $d.f._2$ the degrees of freedom for the two site model (Munson & Rodbard, 1980; Petrash & Bylund, 1986). A two site fit was assumed to be significantly better than a single site fit if the determined F value had a P value of <0.05. Hill slopes were tested for significance by the non-parametric Student's two-tailed t test and significance taken at $P<0.05$. The inhibitory constant (K_i) was calculated from the IC_{50} by the equation of Cheng & Prusoff (1973).

For kinetic experiments, the pseudo first order rate constant (K_{obs}) was calculated from the slope of the plot ln $(B_e/B_e\text{-}B_t)$ versus time where B_e is the binding at equilibrium and B_t is the binding at time t. The association rate constant K_1 was determined from the equation $K_1 = (K_{obs}\text{-}K_2)/[\text{Ligand}]$, where K_2 is the dissociation rate constant calculated from the slope of the plot $\ln(B_t/B_0)$ against time, where B_0 represents binding at time 0 and B_t the binding at time t. The equilibrium dissociation constant K_d was calculated from the equation $K_d = K_2/K_1$.

Protein level was determined by the BSA assay kits, with bovine serum albumin used as the protein standard (Sorenson & Brodbeck, 1986).

Chemicals and drugs

[^{3}H]-RS-15385-197 (57 Ci mmol^{-1}) was synthesized by Dr H. Parnes, Syntex, Palo Alto, [^{3}H]-yohimbine (89 Ci mmol^{-1}) from Du Pont, U.K. Drugs were obtained from the following sources; 5-HT creatine sulphate, yohimbine HCl, clonidine HCl, oxymetazoline HCl, (−)-noradrenaline, (−)-adrenaline, Gpp(NH)p (5'-guanylimidophosphate) and dopamine HCl from Sigma; rauwolsine HCl from Carl Roth; phentolamine HCl from Ciba; RS-15385-197((8a**R**, 12a**S**, 13a**S**)-5, 8, 8a, 9, 10, 11, 12, 12a, 13, 13a-decahydro-3-methoxy-12- (methylsulphonyl)-6H-isoquino [2,1-g][1,6]-naphthyridine), BRL 44409 (2-[5-chloro-1, 3-dihydro-2*H*-isoindol-2-yl) methyl l]-4,5-dihydro-1*H*-imidazole dihydrochloride), SKF 104078 ((6-

chloro-9-[(3-methyl 2 butenyl) oxyl-3-methyl-1*H*-2,3,4,5-tetrahydro-3-benzazepine), idazoxan, and imiloxan from Syntex; WY 26703 (W-methyl-N-(1,3,4,6,7,11b-hezahydro-2H-benzo-αaβ-quinolizin-2-yl)-s-butane-sulphonamide) and indoramin from Wyeth; prazosin HCl from Pfizer; MDL 72222 (1αH, 3αH, 5αH-tropan-3-yl 3,5 dichlorobenzoate methane sulphonate) from Merrell Dow; methysergide bimaleate from Sandoz; WB 4101 (2-[2,6-dichloro(N-beta chloroethyl-N-methyl)-4-methyl amino] phenylimino-2-imidazoline dihydrochloride) from Ward Bleckinsop; ritanserin and haloperidol from Research Biochemicals Incorporated. All other chemicals were of the highest purity commercially available.

Results

Association of [^{3}H]-RS-15385-197 to rat cortex membranes was rapid with $t_{\frac{1}{2}} = 17$ min (Figure 2) and equilibrium reached after 90 min. The mean observed initial rate constant (K_{obs}) calculated from four experiments was 0.045 ± 0.006 min^{-1}. Dissociation of [^{3}H]-RS-15385-197 followed first order kinetics with $t_{\frac{1}{2}} = 64$ min. The mean rate constant for dissociation (K_2) was 0.013 ± 0.001 min^{-1}. The equilibrium dissociation constant determined from the ratio $K_d = K_2/K_1$ where $K_1 = (K_{obs}-K_2)/K_2$[^{3}H]-RS-15385-197 was 0.062 ± 0.015 nM. In the neonatal lung and human platelet [^{3}H]-RS-15385-197 binding was also rapid and reversible and of high affinity with kinetically derived K_d values of 0.056 ± 0.007 nM in the rat neonatal lung and 0.113 ± 0.021 nM in the human platelet (data not shown).

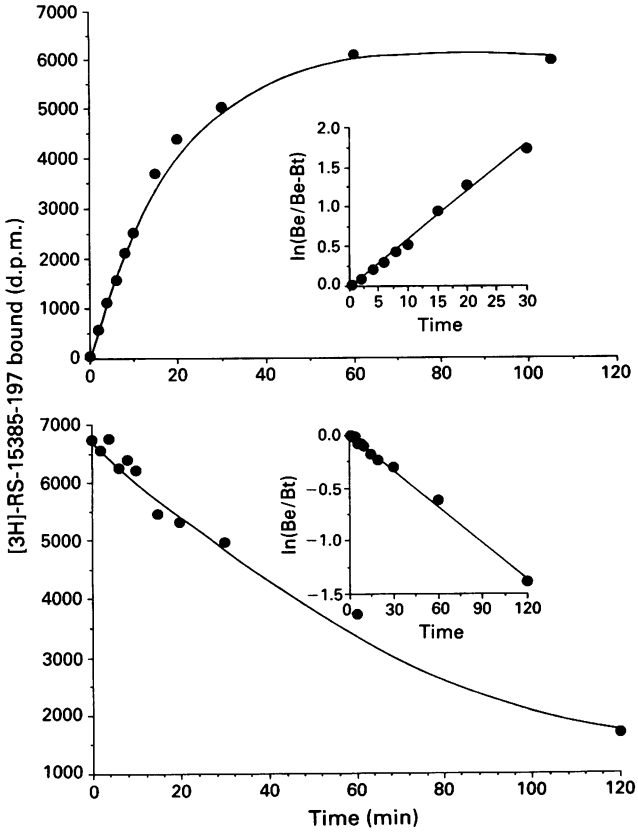

Figure 2 Association and dissociation of 0.15 nM [^{3}H]-RS-15385-197 in rat cortex membranes. The data represent a typical experiment performed in duplicate. The inset shows the pseudo-first order kinetic plot drawn from the data. The association rate constant (K_{obs}) = 0.055 min^{-1}. The dissociation rate constant was followed after addition of 1 μM phentolamine and the rate constant (K_2) = 0.013 min^{-1}. The equilibrium dissociation constant K_d = 0.05 nM.

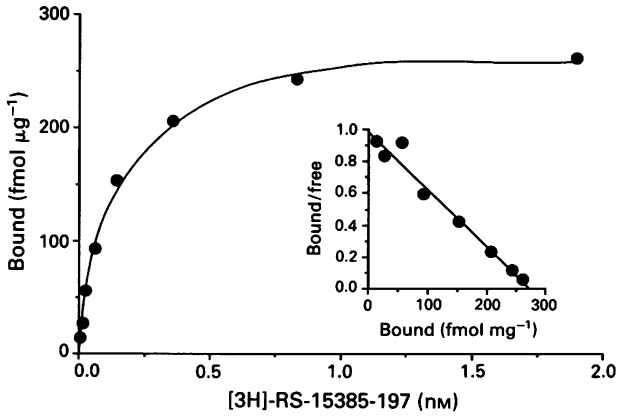

Figure 3 Specific binding of increasing concentrations of [^{3}H]-RS-15385-197 in the rat cortex. The data represent a typical experiment performed in triplicate. The inset shows Scatchard transformation of the specific binding isotherms. Binding parameters K_d and B_{max} were calculated using the non-linear least squares curve fitting programme Ligand (Munson & Rodbard, 1980). K_d = 0.14 nM, B_{max} = 274 fmol mg^{-1}.

Saturation experiments indicated that [^{3}H]-RS-15385-197 bound to a single population of high affinity binding sites in rat cortex (Figure 3, Table 1). The affinity and density of sites labelled by [^{3}H]-RS-15385-197 in the three tissues is given in Table 1, and shows that the highest density was observed in the rat cortex ($B_{max} = 275 \pm 19$ fmol mg^{-1} protein). However, in the same tissue the number of sites labelled by [^{3}H]-yohimbine was significantly less ($B_{max} = 121 \pm 10$ fmol mg^{-1} protein).

In order to determine the nature of the binding site labelled by [^{3}H]-RS-15385-197 in the rat cortex, the affinities of a number of selective ligands were determined at this site and compared with the values obtained for the displacement of [^{3}H]-yohimbine (Table 2 and Figure 4). The rank order of potency of selective α_2-adrenoceptor antagonists to displace [^{3}H]-RS-15385-197 was phentolamine > idazoxan > WY 26703 > rauwolscine = yohimbine >> prazosin, and for agonists was oxymetazoline > clonidine > adrenaline, consistent with [^{3}H]-RS-15385-197 labelling α_2-adrenoceptors in rat cortical membranes. In the presence of 100 μM Gpp(NH)p, the displacement curves for clonidine, (−)-adrenaline and (−)-noradrenaline were shifted to the right and there was a steepening of the Hill slope (Table 3).

The α_1-adrenoceptor antagonists, prazosin and indoramin, displaced [^{3}H]-RS-15385-197 with low affinity and with Hill slopes of unity. In contrast, prazosin but not indoramin displaced [^{3}H]-yohimbine binding with a Hill slope

Table 1 Specific binding of [^{3}H]-RS-15385-197 and [^{3}H]-yohimbine to rat cerebral cortex, rat neonatal lung and human platelet membranes

	K_d (nM)	B_{max} (fmol mg^{-1} protein)
[^{3}H]-RS-15385-197		
Rat cortex	0.12 ± 0.01	275 ± 19
Rat neonatal lung	0.08 ± 0.01	174 ± 20
Human platelet	0.14 ± 0.02	170 ± 37
[^{3}H]-yohimbine		
Rat cortex	5.30 ± 0.90	121 ± 10

Saturation experiments were carried out over the concentration ranges 0.01–5 nM for [^{3}H]-RS-15385-197 and 0.1–15 nM for [^{3}H]-yohimbine. Each value represents the mean ± s.e.mean of at least three separate experiments performed in triplicate.

Table 2 Inhibition of [^{3}H]-RS-15385-197 and [^{3}H]-yohimbine binding to rat cerebral cortex

	[^{3}H]-RS-15385-197		*[^{3}H]-yohimbine*	
	p*K*i	nH	p*K*i	nH
RS-15385-197	9.46 ± 0.04	1.01 ± 0.01	9.45 ± 0.12	1.01 ± 0.08
Phentolamine	8.96 ± 0.20	0.99 ± 0.01	8.40 ± 0.60	0.97 ± 0.09
Idazoxan	8.45 ± 0.23	0.92 ± 0.04	7.67 ± 0.06	1.00 ± 0.05
WY 26703	8.16 ± 0.17	0.98 ± 0.05	7.94 ± 0.07	1.02 ± 0.05
Yohimbine	7.68 ± 0.03	1.00 ± 0.01	7.87 ± 0.07	0.89 ± 0.09
Rauwolscine	7.68 ± 0.04	0.92 ± 0.04	7.86 ± 0.07	0.89 ± 0.09
Clonidine	7.79 ± 0.22	0.77 ± 0.04*	7.85 ± 0.01	0.70 ± 0.05*
Adrenaline	7.23 ± 0.15	0.63 ± 0.01*	7.12 ± 0.13	0.73 ± 0.02*
Noradrenaline	7.01 ± 0.25	0.70 ± 0.06*	6.65 ± 0.10	0.71 ± 0.15*
Oxymetazoline	7.94 ± 0.15	0.74 ± 0.01*	7.70 ± 0.01	0.70 ± 0.08*
Prazosin	6.17 ± 0.18	1.04 ± 0.05	6.96 ± 0.10	0.76 ± 0.09*
Imiloxan	7.14 ± 0.02	0.95 ± 0.04	7.10 ± 0.20	0.98 ± 0.12
WB 4101	7.52 ± 0.05	1.04 ± 0.05	7.24 ± 0.08	0.83 ± 0.10
BRL 44409	7.69 ± 0.06	0.90 ± 0.02	7.18 ± 0.09	0.85 ± 0.10
SKF 104078	7.36 ± 0.02	0.94 ± 0.05	6.70 ± 0.10	0.95 ± 0.06
Indoramin	5.24 ± 0.10	0.97 ± 0.05	5.09 ± 0.04	0.98 ± 0.05
Ritanserin	7.38 ± 0.19	0.87 ± 0.01	7.20 ± 0.01	0.98 ± 0.08
Methysergide	5.94 ± 0.11	0.94 ± 0.07	7.05 ± 0.10	0.77 ± 0.08*
MDL 72222	4.69 ± 0.12	0.96 ± 0.05	ND	
5-HT	4.68 ± 0.18	1.15 ± 0.08	<4.00	
Haloperidol	5.85 ± 0.15	0.95 ± 0.08	<5.00	

Affinity values and Hill slopes (nH) obtained from the displacement of specific binding of 0.1 nM [^{3}H]-RS-15385-197 and 1.5 nM [^{3}H]-yohimbine from rat cerebral cortical membranes.
*denotes a Hill slope significantly different from unity with the respective affinity values representing the pIC_{50} corrected for the free ligand concentration used. Each value represents the mean ± s.e.mean of at least three separate experiments.
ND = not determined.

significantly less than unity. Computer analysis resolved the prazosin and oxymetazoline displacement curves for the inhibition of [^{3}H]-yohimbine binding to rat cerebral cortical membranes into high and low affinity components, consistent with binding to α_{2A}- and α_{2B}-adrenoceptor subtypes (Brown *et al.*, 1990a) (Table 4). The mixed 5-HT_1 and 5-HT_2 ligand, methysergide, also displaced [^{3}H]-yohimbine with high and low affinity but only displaced [^{3}H]-RS-15385-197 with low affinity and a Hill slope that did not deviate from unity.

In order to determine the nature of the binding sites labelled by [^{3}H]-RS-15385-197 in subtype selective tissues the affinity constants (pK_i) of several compounds against [^{3}H]-RS-15385-197 binding in the human platelet (α_{2A}) and neonate lung (α_{2B}) were determined (Table 5).

Rauwolscine and yohimbine were equipotent in the human platelet but rauwolscine was more potent than yohimbine in the neonatal lung. Adrenaline was more potent than noradrenaline in the platelet, although the rank order of potency was reversed in the neonatal lung. Prazosin displayed high affinity in the neonatal lung but only weak affinity in the human platelet, whereas the selective α_{2A} compounds, oxymetazoline and BRL 44409 (Young *et al.*, 1989) showed higher affinity in the human platelet.

A correlation of affinities between compounds for the sites labelled with [^{3}H]-RS-15385-197 in different tissues is shown in Figure 4. There was a poor correlation between affinity estimates obtained in the rat cortex and rat neonate lung ($r = 0.302$), and in the neonate lung and human platelet ($r = 0.389$). The correlation between the human platelet and the rat cortex was better ($r = 0.67$), but the highest degree of homology was observed between the rat cortex and the rat submaxillary gland ($r = 0.80$).

Discussion

The present study demonstrates that [^{3}H]-RS-15385-197 binds with high affinity to a single site in rat cerebral cortical membranes. The finding that the α_2-adrenoceptor antagonists, yohimbine, rauwolscine, idazoxan, WY 26703 and phentolamine display high affinity towards this site whereas a variety of ligands with affinity for a number of other receptor types display low affinity, confirms previous studies showing RS-15385-197 to be a potent and selective α_2-adrenoceptor antagonist (Clark *et al.*, 1989; 1990).

Saturation studies revealed [^{3}H]-RS-15385-197 to be a higher affinity radioligand than [^{3}H]-yohimbine at α_2-adrenoceptors in rat cerebral cortex. The density of α_2-adrenoceptors labelled by [^{3}H]-RS-15385-197 was significantly greater than the number identified with [^{3}H]-yohimbine. A wide range of α_2-adrenoceptor densities, labelled by [^{3}H]-yohimbine have been reported in rat cerebral cortex (90–254 fmol mg^{-1} protein; Cheung *et al.*, 1982; Rouot *et al.*, 1982; Bylund & U'Prichard, 1983; Bylund, 1985; Dickinson *et al.*, 1986), a finding most likely related to differences in the assay conditions employed and the extent to which the membranes have been washed or purified. For this reason it was considered important to compare the binding at equilibrium and under identical conditions. The higher density of α_2-adrenoceptors labelled by [^{3}H]-RS-15385-197 relative to the number of sites identified by [^{3}H]-yohimbine, is unlikely to be caused by [^{3}H]-RS-15385-197 labelling another receptor, as the compound has >800 fold selectivity over any other receptor subtype studied (Clark *et al.*, 1990). Furthermore, all of the α_2-adrenoceptor antagonists fully inhibited the binding of [^{3}H]-RS-15385-197 to rat cortex with Hill slopes not significantly different from unity, confirming that [^{3}H]-RS-15385-197 is binding to probably a single population of α_2-adrenoceptors. Thus if the difference in B_{max} values obtained with [^{3}H]-RS-15385-197 and [^{3}H]-yohimbine is not due to additional binding sites for [^{3}H]-RS-15385-197, then [^{3}H]-yohimbine must not label the total population of α_2-adrenoceptors in rat cerebral cortex under the present experimental conditions. [^{3}H]-yohimbine may dissociate from a proportion of α_2-adrenoceptors during the filtration process owing to its fast dissociation rate, but, previous studies in the human platelet have suggested that [^{3}H]-yohimbine may have some selectivity for the low affinity agonist state of the α_2-adrenoceptor (Daiguji *et al.*, 1981), the lower density of sites labelled by [^{3}H]-yohimbine in the rat cortex may be due to fewer high affinity agonist states being labelled by [^{3}H]-yohimbine, with [^{3}H]-RS-15385-197 labelling the whole

population. It may be possible that the difference in B_{max} observed between [³H]-RS-15385-197 and [³H]-yohimbine may reflect differences in the stability of the ligand-receptor complex. Such an effect has been frequently reported when assessing the B_{max} for dihydropyridine calcium-antagonists (Glossmann & Ferry, 1985). The difference in the binding properties of the dihydropyridines which all bind to the same site, reflects the ability to stabilize the blocked, inactivated, state of the channel. It is possible that a similar phenomenon may take place at α_2-adrenoceptors.

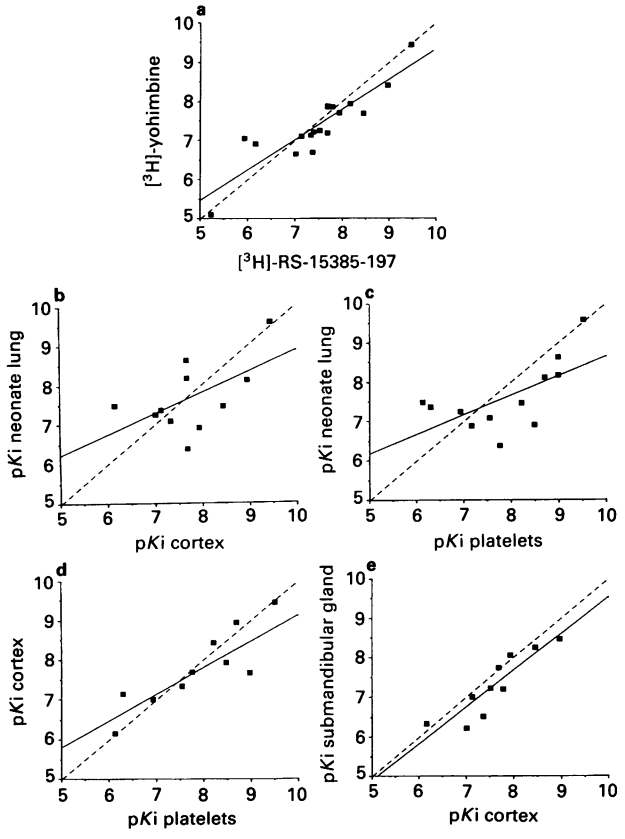

Figure 4 Correlation between affinity estimates obtained at the α_2-adrenoceptor subtypes. The dotted line represents the line of identity. (a) [³H]-RS-15385-197 and [³H]-yohimbine binding in the rat cortex. The data were best described by the expression $y = 0.777x + 1.567$ ($r = 0.789$). (b) [³H]-RS-15385-197 binding in the rat cortex and rat neonate lung. The data were best described by the expression $y = 0.53x + 3.55$ ($r = 0.302$). (c) [³H]-RS-15385-197 binding in the human platelet and rat neonate lung. The data were best described by the expression $y = 0.498x + 3.68$ ($r = 0.389$). (d) [³H]-RS-15385-197 binding in the rat cortex and human platelet. The data were best described by the expression $y = 0.668x + 2.46$ ($r = 0.668$). (e) [³H]-RS-15385-197 in the rat cortex and [³H]-rauwolscine in the rat submaxillary gland. The data were best described by the expression $y = 0.928x + 0.24$ ($r = 0.80$). Data for the submaxillary gland were taken from Michel *et al.*, 1989.

The number of binding sites identified with [³H]-yohimbine is dependent upon the concentration-range chosen for the experiment. Saturation studies carried out over a wider [³H]-yohimbine concentration range (0.1–80 nM) than that used in this study (0.1–15 nM) have demonstrated binding to a second site in rat cortex (Michel & Whiting, 1984). Conditions for [³H]-yohimbine binding to rat cortex have to be carefully defined in order to exclude binding to this second component which if unresolved would increase the density of binding sites. [³H]-rauwolscine, a stereoisomer of yohimbine also binds in a biophasic manner to rat cortical membranes, at high concentrations (Diop *et al.*, 1983; Broadhurst & Wyllie, 1986). Recent studies have shown that [³H]-rauwolscine labels 5-HT_{1A} receptors in human cortex (Convents *et al.*, 1989) and a site that most likely represents a 5-HT_{1A} receptor in rat cerebral cortex (Broadhurst *et al.*, 1988). Rauwolscine and yohimbine also have high affinity for the 5-HT_{1D} binding site identified in non-rodent brain (Heuring & Peroutka, 1987). The low affinity of 5-HT against [³H]-RS-15385-197 indicates that binding to a 5-HT_1-like receptor is not the reason for the greater density of binding sites identified with [³H]-RS-15385-197 in this study.

The pharmacological basis for suggesting that heterogeneity exists within α_2-adrenoceptors is primarily based upon the relative affinities of prazosin or oxymetazoline to displace [³H]-yohimbine and [³H]-rauwolscine binding to sites in a variety of tissues (Cheung *et al.*, 1982; Latifpour *et al.*, 1982; Bylund, 1985) and not upon differences in receptor densities. Prazosin is a more potent inhibitor of [³H]-yohimbine and [³H]-rauwolscine binding to α_2-adrenoceptors in rat neonate lung (Latifpour *et al.*, 1982) and rat cerebral cortex (Cheung *et al.*, 1982) than from α_2-adrenoceptors present on human platelets (Cheung *et al.*, 1982). Oxymetazoline, in contrast, displays higher affinity towards α_2-adrenoceptors on human platelets than at the receptors on rat neonate lung. There are no highly selective antagonists for α_2-adrenoceptor subtypes although a number of α_2-adrenoceptor antagonists have been reported in recent years, including imiloxan (Michel & Whiting, 1981), idazoxan (Doxey *et al.*, 1983), RX 821002 (Stillings *et al.*, 1985), WY 26703 (Lattimer *et al.*, 1984), L-654,284 (Pettibourne *et al.*, 1986), L-657,743 (Pettibourne *et al.*, 1987) and CH-38083 (Vizi *et al.*, 1986). These antagonists have the advantages over yohimbine and rauwolscine of either being more potent and/or selective relative to the other adrenoceptor subtypes. Amongst the new antagonists, idazoxan, RX 821002, L-657,743 and L-654,284 have been radiolabelled. [³H]-idazoxan labels α_2-adrenoceptors in rat cortex with a pharmacological profile consistent with binding selectivity to α_{2A}-adrenoceptor subtype (Brown *et al.*, 1990b). In addition [³H]-idazoxan labels a non-adrenoceptor imidazoline binding site (Brown *et al.*, 1990b) which is not labelled by [³H]-RS-15385-197 (MacKinnon *et al.*, 1990). [³H]-RX 821002, an imidazoline analogue of idazoxan is described as a new radioligand for the identification of α_{2A}-adrenoceptors (Langin *et al.*, 1989). The binding of the non-imidazoline α_2-adrenoceptor radioligands [³H]-L-654,284

Table 3 Effect of Gpp(NH)p on the displacement of [³H]-RS-15385-197 to rat cortical membranes

	Control			+ (100 μM) *Gpp((NH)p*	
	n	pIC_{50}	nH	*n*	pIC_{50}	nH
Adrenaline	6	7.37 ± 0.09	0.66 ± 0.02	3	6.32 ± 0.04*	0.87 ± 0.09*
Noradrenaline	6	7.08 ± 0.13	0.70 ± 0.03	3	6.10 ± 0.11*	0.81 ± 0.03*
Clonidine	6	7.80 ± 0.10	0.75 ± 0.03	3	6.95 ± 0.03*	0.93 ± 0.01*

The affinity values were determined from the displacement of specific binding of 0.15 nM [³H]-RS-15385-197 and 1.5 nM [³H]-yohimbine to rat cerebral cortical membranes in the absence and presence of 100 μM Gpp(NH)p. The results are expressed as pIC_{50} since the compounds showed Hill slopes that were significantly different from unity. Values shown are the mean ± s.e.mean of at least three experiments.

*$P < 0.05$ significantly different from control.

Table 4 Displacement of [^{3}H]-RS-15385-197 and [^{3}H]-yohimbine binding to rat cortical membranes by prazosin, oxymetazoline and methysergide

	pKi			
	[^{3}H]-RS-15385-197	*[^{3}H]-yohimbine*		
		High	*Low*	
Prazosin	6.17 ± 0.18	7.30 ± 0.11	6.00 ± 0.12	(50:50)
Oxymetazoline	7.94 ± 0.15	8.25 ± 0.02	6.92 ± 0.13	(60:40)
Methysergide	5.94 ± 0.11	7.17 ± 0.09	5.34 ± 0.12	(45:55)

The affinity values were obtained for the displacement of 0.1 nM [^{3}H]-RS-15385-197 and 1.5 nM [^{3}H]-yohimbine. Computer analysis resolved prazosin, oxymetazoline and methysergide inhibition curves for the displacment of [^{3}H]-yohimbine into high and low affinity components (Brown *et al.*, 1990b). The values in parentheses represent the proportion of high and low affinity sites differentiated by the ligands. Each value represents the mean ± s.e.mean of at least three separate experiments.

Table 5 Displacement of 0.1 nM [^{3}H]-15385-197 from human platelet and rat neonatal lung membranes

		Human platelet		*Rat neonatal lung*	
	n	p*Ki*	nH	p*Ki*	nH
RS-15385-197	4	9.53 ± 0.14	1.01 ± 0.02	9.77 ± 0.25	0.98 ± 0.02
Yohimbine	4	8.98 ± 0.10	0.89 ± 0.04	8.16 ± 0.08	0.99 ± 0.01
Rauwolscine	4	8.99 ± 0.05	1.03 ± 0.09	8.62 ± 0.07	0.85 ± 0.02
Phentolamine	3	8.70 ± 0.22	1.25 ± 0.35	8.11 ± 0.08	1.01 ± 0.08
Idazoxan	4	8.22 ± 0.03	1.01 ± 0.04	7.46 ± 0.08	0.99 ± 0.01
Adrenaline	4	7.36 ± 0.01	0.80 ± 0.05	7.05 ± 0.04	0.82 ± 0.02
Noradrenaline	4	6.93 ± 0.04	0.75 ± 0.01	7.25 ± 0.03	0.68 ± 0.04
Prazosin	4	6.13 ± 0.08	0.94 ± 0.04	7.49 ± 0.12	1.04 ± 0.09
Imiloxan	3	6.30 ± 0.04	1.30 ± 0.06	7.36 ± 0.02	1.03 ± 0.04
Oxymetazoline	4	8.49 ± 0.01	0.90 ± 0.06	6.91 ± 0.04	0.73 ± 0.07
BRL 44409	4	7.77 ± 0.05	0.98 ± 0.07	6.38 ± 0.05	1.07 ± 0.07

The affinity values were obtained from the displacement of 0.1 nM [^{3}H]-RS-15385-197 from human platelet and rat neonatal lung membranes as described in Methods. Each value represents the mean ± s.e.mean of *n* determinations.

(Randall *et al.*, 1988) and [^{3}H]-L-675,743 (Pettibourne *et al.*, 1988) to rat cerebral cortex have also been characterized. Prazosin displaced each radioligand with low affinity and with Hill slopes that did not deviate from unity, a finding consistent with binding to the α_{2A}-adrenoceptor subtype. In contrast, prazosin shows biphasic displacement curves for [^{3}H]-yohimbine binding in the rat cortex (Bylund, 1985; Brown *et al.*, 1990b).

Thus, the labelling of the α_{2B}-adrenoceptor subtype appears so far to be confined to [^{3}H]-yohimbine and [^{3}H]-rauwolscine. A recent study from our laboratory showed that [^{3}H]-adrenaline binding in rat neonatal lung membranes, a tissue classified as α_{2B}, had characteristics that were not consistent with α_{2B} pharmacology in that prazosin had low affinity and oxymetazoline had high affinity (MacKinnon *et al.*, 1991). Recently, BRL 41992, structurally related to mianserin, has been described as a potent and selective ligand for α_{2B}-adrenoceptors in rat neonatal lung (Young *et al.*, 1989). The synthesis of [^{3}H]-BRL 41992 and its confirmation as a selective, high affinity radioligand for the α_{2B}-adrenoceptor subtype would help resolve the precise nature of the α_{2B}-adrenoceptor subtype and confirm or not its existence in the rat cerebral cortex.

This study showed that [^{3}H]-RS-15385-197 labels both the α_{2A}-adrenoceptor subtype in the human platelet and the α_{2B}-adrenoceptor subtype in the rat neonate lung, as defined by relative affinities of prazosin and ozymetazoline. The lower affinity for prazosin in the rat cortex is consistent, using current classification, with [^{3}H]-RS-15385-197 labelling the α_{2A}-subtype in this tissue. However, the α_2-adrenoceptor in the rat cortex is unlike the α_{2A} site in the human platelet which has very high affinity for yohimbine and rauwolscine and moderate/low affinity for prazosin (Cheung *et al.*, 1982; Brown *et al.*, 1990a and this study). It is also unlike the α_{2A} site described for the hamster adipocyte (MacKinnon *et al.*, 1989) and rabbit spleen (Michel *et al.*, 1989), which show 10 fold lower affinity for prazosin and 50 fold lower affinity for the α_{2B} selective compound imiloxan (Michel *et al.*, 1990). Michel *et al.* (1989) have characterized a site in the rat submaxillary gland which showed intermediate affinity for prazosin, moderate affinity for imiloxan and moderate affinity for yohimbine and rauwolscine, and in this respect shows some similarities to the site in the rat cortex labelled by [^{3}H]-RS-15385-197, and showed a high degree of homology in this study ($r = 0.802$). Recently, Bylund *et al.* (1991) showed the rat submaxilliary site to be similar to the site in the bovine pineal gland and has tentatively termed this site α_{2D}. Future characterization of the rat cortex α_2-adrenoceptor will benefit from more selective compounds, but our studies using [^{3}H]-RS-15385-197 indicating that this site is different from the α_{2A} and the α_{2B}, confirm our previous studies using [^{3}H]-yohimbine and [^{3}H]-idazoxan (Brown *et al.*, 1990b). The precise nature of the subtype(s) of α_2-adrenoceptor in the rat cortex has been disputed. Both α_{2A} and α_{2B} subtypes have been reported to be labelled by [^{3}H]-yohimbine (Bylund, 1985; Brown *et al.*, 1990b). However, a single subtype showing, until now, the greatest similarity with the α_{2A} subtype is labelled with [^{3}H]-idazoxan (Brown *et al.*, 1990b), [^{3}H]-L-654-284 (Randall *et al.*, 1988) and [^{3}H]-L-657-743 (Pettibourne *et al.*, 1988). We would now suggest that like [^{3}H]-RS-15385-197 these ligands label a site in the rat cortex of the α_{2D} subclass, and that this forms the major population of α_2-sites in the rat cortex.

Strong evidence exists for adrenoceptor subtypes being distinct entities. Gene cloning and gene expression experiments have demonstrated that the gene for the human platelet α_{2A}-adrenoceptor subtype is localized on human chromosome 10 (Kobilka *et al.*, 1987) whereas the gene for the human kidney α_2-adrenoceptor subtype is located on chromosome 4 (Regan *et al.*, 1988) and is more similar to the α_{2C} subtype described by Bylund *et al.* (1988). A third α_2-adrenoceptor clone located on chromosome 2 has similarities

to the α_{2B} subtype. Genes homologous to the human genes have been cloned in the rat, the cA2-47 gene (Chalberg *et al.*, 1990), pA2d gene (Voigt *et al.*, 1991) and RNG gene (Zeng *et al.*, 1991), respectively. Two further genes have been cloned RG10 and RG20 (Lanier *et al.*, 1991) suggesting additional subtypes. The RG20 exhibits ligand binding properties distinct from the three other receptor subtypes, although it shows 89% homology with the α_2-C10 human clone. In competition binding studies the rank order of potency for antagonists is phentolamine > idazoxan > yohimbine = rauwolscine >> prazosin (Lanier *et al.*, 1991), and therefore shows strong resemblance to the α_2-adrenoceptor on rat cerebral cortex labelled by [^{3}H]-RS-15385-197 described in this paper.

In summary, this study demonstrates that [^{3}H]-RS-15385-197 is the most selective and potent radioligand available for investigating α_2-adrenoceptors. [^{3}H]-RS-15385-197 labels the α_{2A} subtype on human platelet, the α_{2B} subtype on rat neonatal lung and a subtype in the rat cortex, which does not fit into the current classification, but which we propose may be similar to the α_{2D}-subtype described by Bylund *et al.* (1991).

We thank Dr Howard Parnes, Institute of Organic Chemistry, Syntex, Palo Alto, Ca, U.S.A. for the synthesis of [^{3}H]-RS-15385-197. We also wish to thank our colleagues Dr A. Michel, Ms D. Lowry and Dr R.L. Whiting for the use of their data on the rat submaxillary gland (Michel *et al.*, 1989).

References

BROADHURST, A.M., ALEXANDER, B.S. & WOOD, M.D. (1988). Heterogeneous [^{3}H]-rauwolscine binding sites in rat cortex: two alpha$_2$-adrenergic subtypes or an additional non-adrenergic interaction. *Life Sci.*, **43**, 83–92.

BROADHURST, A.M. & WYLLIE, M.G. (1986). A reassessment of the binding of [^{3}H]-rauwolscine to membranes from the rat cortex. *Neuropharmacology*, **25**, 287–295.

BROWN, C.M., MACKINNON, A.C., MCGRATH, J.C., SPEDDING, M. & KILPATRICK, A.T. (1990a). Heterogeneity of alpha$_2$-adrenoceptors in rat cortex but not human platelets can be defined by 8-OH-DPAT, RU 24969 and methysergide. *Br. J. Pharmacol.*, **99**, 481–486.

BROWN, C.M., MACKINNON, A.C., MCGRATH, J.C., SPEDDING, M. & KILPATRICK, A.T. (1990b). α_2-Adrenoceptor subtypes and imidazoline-like binding sites in the rat brain. *Br. J. Pharmacol.*, **99**, 803–809.

BYLUND, D.B. (1985). Heterogeneity of alpha$_2$-adrenergic receptors. *Pharmacol. Biochem. Behav.*, **22**, 835–843.

BYLUND, D.B., BLAXALL, H.S., MURPHY, T.J. & SIMMONEAUX, V. (1991). Pharmacological evidence for α_{2C} and α_{2D} adrenergic receptor subtypes. In *Adrenoceptors Structure, Mechanisms, Function*. ed. Szabadi, E. & Bradshaw, C.M. pp. 27–36. Basel: Birkhauser Verlag.

BYLUND, D.B., RAY-PRENGER, C. & MURPHY, T.J. (1988). Alpha$_{2A}$- and alpha$_{2B}$-adrenergic receptors: antagonist binding in tissues and cell lines containing only one subtype. *J. Pharmacol. Exp. Ther.*, **245**, 600–607.

BYLUND, D.B. & U'PRICHARD, D.C. (1983). Characterization of the alpha$_1$- and alpha$_2$-adrenergic receptors. *Int. Rev. Neurobiol.*, **24**, 343–431.

CHALBERG, S.C., DUDA, T., RHINE, J.A. & SHARMA, R.K. (1990). Molecular cloning, sequencing and expression of an α_2-adrenergic receptor complementary DNA from rat brain. *Mol. Cell Biochem.*, **97**, 161–172.

CHENG, Y.C. & PRUSOFF, W.H. (1973). Relationship between the inhibition constant (Ki) and the concentration of inhibitor which cuased 50 per cent inhibition (pIC50) of an enzymic reaction. *Biochem. Pharmacol.*, **22**, 3099–3108.

CHEUNG, Y.D., BARNETT, D.B. & NAHORSKI, S.R. (1982). [^{3}H]rauwolscine and [^{3}H] -yohimbine binding to rat cerebral and human platelet membranes: possible heterogeneity of alpha$_2$-adrenoceptors. *Eur. J. Pharmacol.*, **84**, 79–85.

CLARK, R.D., REPKE, D.B., KILPATRICK, A.T., BROWN, C.M., MACKINNON, A.C., CLAGUE, R.U. & SPEDDING, M. (1989). (8a{,12a{,13a{)-5,8,8a,9,10,11,12,12a,13,13a- Decahydro-3-methoxy-12-(methylsulfonyl)-6H-isoquino{2,1-g][1,6]naphthyridine, a potent and highly selective α_2-adrenoceptor antagonist. *J. Med. Chem.*, **32**, 2034–2036.

CLARK, R., SPEDDING, M. & MACFARLANE, C.B. (1990). RS-15385-197, a potent and selective α_2-adrenoceptor antagonist. *Br. J. Pharmacol.*, **99**, 123P.

CONVENTS, A., CONVENTS, D., DE BACKER, J.P., DE KEYSER, J. & VAUQUELIN, G. (1989). High affinity binding of [^{3}H]-rauwolscine and [^{3}H]-RX781094 to α_2 adrenergic receptors and non-stereoselective sites in human and rabbit brain cortex membranes. *Biochem. Pharmacol.*, **38**, 455–463.

DAIGUJI, M., MELTZER, H.Y. & U'PRICHARD, D.C. (1981). Human platelet α_2-adrenergic receptors: labelling with ^{3}H-yohimbine, a selective antagonist ligand. *Life Sci.*, **28**, 2705–2717.

DICKINSON, K.E.J., MCKERNAN, R.M., MILES, C.M.M., LEYS, K.S. & SEVER, P.S. (1986). Heterogeneity of mammalian α_2-adrenoceptors delineated by [^{3}H]yohimbine binding. *Eur. J. Pharmacol.*, **120**, 285–293.

DIOP, L., DAUSSE, J.P. & MEYER, P. (1983). Specific binding of [^{3}H]rauwolscine to alpha$_2$-adrenoceptors in rat cerebral cortex: comparison between crude and synaptosomal plasma membranes. *J. Neurochem.*, **41**, 710–715.

DOXEY, J.C., ROACH, A.C. & SMITH, C.F.C. (1983). Studies on RX 781094: a selective, potent and specific antagonist of α_2-adrenoceptors. *Br. J. Pharmacol.*, **78**, 489–505.

GLOSSMAN, H. & FERRY, D.R. (1985). Assay for calcium channels. *Meth. Enzymol.*, **109**, 513–550.

HEURING, R.E. & PEROUTKA, S.J. (1987). Characterization of a novel [^{3}H]-5-hydroxytryptamine binding site subtype in bovine brain membranes. *J. Neurosci.*, **7**, 894–903.

KOBILKA, B.K., MATSUI, H., KOBILKA, T.S., YANG-FENG, T.L., FRANCKE, U., CARON, M.G., LEFKOWITZ, R.J. & REGAN, J.W. (1987). Cloning, sequencing and expression of the gene coding for the human platelet α_2-adrenergic receptor. *Science*, **238**, 650–656.

LANGIN, D., LAFONTAN, M., STILLINGS, M.R. & PARIS, H. (1989). [^{3}H]-RX821002: a new tool for the identification of α_2-adrenoceptors. *Eur. J. Pharmacol.*, 95–104.

LANIER, S.M., DOWNING, S., DUZIC, E. & HOMCY, C.J. (1991). Isolation of rat genomic clones encoding subtypes of α_2-adrenergic receptor. *J. Biol. Chem.*, **266**, 10470–10478.

LATIFPOUR, J., JONES, S.B. & BYLUND, D.B. (1982). Characterization of [^{3}H]-yohimbine binding to putative alpha$_2$-adrenergic receptors in neonatal rat lung. *J. Pharmacol. Exp. Ther.*, **223**, 606–611.

LATTIMER, N., MCADAMS, R.P., RHODES, K.F., SHARMA, S., TURNER, S.J. & WATERFALL, J.F. (1984). Alpha$_2$-adrenoceptor antagonism and other pharmacological antagonist properties of some substituted benzoquinolizines and yohimbine in vitro. *Naunyn-Schmiedebergs Arch. Pharmacol.*, **327**, 312–318.

MACKINNON, A.C., BROWN, C.M., SPEDDING, M. & KILPATRICK, A.T. (1989). [^{3}H]-idazoxan binds with high affinity to two sites on hamster adipocytes: an alpha$_2$-adrenoceptor and a non-adrenoceptor site. *Br. J. Pharmacol.*, **98**, 1143–1150.

MACKINNON, A.C., BROWN, C.M., KILPATRICK, A.T. & SPEDDING, M. (1990). RS-15385-197 a selective α_2-adrenoceptor antagonist has low affinity for imidazoline binding sites on hamster adipocytes. *Br. J. Pharmacol.*, **102**, 377P.

MACKINNON, A.C., SPEDDING, M. & BROWN, C.M. (1991). [^{3}H]-adrenaline does not label an α_{2B}-adrenoceptor on rat neonatal lung. *Br. J. Pharmacol.*, **104**, 415P.

MICHEL, A.D. & WHITING, R.L. (1981). 2-(2-Imidazolylmethyl0-1,4-benzodioxans, a series of selective α_2-adrenoceptor antagonists. *Br. J. Pharmacol.*, **74**, 255–256P.

MICHEL, A.D. & WHITING, R.L. (1984). Binding of [^{3}H]-yohimbine in rat cerebral cortex. *Br. J. Pharmacol.*, **81**, 95P.

MICHEL, A.D., LOURY, D.N. & WHITING, R.L. (1989). Differences between the α_2-adrenoceptor in the rat submaxilliary gland to the α_{2A}- and α_{2B}-adrenoceptor subtype. *Br. J. Pharmacol.*, **98**, 890–897.

MICHEL, A.D., LOURY, D.W. & WHITING, R.L. (1990). Assessment of imiloxan as a selective α_{2B}-adrenoceptor antagonist. *Br. J. Pharmacol.*, **99**, 560–564.

MUNSON, P.J. & RODBARD, D. (1980). LIGAND: a versatile computerised approach for characterization of ligand-binding systems. *Analyt. Biochem.*, **107**, 220–239.

NAHORSKI, S.R., BARNETT, D.B. & CHEUNG, Y.D. (1985). Alpha-adrenoceptor-effector coupling: affinity states or heterogeneity of the alpha$_2$-adrenoceptor? *Clin. Sci.*, **68**, (Suppl. 10), 395–425.

PETRASH, A.C. & BYLUND, D.B. (1986). Alpha$_2$-adrenergic receptor subtypes indicated by [^{3}H]-yohimbine binding in human brain. *Life Sci.*, **38**, 2129–2137.

PETTIBOURNE, D.J., CLINESCHMIDT, B.V., LOTTI, V.J., MARTIN, G.E., HUFF, J.R., RANDALL, W.C., VACCA, J. & BALDWIN, J.J. (1986). L-654,284 a new potent and selective α_2-adrenoceptor antagonist. *Naunyn-Schmiedebergs Arch. Pharmacol.*, **333**, 110–116.

PETTIBOURNE, D.J., CLINESCHMIDT, B.V., LOTTI, V.J., BALDWIN, J.J., HUFF, J.R., RANDALL, W.C., VACCA, J. & YOUNG, S.D. (1987). Pharmacological profile of a new potent and specific α_2-adrenoceptor antagonist, L-657,743. *Naunyn-Schmiedbergs Arch. Pharmacol.*, **336**, 169–175.

PETTIBOURNE, D.J., FLAGGS, S.D., TOTARO, J.A., CLINESCHMIDT, B.V., HUFF, J.R., YOUNG, S.D. & CHEN, R. (1988). [^{3}H]-L-657,743 (MK-912): a new, high affinity, selective radioligand for brain α_2-adrenoceptors. *Life Sci.*, **44**, 459–467.

REGAN, J.W., KOBILKA, T.S., YANG-FENG, T.L., CARON, M.G., LEFKOWTIZ, R.J. & KOBLIKA, B.K. (1988). Cloning and expression of a human kidney cDNA for an α_2-adrenergic receptor subtype. *Proc. Natl. Acad., Sci. U.S.A.*, **85**, 6301–6305.

RANDALL, W.C., HUFF, J.R., VACCA, J.P., GUARE, J.P., CHEN, R., ROSEGAY, A. & BALDWIN, J.J. (1988). [^{3}H]L-654,284 as a probe of the central alpha$_2$ adrenoceptor. *Naunyn-Schmiedebergs Arch. Pharmacol.*, **338**, 47–52.

ROUOT, B., QUENNEDEY, M.C. & SCHWARTZ, J. (1982). Characteristics of the [^{3}H]-yohimbine binding on rat brain α_2-adrenoceptors. *Naunyn-Schmiedebergs Arch. Pharmacol.*, **321**, 253–259.

SORENSON, K. & BRODBECK, U. (1986). A sensitive protein assay method using microtiter plates. *Experientia*, **42**, 161–162.

STARKE, K. (1977). Regulation of noradrenaline release by presynaptic receptor systems. *Rev. Physiol. Biochem. Pharmacol.*, **77**, 1–124.

STARKE, K. (1987). Presynaptic a-autoreceptors. *Rev. Physiol. Biochem. Pharmacol.*, **107**, 73–146.

STILLINGS, M.R., CHAPLEO, C.B., BUTLER, R.C.M., DAVIS, J.A., ENGLAND, C.D., MYERS, P.L., TWEDDLE, N., WELBOURN, A.P., DOXEY, J.C. & SMITH, C.F.C. (1985). α_2-Adrenoceptor reagents. 3. Synthesis of some 2-substituted 1,4-benzodiaxans as selective presyaptic α_2-adrenoceptor antagonists. *J. Med. Chem.*, **28**, 1054–1062.

VIZI, E.S., HARSING, L.G., GAAL, J., KAPOCSI, J., BERNATH, S. & SOMOGYI, G.T. (1986). CH-33083, a selective, potent antagonist of alpha$_2$-adrenoceptors. *J. Pharmacol. Exp. Ther.*, **238**, 701–706.

VOIGT, M.M., MCCUNE, S.K., KANTERMAN, R.Y. & FELDER, C.C. (1991). The rat α_2-C4 adrenergic receptor gene encodes a novel pharmacological subtype. *FEBS Lett.*, **278**, 45–50.

YOUNG, P., BERGE, J., CHAPMAN, H. & CAWTHORNE, M.A. (1989). Novel α_2-adrenoceptor antagonists show selectivity for α_{2A}- and α_{2B}-adrenoceptor subtypes. *Eur. J. Pharmacol.*, **168**, 381–386.

ZENG, D. & LYNCH, K.R. (1991). Distribution of α_2-adrenergic mRNAs in the rat CNS. *Mol. Brain Res.*, **10**, 219–225.

(Received February 10, 1992
Revised April 22, 1992
Accepted April 23, 1992)

Br. J. Pharmacol. (1992), **106**, 1019–1027 © Macmillan Press Ltd, 1992

Characterization and autoradiographical localization of non-adrenoceptor idazoxan binding sites in the rat brain

[1] N.J. Mallard, [2] A.L. Hudson & D.J. Nutt

Reckitt & Colman Psychopharmacology Unit, Department of Pharmacology, School of Medical Sciences, University Walk, Bristol, BS8 1TD

1 In rat whole brain homogenates, saturation analysis revealed that both [^{3}H]-idazoxan and [^{3}H]-RX821002, a selective α_2-adrenoceptor ligand, bound with high affinity to an apparent single population of sites. However, the B_{max} for [^{3}H]-idazoxan was significantly ($P<0.01$) greater than that for [^{3}H]-RX821002.

2 In competition studies, (−)-adrenaline displaced 3 nM [^{3}H]-idazoxan binding with an affinity consistent with [^{3}H]-idazoxan labelling α_2-adrenoceptors. However, this displacement was incomplete since 23.68 ± 1.11% of specific [^{3}H]-idazoxan binding remained in the presence of an excess concentration (100 μM) of (−)-adrenaline. In contrast, unlabelled idazoxan promoted a complete displacement of [^{3}H]-idazoxan binding with a Hill slope close to unity and an affinity comparable with its K_D determined in saturation studies.

3 Displacement of [^{3}H]-idazoxan binding by the α_2-adrenoceptor antagonists yohimbine, RX821002 (2-(2-methoxy-1,4-benzodioxan-2-yl)-2-imidazoline) and RX811059 (2-(2-ethoxy-1,4-benzodioxan-2-yl)-2-imidazoline) was more complex, with Hill slopes considerably less than unity, and best described by a two-site model of interaction comprising a high and low affinity component. The proportion of sites with high affinity for each antagonist was similar (60–80%).

4 The rank order of antagonist potency for the high affinity component in each displacement curve (RX821002 > RX811059 > yohimbine) is similar to that determined against the binding of [^{3}H]-RX821002 to rat brain, suggesting that these components reflect the inhibition of [^{3}H]-idazoxan binding to α_2-adrenoceptors. The remaining component in each displacement curve exhibiting low affinity towards these antagonists is attributable to the displacement of [^{3}H]-idazoxin from a non-adrenoceptor idazoxan binding site (NAIBS) since a comparable amount of [^{3}H]-idazoxan binding was not displaced by an excess concentration of (−)-adrenaline.

5 The displacement of [^{3}H]-idazoxan binding by RX801023 (6-fluoro-(2-(1,4-benzodioxan-2-yl)-2-imidazoline) was also best described by a model assuming a two site interaction with 20.07 ± 3.11% of the sites labelled displaying high affinity for RX801023. The K_i of RX801023 for the remainder of the sites labelled was similar to its K_i versus [^{3}H]-RX821002, indicating that this drug displays improved affinity and NAIBS/α_2-adrenoceptor selectivity compared with idazoxan.

6 In autoradiographical studies, the distribution of 5 nM [^{3}H]-idazoxan binding to sections of rat whole brain was consistent with that reported from previous studies and resembled the distribution of α_2-adrenoceptors. However, when sections of brain were coincubated with concentrations of α_2-adrenoceptor agonists or antagonists predicted to saturate α_2-adrenoceptors, there remained distinct areas of binding corresponding to discrete brain nuclei. This remaining binding was however displaced by unlabelled idazoxan (3 μM) or RX801023 (3 μM) indicative of the labelling of NAIBS.

7 Quantitative autoradiography of NAIBS revealed several brain nuclei which contained higher densities of these sites than α_2-adrenoceptors, notably the area postrema, interpeduncular nucleus, arcuate nucleus, ependyma and pineal gland.

Keywords: α_2-Adrenoceptors; non-adrenoceptor idazoxan binding sites; radioligand binding; autoradiography; rat brain; idazoxan; interpeduncular nucleus; area postrema; arcuate nucleus

Introduction

During recent years, the tritiated form of the α_2-adrenoceptor antagonist, idazoxan, has been widely employed for the characterization and identification of such receptors in tissue homogenates from a variety of species since it displays enhanced affinity and α_2/α_1 selectivity compared with other antagonists such as rauwolscine (Doxey *et al.*, 1983; 1984). In autoradiographical studies [^{3}H]-idazoxan has also proved useful at the macroscopic level to localize central α_2-adrenoceptors (Boyajian *et al.*, 1987; Bruning *et al.*, 1987). However, recent research has shown that both [^{3}H]-idazoxan and [^{3}H]-rauwolscine also bind with high affinity to non-adrenoceptor sites and that careful definition of the specific component of their binding is essential when using these radioligands in receptor binding and autoradiographical investigations of α_2-adrenoceptors (see Lehmann *et al.*, 1989; Michel & Insel, 1989). Thus, [^{3}H]-rauwolscine has been reported to bind to 5-HT_{1A} receptors as well as to α_2-adrenoceptors in rat (Broadhurst & Wyllie, 1986), rabbit and human frontal cortex membranes (Convents *et al.*, 1989) and in autoradiographic studies its primary distribution is associated with dopaminergic terminals (Boyajian *et al.*, 1987).

Likewise, [^{3}H]-idazoxan binds with equal affinity to α_2-adrenoceptors and phentolamine displaceable non-stereoselective sites in rat, rabbit, guinea-pig and human cortex membranes (Convents *et al.*, 1989; Wikberg, 1989; Brown *et al.*, 1990; Wikberg & Uhlen, 1990; Hamilton *et al.*, 1991).

[1] Present address: Cardiff Clinical Trials Ltd., Dept. of Pharmacology & Therapeutics, University of Wales College of Medicine, Heath Park, Cardiff, CF4 4XN.
[2] Author for correspondence.

Similar non-adrenoceptor idazoxan binding sites or NAIBS (Michel & Insel, 1989) have also been observed in membrane preparations from other tissues such as adipocytes (Langin & Lafontan, 1989; MacKinnon *et al.*, 1989; Langin *et al.*, 1990a,b), kidney (Coupry *et al.*, 1989; Michel *et al.*, 1989; Vigne *et al.*, 1989; Hamilton *et al.*, 1991), smooth muscle (Wikberg *et al.*, 1991; Yablonsky & Dausse, 1991) and liver, where binding studies with subcellular fractions suggest a major localization of NAIBS in mitochondria (Tesson *et al.*, 1991). These non-adrenoceptor idazoxan binding sites show only low affinity for compounds such as cimetidine and imidazole-4-acetic acid indicating they are distinct from the non-adrenoceptor imidazoline binding sites labelled by [^{3}H]-clonidine or [^{3}H]-*p*-aminoclonidine in the ventrolateral medulla (Ernsberger *et al.*, 1987; 1988a,b) which may be responsible for the antihypertensive actions of clonidine and related analogues such as rilmenidine (Bricca *et al.*, 1989; Ersberger *et al.*, 1990; Feldman *et al.*, 1990; Gomez *et al.*, 1991). In contrast, no proven function(s) or endogenous neurotransmitter have yet been described for NAIBS.

Interestingly, whilst the 2-alkoxy substituted analogues of idazoxan, RX821002 (2-(2-methoxy-1,4-benzodioxan-2-yl)-2-imidazoline) and RX811059 (2-(2-ethoxy-1,4-benzodioxan-2-yl)-2-imidazoline) maintain high affinity and selectivity for α_2-adrenoceptors (Stillings *et al.*, 1985; Welbourn *et al.*, 1986), their affinity for NAIBS is at least 1000 fold lower than that of idazoxan (Langin *et al.*, 1989; Galitzky *et al.*, 1990; Vauquelin *et al.*, 1990; Hudson *et al.*, 1992). Conversely, preliminary investigations revealed that the 6-fluoro derivative of idazoxan, RX801023 (6-fluoro-(2-(1,4-benzodioxan-2-yl)-2-imidazoline), displays reduced affinity for α_2-adrenoceptors (Chapleo *et al.*, 1983) whilst that for NAIBS is maintained (Mallard *et al.*, 1991). These observations suggest that the interaction of idazoxan with NAIBS occurs in a structurally specific fashion and, against this background, we have therefore investigated the radioligand binding profile and autoradiographical distribution of NAIBS in the rat brain. Preliminary accounts of some of this work have been given (Hudson & Nutt, 1990; Hudson *et al.*, 1991a,b).

Methods

Membrane preparation

Male Wistar rats (200–300 g) were killed by stunning followed by decapitation. Whole brains were rapidly dissected over ice and homogenized in 10 vol of buffered sucrose (0.32 M in 50 mM Tris HCl, pH 7.4 at 4°C) using a motor driven Teflon-glass homogenizer. The homogenate was then centrifuged at 1000 *g* for 10 min at 4°C. The resultant supernatants were pooled and recentrifuged at 31,000 *g* for 20 min at 4°C. The supernatants were then discarded and each pellet resuspended in 10 vol of assay buffer (50 mM Tris HCl, 1 mM $MgCl_2$, pH 7.4 at 4°C). The pellets were then washed twice by repeated centrifugation at 31,000 *g* for 20 min at 4°C. The final pellets were stored at − 70°C until use.

Saturation binding studies

Membrane aliquots (300–450 μg protein) and nine concentrations of [^{3}H]-idazoxan or [^{3}H]-RX821002, over the range 0.1–60 nM, were incubated, in triplicate, to equilibrium (30 min) in a final volume of 1 ml at 25°C. Bound and free radioligand were then separated by rapid filtration through pre-soaked (0.5% polyethyleneimine) Whatman GF/B filters using a Brandel M-24 cell harvester. Filters were washed twice with 5 ml of ice-cold assay buffer and the radioactivity remaining on the filters determined by liquid scintillation counting. Non-specific binding at each free ligand concentration was determined with either 10 μM or 1 mM phentolamine for [^{3}H]-RX821002 or [^{3}H]-idazoxan respectively.

Competition binding studies

Competition studies were carried out in identical conditions to saturation experiments with either 3–4 nM [^{3}H]-idazoxan or 2–3 nM [^{3}H]-RX821002 and various drugs over the concentration range 0.1 nM–1 mM in a final volume of 1 ml. Non-specific binding was again determined by use of 10 μM or 1 mM phentolamine for [^{3}H]-RX821002 or [^{3}H]-idazoxan respectively. Ascorbic acid (0.05%) was included in the assay buffer for competition studies with (−)-adrenaline.

Analysis of binding data

Saturation and competition binding data were analysed by iterative non-linear regression procedures capable of fitting single and two site models using GraphPad Inplot (ISI Software, 1990). K_i values for competing drugs were calculated from the Cheng & Prusoff (1973) equation: $K_i = IC_{50}/(1 + L/K_D)$. All displacement curves were initially analysed assuming a one site model of radioligand binding. Displacement curves with Hill coefficients significantly less than unity were reanalysed assuming a two site model of radioligand binding and the results compared to the one site model of fit using the differential F value defined by the equation:

$$F = \frac{(SS_1 - SS_2)/(d.f._1 - d.f._2)}{SS_2/(d.f._2)}$$

where SS_1 is the sum of the squares error for the single site fit, SS_2 is the sum of the squares error for the two site fit, $d.f._1$ is the degrees of freedom for the single site model and $d.f._2$ the degrees of freedom for the two site model (Munson & Rodbard, 1980; Petrash & Bylund, 1986). A two site fit was assumed to describe a displacement curve better than a one site fit if the determined F value had a $P<0.05$.

Autoradiography

Male Wistar rats (280–320 g) were anaesthetized with sodium pentobarbitone (40 mg kg^{-1}) and perfused (intracardiac) with 280 ml of ice-cold phosphate (0.01 M) buffered saline (pH 7.4). Brains were rapidly removed, frozen in isopentane at − 40°C and 10 μm thick sections cut on a cryostat at − 15°C. Sections were thaw mounted onto gelatin subbed glass slides, stored at − 70°C for up to three months or used immediately for autoradiography. Additional sections were cut and stained with cresyl-fast violet for histological confirmation of brain structures.

Prior to binding, slide mounted sections were prewashed in buffer (50 mM Tris HCl, 1 mM $MgCl_2$, pH 7.4) for 30 min at 22°C. Dried sections were then incubated in fresh buffer containing 5 nM [^{3}H]-idazoxan, with or without unlabelled drugs, for 20 min at 22°C. Ascorbate (0.05%) was included in the assay buffer for studies with noradrenaline. Assays were terminated by two 20 s rinses in ice-cold buffer followed by one dip in distilled water (4°C) and rapid drying in a stream of cool air. The radioactivity bound to some sections was then determined by liquid scintillation counting. Other sections were apposed to ^{3}H-sensitive film (Hyperfilm, Amersham) with known ^{3}H standards for 6–8 weeks before photographic development and computerised densitometry (Quantimet 970, Cambridge Instruments, UK). Binding densities determined in each brain region were corroborated by quantitative analysis of triplicate experiments derived from a minimum of 3 animals. Brains were prepared, sectioned and analysed, to facilitate structural recognition with a Paxinos & Watson (1986) stereotaxic atlas. Resulting autoradiograms may reveal other brain structures where sections were only close to parasagittal or transverse planes relative to the atlas.

Protein determinations

Protein concentrations were determined with Coomassie blue and bovine serum albumin as the standard (Bradford, 1976).

Drugs and chemicals

[^{3}H]-idazoxan (specific activity 40–41 Ci mmol^{-1}) and [^{3}H]-RX821002 (specific activity 47.5 Ci mmol^{-1}) were produced for Reckitt and Colman by Amersham International.

The following drugs were obtained from external sources; phentolamine mesylate (Research Biochemicals Inc.); rauwolscine hydrochloride (Research Biochemicals Inc.); clonidine hydrochloride (Sigma); (−)-adrenaline (Sigma); noradrenaline (Sigma); yohimbine hydrochloride (Sigma).

Idazoxan, RX811059, RX821002 and RX801023 were synthesized by the Department of Medicinal Chemistry, Reckitt and Colman Products, Hull, UK. All other reagents used were of the highest analytical grade.

Results

Saturation binding studies

Over the concentration range 0.1–60 nM the binding of both [^{3}H]-idazoxan and [^{3}H]-RX821002 to membranes prepared from rat whole brain was saturable and of high affinity (Figure 1a). Iterative non-linear regression (Figure 1a) and Scatchard analysis (Figure 1b) of the binding isotherms suggested that each ligand was labelling a single population of non-interacting sites. However, the maximal number of binding sites (B_{max}) labelled by [^{3}H]-idazoxan was significantly ($P<0.01$) greater than the maximal number of sites labelled by [^{3}H]-RX821002 (Table 1) whereas the equilibrium dissociation constant (K_D) for [^{3}H]-RX821002 was significantly ($P<0.05$) less than that for [^{3}H]-idazoxan (Table 1). Nevertheless, at concentrations approximating to their respective K_D values, greater than 90% specific binding was achieved for both ligands.

Table 1 Specific binding of [^{3}H]-idazoxan and [^{3}H]-RX821002 to rat whole brain membranes

	[^{3}H]-idazoxan	*[^{3}H]-RX821002*
B_{max}	328.95 ± 4.31**	212.46 ± 12.90
K_D	7.14 ± 1.00	1.22 ± 0.25*

Saturation experiments were performed as described in the methods section. Non-specific binding of [^{3}H]-RX821002 and [^{3}H]-idazoxan was defined in the presence of 10 μM and 1 mM phentolamine respectively. Each value represents the mean ± s.e.mean of observations from five separate determinations performed in triplicate. Data were analysed by iterative non-linear regression analysis (GraphPad Inplot) assuming a one-site model of fit.
**$P<0.01$ compared to the B_{max} for [^{3}H]-RX821002; *$P<0.05$ compared to the K_D for [^{3}H]-idazoxan.

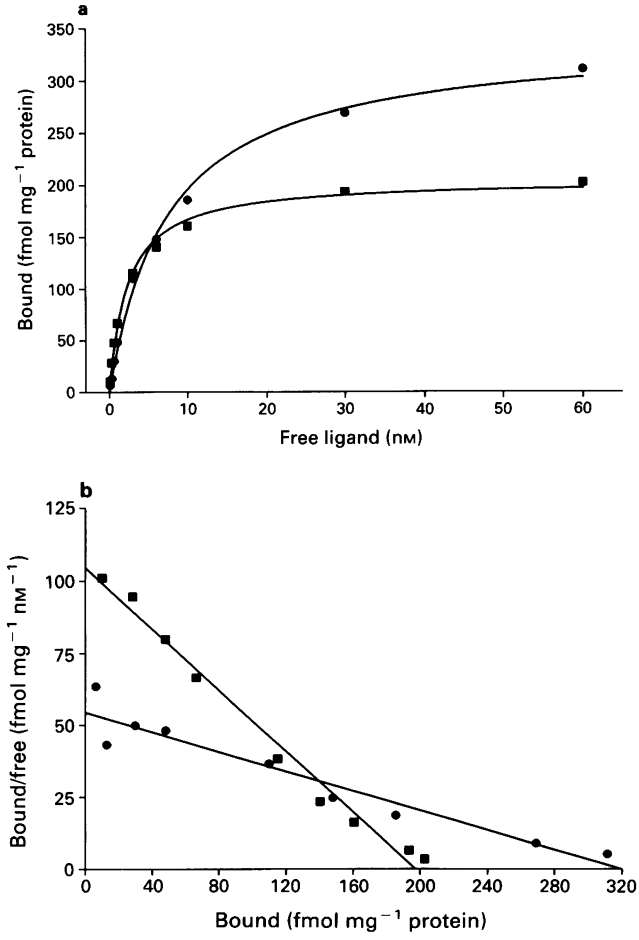

Figure 1 [^{3}H]-idazoxan (●) and [^{3}H]-RX821002 (■) saturation binding to rat whole brain membranes. (b) Scatchard transformation of the data shown in (a). Incubations were performed for 30 min at 25°C in a Tris HCl buffer (50 mM Tris HCl, 1 mM $MgCl_2$; pH 7.4). Non specific binding at each free ligand concentration was determined with either 10 μM or 1 mM phentolamine for [^{3}H]-RX821002 or [^{3}H]-idazoxan respectively. Both curves describe triplicate results from a single experiment with each ligand performed in parallel. A similar profile was obtained in a further five experiments.

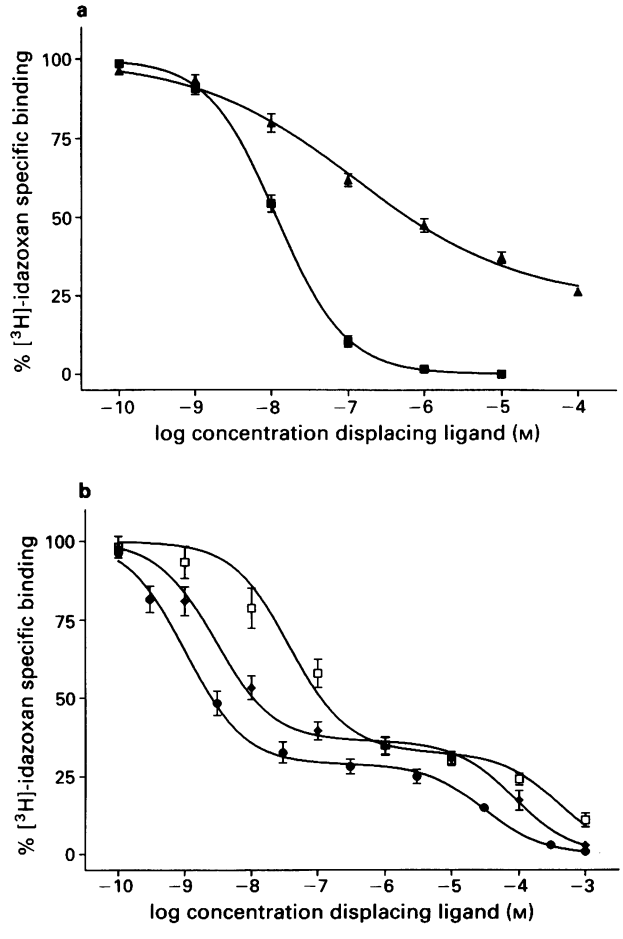

Figure 2 Concentration-dependent displacement of specific [^{3}H]-idazoxan binding to rat whole brain membranes by α-adrenoceptor agonists and antagonists. (a) Idazoxan (■) and (−)-adrenaline (▲); (b) RX821002 (●), RX811059 (◆) and yohimbine (□). Incubations were performed for 30 min at 25°C in a Tris HCl buffer (50 mM Tris HCl, 1 mM $MgCl_2$; pH 7.4) containing 3–4 nM [^{3}H]-idazoxan. Non specific binding was determined with 1 mM phentolamine. Each point represents the mean (± s.e.mean, vertical bars) of observations from 4 or 5 determinations performed in triplicate.

Competition binding studies

In competition experiments, a number of α-adrenoceptor agonists and antagonists produced a concentration-dependent inhibition of specific [^{3}H]-idazoxan binding to rat whole brain membranes (Figure 2a,b). The endogenous adrenoceptor agonist (−)-adrenaline inhibited the binding of [^{3}H]-idazoxan in a monophasic fashion (Figure 2a) with a Hill slope substantially less than unity and affinity (K_i) consistent with [^{3}H]-idazoxan labelling α_2-adrenoceptors (Table 2). Interestingly, however, this displacement was not complete since 23.68 ± 1.11% ($n = 5$) of specific [^{3}H]-idazoxan binding remained in the presence of an excess concentration (100 μM) of (−)-adrenaline (Figure 2a). In contrast, unlabelled idazoxan promoted complete displacement of [^{3}H]-idazoxan binding in a monophasic fashion with a K_i value comparable to its K_D determined in saturation experiments (Table 1) and a Hill slope close to unity (Figure 2a, Table 2).

The displacement of [^{3}H]-idazoxan binding to rat whole brain membranes by the α_2-adrenoceptor antagonists, yohimbine, RX821002 and RX811059 was more complex with Hill slopes considerably less than unity (Figure 2b). Computer assisted analysis of the displacement curves indicated that the inhibition of [^{3}H]-idazoxan binding by each antagonist was best described by a two-site model of interaction comprising both a high and low affinity component (Figure 2b, Table 2). Moreover, the proportion of high affinity sites revealed by each antagonist was similar (Figure 2b) and in the range 60–80% (Table 2). The antagonist rank order of potency of RX821002> RX811059> yohimbine derived from the high affinity component in each displacement curve is similar to that determined against the binding of the selective α_2-adrenoceptor ligand [^{3}H]-RX821002 in this tissue (Hudson *et al.*, 1992), suggesting that this represents the inhibition of [^{3}H]-idazoxan binding to α_2-adrenoceptors. The remaining component (20–40%) in each displacement curve exhibiting only low affinity towards the α_2-adrenoceptor antagonists (Figure 2b, Table 2) is then attributable to the displacement of [^{3}H]-idazoxan binding to a non-adrenoceptor site (NAIBS) since a comparable amount of binding was not displaced by an excess concentration of (−)-adrenaline (Figure 2a). A comparison of the antagonist affinities for these two sites reveals that all three are more than 5000 fold selective for α_2-adrenoceptors (Table 2).

The displacement of [^{3}H]-idazoxan by its 6-fluoro derivative RX801023 was also best described by a model assuming a two site interaction (Figure 3). Unlike the competition curves obtained with the other α_2-adrenoceptor antagonists however, only 20.07 ± 3.11% ($n = 7$) of the sites labelled displayed high affinity for RX801023 ($K_i = 4.79 \pm 0.71$ nM; Figure 3). The remaining 79.93 ± 3.11% of the labelled sites exhibited approximately 54 fold lower affinity for RX801023 ($K_i = 260.71 \pm 25.72$ nM; Figure 3). In concurrent experiments, the displacement of the selective α_2-adrenoceptor ligand [^{3}H]-RX821002 by RX801023 was best described a single site model of interaction with a Hill slope close to unity (1.02 ± 0.03, $n = 4$) and a K_i value of 113.46 ± 19.83 nM (Figure 3). The similarity of this latter K_i value to the K_i value determined for the low affinity component in the biphasic displacement of [^{3}H]-idazoxan by RX801023 is again consistent with the suggestion that 60–80% of [^{3}H]-idazoxan binding to this membrane preparation is to α_2-adrenoceptors. Moreover, compared to unlabelled idazoxan, RX801023 exhibits enhanced affinity and improved selectivity for the NAIBS component of [^{3}H]-idazoxan binding relative to the α_2-adrenoceptor component.

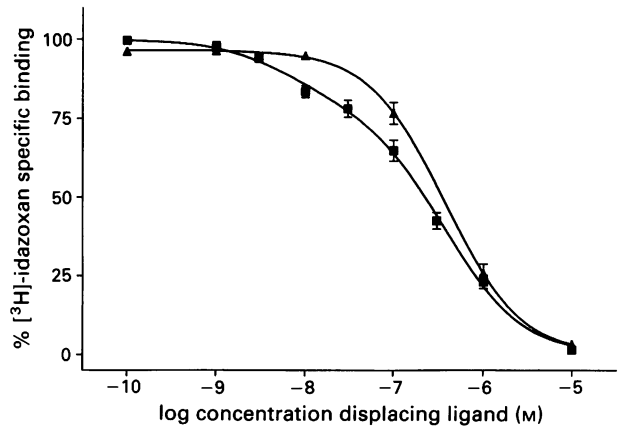

Figure 3 Concentration-dependent displacement of [^{3}H]-idazoxan (■) or [^{3}H]-RX821002 (▲) binding to rat whole brain membranes by RX801023 (6-fluoro-idazoxan). Incubations were performed for 30 min at 25°C in a Tris HCl buffer (50 mM Tris HCl, 1 mM $MgCl_2$; pH 7.4) containing 3–4 nM [^{3}H]-idazoxan or 2–3 nM [^{3}H]-RX821002. Non specific binding was determined with either 10 μM or 1 mM phentolamine for [^{3}H]-RX821002 and [^{3}H]-idazoxan respectively. Each point represents the mean (± s.e.mean, vertical bars) of observations from 4 or 5 determinations performed in triplicate.

Autoradiography of [^{3}H]-idazoxan

In preliminary experiments, sections incubated with 5 nM [^{3}H]-idazoxan alone or in the presence of yohimbine (5 μM) or idazoxan (3 μM) were removed from the glass slides and bound radioactivity estimated by liquid scintillation counting (data not shown). In this manner, the washing procedure employed was determined to be optimal for high specific [^{3}H]-idazoxan binding to both α_2-adrenoceptors and NAIBS. For other labelled sections, a photographic exposure time of 6 to 8 weeks was chosen as this allowed the detection of NAIBS while the images reflecting α_2-adrenoceptor distribution remained within the linear detection phase of the tritium-sensitive film.

Examples of total [^{3}H]-idazoxan (5 nM) binding to sections of brain are shown in Figures 4a, 5 (left hemisections), 6a

Table 2 Affinity constants (K_i) and Hill slopes for the displacement of specific [^{3}H]-idazoxan binding to rat whole brain membranes by α-adrenoceptor agonists and antagonists

Ligand	K_i (nM)		*nH*	*α2/NAIBS*	n
Idazoxan	8.53 ± 1.28		0.97 ± 0.02	1	5
(−)-Adrenaline	106.20 ± 29.94		0.42 ± 0.01	ND	5
RX821002	0.80 ± 0.15	21.76 ± 0.97 μM	(71:29)*	27,200	4
RX811059	2.32 ± 0.48	66.41 ± 1.89 μM	(64:36)*	28,625	4
Yohimbine	32.39 ± 17.24	306.92 ± 129.82 μM	(66:34)*	9.475	5

Affinity values were obtained for the displacement of specific 3 nM [^{3}H]-idazoxan binding to rat whole brain membranes prepared as described under methods. RX821002, RX811059, and yohimbine displaced [^{3}H]-idazoxan binding to rat whole brain membranes with Hill slopes (nH) considerably less than unity (*) which could be resolved by computer-assisted curve fitting into high (α_2-adrenoceptor) and low (NAIBS) affinity components. For each of these ligands, the proportion of high and low affinity sites differentiated is shown in parentheses. Comparison of K_i values for the high and low affinity [^{3}H]-idazoxan labelled sites reveals each antagonist to be more than 5000 fold selective for α_2-adrenoceptors. Each value represents the mean ± s.e.mean of observations from the number of experiments (n) performed in triplicate.

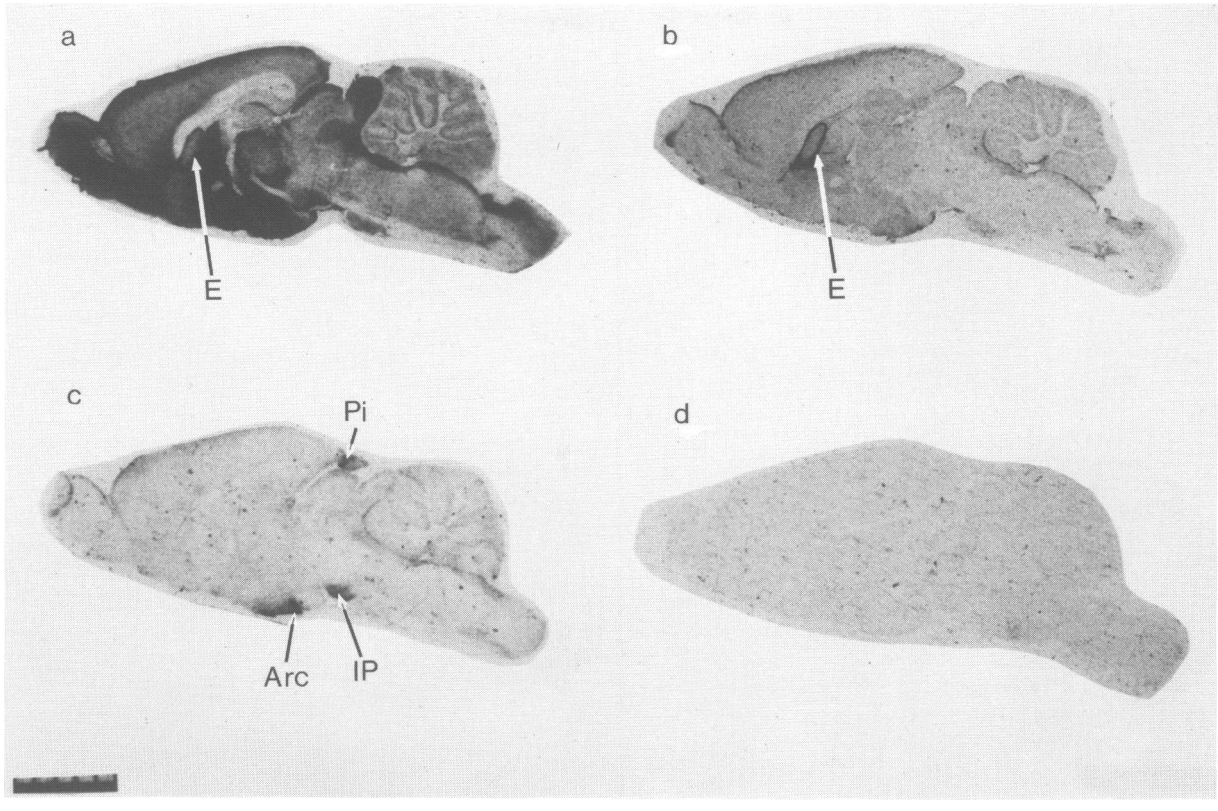

Figure 4 Autoradiograms of [^{3}H]-idazoxan (5 nM) binding to parasagittal sections of rat brain. Sections (a) and (b) lie approximately 1.2 mm from the midline, whilst (c) and (d) were cut 0.5 mm from the midline. Section (a) demonstrates total binding, (b) is that binding remaining in the presence of rauwolscine (5 μM), (c) is that remaining in the presence of RX821002 (3 μM), whilst (d) represents non-specific binding defined in the presence of unlabelled idazoxan (3 μM). See Table 3 for key to abbreviations. Dark areas depict higher levels of bound ligand. Scale bar = 5 mm.

and 6b. These figures are positive prints of the original autoradiograms, so that dense areas of binding are represented as grey to black areas of silver grains. Non-specific binding as defined by unlabelled idazoxan (3 μM) is shown in Figure 4d and is only slightly darker than normal background fogging.

Autoradiographic distribution of NAIBS

Throughout most regions of the rat brain, rauwolscine (5 μM), yohimbine (5 μM), RX821002 (3 μM), clonidine (3 μM) and noradrenaline (10 μM) each displaced much of the bound [^{3}H]-idazoxan. The remaining uneven images indicating [^{3}H]-idazoxan binding to NAIBS were further reduced in density by coincubation with unlabelled idazoxan (3 μM) or RX-801023 (3 μM). This is demonstrated qualitatively by Figures 4, 5 and 6. Whereas Figure 4a shows total 5 nM [^{3}H]-idazoxan binding to a parasagittal section of rat brain approximately 1.2 mm lateral from the midline, Figure 4b shows a similar section from the same animal incubated with [^{3}H]-idazoxan in the presence of rauwolscine (5 μM) to preclude α_2-adrenoceptor binding. Although [^{3}H]-idazoxan binding throughout the section was greatly reduced, a dense area of binding remained over the ependymal layer (E) surrounding the lateral ventricle (Figure 4b). Figure 4c illustrates a section closer to the midline which reveals structures containing [^{3}H]-idazoxan binding insensitive to displacement by RX-821002 (3 μM), namely arcuate nucleus, interpeduncular nucleus and pineal gland. Again, however, this binding to NAIBS was displaced by unlabelled idazoxan (3 μM, Figure 4d), leaving a near undetectable level of non specific binding.

Figure 5 demonstrates [^{3}H]-idazoxan binding to transverse sections of rat brain alone (left hemisections) or in the presence of various α_2-adrenoceptor ligands (right hemisections). In rostral areas of brain (Figure 5a) there remained low but detectable amounts of [^{3}H]-idazoxan binding (in the presence of 5 μM yohimbine) to areas of frontal cortex, cingulate cortex and anterior olfactory nucleus. Sections cut through the level of the caudate putamen (Figure 5b, approx bregma − 0.26 mm) show that whilst clonidine (3 μM) displaced much of the bound [^{3}H]-idazoxan (right hemisection) there again remained a residual image. Additionally, dense binding remained around the surface of the 3rd and lateral ventricles corresponding to the ependymal layer and choroid plexus respectively (Figure 5b). Brain sections through bregma − 3.3 mm (Figure 5c) revealed that total [^{3}H]-idazoxan binding was high in the arcuate nucleus although, unlike binding to surrounding brain structures, this was not attenuated in the presence of noradrenaline (10 μM). Likewise, the medial habenular nucleus and ventral medial thalamus also retained a degree of labelling (Figure 5c). Figure 5d illustrates the intense labelling of the interpeduncular nucleus which, as the right hemisection shows, remained in the presence of RX811059 (3 μM), as did a portion of the [^{3}H]-idazoxan bound in the central gray, especially that adjacent to the aqueduct. A more caudal section (bregma − 13.7 mm; Figure 6b,d and f) revealed binding to be high in the area postrema and the nucleus of the solitary tract (Figure 6b) although only the binding in this latter nucleus was prevented by rauwolscine (5 μM; Figure 6d). Figure 6 also demonstrates that the NAIBS component of [^{3}H]-idazoxan binding to brain structures such as the interpeduncular nucleus and area postrema was displaceable by RX801023 (3 μM), consistent with the NAIBS-selectivity of this compound revealed in radioligand binding studies. Thus, total [^{3}H]-idazoxan binding (Figure 6a,b) was preferentially reduced in the presence of RX801023 (3 μM) in the interpeduncular nucleus (Figure 6e) and area postrema

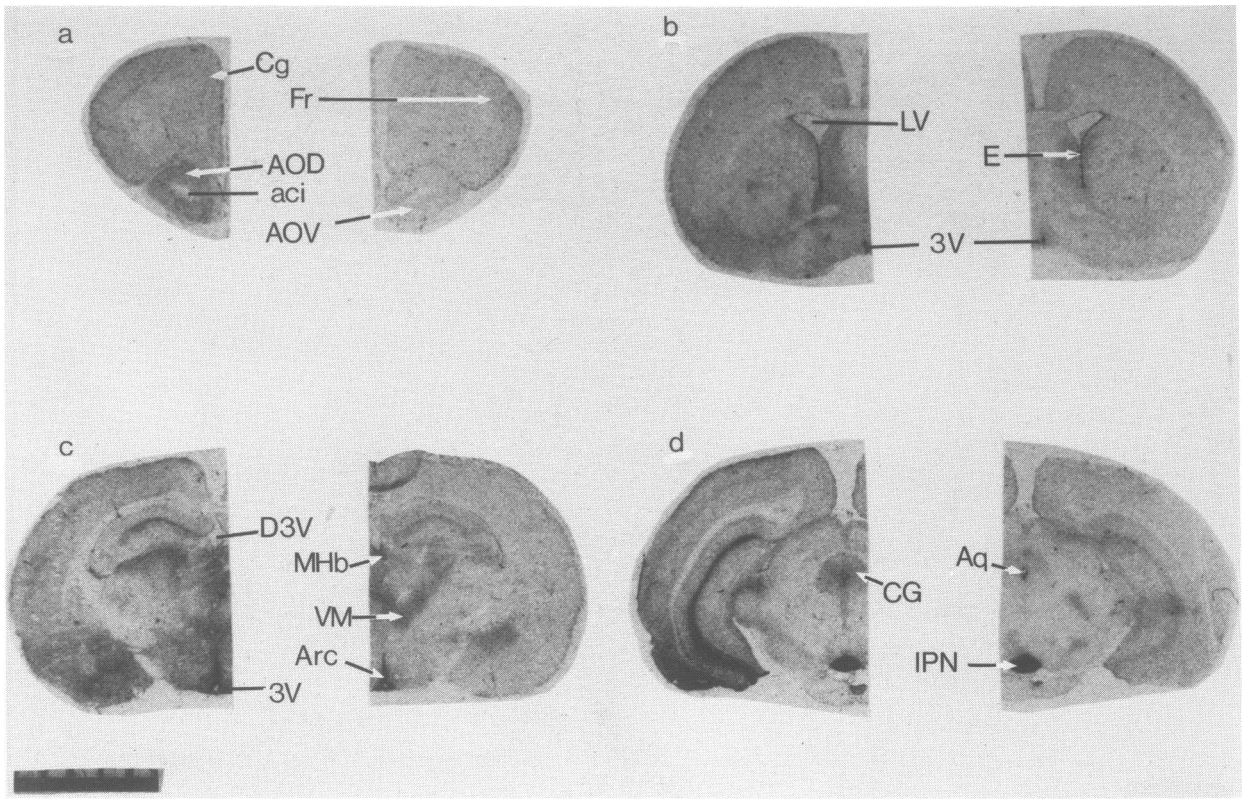

Figure 5 Autoradiographic distribution of [^{3}H]-idazoxan binding in transverse sections of rat brain. Sections are shown in a rostral to caudal manner taken at (a) bregma 4.2 mm; (b) − 0.26 mm; (c) bregma − 3.3 mm; and (d) bregma − 6.0 mm. At each level the left hemisection demonstrates total [^{3}H]-idazoxan (5 nM) binding, whilst the right hemisections have been co-incubated with (a) clonidine (3 μM); (b) yohimbine (5 μM); (c) noradrenaline (10 μM); and (d) RX811059 (3 μM). Key to abbreviations shown in Table 3. Scale bar = 5 mm.

(Figure 6f), structures in which the binding of [^{3}H]-idazoxan was resistant to displacement by 5 μM rauwolscine (Figure 6c,d). In all autoradiographic studies, [^{3}H]-idazoxan binding which remained in the presence of the various α_2-adrenoceptor ligands was reduced to background levels by the addition of RX801023 (3 μM) in an equivalent manner to that found by the addition of unlabelled idazoxan (3 μM).

Quantitative autoradiography of [^{3}H]-idazoxan binding

Table 3 summarises the results of a quantitative analysis of [^{3}H]-idazoxan autoradiography in rat brain. [^{3}H]-idazoxan binding to α_2-adrenoceptors was determined as that component displaced by either rauwolscine (5 μM) or RX821002 (3 μM). That bound to NAIBS was identified as [^{3}H]-idazoxan binding remaining in the presence of rauwolscine or RX821002 which was displaceable by either RX801023 (3 μM) or idazoxan (3 μM). The highest density of [^{3}H]-idazoxan binding not displaced by α_2-adrenoceptor ligands was in the area postrema (Table 3). The ependyma, interpeduncular and arcuate nuclei also contained high levels of [^{3}H]-idazoxan binding, more of which was insensitive to displacement by rauwolscine or RX821002 than by RX801023 or idazoxan (Table 3). The central gray contained moderate levels of both α_2-adrenoceptor and NAIBS binding. Nuclei such as the ventral medial thalamus, hippocampus and entorhinal cortex contained moderate levels of NAIBS binding but were relatively low when compared with the large amount of [^{3}H]-idazoxan binding displaceable by α_2-adrenoceptor agonists and antagonists in these regions (Table 3). Most brain nuclei apart from those shown in Table 3 contained low levels of NAIBS binding (<20 fmol mg^{-1} wet tissue) and have not therefore been listed. Specific [^{3}H]-idazoxan binding in sections of rat spinal cord was completely displaced by rauwolscine (5 μM).

Discussion

The present data demonstrate several clear findings. First it confirms recent observations (Brown *et al.*, 1990) that [^{3}H]-idazoxan labels two distinct binding sites in rat brain, namely α_2-adrenoceptors and additional non-adrenoceptor binding sites or NAIBS. Secondly, autoradiography reveals that there is marked regional variation in the distribution of these two sites. Thirdly, the close structural analogues of idazoxan, RX821002 and RX811059 are high affinity α_2-adrenoceptor antagonists with α_2-adrenoceptor/NAIBS selectivity of more than 5000 fold. Conversely, RX801023 is a moderately selective ligand (54 fold) for the NAIBS site with an affinity around 4–5 nM.

On the basis of observations from both the present and previous investigations (Brown *et al.*, 1990) it appears that in rat whole brain homogenates, 70–80% of specific [^{3}H]-idazoxan binding is to α_2-adrenoceptors whilst 20–30% is to NAIBS. The technique of autoradiography has provided visual evidence that this ratio of the two sites is not constant throughout the rat brain and that the distribution of NAIBS shows a marked degree of heterogeneity. For example, whilst α_2-adrenoceptors were clearly delineated in limbic structures, cortex and olfactory cortex, NAIBS were found to be much less dense. However, NAIBS were clearly visualized in discrete nuclei such as the arcuate and interpeduncular nucleus and pineal gland. A particularly clear demonstration of this differential distribution of α_2-adrenoceptors and NAIBS is given in the autoradiograms of the brain stem (Figure 6d,f) where α_2-adrenoceptor binding is most dense in the nucleus tractus solitarius and almost absent in the area postrema. Conversely, NAIBS binding shows almost opposite localization, with the area postrema exhibiting the highest density of any brain region. What remains unclear from these studies is whether NAIBS are localized to neuronal and/or glial

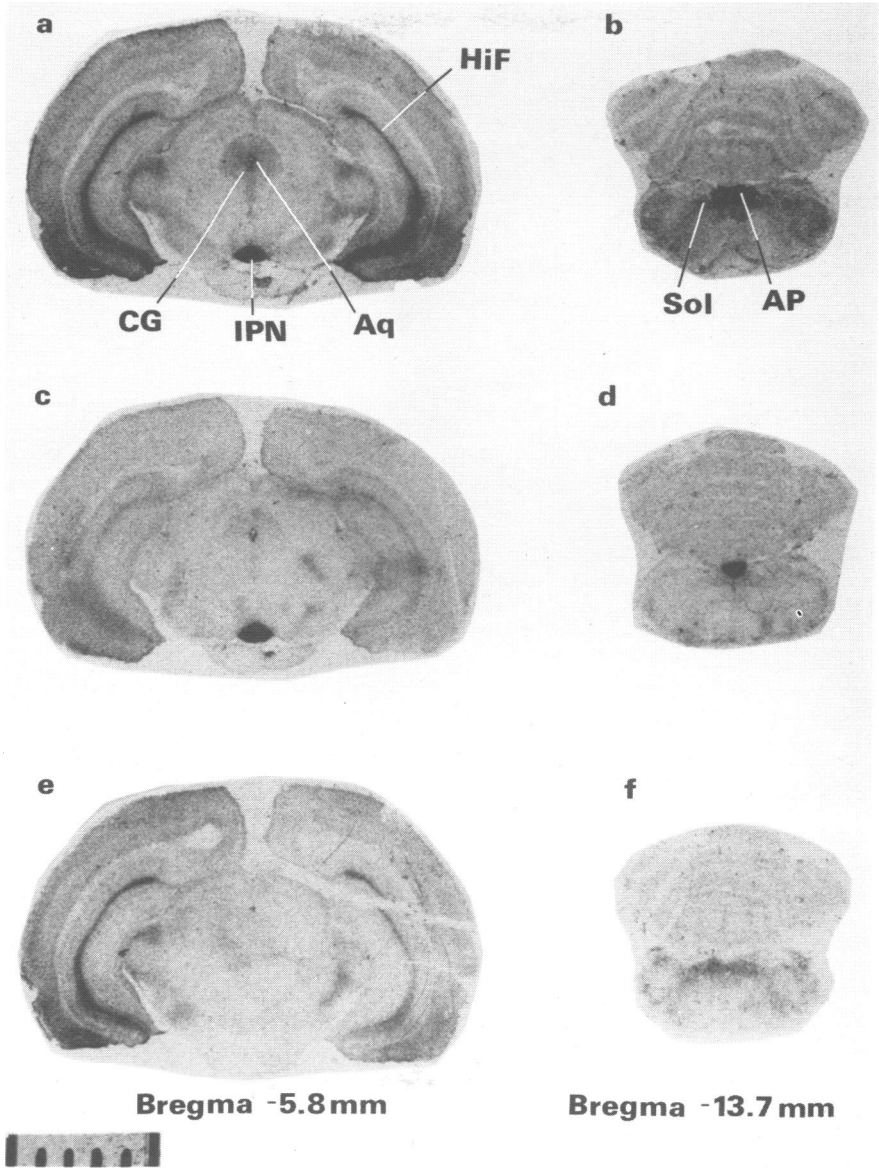

Figure 6 Autoradiographs of [^{3}H]-idazoxan binding in tranverse sections of rat brain at bregma − 3.3 mm (a,c and e) and at bregma − 13.7 mm (b,d and f). Sections (a) and (b) show total [^{3}H]-idazoxan (5 nM) binding. Sections (c) and (d) demonstrate that binding displaced by rauwolscine (5 μM) whilst sections (e) and (f) show the preferential displacement of binding in those brain nuclei containing NAIBS by RX801023. For key to abbreviations see Table 3. Scale bar = 5 mm.

elements or some other cell type. Possibly the high density of NAIBS in the pineal gland, on or close to ventricle surfaces, for instance around the 3rd ventricle, the aqueduct and associated with the ependyma lining the lateral ventricle, indicate a non-neuronal cell type. Interestingly, the distribution of NAIBS shows a striking resemblance to that of peripheral type benzodiazepine sites in rat brain revealed in autoradiographic studies with [^{3}H]-PK11195 (Benavides *et al.*, 1983). However, whilst it is widely accepted that central [^{3}H]-PK11195 binding is primarily associated with glial and non-neuronal elements, assigning NAIBS to a non-neuronal location based on autoradiographical comparisons alone would be premature. Further studies will be needed to clarify their exact cellular location in the brain, possibly utilizing discrete chemical and electrolytic lesions. Interestingly, however, localization of NAIBS to mitochondria has been postulated on the basis of binding studies with subcellular fractions of peripheral tissues (Lachaud-Pettiti *et al.*, 1991; Tesson *et al.*, 1991).

The differential distribution of [^{3}H]-idazoxan binding to α_2-adrenoceptors and NAIBS may help explain many of the actions of this drug. It markedly increases noradrenaline turnover in rat brain (Walter *et al.*, 1984) in regions which possess a high density of α_2-adrenoceptors. It seems likely that the antidepressant actions of idazoxan are mediated through an action at α_2-adrenoceptors (Osman *et al.*, 1989; see Dickinson, 1991) although confirmation of this will depend on demonstrating clinical efficacy with drugs such as RX811059 which show low affinity for NAIBS. There are effects of idazoxan that are not mimicked by the selective α_2-adrenoceptor antagonists RX821002 and RX811059 which may suggest they are mediated by NAIBS. For instance, idazoxan stimulation of eating in rats (Jackson *et al.*, 1991b). This is consistent with the high density of NAIBS in both the area postrema and arcuate nucleus, two regions intimately involved in the control of food intake (see Blundell, 1991). Similarly, idazoxan does not share the typical proconvulsant profile of other α_2-adrenoceptor antagonists and can even lower seizure threshold in mice (Jackson *et al.*, 1991a). This could perhaps be mediated in the hippocampus where NAIBS were located to the surface of hippocampal fissure between the molecular layer of the dentate gyrus and the lacunosum moleculare layer (Figure 6c). The finding that RX801023 is relatively a selective ligand for NAIBS will allow the evaluation of these possibilities.

The distribution of [^{3}H]-idazoxan binding in rat brain

Table 3 Quantitative autoradiographic analysis of [^{3}H]-idazoxan binding to discrete areas of rat brain

Brain region	*Figure symbol*	*α_2-adrenoceptors* (fmol mg^{-1} wet tissue)	*NAIBS* (fmol mg^{-1} wet tissue)
Anterior olfactory nucleus			
dorsal	AOD	235.1 ± 6.4	17.7 ± 0.9
ventral	AOV	206.5 ± 22.2	34.9 ± 1.7
anterior commissure, intrabulbar	aci		
Frontal cortex	Fr	106.5 ± 6.4	24.9 ± 0.7
Cingulate cortex	Cg	54.3 ± 3.2	29.8 ± 1.6
Entorhinal cortex		95.1 ± 12.2	18.6 ± 4.5
Corpus callosum		23.3 ± 5.9	4.6 ± 2.0
Caudate putamen		56.3 ± 3.2	29.7 ± 2.1
Choroid plexus	CP	12.7 ± 6.0	62.3 ± 5.6
Ependymal layer	E	47.2 ± 31.5	101.9 ± 8.1
Hippocampal fissure	HiF	110.6 ± 30.2	61.6 ± 8.2
Arcuate nucleus	Arc	14.5 ± 1.1	102.2 ± 3.3
Lateral hypothalamic area		74.1 ± 2.5	20.0 ± 2.4
Ventromedial hypothalamic nu	VM	56.7 ± 6.5	40.3 ± 6.4
Central gray	CG	51.2 ± 1.4	27.5 ± 2.8
Superior colliculus		73.1 ± 12.7	47.9 ± 11.2
Inferior colliculus		101.5 ± 9.8	16.6 ± 0.7
Interpeduncular nucleus	IPN	55.1 ± 7.1	123.4 ± 12.7
Medial habenular nucleus	MHb	72.9 ± 5.1	45.4 ± 5.9
Lateral habenular nucleus		35.8 ± 8.6	27.6 ± 1.4
Nuc solitary tract	Sol	113.6 ± 5.0	22.5 ± 3.7
Area postrema	AP	18.9 ± 18.4	208.2 ± 18.7
Aqueduct	Aq		
surface of the aqueduct		27.2 ± 7.3	134.8 ± 18.2
Dorsal third ventricle	D3V		
Lateral ventricle	LV		

[^{3}H]-idazoxan binding to α_2-adrenoceptors was taken to be that displaced by rauwolscine (5 μM) or RX821002 (3 μM) whereas that bound to NAIBS was that remaining but displaceable by RX801023 (3 μM) or idazoxan (3 μM). Data represent the mean ± s.e.mean of 3–5 animals, with triplicate determinations in three sections from each rat brain.

shows considerable overlap with that found in the human brain (De Vos *et al.*, 1991). However, there are several intriguing differences. First, the human brain has a relatively higher ratio of NAIBS to α_2-adrenoceptors, with about an equal density of each. In addition, the regions exhibiting the highest NAIBS density in human brain are the dopamine-rich areas such as substantia nigra and caudate nucleus which may explain the therapeutic benefit of idazoxan in the neurodegenerative extrapyramidal condition of progressive supranuclear palsy (Ghika *et al.*, 1991). However, the rat contains sufficient NAIBS binding to allow the opportunity for evaluating the possible role of these binding sites in brain function.

In conclusion, the present results provide further evidence that [^{3}H]-idazoxan can be employed to characterize NAIBS in the rat brain. Moreover, by use of selective α_2-adrenoceptor ligands to preclude [^{3}H]-idazoxan binding to α_2-adrenoceptors, NAIBS can be visualized in discrete nuclei using *in vitro* autoradiography. In combination with the use of a selective ligand such as RX801023, this localization may provide an opportunity to explore possible functions for these binding sites.

References

BENAVIDES, J., QUARTERONET, D., IMBAULT, F., MALGOURIS, C., UZAN, A., RENAULT, C., DUBROEUCQ, M.C., GUEREMY, C. & LE FUR, G. (1983). Labelling of 'peripheral-type' benzodiazepine binding sites in the rat brain by using [^{3}H]PK11195, an isoquinoline carboxamide derivative: Kinetic studies and autoradiographic localization. *J. Neurochem.*, **41**, 1744–1750.

BLUNDELL, J. (1991). Pharmacological approaches to appetite suppression. *Trends Pharmacol. Sci.*, **12**, 147–157.

BOYAJIAN, C.L., LOUGHLIN, S.E. & LESLIE, F.M. (1987). Anatomical evidence for alpha-2 adrenoceptor heterogeneity: differential autoradiographic distributions of [^{3}H]rauwolscine and [^{3}H]-idazoxan in rat brain. *J. Pharmacol. Exp. Ther.*, **241**, 1079–1091.

BRADFORD, M.M. (1976). A rapid sensitive method for the quantification of protein using the principle of protein dye binding. *Anal. Biochem.*, **72**, 248–252.

BRICCA, G., DONTENWILL, M., MOLINES, A., FELDMAN, J., BELCOURT, A. & BOUSQUET, P. (1989). The imidazoline preferring receptor: binding studies in bovine, rat and human brainstem. *Eur. J. Pharmacol.*, **162**, 1–9.

BROADHURST, A.M. & WYLLIE, M.G. (1986). A reassessment of the binding of [^{3}H]-rauwolscine to membranes from the rat cortex. *Neuropharmacology*, **25**, 287–295.

BROWN, C.M. MACKINNON, A.C., MCGRATH, J.C., SPEDDING, M. & KILPATRICK, A.T. (1990). α_2-Adrenoceptor subtypes and imidazoline-like binding sites in the rat brain. *Br. J. Pharmacol.*, **99**, 803–809.

BRUNING, G., KAULEN, P. & BAUMGARTEN, H.G. (1987). Quantitative autoradiographic localisation of α_2-antagonist binding sites in rat brain using [^{3}H]idazoxan. *Neurosci. Lett.*, **83**, 333–337.

CHAPLEO, C.B., MYERS, P.L., BUTLER, R.C.M., DOXEY, J.C., ROACH, A.G. & SMITH, C.F.C. (1983). α-Adrenoceptor reagents. 1. Synthesis of some 1,4-benzodioxans as selective presynaptic α_2-adrenoceptor antagonists and potential antidepressants. *J. Med. Chem.*, **26**, 823–831.

CHENG, Y.C. & PRUSOFF, W.H. (1973). Relationship between the inhibition constant (Ki) and the concentration of inhibitor which causes 50% inhibition (IC_{50}) of an enzymatic reaction. *Biochem. Pharmacol.*, **22**, 3099–3108.

CONVENTS, A., DE KEYSER, J., DE BACKER, J.P. & VAUQUELIN, G. (1989). [^{3}H]rauwolscine labels α_2-adrenoceptors and $5HT_{1A}$ receptors in human cerebral cortex. *Eur. J. Pharmacol.*, **159**, 307–310.

COUPRY, I., ATLAS, D., PODEVIN, R.A., UZIELLI, I. & PARINI, A. (1989). Imidazoline-guanidinium receptive site in renal proximal tubule: asymmetric distribution, regulation by cations and interaction with an endogenous clonidine displacing substance. *J. Pharmacol. Exp. Ther.*, **252**, 293–299.

DE VOS, H., CONVENTS, A., DE KEYSER, J., DE BACKER, J., VAN MEGEN, I.J.B., EBINGER, G. & VAUQUELIN, G. (1991). Autoradiographic distribution of α_2-adrenoceptors, NAIBS, and $5HT_{1A}$ receptors in human brain using [^{3}H]idazoxan and [^{3}H]rauwolscine. *Brain Res.*, **566**, 13–20.

DICKINSON, S.L. (1991). Alpha-2-adrenoceptor antagonists and depression. *Drug News Persp.*, **4**, 197–203.

DOXEY, J.C., LANE, A.C., ROACH, A.G. & VIRDEE, N.K. (1984). Comparison of the α-adrenoceptor antagonist profiles of idazoxan (RX781094), yohimbine, rauwolscine and corynanthine. *Naunyn-Schmiedebergs Arch. Pharmacol.*, **325**, 136–144.

DOXEY, J.C., ROACH, A.G. & SMITH, C.F.C. (1983). Studies on RX781094: a selective, potent and specific antagonist of α_2-adrenoceptors. *Br. J. Pharmacol.*, **78**, 489–505.

ERNSBERGER, P., MEELEY, M.P., MANN, J.J. & REIS, D.J. (1987). Clonidine binds to imidazole binding sites as well as α_2-adrenoceptors in the ventrolateral medulla. *Eur. J. Pharmacol.*, **134**, 1–13.

ERNSBERGER, P., GIULIANO, R., WILLETTE, R.N., GRANATA, A.R. & REIS, D.J. (1988a). Hypotensive action of clonidine analogues correlates with binding affinity at imidazole and not alpha-2-adrenergic receptors in the rostral ventrolateral medulla. *J. Hypertension*, **6**, S554–S557.

ERNSBERGER, P., MEELEY, M.P. & REIS, D.J. (1988b). An endogenous substance with clonidine-like properties: selective binding to imidazole sites in the ventrolateral medulla. *Brain Res.*, **441**, 309–318.

ERNSBERGER, P., GIULIANO, R., WILLETTE, R.N. & REIS, D.J. (1990). Role of imidazole receptors in the vasodepressor response to clonidine analogues in the rostral ventrolateral medulla. *J. Pharmacol. Exp. Ther.*, **253**, 408–418.

FELDMAN, J., TIBIRICA, E., BRICCA, G., DONTENWILL, M., BELCOURT, A. & BOUSQUET, P. (1990). Evidence for the involvement of imidazoline receptors in the central hypotensive effect of rilmenidine in the rabbit. *Br. J. Pharmacol.*, **100**, 600–604.

GALITZKY, J., LARROUY, D., BERLAN, M. & LAFONTAN, M. (1990). New tools for human fat cell alpha-2A adrenoceptor characterization. Identification on membranes and on intact cells using the new antagonist [^{3}H]RX821002. *J. Pharmacol. Exp. Ther.*, **252**, 312–319.

GHIKA, J., TENNIS, M., HOFFMAN, E., SCHOENFELD, D. & GROWDON, J. (1991). Idazoxan treatment in progressive supranuclear palsy. *Neurology*, **41**, 986–991.

GOMEZ, R., ERNSBERGER, P., FEINLAND, G. & REIS, D.J. (1991). Rilmenidine lowers arterial pressure via imidazole receptors in brainstem C1 area. *Eur. J. Pharmacol.*, **195**, 181–191.

HAMILTON, C.A., YAKUBU, M.A., JARDINE, E. & REID, J.L. (1991). Imidazole binding sites in rabbit kidney and forebrain membranes. *J. Auton. Pharmacol.*, **11**, 277–283.

HUDSON, A.L., MALLARD, N.J. & NUTT, D.J. (1991a). [^{3}H] RX821002: a new α_2-adrenoceptor ligand for *in vitro* autoradiography and binding studies in the mammalian CNS. In *Adrenoceptors: Structure, Mechanisms, Functions*. ed. Szabadi, E. & Bradshaw, C.M. pp. 299–300. Basel: Birkhauser Verlag.

HUDSON, A.L., MALLARD, N.J. & NUTT, D.J. (1991b). Autoradiographic localisation of non-adrenoceptor idazoxan binding sites (NAIBS) in the rat brain. *Br. J. Pharmacol.*, **102**, 4P.

HUDSON, A.L., MALLARD, N.J., TYACKE, R. & NUTT, D.J. (1992). [^{3}H]-RX821002: a highly selective ligand for the identification of α_2-adrenoceptors in the rat brain. *Mol. Neuropharmacol.*, **1**, 219–229.

HUDSON, A.L. & NUTT, D.J. (1990). *In vitro* autoradiography of [^{3}H]-RX821002 in the rat CNS, a new ligand for identifying α_2-adrenoceptors. *Br. J. Pharmacol.*, **100**, 345P.

JACKSON, H.C., DICKINSON, S.L. & NUTT, D.J. (1991a). Exploring the pharmacology of the pro-convulsant effects of α_2-adrenoceptor antagonists in mice. *Psychopharmacol.*, **105**, 558–562.

JACKSON, H.C., GRIFFIN, I.J. & NUTT, D.J. (1991b). The effects of idazoxan and other α_2-adrenoceptor antagonists on food and water intake in the rat. *Br. J. Pharmacol.*, **104**, 258–262.

LACHAUD-PETTITI, V., PODEVIN, R.A., CHRETIEN, Y. & PARINI, A. (1990). Imidazoline-guanidinium and α_2-adrenergic binding sites in basolateral membranes from human kidney. *Eur. J. Pharmacol.*, **206**, 23–31.

LANGIN, D. & LAFONTAN, M. (1989). [^{3}H]idazoxan binding at non-α_2-adrenoceptors in rabbit adipocyte membranes. *Eur. J. Pharmacol.*, **159**, 199–203.

LANGIN, D., LAFONTAN, M., STILLINGS, M.R. & PARIS, H. (1989). [^{3}H]RX821002: a new tool for the identification of α_{2A}-adrenoceptors. *Eur. J. Pharmacol.*, **167**, 95–104.

LANGIN, D., PARIS, H., DAUZATS, M. & LAFONTAN, M. (1990a). Discrimination between alpha 2-adrenoceptors and [^{3}H]idazoxan-labelled non-adrenergic sites in rabbit white fat cells. *Eur. J. Pharmacol.*, **188**, 261–272.

LANGIN, D., PARIS, H. & LAFONTAN, M. (1990b). Binding of [^{3}H]idazoxan and of its methoxy derivative, [^{3}H]RX821002 in human fat cells: [^{3}H]idazoxan but not [^{3}H]RX821002 labels additional non α_2-adrenergic binding sites. *Mol. Pharmacol.*, **37**, 876–885.

LEHMANN, J., KOENIG-BERARD, E. & VITOU, P. (1989). The imidazoline-preferring receptor. *Life Sci.*, **45**, 1609–1615.

MACKINNON, A.C., BROWN, C.M., SPEDDING, M. & KILPATRICK, A.T. (1989). [^{3}H]-idazoxan binds with high affinity to two sites on hamster adipocytes: an α_2-adrenoceptor and a non-adrenoceptor site. *Br. J. Pharmacol.*, **98**, 1143–1150.

MALLARD, N.J., TYACKE, R., HUDSON, A.L. & NUTT, D.J. (1991). Comparative binding studies of [^{3}H]-idazoxan and [^{3}H]-RX-821002 in the rat brain. *Br. J. Pharmacol.*, **102**, 221P.

MICHEL, M.C., BRODDE, O.E., SCHNEPEL, B., BEHRENDT, J., TSCHADA, R. & INSEL, P.A. (1989). [^{3}H]Idazoxan and some other α_2-adrenergic drugs also bind with high affinity to a nonadrenergic site. *Mol. Pharmacol.*, **35**, 324–330.

MICHEL, M.C. & INSEL, P.A. (1989). Are there multiple imidazoline binding sites? *Trends Pharmacol. Sci.*, **10**, 342–344.

MUNSON, P.J. & RODBARD, D. (1980). Ligand: A versatile computerized approach for characterization of ligand-binding systems. *Anal. Biochem.*, **107**, 220–239.

OSMAN, O.T., RUDORFER, M.V. & POTTER, W.Z. (1986). Idazoxan: A selective alpha2 : alpha1-antagonist and effective sustained antidepressant in two bipolar depressed patients. *Arch. Gen. Psychiatr.*, **46**, 958–959.

PAXINOS, G. & WATSON, D. (1986). *The Rat Brain in Stereotaxic Coordinates*. New York: Academic Press.

PETRASH, A.C. & BYLUND, D.B. (1986). Alpha-2 adrenergic receptor subtypes indicated by [^{3}H]-yohimbine binding in human brain. *Life Sci.*, **38**, 2129–2137.

STILLINGS, M.R., CHAPLEO, C.B., BUTLER, R.C.M., DAVIS, J.A., ENGLAND, C.D., MYERS, M., MYERS, P.M., TWEDDLE, N., WELBOURN, A.P., DOXEY, J.C. & SMITH, C.F.C. (1985). α-Adrenoceptor reagents. 3. Synthesis of some 2-substituted 1,4-benzodioxans as selective presynaptic α_2-adrenoceptor antagonists. *J. Med. Chem.*, **28**, 1054–1062.

TESSON, F., PRIP-BUUS, C., LEMOINE, A., PEGORIER, J.P. & PARINI, A. (1991). Subcellular distribution of imidazoline-guanidinium-receptive sites in human and rabbit liver. *J. Biol. Chem.*, **266**, 155–160.

VAUQUELIN, G., DE VOS, H., DE BACKER, J.P. & EBINGER, G. (1990). Identification of alpha-2 adrenergic receptors in human frontal cortex membranes by binding of [^{3}H]RX821002, the 2-methoxy analog of [^{3}H]idazoxan. *Neurochem. Int.*, **17**, 537–546.

VIGNE, P., LAZDUNSKI, M. & FRELIN, C. (1989). Guanabenz, guanochlor, guanoxan and idazoxan bind with high affinity to non-adrenergic sites in pig kidney membranes. *Eur. J. Pharmacol.*, **160**, 295–298.

WALTER, D.S., FLOCKHART, I.R., HAYNES, M.J., HOWLETT, D.R., LANE, A.T., BURTON, J.J., JOHNSON, J. & DETTMAR, P.W. (1984). Effects of idazoxan on catecholamine systems in rat brain. *Biochem. Pharmacol.*, **33**, 2553–2557.

WELBOURN, A.P., CHAPLEO, C.B., LANE, A.C., MYERS, P.L., ROACH, A.G., SMITH, C.F.C., STILLINGS, M.R. & TULLOCH, I.F. (1986). α-Adrenoceptor reagents. 4. Resolution of some potent selective prejunctional α_2-adrenoceptor antagonists. *J. Med. Chem.*, **29**, 2000–2003.

WIKBERG, J.E.S. (1989). High affinity binding of idazoxan to a non-catecholaminergic binding site in the central nervous system: description of a putative, idazoxan-receptor. *Pharmacol. Toxicol.*, **64**, 152–155.

WIKBERG, J.E.S. & UHLEN, S. (1990). Further characterisation of the guinea-pig cerebral cortex idazoxan receptor: solubilization, distinction from the imidazole site, and demonstration of cirazoline as an idazoxan receptor selective drug. *J.Neurochem.*, **55**, 192–203.

WIKBERG, J.S., UHLEN, S. & CHHAJLANI, V. (1991). Meditomidine stereoisomers delineate two closely related subtypes of idazoxan (imidazoline) I-receptors in the guinea-pig. *Eur. J. Pharmacol.*, **193**, 335–340.

YABLONSKY, F. & DAUSSE, J.P. (1991). Nonadrenergic binding sites for the α_2-antagonist [^{3}H]idazoxan in the rabbit urethral smooth muscle. *Biochem. Pharmacol.*, **41**, 701–707.

(Received February 12, 1992
Revised March 16, 1992
Accepted April 22, 1992)

Br. J. Pharmacol. (1992), **106**, 1028–1034 © Macmillan Press Ltd, 1992

Human bronchial cyclic nucleotide phosphodiesterase isoenzymes: biochemical and pharmacological analysis using selective inhibitors

Jacob de Boer, *Alison J. Philpott, Ronald G.M. van Amsterdam, [1]* Mohammed Shahid, Johan Zaagsma & C. David Nicholson

Department of Pharmacology and Therapeutics, A Deusinglaan, 9713 AW Groningen, The Netherlands and *Organon Laboratories Ltd., Newhouse, Lanarkshire, ML1 5SH.

1 The aims of the present study were to characterize the cyclic nucleotide phosphodiesterase (PDE) isoenzyme activities present in human bronchi and to examine the ability of selective isoenzyme inhibitors to relax histamine and methacholine precontracted preparations of human bronchi.

2 Three separations of pooled human bronchial tissue samples were performed. Ion-exchange chromatography showed that the soluble fraction of human bronchial preparations contains PDE I, II, III, IV and V isoenzyme activities. Multiple forms of PDE I and PDE IV were observed and PDE IV was the main cyclic AMP hydrolytic activity.

3 3-Isobutyl-1-methylxanthine (IBMX) non-selectively inhibited all separated isoenzyme activities. Zaprinast selectively inhibited PDE V, but also effectively inhibited one of the two PDE I isoforms identified. The PDE IV selective inhibitors rolipram and RO-201724, inhibited the PDE IV activities as did the dual PDE III/IV inhibitor, Org 30029. Org 9935, a PDE III selective inhibitor, potently attenuated part of the PDE IV activity peak in one of three separations performed, indicating that some PDE III activity may co-elute with PDE IV under the experimental conditions employed.

4 PDE IV-selective (rolipram), PDE III-selective (Org 9935) and dual PDE III/IV (Org 30029) inhibitors were effective relaxants of human bronchial smooth muscle. The PDE V/PDE I inhibitor, zaprinast was relatively ineffective.

5 The present study demonstrates in human bronchi, as in animal airways smooth muscle, that inhibitors of PDE III, PDEIV and dual PDE III/IV have potentially useful bronchodilator activity and are worthy of further consideration as anti-asthma drugs.

Keywords: Human bronchi; cyclic nucleotide phosphodiesterase isoenzymes; isoenzyme selective inhibitors; rolipram; Org 30029; Org 9935; zaprinast; IBMX

Introduction

There are five main families of cyclic nucleotide phosphodiesterase isoenzymes which catalyse the hydrolysis of the intracellular second messengers, adenosine 3'5'-cyclic monophosphate (cyclic AMP) and guanosine 3'5'-cyclic monophosphate (cyclic GMP) to 5' nucleotides (Beavo & Reifsnyder, 1990). In addition to showing different regulatory properties, these phosphodiesterase isoenzymes can be distinguished by their sensitivity to a variety of isoenzyme selective inhibitors (Nicholson *et al.*, 1991). Despite the ubiquitous presence of cyclic AMP and cyclic GMP, isoenzyme selective inhibitors do not invariably alter tissue function, possibly because isoenzyme distribution is markedly tissue-dependent (Nicholson *et al.*, 1991). Thus, selective inhibitors may be potentially useful therapeutic agents for a variety of diseases including asthma (Nicholson *et al.*, 1991). Indeed, selective inhibitors of particular phosphodiesterase isoenzymes have been shown both to produce bronchodilatation (Torphy, 1988; Torphy *et al.*, 1988; Harris *et al.*, 1989; Shahid *et al.*, 1991b) and to inhibit mediator release from inflammatory cells (Dent *et al.*, 1991; Souness *et al.*, 1991; Robicsek *et al.*, 1991; Torphy & Undem, 1991).

A combination of bronchodilator and anti-inflammatory activities makes phosphodiesterase isoenzyme inhibition a potentially attractive mechanism for the treatment of asthma. However, isoenzyme selective inhibitors show marked species variation in their airway relaxant effects. Selective inhibitors of the cyclic GMP inhibited phosphodiesterase isoenzyme (PDE III) more effectively relax guinea-pig (Harris *et al.*, 1989) and canine (Torphy *et al.*, 1988) than bovine (Shahid *et al.*, 1991b) tracheal smooth muscle preparations. In contrast, selective inhibitors of the cyclic GMP-insensitive phosphodiesterase isoenzyme (PDE IV) more potently relax bovine (Shahid *et al.*, 1991b) than canine (Torphy *et al.*, 1988) and guinea-pig (Harris *et al.*, 1989) tissues. Although the reasons for the tissue and species variation are not known, they may arise from differences in abundance and/or intracellular localization of functionally important phosphodiesterase isoenzymes. Whether similar species variation exists for the anti-inflammatory effects of isoenzyme-selective phosphodiesterase inhibitors has not been reported.

It is clearly important to clarify the phosphodiesterase isoenzyme profile and the functional activity of selective isoenzyme inhibitors in human airway smooth muscle. Thus, the aims of the present study were to characterize the phosphodiesterase isoenzyme activities present in human bronchi and to examine the functional effects of a variety of known selective isoenzyme inhibitors. A preliminary account of this study has been presented to the British Pharmacological Society (Shahid *et al.*, 1992).

Methods

Separation of cyclic nucleotide phosphodiesterase isoenzymes

Macroscopically normal, human lungs were obtained from lung cancer patients undergoing surgery and were transport-

[1] Author for correspondence at: Organon Laboratories Ltd., Newhouse, Lanarkshire, ML1 5SH

ed to the laboratory in ice cold Krebs-Henseleit solution previously well aerated with 95% O_2 and 5% CO_2. None of the patients had been receiving medication for airways disease, in particular no patient had recently received theophylline containing drugs. Premedication and anaesthetics were the same for all patients. All subsequent steps were performed on ice. Peripheral bronchi (diameter 2–3 mm) were isolated, according to the procedure described by van Amsterdam *et al.* (1990), and carefully trimmed free of vascular and parenchymal tissue before being frozen in liquid nitrogen and stored at − 70°C. Frozen bronchi (9–10 g) obtained from 3 to 4 lung biopsies were pooled, thawed, cut into small cubes and homogenized (Polytron: PT20 probe, 2 × 10 s bursts at speed setting 5 and 2 × 10 s bursts at speed setting 7) in three volumes of buffer A (pH 6.5) containing (mmol l^{-1}): Bistris 20, dithiothreitol 1, benzamidine 2, EDTA 2, NaCl 50 and phenylmethanesulphonyl fluoride (PMSF) 0.1. The extract was centrifuged (107,000 g × 60 min) and the supernatant fraction containing the soluble material was used as the source of phosphodiesterase isoenzymes. The lung tissue was obtained from smokers, hence the particulate material was contaminated and could, therefore, not be analysed. The supernatant fraction was filtered (0.22 μm) and the phosphodiesterase activities separated by ion exchange chromatography on a Mono Q column, pre-equilibrated in buffer A, attached to a fast protein liquid chromatography (FPLC) system essentially as described previously (Shahid *et al.*, 1991b). Bound protein was eluted with a NaCl gradient and 1 ml fractions collected in test tubes kept on ice and containing 0.2 mg bovine serum albumin to protect enzyme activity. Routinely, samples were analysed within 3–4 h after homogenization. For long term storage, the fractions were kept at − 70°C. Three different phosphodiesterase separations were performed.

Cyclic nucleotide phosphodiesterase assay

Phosphodiesterase activity was measured at 37°C as described in detail by Shahid *et al.* (1991b). All assays were performed at 1 μmol l^{-1} substrate concentration and inhibitors were tested with cyclic AMP as substrate except for PDE V where cyclic GMP was used. Drug solutions were prepared as described previously (Shahid *et al.*, 1991b). The drug concentration producing 50% inhibition of phosphodiesterase activity (IC_{50} value) was determined by use of a non-linear regression curve fitting programme. Inhibitors were tested on phosphodiesterase isoenzymes from all three separations.

Bronchial smooth muscle experiments

Human bronchial preparations were prepared as described by van Amsterdam *et al.* (1990). The preparations were mounted (300 mg load) for isotonic recording in 20 ml water jacketed organ baths and equilibrated for 30 min in Krebs-Henseleit solution (37°C) containing (mmol l^{-1}): NaCl 118, KCl 5.6, $MgSO_4$ 1.18, $CaCl_2$ 2.5, NaH_2PO_4 1.29, $NaHCO_3$ 25, and glucose 5.5 aerated with 95% O_2 and 5% CO_2 (pH 7.4). After equilibration, (−)-isoprenaline (0.1 μmol l^{-1}) was applied to establish basal tone. The tissue was washed immediately for 30 min and contracted by cumulative administration of methacholine 10 and 90 μmol l^{-1} followed by 60 min of repeated washings. Subsequently, contraction was induced with either histamine (1 μmol l^{-1}) or methacholine (1 μmol l^{-1}); 15 min later, cumulative relaxation curves were constructed with a phosphodiesterase inhibitor. After completion of the curve (−)-isoprenaline (10 μmol l^{-1}) was added to reestablish basal tone. Only one phosphodiesterase inhibitor was tested on each preparation. Contraction of bronchial muscle was expressed as a % of the first response to 0.1 mmol l^{-1} methacholine. The pD_2 (− log EC_{50}) values of all phosphodiesterase inhibitors were determined from the concentration-relaxation curves according to van Rossum (1963). Maximal relaxation (E_{max}) was expressed as percentage of the full relaxation induced by 10 μmol l^{-1} (−)-isoprenaline given at the end of the experiment.

Chemicals

The following substances were used: 3-isobutyl-1-methyl xanthine (IBMX), calmodulin (Sigma, Poole, Dorset), RO-20-1724 (Gibco BRL, Paisley, Scotland, rolipram (a gift from Schering, Berlin, Germany), Org 30029 (N-hydroxy-5,6-dimethoxy-benzo[b]thiophene-2-carboximidamide HCl) and Org 9935 (4,5-dihydro-6-(5,6-dimethyoxybenzo[b]thien-2-yl-5-methyl-3(2H)pyridazinone) (Chemistry Department, Organon Laboratories Ltd., Newhouse, Lanarkshire), [^{3}H]-cyclic AMP, [^{3}H]-cyclic GMP (Amersham International, Bucks) and Mono Q (Pharmacia, Milton Keynes). All other chemicals were obtained either from Sigma Chemical Co. or BDH Chemicals (both of Poole, Dorset) and of Analar or equivalent grade. Water purified on a Milli-Q (Millipore, Herts.) system was used throughout.

Data analysis

All values are presented as mean ± s.e.mean.

Results

Separation of cyclic nucleotide phosphodiesterase isoenzymes

The cyclic AMP hydrolytic activity in the soluble extract was 4–5 fold greater than that of the cyclic GMP activity. Neither Ca^{2+}/calmodulin nor cyclic GMP significantly affected the cyclic AMP activity of the soluble fraction. Separation of phosphodiesterase isoenzymes revealed an elution profile with, at least, six distinct peaks of activity represented by fractions 12, 24, 29, 34, 45, and 62 (Figure 1). The majority of the cyclic nucleotide hydrolytic activity in the peaks corresponded to phosphodiesterase isoenzymes V, I, I, II, IV and IV, respectively, according to the nomenclature proposed by Beavo & Reifsnyder (1990). In agreement with the phosphodiesterase activity of the soluble extract, the total cyclic AMP activity in the fractions collected from the Mono Q column was much greater than the cyclic GMP hydrolytic activity. Approximately, 80–90% of the activity applied to the ion-exchange column was recovered.

Figure 1 shows the elution profile for phosphodiesterase activity in the cytosolic fraction of human bronchial smooth muscle. Cyclic GMP phosphodiesterase activity determined the position of PDE V which eluted first, fraction 12 (0.13 mol l^{-1} NaCl) represented the peak of activity (Figure 1a). This peak showed higher activity for cyclic GMP than for cyclic AMP, was not activated by Ca^{2+}/calmodulin (Figure 1b), but was potently inhibited by zaprinast (Table 1). The effects of the regulators Ca^{2+}/calmodulin and cyclic GMP on cyclic AMP hydrolysis were examined in an attempt to identify other phosphodiesterase isoenzyme activities. Ca^{2+}/calmodulin stimulated cyclic AMP hydrolysis in fraction 18 to 30 with hydrolytic activity peaks at fractions 24 (0.21 mol l^{-1} NaCl) and 29 (0.24 mol l^{-1} NaCl) (Figure 1b). The two Ca^{2+}/calmodulin stimulated peaks (PDE I) showed differential sensitivity to zaprinast (Table 1). In contrast, the phosphodiesterase activity peaks corresponding to fractions 34, 45 and 62 were not affected by Ca^{2+}/calmodulin. The cyclic AMP hydrolytic activity of the fourth peak, fraction 34 (0.28 mol l^{-1} NaCl) was stimulated 3 fold by 1 μmol l^{-1} cyclic GMP (Figure 1c), suggesting that it contains PDE II. The last two peaks of activity, fractions 45 (0.35 mol l^{-1} NaCl) and 62 (0.65 mol l^{-1} NaCl), eluting at high salt concentration, were not markedly inhibited by cyclic GMP (Figure 1c), suggesting these peaks contain mainly PDE IV. The fifth peak was the largest activity peak and represented 51 ± 4% of the total cyclic AMP hydrolytic activity. A distinct cyclic

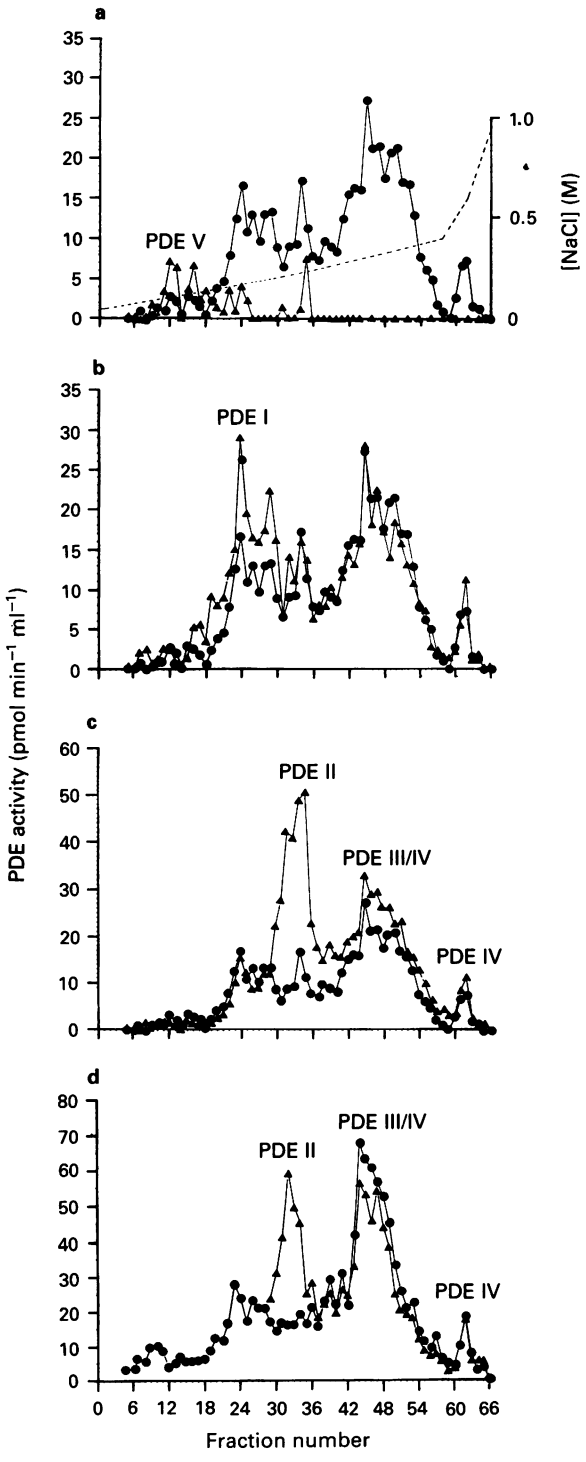

Figure 1 FPLC elution profiles, showing cyclic nucleotide phosphodiesterase activies in human bronchial smooth muscle.The results show the cyclic AMP (●; 1 μmol l^{-1}) and cyclic GMP (▲; 1 μmol l^{-1}) hydrolytic activity of fractions eluted using a NaCl gradient in the absence of any regulator (a) and cyclic AMP hydrolytic activities in the absence (●) presence (▲) of Ca^{2+}/calmodulin (b) and cyclic GMP (c) and (d). The results shown in (c) and (d) were obtained from two different FPLC elutions.

GMP-inhibited phosphodiesterase (PDE III) was not obtained. However, in one separation a small (15–20%) but constant level of inhibition of peak five was observed in the presence of cyclic GMP (Figure 1d). This suggested that PDE III, may be co-eluting with PDE IV in amounts which varied between separations. This suggestion was supported by further experiments using a potent and selective PDE III inhibitor, Org 9935 (Nicholson & Shahid, 1992). Org 9935 produced a biphasic inhibition, with a clear plateau at 0.1 to 3 μmol l^{-1}, of peak five cyclic AMP hydrolytic activity in the separation in which cyclic GMP inhibited hydrolytic activity (Figure 2). As Org 9935 has little ability to inhibit PDE IV at concentrations below 1 μmol l^{-1} (Shahid *et al.*, 1991b), these data suggest the joint presence of both PDE IV and III activities in peak five. At concentrations below 100 μmol l^{-1}, rolipram did not completely inhibit all enzyme activity in those fractions in which Org 9935 displayed significant effects at low concentrations, further indicating the presence of PDE III activity (Figure 2). Kinetic evaluation of human bronchial smooth muscle phosphodiesterase isoenzymes was not possible due to low levels of enzyme activity.

Effects of phosphodiesterase inhibitors on phosphodiesterase isoenzyme activity

The effects of phosphodiesterase isoenzyme inhibitors on human bronchial phosphodiesterase isoenzyme are summarized in Table 1. IBMX was non-selective and inhibited almost equally all phosphodiesterase isoenzymes. Zaprinast selectively inhibited PDE V. This compound also showed differential inhibitory effects on the two PDE I isoforms present in activity peaks two and three, being seventeen times more potent against peak two than peak three. However, the IC_{50} value for peak two was still ten times greater than that for peak one (PDE V). Rolipram, RO-20-1724 and Org 30029 were all potent inhibitors of peak five with rolipram being the most potent. In a few experiments, RO-20-1724 was also tested on peak six; the compound had a slightly higher potency with an IC_{50} value of 7.4 μmol l^{-1}. Org 9935 inhibited peak one and peak five. As discussed above, the effects on the latter activity peak were biphasic in one of the three separations performed (Figure 2).

Relaxation of bronchial smooth muscle

The concentrations of histamine and methacholine employed produced 78.2 ± 6.0% ($n = 11$) and 68.6 ± 4.9% ($n = 11$), respectively, of the maximum response produced by methacholine (0.1 mmol l^{-1}). All phosphodiesterase inhibitors tested produced concentration-dependent relaxation of histamine or methacholine precontracted bronchial segments (Figures 3 and 4); the $-\log EC_{50}$ values are summarized in Table 2. IBMX, zaprinast and Org 9935 were more effective against histamine than methacholine wherease Org 30029 and rolipram equally relaxed contractions produced by these spasmogens. Rolipram and Org 9935 were most potent in causing relaxation. However, both of these drugs produced biphasic concentration-response curves (Figure 3). At concentrations below 1 μmol l^{-1}, Org 9935 invariably partially attenuated histamine-induced, but not always methacholine-induced, contractions. The concentration-response curves for IBMX, zaprinast and Org 30029 were essentially monophasic (Figure 4).

Discussion

The present study has demonstrated that the soluble fraction of human bronchial tissue contains PDE I, II, III, IV, and V isoenzyme activities; this is similar to the results reported for human trachea in a preliminary communication by Cieslinski *et al.* (1988). Bergstrand & Lindquist (1978) have previously examined phosphodiesterase subtypes in human bronchi and shown the presence of four phosphodiesterase activities. However, they did not characterize the regulatory properties of the isoenzymes. Studies on animal airways preparations have also shown the presence of representatives of all five phosphodiesterase isoenzyme families (Shahid *et al.*, 1991b; Torphy & Cieslinski, 1990). However, there are significant species-dependent differences in the exact elution profile and

Table 1 Inhibition of human bronchial smooth muscle cyclic nucleotide phosphodiesterase (PDE) isoenzymes

		$-\log IC_{50}$						
Activity peak	*PDE isoenzyme*	*IBMX*	*Zaprinast*	*Rolipram*	*RO-20-1724*		*Org 9935*	*Org 30029*
1	V	4.72 ± 0.04	6.37 ± 0.08	<3.60	<3.60		4.91 ± 0.03	<3.60
2	I	4.38 ($n = 1$)	5.44 ($n = 2$)	ND	ND		ND	ND
3	I	4.54 ± 0.08	4.16 ± 0.21	ND	ND		ND	ND
4	II	4.64 ± 0.17	3.97 ± 0.06	<3.60 ($n = 2$)	<3.6 ($n = 1$)		<3.60 ($n = 2$)	<3.60 ($n = 1$)
5	III/IV	4.77 ± 0.09	4.17 ± 0.09	5.47 ± 0.07	4.73 ± 0.09	1st phase 2nd phase	7.7 ± 0.1* 4.2 ± 0.2*	4.78 ± 0.08

Values are mean ± s.e.mean
ND - Not determined.
*Data presented for Org 9935 are for the biphasic inhibition curves observed in one separation, values for all other compounds are averaged values for all separations.
All values $n \geq 3$ except when indicated.
IBMX: 3-isobutyl-1-methylxanthine.

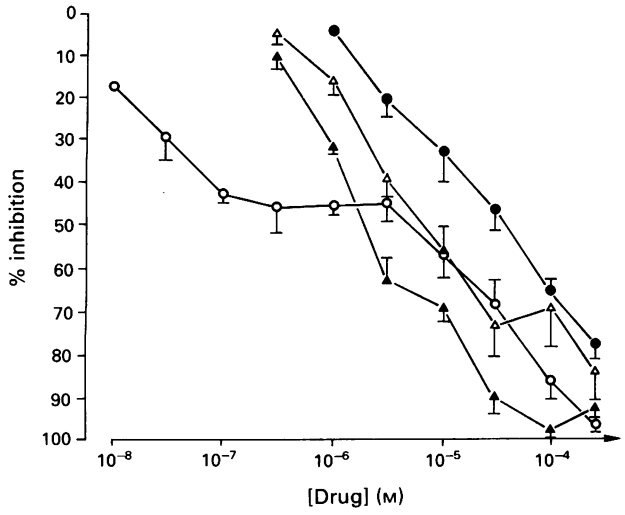

Figure 2 The inhibition of human bronchial smooth muscle peak 5, cyclic AMP hydrolytic activity by Org 9935 (○) and rolipram (△). Open symbols indicate inhibition of peak enzymatic activity from a separation in which cyclic GMP inhibited cyclic AMP hydrolysis; closed symbols indicate pooled data from two further separations in which no cyclic GMP-induced inhibition was observed (see text for details).

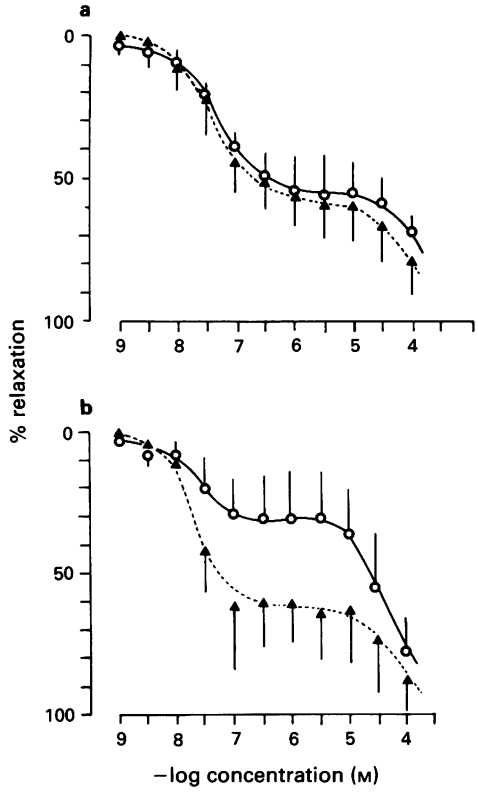

Figure 3 Relaxation of histamine (▲; 1 μmol l^{-1})and methacholine (○; 1 μmol l^{-1}) contracted human bronchial smooth muscle by rolipram (a) and Org 9935 (b).

relative activity levels of different phosphodiesterase isoenzymes.

In contrast to the present study and to human tracheal data (Cieslinski *et al.*, 1988), only one form of PDE I has been detected in canine (Torphy & Cieslinski, 1990) and bovine (Shahid *et al.*, 1991b) tracheal preparations. Human bronchial (the present study) and tracheal (Cieslinski *et al.*, 1988) PDE I isoforms show differential sensitivity to zaprinast, suggesting that they represent distinct PDE I subtypes. Multiple forms of PDE I have been detected in other tissues such as testes (Purvis & Hallgier, 1988), brain (Sharma & Wang, 1986) and cardiac muscle (Shahid *et al.*, 1991a). At least four distinct, but related, genes coding for the PDE I isoenzyme family have been described (Beavo & Reifsnyder, 1990). Human bronchial PDE V eluted well before PDE I; this is different from the elution profile in canine (Torphy & Cieslinski, 1990) and bovine (Shahid *et al.*, 1991b) tracheal smooth muscle where PDE I and PDE V co-elute during ion-exchange chromatography. Furthermore, the relative activity levels of PDE I and PDE V were less than those of PDE IV in the present study, whereas in canine (Torphy & Cieslinski, 1990) and bovine (Shahid *et al.*, 1991b) trachea both PDE I and PDE V activities are much higher than PDE IV.

The main cyclic AMP hydrolytic activity, peak five, contained mainly PDE IV. However, using a highly potent and selective PDE III inhibitor, Org 9935 (Shahid *et al.*, 1991b) a significant presence of PDE III was detected. Co-elution of PDE III, and PDE IV activities has previously been observed in guinea-pig (Harris *et al.*, 1989), canine (Torphy & Cieslinski, 1990) and bovine (Shahid *et al.*, 1991b) trachea. This is despite the fact that the separation techniques used in the present study successfully separate PDE III and PDE IV activities in other tissues such as cardiac muscle (Shahid & Nicholson, 1990). The ratio of PDE III/PDE IV activity level in airways tissue varies between species. As judged by the relative activity of isoenzyme, selective inhibitors the PDE III/IV activity ratio decreases in the order of guinea-pig ≥ man > dog > cow. A second relatively minor, PDE IV activity (peak six) was also insensitive to cyclic GMP and was inhibited by RO-20-1724. Multiple PDE IV activities

Table 2 Relaxation of human bronchial smooth muscle by cyclic nucleotide phosphodiesterase inhibitors in the presence of methacholine (1 μmol l^{-1}) or histamine (1 μmol l^{-1})

		Histamine			*Methacholine*		
		pD_2		E_{max}	pD_2		E_{max}
IBMX		5.58 ± 0.27	(3)	100	5.14 ± 0.13	(3)	> 98.9 ± 1.1
Rolipram	1st phase	7.14 ± 0.17	(3)	60.1 ± 12.2	7.48 ± 0.21	(3)	56.2 ± 13.5
	2nd phase	ca 4		> 79.3 ± 11.6	< 4		> 68.7 ± 5.0
Zaprinast		5.12 ± 0.26	(3)	> 84.0 ± 7.5	4.33 ± 0.36	(3)	> 54.1 ± 11.2
Org 9935	1st phase	7.47 ± 0.19	(3)	60.6 ± 15.6	7.49 ± 0.10	(3)	30.2 ± 17.5
	2nd phase	4.61 ± 0.35	(3)	> 88.1 ± 9.8	4.49 ± 0.26	(3)	> 77.9 ± 12.6
Org 30029		5.18 ± 0.54	(3)	> 84.0 ± 7.3	5.41 ± 7.3	(3)	> 84.0 ± 7.1

pD_2: $-\log EC_{50}$ ± s.e.mean from 3 experiments.
E_{max}: % maximal relaxation.
IBMX: 3-isobutyl-1-methylxanthine.

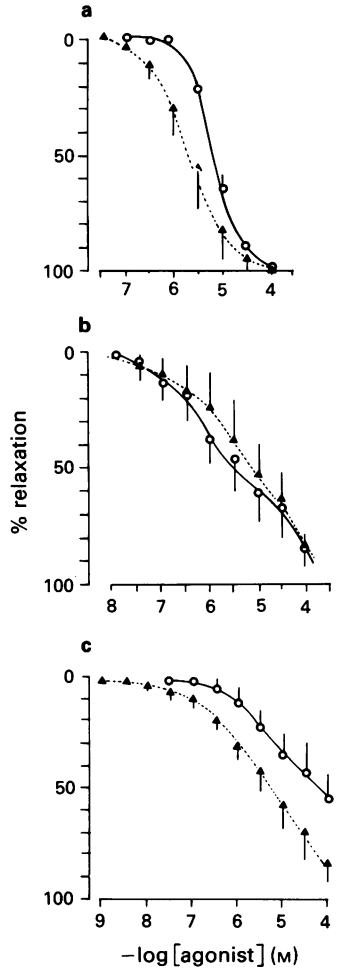

Figure 4 Concentration-relaxation curves of human bronchial smooth muscle contracted with histamine (▲; 1 μmol l^{-1}) and methacholine (○; 1 μmol l^{-1}) by the cyclic nucleotide phosphodiesterase inhibitors isobutyl-methylxanthine (a), Org 30029 (b) and zaprinast (c).

have been reported in airways preparation (Shahid *et al.*, 1991b), and other tissues such as liver (Lavan *et al.*, 1989) and skeletal muscle (Nicholson & Wilke, unpublished data). In liver, the two forms of PDE IV showed differential sensitivity to rolipram and RO-20-1724; one form being inhibited 5–9 fold more potently. A similar result was obtained with RO-20-1724 for peak six in the present study. Recent studies indicate that there may be four gene subfamilies for the PDE IV isoenzyme family (Beavo & Reifsnyder, 1990). As in previous studies using animal airways tissue, the preparation used for phosphodiesterase isoenzyme profiling in the present study does not consist solely of smooth muscle (Bloom & Fawcett, 1968; Bosken *et al.*, 1990). Therefore, the relative amounts of differing isoenzymes in bronchial preparations may not precisely reflect their proportional activities in bronchial smooth muscle. Comparison of isoenzyme activities in preparations of cardiac tissue with those in cardiac myocytes has revealed differences in the relative activity levels in rats (Bode *et al.*, 1991), whilst in guinea-pigs both preparations have similar isoenzyme profiles (Bethke *et al.*, 1991). A further study in human airways smooth muscle cells is required to analyze the phosphodiesterase isoenzyme activities. However, the combination of the elucidation of the isoenzyme profile in human bronchi with the examination of the functional activity of isoenzyme selective inhibitors enables an estimation of the importance of individual isoenzymes for the control of smooth muscle function.

Although all phosphodiesterase inhibitors tested relaxed precontracted bronchi, there were marked differences in their potency and their ability to relax depended on the spasmogen used. Rolipram and Org 9935 were the most potent compounds tested and were active over concentrations maintaining selectivity for inhibition of PDE IV and PDE III isoenzymes, respectively (Reeves *et al.*, 1987; Shahid *et al.*, 1991b). This suggests that in human airway smooth muscle, both PDE III and PDE IV are important in regulating intracellular cyclic AMP and thus for modulation of function. The ability of Org 9935 to relax all the histamine contracted preparations indicates that PDE III is indeed present in human airways smooth muscle; why PDE III was not invariably demonstrated in the separation experiments requires further study. This may be due to the localization of a significant PDE III activity in a particular subcellular compartment or, alternatively, the heterogeneous nature of the tissue preparation used may have partially obscured the detection of PDE III. The ability of both PDE III and PDE IV inhibitors to relax the human airways preparation is more similar to data reported for guinea-pig (Harris *et al.*, 1989) and canine (Torphy & Cieslinski, 1990) than for bovine (Shahid *et al.*, 1991b) trachea. In the present study, both rolipram and Org 9935 produced biphasic concentration-relaxation curves, indicating that selective PDE IV and PDE III inhibition alone is insufficient to relax fully bronchial smooth muscle. However, the ability of phosphodiesterase inhibitors, like β-adrenoceptor agonists, to relax airways preparations is dependent upon the concentration of agonist employed (Torphy *et al.*, 1988). Hence, selective inhibitors may be more effective if a lower concentration of spasmogen were employed. At high concentrations (> 10 μM), both Org 9935 and rolipram lose phosphodiesterase selectivity and also inhibit other isoenzymes (Shahid *et al.*, 1991b). This loss of selectivity may explain the more complete relaxation of airways preparations observed at high concentrations. Alternatively, the biphasic nature of Org 9935 and rolipram relaxation curves could be due to the involvement of mechanisms

other than phosphodiesterase inhibition. A binding site at which rolipram has a higher affinity than the K_i for PDE IV has been reported (Schneider *et al.*, 1986). The nature of this binding site is unknown and until it is clarified, caution should be exercised in assigning all the pharmacological activity of rolipram to phosphodiesterase inhibition. The IBMX and Org 30029 concentration-relaxation curves were monophasic, this is likely to be due to the fact that these compounds are not isoenzyme selective inhibitors. Org 30029 is an equipotent inhibitor of PDE III and PDE IV (Shahid & Nicholson, 1990). Dual inhibition of PDE III and PDE IV seems a more effective mechanism for relaxation of human bronchial smooth muscle than selective inhibition of either enzyme. Zaprinast was not an effective relaxant at concentrations showing selective inhibition of PDE V and PDE I, suggesting that these isoenzymes are relatively less important in the regulation of smooth muscle tone in this preparation.

It has been shown in a number of studies that phosphodiesterase inhibitors are more effective at relaxing histamine-induced contractions than muscarinic agonist-induced contractions (Torphy *et al.*, 1988; Harris *et al.*, 1989; Hall *et al.*, 1990; Shahid *et al.*, 1991). In agreement, the present study showed zaprinast, IBMX and Org 9935 to be less active at relaxing methacholine contractions, although in the case of Org 9935 only the maximum relaxation (first phase; Figure 3) was reduced with no change in the EC_{50} value. Whilst the mechanism(s) underlying the differential sensitivity to phosphodiesterase inhibitors against histamine or methacholine-induced spasms are not clear it may be related to differences in the ability of these agonists to stimulate phosphatidyl inositol metabolism (Hall & Hill, 1988; Madison & Brown, 1988; van Amsterdam *et al.*, 1989; 1990; Hall *et al.*, 1989; 1990). In human bronchial smooth muscle, the maximal increase in inositol phosphate production is smaller after challenge with histamine than after methacholine (van Amsterdam *et al.*, 1990). In contrast to the other compounds used in this study, Org 30029 and rolipram, did not show spasmogen-dependency in the functional experiments. It is conceivable that these compounds possess properties additional to phosphodiesterase inhibition, alternatively PDE IV inhibition may equally attenuate smooth muscle tone generated by muscarinic or histamine receptor agonists in this preparation. Further experiments in intact preparations are required to confirm that the phosphodiesterase inhibitors tested act by increasing cellular cyclic AMP in human bronchial smooth muscle. This is important since a recent communication by Hall *et al.* (1992) has shown that in primary cultures of human tracheal smooth muscle, IBMX and rolipram increased cellular cyclic AMP whilst the PDE III inhibitor SKF 94120 had no effect. In animal tissues, increases in cyclic AMP produced by PDE IV (Hall *et al.*, 1989) and PDE III (Torphy *et al.*, 1988) inhibitors as well as activation of cyclic AMP-dependent protein kinase (Torphy *et al.*, 1988) are observed at concentrations producing tracheal relaxation.

In conclusion, the present study has shown human bronchi to contain representatives of all five presently identifiable phosphodiesterase isoenzyme families. Multiple isoforms of PDE I and PDE IV were observed and PDE IV was the main cyclic AMP hydrolytic activity. Based on inhibitor experiments, significant PDE III activity was identified the level of which was similar to that in guinea-pig airway smooth muscle. Both PDE III and PDE IV selective and dual PDE III/IV (Org 30029) inhibitors were effective relaxants of human bronchial smooth muscle, whereas the PDE V inhibitor, zaprinast was relatively ineffective. The present study confirms data, from experiments using animal tissue, that inhibitors of PDE III, PDE IV and PDE III/IV have potentially useful bronchodilator activity. Experiments with human inflammatory cells (Nielson *et al.*, 1990; Robicsek *et al.*, 1991; Torphy & Undem, 1991) indicate that PDE IV and PDE III/IV inhibitors possess greatest potential as anti-inflammatory agents. Consequently, inhibitors of PDE IV isoenzymes and possibly dual PDE III/IV inhibitors are worthy of further consideration as anti-asthma drugs.

The authors express their appreciation to the Staff of the Pulmonology, Pathology and Surgery Departments of the University Hospital and the Martini Hospital, Groningen and also to the Staff of the Department of Cardiothoracic Surgery, Royal Infirmary, Glasgow for the supply of human lung tissue and thank Ms Karen Cochrane for her secretarial assistance.

References

BEAVO, J.A. & REIFSNYDER, D.H.L. (1990). Primary sequence of cyclic nucleotide phosphodiesterase isoenzymes and the design of selective inhibitors. *Trends Pharmacol. Sci.*, **11**, 150–155.

BERGSTRAND, H. & LINDQUIST, B. (1978). Partial purification of cyclic nucleotide phosphodiesterases from human bronchial tissue. *Mol. Cell. Biochem.*, **21**, 9–15.

BETHKE, TH., SCHMITZ, W., SCHOLZ, H., STEIN, B., THOMAS, K. & WENZLAFF, H. (1991). Phosphodiesterase inhibition in isolated ventricular myocytes and multicellular ventricular preparations from guinea-pig hearts. *Naunyn-Schmiedebergs Arch. Pharmacol.*, **344**, R81.

BLOOM, W. & FAWCETT, D.W. (1968). Respiratory System. In *A Textbook of Histology*. London: W.B. Saunders Co.

BODE, D.C., KANTER, J.R. & BRUNTON, L.L. (1991). Cellular distribution of phosphodiesterase isoforms in rat cardiac tissue. *Circ.Res.*, **68**, 1070–1079.

BOSKEN, C.H., WIGGS, B.R., PARE, P.D. & HOGG, J.C. (1990). Small airway dimensions in smokers with obstruction to airflow. *Am. Rev. Respir. Dis.*, **142**, 563–570.

CIESLINSKI, L.B., REEVES, M.K. & TORPHY, T.J. (1988). Cyclic nucleotide phosphodiesterases (PDEs) in canine and human tracheal smooth muscle (TSM). *FASEB*, **2**, 474.

DENT, G., GIEMBYCZ, M.A., RABE, K.F. & BARNES, P.J. (1991). Inhibition of eosinophil cyclic nucleotide PDE activity and opsonised zymosan-stimulated respiratory burst by 'type IV'-selective PDE inhibitors. *Br. J. Pharmacol.*, **103**, 1339–1346.

HALL, I.P., DONALDSON, J. & HILL, S.J. (1989). Inhibition of histamine-stimulated inositol phospholipid hydrolysis by agents which increase cyclic AMP levels in bovine tracheal smooth muscle. *Br. J. Pharmacol.*, **97**, 603–616.

HALL, I.P., DONALDSON, J. & HILL, S.J. (1990). Modulation of carbachol-induced inositol phosphate formation in bovine tracheal smooth muscle by cyclic AMP phosphodiesterase inhibitors. *Biochem. Pharmacol.*, **39**, 1357–1363.

HALL, I.P. & HILL, S.J. (1988).β-αdrenoceptor stimulation inhibits histamine-stimulated inositol phospholipid hydrolysis in bovine tracheal smooth muscle. *Br. J. Pharmacol.*, **95**, 1204–1212.

HALL, I.P., TOWNSEND, P., DAYKIN, K. & WIDDOP, S. (1992). Control of cyclic AMP content in primary cultures of human airway smooth muscle cells. *Br. J. Pharmacol.*, **105**, 71P.

HARRIS, A.L., CONNELL, M.J., FERGUSON, E.W., WALLACE, A.M., GORDON, R.J., PAGANI, E.D. & SILVER, P.J. (1989). Role of low K_m cyclic AMP phosphodiesterase inhibition in tracheal relaxation and bronchodilation in the guinea pig. *J. Pharmacol. Exp. Ther.*, **251**, 199–206.

LAVAN, B.E., LAKEY, T. & HOUSLAY, M.D. (1989). Resolution of soluble cyclic nucleotide phosphodiesterase isoenzymes, from liver and hepatocyted, identifies a move IBMX-insensitive form. *Biochem. Pharmacol.*, **38**, 4123–4136.

MADISON, J.M. & BROWN, J.K. (1988). Differential inhibitory effects of forskolin, isoproterenol, and dibutyryl cyclic adenosine monophosphate on phosphoinositide hydrolysis in canine tracheal smooth muscle. *J. Clin. Invest.*, **82**, 1462–1465.

NICHOLSON, C.D., CHALLISS, R.A.J. & SHAHID, M. (1991). Differential modulation of tissue function and therapeutic potential of selective inhibitors of cyclic nucleotide phosphodiesterase isoenzymes. *Trends Pharmacol. Sci.*, **12**, 19–27.

NICHOLSON, C.D. & SHAHID, M. (1992). Cyclic nucleotide phosphodiesterase isoenzymes — the potential of selective inhibitors as drugs for asthma. In *New Drugs for Asthma*, Vol. II, ed. Barnes, P.J. London: IBC Press, (in press).

NIELSON, C.P., VESTAL, R.E., STURM, R.J. & HEASLIP, R. (1990). Effects of selective phosphodiesterase inhibitors on the polymorphonuclear leukocyte respiratory burst. *J. Allergy Clin. Immunol.*, **86,** 801–808.

PURVIS, K. & HALLGIER, R. (1988). High-affinity, calmodulin-dependent isoforms of cyclic nucleotide phosphodiesterase in rat testes. In *Methods in Enzymology*, Vol. 159, ed. Corbin, J.D. & Johnson, R.A. pp. 675–684. London: Academic Press.

REEVES, M.L., LEIGH, B.K. & ENGLAND, P.J. (1987). The identification of a new cyclic nucleotide phosphodiesterase activity in human and guinea-pig cardiac ventricle. *Biochem. J.*, **241,** 535–541.

ROBICSEK, S.A, BLANCHARD, D.K., DJEU, J.Y., KRZANOWSKI, J.J., SZENTIVANYI, A. & POLSON, J.B. (1991). Multiple high-affinity cyclic AMP-phosphodiesterase in human T-lymphocytes. *Biochem. Pharmacol.*, **42,** 869–877.

SCHNEIDER, H.H., SCHMIECHEN, R., BREZINSKI, M. & SEIDLER, R. (1986). Stereospecific binding of the antidepressant rolipram to brain protein structures. *Eur. J. Pharmacol.*, **127,** 105–115.

SHAHID, M., BILLINGTON, C. & NICHOLSON, C.D. (1991a). Evidence for two distinct Ca/calmodulin stimulated cyclic nucleotide phosphodiesterases (PDEs) in rabbit cardiac ventricle. *Br. J. Pharmacol.*, **102,** 30P.

SHAHID, M. & NICHOLSON, C.D. (1990). Comparison of cyclic nucleotide phosphodiesterase isoenzymes in rat and rabbit ventricular myocardium: positive inotropic and phosphodiesterase inhibitory effects of Org 30029, milrinone and rolipram. *Naunyn-Schmiedebergs Arch. Pharmacol.*, **342,** 698–705.

SHAHID, M., PHILPOTT, A.J., DE BOER, J., ZAAGSMA, J. & NICHOLSON, C.D. (1992). Cyclic nucleotide phosphodiesterase (PDE) isoenzyme activities in human peripheral bronchi. *Br. J. Pharmacol.*, **105,** 129P.

SHAHID, M., VAN AMSTERDAM, R.G.M., DE BOER, J., TEN BERGE, R.E., NICHOLSON, C.D. & ZAAGSMA, J. (1991b). The presence of five cyclic nucleotide phosphodiesterase isoenzyme activities in bovine tracheal smooth muscle and the functional effects of selective inhibitors. *Br. J. Pharmacol.*, **104,** 471–477.

SHARMA, R.K. & WANG, J.H. (1986). Regulation of cyclic AMP concentration by calmodulin-dependent cyclic nucleotide phosphodiesterase. *Biochem. Cell. Biol.*, **64,** 1072–1080.

SOUNESS, J.E., CARTER, C.M., DIOCEE, B.K., HASSALL, G.A., WOOD, L.J. & TURNER, N.C. (1991). Characterization of guinea-pig eosinophil phosphodiesterase activity. *Biochem. Pharmacol.*, **42,** 937–945.

TORPHY, T.J. (1988). Action of mediators on airway smooth muscle: functional antagonism as a mechanism for bronchodilator drugs. In *New Anti-asthma Drug* ed. O'Donnell, S.R. & Persson, C.G.A. pp. 37–53. Basel: Birkhauser.

TORPHY, T.J., BURMAN, M., HUANG, L.B.F. & TUCKER, S.L. (1988). Inhibition of the low K_m cyclic AMP phosphodiesterase in intact canine trachealis by SKF 94836: mechanical and biochemical responses. *J. Pharmacol. Exp. Ther.*, **246,** 843–850.

TORPHY, T.J. & CIESLINSKI, L.B. (1990). Characterisation and selective inhibition of cyclic nucleotide phosphodiesterase isoenzymes in canine tracheal smooth muscle. *Mol. Pharmacol.*, **37,** 206–214.

TORPHY, T.J. & UNDEM, B.J. (1991). Phosphodiesterase inhibitors: new opportunities for the treatment of asthma. *Thorax*, **46,** 512–523.

VAN AMSTERDAM, R.G.M., MEURS, H., BROUWER, F., POSTEMA, J.B., TIMMERMANS, A. & ZAAGSMA, J. (1989). Role of phosphoinositide metabolism in functional antagonism of airway smooth muscle contraction by β-adrenoceptor agonists. *Eur. J. Pharmacol.*, **172,** 175–183.

VAN AMSTERDAM, R.G.M., MEURS, M., TEN BERGE, R.E.J., VENINGA, C.C.M., BROUWER, F. & ZAAGSMA, J. (1990). Role of phosphoinositide metabolism in human bronchial smooth muscle contraction and in functional antagonism by β-adrenoceptor agonists. *Am. Rev. Respir. Dis.*, **142,** 1124–1128.

VAN ROSSUM, J.M. (1963). Cumulative dose-response curves in isolated organs and the evaluation of drug parameters. *Arch. Int. Pharmacodyn. Ther.*, **143,** 299–329.

(Received February 24, 1992
Revised April 15, 1992
Accepted April 23, 1992)

Br. J. Pharmacol. (1992), **106**, 1035–1040 © Macmillan Press Ltd, 1992

Altered microvascular reactivity to endothelin-1, endothelin-3 and N^G-nitro-L-arginine methyl ester in streptozotocin-induced diabetes mellitus

Elizabeth Lawrence & [1] Susan D. Brain

Pharmacology Group, Biomedical Sciences Division, King's College, Manresa Road, London SW3 6LX

1 We have determined the dermal microvascular effects of the nitric oxide (NO) synthase inhibitor, N^G-nitro-L-arginine methyl ester (L-NAME, 100 nmol/site), endothelin-1 (ET-1, 0.1–10 pmol/site) and ET-3 (0.1–30 pmol/site) in rats with streptozotocin (STZ)-induced diabetes mellitus. Cutaneous blood flow changes as measured by a ^{133}xenon (^{133}Xe) clearance technique, were determined in diabetic rats four weeks after treatment with streptozotocin (STZ) and compared with responses measured in normal rats four weeks after treatment with saline.

2 Resting skin blood flow was similar in diabetic and in normal rats, as measured by ^{133}Xe clearance and laser Doppler flowmetry.

3 Intradermal N^G-nitro-L-arginine methyl ester (L-NAME) reduced skin blood flow in normal rats by $55.2 \pm 2.6\%$ as measured by ^{133}Xe clearance, ($n = 9$). L-NAME was significantly less effective in diabetic rats, inducing a $40.9 \pm 7.7\%$ decrease in blood flow ($n = 9$, $P < 0.05$). The enantiomer D-NAME had no effect in either group of rats.

4 Low doses of ET-1 and ET-3 injected intradermally induced dose-dependent decreases in blood flow, measured by ^{133}Xe clearance, which were similar in both groups of rats. However, the responses to the highest doses of ET-1 (10 pmol/site) and ET-3 (10 and 30 pmol/site) were significantly reduced in the diabetic compared with the normal rats ($P < 0.05$). In addition vasoconstriction to the highest doses of vasopressin (0.3 and 3 pmol/site) and vasodilatation to the neuropeptide calcitonin gene-related peptide (CGRP, 10 pmol/site) were similarly reduced in the diabetic rats ($P < 0.05$).

5 The decrease in blood flow induced by submaximal doses of ET-1 was enhanced by co-injection with L-NAME (100 nmol/site) in both diabetic and normal rats. However, this enhanced response was significantly reduced in the diabetic rats ($P < 0.05$). A similar pattern of responses were observed to ET-3 in the presence and absence of L-NAME.

6 These results indicate that the cutaneous microvasculature of rats with STZ-induced diabetes responds differently to intradermal ET-1 and ET-3 compared with normal rats; a similarly altered vascular reactivity was observed with vasopressin and CGRP. Hence, the diabetic microcirculation has impaired responses to several vasoconstrictors and a vasodilator. The effect of the nitric oxide synthase inhibitor L-NAME is also suppressed in the diabetics, suggesting that there may be decreased local production of, or response, to nitric oxide.

Keywords: Endothelin-1; endothelin-3; N^G-nitro-L-arginine methyl ester; microvascular blood flow; diabetic mellitus

Introduction

The endothelial cell plays a key role in the control of vascular tone. This function is achieved by release of vasoactive agents including endothelium-derived relaxing factor (EDRF, Furchgott & Zawadski, 1980) and also the vasoconstrictor peptide, endothelin-1 (ET-1) (Yanagisawa *et al.*, 1988). EDRF may act as the endogenous functional antagonist of endothelin function and *vice versa*. Intravascular administration of ET-1 and the related peptide ET-3 in particular, has been shown to induce initial vasodilatation in certain microvascular beds *in vivo* (Fortes *et al.*, 1989; Warner *et al.*, 1989; Gardiner *et al.*, 1989) which may be due to the release of EDRF (De Nucci *et al.*, 1988; Warner *et al.*, 1989). Conversely, EDRF inhibits stimulated release of ET-1 from cultured endothelial cells (Boulanger & Luscher, 1990). EDRF has been identified as NO converted from L-arginine (Palmer *et al.*, 1987; 1988; Ignarro *et al.*, 1987). In the present study we are concerned with microvascular blood flow and its control in skin. We have previously shown that intradermal ET-1 is a potent vasoconstrictor of rat skin microvessels *in vivo* (Lawrence & Brain, 1992). In the same study we found that local administration of the selective inhibitor of NO synthesis, N^G-nitro-L-arginine methyl ester (L-NAME) (Moore *et al.*, 1990) constricts microvessels in rat skin (Lawrence & Brain, 1992). This response to L-NAME was reversed by L-arginine and was not observed to D-NAME in our experiments. We concluded that local constitutive NO production is important for maintaining microvascular tone in skin.

Structural, biochemical and functional changes occur in the microcirculation in clinical diabetes mellitus (Porta *et al.*, 1987; Tooke, 1989). In animal models of diabetes, altered microvascular function including impaired gross inflammatory reactions (Garcia-Leme *et al.*, 1973; 1974) and more specifically depressed polymorphonuclear leukocyte chemotactic responses (Pereira *et al.*, 1987; Sannomiya *et al.*, 1990; Fortes *et al.*, 1991) have been observed. In addition the endothelial cells are known to function abnormally in diabetes, this is implicated in the pathogenesis of diabetic microangiopathy (Porta *et al.*, 1987) Microvascular responses to endothelium-dependent vasodilators appear to be altered in diabetic rats (Fortes *et al.*, 1983; Mayhan *et al.*, 1989; Lash & Bohlen, 1991; Kiff *et al.*, 1991a) possibly due to depressed EDRF release. In addition, the decrease in hindquarter blood flow normally observed following systemic

[1] Author for correspondence.

treatment with L-NAME is impaired in diabetic rats (Kiff *et al.*, 1991b), supporting the theory that in diabetes there is diminished production of or sensitivity to NO in specific microvascular regions. In spite of the depressed function of the endothelium in diabetes and the increase in plasma levels of ET-1 observed in both diabetic patients (Takahashi *et al.*, 1990) and rats (Takeda *et al.*, 1990), no change in ET-1 activity in diabetes mellitus has been recorded to date.

We have previously shown that local injections of ET-1 and ET-3 in rat skin induce local vasoconstrictions which are enhanced by co-injection with intradermal L-NAME (Lawrence & Brain, 1992), indicating that locally generated NO functionally antagonizes local vasoconstriction induced by ET-1 and ET-3 in rat skin. Our experiments suggested that a basal release of NO was responsible for these effects. We were interested to extend this study and see whether in a pathological condition such as diabetes mellitus, where endothelial cell damage occurs, the response to L-NAME in the skin would be attenuated, and whether the microvasculature would become more susceptible to vasoconstriction by ET-1 and ET-3. We also investigated whether interactions between L-NAME and the endothelins would still be intact in diabetic rats. This work has been presented in abstract form to the British Pharmacological Society (Lawrence & Brain, 1991).

Methods

Male adult Wistar rats (Bantin & Kingman, Hull, U.K.) weighing between 150 and 180 g were used. Animals had free access to food and water throughout the experimental period. They were housed in a room maintained at a temperature of 20–22°C with lights on from 07 h 00 min to 19 h 00 min.

Induction of experimental diabetes

Experimental diabetes mellitus was induced in rats by a single intraperitoneal injection of streptozotocin (STZ, 70 mg kg^{-1}) dissolved in 1 ml of 0.9% w/v NaCl solution. The age-matched control rats received the same volume of isotonic saline. Experiments were carried out four weeks later. Blood samples were taken at the end of experiments by cardiac puncture, while the rats were under pentobarbitone anaesthesia as described below. Plasma glucose levels were then assayed spectrophotometrically with a quantitative enzymatic (glucose oxidase) commercial blood glucose measuring kit (Sigma).

Blood flow measured by laser Doppler blood flow meter

Basal blood cell flux in uninjected skin microvessels was measured by the use of a dual channel laser Doppler blood flow meter (Moor Instruments, Devon) in both diabetic and age-matched control rats. The technique used was similar to that described previously (Lawrence & Brain, 1992). The rats were anaesthetized by intraperitoneal injection of pentobarbitone sodium (50 mg kg^{-1}), the dorsal skin was shaved and depilated with a widely available commercial depilatory cream (Immac). A pair of sites were marked in equivalent positions on the dorsal skin on both sides of the spine of each rat. Three readings lasting 1 min each were taken at each pair of sites. While the measurements were being made the rats were kept as still as possible on a heating pad at 37°C. The laser Doppler blood flow meter was set at a band width of 14.9 kHz with a time constant of 0.1 s and 0.5 s for flux and concentration respectively. Results were expressed as blood cell flux. The flux value is a measure of the number of red blood cells moving in the path of the laser beam multiplied by the mean cell velocity. This value is used as an index of blood flow. The laser Doppler blood flow meter records blood cell flux in a 1–2 mm^2 area of skin observed by the laser probe.

Blood flow measured by ^{133}xenon clearance

Cutaneous microvascular blood flow was measured at multiple sites in the dorsal skin by a ^{133}Xe clearance technique modified for use in the rat as previously described (Lawrence & Brain, 1992). Rats were anaesthetized by an intraperitoneal injection of pentobarbitone sodium (50 mg kg^{-1}, plus maintenance doses as necessary) and the dorsal skin was shaved. Test agents were dissolved in a modified balanced salt solution (Tyrode). Equal quantities of ^{133}Xe (3.6 MBq) were mixed with each 1 ml sample of test agents or a Tyrode solution control in each experiment. The samples were then given rapidly by intradermal injection (100 µl volumes). Up to nine samples were injected in duplicate in each rat, according to a predetermined balanced site pattern. The site pattern was designed to minimize inter-site variation in basal blood cell flow in a single experiment. Three rats were used in each experiment and the site pattern and order of injection were rotated in the second and third rats. After a 15 min clearance period in each rat, the animals were killed by pentobarbitone overdose. Just prior to overdosing the rat, a sample of blood (250 µl volume) was taken by cardiac puncture for the determination of plasma glucose levels. The dorsal skin encompassing all the skin sites was removed, the injected sites were punched out (16 mm diameter) and counted for radioactivity in an automatic gamma-counter. Results were calculated as percentage change in blood flow at test sites compared with that at control, Tyrode-injected sites according to a calculation detailed in a previous paper (Lawrence & Brain, 1992).

Drugs and chemicals

The following drugs were used: human ET-1 and ET-3, were purchased from Bachem (U.K.) Ltd. (Essex). Human α-calcitonin gene-related peptide (αCGRP) was a gift from Dr U. Ney, Celltech (Bucks). The peptides were all dissolved in water, then diluted in Tyrode solution and stored in aliquots at − 20°C until just before use. Vasopressin, STZ, L-NAME, the enantiomer D-NAME and L-arginine were all purchased from Sigma Chemical Company Ltd. (Dorset). These agents were all made up immediately before use. ^{133}Xenon was obtained from Amersham International (Amersham, Bucks). Pentobarbitone sodium (Sagatal) was purchased from May and Baker Ltd. (Essex). In all the experiments test agents were made up in Tyrode solution of the following composition (mM): NaCl, 137, KCl 2.7, $MgCl_2$ 1.05, NaH_2PO_4 0.4, $NaHCO_3$ 11.9 and glucose 5.6.

Statistical analysis of results

Results are all expressed as mean ± s.e.mean. Significant differences between the plasma glucose levels in the STZ-treated diabetic rats and the saline-treated control rats were assessed by an unpaired Student's t test. The significance of differences between intradermal treatments was assessed by Bonferroni's modified t test, which uses the standard error estimate for the analysis of variance to allow comparison of multiple sites. $P<0.05$ was accepted as statistically significant.

Results

Experimental diabetes

Rats in the test group treated with STZ exhibited polydipsia and polyuria, and four weeks after STZ treatment the plasma glucose levels were significantly higher in the test group: 29.30 ± 0.81 mmol l^{-1}, $n = 29$; compared with the control

group: 6.61 ± 0.04 mmol l^{-1}, $n = 31$; $P < 0.001$. Rats treated with STZ, displaying increased blood glucose levels are termed diabetic, and those rats treated with saline displaying normal blood glucose levels are termed normal.

Resting levels of blood flow

In order to determine whether resting skin blood flow differed between the two groups of rats the following measurements were taken. Blood cell flux in microvessels of uninjected skin was determined with the laser Doppler blood flow meter and was compared in the two groups of rats. The diabetic rats had a blood cell flux value of 80.8 ± 10.4 flux ($n = 6$) which was not significantly different from that observed in the normal rats 89.2 ± 5.7 flux ($n = 6$). Clearance values at control Tyrode-injected sites, estimated as the extent of ^{133}Xe washout over 15 min, were also similar in both groups. Following intradermal injection of Tyrode, ^{133}Xe clearance was $21.0 \pm 1.4\%$ clearance ($n = 23$) in diabetic rat skin and $21.3 \pm 1.2\%$ clearance ($n = 20$) in normal rat skin.

Effect of L-NAME on basal blood flow

L-NAME inhibited cutaneous blood flow in both the normal and diabetic rats. This inhibitory effect was significantly less in the diabetic rats compared with normal rats ($P < 0.05$) as shown in Figure 1. D-NAME, was without effect in either group (Figure 1). We have previously shown that the effects of L-NAME (100 nmol/site) can be reversed by intravenous L-arginine (600 μmol kg^{-1}) suggesting that L-NAME is a selective inhibitor of local NO production in rat skin (Lawrence & Brain, 1992).

Effect of vasoactive substances on blood flow in normal and diabetic rats

ET-1 (0.1–10 pmol/site) induced a dose-dependent decrease in microvascular blood flow in both the normal and diabetic rats, as shown in Figure 2a. At the lower doses used there was no significant difference between cutaneous response obtained in the two groups of rats, however the vasoconstriction induced by the highest dose of ET-1 was significantly diminished in diabetics ($P < 0.05$) compared with the response in normal rats (Figure 2a). Similarly the response to ET-3 was reduced at the higher doses in diabetic rat skin ($P < 0.05$) as shown in Figure 2b. This reduced vascular responsiveness of diabetic rat skin was not a peculiarity of the endothelin isopeptides since it was also observed with the unrelated vasoconstrictor, vasopressin (Figure 2c). The potent vasodilator neuropeptide, CGRP, induced dose-dependent vasodilatation in normal rat skin: CGRP (0.1 pmol/site) $5.6 \pm 4.9\%$ increase in blood flow ($n = 5$ rats); CGRP (1 pmol/site) $23.6 \pm 14.9\%$ ($n = 5$); CGRP (10 pmol/site) $95.7 \pm 18.6\%$ ($n = 5$). In the diabetic rats the responses to lower doses of CGRP were very similar to those in normal rats: CGRP (0.1 pmol/site) $3.4 \pm 6.7\%$ decrease in blood flow ($n = 4$ rats); CGRP (1 pmol/site) $10.7 \pm 10.57\%$ increase in blood flow ($n = 4$); CGRP (10 pmol/site) $58.8 \pm 20.13\%$ increase in blood flow ($n = 4$). However the increase in blood flow induced by the highest dose of CGRP 10 pmol/site was significantly less in diabetic rats compared with normal rats ($P < 0.05$). The effect of the endothelium-dependent vasodilator, acetylcholine, was tested in normal rats; it increased blood flow only at high concentrations (10 nmol/site) and the increase in blood flow at this dose was modest ($20.81 \pm 8.45\%$ increase in blood flow, $n = 11$) relative to that seen with other vasodilators; thus the effect of acetylcholine was not investigated in diabetic rats.

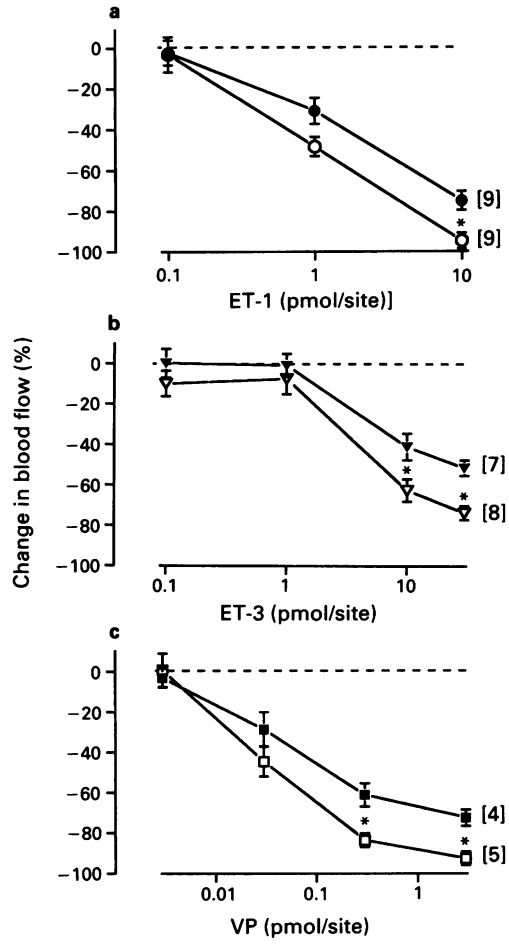

Figure 2 The effect of endothelin-1 (ET-1), ET-3 and vasopressin (VP) on local blood flow in the skin of control rats (open symbols) compared with diabetic rats (closed symbols). The response to Tyrode is represented by the dashed line. The results are mean (± s.e.mean, vertical bars) with the number of rats in each case shown in parentheses. A significant difference between the response in control compared with diabetic rats is indicated by $*P < 0.05$: (a) shows the response to ET-1; (b) shows the response to ET-3; (c) shows the response to VP.

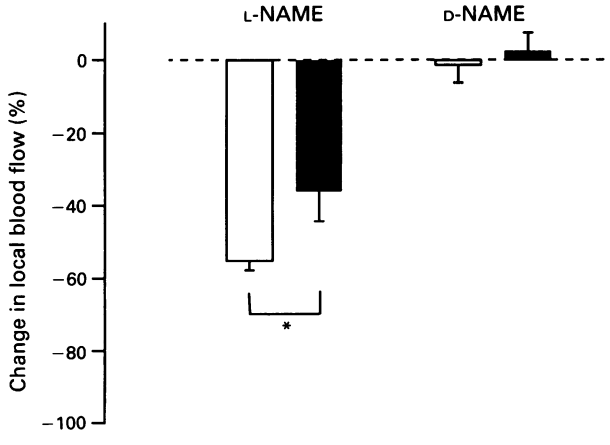

Figure 1 The effect of N^G-nitro-L-arginine methyl ester (L-NAME, 100 nmol/site) and its enantiomer D-NAME (100 nmol/site) on cutaneous blood flow in normal rats (open columns) and in diabetic rats (solid columns). Results are expressed as percentage change in local blood flow at test sites compared with sites injected with Tyrode alone in the same rat. The dashed line indicates the response at sites injected with Tyrode alone. The results are expressed as the mean (± s.e.mean, vertical bars) from $n = 9$ rats in each case. A significant difference between the response in diabetic compared with normal rats is indicated by $*P < 0.05$.

Effect of L-NAME on responses to ET-1 and ET-3

The effect of intradermal L-NAME on the responses to the endothelins was investigated in both diabetic and normal rats. Results are shown in Table 1. Intradermal L-NAME reduced blood flow in a similar manner as described above. L-NAME co-injected with submaximal doses of ET-1 and ET-3 enhanced the decrease in blood flow induced by each endothelin alone, this effect was observed in both the diabetic and normal rats. The combined responses to endothelins and L-NAME were diminished in the diabetic rats in all cases, see Table 1.

Discussion

The results show that the skin microvessels of STZ-induced diabetic rats are less responsive to changes in blood flow induced by the NO synthase inhibitor, L-NAME and to high doses of the endothelins and other vasoactive agents than those in normal rats. We are unable to eliminate a direct effect of STZ, but it has a half life in rat serum of 15 min (Rossini *et al.*, 1977) and is unlikely to exist in an active form or concentration four weeks after treatment. In addition others have found that vascular changes are not present immediately after treatment with STZ but develop a week or longer afterwards (Takeda *et al.*, 1991).

We observed an equivalent resting skin blood flow in diabetic and normal rats despite the altered vascular reactivity. It is interesting that Hill & Larkins (1989) found, in contrast, that resting blood flow to abdominal skin and to certain skeletal muscles in the hindlimbs was depressed in rats four weeks after STZ treatment; they measured blood flow as regional distribution of systemic microspheres. The difference between their finding and ours is surprising and presumably lies in the different technique used to measure blood flow since the rats were of the same species and were examined at the same timepoint after STZ treatment. In our study we measured blood flow in dorsal skin of rats as opposed to abdominal skin: this could be a relevant difference since in diabetic patients more distal capillaries exposed to higher capillary hydrostatic pressure exhibit greater structural changes (Vracko, 1970); therefore it is possible that the severity of dermal microvascular changes is highly dependent on the anatomical region.

Haemodynamic status in rats four weeks after STZ treatment has been described elsewhere. Hill & Larkins (1989) report that in anaesthetized STZ-treated Wistar rats there is no difference in mean arterial blood pressure compared with saline-treated rats. This finding is supported by work on conscious rats where no change in mean arterial blood pressure and a slight bradycardia were recorded in the diabetic animals (Kiff *et al.*, 1991b). However, this point is still controversial since different groups have found that diabetic rats are both hypertensive and hypotensive relative to normal rats.

In the present study, vasoconstriction to a local injection of L-NAME was decreased in the diabetic rat skin. This is consistent with either reduced synthesis and release of NO or decreased sensitivity of cutaneous microvessels to NO. This proposal is supported by a report that endothelium-dependent vasodilatation to acetylcholine was reduced in diabetic rat intestinal arterioles which responded normally to the direct cyclic GMP agonist, sodium nitroprusside (Lash & Bohlen, 1991). This change in sensitivity to acetylcholine occurred within 1 week of hyperglycaemia and would therefore be relevant to our study. We have previously shown that NO is important for maintaining basal blood flow (Lawrence & Brain, 1992) and were therefore surprised to find in the present study that the L-NAME-induced vasoconstriction was reduced in diabetic compared with normal skin despite a normal basal skin blood flow. It is possible that the depressed response to L-NAME represents a non-specific decrease in the reactivity of microvessels in the diabetic skin and basal microvascular blood flow may be less dependent on local production of NO in diabetic than in normal rats; for example, loss of endogenous NO in the disease state could be compensated by release of another vasodilator.

We observed a decrease in the vasoconstrictor response to ET-1 at high doses in diabetic rats. To date, the activity of ET-1 had been found unchanged in diabetic rats both *in vitro* on rat atria (Reid & Lieu, 1991) and *in vivo* following bolus intravenous injection (Kiff *et al.*, 1991b). This was in spite of a decrease in the density of [^{125}I]-ET-1 binding sites in cardiac tissue (Nayler *et al.*, 1989) and an increase in plasma levels of ET-1 (Takeda *et al.*, 1991) in diabetic rats. It is interesting that two structurally related peptides, which if normally present in rat skin, as suggested in man (Bull *et al.*, 1991), are probably derived from different cell types (Inoue *et al.*, 1989), active on different receptor subtypes (Arai *et al.*, 1990; Sakurai *et al.*, 1990) and yet have similarly depressed effects at high doses in diabetic rats. However the depressed response to ET-1 in skin in the present study cannot be explained as a specific decrease in the high affinity ET-1 binding sites described by Arai *et al.* (1990) since a similar decrease was observed to ET-3, and the unrelated peptide, vasopressin. Although arginine-vasopressin is unrelated to endothelin it can stimulate endothelin release from cultured endothelial cells (Masaki *et al.*, 1990) and at high doses decreases ET-1 binding sites on vascular smooth muscle cells (Roubert *et al.*, 1989) therefore the altered response to vasopressin observed in the present study could be linked to the altered endothelin activity observed in diabetic rat skin. We have therefore studied the actions of a potent vasodilator, CGRP, in diabetic skin to try and establish whether the altered response to endothelins represents a general or a more specific decrease in microvascular reactivity to vasoactive agents. CGRP is a neuropeptide and therefore likely to be affected by neuropathy; however, at the time point we studied, there are no significant neuropathological changes observed in skin samples from rats (Karanth *et al.*,

Table 1 Blood flow changes (% decrease compared with Tyrode-injected sites, mean ± s.e.mean) in normal and diabetic rats; the responses are in the absence and presence of N^G-nitro-L-arginine-methyl ester (L-NAME, 100 nmol/site)

Agent	(mol/site)	*Normal*	+L-NAME *Normal*	n	*Diabetic*	+L-NAME *Diabetic*	n
Tyrode		0	− 55.2 ± 2.60	9	0	− 35.9 ± 8.4*	9
ET-1	0.3	− 44.0 ± 8.1	− 72.4 ± 6.1	9	− 39.4 ± 7.7	− 50.6 ± 7.9**	9
ET-1	3.0	− 93.2 ± 1.0	− 90.9 ± 1.7	9	− 73.9 ± 4.2**	− 71.1 ± 6.1*	9
ET-3	0.1	− 9.9 ± 6.3	− 55.8 ± 7.0	7	0.23 ± 7.1	− 36.1 ± 5.1*	7
ET-3	1.0	− 7.3 ± 7.7	− 55.3 ± 7.1	7	− 0.7 ± 5.8	− 35.2 ± 5.7*	7
ET-3	10.0	− 62.4 ± 5.5	− 82.1 ± 3.1	7	− 40.9 ± 6.7*	− 67.3 ± 4.4	7

*$P<0.05$ and **$P<0.01$ indicate a significant difference between diabetic and normal rats, according to a modified t test.

1990). The reduced vasodilatation to CGRP combined with the decreased vasoconstriction to ET-1, ET-3 and vasopressin observed in the present study strongly suggests that the rat skin microvessels show a decrease in general vascular reactivity in diabetes.

We have previously shown that co-injection of L-NAME enhances the vasoconstriction to both ET-1, ET-3 and other vasoconstrictors in normal rats. We have suggested that endothelin could cause a damaging decrease in blood flow when NO production or action is limited in skin. In this study we examined interactions of L-NAME with ET-1 and ET-3 in diabetic rats. The results show that in keeping with a reduced effect of L-NAME in diabetic rats a reduced interaction between L-NAME and endothelin was observed. Thus inhibition of NO production in diabetic skin does not lead to such a dramatic potentiation of endothelin responses and is therefore not accompanied by such a potentially damaging decrease in blood flow as observed in normal rats.

We conclude from the present study that at an acute stage of experimental diabetes a nonspecific decrease in the responsiveness of the skin microvasculature to vasoactive agents has occurred. This decrease in responsiveness is not at present understood but it cannot simply be explained as a similar morphological decrease in density of cutaneous microvessels in diabetes as that observed in patients (Bohlen & Niggl, 1979) since basal blood flow is equivalent in both groups. Fortes *et al.* (1984) have carried out an intravital study of responses of the rat mesenteric microcirculation and oedema formation in skin to vasoactive agents in alloxan-induced diabetic rats compared with normal rats. They showed that vascular reactivity in the diabetic rat could be returned by local application of insulin and that reduced oedema formation in the skin of diabetic rats could be mimicked by 2-deoxyglucose (which inhibits glucose uptake) treatment of normal rats. Thus it is possible that insulin itself plays a pivotal role in maintaining cellular glucose levels at the microvascular levels in skin and in vascular reactivity and this should be the subject of further investigations on rat skin blood flow. Our results suggest that the cutaneous microvasculature of diabetic rats reacts differently to vasoactive factors, although basal blood flow through the microvascular bed is unaffected.

E.L. is in receipt of a British Heart Foundation studentship.

References

ARAI, H., HORI, S., ARAMORI, I., OHKUBO, H. & NAKANISHI, S. (1990). Cloning and expression of a cDNA encoding an endothelin receptor. *Nature*, **348**, 730–732.

BOHLEN, H.G. & NIGGL, B.A. (1979). Arteriolar anatomical and functional abnormalities in juvenile mice with genetic or streptozotocin-induced diabetes mellitus. *Circ. Res.*, **45**, 390–396.

BOULANGER, C. & LUSCHER, T.F. (1990). Release of endothelin from porcine aorta. *J. Clin. Invest.*, **58**, 587–590.

BULL, H.A., BUNKER, C.B., TERENGHI, G., SPRINGALL, D.R., ZHAO, Y., POLAK, J.M. & DOWD, P.M. (1992). Endothelin-1 in human skin: Immunolocalisation, receptor binding, mRNA expression, and effects on cutaneous microvascular endothelial cells. *J. Invest Dermatol.*, **97**, 618–623.

DE NUCCI, G., THOMAS, R., D'ORLEANS-JUSTE, P., ANTUNES, E., WALDER, C., WARNER, T. & VANE, J.R. (1988). Pressor effects of circulating endothelin are limited by its removal in the pulmonary circulation and by the release of prostacyclin and endothelium-derived relaxing factor. *Proc. Natl. Acad. Sci. U.S.A.*, **85**, 9797–9800.

FORTES, Z.B., DE NUCCI, G. & GARCIA-LEME, J. (1989). Effect of endothelin-1 on arterioles and venules in vivo. *J. Cardiovasc. Pharmacol.*, **13** (Suppl 5), S200–S201.

FORTES, Z.B., FARSKY, S.P., OLIVEIRA, M.A. & GARCIA-LEME, J. (1991). Direct vital microscopic study of defective leukocyte-endothelial interaction in diabetes mellitus. *Diabetes*, **40**, 1267–1273.

FORTES, Z.B., GARCIA-LEME, J. & SCIVOLETTO, R. (1983). Influence of diabetes on the reactivity of mesenteric microvessels to histamine, bradykinin and acetylcholine. *Br. J. Pharmacol.*, **78**, 39–48.

FORTES, Z.B., GARCIA-LEME, J. & SCIVOLETTO, R. (1984). Vascular reactivity in diabetes mellitus: possible role of insulin on the endothelial cell. *Br. J. Pharmacol.*, **83**, 635–643.

FURCHGOTT, R.F. & ZAWADZKI, J.V. (1980). The obligatory role of endothelial cells in the relaxation of arterial smooth muscle by acetylcholine. *Nature*, **288**, 373–376.

GARCIA-LEME, J., BOHM, G.M. MIGLIORINI, R.H. & SOUZA, M.Z.A. (1974). Possible participation of insulin in the control of vascular permeability. *Eur. J. Pharmacol.*, **29**, 298–306.

GARCIA-LEME, J., HAMAMURA, L., MIGLIORINI, R.H. & LEITE, M.P. (1973). Influence of diabetes upon the inflammatory response of the rat. A pharmacological analysis. *Eur. J. Pharmacol.*, **23**, 74–81.

GARDINER, S.M., COMPTON, A.M. & BENNETT, T. (1989). Regional hemodynamic effects of endothelin-1 in conscious unrestrained Wistar rats. *J. Cardiovasc. Pharmacol.*, **13** (Suppl 5), S202–S204.

HILL, M.A. & LARKINS, R.G. (1989). Alterations in distribution of cardiac output in experimental diabetes in rats. *Am. J. Physiol.*, **257**, H571–580.

IGNARRO, L.J., BUGA, G.M., WOOD, K.S. & BYRNS, R.E. (1987). Endothelium-derived relaxing factor produced and released from artery and vein is nitric oxide. *Proc. Natl. Acad. Sci. U.S.A.*, **84**, 9265–9269.

INOUE, A., YANAGISAWA, M., KIMURA, S., KASUYA, Y., MIYAUCHI, T., GOTO, K. & MASAKI, T. (1989). The human endothelin family: Three structurally and pharmacologically distinct isopeptides predicted by three separate genes. *Proc. Natl. Acad. Sci. U.S.A.*, **86**, 2863–2867.

KARANTH, S.S., SPRINGALL, D.R., FRANCAVILLA, S., MIRRLEES, D.J. & POLAK, J.M. (1990). Early increase in CGRP- and VIP-immunoreactive nerves in the skin of streptozotocin-induced diabetic rats. *Histochemistry*, **94**, 659–666.

KIFF, R.J., GARDINER, S.M., COMPTON, A.M. & BENNETT, T. (1991a). Selective impairment of hindquarters vasodilator responses to bradykinin in conscious Wistar rats with streptozotocin-induced diabetes mellitus. *Br. J. Pharmacol.*, **103**, 1357–1362.

KIFF, R.J., GARDINER, S.M., COMPTON, A.M. & BENNETT, T. (1991b). The effects of endothelin-1 and N^G-nitro-L-arginine methyl ester on regional haemodynamics in conscious rats with streptozotocin-induced diabetes mellitus. *Br. J. Pharmacol.*, **103**, 1321–1326.

LASH, J.M. & BOHLEN, H.G. (1991). Structural and functional origins of suppressed acetylcholine vasodilation in diabetic rat intestinal arterioles. *Circ. Res.*, **69**, 1259–1268.

LAWRENCE, E. & BRAIN, S.D. (1991). The effect of L-N^G-nitro arginine methyl ester (L-NAME) and endothelins (ET-1 and ET-3) on cutaneous blood flow in the diabetic rat. *Br. J. Pharmacol.*, **102**, 13P.

LAWRENCE, E. & BRAIN, S.D. (1992). Responses to endothelins in the rat cutaneous microvasculature: A modulatory role of locally-produced nitric oxide. *Br. J. Pharmacol.*, (in press).

MASAKI, T., YANAGISAWA, M., GOTO, K. & KIMURA, S. (1990). Role of endothelin in mechanisms of local pressure control. *J. Hypertens.*, **8** (Suppl 7), S107–S112.

MAYHAN, W.G. (1989). Impairment of endothelium-dependent dilatation of cerebral arterioles during diabetes mellitus. *Am. J. Physiol.*, **256**, H621–H625.

MOORE, P.K., AL-SWAYEH, O.A., CHONG, N.W.S., EVANS, R.A. & GIBSON, A. (1990). L-N^G-nitro arginine (L-NOARG), a novel, L-arginine-reversible inhibitor of endothelium-dependent vasodilatation in vitro. *Br. J. Pharmacol.*, **99**, 408–412.

NAYLER, W.G., LIU, J., PANAGIOTOPOULOS, S. & CASLEY, D.J. (1989). Streptozotocin-induced diabetes reduces the density of [^{125}I]-endothelin-binding sites in rat cardiac membranes. *Br. J. Pharmacol.*, **97**, 993–995.

PALMER, R.M.J., ASHTON, D.S. & MONCADA, S. (1988). Vascular endothelial cells synthesise nitric oxide from L-arginine. *Nature*, **333**, 664–666.

PALMER, R.M.J., FERRIGE, A.G. & MONCADA, S. (1987). Nitric oxide release accounts for the biological activity of endothelium-derived relaxing factor. *Nature*, **327**, 524–526.

PEREIRA, M.A.A., SANNOMIYA, P. & GARCIA-LEME, J. (1987). Inhibition of leukocyte chemotaxis by factor in alloxan-induced diabetic rat plasma. *Diabetes*, **36**, 1307–1314.

PORTA, M., LA SELVA, M., MOLINATTI, P. & MOLINATTI, G.M. (1987). Endothelial cell function in diabetic microangiopathy. *Diabetologia*, **30**, 601–609.

REID, J.J. & LIEU, A.T. (1991). The effect of 4-week streptozotocin-induced diabetes on response to endothelin-1 in rat isolated atria. *Neurochem. Int.*, **18**, 461–464.

ROSSINI, A.A., LIKE, A.A., CHICK, W.L., APPEL, M.C. & CAHILL, P. (1977). Studies of streptozotocin-induced insulitis and diabetes. *Proc. Natl. Acad. Sci. U.S.A.*, **74**, 2495–2489.

ROUBERT, P., GILLARD, V., PLAS, P., GUILLON, J.M., CHABRIER, P.E. & BRAQUET, P. (1989). Angiotensin II and phorbol-esters potently down-regulate endothelin (ET-1) binding sites in vascular smooth muscle cell cells. *Biochem. Biophys. Res. Commun.*, **164**, 809–815.

SAKURAI, T., YANAGISAWA, M., TAKUWA, Y., MIYAZAKI, H., KIMURA, S., GOTO, K. & MASAKI, T. (1990). Cloning of a cDNA encoding a non-isopeptide-selective subtype of the endothelin receptor. *Nature*, **348**, 732–735.

SANNOMIYA, P., PEREIRA, M.A.A. & GARCIA-LEME, J. (1990). Inhibition of leukocyte chemotaxis by serum factor in diabetes mellitus: Selective depression of cell responses mediated by complement-derived chemoattractants. *Agents Actions*, **30**, 369–376.

TAKAHASHI, K., GHATEI, M.A., LAM, H.-C., O'HALLORAN, D.J. & BLOOM, S.R. (1990). Elevated plasma endothelin in patients with diabetes mellitus. *Diabetologia*, **33**, 306–310.

TAKEDA, Y., MIYAMORI, I., YONEDA, T. & TAKEDA, R. (1991). Production of endothelin-1 from the mesenteric arteries of streptozotocin-induced diabetic rats. *Life Sci.*, **48**, 2553–2556.

TOOKE, J.E. (1989). Microcirculation and diabetes. *Br. Med. Bull.*, **45**, 206–223.

VRACKO, R. (1970). Skeletal muscle capillaries in diabetics. *Circulation*, **41**, 271–283.

WARNER, T.D., DE NUCCI, G. & VANE, J.R. (1989). Rat endothelin is a vasodilator in the isolated perfused mesentery of the rat. *Eur. J. Pharmacol.*, **159**, 325–326.

YANAGISAWA, M., KURIHARA, H., KIMURA, S., TOMOBE, Y., KOBAYASHI, M., MITSUI, Y., YAZAKI, Y., GOTO, K. & MASAKI, T. (1988). A novel potent vasoconstrictor peptide produced by vascular endothelial cells. *Nature*, **332**, 411–415.

(Received April 9, 1992
Accepted April 24, 1992)

 © Macmillan Press Ltd, 1992

Erratum

Br. J. Pharmacol. (1992) **106**, 387–394

M.D. Ivorra, C. Lugnier, C. Shott, M. Catret, M.A. Noguera, E. Anselmi & P. D'Ocon. Multiple actions of glaucine on cyclic nucleotide phosphodiesterases, α_1-adrenoceptor and benzothiazepine binding site at the calcium channel.

In the above paper, the figure which appeared as Figure 1 on page 388 was incorrect. The correct figure is shown below.

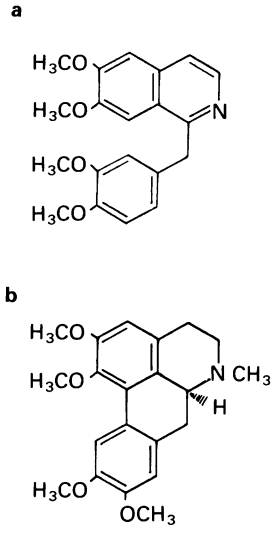

Figure 1 Chemical structures of (a) papaverine and (b) glaucine.

British Journal of Pharmacology

VOLUME 106 (4) AUGUST 1992

SPECIAL REPORTS

D.W.P. Hay. Pharmacological evidence for distinct endothelin receptors in guinea-pig bronchus and aorta 759

E.M. Silinsky, V. Gerzanich & S.M. Vanner. ATP mediates excitatory synaptic transmission in mammalian neurones 762

Y. Ishida, H. Honda & T.X. Watanabe. Ca^{2+} release from isolated sarcoplasmic reticulum of guinea-pig psoas muscle induced by K^+-channel blockers 764

A. Buisson, M. Plotkine & R.G. Boulu. The neuroprotective effect of a nitric oxide inhibitor in a rat model of focal cerebral ischaemia 766

PAPERS

H Sheng, H.H.H.W. Schmidt, M. Nakane, J.A. Mitchell, J.S. Pollock, U. Föstermann & F. Murad. Characterization and localization of nitric oxide synthase in non-adrenergic non-cholinergic nerves from bovine retractor penis muscles 768

E.R. Lazarowski, S.J. Mason, L. Clarke, T.K. Harden & R.C. Boucher. Adenosine receptors on human airway epithelia and their relationship to chloride secretion 774

H. Rogers, P.J. Birch, S.M. Harrison, E. Palmer, G.R. Manchee, D.B. Judd, A. Naylor, D.I.C. Scopes & A.G. Hayes. GR94839, a κ-opioid agonist with limited access to the central nervous system, has antinociceptive activity 783

K. Tazi-Saad, J. Chariot, M. Del Tacca & C. Rozé. Effect of α_2-adrenoceptor agonists on gastric pepsin and acid secretion in the rat 790

S.-M. Yu, S.-Y Hsu, F.-N. Ko, C.-C. Chen, Y.-L. Huang, T.-F. Huang & C.-M. Teng. Haemodynamic effects of dicentrine, a novel α_1-adrenoceptor antagonist: comparison with prazosin in spontaneously hypertensive and normotensive Wistar-Kyoto rats 797

P. Charlesworth, I. Jacobson, G. Pocock & C.D. Richards. The mechanism by which procaine inhibits catecholamine secretion from bovine chromaffin cells 802

J.L. Berry, R.C. Small & R.W. Foster. Tracheal relaxation induced by potassium channel opening drugs: its antagonism by adrenergic neurone blocking agents 813

R.B. Barlow, S. Bond, D.W. Holdup, J.A.K. Howard, D.S. McQueen, A. Paterson & M.A. Veale. The contribution of charge to affinity at functional (M_3) muscarinic receptors in guinea-pig ileum assessed from the effects of the carbon analogue of 4-DAMP methiodide 819

S. Ebihara & N. Akaike. Strychnine-induced potassium current in CA1 pyramidal neurones of the rat hippocampus 823

J.P. Hayes, J. O. Lotvall, P.J. Barnes, A.J. Newman Taylor & K. Fan Chung. Involvement of inflammatory mediators in the airway responses to trimellitic anhydride in sensitized guinea-pigs 828

E. Castro, J. Pintor & M.T. Miras-Portugal. Ca^{2+}-stores mobilization by diadenosine tetraphosphate, Ap_4A, through a putative P_{2y} purinoceptor in adrenal chromaffin cells 833

R.J. Gryglewski, A. Zembowicz, D. Salvemini, G.W. Taylor & J.R. Vane. Modulation of the pharmacological actions of nitrovasodilators by methylene blue and pyocyanin 838

J.V. Espluges, B.J.R. Whittle & S. Moncada. Modulation by opioids and by afferent sensory neurones of prostanoid protection of the rat gastric mucosa 846

R.H. Henning, A. Nelemans, J. van den Akker & A. den Hertog. The nucleotide receptors on mouse C2C12 myotubes 853

S.B. Guild, S. Jenkinson & T.C. Muir. Noradrenaline-stimulated inositol phosphate accumulation in arteries from spontaneously-hypertensive rats 859

J.E. Nally, T.C. Muir & S.B. Guild. The effects of noradrenaline and adenosine 5′-triphosphate on polyphosphoinositide and phosphatidylcholine hydrolysis in arterial smooth muscle 865

T.V. Murphy, S. Foucart & H. Majewski. Prejunctional α_2-adrenoceptors in mouse atria function through G-proteins which are sensitive to N-ethylmaleimide, but not pertussis toxin 871

C.M. Scott, K.T. Bunce & C.F. Spraggs. Investigation of the 5-hydroxytryptamine receptor mediating the 'maintained' short-circuit current response in guinea-pig ileal mucosa 877

C. Advenier, V. Lagente, Y. Zhang & E. Naline. Contractile activity of big endothelin-1 on the human isolated bronchus 883

C.A. Maggi & R. Patacchini. Tachykinin NK_1 receptor in the guinea-pig isolated proximal urethra: characterization by receptor selective agonists and antagonists 888

P. Van den Hooff & M. Galvan. Actions of 5-hydroxytryptamine and $5\text{-}HT_{1A}$ receptor ligands on rat dorso-lateral septal neurones *in vitro* 893

H. Tanaka, Y. Habuchi, M. Nishimura, N. Sato & Y. Watanabe. Blockade of Na^+ current by promethazine in guinea-pig ventricular myocytes 900

Y. Jinno, H. Kasai, H. Ohta, K. Nishikori, H. Fukushima & N. Ogawa. Contribution of cyclic GMP formation to KRN2391-induced relaxation in coronary artery of the pig 906

J.H. Kehne, J.M. Kane, F.P. Miller, H.J. Ketteler, D.L. Braun, Y. Senyah, S.F. Chaney, A. Abdallah, M.W. Dudley, A.M. Ogden & M.G. Palfreyman. MDL 27,531 selectively reverses strychnine-induced seizures in mice 910

D.M. Vanags, S.E. Rodgers, E.M. Duncan, J.V. Lloyd & F. Bochner. Potentiation of ADP-induced aggregation in human platelet-rich plasm by 5-hydroxytryptamine and adrenaline 917

E.R. Petrich, N. Leblanc, F. deLorenzi, Y. Allard & O.F. Schanne. Effects of K^+ channel blockers on the action potential of hypoxic rabbit myocardium 924

D. Salvemini, V. Mollace, A. Pistelli, E. Änggård & J. Vane. Cultured astrocytoma cells generate a nitric oxide-like factor from endogenous L-arginine and glyceryl trinitrate: effect of *E. coli* lipopolysaccharide 931

M.R. MacLean, A.G.B. Templeton & J.C. McGrath. The influence of endothelin-1 on human foeto-placental blood vessels: a comparison with 5-hydroxytryptamine 937

R. Foulkes & S. Shaw. The cardiodepressant and vasodepressant effects of tumour necrosis factor in rat isolated atrial and aortic tissues 942

T.D. Warner, G.P. Budzik, T. Matsumoto, J.A. Mitchell, U. Förstermann & F. Murad. Regional differences in endothelin converting enzyme activity in rat brain: inhibition by phosphoramidon and EDTA **948**

J.B. Warren, M.L. Coughlan & T.J. Williams. Endotoxin-induced vasodilatation in anaesthetized rat skin involves nitric oxide and prostaglandin synthesis **953**

S.P. Connors, E.W. Gill & D.A. Terrar. Actions and mechanisms of action of novel analogues of sotalol on guinea-pig and rabbit ventricular cells **958**

C. Astarie-Dequeker, L. Iouzalen, M. David-Dufilho & M.-A. Devynck. *In vitro* inhibition by endothelins of thrombin-induced aggregation and Ca^{2+} mobilization in human platelets **966**

J.C. Ellory, G.B. Nash, P.C.W. Stone, S.J. Culliford, E. Horwitz & J. Stuart. Mode of action and comparative efficacy of pharmacological agents that inhibit calcium-dependent dehydration of sickle cells **972**

J.R. Thorne & K.J. Broadley. Adenosine-induced bronchoconstriction of isolated lung and trachea from sensitized guinea-pigs **978**

S. Uhlén, Y. Xia, V. Chhajlani, C.C. Felder & J.E.S. Wikberg. [^{3}H]-MK 912 binding delineates two α_2-adrenoceptor subtypes in rat CNS one of which is identical with the cloned pA2d α_2-adrenoceptor **986**

P. Leff & H. Giles. Classification of platelet and vascular prostaglandin D_2 (DP) receptors: estimation of affinities and relative efficacies for a series of novel bicylic ligands. With an Appendix on Goodness-of-fit analyses **996**

S.A. Waterman, M. Costa & M. Tonini. Modulation of peristalsis in the guinea-pig isolated small intestine by exogenous and endogenous opioids **1004**

A.C. MacKinnon, A.T. Kilpatrick, B.A. Kenny, M. Spedding & C.M. Brown. [^{3}H]-RS-15385-197, a selective and high affinity radioligand for α_2-adrenoceptors: implications for receptor classification **1011**

N.J. Mallard, A.L. Hudson & D.J. Nutt. Characterization and autoradiographical localization of non-adrenoceptor idazoxan binding sites in the rat brain **1019**

J. de Boer, A.J. Philpott, R.G.M. van Amsterdam, M. Shahid, J. Zaagsma & C.D. Nicholson. Human bronchial cyclic nucleotide phosphodiesterase isoenzymes: biochemical and pharmacological analysis using selective inhibitors **1028**

E. Lawrence & S.D. Brain. Altered microvascular reactivity to endothelin-1, endothelin-3 and N^G-nitro-L-arginine methyl ester in streptozotocin-induced diabetes mellitus **1035**

ERRATUM

Br. J. Pharmacol. (1992), **106**, 387–394

M.D. Ivorra, C. Lugnier, C. Shott, M. Catret, M.A. Noguera, E. Anselmi & P. D'Ocon. Multiple actions of glaucine on cyclic nucleotide phosphodiesterases, α_1-adrenoceptor and benzothiazepine binding site at the calcium channel **1041**

SPECIAL REPORTS

The purpose of *Special Reports* is to provide rapid publication for **new** and **important** results which the Editorial Board considers are likely to be of special pharmacological significance. *Special Reports* will have publication priority over all other material and so authors are asked to consider carefully the status of their work before submission.

In order to speed publication there is normally no revision allowed beyond very minor typographical or grammatical corrections. If significant revision is required, the Board may either invite rapid re-submission or, more probably, propose that it be re-written as a Full Paper and be re-submitted for consideration. In order to reduce delays, proofs of *Special Reports* will be sent to authors but **essential corrections must reach the Production Office within 48 hours of receipt.** Authors should ensure that their submitted material conforms exactly to the following requirements.

Special Reports should normally occupy no more than two printed pages of the Journal; two illustrations (Figures or Tables, with legends) are permitted. As a guideline, with type face of 12 pitch and double-line spacing, a page of A4 paper could contain about 400 words. The absolute maximum length of the *Special Report* is 1700 words. For each Figure or Table, please deduct 200 words. The manuscript should comprise a Title page with key words (maximum of 10), a Summary consisting of a single short paragraph, followed by Introduction, Methods, Results, Discussion and References (maximum of 10). In all other respects, the requirements are the same as for Full Papers (see current 'Instructions to Authors').

Edited for the British Pharmacological Society by

A.T. Birmingham *(Chairman)*
R.W. Horton *(Secretary)*
W.A. Large *(Secretary)*

EDITORIAL BOARD

J.A. Angus Prahran, Australia
M.L.J. Ashford Cambridge
G.W. Bennett Nottingham
T. Bennett Nottingham
W.C. Bowman Glasgow
N.G. Bowery London
Alison F. Brading Oxford
S.D. Brain London
K.T. Bunce Ware
G. Burnstock London
K.D. Butler Horsham
M. Caulfield London
M.K. Church Southampton
S.J. Coker Liverpool
R.A. Coleman Ware
G.A. Cottrell St Andrews
A.J. Cross London
V. Crunelli Cardiff
T.C. Cunnane Oxford
F. Cunningham London
A. Dray London
J.M. Edwardson Cambridge
W. Feniuk Cambridge
J.R. Fozard Basle, Switzerland
C.J. Garland Southampton
L.G. Garland Beckenham
A. Gibson London
R. Gristwood Barcelona, Spain
P.E. Hicks Leuville-sur-Orge, France
S.J. Hill Nottingham
J.C. Hunter Cambridge
K.A. Kane Glasgow
P. Keen Bristol
D.A. Kendall Nottingham
P. Leff Loughborough
D. Lodge Surrey
H.D. Lux Planegg, Germany
R. McMillan Macclesfield
J. Maclagan London
G. Martin Beckenham
W. Martin Glasgow
D.N. Middlemiss Harlow
R.C. Miller Strasbourg, France
P.K. Moore London
R.J. Naylor Bradford
C.D. Nicholson Newhouse
C.P. Page London
R.M.J. Palmer Beckenham
B.K. Park Liverpool
A.N. Payne Beckenham
F.L. Pearce London
M.H.T. Roberts Cardiff
P.J. Roberts Southampton
C. Robinson London
G.J. Sanger Harlow
M.A. Simmonds London
J.M. Sneddon Sunderland
M. Spedding Edinburgh
K. Starke Freiburg, Germany
P.V. Taberner Bristol
M.D. Tricklebank Harlow
M.B. Tyers Ware
S.P. Watson Oxford
A.H. Weston Manchester
B.J.R. Whittle Beckenham
Eileen Winslow Newhouse

CORRESPONDING EDITORS

P.R. Adams Stony Brook, U.S.A.
C. Bell Melbourne, Australia
F.E. Bloom La Jolla, U.S.A.
A.L.A. Boura Clayton, Australia
N.J. Dun Toledo, U.S.A.
R.F. Furchgott New York, U.S.A.
T. Godfraind Brussels, Belgium
S.Z. Langer Paris, France
R.J. Miller Chicago, U.S.A.
R.C. Murphy Denver, U.S.A.
E. Muscholl Mainz, Germany
R.A. North Portland, U.S.A.
M. Otsuka Tokyo, Japan
M.J. Rand Melbourne, Australia
S. Rosell Södertalje, Sweden
P. Seeman Toronto, Canada
L. Szekeres Szeged, Hungary
B. Uvnas Stockholm, Sweden
P.A. Van Zwieten Amsterdam, Netherlands
V.M. Varagič Belgrade, Yugoslavia
G. Velo Verona, Italy
Wang Zhen Gang Beijing, China
M.B.H. Youdim Haifa, Israel

Papers will be considered for publication on all aspects of pharmacology, including chemotherapy.

Manuscripts (two copies) should be sent to Editorial Office, British Journal of Pharmacology, St. George's Hospital Medical School, Cranmer Terrace, London SW17 0RE. Authors should consult the Instructions to Authors in Vol. 105, 245–251 (1992) and the Nomenclature Guidelines for Authors in Vol. 105, 252–254 (1992). These Instructions and Guidelines also appear with the journal Index for volumes 102–104, 1991.

The *British Journal of Pharmacology* is published monthly by the Scientific & Medical Division, Macmillan Press Ltd.

The journal is covered by *Current Contents*, *Excerpta Medica* and *Index Medicus*.

All business correspondence and reprint requests should be addressed to the Scientific & Medical Division, Macmillan Press Ltd., Houndmills, Basingstoke, Hampshire RG21 2XS, UK. Telephone: (0256) 29242; Fax: (0256) 810526.

Annual subscription prices for 1992 EEC £412, elsewhere £445/US$825 (sterling rate is definitive). Orders must be accompanied by remittance. Cheques should be made payable to Macmillan Press, and sent to: Macmillan Press Ltd., Subscription Department, Brunel Road, Houndmills, Basingstoke, Hampshire RG21 2XS, UK.

Overseas subscribers may make payments into UK Post Office Giro Account No. 5192455. Full details must accompany the payment.

Second Class postage paid at Rahway NJ. US Mailing Agent: Mercury Airfreight International Ltd, Inc., 2323 Randolph Avenue, Avenel, New Jersey, NJ 07001, USA.

Enquiries concerning advertising space or rates should be addressed to: Michael Rowley, Advertisement Manager, Macmillan Press Ltd., 4 Little Essex Street, London WC2R 3LF. Telephone: 071 836 6633; Fax: 071 379 0820.

All rights of reproduction are reserved in respect of all papers, articles, illustrations, etc., published in this journal in all countries of the world.

Authorization to photocopy items for internal or personal use, or the internal or personal use of specific clients, is granted by Macmillan Press Ltd for libraries and other users registered with the Copyright Clearance Center (CCC) Transactional Reporting Service, provided that the base fee of $3.50 per copy is paid directly to CCC, 21 Congress St., Salem, MA 01970, USA.

© The British Pharmacological Society & Macmillan Press Ltd, 1992.
ISSN 0007–1188

0007–1188/92 $3.50 + $0.00

T.D. Warner, G.P. Budzik, T. Matsumoto, J.A. Mitchell, U. Förstermann & F. Murad. Regional differences in endothelin converting enzyme activity in rat brain: inhibition by phosphoramidon and EDTA **948**

J.B. Warren, M.L. Coughlan & T.J. Williams. Endotoxin-induced vasodilatation in anaesthetized rat skin involves nitric oxide and prostaglandin synthesis **953**

S.P. Connors, E.W. Gill & D.A. Terrar. Actions and mechanisms of action of novel analogues of sotalol on guinea-pig and rabbit ventricular cells **958**

C. Astarie-Dequeker, L. Iouzalen, M. David-Dufilho & M.-A. Devynck. *In vitro* inhibition by endothelins of thrombin-induced aggregation and Ca^{2+} mobilization in human platelets **966**

J.C. Ellory, G.B. Nash, P.C.W. Stone, S.J. Culliford, E. Horwitz & J. Stuart. Mode of action and comparative efficacy of pharmacological agents that inhibit calcium-dependent dehydration of sickle cells **972**

J.R. Thorne & K.J. Broadley. Adenosine-induced bronchoconstriction of isolated lung and trachea from sensitized guinea-pigs **978**

S. Uhlén, Y. Xia, V. Chhajlani, C.C. Felder & J.E.S. Wikberg. [^{3}H]-MK 912 binding delineates two α_2-adrenoceptor subtypes in rat CNS one of which is identical with the cloned pA2d α_2-adrenoceptor **986**

P. Leff & H. Giles. Classification of platelet and vascular prostaglandin D_2 (DP) receptors: estimation of affinities and relative efficacies for a series of novel bicylic ligands. With an Appendix on Goodness-of-fit analyses **996**

S.A. Waterman, M. Costa & M. Tonini. Modulation of peristalsis in the guinea-pig isolated small intestine by exogenous and endogenous opioids **1004**

A.C. MacKinnon, A.T. Kilpatrick, B.A. Kenny, M. Spedding & C.M. Brown. [^{3}H]-RS-15385-197, a selective and high affinity radioligand for α_2-adrenoceptors: implications for receptor classification **1011**

N.J. Mallard, A.L. Hudson & D.J. Nutt. Characterization and autoradiographical localization of non-adrenoceptor idazoxan binding sites in the rat brain **1019**

J. de Boer, A.J. Philpott, R.G.M. van Amsterdam, M. Shahid, J. Zaagsma & C.D. Nicholson. Human bronchial cyclic nucleotide phosphodiesterase isoenzymes: biochemical and pharmacological analysis using selective inhibitors **1028**

E. Lawrence & S.D. Brain. Altered microvascular reactivity to endothelin-1, endothelin-3 and N^G-nitro-L-arginine methyl ester in streptozotocin-induced diabetes mellitus **1035**

ERRATUM

Br. J. Pharmacol. (1992), **106**, 387–394

M.D. Ivorra, C. Lugnier, C. Shott, M. Catret, M.A. Noguera, E. Anselmi & P. D'Ocon. Multiple actions of glaucine on cyclic nucleotide phosphodiesterases, α_1-adrenoceptor and benzothiazepine binding site at the calcium channel **1041**

SPECIAL REPORTS

The purpose of *Special Reports* is to provide rapid publication for **new** and **important** results which the Editorial Board considers are likely to be of special pharmacological significance. *Special Reports* will have publication priority over all other material and so authors are asked to consider carefully the status of their work before submission.

In order to speed publication there is normally no revision allowed beyond very minor typographical or grammatical corrections. If significant revision is required, the Board may either invite rapid re-submission or, more probably, propose that it be re-written as a Full Paper and be re-submitted for consideration. In order to reduce delays, proofs of *Special Reports* will be sent to authors but **essential corrections must reach the Production Office within 48 hours of receipt.** Authors should ensure that their submitted material conforms exactly to the following requirements.

Special Reports should normally occupy no more than two printed pages of the Journal; two illustrations (Figures or Tables, with legends) are permitted. As a guideline, with type face of 12 pitch and double-line spacing, a page of A4 paper could contain about 400 words. The absolute maximum length of the *Special Report* is 1700 words. For each Figure or Table, please deduct 200 words. The manuscript should comprise a Title page with key words (maximum of 10), a Summary consisting of a single short paragraph, followed by Introduction, Methods, Results, Discussion and References (maximum of 10). In all other respects, the requirements are the same as for Full Papers (see current 'Instructions to Authors').

PREPARATION OF MANUSCRIPTS

Authors are strongly recommended to read the full *Instructions to Authors* and *Nomenclature Guidelines for Authors* (*Br. J. Pharmacol.* 1992, **105,** 245–254) before submitting a manuscript for publication in the *British Journal of Pharmacology*. The manuscript and cover letter should be checked against the following list before mailing.

The original and one copy of the manuscript must be supplied. Manuscripts must be typed in double-line spacing on one side of A4 paper, in type not smaller than 12 characters per inch or 10 point. Both copies to include Tables and a set of labelled Figures. One set of Figures without numbers or letters is also to be included. The text to be arranged in the following subsections:

1. **Title**—To have no more than 150 characters on a separate page, which should also include a Short Title (50 characters maximum) and the name and address of the author for correspondence.

2. **Summary**—To be arranged in numbered paragraphs (Full Papers) or a single paragraph (Special Reports).
   —to include aims, principal results and conclusions.
   —to include Key words (10 maximum) at end of summary.

3. **Introduction**—To contain concise statements of the problem and the aims of the investigation.

4. **Methods**—To have brief but adequate account of the procedures; *full names of drugs* (*including those referred to by manufacturer's code*), sources of drugs and statistical tests to be stated.

5. **Results**—To have no repetition of data in Figures, Tables and text.

6. **Discussion**—Findings and conclusions to be placed in context of other relevant work.
   NB Simple repetition of results and unwarranted speculation are not acceptable.

7. **Acknowledgments**—Sources of support. Sources of drugs not widely available commercially.

8. **References**—All references in the text to be included in the Reference List and *vice versa*. References in alphabetical order with complete citations; Journals publishing 'in press' papers identified.
   References to manuscripts submitted to other journals but not yet accepted are not allowed.

9. **Tables**—Each on a separate page and prepared in accordance with current requirements of the Journal.

10. **Figures**—Both labelled and non-labelled Figures to be prepared in accordance with current requirements of the Journal (see *Instructions to Authors*, 1992, **105,** 245–251) and provided with Figure Number and Authors' names on back (*in pencil*).
    —each legend to be typed on a separate page and carrying keys to symbols.
    —keys to symbols and histograms must not appear on the figures themselves, but in the respective legends.
    —'box style' figures are not in keeping with the Journal style; line drawings etc must have only left-hand and bottom axes.

11. **Manuscripts**—To be accompanied by a declaration signed by each author that
    (a) results are original
    (b) approval of all persons concerned has been given to submit manuscripts for consideration (see also 12b)
    (c) the same material is neither 'in press' (i.e. is in proof or has definitely been accepted for publication) nor under consideration elsewhere. Furthermore it will not be submitted or published elsewhere before a decision has been reached by the Editorial Board of the *British Journal of Pharmacology* and will not be submitted elsewhere if accepted by the *British Journal of Pharmacology*.
    (d) Copyright assignment is included.

12. **Cover letter**—To state clearly
    (a) Corresponding author's full postal address, telephone, telex or Fax number
    (b) where appropriate, that *either* ethical approval has been given for investigation *or* Company or Institutional permission to publish work has been received.

13. **Reminder**—Packaging to be sufficiently robust to protect Figures and to withstand mailing.

Failure to comply with *Instructions to Authors* may lead to substantial delays in processing, review and publication and may even jeopardize acceptance of the manuscript.

NOMENCLATURE

Authors are reminded that accepted receptor and associated terminology is laid out in *Nomenclature Guidelines for Authors*, as published in the *British Journal of Pharmacology, Br. J. Pharmacol., 1992,* **105,** 245–254.

BRITISH JOURNAL OF PHARMACOLOGY VOLUME 106 (4) 1992

SPECIAL REPORTS

D.W.P. Hay. Pharmacological evidence for distinct endothelin receptors in guinea-pig bronchus and aorta 759

E.M. Silinsky, V. Gerzanich & S.M. Vanner. ATP mediates excitatory synaptic transmission in mammalian neurones 762

Y. Ishida, H. Honda & T.X. Watanabe. Ca^{2+} release from isolated sarcoplasmic reticulum of guinea-pig psoas muscle induced by K^+-channel blockers 764

A. Buisson, M. Plotkine & R.G. Boulu. The neuroprotective effect of a nitric oxide inhibitor in a rat model of focal cerebral ischaemia 766

PAPERS

H Sheng, H.H.H.W. Schmidt, M. Nakane, J.A. Mitchell, J.S. Pollock, U. Förstermann & F. Murad. Characterization and localization of nitric oxide synthase in non-adrenergic non-cholinergic nerves from bovine retractor penis muscles 768

E.R. Lazarowski, S.J. Mason, L. Clarke, T.K. Harden & R.C. Boucher. Adenosine receptors on human airway epithelia and their relationship to chloride secretion 774

H. Rogers, P.J. Birch, S.M. Harrison, E. Palmer, G.R. Manchee, D.B. Judd, A. Naylor, D.I.C. Scopes & A.G. Hayes. GR94839, a κ-opioid agonist with limited access to the central nervous system, has antinociceptive activity 783

K. Tazi-Saad, J. Chariot, M. Del Tacca & C. Rozé. Effect of α_2-adrenoceptor agonists on gastric pepsin and acid secretion in the rat 790

S.-M. Yu, S.-Y Hsu, F.-N. Ko, C.-C. Chen, Y.-L. Huang, T.-F. Huang & C.-M. Teng. Haemodynamic effects of dicentrine, a novel α_1-adrenoceptor antagonist: comparison with prazosin in spontaneously hypertensive and normotensive Wistar-Kyoto rats 797

P. Charlesworth, I. Jacobson, G. Pocock & C.D. Richards. The mechanism by which procaine inhibits catecholamine secretion from bovine chromaffin cells 802

J.L. Berry, R.C. Small & R.W. Foster. Tracheal relaxation induced by potassium channel opening drugs: its antagonism by adrenergic neurone blocking agents 813

R.B. Barlow, S. Bond, D.W. Holdup, J.A.K. Howard, D.S. McQueen, A. Paterson & M.A. Veale. The contribution of charge to affinity at functional (M_3) muscarinic receptors in guinea-pig ileum assessed from the effects of the carbon analogue of 4-DAMP methiodide 819

S. Ebihara & N. Akaike. Strychnine-induced potassium current in CA1 pyramidal neurones of the rat hippocampus 823

J.P. Hayes, J. O. Lotvall, P.J. Barnes, A.J. Newman Taylor & K. Fan Chung. Involvement of inflammatory mediators in the airway responses to trimellitic anhydride in sensitized guinea-pigs 828

E. Castro, J. Pintor & M.T. Miras-Portugal. Ca^{2+}-stores mobilization by diadenosine tetraphosphate, Ap_4A, through a putative P_{2y} purinoceptor in adrenal chromaffin cells 833

R.J. Gryglewski, A. Zembowicz, D. Salvemini, G.W. Taylor & J.R. Vane. Modulation of the pharmacological actions of nitrovasodilators by methylene blue and pyocyanin 838

J.V. Espluges, B.J.R. Whittle & S. Moncada. Modulation by opioids and by afferent sensory neurones of prostanoid protection of the rat gastric mucosa 846

R.H. Henning, A. Nelemans, J. van den Akker & A. den Hertog. The nucleotide receptors on mouse C2C12 myotubes 853

S.B. Guild, S. Jenkinson & T.C. Muir. Noradrenaline-stimulated inositol phosphate accumulation in arteries from spontaneously-hypertensive rats 859

J.E. Nally, T.C. Muir & S.B. Guild. The effects of noradrenaline and adenosine 5'-triphosphate on polyphosphoinositide and phosphatidylcholine hydrolysis in arterial smooth muscle 865

T.V. Murphy, S. Foucart & H. Majewski. Prejunctional α_2-adrenoceptors in mouse atria function through G-proteins which are sensitive to N-ethylmaleimide, but not pertussis toxin 871

C.M. Scott, K.T. Bunce & C.F. Spraggs. Investigation of the 5-hydroxytryptamine receptor mediating the 'maintained' short-circuit current response in guinea-pig ileal mucosa 877

C. Advenier, V. Lagente, Y. Zhang & E. Naline. Contractile activity of big endothelin-1 on the human isolated bronchus 883

C.A. Maggi & R. Patacchini. Tachykinin NK_1 receptor in the guinea-pig isolated proximal urethra: characterization by receptor selective agonists and antagonists 888

P. Van den Hooff & M. Galvan. Actions of 5-hydroxytryptamine and 5-HT_{1A} receptor ligands on rat dorso-lateral septal neurones *in vitro* 893

H. Tanaka, Y. Habuchi, M. Nishimura, N. Sato & Y. Watanabe. Blockade of Na^+ current by promethazine in guinea-pig ventricular myocytes 900

Y. Jinno, H. Kasai, H. Ohta, K. Nishikori, H. Fukushima & N. Ogawa. Contribution of cyclic GMP formation to KRN2391-induced relaxation in coronary artery of the pig 906

J.H. Kehne, J.M. Kane, F.P. Miller, H.J. Ketteler, D.L. Braun, Y. Senyah, S.F. Chaney, A. Abdallah, M.W. Dudley, A.M. Ogden & M.G. Palfreyman. MDL 27,531 selectively reverses strychnine-induced seizures in mice 910

D.M. Vanags, S.E. Rodgers, E.M. Duncan, J.V. Lloyd & F. Bochner. Potentiation of ADP-induced aggregation in human platelet-rich plasm by 5-hydroxytryptamine and adrenaline 917

E.R. Petrich, N. Leblanc, F. deLorenzi, Y. Allard & O.F. Schanne. Effects of K^+ channel blockers on the action potential of hypoxic rabbit myocardium 924

D. Salvemini, V. Mollace, A. Pistelli, E. Änggård & J. Vane. Cultured astrocytoma cells generate a nitric oxide-like factor from endogenous L-arginine and glyceryl trinitrate: effect of *E. coli* lipopolysaccharide 931

M.R. MacLean, A.G.B. Templeton & J.C. McGrath. The influence of endothelin-1 on human foeto-placental blood vessels: a comparison with 5-hydroxytryptamine 937

R. Foulkes & S. Shaw. The cardiodepressant and vasodepressant effects of tumour necrosis factor in rat isolated atrial and aortic tissues 942

T.D. Warner, G.P. Budzik, T. Matsumoto, J.A. Mitchell, U. Förstermann & F. Murad. Regional differences in endothelin converting enzyme activity in rat brain: inhibition by phosphoramidon and EDTA 948

J.B. Warren, M.L. Coughlan & T.J. Williams. Endotoxin-induced vasodilatation in anaesthetized rat skin involves nitric oxide and prostaglandin synthesis 953

S.P. Connors, E.W. Gill & D.A. Terrar. Actions and mechanisms of action of novel analogues of sotalol on guinea-pig and rabbit ventricular cells 958

C. Astarie-Dequeker, L. Iouzalen, M. David-Dufilho & M.-A. Devynck. *In vitro* inhibition by endothelins of thrombin-induced aggregation and Ca^{2+} mobilization in human platelets 966

J.C. Ellory, G.B. Nash, P.C.W. Stone, S.J. Culliford, E. Horwitz & J. Stuart. Mode of action and comparative efficacy of pharmacological agents that inhibit calcium-dependent dehydration of sickle cells 972

J.R. Thorne & K.J. Broadley. Adenosine-induced bronchoconstriction of isolated lung and trachea from sensitized guinea-pigs 978

S. Uhlén, Y. Xia, V. Chhajlani, C.C. Felder & J.E.S. Wikberg. [^{3}H]-MK 912 binding delineates two α_2-adrenoceptor subtypes in rat CNS one of which is identical with the cloned pA2d α_2-adrenoceptor 986

P. Leff & H. Giles. Classification of platelet and vascular prostaglandin D_2 (DP) receptors: estimation of affinities and relative efficacies for a series of novel bicylic ligands. With an Appendix on Goodness-of-fit analyses 996

S.A. Waterman, M. Costa & M. Tonini. Modulation of peristalsis in the guinea-pig isolated small intestine by exogenous and endogenous opioids 1004

A.C. MacKinnon, A.T. Kilpatrick, B.A. Kenny, M. Spedding & C.M. Brown. [^{3}H]-RS-15385-197, a selective and high affinity radioligand for α_2-adrenoceptors: implications for receptor classification 1011

N.J. Mallard, A.L. Hudson & D.J. Nutt. Characterization and autoradiographical localization of non-adrenoceptor idazoxan binding sites in the rat brain 1019

J. de Boer, A.J. Philpott, R.G.M. van Amsterdam, M. Shahid, J. Zaagsma & C.D. Nicholson. Human bronchial cyclic nucleotide phosphodiesterase isoenzymes: biochemical and pharmacological analysis using selective inhibitors 1028

E. Lawrence & S.D. Brain. Altered microvascular reactivity to endothelin-1, endothelin-3 and N^G-nitro-L-arginine methyl ester in streptozotocin-induced diabetes mellitus 1035

ERRATUM

Br. J. Pharmacol. (1992), **106**, 387–394

M.D. Ivorra, C. Lugnier, C. Shott, M. Catret, M.A. Noguera, E. Anselmi & P. D'Ocon. Multiple actions of glaucine on cyclic nucleotide phosphodiesterases, α_1-adrenoceptor and benzothiazepine binding site at the calcium channel 1041

Typeset by Elite Typesetting Techniques, Southampton, Hampshire
and printed in Great Britain by Unwin Brothers Ltd., The Gresham Press, Old Woking, Surrey